ASSOCIATION FOR RESEARCH IN OTOLARYNGOLOGY

FOUNDED IN 1973

FEBRUARY 9–14, 2018

41ˢᵗ Annual MidWinter Meeting

ABSTRACTS

Manchester Grand Hyatt | San Diego, California, USA

ARO OFFICERS FOR 2017-2018

PRESIDENT:

John P. Carey, MD (17-18)
Johns Hopkins School of Medicine
Department of Otolaryngology-HNS
601 North Caroline Street, Room 6161A
Baltimore, MD 21287-0910 USA

PRESIDENT ELECT:

Karen P. Steel, PhD (17-18)
Kings College London
Guys Campus, Wolfson Center For Age Related Diseases
London Central
United Kingdom SE1 1UL

PAST PRESIDENT:

Matthew W. Kelley, PhD (17-18)
NIDCD/NIH-Porter Neuroscience Research Center
Building 35, Room ID-993
35 Convent Drive
Bethesda, MD 20892 USA

SECRETARY/ TREASURER:

Gabriel Corfas, PhD (17-20)
The University of Michigan, Kresge
Hearing Research Institute
1150 West Medical Center. Drive
Medical Sciences 1 Bldg; RM 5424A
Ann Arbor, MI 48109

EDITOR:

Barbara G. Shinn-Cunningham, PhD (15-18)
Boston University
CRESCENT
610 Commonwealth Ave
Boston, MA 02215 USA

HISTORIAN:

David J. Lim, MD
UCLA Geffen School of Medicine
Department of Head & Neck Surgery
1000 Veterans Ave, Rm 31-27
Los Angeles, CA 90024

COUNCIL MEMBERS AT LARGE:

Keiko Hirose, MD (17-20)
Department of Otolaryngology
Washington University School of Medicine
660 S Euclid Ave.
St. Louis, MO 63110

Shi Nae Park, MD, PhD (16-19)
Professor, Dept of Otolaryngology – HNS
Seoul St. Mary's Hospital
The Catholic University of Korea
College of Medicine
505 Banpo-dong, Seocho-su
Seoul, Lorea 137-040

Jennifer S. Stone, PhD (15-18)
Research Associate Professor
Department of Otolaryngology
VM Bloedel Hearing Research Center
CHDD CD 176 Box 357923
University of Washington
Seattle, WA 98195 USA

ARO Executive Director:

Haley J. Brust
Talley Management Group
19 Mantua Road
Mt. Royal, NJ 08061 USA
Ph: 1 (856) 423-7222 Ext. 103
Fax 1 (856) 423-0041
Email: hbrust@talley.com
　　　 headquarters@aro.org

Conference Program of the 41st Annual MidWinter Meeting

Dear colleagues,

On behalf of the ARO Council and our Tally Management team, I would like to welcome everyone to our 41st annual ARO Midwinter Meeting in San Diego! Our Program Committee, under the leadership of Ruth Litovsky, has prepared another outstanding slate of scientific podium presentations, symposia, and posters, as well as an expanded program of mentorship sessions and workshops. Most importantly, there will be time for both formal and informal social gatherings that are so important to the cohesion of ARO. In fact, if you arrive in time on Friday, meet your friends at Bootleggers Pub (5p on) for our 2nd Annual Science Café, where Dr. Susan Shore from the University of Michigan, will talk about "Why are my ears ringing? Multisensory systems contribute to tinnitus," and Dr. Ross Maddox from the University of Rochester, will discuss, "When ears aren't enough: how your eyes help you listen."

The **Presidential Symposium** (Saturday 8a – noon), entitled "From Bench to Boardroom: Perspectives on Commercializing Research in Otolaryngology," is inspired by the growing number of ARO members who are now engaged in efforts bring their scientific and clinical discoveries to products that can benefit patients. In many ways, "we have arrived" at place of intense interest from both pharmaceutical firms and device manufacturers. It seems a fitting moment for the ARO to take a serious look at how, when and why researchers get involved in commercialization, and to learn what lessons are there for us all. I am pleased to have leaders from both industry and academia as well as ARO members who have spanned between those worlds. Dr. Ian Reynolds, CNS Discovery Group Leader at Teva Pharmaceuticals, will discuss how an academic researcher can get industry interested in a potential therapeutic agent. Dr. Vincent Groppi, Director of the Center for the Discovery of New Medicines and the Center for Chemical Genomics at the University of Michigan Life Sciences Institute, will address how to advance academic drug discovery projects from concept to proof-of-concept clinical trials. Dr. David Weber will share his perspective as the CEO of Otonomy on the business, financial and development paths needed to grow a company for the pharmacotherapy of neurosensory diseases. Dr. Lloyd Minor, Dean of the Stanford University School of Medicine, will address how academic leaders view the development of relationships between industry and academia. Two ARO members will then discuss their own experiences in commercializing their ideas into marketable devices. Dr. Sunil Puria will share lessons from development of the light-driven contact hearing aid, which is now marketed, and Dr. Charles Della Santina will discuss his efforts that have brought the multichannel vestibular implant to clinical trials. Finally, we will have a panel discussion and take questions from the audience. Our speakers will be joined by Dr. Edwin Rubel and Dr. Andrea Vambutas, who will add their perspectives in working with industry to develop and apply products for the prevention of ototoxicity and the treatment of autoimmune inner ear disease. Please bring your questions for a lively discussion!

On Saturday afternoon be sure to join us at the **Welcome Get-Together** (5:30-6:30p). Then on Sunday at the ARO Business Meeting (5-5:30p), we will update you on the state of the Association, transfer leadership from the incoming Council, including the new President, Dr. Karen Steele, and hand out our coveted prizes – you can enter the prize drawings when you visit the exhibits. We will also recognize the important contributions of Dr. Ruth Litovsky in expanding our program offerings, Dr. Paul Manis in shepherding the successful growth of JARO, and the decades-long service of Dr. David Lim as our Historian. After that, our External Relations Committee and spARO leaders have organized a double-header of events at the nearby Balboa Theater. From 6-7p they will present the "spARO Reverse Science Fair," where students and postdocs will present interactive science displays and demonstrations that will engage the public in hearing research, hearing loss, speech discrimination, and music perception that will be judged by the public, and prizes will be awarded. Then head inside the Balboa for "Sounds of Music – Symphony and Science," a wonderful evening exploring the relationship between the sounds of music and the science of listening with jazz, classical quartet, and percussion musicians and guest speakers Nina Kraus, Kevin Franck and Michael Santucci. Tickets are now on sale for $15 on Ticketmaster at: www.bit.ly/symphonyscience.

Please take advantage of the daily (Sat-Tues) afternoon **Mentoring Sessions** for young investigators, where mentors and peers exchange ideas on different topics in navigating careers. This has grown into a very popular program geared towards students, post-docs and junior faculty.

At the **Awards Ceremony** (Monday 5:30-7p) and reception (7-8p), we celebrate the people and work that merited several awards, including the Geraldine Dietz Fox Young Investigator Award and the ARO Award of Merit. This year the Award of Merit goes to Prof. Christine Petit, for her pioneering work on understanding the genetic basis of many forms of human hearing loss and other neurosensory deficits.

The annual Hair Ball returns on Tuesday night (8p-12 midnight). This social event with a live band and dance floor remains one of our most fun gatherings of the Meeting, so please don't forget to bring your dancing shoes (and earplugs!).

Finally, I would like to thank the many individuals who have worked to bring this meeting together. Ruth Litovsky, her scientific program co-chairs Carolina Abdala and Christopher Shera, and all of the members of the Program Committee have spent many hours optimizing the schedule. Our spARO leaders and External Relations Committee under Dan Lee have organized three events that promise to enhance our social time and public outreach. There are many others to thank, but please take moment to stop by registration to thank Wendy Stevens for the overall meeting organization, Haley Brust for her diligent management of our organization, and all of the team at Talley Management who allow us to focus on science, fun, and (hopefully) sun at our Midwinter Meeting.

With best wishes for a fulfilling meeting,

John Carey
ARO President, 2017-2018

CONFERENCE OBJECTIVES

At the conclusion of the MidWinter Meeting, participants should be better able to:

- Explain current concepts of the function of normal and diseased states of the ear and other head and neck structures
- Recognize current controversies in research questions in auditory neuroscience and otolaryngology
- Describe key research questions and promising areas of research in otolaryngology and auditory neuroscience

REGISTRATION

The 2018 MidWinter Meeting Registration Desk is located in the Seaport Foyer and will be open and staffed during the following hours:

Friday, February 9	4:00 PM-7:00 PM
Saturday, February 10	7:00 AM-6:00 PM
Sunday, February 11	7:00 AM-6:00 PM
Monday, February 12	7:00 AM-6:00 PM
Tuesday, February 13	7:00 AM-6:00 PM
Wednesday, February 14	7:00 AM-10:00 AM

SPEAKER READY ROOM

The 2018 Program Committee is committed to providing attendees cutting edge technology and coordinated presentations at the MidWinter Meeting. To be fully prepared for your session, each presenter is requested to visit the Speaker Ready Room at least 24 hours prior to your presentation. The Speaker Ready Room is located in the **Show Office #7 in the Palm Foyer** and will be open the following days and times:

Location: Show Office #7 in the Palm Foyer

Friday, February 10	4:00 PM-7:00 PM
Saturday, February 11	7:00 AM-6:00 PM
Sunday, February 12	7:00 AM-6:00 PM
Monday, February 13	7:00 AM-6:00 PM
Tuesday, February 14	7:00 AM-6:00 PM
Wednesday, February 15	7:00 AM-10:00 AM

ADMISSION

Conference name badges are required for admission to all activities related to the 41st Annual MidWinter Meeting, including the Exhibit Hall and social events.

> *Smoking and photography are not permitted in the meeting rooms or poster hall*

MOBILE APP AND ONLINE WEBSITE

Enhance your experience at the 2018 ARO MidWinter Meeting! You'll be able to plan your day by performing detailed abstract searches and can also view the schedule, browse exhibitors, sponsors, maps and general show info. You must create an account in order to view abstracts/save talks to your itinerary.

The app is compatible with iPhones, iPads, iPod Touches and Android devices. Search "ARO MWM" on the App Store/Google Play. You can also access the same information via our website version of the app through any browser on any device! The searchable mobile app is available at your app store, keyword ARO MWM. The online site is available at: https://goo.gl/r2ACf3.

MOBILE DEVICES

As a courtesy to the speakers and your fellow attendees, please switch your mobile device(s) to silent while attending the sessions.

RECORDING POLICY

ARO does not permit audio or photographic recording of any research data presented at the meeting.

BREAKS

Complimentary coffee and tea will be available in the morning and at selected breaks.

ASSISTED LISTENING DEVICES

A limited amount of assisted listening devices are available at the ARO MidWinter Meeting Registration Desk, courtesy of Phonak.

A SPECIAL NOTE FOR THE DISABLED

ARO wishes to take steps that are required to ensure that no individual with a disability is excluded, denied services, segregated or otherwise treated differently than other individuals because of the absence of auxiliary aids and services. If you need any auxiliary aids or services identified in the Americas with Disabilities Act or any assistance please see the ARO staff at the Registration Desk.

2018 ARO MIDWINTER MEETING

PROGRAM COMMITTEE
Ruth Y. Litovsky, PhD, Chair (3/17-2/20)
Carolina Abdala, PhD, Scientific Program Co-chair (3/17-2/20)
Christopher Shera, PhD, Scientific Program Co-chair (3/17 – 3/20)
Jose Antonio Lapez-Escamez, MD (3/17 – 2/20)
Maria Chait, PhD (3/17 – 2/20)
Monita Chatterjee, PhD (3/17 – 2/20)
Rick Friedman, MD, PhD (3/15-2/18)
Ronna Hertzano, MD, PhD (3/15-2/18)
Larry Hoffman, PhD (3/17-2/18)
Nandini Iyer (3/17 – 2/20)
Ingrid Johnsrude, PhD (3/16-2/19)
Achim Klug, PhD (3/16-2/19)
Hubert Lim, PhD (3/16-2/19)
Rebecca Lim, PhD (3/17 – 2/20)
Brian McDermott, PhD (3/15-2/18)
H. Heidi Nakajima, MD, PhD (3/16-2/19)
Sunil Puria, PhD (3/17-2/18)
Konstantina Stankovic, MD, PhD (3/17 – 2/20)
Eric Thompson, PhD (3/17 – 2/20)
Mark Warchol, PhD (3/16-2/19)
Council Liaison: Ruth Y. Litovsky, PhD (3/17-2/20)
spARO Representative: Sophie Nyberg

Animal Research Committee
Steve Eliades, MD, PhD, Chair (3/17-2/20)
Mark Chertoff, PhD (3/16-2/19)
Michael Deans, PhD (3/16-2/19)
Hisayuki Ojima, PhD (3/16-2/19)
Sonja Pyott, PhD (3/15-2/18)
Catherine Weisz, PhD (3/16-2/19)
Council Liaison : Keiko Kirose, MD (3/17-2/20)
spARO Representative: Karolina Charaziak

Award of Merit Committee
Ruth Anne Eatock, PhD, Chair (3/17-2/20)
Kathleen Cullen, PhD (3/16-2/19)
Ana Belen Elgoyhen, PhD (3/15-2/18)
Paul Fuchs, PhD (3/17 – 2/20)
Anna Lysakowski, PhD (3/17 – 2/20)
Michael McKenna, MD (3/15-2/18)
Chris Schreiner, MD, PhD (3/15-2/18)
Edwin Rubel, PhD (3/16-2/19)
Fan-Gang Zeng, PhD (3/16-2/19)
Council Liaison: Past-President Matthew W Kelley, PhD (3/17-2/18)

Diversity & Minority Affairs Commiittee
Lina Reiss, PhD, Chair (3/16-2/18)
Evelyn Davies-Venn, PhD (3/15-2/18)
Amanda Lauer, PhD (3/16-2/19)
Ivan Lopez, PhD (3/16-2/19)
Ramnarayan Ramachandran (3/16-2/19)
Astin Ross, PhD (3/15-2/18)
Suhua Sha, MD (3/16-2/19)
Council Liaison: Shi Nae Park, MD, PhD (3/17-2/19)
spARO Representative: Michelle Valero

External Relations Committee
Dan Lee, MD, Chair (3/15-2/18)
Yuri Agrawal, MD (3/17 – 2/20)
Allison Coffin, PhD (3/16-2/19)
Keith Duncan, PhD (3/15-2/18)
J. Chris Holt, PhD (3/16-2/19)
Hubert Lim, PhD (3/15-2/18)
Yunxia (Yesha) Wang Lundberg, PhD (3/15-2/18)
Stéphane Maison, PhD (3/16-2/19)
Michael Roberts, PhD (3-16 – 2/19)
Shinichi Someya, PhD (3/15-2/18)
Joel Snyder, PhD (3/16-2/19)
Council Liaison: Keiko Hirose, MD (3/17-2/20)
spARO Representative: Judith Kempfle

Finance & Investment Committee
Erick Gallun, PhD, Chair (3/17-2/20)
Thomas Friedman, PhD (3/16-2/19)
Michael Anne Gratton, PhD (3/16-2/19)
Lisa Olsen, PhD (3/17 – 2/20)
Neil Segil, PhD (3/15-2/18)
Ex-officio: Secretary-Treasurer Gabriel Corfas, PhD (3/17-2/20)

International Committee
Alan Brichta, PhD: Australia. Chair (3/16-2/18)
W. Robert J. Funnell: Canada (3/16-2/19)
Jonathan Gale: UK (3/16-2/19)
Hannes Maier, PhD: Germany (3/16-2/19)
ShiNae Park, MD, PhD: Korea (3/15-2/18)
Ulla Pirvola, PhD: Finland (3/16-2/19)
Yilai Shu, MD, PhD: China (3/15-2/18)
Joris Soons, PhD: Belgium (3/15-2/18)
Isabel Varela-Nieto, PhD: Spain (3/16-2/19)
Council Liaison: Jennifer Stone, PhD (3/15-2/17)
spARO Representative: Patrick Atkinson, PhD

2018 ARO MIDWINTER MEETING

The External Relations Committee (ERC) is offering three exciting outreach events for ARO membership and the public.

Friday, February 9 at **5pm**, please join ARO at [Bootlegger](#) for our second annual Science Café. This casual event features two ARO members speaking about their work in a relaxed pub atmosphere, suitable for auditory scientists and non-scientists alike. This year our first speaker is **Susan Shore** from the University of Michigan, speaking on ***"Why are my ears ringing? Multisensory systems contribute to tinnitus."*** The second speaker is **Ross Maddox** from the University of Rochester, speaking on ***"When ears aren't enough: how your eyes help you listen."*** This event is free – come have a drink and catch up with your auditory colleagues while hearing about great work from Susan and Ross!

[Contact Allison Coffin for more information](#)

Sunday, February 11 at **6pm**, the **ERC and spARO** are sponsoring a **"Reverse" Science Fair** at the [Balboa Theater](#). Students and postdocs will present interactive science displays that will be judged by the public and prizes will be awarded.

Following the Science Fair, on **Sunday, February 11** from **7:00pm-8:30pm** at the **Balboa Theater**, the ARO will host a special concert called ***"Sounds of Music: From Symphony to Science."*** Spend a wonderful evening exploring the relationship between the sounds of music and the science of listening with jazz, classical quartet, and percussion musicians and guest speakers **Nina Kraus**, **Kevin Franck** and **Michael Santucci.** Tickets are on sale for $15 on Ticketmaster at: www.bit.ly/symphonyscience.

AWARD OF MERIT

2018 Award of Merit Recipient
Christine Petit, M.D, Ph.D.
Professor at College de France
Professor at Institut PasteurHead, Genetics and Physiology of Hearing Laboratory

AWARD OF MERIT BIOSKETCH: CHRISTINE PETITE

The 2018 Award of Merit winner, Christine Petit, grew up in the vineyards of the Burgundy region of France. Influenced by her father, a brilliant engineer, and his passion for scientific discoveries, she became interested in science early on. During her training as a physician, Christine came to realize that the depth she sought in biological science was likely to be found in genetics and biochemistry courses. She obtained a Master's degree in genetics and biochemistry, in addition to her medical degree, at Paris XI University at Orsay. She continued to work towards her doctoral degree, first with Nobel-winning biologist François Jacob at Institut Pasteur in Paris, and then in an immunology laboratory, to enable her to study the genetic control of cell differentiation. She obtained her doctorate in 1982, and after pursuing postdoctoral training at the Institute of Immunology in Basel, Switzerland, she settled at Institut Pasteur in 1985.

Christine pursued her research as an independent researcher on sex determination, initiated with Jean Weissenbach, but soon moved on to take advantage of human hereditary disorders for elucidating the molecular mechanisms of olfaction, by studying Kallmann syndrome. She then became convinced that genetics could overcome the limits of biochemistry and molecular genetics for elucidating the molecular physiology of hearing, imposed by the small number of cochlear cells. She

began to collaborate with scientists and clinicians in Tunisia, Lebanon, and Jordan to study deaf families suitable for a genetic analysis. She thus mapped the first loci for recessive hearing impairment, DFNB1 and DFNB2, to human chromosomes in 1994. This opened an enormous field of research, led by Christine, with collaborators all over the world. The discovery of the genetic basis of deafness had begun. In 2002, Christine Petit became Professor at Collège de France, holding the chair of "Genetics and Cell Physiology".

Over the years, Christine and her team have discovered dozens of causal genes for non-syndromic and syndromic forms of hearing impairment. The number is daunting, especially considering that these discoveries were made in the early days of gene identification. These genes are responsible for cochlear deficits. Today, Christine with her colleague Nicolas Michalski, focuses on genes underlying hearing disabilities of central origin with the objective to extend the genetic dissection of hearing to the development and functioning of the auditory cortex.

Virtually all the causal genes for deafness Christine identified with her colleagues and European collaborators, especially Steve Brown and Thomas Jentsch, encode previously unknown proteins. Most turned out to encode components of auditory hair cells. These proteins include components of the hair bundles, such as PDZ domain-containing proteins and other scaffold proteins (harmonin, whirlin, Nherf-1, Nherf-2, and sans), transmembrane and membrane-associated extracellular proteins (vezatin, PHR1, and stereocilin), myosin-VIIa, hair-cell synapse proteins (KCNQ4 and otoferlin), components of the tectorial membrane (otogelin and otoancorin), the major otoconial protein (otoconin-95), and several other proteins (pejvakin, EYA1, SIX1, AK2, and CDC14A).

Christine is not only responsible for establishing the research field of human hereditary of deafness, but for putting derived cellular and molecular information to the best use as well. She developed the conditions for multi-scale analysis (from morphology to physiology) of engineered mouse models of human deafness, conditional knockout mice, and mice carrying particularly informative missense mutations, associated with biochemical studies. She pioneered the deciphering of protein complexes in the cochlea, based on her hypothesis that the causal genes for a syndromic form of deafness may encode proteins belonging to the same protein network or complex. With her colleagues, she thus demonstrated that the proteins encoded by genes that are defective in Usher syndrome (sensorineural deafness associated with blindness) type 1, form a protein complex involved in the anchoring of early embryonic hair bundle lateral links and thereafter of tip links to actin filaments of stereocilia. She also demonstrated that the various fibrous links of hair bundles, which had previously been largely ignored, are essential for hair-bundle development and sound processing. She showed that early embryonic hair bundle lateral links are essential for the cohesion of stereocilia during hair-bundle development and that the proteins encoded by three of the known genes for Usher syndrome type II interact to form another type of hair-bundle link, the ankle links. Through the discovery of stereocilin, also encoded by a deafness gene, she revealed the key role played by the uppermost lateral links of the outer hair cell hair bundles, the top connectors. She has also shown that the transduction machinery and F-actin polymerization in hair bundles are coupled, pointing that MET-channel function and hair-bundle architecture are linked. With her colleague, Aziz El-Amraoui, she extended the notion of an Usher-1 adhesion protein complex to photoreceptors. They showed that this module, also in the photoreceptors, is associated with microvilli-like structures, the neglected so called calyceal processes, forming an adhesion belt that controls the sizing of the disks and lamellae of the photoreceptor outer segment.

Her multi-scale vision soon led Christine to expand the seemingly reductionist view of molecules and zoom out to capture the broader picture of integrated physiology. Indeed, it is one lesson of molecular biology, taught to Christine by her mentor, François Jacob, that nature incessantly tinkers, integrating systems from simpler levels, from which novel properties arise, explained by, but not deduced from, those of lower-level elements. Christine's lab thus set out to use the modifications of deafness genes to investigate auditory physiology, in depth, thanks to long-lasting collaborations with physicists, especially Paul Avan in Clermont-Ferrand. For example, with her colleagues and Paul Avan, she used mouse mutants defective in the links that interconnect stereocilia or couple the stereocilia to the tectorial membrane, e.g., mutants defective in stereocilin, to address the roles of these links and explore the possible dissociation of cochlear properties by characterizing which could be preserved (sensitivity and tuning at early stages in Strc-/- mice), and which could not (inability to generate large otoacoustic emissions from the non-cohesive stereocilia bundle in Strc-/- mice, plus abnormal masking strength). She also observed that sensitivity can be lost, whereas some tuning persists, or that emissions can persist, but neither tuning nor sensitivity, in mice carrying mutations in other "deafness genes". These observations teach us that these properties are coupled, not in a straightforward manner, but through subtle arrangements of molecular and cellular structures. Extrapolating these results to patients would suggest that they may experience difficulties in noise, despite subnormal hearing sensitivity, for purely mechanical reasons and that this should not be overlooked.

Christine's team also discovered the first and most frequent cause of auditory neuropathy of genetic origin, a defect in otoferlin, a multi-C2 domain transmembrane protein (1999). They then identified its key role in the synaptic release machinery of the inner hair cell (2006) before finally, its identity as a calcium sensor of synaptic vesicle fusion and replenishment (2017): an almost twenty-year treasure-hunt using state-of-the-art tools to, at last, hit the target. Comprehensive methodology cannot eliminate all (good) surprises. Christine's team discovered a new protein, pejvakin, in 2006, while searching for another gene responsible for neuropathy. The huge dependence of the hearing impairment of pjvk-/- mice on the low acoustic energy delivered during measurements (and even in housing facilities) attracted attention. This initially unwelcome finding found an explanation when peroxisomes entered the limelight (2015), pinpointing the need to consider this organelle and its highly active role in redox metabolism to understand and control reactive-oxygen species production by this sensory system in response to sound-overexposure.

Her research led to major insights not only into mechano-electrical transduction, the structure/function of the hair bundle, and synaptic transmission, but also cell-cell junctions, cochlear ionic homeostasis, and more recently, the development of parvalbumin-positive interneuron precursors of the auditory cortex.

Christine Petit has always focused on the translational aspects of her discoveries and how they can be put into clinical practice. Many of the first known genes for deafness were discovered by Christine's team, dramatically changing the genetic counseling provided to individuals with hereditary hearing loss. During the last five years, Christine's team has additionally focused on the development of gene therapy for preventing and curing hearing impairment. In collaboration with her colleague, Saïd Safieddine, she has made a major contribution towards clinical trials in gene therapy for inner ear defects.

Christine's many contributions to the auditory field have extended far beyond her own laboratory. She has worked with laboratories around the world, especially helping groups that needed human molecular genetics expertise.

As a supervisor, Christine can connect with anyone, and always manages to get the best out of her colleagues. One of her most striking aspects is that she sets her scientific standards very high, and then always finds a way to bring her staff and workmates to actually reach these standards. She is very successful in motivating graduate students and postdocs. Most of her PhD students have gone on to become successful researchers and now have tenured positions. As a person, she is always open, generous, and willing to help her collaborators achieve the best possible career development.

Among her many accomplishments, Christine's vision led her to create a collaborative team of scientists as part of a European Consortium – EuroHear – which incorporated not only geneticists, but also biophysicists, biochemists, electrophysiologists, and other specialists. This remarkable insight brought the EuroHear consortium to the forefront of "deafness gene" discovery for years.

Trained as an MD, Christine would not like all her efforts restricted to mice. She has increasingly felt the need for a permanent research structure in France, where all her collaborations developed over the years can thrive in association with experts from complementary auditory fields. She has thus worked with strength and passion towards developing an interdisciplinary hearing research center associated with a clinical center, a research and innovation center in audiology, and has convinced sponsors to support the project. As a result, a new institute, Institut de l'Audition, will open in Paris in 2019. Christine, whose pastime was mountaineering, when she could get away from the lab, as the Director of this new institute, is about to reach the summit of yet another level of complexity of nature's scale, the sphere of management (including that of construction sites).

Christine has earned many awards prior to the ARO Award of Merit, including the L'Oréal-UNESCO "For Women in Science" Award (2004), Institute for Health Sciences "Research and Medicine" Award (2004), Bristol-Myers-Squibb "Freedom to Discover" Award in Neuroscience (2005), Louis-Jeantet for Medicine Prize (2006), Grand Prix INSERM de la Recherche Médicale (2007), and the Pasarow Foundation Medical Research Award for Extraordinary Achievement in Neuropsychiatry Research (2012). She went on to win the Brain Prize, together with Karen Steel, an international scientific award and the world's largest brain research prize (2012) and received the Hughes Knowles Prize (2016). In 2002, she was elected to the French Academy of Sciences, in 2011 to the US National Academy of Medicine as foreign associate, and in 2016, to the US National Academy of Sciences as foreign associate.

Karen B. Avraham, Aziz El-Amraoui, Paul Avan and Saïd Safieddine

Past Presidents

1973-74	David L. Hilding, MD
1974-75	Jack Vernon, PhD
1975-76	Robert A. Butler, PhD
1976-77	David J. Lim, MD
1977-78	Vicente Honrubia, MD
1978-80	F. Owen Black, MD
1980-81	Barbara Bohne, PhD
1981-82	Robert H. Mathog, MD
1982-83	Josef M. Miller, PhD
1983-84	Maxwell Abramson, MD
1984-85	William C. Stebbins, PhD
1985-86	Robert J. Ruben, MD
1986-87	Donald W. Nielsen, PhD
1987-88	George A. Gates, MD
1988-89	William A. Yost, PhD
1989-90	Joseph B. Nadol, Jr., MD
1990-91	Ilsa R. Schwartz, PhD
1991-92	Jeffrey P. Harris, MD, PhD
1992-93	Peter Dallos, PhD
1993-94	Robert A. Dobie, MD
1994-95	Allen F. Ryan, PhD
1995-96	Bruce J. Gantz, MD
1996-97	M. Charles Liberman, PhD
1997-98	Leonard P. Rybak, MD, PhD
1998-99	Edwin W. Rubel, PhD
1999-00	Richard A. Chole, MD, PhD
2000-01	Judy R. Dubno, PhD
2001-02	Richard T. Miyamoto, MD
2002-03	Donata Oertel, PhD
2003-04	Edwin M. Monsell, MD, PhD
2004-05	William E. Brownell, PhD
2005-06	Lloyd B. Minor, MD
2006-07	Robert V. Shannon, PhD
2007-08	P. Ashley Wackym, MD
2008-09	Paul A. Fuchs, PhD
2009-10	Steven Rauch, MD
2011-12	Karen B. Avraham, PhD
2012-13	Debara L. Tucci, MD
2013-14	John C. Middlebrooks, PhD
2014-15	Jay. T Rubinstein
2015-16	Lawrence R. Lustig, MD
2016-17	Matthew W. Kelley, PhD
2017-18	John P. Carey, MD

Award of Merit Recipients

1978	Harold Schuknecht, MD
1979	Merle Lawrence, PhD
1980	Juergen Tonndorf, MD
1981	Catherine Smith, PhD
1982	Hallowell Davis, MD
1983	Ernest Glen Wever, PhD
1984	Teruzo Konishi, MD
1985	Joseph Hawkins, PhD
1986	Raphel Lorente de Nó, MD
1987	Jerzy E. Rose, MD
1988	Josef Zwislocki, PhD
1989	Åke Flóck, PhD
1990	Robert Kimura, PhD
1991	William D. Neff, PhD
1992	Jan Wersäll, PhD
1993	David Lim, MD
1994	Peter Dallos, PhD
1995	Kirsten Osen, MD
1996	Ruediger Thalmann, MD & Isolde Thalmann, PhD
1997	Jay Goldberg, PhD
1998	Robert Galambos, MD, PhD
1999	Murray B. Sachs, PhD
2000	David M. Green, PhD
2001	William S. Rhode, PhD
2002	A. James Hudspeth, MD, PhD
2003	David T. Kemp, PhD
2004	Donata Oertel, PhD
2005	Edwin W. Rubel, PhD
2006	Robert Fettiplace, PhD
2007	Eric D. Young, PhD
2008	Brian C. J. Moore, PhD
2009	M. Charles Liberman, PhD
2010	Ian Russell, PhD
2011	Robert V. Shannon, PhD
2012	David P. Corey, PhD
2013	Karen P. Steel, PhD
2014	H. Steven Colburn, PhD
2015	Thomas B. Friedman, PhD
2016	Geoffrey A. Manley, PhD
2017	Alan R. Palmer, PhD
2018	Christine Petit, MD, PhD

2018 TRAVEL AWARD RECIPIENTS

Anaam Alkharabsheh
Sean Anderson
Felix Aplin
Meenakshi Asokan
David Baechinger
Catherine Barone
Chama Belkhiria
Shauntelle Cannon
Ryan Casserly
Duncan Chadly
Karolina Charaziak
Zongwei Chen
Margaret Chow
Michael Crompton
Mathilde de Kerangal
Constantino Dragicevic
Michael Ebeid
Philipp Eckert
Fadhel El May
Nnenna Ezeilo
Philippe Fournier
Stacey Frumm
Deepa Galaiya
Iman Ghanad
Sanchez Gilson
Tobias Goehring
Ana Claudia Goncalves
Craig Hanna
Hariprakash Haragopal
Katherine Hardy
Aenea Hendry
Kelli Hicks
Lubos Hladek
Adam Hockley
Emma Holmes
Reuven Ishai
Kelly Jahn
Amanda Janesick
Nicole Jiam
Weitao Jiang
Nopporn Jongkamonwiwat
Christopher Kaufmann
Eun Jung Kim
Ye-Hyun Kim
Min-A Kim
Ye-Ri Kim
Sian Kitcher
Rafael Kochaj
Srinivasa Prasad Kommajosyula
Mikolaj Kozlowski
Andre Landin Malt
Jennifer Lawlor
Zhenjie Liu
Andrew Liu
Andrea Lowe

Hsin-Wei Lu
Wenwei Luo
Sara Madsen
Alexandra Mai
Maggie Matern
Mami Matsunaga
Kate McClannahan
Malinda McPherson
Ainhitze Mendizabal
Amir Nankali
Karli Nave
Kevin Nella
Alexandra Niemczura
Kim Noij
Molly O'Reilly
Monika-Maria Oster
Aaron Oswald
Geng Pan
Clarisse Panganiban
Gloria G. Parras
Pranav Patni
Melissa Polonenko
Silvia Prades I Abadias
Monzilur Rahman
Miguel Ramirez
Cong Ran
Stefan Raufer
Daniel Reijntjes
Darrian Rice
Samantha Rincon Sabatino
Raul Rodriguez
Shefin Sam George
David Sandlin
Aritra Sasmal
Nick Schubert
Adam Schwalje
Ivy Schweinzger
Yilai Shu
James Sinclair
Jenni Sis
Spencer Smith
Emily Spitzer
Danielle Trakimas
Margarete Ueberfuhr
Leticia Vicente
Dillan Villavisanis
Koichiro Wasano
Kelly Whiteford
Tanika Williamson
Lara Wood
Xiaoyu Yang
Anusha Yellamsetty
Shengyang Kevin Yu
Jingyuan Zhang

Table of Contents

Table of Contents

Table of Contents

From Bench to Boardroom: Perspectives on Commercializing Research in Otolaryngology

PRES SYMP 1

Advancing Your New Therapeutic And Getting Industry To Listen

Ian Reynolds, **PhD**, *CNS Discovery Group Leader, Teva Pharmaceutical Industries, West Chester, PA, USA.*

New therapeutics may emerge from many different sources. While the traditional origin of new drugs is the pharmaceutical industry, concepts molecules and devices are being developed in non-traditional locations with increasing frequency. Academic laboratories, research institutes and start-up biotechnology companies are making major contributions to the pipeline of new therapeutics. However, while innovative products may have their origins elsewhere, it is still the case that an industry partner is often essential to advance a new therapeutic because industry has the expertise in regulatory affairs, manufacturing and marketing that are essential for ultimate commercial success.

Given the likely necessity of an industry interaction while advancing a new therapeutic, it becomes important to understand what the industry representatives are looking for when they evaluate new opportunities. As the metrics for success in academia (such as publications and grant awards) are very different from success in industry (a commercially successful product), there is a risk of a "failure to connect" if a therapeutic opportunity is presented purely in academic terms.

In this presentation I will discuss the industry approach to evaluating new therapeutic opportunities, and I will provide a framework for a successful pitch to a potential industry partner. While companies vary considerably in their strategic interests, the key elements of a presentation describing a new therapeutic are similar. My focus will be on small molecule therapeutics, although the principles may potentially apply across multiple therapeutic modalities, and I will emphasize the challenges associated with proposing and developing therapeutics for progressive degenerative diseases.

PRES SYMP 2

The Business, Financial and Development Paths Required for Pharmacotherapy of Neurosensory Disease

David A. Weber, PhD, *President & Chief Executive Officer, Otonomy, Inc., San Diego, CA*

According to the World Health Organization, hearing loss is the fourth leading cause of disability globally, and together with tinnitus and balance disorders, severely impact patients' lives and present a significant socio-economic burden. Despite the clinical and commercial success of pharmacotherapy for retinal diseases over the past two decades, no drug has been approved in the U.S. for treating any inner ear disorder. Yet numerous corollaries can be drawn between these neurosensory fields to inform researchers, physicians, investors, and the pharmaceutical industry as to the path and barriers for successful drug development in otology. This talk will explore business, financial and development factors, using one company as an example. Founded in 2008 by a Meniere's disease patient and his otolaryngologist, Otonomy has progressed from a venture-backed start-up with a narrow focus to a publicly traded company with drug candidates addressing a broad set of otic disorders including Meniere's, hearing loss and tinnitus. This path started by addressing the fundamental need to achieve sustained drug exposure in the inner ear via a simple, in-office injection and led to the sponsorship of large, multi-center, international clinical trials to support regulatory approval. These endeavors required significant private and public investor support and helped to establish today's growing interest in pharmacotherapy for otic diseases. Understanding the important role that each of us, whether patient, physician, researcher, medical society, industry, or investor has in bringing safe and effective drugs to the market is essential to delivering on our common goal of addressing the needs of patients suffering from neurosensory otic disorders.

PRES SYMP 3

Getting a New Drug Through the Clinical Trials Gauntlet

Vincent E. Groppi, PhD, *Director, Center for the Discovery of New Medicines and Director, Center for Chemical Genomics, University of Michigan Life Sciences Institute, Ann Arbor, MI, USA*

The major advantage of academic drug discovery is that it builds upon the knowledge created from years of basic science research in specific disease areas. Groups such as NIH and DOD fund basic research and the subsequent research generates knowledge about the disease. In this way the basic science research sets the stage for carrying out translational drug discovery activities. Currently there is a growing excitement in the opportunity to discover and develop new therapeutic agents to treat impairments in hearing and balance hearing. This excitement is derived from research previously funded by institutes such as NIDCD.

Each drug discovery project starts with the deep understanding of the disease or disorder being studied. Layered on to that disease knowledge is the knowledge of starting and advancing milestone-driven drug discovery, which is different than doing basic science research and best done by cross functional teams. Early in the life cycle of a drug discovery project it is important to create an initial Target Product Profile (TPP) for the drug. A TPP becomes the guidepost to creating a new therapeutic because it captures the most important clinical and commercial attributes needed to be successful. It describes the endpoint and can be used to determine the key go/no decision points. My presentation will provide an established framework for starting and advancing academic drug discovery projects from concept to proof-of-concept clinical trials. The focus will be on establishing translational assays for decision-making and using contract research and/or established core labs to accelerate screening, medicinal chemistry, pharmacokinetics, preclinical safety, IND enabling studies, regulatory science and clinical trials.

PRES SYMP 4

The Perspective of a Dean on Developing Relationships Between Industry and Academia

Lloyd Minor, MD, **Carl and Elizabeth Naumann Dean** *of the Stanford University School of Medicine*

News of large patent windfalls has led to an increased interest in intellectual property and commercialization at universities and non-profits around the United States. And yet, despite stories of multi-million dollar bonanzas, most inventions produce little or no income. For the few that do, financial reward can take many years to materialize. Even for Stanford Medicine, which has been extraordinarily successful in its technology transfer, nearly all royalty income has originated from just a handful of patents. The Stanford experience will be shared in this presentation along with a description why intellectual property cannot be viewed as a reliable source of income for any institution.

Despite the low overall probability of monetary gain, technology transfer is still vitally important for the translation of discoveries. Technology transfer offices have a critically important role in supporting and advising faculty as well as in managing and mitigating, rather than avoiding, conflicts of interest.

Collaborations between academia and industry offer important opportunities for expanding the scope and reach of research studies. Some examples of these collaborations at Stanford Medicine include the Project Baseline study with Verily (formerly Google Life Sciences) and the Apple Heart Study. Both studies demonstrate the potential of collaborations with industry to advance scientific discoveries. They bring us closer to achieving our goal of Precision Health: to predict, prevent, and cure disease, *precisely*.

PRES SYMP 5

Development and Commercialization of the Light-Driven Contact Hearing Aid

Sunil Puria, PhD, Amelia Peabody Scientist *in the Eaton-Peabody Laboratories, Massachusetts Eye and Ear Infirmary, Boston, MA, USA*

The broad frequency ranges unique to mammalian hearing provide important means for localizing speech and sounds. However, conventional hearing aids, limited by output level and feedback, only provide amplification to about 5 kHz. Several decades ago the field of ophthalmology began to provide patients with options other than eyeglasses. Now the treatment of hearing loss may be entering such an era with partially and fully implantable middle-ear hearing devices (MEHDs). The key distinguishing feature of MEHDs is that their output transducers are designed for mechanical vibrational output rather than acoustic output, giving them the potential to achieve wider bandwidths than conventional acoustic hearing aids. A promising non-surgical system is the contact hearing aid (CHA), which was originally designed to use an electromagnetic field to exert force on a small magnetic 'lens' placed on the eardrum. Limitations to this approach required the development of a radically different system that uses light to wirelessly drive a transducer that directly contacts the eardrum. Switching to this new approach was risky, but has paid off in terms of increased output, bandwidth, and energy efficiency. A key clinical finding is that, even with a widely vented fit, the light-transmission system produces minimal feedback as compared to conventional acoustic hearing aids, which therefore allows it to provide significantly more gain. These findings are an outcome stemming from NIDCD-funded middle-ear measurements made by the author in the years leading up to the formation of Earlens Corporation. The author played a critical role in growing the company from 2 to 100 employees over 10+ years, including obtaining early-stage Small Business Innovation Research (SBIR) funding from the NIDCD. In 2015, the company received 510(k) approval from the FDA to market the device. Since its commercial launch in 2016, the device is currently distributed by over 40 otology centers and has been placed in over 350 subjects. The related clinical and engineering results have been reported in several scientific publications (e. g. , Fay et al. , 2013; Puria et al. , 2017; Gantz et al. , 2017). A significant number of clinical, manufacturing, and marketing challenges remain, which will be

discussed. This device has the potential to improve the lives of hearing-impaired individuals by restoring the full spectrum of hearing through innovative technology that is well protected by over 40 issued patents. [Work supported in part by SBIR Phase IIB U44 DC08499 and R01 DCD05960 grants from the NIDCD of the NIH].

PRES SYMP 6

Perspective of a clinician-scientist: The Labyrinth Devices MVI™ Vestibular Implant – A case study on navigating the path from basic science to first-in-human trial

Charles C. Della Santina PhD, MD, *Professor of Otolaryngology-Head and Neck Surgery; Director, Vestibular NeuroEngineering Laboratory; Director, Listening Center, Johns Hopkins University School of Medicine, Baltimore, MD, USA*

Basic and translational research in otolaryngology has led to hearing restoration for nearly a half million cochlear implant users, countless other improvements in diagnosis and treatment of ear disorders, and the advent of a wide array of new small molecule, genetic, stem cell and rehabilitative interventions currently in "preclinical" investigations or first-in-human trials. However, the path from study of normal structure and function to regulatory approval of a new drug, medical device or diagnostic system can be as long and challenging as it is potentially impactful and rewarding. In this presentation, I will discuss development of the Labyrinth Devices MVI™ vestibular implant as a case study of translational research extending from bench to bedside to boardroom, with a particular focus on lessons learned from the perspective of an academic clinician-scientist.

Age-Related Changes in Humans

PS 01

Analysis of Otic Capsule Calcified Tissue by Fourier Transform Infrared (FTIR) Microspectroscopy

Steven Doty[1]; Kenneth Brookler[2]
[1]Hospital for Special Surgery; [2]Mayo Clinic

Abstract
Various spectroscopic methods have been applied to evaluate bone quality. Bone, as a tissue, is subject to change due to aging, disease, genetic variability and mechanical or stress related factors. Using FTIR analysis of bone samples, the mineral content, mineral crystallinity and collagen maturity, have all been shown to change with the aging process. A search of the published literature indicates that FTIR analysis of the bone quality of the otic capsule and inner ear has not been done. Considering the significant loss of hearing ability within the human aging population, we have begun to use FTIR to analyze bone quality of the ear bones to describe any changes which may occur with aging or disease. FTIR reveals the collagen peak at 1660 cm^1 and the collagen distribution (ie, amide 1 intensity image) within the region outlined by the small box overlaying a 2 micron thick section of otic capsule. Sample preparation requires tissue dissection, fixation in formalin or alcohol, embed in poly methyl methacrylate, and sectioning of calcified tissue at 1-2 micron thickness. The FTIR spectra shows mineral crystallinity peak at 1030 cm^1, collagen peak at 1660-1690 cm^1, and combination of peaks to obtain mineral/matrix ratios.

[Doty and Brookler abstract for Otolaryn meeting, San Diego, 2018,-2.doc](#)

PS 02

Association of Cognitive Decline with Basal Ganglia Volume Changes in Presbycusis

Chama Belkhiria[1]; Paul H. Delano[2]; Rodrigo Vergara[1]; Carolina Delgado[3]
[1]Neuroscience Department, Faculty of Medicine, University of Chile; [2]Otolaryngology Department, Clinical Hospital of the University of Chile; [3]Neuroscience Department, Faculty of Medicine, University of Chile. Neurology and Neurosurgery Department, Clinical Hospital of the University of Chile

Structural, functional, and connectivity abnormalities of basal ganglia have been found in a wide range of cognitive disorders including Alzheimer';s disease (Cho et al. 2006), Huntington's disease (Misiura et al., 2017) and depression (Bluhm et al. 2009). Despite accumulating evidences associated dementia and age-related hearing loss (Presbycusis), relatively few studies have examined hearing impairments with cortical volume changes (Lin et al., 2014; Rigters et al., 2017) and no study, to our knowledge, examined the possible relationship between cognitive decline and subcortical volume loss in Presbycusis. The aim of this preliminary study was to assess whether there are differences in basal ganglia volumes in presbycusis and controls subjects ando associate these structural changes with cognitive functions. Based on the anatomical position of the dorsal striatum (putamen and caudate) as primary input to basal ganglia, we hypothesized that dorsal striatum would exhibit prominent volume loss in accordance with cognitive declines in presbycusis patients. We enrolled 17 presbycusis patients and 13 controls over 65 years. All participants underwent pure tone audiometry evaluations, detailed neuropsychological tests and T1-weighted MRI at 3T. We segmented the

volumes of five subcortical structures: thalamus, caudate nucleus, putamen, globus pallidus and nucleus accumbens using the FSL-FIRST integrated registration and segmentation tools. After computing z-scores of target scales (Memory, vision, composite scores in executive functions and processing speed tests), we conducted factor analysis to verify internal structure that supports the unidimensionality. We run internal consistency analysis with Cronbach's alpha to verify whether the scales are highly correlated among each other. The results showed that correlations of basal ganglia volumes with cognitive functions were lower in presbycusis than in controls mainly in putamen, caudate and globus pallidus (Table 1). Our data offer additional explanations in brain and hearing impairment fields of elderly considering that previous neuroimaging studies showed accelerated rates of whole brain atrophy and volume declines only in temporal gyri, primary auditory cortex and temporal lobe (Lin al., 2014). Our findings suggest that in presbycusis patients cognitive and subcortical alterations would involve gradual brain volumes and connectivity affecting the integration of sensory information, language comprehension and emotion association such as fronto-temporal and fronto-pareital networks. The change in volumes and connectivity would be interpreted as a compensation mechanism in Presycusis. The novelty of our study was to highlight the basal ganglia volume changes in presbycusis, however more patients and assessment of other brain regions are needed.

Table 1.docx

PS 03

Hidden Hearing Loss is Associated with Slower Processing Speed in Elderly Subjects

Paul H. Delano[1]; Melissa Martinez[2]; Alexis Leiva[3]; Macarena Ipinza[3]; Ambar Soto[2]; Kattalin Elespuru[3]; Carolina Delgado[4]
[1]*Otolaryngology Department, Clinical Hospital of the University of Chile;* [2]*Neurology and Neurosurgery Department, Clinical Hospital of the University of Chile;* [3]*Neuroscience Department, Faculty of Medicine, University of Chile;* [4]*Neuroscience Department, Faculty of Medicine, University of Chile. Neurology and Neurosurgery Department, Clinical Hospital of the University of Chile*

Previous epidemiological evidence shows an association between age-related hearing loss and cognitive decline in elderly people. Presbycusis subjects with audiometric hearing thresholds (PTA) worse than 40 dB are more likely to develop cognitive decline. The mechanisms that connect this epidemiological association are unknown. Here we propose that hidden hearing loss (HHL), that is the loss of synapses between inner hair cells and auditory nerve neurons without alterations in the audiometric thresholds, is an important factor linking presbycusis and cognitive decline.

Methods
The ANDES (Auditory and Dementia study) study is a prospective cohort of Chilean hispano-mestizo elders ≥65 years, "cognitively" normal (MMSE>24) with different levels of age-related hearing impairment. A total of 94 people have been evaluated with comprehensive neuropsychological and audiological evaluations, including: audiometric thresholds, amplitudes and latencies of ABR waves I and V obtained at 80-90 dB nHL, distortion product otoacoustic emissions (DPOAEs) with and without contra-lateral broad-band noise stimulation.

Results
94 participants (60 women) complied with the inclusion criteria, with a mean age of 73.9 ± 5.2 years, and a mean education of 9.4 ± 4.1 years. The mean pure tone average (PTA) for the right ear was 29.3 ± 12.1 dB HL, while for the left ear was 28.8 ± 12.1 dB HL. Twenty-two subjects had normal PTA (<20 dB HL), while 52 had mild hearing loss (20-40 dB) and 20 individuals had more than 40 dB of hearing loss. Mean HHIE-S was 7.00 ± 7.3 points, while average MMSE was 28.1 ± 1.3 (range between 24 and 30 points). In the group of normal hearing subjects, the amplitude of the left ABR wave I and of the left amplitude ratio between wave I and V correlated with the Trail Making Test A (TMT-A) time (Spearman test, r=-0.45, p=0.04; r=-0.52, p=0.02 respectively), while there was no correlation in the amplitude of DPOAEs and in the contralateral noise effects on DPOAEs from the left ear. In addition, the amplitude of the right ABR wave I and the right wave I/V ratio correlated with the Frontal Assessment Battery (FAB) score (Spearman test, r=-0.471, p=0.03; r=-0.541, p=0.01), while there were non-significant correlations between the amplitude of DPOAEs and the contralateral noise effects in the right DPOAEs with the FAB score.

Conclusions
These results suggest that hidden hearing loss is associated to slower processing speed and diminished frontal functions in elderly humans.

The Effects of Age on Auditory Processing Abilities

Hyesoo Ryu; Haekyung Hwang; Keonseok Yoon; Hyunsook Jang
Hallym University

Title

The Effects of Age on Auditory Processing Abilities Research background Many studies have shown that auditory processing abilities deteriorate with age. The auditory processing abilities of the central nervous system should be examined in various processing areas such as temporal processing, dichotic listening, monaural low-redundancy and binaural interaction areas. The purpose of this study was to observe the effects of age on auditory processing abilities by examining Korean populations in the age groups of 20s through 70s with normal hearing sensitivity. Methods Five auditory processing tests, including Speech-in-Noise Test (SINT), Compressed-Speech Test (CST), Binaural Fusion Test (BFT), Dichotic Digit Test (DDT) and Frequency Pattern Test (FPT), were used on 128 subjects, divided into six age groups between 20s to 70s. Performance on each test was analyzed to examine the changes in auditory processing abilities by age. Correlations between tests were also analyzed. Furthermore, the number of subjects who were below the -2 SD, based on each test result of the age of 20s, were identified to determine the prevalence of suspected auditory processing disorder in each age group. Results The results revealed that the performance decreased in all test areas as age increased from 20s and 70s, especially significantly declined from the age of 50s. It was indicated that performance decreased from the age 50s in SINT, CST, DDT and FPT. However, a significant performance degradation was found in the age of 60s in the BFT. Significant correlations were found between SINT and CST, and also between DDT and FPT. It showed that as age increased, the number of subjects who scored below at-risk criteria (-2 SD) increased. Conclusion The results of all auditory processing tests proved that central auditory processing functions decreased as a function of age. These findings suggest that it is necessary to establish test standards for ages above 50s. These data from the study can be used in attribution towards a development of a standardized test, especially to be used for adults and the elderly population in a clinical setting for effective diagnosis and rehabilitation program.

PS 05

Effects of age on electrophysiological measures of cochlear synaptopathy in humans

Samuele Carcagno[1]; Christopher J. Plack[2]
[1]*Lancaster University*; [2]*University of Manchester*

Background

Recent studies indicate that in rodents cochlear synaptopathy occurs as a result of aging even in the absence of significant noise exposure. This cochlear synaptopathy is thought to affect mainly low-spontaneous rate fibers and result in a reduction of wave I of the auditory brainstem response (ABR) at high stimulus levels, and of the frequency following response (FFR) at high levels and low modulation depths.

Methods

ABRs were recorded from 58 listeners (19 young, 21 middle-aged, 18 elderly) with audiometric thresholds within 40 dB nHL up to 4 kHz. ABRs were collected in response to 80 and 105 dB ppeSPL clicks bandpass filtered between 0.35 and 3 kHz, and presented in quiet, or in the presence of a pink noise highpass filtered at 3.5 kHz. FFRs were recorded from a subset of the same listeners (N=54; 19 young, 18 middle-aged, 17 elderly) in response to 0.6 kHz and 2 kHz 75 dB SPL carrier tones amplitude modulated at 100 Hz with modulation depths of 100%, and 70% in the presence of a pink noise highpass filtered at 3 kHz. For both ABR and FFR recordings the highpass noise level was selected in pilot experiments so that it would completely mask basal cochlear contributions to the electrophysiological response, thus minimizing the effects of age-related audiometric losses above 4 kHz.

Results

The amplitude of wave I in response to the high-level click showed significant age-related declines in quiet, but not in the presence of the highpass masking noise. The ratio of wave I amplitude in the high-level condition to that in the low-level condition, which should decrease with age if synaptopathy affects mostly low-spontaneous rate fibers, did not show significant age-related declines either in quiet or in the presence of highpass masking noise. FFR amplitude at the modulation frequency for the low-frequency carrier showed marked age-related declines for both modulation depths. If cochlear synaptopathy affects mostly low-spontaneous rate fibers the slope of the FFR level as a function of modulation depth should become steeper with age. However, no significant age-related differences were found for this differential measure at either carrier frequency.

Conclusions

Although for some conditions ABRs and FFRs showed robust age-related declines, these declines did not appear to be specific for conditions that drive low-spontaneous rate fibers as predicted by the cochlear synaptopathy hypothesis.

PS 06

The Effect of Distraction on Auditory Change Detection: an Ageing Study.

Mathilde de Kerangal[1]; Deborah Vickers[1], Maria Chait[2]
[1]*University College London - Ear Institute;* [2]*University College London*

Multiple lines of evidence suggest that, in addition to loss of sensory acuity (e.g. peripheral hearing loss) aging is associated with various deficits of cognitive, executive function and sustained-attention, which have expansive perceptual consequences across sensory modalities. In the context of hearing, these deficits may have wide-ranging implications for listening in crowded environments such as ability to attend to a relevant sound source or avoid distraction.

Here, we investigate how aging affects listeners'; ability to detect changes, manifested as a disappearance of a source, within artificial acoustic 'scenes'; comprised of multiple concurrent streams of pure tones. These 'scenes'; model listening in natural situations but in conditions that are devoid of semantic context. To study the effects of distraction, brief (100 ms) AM modulated chords, with frequencies that do not mask the scene sources, are introduced at the time of change (scenes with no change also contain distractors such that the presence of a distractor is not predictive of the occurrence of change).

Initial results suggest that in the absence of the distractor sound the old and young listeners performed similarly. The addition of the distractor lead to a drop in performance for both groups but with a much larger variability for the older listeners: some old listeners performed poorly compared to the young listeners, while others had similar performances.

The study presents a correlation analysis that examines the relation between the change detection performance (and its susceptibility to distraction) and performance on a battery of general attention tests, pure tone audiometry, and speech in noise tests.

PS 07

Age- and Hearing-Loss-Related Deficits in Voice Emotion Recognition

Jenni Sis[1]; Julie Christensen[1]; Aditya Kulkarni[2]; Shauntelle Cannon[1]; Monita Chatterjee[2]
[1]*Boys Town National Research Hospital;* [2]*Auditory Prostheses & Perception Lab, Center for Hearing Research, Boys Town National Research Hospital, Omaha, NE*

Introduction
As the aging population increases, the prevalence of hearing loss also increases. Personal relationships are developed through communication and social interactions that require the ability to recognize others'; emotions. Both aging and hearing loss have been associated with deficits in facial and verbal emotion recognition, which may lead to social isolation resulting in decreased social cognition and poorer quality of life. The mechanism underlying age-related reductions in emotion recognition remains unclear. Hearing loss in the aging population further complicates the question by reducing or eliminating access to the key acoustic cues that convey voice emotion (dynamic changes in voice pitch, speaking rate, intensity, and timbre). The purpose of this study is to investigate the interaction between age-related changes in voice-emotion recognition and the contributions of hearing loss.

Methods
Thirty-two binaural hearing aid wearing listeners with bilateral sensorineural hearing loss (ranging from mild to severe), and 22 normal hearing (NH) listeners participated in this study. Stimuli comprised of 12 sentences, each spoken with one of five emotions (happy, sad, neutral, scared, and angry) by a male and a female talker, for a total of 60 utterances. Stimuli were counterbalanced (two male-talker sets, two female-talker sets) with two sets of passive training prior to each test to familiarize the listener with the speaker';s speaking style. During the test, subjects listened to the 60 sentences within each set (fully randomized order) and judged the emotion using a computer-interface (single-interval, five-alternative forced-choice procedure).

Results
Preliminary analyses show an age-related decline in performance with young NH listeners performing the best. Significant effects of bilateral low-frequency PTA were found, with no effects of talker or emotion. There was no interaction between hearing loss and the age of the listener.

Conclusions
In conclusion, these results suggest that age-related deficits in spoken emotion recognition occur, both in normal hearing and hearing-impaired listeners. Listeners with hearing loss had greater deficits than their NH peers. Reduced emotion recognition abilities due to age and hearing loss may impact social communication and quality of life in the aging population.

PS 08

Aging and Acoustic Trauma: Is There a Synergistic Effect?

Teresa Parsons[1]; Rachal Love[2]; Joseph P. Walton[3]
[1]Dept. of Communication Sciences & Disorders,Global Center for Hearing and Speech Research, University of South Florida, Tampa, FL; [2]Global Center for Hearing and Speech Research, University of South Florida, Tampa, FL; [3]Department of Communication Sciences & Disorders, and Chemical and Biomedical Engineering, Global Center of hearing and Speech Research, University of South Florida, Tampa, FL

Background

Age-related hearing loss (ARHL) can be attributed to different personal and environmental factors, with a history of noise exposure one of the most common co-morbidities. About 46% of adults above the age of 40 have hearing loss, whereas the prevalence increases to 89.5% in adults over the age of 80 years (Cruickshanks, et al. 1998.) The recent discovery of so-called "hidden hearing loss" following moderate noise exposure that does not result in permanent threshold shift, but causes central auditory processing deficits begs the question as to whether advancing age may exacerbate these effects. We hypothesized that the functional effects related to cochlear synaptopathy, following acoustic trauma, would be increased in old CBA mice. We tested this by using a longitudinal research design that measured ABRs prior to and at several time points following noise trauma.

Methods

ABR intensity functions (10-90 dB SPL) were recorded from male and female CBA mice between the ages of 22-27 months using tone bursts with frequencies of 8, 12, 16, 24, and 32 kHz. Thresholds were visually determined in 2 ways: using the complete waveform, minimal response threshold-(MRT), and individually for P1 and P4. All mice which were included in the study had MRTs of 40-50 dB or better at 12 and 16kHz. Acoustic trauma consisted of exposure to an octave band noise centered at 16 kHz at 110 dB for 45 minutes while awake. Subsequent ABRs were performed 24 hours, 2 weeks, and 4 weeks after acoustic trauma. The amplitude and latency of ABR peaks 1, 2, and 4 were analyzed using automated peak detection software (MatLab) which was subsequently verified by a judge blinded to the experimental condition.

Results

ABR thresholds increased significantly by ~20-25 dB following noise exposure and did not recover completely after 2 or 4 weeks, indicating small permanent threshold shifts of ~ 10-15 dB. Threshold shifts were similar for both determination methods. Peak 1 amplitudes were reduced at 24 hour, 2 week and 4 week post acoustic trauma at all frequencies with 16 and 24 kHz having the greatest P1 amplitude reduction compared to P4. P4 effects were both frequency and time dependent with the greatest effects observed for 24 kHz and complete recovery observed for 12 kHz. These functional changes will be supplemented by biomarker analysis in which assays for synaptic ribbons and metabotropic glutamate receptors will be quantified.

Conclusion

As previously reported, young mice exposed to the noise trauma used in the current study show complete to near complete recovery 4 weeks post trauma. Our results suggest that the effects of this exposure on old mice is much more severe. This exposure resulted in increased hearing loss and deficits in auditory nerve and brainstem function suggesting a synergistic effect of NIHL and ARHL when noise trauma occurs later in life. Our conclusions support the need for increased education of older human listeners regarding the importance of noise protection and hearing conservation.

PS 09

Predictability and Reliability of Revised Self-assessment Hearing Screening for the Elderly (R-SHSE)

Saea Kim[1]; Woojae Han[2]; Young Joon Seo[3]
[1]Department of Speech Pathology and Audiology, Graduate School, Hallym University; [2]Division of Speech Pathology and Audiology, College of Natural Science, Hallym University; [3]Yonsei University Wonju College of Medicine

Purpose

Currently hearing-impaired elderly have an opportunity to measure degree of disability, hearing aid benefit, and psycho-social problems using various questionnaires. However, if they wonder how much age-related hearing loss they have, there is no direct screening tool to self-check their severity up to now. In this respect, Self-assessment for Hearing Screening of the Elderly (SHSE, 2017) was developed and validated. The present study was to revise some questions of the original SHSE and Revised SHSE was standardized to be practical for many clinical applications. Method: The R-SHSE questionnaire consisted of 20 questions with 3 categories (i.e., general issue, distracting conditions, and working memory) instead of 4 categories from the SHSE. It was scored by a five point-scale (e.g., never, occasionally, half the time, almost always, and always). To standardize the R-SHSE, total 55 hearing-impaired elderly participated so far. They were conducted by mini-mental

state examination for dementia screening, tympanometry, pure-tone audiometry (PTA), otoacoustic emissions (OAE), and auditory brainstem response (ABR) for obtaining their information of hearing loss by both subjective and objective ways. Based on four-tone average of the pure-tone audiogram, the participants divided into four groups: normal, mild, moderate and moderate-to-severe. They were also tested by three questionnaires - R-SHSE, Korean Evaluation Scale for Hearing Handicap, and Korean Hearing Handicap Inventory for the Elderly. Only R-SHSE was retested 3 weeks later to confirm its reliability. Furthermore, the subjects performed fast speech-rated test, speech perception in noise test, and adaptive digit span test for assessing its validity. Result: The group mean of PTA was 15.00, 34.34, 54.95, and 70.00 dB HL for normal, mild, moderate, and moderate-to-severe groups, respectively. A high correlation was observed between the total scores and pure-tone thresholds, which indicated gradually increased SHSE scores of 30.66%, 39.70%, 63.31%, and 75.00% for normal hearing, mild, moderate, and moderate-to-severe groups, respectively. Either OAE or ABR data also supported total scores of SHSE for each group. With regard to construct validity, R-SHSE showed a negative correlation with speech perception scores in noise, with scores of time-compressed speech perception, and with results of the adaptive digit span. Conclusion: Although current data revealed with only 55 sample size that the R-SHSE scores between normal and mild groups showed no significant difference, we expect that R-SHSE will be a reliable and valid measure to represent the degree of hearing loss in the elderly with a large size of the participants.

PS 10

New battery of audiometric tests used for diagnosis of presbycusis

Oliver Profant; Zbynek Bures; Milan Jilek; Vaclav Vencovsky; Veronika Svobodova; Diana Kucharova; Josef Syka
[1]Department of Auditory Neuroscience, Institute of Experimental Medicine, The Czech Academy of Sciences, [2]Department of Otorhinolaryngology of University Hospital Královské Vinohrady and 3rd Faculty of Medicine, Charles University, [3]Department of Otorhinolaryngology and Head and Neck Surgery, 1st Faculty of Medicine, Charles University in Prague, University Hospital Motol, [4]Department of Technical Studies, College of Polytechnics

Age related hearing loss (presbycusis), is one of the most common sensory impairments in the ageing population. For many years, inner ear pathology was accepted as the main cause of presbycusis. However, deterioration of the speech understanding especially in noisy environments and deficits in temporal processing suggest that there exists also central component of presbycusis.

The aim of our project was to use audiological examination for better characterization of presbycusis

Several regularly used audiologic tests (high frequency audiometry, otoacoustic emissions, speech audiometry) were complemented by novel tests (speech in babble noise, periodically gated speech, laterogram, gap in noise, short click thresholds, auditory thresholds in noise, detection of short tones, difference limen of intensity, frequency modulation thresholds) along with cognitive tests (MoCA, MiniCog) and anamnestic data.

Fifty elderly volunteers (60-75 years of age) were compared with 25 young controls (22-32 years of age) to find out auditory differences. Within the elderly group, data were correlated using multifactorial analysis to identify independent variables to separate peripheral and central auditory functions. These correlations enabled us to differentiate four subtypes of presbycusis regarding peripheral and central auditory dysfunctions.

Complex auditory testing is essential in proper diagnosis of presbycusis. Acquired data will be further used for individualized rehabilitation based on peripheral, central auditory deficits, cognitive impairment or their combination.

PS 11

Initial Teleaudiology Planning Assessment for the State of Arizona: Geographic Workforce Analysis

Laura Coco; Kyle J. Sorlie Titlow; Nicole Marrone
University of Arizona

Access to health care can be affected by a person';s geographic proximity to a provider (Guilliford et al., 2002). Research has shown providers tend to be concentrated in urban areas, with fewer services in rural areas, where aging Americans disproportionately live (Comartie & Nelson, 2009). Hearing loss affects two thirds of Americans age 70 years or older (Goman & Lin 2016). A recent geographic survey of otolaryngologists across the United States found that most providers practice in highly populated urban areas, and 65.7% of counties lack a single provider (Bush 2017). In addition, it has been suggested that the number of practicing audiologists needs to at least double by 2030 to meet demand for services (Windmill & Freeman, 2013), yet we lack a geographic analysis of the audiology workforce distribution. Such data are important for public policy making and developing strategies for decreasing gaps in access to care.

Telehealth is a strategy for connecting patients in rural and under-resourced areas to hearing health care providers that minimizes the barrier of geography (Smith & Gray 2009; Doarn & Merrell 2008). However, in an audiology context, telehealth has been minimally implemented in the United States (Bush et al., 2016). Planning frameworks for telehealth interventions include data collection and needs assessment, as well as a priority setting analysis (Alverson et al., 2008; Krupinksi 2015; AlDossary et al., 2017). In this project, we perform the initial stage of a teleaudiology planning assessment for the state of Arizona. Results include a geographic survey of the distribution of the hearing health care workforce of Arizona using publicly available datasets and mapped to the population of older adults (≥65 years).

Population data was gathered from the U.S. Census and audiologist provider data was obtained from the Arizona Department of Health Services. Detailed population information will be presented for Arizona counties, including population density per square mile for individuals over 65 years old, as well as the distribution of audiologists and hearing aid dispensers by county. The results of the workforce analysis will be tabulated and used to estimate resource accessibility by county. Results will include population-to-provider ratio and estimated travel burden for individuals to reach the nearest audiologist.

Future research will include data from providers and community members on their perceived needs for services to help optimize the implementation and diffusion of teleaudiology.

Auditory Nerve I

PS 12

A Xenograft Model of Vestibular Schwannoma and Hearing Loss

Christine T. Dinh[1]; **Christine Mei**[1]; Olena Bracho[1]; Esperanza Bas[2]; Fred Telischi[1]; Cristina Fernandez-Valle[3]; Xue-Zhong Liu[1]
[1]University of Miami Miller School of Medicine, Department of Otolaryngology; [2]Department of Otolaryngology, University of Miami Miller School of Medicine; [3]University of Central Florida Burnett School of Biomedical Science, Division of Neuroscience

Background
Neurofibromatosis type II (NF2) is an autosomal dominant genetic condition that predisposes individuals to develop bilateral vestibular schwannomas. These tumors develop from mutations in the NF2 gene that encodes for the merlin tumor suppressor protein. Vestibular schwannomas develop from Schwann cells in the cochleovestibular nerve and can lead to hearing loss, dizziness, facial weakness, and life-threatening intracranial complications. The development of effective drug therapies that reduce tumor burden and audiovestibular dysfunction is impeded by the availability of animal models of vestibular schwannoma that develop hearing loss and imbalance.

Objective
Describe a microsurgical technique for implantation of schwannoma cells onto the cochleovestibular nerve that leads to tumor growth, hearing loss, and vestibular dysfunction in immunodeficient rats.

Methods
Ten adult Rowett Nude immunodeficient rats were anesthetized with isoflurane anesthesia and received a right or left microsurgical craniotomy to identify the root entry zone of the cochleovestibular nerve. Merogel impregnated with luciferase reporter merlin-deficient Schwann cells (MD-SCs; N=5) or Merogel alone (N=5) was placed into the cerebellopontine angle cistern and on top of the cochleovestibular nerve. Rats received auditory brainstem response tests and were observed for head tilt at baseline and every two weeks after surgery for a total of 6 weeks. In addition, rats underwent bioluminescence imaging at two week intervals after surgery. Subsequently, the skulls were harvested, fixed, and stained with hematoxylin & eosin and for S100 antigen. The two groups were compared with Mann-Whitney U tests.

Results
Rats implanted with MD-SCs developed significantly higher hearing thresholds shifts and tumor bioluminescence measurements by the 4th and 6th weeks, compared to control rats (p<0.05). Rats implanted with MD-SCs also developed gross tumor, and the tumor volume was significantly higher than nerve volumes in rats in the control group (p<0.05). In addition, all rats with tumors developed a head tilt, while none of the control rats had signs of vestibular dysfunction. The tumors were analyzed with immunohistochemistry and stained positive for S100.

Conclusion
Using this microsurgical technique, this xenograft rat model of vestibular schwannoma develops a cerebellopontine angle tumor, shifts in ABR thresholds, as well as head tilt. This animal model can be utilized for preclinical investigations of potential drug therapies for NF2-associated and sporadic vestibular schwannoma. It can also be valuable in studying the effects of vestibular schwannoma on auditory and vestibular function, in order to identify candidate targets for otoprotective therapies.

PS 13

Differentiating human embryonic and induced pluripotent stem cells towards an auditory neuron-like lineage

Niliksha Gunewardene[1]; Takahisa Watabe[1]; Judith S. Kempfle[2]; Sarah Kassenaar[1]; Albert Edge[3]

1 Department of Otolaryngology, Harvard Medical School, Boston, MA, USA 2 Eaton-Peabody laboratories, Massachusetts Eye a; [2]1, Department of Otolaryngology, Massachusetts Eye and Ear, Boston, MA, USA. 2, Department of Otology and Laryngology, Harvard Medical School, Boston, MA, USA. 3, Department of Otolaryngology, University Tübingen Medical Center, Germany; [3]Harvard Medical School

The development of a stem cell–based therapy for auditory neuron replacement requires overcoming several major challenges, one being to successfully differentiate stem cells to an appropriate neurosensory lineage. In the current study, we used two neural differentiation protocols to specify cells towards an otic progenitor and subsequently an auditory neuron lineage. The first protocol is a published protocol designed to generate a pure population of stem cell-derived otic progenitors with very high efficiency. Specifically, hiPSCs and hESCs treated with BMP4 together with otic induction factors FGF2, FGF3, FGF10, and FGF19 for 11 days *in vitro* (DIV) expressed a cohort of otic progenitor markers, PAX2, PAX8, SOX2, OTX1, FOXG1, EYA1, GATA3, and TBX1, confirmed by immunocytochemistry and qRT-PCR. These cells were subsequently differentiated into sensory-like neurons. The second protocol employed was a traditional neural induction protocol designed to generate dorsal-caudal hindbrain neurons. Following treatment of cells with transforming growth factor (TGF)-β inhibitor SB431542, BMP inhibitor DMH1 and GSK3-β inhibitor CHIR99021 for 6 DIV, we observed significant upregulation of the otic progenitor markers, PAX2 and PAX8. Subsequent treatment of the cells with neurotrophins BDNF and NT-3 prompted upregulation of neural markers NFM, ßIII-TUBULIN and the auditory neuron markers MAFB and NPR2. We are currently testing the capacity for these cells to innervate their peripheral and central targets both *in vitro* and *in vivo*.

PS 14

A Mouse Model of the Auditory Nerve to Study Cochlear Synaptopathy

Gerard Encina-Llamas[1]; James M. Harte[2]; Torsten Dau[3]; Bastian Epp[1]

[1]Hearing Systems group, Department of Electrical Engineering, Technical University of Denmark; [2]Interacoustics Research Unit; [3]Hearing Systems group, Technical University of Denmark

Background
Cochlear synaptopathy, the loss of auditory nerve (AN) fiber synapses after a temporary threshold shift, has been demonstrated in several non-human mammals. By far, the mouse is the most used and best characterized species in connection with cochlear synaptopathy. Studies in human listeners are, however, inconclusive. The impossibility to directly assess the status of the AN in humans is a major challenge. Hence, similar studies carried out in humans and mice are of great interest. Previously, we proposed the use of envelope following responses (EFR) as a tool to investigate synaptopathy both in mice and humans. We reported similar patterns in synaptopathic mice and humans, which could be explained by a humanized model of the AN with simulated synaptopathy. In this study, the original animal version of the AN model developed using cat data was evaluated and modified to account for the EFRs recorded in mice.

Methods
The cat version of the AN model by Zilany et al. (2009, 2014) was used to simulate EFR level-growth functions using sinusoidally amplitude modulated tones with strong (m=85%) and shallow (m=25%) modulation depths in noise-exposed and control mice. The stimuli used in the mice recordings were adapted to the cat AN model by transposing them to the cat's relative cochlear place. A mouse model was proposed by modifying the middle-ear response, the AN tuning, and the sensitive frequency range of the model.

Results
The cat AN model could account for the overall effect of synaptopathy on the recorded EFRs in noise-exposed mice. However, the shape of the recorded EFR level-growth functions both in the noise-exposed and the control mice did not fully agree with the simulated EFRs using the cat model. The mouse model also showed deviations from the data.

Conclusions
The analysis of the simulated results suggested that the inaccuracy of the model outcome may be caused by the differences in AN tuning between the model (cat) and the data (mouse). In addition, at supra-threshold levels, the total EFR is dominated by the off-frequency contributions (i.e., neuronal activity away from the characteristic place of the stimulus), which are limited in the high frequencies of the cat AN model. The proposed modifications of the model showed improvements which were not sufficient to entirely account for the data.

Funding

PS 15

The effect of an extended recording window on the eCAP recovery function in deaf guinea pigs

Dyan Ramekers; Henk A. Vink; Sjaak F. L. Klis; Huib Versnel
University Medical Center Utrecht, Brain Center Rudolf Magnus, Utrecht University

Successful cochlear implant performance requires adequate responsiveness of the auditory nerve to prolonged pulsatile electrical stimulation. Degeneration of the auditory nerve associated with severe hair cell loss may considerably deteriorate this ability. As a relevant measure of responses to multiple pulses, we have previously characterized two-pulse masker-probe recovery functions of the electrically evoked compound action potential (eCAP) in both normal-hearing and deafened guinea pigs (Ramekers et al. 2015, Hear Res 321:12-24). These recovery functions, however, could not be described by a simple exponential function as is conventionally used for human data (e.g., Morsnowski et al. 2006, Audiol Neurotol 11:389-402). A nonmonotonic recovery pattern was invariably observed, which could best be described using the product of two separate exponential functions, thereby assuming a fast facilitatory mechanism around 1 ms masker-probe interval. Novel experiments using elongated masker-evoked eCAP recordings show a reduction of the previously observed nonmonotonicity in the recovery function, suggesting that its origin lies in long-latency activity in response to the masker pulse. Conversely, since the nonmonotonic behavior is noticeably less pronounced than previously assumed based on the short eCAP recordings, but often by no means eliminated by the subtraction of long masker-evoked eCAP recordings, it may have a secondary origin. We conclude facilitation is additionally present: the preferred inter-pulse interval of approximately 1 ms would fit with experimentally obtained single fiber data (Prijs et al. 1993, Hear Res 71:190-201).

PS 16

Deconvolution of Longitudinally Recorded Electrically Evoked Compound Action Potentials in Normal-Hearing and Subsequently Deafened Guinea Pigs

Dyan Ramekers[1]; Stefan B. Strahl[2]; Konrad E. Schwarz[2]; Huib Versnel[1]
[1]*University Medical Center Utrecht, Brain Center Rudolf Magnus, Utrecht University;* [2]*Research and Development, MED-EL Medical Electronics, Innsbruck, Austria*

The electrically evoked compound action potential (eCAP) is a direct measure of the responsiveness of the auditory nerve to electrical stimulation. It can be easily obtained from a cochlear implant (CI), and as such it offers a unique opportunity to study the auditory nerve's electrophysiological behavior in individual subjects over time. Although traditional eCAP measures have shown not to be overly informative of speech perception with a CI (van Eijl et al. 2017, Laryngoscope 127:476-487), we have previously shown in guinea pigs that by applying more sophisticated stimulation paradigms robust differences in eCAP measures can be observed between healthy and degenerating auditory nerves (e.g., Ramekers et al. 2014, J Assoc Res Otolaryngol 15:187-202; Ramekers et al. 2015, Hear Res 321:12-24). However, these measures largely ignore the eCAP morphology, which may contain valuable information about neural subpopulations, site of excitation and firing synchrony - all of which may be subject to neurodegeneration. We have recently shown that the entire eCAP waveform can be mathematically analyzed using a convolution model (Strahl et al. 2016, Adv Exp Med Biol 894:143-153). The data we present here are derived from weekly eCAP recordings in chronically implanted guinea pigs. Additionally, we extended the traditional 1.7-ms eCAP recording time window to 8 ms, thereby including possible electrophonic responses. Four weeks after cochlear implantation the animals were systemically deafened (using kanamycin and furosemide), after which the eCAP recordings were continued for up to seven weeks. Using a mathematical unit response based on experimental findings, deconvolution of the experimentally obtained eCAP yield a compound latency discharge distribution (CDLD), which is a representation of the temporal distribution of excitation of all individual cells forming the auditory nerve. Using the traditional (i.e., short) eCAP recording window, the analysis of these CDLDs revealed two distinct firing populations approximately 1 ms apart. The slower of these two populations was the smallest, but gradually increased in size after deafening, consistent with our previous findings in acutely implanted animals. When using the extended recording window, a third distinct firing population was observed approximately 2 ms post-stimulus in the deafened animals, which was faster in the normal-hearing animals, thereby largely overlapping with the second population. We conclude that, by using a wide eCAP recording window, late evoked responses are revealed that may be informative of neural health.

PS 17

Three-dimensional electron microscopy of hair cell synapses in the inner spiral plexus

Shelby Payne; Mark Rutherford
Washington University in St. Louis

Classic measurements of serial sections from the inner spiral plexus of the cat showed morphological differenc-

es among auditory nerve fibers (Liberman 1980a), suggesting a widely-accepted fiber classification scheme that correlates with auditory nerve fiber threshold and spontaneous rate (Liberman, 1978). Additional measurements were made of efferent innervation onto the unmyelinated afferent fibers (Liberman 1980b).

To further study synaptic anatomy and to compare anatomically the afferent and efferent synapses in the inner spiral plexus between cat and mouse, we are undertaking a similar approach. We began by acquiring a ~30 μm^3 volume of the inner spiral plexus from a p17 C57Bl6 mouse. Postnatal day 17 is an age after the onset of hearing function, commonly used for ex vivo patch-clamp experiments, when synaptic and spike generator structure and function seems largely but not entirely mature (Wong et al., 2013; Kim and Rutherford, 2016). After preparing the sample for electron microscopy, we used a focused ion beam scanning electron microscope to image the volume with 8 nm pixels in X, Y, and Z. The aligned image stack consisted of more than 2 thousand images containing the inner spiral plexus from the habenula to the nuclei of 3 inner hair cells. For one inner hair cell, the entire basolateral membrane below the nucleus and all the afferent and efferent innervation were included. In addition, the other two inner hair cells and their synapses were mostly but not entirely contained in the volume, for a total of approximately 40 ribbon synapses and afferent fibers.

The data set was segmented in Amira, where renderings and measurements were made. We segmented presynaptic ribbons, presynaptic densities, and postsynaptic densities for each contact. On the cellular level, we segmented the hair cell and began segmenting the afferent and efferent neurons. Synapse size and shape will be compared with position on the inner hair cell, as well as afferent fiber volume and density of efferent innervation.

PS 18

Effects of a noise precursor on signal-to-noise ratios measured from the human auditory nerve

Skyler G. Jennings
University of Utah

In laboratory animals, the neural signal-to-noise ratio (SNR) improves as a sinusoidal increment is delayed from the onset of a sinusoidal pedestal of the same frequency [Smith and Zwislocki, Biol. Cybern. **17**, 169-182 (1975)]. This improvement occurs because the neural response to the increment remains constant as the response to the pedestal undergoes short-term adaptation. A similar improvement in neural SNR is observed in laboratory animals when the medial olivocochlear

(MOC) reflex is elicited by contralateral acoustic stimulation [Kawase et al., J. Neurophysiol. **6**, 2533-2549 (1993)]. Unlike short-term neural adaptation, improvements in SNR from the MOC reflex are due to a rapid decrease in cochlear amplifier gain, which affects the lower-level masker more than the higher-level probe. This study measured temporal changes in the neural SNR in humans by measuring the compound action potential (CAP) in response to a series of clicks in noise. Click series are preceded by silence or by a noise precursor. Preliminary results show that neural SNRs are improved for clicks preceded by noise precursors compared to clicks preceded by silence. Further research is needed to determine if these improvements in SNR are facilitated by short-term adaptation, or MOC efferents. These findings are consistent with the human auditory system quickly adapting to the local soundscape to improve the neural SNR. Such an improvement may facilitate speech perception in noisy backgrounds.

PS 19

Familial Neurofibromatosis Type 2 with Lumbosacral Plexiform Neurofibroma and a Novel NF2 Gene Mutation

Liang Zong[1]; Weiwei Guo[2]; **Shiming Yang**[2]
[1]*University of Kentucky Medical Center;* [2]*Chinese PLA Medical School*

Background

Neurofibromatosis type 2 (NF2) is a rare autosomal-dominant inherited disorder characterized by bilateral vestibular schwannomas, along with multiple meningiomas and ocular abnormalities. The disease is caused by mutations in the tumor suppressor gene NF2 on chromosome 22, and its incidence at birth is estimated to be 1:25 000 to 1:40 000. The NF2 mutations could be identified in most familial cases, although about 50% of the sporadic patients harbor de novo mutations. These causative mutations include many different types of change in coding sequences. Previous studies have suggested that the mutation of insertion or deletion resulting in truncated protein tends to induce more severe and aggressive phenotypes than the missense mutation. However, the genotype-phenotype correlations and the underlying pathological mechanisms still remain unclear.

Methods

In the study, we ascertained and clinically evaluated a three-generation Chinese family with NF2. Mutation screening of NF2 gene was performed on DNA samples from the family by using next-generation sequencing joint gene chip method. The pathogenic role of the detected mutation was assessed using the prediction approach of Mutation-Taster. Results: Affected family

members showed classical bilateral vestibular schwannomas and lumbosacral plexiform neurofibromas, as well as sporadic cutaneous nodular formations on the trunk. The proband, with the age of onset at four years, also showed unilateral facial nerve palsy. Two patients had mobility impairment resulting from lumbosacral neurofibromas. A novel deletion mutation (c.1634delA; p.Glu545GlufsX5) in exon 15 of the NF2 gene was present in the affected family members. The mutation is absent in 1000 Genomes, NHLBI EVS and ExAC databases, as well as 100 ethnically matched controls. The deletion leads to a frameshfit and an early stop codon, which obviously shortens the resultant protein. Conclusions: These data expand the mutation spectrum of NF2 gene in neurofibromatosis type 2, and help to further understand the genotype-phenotype relationships in this disease. Further studies on specific animal model with the novel mutation are required to detect the underlying pathological changes.

PS 20

Effects of auditory-nerve damage on behavioral tone detection by budgerigars in quiet and in noise

Stephanie Wong; Kenneth Henry
University of Rochester

Auditory-nerve (AN) fibers are lost with increasing age and with sound overexposure. This may happen even in the absence of hair-cell damage, which could produce 'hidden hearing loss';, i.e., deficits in complex sound perception without elevation of audiometric thresholds. The use of an avian model, such as the budgerigar (*Melopsittacus undulatus*), is advantageous due to their auditory sensitivity in the low frequency (Intracochlear infusions of kainic acid were performed bilaterally in budgerigars to induce permanent AN damage in both ears. Auditory brainstem response (ABR) tests were used to establish the level of AN damage, which ranged from moderate to severe across animals. The animals were trained to detect single tone frequencies with and without simultaneously gated background noise using operant conditioning procedures and a single-interval, two-alternative, non-forced discrimination task.

Minimum tone detection levels were established with and without background noise using two-down, one-up adaptive threshold tracking procedures. Thresholds were estimated across behavioral test sessions and compared between control animals and animals with varying degrees of AN damage.

The results of this ongoing study will determine the extent of AN damage for which tone detection becomes impaired (1) in quiet and (2) under more realistic, noisy listening conditions. If AN damage indeed causes hidden hearing loss, animals with AN lesions are predicted to show substantial elevation of tone detection thresholds in noise, but not under quiet listening conditions.

PS 21

Effects of auditory-nerve damage on behavioral sensitivity to amplitude modulation in the budgerigar

Kenneth Henry; Kristina Abrams; Kassidy Amburgey
University of Rochester

Auditory-nerve (AN) synapses are lost with age and with overexposure to loud sound, even in the absence of hair-cell damage. AN loss without hair-cell damage might produce 'hidden hearing loss';, i.e., deficits in complex sound perception without elevation of audiometric thresholds. However, support for this hypothesis is presently mixed. Behavioral studies in nonhuman animal models could be informative, but most existing model systems have limited capacity to discriminate low-frequency (Melopsittacus undulatus). Budgerigars are open-ended vocal learners with sensitive low-frequency hearing and human-like behavioral sensitivity to many speech-like sounds. The goal of the present study was to quantify the effects of AN damage on behavioral sensitivity to a key speech component: amplitude modulation.

Kainic acid is a glutamate analog that damages neurons through excitotoxicity, similar to the mechanism for noise-induced neuropathy. Kainic acid was infused into both cochleae to induce AN damage in budgerigars. Resulting damage was permanent, without recovery, and ranged from 40-75% across animals, as assessed from wave I of the auditory brainstem response. Animals were trained to discriminate fully modulated target stimuli from an unmodulated standard using operant conditioning procedures and a single-interval, two-alternative, non-forced discrimination task. Stimuli had a carrier frequency of 2 kHz and modulation frequency of 16, 45, or 128 Hz. Modulation detection thresholds were assessed by systematically varying the modulation depth of target stimuli using two-down, one-up, adaptive tracking procedures.

All test subjects, independent of AN status, learned to discriminate fully modulated stimuli from unmodulated stimuli with >90% correct performance. For each condition, modulation detection thresholds improved across test sessions and approached -20 dB (10% modulation depth) in two control animals after ~3 weeks of testing. One animal with severe (75%) AN damage showed substantial impairment of modulation detection thresholds

(elevation by ~5 dB), while two others with moderate (40-45%) damage performed more similarly to controls.

These preliminary results suggest a correlation between the extent of AN damage and behavioral impairment of modulation detection thresholds. Minimal behavioral impairment in animals with 40-45% AN damage is intriguing, and consistent with a recent modeling study based on signal detection theory. Future studies in this new model system will assess (1) changes in behavioral sensitivity to speech-like sounds in complex maskers and (2) effects of excitotoxic AN damage on central processing.

PS 22

Test-retest reliability of measures used to identify hidden hearing loss in humans

Daniel Rasetshwane[1]; Judy Kopun[2]; Stephen Neely[2]
[1]*Boys Town National Reaserch Hospital;* [2]*Boys Town National Research Hospital*

Background
Recent animal studies have shown that noise exposure can cause synaptopathy without permanent threshold shift. Because the noise exposure preferentially damaged auditory nerve fibers that processes suprathreshold sounds (low-spontaneous rate fibers), it has been suggested that synaptopathy may underlie hidden hearing loss (HHL) in humans. Recently, several researchers have suggested measures to identify HHL in humans, based on results from animal studies. However, the reliability of these measure have not been assessed in relation to HHL. The purpose of this study was to assess the test-retest reliability of measures that may have the potential to identify HHL in humans.

Methods
Adults with audiometric normal hearing were tested on a battery of psychophysical, physiological, electrophysiological, and speech tests that included (1) toneburst auditory brainstem response (ABR), (2) speech-ABR, (3) frequency-following response (FFR), (4) middle-ear muscle reflex (MEMR), (5) frequency-modulation detection thresholds (FMDT), (6) thresholds in noise (TIN), (7) thresholds in quiet (TIQ), (8) word recognition with or without noise or time compression or reverberation, and (9) distortion-product otoacoustic emissions (DPOAEs). Data collection for each measure was repeated over two visits separated by at least one day. The residuals of the correlation between TIQ and the other measures was obtained using correlational analysis. The residuals provide for a functional and quantitative proxy for HHL because they represent the portion of the raw measures that is not dependent on thresholds in quiet. Reliability of the raw and residual measures was assessed using root mean square (RMS) deviation of the standardized measures, Pearson correlation coefficient (r), and Cronbach';s α.

Results
Reliability for the raw measures was strong (RMS deviation0.5; α>0.5) for all the measures, except recognition of words in noise, which had moderate reliability (RMS deviation 1 SD; r0.5 and α>0.5 for all residual measures. (Results from ABR and FFR measurements will also be reported.)

Conclusions
Psychophysical and physiological measures were more reliable compared to speech tests, suggesting that, care should be taken when including speech tests in diagnostic tests for HHL. Quantifying HHL as the variance in suprathreshold measures of auditory function that is not due to thresholds in quiet may provide a reliable estimate of HHL in humans.

Funding

PS 23

Effects of noise exposure in young adults with normal hearing: Speech-in-noise deficits in non-musicians but not musicians, and no evidence of cochlear synaptopathy

Samuel Couth[1]; Garreth Prendergast[2]; Christopher J. Plack[2]; David R. Moore[3]; Kevin J. Munro[2]; Piers Dawes[1]
[1]*Manchester Centre for Audiology and Deafness, University of Manchester;* [2]*University of Manchester;* [3]*Cincinnati Children's Hospital*

Background
Previous research has suggested that high levels of noise exposure may lead to speech-in-noise processing difficulties, whilst the audiogram may be unaffected. It has been proposed that this is related to a loss of synapses between inner hair cells and auditory nerve fibers (cochlear synaptopathy), which can be assessed using electrophysiological measures. Musicians may be at risk of noise-induced hearing loss; however there is evidence that musical experience may improve spatial auditory processing abilities, and this may reduce some of the detrimental effects of high noise exposure.

Methods
Fifty-eight early-career musicians (female n = 26; age = 18-26 years) and thirty non-musicians (female n = 19;

age = 18-26 years) completed a test battery including pure-tone audiometry (PTA; 0.25-8 kHz), extended high frequency audiometry (EHF; 12 and 16 kHz), distortion product otoacoustic emissions (DPOAEs; 1-8 kHz), and click-evoked auditory brainstem responses (ABRs). Speech-in-noise processing was assessed using the coordinate response measure (CRM) with maskers presented centrally or spatially offset. A lifetime noise immission rating (NIR) was obtained by structured interview, which was used to classify participants into low (n = 58) and high (n = 30) noise exposure groups. The total NIR did not differ between musicians and non-musicians in either low or high noise exposure groups.

Results
There were no effects of musicianship or noise exposure on PTA, EHF, or DPOAEs. There was a significant interaction between musicianship and noise exposure on CRM performance; overall, performance was improved for spatially offset maskers compared to central (mean difference = -13.4 dB), but non-musicians with high noise exposure showed significantly less improvement for spatially offset maskers (mean difference = -8.0 dB) compared to all other groups. Total NIRs were significantly correlated with the amount of improvement for spatially offset maskers (i.e. higher NIR = less improvement), but only for the non-musicians (r = 0.593, p = 0.002). There was no effect of musicianship or noise exposure on the summating potential (SP), action potential (AP) or Wave V amplitude of the ABR. There was a borderline significant increase in the SP/AP ratio for the high noise exposure non-musicians, which appears to be due to larger SPs.

Discussion
High levels of noise exposure could impact on speech-in-noise processing, but musical experience may help to negate these perceptual effects. In agreement with other recent findings, there is little evidence that noise exposure produces large deficits in auditory nerve function consistent with cochlear synaptopathy.

Acknowledgements

PS 24

Estimating auditory-nerve activity in younger and older adults using forward-masked recovery functions and computational modeling

Carolyn M. McClaskey[1]; James W. Dias[1]; Judy R. Dubno[2]; Kelly C. Harris[1]
[1]Medical University of South Carolina; [2]The Medical University of South Carolina

Older adults often have difficulty processing suprathreshold stimuli and listening in complex environments. These findings may relate to changes in the function of the auditory nerve (AN), specifically the loss or diminished activity of AN fibers with low spontaneous rates (SR). Low-SR fibers are thought to be responsible for encoding sound in the presence of noise but may be more vulnerable to injury and aging than high-SR fibers. Low-SR fibers are also known to recover more slowly from prior stimulation. To better understand how changes in AN function may contribute to listening difficulties in older adults, we used a forward masking paradigm to characterize AN function in younger (aged 19-30) and older (aged 58-85) adults using the compound action potential (CAP). CAPs were elicited by a 3000 Hz signal ("probe") that was preceded by a 3000 Hz masker, and the time interval (Δt) between the masker and the probe was varied between 30 ms and 700 ms. Responses to the masked probe were normalized to the amplitude of the isolated probe and plotted as a function of Δt, which is known as a "recovery function". Results of studies with laboratory animals suggest that a change in the slope of the recovery function represents differences in the recovery rates of low-SR and high-SR fibers. That is, the slope of the function is steeper at smaller values of Δt, which may reflect the rates of recovery of both low- and high-SR fibers. The function begins to plateau for larger values of Δt after the majority of high-SR fibers have recovered, and subsequent shallower slopes or slowed growth has been attributed to the slower recovery of low-SR fibers. Consistent with these predictions, we found that, for both younger and older adults, mean normalized CAP amplitudes increased as Δt increased and the slope of this recovery function was steeper for Δt ≤ 100 ms than for Δt > 100ms. Slopes were steeper for older than younger adults for Δt ≤ 100 ms and Δt > 100 ms, indicating a greater contribution (or a larger representation) of high-SR fibers for older adults. An auditory nerve model was then used to describe the recovery functions of younger and older adults in an attempt to estimate the relative distribution of low- and high-SR fibers for each age group. Preliminary results are consistent with a loss or inactivity of low-SR fibers in older adults. Supported by NIH/NIDCD.

PS 25

Auditory Nerve Fiber Spontaneous Rate is Decreased in an Animal Model for Presbyacusis

Amarins N. Heeringa; Lichun Zhang; Christine Koeppl
Carl von Ossietzky University Oldenburg

Background
As our society ages, presbyacusis is becoming more prevalent. To study the underlying mechanisms of pres-

byacusis, the Mongolian gerbil is frequently used as an animal model because of a similar low-frequency sensitivity to that of humans. In gerbils, high- and low-spontaneous rate (SR) auditory nerve fibers (ANFs) are unevenly distributed along the cochlea. Basal, high-frequency inner hair cells are contacted by approximately equal numbers of high- and low-SR ANFs, whereas apical, low frequency inner hair cells are innervated primarily by high-SR ANFs. Here, we aim to understand whether the large population of high-SR ANFs in the low-frequency hearing range is affected by aging.

Methods

Eighty single-unit ANF recordings were obtained from 14 gerbils (including 5 "old" > 23 months). Single units were mostly tuned to low frequencies, <6kHz. Firing rates in quiet, during pure-tone stimulation, and during 1-s noise bursts (80 dB SPL band level, 400Hz-12kHz) were collected and SR, best frequency (BF), and threshold were derived. REVCORs (reverse correlations) were constructed from responses to noise and the maximum amplitude in the power spectrum defined phase locking strength.

Results

Thresholds of auditory nerve fibers were significantly elevated in old gerbils, indicative of presbyacusis (two-sample T-test: $T(37) = 7.023$, $p < 0.001$). ANFs of old gerbils had a decreased SR ($T(70) = 4.297$, $p < 0.001$) and low-SR fibers appeared more frequently in low-BF ANFs of old gerbils (figure). Noise-evoked firing rates were not significantly different between young and old gerbils, suggesting that these fibers were still capable of high firing rates. Furthermore, phase locking amplitudes were also not affected by aging.

Conclusion

Whereas low-BF fibers had decreased SR, previous research showed that high-BF fibers in the same species have an increased SR with aging (Schmiedt et al., J Neurophysiol, 1996). This highlights further that the gerbil';s basal and apical cochlear regions are discrete and may behave quite differently. Aging did not affect phase locking, which is consistent with low-SR fibers being superior at phase locking when compared to high-SR fibers in young animals (Louage et al., J Neurophysiol, 2004). High-SR fibers in young animals, however, are superior in synchronizing to sound onset (Bourien et al., J Neurophysiol, 2014). Therefore, future experiments will aim at studying onset coding of aged gerbils. These findings should shed light on neural mechanisms of presbyacusis and associated suprathreshold listening problems.

SR of low-BF auditory nerve fibers
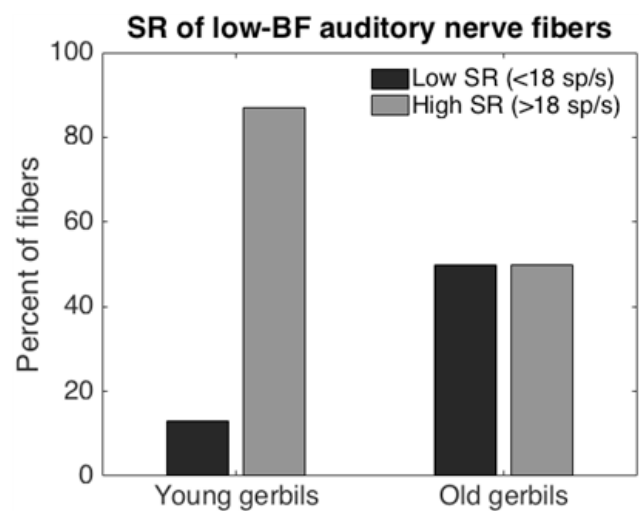
PS 26

Introcochlear Delivery of CNTF Promotes Regeneration of Cochlear Synapse after Noise-induced Cochlear Synaptopathy

Ning Hu; Steven H. Green
The University of Iowa

Introduction

Moderate noise exposure can cause cochlear afferent synapse loss of spiral ganglion neurons (SGN) under inner hair cells (HC), even though it does not cause HC loss. Significant regeneration has not been observed and the synapse loss appears to be permanent. Application of neurotrophic factors may promote synapse regeneration after noise-induced cochlear synaptopathy (NICS). In particular, NT-3 has been shown to be effective in this regard. However, NT-3 has also been shown to affect the physiological properties of SGNs, so alternatives may be desirable. We have shown that ciliary neurotrophic factor (CNTF) is expressed in organ of Corti at high levels and is nearly as effective as NT-3 in promoting SNG survival, neurite outgrowth and cochlear synapse regeneration in vitro. Here we extend these results to NICS *in vivo*.

Methods

12 to 14 week-old CBA/CaJ male mice were exposed to 100 dB SPL 8-16 kHz octave band noise for 2 hours to generate NICS. CNTF, dissolved in 0.1% mouse serum albumin (MSA) in artificial perilymph, was perfused into the left cochleae via the round window by a minipump/cannula system. Auditory brain responses (ABR) were measured at 8, 16, and 32 kHz prior to noise exposure, immediately after noise, and post-noise days 12-14 (PND14) to obtain measures of baseline, temporary threshold shift (TTS), and threshold recovery in a within-subject design. Intracochlear perfusion was initiated within 3 hours postnoise. Postsynaptic densities, presynaptic ribbons, and HCs were visualized, respectively,

with anti-PSD95, anti-Ribeye/CTBP2, and anti-myosin antibodies for quantitation of synapses/IHC at PND14 in organ of Corti wholemounts at 8, 16 and 32 kHz locations.

Results
ABR thresholds: TTS was confirmed for all mice. On PND14, in unoperated right ears, ABR thresholds recovered to prenoise baseline; in operated left ears, ABR thresholds recovered to baseline in 2/3 of ears; the other ears were excluded. ABR amplitudes: On PND14, wave I amplitudes were significantly decreased in all groups, in part due to the surgery in operated ears. The wave I amplitude decline was significantly smaller in CNTF-treated ears than in MSA-only controls and close to prenoise amplitude. Synapse counts: Cochlear synapse counts in CNTF-treated ears were close to normal control ears and significantly greater than in unoperated ears or MSA-only ears.

Conclusions
These data show that ears receiving CNTF intracochlearly postnoise exhibit significant recovery of ABR wave I amplitudes and morphological synapses after acute NICS, suggesting CNTF as an effective postnoise therapeutic for NICS.

PS 27

Cochlear Nerve Hypotrophy and Degeneration in a Mouse Model of Charcot-Marie-Tooth Type 2E Disease

Kye Hoon Park[1]; Hunki Paik[2]; Jian Zhao[3]; Wei Dong[4]; Elizabeth S. Olson[5]; Ronald KH. Liem[3]; Ana H. Kim[2]
[1]Department of Otolaryngology-HNS, Soonchunhyang University Cheonan Hospital; [2]Department of Otolaryngology-HNS, Columbia University Medical Center; [3]Department of Pathology and Cell Biology, Columbia University Medical Center; [4]VA Loma Linda Health Care System and Otolaryngology, Loma Linda University; [5]Columbia University

Introduction
Charcot-Marie-Tooth disease (CMT) is the most common inherited peripheral neuropathy. Mutations in the neurofilament light polypeptide gene (*NEFL*) have been reported to cause CMT type 2E. Neurofilaments (NFs) are heteropolymers made of three different subunits—NFL, NFM and NFH (Light, Medium and Heavy), and these subunits assemble into 10 nm filaments that compose the main part of the axonal cytoskeleton. Mutations in NFL are thought to result in neurofilamentous accumulations that disrupt axonal transport, which contribute to CMT mechanisms leading to axonal degeneration. CMT2E patients with one of the *NEFL* mutations (N98S) were reported to have hearing loss. Recently, a knock-

in mouse model bearing the N98S mutation has been generated, and its behavioral phenotypes and histological results have been reported. Initial studies have been conducted to investigate hearing in this CMT mouse model. In this study, we confirmed the presence of hearing loss in this mouse model, and evaluated the cause of hearing loss histologically.

Methods
Nefl[N98S/+] mice (heterozygote, HT) were compared to *Nefl*^{+/+} (wild type, WT) to evaluate hearing thresholds using auditory brainstem response (ABR) at 1, 2, 4, and 6 months of age. The cochleae were extracted at 4 months or 6 months of age for histologic evaluation of hair cells, peripheral processes and cochlear nerve.

Results
HT showed a significant higher hearing threshold and more delayed latency than WT from 1 month of age, and their hearing became worse with age. Immunohistochemistry of cochlear whole mounts revealed that hair cells in both genotypes were intact except in the basal turn. However, severe accumulations of NFs, as seen by neurofilament (NFL, NFH) staining, were observed at the distal peripheral processes under inner hair cells in every turn of HT cochlea, but not in WT. The efferent fibers to outer hair cells in HT were fewer and thicker than in WT. Immunostaining of transverse-sectioned cochlear nerve showed that the stained area of NFL and NFH was significantly reduced in HT, but no differences were found when the stained area of -tubulin was compared. Furthermore, the diameter of the cochlear nerve was significantly smaller in HT.

Conclusions
The *Nefl*[N98S/+] mice showed hearing loss compatible with auditory neuropathy that is similar to CMT2E clinical results. The cause of hearing loss is likely cochlear neuropathy following the pathological accumulation of NF aggregates in peripheral processes. This mouse model could be useful for testing a potential treatment to hearing loss resulted from NF assembly disruption.

PS 28

Effects of acoustic overexposure on the human auditory system -- Measurements in a clinical setting

Alexandra Mai[1]; Jennifer Simpson[1]; Brooke Flesher[2]; Michael Heinz[1]; Hari Bharadwaj[2]
[1]Department of Speech, Language, and Hearing Sciences, Purdue University; [2]Purdue University

Currently, the audiogram is the basis for hearing evaluation in the clinic. However, many patients present with normal thresholds but complain of difficulty understand-

ing speech in noise, i.e., at restaurants, cocktail parties, and other crowded environments. A possible explanation for this difficulty is cochlear synaptopathy from noise exposure or early aging, as robustly demonstrated in animal models. However, as of right now, it is unclear if synaptopathy affects humans and how it may be diagnosed. Currently, we are working on a large scale study comparing young adults regularly exposed to significant amounts of loud sounds, i.e., student members of the Purdue bands, to age-matched controls with nominal acoustic exposure from the general population, with the aim of determining the presence of cochlear synaptopathy in humans. The study includes both an elaborate battery of measures performed in a laboratory setting, and a shorter battery of measures performed in a clinical setting. Clinical measures being used include extended high-frequency audiometry, middle-ear muscle reflexes with high-frequency tonal and noise elicitors, auditory brainstem responses, and speech-in-noise measures using monosyllabic words in speech-shaped stationary noise, and low-context sentences in babble. Here, we describe the preliminary results from our measures performed with equipment available in most clinics.

PS 29

Apoptosis is Associated with Decreased BDNF Signal in the Spiral Ganglion of Otof -deficient Mouse

Kazunori Namba[1]; Hideki Mutai[2]; Tatsuo Matsunaga[3]
[1]Division of Hearing and Balance Research, National Institute of Sensory Organs, National Tokyo Medical Center; [2]Division of Hearing and Balance Research, National Institute of Sensory Organs, National Hospital Organization Tokyo Medical Center; [3]Division of Hearing and Balance Research, National Institute of Sensory Organs/ Medical Genetics Center, National Hospital Organization Tokyo Medical Center

Background
OTOF is responsible for hereditary hearing loss (DFNB9). Otoferlin, which is encoded by *OTOF*, is localized at presynaptic particles in inner hair cells and regulates the secretion and recycling of neurotransmitters in the ribbon synapse. Although the proper function of spiral ganglion neurons (SGNs) are critical for the efficacy of cochlear implantation, there has not been a detailed study on whether SGNs are affected by otoferlin dysfunction. We studied the number and apoptotic status of SGNs in *Otof*+/+ and *Otof*-/- mice during various developmental stages.

Methods
Thick (5 μm) paraffin sections from the inner ear of *Otof*+/+ and *Otof*-/- mice, at embryonic day 18.5 (E18.5), postnatal (P) days 1 to 7, 28, 42, and 84, were prepared.

TUNEL labeling for apoptotic cells were performed on each section, which then underwent sequential immunostaining for NeuN and peripherin. Cells that were NeuN(+)-peripherin(-) and NeuN(+)-peripherin(+)were defined as type I and II SGNs, respectively. Inner ear sections (obtained on E18.5, P1–P7, and P42) were also immunostained for BDNF and TrkB (i.e., BDNF receptor), and their signal intensities were compared.

Results
The number of type I SGNs was stable at first and gradually decreased between P7 and P28. During this period, there were no significant differences between *Otof*+/+ and *Otof*-/- mice. At P42 and P84, the number of type I SGNs in *Otof*-/- mice were approximately 50% lower than that in *Otof*+/+ mice. In contrast, the number of type II SGNs gradually decreased during development, with no significant difference between *Otof*+/+ and *Otof*-/- mice through the experimental period. The number of TUNEL(+) type I SGNs in *Otof*+/+ and *Otof*-/- was similar from E18.5 to P7. However, although not observed in *Otof*+/+ mice during the same period, TUNEL(+) type I SGNs in *Otof*-/- mice significantly increased from P28 to P84,. There was no significant difference in TUNEL(+) type II SGNs between *Otof*+/+ and *Otof*-/- mice throughout the experimental period. The expressions of TrkB and BDNF signals in the type I SGNs were the most intense at P3 and P4 in *Otof*+/+ mice. However, these signals were significantly small in the SGNs of *Otof*-/- mice at any of the time points that were examined.

Conclusion
Increased apoptosis in type I SGNs were observed in the *Otof*-/- mouse from P28 to P84.

Auditory Pathways Brainstem I

PS 30

Relative contributions of auditory nerve, brainstem, and cortical generators to the auditory frequency-following response revealed by EEG

Gavin M. Bidelman
University of Memphis

The auditory frequency-following response (FFR) is a neurophonic potential reflecting sustained, phase-locked neural activity to the spectrotemporal features of complex sounds. Despite providing a unique window in the encoding of speech/music, auditory disorders, and neuroplasticity, the neural origins of the FFR remain controversial. To elucidate the underlying sources of the FFR, we recorded responses to speech sounds using high-density (64 ch) EEG and applied state-of-the art source imaging techniques to the multichannel data (discrete dipole modeling, distributed imaging, indepen-

dent component analysis, computational simulations). We confirm a mixture of generators localized to bilateral auditory nerve (AN), brainstem inferior colliculus (BS), and bilateral primary auditory cortex (A1). However, frequency-specific scrutiny of source waveforms showed that the relative contribution of these nuclei to the aggregate FFR varied systematically with stimulus frequency. Whereas AN and BS sources produced robust FFRs up to about the sixth or seventh harmonic (~600-700 Hz), A1 showed much weaker phase-locking with little energy for frequencies above the speech fundamental (F0≈100 Hz). Findings were corroborated by functional CLARA imaging, which showed A1 activation was eradicated for FFRs >150 Hz, above which only subcortical sources remained active. Our results reveal that the site of FFR generation varies critically with stimulus frequency but subcortical structures make the largest contribution to the electrically recorded FFR (i.e., AN ≥ BS > A1). While some (albeit weak) cortical FFRs are apparent for low frequency stimulation (~100 Hz), subcortical FFRs (AN, BS) dominate for a majority of the speech bandwidth (>150 Hz). We infer that cleanly separating subcortical from cortical FFRs can be achieved by ensuring stimulus frequencies are >150-200 Hz, above the known phase-locking limit of cortical neurons.

PS 31

The Influence of Noise Exposure on Auditory Efferent Function Measured using Modulated Signals

Sriram Boothalingam[1]; Tim Schoof[2]
[1]University of Wisconsin-Madison; [2]University College London, London, UK

Emerging evidence suggests that noise exposure, even when it does not lead to elevated audiometric thresholds, may result in the loss of auditory nerve synapses (cochlear synaptopathy). Animal models indicate that this damage is selective to high-threshold auditory nerve fibers that respond to moderate-to-high sound levels. Evidence also suggests that auditory efferents may reduce the incidence of synaptopathy, although evidence for such protective role in humans is currently unavailable. Counterintuitively, efferent activity appears to be larger in individuals with more noise exposure. In the event of damage to high-threshold fibers, one would expect a decrease - not an increase - in efferent activity. On the other hand, it is also possible that larger noise exposure could strengthen efferents, as in musicians. At this juncture, the relationship between peripheral changes in the afferent synapses and changes in the efferent neurons is unclear. To further understand the relationship between the input drive to the efferents and their sensitivity to noise exposure, the relative roles of low- and high-threshold fibers in activating efferents must be delineated. The present study sought to address this gap by activating efferents using noise modulated at different depths (no modulation, 8 dB, 4 dB, and 0 dB). The rationale was that progressively shallower modulation depths will not be encoded as the low-threshold fibers would be driven to saturation leaving the damaged high-threshold fibers to encode modulation depth. We hypothesize that damage to high-threshold afferent fibers will restrict the availability of modulation cues to the efferent neurons at moderate-to-high sound levels. We used click-evoked otoacoustic emissions (CEOAE) to index efferent activity with elicitor noise presented to the contralateral cochlea. Efferent strength as a function of modulation depth (slope) was obtained and correlated with noise exposure history. We predict that individuals with greater noise exposure will depend heavily on the 'saturated'; low-threshold fibers which would provide a constant drive to the efferent neurons regardless of the modulation depth, resulting in a shallower slope. Pilot data in 6 individuals indicates a progressive reduction in efferent strength with increasing modulation depth as expected. However, the relationship between efferent strength and noise exposure is unclear in this small sample. Further data collection is ongoing.

PS 32

Characterisation of auditory brainstem neurons in a murine model of gap-detection deficits, the BXSB/Mpj-Yaa mouse

James Sinclair[1]; Jennifer F. Linden[1]; Conny Kopp-Scheinpflug[2]
[1]UCL Ear Institute; [2]LMU Munich

Background
In the auditory brainstem, midbrain, thalamus and cortex, there are subsets of cells that respond to the offsets (disappearances) of sounds (Behrend et al., 2002, Fuzessery & Hall, 1999, He, 2001, Rencanzone, 2000). Encoding brief silences accurately is likely to be important for correctly interpreting human speech.

The BXSB/MpJ-*Yaa* mouse strain is a powerful animal model for studying the role of gap detection and offset-sensitivity in auditory processing. In this strain, approximately half of male animals exhibit stereotyped, highly localized disorganization in the layers of their neocortex, termed ectopias. Ectopic male BXSB/MpJ-*Yaa* mice perform worse than their non-ectopic littermates in behavioural tests involving detection of short (5ms) gaps in noise (Clark et al., 2000). In extracellular recordings from the medial geniculate body, neurons are less sensitive to short gaps in noise in ectopic than non-ectopic mice, with the deficit most pronounced for gap durations of 2 to 8 milliseconds (Anderson & Linden, 2016).

Methods

We used whole-cell patch clamp to study the cellular mechanism giving rise to the deficit in offset firing in ectopic BXSB/MpJ-*Yaa* mice. Many neurons of the superior paraolivary nucleus (SPN) of the auditory brainstem generate action potentials (APs) following the offset of sounds (Kopp-Scheinpflug et al., 2011). We performed whole-cell patch clamp on SPN neurons in brainstem slices from male BXSB/MpJ-*Yaa* mice sacrificed after the onset of hearing (P12-19). During patching, offset firing was triggered by injecting negative current pulses of 200ms.

Results

In SPN neurons from an ectopic male mouse, the number of offset APs evoked following a -1nA pulse (1.2 ± 0.5 APs, n = 5 cells, mean ± S.E.M) was lower than those from two ectopic mice (3.1 ± 0.6 APs, n = 13 cells Mann-Whitney U, p = 0.049). However, we observed that SPN cells from ectopic mice required similar levels of negative current to evoke any offset firing (-690 ± 174pA) compared to those from non-ectopic mice (-469 ± 86pA, p = 0.225, unpaired t-test) and that the latency from current offset to AP peak was similar between ectopic (3.03 ± 0.49ms) and non-ectopic male mice (5.38 ± 0.77ms, p = 0.089, unpaired t-test).

Conclusions

Ongoing electrophysiological and immunohistochemical experiments aim to investigate these preliminary results further to determine what physiological differences give rise to the gap detection deficit exhibited by the ectopic BSXB/Mpj-*Yaa* mice.

PS 33

Enhancing wave-I of auditory brainstem response by choosing the latency of rising-frequency chirp

Takashi Morimoto[1]; Yoh-ichi Fujisaka[2]; Yasuhide Okamoto[3]; Toshio Irino[4]

[1]*Rion Co., Ltd. / Wakayama University;* [2]*Rion Co., Ltd.;* [3]*Tokyo Saiseikai Central Hospital / Keio University Hospital;* [4]*Faculty of Systems Engineering, Wakayama University*

A defect in the cochlear afferent synapses between inner hair cells and spiral ganglion neurons without hair cell loss or permanent threshold shift has been reported. This "cochlear synaptopathy" may affect the encoding of temporally complex stimuli in the conditions of background noise. Recent animal studies have shown that "cochlear synaptopathy" is associated with amplitude reductions in the wave-I of the auditory brainstem response (ABR) [Kujawa and Liberman, J Neurosci, 2009, pp. 14077–14085]. Thus, "cochlear synaptopathy" may

be diagnosed via observing a degree of wave-I amplitude reduction. However, the estimation of the amplitude of wave-I is not easy because the wave-I is not very salient and is much smaller than wave-V when measured with low-level click signals. Elberling and Don [JASA, pp. 3022–3037, 2008] reported that raising-frequency chirp signals, in particular, the "Don-Chirp," enhance the amplitude of wave-V.

This study aims to find an optimal chirp that enhances the amplitude of wave-I. We produced a set of ten chirp signals with various latencies. They were modified from the "Don-Chirp": $t\_g(f) = k*f^{\wedge}(-d)$, where d = 0.4356 and $k = 0.0902*(n\_k - 1)/9$ with an integer n_k between zero to nine. The signal becomes a click when n_k = 0 and a Don-Chirp when n_k = 9. The chirp level was set to 110 dB in peak equivalent SPL to make wave-I salient and measurable. The ABRs were estimated via averaging the sweeps which are evoked by an alternating polarity chirp signal repeated 1000 times. Six normal-hearing listeners participated in the experiment.

Figure 1 shows the averages and standard deviations of wave-I and wave-V amplitudes across listeners. The amplitude of wave-I is smaller than that of wave-V and becomes maximum when n_k = 4, while the amplitude of wave-V becomes maximum when n_k = 6. A two-way ANOVA with factors of n_k and subject was performed for the amplitudes of wave-I and wave-V. There is main effect of n_k for wave-I ($F_{(9,45)}$ = 14.86, p < 0.001,) but not for wave-V ($F_{(9,45)}$ = 2.03, p = 0.058). Multiple-comparison showed that the mean value at n_k = 4 is significantly different from the mean values at n_k = 0, 7, 8, and 9. The moderate chirp signal increases the amplitude of wave-I but at a latency approximately half of the Don-Chirp. The optimal choice of chirp signals may help in diagnosing of "cochlear synaptopathy."

PS 34
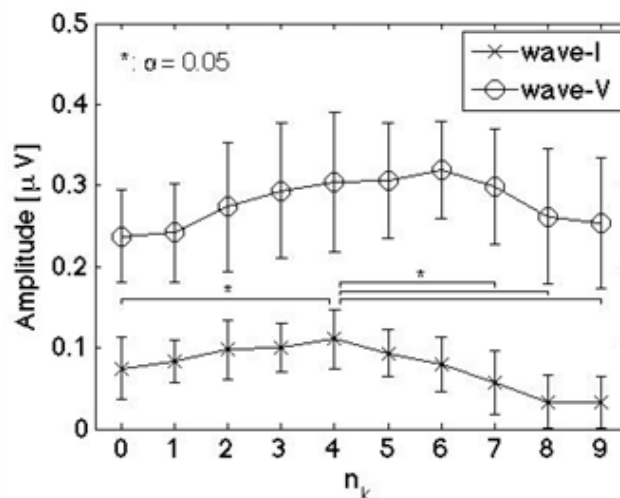
Effect of noise exposure on neurons of the superior paraolivary nucleus

Ezhilarasan Rajaram[1]; Matthew Fischl[2]; Conny Kopp-Scheinpflug[1]

[1]LMU Munich; [2]NIH / NIDCD Section on Neuronal Circuitry

Background

Neurons in the superior paraolivary nucleus (SPN) are under strong inhibitory constraint by the medial nucleus of the trapezoid body (MNTB), resulting in low spontaneous activity and phasic offset responses to contralateral sound. MNTB neurons increase firing rates in response to increased synaptic activity by switching the use of potassium channels (Steinert, 2011). Furthermore, neuronal activity in the MNTB has been shown to release the neuromodulator nitric oxide, which can modify the strength of inhibition in the SPN via the potassium-chloride co-transporter 2 (KCC2) (Yassin, 2014). This raises the question of whether increased activity in the MNTB evoked by sound exposure will increase the strength of inhibition in the SPN via increased firing rates or decrease the strength of inhibition via nitric oxide action on KCC2?

Methods

In C57BL/6J mice with ages ranging from postnatal day 15 to 22 (P15-22), we used in vitro whole-cell patch-clamp recording to study intrinsic and synaptic properties of SPN neurons. Inhibitory postsynaptic currents (IPSCs) were evoked by stimulating the MNTB, in the presence of the AMPA receptor antagonist DNQX (10µM) and NMDA receptor antagonist D-AP5 (50µM). We recorded IPSC amplitudes and time constants, input-output functions, reversal potential, synaptic depression, and miniature IPSCs between animals that underwent acoustic over exposure 24 hours prior to the experiment and control animals that were not exposed to noise. *In vivo* single-unit recordings of SPN neurons were also compared between noise exposed and control animals. All experiments were performed in accordance with the German guidelines for the care and use of laboratory animals as approved by the Regierung of Oberbayern (AZ 55.2-1-54-2532-38-13, Bavaria, Germany).

Results

Preliminary data indicates that SPN neurons in the noise exposed animals have more depolarized resting membrane potentials. In addition, SPN neurons from exposed animals have more depolarized reversal potentials for chloride, hinting towards a shift in the balance between excitation and inhibition. Incidentally, we also observed an increase in the number of spontaneously firing cells in the noise exposed animals, which is only rarely seen in controls.

Conclusions

Noise exposure seems to disturb the balance of excitation and inhibition in the SPN. These preliminary data suggest that acoustic trauma might result in a switch from phasic to tonic firing patterns in SPN neurons. Whether this switch results in changes in the efferent feedback system or whether it is part of the generation of phantom sounds as found in tinnitus is currently investigated.

PS 35

Frequency Following Responses to Complex Stimuli: Effects of Audiometric Configuration

Emily Spitzer[1]; John Grose[2]; Emily Buss[1]

[1]University of North Carolina - Chapel Hill; [2]UNC School of Medicine

Purpose

Harmonic complexes with an absent fundamental frequency (F0) can generate a frequency following response (FFR) with a component at F0 for complexes comprising either resolved or unresolved harmonics. However, the mechanisms that contribute to the origin of this response remain unclear. The purpose of this study was to examine the relative contributions of: (1) the 2f1-f2 cochlear distortion product; and (2) for resolved harmonics, the component interactions in the low-frequency tails of auditory filters tuned to high frequencies.

Methods

Three groups of adults participated: (1) normal hearing (NH); (2) cochlear hearing loss with moderate flat losses (CHL-F), targeting listeners unlikely to generate cochlear 2f1-f2 distortion products; and (3) cochlear hearing loss with steeply sloping high-frequency losses above about 1 kHz (CHL-S), targeting listeners unlikely to exhibit the interaction of resolved components in the tails of high-frequency filters. Following screening with distortion product otoacoustic emissions (DPOAEs), FFRs were recorded to harmonic or inharmonic tonal complexes. The harmonic complexes had a missing F0 of 245 Hz and comprised harmonics 2-4 (resolved), 11-13 (unresolved), or all 6 combined. Three complementary inharmonic complexes comprised components upshifted by 61 Hz from these harmonic frequencies; the envelope rate remained 245 Hz. Stimuli were presented monaurally at 3.9 Hz in alternating phase at either 70- or 80-dB SPL. A 1-channel vertical recording montage was used, and 4000 artifact-free sweeps were collected for each polarity. Dependent variables were component amplitudes at the frequencies of F0 and 2f1-f2.

Results

DPOAEs were present for the entire NH group, indicating normal non-linear cochlear function, but were ab-

sent in the CHL-F group and for high frequencies in the CHL-S group. All three groups exhibited a robust FFR component at 245 Hz. Whereas a component at 2f1-f2 was present for the resolved inharmonic complexes in the NH group, this was not consistently the case in the CHL-F group. For the CHL-S group, the amplitude of the F0 component tended to be smaller than for comparable conditions in the NH group.

Conclusions

The presence of cochlear hearing loss does not preclude the generation of an FFR component at the missing F0 or envelope rate. However, amplitude differences across groups suggest that this response likely depends on cochlear status. This study demonstrates that audiometric configurations which diminish the likelihood of cochlear distortion products or interactions in high frequency regions can shed light on the relative contributions of the different putative mechanisms responsible for generating the FFR.

PS 36

Nonmusicians with innate musicality exhibit enhanced subcortical encoding of speech

Kelsey Mankel; Gavin M. Bidelman
University of Memphis

Previous studies have established that trained musicians exhibit superior auditory encoding of normal and noise-degraded speech at both subcortical and cortical levels of processing. What remains uncertain is whether this "musician advantage" results from formal musical training itself or innate sensitivities of the auditory system that precede music engagement. In the present study, we compared frequency-following responses (FFRs), which reflect phase-locked neural activity to the spectrotemporal features of auditory stimuli, in a group of nonmusicians to speech and music sounds in quiet and noisy backgrounds. Participants were assessed objectively on their degree of musicality via the Profile of Music Perception Skills (PROMS). Nonmusicians with high musicality (i.e., high PROMS scores) demonstrated stronger neural pitch salience in their speech-evoked FFRs that was more resilient to noise than those with low musicality scores. "Neural noise," spontaneous brain activity measured in pre- and post-stimulus intervals, was significantly lower in participants with high musicality. Both reduced neural noise and more robust FFR voice pitch encoding predicted higher musicality scores. These results demonstrate that brainstem responses to speech are related to enhanced auditory skills, even in listeners without formal musical training. Our results parallel those reported in trained musicians but suggest that certain individuals are "musical sleepers" who have innate, musician-like listening capabil-

ities that provide increased sensitivity to auditory and linguistic brain processing.

PS 37

Objective detection of auditory steady-state responses based on mutual information: Receiver operating characteristics and validation across modulation rates and levels

Gavin M. Bidelman; Claire McElwain
University of Memphis

Auditory steady-state responses (ASSRs) are sustained potentials used to assess the physiological integrity of the auditory pathway and rapidly estimate hearing thresholds. ASSRs are typically analyzed using statistical procedures in order to remove the subjective bias of human operators. Knowing when to terminate signal averaging in ASSR testing is also critical for making effcient clinical decisions and obtaining high-quality data in empirical research. Here, we investigated a new detection metric for ASSRs based on mutual information (MI) [Bidelman, G. M. (2014). Objective information-theoretic algorithm for detecting brainstem evoked responses to complex stimuli. *J. Am. Acad. Audiol.*, 25(8), 711-722], previously bench tested using only a single suprathreshold stimulus. ASSRs were measured in *n*=10 normal hearing listeners across a broad range of stimuli varying in modulation rate (40, 80 Hz) and level (80 – 20 dB SPL). MI-based classifiers applied to ASSRs recordings showed that accuracy of ASSR detection ranged from ~75 - 99% and was better for 40 compared to 80 Hz responses and for higher compared to lower stimulus levels. Detailed receiver operating characteristics were used to establish normative ranges for MI for reliable ASSR detection across levels and rates (MI=0.9-1.6). Our new results confirm that MI can be applied across a broad range of ASSR stimuli and might offer improvements to conventional objective techniques for ASSR detection.

PS 38

Visualization of Functional Connections within an Isofrequency Lamina

Lin Lin; Yihe Ma; Xiao-Jie Cao; Meyer Jackson; Donata Oertel
University of Wisconsin School of Medicine and Public Health

We have combined two genetic approaches to understand the function of neuronal circuits in the ventral cochlear nucleus (VCN), the first integrative stage in the auditory pathway. The topographic innervation of the VCN by auditory nerve fibers imposes a tonotopic organization on their synaptic targets so that a tone activates cells along the isofrequency lamina that is tuned to that tone.

We marked cells activated by a tone and then explored synaptic connections among them optically. We marked active cells by a genetic approach, targeted recombination in active population (TRAP), pioneered by Guenthner et al. (Neuron 78:773-784, 2013). In mice that express the tamoxifen-dependent Cre recombinase, CreER[T2], under the control of the immediate early gene *Fos*, and a fluorescent reporter after a floxed stop codon on a *Rosa26* locus, the fluorescent protein is expressed only in activated neurons. Cre was then used to drive the expression of a hybrid voltage sensor (hVOS) probe (Wang et al., Biophys. J. 99:2355-2365, 2010) in hVOS::Fos-Cre mice in order to measure voltage changes optically in neurons activated by sound. In VCN slices from hVOS::Fos-Cre mice that were first kept in quiet in a sound isolated chamber for 3 hours, then stimulated with a tone at 15,000 Hz at 85 dB for 3 hours, administered tamoxifen, and stimulated for a further 3 hours, labeled neurons lay parallel to the path of auditory nerve fibers in an isofrequency lamina. Trains of electric shocks to auditory nerve fibers evoked fluorescence changes in the hVOS-probe expressing cells in the same isofrequency lamina with synaptic delays and synaptic depression as expected from previous electrical measurements. In the VCN from animals presented with sound immunohistochemistry confirmed a successful, activity-dependent expression of the hVOS probe within an isofrequency lamina. The results indicate that hVOS-detectable synaptic potentials can be induced through synaptic connections between auditory nerve fibers and principal cells defined by responsiveness to a specific auditory stimulus. This work was supported by a grant from the NIDCD R21 DC014858.

PS 39

Subcortical Amplitude Modulation Encoding Deficits in Young Adults with Greater Noise Exposure History Suggest Evidence of Cochlear Synaptopathy

Brandon Paul[1]; Sajal Waheed[2]; Ian C. Bruce[2]; Larry E. Roberts[2]
[1]University of Montreal; [2]McMaster University

Animal studies have shown that moderate noise exposure can permanently damage synapses that connect auditory nerve fibers to inner hair cells while leaving the hair cell intact. Noise damage is greatest for synapses on auditory nerve fibers with high thresholds for firing, which impairs suprathreshold listening.

Synapses on fibers with low thresholds are less affected, leaving threshold hearing as measured by the audiogram intact. However, there is to date only limited evidence that suprathreshold listening deficits observed in individuals with audiometrically normal hearing are related to noise exposure history.

Twenty-five 18- and 19-year olds with normal audiograms (< 25 dB HL to 14 kHz) were divided into a high-exposure (N = 12) or low-exposure (N = 13) group on the basis of their replies to validated lifetime noise exposure questionnaire (Jokitulppo et al., 2006, Mil. Med., 171). Thresholds for detecting the presence of amplitude modulation (AMD) in a 5 kHz 75 dB SPL tone AM at 19 Hz were obtained in quiet and in narrowband background noise (NBN) at spectrum levels of 25, 40, and 45 dB. Thereafter we measured the 86 Hz Envelope Following Response (EFR), an auditory midbrain potential measured by EEG that is sensitive to synaptopathy. EFRs were similarly evoked by 5 kHz, 75 dB SPL AM tone (full modulation depth) in conditions of quiet and in 25, 40, and 45 dB spectrum level NBN.

Participants in the high exposure group had smaller EFR amplitudes than did participants in the low exposure group (main effect p = 0.029). The high exposure group also tended to have overall poorer AMD thresholds, although this finding fell short of significance (p = 0.06). Correlations between AMD thresholds and EFR amplitude did not reach significance. Auditory peripheral modeling (Zilany et al 2014; JASA, 135) suggested that the significant group difference in EFR amplitude could be explained by a mild degree of synaptopathy in the high noise exposure group.

Modulations of sound at AMD thresholds are typically shallow and are thus likely to engage a smaller range of auditory nerve synapses compared to EFRs evoked by fully-modulated tones. For this reason EFRs evoked by fully modulated tones may be more sensitive to synaptopathy than AMD, as we observed. At the ARO meeting we will present new data comparing EFRs to AM discrimination thresholds, which are measured at comparatively similar modulation depths used to evoke EFRs. (Supported by NSERC of Canada)

PS 40

Searching for Sources of Speech-in-Noise Performance Variability in Listeners with Normal Audiograms

Spencer B. Smith; Christine Liu; Jen Krizman; Travis White-Schwoch; Nina Kraus
Northwestern University

Background
Audiologists routinely encounter patients complaining of speech-in-noise (SIN) deficits despite normal audiograms. Three physiologic mechanisms underlying this so-called "*hidden hearing loss*" (HHL) have been proposed: (1) *synaptopathy*, whereby noise exposure predominately insults high threshold auditory nerve fibers

but spares low threshold fibers and hair cells, (2) *"subclinical" hearing loss* resulting from hair cell damage that is undetectable by conventional audiometry, and/or (3) deficits in *central* auditory neurophysiologic functions such as temporal encoding. Our goal is to test the extent to which these three hypotheses can account for speech-in-noise (SIN) perception difficulties using data collected over multiple experiments in the past decade.

Methods

This retrospective analysis of over 350 adults includes otoacoustic emissions, auditory evoked potentials, standard and extended high frequency audiograms, and SIN performance.

Part I of this investigation tested the following predictions from the HHL literature:

1. ABR wave I amplitudes, a proxy of *synaptopathy*, are significantly correlated with SIN performance.

2. High frequency hearing thresholds (> 8 kHz) and distortion product otoacoustic emission amplitudes, both proxies of *subclinical hearing loss*, are significantly correlated with SIN performance.

Part II of this investigation tested predictions regarding the relationship between central auditory processing and SIN performance:

1. Frequency following response (FFR) temporal encoding is stronger in good SIN performers than in poor SIN performers

Results

The prevalence of HHL in our normal hearing adult cohort was approximately 9% based on SIN performance. No significant relationships between ABR wave I amplitudes or extended high frequency thresholds and SIN performance were observed. Measures of FFR temporal encoding were stronger in better SIN performers.

Conclusions

Our results indicate that HHL is poorly explained by synaptopathy or subclinical hearing loss, to the extent that these can be reliably measured non-invasively in humans. In contrast, the FFR, a measure of midbrain sound processing influenced by sensory and cognitive factors, provides insight into individual variation in SIN performance.

PS 41

Assessment of Cochlear and Auditory Brainstem Neural Integrity in Children Suspected of Auditory Processing Disorder

Sangamanatha Ankmnal Veeranna; Chris Allan; Prudence Allen
Western University

Background

The click evoked auditory brainstem response (ABR) is a widely used objective measure to assess the neural integrity of the auditory brainstem. Published evidence indicates that 10-20 % of children suspected of auditory processing disorder (sAPD) have clinically abnormal (> 2 SD from age matched children) wave I [or action potential (AP)] latency. The AP reflects synaptic transmission between inner hair cells and the auditory nerve. The quality (amplitude/latency) of the AP depends on coordinated activity within the cochlea. Any disruption in activity may compromise the quality of the AP. A significantly prolonged AP in children sAPD can often be attributed to impaired cochlear processing. Electrical events within the cochlea can be recorded by placing the electrode close to the cochlea, a technique called Electrocochleography (ECochG). The objective of this study was to simultaneously record both the cochlear and neural responses to acoustic stimuli in typically developing (TD) children and children sAPD.

Methods

Seventeen normal hearing TD children and 12 children sAPD participated in this study. Auditory evoked potentials were recorded using the two channel Vivosonic Integrity system. The click evoked (alternating polarity) ECochG was recorded by placing gold foil electrodes in the ear canal. Stimuli were presented to right and left ears at 80dB nHL (13.3 and 57.7 clicks/sec). Cochlear integrity was assessed by measuring the summating potential (SP), AP amplitude ratio, SP-AP latency difference, and the AP latency difference to condensation and rarefaction stimuli. Auditory brainstem neural integrity was assessed by measuring the ABR wave latencies, interwave intervals, wave V shifts at faster stimulation rate and V/I amplitude ratios.

Results

No statistically significant differences were found between groups. However, several individual children sAPD demonstrated clinically abnormal (> 2 SD from TD children';s data) cochlear and/or auditory brainstem potentials. Two children sAPD (16.66%) showed a clinically abnormal response in at least one of the cochlear potential components. Four children sAPD (33.33%) showed clinically abnormal cochlear and neural potentials. Three children sAPD (25%) showed clinically abnormal auditory brainstem potentials.

Conclusions

Results of this study provide new evidence of abnormal cochlear potentials in individual children sAPD. The atypical ECochG findings in children sAPD may be due to poor coordination in the cochlear mechanism. The co-occurrence of abnormal responses in both cochlear and neural responses suggests that atypical cochlear function may contribute to poor neural representation.

PS 42

Frequency-following responses of three component consecutive odd-harmonic stimuli reveal frequency dependent differences in cochlear nonlinearities

Dameon Harrell; Erika Skoe
University of Connecticut, Department of Speech, Language, and Hearing Sciences

Studies examining the pitch of tonal stimuli consisting of only odd harmonics have found that the pitch of such stimuli matches the fundamental frequency (F0) when the F0 is above 200 Hz, but is perceived as being approximately an octave above the F0 when the F0 is below 200 Hz. A study conducted by Bashford and Warren (J. Acoust. Soc. Am., 1990) explored the possibility that this shift in pitch is caused by interactions between harmonics in the "dominant region" when the F0 is below 200 Hz. Listeners were presented triplets of consecutive odd harmonics (for example 3rd, 5th, and 7th, or 7th, 9th and 11th) with missing fundamentals between 100 and 200 Hz. The authors found that low order triplets were pitch matched to the missing fundamentals, while higher order triplets (those beginning with the 9th harmonic or above) were matched to pitches almost an octave higher. The current study recorded frequency following responses (FFR) to similar triplet stimuli in adults with normal hearing. The FFR reflects sustained, phase-locked neural activity in the brainstem and possibly the cortex. FFRs have been shown to carry pitch relevant information, with one school of thought considering FFRs to be neural correlates of pitch. All triplet stimuli produced FFRs with spectral energy at the difference tone distortion product, which corresponds to the second harmonic of the missing fundamental. However, only the responses to stimuli containing higher order triplets, e.g. 11th, 13th, and 15th harmonics, produced an FFR spectrum with additional distortion products at frequencies that are even harmonics of the missing fundamental. Alternatively, these additional distortion products could be interpreted as harmonics of a complex waveform with twice the missing fundamental that is produced by an interaction between the harmonics of higher order triplets. This interpretation lends support to the theory proposed by Bashford and Warren that the change in pitch as the triplets increase in frequency is due to an interaction between harmonics.

PS 43

Neural Pitch Coding in Multi-lingual Population: Language Effect

Esther Pugh[1]; Melanie Rosenblatt[1]; Jiong Hu[2]
[1]University of the Pacific; [2]Department of Audiology, University of the Pacific

Background

Previous studies have shown that adults who speak tonal language such as Mandarin Chinese show stronger neural pitch coding ability at the brainstem level, compared to adults who speak non-tonal language such as English. Long-term auditory exposure to certain characters in those languages have been suggested to be the underline reason. At the same time, some behavioral studies have suggested that people who speak multiple languages are thought to process certain auditory features better than monolingual adults. The question that is it the multilingualism or is it certain language that (re)shapes the auditory brainstem remains unanswered. The purpose of this study was to examine the effect of multilingualism on adults'; pitch processing ability.

Method

Three language groups were recruited in this study: 1) monolingual adults who speak only American English, 2) bilingual adults who speak English and a tonal language and 3) bilingual adults who speak English and a non-tonal language. They all had normal audiometric test results as well as normal supra-threshold click-evoked ABR. None of the subjects identified themselves as had long time music or auditory trainings. To obtain scalp recorded Frequency Following Response, two Mandarin Chinese syllables with different fundamental frequency pitch contours (Flat Tone and Falling Tone) were presented at 70 dB SPL. Fundamental frequencies (f0) of both the stimulus and the responses were extracted and compared to individual brainstem responses. Two indices were used to examine different aspects of pitch processing ability at the brainstem level: Pitch Strength and Pitch Correlation.

Results

Measured by Pitch Strength and Pitch Correlation, lexical tone elicited FFR was found to be stronger in bilingual tonal language speakers, compared to both monolingual speakers and bilingual non-tonal language speakers. However, there was no statistically significant difference between the monolingual group and bilingual non-tonal group.

Conclusion

Results of this study demonstrated that pitch processing ability at the brainstem level is primarily influenced

by specific auditory features in the languages that they speak, not the number of languages they speak. Furthermore, comparable FFR results obtained from both mono-lingual and non-tonal bilingual speakers group suggest that although behaviorally bilingualism or multi-lingualism could show some differences in certain tests or assessment, they likely did not affect speakers'; pitch processing mechanism, at least not reflected by auditory electrophysiological tests such as FFR. Future directions include examine effect of bilingualism that consists different tonal languages, such as Mandarin Chinese and Cantonese Chinese.

PS 44

The Development of A Multi-Channel ABR Testing System and Its Efficacy Evaluation

Dingxuan Zeng[1]; Changquan Wang[1]; Wei Liu[2]; Fangyi Chen[1]
[1]Department of Biomedical Engineering, Southern University of Science & Technology; [2]Department of surgical sceinces, Uppsala university, Uppsala, Sweden

To develop therapeutic strategies against hearing loss, chemical and genetic approaches have been intensively used to generate deaf animal models, which play essential roles in evaluation of hearing-protecting drugs, gene delivery, stem cell transplant, and so on. Hence, a highly efficient system for testing the auditory function of the diseased and treated animals is strongly demanded in both basic and translational studies. The commercial TDT auditory working station series have been widely used and becoming one of the most popular facilities for evaluating mammalian hearing. However, these systems are designed as single-channel ones that can only measure one animal at a time, which limits the efficiency of the screening. In order to solve this problem, we developed a multi-channel ABR system, which can monitor several animals simultaneously. The system includes multiple highly sensitive micro-volt EEG amplifiers, a high-resolution multi-channel analog-to-digital converter, a dual-channel digital-to-analog converter, two programmable attenuators, power amplifiers, and the high-speed Ethernet connection between the instrument and PC. A software system was also developed for setting up the testing parameters, such as designing stimulus profile, setting the intensity range, and so on. To validate the efficacy of the system, we firstly tested the sub-systems. With the same animal and the same speaker, results from our amplifier showed less-noisy waveform and discernible ABR signal under 5 dB lower sound intensity than its TDT counterpart. More testing results on other sub-systems will be provided. Results from multi-animal ABR tests will also be provided to demonstrate the high-throughput capability of the system.

PS 45

The Importance of Within-Subject Measures of Brainstem Envelope Following Responses in Characterizing Individual Differences in Suprathreshold Encoding

Scott Bressler; Bennett O'Brien; Barbara Shinn-Cunningham
Boston University

Envelope following responses (EFRs), here defined as the auditory brainstem';s ability to faithfully represent low frequency envelope fluctuations from harmonic acoustic stimuli, are often utilized as a biomarker for a type of sub-clinical hearing dysfunction thought to be linked to neuropathy of a subset of auditory nerve fibers that respond to suprathreshold levels of sound--more commonly referred to as "hidden hearing loss." The EFR is generally thought to represent the collective neural response of the peripheral auditory pathway from auditory nerve bundle up to the inferior colliculus. To isolate the contribution of the suprathreshold-responding fiber population from other brainstem processes, we measured the EFR to various amplitude modulated stimuli whose peak-to-peak pressures were kept constant, and compared the responses across three different modulation depths corresponding to modulation indices of 100%, 79.4%, and 63.1%. The same 102.4-Hz half-wave rectified sinusoid was used to modulate two different carriers: a 4096 Hz pure tone with and without an 800-Hz wide notched noise masker at 20 dB SNR, and 3-10 kHz band passed Gaussian white noise. EFR magnitudes and phase locking values (PLVs), a normalized measurement of inter-trial response synchrony, to the envelope fundamental frequency were computed from 32-channel EEG data using complex principal component analytical methods described in Bharadwaj *et al.* (2014). These measures were compared relative to an estimated noise floor constructed from phase-randomized individual trial data.

We found that generally responses to the modulated noise stimuli generated larger overall responses, with the smallest responses resulting from the modulated tone stimuli. Both measures of EFR magnitude and PLV exhibited a high degree of correlation across all three different stimulus types (i.e., subjects who exhibited high magnitudes and PLVs from one stimulus generally had equivalently high response measures from the other two stimuli), particularly at the deeper modulation depths of 100% and 79.4%. However, how these EFR measures changed as a function of modulation depth exhibited no correlation across the three different stimuli. These findings suggest that while differences in intensity of the EFR reflect the level of cochlear excitation due to spread of excitation and stimulus bandwidth, the absolute EFR

measures appear to be related more to response SNR than with suprathreshold encoding. Individual differences in suprathreshold encoding, however, do appear to be captured in the way the EFR strength changes as the modulation depth is reduced. Collectively these results highlight the importance of incorporating within-subject measures when quantifying brainstem responses.

Auditory Pathways: Midbrain I

PS 46

Auditory Cortex Projects to Brainstem Cholinergic Cells That Innervate the Thalamus and the Cochlear Nucleus

Brett R. Schofield; Nichole L. Beebe
Northeast Ohio Medical University

We showed previously that auditory cortex (AC) projects directly to cholinergic cells in the pontomesencephalic tegmentum (PMT) that project to the inferior colliculus or cochlear nucleus (CN). That work suggests that AC axons could elicit release of ACh in multiple brainstem nuclei. The PMT also is the main source of ACh input to the medial geniculate body (MG). Here, we ask several questions about cholinergic circuits in pigmented guinea pigs: 1) Do AC axons contact cholinergic PMT cells that project to the MG? 2) Do cholinergic cells have branching axons that innervate the CN and MG? 3) Do AC axons contact these latter cells? We use double retrograde tracing and immunochemistry to identify cholinergic cells with branching axonal projections. We add anterograde tracing to identify AC axons that contact the cholinergic cells that project to one or two auditory nuclei.

First, we found that AC axons contact PMT cells that project to the MG. The contacts occur most often ipsilateral to the AC of origin, and on PMT cells that project to the ipsilateral MG. Second, individual cholinergic cells can have branching projections to the MG and CN. The most common projection pattern is to the MG and CN ipsilateral to the PMT cell. Third, AC projections contact cholinergic PMT cells that innervate both the CN and the MG. Such contacts were more numerous ipsilateral to the labeled AC cells, and the contacted cells projected most often to the ipsilateral MG and CN.

We conclude 1) that individual cholinergic PMT cells can have widely divergent projections, extending from the CN to the MG (the full extent of the subcortical central auditory pathway), and 2) that AC axons contact cholinergic PMT cells that project to the MG or to the MG and the CN. Divergent projections from PMT neurons suggest that ACh is released concurrently across multiple sites in the subcortical auditory pathways. Via direct projections from the AC, top-down influences could activate these PMT cholinergic cells and trigger widespread release of ACh. In the short term, ACh release may support arousal and quick action. On a longer time scale, ACh release could support subcortical plasticity, perhaps to fine-tune circuitry for stronger responses and efficient gating of salient signals, or to adapt to alterations in sensory input during development, aging or after damage to the cochlea or central pathways. Supported by NIH R01DC004391.

PS 47

Cholinergic Inputs to Ascending and Descending Pathways From the Inferior Colliculus

William A. Noftz[1]; Nichole L. Beebe[2]; Brett R. Schofield[2]
[1]*Kent State University; Northeast Ohio Medical University;* [2]*Northeast Ohio Medical University*

Acetylcholine (ACh) is associated with attention, arousal and plasticity, and alters responses to sound of many neurons in the inferior colliculus (IC). The IC is the primary source of ascending projections to the medial geniculate body (MG) and descending pathways to the superior olivary complex (SOC). Do cholinergic inputs to the IC contact the ascending pathways, the descending pathways, or both? Here, we used fluorescent tracers and immunohistochemistry for vesicular acetylcholine transporter (VAChT) to determine whether cholinergic axons contact IC cells that give rise to ascending or descending pathways. Moreover, ACh has been shown to act directly on GABAergic cells in the IC. Because GABAergic cells contribute to numerous IC output pathways, we immunostained for glutamic acid decarboxylase (GAD) to distinguish GABAergic from non-GABAergic (presumptive glutamatergic) cells in the output pathways.

Fluorescent retrograde tracer was stereotaxically injected into the MG or SOC of adult Long Evans rats. Following fixation, brains were cut at 40 μm and immunostained for GAD to label GABAergic neurons and VAChT to label cholinergic terminals. Retrogradely-labeled cells were analyzed for GAD reactivity and for VAChT-immunopositive (VAChT+) boutons in close apposition to the labeled cells.

Injections into the MG labeled cell bodies in the central nucleus, lateral cortex and dorsal cortex of the IC. Throughout these regions, VAChT+ boutons appeared in close contact with somas and proximal dendrites of a subset of retrogradely-labeled neurons. Most of the contacted cells were GAD-negative, reflecting the predominance of GAD-negative cells in the IC-MG pathway, but GAD+ IC-MG cells were also contacted by VAChT+ boutons.

Injections into the SOC labeled cell bodies in all three subdivisions of the IC and in the ventral tectal longitudinal column (TLCv). VAChT+ boutons contacted cell bodies and/or dendrites of GAD-negative retrogradely-labeled IC neurons in all these regions.

We conclude that cholinergic axons are likely to make direct contact with both ascending and descending pathways from the IC. The cholinergic axons appear to contact both the predominant excitatory neurons as well as GABAergic neurons that contribute to these pathways. Cholinergic inputs to the ascending pathways could provide for modulation of bottom-up processing whereas inputs to the descending pathways could provide for top-down influences on early auditory processing. Supported by NIH R01DC004391.

PS 48

Anatomical Basis for Parallel and Interconnected non-ITD Pathways from the Inferior Colliculus to the Medial Geniculate in the Mongolian Gerbil

Kendall A. Hutson; Gilberto D. Graña; Douglas C. Fitzpatrick
University of North Carolina

In the gerbil, the constituent nuclei of the inferior colliculus (IC) can be identified in cytochrome oxidase (CO) stained material as "core" and "belt" regions based on levels of activity. The core region is the central nucleus, which can be further parceled into a core region 1 (C1) of very high CO activity bordered medially by a less active region, core 2 (C2). C1 is also bounded laterally by a less active region, the lateral nucleus (L), which appears to have both "core" and "belt" features (see below). C1 has a similar pattern of ascending inputs as L and C2 (including contralateral cochlear nucleus, ipsilateral superior paraolivary nucleus and bilaterally from dorsal nucleus of the lateral lemniscus) except it is heavily innervated by the lateral and medial superior olives, while C2 and L are not. Physiologically, we have found L and C2 neurons share common features differing from those in C1. Whereas C1 neurons are often sensitive to interaural time difference (ITD), neurons in L and C2 while binaural, are largely non-ITD sensitive. We have placed biotinylated dextran amine injections into the IC, medial geniculate (MG) and auditory cortex to gain a better understanding of the anatomical basis underlying these physiological observations and to examine how L and C2 distribute their efferent projections to the MG. Injections restricted to L show the inputs described above, but also demonstrate significant projections to and from C2 (bilaterally) as well to and from the contralateral L. Small injections in C2 show a similar pattern of ascending inputs and that C2 receives projections from L bilaterally and from the contralateral C2. Both L and C2 project to the ventral division of the MG (MGv), but differ in their primary targets in MGv. L preferentially innervates rostral MGv, particularly its rostral pole (RP). In contrast, C2 while also projecting to the RP, preferentially innervates the most caudal MGv. C1 primarily projects to the central regions of MGv. Thus, areas L and C2 form parallel and interconnected pathways to the MGv for conveying information from neurons that are largely not sensitive to ITDs. Projections to the MGv are characteristic of core pathways, however L receives projections from auditory cortex, a characteristic of belt regions, while cortical projections to C2 are meager. Thus, L has features which place it intermediate between core and belt areas as previously described.

PS 49

Pathways for the Transmission of Frequency and ITD Information from the Central Nucleus of the Inferior Colliculus to the Ventral Division of the Medial Geniculate Body in the Gerbil

Gilberto D. Graña; Kendall A. Hutson; Brendan T. Lutz; Douglas C. Fitzpatrick
University of North Carolina

A characteristic finding in mammals is that there is a transformation from a single tonotopic organization in the central nucleus of the IC (ICc) to multiple tonotopic representations in the core regions of auditory cortex. For most species, it is not known if this transformation happens between the IC and thalamus, or between the thalamus and cortex. In the mustached bat, the transformation from a representation according to frequency in the IC to one according to function in the thalamus and cortex happens in the output pathways of the IC. To test if this is also the case in an auditory system not specialized for echolocation, pathways between the central nucleus of the IC and ventral division of the MG (MGv) were studied in the Mongolian gerbil using a combination of anatomical and physiological methods.

Biotinylated dextran amine was injected into different locations within the MGv. The location and distribution of retrogradely labeled cells in the IC were plotted from 40 µm thick sections. A magnetic resonance image (MRI) of a gerbil brain served as a digital framework to chart the location and size of the injection sites across cases, and to compare the locations of the labeled cell bodies within this digital framework to the locations and properties of physiological recordings obtained previously in the IC.

Preferential labeling in each subdivision of the central nucleus was found after injections in specific parts of the MGv. Injections into the lateral portion of the MGv labelled cells in the dorsal region of the central nucle-

us (C1d) which contains low-frequency, ITD-sensitive cells, and those in the caudal portion of the MGv (MGvc) tended to label cells in the medial region of the central nucleus (C2), which contains primarily high-frequency, non-ITD sensitive cells. Segregation based on function rather than topography might have been expected in the outputs from the ventral part of the central nucleus (C1v), whose cells respond to middle to high frequencies and possess a mixture of ITD and non-ITD sensitive neurons. However, injections in MGv that primarily labelled cells in C1v were located in the ventral part of the MGv, medial to those that labelled C1d and rostral to MGvc; in aggregate, this suggests an organization based primarily on topographic projections from ICc to MGv, rather than a major reorganization of projections as in the mustached bat. However, in previous studies some divergence of anterograde projections in MGv were seen following BDA injections in the ICc. Our injections in the MGv produced some labeled cells in multiple subdivisions of the ICc, so there is a substrate for a complex organization of the output pathways of the ICc to reorganize tonotopic information to a degree in the MGv.

PS 50

Unilateral and Bilateral Projections to the Auditory Thalamus from Individual Neurons in the Inferior Colliculus

Jeffrey G. Mellott; Nichole L. Beebe; Brett R. Schofield
Northeast Ohio Medical University

The inferior colliculus (IC) is the source of a large projection to the ipsilateral medial geniculate body (MG) and a smaller projection to the contralateral MG. We injected different fluorescent retrograde tracers into the left and right MGs in adult guinea pigs to identify individual IC cells that project bilaterally. We found cells in the IC that contained both retrograde tracers, indicating that they project to both MGs. We quantified retrogradely labeled cells from 8 ICs (2 sections/IC) in 4 animals that had substantial IC cell labeling. Of 9396 retrogradely labeled cells, bilaterally-projecting cells constituted up to 37% (average 12%) of the cells that projected to the ipsilateral MG and up to 81% (average 41%) of the cells that projected to the contralateral MG. Bilaterally-projecting cells were located in all major IC subdivisions, including the central nucleus, dorsal cortex and external cortex.

IC projections to the MG are either GABAergic or glutamatergic (Bartlett and Smith, ';99, J Neurophysiol. 81:1999-2016). GABAergic cells contribute to both the crossed and uncrossed projections, but are outnumbered by glutamatergic cells in both pathways. We used immunohistochemistry for glutamic acid decarboxylase (GAD) to distinguish GABAergic from glutamatergic cells. We interpreted triple-labeled cells (two retrograde

tracers plus GAD-immunopositive) as GABAergic cells that project bilaterally to the two MGs. Nearby double-retrograde cells that were GAD-immunonegative were interpreted as likely glutamatergic bilaterally-projecting cells. GABAergic cells averaged 20% (range: 14-28%; n = 476 cells) of the bilaterally-projecting population in the IC overall. GABAergic bilaterally-projecting cells were found in all three IC subdivisions, where they averaged 12-26% of the bilaterally-projecting population within the individual subdivision.

We conclude that there is a distinct pathway comprising IC cells with branching axons that innervate the auditory thalamus bilaterally. Both glutamatergic and GABAergic cells contribute to this projection. While an IC projection to the *contralateral* MG has been known for many years, it is usually treated as separate from the ipsilateral projection. Our results suggest that the tectothalamic projection may be better viewed as a large ipsilateral projection and a smaller bilateral projection. The bilaterally-projecting cells undoubtedly serve functions different from the ipsilateral projections, perhaps synchronizing activity on the two sides of the auditory brain. Supported by NIH R01DC004391.

PS 51

Neurons projecting from the lateral cortex of the inferior colliculus to the superior colliculus are found in auditory-recipient extramodular zones

Alexandria Lesicko[1]; Daniel A. Llano[2]
[1]*Neuroscience Program, University of Illinois at Urbana-Champaign;* [2]*Department of Molecular and Integrative Physiology, University of Illinois at Urbana-Champaign*

The lateral cortex of the mouse inferior colliculus contains periodic, neurochemically dense zones, or modules, that stain positive for markers associated with inhibition, plasticity, and high metabolic activity. While the exact function of these modules remains unknown, previous studies in our laboratory have shown that the termination patterns of extrinsic multimodal inputs to the lateral cortex are correlated with the distribution of neurochemical modules: somatosensory inputs target these regions, while auditory inputs avoid them. In the present study, we sought to determine whether the cell bodies of projection neurons in the lateral cortex are also arranged in a modular fashion. The retrograde tracer, Fluorogold, was injected iontophoretically into the superior colliculus of the GAD67-GFP mouse, in which modules are readily distinguishable as high-density clusters of GFP-labeled terminals and cell bodies. Following a week-long survival period, animals were sacrificed and brains were cut into 40 μm thick sections. For each tissue section containing retrograde label, 20X mosaic Z-stacks of

the Fluorogold and GFP labeling were taken throughout the entire depth and x–y plane of the lateral cortex. The stacks were collapsed into 2D maximum intensity projections and individual mosaic tiles were merged to form a composite image. Overlay images revealed that Fluorogold-labeled cells in the lateral cortex were found almost exclusively outside of the GFP-labeled modules. Injections into medial portions of the superior colliculus produced stronger labeling in the lateral cortex than more lateral injection sites. In all cases, retrogradely labeled cells were most prominent in rostral regions of the lateral cortex. In conjunction with our previous data, these results indicate that cells that project to the superior colliculus are found in regions of the lateral cortex that predominately receive auditory input. The present study further supports the hypothesis that the lateral cortex exhibits connectional as well as neurochemical modularity, and shows that the pattern of projection neurons in this structure is correlated with the distribution of neurochemical modules.

PS 52

GABAergic Components in the Descending Pathway from the Inferior Colliculus to the Superior Olivary Complex

Nichole L. Beebe[1]; William A. Noftz[2]; Brett R. Schofield[1]
[1]Northeast Ohio Medical University; [2]Kent State University; Northeast Ohio Medical University

The inferior colliculus (IC) contains glutamatergic and GABAergic neurons. Both types project to the thalamus or the contralateral IC, whereas glutamatergic cells are thought to be the source of projections to the cochlear nucleus. Little is known about the cells that give rise to the largest descending pathway from the IC, which terminates in the superior olivary complex (SOC). The primary target of this colliculo-olivary projection is the ventral nucleus of the trapezoid body (VNTB), which contains many GABAergic cells as well as other neurotransmitter phenotypes. Here, we address two questions: 1) are the colliculo-olivary cells glutamatergic or GABAergic; and, 2) do colliculo-olivary axons contact GABAergic cells in the VNTB? To address these questions, we combined retrograde or anterograde tracing with immunohistochemistry for glutamic acid decarboxylase (GAD) in pigmented guinea pigs and Long-Evans rats. We also used adeno-associated viral vectors in VGAT-cre transgenic rats to examine GABAergic projections selectively.

In rats and guinea pigs, injections of retrograde tracer into the SOC labeled cells throughout the IC, especially in the central and lateral regions. Few (<5%) of retrogradely labeled cells in the IC were GAD-immunopositive (GAD+). In both species, many of the retrogradely-labeled, GAD-negative somas were densely surrounded by GAD+ terminals. Such GAD+ perisomatic rings were much less common around guinea pig IC cells that were retrogradely labeled from the thalamus or contralateral IC. Anterograde tracing from the IC in both species labeled many boutons in the ipsilateral VNTB, where some formed putative contacts with GAD+ and GAD-negative cells. We injected a viral vector carrying a cre-dependent fluorescent protein gene into the IC of VGAT-cre transgenic rats to label GABAergic projections selectively. We observed labeled axons in the lateral lemniscus and some axons and boutons in the ipsilateral VNTB.

We conclude that 1) most colliculo-olivary cells are glutamatergic, and 2) colliculo-olivary axons appear to contact both GABAergic and non-GABAergic VNTB cells. These data suggest that the large colliculo-olivary pathway could exert inhibitory and excitatory effects on lower brainstem nuclei via the projections from IC-targeted VNTB cells. In addition, many of the colliculo-olivary cell bodies are surrounded by GABAergic boutons, suggesting that this descending pathway could be subject to intense inhibition within the IC. Thus, our data support the general assumption that the colliculo-olivary projection is excitatory, and demonstrate that GABAergic inhibition is likely to be a key component at several points within this descending system.

PS 53

Optogenetic Circuit Mapping of Commissural and Ascending Projections to VIP Neurons in the Inferior Colliculus of Mice

David Goyer; Peter T. Malinski; Alexander P. George; Michael T. Roberts
Kresge Hearing Research Institute, Dept. of Otolaryngology - Head and Neck Surgery, University of Michigan

The central nucleus of the inferior colliculus (ICC) is the hub of the ascending auditory system and a critical site for sound processing. By using a combination of genetic, anatomical, and physiological methods, we recently identified a novel class of stellate cells that are labeled in Vasoactive Intestinal Peptide (VIP)-IRES-Cre mice. VIP neurons in the ICC have a sustained firing pattern, a moderate input resistance (223.07 ± 141.58 MΩ; mean ± SD) and membrane time constant (13.28 ± 7.31 ms), and only little I_h (sag ratio = 0.85 ± 0.17; n=89). Post-hoc reconstructions showed that VIP neurons are stellate and ~90% have spiny dendrites. Absence of immunostaining by an antibody against the GABA-synthetic enzyme GAD67 suggests that VIP neurons are glutamatergic. Currently, we are using long-range optogenetic circuit mapping to identify the sources and functional

impact of synaptic input to VIP neurons. Based on the distribution of VIP neurons in the ICC, we hypothesize that VIP neurons integrate input from the dorsal cochlear nucleus (DCN) and contralateral ICC. To test this hypothesis, we are using stereotaxically targeted, intracranial injections of a recombinant adeno-associated virus (rAAV.1.Syn.Chronos-GFP.WPRE.bGH) to express the optogenetic protein Chronos in the right DCN or right IC of VIP x Ai14 mice. After allowing 3-4 weeks for Chronos expression, we make in vitro patch clamp recordings from VIP neurons in the left IC while activating Chronos in presynaptic terminals with blue light flashes. Our data show that VIP neurons receive long-range synaptic input from the DCN (n=9). EPSPs evoked by optical stimulation of DCN afferents were excitatory and surprisingly slow (2.39 ± 0.52 mV, halfwidth: 15.8 ± 9.8 ms, risetime: 2.22 ± 0.42 ms, tau: 18.1 ± 6.9 ms). In a few cases, activation of DCN afferents also elicited feed-forward inhibition, which acted to limit EPSP duration. Additionally, we have found that VIP neurons receive input from the contralateral IC (n=6). Commissural inputs could be excitatory (EPSPs: 1.15 ± 0.28 mV, halfwidth: 12.9 ± 7.2 ms, tau: 47.59 ± 54.62 ms, risetime: 4.28 ± 1.18 ms) or inhibitory (IPSPs: -2.61 +/- 0.65 mV, halfwidth: 36.44 ± 11.23 ms, tau: 87.07 ± 64.92 ms, risetime: 7.53 ± 1.16 ms). We are now working to identify whether and how inputs from the DCN and contralateral IC combine to shape the output of VIP neurons. These experiments are a critical step toward defining how ICC neurons integrate diverse streams of inputs.

PS 54

Alignment of Eph-ephrin Guidance Patterns with Modular-Extramodular Framework in the Lateral Cortex of the Inferior Colliculus.

Sean M. Gay; Isabel D. Lamb-Echegaray; Mark L. Gabriele
James Madison University

Background
Eph-ephrin signaling instructs the ordering of patterned inputs in a variety of systems. Previously, we reported graded Eph-ephrin expression along the central nucleus of the inferior colliculus (CNIC) that influences frequency-mapping of its layered afferents. In contrast to gradients and continuous mapping exhibited in the CNIC, recent findings from our lab suggest discrete Eph-ephrin patterns in the neighboring lateral cortex of the inferior colliculus (LCIC). EphA4 and ephrin-B2 expression appears patchy, or modular in the nascent LCIC, while ephrin-B3 is concentrated in surrounding extramodular zones. These seemingly segregated guidance patterns appear strikingly similar to the complementary, modular-extramodular neurochemical framework we recently described in developing mouse. Acetylcholinesterase

(AChE), cytochrome oxidase (CO), glutamic acid decarboxylase (GAD), and nicotinamide adenine dinucleotide phosphate-diaphorase (NADPH-d) are all reliable modular markers, while calretinin (CR) serves as a specific extramodular marker. Multimodal input-output streams appear to exhibit similar patch-matrix-like patterns, and thus likely reflect this LCIC micro-organization. The present study examines the spatial registry of Eph-ephrin patterns with that of neurochemically-defined LCIC modular-extramodular fields. Understanding how guidance cues interface with identified modular-extramodular markers will provide a necessary foundation for elucidating mechanisms that shape early LCIC multisensory circuits.

Methods
A developmental series of early postnatal C57BL/6J and GAD67-GFP mice were utilized. The GAD67-GFP knock-in line specifically labels GABAergic neurons, facilitating easy visualization of LCIC modules. Brains were fixed in 4% paraformaldehyde, cryoprotected, and sectioned on a sliding freezing microtome at 50µm. Peroxidase and fluorescent immunocytochemistry were performed with a variety of antibody combinations (Eph-ephrin primary antibodies, R&D Systems and ThermoFisherScientific; calretinin primary antibody, SWANT; biotinylated secondary antibodies and streptavidin fluorescent conjugates, Vector Laboratories and ThermoFisherScientific). A Nikon C1si TE2000 microscope equipped with appropriate filter sets was used to acquire fluorophores in separate channels, as well as for brightfield imaging.

Results
GAD-positive LCIC modules were apparent at all examined ages. Single Eph-ephrin labeling confirmed previous findings that guidance expression is strong during the early postnatal period, prior to downregulation around hearing onset. Immunocytochemistry in GAD67-GFP tissue shows alignment of Eph-ephrin patterns with the modular-extramodular neurochemical framework. For example, discontinuous EphA4 patchy expression overlaps GAD-positive LCIC modules. EphA4 was confined to modular boundaries and terminal-like in its appearance, forming a network between GABAergic neurons.

Conclusion
The present study provides evidence that Eph-ephrin guidance patterns align with neurochemically-defined modular-extramodular zones. Ongoing studies utilizing Eph-ephrin mutants aim to determine their precise role in guiding LCIC modular-extramodular connectivity patterns.

PS 55

Central Nucleus Projection Patterns to the Lateral Cortex of the Inferior Colliculus Target Calretinin-Positive Extramodular Zones in Developing Mouse.

Isabel D. Lamb-Echegaray[1]; Sean M. Gay[1]; William A. Noftz[2]; Mark L. Gabriele[1]
[1]James Madison University; [2]Kent State University; Northeast Ohio Medical University

Background

The multimodal lateral cortex of the inferior colliculus (LCIC) exhibits a modular-extramodular micro-organization that is evident early in development. In addition to a set of neurochemical markers that reliably highlight layer 2 LCIC modular domains, we recently identified calretinin (CR) as a complementary marker of surrounding extramodular fields. Studies of mature projection patterns in a variety of adult species suggest that major LCIC afferents recognize and adhere to such a framework, terminating in either modular or extramodular distribution patterns. This patch-matrix-like arrangement appears to segregate distinct afferent streams, with somatosensory inputs targeting LCIC modules and auditory inputs surrounding extramodular zones. Currently lacking is a detailed understanding of the development and shaping of multimodal LCIC afferents with respect to its modular-extramodular framework. The present study examines the ontogeny of one auditory input to the LCIC, that arising from the CNIC, and confirms an early projection specificity and preferential targeting of CR-positive extramodular zones.

Methods

Fluorescent tract-tracing in fixed tissue preparations and biocytin labeling in living slices was performed on a developmental series of C57BL/6J mice. Animals were either transcardially perfused with 4% paraformaldehyde, or cold, artificial cerebrospinal fluid (95% O_2/5% CO_2). NeuroVue dyes or biocytin crystals were positioned in the CNIC. Fixed tissue blocks containing NeuroVue dyes were incubated at 37°C for several weeks to facilitate adequate diffusion, while biocytin slices were bubbled in aCSF at room temperature overnight. Tissue was then sectioned on either a vibratome or sliding freezing microtome. After confirmation of CNIC to LCIC projection labeling, immunocytochemistry was performed for CR (SWANT, 1:5000). Fluorescence and brightfield imaging was performed on a Nikon C1si TE2000 microscope.

Results

CNIC tracer placements were verified by the presence of retrogradely-labeled cells in downstream nuclei of the lateral lemniscus, the superior olivary complex, and the cochlear nuclei. CNIC to LCIC projections were bilateral, occupying extramodular domains surrounding LCIC

layer 2 modules. Discrete extramodular patterning became increasing clear over the early postnatal period, and readily apparent by hearing onset. Double-labeling studies confirm axonal distributions within the LCIC align with CR-positive extramodular fields.

Conclusions

The present findings suggest an early specificity of patterned inputs to the LCIC that exhibit discrete modular-extramodular mapping characteristics. Ongoing studies aim to determine the spatial arrangement of multiple LCIC input arrays with respect to each other, as well as how each interface with and are potentially influenced by similarly configured Eph/ephrin guidance patterns.

Auditory Prostheses I

PS 56

The Effect of Phantom Stimulation and Asymmetric Pulse Shapes on the Upper Limit of Temporal Pitch in Cochlear Implant Listeners

Wiebke Lamping[1]; John M. Deeks[2]; Jeremy Marozeau[3]; Sébastien Santurette[4]; Robert P. Carlyon[2]
[1]Hearing Systems group, Department of Electrical Engineering, Technical University of Denmark; [2]MRC Cognition and Brain Sciences Unit, University of Cambridge; [3]Hearing Systems Group, Department of Electrical Engineering, Technical University of Denmark; [4]Hearing Systems, Department of Electrical Engineering, Technical University of Denmark & Department of Otorhinolaryngology, Head and Neck Surgery, and Audiology, Copenhagen University Hospital

Cochlear implants (CIs) can convey pitch along two independent perceptual dimensions, corresponding to the place-of-excitation in the cochlea and the temporal pattern of stimulation. Pitch remains poor for CI recipients: the range of place pitches is limited by the number of implantable electrodes, shallow insertion depths and current spread while temporal pitch deteriorates above an "upper limit" of about 300 pulses per second (pps). Recently, by stimulating an apical electrode pair in bipolar mode using "pseudomonophasic anodic (PSA)" pulses, Macherey et al (2011) could evoke a place-pitch sensation lower than obtained by stimulation of the most apical electrode. Further, a significant increase in the upper limit of temporal pitch was found using these stimuli, consistent with improved temporal processing when information originates from the cochlear apex.

One can also steer the locus of excitation beyond the most apical electrode using so-called phantom stimulation. Here, current is injected through the "primary" member of an apical bipolar electrode pair and a propor-

tion σ is returned by the other, with 1-σ returned via an extra-cochlear electrode. Experiment 1 investigated the effect of phantom stimulation on the perception of place and temporal pitch. For a 20-pps rate, the σ needed to elicit the lowest and highest possible place pitches was determined with the primary electrode being the more apical and more basal member of the pair, respectively. For each of these focusing coefficients, σA and σB, the upper limit of temporal pitch was then measured using the midpoint comparison (MPC) procedure whereby subjects pitch-ranked pulse trains having rates ranging from 142 to 1159 pps. Experiment 2 utilized the MPC procedure to compare the upper limit between PSA and "pseudomonophasic cathodic (PSC)" stimuli, as used by Macherey et al (2011), again using an apical bipolar pair.

Experiment 1 showed that phantom stimulation could elicit place-pitch percepts lower and higher than the most apical electrode in monopolar mode (σ=0). The value of σA was significantly larger than σB, perhaps due to better neural survival at apical cochlear regions. However, no consistent difference in the upper limit was observed. In contrast to Macherey et al (2011), experiment 2 did not reveal differences in the upper limit between PSA and PSC stimuli. In both experiments the upper limit could differ substantially between conditions for individual listeners. A series of experiments investigating possible reasons for these individual differences, particularly with regards to the electrode-neuron interface, will be carried out.

PS 57

The Effect of Polarity Order and Electrode Activation Order on Loudness with Multi-Channel Stimulation

Ann E. Todd; David M. Landsberger
New York University School of Medicine

Background
Electrical current pulses used for cochlear implant stimulation are typically biphasic and symmetrical with each phase having opposite polarity (i.e., an anodic and a cathodic phase) and are presented with a consistent order of the polarity phases across pulses (i.e., pulses are either all anodic first or all cathodic first). Previous research has shown that when polarities alternate across pulses, lower current amplitude is needed to achieve thresholds and in some cases, most comfortable loudness given that pulses occur close enough in time. It has been suggested that this is due to residual neuronal polarization from the second phase of the preceding pulse lowering the current amplitude needed to activate neurons from the first phase of the following pulse. Potentially this mechanism could be used to improve power efficiency of cochlear implants. In the present study, we

examine how alternating polarities across 16 channels affects the current amplitude needed for most comfortable loudness.

Methods
Participants will be 8 adults with Advanced Bionics cochlear implants. Stimuli will be 500-ms pulse trains presented at 900 pulses per second per channel using 16 channels. Pulses will be presented in one of three polarity order conditions: alternating polarities (Alt), constant polarities with anodic phases first (Con-An), and constant polarities with cathodic phases first (Con-Cat). Electrodes will be activated in a consecutive order (i.e., 1, 2, 3,…) or one of three non-consecutive orders (1) 1, 9, 2, 10…, (2) 1, 7, 13, 2, 8, 14…, (3) 1, 5, 9, 13, 2, 6, 10, 14…. Participants will loudness balance the stimuli by adjusting the current amplitude of all channels in dB, with the Con-Cat stimuli in the consecutive electrode activation order at most comfortable loudness as the reference.

Results
Preliminary results with two cochlear implant users indicate that with the consecutive electrode activation order, the current amplitude needed for most comfortable loudness is lower with the Alt polarity order than with the Con-An or Con-Cat polarity orders. Further data will be collected to evaluate whether stimuli in the Alt polarity order require lower current amplitudes for most comfortable loudness than the Con-An or Con-Cat polarity order with the non-consecutive electrode activation orders.

Conclusion
The results support the idea that alternating polarity order across channels may be a way to reduce current amplitudes required for cochlear implant stimulation, which has implications for improved power efficiency of cochlear implants.

PS 58

Focused Thresholds and Psychophysical Tuning Curves Predict Electrode Position in Cochlear Implant Listeners

Lindsay DeVries[1]; Julie G. Arenberg[2]
[1]University of Washington; [2]Department of Speech and Hearing Sciences, University of Washington

Perceptual abilities vary widely among cochlear implant (CI) listeners, likely due to increased channel interaction, which leads to distorted speech signals and may reduce speech understanding. A high degree of chan-

nel interaction may be caused by either poor electrode position and/or reduced neural integrity. While it is not possible to directly measure neural integrity in humans, electrode position can be estimated via CT imaging; however, CT imaging is costly and typically unavailable to clinicians. Alternate methods for assessing electrode position may be obtained using behavioral measures, such as signal detection thresholds and psychophysical tuning curves (PTCs). The purpose of this study was to 1) quantify the relationship between electrode-to-modiolus distance, scalar location, focused detection thresholds, PTC bandwidths, and PTC tip shifts, and 2) determine whether these measures are predictive of clinical outcomes in CI listeners. Thirteen unilaterally implanted adults with the Advanced Bionics HiRes90K device participated. CT scans were obtained and reconstructed in three-dimensions to estimate the distance of each electrode from the modiolus and scalar location. PTCs were collected using a forward-masking paradigm using a focused masker followed by a brief monopolar probe. Degree of channel interaction was quantified using equivalent rectangular bandwidths; the presence of PTC tip shifts was evaluated, as tip shifts are thought to reflect local neural integrity. Detection thresholds were obtained using focused stimulation to better capture local variability between electrodes. PTCs and detection thresholds were obtained for electrodes 215 using a Békésy-like sweep procedure. Word recognition was obtained using consonant-nucleus-consonant (CNC) word scores. Results from a linear mixed effects model show a predictive relationship between electrode-to-modiolus distance, detection thresholds and PTC bandwidths; in other words, electrodes with higher behavioral thresholds and broader PTCs were further from the modiolus. There was no significant relationship between PTC bandwidths and detection thresholds. For electrodes translocated to scala vestibuli, detection thresholds were higher, electrode-to-modiolus distances were greater, and PTC bandwidths were broader. Electrodes with larger electrode-to-modiolus distances were more likely to have tip-shifted PTCs. There was no significant relationship between detection thresholds and the presence of a PTC tip-shift. Higher CNC word scores were observed for listeners with, on average, lower detection thresholds, but not with electrode-to-modiolus distance or PTC ERBs. The long-term goal of this research is to develop a non-radiologic method for estimating electrode position, to individualize device programming by reducing unwanted channel interaction.

PS 59

Pulse train integration in CI-users and effects of high stimulation rates

Miguel Obando[1]; Daniela Schwanda[2]; Werner Hemmert[1]
[1]Technical University of Munich; [2]Hochschule München

The broad spread of the electric fields in the implanted cochlea can greatly increase the effective rate with which individual neurons are stimulated, because every neuron is exposed to the stimulation from several nearby electrode contacts. In order to assess the effects of these increased effective stimulation rates on loudness perception, we conducted a psychophysical experiment to assess the integration of pulse trains as a function of the number of pulses. Particularly, we compared the behavior of normal and very high stimulation rates. Measurements at these high rates are novel, and can shed light on the temporal behavior of the electrically stimulated auditory nerve.

Four subjects (five ears) with Med-El cochlear implants participated in the experiment. We measured threshold levels (THR), maximum comfortable levels (MCL) and a curve of equal loudness (ISO) for biphasic pulse trains. The durations of the trains varied from a single pulse up to 500 ms trains. Stimuli were repeated at a rate of 1 Hz. Subjects freely set the stimulation amplitudes (method of adjustment) for a total of three repetitions per parameter combination. The stimulations occurred at either apical or basal electrodes (E3 and E10, Med-El arrays have 12 electrode contacts), and at pulse rates of either 1200 or 25000 pulses per second (pps). During loudness balancing, subjects compared a reference stimulus with 200 ms duration to test stimuli with different durations at the same electrode and with the same stimulation rate. The amplitude of the reference pulse was fixed at 60% of the dynamic range (DR) between THR and MCL. Reference-test pairs repeated continuously, with 500 ms between reference and test trains, and 1000 ms between pairs.

The pulse-integration curve (THR as a function of the number of pulses in a train) was fitted with a power-law for short durations. This curve decayed more steeply for the 25000 pps than for the 1200 pps stimulation rate before flattening out: the exponents were -0.24 ± 0.03 for 25000 pps and -0.16 ± 0.08 for 1200 pps. This indicates a higher interaction between individual pulses at the higher stimulation rate. The DR was also much higher for the higher stimulation rate. For pulses of 200 ms duration, the DR was on average (12.2 ± 1.1) dB at 1200 pps, and it increased by (8.3 ± 0.9) dB for the 25000 pps stimulation.

PS 60

Effects of electrode position on functional measures of cochlear health in cochlear implant listeners

Kara C. Schvartz-Leyzac[1]; H. Alexander Arts[1]; Timothy A. Holden[2]; Christopher J. Buswinka[1]; Jill B. Firszt[2]; Teresa Zwolan[3]; Aaron P. Hughes[1]; Deborah J. Colesa[1]; Bryan E. Pfingst[1]

[1]Department of Otolaryngology - Head and Neck Surgery, University of Michigan; [2]Department of Otolaryngology - Head and Neck Surgery, Washington University School of Medicine; [3]University of Michigan

Introduction

Studies show that about 50% of the variance observed for specific electrophysiological and psychophysical measures (which we term "functional measures") can be accounted for by variance in spiral ganglion cell density in the implanted guinea pig cochleae. There is evidence that some of these functional measures are predictive of speech recognition. It is hypothesized that functional measures also depend on non-neural factors such as location of the electrodes with respect to the neurons. The purpose of the current study was to determine the extent to which electrode placement affects functional measures of neural health.

Methods

Human participants were adult cochlear implant recipients who had been unilaterally-implanted for at least 6 months. Electrically-evoked compound action potentials (ECAPs) were recorded from each available electrode in each subject using a forward-masking technique for artifact reduction. ECAP amplitude-growth functions (AGFs) were collected using a cathodic-leading biphasic pulse and two interphase-gap (IPG) conditions. The slope change when increasing the IPG (IPG Effect) was calculated. Psychophysical thresholds were measured on each available electrode using a 2-AFC adaptive procedure using two stimulation rates and the multipulse integration (MPI) slope was calculated. Post-operative CT scans were performed using methods detailed in previous studies (Long et al., 2014). Derived measures included estimated electrode distances from (a) the medial wall of the scala and (b) the midmodiolar axis.

Results

In agreement with previous studies, the within-subject, across-site pattern in psychophysical detection thresholds were related to the across-site pattern of estimates of electrode distance from the medial wall of the scala. Psychophysical thresholds showed little or no relationship to estimates of electrode distance from the midmodiolar axis. The within-subject, across-site pattern in slope of the ECAP AGF was related to estimates of electrode distance to the midmodiolar axis, but not the medial wall. Measures of MPI and ECAP IPG Effect were seemingly unrelated to estimated electrode distance from the medial wall or midmodiolar axis.

Conclusions

Previous studies from our lab suggest that two measures in particular, MPI and IPG Effect were strongly related to speech recognition performance in bilaterally-implanted listeners. The current study suggests that neither measure is strongly dependent on electrode location. In contrast, other functional measures found not to be related strongly to speech recognition (e.g., ECAP AGF slope) were more dependent on electrode location. The results also suggest a possible difference in site of excitation for low-level (i.e., threshold) measures versus high-level (.i.e., suprathreshold) measures.

PS 61

Comparing Modulation Detection Thresholds in Children and Adults with Cochlear Implants

Natalia Stupak[1]; Janet Green[2]; Kaitlyn Tona[2]; Susan B. Waltzman[2]; David M. Landsberger[2]

[1]NYU School of Medicine; [2]New York University School of Medicine

Introduction

The auditory experience of post-lingually deafened adult CI users is very different to that of early implanted children. The auditory system of post-lingually deafened adults developed in response to a rich acoustic input but then had to adapt to a CI later in life. Early implanted children, by contrast, have the advantage of adapting to the CI as a young child but have the potential disadvantage of never having developed in response to a rich acoustic input. Therefore, it is likely that the capabilities and limitations of the auditory systems for each of these populations will be different. Landsberger et al. (2017) demonstrated that children with cochlear implants have poorer spectral resolution abilities than post-lingually implanted adults. As spectral resolution is correlated with speech outcomes for post-lingually deafened adults (e.g, Holden et al., 2017; Gifford et al., 2017), no correlations has been found between spectral resolution and speech performance for children (e.g. Gifford et al., 2017). We therefore hypothesize that children may instead be relying on temporal cues. Therefore, further investigation into the differences between the temporal abilities of children and post-lingually deafened adults with CIs is necessary. In this study, we measured temporal modulation thresholds in adult and pediatric populations to determine a) if temporal modulation thresholds improve with age for children with CIs and b) if children perform differently than post-lingually defended adults.

Methods
Prelingually implanted children and post-lingually deafened adult CI users were tested on a 3-interval forced choice adaptive modulation detection task. The target stimuli were amplitude modulated broadband noise at 100 Hz and the reference stimuli were unmodulated broadband noise.

Results and Conclusions
Preliminary data with 10 children (aged between 9 and 16 years) have similar or higher modulation thresholds than the 9 post-lingually tested adult CI users (p=0.0515). No correlation is observed between age and modulation detection for children. However, given that auditory maturation for spectral resolution occurs at approximately 10 years of age (Landsberger et al., 2017), younger subjects need to be recruited to evaluate this relationship. These results suggest that, unlike spectral resolution, temporal abilities of pediatric CI users are similar or better when compared to the adult CI population. These findings are compatible with the idea that implanted children might rely more heavily on temporal information for speech understanding.

PS 62

Spectral-Temporal Modulated Ripple Discrimination by Children with Cochlear Implants

David M. Landsberger[1]; Monica Padilla[2]; Amy Martinez[2]; Camille Dunn[3]; Janet Green[1]; Susan B. Waltzman[1]; Laurie S. Eisenberg[2]
[1]New York University School of Medicine; [2]Keck School of Medicine, USC; [3]University of Iowa

Introduction
A post-lingually implanted adult typically develops hearing with an intact auditory system, followed by periods of deafness and adaptation to the implant. For an early implanted child whose brain is highly plastic, the auditory system matures with consistent input from a cochlear implant. It is likely that the auditory system of early implanted cochlear implant users is fundamentally different (with different limitations and bottlenecks) than post-lingually implanted adults. The purpose of this study is to compare the basic psychophysical capabilities and limitations of these two populations on a spectral resolution task to determine potential effects of early deprivation and plasticity.

Methods
Performance on a spectral resolution task (SMRT) was measured for twenty implanted children (aged between 5 and 13 years) and twenty hearing children within the same age range. Additionally, 15 post-lingually deafened cochlear implanted adults and 10 hearing adults were tested. Hearing listeners (adult and children) were tested with the unprocessed SMRT and a vocoded version. In a follow up pilot experiment, implanted children with ipsilateral or contralateral hearing are being tested with their CI alone to determine the effect of acoustic input on electric only spectral resolution.

Results
A positive correlation was found between age and both unprocessed and vocoded SMRT for normal hearing children. Older hearing children performed similarly to hearing adults in both the unprocessed and vocoded test conditions. However, for children with CIs, no relationship was found between SMRT and chronological age, age at implantation, or years of implant experience. Pediatric CI performance was poorer than adult CI performance. Pilot data with children with a CI and residual hearing suggests that having residual hearing may yield better electric only spectral resolution outcomes than for children without residual hearing.

Conclusions
Results suggest that basic psychophysical capabilities of early implanted children and post-lingually implanted adults differ when assessed through their implant processors. Because spectral resolution does not improve with age for early implanted CI users, it seems likely that the sparse representation of the signal provided by a CI limits spectral resolution development. These results are consistent with the finding that post-lingually implanted adults, who developed their auditory system from normal auditory inputs but now receive the same sparse signal as the implanted children, perform significantly better than children on the spectral resolution test.

PS 63

Temporal modulation sensitivity in cochlear implant users: effects of stimulation mode, carrier rate, and cochlear place

Shaikat Hossain; Susan Bissmeyer; Raymond L. Goldsworthy
University of Southern California

Previous research has found that using temporal modulation sensitivity to select channels in clinical cochlear

implant (CI) programming can improve speech reception performance (Garadat et al., 2013). The present study examines factors that may affect temporal modulation sensitivity in CI users. We hypothesized that modulation sensitivity will be greater in monopolar stimulation mode compared to bipolar stimulation mode due to a greater population of neurons encoding modulations, a trend previously observed by Middlebrooks (2008) in a study on guinea pigs. We also hypothesized that sensitivity would be better at lower carrier rates due to the greater size of pulse-to-pulse current steps. Lastly, we predicted a basal advantage to modulation sensitivity based on previous data collected in our lab on spatial forward masking (FM) and multi-pulse integration (MPI) (Bissmeyer et al., 2017). One possible mechanism for this basal advantage might be a resynchronization of ascending inputs to the cochlear nucleus to correct for cochlear traveling wave dispersion. Since such traveling wave dispersion is absent in CI users, this reduction in synchrony may be detrimental to temporal sensitivity.

Modulation sensitivity thresholds were measured in adult patients implanted with Cochlear Nucleus cochlear implant devices. The USC Cochlear Implant Research Interface (CIRI) was used to provide direct electrical stimulation. Threshold and comfort current levels were determined by adjusting the phase duration of 10 Hz amplitude modulated pulse trains of 400 ms duration with rates of either 400 or 800 pps. After mapping the participants, modulation detection thresholds were measured on a basal and apical electrode in in pseudomonopolar and bipolar stimulation modes using 2 carrier frequencies (400 and 800 pulses per second) and 3 modulation frequencies (10, 100, 200 Hz). In addition to the direct stimulation testing, participants also completed the modulation sensitivity testing using their clinical processors with acoustic stimuli to assess how effectively modulations are encoded in current devices. An analysis of variance statistical analysis of the collected data will be performed to analyze the effects of the different factors. In addition, the modulation sensitivity data will be correlated with previously collected measures of neural health (FM and MPI). Outcomes will have implications for the development of next generation CI devices which are more robust in the presence of background noise.

S.N. Garadat, T.A. Zwolan, B.E. Pfingst. (2013). Using temporal modulation sensitivity to select stimulation sites for processor maps in cochlear implant listeners. Audiol. Neurotol., 18, pp. 247-260

J.C. Middlebrooks. (2008). Cochlear-implant high pulse rate and narrow electrode configuration impair transmission of temporal information to the auditory cortex. J. Neurophysiol. 100, 92–107.

S. Bissmeyer, S. Hossain, and R. Goldsworthy. "Factors Affecting Rate Sensitivity in Cochlear Implant Users". Presented at the 2017 Conference on Implantable Auditory Prostheses.

PS 64

Ipsilateral and Contralateral Modulation Masking/Modulation Interference with Speech Temporal Envelopes With Direct Electrical Stimulation

Monita Chatterjee; Aditya Kulkarni
Auditory Prostheses & Perception Lab, Center for Hearing Research, Boys Town National Research Hospital, Omaha, NE

It is known that cochlear implant (CI) users experience modulation masking and modulation interference (MDI). The objective of the present study is to investigate these effects under conditions in which the target to be detected is either a single- or multi-channel signal with a speech temporal envelope. The interferer was modulated by either speech or noise, was single or multi-channel, and presented in the same ear or the contralateral ear.

Here, we present preliminary results (proof of concept) in one adult, post-lingually deaf CI user. Stimuli were 600-ms long, 900-Hz pulse trains with different temporal envelopes. Masker and target pulse trains were presented concurrently (interleaved when in the same ear, simultaneous when in opposite ears). The target carrier pulse train was amplitude-modulated by a temporal envelope derived from a 600-ms long segment of speech. Loudness-balanced, unmodulated versions (SS) were also created. The task was to detect the speech envelope in the target in a three-interval, three-alternative, forced choice paradigm, in which two of the intervals contained the SS stimuli, and a third (random) interval contained the speech-modulated target. The masker was otherwise identical to the target, but was modulated by 1) the same speech envelope or 2) noise or 3) unmodulated with amplitude fixed at the peak of the modulated versions (SSP). The masker was present in all three intervals. Each condition was repeated multiple times, and percent correct scores were obtained in each case. In one condition, the target consisted of 6-channel speech (based on the word "frog"), using a CIS-processor and the patient';s everyday frequency-to-electrode allocation table. An unmodulated version of the 6-channel target was also created. The masker was a concurrent 6-channel pulse train, modulated by noise or SSP. Masker and target were presented to the same ear. The task was again to detect the target envelope in a 3I, 3AFC procedure.

Results showed poorer performance with the speech- or noise-modulated maskers than with the SSP maskers in all conditions, indicating MDI. These results provide proof of concept that MDI occurs in CI users when the target is a speech signal and the masker is either speech or noise, presented either in the same ear or in the contralateral ear. [This work was funded by the American Hearing Research Foundation]

What Is the Sensitive Period to Initiate Auditory Stimulation for the Second Ear in Sequential Cochlear Implantation?

Byung Chul Kang; Jun Woo Park; Hong Ju Park
Asan Medical Center

Objectives
Bilateral cochlear implants is the standard treatment for bilaterally deaf children, but it is unclear how late the second CI (CI-2) in the second ear can be delayed in sequential bilateral CI. We investigated the performances of sequential CI to answer this question.

Study Design
Retrospective case series review.

Setting
Tertiary referral center.

Methods
We studied a cohort of congenitally deaf children (n = 73) who underwent sequential CI without any inner ear anomaly or combined disabilities. Hearing threshold levels and speech perception was evaluated by aided pure tone audiometry and an open-set monosyllabic word recognition test. The scores were analyzed by the ages at surgery and compared among the different age groups.

Results
When the CI-2 was performed before 3.5 years (the optimal period for CI-1), CI-2 scores (96.9%) were comparable to CI-1 scores. Although CI-1 scores were ≥80% when CI-1 was implanted before the age of 7 years, CI-2 scores were ≥80% when CI-2 was implanted before the age of 13 years. The hearing threshold levels were not different regardless of the ages and sides.

Conclusion
Our cohort demonstrated that CI-2 showed comparable results to CI-1 when implanted before 3.5 years, suggesting optimal periods for CI-1 and CI-2 are same. However, the sensitive period (13 years) for CI-2, resulting in relatively good results and decline thereafter, was much longer than that (7 years) of CI-1, suggesting that CI-1 prolongs the sensitive period for CI-2 and CI-2 should be implanted early, but considered even at a later age.

Attentional Modulation of Event Related Potentials as a Measure of Stream Segregation for Cochlear Implant Listeners

Andreu Paredes-Gallardo[1]; Hamish Innes-Brown[2]; Sara M. K. Madsen[1]; Torsten Dau[3]; Jeremy Marozeau[1]
[1]Hearing Systems Group, Department of Electrical Engineering, Technical University of Denmark; [2]Bionics Institute; [3]Hearing Systems group, Technical University of Denmark

Cochlear implants (CI) significantly improve the ability to understand speech in quiet. However, listening to music or a single voice in a crowded room is still challenging. To succeed in such scenarios, the listener needs to be able to segregate competing streams and selectively attend to the target. Selective attention is known to modulate auditory-evoked event related potentials (ERPs) in normal-hearing (NH) listeners, and recent studies have used this modulation to objectively estimate which stream the listeners are attending to. The present study combined a behavioral task with ERP recordings to determine whether the attentional modulation of ERPs can be used as an objective measure of stream segregation for CI listeners. Nine CI listeners participated in a melodic contour identification task, where they were asked to focus on and attend to a pattern of bursts of pulses presented on electrodes 9, 11 and 13. This pattern was repeated three times in the presence of interleaved distractor sounds. A deviant was randomly introduced in 75% of the trials by reversing the target pattern in any of the three repetitions, resulting in four different melodic contours which the listeners were asked to identify. In the behavioral task, the electrode range for the distractor sounds was varied, resulting in different amounts of overlap between target and distractor. We hypothesized that if listeners used place cues to segregate the target stream, performance would improve as the electrode separation between the target and the distractor increases. The results supported this hypothesis, suggesting that larger electrode differences facilitate the segregation process. In a second experiment, the same stimuli were presented to the listeners and ERPs were recorded under active and passive listening conditions. The listeners were asked to perform the behavioral task for the active listening condition and encouraged to watch a muted movie for the passive listening condition. It was hypothesized that if the listeners would segregate the streams, the ERPs to the target stream would be enhanced in the active condition relative to the passive

recording, as reported in earlier studies with NH listeners. An analysis of the ERP waveforms supported this hypothesis. Overall, the results from this study suggest that CI listeners are able to use place cues to segregate and to attend to a sound sequence in the presence of interleaved distractor sounds. Moreover, the segregation of a simple sound sequence could be assessed through the attentional modulation of the ERP responses.

PS 67

Initial findings on the influence of onset cues on auditory object formation and sound lateralization in bilateral cochlear implant listeners

Tanvi Thakkar; Alan Kan; Ruth Y. Litovsky
University of Wisconsin-Madison

Sensitivity to interaural time differences (ITDs) in bilateral cochlear implants (BiCI) listeners is poorer than in normal hearing (NH) listeners, due to a combination of patient and device limitations. In NH listeners, ITDs are robust in quiet, but imprecise in reverberant and noisy environments, rendering poor lateralization and auditory object formation (AOF) abilities. Further, in noisy environments, onset ITDs can dominate, driving responses to the correct location. Similarly, BiCI listeners experience dominance from onset ITDs but noisy, multi-source environments are even more detrimental to their binaural hearing abilities, in comparison to their NH counterparts. Previous work in our lab, using research processors to deliver electrical pulse trains, showed that periodic and consistent ITDs lead to good lateralization and AOF. However, when ITDs dynamically change, listeners report a single auditory object but are unable to lateralize the sound. This is inconsistent with what is seen in NH listeners when presented with the same stimulus, because they do not perceive the sound as a single auditory object nor can they use ITDs to perceptually lateralize the sound. The present study aimed to bridge the gap in knowledge using stimuli that change from consistent periodic ITDs to dynamically-changing ITDs. The goal was to construct stimuli that increase the salience of the ITD, such that BiCI listeners correctly lateralize the sound, and perceive a single auditory object. We investigated whether an increased number of repetitions of consistent onset pulses would improve lateralization while maintaining AOF.

Stimuli were pulsatile trains of biphasic pulses, presented to a bilateral pair of pitch-matched electrodes (100 pulses-per-second, 300-millisecond duration). We systematically manipulated the number of pulses starting from the onset that carried the same ITD, while the remaining pulses had a different ITD. The consistent ITDs were either 0, -500 µs or +500 µs. Using a single interval, six-alternative forced-choice

task, listeners reported where the sound was heard, and how many (one vs. two) sounds were heard. Results suggest that BiCI listeners were more accurate in reporting the lateral position of the sound with increasing number of consistent onset pulses. Similar to previous work, listeners also reported hearing only "one sound," regardless of the number of pulses with a different ITD. This suggests that BiCI listeners may benefit from a strategy where a few samples of a repeated onset ITD might result in improved lateralization.

PS 68

Across-frequency interaural-level-difference processing in bilateral cochlear-implant users

Olga Stakhovskaya; Matthew Goupell
University of Maryland, College Park

Introduction
Bilateral cochlear-implant (BiCI) listeners use interaural level differences (ILDs) as their primary cue for sound localization. Unlike interaural time differences, ILDs are highly frequency-dependent, near negligible below 500 Hz and about 25 dB at 8000 Hz. This frequency-dependence of naturally occurring ILDs suggests that different electrodes might have different weights in the final determination of the sound location in BiCI listeners. Additional across-frequency inconsistencies in ILDs may be introduced by the differences in loudness growth. This study investigates how multi-electrode ILD lateralization is affected by differences in perceptual loudness growth functions or electrically evoked compound action potentials (ECAP) amplitude growth functions.

Methods
Seven BiCI listeners with Cochlear-brand devices were tested in an ILD lateralization experiment using direct stimulation. Stimuli were 1000-pulses/second, 300-ms, constant-amplitude pulse trains. Thresholds, most-, and maximum-comfortable levels were obtained for five electrode pairs (electrodes 4, 8, 12, 16, and 20). Stimuli were presented at 70-80% of the dynamic range. Frequency-dependent ILDs were derived from behind-the-ear (BTE) microphone head related transfer functions (HRTFs) using the bandwidths from a standard frequency-to-electrode allocation table for sources at 0, ±30, ±45, ±60, ±80, ±90°. The stimuli were presented using combinations of one to five electrode pairs. The listeners reported the intracranial image lateralization. Single-electrode loudness growth functions and ECAP amplitude growth functions were measured in separate tasks.

Results
An analysis of HRTFs showed that ILDs from BTE-level microphones are smaller than natural ILDs in nor-

mal-hearing listeners, and thus reduced the perceived ILD lateralization range. Relatively large ILDs in high-frequency channels produced larger lateralization ranges. Lateralization ranges obtained with multi-electrode stimulation were like the lateralization ranges obtained on just the high-frequency channels, suggesting that the high-frequency channels dominated the multi-electrode response. The relationship between the lateralization, perceptual loudness growth, and ECAP amplitude growth functions will be investigated by assessing the interaural difference in the functions for individual electrodes.

Discussion
Naturally occurring frequency-specific ILDs from BTE microphones produce lateralization percepts in BICI listeners that vary across electrode pairs and that different weighting for high-frequency channels should be incorporated in binaural models that predict across-channel ILD processing in BICI listeners. Moreover, differences in loudness growth functions on individual electrodes within the ear and their asymmetry across the ears may also contribute to the inconsistencies in ILDs processing in BiCI listeners. These interaural inconsistencies, particularly at the high-frequency channels, may explain the diminished sound localization capabilities in BiCI listeners compared to normal-hearing listeners.

PS 69

Cortical Auditory Network Connectivity in Bilateral Cochlear Implant Users

Daniel Smieja[1]; Benjamin Dunkley[1]; Blake Papsin[2]; Karen Gordon[2]
[1]The Hospital for Sick Children; [2]The University of Toronto; The Hospital for Sick Children

Objectives
The present research investigates the cortical auditory network in children with bilateral deafness who received bilateral cochlear implants simultaneously, by characterizing functional connectivity between active neural sources.

Background and Rationale
We are asking: Are long-range functional connections within the auditory network compromised in children using bilateral implants compared to their normal hearing counterparts?

Recent animal studies suggest that local functional connections remain strong in auditory areas despite deafness, however long-range connections are reduced. We have found that expected cortical synchrony is promoted in temporal areas in children receiving bilateral cochlear implants but it is not clear whether these areas maintain long-range connectivity with cortical areas known to be important for spatial hearing and attention to sound. In the present study, we aimed to develop a technique to identify cortical areas and determine long-range connectivity involved in this network from EEG responses in children with normal hearing and using bilateral cochlear implants.

Methods
Precise time resolution, required for functional connectivity was provided by 64-channel electroencephalography (EEG). Responses were recorded from children who use bilateral cochlear implants and an age-matched control group evoked by electrical pulse-train stimuli and broadband click stimuli, respectively.

The phase-locking value (PLV) was calculated between non-adjacent scalp electrodes as an initial measure of the underlying connectivity. Surface potential data were compared with the PLVs and imaginary coherence of reconstructed cortical source responses. These "virtual" responses were obtained by spatial filtering, using the *time restriction and artifact and coherent source suppression* (TRACS) beamformer. This technique removes the CI artifact by adding a constraint that minimizes components of the artifact lead field. By interpolating the result onto a structurally labelled anatomical atlas, sources were mapped directly to their anatomical correlates. Connectivity was assessed across all pairs of anatomical sources as a function of frequency.

Results
Preliminary source data revealed the underlying sources and connections that give rise to synchrony in the surface data. The source reconstruction mitigated volume conduction effects and allowed identification of the regions-of-interest based on their signal-to-noise ratios. Assessment of the timing and strength of functional connectivity as a function of frequency is ongoing in several higher order areas within the prefrontal cortex and precuneus region.

Significance
Source reconstruction from EEG measures can add important spatial information to functional connectivity analyses to better understand the unique hearing network in children using bilateral cochlear implants.

PS 70

Sound Coding Strategy for Cochlear Implants Inspired by Speech Statistics

Tarik Siebe[1]; **Jacques A. Grange**[2]; Tim Juergens[1]; John F. Culling[2]
[1]*Oldenburg University;* [2]*Cardiff University*

Typically, cochlear implant processors first analyse sound through a bank of evenly spaced filters on a log-frequency scale, before each extracted temporal envelope is used to modulate the excitatory current passed through each implanted electrode. However, factor analysis (FA) of speech shows that the information carried by the temporal modulations of speech is distributed in bands whose width grows non-monotically with frequency on a logarithmic scale. Given that the spread of excitation (SOE) along the spiral ganglion limits the number of independent channels in CI users to eight or less, optimizing transmission of information within those eight channels must be considered in the design of sound coding strategies. A scree plot derived from factor analysis shows that six channels should suffice to transmit most of the speech information. This outcome may explain why speech-reception thresholds (SRTs) using a cochlear implant simulation improve markedly more slowly as a function of number of channels beyond 7 simulated channels. The present study tests whether FA-inspired channel bandwidths might improve speech intelligibility. Simulations with normal-hearing listeners employed a pulsatile vocoder (Oldenburg) and adaptively measured SRTs for the following factors: two levels of SOE (200 dB/oct and 8 dB/oct) x two numbers of channels (8 or 11) x three channel definition/allocation strategies. The first strategy (CIS) used evenly-spaced channels and simulated electrodes aligned with the channel center frequencies. The second and third strategies used FA-selected channels, with simulated electrodes selected from a fixed 22-electrode array; in the second (FA$_w$), selected electrodes were evenly spaced, thereby limiting channel interaction, but leading to spectral warping; in the third (FA$_u$), the selected electrodes were those with a place frequency closest to each of the channel center frequencies, leading to an almost unwarped electrode map. Simulating SOE significantly elevated thresholds and caused extra channels (from 8 to 11) to be detrimental to SRTs. Although no effect of strategy was found, spectral warping would be expected to elevate SRTs. However, with 8 channels and SOE typical of CI users, the CIS and FA$_w$ strategies led to the two lowest thresholds. A perceptual learning experiment would help elucidate whether a FA-inspired strategy requires more listener adaptation to reveal its full potential over time in CI users.

PS 71

Optimizing a Machine Learning Algorithm to Mitigate Reverberation in Cochlear Implant Users

Boyla O. Mainsah; Kedar S. Prabhudesai; Leslie M. Collins; Chandra S. Throckmorton
Duke University

Background

peech recognition degrades significantly in cochlear implant (CI) users under reverberant conditions. Reverberant effects can be categorized into two types, as illustrated in Figure 1: self-masking, which represents early signal reflections that interfere with active speech, and overlap-masking, which represents late reflections that occur between active speech segments. Desmond (Ph.D. dissertation, Duke University, 2014) proposed a reverberation mitigation strategy based on using channel-specific classifiers to discriminate between self- and overlap-masking patterns in CI pulse segments, with deletion of overlap-masking segments when detected. Detection is achieved by scoring pulse-based features and comparing the score to a threshold value, termed a classifier operating point, to categorize features. Classifier operating points associated with the same probability of detection (PD) of overlap-masking segments were used across channels. However, operating at the same PD across channels might not necessarily be optimal as the information provided by each channel may vary in importance for speech intelligibility. In this study, we investigate the utility of optimizing channel-specific operating points in the reverberation mitigation algorithm.

Methods

Channel-specific classifiers were trained on pulse-based features generated post CI-processing of speech signals under simulated room reverberation (Lehmann and Johansson, JASA 2008(124):269-277), with varying room parameters and reverberation times. Studies suggest that speech intelligibility is robust to some amount of channel information loss, especially if lost segments are of short duration and distributed uniformly (Kressner et al., JASA 2016(139):800-810). Channel-specific PDs were independently optimized by selecting the largest PD value that resulted in less than 15% loss of self-masking segments in a channel upon algorithm implementation, with and without knowledge of the test reverberant signals. Channel loss tolerance level was subjectively chosen based on empirical analysis from a previous study (Mainsah et al., CIAP 2017). Vocoded speech signals with simulated room reverberation were used to evaluate the reverberation mitigation algorithm with varying degrees of channel-specific parameter optimization.

Results

Figure 2 shows preliminary speech recognition results in normal-hearing (NH) listeners. Results indicate that the various implementations of the reverberation mitigation algorithm statistically significantly improved speech intelligibility from the unmitigated condition, with channel-specific parameter optimization providing additional benefits when compared to a non-optimized algorithm.

Conclusions

Preliminary results in NH listeners demonstrate that channel-specific parameter optimization has the potential to enhance the performance of a reverberation mitigation algorithm that identifies and deletes non-informative speech segments from CI pulse trains. This reverberation mitigation strategy will be tested in CI users. Funded by NIH grant R01-DC014290-02.

mainsahARO2017-Fig1.pdf

mainsahARO2017-Fig2.pdf

PS 72

Phonetic Cue Weighting in Children and Adults with Cochlear Implants

Mishaela DiNino; Matthew B. Winn; Annie Duchen; Julie G. Arenberg
Department of Speech and Hearing Sciences, University of Washington

Phonetic cue weighting assesses the weight an individual places on a cue when categorizing speech sounds. Such a test can be used to measure one';s reliance on the various frequency and temporal components of an auditory signal. In this study, a continuum of speech sounds was used, which ranged from /ba/ to /da/ based on a fine-resolution cue, formant transitions, and a coarse-resolution cue, spectral tilt. Higher reliance on the formant cue compared to the spectral tilt cue indicates likelihood of better spectral resolving capabilities. In prior studies, normal hearing (NH) adults relied almost exclusively on the formant cue, but CI listeners, who have poor spectral resolution, relied more on the spectral tilt cue to categorize the sounds. The aim of the current study was to determine whether prelingually-deafened, early-implanted children with CIs and children with NH showed a similar cue-weighting pattern as that found in adults tested in previous experiments.

Participants in this study were 34 NH children, 12 prelingually-deafened, early-implanted children with CIs, and 10 postlingually-deafened adults implanted later in life. All participants performed the speech categorization test as well as a standardized measure of spectral ripple discrimination.

Comparison of group results showed that, compared to adults with CIs, NH children relied much more on the formant cue and less on the spectral tilt cue, similar to results of previous studies in adults. On average, children with CIs demonstrated less efficient use of both cues compared to both NH children and adults with CIs. Analysis of individual CI user results revealed greater variability among children than among adults. Notably, some pediatric CI users were able to rely on the formant cue as highly as NH children did. These results indicate that prelingually-deafened, early-implanted children may differ from postlingually-deafened, later implanted adults in their integration of acoustic cues for speech sounds. We offer further analysis of sequentially implanted children for whom cue weighting strategies were not the same in each ear, suggesting that peripheral factors affect cue weighting of CI users. Additionally, formant cue coefficients were positively related to spectral ripple discrimination thresholds of CI listeners, suggesting that both measures might tap into common auditory processing mechanisms. Future directions include examinations of variables that could contribute to cue-weighting strategies of children and adults with CIs.

PS 73

Effect of a Channel-Selection Strategy based on Polarity Sensitivity on Speech Perception by Cochlear Implant Users

Tobias Goehring[1]; Julie G. Arenberg[2]; John M. Deeks[1]; Robert P. Carlyon[1]
[1]MRC Cognition and Brain Sciences Unit, University of Cambridge; [2]Department of Speech and Hearing Sciences, University of Washington

Cochlear implants (CIs) allow many users to understand speech well in quiet acoustic situations. However, there is still a large variability in the performance between users and even the most successful struggle to understand speech in background noise. Two reasons for this variable outcome are the user-specific pattern of neural survival and the broad spread of neural activation along the auditory nerve.

Results from studies using acutely deafened animals indicated a higher sensitivity to cathodic than to anodic current. In contrast, human CI users are usually more sensitive to anodic than to cathodic stimulation. Our hypothesis is that this difference may result from a greater survival of the auditory nerve';s peripheral processes in animals, which are responsible for the higher sensitivity to cathodic stimuli, but which may have degenerated in human CI users that have been deaf for longer periods. Thus the effect of stimulus polarity on thresholds, the polarity effect (PE), may serve as an estimate of the local neural survival at each electrode position.

In this study, we measured behavioural detection thresholds in 8 users of Advanced Bionics devices for 80-pps, tri-phasic, monopolar pulse trains in which the central high-amplitude phase was either anodic or cathodic. The cathodic-anodic electrode difference defined the PE for each electrode. Detection thresholds were measured using an adaptive tracking procedure similar to Békésy tracking. The pattern of PEs across electrodes were then used to identify the electrodes with the best and worst hypothesised local neural survival for each subject. Two experimental maps were generated for each subject by deactivating the five electrodes with either the highest or the lowest magnitudes of the PE. The subjects'; performance with the two experimental maps was evaluated using spectro-temporal tests, that have been proposed as predictors for speech perception (SMRT, Aronoff and Landsberger, 2013; STRIPES, Archer-Boyd et al., 2017) and subjective measures of speech understanding in quiet (percentage correct) and in background noise (speech-reception-threshold, SRT).

Results revealed that the PE varied substantially across electrodes, with magnitudes from -2 to +2 dB and approaching the electrical dynamic range of some users. PE measures showed an individual pattern for each subject that was distinct to their impedance profile and clinical map. The evaluation tests are currently underway and the presented results will indicate whether channel selection based on the PE is an effective method for improving speech perception by CI users.

PS 74

Effects of Auditory Degradation on Verbal Short-Term Memory

Mary C. Luckasen; Adam K. Bosen
Boys Town National Research Hospital

Immediate serial recall is frequently used to measure short-term memory capacity in listeners with normal hearing and listeners with cochlear implants, but the interaction between auditory degradation and test material in short-term memory remain uncharacterized. When speech sounds can be unambiguously mapped to a known word then they can be readily stored in memory as a whole word, but when possible mappings are ambiguous due to auditory degradation, additional processing is required. This additional processing should impair memory capacity only when the speech sounds are indistinct. Confusability between words is dependent on lexical neighborhood density, so if the set of possible words to be recalled is small, because the lexical neighborhood density of possible responses is low, there should be low confusability, even with degraded auditory input. As the word set size increases, confusion rates should increase, especially with degraded speech cues.

Therefore, we hypothesize that auditory degradation should differentially impact short-term memory depending on the stimuli to be recalled. To test this hypothesis, we measured normal hearing adults'; immediate serial recall of spoken lists of digits, Consonant-Vowel-Consonant (CVC) words, and CVC non-words which were either unprocessed or vocoded. Preliminary results indicate that memory capacity for digits, words, and non-words decreases in that order, and that capacity for non-words is more heavily impacted by vocoding than capacity for words. These results indicate that reductions in memory capacity in listeners with cochlear implants may not generalize across conditions, but rather should be considered with respect to the stimuli used to test capacity.

PS 75

Modeling Verbal Short-Term Memory Deficits Caused by Auditory Degradation

Adam K. Bosen; Mary C. Luckasen
Boys Town National Research Hospital

Connectionist models of verbal short-term memory have been previously demonstrated to reproduce several phenomena that have been observed in listeners with normal hearing, but have not yet been used to predict the impact of auditory degradation on short-term memory. The goal of this project was to usea connectionist model to simulate the impact of acute and chronic auditory degradation on verbal short-term memory. Model predictions were compared to experimental results, to determine the utility of this model in predicting the effects of hearing loss on memory. The model was trained and tested on an immediate serial recall task both with and without simulated auditory degradation. Auditory degradation was simulated by swapping phoneme features, such as place and manner, at a rate that matches information transmission rates for those features in listeners with cochlear implants. Training and testing the model with these degradations was expected to produce deficits in immediate serial recall beyond those observed in a model that was trained without degradation, but tested with degradation. This comparison was intended to mimic the relationship between pre-lingually deafened listeners with cochlear implants and listeners with normal hearing who hear vocoded speech, to demonstrate whether experimental differences across these groups can be explained by development (simulated by model training) with degraded auditory input. Additional predictions about the impact of auditory degradation on short-term memory were made, which can be used to guide future experimentation.

PS 76

Assessing cognitive measures in high performing cochlear implant users.

Alexandra Parbery-Clark[1]; Elizabeth Elkins[1]; Jake Hillyer[2]; Cody Buchanan[3]; Soo Jang[1]; Stacey Watson[1]; Chantel Hazlewood[4]; Julie G. Arenberg[5]; Douglas Backous[6]

[1]*Swedish Neuroscience Institute;* [2]*Oregon Health & Science University;* [3]*St. John Clinic;* [4]*Swedish Medical Center;* [5]*University of Washington;* [6]*Proliance Surgeons*

Introduction

Despite being considered one of the most successful neural prostheses, cochlear implant (CI) recipients reveal a wide range of speech understanding abilities. While some CI users are able to understand speech even in the absence of visual cues, other recipients exhibit more limited speech comprehension. Although cognitive skills have been documented as a fundamental contributor to complex auditory processing such as language understanding, these skills have received little attention in CI users. Currently, no standardized clinical tests exist for determining the cognitive ability of adult CI users. Here, we evaluate the feasibility of assessing cognitive skills in high-performing CI recipients using the visual rather than the auditory-visual modality to avoid using the deficient auditory modality for CI users.

Methods

19 adult cochlear implant users (3 CI only, 11 bimodal and 5 bilateral; all post-lingual hearing loss) with clinical speech understanding scores in quiet of > 60% on AzBio sentences (in first ear if implanted bilaterally) were recruited. All participants demonstrated normal nonverbal IQ (mean = 106, SD = 5.99, range: 99-118). A cognitive test battery assessing auditory and visual working memory, processing speed and cognitive efficiency were administered in addition to clinical measures of speech understanding (i.e., AzBio and Consonant-Nucleus-Consonant CNC test).

Results

High-functioning CI users demonstrated significantly greater visual working memory than auditory-visual working memory. Visual and auditory-visual working memory measures were not related. Visual working memory significantly related to clinical measures of speech understanding as measured by AzBio in quiet, unlike auditory-visual working memory. Processing speed, cognitive efficiency, and IQ did not relate to any measures of speech perception.

Conclusions

In high-performing cochlear implant users, assessing visual working memory is more predictive of speech understanding ability than auditory-visual working memory. In this population, measures of cognitive efficiency and processing speed did not relate with cochlear implant speech understanding.

PS 77

Across- and Within-Gender Talker Identification in Cochlear Implant Listeners

Sara I. Duran; Zachary M. Smith
Denver Research & Technology Labs, Cochlear Ltd.

In order for listeners to follow a conversation in a complex multi-talker environment, they should correctly identify what is said as well as who said which parts. Associating an utterance with a specific talker provides context that helps the listeners'; interpretation. Correctly identifying each talker may also aid listeners in forming discrete auditory objects that are easier to track, thereby reducing the amount of effort required to follow the conversation. Despite this potential impact on functional listening, the ability of cochlear implant listeners to identify talkers has not been extensively studied. The available data suggest that performance on talker identification tasks is highly variable for cochlear implant recipients, and it has been hypothesized this variability may be related to spectral resolution. In this study, we provide additional insight into the within- and across-gender talker identification abilities of cochlear implant listeners and investigate their relationship to spectral resolution.

Experiments were conducted in Nucleus recipients using their clinical maps and stimuli presented in the free field. Talker identification was measured using IEEE sentences presented in quiet. Four different multi-talker conditions were tested: 1 male, 1 female; 2 male, 2 female; 3 male; and 3 female. Subjects were presented with one target sentence followed by multiple reference sentences with different linguistic content. Each of the reference sentences was spoken by a different talker, one of whom was also the target talker. Subjects were instructed to identify the reference talker who uttered the test sentence. Spectral resolution was measured using an adaptive spectral ripple phase detection task. Preliminary results from this ongoing study suggest that listeners with better spectral resolution also perform better on the talker identification task.

PS 78

Voice Emotion Recognition to Child-directed and Adult-Directed Speech in Pediatric Cochlear Implant Users

Karen Chan. Barrett[1]; Meredith Caldwell[2]; Patpong Jiradejvong[1]; Aditya Kulkarni[3]; Monita Chatterjee[3]; Charles Limb[4]

[1]*Sound & Music Perception Lab, Department of Otolaryngology- Head & Neck Surgery, University of California - San Francisco, San Francisco, CA;* [2]*Johns Hopkins University School of Nursing;* [3]*Auditory Prostheses & Perception Lab, Center for Hearing Research, Boys Town National Research Hospital, Omaha, NE;* [4]*Sound & Music Perception Lab, Department of Otolaryngology-Head & Neck Surgery, University of California - San Francisco, San Francisco, CA*

Cochlear implants (CIs) are remarkable in allowing individuals with severe-to-profound hearing loss to perceive speech. Despite these gains in speech understanding, however, CI users often struggle to perceive elements such as vocal emotion and prosody, as CIs are unable to transmit the spectro-temporal detail needed by the listener to decode the voice pitch changes that are a critical component of these cues. Research has found that voice emotion production is poorer in child cochlear implant users compared to their normal-hearing (NH) peers (Nakata et al., 2012). Regarding voice emotion perception, pediatric CI users show a range of performance in voice emotion recognition when listening to child-directed human speech where the prosody is greatly exaggerated (Chatterjee et al., 2015), with mean performance falling significantly below that of NH listeners. In the present study, voice emotion recognition was measured using both child-directed (CDS) and adult-directed (ADS) speech conditions, in pediatric cochlear implant users aged 7-19 years. It was predicted that the reduced prosodic variations found in the ADS condition would result in lower vocal emotion recognition scores compared to the CDS condition, which featured greater prosodic changes.

Pediatric CI users with no cognitive or visual impairments and who communicated through oral communication with English as the primary language participated in the experiment (n= 27). Stimuli comprised twelve sentences selected from the HINT database. The sentences were spoken by male and female talkers in a child-directed or adult-directed manner, in each of the five emotions (i.e., 60 sentences per talker). The chosen sentences were semantically emotion-neutral. Percent correct emotion recognition scores were analyzed for each participant in each condition (CDS vs. ADS). Children also completed cognitive tests of nonverbal IQ (PPVT and WASI) while parents completed questionnaires of CI and hearing history.

Preliminary data analysis indicates that pediatric CI users scored higher on CDS compared to ADS. Significant talker effects were also observed. Additional analysis will examine what factors may serve as predictors of voice emotion scores—factors such as age of CI implantation, duration of experience using the CI, nonverbal IQ scores, and socioeconomic status. Results have broad implications for understanding how cochlear implant users perceive emotions in others both from an auditory communication standpoint as well as from a socio-developmental perspective.

PS 79

Aging and Voice Emotion Recognition with Spectrally-Degraded Speech

Shauntelle Cannon[1]; Monita Chatterjee[2]

[1]*Boys Town National Research Hospital;* [2]*Auditory Prostheses & Perception Lab, Center for Hearing Research, Boys Town National Research Hospital, Omaha, NE*

Introduction

Aging has a negative impact on facial emotion and voice emotion recognition, as well as on social cognition in general, in normally hearing (NH) adults. NH older adults also demonstrate deficits in phoneme discrimination, gender discrimination and voice pitch discrimination in cochlear implant (CI) simulation studies. These deficits may also impact their perception of emotional prosody. Recent studies have investigated voice emotion recognition by adults and children with NH and CIs using unprocessed stimuli. Although parallel experiments have also been conducted with CI-simulated speech in children and young adults with NH, the effects of aging on voice emotion recognition using spectrally-degraded stimuli are not known. The objective of the present study is to gain a better understanding of how aging affects NH listeners'; voice emotion recognition in speech with varying levels of spectral degradation, and how such age-related changes may influence older CI users'; perception of voice emotions.

Methods

Nine normally hearing adults participated in preliminary data collection for this study. They were split into two groups by age: younger (age 21-35) and older (age 50-76). Participants listened to a series emotion neutral sentences presented in two conditions: 1) unprocessed (full spectrum) or 2) with 8- channel noiseband vocoding. Stimuli consisted of 12 emotion-neutral sentences spoken by a male and female talker in 5 emotions

(happy, sad, scared, angry, neutral) in an adult-directed manner, for a total of 60 sentences. The participant';s task was to identify the emotion associated with each of these recordings within a single-interval, five-alternative, forced-choice paradigm.

Results
Preliminary data confirm declines in overall percent correct scores with both age and increasing spectral degradation. The younger adult group showed better performance than the older adult group on voice emotion recognition in both conditions of spectral degradation.

Conclusions
These results suggest that age-related declines are present in normally hearing older adults. Additional data with adults with NH, as well as results of ongoing studies with middle-aged and older adults with CIs, will be presented. Reduced ability to identify a talker';s intended emotion can negatively impact social interactions as adults age. These results have important implications in the aging population of adults with NH and hearing loss as declines in the quantity and quality of social interactions and in social cognition have been associated with declines in quality of life.

PS 80

Brain oscillations and entrainment in cochlear implant users while watching the television series, "The Office": relations to self-reported listening effort and performance.

Andrew Dimitrijevic; Varia Sajeniouk; Joseph Chen
Sunnybrook Hospital Otolaryngology Head and Neck Surgery, University of Toronto

Background
Cochlear implant (CI) users often struggle while listening to a conversation in adverse listening environments such as a noisy room and often report that they feel exhausted after a day of listening. In order to follow conversations, especially in the presence of noise, attention and effort must be exerted and may be related to listening effort (LE). The physiological mechanisms of LE are not well understood. Previous work has also shown that cortical entrainment to an auditory stimulus such as a sentence is related to speech understanding.

Methods
Adult CI users were tested in free field using their everyday CI setting while watching the television series "The Office". The sound was delivered in a circular 8 speaker array. The front facing speaker played the sound of the movie stimulus while the other 7 speakers played multitalker babble noise. Three signal-to-noise ratios (SNR) were used +5, +10, and +15 dB. High density EEG recording were used to quantify neural responses while watching the movie. The audio output of the movie stimulus was simultaneously digitized as a channel on the EEG amplifier. This allowed for the acquisition of the reference signal for the cortical entrainment measure. EEG was recorded for 15 minutes for each of the SNRs. Subjective reports of task difficulty (i.e., watching and following the television show) were assessed using the NASA Task Load Index for each of the SNRs. These measures included effort, demand and frustration.

Results
Two types of analyses were performed: (1) spontaneous EEG, not time-locked to the movie audio, and (2) cortical coherence phase locked to the audio envelope. Increased power in the alpha rhythm frequency (8-12 Hz) was observed with increased listening effort in frontal regions. Significant coherence was observed between the movie audio and brain rhythms in the 4-6 Hz range. This increased coherence was observed bilaterally in the temporal cortex with largest magnitude at the right pole. Significant correlations between the degree of coherence and listening effort were observed in left frontal regions.

Conclusions
The results of this study show that audio-brain coherence can be measured in cochlear implant users. The degree of coherence and the alpha rhythm appear to be potential biomarkers of listening effort in the cochlear implant population. This may be useful for assessing different types of rehabilitative interventions for CI users.

PS 81

Getting the Feeling? Salience Of Music Emotion With A Cochlear Implant

David R. Friedmann[1]; Daniel Jethanamest[2]; Natalia Stupak[3]; David M. Landsberger[1]; Susan B. Waltzman[1]; J Thomas Roland[3]
[1]New York University School of Medicine; [2]NYU School of Medicine, Dept Otolaryngology; [3]NYU School of Medicine

Introduction
Music, like all forms of art, seeks to communicate emotional content to its audience. Prior studies demonstrate the signal provided by cochlear implants do not faithfully represent the psychophysical relationships inherent in music. We sought to determine whether targeted musical emotions are conveyed through electric

only stimulation with a cochlear implant and whether this ability correlates with spectral and temporal abilities.

Methods
Twenty musical pieces for which there was concordance among normal hearing (NH) listeners as to the emotion conveyed: (1)happy, (2)sad, (3)scared or, (4) peaceful were presented to cochlear implant (CI) subjects (n=20) via a sound field speaker through a specifically designed application administered on an iPad.

The musical clips were original recordings and orchestrations of western music from various musical genres but not widely familiar to participants. Subjects also completed a music background questionnaire (MBQ). Subset of patients also completed tests of spectral resolution and temporal modulation to determine whether these skills were correlated to the ability to detect music emotion

Results
CI users identified the target emotion in only 53% of cases compared to NH listeners who correctly identified the target emotion in 87% of pieces. Musical pieces with the target emotion of happy were recognized in **86**% of cases by CI users compared to **92%** among NH while the remaining target emotions were much more difficult for CI users sad (**44%**), scary (**38%**) and peaceful (**41%**) compared with NH raters. Length of CI experience and speech perception scores did not correlate with performance on this task. Prior music training and reported listening habits also did not correlate with music emotion identification. We will also report on correlations with spectral and temporal tasks and the music emotion identification.

Conclusions
Current CI technology and processing strategies do not convey the range of emotions conveyed in music as recognized by NH subjects. This difficulty may explain the reported lack of interest many patients have in music after CI despite a passion for music before onset of hearing loss. This ability may be unrelated to prior psychophysical measures of music perception or linked to temporal and spectral abilities.

PS 82

Auditory-motor Interactions in the Music Production of Adults with Cochlear Implants

Tara Vongpaisal
MacEwan University

Overview
Cochlear Implants (CIs) constrain the perception of pitch in us.. many continue to participate in musical ac-

WITHDRAWN

tivities after receiving their implants. To date, there has been no research examining the basis upon which adult CI users integrate electrical hearing input with motor skill to perform a musical instrument.To understand the basis of CI users'; music production and to what extent auditory and motor systems contribute to this process, we trained adult CI users and hearing controls to learn short sequences on a piano keyboard. We examined how their performance is affected by changes in the melodic and motor sequences in the learned patterns.

Methods
Using a computer animated learning procedure that removes the constraints of reading standard music notation, we trained participants to perform short melodic sequences on the piano, and examined their transfer of learning to novel sequences involving a change in the following: 1) melodic pattern only, 2) finger pattern only, 3) melodic and finger patterns, 4) no change.

Results
Hearing controls demonstrated the same pattern of difficulty in the transfer of learning across conditions as trained pianists in previous reports. That is, retaining the same melodic and finger patterns enabled the greatest transfer of learning, while those that altered both of these components yielded the poorest transfer of learning. Sequences involving a change in either the melodic or finger pattern yielded intermediate transfer performance. A number of CI participants demonstrate similar learning patterns across auditory and motor dimensions as those of hearing controls, however, much variability in performance was observed.

Conclusion
Our findings indicate that CI users'; can integrate auditory and motor processes to produce melodic sequences on a piano keyboard. For many, these processes are subject to similar learning effects observed in hearing controls. However, the large variability in performance likely stems from their unique hearing histories, musical experience, and reliance on hearing input for musical performance.

PS 83

The benefit of a second ear; directional hearing with a hearing implant and a contralateral normal hearing ear

Martijn Agterberg[1]; Myrthe Hol[1]; John Van Opstal[2]; Ad Snik[1]
[1]Radboudumc; [2]Radboud University

Treatment options for patients with conductive and mixed hearing loss are expanding. Due to development

of new technologies multiple implantable devices have been introduced during the last three decennia. However, several implantable devices have already been rejected by the industry. Recently the production of the Codacs, a powerful device with the actuator directly coupled to the cochlea fluids, has been stopped. The present study shows how direct cochlear stimulation with a middle-ear implant can improve directional hearing in children with unilateral conductive hearing loss. In patients we rely on psychophysical measurements to demonstrate accurate binaural hearing. One of the most accurate methods to demonstrate binaural hearing abilities is a method that investigates sound localization in the horizontal plane (Snik et al., 2015). Unfortunately, sound localization tests differ remarkably from clinic to clinic, ranging from setups with speakers positioned 60 degrees apart (Lovett et al. 2009), 45 degrees apart (Schoonhoven et al., 2016), 30 degrees apart (Heyning et al., 2016; Bosman et al., 2011; Priwin et al., 2007), 15 degrees apart (Van Deun et al., 2010), 10 degrees apart (Grieco-calub and Litovsky, 2012), to setups were stimuli can be presented from every possible position (Agterberg et al., 2011; Kuhnle et al., 2013). Furthermore, the setups differ in the stimulus duration, pointing method, bandwidth of the stimuli, visibility of the speakers and amount of roving of the sound level. These differences result in conflicting outcomes and in results that are difficult to compare. The present study investigates binaural hearing (i.e. the accurate neural processing at the level of the brainstem) in patients with middle ear implants. The proposed psychophysical tests are built in a mobile lab, so the same method can be applied when children are tested in different clinics in different countries (Belgium, Germany, The Netherlands).

PS 84

Evaluation of a Research Sound Coding Strategy Using the Research Interface Box II

Fang Du[1]; Yi Hu[1]; Christina L. Runge[2]
[1]University of Wisconsin - Milwaukee; [2]Medical College of Wisconsin

Background
Investigating the effects of sound processing changes on speech perception with cochlear implants (CIs) is highly challenging in an acute setting. When testing experimental strategies, patients'; familiarity with their own strategy, ceiling effects, and the need to acclimate to novel sound coding over time can add significant delays to data collection and confound results. Thus, acute experiments are often desirable, and a research strategy that is easily manipulated can greatly facilitate progress in CI research. To address this issue, we have implemented a research Continuous Interleaved Sampling (CIS) strategy with the Research Interface Box II (RIB II)

platform that can be used in acute experiments for MED-EL recipients. The purpose of this study was to compare sentence perception between our research CIS strategy and clinical strategies.

Methods
MATLAB code was developed that utilized patients'; maps to create customized CIS versions of sentences for direct stimulation using the RIB II platform. IEEE sentences were processed in both quiet and 4-talker babble background noise (SNR +10). IEEE sentences were chosen because of the large number of lists, and because they are not used clinically and therefore would be unfamiliar to subjects. Nine experienced MED-EL recipients using one of the Fine Structure Processing (FSP) sound coding strategies (FSP, FS4, FS4-p) were included in this study (average length of CI use 5 ±1 years). Performance for IEEE sentences with the research CIS strategy was measured acutely and compared to the most recent clinical AzBio scores in quiet and 4-talker babble (SNR +5 or +8 dB).

Results
Significant correlations were found between research CIS and clinical FSP map conditions in both quiet and in noise (p

Conclusions
This study shows that a research CIS strategy can be implemented with the RIB II interface to promote acute experimental testing of sound processing manipulations in MED-EL recipients. Currently, we are using this research CIS strategy as a baseline to create experimental manipulations for acute testing in our lab.

PS 85

An Open FPGA-based Computational Platform for Developing Real-Time Cochlear and Hearing-Aid Processors

Christopher Casebeer[1]; Raymond J. Weber[2]; Ross K. Snider[1]
[1]Montana State University - Bozeman; Flat Earth Inc.; [2]Flat Earth Inc.

Field Programmable Gate Arrays (FPGAs) provide flexible computational architectures that are ideal for digital signal processing (DSP). With support of a NIH/NIDCD SBIR grant*, we are developing an open FPGA platform

for the speech and hearing research community where one of the objectives is to develop open hearing-aid and cochlear processors. The advantage of the FPGA computational platform over conventional CPU approaches is the ability to implement low-latency high-performance signal processing with deterministic latencies.

The hardware portion of the platform includes audio I/O, an audio codec, and an Intel FPGA with flexible I/O. Development of signal processing algorithms uses Mathwork';s Simulink, which allows exploration and modeling of signal processing algorithms. Once a Simulink model has been developed, VHDL code can be generated that implements the signal processing in the FPGA fabric where the FPGA functions as a real-time signal processor.

We are currently soliciting ideas/feedback from the speech and hearing community as to what features they would like to see in the next iteration of the open FPGA-based computational platform.

 www.openspeechtools.com

PS 86

Loudness perception for simultaneous electrical stimulation

Florian Langner[1]; Colette McKay[2]; Andreas Büchner[1]; Waldo Nogueira[3]
[1]Department of Otolaryngology, Hannover Medical School, Germany; Cluster of Excellence; [2]Bionics Institute Melbourne; [3]Department of Otolaryngology, Hannover Medical School, Germany; Cluster of Excellence Hearing4all

Models of the loudness elicited by cochlear implant (CI) electrical stimulation are useful for the optimization of sound coding strategies. The balance between performance and power consumption must be considered in new strategies and improved so that advances towards a fully implantable device can be achieved in the future. One step towards this is the utilization of parallel stimulation of channels, which increases electrical interaction and decreases the levels of stimulation. In the past, a loudness model was successfully developed for the prediction of loudness for sequential electrical stimulation by McKay et al. (JASA, 2003). This study aimed to extend this model by investigating the loudness perception of parallel channel stimulation and to apply the model to reduce power consumption in CIs.

Thirteen Advanced Bionics CI users participated in the study and were directly stimulated via the HRStream interface. A loudness balancing was assessed by a self-adjustment method using a rotational controller without anchors. The balancing was performed between a reference, (composed of a single channel located on either the most apical/basal or middle location of the array) and the target stimulus (same configuration but with an additional parallel channel with fixed distance in electrode steps to the original channel). Across conditions, the distance between the two channels of the target stimulus was altered to cover the complete array. Each condition was finished when the participant set the target stimulus to the same loudness as the reference. The loudness balancing was performed having the reference stimuli set to most comfortable level (9 subjects) and threshold level (7 subjects).

Adding a second parallel channel adjacent to the reference stimulus reduced the current necessary for equal loudness by 4.9 dB (smallest distance). With greater distance between each channel, more current was necessary for the same loudness percept (average of 0.33 dB / electrode distance). For the greatest distance, a current reduction of 2.7 dB was necessary. There was a significant linear relationship between current adjustment and distance, which was independent from the site of the reference stimulation and presentation level. This finding was incorporated into an extended loudness model for simultaneous stimulation and used to predict loudness adjustments between different parallel channel sound coding strategies. The outcomes of the model have been validated using additional experimental data demonstrating the effective use of the model.

Clinical Otolaryngology & Pathology I

PS 87

RNA-Seq Analysized Genes related to Middle ear primary papilloma

Xiaoyu Yang[1]; Xiaoqing Qian[2]; Rui Ma[2]; Ning Cong[2]; Fanglu Chi[1]; Dongdong Ren[1]
[1]EYE & ENT Hospital of Fudan University; [2]Eye & ENT Hospital of Fudan University

Background

Middle ear papilloma is a rare disease with a incidence of 0.63/100000. It can be divided to primary and secondary tumor. While middle ear papilloma mostly occurs in the ipsilateral ear of female and causes destruction of ossicular chain and nerve. Recent study showed that sinonasal and laryngeal papilloma has a close relationship to HPV infection. Nevertheless, the causation of middle ear primary papilloma is not fully established.

Object
To discover genes related to middle ear primary papilloma in patients.

Methods
To study pathogenesis in patients with middle ear papilloma, we collected the tumor tissue from three patients, with middle ear, laryngeal and maxillary sinus primary papilloma respectively, and normal middle ear mucosa as control. We performed a high throughout RNA-Seq study of gene expression.

Results
Our bioinformatics analysis identified 279 unreported genes remarkably upregulated in patients with middle ear primary papilloma compared with the control group, including TACR1, BAX, MMP7, MAPK8, RRAS, PLA-2G4A and DUSP12 . The results were inconsistent with abnormal genes in sinonasal and laryngeal papilloma. We found that middle ear papilloma is more like a result of the interaction of virus, inflammatory response and allergy.

Conclusion
RNA-Seq and bioinformatics techniques can be used as a powerful tool for overall gene-transcription in patients with middle ear primary papilloma. Middle ear papilloma and larynx or sinus papilloma probably not share the same origin. Some key genes screened in this study may become candidate genes or operating targets in the future research.

Keywords
Middle ear; Papilloma; RNA-Seq; transcriptome

PS 88

Valnoctamide Inhibits Cytomegalovirus Infection in the Developing Auditory System and Rescues Virally Induced Hearing Loss.

Sara Ornaghi[1]; Jun-Ping Bai[2]; Winston Tan[3]; **Joseph Santos-Sacchi**[4]; Dhasakumar Navaratnam[5]; Michael Paidas[6]; Anthony van den Pol[7]
[1]PhD program in Neuroscience, University of Milan-Bicocca, Italy; Dept. of Neurosurgery and Obstetrics, Gynecology, and Reproductive Sciences, Yale University School of Medicine, USA; [2]Department of Neurology, Yale University School of Medicine, New Haven, Connecticut, USA; [3]Department of Surgery (Otolaryngology), Yale University School of Medicine, New Haven, Connecticut, USA; [4]Department of Surgery (Otolaryngology), Neuroscience, and Cellular and Molecular Physiology, Yale University School of Medicine, New Haven, Connecticut, USA; [5]Department of Neurology and Neuroscience, Yale University School of Medicine, New Haven, Connecticut, USA; [6]Dept. of Obstetrics, Gynecology, and Reproductive Sciences, Yale University School of Medicine, USA; [7]Department of Neurosurgery, Yale University School of Medicine

Objective
Congenital cytomegalovirus (CMV) is the leading infectious cause of non-hereditary sensorineural hearing loss in newborns and children. No treatments are currently recommended for affected fetuses during pregnancy and postnatal therapy is only available for the most severe cases of infection due to substantial safety concerns. We showed that valnoctamide (VCD), a mood stabilizer, effectively blocks CMV. Here we investigate CMV infection in the developing auditory system of newborn mice and the potential benefits of VCD on long-term hearing outcomes. **Study Design:** Pups inoculated intraperitoneally (i.p.) with murine CMV (mCMV, 750 PFU in 20 µL of media) on the day of birth received VCD (n=6) or vehicle (VEH, n=6) daily (1.4mg/mL) from p1 to p21. Media-inoculated animals served as controls (n=6). Newborn mice were chosen because their brain development parallels that of a human fetus during the early 2nd trimester, critical period of neurontogeny where CMV can cause substantive dysfunction. mCMV load and distribution in the cochlea and central auditory regions were assessed by qPCR and histochemistry at multiple timepoints post-infection. Hearing was investigated blindly with respect to the experimental group using Auditory Brainstem Responses (ABRs) in 7 week-old mice. Statistical significance was determined by Student';s t-test and mixed-model ANOVA with Repeated Measures and Newman Keuls'; post-hoc test, and set at $p<.05$; all analyses were conducted with GraphPad Prism version 6.0.

Results
After i.p. inoculation, mCMV was detected in the cochlea as early as 2 dpi, with viral load peaking at p16-21 and viral particles still measurable at p50. mCMV-infected cells were identified in multiple areas of the inner ear, including the stria vascularis, the temporal bone, and the cochlea. mCMV-positive cells were also recognized in central components of the auditory system, such as the cochlear nuclei, the inferior colliculus, and the auditory cortex. Infected mice showed significantly increased hearing thresholds at multiple frequency tone stimuli. VCD administration substantially reduced mCMV load in the cochlea and the brain, and ameliorated hearing development with restoration of normal auditory responses.

Conclusion
VCD effectively blocks mCMV infection in the developing auditory system, and rescues virally induced hearing impairment. VCD has already been clinically used for treating neuropsychiatric disorders and lacks teratogen-

ic activity. Thus, it may merit consideration as a novel therapeutic approach in CMV-mediated deafness during early development.

PS 89

Guinea pig model of middle ear infusion and hair cell injury: histopathological evaluation and cytocochleogram.

Jean-Francois Lafond; Kelly Tenneson
Charles River Laboratories

Local drug administration to the middle ear by transtympanic injection is often the preferred method but is not optimal in long term animal studies investigating toxicity or efficacy of new compounds being developed for the treatment of hearing disorders. Surgical techniques for middle ear catheterization have previously been used but these have been associated with severe local trauma and inflammation which can be detrimental to hearing, the general condition of the animal and can adversely impact the integrity of the results obtained. In order to improve animal welfare and to permit long-term middle ear dosing, we refined a surgical procedure for middle ear catheterization and infusion and used it to produce an aminoglycoside-induced model of hair cell injury. Histopathological evaluation and cytocochleograms showed this model was associated with mild procedure-related inflammatory changes in the middle ear 9 weeks after catheter implantation and minimal hair cell loss. Severe hair cell loss was confirmed histopathologically and by cytocochleograms in animals given aminoglycoside (gentamicin). In conclusion, this refined surgical model resulted in only minor microscopic changes related to surgical procedures and inflammation. These did not affect the interpretation of potential treatment-related changes in the middle and inner ear following repeat middle ear dosing in the Guinea Pig, and therefore the model is suitable for use in toxicity and efficacy studies.

Gene Regulation in the Inner Ear I

PS 90

Chromatin Accessibility Landscape of Adult Cochlear Hair Cells

Lei Chen[1]; Huizhan Liu[1]; Kimberlee P. Giffen[1]; Silu Hu[2]; Tinghuan Zhang[2]; Wenyang Sun[3]; Qianzi Tang[2]; David Z. He[1]
[1]Creighton University; [2]Sichuan Agricultural University; [3]Chongqing Academy of Animal Sciences

Introduction

While the genome is identical for nearly every cell in multicellular organisms, the gene expression profile for each cell is different. This orchestrated gene activity plays a central role in controlling the functional complexity and morphological diversity seen among different cells. Transcription factors (TFs) and cis-regulatory elements (CREs) are key components in the gene regulatory networks that control gene expression. Cochlear inner hair cells (IHCs) and outer hair cells (OHCs) have different morphology and function. The genetic mechanisms controlling their morphological and functional specializations are largely unknown. We examined the accessible chromatin regions, which coincide with CREs, in the genome of adult mouse IHCs and OHCs to gain insight of the gene regulatory mechanisms in IHCs and OHCs.

Methods

Isolated IHCs and OHCs (~200) were separately collected for each of three biological replicates from adult FVB mice using a suction pipette technique. Cells were lysed and digested by DNase I. DNA fragments were extracted and the DNase-seq libraries were prepared using NEBNext Ultra II DNA Library Prep Kit (Illumina NEB). After library amplification, small fragments (< 200 bp) drived from DNase I hypersensitive sites (DHSs) were enriched by gel-based size selection and second-round amplification. Libraries were sequenced by SE50 (Illumina HiSeq2500).

Results

DNase I accessible chromatin landscape were mapped. 30,831 and 31,851 DHSs were identified in IHCs and OHCs, respectively. DNase-seq tag density correlation analysis showed a high similarity of DNase I accessible chromatin landscape between the two cell types (r=0.97). 708 of 31,620 combined DHSs showed differential signal (PDe novo motif analysis showed an enrichment of KLF5 binding site in differential DHSs. It suggested an important role of KLF5 in hair cell differentiation. Besides, significant higher DNase I hypersensitivity around the TSS of *Slc26a5* (*Prestin*) were identified. These regions may be responsible for transcriptional control of *Slc26a5*.

Conclusions

Our studies provide the first CRE landscape in IHCs and OHCs. Experiments using mouse genetics, gel-shifting assay, ChiP-seq and various reporter as well as electrophysiology are under way to elucidate the mechanisms of transcription regulation of unique morphological and functional specializations of IHCs and OHCs and their development. (Supported by NIH grant DC004696 from the NIDCD to DH and by National Natural Science Foundation of China 31771376 to LC)

PS 91

Computational Repositioning and Preclinical Validation of Mifepristone for Human Vestibular Schwannoma

Jessica E. Sagers[1]; Adam S. Brown[2]; Sasa Vasilijic[3]; Rebecca Lewis[3]; Mehmet I. Sahin[3]; Lukas D. Landegger[3]; Roy H. Perlis[4]; Isaac S. Kohane[2]; Bradley Welling[3]; Chirag J. Patel[2]; Konstantina M. Stankovic[3]
[1]Department of Otolaryngology, Eaton Peabody Laboratories, Massachusetts Eye and Ear, Program in Speech and Hearing Bioscience and Technology, Harvard Medical School; [2]Department of Biomedical Informatics, Harvard Medical School; [3]Department of Otolaryngology, Massachusetts Eye and Ear; [4]Department of Psychiatry, Massachusetts General Hospital

The computational repositioning of existing drugs represents an appealing avenue for identifying effective compounds for diseases with no FDA-approved pharmacotherapies. Here we present the largest meta-analysis to date of differential gene expression in human vestibular schwannoma (VS), a debilitating intracranial tumor, and use these data to inform the first application of algorithm-based drug repositioning for this tumor class. We apply an open-source computational drug repositioning platform to gene expression data from 80 patient tumors and identify eight promising FDA-approved drugs with potential for repurposing in VS. Of these eight, mifepristone, a progesterone and glucocorticoid receptor antagonist, consistently and adversely affects the morphology, metabolic activity, and proliferation of primary human VS cells and HEI-193 human schwannoma cells. Mifepristone treatment reduces VS cell viability more significantly than cells derived from patient meningiomas, while healthy human Schwann cells remain unaffected. Our data recommend an immediate Phase II clinical trial of mifepristone in VS.

PS 92

High-throughput Perturbation of Genes in an Organoid Model of Hair Cell Differentiation

Kathy S. So[1]; Tyler M. Gibson[2]; Matthew N. Nguyen[1]; Danielle Lenz[3]; Barbara Bryant[1]; Gabriela Pregernig[1]; Adam T. Palermo[1]; Joseph C. Burns[1]; Albert Edge[4]
[1]Decibel Therapeutics; [2]Eaton-Peabody Laboratories, Massachusetts Eye and Ear Infirmary; and Department of Otology and Laryngology, Harvard Medical School; [3]Eaton-Peabody Laboratories, Massachusetts Eye and Ear Infirmary; [4]Harvard Medical School

Studies in the development of the sensory hair cells in the organ of Corti are limited in their scope by the dual technical challenges of both a severely limited number of cells available for study, and limited success delivering synthetic genetic constructs required to run targeted perturbations. Thus, expensive and time-intensive genetically engineered animal models are most frequently employed. While recent advances in viral vector design have begun to facilitate *in vivo* studies on hair cells, there are still limited tools available to study the cochlear supporting cells that can serve as a progenitor population for hair cells.

To address these limitations, we took advantage of our recently-developed method for expanding neonatal supporting cells in organoid culture and differentiating them into hair cells. Using an unbiased clustering analysis of single-cell RNA-Seq (scRNA-seq) data collected from P1 whole cochlea, we demonstrate that the transcriptomes of the organoid culture hair cells are very similar to the neonatal hair cells. We have also found that these organoids, in contrast to the intact organ of Corti, can be efficiently transduced using conventional lentivirus at moderate titers.

New methods in scRNA-Seq and genome editing have produced a promising technique known as Perturb-Seq that combines high-throughput genomic perturbations with a transcriptional readout. By developing a novel vector, optimizing a short guide RNA (sgRNA) barcode recovery strategy, and implementing custom bioinformatics, we report here a Perturb-Seq-like screening system for cochlear organoids. As a proof of concept, we derived organoids from neonatal transgenic mice with constitutive organism-wide expression of the RNA-guided nuclease Cas9 and transduced them with lentivirus encoding sgRNAs targeting either the Atoh1 gene or an off-target control. Cells with expression of the Atoh1-targeting sgRNA showed disruption of the Atoh1 gene in the genomic locus, as well as a decrease in generation of hair cells measured using both fluorescence-based markers and scRNA-Seq analysis.

Ongoing work in our labs aims to scale these proof-of-concept experiments to attain a systems-level understanding of the process by which supporting cells differentiate into cochlear hair cells. The information gained from these studies will provide an effective resource to guide future discovery in the identification of targets that promote hair cell reprogramming.

PS 93

Role of Neuropilin-1/Semaphorin-3A Signaling in Age-Related Hearing Loss and the Functional and Morphological Integrity of the Cochlea

Pezhman Salehi[1]; Marshall Ge[2]; Usha Gundimeda[3]; Homero Cantu[4]; Litao Tao[2]; Carolina Abdala[5]; Joel Lavinsky[6]; Matthew W. Kelley[7]; Takahiro Ohyama[2]; Thomas M. Coate[8]; **Rick Friedman**[9]
[1]NEOMED; [2]University of Southern California, Caruso Dept. of Otolaryngology, Keck School of Medicine; [3]Caruso Department of Otolaryngology, USC; [4]George Town University Medical Center; [5]Auditory Research Center, Caruso Department of Otolaryngology, University of Southern California; [6]Graduate Program in Surgical Sciences, Federal University of Rio Grande do Sul; [7]NIDCD/NIH; [8]Department of Biology, Georgetown University; [9]UCSD Division of Otolaryngology

Background

Neuropilin-1 (Nrp1) encodes the transmembrane cellular receptor neuropilin-1, which is associated with cardiovascular and neuronal development and was within the peak SNP interval on chromosome 8 in our prior GWAS study on age-related hearing loss (ARHL) in mice [1].

Methods

In this study, we generated and characterized an inner ear-specific *Nrp1* conditional knockout (CKO: *Nrp1$^{fl/fl}$;-Pax2^{Cre}*) mouse line because *Nrp1* constitutive knockouts are embryonic lethal. All experiments were performed on mutants and littermate controls. *In situ* hybridization using sense and antisense probes for *Sema3A* and *Nrp1* were hybridized to midmodiolar cochlear sections. For quantitative neuronal and hair cell assays, cochlear whole mounts and frozen section immunostaining was performed using the following antibodies: anti-TUJ1, anti-Nrp1, anti Sema3A, anti-CtBP2, anti- myosin VI, anti-Sox2, anti-synaptotagmin-1, and anti-GAP43 using standard protocols. SGN explant three dimensional cultures were performed to assess the *in vitro* responses to Sema3A and Nrp1.

Results

In situ hybridization demonstrated weak *Nrp1* mRNA expression late in embryonic cochlear development, but increased expression in early postnatal stages when cochlear hair cell innervation patterns have been shown to mature. At postnatal day 5, *Nrp1* CKO mice showed disorganized outer spiral bundles and enlarged microvessels of the stria vascularis (SV) but normal spiral ganglion cell (SGN) density and presynaptic ribbon body counts; however, we observed enlarged SV microvessels, reduced SGN density, and a reduction of presynaptic ribbons in the outer hair cell region of 4-month-old *Nrp1* CKO mice. In addition, we demonstrated elevated hearing thresholds of the 2-month-old and 4-month-old *Nrp1* CKO mice at frequencies ranging from 4 to 32kHz when compared to 2-month-old mice.

Conclusions

These data suggest that conditional loss of *Nrp1* in the inner ear leads to progressive hearing loss in mice. We also demonstrated that mice with a truncated variant of *Nrp1* show cochlear axon guidance defects and that exogenous semaphorin-3A, a known neuropilin-1 receptor agonist, repels SGN axons *in vitro*. These data suggest that Neuropilin-1/Semaphorin-3A signaling may also serve a role in neuronal pathfinding in the developing cochlea. In summary, our results here support a model whereby Neuropilin-1/Semaphorin-3A signaling is critical for the functional and morphological integrity of the cochlea and that *Nrp1* may play a role in ARHL.

Acknowledgements

PS 94

Targeted next-generation sequencing analysis of the genotype-phenotype correlation of DFNA8/12 caused by TECTA mutations in 990 autosomal dominant hearing loss patients

Rika Yasukawa; Ken Hiramatsu; Hideaki Moteki; Shinya Nishio; Shin-ichi Usami
Department of Otorhinolaryngology, Shinshu University School of Medicine

Background

TECTA mutations are one of the most frequent causes of autosomal dominant (AD) hearing loss (DFNA8/12), and mostly lead to late-onset hearing loss ofvarious types. Many mutations have been reported from various population-based genetic analyses. According to the previous reports, mutations in the TECTA are thought to be characterized by mid-frequency or high frequencyhearing loss. In this study, we used targeted next-generation sequencing for 68 known hearing loss genes for the comprehensive genetic testing for 6,004 Japanese hearing loss patients, and investigated the prevalence ofTECTA mutations and the genotype-phenotype correlationamong patients with hearing loss caused by TECTAmutations.

Methods

Six thousand and four (6,004) hearing loss patients with sensorineural hearing loss (SNHL) were enrolled in this

study. We examined DNA samples using targeted genomic enrichment and next-generation sequencing of 68 candidate genes. We performed target-capture and sequencing using an AmpliSeq custom primer poolfollowed by customized analysis pipeline screening withIon PGM/Ion Proton (Thermo Fisher Scientific). We focused on those patients with TECTA mutations implicated in autosomal dominant inheritance, and examined the genotype-phenotype correlations.

Results
We identified 28 patients (26 probands) with causative mutations in the TECTA gene from among 990 SNHL families with AD inheritance. TECTA mutations were detected in 2.5% (26/990) of Japanese ADNSHL families, and most patients showed typical genotype-phenotype correlations with mid- or high-frequencyhearing loss. Twenty-six mutations we found, 16 of which were novel, while several were previously reported from different ethnic groups. Those recurrent mutations were considered to be due to a mutational hot spot in TECTA.

Conclusion
We revealed that TECTA mutations were prevalent among Japanese AD hearing loss patients, particularly among those with AD inherited causative genes. Most of the patients with TECTA mutations showed typical genotype-phenotype correlations with SNHL. Severalmutations were suggested to be caused by a possible mutational hot spot.

PS 95
CHD7 Maintains Expression of Long Genes During Early Ear Development

Gilson J. Sanchez[1]; Ethan D. Sperry[2]; Robert Durruthy-Durruthy[3]; Daniel R. Fuentes[4]; Margot E. Bowen[5]; Adrienne N. Niederriter-Shami[6]; Jennifer M. Skidmore[1]; Anshika Srivastava[7]; Laura D. Attardi[8]; Tomasz Swigut[9]; Joanna Wysocka[10]; Stefan Heller[11]; Peter C. Scacheri[12]; Donna M. Martin[13]
[1]Departments of Pediatrics and Communicable Diseases University of Michigan, Ann Arbor, MI, USA.; [2]Department of Human Genetics and the Medical Scientist Training Program University of Michigan, Ann Arbor, MI, USA.; [3]Stanford | School of Medicine |Department of Otolaryngology - Head & Neck Surgery; [4]Chemical and Systems Biology Stanford University, Stanford; [5]Radiation and Cancer Biology Stanford University, Stanford, CA, USA.; [6]Departments of Pediatrics and Communicable Diseases and Human Genetics University of Michigan, Ann Arbor, MI, USA.; [7]Department of Human Genetics University of Michigan, Ann Arbor, MI, USA.; [8]Radiation and Cancer Biology, Stanford University, Stanford, CA, USA.; [9]Chemical and Systems Biology, Stanford School of Medicine, Stanford; [10]Chemical and Systems Biology and Developmental Biology and the Howard Hughes Medical Institute, Stanford School of Medicine, Stanford, CA, USA.; [11]Stanford | School of Medicine | Department of Otolaryngology - Head & Neck Surgery; [12]Department of Genetics, Case Western Reserve University, , Cleveland, OH, USA.; [13]Departments of Pediatrics and Human Genetics, University of Michigan, Ann Arbor, MI, USA

CHD7 is an ATP-dependent helicase that is critical for proper development of the mammalian inner ear. Humans with CHARGE syndrome and heterozygous pathogenic variants in *CHD7* exhibit mixed conductive-sensorineural hearing loss and inner ear dysplasia, including abnormalities of the semicircular canals and Mondini malformations. *Chd7*$^{Gt/+}$ mice are an excellent model for CHARGE syndrome as they exhibit dysplastic semicircular canals and mild mixed conductive-sensorineural hearing loss. Chromatin remodelers such as CHD7 reposition nucleosomes to modulate DNA access for the transcriptional machinery. Consequently, they affect transcription initiation, elongation, termination and RNA processing. Indeed, reduced *Chd7* function in the ear disrupts expression of genes involved in developmental patterning and neurogenesis. Because the underlying mechanisms of CHD7 remain unknown, we sought to define roles for CHD7 in global regulation of gene expression and histone mark maintenance during the embryonic stage of ear organogenesis. We performed RNA-seq based transcriptome analysis on *Chd7*$^{+/+}$ and *Chd7*$^{Gt/+}$ E10.5 otocysts and discovered a transcript length-dependent gene misregulation in *Chd7*$^{Gt/+}$ ears compared to wild type (*p*Chd7 loss. ChIP-seq analyses on *Chd7*$^{+/+}$ and *Chd7*$^{Gt/+}$ E10.5 otocysts revealed 37 and 91 genomic locations that were enriched or depleted for the histone marks H3K27ac and H3K4me3 in *Chd7*$^{Gt/+}$ ears, respectively, whereas enrichment of histone tri-methylation on H3K36 was unchanged. Among the 37 genomic sites with altered H3K27ac and 91 genomic sites with altered H3K36me3, roughly half were enriched and half were depleted in *Chd7*$^{Gt/+}$ ears. Unexpectedly, none of the CHD7-dependent histone modification changes identified in the chromatin of *Chd7*$^{Gt/+}$ ears were in close proximity to misregulated long genes. Taken together, our findings support a model in which CHD7 regulates transcription in the developing ear independent of histone H3K27 acetylation or tri-methylation of H3K4 and H3K36. Our findings are in agreement with a recent report demonstrating cooperativity between CHD7 and the topoisomerase TOP2B to sustain expression levels of over 200 long genes (~250 kb) in cerebellar neurons. Interestingly, length-dependent gene misregulation has also been described in Rett syndrome, Autism Spectrum Disorder, and Fragile X syndrome, suggesting possible links between the molecular etiologies of these disorders and CHARGE syndrome.

PS 96

Enrichment of familial MD genes in cochlear and vestibular epithelial non-sensory cells

Teresa Requena; Alvaro Gallego-Martinez; Jose Antonio Lopez-Escamez
Centre for Genomics and Oncology Research (Genyo)

Background

Cochlear and vestibular epithelial non-sensory cells are essential to maintain the cellular architecture in the Organ of Corti and the vestibular epithelium integrity in the vestibular sensory organs. Intercellular junctions and extracellular matrix interactions are essential to prevent an abnormal ion redistribution resulting in loss of endocochlear potential. Diseases as Meniere';s disease (MD) could involve a dysfunction in supporting cells, since hair cells (HCs) do not show degeneration in MD human temporal bones. The aim of this study is to generate molecular networks maps and pathways in cochlear and vestibular non-sensory cells to define clusters of proteins involved in hearing or vestibular loss in MD.

Methods

We retrieved microarray and RNA-seq datasets from P0 mouse epithelial sensory and non-sensory epithelial cells from gEAR portal (http://umgear.org/index.html)([1](1)) and obtained gene expression fold-change between epithelial non-HCs (ENHCs) and non-epithelial cells (NECs) against HCs for each gene. Differentially expressed genes (DEG with a log2 Fold Change>1) between both non-sensory and HC were selected to search for interactions using the STRING database (https://string-db.org/). Specific molecular networks for non-sensory HCs in the cochlea and the vestibular organs were generated and significant pathways were identified. Candidate familial MD genes identified by whole exome sequencing, were manually searched in these pathways..

Results

Between 586 and 1245 genes were up regulated in ENHCs or NECs in both cochlear and vestibular datasets in the early neonatal mouse. Molecular networks had a significant enrichment of GO biological functions, cellular components and functional processes and specific protein clusters were identified in both cochlear and vestibular non-sensory cells. From these datasets, we have found 57 molecular pathways and 23 of them were associated with some of the MD genes. Candidate genes for familial MD combined with these datasets showed enrichment in 3 pathways: focal adhesion, gap junction in both cochlear and vestibular datasets and axon guidance pathway only found in cochlear supporting cells.

Conclusions

We have predicted molecular networks map with several protein clusters for non-sensory epithelial cells of the Organ of Corti and vestibular organs. This map will facilitate the functional studies of novel candidate genes for hearing or vestibular loss in non-sensory epithelial cells for MD. In addition we have identified 3 pathways that could explain MD phenotype.

References

Elkon, R., Milon, B., Morrison, L., Shah, M., Vijayakumar, S., Racherla, M., Leitch, C.C., Silipino, L., Hadi, S., Weiss-Gayet, M. *et al.* (2015) RFX transcription factors are essential for hearing in mice.

Nature communications, 6, 8549.

PS 97

Changing Gene Expression Modes During Organ of Corti Maturation

Joerg Waldhaus[1]; Daniel C. Ellwanger[2]; Robert Durruthy-Durruthy[3]; Stefan Heller[2]
[1]*University of Michigan;* [2]*Stanford | School of Medicine | Department of Otolaryngology - Head & Neck Surgery;* [3]*Stanford | School of Medicine | Department of Otolaryngology - Head & Neck Surgery*

Development of any tissue or organ is associated with dynamic changes of gene expression patterns. In general, studies investigating the transcriptome at single cell level observe a global reduction in numbers of genes expressed per cell while development proceeds from the embryo towards adulthood. We hypothesize that the decrease in genes per cell counts may not solely correspond to a fraction of genes simply being shut off once development is completed, but rather due to well-coordinated modulation of gene expression from constitutively ON, at varying levels, towards a binary ON/OFF mode, also known as bursting. We specifically addressed this hypothesis in the maturing mouse organ of Corti.

Gene expression in mammalian cells is modulated by various factors including promoter activity, transcription rates, and transcript lifetime. Thus far, these parameters were assessable through low throughput measures such as single molecule *in situ* hybridization, which allows single transcript counting. Using high-multiplexed single cell qRT-PCR, we analyzed in parallel the expression of 96 candidate genes from flow-sorted pillar and Deiters'; cells at three time points during late organ of Corti development and maturation. Concordant with the general view, we measured a decrease in the number of detectable genes expressed as supporting cells differentiated. Comparing mRNA-expression levels from select

candidate genes with protein and fluorescent reporter expression levels we found evidence for the occurrence of distinctive modes of gene expression in the adult organ of Corti. Specifically, we found that expression of various genes changed from a continuous expression to a previously described "bursting mode" that is characterized by undulating transcript levels over time. We applied a novel data analysis strategy to predict bursting rate, bursting intensity and length of each bursting event for the 96 genes analyzed.

The results of this study contribute to the rapidly growing field of single cell analysis and highlight that the maturation state of a cell needs to be considered in comparative studies using single cell transcriptomic data. Moreover, our results show that substantial changes in gene expression regulation exist between neonatal and mature organ of Corti supporting cell types. Our data analysis strategy allows the quantitative assessment of transcription kinetics with single cell and single gene resolution with a throughput of up-to 300 genes per cell. A fundamental understanding of the changes that happen when organ of Corti supporting cells mature from neonatal stages is going to be useful for the development of regenerative therapies.

PS 98

Autogenous Regulation of the Fragile X Mental Retardation Gene During Embryonic Development of the Auditory Brainstem

Diego A. R. Zorio[1]; Xiaoyu Wang[2]; Hitomi Sakano[3]; Yuan Wang[2]
[1]Department of Biomedical Sciences, College of medicine, Florida State University; [2]Department of Biomedical Science, Program in Neuroscience, Florida State University College of Medicine; [3]Virginia Merrill Bloedel Hearing Research Center, Department of Otolaryngology-Head and Neck Surgery, University of Washington, School of Medicine

Fragile X mental retardation protein (FMRP) is an mRNA-binding protein that regulates a multitude of synaptic proteins and signaling pathways involved in neurological diseases. Loss of FMRP leads to abnormal auditory processing in the fragile X syndrome (FXS). In this study, we discovered that the intensity of FMRP protein in auditory neurons is tightly regulated during development and we identified a novel autogenous regulation of FMRP expression. All experiments were performed in the chicken auditory brainstem particularly the nucleus magnocellularis (NM), the avian analogue of the mammalian anteroventral cochlear nucleus (AVCN).

To examine FMRP protein level during development, we produced a rabbit polyclonal antibody specifically recognizing the chicken FMRP. Western blot on chicken brainstem samples revealed that FMRP protein level is largely stable from embryonic day 9 (E9; the earliest stage that NM can be identified) to post-hatch day 4 (P4; when auditory brainstem is considered mature-like structurally and functionally). Immunocytochemistry demonstrated that the total amounts of FMRP immunoreactivity per individual NM neuronal cell body are relatively stable from E9 to E19 and increase at P4. Interestingly, the average FMRP immunoreactivity intensity in NM cell bodies displays a significant reduction from E9 to E15, and then restores gradually. These observations indicate that FMRP protein synthesis does not accompany appropriately with the increase of the cell body size during this developmental windows.

We next explored the underlying mechanisms responsible for this reduced FMRP intensity. Using quantitative PCR (qPCR), we found that total Fmr1 RNA levels in the brainstem are stable from E3 to P4. However, we discovered a developmentally regulated alternative splicing event that caused retention of intron 8. This event first appears at E7 and it is less evident at P4. In addition, we demonstrated for the first time that FMRP is capable binding to the 3'; region of the intron in a very specific manner, leading to a hypothesis that FMRP protein inhibits its own expression from E7 to E19 by producing a premature stop codon. This hypothesis was corroborated by nuclear localization of FMRP immunoreactivity at the ages before and during FMRP intensity reduction.

In summary, NM neurons actively down regulate FMRP protein synthesis during a critical developmental window and this down regulation is likely governed by a novel FMRP autogenously regulation.

PS 99

Neuronal diversity in the inner ear revealed by single-cell RNA sequencing

Charles Petitpre[1]; Anil Sharma[1]; Anna Tokarska[1]; Haohao Wu[1]; Francoise Helmbacher[2]; Gilad Sildeberg[1]; Saida Hadjab[1]; Francois Lallemend[1]
[1]Karolinska Institutet; [2]IBDM (Developmental Biology Institute of Marseille

Our ability to encode acoustic signals to the brain depends on a highly specified and functional cochlear nervous system. Two types of neurons coexist in the cochlea. The type I neurons constitute the majority of the neurons and are the principal carrier of the auditory signal. On the other hand, despite much speculation, the contribution of the type II population to hearing in vivo

is still largely unknown. Moreover, the heterogeneous physiological features within type I SGNs has suggested the existence of distinct classes of type I auditory afferents, with different functions in hearing. Here, by using the single-cell RNA sequencing technique, we characterize the genetic profile of type II SGNs and reveal the presence of distinct populations of type I SGNs. Combining mouse genetics with RNAscope and immunostaining, we provide anatomical evidence of three distinct subtypes of type I SGNs and of their differential projection pattern at the inner hair cell level. Our data suggest a genetic determination, independent of sensory activity, of different classes of type I SGNs that could explain the large heterogeneity in the electrophysiological profile of the type I afferents and could in vivo encode distinct auditory features in the periphery.

PS 100

The Intrinsically Disordered Region within Prestin's C-terminal Impacts Protein Expression in Outer Hair cells

Tetsuji Yamashita[1]; **Satoe Takahashi**[2]; Kazuaki Homma[2]; Yingjie Zhou[3]; Jian Zuo[1]; Jing Zheng[2]; Mary Ann Cheatham[3]
[1]Department of Developmental Neurobiology, St. Jude Children's Research Hospital, Memphis, Tennessee, USA; [2]Northwestern University; [3]Department of Communication Sciences and Disorders, Northwestern University

Background

Outer hair cells (OHC) express the motor protein, prestin, which is required for sensitivity and frequency selectivity, the hallmarks of mammalian cochlear function. Our previous work shows that a calmodulin binding site (CBS) is located in prestin's C-terminal, and specifically within the intrinsically disordered region (IDR). Because prestin's function could potentially be influenced by calmodulin, we sought to investigate the role of prestin's CBS on motor function. Hence, a prestin knockin mouse with this region deleted was developed to study the functional significance of calmodulin binding, which is known to be calcium dependent.

Methods

The targeting construct was evaluated using patch clamp recordings in HEK293T cells prior to developing the homologous recombinant ES cells. The phenotype of mutant mice was defined using distortion product otoacoustic emissions (DPOAE) and auditory brainstem responses (ABR). Anatomical evaluations were obtained by constructing cytograms to document OHC loss and by using immunofluorescence to evaluate protein expression. Multiple primer pairs were then designed to interrogate prestin's mRNA using RT-PCR.

Results

The targeting construct was designed to create hybrid exons 17 and 18 by deleting amino acids 571-635, i.e., the CBS and some of the IDR. When a similar cDNA construct was transfected into HEK293T cells, it targeted the membrane and exhibited nonlinear capacitance (NLC) that maintained fast motor kinetics and sensitivity to cholesterol. After confirming homologous recombination, a ΔIDR prestin knockin mouse was developed and the neomycin cassette used to facilitate ES cell screening was removed. The phenotype in homozygous mice was similar to that in prestin knockouts as DPOAE and ABR thresholds were elevated 40-50 dB, NLC could not be measured and OHCs were missing from basal regions of the cochlea. Although ΔIDR prestin mRNA was measured, RT-PCR showed that exons 17 and 18 were absent, rather than only those portions targeted for deletion. Despite the presence of mRNA, no prestin protein was observed using both anti-N-mprestin and anti-C-mprestin in neonatal (P5-8) and adolescent mice.

Conclusions

Given the presence of ΔIDR mRNA, the lack of prestin protein is provocative and implies that the IDR may include regulatory elements that influence mRNA splicing and protein expression. Even though several RNA surveillance mechanisms serve to minimize the production of potentially toxic mutated proteins, these mechanisms do not provide a clear explanation of our results. Hence, further investigations are required to learn the implications of IDR removal on prestin's translational efficiency. (Supported by NIDCD DC000089 and DC006471).

PS 101

Unique Expression of Gene Orthologs in Zebrafish and Mouse Non-sensory Supporting Cell Populations of the Inner Ear

Kimberlee P. Giffen[1]; Huizhan Liu[1]; Lei Chen[1]; Sean T. Stringham[2]; Kenneth L. Kramer[1]; Kirk W. Beisel[1]; David Z. He[1]
[1]Creighton University; [2]Creighton University School of Medicine

Background

Non-mammalian vertebrates, including zebrafish, retain the ability to regenerate hair cells (HCs) due to unknown molecular mechanisms that regulate proliferation and conversion of non-sensory supporting cells (SCs) to HCs, while mammals lack the ability to do so. We hypothesize that identification of uniquely expressed orthologous genes in mouse and zebrafish SCs will reveal gene candidates involved in the transdifferentiation of SCs to HCs.

Methods

Homogenous populations of zebrafish non-sensory surrounding cells (zSCs) and mouse non-sensory supporting cells (mSCs) (pillar and Deiters cells) from the inner ear were isolated (~1,000 cells of each type with three biological replicates) using our novel suction-pipette technique. Total RNA was collected and sequenced (Illumina). Gene expression values, derived from reads mapped to the zebrafish genome (GRCz10) and mouse genome (GRCm38.5), were merged and analyzed. A list of orthologous zebrafish and mouse protein-coding genes was generated using Ensembl Biomart. Expressed ortholog genes had a value greater than 0.1 RPKM (p < 0.05).

Results

Comparison of mouse and zebrafish genomes revealed that 79% of mouse protein-coding genes have at least one zebrafish ortholog, and over 50% of those have a one-to-one zebrafish ortholog. Out of 17,497 orthologs, a total of 13,177 protein-coding genes were expressed in zSCs. A total 13,782 orthologous genes were expressed in mSCs. Analysis of uniquely expressed genes revealed 710 one-to-one orthologs that were expressed in zSCs compared to mSCs. Of these, 101 transcription factor genes, including *zic1*, *zic3*, *dmrt2a*, and *bcl11ba,* were solely expressed in zSCs and not in other zebrafish inner ear cell types.

Discussion

Critical analysis of these unique orthologous gene expression profiles of zebrafish and mouse inner ear cells will reveal critical transcription factors and potential downstream targets that may initiate conversion of SCs to HCs. This research shows further promise for identifying potential therapeutic targets for conversion and proliferation of supporting cell populations to regenerate mammalian hair cells *in vivo*.

PS 102

Mocha: A Novel Microglial Cell Line From Rat Cochlea

Gail Seigel[1]; **Senthilvelan Manohar**[1]; Bai Yingying[2]; Dalian Ding[1]; Richard Salvi[3]
[1]University at Buffalo, USA; [2]Southeast University, Nanjing, China; [3]Center for Hearing and Deafness; State University of New York at Buffalo

Background

Microglia are phagocytic mononuclear cells of the central nervous system that play a critical role in neural development, neuroprotection and immune function. However, little is known about the biology of microglia that reside in the cochlea, a site vulnerable to damage by aging, noise and ototoxic compounds. The goal of this project was to develop a novel microglial cell line derived from rat cochlea as a novel in vitro model for the study of neuroprotective and ototoxic processes. Methods: We isolated and enriched a subpopulation of CD11b+ cells from the rat cochlea and immortalized these cells with the 12S E1A gene of adenovirus in a replication-incompetent retroviral vector to derive a novel microglial cell line, designated Mocha (microglia of the cochlea). Mocha cells were selected for two weeks on the basis of neomycin resistance and then examined for the presence of microglial characteristics by immunocytochemistry, gene array analysis, lipopolysaccharide (LPS) response, and the ability to phagocytose fluorescent beads. Results: Mocha cells expressed a number of markers consistent with microglia as shown by gene array analysis [TMEM119, IGF-1, CD68, TNFR1, CD54 (ICAM-1), CD40, CD74, Ccl2, B7-1, IF-NgR , Sgpp1, IL1R1, IL13RA1, IL15RA, CCR5, Cox2, P2Y12, Il6R and MAP2], which was further validated by immunocytochemistry [CD68, Sox10, CD11b, CD40, Iba1, TMEM119, IL-1beta, CD45 and F4/80]. Mocha cells responded to LPS stimulation by upregulation of genes [Cox2, ICAM-1, Il6r, Ccl2, Il13Ra and Il15Ra] as well as release of cytokines [IL-1beta, IL-12, IL-13 and RANTES] as detected by ELISA. Mocha cells exhibited typical microglial behavior by phagocytosis of fluorescent beads at 37 ºC, but not at 4 ºC. The expression pattern of microglial markers in Mocha cells suggests that immortalization may lead to a more primitive phenotype, a common phenomenon in immortalized cell lines. Conclusions: Mocha cells demonstrate important characteristics of microglia, including expression of microglial markers, cytokine release in response to LPS, as well as phagocytosis. Mocha cells are now available as a useful in vitro model system for the study of microglial behavior.

PS 103

The Identification of Cholesterol Metabolic Pathways of the Inner Ear that Impact Hearing

Karen S. Pawlowski; **Joyce J. Repa**
UT Southwestern Medical Center

A limited number of clinical studies have suggested a correlation between circulating lipid levels and sensorineural hearing loss, but this finding has not been consistent. In instances where effects were observed, any sterol-associated decline in hearing was suggested to result from diminished blood flow secondary to angiopathic mechanisms. However, recently, three human genetic disorders resulting from aberrant cellular cholesterol metabolism have been associated with hearing loss: Niemann-Pick type C disease (NPC, OMIM#257220), MEGDEL syndrome (OMIM#614738), and DFNA67

(OMIM#616340). In addition, 2-hydroxypropyl-beta-cy-clodextrin, a cholesterol-chelating agent and therapy for NPC disease, causes immediate and irreversible hearing loss coincident with outer hair cell loss in mice and humans. Thus accumulating evidence supports a role for cholesterol in hearing.

Taking advantage of the numerous genetic mouse strains developed at UT-Southwestern for cholesterol research, we have initiated hearing screens to identify sterol metabolic pathways that impact inner ear function. Here we will present initial data from three of our knockout mouse strains (*Abcg1-/-, Abca1-/-* and *LXR-/-*) to suggest that cholesterol efflux pathways impact cells of the inner ear to affect hearing.

ATP-binding cassette transporter G1 (ABCG1) is an intracellular protein that promotes cholesterol trafficking and efflux from cells to preformed HDL particles. Mice lacking ABCG1 exhibited abnormal auditory brainstem response (ABR) thresholds by 2.5-months (males) and 6-months (females) of age at all frequencies tested (4, 16, 32 kHz) compared to wildtype littermate controls. Analyses for localization of ABCG1 in the mouse cochlea revealed that ABCG1 is very highly expressed ~exclusively in inner and outer hair cells and marginal cells of the stria vascularis. The absence of ABCG1 elicits a change in RNA levels of the inner ear consistent with an increase in cellular cholesterol content (increased ABCA1, decreased SREBP2 and LDLR mRNA species). There is a modest loss of outer hair cells observed in mice lacking ABCG1, but no significant change in markers of inflammation in the inner ear (as observed in the lungs of these mice).

The other cholesterol efflux protein, ATP-binding cassette transporter A1 (ABCA1), resides in plasma membranes to facilitate the egress of cellular cholesterol to apoprotein acceptors in the formation of nascent HDL particles. The sterol-sensing transcription factor, LXR, regulates the expression of both ABCA1 and ABCG1. Mice lacking ABCA1 or LXR also exhibit significant hearing loss as revealed by ABR testing. These studies implicate the importance of cholesterol elimination/efflux pathways in cells of the inner ear to impact hearing function.

PS 104

Whole Exome Sequencing to Discover Novel Genes Associated with Hearing Loss

Hideki Mutai[1]; Yukihide Momozawa[2]; Yoichiro Kamatani[3]; Michiaki Kubo[4]; Tatsuo Matsunaga[5]
[1]*Division of Hearing and Balance Research, National Institute of Sensory Organs, National Hospital Organization Tokyo Medical Center;* [2]*Laboratory for Genotyping Development, Center for Integrative Medical Sciences, RIKEN;* [3]*Laboratory for Statistical Analysis, Center for Integrative Medical Sciences, RIKEN;* [4]*Center for Integrative Medical Sciences, RIKEN;* [5]*Division of Hearing and Balance Research, National Institute of Sensory Organs/ Medical Genetics Center, National Hospital Organization Tokyo Medical Center*

Background
Targeted next-generation sequencing (NGS) has been applied for diagnostic test of deafness genes. Focusing on up to approximately 100 deafness genes can efficiently detect pathogenic mutations. However, number of genes associated with nonsyndromic and syndromic hearing loss is several hundred and still counting, indicating that as for gene research, wider range of genes should be analyzed to detect cause of hereditary hearing loss. In this study, we conducted whole exome analysis (WES) to the patients with hearing loss.

Methods
Japanese subjects with hearing loss and their parents (72 families, 215 individuals) participated the study after written informed consent from the patients and/or their parents. They had been subjected to genetic screening of either m.1555A>G, m.3243A>G and *GJB2* mutation, cytomegalovirus in the umbilical cord, Sanger sequencing of candidate genes based on the clinical features, genetic test of up to 154 mutations in 19 genes (GeneticTestMolBiomark 2015(19) 209), or NGS analysis targeting 119 deafness genes (OJRD 2103(8) 172) with no results. Genomic DNA was subjected to capture whole exome region using Illumina Nextera Kit and sequencing using HiSeq2500 (Illumina). Paired-end read sequences were mapped on human reference sequence GRCh37, and variants were joint-called using in house sequencing data (WES, n= 348 and whole genome sequencing, n= 1037). Variants were filtered by MAF (

Results
WES analysis identified 22 candidate genes in 34 out of 72 family. Among them, 12 genes categorized in Tier 1 were identified in 22 families. In addition, 10 novel candidate genes were identified in 12 families, including 2 genes previously reported to associate with hearing loss in animal models (Tier 2) and a gene predominantly expressed in macaque cochlea (Tier 3). Accumulation of the subjects, *in vivo*, and *in vitro* analysis would prove the association of these genes with hearing loss.

Conclusions
WES analysis is useful for discovering novel deafness genes and has important implication for future diagnostic test.

PS 105

Biochemical evidence for the tRNAIle 4317A>G mutation in the phenotypic manifestation of deafness-associated mitochondrial 12S rRNA mutation

Feilong Meng[1]; Jing Zheng[2]; **Min-Xin Guan**[1]
[1]*Zhejiang University;* [2]*Northwestern University*

Mitochondrial 12S rRNA 1555A>G mutation has been associated with aminoglycoside-induced and nonsyndromic deafness in many families worldwide. Mitochondrial modifiers are proposed to modify the phenotypic expression of deafness-associated m.1555A>G mutation. In this study, we demonstrated that the deafness susceptibility allele (m.4317A>G) in the tRNA[Ile] gene modulated the phenotypic expression of m.1555A>G mutation. One Chinese pedigree carrying both m.4317A>G and m.1555A>G mutations exhibited much higher penetrance of deafness than those carrying only m.1555A>G mutation. It was hypothesized that the m.4317A>G mutation at a highly conserved adenine at position 59 at the T-loop altered both the structure and function of tRNA[Ile]. Using lymphoblastoid cell lines cell lines derived from members of these Chinese families (three carrying both m.1555A>G and m.4317A>G mutations, three harboring only m.1555A>G mutation and three control subjects lacking these mutations), we demonstrated that these cell lines bearing both m.4317A>G and m.1555A>G mutations exhibited more severe mitochondrial dysfunctions than those carrying only m.1555A>G mutation. Especially, the m.4317A>G mutation perturbed the conformation, stability and aminoacylated efficiency of tRNA[Ile]. These alterations in tRNA[Ile] metabolism caused by the m.4317A>G mutation aggravated the defective mitochondrial protein synthesis and respiratory phenotypes associated with m.1555A>G mutation. Furthermore, more reductions in the levels of mitochondrial ATP and membrane potentials, increasing production of reactive oxygen species were also observed in mutant cells bearing both m.4317A>G and m.1555A>G A mutations than those carrying only m.1555A>G mutation. Our findings provided new insights into the pathophysiology of maternally inherited deafness that were manifested by interaction between 12S rRNA and tRNA mutations.

Guan Abstract 2.docx

PS 106

a Nuclear Modifier Allele (A10S) in TRMU (Methylaminomethyl-2-thiouridylate-methyltransferase) Related to Mitochondrial tRNA Modification in the Phenotypic Manifestation of Deafness-associated 12S rRNA Mutation

Feilong Meng; **Min-Xin Guan**
Zhejiang University

Nuclear modifier gene(s) was proposed to modulate the phenotypic expression of mitochondrial DNA mutation(s). Our previous investigations revealed that a nuclear modifier allele (A10S) in TRMU (methylaminomethyl-2-thiouridylate-methyltransferase) related to tRNA modification interacts with 12S rRNA 1555A→G mutation to cause deafness. The A10S mutation resided at a highly conserved residue of the N-terminal sequence. It was hypothesized that the A10S mutation altered the structure and function of TRMU, thereby causing mitochondrial dysfunction. Using molecular dynamics simulations, we showed that the A10S mutation introduced the Ser10dynamic electrostatic interaction with the Lys106 residue of helix 4 within the catalytic domain of TRMU. The Western blotting analysis displayed the reduced levels of TRMU in mutant cells carrying the A10S mutation. The thermal shift assay revealed the *T*m value of mutant TRMU protein, lower than that of the wild-type counterpart. The A10S mutation caused marked decreases in 2-thiouridine modification of U34 of tRNALys, tRNAGlu and tRNAGln However, the A10S mutation mildly increased the aminoacylated efficiency of tRNAs. The altered 2-thiouridine modification worsened the impairment of mitochondrial translation associated with the m.1555A→G mutation. The defective translation resulted in the reduced activities of mitochondrial respiration chains. The respiratory deficiency caused the reduction of mitochondrial ATP production and elevated the production of reactive oxidative species. As a result, mutated TRMU worsened mitochondrial dysfunctions associated with m.1555A→G mutation, exceeding the threshold for expressing a deafness phenotype. Our findings provided new insights into the pathophysiology of maternally inherited deafness that was manifested by interaction between mtDNA mutation and nuclear modifier gene.

Guan Abstract 1.docx

PS 107

Developmental Profiling of the Human Embryonic Inner Ear by MicroRNA Sequencing and Pathway Analysis using a Formalin-Fixed Paraffin-Embedded (FFPE) Specimen

Cong Ran[1]; Duncan Chadly[2]; Jennifer Best[1]; Małgorzata Bruska[3]; Adam Piortowski[3]; Bartosz Kempisty[3]; Mark Schwartz[4]; Bonnie LaFleur[4]; Bj Kerns[4]; John Kessler[1]; Akihiro Matsuoka[5]
[1]Feinberg School of Medicine at Northwestern; [2]California Instituite of Technology; [3]Poznań University; [4]HTG Molecular Science; [5]Northwestern University Feinberg School of Medicine

Background

The advancement of stem cell replacement therapies for sensorineural hearing loss is contingent on outlining the regulatory and developmental pathways of the human inner ear in order to direct differentiation of progenitors. Due to the extreme inaccessibility of fetal human inner ear tissue, in vivo animal studies have been utilized to investigate key microRNAs (miRNAs) that regulate developmental pathways of the inner ear. In this study, we harnessed a unique opportunity to perform the first miRNA sequencing of otic precursors in human specimens.

Methods

We obtained paraffin embedded (FFPE) human embryonic specimen at Carnegie developmental stages 13-15, which corresponds to embryonic day 11 (E11), E11.5 and E12. Three FFPE slides were used for obtaining enough material from each tissue type. Laser catapulting micro-dissecting technique was used to specifically identify and acquire tissue areas of interest, which are cochlear vestibular ganglion (CVG), neural crest (NC), and otic vesicle (OV). Subsequently, using HTG miRNA Whole Transcriptome assay, we obtain miRNA expression profiles of CVG, NC and OV at three developmental stages. Overexpression analysis and gene set enrichment analysis were performed on the transcriptome results to decipher the most differentially expressed miRNAs and the associated functional gene expression pattern.

Results

We identified that differentially expressed miRNAs of the CVG included miRNA-183 family (miRNA-96, miRNA-182, and miRNA-183) when comparing the miRNA profile using the overexpression analysis. When examining the gene expression predicted by the miRNA profile in these samples, Dicer pathway found to be most significantly upregulated in CVG over NC at stage 13, which could have developmental significance in the human inner ear. Other specific pathways found differentially expressed in CVG compared to NC or OV included FGF, IGF and Wnt pathways at various developmental stages. Additionally, genes that are functionally related to auditory development or neuronal development in CVG are more differentially regulated earlier at stage 13 when compared to the later stages.

Conclusions

For the first time in human embryonic tissues, we were able to demonstrate that miR-183 family are differentially expressed in the CVG comparing to NC or OV, which was previously postulated from murine models. We further identified other transcription factors that are differentially targeted in the CVG compared to the other tissues in a temporal manner. Our results provide the starting point for more detailed investigations of the role of these many pathways in spiral ganglion regeneration and for a description of their possible interactions.

PS 108

Whole Exome Sequencing Identified a Novel Mutation in HOMER2 for Autosomal Dominant Nonsyndromic Deafness in a Chinese Family

Xingxing Lu; Qi Wang; Hongbo Gu; Xiao Zhang; Yanmei Zhang; Yuhe Liu
Department of Otolaryngology,Head & Neck Surgery Peking University First Hospital

Hearing loss is one of the most common sensory disorders worldwide, and about half of cases attributable to genetic factors. Hereditary hearing loss is an extremely heterogeneous disease with variable pathogenesis. To date, more than 150 genes were found to be related with hearing loss. *HOMER2* gene was reported newly to be a gene, which';s mutation results in autosomal dominant hearing loss. Here, we identified a novel mutation in *HOMER2* in a Chinese family with autosomal dominant, non-syndromic, progressive sensorineural hearing loss. It was the second reported family with hearing loss caused by mutation in *HOMER2* in the world. After excluding plausible variants in known deafness-causing genes using a deafness-specific panel of 140 genes in the proband, we performed whole exome sequencing in two hearing-impaired and one normal family members. The mutation c.840_841insC in *HOMER2*, segregating with the hearing loss phenotype in the extended family, was most probably a disease-causing mutation. The mutation was not found in the dbSNP database and the 1000 genomes SNP database, in 76 patients with sporadic hearing loss, or in 100 normal individuals. The insertion mutation leads to a frameshift and a premature stop codon producing a truncated HOMER2 protein (aa288) with abnormal protein sequence from aa280. HOMER2 belonged to the homer family of post-synaptic density scaffolding proteins. The coiled-coil domain in C-terminal of HOMER2 protein was essential for protein multimerization and the HOMER2-CDC42 interaction.

We performed QRT-PCR, western blot and immuno-fluorescence to investigate the potential pathogenic mechanisms. We found that mutant HOMER2 protein is less stable than wild-type HOMER2. The ability to multimerize of $HOMER2_{MU}$ decreased significantly than $HOMER2_{WT}$ and $HOMER2_{G587C}$. In HEI-OC1 hair cells and HEK 293T cell lines, $HOMER2_{MU}$ tended to distribute in a diffuse manner, whereas $HOMER2_{WT}$ and $HOMER2_{G587C}$ proteins tended to cluster together at a side of the nucleus. HOMER2 was involved in calcium homeostasis and stereocilia maintenance, and homo/hetero-multimerization might be its first step to exert its normal functions. Reduced multimerization capability of mutant HOMER2 might be the key pathogenic mechanism. The *HOMER2* deafness-causing Chinese family provided compelling evidence that *HOMER2* is indeed required for normal hearing and its sequence alteration is responsible for late-onset autosomal dominant non-syndromic sensorineural hearing loss in humans.

Key words
Hearing loss , HOMER2 , Insertion mutation, Multimerization, CDC42

PS 109

RNA-seq analysis of gene expression profiles in isolated stria vascularis from wild type and Alport mice reveals key pathways underling Alport strial pathogenesis.

Dominic Cosgrove[1]; Brianna Dufek[1]; Daniel Meehan[1]; Duane Delimont[1]; Grady Phillips[2]; Michael Anne Gratton[2]
[1]Boys Town National Research Hospital; [2]Washington University

RNA-seq analysis of gene expression profiles in isolated stria vascularis from wild type and Alport mice reveals key pathways underling Alport strial pathogenesis. Dominic Cosgrove*, Brianna Dufek*, Daniel T. Meehan*, Duane Delimont*, Grady Phillips# and Michael Anne Gratton# *Boys Town National Research Hospital, Omaha, NE; #Washington University, Saint Louis MO Previous work from our labs demonstrate that the hearing loss in Alport mice is caused by defects in the stria vascularis. As the animals age, progressive thickening of the strial capillary basement membranes (SCBMs) occurs associated with elevated levels of extracellular matrix expression and elevated levels of hypoxia-related gene and protein expression. These conditions render the animals susceptible to noise-induced hearing loss associated with a significant drop in endocochlear potential, again pointing to reduced capacity of lateral wall function. In an effort to develop a more comprehensive understanding of how the underlying mutation in the COL4A3 gene influences homeostasis in the stria vascularis, we per-formed RNA-seq analysis using isolated stria vascularis from 7-week old wild type and Alport mice on the 129 Sv background. The stria from 6-8 mice were pooled and two independent experiments were performed. RNA-seq and bioinformatics analysis were performed at the University of Nebraska Medical Center's genomics and bioinformatics core facilities. Hundreds of genes were induced (5 to 48-fold) or suppressed (5 to 20-fold) in the stria from Alport mice relative to wild type. These included transcription factors associated with the regulation of pro-inflammatory responses including (but not limited to) Gata2, STAT-1, JUNB, which regulate a large number of cytokines, chemokines, and chemokine receptors, as well as transcription factors involved in developmental pathways including POU4F1, POU4F2 and FOXA1. Canonical pathways included modulation of genes associated glucose and glucose-1-PO4 degradation, NAD biosynthesis, histidine degradation, calcium signaling, and glutamate receptor signaling (among others). In all, the data point to the Alport stria being in an inflammatory state with disruption in numerous metabolic pathways indicative of metabolic stress, a likely cause for the susceptibility of Alport mice but not age-matched wild type controls to permanent noise-induced hearing loss. The work lays the foundation for studies aimed at understanding the nature of strial pathology in Alport mice which could provide important biomarkers for therapies aimed at ameliorating hearing loss associated with the Alport mouse. The modulation of these biomarkers under condition of therapeutic intervention may provide important pre-clinical data to justify trials in humans afflicted with the disease.

PS 110

Mitochondrial 12S rRNA 1555A>G mutation caused abnormal morphology and dysfunction of the derived hair cell-like cells from iPSCs

Feilong Meng; Xiaoli Zhao; Min-Xin Guan
Zhejiang University

The mitochondrial 12S rRNA 1555A>G (m.1555A>G) mutation has been associated with both aminoglycoside-induced and nonsyndromic hearing loss. However, the tissue-specific effect of this mutation remains poorly understood. In this report, we generated iPSCs from dermal fibroblasts derived from one symptomatic and one asymptomatic matrilineal relatives of a Chinese family carrying m.1555A>G mutation and one control subject lacking this mutation. The iPSCs were subjected to hair cells differentiation with a two step-induction protocol. Firstly, the iPSCs differentiated into the otic epithelial progenitors (OEPs). Immunocytochemistry showed that OEPs expressed early otic markers, including PAX2, PAX8 and SOX2. The OEPs were then induced into hair cell-like cells on mitotically inactivated chicken utricle

stromal cells. Immunocytochemistry revealed that the hair cell-like cells induced from mutant and control iPSCs expressed hair cell markers, including BRN3C and MYO7A. Reverse transcriptional PCR analysis showed that the induced cells expressed hair cell marker genes *BRN3C*, *MYO7A* and *ESPIN*. Furthermore, the hair cell-like cells can rapid take up the FM1-43 dye, indicating the functional activity of mechanotrasduction channels. The m.1555A>G mutation resulted in abnormal morphology and dysfunction of the derived hair cell-like cells. Our finding may provide new insight into pathophysiology of maternally inherited hearing loss and valuable information and technology for the therapeutic approaches for hearing loss.

PS 111

Delivery of Adeno-Associated Viral Vectors in Adult Mammalian Inner Ear Cell Subtypes without Auditory Dysfunction

Yong Tao[1]; Mingqian Huang[2]; Yilai Shu[3]; Adam Ruprecht[4]; Hongyang Wang[5]; Yong Tang[6]; Luk Vandenberghe[6]; Qiuju Wang[7]; Guangping Gao[8]; Weijia Kong[9]; Zheng-Yi Chen[10]
[1]*Shanghai Jiao Tong University;* [2]*1. Department of Otolaryngology, Harvard Medical School, 2. Eaton-Peabody Laboratory, Massachusetts Eye and Ear Infirmary;* [3]*1. Department of Otolaryngology, Harvard Medical School, 2. Eaton-Peabody Laboratory, Massachusetts Eye and Ear Infirmary, 3. Department of Otolaryngology, Hearing Research Institute, Affiliated Eye and ENT Hospital of Fudan University;* [4]*Eaton Peabody Laboratory, Massachusetts Eye and Ear Infirmary;* [5]*Eaton Peabody Lab, MEEI, Harvard Medical School/Chinese PLA General Hospital;* [6]*Massachusetts Eye and Ear Infirmary;* [7]*Chinese PLA General Hospital;* [8]*University of Massachusetts Medical School;* [9]*Huazhong University of Science and Technology;* [10]*1. Department of Otolaryngology, Harvard Medical School, 2. Eaton Peabody Laboratory, Massachusetts Eye and Ear Infirmary*

Background

Adeno-associated virus (AAV)-mediated gene transfer has been shown to effectively restore auditory functions in mouse models of genetic deafness when delivered at neonatal stages. However, the mouse cochlea is still developing at those time points whereas in human the newborn inner ears are already fully mature. Surgical procedure cochleostomy, which is effective for neonatal delivery, has been shown to be detrimental to outer hair cell survival with hearing loss. Therefore it is important to determine the effectiveness of AAV infection in adult mouse cochlea for the route of delivery and the cell types to be targeted.

Methods

Ten-week-old male C57BL/6J mice were randomly assigned to the different experimental groups, with at least three mice in each group. 1 μL of AAV1, 2, 6.2, 8, 9, rh.39, rh.43-CMV-EGFP or AAV2/Anc80L65.CMV. EGFP.WPRE was injected via the posterior semicircular canal. 2 weeks later, auditory brainstem response (ABR) and distortion product otoacoustic emission (DPOAE) were performed. Cochleae were harvested and dissected, and MYO7A and GFP antibodies were used to label hair cells and infected cells. Hair cells and GFP positive cells were quantified for each individual AAV serotype for comparison.

Results

Canalostomy preserves hair cells and maintains normal hearing after injection. AAV serotypes AAV2, 8, 9, rh.39, rh.43 and Anc80 transduce the sensory inner hair cells efficiently, but with lower efficiency in transducing outer hair cells. AAV1 and 6.2 transduce inner or outer hair cells inefficiently. A subset of AAVs, including AAV1, 2, 6.2, 8, rh.43 and Anc80, also transduces some supporting cells and non-sensory cochlear cell types with generally lower efficiency.

Conclusions

Canalostomy approach establishes an efficient and safe route for inner ear delivery in adult cochlea without hearing impairment.Multiple AAV vectors can infect hair cells, as well as some supporting cells and non-sensory cells. The infection efficiency is the highest in the inner hair cells, and is reduced in other cell types. The ability of different AAV vectors that target diverse adult cochlea cell types with varying efficiencies provides an opportunity for their use in gene therapy to treat genetic deafness in mature mice. Future study to identify new AAV vectors to target other cell types efficiently should be a priority in order to broaden their application to treat hearing loss as the results of genetic defects in non-hair cells.

PS 112

Comprehensive analysis of alternative splicing variants identified from tonotopical differences in the mouse cochlea

Shin-ya Nishio; Shin-ichi Usami
Department of Otorhinolaryngology, Shinshu University School of Medicine

Background

The mammalian cochlea is a spiral shaped auditory sensing organ, with the mouse cochlea forming 2.5 turns around its axis. This cochlear structure has an important role in the mechanism for distinguishing sound frequency. This mechanism, based on the synchronized vibra-

tion of the basilar membrane, is thought to be caused by differences in the thickness and width of the basilar membrane. Of course, these morphological and physiological characteristics of the inner ear are related to differences in gene expression along the tonotopic axis. We previously reported the gene expression profiles in the apical, middle and basal turn of cochlea and identified a number of genes associated with high frequency hearing loss the expression of which increased in a gradient along the tonotopic axis. In this study, we performed exon-level gene expression analysis using the cDNA microarray to identify alternative splicing variants in specific regions of the cochlea.

Methods

Temporal bone samples from 6-week-old C57BL/6 mice (n=4) were extracted under deep anesthesia. The inner ears were extracted from the temporal bone, transferred into RNAlater solution and then separated into the apical, middle and basal turns. Total RNA samples were extracted from each part of cochlea and gene expression levels for each exon were analyzed using SurePrint G3 Mouse Exon Microarrays (165,984 exon probes for 24,547 genes).

Results

As a result, we identified cochlear turn-specific alternative splicing variants in many genes. Among these genes, 44 genes fulfilled the criteria for confident splicing variants, which were set at a splicing index of over 1.0 (i.e., a 2-fold or more change in signal intensity was observed for each turn of the cochlea) and a p-value of under 0.05 (i.e., a statistically significant difference was observed). Among the 44 confident alternative splicing genes, *Otog* and *Strc* were previously reported to be responsible for hearing loss. We also identified the following suspected alternative splicing variants in each turn of cochlea; *Col2a1*, *Col4a3*, *Col11a1*, *Col11a2*, *Eya1*, *Myh9*, *Myh14*, *Myo7a*, *Otof*, *Slc26a4*, *Slc26a5*, *Tjp2*, *Ush1c*, and *Whrn.*

Conclusion

We identified many candidate alternative splicing variants that are speculated to be associated with tonotopy. This dataset will provide a useful base for more detailed studies of cochlear function. However, these results were based on cDNA microarray data and further study is required to confirm their involvement.

PS 113

Novel Computational Molecular Biophysics Algorithms to Classify Missense Variants: Application to GJB2

Hernan Bernabe[1]; Michael Schnieders[1]; Richard J. H. Smith[2]
[1]Department of Biomedical Engineering; [2]Molecular Otolaryngology and Renal Research Laboratories, Department of Otolaryngology—Head and Neck Surgery, Carver College of Medicine, University of Iowa

The most common genetic birth defect diagnosed in the developed world today is hereditary hearing loss. In many different ethnic groups, when the hearing loss is severe-to-profound, the majority of newborns will carry genetic variants in the gene *GJB2*, which encodes the protein connexin 26. Connexin 26 participates in the recycling of potassium in the cochlea, however because functional studies are not available on most genetic variants in this gene, these variants are classified as variants of uncertain significance (VUS). Herein we use computational biophysical techniques to measure the predicted effects of VUSs on Connexin 26 function to facilitate refined classification of these VUSs. We hypothesized that a significant change in free energy (>1 kcal/mol), which is indicative of protein misfolding, would correlate with pathogenicity. We tested and verified this hypothesis on control variants of a known status using our computational biophysical technique. Side-chain optimization of the native and mutant model structures of connexin 26 provided a stable starting state for our comparative computational analysis. This optimization was accomplished using the AMOEBA polarizable force field in conjunction with an innovative, hybrid Force Field X (FFX) and OpenMM side-chain repacking algorithm, which offered significant speed compared to prior optimization efforts. Changes in protein folding stability were calculated between the wildtype and mutant models. We demonstrate that our hybrid algorithm offers a faster exploration of the free energy surface associated with a mutation, as well as faster convergence on the total change in free energy when compared to non-hybrid approaches. Results of these calculations indicate whether a mutation causes significant destabilization of native folding thus leading to impaired function and ultimately hearing loss. We conclude from this study that this approach provides a valuable tool for VUS classification in hearing loss. As such, we expect our algorithm to prove advantageous in interpreting genetic data associated with hearing loss and other diseases. (Supported in part by NIDCD R01 DC012049).

PS 114

OtoProtein: Protein Optimization and Physics-Based Analysis of Genetic Missense Variants Associated with Deafness

Mallory Tollefson[1]; Hernan Bernabe[1]; Kevin Booth[2]; Hela Azaiez[3]; Jill Hauer[4]; Carla Nishimura[3]; E Ann Black-Ziegelbein[4]; Jacob Litman[5]; Terry Braun[1]; Richard J. H. Smith[3]; Michael Schnieders[1]
[1]Department of Biomedical Engineering; [2]Molecular Otolaryngology and Renal Research Laboratories, Department of Otolaryngology—Head and Neck Surgery; Interdisciplinary Graduate Program in Molecular Medicine, Carver College of Medicine, University of Iowa; [3]Molecular Otolaryngology and Renal Research Laboratories, Department of Otolaryngology—Head and Neck Surgery, Carver College of Medicine, University of Iowa; [4]Department of Otolaryngology-Head and Neck Surgery; [5]Department of Biochemistry

Accurate classification of missense variants as pathogenic or benign is a crucial step in translational genetic research. Current classification schemes often use a combination of bioinformatics tools such as SIFT, CADD, and FoldX to analyze genetic variants of unknown significance in patients with hearing loss. These prediction tools assess the pathogenicity of a variant based primarily on sequence conservation; however, they often yield ambiguous or even contradictory results. Computational molecular biophysics provides a complementary approach by incorporating three-dimensional protein structures and first principles thermodynamic assessment into variant classification algorithms. We applied free energy perturbation (FEP) to calculate the mutational folding free energy ($\Delta\Delta G_{WT>Variant}$) of sixty USH2A variants from the Deafness Variation Database (DVD), which are associated with hearing loss. We hypothesized that a significant (>1 kcal/mol) free energy change, indicative of substantial protein folding destabilization and/or misfolding, correlates with pathogenicity. Assessment of this hypothesis was tested using thermodynamic predictions on positive and negative control variants of known status, *i.e.* those classified specifically as benign or pathogenic according to the DVD. FEP calculations on positive and negative controls showed agreement with the DVD. We recently designed a parallelization scheme utilizing Nvidia graphical processing units (GPUs) to accelerate our atomic resolution assessment algorithms. With the use of one GPU, our side-chain optimization algorithm achieved a 67 times speed-up compared to using two Intel Xeon E5-2680v4 central processing units (CPUs). These simulations remain time consuming to prepare, troubleshoot, and analyze, and thus require the attention of experienced computational scientists. To address this challenge, we designed a web-based application called "OtoProtein", the goal of which is to provide user-friendly access to biophysical algorithms while requiring little specialized knowledge of simulation methods. In its current state, OtoProtein provides intuitive access to cutting-edge biophysical optimization algorithms. Ultimately, we expect OtoProtein to provide access to missense variant classification algorithms, which will complement and augment diagnostic capabilities.

PS 115

Expression of LOXHD1b gene in the Hair Cell Bundles of Zebrafish

Shunsuke Tarumoto; Kazuma Sugahara; Yoshinobu Hirose; Yosuke Takemoto; Hiroshi Yamashita
Department of Otolaryngology, Yamaguchi University Graduate School of Medicine

Background
It is known that the incidence of congenital hearing impairment is about 1 in 1,000 live births. Hereditary hearing loss accounts for a large frequency among them. Grillet et al.reported that a causative gene of hereditary hearing loss, the LOXHD1b gene expressed in hair cells was the causative gene of DFNB77. But there are many unclear points.

Deafness caused by LOXHD1b gene mutation is clinically autosomal recessive inheritance and progressive. Hereditary families caused by LOXHD1 gene mutation has been also reported in Japan. In this study, we will investigate the effects of the LOXHD1b gene in the hair cell bundle of zebrafish. I discussed about the present and report it.

Method
The zebrafish information network suggested that LOXHD1 gene was present in zebrafish. RNA was extracted from 5-day post-fertilization (5-dpf) zebrafish larvae, and cDNA was reverse-transcribed from RNA. Using the LOXHD1b primer, cDNA of LOXHD1b gene was amplified by PCR. We confirmed by electrophoresis that the aimed cDNA was amplified. Fragments of LOXHD1b were obtained by PCR and inserted into the pGEM vector. The inserted fragments were amplified with the T7 and SP6 primers by PCR, and the respective products were used as templates for in vitro transcription with T7 or SP6 RNA polymerase in the presence of digoxigenin (DIG)-UTP, to respectively synthesize sense and antisense probes. Larvae were then immunoreacted with an alkaline phosphatase-coupled anti-DIG antibody and stained with BM Purple.

Result

LOXHD1b mRNA was expressed by neuromasts of 5-dpf larvae. No signal was found in larval skin with the sense probe.

Discussion

We used Anion Exchanger 1b gene (AE1b gene) as a positive control about the expression of LOXHD1b gene. Yuan-Hsiang Lin et al reported that in situ hybridization was enfoced in zebrafish for AE1b gene and the gene was expressed in hair cell bundles of zebrafish. Because the localization of LOXHD1b stained by in situ hybridization accorded with the localization of AE1b, it became clear that the LOXHD1b gene was expressed in hair cell bundles.

PS 116

PAK1 Disruption Causes Stereocilia Disorganization, Hair Cell loss And Deafness in Mice

Cheng Cheng[1]; Xia Gao[2]; Yanfei Wang[3]; Renjie Chai[1]; Wei Xie[4]
[1]Southeast University; [2]Affiliated Drum Tower Hospital of Nanjing University; [3]Shandong University; [4]Southest University

Several clinical studies reported that hearing loss might be related with autism in children; around 3.5% of autism children have different degrees of hearing loss, which is higher than general population. However little is known about the relationship between the hearing loss and autism; and the detailed genes leading to both autism and hearing loss have never been investigated before. p21-activated kinases (PAKs) are a family of serine/threonine proteins that can be activated by multiple signaling molecules, particularly the Rho family small GTPases. It has been shown that PAK1 mutations are associated with autism. In the present study, we took advantage of PAK1 knockout mice to investigate the role of PAK1 in hearing. We found PAK1 extensively expresses in the postnatal mice cochlea. Knockout of PAK1 leads to the significant hearing loss and hair cell (HC) loss. Our data also showed that PAK1 disruption leads to the apoptosis of HCs. Further investigation showed that the synapse density is decreased in the basal turn of PAK1 knockout mice, and the stereocilia of HCs are disorganized in all three turns. The phosphorylation of cofilin and Ezrin-radixin-mesin (ERM) are both significantly decreased in PAK1 knockout mice, which might contribute to the stereocilia deficit. In conclusion, our result demonstrated that PAK1 disruption causes stereocilia disorganization, HC loss and deafness in mice, and suggested that the autism-related gene PAK1 plays an important role in hearing. This study provides the first evidence about the gene both involved in hearing loss and autism.

Hair Cells I

PS 117

Molecular Mechanisms Underlying Differences Between Zebrafish and Mouse Hair Cell Specializations

Huizhan Liu[1]; Lei Chen[1]; Kimberlee P. Giffen[1]; Yi Li[2]; Kenneth L. Kramer[1]; Kirk W. Beisel[1]; **David Z. He[1]**
[1]Creighton University; [2]Beijing Tongren Hospital

Introduction

Hair cells (HCs) are the sensory receptors of the auditory and vestibular systems in the ears of all vertebrates. HCs transduce mechanical stimuli into electrical activity. Although all HCs have the hallmark stereocilia bundle for mechanotransduction, HCs in non-mammals and mammals are different in many ways. HCs of non-mammals (such as zebrafish) are electrically tuned to specific frequencies and possess an active process in the stereocilia bundle to amplify sound signals. Mammalian HCs, in contrast, are not electrically tuned and achieve amplification by somatic motility of outer HCs. The molecular mechanisms that underlie these differences between non-mammalian and mammalian hair cells are largely unknown.

Methods

Hair cells were isolated from adult zebrafish and mouse inner ears. 1,000 zebrafish HCs, and 1,000 mouse inner and outer HCs were isolated using a suction pipette technique and their transcriptomes were examined using RNA-seq. Real-time PCR, *in situ* hybridization and confocal microscopy were used to validate expression of some genes and proteins. Whole cell currents, nonlinear capacitance and motility were measured using whole cell voltage-clamp techniques.

Results

An analysis of genes related to HC specializations showed that zebrafish and mouse HCs both express *Tmc1*. *Tmc2* was not detected in mouse HCs but *tmc2a* and *tmc2b* were highly expressed in zebrafish HCs. Mouse HCs expressed *Cacng5*, *Kcnj13*, *Kcnj16*, and *Kcnq4*, while zebrafish HCs did not. However, robust expression of *cacnb3b*, *kcng4a*, and *kcnj2a* was detected in zebrafish HCs. Both *Chrna9* and *Chrna10* were expressed in mouse HCs. In contrast, *chrna10* was not expressed in zebrafish HCs. *Slc17a8* and *Slc1a3* were highly expressed in all HCs. *Slc26a5*, highly expressed in mammalian outer HCs, was weakly expressed in zebrafish HCs; however, neither nonlinear capacitance nor somatic motility was detected.

Conclusion

Our analyses unveil substantial differences in gene expression patterns that may explain different phenotypes

of zebrafish and mouse HCs. Our datasets also establish a framework for future characterization of genes expressed in HCs of these two species, as well as for the study of HC evolution from non-mammals to mammals. (Supported by NIH grant R01 DC 004696 from the NIDCD/NIH)

PS 118

Noise-Induced Upmodulation of Annexin A2 and Dysferlin in Stereocilia of Cochlear Outer Hair Cells

Dennis G. Drescher; Marian J. Drescher
Wayne State University School of Medicine

Background
Cochlear hair cells are vulnerable to injury by sound and their membranes become reversibly porous with noise exposures that cause auditory threshold shifts (Mulroy et al., Hear Res 115:93-100, 1998). We sought molecular correlates of presumptive resealing of hair-cell membranes by examining proteins involved in membrane repair before and after exposure to noise.

Methods
Adult Black Agouti rats were exposed to 103 dB SPL 10-20 kHz octave-band noise for 4 hours, followed by 0.5-2.5 hour recovery. Controls were maintained in silence for the same duration. The cochleas were isolated and fixed with 4% paraformaldehyde infused through the round window. A microdissected organ of Corti surface preparation was processed as described (Selvakumar et al., Biochem J 474:79-104, 2017). Tissues were incubated with antibodies for annexin A2 or dysferlin overnight at 4 ºC, followed by appropriate secondary antibody with fluorophore and Z-stack fluorescence confocal microscopy. Dysferlin immunoreactivity was additionally detected with diaminobenzidene (DAB) staining.

Results
We found that the largest effect of noise was to upmodulate immunofluorescence-detected expression of annexin A2 in stereocilia of cochlear outer hair cells with a lesser increase of annexin A2 in stereocilia of cochlear inner hair cells. These increases of annexin A2 expression were accompanied by modest increases in dysferlin, which in noise-exposed animals was immunolocalized to the tops of individual stereocilia in stereociliary arrays, consistent with the localization observed with DAB detection of dysferlin in control animals. Interestingly, a major site for expression of both dysferlin and annexin A2, in non-exposed animals, was the outer pillar cells, possibly correlating with the marked susceptibility of these cells to damage in noise-induced hearing loss (Harding et al., Hear Res 63:26-36, 1992). We obtained evidence in controls for co-localization of dysferlin with annexin A2 at the base of cochlear inner hair cells. With noise exposure, there was a *decrease* in annexin A2 at these basal sites and its co-localization with dysferlin.

Conclusions
The discovery of molecules that function directly in the repair of hair-cell lesions produced by noise exposure would be an important missing link in our understanding of overall noise damage and recovery from noise-induced hearing loss. Known membrane-repair proteins, such as the annexins and ferlins, are good candidates for cochlear repair. An enhancement in the expression of these proteins in hair cells elicited by noise exposure is consistent with their function as membrane-repair catalysts at specific hair cell membrane targets, reversing hearing loss.

PS 119

A Photoreceptor-like cGMP Pathway in Inner Ear Hair Cells Points to Rhodopsin-linked Signal Transduction

Marian J. Drescher; Dennis G. Drescher
Wayne State University School of Medicine

Background
A cGMP-gated cyclic nucleotide channel subunit CNGA3, the cone photoreceptor transduction alpha subunit, and CNGB1 subunit, the rod photoreceptor transduction beta subunit, were previously identified in purified saccular hair cells (IEB Abstr. 52:011, 2015). A photoreceptor-like membrane guanylyl cyclase pathway for synthesizing cGMP, required to gate this CNG channel, has been documented in both teleost vestibular and mammalian cochlear hair cell models (ARO Abstr. 38:PS-772, 2015). Direct protein-protein interaction analysis by competitive pull-down assays and SPR indicated CNGA3 tightly interacts with myosin VIIA in competition with tip-link-protein cadherin 23 (Selvakumar et al., J. Biol. Chem. 288:7215-7229, 2013). The nature of the proteins interacting with CNGB1 mediating photoreceptor transduction adaptation has now been assessed in hair cells.

Methods
PCR was carried out with degenerate primers on teleost saccular hair cell cDNA to identify hair cell expression of rod photoreceptor transduction proteins. Hair cell transcript sequences (crossing introns) were submitted to GenBank. Rhodopsin has been immunolocalized in teleost vestibular and mammalian cochlear hair cell models.

Results
In rod phototransduction, each activated molecule must undergo inactivation before absorption of the next photon. Thus, rhodopsin is phosphorylated at its C-termi-

nus by rhodopsin kinase (GRK1), followed by binding of visual S-antigen form of arrestin (SAG). Both photoreceptor GRK1 and SAG transcripts are expressed in saccular hair cells, but not GRK7, which phosphorylates cone photoreceptor opsin. RDH8, which converts all-trans retinal to all-trans retinol, rate-limiting in the visual cycle, is not expressed. Two specific CNGB1-binding partners are expressed: the tetraspan flippase ABCA4 described as "expressed exclusively in retina photoreceptor cells," mediating transport of **11-cis-retinylidene** phosphoethanolamine (PE), the Schiff-base conjugate of 11-cis-retinal and PE, from lumen to cytoplasmic leaflet of rod photoreceptor disk membranes. In phototransduction, 11-cis-retinylidene is photoisomerized to all-*trans* configuration. CNGB1-binding photoreceptor-specific peripherin-2 (RDS) is also expressed in saccular hair cells. Peripherin-2 (RDS) is found in outer segments of rod and cone photoreceptors, putatively generating membrane curvature and disk-disk tethering. Rhodopsin protein has been immunolocalized to both mammalian cochlear and teleost saccular hair cells.

Conclusions

Given that a membrane guanylyl cyclase with identity to GC-F and GC-E, activating proteins GCAP1 and GCAP2, transducins GNAT1 and GNAT2 coupling rhodopsin and PDE6, cone PDE6C degrading cGMP, and now GRK1, SAG, ABCA4, and RDS are all expressed by saccular hair cells, with rhodopsin immunolocalized to mammalian and teleost hair cells, the conclusion would be that a rod phototransduction pathway exists in hair cells, supporting CNGA3/CNGB1 physiological function.

PS 120

Spontaneous Activity Drives Functional Maturation in Developing Outer Hair Cells

Aenea Hendry[1]; Federico Ceriani[1]; Jing-Yi Jeng[1]; Dwayne Simmons[2]; Walter Marcotti[1]
[1]University of Sheffield; [2]Baylor University

Background In mammals, the sense of hearing relies on mechanoelectrical transduction performed by the primary sensory receptor inner hair cells (IHCs) and the outer hair cells (OHCs), in response to acoustic stimuli. Before the onset of hearing, spontaneous activity generated in the cochlea is thought to be crucial for the refinement of tonotopic maps in the auditory pathway, as well as maturation of sensory cells. This activity has so far been ascribed uniquely to IHCs, which are known to exhibit spontaneous calcium (Ca2+) action potentials before becoming mature sensory receptors. OHCs, the highly specialised sensory cells conferring fine tuning and high sensitivity to the mammalian cochlea, have not thus far been found to exhibit this property. How these specialised sensory cells and their innervation patterns are refined during pre-hearing stages of development is currently unknown. Methods Whole-cell, cell attached patch-clamp recordings and 2-photon calcium imaging were performed from OHCs of C57B, Cx30 (-/-) and Cav1.3 (-/-) mice. OHCs were studied in acutely dissected cochleae from postnatal day 0 (P0) to P13, where the day of birth is P0. Recordings were performed using near-physiological solutions (1.3 mM extracellular Ca2+). Animal work was performed following UK regulation procedures. Results We show that, similarly to IHCs, immature OHCs exhibit spontaneous Ca2+ spikes, which were associated with action potential firing. This activity, which is mediated by L-type Ca2+ channels, is present during the first postnatal week, before OHCs become electromotile and fully acquire their mature ion channel profile, and disappears progressively from base to apex. We demonstrate that spontaneous Ca2+ spikes are required for OHC functional differentiation into sensory receptors. We also show that spontaneous release of ATP from Deiters' cells directly coordinates the firing activity of adjacent OHCs. In knockout mice for connexin 30, in which ATP release from connexin hemichannels in non-sensory cells is largely reduced, the normal maturation of OHC afferent and efferent innervation pattern is impaired. Conclusions Our results indicate that, before the onset of OHC function, the acquisition of the mature physiological characteristics of OHCs and their neuronal connectivity is coordinated by experience-independent electrical activity involving both sensory and non-sensory cells of the mammalian cochlea.

PS 121

Transgenic Tmc2 expression partially rescues auditory function in a mouse model of DFNB7/B11 deafness

Hiroshi Nakanishi[1]; Kiyoto Kurima[1]; Bifeng Pan[2]; Philine Wangemann[3]; Tracy S. Fitzgerald[1]; Jeffrey R. Holt[4]; Andrew J. Griffith[5]
[1]NIDCD, NIH; [2]Boston Children's Hospital, Harvard Medical School; [3]Kansas State University; [4]Boston Children's Hospital, Harvard Medical School; [5]Otolaryngology Branch, National Institute on Deafness and Other Communication Disorders (NIDCD), Bethesda, MD, USA

Background

Mouse *Tmc1* and *Tmc2* are required for mechanoelectrical transduction (MET) in cochlear and vestibular hair-cells (HCs). $Tmc1^{\Delta/\Delta}$ homozygotes are deaf, $Tmc2^{\Delta/\Delta}$ mice have normal hearing, and double homozygous $Tmc1^{\Delta/\Delta}$;$Tmc2^{\Delta/\Delta}$ mice have deafness and profound vestibular dysfunction. *Tmc1* expression persists in mature cochlear and vestibular HCs, whereas *Tmc2* expression is transient in neonatal cochlear HCs but persists in mature vestibular HCs. These results suggested that *Tmc2*

expression in mature vestibular HCs preserves vestibular function in $Tmc1^{\Delta/\Delta}$ mice. We hypothesized that persistent $Tmc2$ expression in mature cochlear HCs could rescue auditory function in $Tmc1^{\Delta/\Delta}$ mice.

Methods

We generated a bacterial artificial chromosome transgenic mouse line, Tg(P$_{Tmc1}$-$Tmc2$), in which $Tmc2$ is expressed under the control of the $Tmc1$ promoter so that it is expressed in mature cochlear HCs. We crossed Tg(P$_{Tmc1}$-$Tmc2$) and $Tmc1^{\Delta/\Delta}$ to generate Tg(P$_{Tmc1}$-$Tmc2$);$Tmc1^{\Delta/\Delta}$mice for further analyses.

Results

$Tmc1^{\Delta/\Delta}$mice had no detectable auditory brainstem responses (ABRs) at 90 dB SPL, whereas the ABR thresholds of Tg(P$_{Tmc1}$-$Tmc2$);$Tmc1^{\Delta/\Delta}$mice were approximately 80 dB SPL at postnatal day 16 (P16). However, no responses were present at 90 dB SPL at P25. Hair-cell transduction currents were detected at P7-P8 and FM1-43 uptake was observed in both inner and outer HCs at P16, suggesting that functional MET channels were present. Outer, but not inner, HCs took up FM1-43 at P25. Distortion product otoacoustic emissions were absent at P16, indicating that active amplification by outer HCs was not rescued even though prestin expression and the endocochlear potential were intact. Hair-cell stereocilia were intact in inner and outer HCs at P16. At P25, the stereocilia bundles were intact in inner HCs, but were degenerating in basal-turn outer HCs. KCNMA1 expression, required for $I_{k,f}$ currents in mature inner HCs, was detected at P16, but disappeared at P25. KCNQ4 expression, underlying $I_{k,n}$ currents in mature outer HCs, remained intact at P16 and P25.

Conclusion

$Tmc2$ expressed in mature cochlear HCs partially and transiently rescues auditory function in $Tmc1^{\Delta/\Delta}$ mice. Elevation of ABR thresholds was associated with a complex and progressive loss of inner and outer HC functions. There was a progressive loss of MET channel function in inner but not outer HCs between P16 and P25. However, there was no detectable active amplification by outer HCs at P16. We conclude that $Tmc1$ and $Tmc2$ mediate partially redundant functions in outer and inner HCs. $Tmc2$ expression can only partially compensate for loss of $Tmc1$ expression in cochlear hair-cells.

Mass Loading Engenders Spontaneous Oscillation by Hair Bundles

Andrew Milewski[1]; Daibhid O Maoileidigh[2]; Joshua Salvi[1]; A. James Hudspeth[1]
[1]*Howard Hughes Medical Institute and Laboratory of Sensory Neuroscience, The Rockefeller University;*
[2]*Department of Otolaryngology - Head and Neck Surgery, Stanford University School of Medicine*

Introduction

Spontaneous hair-bundle oscillations, which occur in fishes, amphibians, and reptiles, emanate from an active process that endows the bundles with frequency selectivity, enhanced sensitivity, and a broadened dynamic range. Because spontaneous oscillations have not been observed in mammalian hair bundles, it remains uncertain whether the same active process operates in mammals. Theoretical analysis suggests that spontaneous bundle oscillations occur for only a limited set of conditions. That mammalian hair bundles can be tenfold as stiff as amphibian bundles may account in part for the apparent absence of spontaneous oscillations in the former. The theoretical work, however, predicts that loading a hair bundle with a mass comparable to its load *in vivo* can induce the bundle to self-oscillate.

Methods

We tested this prediction by placing tungsten particles onto hair bundles of the bullfrog's sacculus. Because tungsten is 32 times as dense as water, a particle of radius 5 mm imparts a mass of 10 ng to a bundle. In a two-chamber preparation, particles were delivered to individual hair bundles with a sticky probe or to the entire sensory epithelium by fluid exchange. Projecting the image of the bundle or of the attached tungsten particle onto a dual photodiode allowed determination of the bundle';s motion.

Results

Mass loading was found to engender spontaneous oscillations in previously quiescent hair bundles. These oscillations could be abolished by severing tip links or by blocking mechanotransduction channels. We showed additionally that the oscillations stemmed from the active process and were not the result of thermal fluctuations filtered by the passive properties of a loaded hair bundle. Moreover, the bundle';s force-displacement relation did not exhibit negative stiffness either with or without mass loading.

Conclusions

Although negative stiffness is a necessary ingredient for generating spontaneous oscillations in unloaded

hair bundles, such a strong nonlinearity is not needed for mass-loaded bundles to self-oscillate. The weak nonlinearity seen in mammalian bundles is theoretically sufficient for their spontaneous oscillation. Furthermore, because they are coupled to the massive tectorial membrane, the bundles of outer hair cells may have the capacity to oscillate spontaneously in their native environments and thus to contribute to the cochlear active process.

PS 123

The role of Calcium and ATPase in slow adaptation and set point regulation.

Giusy Caprara[1]; Andrew Mecca[2]; Anthony Peng[3]
[1]*University of Colorado Anschutz Medical Campus;*
[2]*Neuroscience Program, University of Colorado Anschutz, Aurora, CO;* [3]*Department of Physiology and Biophysics, University of Colorado Anschutz, Aurora, CO*

Hair cells of the inner ear are mechanosensors that transduce mechanical forces arising from sound waves and head movement to provide our senses of hearing and balance. Sound deflects the hair bundle, a cross-linked cluster of stereocilia on the apical surface of a hair cell, and causes the opening of mechanically sensitive ion channels to start the mechanotransduction (MET) process. The MET complex is built around the tip-link, an extracellular filament that connects the top of the shorter stereocilia with the side of the next taller row. One important property of the kinetics of MET currents is a decline in current during a sustained displacement stimulus, a process called adaptation. Two major adaptation processes are commonly recognized: fast adaptation operates on a millisecond time scale and slow adaptation acts over tens of milliseconds. The general thought was that the adaptation process is regulated by intracellular Ca^{2+}, but a recent study demonstrated that in mammalian auditory system Ca^{2+} is not directly involved in fast adaptation [1]. The mechanism underlying slow adaptation has been well documented in nonmammalian and low frequencies hair cells with a model that proposes a direct link between Ca^{2+} influx through MET channels and the movement of unconventional myosin 1C (Myo1C) to release tension and close the channel[2]. Recent evidence shows that in mammalian species, MET channels and Myo1C have a different localization and that the expression during development of Myo1C does not match the onset of slow adaptation [3-5]. For these reasons, it seems unlikely that the specific mechanisms described in low frequencies hair cells translates to cochlear hair cells. Using rat and mouse auditory hair cells, high-speed imaging, different pharmacological approaches, and internal Ca^{2+} manipulations, we clarify the role of Ca^{2+} and myosin motors in cochlear hair cell slow adaptation.

The increase of $[Ca^{2+}]_i$ by lowering the Ca^{2+} buffering or blocking calcium pump activity leads to increased adaptation and reduces the resting P_{open} with fluid jet stimulation. Application of certain ATPase inhibitors results in a decreased Ca^{2+}-induced adaptation without the concomitant modulation of the resting P_{open}. Our data indicate that myosin motors modulate slow calcium-dependent adaptation.

1. Peng, A. W. *et al*. Neuron (2013).

2. Holt, J. R. *et al.* Cell (2002).

3. Beurg, M. *et al*. Nature neuroscience (2009).

4. Grati, M. *et al*. PNAS (2011).

5. Waguespack, J. *et al*. J Neurosci (2007).

PS 124

How to build a fast and highly sensitive sound detector that remains robust to temperature shifts.

Minghui Chen[1]; Henrique von Gersdorff[2]
[1]*Oregon Health and Science University;* [2]*Vollum Institute, Oregon Health and Science University*

Frogs quickly adapt to a wide range of body temperature during their normal activities. To successfully find mating partners their hearing abilities must be sharp during the warm summer months. *In vivo* single auditory nerve fiber recordings in frogs have revealed strong temperature sensitivity of the afferent fiber spike activity. To understand how frog hair cells preserve both sensitivity and temporal precision at higher temperatures, we performed *in vitro* patch-clamp recordings of hair cells and their afferent fibers in bullfrog amphibian papillae under both room (23-25°C) and high (30-33°C) temperature. Afferent fiber recordings revealed heterogeneity in the temperature dependence of spontaneous spikes. 71% of fibers showed increased spiking rates with lower threshold at high temperature and 29% of fibers showed decreased spiking rates without threshold changes at high temperature. Different from spikes, EPSP and EPSC frequency increased at high temperature for all fibers, suggesting more spontaneous vesicle release from hair cells. We next tested whether increasing temperature depolarizes hair cells, as occurs in some neurons and nerve terminals (e.g. the calyx of Held). However, surprisingly, whole-cell recording revealed hyperpolarization of resting membrane potential at higher temperatures, while gramacidine-perforated patch revealed no significant change. Furthermore, both inward Ca^{2+} current and outward K^+ current at the resting membrane potential of -60 mV were increased at higher temperatures.

Two consequences of this increased current flux: First, an increase of $[Ca^{2+}]$ at hair cell release sites under high temperature that induces more spontaneous exocytosis. Second, more "leaky cells" decreases hair cell input resistance (R_{in}). A decreased R_{in} sacrifices sensitivity in sound detection ($V_m = R_{in} \times I$), while a smaller R_{input} benefits temporal precision ($\tau = R_{in} \times C_m$). Are there mechanisms that compensate for a drop in sensitivity? Using membrane capacitance measurements, we found that the temperature dependence of exocytosis ($Q_{10} = 2.4$) was larger than the temperature dependence of Ca^{2+} charge transfer (; $Q_{10} = 1.5$), indicating increased exocytosis efficiency ($\Delta C_m/$). This suggests a reduction in the intrinsic energy barrier for membrane fusion at higher temperatures compensates for the potential loss of sensitivity caused by a smaller R_{in}. Estimation of hair cell passive membrane properties using both voltage- and current-clamp recordings confirmed that R_{in} and membrane time constant (τ) decreased at higher temperatures, while cell capacitance (C_m) remained unchanged. Altogether, our results suggest that adaptations to higher temperature can enhance both exocytosis efficiency and improve temporal precision in sound information transfer at hair cell ribbon synapses.

PS 125

Myosin-XVa is Essential to Form the Gradation of Stereocilia Diameters Within the Hair Bundles of Inner but not Outer Hair Cells

Shadan Hadi; Andrew J. Alexander; A. Catalina Velez-Ortega; Gregory I. Frolenkov
Department of Physiology, University of Kentucky

During the postnatal development in rodents, hair cell stereocilia elongate to form a characteristic staircase bundle. Concurrent with this elongation, taller stereocilia in the bundle grow in diameter, while supernumerary stereocilia retract. Although a number of molecules involved in stereocilia elongation were identified — such as myosin-XVa, whirlin, Eps8, Eps8L2, espin-1, ES-PNL, twinfilins — significantly less is known about the molecular mechanisms of stereocilia thickening and of supernumerary stereocilia retraction. Our previous observations hinted that mutations in myosin XVa and its cargoes may disrupt not only the normal elongation of stereocilia but also their thickening and the retraction of supernumerary stereocilia. Therefore, we quantified postnatal changes of stereocilia diameters and the number of stereocilia per bundle/row in the auditory hair cells of *shaker2* mice, which carry a mutation in the "long" and "short" isoforms of myosin-XVa ($Myo15^{sh2}$), and in the isoform-specific knockout mice ($Myo15^{\Delta N}$) that lack only the "long" isoform of myosin-XVa (Fang et al., 2015).

Using scanning electron microscopy, we imaged inner (IHC) and outer (OHC) hair cell bundles in the mid-cochlear region of homozygous and control heterozygous mice at postnatal days 0 through 20 (P0-P20). Stereocilia counts showed identical developmental retraction of supernumerary stereocilia in control, $Myo15^{sh2/sh2}$ and $Myo15^{\Delta N/\Delta N}$ mice, suggesting that myosin-XVa is not involved in this process, at least in OHCs. Likewise, we did not observe an effect of myosin-XVa deficiency on stereocilia diameters in the OHCs. We also determined that OHC stereocilia have equal thickness in the first, second, and third rows of the bundle, and their postnatal thickening was largely completed by P1. In contrast to OHC, the first (tallest) and second row stereocilia of IHCs grow in diameter until approximately P10, while the third row stereocilia decrease their diameters after P1. By P10, IHC stereocilia have a ~2.5-fold difference in diameter between the first and third rows. This developmental thinning of the third row stereocilia was disrupted in the IHC of $Myo15^{sh2/sh2}$ but not $Myo15^{\Delta N/\Delta N}$ mice.

We concluded that, besides being essential for the normal elongation of stereocilia, myosin-XVa is also required for the gradation of stereocilia diameters, which are normally present in the IHCs but not OHCs. Since stereocilia thickness abnormalities are observed in young postnatal $Myo15^{sh2/sh2}$ but not $Myo15^{\Delta N/\Delta N}$ mice, we believe that it is the "short" isoform of myosin-XVa that is essential for the normal thinning of the third row stereocilia during IHC development.

PS 126

The CIB2/USH1J protein, defective in isolated deafness without vestibular and retinal deficits, is key for auditory hair cell mechanotransduction and survival

Pranav Patni[1]; Vincent Michel[2]; Matteo Cortese[1]; Amel Bahloul[3]; Michael R. Bowl[4]; Steve Brown[5]; Paul Avan[6]; Christine Petit[7]; Aziz El-Amraoui[1]
[1]Pasteur Institute; [2]Institut Pasteur, INSERM UMRS 1120, Université Pierre et Marie Curie; [3]Unité de Génétique et Physiologie de l'Audition, Institut Pasteur and UMRS 1120, Institut National de la Santé et de la Recherche Médicale; [4]MRC Harwell Institute, Mammalian Genetics Unit, Harwell, Oxford; [5]MRC Harwell Institute; [6]Centre Jean Perrin, Université Clermont Auvergne, INSERM UMR 1107; [7]Institut Pasteur, INSERM UMRS1120, Université Pierre et Marie Curie, Institut de la Vision, Collège de France

Defects in CIB2, the calcium- and integrin-binding protein 2, cause isolated deafness, DFNB48, and the Usher

syndrome type-IJ, characterized by congenital profound deafness, balance defects and blindness. We show here that a ubiquitous, early gene inactivation (*CIB2*^{−/−} mice) of CIB2 in mouse causes profound deafness without any sign of balance and retinal dysfunctions. In these mice, the mechanoelectrical transduction currents are totally abolished in the auditory hair cells, whilst they remain unchanged in the vestibular hair cells. The hair bundle morphological abnormalities of *CIB2*^{−/−} mice, unlike those of mice defective for the other five known USH1 proteins, begin only after birth, and leads to regression of the stereocilia and rapid hair cell death. The mislocalisation of two key CIB2-partners in the hair bundle, whirlin and integrin α8, in *CIB2*^{−/−} mice point to a key scaffolding role of CIB2 in the hair bundle. Unlike other USH1 mutant mice, the structural abnormalities in *CIB2*^{−/−} mice began after birth, leading to stereocilia regression and, rapidly afterwards, to hair cell death. This essential role of CIB2 in mechanotransduction and cell survival that, we show, is restricted to the cochlea, probably accounts for the presence in *CIB2*^{−/−} mice and *CIB2*patients, unlike in Usher syndrome, of isolated hearing loss without balance and vision deficits.

Acknowledgements

[Patni et al. Abstract ID- 383063.docx](#)

Hair Cells II

PS 127

The Role of Calcium-Binding Protein 2 in Sound Encoding

Tina Pangrsic[1]; Maria Magdalena Picher[2]; Anna Gehrt[3]; Nicola Strenzke[3]; Tobias Moser[4]
[1]University Medical Center Göttingen, Institute for Auditory Neuroscience and InnerEarLab; [2]IST Austria and University Medical Center Göttingen, Institute for Auditory Neuroscience and InnerEarLab; [3]University Medical Center Göttingen, Department of Otolaryngology, InnerEarLab; [4]Institute for Auditory Neuroscience

Calcium binding proteins (CaBPs) shape presynaptic calcium signals by binding to voltage-gated calcium channels and reducing their inactivation upon cell depolarization. Inner hair cells (IHCs) express several CaBPs, which may be partially redundant, but isolated mutations in *CaBP2* were identified to cause moderate to severe hearing impairment in humans, DFNB93. To gain insight into the pathological mechanisms of DFNB93, *Cabp2* knock-out mice were generated and investigated for a hearing deficit. These mice show increased auditory brainstem response (ABR) threshold. Recordings from single auditory fibers reveal decreased spontaneous and evoked spiking rates with increased first spike latency and jitter, likely explaining reduced ABR wave I amplitude. Patch-clamp measurements of calcium and barium currents in near physiological conditions demonstrate an increased voltage-dependent inactivation (VDI) of $Ca_V1.3$ channels in Cabp2-deficient IHCs and show a trend towards increased calcium-dependent inactivation (CDI). We propose that hearing impairment in the absence of CaBP2 is caused by enhanced steady-state inactivation of $Ca_V1.3$ channels, which reduces the availability of channels to trigger exocytosis at the first synapse in the auditory pathway. This in turn degrades temporal precision of sound encoding and results in hearing impairment as observed in knock-out mice and human patients.

PS 128

Mitochondrial Morphology in Outer Hair Cells

Teresa Wilson; Sarah Foster; Sean Elkins; Alfred L Nuttall
Oregon Health & Science University

Background

Mitochondria are highly dynamic organelles that are maintained by the opposing processes of fusion and fission, events which directly influence mitochondrial biogenesis, energy metabolism, autophagy, calcium and reduction/oxidation homeostasis, and cell death. Mitochondrial dysfunction, including the deregulation of fission and fusion processes, is implicated in many pathological conditions including hearing loss. Cellular stress can affect mitochondrial dynamics resulting in increased mitochondrial fragmentation, production of excessive oxidative free radicals, and cell death. Whether mitochondrial dynamics are altered in response to increased energy needs of outer hair cells (OHCs) with loud sound exposure has not been well-characterized

Methods and Results

For visualization of OHC mitochondria, PhAM[floxed] mice (C57Bl/6 background) were crossed with prestin-CreER[T2] mice to generate mice that express a mitochondrial-specific version of the Dendra2 fluorescent

protein (Mito-Dendra2). These mice were exposed to loud sound and the cochlea harvested at various times following noise exposure. Airyscan imaging revealed primarily punctate mitochondria in the OHCs of control animals. Further, distinct populations of mitochondria were observed: infranuclear, lateral, and apical. In basal OHCs, the infranuclear mitochondria were significantly smaller than those located in the apical region. Additionally, the apical and lateral mitochondria decreased in size progressing from the base to the apex of the cochlea. Following noise exposure, the apical mitochondria in basal OHCs acquired a more punctate morphology and an altered spatial organization.

Conclusions

Regulation of mitochondrial fusion and fission processes, and therefore the morphological state of mitochondria, is believed to modulate mitochondrial function and health. The presence of fragmented mitochondria in normal OHCs suggests that the balance of fission and fusion processes are altered, potentially due to a higher oxidant environment being present in these cells. The existence of distinct populations of mitochondria in OHCs, particularly OHCs in the high frequency region of the cochlea, likely reflects the regional metabolic needs within these cells, and may provide a clue as to the basis for the increased sensitivity of these OHCs to damage from loud sound exposure.

Funding

PS 129

Auditory Studies on MAP1S Knock Out Mice

Jun-Ping Bai[1]; Lei Song[2]; Alexei Surguchev[3]; Joseph Santos-Sacchi[4]; Dhasakumar Navaratnam[5]
[1]Department of Neurology, Yale University School of Medicine, New Haven, Connecticut, USA; [2]Department of Otolaryngology - Head & Neck Surgery, Shanghai Ninth People's Hospital; Ear Institute, Shanghai JiaoTong University School of Medicine; Shanghai Key Laboratory of Translational Medicine on Ear and Nose diseases, Shanghai, China; [3]Department of Surgery (Otolaryngology), Yale University School of Medicine, New Haven, Connecticut, USA; [4]Department of Surgery (Otolaryngology), Neuroscience, and Cellular and Molecular Physiology, Yale University School of Medicine, New Haven, Connecticut, USA; [5]Department of Neurology and Neuroscience, Yale University School of Medicine, New Haven, Connecticut, USA

Prestin is a member of the SLC26 family of anion transporters that is responsible for outer hair cell (OHC) electromotility (eM). Microtubule-associated protein 1S (MAP1S), a protein that binds both actin and tubulin also interacts with prestin. Co-expression of MAP1S with prestin resulted in both an increase in nonlinear capacitance (NLC) and in surface expression of prestin. We hypothesize that MAP1S links prestin to the underlying cytoskeleton. To better characterize the nature of their interactions, we used a germline MAP1S knockout (MAP1S KO) mouse generated by Layuan Liu and performed a series of studies on these mice.

C57BL/6 MAP1S KO mice aged from 19 postnatal days (P) to 13-month were used for experiments. The developmental change in auditory thresholds of MAP1S KO mice and wild type (WT) mice were assessed using auditory brainstem responses (ABR) recorded at different ages. NLC was recorded using whole cell voltage clamp in OHCs from the apical turn of the organ of Corti explant. Both bath solution and pipette solution contained ion channel blockers to prevent interference from ionic currents. Cells were recorded in the presence of 140mM intra and extracellular chloride solutions. OHCs were recorded at room temperature using jClamp software and an Axopatch 200B amplifier. Data were low pass filtered at 10 KHz and digitized with a Digidata 1320A at 100 kHz.

ABR recordings from P19 onwards confirm hearing loss in the high frequencies that then extended to the lower frequencies at 2 months and older. Interestingly, the reduced ABR responses were most significant at high frequencies and at suprathresholds where eM is robust. Importantly, these effects mimic those of the Spectrin V (a component of OHC cortical cytoskeleton) knockouts and corroborates our hypothesis that MAP1S links prestin to the underlying cytoskeleton in OHCs. Prestin';s signature NLC, a measure of charge movement in the membrane, was preserved, indicating that MAP1S KO induced hearing loss is not directly linked with prestin';s proper folding and insertion in the membrane.

PS 130

Otoferlin is the Ca2+ sensor for vesicle fusion and vesicle pool replenishment at auditory hair cell ribbon synapses

Nicolas Michalski[1]; Juan Goutman[2]; Sarah Auclair[3]; **Jacques Boutet de Monvel**[1]; Margot Tertrais[4]; Alice Emptoz[5]; Alexandre Parrin[6]; Sylvie Nouaille[6]; Marc Guillon[7]; Martin Sachse[8]; Danica Ciric[6]; Amel Bahloul[6]; Jean-Pierre Hardelin[6]; R. Bryan Sutton[9]; Paul Avan[10]; Shyam S. Krishnakumar[3]; James E. Rothman[3]; Didier Dulon[11]; Saaid Safieddine[12]; Christine Petit[13]

[1]Institut Pasteur, INSERM UMRS 1120, Université Pierre et Marie Curie; [2]Instituto de Investigaciones en Ingeniería Genética y Biología Molecular, Consejo Nacional de Investigaciones Científicas y Técnicas-Universidad de Buenos Aires; [3]Department of Cell Biology, Yale University School of Medicine; [4]Laboratoire de Neurophysiologie de la Synapse Auditive, Université de Bordeaux, and UMRS 1120, Inserm; [5]Institut Pasteur; [6]Unité de Génétique et Physiologie de l'Audition, Institut Pasteur and UMRS 1120, Institut National de la Santé et de la Recherche Médicale; [7]Wave Front Engineering Microscopy Group, Neurophotonics Laboratory, CNRS UMR 8250, University Paris Descartes, Sorbonne Paris Cité; [8]Center for Innovation & Technological Research, Ultrapole, Institut Pasteur; [9]Department of Cell Physiology and Molecular Biophysics, Texas Tech University Health Sciences Center; [10]Centre Jean Perrin, Université Clermont Auvergne, INSERM UMR 1107; [11]INSERM and University of Bordeaux; [12]Unité de Génétique et Physiologie de l'Audition, Institut Pasteur, UMRS 1120 Inserm; [13]Institut Pasteur, INSERM UMRS1120, Université Pierre et Marie Curie, Institut de la Vision, Collège de France

Hearing relies on extremely fast and sustained neurotransmitter release at the ribbon synapses of the cochlear inner hair cells (IHCs), endowing the mammalian ear with exquisite temporal precision. This process requires otoferlin, a six C_2-domain, Ca^{2+}-binding transmembrane protein of synaptic vesicles. To decipher the role of otoferlin in the synaptic vesicle cycle, we produced knock-in mice ($Otof^{Ala515,Ala517/Ala515,Ala517}$) with lower Ca^{2+}-binding affinity of the C_2C domain. While the mutation had no effect on the IHC ribbon synapse structure, the synaptic Ca^{2+} currents, or the otoferlin cellular distribution, the auditory brainstem response wave-I amplitude was reduced. Lower Ca^{2+} sensitivity and delays of the fast and sustained components of IHC synaptic exocytosis were observed by membrane capacitance measurement under various conditions of calcium changes in the IHCs including, modulations of intracellular Ca^{2+} concentration, local Ca^{2+} influx through voltage-gated Ca^{2+}-channels, and release of intracellular

Ca^{2+} by uncaging. Our results reveal that otoferlin functions as a dual Ca^{2+}sensor at the IHC synapse, setting both the rates of vesicle fusion and of synaptic vesicle pool replenishment in the active zone.

ARO2018_abstract_synapse_KIC2C.doc

PS 131

Inner Hair Cell Auditory Neuropathy in Klhl18 Mutant Mice

Navid Banafshe[1]; Neil Ingham[2]; Morag Lewis[1]; Karen Steel[2]
[1]King's College London; [2]King's College London and Wellcome Trust Sanger Institute

Background

Following a large-scale screen of new mouse mutants using Auditory Brainstem Response recording (Sanger Institute Mouse Genetics Project), we discovered two mutant alleles of the Klhl18 gene, $Klhl18^{tm1a(KOMP)Wtsi}$ and $Klhl18^{lowf}$, with progressive hearing loss predominantly affecting low frequencies. The first allele was a targeted mutation leading to knockdown of Klhl18 expression, and the second allele was a spontaneous missense mutation of Klhl18 (9:110455454 C>A; V55F), predicted to have a damaging effect on protein structure. Compound heterozygotes for the two alleles also showed low frequency hearing impairment. Mutants had normal middle and external ears and the gross structure of the inner ear was also normal. Mutants had normal ABR thresholds at 3 weeks old but showed progressive increase in ABR thresholds from 4 weeks onwards affecting low frequencies first. DPOAE recordings up to 14 weeks old revealed normal thresholds.

Objectives

To elucidate whether the low frequency hearing impairment includes a reduction or change in frequency tuning and whether this hearing impairment is associated with a synaptic defect.

Methods

Six week old mice homozygous and heterozygous for the $Klhl18^{lowf}$ were used for an ABR forward masking paradigm to assess frequency tuning at 12 kHz and 24 kHz probe tones. Sharpness of tuning was measured by calculating Q10 dB (best frequency divided by the bandwidth 10 dB above the tuning curve tip). Presynaptic ribbons and postsynaptic densities of inner hair cells were stained for Ribeye and GluR2, respectively. Whole mount cochleae were visualized with a confocal microscope and numbers of synapses (colocalized pre- and postsynaptic components), presynaptic ribbons and postsynaptic components were counted at 12 kHz and 24 kHz best frequency regions with FIJI.

Results

In homozygous mutants broader frequency tuning was observed for the 12 kHz probe, while tuning was not well tuned at the 24 kHz probe for both homozygous and heterozygous *Klhl18^lowf*. Immunohistochemistry revealed a reduced number of synapses in homozygous *Klhl18^lowf* at the 12 kHz cochlear region compared with controls. Numbers of orphan postsynaptic densities were increased at both 12 kHz and 24 kHz regions in homozygous mutants compared with controls.

Conclusions

Our observations suggest that the progressive low frequency hearing impairment in *Klhl18* mutant mice is an auditory neuropathy affecting the inner hair cells or their synapses with afferent neurons. These findings suggest that *Klhl18^lowf* is not required for development of cochlear responses and that outer hair cells function normally.

PS 132

Generation and Characterization of a Novel Mouse Model Expressing a Fused Prestin-YFP-Chloride Sensor in Outer Hair Cells

Winston Tan[1]; Jun-Ping Bai[2]; Na Xue[3]; Alexei Surguchev[1]; Sheng Zhong[4]; Jennifer Dearman[5]; Tetsuji Yamashita[5]; Jian Zuo[5]; Dhasakumar Navaratnam[6]; Joseph Santos-Sacchi[7]

[1]Department of Surgery (Otolaryngology), Yale University School of Medicine, New Haven, Connecticut, USA; [2]Department of Neurology, Yale University School of Medicine, New Haven, Connecticut, USA; [3]Department of Otolaryngology - Head & Neck Surgery, Shanghai Ninth People's Hospital; Ear Institute, Shanghai Jiao Tong University School of Medicine; Shanghai Key Laboratory of Translational Medicine on Ear and Nose diseases, Shanghai, China; [4]Department of Cellular and Molecular Physiology, Yale University School of Medicine, New Haven, Connecticut, USA; [5]Department of Developmental Neurobiology, St. Jude Children's Research Hospital, Memphis, Tennessee, USA; [6]Department of Neurology and Neuroscience, Yale University School of Medicine, New Haven, Connecticut, USA; [7]Department of Surgery (Otolaryngology), Neuroscience, and Cellular and Molecular Physiology, Yale University School of Medicine, New Haven, Connecticut, USA

Prestin is a motor protein within the lateral membrane of outer hair cells (OHCs). It is a key element for mammalian cochlear amplification, a mechanism responsible for our exquisite hearing sensitivity and frequency selectivity. Chloride (Cl^-), a major anion in cells, plays an important role in modulating prestin activity and hence the electrophysiological properties of OHCs in establishing normal hearing. In our earlier study, we developed a YFP-based chloride sensor (mCl-YFP) that has enhanced chloride sensitivity and photostability, while having reduced pH interference. We collaborated with Dr. Zuo';s lab to create a knockin mouse model on a C57BL/6 background, which expresses mCl-YFP in OHCs, by fusing the Cl^- sensor with prestin. This provides us with an ideal animal model to perform *in vivo/vitro* studies on understanding chloride';s role in hearing. The expression of mCl-YFP in OHCs was confirmed by YFP fluorescence in the lateral membrane of OHCs. In this Cl^- sensor mouse, there is a negative correlation between fluorescence intensity and intracellular Cl^- concentration of OHCs. To assess the *in vivo* function of OHCs, auditory brainstem response (ABR) measurements were performed on postnatal day 44 mice to determine their hearing sensitivity. There was no significant difference ($p > 0.05$, *t*-test) in ABR thresholds across the frequency range (2-32 kHz) between Cl^- sensor mice and age-matched WT mice of the same background. The function of prestin was also assessed by measuring nonlinear capacitance (NLC) of OHCs, an electrical correlate of OHC electromotility. Whole-cell voltage-clamp recording was performed on OHCs in the apical turn of the explant organ of Corti from postnatal day 44 mice. Both the bath and pipette solutions contained ionic blocking components to remove the interference of ionic current on NLC recording. We show that OHCs from Cl^- sensor mice displayed the typical bell-shaped NLC curve in response to voltage perturbation. These results demonstrate that the prestin Cl-YFP fusion construct is functional in these mice and does not interfere with OHC function. Using fast confocal imaging we also determine that mCl-YFP shows the expected decrease in fluorescence (increased intracellular Cl^-) when extracellular Cl^- bathing OHCs was increased to high levels. Our Cl^- sensor mouse is a valuable animal model for future studies of Cl^- on cochlea amplification and the molecular mechanism of this ion';s movements through prestin itself.

PS 133

A rescuable auditory synaptopathy in mice lacking CLARIN-1

Didier Dulon[1]; Samantha Papal[2]; Alice Emptoz[3]; Pranav Patni[2]; Matteo Cortese[2]; Paul Avan[4]; Saaid Safieddine[5]; Aziz El-Amraoui[2]; Christine Petit[6]

[1]INSERM and University of Bordeaux; [2]Pasteur Institute; [3]Institut Pasteur; [4]Centre Jean Perrin, Université Clermont Auvergne, INSERM UMR 1107; [5]Unité de Génétique et Physiologie de l'Audition, Institut Pasteur, UMRS 1120 Inserm; [6]Institut Pasteur, INSERM UMRS1120, Université Pierre et Marie Curie, Institut de la Vision, Collège de France

Clarin-1, a tetraspan-like membrane protein defective in Usher syndrome type IIIA (USH3a) associating progressive deafness and blindness, is essential for

the hair-bundle morphogenesis of auditory hair cells. Here, we addressed a possible role of clarin-1 at the inner hair cell (IHC) ribbon synapses by characterizing two *Clrn1* mouse mutants, a constitutive knockout (*Clrn1*$^{ex4-/-}$) and a postnatal, hair cell-specific conditional knockout (*Clrn1*$^{ex4fl/fl}$*Myo15-cre*$^{+/-}$) mice. Whereas *Clrn1*$^{ex4-/-}$ mice were profoundly deaf, *Clrn1*$^{ex4fl/fl}$*Myo15-cre*$^{+/-}$ mice displayed progressive hearing threshold elevation which develops with normal otoacoustic-emissions and hair bundle morphology, thus indicating an auditory neuropathy.

Both mutant IHCs displayed reduced exocytotic Ca^{2+}-efficiency due to a spatial disorganization of Ca^{2+} channels, and a loss of afferent dendrites associated with an abnormal enlarged distribution of postsynaptic AMPA-receptors.

Protein-protein interactions suggested that clarin-1 interacts with the synaptic Ca$_v$1.3 Ca^{2+} channel complex through the Ca$_v$β2 auxiliary subunit and the PDZ domain-containing protein, harmonin (defective in Usher syndrome type 1C).

Cochlear gene therapy strategy in newborn mutant mice, through AAV-mediated transfer of the clarin-encoding cDNA into hair cells, prevented the synaptic defects and reduced hearing loss at adult age. Our results reveal clarin-1 as a key organizer of the IHC ribbon synapses, and suggest new perspectives for USH3a patients'; hearing treatment.

PS 134

A dual AAV viral vector approach partially restores exocytosis and rescues hearing in deaf otoferlin knock-out mice

Hanan Al-Moyed[1]; Andreia P. Cepeda[1]; Sangyong Jung[2]; Tobias Moser[3]; Sebastian Kügler[4]; Ellen Reisinger[1]
[1]*Molecular Biology of Cochlear Neurotransmission Group, Department of Otorhinolaryngology, University Medical Center Gottingen, Germany, and Collaborative Research Center 889, University of Göttingen, Göttingen, Germany.;* [2]*InnerEarLab, Institute for Auditory Neurosciences, University Medical Center Goettingen, Germany;* [3]*Institute for Auditory Neuroscience;* [4]*Viral Vectors Lab, Dept. of Neurology, University Medical Center Goettingen, Germany*

Normal hearing and rapid synaptic transmission in auditory inner hair cells (IHCs) requires otoferlin. Mutations in otoferlin have been associated with deafness DFNB9, a form of nonsyndromic recessive auditory synaptopathy. Cochlear implants are the only available treatment for hearing impaired patients suffering from this kind of deafness. Because of the limited frequency resolution of these implants, DFNB9 patients would benefit from gene replacement therapy. Gene transfer mediated by recombinant adeno-associated viruses (rAAVs) is considered to be a safe and promising tool to treat several inherited diseases like blindness, muscular dystrophy, and deafness. However, all previous attempts to transfer the 6 kb long coding sequence (CDS) of the full length otoferlin into IHCs to restore hearing in deaf *Otof*$^{-/-}$ mice have failed. Dual rAAV vectors have been developed specially to transfer large genes exceeding the packaging capacity of rAAVs (~5kb). To date, these viral vectors had only demonstrated efficacy in various other cell types, not in IHCs.

In this study we demonstrate, for the first time, that a dual AAV approach can be used to transfer the large full-length otoferlin CDS into auditory IHCs by co-injecting two split-otoferlin AAV half vectors into mice lacking this protein. Transduced *Otof*$^{-/-}$ IHCs not only showed specific full-length otoferlin expression, but also partially restored fast and sustained exocytosis levels as measured by patch clamp recordings. Auditory brainstem response (ABR) amplitudes and thresholds were improved in these animals when subjected to click sound stimuli. Our data suggest that gene delivery mediated by dual AAV viral vectors could be a promising tool for future gene therapy treatments of deafness forms caused by mutations in large genes.

PS 135

Viral gene transfer of short otoferlins partially restores the fast component of synaptic exocytosis in auditory hair cell from OTOF knock-out mice

Margot Tertrais[1]; Alice Emptoz[2]; Yohan Bouleau[3]; Christine Petit[4]; Saaid Safieddine[5]; Didier Dulon[6]
[1]*Laboratoire de Neurophysiologie de la Synapse Auditive, Université de Bordeaux, and UMRS 1120, Inserm;* [2]*Institut Pasteur;* [3]*University of Bordeaux;* [4]*Institut Pasteur, INSERM UMRS1120, Université Pierre et Marie Curie, Institut de la Vision, Collège de France;* [5]*Unité de Génétique et Physiologie de l'Audition, Institut Pasteur, UMRS 1120 Inserm;* [6]*INSERM and University of Bordeaux*

Transmitter release at auditory inner hair cells (IHCs) ribbon synapses involves sustained exocytosis of glutamatergic vesicles during voltage-dependent activation of L-type (Cav1.3) calcium channels (Glowatzki and Fuchs, 2002; Brandt et al., 2003). Remarkably, IHCs do not use

the conventional two-C2 domains synaptotagmins (Syt1 and Syt2) as calcium (Ca^{2+}) sensors to trigger synaptic vesicle fusion (Beurg et al., 2010). Otoferlin, a large six-C2 domains protein (C2A-F), has been proposed to function as a high affinity Ca^{2+} sensor that controls the fast and indefatigable release of synaptic vesicles at the IHCs ribbon synapses (Roux et al., 2006; Beurg et al., 2010; Pangrsic et al., 2010; Vincent et al., 2014). However, the precise molecular events by which individual otoferlin C2-domains contributes and/or regulates the synaptic vesicle cycle is still incompletely understood.

In the present study we have characterized the role of the C-terminal C2-domain of otoferlin. For that purpose, we used an *in vivo* cochlear viral gene transfer to newborn mutant mice. The Adeno-Associated Virus (AAV) mediated efficient transfer of several otoferlin short forms (otoferlin C2-EF, C2-DEF, C2-ACEF or C2-ACDF) into mouse IHCs lacking otoferlin. The expression of these various otoferlin short forms failed to restore hearing. Surprisingly, IHC patch-clamp recordings showed that the expression of these short otoferlin forms resulted in a partial restoration of the fast component of synaptic exocytosis but not of the sustained component. These results confirm that otoferlin is involved in both the fast vesicle fusion and vesicle replenishment (Pangrsic et al. 2010), and suggest that a cooperativity between the six-C2 domains structure is required for an efficient priming-mobilization of synaptic vesicles in IHCs. Interestingly, the partial exocytotic restoration of the fast component was associated with a recovery to near normal amplitude of the fast inactivating Ca^{2+} currents (Vincent et al., 2017), suggesting that Cav1.3 channel short isoforms interacts with otoferlin.

Hearing with Prostheses

PS 136

Frontal and auditory cortex interplay predicts variances of speech-in-noise understanding in cochlear implant users

Inyong Choi[1]; Subong Kim[2]; Adam Schwalje[3]; Youngmin Na[4]; Phillip Gander[5]; Andrew S. Liu[6]; Jihwan Woo[4]; Bob McMurray[1]; Timothy Griffiths[7]
[1]*The University of Iowa;* [2]*University of Iowa;* [3]*University of Iowa Hospitals and Clinics Department of Otolaryngology;* [4]*University of Ulsan;* [5]*Human Brain Research Laboratory, Department of Neurosurgery, The University of Iowa;* [6]*Human Brain Research Laboratory, Department of Otolaryngology-Head and Neck Surgery, University of Iowa Hospitals and Clinics;* [7]*Newcastle University*

Understanding speech in background noise is challenging especially for hearing-impaired listeners. The variance in the speech-in-noise (SiN) understanding ability is significant in cochlear implant (CI) users, which is a critical problem in CI clinics. Variation in the neural encoding of acoustic information, measured as early auditory-cortical evoked responses, is known to contribute to the behavioral variance, while its interaction with cognitive processing mediated by frontal cortex is unclear. Understanding the relative contributions of sensory encoding fidelity and cognitive factors can guide clinical interventions. Here, we explored relationships between the evoked responses from auditory cortex (AC), frontal cortex, and behavioral performance in SiN understanding. Previous electroencephalographic (EEG) studies showed increased inferior frontal gyrus (IFG) activity in the clean speech condition, whereas an fMRI study showed increased IFG activity associated with the increased listening effort. We hypothesized that stronger and faster AC responses predict better performance, and increased amplitude and latency of evoked responses from frontal cortex predict difficulty in SiN understanding. We tested evoked responses to words in multi-talker babble background in 109 CI users (50 male, aged 53-75). Unlike previous evoked-potential studies that used simple nonsense speech tokens, we used one hundred consonant-vowel-consonant spoken words that are standardly used in the clinic and heterogeneous across different manner and place of articulation. Given that the morphology of speech-evoked response is affected by the temporal envelope of words, k-means clustering was applied to partition the word lists into several clusters based on the temporal envelope. A word cluster with steepest attack curves followed by shortest decay contours that mostly included initial stop consonants was included for evoked potential analysis. We found that poor CI performers exhibit stronger late response (later than around 600ms after the word onset) in the frontal area as well as weaker and delayed N1 response at the auditory cortex region. Our results suggest that frontal cortical activity can predict SiN understanding performance of CI users. This study will define several fundamental mechanisms of neural processes required for successful speech-in-noise understanding and will provide an insight to a better understanding of individual variances in CI benefits.

PS 137

Cortical evoked responses reflect cochlear implant-induced improvement of speech-in-noise understanding in single-sided deafness

Inyong Choi[1]; Subong Kim[2]; Adam Schwalje[3]; Camille Dunn[2]; Bruce Gantz[4]
[1]The University of Iowa; [2]University of Iowa; [3]University of Iowa Hospitals and Clinics Department of Otolaryngology; [4]University of Iowa Hospitals and Clinics

Listeners with single-sided deafness (SSD) experience significant difficulties in understanding speech in background noise. This study aimed to investigate neural correlates of SSD listeners'; impaired speech-in-noise understanding and find neurophysiological evidence of recovery of such ability after cochlear implantation (CI) in the deafened ear. We explored CI effect on the evoked responses from auditory cortex (AC), frontal cortex, and behavioral performance in a speech-in-noise understanding task. We hypothesized that CI induces stronger and faster AC responses that predict better performance, and decreased amplitude and latency of evoked responses from frontal cortex reflecting reduced listening effort. In our speech-in-noise test, listeners heard a target word in multi-talker babble, followed by a 4AFC recognition task. The noise started 1 second before the target arises from one of three directions (-30°, 0°, and 30°azimuth: L, C, and R). Target words from California Consonant Test were presented at +3 dB SNR, always arising at 0°azimuth. On each trial, listeners choose between four written words on a screen. Subjects completed 150 trials (50 at each noise direction, presented randomly). We examined accuracy, reaction time, and the distribution of errors. Simultaneously, cortical evoked responses following speech and noise onsets were measured using 64-channel electroencephalography. Our data from 13 SSD-CI listeners demonstrate that evoked response to target word onsets in the auditory cortex increases with CI-on versus CI-off. In the average response of the condition with the CI on, we observed a strong peak at approximately 150 ms in the auditory cortex, whereas the peak is later and less strong in the CI-off condition. The data also demonstrate significant activity in inferior frontal gyrus for the CI-on and CI-off conditions, with a longer latency (of approximately 500 ms) and increased amplitude in the CI-off condition. This region is similar to prior normal-hearing studies showing correlations with attention to degraded speech or increased listening effort. This study will promote our understanding of how the processing deteriorates in unilateral listening and exhibit CI benefit in the neural processes required for successful speech-in-noise understanding.

PS 138

Temporal Coherence, But Not Spectral Coherence, of Background Noise Improves Speech Discrimination for Cochlear Implantees

Adam Schwalje[1]; Subong Kim[2]; Kate Gfeller[1]; Inyong Choi[3]
[1]University of Iowa Hospitals and Clinics Department of Otolaryngology; [2]University of Iowa; [3]The University of Iowa

Background
In real-world situations, speech occurs in many different background sounds, including in background music. Music consists of sounds which are organized in time (temporal coherence) and/or frequency (harmonic or spectral coherence). Competing hypotheses predict different results from speech understanding in background music: Informational masking might make speech in background music harder to understand than speech in background babble that conveys less information than music; on the other hand, co-modulation release from masking might make background music the easier condition. Since cochlear implant (CI) users have relatively preserved gross temporal structure, but impaired pitch perception, we hypothesized that temporal coherence of background music would benefit their speech-in-noise performance, but that spectral coherence would not.

Methods
Ten-second rhythmic (temporally and spectrally coherent) and non-rhythmic (spectrally coherent) music samples were selected to match the long term spectrum of multitalker babble. Low and high signal-to-noise ratio (SNR) babble, along with the "babble-shaped music" samples (presented at the same RMS level as the low SNR babble), were used as background for the California Consonant Test (CCT). Five CI users and ten normal hearing (NH) listeners were asked to select the correct word from four answer choices while 64-channel cortical electrical activity (EEG) was recorded to measure target word-evoked responses.

Results
Behavioral results revealed that, for NH listeners, the easiest condition on average was high SNR babble, followed by rhythmic music, non-rhythmic music, and low SNR babble. For CI listeners, the non-rhythmic music condition was, on average, the most difficult condition. Rhythmic music was easier than non-rhythmic music for most NH and CI subjects. Preliminary cortical evoked response analysis for the NH subjects revealed significantly stronger late (~550ms after word onset) right frontal negative deflection in the nonrhythmic music condition compared to the rhythmic music condition.

Conclusions

Temporal coherence of the music background improved speech-in-noise discrimination for both cochlear implantees and normal hearing listeners, while spectral coherence of the music background improved performance, relative to multitalker babble, only for normal hearing listeners. The nonrhythmic but spectrally coherent music sample was more difficult to segregate from a speech stream than multitalker babble for cochlear implantees. Spectral coherence of the background music therefore degraded performance for CI users. EEG results show increased right frontal activity in the more difficult music condition, which may indicate listening effort. Further analysis of the neural pathways involved in this performance decrease might lead to targets for intervention.

PS 139

Electric and Acoustic Pitch Fusion Ability Predicts Speech-in-Noise Performance in Hybrid Cochlear Implant Users

Adam Schwalje[1]; Damien Bonnard[2]; Bruce Gantz[3]; Inyong Choi[4]
[1]University of Iowa Hospitals and Clinics Department of Otolaryngology; [2]University of Bordeaux, Department of Otolaryngology; [3]University of Iowa Hospitals and Clinics; [4]The University of Iowa

Background

Complex pitch perception relies on place or temporal fine structure-based mechanisms from resolved harmonics and the temporal envelope of unresolved harmonics. Combining this information is essential for speech-in-noise performance, as it allows segregation of a target speaker from background noise. In hybrid cochlear implant (H-CI) users, low frequency acoustic hearing should provide pitch from resolved harmonics while high frequency electric hearing should provide temporal envelope pitch from unresolved harmonics. How the acoustic and electric auditory inputs interact for H-CI users is largely unknown. We hypothesized that some H-CI users would be able to fuse acoustic and electric information for complex pitch perception, and that this ability would be correlated with speech-in-noise performance. In this study, we used perception of inharmonicity to demonstrate this fusion.

Methods

Harmonicity and inharmonicity are emergent features of sound in which overtones are concordant or discordant with the fundamental frequency. Thirteen H-CI users with only acoustic hearing below 500 Hz, only electric hearing above 1KHz, and more than 6 months CI experience, along with twelve normal hearing (NH) controls, were presented with harmonic and inharmonic sounds. The stimulus was created with a low frequency compo-

nent, corresponding with acoustic hearing (f0 between 125-175 Hz), and a high frequency component, corresponding with electric hearing. Subjects were asked to identify the more inharmonic sound, which requires the perceptual fusion of the low and high components, while 64 channels of cortical electrical activity (EEG) were recorded. Speech-in-noise performance was tested in both groups using the California Consonant Test (CCT), and perception of CNC words in quiet was tested for the CI users.

Results

Seven of the H-CI subjects (54%), and all of the NH subjects, scored significantly above chance level for inharmonicity detection. These results were significantly correlated with speech scores in both quiet and noise for H-CI users, but not for NH listeners. Preliminary analysis of EEG recordings revealed a significant difference in P2 amplitude between high and low performing H-CI users. NH controls had increased mid-latency frontal activity (at ~300 ms after sound initiation) in the harmonic condition.

Conclusions

We demonstrate fusion of acoustic and electric information in H-CI users for complex pitch sensation. The correlation with speech scores in H-CI users might be associated with the ability to segregate a target speaker from background noise using the speaker';s fundamental frequency. Further analysis of cortical pathways will help guide our understanding of the mechanisms underlying this fusion and associated perceptual improvement.

PS 140

The window of tempral integration for bone-conducted ultrasound

Tadao Okayasu[1]; Tadashi Nishimura[2]; Yuka Uratani[1]; Akinori Yamashita[3]; Seiji Nakagawa[4]; Hiroshi Hosoi[1]; Tadashi Kitahara[3]
[1]Nara Medical University; [2]Otolaryngology - Head and Neck Surgery, Nara Medical University; [3]Department of Otolaryngology - Head and Neck Surgery, Nara Medical University; [4]Center for Frontier Medical Engineering, Chiba University

Some profoundly deaf can perceive bone-conducted ultrasound (BCU) over 24k Hz which is the upper limit of air-conducted audible sound (ACAS). Moreover, they can recognize the speech signals through the amplitude-modulated BCU. This characteristic of BCU provides the possibility of the creating a bone-conducted ultrasonic hearing aid which is the alternative to a cochlear implant. However, the characteristic of ultrasonic perception has not been enough studied. In ACAS, the central auditory system can integrate the closely pre-

sented sounds into single information units such as temporal integration. The window of the temporal integration estimated by loudness summation and backward masking are considered about 200ms. This study investigated the temporal integration window (TWI) of BCU estimated by stimulus omission using magnetoencephalography (MEG). Eight subjects with normal-hearing took part in this study. We measured the MMFs evoked by stimulus omission in the BCU train in the steady onset-to-onset time (SOA) at 100, 125, 150, 175, 200, or 350ms. The frequency of the ultrasound signal was set at 30-kHz. The duration was set at 50 ms, including rise and fall ramps of 5 ms. The intensity was set at 15 dB sensation level. MEG recordings were performed with a 122-channel whole-head neuromagnetomater (Neuromag-122TM). All participants obtained sufficient MMF for omission with the three shortest SOAs at 100 to 150 ms. However, with the SOA 175 ms only 4 participants and with the SOAs 200 to 350 ms no participant obtained sufficient MMF. On the other hand, a few participants obtained sufficient N1m for BCU stimuli next the omission with shorter SOAs at 100 to 175 ms. All participants obtained sufficient N1m with the longest SOA at 350 ms. The MMF peak amplitude for all subjects was larger for the three shortest SOAs than for the longer SOAs (p < 0.01). On the MMF latency, revealed no significant main effects of SOA. Previous studies reported that TWI for ACAS estimated by MMF omission was approximately 150-200 ms. Since all participants found definite MMF elicited by stimulus omission with the SOA 100 to 150 ms and without SOA 200 and 350 ms, the TWI for BCU was estimated to 150 to 200 ms which was similar to that of ACAS. In ordinary conversation, stimulus duration and omission are important cues of prosody. These similarities of TWI and the detection of omission may support the possibility of the creating the transmission system using BCU.

PS 141

Speech Intelligibility of Speech-Modulated Bone-Conduction Ultrasound

Akinori Yamashita[1]; Tadashi Nishimura[2]; Yoshiki Nagatani[3]; Hiroshi Hosoi[4]; Tadashi Kitahara[1]
[1]*Department of Otolaryngology - Head and Neck Surgery, Nara Medical University;* [2]*Otolaryngology - Head and Neck Surgery, Nara Medical University;* [3]*Kobe City College of Technology;* [4]*Nara Medical University*

Background

Since Gavreau reported that ultrasound could be perceived through bone- conduction, many interesting characteristics have been reported about bone conducted ultrasonic perception. Especially, recent studies indicated that Bone-conducted ultrasound(BCU) modulated by different speech sounds could be discriminated by some profoundly deaf subjects as well as the normal hearing. These findings suggest the usefulness of developing a bone conducted ultrasonic hearing aids(BCUHA). Recently, a prototype for a bone-conducted ultrasonic hearing aid for the profoundly deaf have been developed. However, the characteristics of BCU are still poorly understood. The first aim of this present study was to compare BCU and air-conducted audible sound(ACAS) in terms of their associated speech perception tendency and to investigated the difference perceptual characteristics of BCU and ACAS. The second aim was to investigate the effects of visual information(lip-reading information) on intelligibility in BCU perception.

Methods

（1）Speech discrimination tests using Japanese 20 monosyllables were performed with normal hearing subjects at both BCU and ACAS. The results were compared for intelligibility and hearing confusion.（2）Speech discrimination tests were performed in audio alone condition, aidio-visual condition and visual condition. The results were compared.

Results

Hearing confusion with ACAS and BCU according to the individual syllabic nuclear group showed a clear difference in incorrect rates. Moreover, the stimulus nuclear groups were often perceived in other nuclear group in BCU.Our results showed that lip-reading information strongly affected speech intelligibility of speech-modulated bone-conduction ultrasound.

Conclusion

We found that it is possible to transmit language information using BCU in normal haring subjects. Our findings indicate that BCUHA has potential as one possible option for deaf individuals to obtain hearing information. On the other hand, our findings also suggested the efficacy of use of signal processing techniques in improving the intelligibility of prior consonants.

PS 142

Brain Computer Interface for Cochlear Implants: First Results of Epidural Recording

Magnus Teschner[1]; Sabine Haumann[2]; Günther Bauernfeind[1]; Jochem Rieger[3]; Martin Bleichner[4]; Thomas Lenarz[5]

[1]Department of Otolaryngology, Hannover Medical School, Germany; Cluster of Excellence "Hearing4all"; [2]Department of Otolaryngology, Hannover Medical School, Germany; Cluster of Excellence; [3]Applied Neurocognitive Psychology, Carl-von-Ossietzky-University, Oldenburg, Germany; Cluster of Excellence "Hearing4all"; [4]Applied Neurocognitive Psychology, Carl-von-Ossietzky-University, Oldenburg, Germany; Cluster of Excellence Hearing4all; [5]Department of Otolaryngology, Hannover Medical School, Germany and DFG Cluster of Excellence Hearing4all

Introduction

Brain Computer Interface systems are an important step for the optimization of hearing implants. These systems would allow a direct control feedback between the physiological response and the Implant. Compared to conventional EEG electrodes, the use of implanted epidural electrodes offers numerous advantages since it allows better signal quality and near-field recording from the auditory cortex. The aim of the present study was therefore to test concepts for the implementation of epidural closed loop systems for hearing implants. Methods: In 9 patients, epidural electrodes were placed during a cochlear implantation temporarily between the dura mater and the cranial vault over primary auditory cortex. Intraoperatively, BERA and MLR were recorded. In addition, postoperatively, measurements of BERA, MLR, CERA, MMN and P300 were recorded. Stimulation was performed acoustically via the cochlear implant from the ipsilateral side. The epidural electrodes were removed after a few days.

Results

To date, 9 patients were temporally implanted. These data show promising results; particularly with the CERA, epidurally clearer waves could be recorded which were clearly recognizable even at lower stimulation intensities. There was a strong dependence on the location and the type of stimulus. Conclusions: Epidural recordings pursued here could be carried out well and provides clearly recognizable AEP waves. The results represent an important step in the development of closed loop systems for hearing implants, especially for cochlear implants.

PS 143

Optical Neuroimaging of Speech Perception in Listeners with Cochlear Implants

Arefeh Sherafati[1]; Mahlega S. Hassanpour[2]; Adam T. Eggebrecht[3]; Joseph P. Culver[4]; Jill B. Firszt[5]; Jonathan E. Peelle[6]

[1]Departments of Physics, Washington University School of Medicine, St. Louis, Missouri 63110, USA; [2]Departments of Physics, Washington University School of Medicine, St. Louis, Missouri 63110, USA. Moran Eye Center, University of Utah, Salt Lake City, Utah, 84112, USA; [3]Departments of Radiology, Washington University School of Medicine, St. Louis, Missouri 63110, USA; [4]Departments of Physics, Radiology, Biomedical Engineering, Division of Biology and Biomedical Sciences, Washington University School of Medicine, St. Louis, Missouri 63110, USA; [5]Department of Otolaryngology - Head and Neck Surgery, Washington University School of Medicine; [6]Departments of Otolaryngology. Washington University School of Medicine, St. Louis, Missouri 63110, USA

There is tremendous variability in how well listeners with cochlear implants (CIs) understand speech, especially in the presence of background noise. One possibility is that individual differences in the engagement of higher-level cortical networks contribute to speech comprehension success. Our goal was to map the neural systems supporting speech comprehension in listeners with CIs using High Density Diffuse Optical Tomography (HD-DOT), an optical neuroimaging technique with a spatial resolution comparable to that of fMRI [1]. HD-DOT is ideal for studying people with implanted medical devices because it poses no safety risk, and artifacts in the measured signal are minimal. We recorded the brain';s hemodynamic response to the audition of single words and short sentences in both listeners with CIs and normal-hearing participants using a previously described HD-DOT system (Fig. 1) [3]. The sentence processing task contained 20 noise trials (1-channel noise-vocoded speech as a control condition) and 40 AzBio sentences (a set of sentences designed for speech perception evaluation in hearing impaired listeners) [2]. Eight of the sentences were followed by a visually presented probe word. Listeners were instructed to press a key if the probe word was semantically related to the last sentence presented. During each hearing words task, participants listened to a total of 90 words during six trials. Each trial contained 15 words, followed by 15 seconds of silence. We studied five control subjects and two participants with a right side unilateral CI (two sessions for each participant). We used a General Linear Model (GLM) to analyze the data. Our results demonstrate left and right superior temporal gyri activation in response to the hearing words task for control participants, and right superior temporal gyrus

activation for participants with a CI (Fig. 2a). In response to the sentences, we saw left middle and superior temporal gyri, right superior temporal gyrus, and left inferior frontal gyrus activations in controls. However, for participants having a CI, in addition to the left inferior frontal gyrus, left and right occipital cortex activations were also observed (potential compensatory activation observed only in participants having a CI) (Fig. 2b). We also subtracted the responses to noise from the responses to sentences and we found very similar regions to those for sentences only (Fig. 2c). In summary, we designed an experimental paradigm that enabled us to investigate the neural substrate for speech processing in listeners with a CI using HD-DOT.

ARO 2018_Figures.docx

ARO 2018_References.docx

PS 144

Role of Cognitive Factors in Variability of Hearing Outcomes in Cochlear-Implant Users and Normal-Hearing Listeners with Simulated Current Spread

Erin O'Neill; Heather A. Kreft; Andrew J. Oxenham
University of Minnesota

Background
Anatomical, physiological, and surgical factors at the level of the auditory periphery have been studied extensively in an attempt to explain the substantial individual differences in performance between cochlear implant (CI) users. Despite these efforts, the proportion of variance in speech perception abilities accounted for by other measures, such as spectral resolution, is generally small. In this study, our aim was to determine the degree to which non-peripheral factors, unrelated to cochlear implantation, may affect performance.

Methods
CI users were tested in measures of high- and low-context sentence recognition in quiet and noise, working memory, intellectual efficiency, and spectral resolution. We compared their results with those from normal-hearing (NH) younger and older adults, who were presented with sounds via tone-excited vocoders designed to simulate the poor spectral resolution experienced by CI users.

Results
The data suggests that CI users make more use of context in sentences than do NH listeners, but also demonstrate poorer overall performance on cognitive measures of working memory and intellectual efficiency than both young and older NH controls. CI users also showed significantly greater variance in some, but not all of the measurements, indicating that performance variability seen in the CI population may not be so different from that found in the NH population when performing auditory and cognitive tasks of equated difficulty.

Conclusion
Overall, the work suggests that it is important to determine the extent of more central contributions to variability when attempting to understand the effects of more peripheral factors.

PS 145

Novel computer-based therapy enhances speech perception in Cochlear Implant users

Akshay R. Narayan
University College London

Introduction
Auditory therapy is offered post-surgery to cochlear implant users and helps them to differentiate between specific sounds,phonemes, and identify words. In the UK, there are very limited facilities for provision of auditory therapy. The main limitations of auditory therapy in the UK are twofold: 1) they mostly require face-to-face interaction which requires patients to come into healthcare centres to receive therapy and 2) computer-based programmes utilise the same pitch and tone. Since we explored the possibility of providing personalized auditory therapy in the comforts of patient';s homes, we aimed to investigate if our new computer-based therapy,which adapts its tone and pitch based on each patient';s unique deficiencies,is more effective at improving speech perception.

Methods
In this randomized control trial, candidates were split into two groups and underwent three rounds of testing. In the first round,all candidates underwent testing where they identified words that they heard and the percentage of correctly identified words was recorded. Subsequently in the second round,they received training where they practised listening to sentences and identifying the words in the sentence. If they failed to identify a word correctly,the sentence was replayed identically for candidates in the first group. In the second group, specific emphasis was placed on the word in the sentence candidates could not identify by varying its tone and pitch. In the third round, they underwent testing again and the percentage of words they were able to correctly identify before and after training was compared. A paired t-test was used to analyse the data and see if there was any significant difference in the levels of improvements between the two groups.

Results

There were 8 and 9 candidates in the first (those who received standard computer-based auditory therapy) and second group (those who received our therapy that modifies the pitch and tone based on the patient';s performance in the initial round) respectively. The mean percentages for candidates in the first round of testing in the first and second groups were 50.63%(95%CI 37.3-65.2) and 53.5%(95%CI 38.1-69.3). The mean percentages for candidates in the second round of testing were 52.5%(95%CI 38.4-68.2) and 67.78%(95%CI 54.6-80.9).The mean improvement in scores was greater in those in the second group than first group(p=0.0432).

Conclusion

Our new computer program improves their speech perception to a greater extent with the same amount of training. Given the promising results, broadening the study to a larger patient population would be ideal.

PS 146

Pilot Trial Exploring AUT00063, an Oral Modulator of Voltage-gated Potassium Channels, in Cochlear Implant Users: QuicK+fire

Victoria A. Sanchez[1]; Alice Sharman[2]; Sornaraja Thasma[2]; John Hutchison[2]; Shakeel R. Saeed[3]; Charles H. Large[2]; Peter Harris[2]
[1]*University of South Florida;* [2]*Autifony Therapeutics;* [3]*University College London*

Although cochlear implants (CIs) bypass damaged parts of the inner ear and provide access to sound, many CI users still struggle to recognize speech, especially in noisy environments. We conducted a Phase IIa clinical trial (QuicK[+]fire; clincaltrial.gov ID# NCT02832128), which was a multi-site, randomized double-blind, placebo-controlled, crossover design, pilot trial that examined an orally taken investigational medicinal product (AUT00063) in 12 post-lingual CI users (26-82 years; 5 MedEl and 7 Cochlear). AUT00063 is a novel molecule that positively modulates Kv3.1b fast-activating potassium channels that are important for returning the cell membrane to its resting state soon after an action potential, and are found at all levels in the auditory system. Kv3.1b channels are important in central auditory neurons that must fire rapidly and with precise timing such as in circuits involved in decoding speech. In a mouse model of auditory neuropathy in which auditory input from the cochlea is drastically reduced, leading to central adaptive changes, AUT00063 improved the timing of firing and synchronization of neurons in the inferior colliculus in response to auditory stimuli (Polley et al. 2014, Soc. Neurosci.). It was thought that by increasing the precision and timing of neural firing (allowing neurons to "quickfire"), AUT00063 may enhance the central auditory performance and could be a potential therapy for CI users by improving neural synchrony, temporal processing, and speech recognition in noise. Here we report the safety and efficacy results of AUT00063 versus a matching placebo using The Minimum Speech Test Battery (MSTB; Auditory Potential, 2011). The MSTB collects performance on the AzBio sentences in quiet and in noise, Consonant-Nucleus-Consonant (CNC) words in quiet, and the Bamford-Kowal-Bamford Speech-in-Noise (BKB-SIN) test. From baseline to 28 days, both active and placebo periods improved on the MSTB, but the between-treatment difference was not statistically significant. The crossover design allowed for the evaluation of the MSTB stability and the outcome measures showed strong test, re-test reliability. In addition, AUT00063 was found to be safe and well tolerated and the trial data were of high quality, with excellent compliance and retention; thus, allowing for a conclusive outcome. Logistical lessons learned including design, recruitment, and outcome measures will be discussed and implications for future pharmaceutical studies.

Middle Ear Cavity & Pathology

PS 147

Cilia polarity in the epithelial lining of ~~~~~ce middle ear and eustachian tube

Wenwei Luo[1]; Dongdong Ren[1]; ~~~~ ~hen[2]; Fanglu Chi[1]
[1]*EYE & ENT Hospital of ~~~ University;* [2]*Department of Cell Biology, Emo~~ ~~rsity, Atlanta, GA 30322, USA*

Motility a~~ ~~~~~~ar polarity are essential features of multicilia t~~ ~~~~ntee coordinated beating and proper mucociliary clearance in epithelium of mammalian airway, ependymal, and oviduct. Defects in cilia ploarity or motility lead to recurrent respiratory infection,chronic nasal congestion, infertility,and hydrocephaly. In mammals, the middle ear cavity and the eustachian tubes are covered with a comparable multiciliated cells, which allows air pressure on the eardrum to be equalized and elimination of debris or infectious particles from middle ears. Chronic otitis media with effusion (COME) is the leading cause of conductive hearing loss. However, ciliation and polarity information of the motile cilia in the middle ear cavity and the eustachian tubes is limited. In our study, we confirmed the presence of a ciliated region near the eustachian tube orifice at the ventral region of the middle ear cavity. In addition, we found that the epithelial of eustachian tube was discontinuously ciliated along the middle ear-to-nasopharynx axis. We also demonstrated that both middle ear and Eustachian tube epithelium consist of a lumen layer of multi-ciliated and a layer of Keratin- 5-positive basal cells. Further more, we con-

firmed that the motile cilia in epithelium of middle ear and the eustachian tubes were polarized coordinately and displayed a planar cell polarity. We also detected the asymmetric localization of core PCP proteins in the these epithelium. Our study revealed for the first time coordinated polarity of cilia in the epithelium of themammalian middle ear and the eustachian tubes, thus illustrating novel structural features that may lead tochronic otitis media and related to OM susceptibility.

Middle Ear Cavity & Pathology

PS 148

Redistribution of Tight Junction Molecules by Diesel Exhaust Particles in Upper Respiratory Epithelial Cells

Nahyun Kim[1]; Moo Kyun Park[2]
[1]Center for Medical Innovation, Seoul National University Hospital, Seoul, South Korea; [2]Seoul National University Hospital

Objectives
Tight junction (TJ) in epithelium plays a critical role to form the epithelial barrier against extracellular environment. Diesel exhaust particles (DEP) have been reported that disrupt the epithelial barrier. However, the signaling pathway involved in the process remains unclear. The aim of this study is to investigate whether the pattern recognition receptors such as TLRs affect diesel exhaust particles (DEP) - induced epithelial barrier dysfunction in primary human nasal epithelial cells (PHNECs) and human middle ear epithelial cells (HMEEC).

Methods
PHNECs and HMEEC cultured at an air/liquid interface (ALI) create a fully differentiated, in-vivo-like model of the human nasal epithelium and then were exposed to DEP (PM<4μm) and lipopolysaccharide (LPS). Cell vitality was determined by MTT assay. TJ paracellular permeability was assessed using fluorescently labelled dextrans. TJ molecules ZO1 and occludin expressed membrane surface were observed by confocal microscopy and detected by biochemistry assay. Results: TJ paracellular permeability was significantly increased after 24h of exposure to 25, 50, 100, 200μg/cm2 of DEP in PHNEC and HMEEC epithelium. In the presence of DEP, membrane expression of ZO1 and occludin in differentiated nasal epithelium were significantly decreased when compared to the control. Cell viability was not affected up to 20ug/ml of LPS treatment for 24h in PHNEC. Treatment of 10ug/ml of LPS at the same time with DEP significantly increased membrane expression of occludin but not ZO1. Colocalization of ZO1 and Occludin was also increased by simultaneous treatment of LPS with DEP. TJ paracellular permeability increased by exposure to DEP was also decreased by si-

multaneous treatment of 10ug/ml of LPS with DEP in both PHNEC and HMEEC epithelium. Conclusion: Activation of TLR by LPS can affect redistribution of tight junction molecules induced by DEP, leading to modulate paracellular permeability to small molecules, which might increase cell survivability in harsh environmental conditions.

PS 149

The clinical implication of poloxamer 407 as packing material in an animal model

Ji-Eun Choi[1]; So-Young Chang[2]; Jae-Hun Lee[3]; Min Young Lee[1]; Jae Yun Jung[1]
[1]Dankook University College of Medicine; [2]Beckman Laser Institute Korea; [3]Beckman Laser Institute Korea, Dankook University

Background and Objective
The primary aims of middle ear packing are to support the grafts and provide hemostasis. Gelfoam® is now commonly used in the otorhinolaryngology field around the world. However, gelfoam can provoke severe connective tissue hyperplasia, resulting in adhesion and fibrosis surrounding the tympanic membrane (TM) and grafts. Previous studies have reported that unexpected fibrosis and adhesion was found in patients who underwent second look or revision ear surgery. Recently, endoscopic ear surgery has become popular, and packing materials that can easily be packed with one-hand are needed. Poloxamer 407 (P407) is one of the thermos-reversible gels and has been proposed as a matrix for drug delivery. P407 also have been shown to have antiadhesive activity and to prevent postsurgical tissue adhesion. Therefore, we aim to investigate the clinical implication of P407 as packing material in animal model.

Materials and Methods
Eight male Hartley guinea pigs (350 and 400 g) were utilized in this study. The animals were randomly divided into four groups according to packing materials, the control group (n=2), the P407 group (n=3), and the gelfoam group (n=3). To assess the role of packing materials on bacterial colonization, left ears were inoculated with Streptococcus pneumoniae through the TM using 0° endoscope. On the 5 day post-inoculation, the middle ear cavity was packed through transbullar approach using 18% P407 and gelfoam on both ears. In the control group, no ear pack was inserted. The eardrum was examined TM every week using 0° 1.9-mm endoscope. Three animals per each group were sacrificed 3 weeks after placement of the packing material.

Results
Two of three in gelfoam group showed severe otorrhea after packing gelfoam in the left ears. Histological anal-

ysis showed inflammation, granulation tissue formation, and foreign body reaction was severe in gelfoam group than P407 group.

Conclusion

This study demonstrated that P407 is feasible as a packing material to prevent adhesion, especially infected middle ear mucosa. This study was supported by Basic Science Research Program through the National Research Foundation of Korea (NRF) funded by the Ministry of Science, ICT & Future Planning (NRF-2015R1C1A1A01052624)

PS 150

Sensorineural Hearing Loss observed in Patients with Glomus Tympanicum

Dhrumi Gandhi; Danielle R. Trakimas; Iman Ghanad; Elliott D. Kozin; Barbara S. Herrmann; Michael McKenna; Aaron K. Remenschneider
Massachusetts Eye and Ear Infirmary, Harvard Medical School

Background

Glomus tympanicum, a paraganglioma typically arising over the cochlear promontory, is the most common middle ear tumor. While glomus tumors often present as an asymptomatic mass, they may also cause pulsatile tinnitus, otalgia, or hearing loss. Tumor-associated hearing loss is typically attributed to disruption of the conductive pathway, or through labyrinthine fistula. Little is known about the incidence and mechanisms of sensorineural hearing loss in glomus tumors without fistulae. We hypothesize that a subgroup of low grade glomus tympanicum tumors may be associated with ipsilateral sensorineural hearing loss and that hearing losses may resolve following surgical removal.

Methods

Consecutive adult patients with unilateral glomus tympanicum tumors diagnosed during a 10-year period (2007-2017) from a single academic center were reviewed. Cases were included if 1) tumor was treated with surgical resection alone and 2) pre and post-operative audiometry was available. Clinical, surgical, and radiologic records were reviewed. Pre-operative hearing status was reported as sensorineural (SNHL) (≥10 dB difference in bone pure tone average (PTA) on tumor vs non-tumor side), conductive (CHL) (air-bone gap ≥10 dB on tumor side), or normal. Tumor size was graded using the Glasscock-Jackson classification scale. Additionally, specimens with a diagnosis glomus tympanicum tumor from a human temporal bone repository were studied by light microscopy and histologically described.

Results

Fifteen patients met inclusion criteria for the study. Pre-operatively, five patients (33%) showed SNHL, seven patients showed CHL, and three patients had normal hearing. Patients with pre-operative SNHL or normal hearing tended to have lower tumor grades than those with CHL. Following tumor resection, one patient with SNHL showed an improvement of 15dB PTA and increase of 14% in WRS, while the remainder of patients were unchanged. Otopathologically, three ears containing glomus tympanicum tumors were identified. Inner and outer hair cells appeared to be well preserved, but patch atrophy of the stria vascularis was observed in one specimen. This specimen also demonstrated asymmetric SNHL on pre-mortem audiogram.

Conclusions

Review of a small cohort of patients with glomus tympanicum identified a subset with SNHL. Histological analysis of temporal bones showed a greater atrophy of the stria vascularis in the one patient with hearing loss. Mechanisms of SNHL in patients with glomus tympanicum is unknown but could include tumor secreted ototoxins. Larger studies are needed to replicate findings and identify the natural history of postoperative hearing.

PS 151

Volumetric Analysis of Cholesteatoma Induced with a Novel Ear Canal Ligation Approach in a Gerbil Model

Ivy Schweinzger[1]; Brian Earl[2]; Ravi Samy[1]; Joseph Pinkl[2]; Randi Wray[1]
[1]*University of Cincinnati;* [2]*2. University of Cincinnati*

Background

Cholesteatomas (CHST) are lesions of the temporal bone that, if left untreated, can cause hearing loss, dizziness, facial paralysis, or death. Surgical removal has been the standard of care for over 100 years; however, the recurrence rate can be as high as 70%. Recent *in vitro* research has shown that virotherapy with an oncolytic herpes simplex virus (oHSV) could be effective in selectively eliminating CHST cells. The objective of this pilot study was to establish an *in vivo* CHST model using a novel ear canal ligation approach in gerbil with 3D volumetric analysis of CHST growth.

Methods

A novel double-ligation approach was completed in 16 Mongolian gerbils, bilaterally, to induce CHST growth. Post-auricular incisions were made to access the cartilaginous portion of the external auditory canals. The canals were transected 2-3 mm lateral from the osseo-cartilaginous junction followed by a 20 ul inoculation of

Pseudomonas aeruginosa (PA; which expedites CHST growth) into the bony canal. The medial and lateral edges of the transected canals were then ligated with silk sutures and the skin incision was closed with absorbable sutures. At six weeks post-inoculation, gerbils were euthanized and microCT imaging was completed. Volumetric analyses were completed using Siemens Iveon analysis software to determine the size of CHST and the associated bone erosion and/or bone growth.

Results

Preliminary data showed that the double ligation plus PA inoculation led to CHST growth in 93% of ears within the six-week time frame. The medial ligation was still intact for 66% of ears, while the lateral ligation was intact for 71%. Of those ears with an intact medial ligation, 70% had CHST growth ranging from Stage I-V (per the McGinn et al., 1982 CHST classification) with 62.5% of experimental gerbils exhibiting different stages across ears. MicroCT images showed that 31% of ears exhibited osteoblastic effects while only 6% exhibited osteolytic effects as a result of CHST presence.

Conclusion

Overall, the double-ligation plus PA inoculation technique was highly successful in inducing CHST in gerbil. Given that a larger percentage of lateral ligations remained intact compared with medial ligations, there is a relative advantage of the double- vs. single ligation approach. The 3D volumetric analysis provides high-resolution assessments of CHST volume that will be useful in evaluating the effect of treatment with oHSV on CHST growth and the resultant osteolytic and osteoblastic processes in future experiments.
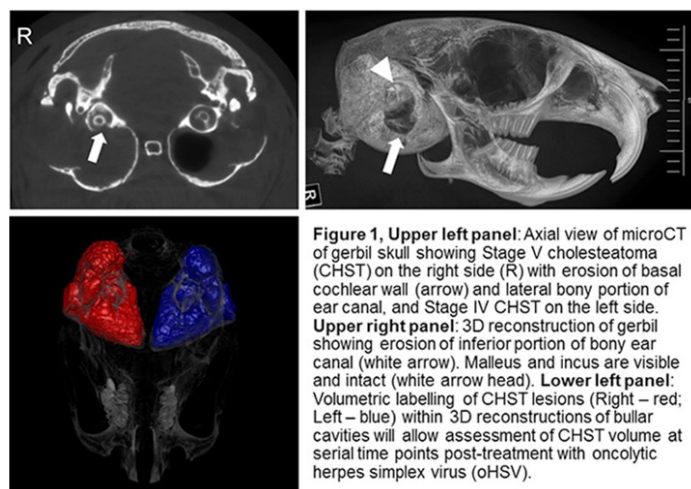
Figure 1, Upper left panel: Axial view of microCT of gerbil skull showing Stage V cholesteatoma (CHST) on the right side (R) with erosion of basal cochlear wall (arrow) and lateral bony portion of ear canal, and Stage IV CHST on the left side. **Upper right panel**: 3D reconstruction of gerbil showing erosion of inferior portion of bony ear canal (white arrow). Malleus and incus are visible and intact (white arrow head). **Lower left panel**: Volumetric labelling of CHST lesions (Right – red; Left – blue) within 3D reconstructions of bullar cavities will allow assessment of CHST volume at serial time points post-treatment with oncolytic herpes simplex virus (oHSV).

An Animal Model of Cholesteatoma for Improvement of Middle Ear Surgical Reconstruction

Rong Z. Gan[1]; Tao Chen[1]; Kyle Smith[1]; Shangyuan Jiang[1]; Zachary Yokell[1]; Betty Tsai Do[2]; Robert Jyung[3]
[1]University of Oklahoma; [2]University of Oklahoma Health Sciences Center; [3]Rutgers New Jersey Medical School

Introduction

Acquired cholesteatoma is an invasive, destructive disease of the temporal bone which causes conductive hearing loss through various mechanisms such as the erosion of ossicular bones and retraction of the tympanic membrane (TM). Cholesteatoma is morphologically characterized by epithelial cell proliferation and granulation tissue formation due to chronic Eustachian tube dysfunction. Only surgical treatment is effective, but recurrence is common. Hearing restoration following surgical eradication of cholesteatoma critically depends on middle ear reconstruction using TM grafts and ossicular replacement prostheses. However, the outcomes from middle ear reconstruction depend on the disease severity. Understanding the mechanism of cholesteatoma formation and developing patient-specific prostheses will optimize hearing outcomes. This paper reports our preliminary studies on development of an animal model of cholesteatoma at different stages of disease severity and innovation of 3D printed middle ear prostheses for reconstruction of diseased ears. The goal is to provide an animal model for mapping the cholesteatoma progression and enhancing middle ear prosthesis design for surgical reconstruction.

Methods

The cholesteatoma was established in chinchillas through administration of propylene glycol (PG) as reported by Vassalli et al. (1988). 20 animals were included and the PG solution was injected into the right ear with untreated left ear as control. Different PG concentrations (50%, 70%, and 90%) with variable inoculation length (10 days, 2 and 6 weeks) were used to examine the severity of cholesteatoma. Endoscopic photography and histologic images of chinchilla temporal bones/bullae documented the cholesteatoma formation. Surgery to remove cholesteatoma and implant 3D-printed middle ear prostheses prototyped in our lab were performed at the end of inoculation period following the micro-CT scanning of the ear. Middle ear and cochlear functions were tested after one week of recovery.

Results and Discussion

Histological sections and endoscopic photos show that the inflammation, epithelial cell proliferation, keratin layers, and matrix of cholesteatoma were formed near the

bony septa and bulla/cavity wall after 10 days of inoculation at 70% or 90% PG. Fig. 1 shows histologic section images of cholesteatoma developed during the inoculation time course. Results indicate that the PG injection volume/frequency and the inoculation length affect cholesteatoma severity, in addition to PG concentration. However, there was no obvious difference between 70% and 90% concentrations. The extent of destruction by the cholesteatoma identified in our preliminary studies will be used for further investigation of middle ear cholesteatoma and surgical treatment. (Supported by NIH R01DC011585)

ARO 2018 abstract-Rong Gan-Figure 1.doc

PS 153

Keratinocyte Growth Factor (KGF) Modulates Epidermal Progenitor Cell Kinetics Through activation of p63 in middle ear cholesteatoma.

Tomomi Yamamoto-fukuda[1]; Naotaro Akiyama[2]; Hiromi Kojima[1]
[1]Department of Otorhinolaryngology, Jikei University School of Medicine; [2]Department of Otorhinolaryngology, Toho University School of Medicine

Research Background

The basal stem/progenitor cell maintains homeostasis of epidermis and progressive disturbance of this homeostasis has been implicated as a possible cause in the pathogenesis of epithelial diseases such as middle ear cholesteatoma. In many cases of stem/progenitor cell regulations, the importance of extracellular signals provided by surrounding cells is well recognized. Keratinocyte growth factor (KGF) is a mesenchymal-cell-derived paracrine growth factor that specifically participates in skin homeostasis, but over expression of KGF induced middle ear cholesteatoma. In this study, we investigated the effect of over-expressed KGF on cell kinetics of stem cells, progenitor cells and more differentiated cells.

Methods

In this study, the expression levels of p63 (stem/progenitor cell marker) and phosphorylated p63 (pp63) (progenitor cell marker) were examined by immunohistochemical analysis of cholesteatomas and skin tissues obtained from patients during ear surgery. And more we investigated in vivo study, mice ear skin tissues were transfected with FLAG-hKGF expression vector or null vector by electroporation and analyzed at 1, 4 and 7 days following transfection. 5-bromo-2'-deoxyuridine (BrdU) was injected intraperitoneally at 24 hours prior to transfection and to label proliferative cells such as stem cells and progenitor cells 5-ethynyl-2'-deoxyuridine (EdU) was injected intraperitoneally at 2 hours prior to each sacrifice.

Results

As a result, increased number of pp63 positive cells detected in human cholesteatoma tissue. Over-expression of KGF increased proliferative activity of basal and suprabasal cells in the epithelium accompanying a high expression of p63. BrdU(+)EdU(+) cells (stem/progenitor cell) were detected in thickened epithelium in KGF transfected specimens. Use of a high resolution microscope permits us to analyze phosphorylated level of p63 in individual nuclei, and the results clearly demonstrated that the BrdU(+)EdU(+) cells were regarded as progenitor cells. Under the over-expression of KGF, stimulation of progenitor cell proliferation was inhibited by SU5402, an inhibitor for tyrosine kinases of KGFR.

Conclusions

These findings indicated that KGF overexpression may possibly increase stem/progenitor cell proliferation and block terminal differentiation, resulting in epithelial hyperplasia, which was typical in middle ear cholesteatoma.

ARO 2018 abstract T Yamamoto-Fukuda.doc

PS 154

Evaluation of Mechanotransduction in a Rat Tympanic Membrane Under a Continuous Negative Pressure Load and in Human Middle Ear Cholesteatoma

Naotaro Akiyama[1]; Tomomi Yamamoto-fukuda[2]; Mamoru Yoshikawa[1]; Hiromi Kojima[2]
[1]Department of Otorhinolaryngology, Toho University School of Medicine; [2]Department of Otorhinolaryngology, Jikei University School of Medicine

Background

Mechanotransduction plays an important role in cell-proliferative activities. Negative pressure in the middle ear is thought to be an important factor related to the etiology of acquired middle ear cholesteatoma. However, the correlation between negative pressure in the middle ear and the mechanism of middle ear cholesteatoma formation remains unclear. In this study, we investigated the expression of key molecules for mechanotransduction immunohistochemically.

Methods

Four male Sprague-Dawley rats (8 weeks old) were used and continuous negative pressure in the middle ear was given through the supply route of a micro infusion

pump continuously during 24 hours for five consecutive days per week. All of the rats were euthanized at seven days after surgery and the temporal bones were collected. Animal care and experimental procedures were performed in accordance with the Guidelines for Animal Experimentation of Nagasaki University with the approval of the Institute of Animal Care and Use Committee (approval number is 1304301058). The study subjects of human samples were eight ears with acquired Pars flaccida (PF)-type cholesteatoma, and the patients consisted of five men and three women (34-67 yr). All patients were treated surgically at the Department of Otolaryngology Department of Otorhinolaryngology, Jikei University Hospital, between May 2016 and September 2016. The study protocol was approved by the Human Ethics Review Committee of Jikei University School of Medicine, and signed informed consent was obtained from all the patients for this study (approval number is 27-344 8229). An immunohistochemical analysis was performed using anti-Wnt5a (a marker of the alternative Wnt signaling pathway), - Yes-associated protein (YAP) (a marker of mechanosensing) and - phosphorylated YAP (inactivated YAP) antibody.

Results
The number of Wnt5a-positive cells had increased and YAP nuclear translocation was observed in epithelial and mesenchymal cells in the thickened TM of the PF under a negative-pressure load and in human middle ear cholesteatoma tissues.

Conclusions
In conclusion, YAP could be one of the therapeutic targets for this disease, although further studies are necessary to elucidate the role of YAP in the pathophysiology of retraction-type cholesteatoma.

PS 155

Prostaglandin E2 regulates osteoclastogenesis through the induction of RANKL in middle ear cholesteatoma.

Ryusuke Imai[1]; Takashi Sato[1]; Yasuhiro Osaki[1]; Yumi Ohta[1]; Takao Imai[2]; Hidenori Inohara[3]
[1]Department of Otorhinolaryngology-Head and Neck Surgery, Osaka University Graduate School of Medicine; [2]Department of Otorhinolaryngology—Head and Neck Surgery, Osaka University Graduate School of Medicine; [3]Department of Otorhinolaryngology-Head and Neck Surgery, Graduate School of Medicine, Osaka University

Background
Cholesteatoma destructs adjacent bones and causes various complications such as hearing loss, vertigo, facial nerve palsy and brain abscess. Although mechanism of bone destruction by cholesteatoma has been explored for many years, it has not been cleared. In inflammatory bone diseases such as periodontitis and rheumatoid arthritis, receptor activator of nuclear factor κB ligand (RANKL)-mediated osteoclastogenesis is well known to play an important role in bone destruction. Infiltrated leukocytes produce PGE2 which induce RANKL expression in osteoblasts, synovial fibroblasts and gingival fibroblasts. In this study, we investigated that RANKL-mediated osteoclastogenesis and PGE2 pathway were involved in bone destruction by cholesteatoma with human clinical sample. Also we confirmed whether PGE2 regulated RANKL expression in a model mouse for cholesteatoma, epidermal cyst-like tissue which was reported before (Mol Cell Biol. 2016).

Methods
Cholesteatoma tissues were obtained from patients with acquired cholesteatoma who underwent surgery in Department of Otorhinolaryngology-Head and Neck Surgery, Osaka University Hospital. Mastoid bone far from cholesteatoma and postauricular skin specimens were acquired from same patients as control tissue. We examined the expression of osteoclasts, RANKL and PGE2 in both samples by TRAP stain, PCR, immunostaining and ELISA method. Model mouse for cholesteatoma was obtained in same protocol of previous papers. Mouse fibroblasts were isolated from ear pinnae, same as production of model mouse for cholesteatoma.

Results
Tartrate-resistant acid phosphatase stain method revealed that the number of osteoclasts on the surface of bone adjacent to cholesteatoma was significantly increased, compared with control bone. RANKL mRNA expression in cholesteatoma prematrix tissue corrected by GAPDH mRNA was higher than in skin dermal tissue by Droplet Digital PCR. RANKL was also expressed in spindle shaped vimentin positive fibroblasts by immunohistological analysis of cholesteatoma. The PGE2 concentration of extraction from cholesteatoma was higher than that from control skin by ELISA method.

The PGE2 concentration of extraction from the epidermal cysts like cholesteatoma in model mouse was higher than that from control tissue injected PBS by ELISA. In vitro culture system, it was confirmed that PGE2 significantly upregulated RANKL expression in primary fibroblasts. Furthermore, the upregulation of RANKL expression was inhibited by EP3 and EP4 antagonists which were known for the PGE2 receptor antagonists.

Conclusions

These data suggested that PGE2 regulated osteoclast differentiation through the induction of RANKL expression in fibroblasts of cholesteatoma. Furthermore, these were implicated that cyclooxygenase-2 inhibitors or EP antagonists have possibility of new therapeutic agent against cholesteatoma-induced bone destruction.

PS 156

The Expression of Thymic Stromal Lymphopoietin in Eosinophilic Otitis Media

Tomoya Miura; Atsushi Matsubara; Naomi Kudo; Ryutaro Hara
Department of Otorhinolaryngology, Hirosaki University Graduate School of Medicine

Background

Eosinophilic otitis media (EOM) is known as an intractable otitis media characterized by eosinophil dominant highly viscous middle ear effusion. Recent studies have revealed Th2 type allergy involving in the pathogenesis of EOM. The aim of the present study is to investigate the expression of the epithelium-derived factor thymic stromal lymphopoietin (TSLP), key molecule as the trigger of Th2 type allergic reaction, in the middle ear mucosa of EOM.

Methods

Immunohistological study for TSLP was performed in patients with EOM and model animal of EOM. Ovalbumin (OVA) was administered to Hartley Guinea pigs intraperitoneally for general sensitization, and afterwards, nasal OVA drips (airway sensitization) and intratympanic injection of OVA were carried out (topical stimulation) for 7 days and 14 days. Moreover, expression of messenger RNA (mRNA) for TSLP in the middle ear mucosa of the model animal was analyzed by real time PCR, and compared with that of the control animal.

Results

Immunoreactivities for TSLP were observed in the middle ear mucosa around the tympanic ostium of the Eustachian tube of EOM patients. In the model animal, strong immunoreactivity for TSLP was also found in the Eustachian tube epithelium. TSLP mRNA expression in the 7-day stimulated animal was significantly higher than that of the control animal.

Conclusions

The present results have revealed that TSLP is localized in the middle ear mucosa of EOM patients and model animal of EOM. In addition, gene expression of TSLP was also identified at the early stage of OVA stimulation. These results suggest that TSLP of Eustachian tube plays an important role in the onset of EOM as well as other allergic diseases.

PS 157

Single-Cell RNA-Seq Reveals The Role Of Mucosal Cells And Leukocytes During Otitis Media

Allen F Ryan[1]; Nicholas Webster[2]; Kwang Pak[2]; Arwa Kurabi[3]
[1]UCSD and San Diego VA Medical Center; [2]UCSD; [3]University of California, San Diego

Our prior study of middle ear (ME) gene expression during an episode of acute otitis media (OM) in mice evaluated the entire contents of the ME. It revealed that approximately 3600 genes define the ME response to infection with nontypeable *Haemophilus influenzae* (NTHi). However, these results did not address the cellular diversity of the ME. While the normal ME contains primarily a thin squamous epithelial mucosa and a few resident leukocytes, infection induces dramatic growth and differentiation of the ME mucosa into a complex, respiratory-type epithelium with a well-organized stroma. In addition, large numbers of leukocytes are recruited into the mucosa and ME lumen. The many different cell types present in the ME during the course of OM presumably play distinct roles in pathogenesis and recovery. These roles are obscured in the transcriptome of the entire ME.

To unravel this cellular complexity we generated single-cell transcriptomes and evaluated the expression profiles of different ME cell populations. OM was induced in the MEs of mice by inoculation with NTHi. ME tissue and effusion were harvested at various times and dissociated into single-cell suspensions. Using the Fluidigm C1 Single-Cell mRNA Amplification System, cells were FACS-sorted into individual wells, and single-cell cDNAs generated. The tagged cDNAs were amplified, pooled and sequenced. The MEs of untreated mice serve as pre-infection controls. Unbiased, hierarchical cluster analysis of uninfected ME cell transcripts revealed a single cluster expressing genes consistent with epithelial cells that differed primarily along a mesenchymal-to-epithelial transition, including variation in ability to produce mucin and secrete cytokines, with a few monocyte/macrophages. By 24 and 48 hours after infection, five clusters of cells had emerged, and different cell types could be identified based on the expression of marker genes. Approximately 500 genes that were differentially regulated generated these five clusters. The differences in cellular responses were thus generated by only a subset of the ~3600 genes that define the OM transcriptome of the entire ME. Moreover, both mucosal cells and leukocytes exhibited upregulation of many immune and inflammatory genes. The results indicate that multiple cell

types in the ME participate in pathogenesis and resolution of acute OM, mediated primarily by innate immune responses to NTHi.

PS 158

Expression of Macrophage Migration Inhibitory Factor and CD74 in Lipopolysaccharide-induced Otitis Media

Shin Kariya; Mitsuhiro Okano; Yukihide Maeda; Hisashi Ishihara; Kazunori Nishizaki
Okayama University

Objectives
The inner ear dysfunction secondary to otitis media has been reported. However, the specific mechanisms involved are not clearly understood. The aim of this study is to investigate the expression of macrophage migration inhibitory factor and CD74 in the middle ear and inner ear in lipopolysaccharide-induced otitis media.

Method
BALB/c mice received a transtympanic injection of either lipopolysaccharide or phosphate-buffered saline (PBS). The mice were sacrificed 24 h after injection, and temporal bones were processed for polymerase chain reaction (PCR) analysis, histologic examination, and immunohistochemistry.

Results
PCR examination revealed that the lipopolysaccharide-injected mice showed a significant up-regulation of macrophage migration inhibitory factor in both middle ear and inner ear as compared with the PBS-injected control mice. Immunohistochemical study showed positive reactions for macrophage migration inhibitory factor and CD74 in infiltrating inflammatory cells, middle ear mucosa, and inner ear in the lipopolysaccharide-injected mice.

Conclusion
Significant expression of macrophage migration inhibitory factor and its receptor (CD74) was observed in both the middle ear and inner ear in experimental otitis media in mice. Modulation of macrophage migration inhibitory factor and its signaling pathway might be useful in the management of inner ear inflammation due to otitis media.

PS 159

Lower Beclin-1 mRNA Levels in Pediatric Compared to Adult Patients with Otitis Media with Effusion

Sanghoon Kim; Seung Geun Yeo
Department of Otorhinolaryngology, School of Medicine, Kyung Hee University

Background
The role of autophagy in the pathophysiology of otitis media with effusion (OME) is unclear, especially the difference between pediatric and adult patients. This study analyzed expression levels of autophagy-associated mRNAs in effusion fluids obtained from pediatric and adult patients with OME.

Methods
Middle ear fluid samples were collected from 76 pediatric patients and 41 adult patients with OME and the levels of mRNAs encoding autophagy-related genes were measured by real-time RT-PCR. The relationships between the levels of autophagy-associated mRNAs and the frequency of ventilating tube insertion, the characteristics of middle ear fluids, and bacterial culture results were analyzed.

Results
Autophagy-associated mRNAs were present in the effusion fluid of all patients. The level of Beclin-1 mRNA was significantly lower in pediatric than in adult patients, regardless of the frequency of surgery or of fluid characteristics ($p < 0.05$).

Conclusion
Autophagy-associated mRNAs were expressed in effusion fluids of both pediatric and adult patients with OME. However, the level of Beclin-1 mRNA was significantly lower in the effusion fluid of pediatric than of adult patients.

Table 1-6.doc

PS 160

Role of Endoplasmic Reticulum Stress in Otitis Media

Hongchun Zhao[1]; Xiaolin Zhang[2]; Juan Che[2]; Tihua Zheng[3]; Jun Chen[2]; Haibo Wang[1]; Zhaomin Fan[1]; **Qing Zheng**[4]
[1]Shandong Provincial Hospital Affiliated to Shandong University; [2]Affiliated Hospital of Binzhou Medical University; [3]Binzhou Medical University; [4]Case Western Reserve University

Background & Aims

Endoplasmic reticulum (ER) stress has been shown to occur in many inflammatory responses. Here, we investigated the role of ER stress and associated apoptosis in otitis media (OM) to elucidate the mechanisms of OM and signaling crosstalk between ER stress and other signal pathways, including cytokines and apoptosis OM.

Methods

We examined the inflammatory cytokines and ER stress-related genes and proteins by RT-PCR, western-blot, Immunohistochemistry (IHC) of middle ears in C57BL/6J mice after challenged with peptidoglycan-polysaccharide (PGPS). Then, we evaluated the treatment effect of ER stress inhibitor-tauroursodeoxycholic acid (TUDCA).

Results

ER stress and apoptosis-related genes and proteins were up-regulated by PGPS. These genes include the cleaved nuclear form of ATF6. CHOP, Bip, Caspase12 and Caspase3. TUDCA treatment reduced expression of CHOP, Bip tumor necrosis factor-α (TNF-α), Interleukin-6 (IL-6) and Caspase3. Reduced signs of ER stress in these mice were associated with PGPS-induced inflammation and apoptosis in middle ear epithelial cells.

Conclusions

These results suggest that PGPS triggers ER stress in middle ear epithelial cells, which augments inflammation. Therefore, ER stress plays a critical role in inflammation and cell death, leading to the development of OM. Our results suggest that the correction of ER stress could be a potential therapeutic target for OM.

PS 161

Newly Developed Hand-held Probe for Objective Intra-operative Assessment of Ossicular Mobility

Sho Kanzaki[1]; Takuji Koike,[2]; Yuuka Irie[2]; Sinyoung Lee[2]; Chee Sze Keat[3]; Kenji Higo[4]; Kenji Ohoyama[5]; Masaaki Hayashi[6]; Hajime Ikegami Ikegami[6]
[1]Keio University; [2]The University of Electro-Communications; [3]Mechano Transformer Corp; [4]Leadence Corp.; [5]Leadence Corp; [6]Daiichi Medical Co.

Evaluating the mobility of the ossicles is important during the tympanoplasty surgery, because the ossicular mobility affects the prognosis for the improvement of the hearing level. The assessments of ossicular mobility have been made with palpation by otologic surgeon. However, the palpation is inherently subjective and may not always be reliable, especially in milder degrees of ossicular fixation. We have developed a mechanical, hand-held probe that can provide an objective and quantitative assessment of the mobility of each ossicle during middle ear surgery. In this study, an improved probe was presented and its reliability and practical performance were evaluated through the measurements of artificial ossicles and cadavers. The hand-held probe consists of a force censor, an actuator and an ear pick, which is usually used in ear surgery. The end point of the ear pick is attached to the piezoelectric force sensor, which, in turn, is connected to the high precision piezoelectric actuator. The probe is connected to a computer-driven control unit. When the tip of the ear pick contacts an object like an ossicle, the actuator vibrates the ear pick at a frequency of 20 Hz. The reaction force from the ossicle is detected by the force sensor. A fixed ossicle is expected to generate a greater reaction force than one that is mobile. The equivalent spring constant (or compliance) of the ossicle is determined from the reaction force by use of a preliminarily formed calibration curve. Each measurement takes 0.7 seconds. Measurements were performed on artificial ossicles and fresh cadavers. The spring constants of the artificial ossicles were determined based on the results which were preliminary measured with the previous version of the probe in patients during surgery. The spring constants of the artificial ossicles were measurable without being influenced by hand trembling. The real ossicles are considered as rigid body, and the ossicular chain is supported by the ligaments and tendons in the tympanic cavity. The spring constant measured with our system therefore reflects the stiffness of the ligaments and tendons. Assessment of the degree of ossification of the ligaments and/or tendons is important for selection of a better surgical method and for improving the prognosis after surgery. Our device can provide valuable information of the status of the ossicles to the surgeons. This work was supported by Saitama Leading Edge Project 2016 (Medical Innovation), and Strategic Core Technology Advancement Program 2017 (Supporting Industry Program).

The hand-held probe consists of a force censor, an actuator and an ear pick, which is usually used in ear surgery. The end point of the ear pick is attached to the piezoelectric force sensor, which, in turn, is connected to the high precision piezoelectric actuator. The probe is connected to a computer-driven control unit. When the tip of the ear pick contacts an object like an ossicle, the actuator vibrates the ear pick at a frequency of 20 Hz. The reaction force from the ossicle is detected by the force sensor. A fixed ossicle is expected to generate a greater reaction force than one that is mobile. The equivalent spring constant (or compliance) of the ossicle is determined from the reaction force by use of a preliminarily formed calibration curve. Each measurement takes 0.7 seconds.

Measurements were performed on artificial ossicles and fresh cadavers. The spring constants of the artificial ossicles were determined based on the results which were preliminary measured with the previous version of the probe in patients during surgery. The spring constants of the artificial ossicles were measurable without being influenced by hand trembling. The real ossicles are considered as rigid body, and the ossicular chain is supported by the ligaments and tendons in the tympanic cavity. The spring constant measured with our system therefore reflects the stiffness of the ligaments and tendons. Assessment of the degree of ossification of the ligaments and/or tendons is important for selection of a better surgical method and for improving the prognosis after surgery. Our device can provide valuable information of the status of the ossicles to the surgeons.

Measurement probe for ossicular mobility.docx

Ototoxicity

PS 162

TLR4: A Potential Mediator of the Protective Effect of Heat Shock Against Aminoglycoside-Induced Hair Cell Death

Shimon Francis; Lisa Cunningham
National Institute on Deafness and Other Communication Disorders

Background
Our lab has previously shown that aminoglycoside-induced hair cell (HC) death can be inhibited by preconditioning with a sub-lethal heat shock, and this protective effect is mediated by heat shock protein 70 (HSP70). Using the adult mouse utricle as a model system we observed HSP70 induction in the glia-like supporting cells (SCs) after heat shock, with little induction in HCs. Furthermore, this protective HSP70 was found to be secreted from SCs in a paracrine-like fashion, but not internalized by HCs (May et al 2013 JCI). These data suggest that secreted HSP70 may be binding a HC cell surface receptor. We have identified Toll-like receptor 4 (TLR4) as a potential binding partner for extracellular HSP70 in the inner ear. HSP70 is an endogenous ligand for TLR4, and signaling through this pathway is protective in models of lung and cardiac injury. Therefore, we evaluated whether signaling through TLR4 is required for the protective effect of heat shock.

Methods
Whole-organ explants utricles from adult CBA/J mice were incubated with (or without) COBRA, an inhibitor of TLR4 and preconditioned with a 43° C sub-lethal heat shock. The explants were allowed to recover for 6h before being exposed to neomycin. In addition to a small molecule inhibitor, we also analyzed the effects of HC-specific knockout of TLR4. We crossed mice bearing a floxed allele of exon 3 of the Tlr4 gene with a HC-specific Atoh-1Cre mouse. Explants from Tlr4 conditional knockout mice and their WT littermates were preconditioned with heat shock before being exposed to neomycin. Hair cell viability was assessed using myosin VIIa immunoreactivity.

Results
Co-incubation with COBRA, an inhibitor of TLR4 signaling abolished the protective effect of heat shock against neomycin-induced HC death. Heat shock was protective in utricles from WT mice, but it was not protective in Tlr4 conditional knockout mice.

Conclusions
These results indicate that the protective effect of heat shock requires TLR4 expression in HCs, and they suggest that HSP70 may be signaling via TLR4. Current experiments are designed to test downstream mediators of TLR4 activation in HCs.

Shimon ARO Abstract 2018 Final.docx

PS 163

Cisplatin Pharmacokinetics Underlie Ototoxicity

Andrew M. Breglio[1]; Aaron Rusheen[2]; Katharine Fernandez[3]; Eric Shide[4]; Katie Spielbauer[5]; Katherine McLachlin[6]; Matthew Hall[7]; Lauren Amable[4]; Lisa Cunningham[3]
[1]*National Institute on Deafness and Other Communication Disorders & University of Oxford;* [2]*Mayo Clinic School of Medicine;* [3]*National Institute on Deafness and Other Communication Disorders;* [4]*National Institute on Minority Health and Health Disparities;* [5]*Michigan State University College of Human Medicine;* [6]*Electro Scientific Industries, Inc.;* [7]*National Center for Advancing Translational Sciences*

Background
Cisplatin-based chemotherapy has been central to the treatment of pediatric and adult cancers for decades. Unfortunately, permanent hearing loss remains a common and serious adverse effect. Current understanding of this cisplatin ototoxicity is largely limited to reports of the resultant changes in cochlear morphology and cellular states. We investigated cisplatin pharmacokinetics and tissue distribution in order to understand how local drug levels may contribute to ototoxicity.

Methods

Mice were administered three cycles of cisplatin in order to induce ototoxicity. Human cochlear sections were obtained from the NIDCD National Temporal Bone, Hearing and Balance Pathology Resource Registry at Massachusetts Eye and Ear. Inductively coupled plasma mass spectrometry (ICP-MS) was utilized to measure total cisplatin content in cochleae and other whole organs from mice, as well as cochlear tissue sections from human donors. Additionally, laser ablation ICP-MS was utilized to map the distribution of cisplatin in sectioned cochlear tissue from both experimental mice and human donors.

Results

In most organs, cisplatin was detected within one hour after injection, and was eliminated over the following days to weeks. In contrast, the cochlea retained cisplatin for months-to-years after treatment in both mice and human patients. Cisplatin did not distribute evenly throughout the cochlea, but rather preferentially accumulated in specific cochlear regions. Accumulation was highest in the stria vascularis and towards the cochlear base.

Conclusions

Our data demonstrate that cisplatin remains in the cochlea long after cessation of chemotherapy, and thus prolonged cisplatin exposure may be a previously unrecognized contributor to ototoxicity. The stria vascularis is the cochlear region with the highest levels of cisplatin, and thus it represents a promising target for prevention of cisplatin ototoxicity. Together our results (1) illustrate parallels between tissue concentrations of cisplatin and observed patterns of damage, (2) highlight the importance of investigating cisplatin cochleotoxicity in regions outside the organ of Corti, and (3) demonstrate the utility of ICP-MS to help better understand cisplatin ototoxicity.

Funding

PS 164

Pharmacological Induction of Stress Granule Formation Ameliorates Aminoglycoside-Induced Ototoxicity in Cochlear Explants

Ana Claudia Goncalves[1]; Naila Haq[2]; Sally Dawson[1]; Jonathan Gale[2]
[1]University College London; [2]UCL Ear Institute

Cellular stressors such as ototoxic drugs, noise exposure and ageing contribute to the deterioration of the cochlear structures, thereby leading to the development of hearing loss. Some types of cellular stress trigger the formation of stress granules (SGs), dynamic cytoplasmic aggregates of mRNA and RNA-binding proteins. By recruiting mRNAs for translational silencing, SGs can actively promote the translation of key stress-responsive proteins. Dysregulation of known SG-components has been associated with pathological inclusions observed in neurodegenerative diseases such as ALS and Alzheimer';s.

Previously, we have shown that the SG-pathway is activated in mammalian cochlear hair cells following aminoglycoside antibiotic treatment (Towers *et al*., 2011), noise exposure and ageing, suggesting that SGs are involved in the cochlea';s response to stress.

Here, we have used the inner ear-derived UB/OC-2 cell line and cochlear explants from C57BL/6 mice to investigate the formation and regulation of SGs. We confirmed co-localisation of polyA$^+$ mRNA with two known SG-components, TIA-1 and Caprin-1. The induction and subsequent recovery of SGs were quantified by image analysis.

To assess the effect of modulating the SG-pathway on hair cell survival, we first showed that we could: (i) pharmacologically activate SG-formation using a hydroxamate derivate[1] that impairs translation initiation (Rodrigo et al., 2012) and (ii) reduce SG formation with the integrated stress response inhibitor, ISRIB (Sidrauski et al, 2015). Neither of these manipulations alone affected hair cell survival in cochlear explants. During neomycin-induced toxicity we found significant protection in explants incubated with hydroxamate(-)-9: ~30% of outer hair cells remained 48h after the end of treatment compared with 6% in sham-treated controls (*p*=0.002). The same protective effect was not observed in inner hair cells. Reducing SG formation by treatment with ISRIB further reduced the number of surviving outer hair cells to 0.2% (*p*=0.04).

Our results show, for the first time in mammalian native tissue, that pharmacological induction of SG may promote outer hair cell survival. This implicates the SG-pathway not only in the maintenance of auditory function but also as a potential therapeutic target during various forms of age and trauma-evoked cochlear degeneration.

[1] The hydroxamate(-)-9 was a kind gift from Dr Jerry Pelletier

PS 165

Potassium Depolarisation Protects Cochlear Hair-Cells against Aminoglycoside but not Cisplatin-Induced Cell Death

Sian R. Kitcher; Abigail Secker; Corné J. Kros; Guy P. Richardson
University of Sussex

Background

Aminoglycoside (AG) antibiotics and platinum-based compounds are used, respectively, for the successful treatment of life-threatening infections and certain types of cancer. The AG gentamicin and the chemotherapy drug cisplatin, however, cause permanent hearing loss due to death of sensory hair-cells in the inner ear. AGs are permeant blockers of the hair-cell';s mechano-electrical transducer (MET) channel, with the positively charged AGs being driven into the hair-cells by the large potential difference across their apical plasma membrane. The entry route of cisplatin into hair-cells is less well explored, but recent evidence from zebrafish (Thomas et al, 2013) suggests it too may enter via the MET channel.

Methods

To investigate whether partial depolarisation of hair-cells offers protection against cell death induced by either gentamicin or cisplatin we prepared organotypic cochlear cultures from P2 CD-1 mice and after 24 hours applied the ototoxic compounds in the presence of low-serum cochlear culture medium (LSM) or LSM containing an additional 18 mM KCl, expected to depolarise outer hair-cells by around 15 mV, for a further 48 hours. To control for changes in osmolality, cisplatin and gentamicin were also applied in LSM containing an additional 18 mM NaCl. Cultures where then fixed and stained to visualise both the hair-bundles and cell bodies and counts were performed to assess hair-cell survival.

Results

After 48 hours, hair-cell numbers in cultures grown in LSM with an additional 18 mM of KCl or NaCl were comparable to those grown in LSM alone. Cultures exposed to 5 μM of gentamicin or cisplatin in either LSM or LSM containing an additional 18 mM NaCl showed similar and significant levels of hair-cell loss. In cultures grown in LSM with 18 mM KCl, a significant increase in hair-cell survival was observed when the cultures were exposed to 5 μM gentamicin. Significant protection was not, however, observed when cultures were exposed to 5 μM cisplatin in LSM containing 18 mM KCl.

Conclusion

These results provide evidence that partially depolarising mouse cochlear hair-cells with elevated extracellular KCl offers protection against the damaging effects of gentamicin. This result is consistent with existing research that supports the MET channel as an entry route for AGs into mouse cochlear hair-cells. K$^+$ depolarisation of hair-cells does not, however, offer protection against cisplatin suggesting this compound may employ a different route of entry.

PS 166

The Protective Effect of Galangin on Amikacin-induced Ototoxicity by Decreasing Mitochondrial Production of Reactive Oxygen Species in Mouse Cochlear Explants

Ye-Ri Kim; Kyung-Hee Kim; Tae-Hyeong Kim; Da Jung Jung; Myung Hoon Yoo; Un-Kyung Kim; Kyu-Yup Lee
Kyungpook National University

Aminoglycosides are among the oldest antibiotics available to treat serious infections caused by primarily, Gram-negative bacteria. The most commonly utilized parenteral agents in this class include gentamicin, tobramycin and amikacin. However, aminoglycoside antibiotics are known to have ototoxic effects and may induce sensorineural hearing loss. In this study, the effect of galangin on amikacin-induced ototoxicity was examined using cultures of cochlear explants. The organ of Corti explants were exposed to amikacin with or without galangin. Immunofluorescent staining showed that treating both inner hair cells (IHCs) and outer hair cells (OHCs) with galangin significantly decreased their damage induced by amikacin, especially OHCs than IHCs and base than apex. Moreover, pretreatment with galangin resulted in decreased mitochondrial ROS production in both hair cell types, as measured by mitoSOX-red staining. We also investigated whether galangin could attenuate the disruption of mitochondria by amikacin-induced mitochondrial ROS production in inner ear using MitoProbe^{TM} JC-1 as well as detection of potential-dependent accumulation in the mitochondria. To clarify the protective effect of galangin, we used MitoQ10, a mitochondrial ROS scavenger, as the positive control. We confirmed that in the cochlear explants treated with CCCP, which is a mitochondrial membrane potential disrupter, fluorescence emission did not shift from green to red. The ratio of the red/green signal significantly decreased in the AK and AK + dTPP groups compared to the CT group, whereas the AK + MitoQ10 and AK + GG groups showed similar ratio compared to the CT group. Using the ratio of red to green fluorescence intensity, we found that galangin could prevent mitochondrial membrane potential disruption caused by amikacin ($P < 0.05$). Attenuation of apoptotic cell death was assessed

immunohistochemically using active caspase 3 antibodies and also with terminal deoxynucleotidyl transferase dUTP nick end labeling (TUNEL) assay, compared to explants exposed to amikacin alone ($P < 0.05$). These results indicate that galangin protects hair cells in the organ of Corti from amikacin-induced toxicity by reducing the production of mitochondrial ROS. The results of this study suggest that galangin can potentially be used as an antioxidant and antiapoptotic agent to prevent hearing loss caused by aminoglycoside induced-oxidative stress.

PS 167

Characterization of Cisplatin-Induced Ototoxicity in a Mouse Model of Repeated Cisplatin Administration

Ann E. Hickox[1]; Xichun Zhang[1]; Trang Nguyen[1]; Ning Pan[1]; Samantha Palmer[2]; Collin Polucha[3]; Jason Le[1]; Arun Senapati[1]; Brendan Arsenault[1]; John Soglia[1]; Ada Silos-Santiago[1]

[1]Decibel Therapeutics; [2]Stony Brook University School of Medicine; [3]Brown University

Background
For many chemotherapy patients, cisplatin provides efficacious anti-cancer treatment but also induces permanent hearing impairment. Understanding the relationship between cisplatin exposure and progression of hearing loss is critical for determining therapeutic strategies. Here, we use a chronic, low-dose mouse model of cisplatin ototoxicity (Roy et al. 2013, J Clin Invest) and pharmacokinetic/pharmacodynamic (PK/PD) approaches to investigate this relationship.

Methods
Male CBA/CaJ mice (6-14 wks at study onset) were administered 3.5 mg/kg cisplatin i.p. over three cycles (each cycle consisting of 1 cisplatin injection/day for 4 days, followed by ~10 days recovery). Primary readouts for ototoxicity were distortion-product otoacoustic emission (DPOAE) thresholds and outer hair cell (OHC) count. Total platinum was quantitated by inductively coupled plasma mass spectrometry for several sample matrices (whole cochlea, perilymph, plasma, and whole blood) taken at specific timepoints throughout the cisplatin regimen. Pharmacokinetic parameters used for modelling and simulation were determined based on experimental results. A two-compartment PK model was used to simulate the pharmacokinetics of total platinum in plasma and cochlea for individual animals over the entirety of the study. PK/PD analysis was conducted by comparing the pharmacokinetics of each animal to the primary functional readout for ototoxicity (DPOAE thresholds).

Results
This cisplatin regimen resulted in significant DPOAE threshold shifts with lower morbidity/mortality (<5%) compared to acute, high-dose cisplatin models. DPOAE threshold shifts (up to 40-50 dB) and OHC loss (up to 40-100%) were highly correlated in the cochlear base (>22 kHz), although onset and degree of ototoxicity varied across cohorts. Total platinum levels in cochlea were significantly higher than in perilymph (>100X), plasma (~40X), or blood (~20X). Pharmacokinetic profiles for total platinum showed no significant accumulation in plasma. In contrast to extracellular fluid platinum levels, cochlear platinum accumulated significantly with repeated cisplatin administrations and varied widely across animals.

Conclusions
Within this inbred strain, this cisplatin regimen produced ototoxicity with variable onset and severity, which can potentially be harnessed to understand the nature of the mechanisms driving hearing loss. Examination of cochlear cisplatin PK profiles and severity of hearing loss on an individual-animal basis reveals a potential "threshold" for ototoxicity based on total platinum in cochlear tissue. Ongoing studies with the cisplatin chelator sodium thiosulfate (STS) may provide additional insight into this emerging hypothesis. Taken together, these findings indicate that an improved PK/PD understanding may help predict susceptibility to cisplatin ototoxicity and determine the therapeutic intervention for cisplatin-treated patients.

Background
For many chemotherapy patients, cisplatin provides efficacious anti-cancer treatment but also induces permanent hearing impairment. Understanding the relationship between cisplatin exposure and progression of hearing loss is critical for determining therapeutic strategies. Here, we use a chronic, low-dose mouse model of cisplatin ototoxicity (Roy et al. 2013, J Clin Invest) and pharmacokinetic/pharmacodynamic (PK/PD) approaches to investigate this relationship.

Methods
Male CBA/CaJ mice (6-14 wks at study onset) were administered 3.5 mg/kg cisplatin i.p. over three cycles (each cycle consisting of 1 cisplatin injection/day for 4 days, followed by ~10 days recovery). Primary readouts for ototoxicity were distortion-product otoacoustic emission (DPOAE) thresholds and outer hair cell (OHC) count. Total platinum was quantitated by inductively coupled plasma mass spectrometry for several sample matrices (whole cochlea, perilymph, plasma, and whole blood) taken at specific timepoints throughout the cisplatin regimen. Pharmacokinetic parameters used for

modelling and simulation were determined based on experimental results. A two-compartment PK model was used to simulate the pharmacokinetics of total platinum in plasma and cochlea for individual animals over the entirety of the study. PK/PD analysis was conducted by comparing the pharmacokinetics of each animal to the primary functional readout for ototoxicity (DPOAE thresholds).

Results
This cisplatin regimen resulted in significant DPOAE threshold shifts with lower morbidity/mortality (<5%) compared to acute, high-dose cisplatin models. DPOAE threshold shifts (up to 40-50 dB) and OHC loss (up to 40-100%)were highly correlated in the cochlear base (>22 kHz), although onset and degree of ototoxicity varied across cohorts. Total platinum levels in cochlea were significantly higher than in perilymph (>100X), plasma (~40X), or blood (~20X). Pharmacokinetic profiles for total platinum showed no significant accumulation in plasma. In contrast to extracellular fluid platinum levels, cochlear platinum accumulated significantly with repeated cisplatin administrations and varied widely across animals.

Conclusions
Within this inbred strain, this cisplatin regimen produced ototoxicity with variable onset and severity, which can potentially be harnessed to understand the nature of the mechanisms driving hearing loss. Examination of cochlear cisplatin PK profiles and severity of hearing loss on an individual-animal basis reveals a potential "threshold" for ototoxicity based on total platinum in cochlear tissue. Ongoing studies with the cisplatin chelator sodium thiosulfate (STS) may provide additional insight into this emerging hypothesis. Taken together, these findings indicate that an improved PK/PD understanding may help predict susceptibility to cisplatin ototoxicity and determine the therapeutic intervention for cisplatin-treated patients.

PS 168

Pharmacokinetics of an Ototoxic Cyclodextrin in the Inner Ear Measured by LC/MS-MS

Mark A. Crumling[1]; Daniel S. Ory[2]; Xuntian Jiang[2]; **Robert K. Duncan**[1]
[1]University of Michigan; [2]Washington University School of Medicine

Cyclodextrins are oligosaccharides that have many medical uses arising from their ability to hold guest compounds inside their ring-shaped structures. Contrary to their general safety, two medically used cyclodextrins have been found ototoxic at high doses. One of these, 2-hydroxypropyl-β-cyclodextrin (HPBCD), is being used to treat patients with Niemann-Pick Disease Type C (NPC), a cellular lipid processing disorder that is usually fatal in the teenage years. In a recent NPC clinical trial, all patients receiving intrathecal HPBCD suffered clinically significant hearing loss, underscoring the dire need to uncover the mechanism of the ototoxicity, since HPBCD is the most effective NPC therapy available.

In both humans and mice, the site of damage is thought to be the outer hair cell (OHC). In mice, HPBCD dosing into cerebrospinal fluid or via subcutaneous injection produces similar cochlear damage. Therefore, we used subcutaneous injection of HPBCD in mice to model human HPBCD ototoxicity. HPBCD was dosed at 8,000 mg/kg, which eliminates ~85% of OHCs in ~8 hours. To understand the exceptionally fast destruction of OHCs, we undertook a pharmacokinetic study of HPBCD in blood plasma, the cochlear and vestibular labyrinths, cochlear fluid, the kidney, and skeletal muscle. This was accomplished by sampling at time points from 0.5 to 24 hours after HPBCD injection. A clinical-grade LC/MS-MS method of quantifying HPBCD content was used to analyze the samples.

The concentration of HPBCD in the tissues and plasma was highest in the first two hours post-injection. The time constant (τ) of HPBCD decline was 1.0-2.5 hours for all samples except kidney which had a τ of 5.5 hours. Surprisingly, the concentration of HPBCD detected in cochlear fluid 3 hours post-injection was 128±31 μM (n=3), far below typical cytotoxic levels of HPBCD. Estimates of molar concentration in the membranous cochlear labyrinth derived from the cochlear samples at 3 and 9 hours are in good agreement with the measured fluid concentration at those times. This suggests the tissue samples are a good proxy for cochlear fluid and allows an estimate of peak fluid concentration of ~1 mM. In other cell systems, LC_{50} values for HPBCD are on the order of 100 mM, so the results prompt the question of what makes OHCs succumb to so little HPBCD.

PS 169

Knockdown of Slc31a1 gene by RNAi prevents cisplatin ototoxicity

Weidong Qi[1]; Chenqiang Jia[2]; Renji Zhang[2]; Fang Yuan[3]; Dalian Ding[4]
[1]Department of Otolaryngology, Huashan Hospital Fudan University; [2]Fudan University; [3]huashan hospital fudan university; [4]University at Buffalo, USA

The copper transporter Ctr1 expressed by Slc31a1 gene in mammal';s auditory cells is a major transporter for cisplatin influx. We developed a siRNA delivery recombination protein, TAT double stranded RNA-binding domains (TAT-DRBDs), which can transfect siRNA into cells of the inner ear to knockdown Slc31a1 and observed the protection effect for cisplatin ototoxity.

There were no morphological damages after 72 hours of transfection using TAT-DRBDs in vitro, and we observed almost 100% transfection efficiency of Cy3 labled siRNA in inner hair cells and outer hair cells under confocal. We screened and selected a valid siRNA targeted Slc31a1 gene (know down >90%) in rat BRL cells in vitro, then transfected the siRNA by TAT-DRBDs into basilar membrane. The result of RT-PCR showed the expression of gene 60% know down. We found apparent protection in pretreatment group with TAT-DRBDS /siRNA 12 hours than cisplatin treatment(10μm) 48h only（P

We illustrated that TAT-DRBD could transform Cy3-labeled siRNA into the inner and outer hair cells in vitro, and there was no apparent morphological damage for the time of observation. Therefore, as a non-viral vector, TAT-DRBDs, has great potential for siRNA delivery to the cochlea. Block cisplatin influx by Slc31a1 silencing supply a new strategy for cisplatin ototoxity.

PS 170

Protection against cisplatin ototoxicity through antioxidation and vasodilation.

Alejandro Gibaja[1]; Liliana Carles[2]; Juan C Alvarado[1]; Carlos Almodovar[2]; **Jose M Juiz**[1]
[1]Med School/IDINE, University of Castilla-La Mancha, Albacete, SPAIN; [2]Dpt. of Otolaryngology, Hospital 12 de Octubre, Madrid, SPAIN

Cisplatin, used as an antineoplastic agent, causes permanent sensorineural hearing loss, which has been linked to increased excess oxidative stress leading to cell death in the auditory receptor. In the context of a program aimed at exploring similarities and differences in cellular and molecular events related to cisplatin and aminoglycoside antibiotics ototoxicity and otoprotection strategies, we provide evidence of the reduction of cisplatin-induced ototoxic damage to the auditory receptor synergistically combining the antioxidant and vasodilator properties of a combination of Vitamin A, E and N-acetlylcysteine, along with $MgSO_4$. (AENaMg)

Wistar rats were treated with a single intraperitoneal injection of cisplatin at 16 mg/Kg. At the same time of the injection or a few hours earlier, two groups of rats received AENaMg, administered either systemically (s.c.) or by transtympanic injection at previously adjusted doses. Two groups of animals received vehicle injections, systemic or intratympanic. An additional group of animals received only cisplatin injections. Rats were allowed to survive for three days. ABRs and otoacoustic emissions were recorded before and after the injections, and immediately before euthanasia after three days, at which time cochleas were collected for quantitative histology, aimed at analyzing numbers and structural preservation of hair cells, and immunocytochemistry and PCR, aimed at identifying pathways to auditory receptor damage and protection.

So far, 25% of the rats treated with AENaMg show significant improvement in ABR thresholds compared with control groups. There is an apparent paradox, currently being analyzed in detail, in that there seems to be no significant changes in the number of missing hair cells, although there is a trend towards a better preservation. This suggests that, under current conditions, treatment with AENaMg improves the functional status of sensory cells in the auditory receptor with sub-lethal ototoxic damage after cisplatin treatment.

PS 171

Characterization of Moringaceae Antioxidant Protection Against Gentamicin and Kanamycin-Induced Ototoxicity in Organ of Corti

Peng Jiang[1]; Julia Brennan[1]; Samantha Cohen[1]; **Michael Brenner**[2]
[1]University of Michigan; [2]Kresge Hearing Research Institute, University of Michigan

Background
Formation of reactive oxygen species in the inner hear is associated with acquired hearing loss from the aminoglycoside antibiotics, gentamicin and kanamycin. Flavonoids, which account for much of the antioxidant activity in plants, demonstrate protective effects in explant cultures and in vivo models of hair cell injury. Moringa Oleifera, a plant rich in the flavonoid quercetin, vitamin C and beta-carotene, is an important source of phenolic antioxidants. Combining these antioxidants may minimize toxicity while achieving protective effects for hearing. We therefore investigated Moringa Oleifera extract as a potential otoprotectant for gentamicin-induced and kanamycin-induced injury.

Methods

Moringa extract protection from gentamicin ototoxicity was investigated in P2-P3 neonatal murine organ of Corti explants. Gentamicin (4. 2 μM) was administered for 72 hours alone or in combination with Moringa (25-300 μg/mL). Explants were stained with Rhodamine-phalloidin and cytocochleograms evaluated. Dihydroethidium (DHE), cytochrome oxidase, mitochondrial membrane potential, and caspase activity assays were used to investigate reactive oxygen species, bioenergetics, and cell death pathway activation. For in vivo investigation, kanamycin was administered 700mg /kg body weight to 4 week old CBA/J mice subcutaneously, twice daily for 14 days. Moringa was administered daily 500 mg/kg body weight for 15 consecutive days, starting one day before kanamycin, by gavage feeding or intraperitoneal injection. ABRs at 12 and 24 kHz recorded at baseline, 2, 3, and 5 weeks after initiation of kanamycin therapy for the groups.

Results

Moringa was well-tolerated in explants up to 300 μM and conferred near complete protection from 4. 2 μM gentamicin. Assays demonstrated suppression of ROS on DHE and intact mitochondrial membrane potential with DePsipher reagent red aggregated fluorescence. There was decreased caspase activation with Moringa, using FAM-VAD-FMK fluorescein-labeled peptide inhibitor of caspase assay, and cytochrome oxidase activity was preserved on 3,3' diaminobenzidine (DAB) staining. No toxicity or elevation in ABR thresholds was observed with Moringa alone relative to untreated controls. ABR threshold shifts most allevaited at 12 kHz among animals receiving Moringa via intraperitoneal or gavage route, although protection was not consistent across all animals. Mean ABR thresholds shifts were decreased 17 (24 kHz) and 14 dB (12 kHz) in Moringa treated animals.

Conclusions

Moringa extract demonstrated potent antioxidant properties in cochlear explants and protected against gentamicin ototoxicity while stabilizing mitorchondrial bioenergetics, with more limited protective effect with in vivo kanamycin studies. Further research is needed to investigate uptake patterns in the inner ear and pharmacokinetics of different Moringa administration regimens.

PS 172

Protective effects of concurrent statin use against ototoxicity in cisplatin-treated mice

Katharine Fernandez[1]; Katie Spielbauer[2]; Charis Williams[1]; Lauren Amable[3]; Lisa Cunningham[1]
[1]*National Institute on Deafness and Other Communication Disorders;* [2]*Michigan State University College of Human Medicine;* [3]*National Institute on Minority Health and Health Disparities*

Background

Worldwide, cisplatin is used to treat a variety of solid tumors, including lung, bladder, testicular, ovarian, and head and neck cancers. However, the commonly-associated hearing loss secondary to treatment has yet to be resolved. Our current research is aimed at developing a clinical co-therapy that will protect against cisplatin-induced hearing loss without reducing the efficacy of cisplatin therapy.

Statin drugs, used to treat hypercholesterolemia, have been in use since the 1970s. They have good safety profiles in humans, and they do not inhibit the therapeutic efficacy of cisplatin. Statins induce heat shock protein 32 (HSP 32), which we have shown to be protective against cisplatin and aminoglycoside ototoxicity. Here we have examined the extent to which Lovastatin reduces cisplatin-induced ototoxicity in mice.

Methods

Adult CBA/CaJ mice were pretested using distortion product otoacoustic emissions (DPOAE) and auditory brainstem response (ABR) testing. Mice were pre-treated once daily with Lovastatin (40 mg/kg or 60mg/kg) for two weeks prior to 3 cycles of cisplatin treatment consisting of 3.5 mg/kg/day for 4 days followed by 10 recovery days totaling 6 weeks. Upon completion of treatment, hearing was reevaluated using DPOAE and ABR. Endocochlear potential (EPs) were recorded in a subset of mice. Cochleas were collected for either immunohistochemistry and hair cell quantification or to analyze platinum levels via inductively coupled plasma mass spectrometry (ICP-MS) at separate locations along the length of the cochlea or in the isolated stria vascularis.

Results

Our cisplatin paradigm induced a 35-55 dB SPL permanent hearing loss confirmed by both DPOAE and ABR at all frequencies assayed from 8 to 40 kHz. In cisplatin-treated mice receiving lovastatin co-treatment, ABR response thresholds in the low to mid frequencies were significantly protected relative to cisplatin-only treated mice. DPOAEs were preserved, though reduced, at analogous frequencies. EP voltages were inversely

related to the ABR threshold shift (TS) at 40 kHz. The greater the TS, the greater the reduction in EP, regardless of treatment group.

Discussion

Concurrent use of statins during cisplatin-based chemotherapy offers a low risk opportunity to protect against ototoxicity. Based on these results in mice, we are conducting a prospective clinical study to determine if statin use reduces ototoxicity in patients undergoing cisplatin therapy for head and neck cancer.

PS 173

Berbamine Derivatives Attenuate Ototoxic Hair Cell Damage in the Zebrafish Lateral Line

Alexandria M. Hudson[1]; Bruce E. Blough[2]; Allison B. Coffin[1]
[1]Washington State University Vancouver; [2]RTI International

Aminoglycoside-induced hearing loss affects 20% of the patients requiring these life-sustaining antibiotics. Although aminoglycosides are efficacious in treating bacterial infections in life threatening diseases such as cystic fibrosis and sepsis, they often result in the adverse side effect of hair cell damage. To date, there are no FDA-approved drugs that prevent damage from aminoglycosides. Our goal is to develop a drug that prevents aminoglycoside-induced hearing loss, using a natural product as the chemical scaffold. A previous study by our lab identified four natural compounds that share a modified quinolone scaffold and strongly protect zebrafish lateral line hair cells by attenuating aminoglycoside uptake, likely via partial block of the mechanotransduction channel. The present study builds on previous work, investigating analogs of our berbamine compounds to determine the core protective structure and the specific molecular targets that are responsible for protection. Recent findings suggest that co-treatment of our analogs with aminoglycosides robustly protect hair cells from ototoxic damage at higher potencies than the parent compounds. Some analogs were found to be particularly efficacious and blocked uptake of aminoglycosides, implying those structures might play a crucial role in protection and that they likely mitigate damage via a transient block of the mechanotransduction (MET) channel. Additional gentamicin washout experiments further imply that some analogs may be mitigating aminoglycoside hair cell damage via intracellular mechanisms in addition to transiently blocking the MET channel. Hair cell protection also varied depending on the combination of analog and aminoglycoside. Certain analogs protected hair cells from multiple aminoglycosides while others protected from neomycin only. This suggests multiple pathways of protection and is consistent with the literature on aminoglycosides having different mechanisms of damage. Future studies will continue exploration of the quinolone-ring derivative chemical structure to refine the functional groups for lead optimization as an otoprotectant for aminoglycoside toxicity. This work demonstrates that we have promising lead compounds for further development to meet the therapeutic goal of devising a protective hearing loss drug candidate.

PS 174

Live Cell Imaging of Cisplatin Induced Ototoxicity in Organ of Corti Explant Cultures Reveals Differences in Sensitivity and Lesion Kinetics between Hair Cells and Supporting Cells

Audrey Broussy; Jessica Madern; **Montserrat Bosch-Grau**; Jonas Dyhrfjeld-Johnsen
Sensorion

Ototoxicity, leading to hearing loss and tinnitus, is one of the most frequent and disabling side-effects of chemotherapy, particularly in pediatric oncology patients. While in vivo models of cisplatin-induced hearing loss are well-established (Petremann et al., 2017), screening for potential drug targets and candidates would be more ethically and efficaciously achieved in vitro. We here present live-cell imaging data quantifying effects of cisplatin exposure duration in phenotypic Organ of Corti explant cultures and differential sensitivity of hair cells and supporting cells to ototoxic insult.

Organ of Corti explant cultures were plated in 24 well culture plates following microdissection of the cochlea from P5 Wistar rat pups. Hair cells were loaded with FM1-43 for 2h after which the culture medium was changed and the apoptosis marker Annexin V added. After 24h of incubation, a baseline scan was performed and groups of cultures (n=3-4) were exposed to either control medium or 50 µM cisplatin (CDDP) for 7 or 24h. Live cell imaging was performed every 6h for 120h using a live-cell imaging system with the area of fluorescence of FM1-43 and Annexin V normalized to the group mean at t=0 h. Fluorescent label area changes were quantified using time to half-maximal change (t_{50}) and maximal change of fluorescent area at t=90h.

Loss of FM1-43 labelled hair cells was clearly observed in exposed cultures from t=40h after cisplatin addition, while clear increase of Annexin V fluorescence was already evident at t=20h after beginning of cisplatin exposure. The maximal change of both markers was achieved at t=90h after initial exposure. The remaining FM1-43 labelling relative to control at t=90h (20.0 ±3.5% and 4.7±1.1% for 7 and 24h exposure) and t_{50} (72±0.0h and 62±2h for 7 and 24h exposure) both decreased with

increasing cisplatin exposure duration. The Annexin V labeling relative to control at t=90h (280.7±40.2% and 259.9±80.8% for 7 and 24h exposure) appeared saturated already after 7h exposure, while the t_{50} (respectively 72±0.0h and 62±2h for 7 and 24h exposure) decreased from 7 to 24h.

These preliminary data demonstrates the feasibility of a High Content Screening approach to quantifying ototoxic lesions in Organ of Corti explant cultures. Furthermore, the differences in kinetics of loss of sensory hair cells (loss of FM1-43 labeling) versus the overall increase in apoptosis suggest that supporting cells are more sensitive to cisplatin ototoxicity than hair cells, which could be of relevance to future screening for drug targets and candidates.

PS 175

Regulator of G-protein Signaling 17 (RGS17), a Novel Mediator of Cisplatin-induced Ototoxicity

Asmita Dhukhwa[1]; Debashree Mukherjea[1]; Kelly Sheehan[1]; Sumana Ghosh[1]; Sandeep Sheth[1]; Leonard Rybak[2]; Vickram Ramkumar[1]
[1]*SIU School of Medicine;* [2]*Southern Illinois University School of Medicine*

Background
Regulator of G-protein signaling (RGS) catalyzes the hydrolysis of GTP bound to G proteins and terminates the actions of the associated G-protein coupled receptor (GPCR). RGS17, a member of RGS-RZ subfamily, is highly expressed in the central nervous system. Data from the transcriptome analyses of cisplatin treated rat cochlea showed up-regulation of various RGS proteins, including RGS17. RGS17 generally targets GTP bound Gαz for hydrolysis and signal termination. Previous data from our laboratory have implicated GPCRs such as the adenosine A_1 receptor (A_1AR) and cannabinoid receptor 2 (CB2) in mediating protection against hearing loss. As these receptors interact with G-proteins, including Gi and Gz, we propose that induction of RGS17 would serve to negate the protective actions of these receptors. The goal for this study was to examine what role, if any, RGS17 plays in cisplatin-induced ototoxicity.

Methods
Animals used were male Wistar rat for cisplatin ototoxicity and mice for RGS17 immunolabeling. Auditory brain response (ABR) threshold shifts were measured in naïve rats, which were treated with siRNA for RGS17 or SCR (scrambled sequence) trans-tympanically (TT) for 24h prior to cisplatin (11mg/kg, i.p) administration. Cochleae were collected and processed for either RNA or immunohistochemistry. *In vitro* studies were performed in immortalized organ of Corti (UB/OC1) cell line. ROS generation was determined using CellROX assay. Apoptosis was determined by Annexin V/PI and MTS assays. Gene expression studies were determined by quantitative PCR.

Results
RGS17 expression was verified in the mouse and rat cochlea by immunohistochemistry. Increased cochlear RGS17 expression by cisplatin (159.2±10.3%) was determined by immunofluorescence. Cochlear gene expression analyses corroborated cisplatin induced up-regulation of *RGS17* (5.9±1.2 fold), which was decreased to basal level by pre-treatment with CB2 agonist JWH015 (TT) prior to cisplatin. Furthermore, pre-treatment of rats with trans-tympanic siRGS17 reduced cisplatin-induced elevations in ABR thresholds. *In vitro* data from UB/OC1 cells indicate that overexpression of *RGS17* increased ROS generation (230±17%), RGS17 immunostaining by (378±35%) and increased gene expression of *NOX3* (2.6±0.2), *KIM1* (1.5±0.1) and *iNOS* (1.9±0.2) compared to empty vector controls. Overexpression of *RGS17* also increased cell apoptosis by (25±2%) and exacerbated cisplatin-induced apoptosis. Pretreatment with JWH015 significantly reduced basal and cisplatin-induced death in *RGS17*-overexpressed cells.

Conclusions
Our findings suggest that cisplatin-induced RGS17 lead to increased oxidative stress, cell apoptosis and hearing loss. This process is negated by activation of CB2 agonist which likely opposes the function of RGS17 at the level of the G protein.

PS 176

Genetic Inhibition of Necroptosis and Receptor-mediated Apoptosis ameliorates Cisplatin- and Aminoglycoside Ototoxicity in an in vivo mouse model

Doug Ruhl; Tingting Du; Jeong-Hwan Choi; Sihan Li; Robert Reed; Michael Freeman; John Lukens; Jung-Bum Shin
University of Virginia

The ototoxic side effects of cisplatin and aminoglycosides have been extensively studied, but no therapy is available to date. Blocking various cell death pathways such as apoptosis and necrosis have therapeutic potential in theory, but incomplete protection, the toxicity of inhibitors, and lack of druggable targets in the case of necrosis, have hampered the development of clinically applicable drugs. Here, we are testing the hypothesis that a more recently discovered cell death pathway called necroptosis is involved in ototoxicity. Necroptosis

is distinguished from passive necrotic cell death, in that it follows a cellular program, involving distinct molecules and pathways, the inhibition of which leads to a block of the necroptosis pathway. Furthermore, necroptosis was shown to be triggered when apoptosis is inhibited, suggesting that an effective prevention of ototoxic cell death might require the simultaneous inhibition of both apoptosis and necroptosis pathways.

The receptor-interacting protein kinase 3 (RIP3/RIPK3) has emerged as a crucial mediator of necroptosis. In this study, we thus used *Ripk3 null* mice to test whether genetic inhibition of necroptosis alleviates hearing loss in mouse models for cisplatin and aminoglycoside ototoxicity. Furthermore, *Ripk3/Casp8 double ko* mice were utilized to investigate the protective potential of blocking both necroptosis and receptor-mediated apoptosis. First, we demonstrated that *Ripk3/Casp8 double ko* and *Ripk3 single ko* mice, without ototoxic insult, display normal hearing thresholds up to 20 weeks of age. Strikingly, our study demonstrates that *Ripk3/Casp8 double ko* are strongly protected from both types of ototoxicity, while *Ripk3 ko* mice show a more moderate, but significant level of protection. Future studies will elucidate the cell types involved in this process, and explore whether known pharmaceutical inhibitors of necroptosis can recapitulate the otoprotection evident in the genetic mouse models.

Perception of Complex Sounds

PS 177

Sensitivities of Pupillary Dilation Responses and Microsaccade Rates to Alert Sounds

Haruna Fujihira; Shimpei Yamagishi; Hsin-I Liao; Shigeto Furukawa
NTT Communication Science Laboratories

Alerting signals, either artificially generated (e.g. a fire alarm) or naturally uttered (e.g. a human scream), are thought to have common features that attract people';s attention (Arnal et al., 2015). To explore this, the present study examined the sensitivities of pupil dilation responses (PDRs) and microsaccade rates to alerting sounds and the effects of top-down attention, which have been suggested to reflect attention-related mechanisms.

The stimuli were a 1000-Hz tone, a white noise, a fire alarm, and screams made by a woman and a man, with a duration of 2 s, presented in intervals of 4 - 8 s and equalized in loudness level. During a session, participants were asked to fixate a light-gray disk presented at the center of a monitor, and pupil diameter and eye movement were recorded. In the attend-audition condition, participants were   instructed to press a key as

fast as possible when they detected a silent gap of 100 ms, which was inserted into randomly selected (16.7% probability) sounds. In the attend-vision condition, the participant';s task was to respond similarly to a random 100-ms change in the luminance of the fixation disk, occurring during the sound period. Analyses were performed only for sound presentations without the silent gap or luminance change.

Genereally, the PDR occurred immediately after the stimulus onset and reached a near-maximal state in around 0.5 s. The response afterwards varied somewhat with stimulus type. The PDRs were larger in the attend-audition than in the attend-vision conditions. The interaction between the attention condition and stimulus type was significant: The PDRs were larger in the attend-audition than in the attend-vision conditions, only for the fire alarm and the screams. There were indications that the PDR magnitudes correlated with the modulation power within the roughness domain (30 - 150 Hz), as reported in the study on the perception of screams (Arnal et al., 2015).

The sound presentation generally reduced the microsaccade rate. The time course of the rate consisted of an initial sharp decline (onset response) followed by a higher-rate steady period during the sound presentation (sustained response). Unlike for the PDR, stimulus type had no significant effect on either the onset or sustained response. A significant effect of the attentional state was observed only for the sustained response. The results imply that the PDRs and microsaccades reflect (partially) different mechanisms related to attention.

PS 178

Pupil Dynamics during Auditory Incidental Learning

HiJee Kang; Daniel Pressnitzer
Laboratoire des Systèmes Perceptifs (CNRS UMR 8248), École normale supérieure

Auditory memory may be a general by-product of auditory processing, as suggested by a series of studies showing rapid incidental learning for tokens of white noise after a few repeated presentations (Agus et al., 2010). While EEG correlates of the phenomenon have been found (Andrillon et al., 2015), the underlying neural mechanisms remain to be specified. Here, we tracked pupil size during the incidental learning of noise tokens, to test for another physiological index that is known to be modulated during intentional auditory learning (Goldinger & Papesh, 2012).

We used a typical memory for noise paradigm. Noise sequences lasting 1.5s. were presented to adult participants. Each sequence was either 1.5s of purely random

noise (Noise, N), or consisted of 3 seamless repeats of the same, 0.5s random noise token, generated afresh for each trial (Repeated Noise, RN). A last condition was like RN, but with the same noise token used in all trials of an experimental block (Reference RN, RefRN). Participants were instructed to report within-trials repeats. We used an eye tracker (Eyetribe, 60 Hz) to record pupil size while participants performed the task. After each trial, there was 5s of silence to allow the pupil size to return to baseline. Pupil diameter was recorded and baseline-corrected for each trial.

Behavioral results replicated previous findings. A large advantage at the end of each block for RefRNs compared to RN indicated perceptual learning of the RefRN tokens, which were heard multiple times during a block. Pupil dilation was modulated by stimulus condition. Pupil dilation was equivalent for all conditions at the beginning of a block, but was markedly reduced at the end of a block for RefRN only. Thus, sounds that had been learnt induced less pupil dilation than highly similar but novel sounds.

The effect of auditory learning on pupil dilation was opposite to what was observed during intentional learning (Goldinger & Papesh, 2012). A possible interpretation is that pupil dilation here reflected listening effort (e.g. Koelewijn et al., 2015), as RefRNs were associated to near-perfect task performance after incidental learning. Future experiments may be able disentangle memory effects from listening effort using a similar paradigm, but without a task (Andrillon et al., 2015).

References
Agus, T. R., Thorpe, S. J., & Pressnitzer, D. (2010). Rapid formation of robust auditory memories: Insights from noise. *Neuron, 66*, 610-618.

Andrillon, T., Kouider, S., Agus, T., & Pressnitzer, D. (2015). Perceptual learning of acoustic noise generates memory-evoked potentials, *Current Biology, 25*(21), 2823-2829.

Goldinger, S. D., and Papesh, M. H. (2012). Pupil Dilation Reflects the Creation and Retrieval of Memories, *Current Directions in Psychological Science, 21*, 90–95.

Koelewijn, T., de Kluiver, H., Shinn-Cunningham, B. G., Zekveld, A. A., and Kramer, S. E. (2015). "The pupil response reveals increased listening effort when it is difficult to focus attention," *Hearing Research, 323*, 81–90.

PS 179

Dynamic modulation of pupil size reflects the integration of contextual information during continuous change detection task

Jennifer Lawlor[1]; Agnès Zagala[2]; Celian Bimbard[2]; Shihab Shamma[3]; Yves Boubenec[1]
[1]Ecole Normale Supérieure, Paris, France; [2]Ecole Normale Supérieure; [3]Ecole Normale Supérieure, University of Maryland

In humans, pupil dilation has been associated with a number of underlying cognitive processes, such as decision-making and attentional load. Here we want to test how online modulation of pupil diameter can reflect subject';s expectation during a perceptual decision-making task. For this purpose we recorded the pupil diameter of 18 individuals performing a change detection reaction time task. Subjects had to monitor a continuous and complex acoustic scene to detect a change in its statistical properties. Unbeknownst to the subjects, change time blocks were introduced. In each of these blocks, the change could arise only after a fixed pre-change period (0s, 1.5s and 3s from trial onset). We found a decrease in false alarm rate during these pre-change periods, indicating that subjects implicitly incorporated in their decision strategy the contextual information available at the block level. Onset-related pupil dilation was delayed with increasing pre-change period durations, correlating with subjects'; decreased false alarm rate during this time period. Interestingly, a similar observation could be made in ferrets performing a similar task. All together, this suggests that the pupil-related modulation can reflect time-dependent adaptation of decision threshold.

PS 180

The Pupillary Light Response Reveals the Focus of Auditory Spatial Attention

Hsin-I Liao; Haruna Fujihira; Shigeto Furukawa
NTT Communication Science Laboratories

A recent study (Mathôt et al., 2013) indicates that the pupillary light response (PLR) reflects the luminance of the target location to which the participant covertly attends without actually moving his/her gaze. This suggests a visual attentional orienting mechanism that accounts for a preparation of an upcoming eye movement. Assuming a unified attentional orienting processing across different modalities, we hypothesize that the PLR also reflects the luminance of a location to which auditory spatial attention is directed.

Participants performed an auditory task while their pupillary responses were recorded by an infrared eye-camera. The auditory task consisted of two events separat-

ed by a 5-s interval. First, a cue, a voice saying 'left'; or 'right';, was presented diotically via headphones. Second, a target, a dog barking sound or a phone ringing sound, was presented dichotically. Participants were instructed to pay attention to their left or right ear according to the voice cue, and report whether the target sound, i.e., the one presented to the cued ear, was a dog barking or phone ringing. They answered by pressing a corresponding key on the keyboard as soon as and yet as accurately as possible. Throughout the experiment, they fixated a gray cross positioned at the center of a monitor. The background of the visual display had a disparity in luminance between the left and right halves of the monitor. The display disparity (black on left or right visual field), cue direction (left or right ear), and target identification were all counterbalanced across trials.

As expected, the participant performed the task well (mean accuracy = 98%, mean RTs = 1165 ms), regardless of the conditions. Most importantly, the mean pupil diameter during the interval between the cue and target events showed an interaction between the display disparity and cue direction ($p < .001$). That is, pupil size was larger when the attended ear and darker visual field were on the same side than when they were not. The result cannot be explained by (purely) visual attentional shift or by the difference in the physical luminance of inputs to the eyes: The task did not require moving visual attention, and participants maintained their gaze at the center (controlled by data screening).

The PLR reveals not only the focus of covert visual attention but also that of auditory attention. Spatial attention across visual and auditory modalities is unified.

PS 181

Statistics of Resonant Modes Allow Auditory Inference of Material from Impact Sounds

James Traer[1]; Josh H. McDermott[2]
[1]MIT; [2]Department of Brain and Cognitive Sciences, MIT; Center for Brains, Minds, and Machines, MIT; Program in Speech and Hearing Biosciences and Technology, Harvard

Humans infer physical properties of objects, such as their material and size, from the sounds they make when colliding. We explored the acoustic underpinnings of auditory physical inferences by recording impact sounds and modeling the relevant physics. We recorded the sounds of a set of balls (i.e. small projectiles) falling upon a set of plates, both of which varied in size, shape and material. We also synthesized impact sounds by convolving a simulated contact force (synthesized via a spring-model) with object impulse responses (IRs) that modeled the object acoustic resonances. The synthetic IRs either conformed to, or deviated from, the statistics of measured object IRs. We presented listeners with recorded and synthetic impact sounds and asked the listeners to judge physical properties (e.g. which mallet was the heaviest? Which hit with most force?). We found that humans were able to accurately judge material from sound, and that their abilities could not be explained by null models using simple acoustic features (e.g. amplitude or spectral centroid). Listeners attributed similar material properties to synthetic impact sounds as to the real objects upon which they were based, suggesting that the resonant modes modeled in the synthetic IRs underlie the perception of material properties.

PS 182

Multi-feature regularity extraction from stochastic sequences

Benjamin Skerritt-Davis; Mounya Elhilali
Johns Hopkins University

The brain is able to easily interpret its surroundings, parsing ongoing sounds into distinct sources and tracking these sources through time. To effectively perform this task, the brain collects information about regularities from sounds sequentially over time, building representations that are both invariant to the randomness present in real-world sounds and flexible to adapt to changes in a dynamic environment. Real-world, complex sounds vary along multiple acoustic features, but not all of them are necessarily informative for auditory scene analysis. In a series of change detection experiments, we investigate how information is combined across acoustic features. Employing stimuli based on random fractals, listeners are tasked with detecting changes in the stochastic properties of a sequence of complex tones, where change information is present in one or more acoustic feature. We investigate both spectral and spatial features, and use these results to infer at what computational level information for regularity extraction along multiple features is combined in the brain.

PS 183

Complexity Perception of Realistic Listening Environments

Adam Weisser; Jorg Buchholz
National Acoustic Laboratories

Background
Psychoacoustic research tends to focus on well-controlled acoustic stimuli that can be readily produced in the laboratory. While knowledge from this research is vital to understand the basic processing of the hearing system, it has low predictive power to listening or com-

municating in the real world. Whenever the realistic, and often uncontrolled, nature of a given acoustic situation is emphasized, the term "complex acoustic environments" is regularly invoked, but usually without providing any definition or further clarification. This is a particular problem when investigating the effect of realistic acoustic environments on a listener';s hearing abilities and the benefit provided by hearing devices. The goal of this project is therefore to obtain a more complete understanding of the factors that make acoustic environments appear complex to listeners. The results will help to derive an appropriate subjective model and a working definition of complexity in the context of realistic acoustic environments.

Methods

A novel three-part questionnaire was developed and applied for subjective evaluation of 14 acoustic environments that were reproduced in an anechoic chamber using a higher-order Ambisonics system. Normal hearing subjects (N=66) were asked to rate different attributes (loudness, annoyance, variability, complexity, etc.) of the environments, indicate where they were recorded, and identify the sound objects they contained. They had to answer similar questions also with target speech that was planted in the scenes at realistic vocal effort and level.

Results

The underlying structure of the data was analyzed using an exploratory three-way principal component analysis. Two components explained most of the variability in the rating data, in addition to three scene and two subject components. The primary component may be referred to as "listening comfort" and is highly correlated with perceived loudness, annoyance and intelligibility, among others. The second component was primarily driven by the number of sources in the scenes and their perceived variability. Complexity could be explained as a composite variable of both components, and mapped closely to busyness.

Conclusions

Test subjects made sense of the complexity rating. Their data indicated that it is indeed not a simple attribute of the acoustic scenes. This confirms that the subjective listening experience is not driven solely by the sound pressure level, but also by more informational elements in the acoustics, as the variability of the scene. This may have implications on the understanding and design of speech-communication tests and on hearing device design more suitable to realistic conditions.

Motor Modulation of Auditory Spatial Perception

John Myers; Jeff Mock; Ed Golob
University of Texas at San Antonio

A key function of the auditory system is identifying sounds in 360 degrees of space. Predicting the location of self-generated sounds is critical to functioning in the world[EG1] . Previous work suggests that the brain estimates the frequency and intensity of self-generated sounds before they occur. Few studies have tested whether sensorimotor predictions of a sound';s spatial location could affect how it is perceived. We tested whether intensity discrimination performance was affected by a motor (*active*) versus a non-motor control condition (*passive*). Intensity discrimination is a perceptual test that has been linked to sensory neuron response patterns. Subjects (n = 22) first learned to associate left- vs. right button presses with 600 Hz pure tone feedback to the ear on the same side as the button press. Subjects were then asked to discriminate between a standard tone (70dB) and a higher intensity comparison tone (71-75dB). In the *active* condition, participants pressed a button to generate the standard tone. In the *passive* condition, the identical tones were computer-generated. We hypothesized that loudness perception would depend upon whether the tones were self- vs. computer generated. We observed a main effect of condition (p = 0.010, η^2 = 0.341) indicating that intensity discrimination thresholds were higher in the active (M = 2.5dB) than the passive condition (M = 1.9dB). This study provides evidence that the perception of self-generated sounds can be altered by sensorimotor predictions of sound locality.

Behavioural evidence for a relationship between auditory object grouping and speech-in-noise processing

Phillip Gander[1]; Inyong Choi[2]; Bob McMurray[2]; Timothy Griffiths[3]
[1]Human Brain Research Laboratory, Department of Neurosurgery, The University of Iowa; [2]The University of Iowa; [3]Newcastle University

A persistent problem in hearing impairment (HI) is the fact that peripheral measures do not fully account for outcome variability with speech in noisy real-world environments. We sought to understand the cognitive mechanisms by which listeners detect complex auditory objects (both speech and non-speech) in noisy environments, by examining intermediate cognitive processes as indexed by auditory figure-ground segregation. We hypothesized that the detection of speech in noise (SIN) depends critically on mechanisms for cross-frequency

grouping which tap listeners'; ability to abstract coherent signals from unpredictable and noisy backgrounds that provide the first stage of auditory object analysis.

We investigated whether frequency grouping, indexed by a stochastic figure-ground (SFG) stimulus, predicts SIN ability in normal hearing and hearing impairment. In the SFG single-interval detection task each trial consisted of either background-only or background+figure. The background was heard first and comprised a sequence of random complex tones. On half the trials (figure-present) specific tones remained constant after a transition. The SIN measure adapted the California Consonant Test 4AFC CVC word recognition task, embedding the words in multi-talker babble at two SNR values.

We found a significant correlation between SFG and low SNR SIN in the normal hearing group (N=89, r=.259, p=.014). General intelligence (indexed by the WAIS) did not correlate with either of the SIN or SFG task scores. A significant correlation between SFG and low SNR SIN was also observed in the two groups of hearing impaired subjects (hearing aid, N=10, r=.842, p=.002; cochlear implant, N=43, r=.316, p=.039).

The correlation between auditory object detection (SFG) and SIN may form a vital bridge between peripheral auditory measures and speech outcomes and allow specification of deficits in hearing impaired listeners in a way that is both precise and reflects how people might manage in the acoustic world.

PS 186

The Relationship between Stream Segregation of Complex Tones, Fundamental Frequency Discrimination, and Frequency Selectivity

Sara M. K. Madsen[1]; Torsten Dau[2]; Brian C. J. Moore[3]
[1]Hearing Systems Group, Department of Electrical Engineering, Technical University of Denmark; [2]Hearing Systems group, Technical University of Denmark; [3]Department of Psychology, University of Cambridge

The discrimination of changes in fundamental frequency (F0) is better for complex tones with low than with high harmonics, perhaps because the low harmonics are resolved (Bernstein and Oxenham, 2006). The reduced frequency selectivity of hearing-impaired (HI) listeners may lead to poorer resolution of low and medium harmonics. Furthermore, the extent of perceptual stream segregation of a rapid sequence of complex tones may depend on the discriminability of the difference in F0, DF0, between successive tones. We assessed how the stream segregation of complex tones is affected by harmonic rank and whether tones with low and medium har-

monics are more likely to be segregated for HI than for near normal-hearing (NH) listeners. The listeners were matched in age and working memory capacity as measured by the Reading Span Test (Santurette and Dau, 2012).

Subjective stream segregation and F0 difference limens (F0DLs) were assessed for complex tones that were bandpass filtered between 2 and 4 kHz. The overall level of the complex tone was 80 dB SPL and the level of the threshold equalizing noise used to mask combination tones and to limit the audibility of harmonics falling on the filter skirts was 55 dB SPL/ERBn. Harmonic rank was varied by changing the baseline F0 (with DF0 from 1 to 11 semitones). Auditory filter shapes were estimated from notched-noise masking (Rosen *et al.*, 1998) using a 2-kHz signal.

Stream segregation performance and F0DLs worsened with increasing harmonic rank. The stream-segregation scores and F0DLs were similar for the two groups, but the auditory filters were wider for the HI than for the NH group. Stream segregation scores were neither correlated with auditory filter bandwidths nor F0DLs. These results suggest that the effects of harmonic rank on stream segregation cannot be explained in terms of resolvability and that the ability to segregate sequences of complex tones is not limited by the ability to discriminate between them.

Bernstein, J. G., and Oxenham, A. J. (**2006**). "The relationship between frequency selectivity and pitch discrimination: sensorineural hearing loss," J. Acoust. Soc. Am. **120**, 3929-3945.

Rosen, S., Baker, R. J., and Darling, A. (**1998**). "Auditory filter nonlinearity at 2 kHz in normal hearing listeners," J. Acoust. Soc. Am. **103**, 2539-2550.

Santurette, S., and Dau, T. (**2012**). "Relating binaural pitch perception to the individual listener's auditory profile," J. Acoust. Soc. Am. **131**, 2968-2986.

PS 187

Effects of hearing loss on maintaining and switching attention

Nicole Whittle; Eric Larson; Christi Miller; Adrian K.C. Lee
University of Washington

Introduction
Active listening in a real-world multi-talker setting requires both maintaining and switching of attention between auditory objects. Individuals with normal hearing

can often seamlessly accomplish this task. However, when a person has a damaged auditory system, such as with hearing loss, auditory objects may not be well formed, making it more difficult to attend to different auditory objects in their environment. We tested the hypothesis that individuals with hearing loss would have more difficulty when switching attention in comparison to an age-matched individual with normal hearing.

Participants
Of the 26 (out of a planned 30) adults tested, 13 had normal hearing and 13 had hearing loss. Participants with normal hearing were age-matched (+/- 3 years) to participants with hearing loss, and ranged from 18-64 years.

Methods
Participants were required to identify when they heard a target sound by pressing a button while listening to two simultaneous talkers. For half of the trials, they were instructed to maintain attention on one talker and for the other half of the trials, they were instructed to switch attention midway through the trial. Behavioral accuracy and reaction time were analyzed.

Results
Participants with hearing loss and normal hearing were equally accurate in each condition, confirming audibility of the stimuli. As expected, participants in both groups found switching attention more difficult than maintaining attention, responding with lower accuracy and longer reaction times. However, there was also an increase in reaction time for maintaining of auditory attention for participants with hearing loss, regardless of age.

Conclusion
Persons with hearing loss require more time to react when listening in a multi-talker environment compared to persons with normal hearing, even when attending to a single talker. This suggests a difference in ability to attend to auditory objects in a complex scene due to hearing loss, beyond the issue of audibility.

Funding

PS 188

A measure of selective auditory attention as revealed through functional near-infrared spectroscopy

Min Zhang[1]; Antje Ihlefeld[2]
[1]New Jersey Institute of Technology and Rutgers University; [2]New Jersey Institute of Technology

Background
For speech identification in a background of competing talkers, intelligibility typically improves when a listener can direct auditory attention to spatial and/or pitch cues of the target. Functional magnetic resonance imaging (fMRI) work in normal-hearing (NH) listeners demonstrates that auditory attention can alter Blood Oxygenation Level Dependent (BOLD) signals in lateral frontal cortex (LFCx; Michalka et al., Neuron 2015), at least when directed to spatial cues. Here, we extend this work to attention to pitch, using functional near-infrared spectroscopy (fNIRS).

Methods
We recorded BOLD responses from LFCx in 36 NH participants performing two auditory experiments. In the task condition of Experiment 1, two competing streams of utterances were presented to 17 participants. Target and masker utterances consisted of randomly interleaved color (N=4) and object words (N=16), constrained to differ from each other, and processed to be of 300 millisecond duration each. The two competing talkers differed in pitch (115 versus 144 Hz) and direction (left- versus right-leading interaural time differences, ITDs, of 500 μs). Each trial lasted 15 seconds. Participants were instructed to attend to both pitch and location of the target voice and push colored response buttons each time a color word was uttered by the target talker. In a control condition, participants listened passively to speech-shaped noise (SSN). Experiment 2 consisted of two task conditions. The first condition was identical to the task condition of Experiment 1, the second condition was similar, except that both sources had 0 μs ITD. 19 participants were instructed to direct attention to both pitch-and-space versus pitch-only cues. General linear modeling (GLM) was then applied to fNIRS recordings of LCFx activity, obtained during task performance versus passive listening. The GLM fits of the recorded oxy-hemoglobin responses were then compared across task conditions, using analysis of variance.

Results
In Experiment 1, when listeners directed selective auditory attention to pitch-and-space, both left and right LFCx showed significant changes in activation, as revealed through fNIRS. In contrast, passive listening to SSN did not cause significant changes in LFCx activation. Experiment 2 confirmed these results and revealed comparable GLM fits when attending to pitch alone, versus attending to pitch-and-space.

Conclusions
Result suggests that LFCx underlies auditory attention to space or pitch. fNIRS is a viable tool for assessing whether or not a listener selectively directs auditory attention to perform a task.

Behavioral Enhancement from Ambiguous Visual Cues in an Auditory Spatial Discrimination Task

Madeline S. Cappelloni; Ross K. Maddox
University of Rochester

Auditory and visual location cues are integrated, when both present, to estimate a stimulus's location. Several studies have shown that this integration is well described by an optimal Bayesian observer. Notably, the visual stimulus influences the observer';s perception of the auditory stimulus';s location. It is unclear how this phenomenon changes when there are multiple simultaneous sources, or whether it could offer any benefits to the listener. We tested for a perceptual benefit from two pairs of audiovisual stimuli, aiming to determine whether such an effect would be consistent with Bayesian predictions.

We engaged listeners in an auditory spatial discrimination task. We presented two concurrent auditory stimuli (a pink noise token and a tone complex) located symmetrically in the azimuthal plane using head-related transfer functions, and asked participants to report the side of the tone. Simultaneously with the auditory stimuli, subjects were shown two small visual stimuli of random shape and color which varied from trial to trial and provided no information about the auditory task. The two experimental conditions were designated as matched or central. In the matched condition, the shapes were spatially aligned with the auditory stimuli. In the central (control) condition, the shapes were both at zero degrees azimuth. Presenting the sounds over a range of separations from 1.25 to 20 degrees, we performed a maximum likelihood fit of the data to generate psychometric functions and the corresponding discrimination thresholds for each condition. Preliminary results suggest that there is a behavioral enhancement in some subjects when the visual stimuli are presented at the same locations as the auditory stimuli, even though they were uninformative as to which side the tone was on.

How could a Bayesian observer benefit from an uninformative stimulus? Perhaps counterintuitively, the model predicts that the symmetric bimodal prior provided by the visual stimuli in the matched condition can bias the subject towards reporting the correct answer in the presence of weak auditory evidence. Thus, demonstrating an effect of a task-uninformative visual cue on an auditory spatial discrimination task seems to confirm the validity of what at first appear to be implausible predictions of the Bayesian model.

Behavioral Evidence for a Build-up of Auditory Streaming in Budgerigars (Melopsittacus undulatus)

Huaizhen Cai; Micheal L. Dent
State University of New York at Buffalo

Introduction
Sequential auditory streaming is a classic psychoacoustic phenomenon in auditory scene analysis, which relates to grouping a sound signal consistently radiated by the same sound source as one auditory object. Humans and multiple animal species have shown behavioral evidence of auditory streaming, which supports the idea that auditory streaming is an essential perceptual ability for survival. The build-up process in auditory streaming is elucidated by an increasing probability of streaming perception when hearing the ABA-ABA-… pure tone sequences for a longer time period, which is most apparent for intermediate frequency separations between the A and the B tones. Psychophysical neural recordings in macaques have demonstrated an enhancement of neural adaptation for longer ABA-ABA-… sequence presentation. This adaptation occurs as early as the ventral cochlear nucleus and up to the primary auditory cortex. However, it is yet to be known whether animals perceptually experience the build-up effect when hearing the ABA-ABA-… pure tone sequences. The present study aims to uncover perceptual evidence of the build-up effect in animals'; perception, and to explore how different acoustic features such as frequency separation and repetition rate impact the build-up process.

Methods
The birds were trained to categorize 3 tempos of pure tone sequences of different frequencies: fast isochronous (X-X-…), slow isochronous (X--X--…), and gallop (XXX-XXX-…). Birds were tested on ABA-ABA-… pure tone sequences interspersed with the training stimuli. The birds were able to generalize the streaming perception of testing stimuli to an isochronous category and the coherent perception to a gallop category. The build-up effect was investigated by changing the number of repetitions of stimuli across sessions.

Results
As the testing stimuli became longer, the birds tended to categorize the testing stimuli as isochronous more than gallop. Similar to what is observed in humans, the build-up effect was more apparent for ambiguous frequency separation (6-8 semitones) in birds. Additionally, as the alternating rate between the A and B tones increased in the testing sequences, the build-up process was found to occur faster than for slow alternation rates.

Conclusions

Budgerigars experience a build-up effect in perception when presented with ABA-ABA-… pure tone sequences. Additionally, the birds show a faster build-up process for the tone sequences with a larger frequency separation and faster alternation rate. These perceptual results were congruent with the process of neural adaptation along the auditory pathway of macaques, which were affected by these parameters in the same way.

PS 191

Talker similarity affects head-turn efficiency

Yi Shen; Carly Gurnik
Indiana University Bloomington

In a multi-talker environment, listeners could gain advantageous signal-to-noise ratios (SNRs) by orienting their heads according to the target and interferer locations. However, it is not clear how listeners initiate head turns while localizing the target and interferer talkers in space and identifying the target talker. In the current experiment, listeners were surrounded by six loudspeakers with 60° separations. A target sentence spoken by a female talker was presented from one of the six loudspeakers at random on a given trial, and the listeners were asked to recognize keywords in the target sentence in a closed-set task. A masker was simultaneously presented with the target from the loudspeaker that was 180° away from the target. In separate condition, the masker was a multi-talker babble noise (i.e. Noise masker), or a sentence. The masker sentence was spoken by either a male talker (i.e. Different-Sex masker), a female talker who was different from the target talker (i.e. Same-Sex masker), or the target talker (i.e. Same-Talker masker). The SNR was -10, -15, or -20 dB, varied from trial to trial. Before the experiment, all listeners were provided with ample opportunities to identify their preferred head orientation per target location. Even when the target location was randomly varied, listeners were still able to benefit from head orientation. Head turns were initiated earlier and were less complex in response to target sentences presented from the loudspeakers at more lateral angles. In addition, the masker types also influenced head-turn latency and complexity. The Same-Talker masker corresponded to later initiations of head turns than other masker conditions, suggesting an effect of target-masker similarity on the efficiency of head movements.

PS 192

Brain Signals on Vocoded-Phoneme Recognition

Yue Dong[1]; Guangxin Hu[2]; Yan Gai[1]
[1]Saint Louis University; [2]saint louis university

Noise vocoding is a technique to simulate sound generated by cochlear implants with normal-hearing listeners. When vocoded speech is presented without background noise, high intelligibility can be achieved with as few as four frequency channels. When the listening condition gets difficult (e.g., the addition of background noise), more channels would be required to understand the vocoded speech. This study examined features of brain signals recorded by Electroencephalography (EEG) that may explain the psychophysical observations. Six vocoded phonemes (three vowels and three consonants) were presented as non-vocoded/naturall sound of vocoded sound with 22 or 4 channels to normal-hearing subjects via headsets. The subjects were required to perform a closed-set phoneme discrimination task, while their auditory-evoked potentials (AEPs) were recorded using a 32-channel EEG system. We examined the correlation between the AEPs of non-vocoded phonemes and the AEPs of the vocoded phonemes to see how the number of channels affected the EEG response. We also identified the brain areas that can be used to classify different phoneme responses. When a broadband noise was introduced, we also explored neural responses underlying the psychophysical behavior---binaural release from masking. Taken together, this project aims to cast insight on cortical responses to cochlear-implant sound under diotic or dichotic conditions.

PS 193

Uncertainty in Location, Level and Fundamental Frequency leads to Informational Masking in a Vowel Discrimination Task in young and elderly Listeners

Lena Eipert[1]; Antonia Selle[1]; Georg M. Klump[2]
[1]Cluster of Excellence Hearing4all and Carl-von-Ossietzky University Oldenburg; [2]University of Oldenburg

The ability to perceive and analyze signals from a single sound source in a cacophony of sounds from other sources can be compromised even if these signals are well separated from the sounds from other sources in the excitation patterns in the auditory periphery. This observation defines informational masking (IM). IM may emerge in the presentation of sequential sounds (e.g., Watson, Acta Acust united Ac, 2005, 91: 502–512) in which the temporal separation of masker and target prevents energetic masking in the auditory periphery. IM that causes an elevation of discrimination thresholds is affected by the similarity between target and masker

and stimulus uncertainty. IM strongly influences the perception of phonetic information in complex listening situations. Especially for elderly people speech understanding can be impaired under difficult acoustic conditions which may be related to an increased susceptibility to IM.

To investigate IM we applied a sequential vowel discrimination task with listeners discriminating between the formants of a reference vowel and the formants of a target vowel under various uncertainty conditions. Target vowels were created by shifting formants and thereby morphing a reference vowel into a target vowel. Six young and six elderly listeners were tested to discriminate between vowel pairs /I - i/ and /æ - ɛ/. After a random sequence of reference vowels a target vowel was presented. This target vowel could be presented either with no variation of features (i.e., no uncertainty), uncertainty in fundamental frequency, uncertainty in spatial cues, uncertainty in level, or uncertainty in all three features.

IM resulting in increased vowel discrimination thresholds was observed for both vowel pairs and all three uncertainty factors in young and elderly listeners. Elderly listeners showed higher vowel discrimination thresholds in all conditions. However, the increase in vowel discrimination thresholds due to IM did not differ between young and elderly listeners. Discrimination threshold did not differ between vowel pairs.

PS 194

Enhanced temporal binding of audiovisual information in the bilingual brain

Gavin M. Bidelman; Shelley Heath
University of Memphis

Bilingualism is associated with behavioral and neurophysiological enhancements in auditory-perceptual and cognitive processing necessary for juggling multiple languages. Here, we asked whether bilinguals'; benefits reach beyond the auditory modality and confer advantages in multisensory (e.g., audiovisual) processing. We measured multisensory integration of auditory and visual cues in monolinguals and bilinguals via the double-flash illusion in which the presentation of multiple auditory stimuli concurrent with *single* visual flash induces an illusory perception of multiple flash events. We parametrically varied the stimulus onset asynchrony (SOA) between auditory and visual stimuli (leads and lags of ±300 ms) to assess the temporal binding window where

listeners fuse a single percept. We found that bilinguals were faster and more accurate at perceiving audiovisual stimuli than monolinguals. Moreover, monolinguals showed higher susceptibility for responding to audiovisual illusions and perceived double flashes over an extended range of SOAs indicating poorer AV processing compared to bilinguals. Bilinguals'; temporal integration window was ~1.25-2x shorter than monolinguals'; for both leading and lagging SOAs. Results suggest the plasticity afforded by speaking multiple languages enhances multisensory integration and audiovisual binding in the bilingual brain.

PS 195

Changes in Perception of Ultrasonic Vocalizations as a Consequence of Experience

Laurel A. Screven[1]; Micheal L. Dent[2]
[1]*University at Buffalo;* [2]*State University of New York at Buffalo*

Mice emit ultrasonic vocalizations (USVs) which vary in spectrotemporal parameters (e.g., frequency, amplitude, and duration) in various social situations. Despite their widespread use as a model for human communication, not much is known about how mice use their vocalizations for communication. The effects of social experience have been illustrated by changes in auditory cortex activity in maternal females to pup calls, but it is currently unknown how social experience with other mice affects the perception of adult vocalizations. To test the effects of socialization, we determined if discrimination of USVs was negatively impacted by chronic social isolation compared to mice that were group housed throughout their lifespan. We expected that socially experienced animals would perform better on a vocalization discrimination task than animals that had been chronically socially isolated. Investigating if mice are able to discriminate between vocalizations is a critical step in discovering how mice are using their vocalizations for communication, and if socialization is a necessary component for normal USV perception. Female CBA/CaJ mice were trained and tested using operant conditioning procedures and positive reinforcement to discriminate between natural female USVs of three categories. Mice were tested on all combinations of USVs, with each USV serving as both a background and target stimulus across sessions. The animals were required to respond when they heard a change in the repeating background, and sham trials were included to ensure the mice were under stimulus control. Percent discrimination of calls was measured and compared for isolated and socially housed mice. Isolated mice showed differences in discrimination of USVs relative to socially experienced mice. Additionally, socially isolated mice initially required more training and testing, and more trials to

complete the task than socially experienced mice, with improvements in performance associated with experience with the experimental stimuli. As isolated animals completed more conditions, they became more similar to the socialized animals. These results indicate that active experience with USVs, through either social interactions or from repeated exposure during the operant task, can affect how mice perceive vocalizations. Previous exposure to USVs gives socialized mice an advantage early in testing, but experience with USVs throughout testing also leads to a change in the perception of calls in isolated animals. Socialization appears to be a critical factor in normal USV perception, as our findings indicate that experience with USVs is a necessary component to understanding USVs. This work was supported by NIH DC012302.

PS 196

Responses of Male Mice to Female Broadband Vocalizations Depends on Call Structure

Kayleigh E. Hood; Laura M. Hurley
Indiana University

During courtship interactions, male mice (*Mus musculus*) produce ultrasonic vocalizations (USVs) that attract females. In the initial stage of opposite-sex interaction, females may produce broadband vocalizations (BBVs) paired with rejection behaviors such as kicking and lunging. A recent study has shown that a high initial rate of female BBVs corresponds to reduced male mounting success, while the opposite is true of interactions with low initial BBV production. These results indicate that BBVs may be a behaviorally salient vocalization to males. Using a novel behavioral paradigm in which males were separated from a female by a Plexiglas barrier with a small opening for olfactory investigation, males continued to produce USVs while females did not produce BBVs. This paradigm was used to measure male response to the playback of BBVs isolated from other rejection behaviors that occur during direct male-female contact. Males were presented with a variety of BBV playbacks in this paradigm. Playbacks were 1) an unmanipulated recording of a rejection interaction filtered to remove ultrasonic noise (Natural), 2) a recording in which the varying BBVs from the Natural file were replaced with an exemplar BBV (Exemplar), a recording in which the exemplar was manipulated to 3) increase or 4) decrease structural non-linearity (HighNL and Low NL, respectively), and 5) white noise bursts (White Noise). USVs produced by the same male during playback and non-playback trials were compared. In addition to vocal behaviors, nonvocal behaviors of both male subjects and female social partners were measured. Males significantly reduced their production of USVs when presented with Natural and Exemplar playbacks, indicating that variation in BBV structure is not necessary for USV suppression. Additionally, non-vocal behaviors were not significantly different between playback and no playback conditions, providing support that USV suppression is a specific modification of social behavior in response to a social vocalization rather than a general response to an aversive stimulus. BBVs that were manipulated in structure did not have the same effect. LowNL playbacks increased USV output, while White Noise and HighNL playback had no effect on USV production. Our results indicate that BBVs are a signal of female rejection, and that males respond to BBVs by modifying their courtship behavior.

Regeneration I

PS 197

Large-scale genetic screen identifies heat shock proteins essential for triggering hearing regeneration through cell signaling and metabolic regulation

Wuhong Pei; Jason Sinclair; Erin Jimenez; Lisha Xu; Zelin Chen; Alberto Rissone; **Shawn Burgess**
National Human Genome Research Institute

Regenerative medicine holds great promise for both degenerative diseases and traumatic tissue injury which represent significant challenges to the health care system. Hearing loss, which affects hundreds of millions of people worldwide, is caused primarily by a permanent loss of the mechanosensory receptors of the inner ear known as hair cells. This failure to regenerate hair cells after loss is limited to mammals, while all other vertebrates are able to completely regenerate these mechanosensory receptors after injury. To understand the mechanism of hair cell regeneration and its association with regeneration of other tissues, we performed a guided large-scale mutagenesis screen using zebrafish lateral line hair cells as a screening platform to identify genes that are essential for hair cell regeneration, and further investigated how genes essential for hair cell regeneration were involved in the regeneration of other tissues. We initiated the screening by specifically targeting genes transcriptionally regulated during hearing regeneration in adult zebrafish and expanded gene targets based on initial positive hits. We created genetic mutations either by retroviral insertion or CRISPR/Cas9 approaches, and developed a high-throughput screening pipeline for analyzing hair cell development and regeneration. We screened 253 gene mutations and identified 7 genes specifically affecting hair cell regeneration. Surprisingly these hair cell regeneration genes fell into distinct functional categories. Interestingly, three heat shock related genes (*hspd1*, *hspe1*, and *hspa14*) all showed specific deficits in hearing regeneration. We will present data to show the function of the heat shock

proteins is linked to both cell signaling and metabolic shifts from glycolysis to oxidative phosphorylation that are critical to triggering the regeneration response.

PS 198

Is hair cell regeneration linked to evolutionarily changes within protein sequences?

Robby Boney[1]; Rahul Ram[1]; Matt Lambert[2]; Allison B. Coffin[1]; Phillip Uribe[1]
[1]*Washington State University Vancouver;* [2]*Oregon Health & Science University*

Sensory hair cells, critical for hearing, are vulnerable to multiple damaging agents, such as noise and drugs. In humans and other mammals, which lack regenerative abilities, hair cell loss leads to permanent hearing impairment. In contrast, non-mammalian vertebrates exhibit robust regeneration. We set out to characterize amino acid-level differences between regenerating and non-regenerating species, thereby identifying similar protein sequences in regenerators that are not present or altered in mammals and may contribute to differential regenerative capacity. In this study, we queried NCBI for 6032 proteins that have previously been identified as expressed during regeneration in larval zebrafish lateral line supporting cells. Using the best reciprocal BLAST hits we identified 3250 proteins as having true orthologs across at most 68 species (20 regenerating species (RS), 48 non-regenerating species (NRS)). Multiple sequence alignments were generated for all associated true orthologs. We determined the number of allowable amino acids per aligned site for regenerating and non-regenerating species and calculated the difference between the two groups. We then determined the average difference value per protein and normalized to protein length to calculate the standard deviation of our entire dataset. Using two times standard deviation as a threshold, we identified protein sites that exhibit stringent amino acid selection in RS compared to NRS. We then analyzed these conserved sites to determine the overall proportion of each protein that had a large percentage of these stringently selected sites. From this analysis, gar1 and col6a1 had the highest percentage of stringently selected sites, and neither protein has a known role in hair cell regeneration. These results suggest that our analysis may identify novel genes that are critical for hair cell regeneration.

PS 199

Regeneration and functional recovery of the adult mammalian utricle

Zahra N. Sayyid[1]; Tian Wang[1]; Leon J. Chen[2]; Sherri Jones[3]; Alan G. Cheng[1]
[1]*Department of Otolaryngology-Head and Neck Surgery, Stanford University;* [2]*Stanford University;* [3]*Department of Special Education and Communication Disorders College of Education and Human Sciences, University of Nebraska-Lincoln*

Background

In the vestibular system, the utricle requires sensory hair cells to detect gravity. Prior work showed that the mature organ partially regenerates lost hair cells months after damage. However, the time-course of regeneration, whether organ function is restored, and if enhancing hair cell regeneration improves function are currently unclear. We investigated the histology and function of the mature utricle 7-180 days after damage. Using a fate-mapping approach, we analyzed the time-course and degree of maturation of regenerated hair cells. Furthermore, we examined the effects of Atoh1 overexpression on hair cell regeneration and functional recovery.

Methods

Postnatal 30-day-old mice ($Plp1^{CreERT/+}$; $R26R^{tdTomato/+}$ and $Plp1^{CreERT/+}$; $CAG^{flox-Atoh1-HA/+}$) received the vestibulotoxin IDPN and tamoxifen. Vestibular evoked potentials (VsEPs) were recorded 7-180 days post-injection. Utricles were immunostained for markers of hair cells, supporting cells, stereociliary bundles, pre- and post-synaptic proteins, and neurons. Densities of hair cells, supporting cells, and fate-mapped cells were further analyzed for markers of maturation.

Results

From 7 to 180 days post damage, hair cells significantly increased from 22.9% to 46.1% of age-matched undamaged controls. Using $Plp1^{CreERT/+}$; $R26R^{tdTomato/+}$ mice to fate-map supporting cells, we found a gradual increase in traced hair cells, suggesting that supporting cells replenish lost hair cells over many months. Most traced hair cells were found in the extrastriola and displayed short, disorganized bundles, markers of type 2 hair cells, and pre- and post-synaptic proteins. Six months after damage, $Plp1^{CreERT/+}$; $CAG^{flox-Atoh1-HA/+}$ (Atoh1-OE) organs had significantly more hair cells in both the extrastriolar and striolar regions than damaged organs without Atoh1 overexpression. Atoh1-OE organs also had significantly more fate-mapped hair cells with long stereociliary bundles at 3 and 6 months (44.1% and 45.4%, respectively) compared to damaged only organs (9.7% and 12.7%).

IDPN-treated mice lost VsEP thresholds whereas age-matched, saline-treated controls did not (n=36 controls and 80 IDPN-treated). After 30-180 days, VsEP thresholds of a subset of IDPN-treated animals improved. Serial assessment of 29 IDPN-treated mice demonstrated that 37.9% had recovered thresholds by 6 months, 17.2% showed no improvement, and 44.8% displayed an initial functional improvement followed by a loss of function. By contrast, among the 19 IDPN-treated Atoh1-OE mice, significantly more mice recovered thresholds (68.4%), and fewer animals showed no recovery or unsustained recovery of thresholds (21.1 and 10.5%, respectively).

Conclusions

The adult mouse utricle partially regenerates hair cells and restores function after damage. Atoh1 overexpression improves hair cell regeneration, maturation, and functional recovery.

PS 200

Atoh1 is required in supporting cells for regeneration of type II hair cells in utricles of adult mice

Kelli Hicks[1]; Serena Wisner[2]; Brandon C. Cox[3]; Jennifer Stone[2]
[1]*Department of Otolaryngology, University of Washington School of Medicine; [2]University of Washington; [3]Department of Pharmacology and Department of Surgery, Division of Otolaryngology, Southern Illinois University School of Medicine*

In mature rodents, type II vestibular hair cells are regenerated after near-complete hair cell destruction. In adult mice, utricular type II hair cells also undergo turnover (clearance and replacement). The signals that control type II hair cell turnover and regeneration have not been defined. *Atoh1* is a basic helix-loop-helix transcription factor that is required in mammals for hair cell development and maintenance (Bermingham et al, 1999; Pan et al, 2012; Cai et al, 2013; Chonko et al, 2013). *Atoh1* is expressed in some type II hair cells and a small number of supporting cells under normal conditions in adult mice, which may reflect hair cell turnover (Bucks et al, 2017). After hair cell damage, *Atoh1* becomes highly expressed in supporting cells as they convert into regenerated type II hair cells (Lin et al, 2011; Golub et al, 2012).

Using adult mice, we tested whether *Atoh1* expression in supporting cells is required for type II hair cell turnover under normal conditions or for type II hair cell regeneration after damage. We generated *Sox9-Cre^{ERT2}::Atoh1$^{loxP/loxP}$::Rosa26^{tdTomato}* mice and *Pou4f3^{DTR}::Sox9-Cre^{ERT2}::Atoh1$^{loxP/loxP}$::Rosa26^{tdTomato}*

mice, where the *Pou4f3^{DTR}* allele enabled diphtheria toxin (DT)-mediated destruction of utricular hair cells to stimulate the regeneration process. On average, 76% of supporting cells and 3% of type II hair cells in adult *Sox9-Cre^{ERT2}::Rosa26^{tdTomato}* mice had tdTomato expression 1 week after tamoxifen injection at 6 weeks of age. To conditionally delete *Atoh1* from supporting cells, tamoxifen was administered to 6 week-old *Pou4f3^{DTR}::Sox9-Cre^{ERT2}::Rosa26^{tdTomato}* mice that were either *Atoh1$^{loxP/loxP}$* or *Atoh1$^{+/+}$*. One week later, at 7 weeks of age, DT was administered. In *Atoh1$^{+/+}$* mice at 3 weeks post-DT, there were on average 216 type II hair cells per utricle that were tdTomato-positive, indicating that they were regenerated hair cells derived from *Sox9-Cre^{ERT2}*-expressing supporting cells. By contrast, in *Atoh1$^{loxP/loxP}$* mice, there were on average 10 regenerated type II hair cells per utricle. We detected no significant difference in total numbers of type I hair cells between experimental and control groups. These findings demonstrate that *Atoh1* is necessary for mammalian type II hair cell regeneration. We are currently exploring the effects of *Atoh1* deletion during hair cell regeneration in other vestibular organs and during utricular hair cell turnover.

PS 201

Behavioral and Cell Fate Change after Selective Hair Cell Ablation in the Adult Mouse Utricle

Davood K. Hosseini; Tian Wang; Zahra N. Sayyid; Alan G. Cheng
Department of Otolaryngology-Head and Neck Surgery, Stanford University

Background

Hair cells (HCs) are mechanoreceptors required for hearing and balance. Damage to hair cells in the vestibular system results in balance impairment. In contrast to the mature mammalian cochlea where no hair cell regeneration occurs, the mature utricle can non-mitotically replace lost hair cells. However, it is unknown whether this low level of regeneration depends on the degree of hair cell loss. In this study, we ablated utricular hair cells in *Pou4f3$^{DTR/+}$* transgenic mice with varying doses of diphtheria toxin (DT) and assessed for behavioral changes via observation and swim testing as well as for histologic changes to the utricle via immunohistochemistry.

Methods

P30 *Pou4f3$^{DTR/+}$* transgenic mice were treated with varying doses of DT to ablate hair cells. Behavioral analysis included observation for head bobbing and spinning as well as swim testing two weeks after administration of DT (P44). Histologic analysis of utricles included quan-

tification of hair cells and supporting cells (SCs), as well as hair cell markers Pou4f3, Gfi1 and Atoh1 in hair cells and in supporting cells.

Results

Three doses of DT (low, medium, high) caused incrementally higher degrees of hair cell loss (44.2, 80.6 and 94.7%) in $Pou4f3^{DTR/+}$ mice after two weeks. The number of supporting cells did not significantly change with the doses tested. After treatment with low and medium doses of DT, animals exhibited normal behavior with no spinning or head bobbing. However, two weeks after treatment with high dose DT, mice displayed spinning movements (87.5%) and all had head bobbing. When presented with the swim challenge, 50.0% of the medium dose group had moderately impaired swimming ability including circular swimming and immobile floating; in contrast, 87.5% of the high dose group had severely abnormal swimming such as underwater tumbling. Medium and high doses of DT led to upregulation of hair cell markers (Atoh1, Gfi1, and Pou4f3) in supporting cells, which were rarely found in undamaged controls.

Conclusions

Diphtheria toxin causes a dose-dependent ablation of hair cells in the adult mouse utricle and behavioral change suggestive of vestibular dysfunction. Damage stimulates supporting cells to acquire a hair cell fate.

PS 202

Aminoglycoside Damage and Hair Cell Regeneration in the Chicken Utricle

Mirko Scheibinger[1]; Daniel C. Ellwanger[1]; C. Eduardo Corrales[2]; Stefan Heller[1]
[1]*Stanford | School of Medicine | Department of Otolaryngology - Head & Neck Surgery; [2]Division of Otolaryngology-Head and Neck Surgery, Brigham and Women's Hospital, Harvard Medical School, Boston, MA.*

Inner ear sensory hair cells are essential for hearing and balance. Loss of hair cells results in hearing loss and balance disorders in mammals. Conversely, the study of avian inner ears, which regenerate hair cells, has provided valuable insights into the process of hair cell regeneration. New hair cells in chicken inner ears are produced from supporting cells by two distinct modes: direct transdifferentiation and asymmetric division. Despite identification of signaling pathways potentially involved in hair cell regeneration, a thorough mechanistic insight of regeneration from the earliest events of initiation, realization, and ultimately termination, is not known.

To control a precise temporal onset of hair cell loss, we established a single unilateral surgical delivery of streptomycin and present here a systematic characterization of the regenerative process in the chicken utricle *in vivo*. We observed a robust decline of hair cell numbers in striolar as well as extrastriolar regions. Loss of hair cells in the striola was already detected six hours post-insult. During the initial 12 hours of damage response, we observed global repression of DNA replication, in contrast to the natural, mitotic hair cell production in undamaged control utricles. Regeneration of hair cells in striolar and extrastriolar regions occurred via high rates of asymmetric supporting cell divisions, accompanied by delayed replenishment by symmetric division. While asymmetric division of supporting cells is the main regenerative response to aminoglycoside damage, the detection of symmetric divisions suggests that supporting cells must be replenished after their direct transdifferentiation into new hair cells. Supporting cell divisions appear to be well coordinated because total supporting cell numbers throughout the regenerative process were invariant, despite the initial large-scale loss of hair cells. This work provides an experimental framework to study the precise onset and timing of utricle hair cell regeneration *in vivo*. Initial triggers and signaling events occur already within a few hours after aminoglycoside exposure. Direct transdifferentiation and asymmetric division of supporting cells to generate new hair cells subsequently happen largely in parallel and persist for several days.

PS 203

YAP signaling is activated by hair cell injury and is associated with regenerative proliferation in the avian inner ear

Mark Warchol[1]; Tejbeer Kaur[1]; Matthew Barton[1]; Michael Lovett[2]
[1]*Washington University School of Medicine; [2]Imperial College London*

Background

The YAP1 transcriptional co-activator regulates cell cycle entry and contact inhibition in many cell types and epithelial tissues. Upstream Hippo signaling and/or mechanical tension in the cytoskeleton can evoke translocation of YAP1 from the cytoplasm to the nucleus, resulting in changes in gene expression and enhanced cell division. Hair cell loss from the cochlea and vestibular organs is accompanied by rapid epithelial closure via expansion of adjacent supporting cells, and it is possible that such mechanical stimulation can cause activation of YAP1. The present study characterized YAP pathway genes and the distribution of YAP1 protein in the auditory and vestibular organs of chicks and mice.

Methods

Studies examined YAP1 localization in chick utricles and basilar papillae before and after ototoxic injury. Organo-

typic cultures were treated for 24 hr in 1 mM streptomycin or neomycin, followed by incubation in drug-free medium for 0-48 hr. Hair cell lesions in vivo were created by giving chickens three daily streptomycin injections. Hair cell lesions were generated in Pou4f3-huDTR transgenic mice by administering a single injection of diphtheria toxin. Inner ear tissue from both species was fixed and processed for YAP1 immunolabeling, using a monoclonal antibody (clone 63.7, Santa Cruz). In addition, YAP1/TEAD interaction in organotypic cultures of chick utricles was blocked via treatment with verteporfin, and resulting effects on cell proliferation were assessed by BrdU uptake.

Results

Cytoplasmic immunoreactivity for YAP1 protein was observed in cochlear and utricular supporting cells in both chicks and mice, but YAP1 labeling was not observed in hair cells. Nuclear immunoreactivity for YAP1 was very rare in the undamaged ear, but was enhanced after hair cell injury. Treatment of regenerating chick utricles with verteporfin reduced supporting cell proliferation in a dose-dependent fashion. RNA-Seq profiling of the regenerating chick utricle (see Ku et al., J Neurosci 2015) revealed enhanced expression of numerous Hippo/YAP pathway genes following hair cell lesion.

Conclusions

Data from both chick and mouse indicate that YAP1 protein is present in the cytoplasm of supporting cells and that YAP1 enters the nucleus after hair cell injury. Small molecule inhibition of YAP1 reduced regeneration in the chick utricle. These results suggest that nuclear translocation of YAP1 is an early response to hair cell injury and may be a necessary step in the initiation of regenerative proliferation.

PS 204

Discordant Maturation of Regenerating Mammalian Vestibular Hair Cells

Tian Wang[1]; Mamiko Niwa[1]; Zahra N. Sayyid[1]; Davood K. Hosseini[1]; Nicole Pham[1]; Sherri Jones[2]; Anthony Ricci[1]; Alan G. Cheng[1]
[1]Department of Otolaryngology-Head and Neck Surgery, Stanford University; [2]Department of Special Education and Communication Disorders College of Education and Human Sciences, University of Nebraska-Lincoln

Background

The mammalian vestibular system, including the gravity-sensing utricle, exhibits limited capacity to regenerate hair cells (HCs). Our recent work using lineage tracing experiments characterized the time-course of specific supporting cells/progenitors acquiring a hair cell fate in the damaged, neonatal utricle. However, we lack knowledge of the degree of functional maturation of regenerated HCs and the overall functionality of the organ. Here we have examined the apical and basolateral features of regenerating HCs using immunohistochemistry, electrophysiology including single cell recordings, and vestibular evoked potentials (VsEPs).

Methods

P1 $Pou4f3^{DTR/+}$ transgenic mice were treated with DT to ablate HCs, VsEPs were measured at P15, P30 and P60 before tissue collection for immunohistochemistry. For lineage tracing, $Plp1^{CreERT/+}$; $Rosa26R^{tdTomato/+}$; $Pou4f3^{DTR/+}$ and $Lgr5^{CreERT2/+}$; $Rosa26R^{tdTomato/+}$; $Pou4f3^{DTR/+}$ mice were treated with DT at P1, followed by tamoxifen at P3 or P8 to fate-map SCs.

Results

After DT treatment of P1 $Pou4f3^{DTR/+}$ mice, only 8.0% of Myosin7a+ HCs remained at P15 (in comparison to age-matched controls). HC numbers recovered to 25.1 and 42.5% at P30 and P60, respectively. At P15, 94.1% of mice had no detectable VsEP thresholds and these animals'; thresholds improved to 4.0±5.4 and 1.7±5.5 dB at P30 and P60. Fated-mapping Plp1+ supporting cells (SCs) resulted in tracing of 17.4% and 14.0% of HCs in extrastriola and striola in the P30 damaged utricle, which are significantly higher than undamaged controls (4.6% and 2.5%, respectively). Almost all (95.8%) Plp1-fate-mapped hair cells expressed the type II HC marker annexin A4 and displayed the basolateral potassium currents gDR and gH. 16.3% expressed the type I HC marker osteopontin but none showed gKL currents. At the synaptic level, all traced HCs expressed the presynaptic marker Ctbp2, innervated by Tuj1+ boutons, displayed capacitance change via electrophysiology suggestive of vesicle release. By contrast, most traced HCs showed immature or no stereocilia (82.3% and 7.3%).

By fate-mapping Lgr5+ progenitor cells which primarily occupied the striola, we found that 46.9% of Lgr5 fate-mapped HCs expressed annexin A4, 50.1% expressed the type I marker osteopontin, and 19.6% associated with Tuj1+ calyx. In addition to gH, gDR currents, 21.4% of Lgr5-traced hair cells displayed gKL currents characteristic of Type I HCs.

Conclusions

Regenerated hair cells have basolateral features indicative of maturation, innervation and specialization, but appear immature on their apical surface. The regenerating neonatal utricle achieves a recovery in function.

PS 205

In vivo infusion of gentamicin via the posterior semi-circular canal yields rapid and total tonotopic damage in the chicken cochlea followed by highly synchronized regeneration

Amanda Janesick[1]; Stefan Heller[2]
[1]Stanford University School of Medicine; Department of Otolaryngology-Head & Neck Surgery; [2]Stanford | School of Medicine | Department of Otolaryngology - Head & Neck Surgery

The linchpin of hearing loss is the cochlear sensory hair cell: mammalian hair cells cannot regenerate after they have been lost, and these same cells are exquisitely sensitive to damage by environmental insults. The fragility of the auditory sensory epithelium is observed across all chordates, however, many non-mammalian species, such as the chicken, have repair and regeneration mechanisms to fully restore hearing after damage. I have established a reliable, *in vivo* damage model in the post-hatch day 7 chicken by infusing a single dose of gentamicin via the posterior semi-circular canal. Hair cell extrusion and death occurs quickly within 1 day across the entire tonotopic axis of the chicken cochlea. Using this damage model, in combination with EdU lineage tracing, I have found that proliferation in the supporting cell layer exhibits a sharp peak within the first 2-3 days of regeneration, and occurs predominantly on the neural, afferent side of the epithelium. Direct trans-differentiation of supporting cells into young hair cells is readily observed 5 days post-damage. This *in vivo* damage model is amenable to single cell transcriptomics, where synchronicity of the regenerative process is critical for the temporal ordering of the molecular pathways responsible for reconstructing the cochlear sensory epithelium. Uncovering the mechanism underlying regeneration in birds will bring us closer to the goal of identifying and unearthing rudimentary parts of the regenerative machinery in mammals.

Damage, Chicken Cochlea.pdf

Surgery.pdf

Regenerating Epithelium.pdf

PS 206

Hair cell regeneration model in P1 chicks for single-cell RNA-Seq analysis

Mami Matsunaga[1]; Takayuki Nakagawa[2]; Tomoko Kita[3]; Hiroe Ohnishi[4]; Norio Yamamoto[5]; Koichi Omori[6]
[1]Kyoto University Hospital Department of Otolaryngology, Head and Neck Surgery; [2]Department of Otolaryngology - Head and Neck Surgery, Graduate School of Medicine, Kyoto University; [3]Department of Otolaryngology, Head and Neck Surgery, Kyoto University Graduate School of Medicine; [4]Department of Otlaryngology, Head and Neck Surgery, Graduate School of Medicine, Kyoto University; [5]Department of Otolaryngology, Head and Neck Surgery, Graduate School of Medicine, Kyoto University; [6]Department of Otolaryngology-Head and Neck Surgery, Graduate School of Medicine, Kyoto University

Introduction

The regenerative capacity of mammalian auditory hair cells (HCs) is limited after birth, resulting in the loss of ability to recover from sensorineural hearing loss (SNHL) in mammals. In contrast, birds are able to regenerate damaged HCs through the proliferation or trans-differentiation of supporting cells (SCs), providing us a hint to achieve the recovery from SNHL in mammals. To reveal the HC regeneration mechanism, single-cell RNA-Seq has emerged as a powerful tool. Single-cell analysis is more useful than whole-tissue analysis because HCs and SCs are aligned within sensory epithelia next to each other. Comprehensive analysis of gene expression will provide the information about the network of molecules involved in the HC regeneration. To achieve this purpose, we established the HC regeneration model using the organotypic culture of chick basilar papilla (BP) for single-cell RNA-Seq analysis.

Methods

BPs were dissected from post-hatch day 1 chicks and cultured in DMEM with 1%FBS for 8 days. The explant was treated with/without 78 mM streptomycin (SM) for the first two days. BP samples were collected before culture and days 2 and 8 after culture, fixed with 4%PFA and stained with the marker for HCs and SCs (myosinVIIa, sox2, phalloidin, and DAPI). HC numbers were counted in 3 regions at the distance of 20%, 30% and 40% from the distal end of BP. For the single-cell analysis, the sensory epithelium was isolated from the cartilaginous plate using thermolysin, and single-cell suspensions were obtained by incubating with Accutase and TrypLE Select.

Results

Complete HC loss was observed with two-day SM treatment for BP. In the control samples, HCs labeled with anti-myosinVIIa antibody, phalloidin and DAPI, looked normal in three distal regions, except the proximal end of BP. There are statistically significant differences in HC numbers on day2 between control and SM- treated samples, or non-culture samples and SM-treated samples in the distal region. As for BP samples of cultured for 8 days after SM treatment, regenerated HCs, double-labeled with anti-sox2 and anti-myosinVIIa antibodies were observed. After the cell dissociation, 8,000

to 10,000 single-cells were collected from four BPs of non-culture or SM-treated samples on day 8. The quality of RNA prepared from these samples was good enough to perform single-cell RNA-Seq analysis of BP.

Conclusion
We have established the HC regeneration model of P1 chick BP cultures, which provides sufficient cell number and quality of RNA for single-cell RNA-Seq analysis.

PS 207

Co-activation of Hedgehog and Wnt/β-catenin Signaling Enhanced Cochlear Hair Cell Regeneration After Neomycin Damage

Yan Chen[1]; Wenli Ni[1]; Wenyan Li[2]; Renjie Chai[3]; Huawei Li[4]
[1]ENT and Eye Hospital of Fudan University; [2]1. Department of Otolaryngology, Harvard Medical School, 2. Eaton-Peabody Laboratory, Massachusetts Eye and Ear Infirmary, 3. Department of Otolaryngology, Hearing Research Institute, Affiliated Eye and ENT Hospital of Fudan University; [3]Southeast University; [4]Department of Otolaryngology, Hearing Research Institute, Affiliated Eye and ENT Hospital of Fudan University

Sensorineural hearing loss is one of the universal disabilities that seriously affect the quality of life. Unlike lower vertebrates, mammalian inner ear have limited hair cell regeneration capacity after damage, as a result, hair cell loss is the major cause of permanent sensorineural hearing loss. In situ cochlear hair cell regeneration should be explored as one of the main approaches to restore hearing that is lost due to hair cell loss. Hedgehog and Wnt/β-catenin signaling play important roles in the proliferation, differentiation, and cell fate decision of embryonic inner ear progenitor cells. In this study, we aim to explore whether co-regulation of Hedgehog and Wnt signaling could promote cochlear hair cell regeneration by using transgenic mice. Up-regulation of Wnt/beta-catenin signal in mouse neonatal cochlear support cells could promote precursor cells to proliferate, but a very low proportion of the proliferating cells differentiated into hair cells, and while up-regulation of Hedgehog signaling induced few proliferating cells, but higher percentage of proliferating cells differentiated into hair cells. When the Hedgehog and Wnt signaling were activated simultaneously, hair cell regeneration was enhanced significantly demonstrated by the number of EdU-Myo7a double positive cells. Results showed that Hedgehog signaling promoted hair cell differentiation of Wnt activation induced proliferating supporting cells. This study has important scientific value and application prospect for the treatment of sensorineural hearing loss.

PS 208

Proliferative regeneration after ablation of Lgr5-positive cochlear supporting cells

Tomokatsu Udagawa[1]; Patrick J. Atkinson[1]; Alan G. Cheng[2]
[1]Department of Otolaryngology-HNS, Stanford University; [2]Department of Otolaryngology-Head and Neck Surgery, Stanford University

Background
Cochlear supporting cells (SCs) are required for hair cell development, maintenance and ion homeostasis. Degeneration of SCs as a result of genetic mutation or specific ablation causes secondary hair cell death. While hair cell loss is irreversible, recent studies demonstrated that the neonatal mouse cochlea exhibits the capacity to regenerate lost SCs. However, the progenitor cell pool contributing to supporting cell regeneration is unknown. Here, we have characterized a novel SC ablation model using the Lgr5$^{DTR-EGFP/+}$ mice and fate-mapped specific candidate progenitors.

Methods
Lgr5$^{DTR-EGFP/+}$ mice were injected with different concentrations of diphtheria toxin (DT) at P1 and EdU at P3-5 to detect mitotic activities. Cochleae were harvested for histological analysis at P4-21. Immunostaining was performed for various markers of SCs and hair cells. For fate-mapping, Lgr5$^{DTR-EGFP/+}$; Rosa26R$^{tdTomato/+}$ mice were crossed with Plp1$^{CreER/+}$, Glast$^{CreER/+}$, or Sox-2$^{CreERT2/+}$ mice. To induce Cre recombination, tamoxifen was administered at P1.

Results
The P4 DT-treated Lgr5$^{DTR-EGFP/+}$ cochleae had a dose-dependent reduction of various supporting cells (inner phalangeal cells (IPhCs), pillar cells and Deiters'; cells). We also detected EdU-labeled Sox2+ SCs among the remaining supporting cells and also the GER in a dose-dependent manner. At P7-21, the number of pillar and Deiters'; cells remained low, whereas those of IPhCs returned to normal. Significantly more EdU+ cells were detected in the IPhCs region compared to P4, suggesting mitotic regeneration of these supporting cells.

To determine the source of regenerated cells, we fate-mapped IPhCs, pillar cells, Deiters'; cells, and GER cells using three mouse lines. First, fatemapping of Plp1-td-Tomato+ IPhCs after cell ablation showed the disappearance without later replenishment, suggesting that Plp1+ IPhCs do not self-regenerate. Next, fate- Sox2+

cells, which broadly represent IPhCs, Deiters'; cells, pillar cells, and GER cells found many EdU+ tdTomato+ cells in the IPhCs region at P7 and P14. Lastly, fate-mapping experiments of Glast+ SCs, which represent IPhCs and the GER, showed the initial disappearance of Glast-tdTomato+ IPhCs but re-emergence of many EdU+ Glast-tdTomato+ cells in the IPhCs region at P7 and P14. Together, our fate-mapping results suggest that proliferative cells in the GER act as progenitors for regenerated IPhCs.

Conclusions
Selective ablation of Lgr5-positive cochlear SCs results in proliferation in the organ of Corti and GER in a dose-dependent manner. Proliferative cells in the GER are capable of replacing lost IPhCs.

Funding

PS 209

Comparison of moderate and severe models of aminoglycoside-induced hair cell loss in neonatal cochlear explants

Bonnie Jacques; Anne Harrop-Jones; Alan C. Foster; Fabrice Piu
Otonomy Inc

Background
Hair cell death is a significant contributor to hearing loss. To better understand the mechanisms of hair cell restoration or protection for the purpose of identifying drug targets and to evaluate the efficacy of potential therapeutic compounds, reliable and reproducible models of cochlear hair cell loss are essential. Ex-vivo cochlear explant models in which aminoglycoside antibiotics induce hair cell death are commonly used. Typically, however, these models involve the nearly complete elimination of all hair cells from an explant, which may be relevant to only very severe forms of deafness. Here, to help characterize the efficacy of potential therapeutic compounds for hair cell regeneration or protection, two gentamicin-based models of aminoglycoside-induced hair cell loss were developed: a moderate damage model (<50% hair cell loss) and a severe damage model (>50% hair cell loss). Several different aminoglycosides and their performance in moderate and severe models of hair cell loss were compared.

Methods
Neonatal rat cochlear explants were treated with a range of gentamicin, kanamycin, neomycin or tobramycin concentrations for different lengths of time to induce moderate or severe hair cell damage. After aminoglycoside treatment, explants were rinsed well in aminoglycoside-free media, then allowed to recover for 48-72 hours. Cochleae were fixed and stained for hair cell and support cell markers and the number of both inner and outer hair cells was quantified in 200 μm length segments from the basal, mid and apical regions. Additionally, the application of a gamma-secretase inhibitor was used to evaluate the regenerative potential to form new hair cells under these different conditions.

Results
In both moderate and severe damage conditions, a time and dose-dependent decrease in the number of inner and outer hair cells was observed after aminoglycoside treatment. Hair cell loss was typically restricted to the basal and middle turns as apical hair cells are less susceptible to aminoglycoside damage, and outer hair cells were more affected than inner hair cells. Some damaged explants were treated with a known gamma-secretase inhibitor to induce new hair cell formation; a greater increase in hair cell numbers in the moderate gentamicin model compared to the severe model was noted.

Conclusions
Altering both the concentration and time course of aminoglycoside treatment may affect inter-cochlear reliability in these hair cell damage models. Results with a known gamma-secretase inhibitor suggest an enhanced capacity for hair cell formation under less damaging conditions.

PS 210

Maintaining Active Notch Signaling in Supporting Cells Prevents Spontaneous Hair Cell Regeneration in vivo

Melissa McGovern[1]; Michelle Randle[2]; Luyi Zhou[2]; Brandon C. Cox[3]
[1]*Department of Pharmacology, Southern Illinois University School of Medicine, Springfield, Illinois;* [2]*Department of Pharmacology, Southern Illinois University School of Medicine;* [3]*Department of Pharmacology and Department of Surgery, Division of Otolaryngology, Southern Illinois University School of Medicine*

During embryonic development, progenitor cells differentiate into hair cells (HCs) or supporting cells (SCs) by Notch-mediated lateral inhibition. Many studies have shown that inhibition of Notch signaling allows SCs to convert into HCs in both normal and drug damaged neonatal mouse cochleae. This mechanism is also implicated during spontaneous HC regeneration in non-mam-

malian vertebrates. We and others have observed that spontaneous HC regeneration can occur in the neonatal mouse cochlea. While the inhibition of Notch signaling can force SCs to convert into HCs, it is currently unknown whether loss of Notch signaling is the mechanism underlying spontaneous HC regeneration observed *in vivo*. Therefore, to investigate the role of Notch signaling during the spontaneous HC regeneration process, we used *Atoh1-CreER*[TM]*::Rosa26*[loxP-stop-loxP-DTA/+] mice with tamoxifen administered at postnatal day (P) 0/P1 to ablate HCs and stimulate the spontaneous HC regeneration process. Changes in the expression of genes in the Notch pathway were measured using real time qPCR, immunostaining, and *in situ* hybridization, with most changes limited to the apical one-third of the cochlea. Expression of the Notch effector *HeyL* was increased, while the ligand *Jagged 1* and the effector *Hes5*, which is directly responsible for inhibiting HC fate, were decreased. We also investigated whether inhibition of Notch signaling is required for spontaneous HC regeneration to occur by maintaining active Notch signaling in all SCs in the context of HC damage. The mouse model, *Atoh1-CreER*[TM]*::Rosa26*[loxP-stop-loxP-DTA/+]*::Sox10*[rtTA]*::TetO-LacZ::TetO-NICD,* was injected with tamoxifen at P0-P1 to stimulate spontaneous HC regeneration and given doxycycline, in the diet to nursing mothers from P0-P7 and injected in pups on P1, to induce expression of the *Notch1 intracellular domain* (*N1ICD*) and *LacZ* in all non-HCs. Fewer fate-mapped regenerated HCs were detected after HC loss with *N1ICD* overexpression compared to HC damage alone. Therefore we conclude that loss of Notch-mediated lateral inhibition is required for the majority of spontaneous HC regeneration to occur. Understanding how Notch signaling regulates this regenerative plasticity will allow more directed investigation into why HC regeneration does not occur in the mature cochlea. This understanding will help identify therapeutic targets to treat hearing loss due to HC loss.

PS 211

A High-Throughput Screen Identifies POU4F3 Transcriptional Agonists for Hair Cell Regeneration in Mammalian Cochleae

Shiyong Diao[1]; Pei-i Ho[2]; Marta Jimenez[2]; Douglas Auld[2]; Jian Zuo[3]
[1]*St. Jude Children's Research Hospital;* [2]*Novartis Institutes for BioMedical Research, Inc.;* [3]*Department of Developmental Neurobiology, St. Jude Children's Research Hospital, Memphis, Tennessee, USA*

Background

POU4F3 is required for the differentiation and maturation of cochlear and vestibular hair cells. Dysfunction of POU4F3 results in DFNA15 deafness in humans. We recently showed that ectopic overexpression of POU4F3 can promote regeneration of new hair cells from the mature supporting cells in adult cochleae in vivo. The conversion of supporting cells (Deiters and pillar cells) to new hair cells by POU4F3 overexpression is more efficient than overexpression of Atoh1 alone. These results indicate that POU4F3 might be a therapeutic target for hearing restoration. Here, we therefore aim to identify POU4F3 transcriptional agonists by high-throughput screening (HTS) of large libraries of small molecule compounds.

Methods

We cloned human 6kb POU4F3 promoter into PNL-Col1 vector, a second generation of coincidence luciferase (Firefly & Nano-Luc) reporter vector, transfected it into Hela cells and generated stable cell lines of the POU4F3 promoter reporter with selection of hygromycin resistance. MS-275 and sodium butyrate were chosen as positive controls, which increased 2 to 5 times of the luciferase activity, and data was normalized by DMSO (negative control). Cell viability was detected by Cell-Titer-Glo® Luminescent activity in the primary screen and Alamar Blue in the secondary screen. At Novartis, a ~40K library of compounds published in PubChem and a library of ~3,000 purified natural product compounds were first screened at 10 μM (n=1). Additionally, a Mechanism of Action (MoA) library of ~2,800 compounds was screened from a 10 μM top concentration with 8 concentration points. The MoA library contains well annotated tool compounds and some known drugs. Validation at four concentrations for determining concentration-response curves for each of the primary hits from Pubchem and natural product libraries was performed in Novartis as well. At St. Jude, top hits were further validated for dose responses and non-specific agonist activity by transfecting Hela cells with a SV40-promoter driven LacZ vector and measuring the luminescence signals. We also examined top hits for Atoh1 agonist activity in HeLa cells transfected with an Atoh1-enhancer and promoter driven PNL-Col1 reporter.

Results

A total of 173 primary hits from Pubchem and natural product libraries demonstrated ≥ 50% luciferase activation, which included 76 hits with Firefly Luc (Fluc) & Nano-Luc (Nluc), 80 hits with Fluc only (no Fluc inhibition) and 17 hits with Nluc only (no Nluc inhibition). From the MOA library, 12 compounds showed agonist activity in both Fluc & Nluc signals and 76 compounds showed ≥ 50% agonist activity in either Fluc or Nluc signals. After dose response validations at Novartis, we further validated 16 top hits at St Jude. We have identified 3 top compounds which have POU4F3 agonist activity (≥ 50%) and two of them have Atoh1 agonist activity (≥ 50%, ≥ 500%).

Further validation is currently undergoing for those top hits and additional compounds we identified at Novartis. The POU4F3 agonists will facilitate regeneration of functional hair cells in adult mammalian cochleae when combined with other compounds for clinical applications.

PS 212

Assaying sensory cell regeneration in adult mouse cochlea after noise damage and activation of ErbB2

Jingyuan Zhang[1]; Patricia White[2]
[1]*University of Rochester;* [2]*Dept. of Neuroscience, University of Rochester School of Medicine*

Background
Outer hair cell (OHC) loss is a primary cause of hearing loss, as little regeneration occurs in the mammalian system. To achieve OHC regeneration, we aim to drive replacement from supporting cells (SCs) that are closely interacting with OHCs. Our lab has previously found that activation of ErbB2 signaling is sufficient to drive SC proliferation in the neonatal mouse cochlea *in vitro*. Moreover, it also drives OHC differentiation in neonatal mouse cochleae *in vivo*. Here, we want to understand some challenging questions. First, can SCs in the older animal proliferate after damage if ErbB2 activation is supplied to the system? Second, can adult SCs serve as HC progenitors to compensate hair cells loss after damage if ErbB2 is activated?

Methods
Mice. Several transgenic mouse lines were bred to overexpress a rat constitutively active (CA) ErbB2 in mouse cochlea *in vivo*. Transgenic CA-ErbB2 activation in SCs was accomplished via two strategies: 1) Crossing Tet-on CA-ErbB2 line with a cochlear specific rtTA line, Sox-10rtTA 2) Crossing Tet-on CA-ErbB2/ ROSA-floxed-rtTA-GFP with SC specific Cre lines: Sox2CreER and Fgfr3CreERi. **Noise damage and hearing test.** We used 110dB for 2 hours. ABR and DPOAE were measured 3 days prior to noise, 1-day post noise, 1-week post noise and 1-month post noise. We used immunochemistry to investigate Cre activity (GFP), ErbB2 phosphorylation; SCs, HCs, and synapses makers. Proliferation was revealed by EdU nuclear incorporation and quantified using FLUOVIEW.

Preliminary results and hypothesis
Our transgenic strategy established a way to activate CA-ErbB2 signaling under spatial and timely control *in vivo*. We can transiently activate CA-ErbB2 under three different promoters that express specifically in the cochlea. From the previous study in our lab, 110dB noise lasting for 2 hours was devastating to mouse hearing ability. OHCs are especially vulnerable undergoing apoptosis as early as post-noise one week. Recent data from our lab suggest that one of the immature HC marker: Myosin7 emerged from SC layer directly underneath OHCs in consequence of ErbB2 activation. In combination with noise exposure and CA-ErbB2 treatment to adult animals, we are testing whether CA-ErbB2 can be induced in mature SCs, whether CA-ErbB2 can trigger new Myo7+ cells production, whether CA-ErbB2 can prevent hair cell loss or regenerate hair cells after noise damage, and most importantly whether CA-ErbB2 can be used as a potential therapy to restore auditory function.

PS 213

Isl1 and Atoh1 Synergistically Mediate Cochlear Hair Cell Transdifferentiation in Mice

Fei Zheng[1]; Tetsuji Yamashita[2]; Jian Zuo[2]
[1]*St. Jude Children's Research Hospital;* [2]*Department of Developmental Neurobiology, St. Jude Children's Research Hospital, Memphis, Tennessee, USA*

Hearing loss, as the third most common physical problem in the world, mostly results from the dysfunction and/or loss of cochlear hair cells (HCs) in the inner ear. To regenerate HCs and to restore hearing, we and others have attempted to reprogram cochlear supporting cells (SCs) to HCs. We found that Atoh1, a transcription factor that is involved in the spontaneous HC regeneration in non-mammalian vertebrates, can convert SCs to HCs in the neonatal and juvenile cochleae. However, the conversion is not efficient - only about 6-20% of Atoh1-overexpressing SCs were reprogrammed to the HC fate. Comparing the regeneration in other tissues, we reasoned that reprogramming requires a combination of transcription factors. By analyzing the transcriptome of endogenous SCs, outer hair cells (OHCs), and Atoh1-converted hair cells (cHCs) from the adult murine cochlea, we identified Isl1, a transcription factor that is critical for the differentiation of many cell types, as a potential modifier for Atoh1-induced HC conversion. Here we show both in explants and in transgenic mice that Atoh1 and Isl1 synergistically increased the transdifferentiation efficiency in the cochlea. Moreover, we observed the physical interaction of the two transcription factors in vivo, indicating they may form a complex to regulate Atoh1-target genes for cochlear HC transdifferentiation.

PS 214

Regeneration of Cochlear Hair Cells and Hearing Recovery through Hes1 Modulation with siRNA Nanoparticles in Adult Guinea Pigs

Xiaoping Du[1]; Matthew West[1]; Qunfeng Cai[2]; Ibrahima Youm[1]; Xiangping Huang[2]; Wei Li[1]; Weihua Cheng[1]; Don Nakmali[1]; Donald Ewert[1]; Richard Kopke[3]
[1]Hough Ear Institute; [2]Hough Ear Institute and Otologic Pharmaceutics Inc; [3]Hough Ear Institute, Oklahoma Medical Research Foundationand, Departments of Physiology and Otolaryngology, University of Oklahoma Health Sciences Center, Otologic Pharmaceutics Inc

Background

Deafness is commonly caused by loss of cochlear hair cells (HCs) in the inner ear due to noise trauma, toxins or infections. Once lost, cochlear HCs in mammals do not spontaneously regenerate,resulting in permanent hearing impairments. However, recent studies have demonstrated that mammalian cochlear HCs can be regenerated through genetic manipulation of key regulatory factors, such as Atoh1 and genes in the Notch, FGF, Shh and Wnt pathways. We previously used *Hes1* siRNA (*siHes1*) poly(lactide-*co*-glycolide acid) nanoparticles (PLGA NPs) to regenerate mouse cochlear HCs *in vitro*.

Methods

In the present study, we delivered *siHes1* PLGA NPs to the cochleae of adult guinea pigs by Mini-Osmotic pumps for 24 hours initiated three days after acoustic trauma (125 dB SPL octave-band noise centered at 4 kHz for 3 hours). Noise-injured animals infused with non-targeting (scrambled) siRNA (scRNA) NPs served as controls. Auditory functional recovery was measured by auditory brainstem responses (ABR). HCs were examined by immunolabeling against myosin VIIa, prestin and vGlut3 and scanning electron microscope (SEM).

Results

Significantlygreater HC restoration and hearing recovery were observed in ears treated with *siHes1* NPs compared to ears treated with sham scRNA NPs beginning at three weeks and extending out to nine weeks post-treatment. Ectopic and immature HCs were uniquely observed in the organ of Corti of noise-injured cochleae treated with *siHes1* NPs.

Conclusions

Our results indicate that durable cochlear HCs were regenerated and promoted hearing recovery in noise-deafened cochleae of adult guinea pigs through modulation of *Hes1* expression. Biodegradable PLGA NPs delivering siRNA to the cochlea represent a promising pharmacologic approach to regenerate functional and sustainable mammalian HCs.

PS 215

Induction of proliferation in adult and aged mouse cochlea

Yilai Shu[1]; Wenyan Li[1]; Yi-Zhou Quan[2]; Mingqian Huang[3]; Zhengmin Wang[4]; Huawei Li[4]; Zheng-Yi Chen[5]
[1]1. Department of Otolaryngology, Harvard Medical School, 2. Eaton-Peabody Laboratory, Massachusetts Eye and Ear Infirmary, 3. Department of Otolaryngology, Hearing Research Institute, Affiliated Eye and ENT Hospital of Fudan University; [2]1. Department of Otolaryngology, Harvard Medical School; 2. Eaton-Peabody Laboratory, Massachusetts Eye and Ear Infirmary; [3]1. Department of Otolaryngology, Harvard Medical School, 2. Eaton-Peabody Laboratory, Massachusetts Eye and Ear Infirmary; [4]Department of Otolaryngology, Hearing Research Institute, Affiliated Eye and ENT Hospital of Fudan University; [5]1. Department of Otolaryngology, Harvard Medical School, 2. Eaton Peabody Laboratory, Massachusetts Eye and Ear Infirmary

Introduction

Complete quiescence state of adult mammalian cochlea makes it particularly challenging to induce proliferation. We hypothesize that to achieve cell cycle re-entry in adult cochlea need to be reprogrammed to re-gain the properties similar to young inner ear. We have previously identified MYC as a proliferation master gene in zebrafish hair cell regeneration. Studies have shown Notch1 is a potent progenitor gene in embryonic development. We study the combinatory effect of MYC and Notch1 activation in induction of proliferation in adult mouse cochlea *in vit*ro and *in vivo*.

Methods

Whole cochlea explant organ culture and microinjection into adult cochlea were used for the study *in vitro* and *in vivo*, respectively. *Notch1* and *c-Myc* were activated in adult mice by virus-mediated delivery, or in adult doxycycline-inducible rtTA/tet-*Myc*/tet-*NICD* transgenic mice through supplement of doxycycline. EdU and BrdU

incorporation was used to study proliferation. Lineage tracing using *Sox2*-promoter-driven *Cre* mice (Sox2-CreER) crossed with the tdTomato (tdT) reporter mice was conducted to identify the origin of proliferating cells. The mechanisms underlying reprograming were studied by qRT-PCR, immunolabeling and the effectors that modulate mTOR pathway. Survival was studied by analysis of apoptosis.

Results
We demonstrate that co-activation MYC and Notch1 leads to cell cycle re-entry shown by EdU and BrdU incorporation in adult cochlea *in vitro* and *in vivo.* Lineage tracing shows diverse cochlear cell types, including inner hair cells, pillar cells, Deiters cells, Hensen cells, Claudius cells, cells from limbus region and from stria vascularis are capable of renewed proliferation. Study with specific markers, including Ki67, pH3, Aurora B as well as the mitotic figure by the spindle marker α-tubulin, shows that dividing cells undergo DNA synthesis and different phases of proliferation and complete cell cycle. A majority of the proliferating cells are MYC/NICD double positive and maintain their identities after mitosis by expressing respective cellular markers. Survival of proliferating cells depends on duration of MYC/NICD activation: transient MYC/NICD function results in long-term survival of proliferating cells whereas sustained MYC/NICD activation induces apoptosis. Reprogramming by MYC/NICD is shown by upregulation of inner ear progenitor genes such as Six1, Eya1, Gata3 and Isl1, whereas the stem cell genes and differentiation genes were not. mTOR pathway is activated in the non-sensory epithelial region upon MYC/NICD activation, and inhibition of mTOR by rapamycin suppresses proliferation in those regions, demonstrating mTOR is downstream of MYC/NICD and is required for renewed proliferation. Finally in aged inner ear (12 month) proliferation is induced.

Conclusion
Reprogramming by MYC and Notch1 in adult and aged mammalian cochleae results in renewed proliferation in diverse cell types. Cell survival is enhanced by transient action of MYC/NICD. Renewed proliferation in fully mature mammalian cochlea provides the opportunities to regenerate diverse inner ear cell types, opening the possibility using regeneration to treat some forms of deafness.

PS 216

Limited Hair Cell Recovery After Gamma-Secretase Inhibition in the Damaged Rodent Cochlea

Naila Haq[1]; Lisa Nolan[1]; Rick Cousins[2]; **Jonathan Gale**[1]
[1]*UCL Ear Institute;* [2]*GSK*

Mechanosensory hair cells (HC) are susceptible to death from a variety of insults, including noise, ototoxic drugs, and aging. The loss of HC leads to irreversible hearing loss, hence interventions that can enable HC regeneration to re-establish hearing would be of transformation value to patients. Induction of Atoh1 expression in cochlear supporting cells following inhibition of Notch signalling by gamma secretase inhibitors (GSIs) can induce trans-differentiation into HCs, although the age of the tissue appears to be critical. We set out to test this potential regenerative strategy.

We used rat cochlear explants to investigate recovery after aminoglycoside antibiotic exposure. HC survival was measured by two independent mechanisms, either by quantification of FM1-43 labelling, allowing assessment of HCs before and after neomycin challenge or by immunocytochemical (ICC) analysis using antibodies to myosin VIIA (Myo7a, HC marker), SOX2 (SC marker) and also using phalloidin (for F-actin). Using this approach, we first determined the neomycin-induced hair-cell death-dose relationship, measured 24 hours after neomycin exposure. The two different analyses revealed similar results for 50% survival concentration (and slope) indicating that FM1-43 fluorescence can be used as a quick and simple assay for HC survival. Subsequently, we used 125μM neomycin for 24 hours to test whether a putative small molecule GSI could stimulate hair cell regeneration';. After 24 hours, neomycin was washed out and explants were placed in GSI or in control media (with DMSO vehicle) for a further 48 hours. Using the ICC analysis, we found no significant difference in the number of hair cells between GSI-treated (0.1 to 10μM) and DMSO controls. However, we did observe a small number of SOX2 and Myo7a double-positive cells in GSI-treated, neomycin-exposed explants whereas there were almost none were observed in vehicle-treated, neomycin-exposed explants. The latter data suggest that the GSI was able to induce the conversion of supporting cells to hair cells but to a very limited extent. Separate experiments confirmed that the small molecule GSI was able to induce hair cell formation in naïve undamaged cochlear explants from younger (P0-1) rats.

In conclusion, our data indicate that there is a developmental decline in the "notch-responsiveness" of rat cochlear cells in the first few post-natal days as has been

observed in mice (Maas et al, Front Cell Neurosci 2015) suggesting that this decline is common to rodents and most likely, all mammals.

PS 217

A Cocktail of EGF, FGF2 and IGF1 with Inhibitors of GSK3B, HDAC, and TGFBR1 Induces Robust Proliferation of Supporting Cells Dissociated from and Residing Within Utricles of Neonatal Mice, but Not in Those That Have Matured

Mikolaj Kozlowski; Mark Rudolf; Christina Kim; Jeffrey Corwin
University of Virginia

Background
McLean *et al.* (2017) recently reported a promising approach for expanding progenitor cells from neonatal mouse cochleae. We tested this approach in supporting cells of neonatal and mature utricles as a means to investigate the maturational changes in hair cell epithelia that are hypothesized to limit hair cell regeneration in mammals.

Methods
To test whether McLean et al.';s cocktail of mitogenic growth factors and pharmacological agents could expand vestibular supporting cells, we dissected, delaminated, and trimmed utricular sensory epithelia from P0 mice. We then used enzymatic dissociation and trituration to isolate single cells and small aggregates, which we suspended in 3D Matrigel domes and cultured in a chemically defined medium containing EGF, FGF2, IGF1, vitamin C, and inhibitors of GSK3B, HDAC, and TGFBR1. We also tested whether the cocktails with and without vitamin C and the inhibitors would induce S-phase entry in intact utricles explanted from neonatal and mature mice by supplementing those media with BrdU for three days.

Results
Dissociated cells from P0 utricles expanded markedly when treated with the cocktail and formed small vesicles with lumenal cell apices. Most cells stained positive for Sox2. When we next cultured intact utricles from P0 mice in that complete medium, numbers of BrdU+ supporting cells increased over 20-fold as compared with utricles cultured with medium containing EGF, FGF2, and IGF1 but lacking the vitamin C and inhibitors (954±131 BrdU+ cells vs 36±24, mean±SD). In sharp contrast, preliminary results in explants from one-month-old mice revealed that even the highly mitogenic, complete cocktail had negligible effects on proliferation of supporting cells in mouse utricles once those supporting cells had matured (39±6 BrdU+ cells vs 41±13).

Conclusions
Our findings show that a potent cocktail of growth factors and pharmacologic agents described by McLean *et al.* (2017) also induces rapid proliferation in 3D cultures of Sox2+ cells dissociated from neonatal mouse utricles. The cocktail also stimulates robust proliferation in undamaged P0 utricles. However, our preliminary findings in older utricles suggest that even when the EGF, FGF2, IGF1, and Wnt pathways are simultaneously stimulated in the presence of TGFB inhibition, the proliferative responses of supporting cells are limited by postnatal maturational changes that occur within the mammalian ear.

PS 218

Expression of the Survival Factor Pou4f3 in Regenerated Hair Cells of the Neonatal Mouse Cochlea

Michelle Randle[1]; Brandon C. Cox[2]
[1]*Department of Pharmacology, Southern Illinois University School of Medicine;* [2]*Department of Pharmacology and Department of Surgery, Division of Otolaryngology, Southern Illinois University School of Medicine*

Mice have the capacity to regenerate cochlear hair cells (HCs) after damage within the first postnatal week. In response to HC death, supporting cells (SCs) undergo mitotic regeneration or direct transdifferentiation to regenerate HCs. However, the majority of regenerated HCs die within the first week of differentiation from unknown reasons. *Pou4f3* is a transcription factor that is believed to be necessary for HC survival based on studies where *Pou4f3* was deleted or mutated in the germline. We previously reported that only ~14% of HCs in our model (*Atoh1-CreER*[TM]*::ROSA26*[DTA] mice injected with tamoxifen at postnatal day (P)0 and P1) expressed *Pou4f3* at P6, however fate-mapping was not included to distinguish between original/surviving HCs and regenerated HCs. Therefore, we investigated the ability of regenerated HCs to express *Pou4f3* using fate-mapping methodsas a potential explanation for their impaired survival. To fate-map mitotically regenerated HCs, we injected *Atoh1-CreER*[TM]*::ROSA26*[DTA] mice with tamoxifen at P0 and P1 (to ablate HCs and stimulate the spontaneous HC regeneration process), followed by 5-Bromo-2';-deoxyuridine (BrdU) twice a day (~6hrs apart) from P3-P6 (to label dividing cells) and collected temporal bones at P7. Using immunofluorescence, we observed that less thanone third of the BrdU-positive/myosin VIIa-positive cells expressed Pou4f3. We also fate-mapped SCs using *Prox1*[CreERT2]*::ROSA26*[tdTomato/+]*::Pou4f3*[DTR] mice that were injected with tamoxifen at P0 (to label ~71% of pillar and Deiters'; cells with tdTomato) and diphtheria toxin at P1 (to ablate of HCs) and collected temporal bones at P7. Similar to our previous study, only ~12% of myosin

VIIa-positive HCs expressed Pou4f3. However when td-Tomato expression was included in the analysis to fate-map SCs that regenerated HCs, we found that ~93% of tdTomato-positive/myosin VIIa-positive cells also expressed Pou4f3, while only ~7% of tdTomato-negative/myosin VIIa-positive cells expressed Pou4f3. Therefore, we conclude that the majority of regenerated HCs are capable of expressing Pou4f3, yet the cells formed by mitotic regeneration are less likely to do so. Therefore impaired survival of regenerated HCs is not caused by lack of Pou4f3 expression. In addition, the large number of tdTomato-negative/myosin VIIa-positive/Pou4f3-negative cells observed may be HC "corpses" that remain in the cochlea after death, similar to what has been shown in vestibular organs.

PS 219

In vivo single cell and bulk RNA-seq profiling of Atoh1-mediated cochlear hair cell conversion

Tetsuji Yamashita[1]; Fei Zheng[2]; David Finkelstein[3]; Zoe Kellard[2]; Carter Robert[2]; Celeste Rosencrance[2]; Ken Sugino[4]; John Easton[2]; Charles Gawad[2]; **Jian Zuo**[1]
[1]Department of Developmental Neurobiology, St. Jude Children's Research Hospital, Memphis, Tennessee, USA; [2]St. Jude Children's Research Hospital; [3]Department of Computational Biology, St. Jude Children's Research Hospital; [4]Howard Hughes Medical Institute

In vivo direct conversion of differentiated cells holds promise for regenerative medicine; however, improving its efficiency and completion remains challenging. Ectopic expression of Atoh1 in non-sensory supporting cells (SCs) in mouse cochleae induces their conversion to hair cells (HCs) in vivo. Here, we performed a detailed transcriptome analysis of converted HCs (cHCs), mature SCs, neonatal and mature HCs in mouse cochleae. We utilized bulk RNA-seq, single cell multiplex qPCR (Fluidigm BioMark HD) and single cell RNA-seq (10XGenomics) for transcriptome profiling. The mouse models used were Fgfr3i-CreER; CAG-loxP-Stop-loxP-Atoh1-HA and other GFP/tdTomato reporters. Tamoxifen induction was at P12-13 while cochleae were dissociated at P12, P26 and P33 for analysis. All analyses identified cHCs in multiple intermediate transcriptome states of the conversion process that most closely resembled neonatal differentiating HCs, but differed from the progenitors, mature SCs and mature HCs. We further identified 52 transcription factors that are differentially expressed in cHCs, mature SCs and HCs that likely promote the efficiency and completion of Atoh1-mediated HC conversion. Similarly, we also identified signaling pathways and ligand-receptor pairs likely important for Atoh1-mediated HC conversion. Our results support the notion that in vivo direct HC conversion from SCs bypasses the progenitor states and requires multiple factors to efficiently reach completion.

PS 220

A small molecule regenerative therapy for adult onset sensorineural hearing loss; the REGAIN Horizon 2020 consortium approach

Anne Schilder[1]; Shakeel R. Saeed[1]; Thanos Bibas[2]; Dimitris Kikidis[2]; Stephan Wolpert[3]; Leonie Middlelink[4]; Joanne Palmer[1]; Helen Blackshaw[1]; Matthew Topping[1]; Katherine Lazarides[4]; Helmuth Van Es[4]
[1]University College London; [2]University of Athens; [3]University of Tubingen; [4]Audion Therapeutics

Introduction

Hearing loss affects 500 million adults worldwide and has therefore become a public health priority[1]; the most common cause is sensorineural hearing loss (SNHL) due to auditory hair cell loss. Importantly, this type of hearing loss is linked to dementia[2]. Current treatment is limited to hearing aids and cochlear implants; neither device restores natural hearing nor prevents further hearing deterioration. There is therefore an urgent need for novel hearing therapies.

Preclinical studies have demonstrated that inhibition of Notch signalling with a gamma-secretase inhibitor (GSI) can regenerate outer hair cells and partially restore hearing[3]. Supported by a €5.8 million EU Horizon 2020 grant, the international REGAIN (REgeneration of inner ear hair cells with GAmma-secretase INhibitors) Consortium seeks to translate these preclinical findings into a potential hearing therapy.

Methods

Preclinical development included GSI candidate selection, drug synthesis optimisation, formulation, inner ear pharmacokinetics (PK) and local and systemic toxicology according to FDA guidance. This is to be followed by a phase I safety study conducted in the UK and a phase II efficacy study in the UK, Germany and Greece. The GSI will be administered locally in three doses, one week apart, to the worst hearing ear of adults with

adult-onset mild to moderate SNHL. Local safety and efficacy assessments include a large range of hearing, tinnitus and balance tests.

Results

Preclinical inner ear PK studies with the formulated drug product revealed good cochlear drug exposure as measured by sampling the perilymph and provided the data for patient dosing. Genotoxicity, ototoxicity, systemic toxicity tests and dermal irritation studies showed no evidence of toxicity. The safety study has received regulatory approval in the UK and is scheduled to open late 2017.

Conclusions

Small molecule drugs safely targeting the underlying biological causes of SNHL have the potential to meet a significant need for millions of patients. The REGAIN consortium is progressing the pharmaceutical treatment of SNHL through rigorous clinical testing.

References

Wilson B.S. et al. Global hearing health care: new findings and perspectives. Lancet. 2017 Jul 10. pii: S0140-6736(17)31073-5

Livingston G. et al. Dementia prevention, intervention, and care. Lancet. 2017 Jul 19. pii: S0140-6736(17)31363-6

Mizutari K et al. Notch inhibition induces cochlear hair cell regeneration and recovery of hearing after acoustic trauma. Neuron. 2013 Jan 9;77(1):58-69.

Speech Intelligibility

PS 221

Behavioral and physiological pupil responses reveal audiovisual noise differentially challenges speech recognition

Gavin M. Bidelman; Bonnie Brown; Kelsey Mankel
University of Memphis

In noisy environments, listeners benefit from both seeing and hearing a talker, demonstrating audiovisual (AV) cues enhance speech-in-noise (SIN) recognition. Here, we examined the relative contribution of auditory (A) and visual (V) information to SIN recognition amidst multimodal noise stressors. Listeners performed an open-set sentence recognition task while viewing AV TIMIT sentences presented under different combinations of signal degradation including visual (+Vn), audio (+An), or multimodal (+AnVn) noise. Pupillometry and eyetracking monitored participants'; listening effort and gaze to different parts of the speaker';s face during SIN perception. As expected, behavioral performance for clean sentence recognition was better for A-only and AV compared to V-only speech. For +An (noise in auditory channel of AV speech), performance was aided by the addition of clear and degraded visual cues of the talker, confirming a multimodal benefit to SIN recognition. Interestingly, the addition of visual noise (+Vn and +AnVn)—obscuring the speaker';s face—had little effect on speech recognition regardless of whether the auditory channel was degraded or intact. Physiologically, we observed a graded increase in pupil dilation (+An > +Vn > +AnVn), suggesting multimodal noise increased listening effort (produced greater perceptual difficulty) for auditory relative to visual noise degradations. Similarly, listeners'; gaze fixations increased at the eyes (decreased toward the mouth) whenever the auditory channel was compromised. Nonlinear regression further revealed that this biasing in gaze toward the eyes was associated with a decrease in behavioral recognition, suggesting that SIN performance depends critically on the quality of visual cues at the speaker';s mouth. Collectively, our data suggest that listeners (i) depend heavily on the auditory over visual channel when seeing and hearing clean and noise-degraded speech, (ii) alter their visual strategy when monitoring a talker';s face (clean→noise :: mouth→eyes), and (iii) experience increased cognitive listening effort for speech containing degraded acoustic relative to degraded visual information.

PS 222

Low- and high-frequency cortical brain oscillations reflect dissociable mechanisms of concurrent speech segregation in noise

Anusha Yellamsetty; Gavin M. Bidelman
University of Memphis

Parsing simultaneous speech requires listeners use pitch-guided segregation which can be affected by signal-to-noise ratio (SNR) in the auditory scene. The interaction of these two cues may occur at multiple levels within cortex. The aims of the current study were to assess the correspondence between oscillatory brain rhythms and determine how listeners exploit pitch and SNR cues to successfully segregate concurrent speech. We recorded electrical brain activity while listeners heard double-vowel stimuli whose fundamental frequencies (F0s) differed by zero or four semitones (STs) presented in either clean or noise-degraded (+5dB SNR) conditions. Behaviorally, listeners were more accurate identifying vowel mixtures for larger pitch separations but F0 benefit interacted with noise. Time-frequency analysis parsed spectrotemporal EEG into different frequency bands. Low-frequency bands (θ, β) responses were elevated when speech did not contain pitch cues (0ST>4ST) or

was noisy, suggesting a correlate of increased listening effort. Contrastively, γ power modulations were observed for changes in both pitch (0ST>4ST) and SNR (clean>noise), suggesting high frequency bands carry information related to acoustic features and the quality of speech representations. Brain-behavior associations corroborated these effects showing that modulations in low-frequency rhythms predicted the speed of listeners'; perceptual decisions with higher bands predicting identification accuracy. Results demonstrate that neural oscillations reflect both automatic (pre-perceptual) and controlled (post-perceptual) mechanisms of speech processing that are largely divisible into high- and low-frequency bands of brain rhythms.

PS 223

Subcortical and cortical neural encoding of speech is differentially challenged by noise and reverberation

Gavin M. Bidelman; Megan Howell; Mary Katherine Davis
University of Memphis

Everyday speech perception is challenged by interfering noise and adverse room acoustics (e.g., reverberation) that prevents audible access to perceptual cues and hinders verbal communication. A mechanistic understanding of the hierarchical processing and how the brain extracts speech from different forms of acoustic interference is not well established. Here, we directly compared how different levels of the auditory system (brainstem vs. cortex) code speech and how their neural representations are affected by the acoustic stressors of noise and reverberation. We recorded multichannel (64 ch) brainstem frequency-following responses (FFRs) and cortical event-related potentials (ERPs) simultaneously in normal hearing individuals to speech sounds presented in mild and medium levels of noise and reverberation. Importantly, we matched signal-to-noise and direct-to-reverberant ratios to equate the overall "noisiness" between interference classes. Electrode recordings were parsed into source waveforms to assess the relative contribution of region-specific brain areas [i.e., brainstem (BS), primary auditory cortex (A1), inferior frontal gyrus (IFG)] to degraded speech processing. We found that reverberation was detrimental to (and in some cases facilitated) the neural encoding of speech compared to additive noise in brainstem. This reverb advantage was maintained in left lateralized auditory-language regions of cortex (A1, IFG). Across interferences, correlations revealed associations between BS-FFRs and A1-ERPs, suggesting subcortical speech representations influence higher auditory-cortical areas downstream. Interestingly, we found listeners'; degraded speech perception abilities were predicted based on in-

dependent contributions of intra- and inter-region activity including cortico-collicular (BS→A1) and cortico-cortical (A1→IFG) response interactions. Our findings demonstrate changes in the functional interplay among regions of the speech network that depend on the form and severity of acoustic interference. We infer that listeners'; success at the "cocktail party" is modulated based on how well information is transferred between subcortical and cortical hubs of the auditory-linguistic network.

PS 224

The role of harmonicity in the masking of speech

Stuart Rosen[1]; Kurt Steinmetzger[2]; David Perry[2]
[1]Department of Speech, Hearing & Phonetic Sciences, UCL; [2]UCL

Background
Harmonic tone complexes, whether dynamic or static, are much less effective maskers than a noise with the same overall spectral envelope. There are at least three possible explanations. Firstly, harmonic complexes consist of discrete spectral components possibly allowing 'glimpsing'; into frequency regions between harmonics where there is little masker energy, at least at low frequencies. Secondly, the periodicity of the complex may allow it to be more effectively segregated or 'cancelled out';. Finally, the masking of modulations in the speech by modulations in the masker may be important, and the modulation spectra of noises and harmonic complexes are very different.

Methods
We compared the relative masking effectiveness of static and dynamic complexes in which the discrete spectral components form either a harmonic or inharmonic series. The harmonic dynamic complexes have continuous modulations in fundamental frequency (F0) modelled on genuine F0 contours found in connected speech. Static complexes varied in F0 from trial to trial to match the distribution of F0s in the dynamic ones. In addition, median F0s were varied in relation to the target sentences spoken by a relatively high-pitched male speaker (F0 ≈ 150 Hz), to be low (≈ 100 Hz), medium (≈ 150 Hz) or high (≈ 225 Hz).

Inharmonic complexes were created in two ways, either by shifting all the components in the harmonic series up or down by 25% of the median F0, or by spectrally rotating the harmonic complexes around a centre frequency near 2 kHz. For static contours, these two methods are equivalent for an appropriate choice of parameters. For dynamic contours, the actual shift in component frequencies changes throughout the stimulus, sometimes more and sometimes less than 25%, but the resulting sound is

always inharmonic. Crucially, the modulation spectra of all three variants of the static complexes are essentially identical, but are very different for the frequency-shifted and spectrally-rotated dynamic complexes.

Results & Conclusion
Speech Reception Thresholds (SRTs), determined adaptively, revealed the following: SRTs tend to decrease with increasing masker F0. SRTs are generally worse for dynamic as opposed to static contours. Inharmonic and harmonic complexes lead to similar SRTs, except for the rotated dynamic complexes, which are more effective maskers than the other types, especially for the two higher masker F0s. It thus appears that only theories which consider the role of modulations will be adequate to account fully for the pattern of results obtained.

PS 225

The Effect of Noise and Reverberation on Speech Perception and Listening Effort for Young and Old Adults

Chanbeom Kwak[1]; Woojae Han[2]
[1]Division of Speech Pathology and Audiology, College of Natural Sciences, Hallym University; [2]Division of Speech Pathology and Audiology, College of Natural Science, Hallym University

Purpose
Because of the aging affects sensory, perceptual, and cognitive functions declining, older listeners spend more exertion than younger listeners especially in the distracting listening situations such as background noise and reverberation. The purpose of present study was to compare speech perception ability and listening effort required to young and old adults using sentence recognition scores and a five-point scale questionnaire as a function of signal-to-noise ratio (SNR) and reverberation time.

Methods
Forty-eight young and old adults with normal hearing participated in the current study. For the sentence recognition, Korean Speech Perception in Noise (KSPIN) test in which a question tag was removed and equal root mean square (RMS) was adjusted by -35 dB was applied to total 20 conditions: four SNRs (e.g., quiet, +6, +3, 0 dB) and five reverberation times (i.e., no, 500, 1000, 1500, 2000ms). In addition, the five-point Likert scale questionnaire that designed to estimate degree of listener's exertion was asked right after completing each condition of the recognition task. The participants were seated at 1 meter and 0 degree azimuth from a speaker in the sound isolation room. All data were collected and analyzed in terms of error percent and scale.

Results: In general, both error percent of the sentence recognition and effort scales increased as the level of background noise and reverberation time increased. In SNR conditions, both the error percent and scale of two groups was increased as the noise level was lower. Age difference was remarkable in that 23.01% (0.70 scale), 22.97% (0.90 scale), 17.56% (0.80 scale), and 12.26% (0.40 scale) for quiet, +6, +3, and 0 dB SNR, respectively. The reverberation time conditions showed s similar pattern of the noise conditions. As reverberation time was higher, especially in in the condition of no reverberation and 500ms reverberation, both error percent and scale dramatically increased for two groups. Age difference showed that 14.21% (0.50 scale), 20.82% (0.70 scale), 23.10% (0.90 scale), 23.36% (0.80 scale), and 13.12% (0.60 scale) for no, 500, 1000, 1500, and 2000 ms, respectively.

Conclusion
The results confirms that the old listeners face much challengeable situation and have listening difficulty, while requiring more effort, compared to young counterparts.

PS 226

Speech intelligibility and its relationship to communication effectiveness in noisy environments

Nandini Iyer[1]; Abigail Willis[2]; Eric Thompson[2]; Brian D. Simpson[3]
[1]U.S. Air Force Research Laboratory; [2]Air Force Research Laboratory; [3]Air Force Research Lab, 711th HPW

Background
In many military and civilian domains, individuals are required to communicate in noisy environments, where speech is severely degraded, in order to succeed in their missions. While there are several research studies that quantify the effects of background noise on speech intelligibility, very few studies exist on adequate speech intelligibility needed for effective communication among teams in order to complete complex tasks successfully. The current study was designed to quantify the effects of parametrically degraded speech on communication effectiveness, as well as examine patterns of communication behavior that would be suggestive of communication difficulties.

Methods
Speech intelligibility was parametrically degraded as five pairs of interlocutors completed a "spot-the-difference"

Diapix task (Van Engel et al., 2010). The Adjustable Intelligibility Modification System (AIMS) software (Keller et al., 2017) was used to add noise adaptively to interlocutors' communication channels so as to maintain a constant signal-to-noise ratio (SNR) and therefore constant speech intelligibility. SNR was adjusted to produce target speech intelligibility levels of 100% (no added noise), 80%, 60% or 40%, as measured using the Modified Rhyme Test (MRT) words. These four levels of intelligibility, obtained individually for each interlocutor pair, were then subsequently used as listening conditions in the Diapix task. Pairs of interlocutors completed the task with SNR randomly assigned to the pair; time for task completion, linguistic properties (word count, syntactic complexity etc.), and acoustic properties (frequency and intensity changes) were measured for each interlocutor pair in each SNR condition.

Results

The time taken to complete the Diapix task increased systematically as speech intelligibility decreased, thereby showing reduced communication efficiency. Interlocutors also adapted their utterances relative to the no-noise condition in the acoustic and linguistic dimensions in degraded speech intelligibility conditions to complete the task.

Conclusions

The current paradigm can be used to quantify the minimum speech intelligibility needed for communication effectiveness in several noise environments, thereby demonstrating the need for noise mitigation strategies in military environments and informing the design of such mitigation systems.

PS 227

A Comparison of Automatic Speech Recognition and Human Performance with Vocoded Speech

Guangxin Hu[1]; Sarah Determan[2]; Alec Beeve[3]; Joshua Collins[3]; Yan Gai[3]
[1]saint louis university; [2]Saint louis university; [3]Saint Louis University

Human ears and cochlear implants transform speech information into multiple frequency channels. Acoustical features of speech can be characterized into various spectral and temporal cues. Human listeners can recognize speech even when one or more features are misrepresented. The present study used noise vocoding to simulate implant speech and compared the sentence recognition between humans and a speech-recognition software. The software mostly relied on spectral information for sentence recognition. When the vocoding algorithm contained 22 channels, listeners showed

near-perfect performance for speech in quiet and in noise. The software only detected 60% of the keywords in quiet, and the performance dropped to 14% when noise was introduced. When the number of channels was reduced to four, the human performance was significantly lowered by noise, while the software failed to detect any keyword. Human listeners and the software apparently used different listening strategies. When the spectral profile was improved by doubling the number of channels, the software showed a high recognition performance in quiet, but the correct rate was reduced to near zero when noise was added. The result indicated that even though spectral cues may be used for detecting vocoded speech in quiet, the strategy was unreliable in noise.

PS 228

A Model of Concurrent Vowel Identification Without Segregation Predicts Perceptual Errors

Samuel Smith[1]; Ananthakrishna Chintanpalli[2]; Michael Heinz[3]; Christian Sumner[1]
[1]MRC Institute of Hearing Research, University of Nottingham; [2]Birla Institute of Technology & Science; [3]Department of Speech, Language, and Hearing Sciences, Purdue University

When positioned in a complex auditory environment, individuals with normal hearing are able to identify and concentrate on specific components within that environment, famously termed the cocktail-party phenomenon. There are a multitude of cues which can be used to facilitate auditory stream segregation (e.g., pitch differences, dynamics, onset/offset asynchronies, differences in speech spectral characteristics). Particular attention has been paid to the positive effect that differences in fundamental frequency (F0) between two vowels (steady-state harmonic complexes), presented concurrently, has on their identification (review: Micheyl and Oxenham, 2010).

Computer models exist that predict with some success the improvement in concurrent-vowel identification observed with increasing F0 differences (Meddis & Hewitt, 1992). However, these existing models are poor at predicting listener confusions (Chintanpalli and Heinz, 2013).

Presented is our model of concurrent-vowel identification, which incorporates a naïve Bayesian classifier. This model directly predicts the probabilities of different combinations of two vowels giving rise to an integrated representation of the concurrent-vowel pair presented. This contrasts with previous models, which were deterministic and assumed that a segregation process separated out individual vowel representations based on F0 differences, followed by a comparison with templates of

individual vowels. Our model also incorporates a pitch estimation process, but this is used to restrain the concurrent-vowel pair categories used in classification. Our new synthesis'; based model was tested for both temporal (autocorrelation-based) and spectral (rate-based) internal representations.

The new model was able to successfully predict confusions with a high degree of accuracy (confusions: R>0.9). In the case where there was no difference in F0 between the vowels, performance was slightly better for the spectral model (R=0.96) than the temporal model (R=0.91). However, only when temporal processing was implemented, our model qualitatively replicated the positive effect that differences in F0 have on human concurrent-vowel identification. In our model, pitch estimation was the least accurate for small F0 differences (≤1 semitone), corroborating previous psychoacoustic findings regarding the perception of pitch in concurrent vowels (Assmann and Paschall, 1998). Overall, our model is much closer to predicting human performance than previous models, and hints at a process that seeks to optimally predict which concurrent-vowel pair led to a corresponding internal representation, rather than to segregate the representation and recognise individual vowels separately.

PS 229

Predicting Speech Intelligibility based on Fluctuations in Simulated Auditory-Nerve Responses

Johannes Zaar[1]; Christoph Scheidiger[1]; Laurel H. Carney[2]; Torsten Dau[3]
[1]*Hearing Systems group, Department of Electrical Engineering, Technical University of Denmark;* [2]*Departments of Biomedical Engineering, and Neurobiology & Anatomy, University of Rochester , Rochester;* [3]*Hearing Systems group, Technical University of Denmark*

Various speech intelligibility (SI) models have been proposed to predict the ability of normal-hearing (NH) listeners to understand speech in adverse listening conditions. However, most current SI models are based on a strongly simplified linear simulation of the highly non-linear auditory periphery, which limits their ability to predict effects of hearing impairment on SI. At the same time, the models'; decision stages typically interact strongly with the type of auditory front-end processing applied. The present study attempted to incorporate a non-linear auditory-nerve (AN) model (Zilany *et al.*, 2014) in the framework of the multi-resolution speech-based envelope power spectrum model (mr-sEPSM; Jørgensen *et al.*, 2013), which has been shown to provide accurate predictions of SI measured in NH listeners

in a wide range of acoustic conditions. The mr-sEPSM receives the noisy speech and the noise alone as inputs and assumes SI to be related to the signal-to-noise ratio in the envelope domain (SNR_{env}). Two approaches were used: First, the linear front end of the mr-sEPSM was replaced by the non-linear AN model, keeping the SNR_{env}-based decision process from the original mr-sEPSM. Second, the same input signals and AN front end as before were used in combination with a correlation-based decision process inspired by the vowel-coding hypothesis based on fluctuation sensitivity in the inferior colliculus (Carney *et al.*, 2015). Predictions of sentence recognition in stationary noise, sinusoidally amplitude-modulated noise, and a speech-like interferer were obtained based on firing rates at the output of the AN model in NH configuration. The SNR_{env}-based model yielded accurate predictions of the NH perceptual data at low presentation levels. However, it strongly overestimated SI for the non-stationary interferers at realistic (medium) presentation levels. This limitation could partly be overcome by reducing the modulation-frequency range considered in the mr-sEPSM. In contrast, the correlation-based model yielded stable predictions of NH listeners'; SI data, showing plausible trends across presentation levels. A further investigation of SI data obtained in the same conditions in hearing-impaired (HI) listeners indicated that the correlation-based model could account for some of the main features in the HI data. The AN model includes the effect of HI on the amplitudes of low-frequency fluctuations in AN responses to speech. The work may provide a valuable basis for quantitatively modeling consequences of inner and outer hair-cell loss on speech intelligibility.

PS 230

Predicting Speech Intelligibility Using a Nonlinear and Level-Dependent Auditory Processing Front End

Helia Relaño-Iborra[1]; Johannes Zaar[1]; Torsten Dau[2]
[1]*Hearing Systems group, Department of Electrical Engineering, Technical University of Denmark;* [2]*Hearing Systems group, Technical University of Denmark*

Relaño-Iborra et al. [2016, J. Acoust. Soc. Am., 140(4), 2670-2679] proposed a model, termed sEPSM[corr], which showed that the correlation between the envelope representations of clean and degraded speech is a powerful predictor of speech intelligibility in a wide range of listening conditions. However, due to its simplistic linear preprocessing, sEPSM[corr] cannot account for the level-dependent effects and nonlinear properties of the sound transduction in the auditory periphery, which is a prerequisite for accounting for the consequences of sensorineural hearing loss. Thus, in the present study, a more realistic, nonlinear preprocessing was combined

with the correlation-based back end. Specifically, the front end of the computational auditory signal processing and perception model [CASP; Jepsen et al. (2008), J. Acoust. Soc. Am. 124(1), 422-438] was employed, which has been shown to successfully account for psychoacoustic data in conditions of, e.g., spectral masking, amplitude-modulation detection as well as forward masking, for both normal-hearing (NH) and hearing impaired listeners. The proposed speech-based CASP model, denoted sCASP, receives the clean and degraded speech signals as input. The signals are processed through outer- and middle-ear filtering, a nonlinear auditory filterbank including inner- and outer hair-cell processing, adaptation, as well as a modulation filterbank. The internal representations at the output of these stages are analyzed using a correlation-based back end.

Speech intelligibility predictions obtained with the speech-based CASP implementation are presented and compared to NH listener data obtained in conditions of additive noise, phase jitter, ideal binary mask processing and reverberation. The results demonstrate a large predictive power of the model. As the front end of sCASP can - unlike the front end of its predecessor sEPSM^{corr}- be parametrized to account for sensorineural hearing loss, the proposed framework may provide a valuable basis for evaluating the consequences of different aspects of hearing loss on speech intelligibility in the various experimental conditions.

PS 231

Classifying Attended Talker from EEG Using Artificial Neural Networks

Daniel D.E. Wong[1]; Søren A. Fuglsang[2]; Jens Hjortkjaer[3]; Giovanni M. di Liberto[4]; Alain de Cheveigné[1]
[1]Equipe Audition, Departement d'Études Cognitives, Ecole Normale Supérieure; [2]Hearing Systems group, Department of Electrical Engineering, Technical University of Denmark; [3]Hearing Systems group, Technical University of Denmark; [4]Ecole Normale Supérieure

Auditory cortical activity is known to time-lock to speech. In a multiple-talker environment the activity is enhanced in response to the attended stream relative to the competing stream. Using this, a number of approaches have been recently developed to detect which stream is the focus of attention from the EEG. Most previous methods compute a temporal response function to map either audio features to the EEG, or vice-versa. More recently we have used canonical component analysis (CCA) to transform both audio and EEG so as to maximize mutual correlation. This provides a significant improvement in classification performance. Furthermore, the CCA

methodology makes it easy to harness additional audio features beyond the waveform envelope, such as cochleogram envelopes, or phonemic features. However, applying CCA to these higher order features has so far not yielded better results, possibly due to the large number of parameters, resulting in over-fitting. This issue can be addressed by using a convolutional neural network to minimize the number of parameters that need to be learned.

We applied this idea to a two-talker dataset where normal-hearing subjects were presented with two simultaneous speech streams coming from two speakers positioned at ±60 degrees azimuth relative to the listener. Stories were presented in 50s trials, with a total of 60 trials, while 64-channel scalp EEG was recorded. The position and the gender of the attended speaker were randomized across trials.

When the broad-band waveform envelope of the speech stream is used as an audio feature, the neural network performs no better than CCA in classifying the attended talker. However, when multi-channel cochleogram or phoneme features are used, the neural network outperforms CCA by an average of 7 percentage points (33% error reduction) with a data duration of 7s, for two pilot subjects. We present the neural network structure and training methods, and examine the neural network weights to gain insights on relationships between the auditory features and the cortical responses.

PS 232

Cortical Activity and Incidental Memory for Speech in Noise

Kenneth I. Vaden[1]; Susan Teubner-Rhodes[1]; Jayne B. Ahlstrom[1]; Judy R. Dubno[2]; Mark A. Eckert[1]
[1]Medical University of South Carolina; [2]The Medical University of South Carolina

Background
Memory is poorer for correctly understood speech in noisy conditions, compared to less difficult listening conditions. A prominent hypothesis for this memory deficit is that fewer cognitive resources are available for memory encoding when those resources are required to understand speech in noise. Understanding speech in noise consistently results in elevated activity throughout cingulo-opercular regions of frontal cortex, which are proposed to optimize task performance through adaptive control of behavior and attention. In the context of the cognitive resource hypothesis, these observations guide the prediction that speech understood in noise is less likely to be remembered when cingulo-opercular activity

increases. However, memory experiments that control the perceptual difficulty of stimuli have shown that cingulo-opercular activity increases during encoding for items that are remembered. The current study used a delayed recognition memory task to test the competing predictions that cingulo-opercular activity during word identification in noise relates to better or worse memory.

Methods
Twenty healthy adult participants (10 females, average age = 29.8 ± 5.9 years) with normal hearing participated in an fMRI study. Each participant performed a word identification in babble task (Task 1), then a delayed recognition memory task (Task 2). During Task 1, a single word in multi-talker babble was presented on each trial (+3 or +10 dB signal-to-noise ratio; SNR) and participants repeated the word aloud or said nope if they could not understand. Memory test instructions were given after completing Task 1 to prevent maintenance strategies. During Task 2, a single band-pass filtered word was presented on each trial and participants pressed a button to indicate whether they 1) remembered the word from the earlier task, 2) did not remember, or 3) could not understand the band-pass filtered word.

Results
During word identification, cingulo-opercular activity was higher and average memory scores were lower (95% BCI = 0.16 to 0.28 A' difference) in the more difficult +3 dB SNR. Nonetheless, cingulo-opercular activity decreased on trials for the correctly identified words that were not remembered at test. These results indicate that memory encoding was poorer for correctly identified words during lapses in cingulo-opercular activity.

Conclusion
Although attention to speech in noise appears to limit active memory maintenance, we conclude that sustained performance monitoring and elevated attention can support incidental memory encoding in difficult listening conditions. We will also discuss preliminary findings from older adults, who often exhibit larger memory deficits for correctly identified speech in noise.

Funding

PS 233

Are objective measures of temporal fine structure and auditory nerve correlated with listening performance in noise? Evidence for Hidden Hearing Loss

Macarena Bowen; Jaime A. Undurraga; David McAlpine
Macquarie University

Background
Individuals with hearing loss have difficulties in everyday listening situations. However, many normal-hearing subjects also complain about hearing problems, especially when listening to speech in background noise. This problem has been called 'hidden hearing loss'; (HHL) or cochlear synaptopathy. Animal studies have demonstrated that noise exposure can lead to degeneration and loss of ribbon synapses of auditory nerve fibers, before hair cell damage occurs. Sensitivity to the temporal fine structure (TFS) of sounds is critical to high performance in background noise. This implies that any brain deficit in conveying either slow or fine modulations will reduce speech understanding and binaural integration. Although an increasing number of reports exist on objective measures to diagnose synaptopathy/HHL in humans, there is still no enough evidence linking these measures (e.g. ABR) and perceptual deficits reported/founded by subjects. Here we used monoaural auditory brainstem responses (ABRs) and a measure of binaural temporal processing assessing Interaural Phase Modulations (IPM), in order to provide evidence to this topic.

Methods
15 normal hearing subjects were tested. IPM - Following Responses (IPM-FRs) (Undurraga et al., 2016) were recorded using a 64-channel BioSemi Active Two EEG system. IPM-FR were obtained using a carrier frequency of 520 Hz amplitude-modulated at 41 Hz with an IPD switching rate of 6.8 Hz and six different IPM depths. Stimuli were presented at 65 dB SPL with and without background noise. Different protocols of background noise were used including intensities of 0 to 65 dB SPL, interaurally correlated/uncorrelated, different low-pass filters. ABRs were recorded using the same system with 32-channels at 90 and 60 dB ppeSPL. Speech discrimination in noise were tested with a vowel-consonant-vowel (VCV) task. VCVs stimuli were presented at two different sound levels and signal-to-noise ratios. All subject also completed PTA and an on-line questionnaire about lifetime noise exposure.

Results
IPM-FR amplitude, IPM-FR ratio between two depths as a measure of temporal processing dynamic range, IPM-FR growth curve with background noise and amplitude

and wave I/V ratio of ABR were compared between subjects and correlated with performance in the VCV discrimination task.

PS 234

Neuromodulation for enhancing the comprehension of speech in babble noise

Shabnam N. Kadir; Chrysoula Kaza; George Allaway; Hugo Weissbart; Tobias Reichenbach
Imperial College London

Background
The cocktail party problem can be formulated as follows: how does a partygoer focus attention on a single speaker in a noisy room where several people are speaking simultaneously? The brain is able to solve this problem far better than any current machine-learning algorithm. Recent research has identified that cortical activity in the delta and theta frequency band tracks the rhythm of speech, manifest in its envelope, and this may help to solve the cocktail party problem. Since cortical activity can be evoked through transcranial current stimulation, this method may enhance speech in noise comprehension when the electrical signal is designed to enhance the natural cortical response to the speech rhythm. A recent study did indeed employ transcranial current stimulation with the speech envelope at different temporal delays while human volunteers listened to speech in background noise, and found a modulation of speech-in-noise comprehension. However, in addition to temporal lags, phase shifts between the electrical signal and the speech envelope can also matter for driving the cortical response effectively.

Methods
We investigated the use of transcranial electrical stimulation for modulating the comprehension of speech in four-speaker babble noise. In particular, we employed an electrical current that was proportional to the speech envelope of the target speaker, but shifted by different phases. We used temporal delays of 100 ms and 250 ms. Sham stimulation was applied as well. We then employed an adaptive procedure to determine at what signal-to-noise ratio participants' comprehension dropped to 50% during the different stimulation types. To minimize the effect of guessing words from context, we used 'semantically-unpredictable sentences' for creating both the four-speaker babble noise and the target speech. These sentences were generated using the NLTK (Python Natural Language Toolkit) with the Brown linguistic corpus and various chosen syntactic structures. They were synthesized to audio signals using TextAloud.

Results and Conclusion
We found that our adaptive procedure for determining speech-in-noise comprehension using the computer-generated, semantically-unpredictable sentences gave consistent results that matched those described in the literature. We also found preliminary evidence that transcranial alternating current stimulation modulates speech comprehensibility. In particular, every participant';s best performance was obtained when the electric current had a phase in advance of 60° compared to the speech envelope, at a temporal lag of 250 ms. This shows that transcranial current stimulation can be effective for modulating speech processing and that it depends crucially on the phase of the applied current with respect to the speech signal.

PS 235

Neural and perceptual signatures of temporal fine structure processing underlying speech-in-noise intelligibility

Aravindakshan Parthasarathy[1]; Kenneth Hancock[1]; Daniel B. Polley[2]
[1]*Eaton-Peabody Laboratory, Massachusetts Eye and Ear Infirmary/ Department of Otolaryngology, Harvard Medical School;* [2]*Massachusetts Eye and Ear Infirmary, Harvard Medical School*

Introduction
Encoding of stimulus temporal fine structure (TFS) cues is vital for hearing in noise. Degraded TFS processing in the peripheral auditory pathway may also result in the need for increased allocation of top-down cognitive resources like listening effort, to aid in speech-in-noise intelligibility. However, objective neurophysiological measures of TFS processing and their relationship to perceptual performance are poorly understood. Here we directly compare behavioral and neurophysiological measures of monaural and binaural TFS processing, and their contributions to hearing in noise in normal hearing subjects.

Methods
Electrophysiological encoding of monaural TFS cues were characterized by measuring synchronization in the frequency following response (FFR) to a 500Hz tone with frequency modulation (FM) ranging from 0Hz to 20Hz. Binaural processing of TFS cues were characterized by measuring the following response to changes in interaural phase delays (IPDs) of a 500Hz tone. By simultaneously recording from multiple channels and different electrode-montages, we could emphasize different

generators along the auditory pathway, and explore the contributions of each to temporal coding. Parallel behavioral tests assessed FM and binaural IPD psychophysical detection thresholds. Hearing in noise abilities were assessed using sentences or digit sequences in speech babble noise paired with measures of pupil diameter to assess cognitive load. All measurements were made in adult listeners with normal audiograms up to 8 kHz.

Results

Mean behavioral detection thresholds for the FM deviation was 0.66% (3.3$\pm$1 Hz) and for the IPD detection was 14.4$\pm$1.8°. The FFR measured in these listeners exhibited robust phase-locking to the FM stimuli and modulation in the IPD. The neural phase-locking component of the FM stimulus near threshold (5 Hz FM) was a strong indicator of behavioral performance in the FM detection task and the phase-locking to the IPD at $\pm$90° was correlated with the IPD detection task. The cognitive load as measured by pupil diameter was modulated by signal-to-noise ratio when performing hearing in noise tasks.

Conclusions

These brainstem measures of FM and IPD phase-locking serve as a useful biological marker, and may identify neural predictors for suprathreshold hearing impairments associated with aging or hearing loss. Changes in these responses can also be studied to explore the neural bases for perceptual changes following auditory training. Measuring isoluminous task-correlated changes in pupil diameter during task performance in the same subjects can help understand the interplay between bottom-up temporal processing and top-down cognitive load in speech-in-noise intelligibility.

PS 236

Speech Perception Analysis via Automated Phoneme Alignment

Lydia Wang[1]; Zachary Heiman[2]; Daniel Tward[2]; **Tilak Ratnanather**[2]
[1]Montgomery Blair High School; [2]Johns Hopkins University

Intro

Clinical speech perception tests are commonly used to assess or track the ability of people with hearing loss to hear with hearing aids or cochlear implants. They are generally based on lists of words or sentences, and are presented in a sound booth, sometimes with noise. As a person may not get the whole sentence correct, but most of the words correct, it would be beneficial to analyze the erroneous phonemes, which can be classified based on features of sound production. To this end, an automated

program for computing the accuracy of phonemes from responses in clinical speech perception tests is developed and implemented.

Methods

The program takes a set of true sentences or words, and the corresponding set guessed by a person with hearing loss. An electronic pronouncing dictionary (known as CMU Dict) translates the sentences into phonemes, and a variant of the Levenshtein Minimum Edit Distance algorithm aligns phonemes in the guessed sentences with those in the correct ones. It then displays the accuracy for each phoneme, as well as perception information based on frequency-specific phoneme attributes.

Results

The program was tested with several people with hearing loss, with and without hearing aids or cochlear implants. Some users responded to different sets of 30 sentences, recorded in Clear Speech by male and female American English speakers; other users responded to AzBio sentences with talker babble. Results are also shown for a monosyllabic word test key for an adult cochlear implant user.

Conclusion

The automation and output of this program could permit speech language pathologists and audiologists, particularly in telepractice, to measure phoneme perception in real time. Future work includes evaluation and validation for clinical usage, implementation in mobile auditory training apps such as SpeechBanana, and implementation in other languages, such as Korean.

PS 237

Evaluating Vowel and Consonant Speech Reception Thresholds with a Closed-Set Keyword Triplet Test

Douglas Brungart[1]; Matthew Makashay[2]; Daniel Shub[2]; Hector Galloza[3]
[1]Walter Reed National Military Medical Center; [2]Walter Reed National Millitary Medical Center; [3]Resound Inc.

Most clinical speech perception tests use an open-set response format. Speech materials are presented to listeners over headphones or loudspeakers and then verbally repeated back to a test administrator for manual scoring. However, in many clinical or research settings it would be very helpful to replace these open-set response formats with closed-set ones so tests could be scored automatically and repeated an indefinite number of times without the listeners learning the speech materials. Current tests with closed-speech response sets, which are based on either digit triplets or matrix sentences, tend to generate speech reception thresh-

olds much lower than those obtained with open-speech response sets. They may also produce different patterns of impaired performance when the speech materials are distorted by time compression, reverberation, or other degradations.

One possible explanation for this difference is that open-set speech tests typically require listeners to understand both the consonants and vowels in the stimulus to obtain a correct response, whereas most closed-set speech tests incorporate some redundancies that allow listeners to narrow down the response set (or in some cases obtain the correct answer) with the correct perception of a single phoneme. In order to examine this issue, we constructed two different speech tests designed to obtain independent measurements of vowel and consonant intelligibility in noise. The first was a vowel test that asked listeners to identify three vowels presented in the /hVd/ context. The second was a consonant test that asked listeners to identify three consonants from lists of six rhyming words extracted from the Modified Rhyme Test. Both were designed to adaptively change SNR after each trial to track the 70% Speech Reception Threshold (SRT).

One unexpected problem with the vowel triplet test was that many listeners had difficulty responding to the vowels in the correct order, which resulted in large variability in the normal population. This was addressed by switching to a scoring system that did not require the listeners to identify the vowels in the correct order.

Preliminary results collected on these two tests in speech-shaped noise, in background speech with reverberation, and in background speech with both reverberation and time compression suggest that the consonant SRT rises much faster in increasing complex masking conditions than the vowel SRT. This suggests that performance in complex listening environments may be limited primarily by consonant intelligibility, which may not be accurately captured by current closed-set sentence materials.

PS 238

Phoneme Categorization Relying Solely on Frequencies Beyond 6 kHz

Brian B. Monson
University of Illinois, Urbana-Champaign

Background
Over phylogeny the human cochlea has obtained and retained sensitivity to acoustical energy at frequencies spanning 20 Hz to 20 kHz. Despite this fact, speech energy produced at frequencies beyond 6 or 8 kHz is often cast as having little relevance to speech perception. We hypothesized that human sensitivity to these very high frequencies has been retained, in part, because the information provided by the high frequencies is valuable for the perception of conspecific vocalizations (*i.e.*, human speech). To examine this hypothesis, we assessed listeners'; ability to extract phonetic information from tokens consisting of *only* high-frequency energy produced in speech.

Methods
Consonant-vowel (CV) tokens were recorded from a male and female talker in a soundproof booth and band-pass filtered with cutoff frequencies of 5.7 kHz and 20 kHz. The CV combinations were presented to listeners in separate consonant categorization and vowel categorization tasks. Stimuli were presented with a low-frequency speech-shaped noise masker to help prevent listeners from using distortion products that may have been present in the lower frequencies.

Results
Listeners'; mean accuracy was 15.8% correct for the vowel categorization, which was significantly above chance for our task (p<0.005). There was no significant difference in accuracy between the male (14.3%) and female voice (17.3%) stimuli. Listeners'; mean accuracy was well above chance at 51.5% correct (p<0.001) for the consonant categorization. There was a small but significant difference in accuracy for male (49.5%) versus female (53.5%) stimuli (p<0.05).

Conclusion
Despite the absence of acoustic attributes that are the traditional focus of speech perception research (*e.g.*, the first three formants), listeners performed above chance on both vowel and consonant categorization. As may be expected given the absence of lower frequency formant information, vowel categorization performance was poorer than consonant categorization performance, but was still significantly above chance. These findings suggest that high-frequency energy may be of some utility in speech intelligibility, which seems reasonable from a phylogenetic viewpoint. (Vitela *et al.*, 2015, *J Acoust Soc Amer* 137, EL65-EL70)

PS 239

Theta band of stimulus-driven information and delta band of attention-directed modulation in multi-talker conditions

Yayue Gao[1]; Nai Ding[1]; Liang Li[2]
[1]*College of Biomedical Engineering & Instrument Science, Zhejiang University;* [2]*School of Psychological and Cognitive Sciences, Peking University*

Understanding a conversation in a noisy environment requires a precise neural representation of the sensory input and attentional selection. Here, we distinguish bottom-up (stimulus-driven) and top-down (attention-directed) processing by applying a novel inter-trial coherence (ITC) analysis of magnetoencephalography (MEG) recordings in a multi-talker environment. In the ITC analysis, talkers are divided into stimulus-driven pairs, attention-directed pairs, and baseline pairs. Stimulus-driven pairs were composed of the same two-talker stimulus with different targets, whereas attention-directed pairs were composed of same target with different maskers. Comparing with the baseline pairs, bottom-up processing was observed mainly in the theta band in Pars Orbitalis, Superior Temporal Gyrus and Transverse Temporal Gyrus / Heschl's gyrus, whereas top-down processing in the delta band in right Pars Opercularis. These results demonstrate the separation of bottom-up processing and top-down processing in speech perception and attention.

PS 240

Comparing Speech Modulation Spectra across Languages

Léo Varnet[1]; Maria C. Ortiz-Barajas[2]; Ramón G. Erra[2]; Judit Gervain[2]; Christian Lorenzi[3]
[1]*Laboratoire des systèmes perceptifs, Département détudes cognitives, École normale supérieure, PSL Research University, CNRS;* [2]*Laboratoire Psychologie de la Perception, Université Paris-Descartes, CNRS;* [3]*Laboratoire des systèmes perceptifs, Département d'études cognitives, École normale supérieure, PSL Research University, CNRS*

Languages show systematic variation in their sound patterns and grammars. Accordingly, they have been classified into typological categories such as stress-timed vs. syllable-timed, or Head-Complement (HC) vs. Complement-Head (CH). To date, it has remained incompletely understood how these linguistic properties are reflected in the acoustic characteristics of speech in different languages. In the present study, the amplitude-modulation (AM) and frequency-modulation (FM) spectra of 1797 utterances in 10 languages were analyzed. Overall, the spectra were found to be similar in shape across languages. However, significant effects of linguistic factors were observed on the AM spectra. These differences were magnified with a perceptually plausible representation based on the modulation index (a measure of the signal-to-noise ratio at the output of a logarithmic modulation filterbank): the maximum value distinguished between HC and CH languages, with the exception of Turkish, while the exact frequency of this maximum differed between stress-timed and syllable-timed languages. An additional study conducted on a semi-spontaneous speech corpus showed that these differences persist for a larger number of speakers but disappear for less constrained semi-spontaneous speech. These findings reveal that broad linguistic categories are reflected in the temporal modulation features of different languages, although this may depend on speaking style.

Tinnitus I

PS 241

Electrical Stimulation of the Cochlea to Suppress Tinnitus in Rats: Behavioral and Electrophysiological Studies

Hao Luo[1]; Syed Ahsan[2]; Zhiguo Zhao[1]; Edward Pace[1]; Mehdi Swaid[1]; Yong Xu[1]; Lin Chen[3]; Jinsheng Zhang[1]
[1]*Wayne State University;* [2]*Henry Ford Health Systems;* [3]*University of Science and Technology of China*

Clinical studies have shown that cochlear electrical stimulation (CES) for hearing restoration can significantly suppress tinnitus in 45-78% of patients. However, the underlying mechanisms of (CES)-induced tinnitus suppression remain unclear. To address this issue, we have developed a rat model of cochlear electrical stimulation. We induced tinnitus in rats by exposing them to intense noise (2 hours, 8-16 kHz, 115 dB SPL), followed by implantation in the apical and basal turns of the cochlea. The rats'; tinnitus was behaviorally monitored before, during and after CES using either gap-detection acoustic startle reflex or conditional licking suppression paradigms. Finally we measured neural activity changes in the auditory cortex before and after CES. Our behavioral results showed that half hour tonic CES of the basal turn significantly suppressed tinnitus in the high-frequency region, whereas CES of the apical turn suppressed tinnitus in the middle-frequency region. Electrophysiologically, we found significant neural activity changes in the auditory cortex immediately after CES. The basal turn stimulation caused a decrease in spontaneous firing rate and neurosynchrony at middle and high frequency regions, but an increase in bursting activity at all frequency regions. The apical turn stimulation decreased spontaneous firing rate, bursting activity and neural synchrony at broad frequencies, but more prominently at low and middle frequency regions. These results confirm that CES can suppress tinnitus and that stimulation of

different locations in the cochlea tend to suppress neural activity at different frequency areas in the auditory cortex. This suggests that peripheral modulation of the auditory pathway by CES may lead to changes in neural correlates of tinnitus at the cortical level. Altogether, this demonstrates that bottom-up modulation is a worthy approach to managing tinnitus.

PS 242

The Development of Tinnitus from Chronic Non-Traumatic Noise Exposure in Mice

Laurel A. Screven[1]; Kali Burke[2]; Matthew A. Xu-Friedman[3]; Micheal L. Dent[4]
[1]University at Buffalo; [2]University at Buffalo, SUNY; [3]University at Buffalo, Department of Biological Sciences; [4]State University of New York at Buffalo

Tinnitus is a pervasive auditory dysfunction characterized by the perception of a ringing or hissing noise in the absence of a physical stimulus. It can develop in one or both ears following acute or chronic noise exposure, head trauma, or as the result of natural aging. Stolzberg et al. (2013) developed a categorization paradigm to assess tinnitus, and validated its efficacy following salicylate administration. The present experiment used this categorization paradigm to test if mice would show symptoms of tinnitus in response to a common risk factor: long-term, non-traumatic noise exposure. Adult CBA/CaJ mice were trained to categorize three stimuli types using a two-alternative forced choice operant conditioning task. Mice responded to narrowband white noise (4, 8, 16, 22.6, and 32 kHz) as one category, and responded to both amplitude modulated broadband noise and silent stimuli as another category. Mice were reinforced for correct responses, and punished with a 30 s blackout for incorrect responses. When mice reached 80% correct responses for all training stimuli, they were housed in 85 dB SPL broadband white noise for 22 hours/day. Following the onset of the noise exposure, the silence targets were always reinforced regardless of response, while the narrowband and amplitude modulated noise were only reinforced for correct categorizations. Most of the mice developed tinnitus, as shown by the shift in their response to the silent trials from the amplitude modulated category to the narrowband noise category. The onset of tinnitus ranged from one to ten days, operationalized by mice categorizing silence as narrowband noise more than 50% of the time. Their responses to narrowband and amplitude modulated noise remained comparable to their pre-exposure levels, demonstrating that the change in response was not due to hearing loss or a failure to do the task correctly. The present experiment found that chronic, non-traumatic noise exposure could induce tinnitus in mice, which represents a new and under-appreciated risk factor. Mice are capable of being trained to report the percept of tinnitus using operant conditioning. The results of this experiment show that chronic noise exposure can cause tinnitus in mice in a similar way to salicylate. Furthermore, tinnitus can be induced under naturalistic conditions that are not associated with cochlear damage. This work was supported by a UB IMPACT grant to MXF and MLD.

PS 243

Neural Mechanisms of Transcranial Magnetic Stimulation in the Treatment of Tinnitus

Andrea Lowe[1]; Elliott Brecht[1]; Joseph P. Walton[2]
[1]Department of Chemical and Biomedical Engineering, University of South Florida, Tampa, FL; [2]Department of Communication Sciences & Disorders, and Chemical and Biomedical Engineering, Global Center of hearing and Speech Research, University of South Florida, Tampa, FL

Background

Tinnitus is the chronic perception of a phantom sound and affects a substantial proportion of the population. Successful treatment of this condition has been reported in preliminary trials of transcranial magnetic stimulation (TMS), an emerging brain therapy with FDA approval for treatment of depression. Advancement of this technology has been hindered by the absence of research into mechanisms underlying the positive outcomes. A collaboration with the Rodger';s lab resulted in a custom-built rodent specific TMS coil, consisting of multi-turn copper wire around an iron core. A follow-up study by Rodgers and Mulder';s found that TMS reduced behavioral measures of tinnitus in guinea pigs, but the treatment did not affect neural measures originating from the auditory midbrain. Their interpretation was that TMS reduced hyperactivity in the auditory cortex (AC) and could therefore alleviate tinnitus despite increased activity in lower structures. The purpose of this study was to assay TMS-induced changes in a mouse model through behavioral responses and neural activity in the brainstem and AC.

Methods

Young CBA/CaJ mice were anesthetized and exposed bilaterally to a 116-dB SPL, 8-16 kHz noise for 45-min. Assays for evidence of tinnitus were performed 4-8 weeks later. The assays were gap pre-pulse inhibition of the acoustic startle response (GPIAS) and the auditory brainstem response (ABR) peak-2 to peak-1 ratio, shown to correlate with drug-induced tinnitus in our previous research. A control group of mice received the same assays, but were not noise exposed. Tinnitus positive mice were treated with either 10-min of sham-stimulation or TMS comprising a 120-mT magnetic field over the left AC for 12+ continuous days. Our finite element modeling results indicated that the coil produced an electric

field above the neural activation threshold extending to a brain depth of over 0.7-mm, encompassing all cortical layers in the mouse.

Results/Conclusions
Post-treatment GPIAS, ABRs, and direct recordings of extracellular multiunit activity in the left AC were obtained. These recordings included local field potentials (LFPs) taken from 16 electrode contacts (50-µm spacing) that spanned the AC, which give a measure of net ionic flow and activity across cortical layers. We found that TMS significantly reduced behavioral measures of tinnitus, including increased salience of the GPAIS test. While there was no change in ABRs, as expected, LFPs from the upper layers of the AC in the sham-treated tinnitus group had significantly different LFP amplitudes than the controls, with responses from TMS-treated mice more closely resembling the controls. These findings are the first to report a neural correlate in the AC of the reduction in the tinnitus precept following treatment with rTMS.

PS 244

Addressing Variability in the Acoustic Startle Reflex for Accurate Gap Detection Assessment

Ryan Longenecker[1]; Inga Kristaponyte[2]; Gregory Nelson[1]; Jesse Young[1]; **Alexander Galazyuk**[2]
[1]Northeast Ohio Medical University; [2]Northeast Ohio Medical University (NEOMED)

Background
A reliable animal model of tinnitus is a prerequisite for tinnitus related therapies. Due to its relatively minor time commitment gap-induced prepulse inhibition of the acoustic startle reflex (GPIAS) has quickly become one of the predominant behavioral assessments for tinnitus in laboratory animals. However, several studies have challenged the GPIAS methodology for tinnitus assessment, which suggests that this method is not as straightforward as originally thought. It relies heavily on fine control of data collection, data analysis, and interpretation. Further development of this method is slow due to a lack of details on data collection and analysis provided in published GPIAS studies. The goal of this study was to elucidate several key features of GPIAS data collection and analysis in attempt to improve its reliability.

Methods
Fourteen CBA/CaJ mice were tested across a two month period over 21 testing sessions to assess their baseline gap detection performance. Effects of factors

such as inter-trial interval, circadian rhythm, sex differences, startle response habituation and sensory adaptation on the performance were evaluated. The contribution of gap-induced facilitation and various approaches for GPIAS data analysis were also examined and compared. These approaches were further tested to assess gap detection deficits induced by sound over-exposure which are thought to be associated with the presence of tinnitus.

Results
We found that the absolute acoustic startle reflex magnitude is highly variable (up to three fold) in mice even within a single one hour testing session. This variability is affected by inter-trial intervals, sex differences, circadian rhythm, and other factors. Certain data collection approaches can minimize the variance. We also found that inclusion multiple testing sessions into analysis can greatly enhance precision of GPIAS assessment.

Conclusions
This study provides a guide of how to minimize the effect of variance on GPIAS assessment and to improve the diagnostic power of the test. This knowledge might help to enhance GPIAS reliability and potentially avoid inconclusive or misleading results in gap detection assessment.

PS 245

Gap Detection Data Analysis & Tinnitus Assessment: Animal Grouping and Downstream Experimental Work

Christopher Neal; Andrea Freemyer; Hinrich Staecker; Dianne Durham
Department of Otolaryngology , University of Kansas School of Medicine
Background

Animal subjects cannot directly communicate their perception of tinnitus, and behavioral testing (e.g. gap detection) functions as a surrogate for direct communication. Methods of analysis for behavioral data vary, yielding different findings. Methods used to sort animals into tinnitus groups are critical for studying tinnitus-related changes in anatomy and physiology. Here we explore the effects of two different behavioral analysis methods on identifying individual animals with tinnitus.

Methods
Days 1-4
• Gap detection (GD) recording sessions using three 1 kHz wide narrowband background tones centered at

12, 16, and 20 kHz
 • Hearing thresholds were assessed at 7 frequencies (2, 4, 8, 11.3, 16, 22.6, and 32 kHz) using ABRs
Day 5
 • 16 kHz pure-tone sound exposure (118 dB SPL, 4 hour [n=16] or 114 dB SPL 1 hour [n=24])
Days 6-20
 • 2 week post-exposure recovery period
Days 21-24
 • Post-exposure data acquisition mirroring days 1-4

Statistically significant outliers were removed from raw GD data using a single iteration of the Grubbs outlier detection test (Grubbs, 1950). Animals presenting with more than one instance of baseline gap/nogap ratios >1 were excluded (impaired baseline startle reflex). Using the same raw data, baseline and post-exposure gap/no-gap ratios were calculated using both the gap condition based grand average and the daily gap/nogap ratio based average methods. Post-exposure gap/nogap ratios were divided by baseline gap/nogap ratios to generate normalized GD scores for each individual animal. GD performance was assessed using normalized GD scores, and animals were sorted into tinnitus groups based on performance relative to control animals (n=7).

Results & Conclusion
Using the same raw data, the two methods of gap/nogap ratio calculation can produce distinct gap/nogap ratio values, altering the spread of control animal scores and the assignment of a tinnitus status to sound exposed animals. In control animals, gap condition based averages suggested improvement in performance across all 3 backgrounds with the greatest improvement occurring at 12 kHz, while daily gap/nogap ratio based averages suggested mild impairment in performance of equal magnitude for all 3 backgrounds. Furthermore, gap condition based grand averages could *mask* the presence of tinnitus in a given animal if the tinnitus only presented in a subset of recording sessions. Conversely, daily gap/nogap based averages can *reveal* daily fluctuations in gap detection performance.

Grubbs, F.E. 1950. Sample criteria for testing outlying observations. The Annals of Mathematical Statistics, 27-58.

Named Gap Detection Equations for ARO.pdf

PS 246

Longitudinal Evaluation of Tinnitus Behavior and Alterations in Neuronal Activity in Auditory and Non-auditory Brain Regions using Manganese-enhanced MRI in an Animal Model of Tinnitus

Andrea Freemyer; Christopher Neal; Jennifer Nelson-Brantley; Hinrich Staecker; Dianne Durham
Department of Otolaryngology , University of Kansas School of Medicine

Background
Tinnitus is the perception of sound with no corresponding external stimulus. Tinnitus often accompanies hearing loss, but not all individuals with hearing loss also present with tinnitus. Additionally, the time course of altered CNS activity due to hearing loss or tinnitus is not well understood. Here, we exposed animals to intense sound and documented the time course of hearing loss, tinnitus behavior, and CNS spontaneous activity in three auditory and three non-auditory brain regions at 1 and 3.5 months after sound exposure.

Methods
Male, Long-Evans rats were anesthetized and exposed unilaterally to a 114 dB, 16 kHz pure tone for 1 hour. ABR thresholds were measured at 7 frequencies between 2 and 32 kHz. Tinnitus behavior was evaluated with gap detection over 4 consecutive days. We measured spontaneous brain activity using Manganese enhanced MRI (MEMRI). One day prior to MRI, animals were injected with 66 mg/kg manganese chloride and placed in a soundproof booth for 24 hours. Following MRI acquisition in a 9.4T horizontal bore scanner, brain activity was evaluated in dorsal cochlear nucleus, inferior colliculus, auditory cortex, basolateral amygdala, hippocampus and the cerebellar paraflocular lobe (PFL). All measurements described above were taken prior to sound exposure and at 1 and 3.5 months after exposure.

Results and Conclusions
All sound exposed animals showed mild to moderate hearing loss across most frequencies at 1 month post damage which remained unchanged at 3.5 months. 1 month post damage, 60% of animals displayed behavioral evidence of tinnitus at one or more background frequencies. At 3.5 months, 50% of animals displayed behavioral evidence of tinnitus, and in some cases, an animal';s tinnitus status changed over time. MEMRI revealed a bilateral increase in neuronal activity at 1 month post damage relative to baseline in the IC regardless of tinnitus status (p = .07). When animals were grouped according to tinnitus status, tinnitus + animals had decreased neuronal activity in the ipsilateral PFL relative to tinnitus – animals (p = .07). At 3.5 months post damage, there was a bilateral decrease in neuronal activity

of the PFL (ipsilateral p = .03, contralateral p = .06). At this later time point, these changes appear to be related to hearing loss alone and not tinnitus status. Across all brain regions, there was greater variation in measured neuronal activity between animals at the later time point relative to the early time point post damage.

PS 247

The putative involvement of the middle ear in hyperacusis and tinnitus

Philippe Fournier[1]; Damien Ponsot[1]; Alain Londero[2]; Laurent Pezard[1]; Nicolas Charpentier[3]; **Arnaud Norena[1]**
[1]Université d'Aix-Marseille, Centre national de la recherche scientifique (CNRS); [2]Hôpital Européen Georges-Pompidou, France; [3]Université de Lorraine

We report the case of an acoustic shock injury (ASI), which did not result in a significant hearing loss, but was followed by manifold chronic symptoms both within (tinnitus, otalgia, tingling in the ear, tension in the ear, and red tympanum) and outside the ears (blocked nose, pain in the neck/temporal region). The pathophysiological mechanisms underlying these symptoms remain unknown, even though some authors have hypothesized a dysfunction in the tensor tympani muscle (TTM). The patient described here was able to precisely report his symptoms, their temporal evolution, and take pictures of his eardrums over time during symptom severity fluctuations. The psychoacoustic characteristics of his tinnitus and the functional integrity of the middle ears were also investigated. We suggest that these symptoms may result from a loop involving injury to middle ear muscles, peripheral inflammatory processes, activation and sensitization of the trigeminal nerve, the autonomic nervous system, and central feedbacks. The pathophysiology of this ASI is reminiscent of that observed in post-traumatic trigeminal-autonomic cephalalgia. This framework opens new and promising perspectives on the understanding and medical management of ASI. In addition, we report the case of a subject who is able to voluntary contract the tensor tympani bilaterally. The experiments carried out in this subject, with and without tensor tympani contraction, was aimed at exploring different means to objectify the tensor tympani contraction, namely changes in compliance, acoustic recordings in the ear canal and electromyography.

PS 248

Improved Sound Level Tolerance Accompanies Remission of Persistent Tinnitus in Adolescents with Clinically Normal Audiometry

Larry E. Roberts[1]; Tanit Ganz. Sanchez[2]
[1]McMaster University; [2]University of São Paulo School of Medicine, São Paulo, Brazil

Sanchez et al. [1] found that 27.5% of 170 adolescents in a private school experienced verified tinnitus and reduced sound level tolerance (SLT) during psychoacoustic assessment with no impairment of otoacoustic emissions or clinical audiometry. Risky listening habits were near universal and not more prevalent among those experiencing tinnitus and reduced SLT. However, new cases of tinnitus can resolve over time without explicit treatment in an undetermined percentage of young adults [2]. We therefore carried out repeat measurements on 54 adolescents who returned voluntarily for study one year later. In both studies SLT was measured as Loudness Discomfort Level (LDL).

Results
(1) Of the 14 subjects with verified tinnitus in the first study who returned for a second psychoacoustic measurement, 42.9% experienced verified tinnitus on retest while 57.1% did not. (2) SLT measured as LDL was reduced by 17.2 dB in repeating cases (p < 0.0001) and normal in resolving cases. (3) Hearing thresholds measured to 16 kHz were < 20 dBHL in 98.3% of ears, with only one tinnitus subject showing thresholds > 20 dBHL above 11.2 kHz. However, hearing thresholds > 4 kHz were higher in the left ear (8.33 dBHL) than the right ear (3.05 dBHL) of repeating compared to resolving tinnitus subjects (p = 0.037; all bilateral tinnitus). (4) Otoacoustic emissions did not differentiate between adolescents with or without verified tinnitus in either study. (5) Among returning adolescents those without tinnitus reported attending fewer parties and raves per week than did those with tinnitus (42.3% versus 62.5% respectively), but this difference was not statistically significant.

Conclusions
There was a notable remission of persistent tinnitus in this sample (57.1% of cases), confirming previous reports that persisting tinnitus can resolve without explicit treatment in new cases in young adults [2]. Audiometric thresholds and otoacoustic emissions were clinically normal in repeating cases, although thresholds >4 kHz were elevated by ~5 dB in the left ear in repeating tinnitus. SLT was decreased in repeating tinnitus and recovered to normal levels in resolving tinnitus, confirming previous reports of a relationship to tinnitus [1]. The time course of SLT and tinnitus could

reflect hidden hearing loss followed by synaptic recovery which has been reported in animal models [3].

[1] Sci Rep, DOI: 10.1038/srep27109 1; [2] Roberts (2016), in D. Baguley & M. Fagelson, *Tinnitus.* Plural Press, pp. 13-33; [3] Song et al. (2016), Sci Rep DOI: 10.1038/srep25200. Assisted by NSERC of Canada.

PS 249

Tinnitus after Cerebellopontine Tumor Surgery: The Relation Between Flocculus Volume and Tinnitus Characteristics in Humans

Lilian Mennink[1]; Marc Van Dijk[2]; Bernard Van der Laan[1]; Jan D.M. Metzemaekers[3]; Peter Jan Van Laar[4]; **Pim van Dijk**[5]
[1]University Medical Center Groningen, Dept. of Otorhinolaryngology; [2]University Medical Center Groningen, Dept. of Neurosurgery; [3]Department of Neurosurgery, University Medical Center Groningen, The Netherlands; [4]University Medical Center Groningen, Dept. of Radiology; [5]Department of Otorhinolaryngology, University Medical Center Groningen, The Netherlands

Tinnitus is a common condition in patients that underwent surgery to remove a cerebellopontine angle (CPA) tumor. This surgery involves manipulation of the flocculus, a cerebellar structure that has been implied in tinnitus in rats (Brozoski et al., 2007, Hear Res 228, 168-179) and has been suggested to be involved in gaze-modulated tinnitus (Chen et al., 2017, Hear Res 349, 208-222). Either the tumor or the surgical procedure may cause hypotrophy of the flocculus on the surgery side. This could compromise the function of the flocculus. If the flocculus plays a role in tinnitus after CPA tumor removal, there may be a relation between the volume of the flocculus and tinnitus characteristics. We investigated the relation between flocculus volume and tinnitus characteristics. To evaluate tinnitus characteristics, a questionnaire was sent to 70 patients who underwent CPA tumor surgery. This questionnaire included the Tinnitus Functionality Index (TFI) and questions on gaze-modulation of tinnitus. The questionnaire was completed by 51 patients, of which 36 (71%) described hearing tinnitus. The tinnitus could be modulated by eye gaze in 29 of these 36 patients (81%). Bilateral flocculus volumes could be obtained from CISS T2 MRI scans in 34 patients, of which 25 experienced tinnitus, which was gaze-modulated in 21. There was no difference between flocculus volumes of patients with and without tinnitus. In the patients with tinnitus, the flocculus volume on the surgery side and the contralateral side were correlated with the TFI, respectively (ipsi: R=0.52, p<0.01; contra: R=0.43, p=0.03). The ipsi-to-contralateral flocculus volume ratio was smaller in patients with gaze-modulated tinnitus as compared to those where gaze did not affect tinnitus (t=3.3, p<0.01). These results suggest that the flocculus mediates the severity of tinnitus. In addition, hypotrophy of the flocculus on the tumor side may be involved in the generation of gaze-modulated tinnitus.

PS 250

Hyperexcitability of Caudal Pontine Reticular Nucleus (PnC) Caused by Age-related Hearing Loss

Ning Zhao[1]; Anaam Alkharabsheh[2]; Fei Xu[3]; Wei Sun[4]
[1]the First Affiliated Hospital of China Medical University; [2]University at Buffalo; [3]Zhejiang Chinese Medicine University; [4]State University of New York at Buffalo

Object
There is a high incidence of chronic tinnitus and hyperacusis in elderly population. Increased acoustic startle responses, indicative of hyperacusis behavior, have been reported in middle age C57BL/6J mice which showed early onset hearing loss. However, the central auditory system causing sound perception changes is still not clear.

Methods
Acoustic startle and auditory brainstem responses (ABR) were tested in C57BL/6J mice at 2 months and 6 months of age. The neural function of the caudal pontine reticular nucleus(PnC), which was correlated with startle response, were recorded in these mice.

Results
The averaged ABR threshold increased about 20 dB in the 6 months group compared to the 2 months group. The startle response amplitude increased and the threshold decreased in the old mice. Interestingly, noise-burst induced PnC responses in the 6 months mice were significantly higher than the 2 months group; whereas the threshold were lower in the old group. These data are consistent with the acoustic startle response changes with age. The PnC response induced by tone-bursts showed a frequency dependent change with age: the PnC responses at lower frequencies (20 kHz) were significantly decreased in the 6 months group. These data suggested that the PnC neurons become hypersensitive to sound stimuli at low frequencies after developing high frequency hearing loss.

Conclusion
Our results suggest that the hyperexcitability of PnC caused by high frequency loss in the C57 mice may cause enhanced acoustic startle response. These functional changes may be also related to tinnitus and hyperacusis seen in aging population.

PS 251

Long-term exposure of adult CBA/Ca mice to borderline-synaptopathic 70-75 dB SPL, 8-16 kHz noise does not lead to hyperacusis or tinnitus as assessed using tone and gap prepulse inhibition of the acoustic startle reflex

Martin Pienkowski
Salus University

Hearing loss changes the auditory brain, sometimes in maladaptive ways. In response to a drop in cochlear output, central auditory neurons can become more active spontaneously, and begin to respond more strongly and synchronously to better-preserved cochlear regions, which become over-represented in the brain. This spontaneous and sound-evoked central hyperactivity has been postulated to trigger tinnitus and hyperacusis, respectively. Regional hyperactivity in the auditory brain has also been observed after long-term exposure to noise levels that do not damage the cochlea. Mature animals exposed to various bands of non-damaging noise exhibited suppressed spontaneous and evoked activity in the area of primary auditory cortex (A1) tonotopically mapped to the noise band, but had increased spontaneous and evoked activity in neighboring areas of A1, mapped to sound frequencies above and below the exposure band. We hypothesized that the cortically-suppressed frequencies should for some time be perceived as less loud than before exposure (hypoacusis), whereas the hyperactivity at frequencies outside of the exposure band might lead to hyperacusis and/or tinnitus. To investigate this, mature CBA/Ca mice were exposed for >2 months to 8–16 kHz noise at 70 or 75 dB SPL, and tested for hypo/hyperacusis and tinnitus using tone- and gap-based prepulse inhibition of the acoustic startle reflex. Auditory brainstem responses and distortion product otoacoustic emissions showed evidence of cochlear synaptopathy after exposure at 75 but not 70 dB SPL, putting a lower bound on damaging noise doses (for CBA/Ca mice). Contrary to hypothesis, neither exposure significantly shifted startle results from baseline. These negative findings nevertheless have implications for startle test methodology, and for the putative role of central hyperactivity in hyperacusis and tinnitus.

PS 252

Tinnitus in a Cohort of Occupational noise exposed Workers: Analysis of Demographic and Audiological Characteristics

Xiaowen Tan[1]; Qixuan Wang[1]; Xueling Wang[1]; Zhuwu Huang[1]; Hao Wu[2]
[1]1.Department of Otolaryngology Head & Neck Surgery, Shanghai 9th People's Hospital /Shanghai Ninth People's Hospital , School of medicine, Shanghai Jiao Tong University 2. Ear Institute Shanghai JiaoTong University School of Medicine ） 3.; [2]Department of Otolaryngology Head & Neck Surgery, The Ninth People's Hospital, Shanghai Jiao Tong University School of Medicine, Shanghai, China. Ear Institute, School of Medicine, Shanghai Jiao Tong University, Shanghai, China. Shanghai Key Laborato

Objective
Noise is believed to be one of the induced factor of tinnitus and most commonly among adults with tinntius. The aim of this study was to analyze the relationship between noised induced hearing loss and tinnitus along with other associated factors (characteristic of hearing loss, age, exposure time and sound intensity) of noise exposed workers.

Method
4000 Workers from a dockyard in Shanghai exposed in noise environment were enrolled and required to finish a questionnaire containing basic information (age, name, history of disease, etc.). Inclusion criteria is: Age between 20-60 years ; working period less then 30 years; without otology disease history and ototoxic drug usage. Then subjects selected were performed pure tone audiometry(PTA) in removable sound-proofed room with environment sound

Result
1992 samples met the final criteria with 1837males and 155female; average age is 36.27±8.25 yrs; average length of service is 9.10±6.5yrs. The morbidity of tinnitus among those samples are: 20.6%. All groups showed a notch at 4-6 kHz in PTA--which is the symbol of Noise-induced hearing losswith increasing threshold at 3,4,6,8 kHz followed the severity of tinnitus. The difference at high frequency (3,4,6,8 kHz) among groups and control were significant($P0.25=0.38,P_{0.5}=0.02$). Correlation between age, length of service(exposure years) and mild tinnitus and worse hearing were found, with $R^2=0.89$ and 0.99 respectively. MOT group also show correlation with exposure time ($R^2=0.40$) but remain almost the same in different age group. The cumulative noise exposure (CNE) calculated by sound level were involved. When the noise level were lower than 105dB(A) both MIT and MOT showed a good correlation with $R^2=0.93$ and 0.78 respectively.

Conclusion
Our study shows that noise induced hearing loss has a symbol notch at 4-6kHz. Meanwhile, noise has both direct influence and cumulative effect on tinnitus and it appears more significant in mild tinnitus, and the morbidity is higher(20.6%) than normal(17%). But when the sound is too loud people will tend to acquire moderate tinnitus.

PS 253

Bimodal Stimulation Alters Excitatory-Inhibitory Balance in Dorsal Cochlear Nucleus Fusiform Cells

Annabel S. Lemke[1]; David T. Martel[2]; Calvin Wu[1]; Susan Shore[3]
[1]*University of Michigan Ann Arbor;* [2]*University of Michigan, Ann Arbor;* [3]*University of Michigan*

To examine the neural consequences of noise exposure, tinnitus development, and experimental treatment, this project focuses on changes in excitation and inhibition reflecting long-term depression induction in dorsal cochlear nucleus (DCN) fusiform cells. Inhibition of fusiform cells by neighboring cells (cartwheel, D-Stellate and vertical cells), varies with synaptic strength, and may be altered in tinnitus. Fusiform cells, the principal output neurons of the DCN, exhibit increased spontaneous firing rates, synchrony, and burst rates after tinnitus induction (Wu et al., J Neurosci 2016). They also exhibit stimulus-timing-dependent plasticity, which is induced through bimodal auditory-somatosensory stimulation with varying stimulus orders and intervals (Koehler and Shore, J Neurosci 2013). Here, we examined fusiform-cell receptive fields and their interaction with documented neural correlates of tinnitus. Four groups of guinea pigs were examined: 1) normal (control), 2) noise-exposed animals that developed tinnitus as assessed by gap-prepulse inhibition of the acoustic startle, 3) noise-exposed animals that did not develop tinnitus, and 4) tinnitus animals treated with bimodal stimulation designed to elicit long-term depression to reduce tinnitus. Degree of inhibition was quantified by an inhibitory/excitatory (IE) index defined as $(SE-SI)/(SE+SI)$, where SE and SI are the sums of excitatory and inhibitory responses, respectively, across levels for each frequency in the receptive field (Li et al., JARO 2015). Compared to the other groups, the bimodal-treatment group exhibited a reduced range of excitation-dominated activity, shifting the balance towards inhibition. In contrast, IE indices from noise-exposed animals that did and did not develop tinnitus were indistinguishable, as noise exposure alone, independent of whether or not animals developed tinnitus, increased inhibition-dominated activity. This suggests that disinhibition may not be a prerequisite for tinnitus development. Further investigation is needed to understand the mechanisms underlying bimodal-treatment, as our results suggest alternative pathways for induction and alleviation of tinnitus.

PS 254

Effect of sound generator on tinnitus and hyperacusis

Jung Mee Park[1]; Woo Jin Kim[2]; Jin-Bu Ha[3]; Jung Ju Han[4]; Sang Won Yeo[5]; Shi Nae Park[6]

Background
Sound generator (SG) plays a role as effective sound therapy of TRT in patients with severe tinnitus (Category 1) or hyperacusis (Category 3). This study was performed to evaluate the therapeutic effect of SGs on tinnitus and hyperacusis during their tinnitus retraining therapy (TRT).. Methods: A total of 120 tinnitus patients who visited our tinnitus clinic and were treated with SG along with TRT from January 2008 to December 2016 were included. The patients were divided into two groups by tinnitus category; 78 patients of category 1 and 42 patients of category 3. Their medical records including questionnaires regarding tinnitus severity were retrospectively reviewed to evaluate the therapeutic effect of SGs on tinnitus and hyperacusis. Results: Category 3 patients included more female, were younger than category 1 patients (P < .001), and were prescribed SG earlier due to their severe symptom of hyperacusis. (P = .004) All patients showed significant improvements on all categories of tinnitus VAS scores and THI scores after 6 months use of SG (P < .05). Loudness discomfort levels measured by pure tone audiometry were significantly improved in category 3 group after 6 months use of SGs. Conclusion: Six months use of SGs effectively alleviated distresses of tinnitus symptoms as well as abnormal sensitivity to sounds. This study shows that SG with TRT is an effective treatment modality for all tinnitus patients, especially those with comorbid hyperacusis.

!SG_ARO_JMPARK.docx

PS 255

A New Approach to Diagnosing Hyperacusis

Sarah Theodoroff[1]; Frederick Gallun[1]; Dawn Konrad-Martin[1]; Stephen Neely[2]; Walt Jesteadt[2]
[1]*VA RR&D NCRAR;* [2]*Boys Town National Research Hospital*

Background
Hyperacusis, a problem tolerating the loudness of everyday sounds, is an important and under-researched disorder that commonly co-occurs with tinnitus. No universally accepted framework exists to evaluate hyperacusis and there is not a reliable clinical metric, no gold standard, for diagnostic purposes. Another barrier to diagnosing hyperacusis is the lack of an agreed upon nomenclature to use to define and classify hyperacusis. Commonly used clinical procedures are tests

of loudness discomfort and to rely on self-report questionnaires, but neither of these approaches has widespread acceptance. Therefore, there is a critical need to develop an effective paradigm to diagnose and assess hyperacusis and distinguish it from other disorders of decreased sound tolerance especially in tinnitus patients. A pilot project is underway that takes an innovative approach to characterizing hyperacusis. Methods: Data collection is ongoing and the most recent dataset will be presented. Two behavioral measures and three questionnaires will be compared to identify a reliable metric to diagnose hyperacusis in tinnitus patients: (1) a commonly performed clinical procedure, Loudness Discomfort Levels (LDL); (2) a new computerized loudness scaling procedure, Categorical Loudness Scaling (CLS) that obtains judgments at eleven loudness categories; (3) the Tinnitus and Hearing Survey, a 10-item questionnaire evaluating the impact of tinnitus, hearing problems, and hyperacusis over the last week; (4) a 14-item Hyperacusis Questionnaire evaluating the impact on attention, social, and emotional domains; and (5) a 25-item Noise Avoidance Questionnaire that quantifies sound avoidance in everyday situations. Impact: This research takes a systematic approach evaluating behavioral psychoacoustic techniques to identify the best metric to capture abnormal loudness judgments as well as using questionnaires to evaluate the degree hyperacusis impacts overall well-being in tinnitus patients. The next step will be to further develop this new framework for assessing hyperacusis and expand the test battery to include a physiological measure of auditory function that will complement the identified optimal behavioral metric (CLS vs. LDL). Including physiological measure(s) will provide additional information to help characterize hyperacusis and possible subtypes, specifically in terms of potential auditory peripheral and central contributions. Overall, this avenue of research will result in creating a multi-dimensional framework for assessing hyperacusis and will also assist with modeling abnormal loudness perception at both peripheral and central stages of auditory processing. Supported by a grant from the American Tinnitus Association

Vestibular: VOR, SHIMP, VEMP

PS 256

The Effect of Visual Contrast on Human Vestibulo-Ocular Reflex Adaptation

M M. Mahfuz[1]; Michael C. Schubert[2]; C J. Todd[1]; W V. C. Figtree[1]; S I. Khan[1]; A A. Migliaccio[1]
[1]Neuroscience Research Australia; [2]Johns Hopkins University

The vestibulo-ocular reflex (VOR) is the main retinal-image stabilising mechanism during rapid head movement. When the VOR does not stabilise the world or target image on the retina, retinal image slip occurs generating an error signal that drives the VOR response to increase or decrease until image slip is minimised, i.e., VOR adaptation occurs. Visual target contrast affects the human smooth pursuit and optokinetic reflex responses. We sought to determine if contrast also affected VOR adaptation. We tested 12 normal subjects, each over 16 separate sessions. For sessions 1-14, the ambient light level (lx) during adaptation training was: dark, 0.1, 0.2, 0.3, 0.5, 0.7, 1, 2, 8, 16, 32, 64, 128 and 255 lx (light level for a typical room). For sessions 15-16, the laser target power (related to brightness) was halved with ambient light at 0 and 0.1 lx. The adaptation training lasted 15 minutes and consisted of left/right active head impulses. The VOR gain was challenged to increment, starting at unity, by 0.1 every 90 seconds for rotations to the designated adapting side and fixed at unity towards the non-adapting side. We measured active and passive VOR gains before and after adaptation training. We found that for both the active and passive VOR there was a significant increase in gain only towards the adapting side due to training at contrast level 495 (8 lx) and above. At contrast level 261 (16 lx) and below, adaptation training resulted in no difference between adapting and non-adapting side gains. Our data suggest that there is a contrast threshold between 261 and 495, which is higher than that provided by typical room lighting (16) that must be surpassed for active and passive VOR adaptation. Our findings suggest contrast is an important factor for adaptation, which has implication for rehabilitation programs.

PS 257

Optimal Human Passive Vestibulo-Ocular Reflex Adaptation does not Rely on Passive Training

M M. Mahfuz[1]; Michael C. Schubert[2]; C J. Todd[1]; W V. C. Figtree[1]; S I. Khan[1]; A A. Migliaccio[1]
[1]Neuroscience Research Australia; [2]Johns Hopkins University

The vestibulo-ocular reflex (VOR) is our main vision stabilising system during rapid head movements. A visual-vestibular mismatch stimulus can be used to train or adapt the VOR response because it induces a retinal image slip error signal that the VOR seeks to minimise. The training context has been shown to affect VOR adaptation. We sought to determine whether active (self-generated) versus passive (externally imposed) head rotation vestibular stimuli would differentially affect adaptation and short-term retention of the active and passive VOR responses. We tested 10 subjects, each over 5 separate 1.5 hour sessions. We compared active versus passive head impulse (transient, rapid head rotations with peak velocity ~150o/s) VOR adaptation training lasting

15 minutes with the VOR gain challenged to increment, starting at unity, by 0.1 every 90 seconds towards one side only (this adapting side was randomised to be either left or right). We measured the VOR response in darkness at 10 minute intervals, 20 minute intervals, and a single 60 minute interval for 1 hour post-training. The training was active or passive for the 10 and 20 minute interval sessions, but only active for the single 60 minute interval session. The mean VOR response increase was ~10% towards the adapting side versus ~2% towards the non-adapting side. There was no difference in VOR adaptation and retention between active and passive VOR training. The only factor to affect retention was exposure to a de-adaptation stimulus. Our data suggest that active VOR adaptation training can be used to optimally adapt the passive VOR and that adaptation is completely retained over 1 hour as long as there is no visual feedback signal driving de-adaptation.

PS 258

The Effect of Stimulus Repetition Rate and Duration on Human Vestibulo-Ocular Reflex Adaptation

M M. Mahfuz[1]; Michael C. Schubert[2]; C J. Todd[1]; W V. C. Figtree[1]; S I. Khan[1]; A A. Migliaccio[1]
[1]*Neuroscience Research Australia;* [2]*Johns Hopkins University*

The vestibulo-ocular reflex (VOR) is the main gaze stabilising system during rapid head movements. The VOR is highly plastic and its gain (eye / head velocity) can be increased via training that induces an incrementally increasing retinal image slip error signal to drive VOR adaptation. Using the unilateral incremental VOR adaptation technique and horizontal active head impulses as the vestibular stimulus, we sought to determine the factors important for VOR adaptation including: the total training time, ratio and number of head impulses to each side (adapting and non-adapting sides; the adapting side was pseudo-randomized to be left or right) and exposure time to the visual target during each head impulse. We tested 12 normal subjects, each over 5 separate sessions. For session 1, unilateral incremental VOR adaptation training lasted 15 minutes and the ratio of head impulses to each side was 1:1. Session 2 was similar to 1, except the ratio of head impulses were in favor of the adapting side by 2:1. Session 3 was also similar to 1, except all head impulses were towards the adapting side. Session 4 was similar to 3, except the training lasted only 7.5 minutes. Finally, session 5 was also similar to 3, except that the exposure time to the visual target during each head impulse was doubled. We measured the active and passive VOR gain before and after the training. Our data suggest that the total training time and the visual target exposure time for each head impulse affected adaptation, whereas the total number and ratio of head impulses did not. These data have implications for vestibular rehabilitation, suggesting that quality and duration of VOR adaptation exercises are more important than rapid repetition of exercises.

PS 259

The Role of the Otoliths in Vestibulo-ocular Reflex Adaptation

S I. Khan; A A. Migliaccio
Neuroscience Research Australia

The aim of this study was to determine the role of the otoliths in vestibulo-ocular reflex (VOR) adaptation. Until recently the role of the otoliths has been difficult to determine because there is no surgical or chemical technique that can selectively ablate the otoliths without damaging the semicircular canals. The tilted mouse (Otop 1) lacks functioning otoliths, but has normal semicircular canals, and do not show any permanent phenotype in organ systems other than the otoliths. In 4 Otop 1 mice and 4 control littermates we measured: 1) baseline ocular counter-tilt about the 3 primary axes; 2) baseline horizontal sinusoidal (0.2-10Hz, 20-100°/s) VOR gain (= eye / head velocity); 3) baseline vertical (left-ear-down [LED] and [RED]) sinusoidal VOR; 4) horizontal VOR after gain-increase (x1.5) and gain-decrease (x0.5) adaptation training at 0.5Hz with peak-velocity 20°/s; 5) vertical (left-ear-down and right-ear-down) VOR after gain-increase (x1.5) and gain-decrease (x0.5) adaptation training to one side (LED or RED). Counter-tilt responses in tilted mice were significantly reduced compared to controls, confirming that tilted mice had minimal otolith function. Baseline horizontal and vertical VOR gains were similar between the two mouse types, confirming that the semicircular canals in titled mice were similar to normal. Horizontal VOR adaptation was similar between both mouse types, suggesting that otoliths played a minor role during horizontal VOR adaptation. However, there was a significant difference in vertical VOR adaptation between both mouse types. For the control mouse, adaptation of the VOR gain was most evident when the testing context (LED or RED) was the same as the training context (LED or RED), i.e., they showed context-specific adaptation. Whereas, although the tilted mouse showed the same level of vertical adaptation as the control mouse, context specific adaptation was absent. Our results suggest that context-specific VOR gain adaptation is almost entirely reliant on otolith input and not other contextual cues, e.g., proprioceptive signals.

Direct Current/Pulse Frequency Co-modulation Increases the Inhibitory Range of Electrically Evoked VOR Head Velocities

Dilawer Singh[1]; Felix P. Aplin[1]; Charles C. Della Santina[1]; Gene Y. Fridman[2]
[1]Johns Hopkins University; [2]Johns Hopkins University School of Medicine

Introduction

Bilateral vestibular deficit results in dizziness and disequilibrium and could be aided by electrically evoked pulse frequency modulation (PFM). PFM delivered to surviving afferent fibers of the vestibular nerve evokes the sensation of head rotation, eliciting vestibulo-ocular reflex (VOR) eye rotations. However, the range of electrically evoked VOR eye velocities is small. We propose that as vestibular nerve afferents maintain a baseline of spontaneous activity, PFM can increase the firing rate but cannot decrease it below this activity baseline. Our lab has developed a method of delivering charge-balanced direct current (DC) to living tissue without harmful reactions via a microfluidic device that is capable of both exciting and suppressing spontaneous neural activity. The aim of this study is to investigate the effect of DC on VOR eye rotations elicited by stimulation via PFM.

Methods

Prior to experiments, electrodes were surgically implanted in the left SCCs of bilaterally gentimicin treated chinchillas. Vestibular afferents were stimulated using PFM ramps around an artificially elevated baseline that evoke excitatory and inhibitory VOR responses. A series of PFM ramps was delivered to vestibular afferents while delivering no DC and then repeated with cathodic and anodic DC offsets. During each trial, an eye marker placed on the left eye was detected by a camera. The change in pixel position of the eye marker was used to determine VOR eye velocities.

Results

Delivering excitatory and inhibitory PFM ramps to an SCC proved to elicit a VOR response in the plane of the SCC, but the inhibitory motion was small. Experiments using PFM along with an anodic DC offset, when compared to using PFM alone, improved the inhibitory dynamic range of head velocities by evoking a larger inhibitory VOR response. VOR responses to PFM with a cathodic DC offset showed no increase in inhibitory motion. These results suggest that DC can influence spontaneous neural activity in vestibular afferents and thus improve the inhibitory range of PFM.

Conclusions

Our results showing an improved dynamic range for inhibitory head motions when anodic DC is used with PFM aligns with our hypothesis that anodic DC can suppress spontaneous neural firing. We propose that, by reducing spontaneous activity in the vestibular afferent, DC-offset PFM can better down-modulate firing rate to encode contralateral head rotations. For neural systems that encode information via both excitation and inhibition of neural firing rate, DC may be a beneficial method for reducing a spontaneous activity baseline.

Direct current modulation of vestibular system afferents increases dynamic range of eye rotations

Felix P. Aplin[1]; Dilawer Singh[1]; Gene Y. Fridman[2]
[1]Johns Hopkins University; [2]Johns Hopkins University School of Medicine

Introduction

Bilateral vestibulopathy is a debilitating condition with a profound effect on quality of life. Few treatment options are available beyond rehabilitation therapy. One treatment under development is the use of a neuroelectric prosthesis to stimulate surviving vestibular afferents. Current prostheses use charge-balanced biphasic pulses that excite nearby neural tissues but cannot inhibit them. As the vestibular system encodes information by modulation around a firing rate baseline, a prosthetic system that could also inhibit firing rate would be ideal. We previously developed a novel system that allows for safe delivery of ionic DC current, capable of both exciting and inhibiting neurons. Here we demonstrate DC stimulation to modulate output of the semicircular canals via excitation and inhibition of semicircular canal afferents.

Methods

Adult wild-type chinchillas were bilaterally treated with intratympanic injections of gentamicin to emulate human bilateral vestibular dysfunction. Current was delivered via gel-filled microcatheter tubes implanted into the semicircular canals of the left ear, that served to isolate hazardous byproducts caused by electrolysis at the metal interface. After adaptation to a range of tonic pulse frequencies or DC current steps, animals were stimulated with stepped anodic and cathodic DC current and pulse frequency modulated (PFM) biphasic waveforms. Vestibulo-ocular reflex eye movements associated with the sensation of head rotation were recorded using an eye-tracking rig and analyzed to compare PFM and DC neural modulation.

Results

DC and PFM stimulation resulted in vestibulo-ocular reflex mediated eye rotations associated with head

movement corresponding to the modulated semicircular canal. PFM and cathodic DC steps effectively elicited eye rotation vectors associated with excitation of vestibular afferents. When modulating down from an adapted baseline, PFM stimulation elicited inhibitory eye rotation vectors but this increased baseline limited the dynamic range of achievable eye rotation velocities. Anodic DC current steps also elicited inhibitory eye rotations and, when paired with an adapted cathodic offset, resulted in an increased dynamic range of eye rotation velocities in comparison to PFM.

Conclusion

These results suggest that DC stimulation can effectively stimulate and inhibit the degenerated vestibular system. In conjunction with a safe DC delivery system, DC stimulation could potentially increase the range of simulated head rotation velocities in neuroelectric prostheses designed to mimic vestibular function. Continued research is necessary to fully characterize this response and determine the chronic safety of the DC delivery system. Beyond the vestibular system, direct current has many potential applications where inhibition of a nerve is desirable.

PS 262

Noninvasive Evaluation of Vestibular Dysfunction with Surgery-Free Animal Immobilization - A Binocular VOR-Measuring System

Xiaojie Yang[1]; Qun Liao[1]; Jiaojiao Wu[1]; Shiyue Zhou[1]; Changquan Wang[1]; Lei Qu[2]; Fangyi Chen[1]
[1]*Department of Biomedical Engineering, Southern University of Science & Technology;* [2]*Department of Biomedical Engineering, Hebei University of Technology*

Vestibulo-ocular reflex (VOR) is an involuntary eye movement that helps to stabilize images on the retina by compensating head motion. Therefore, detection of head motion, which is achieved by the vestibular sensory system, is crucial to VOR. Deficits on the vestibular system usually result in reduced amplitude and other abnormalities of VOR.

In order to evaluate the damage to the vestibular system induced by drug treatment or gene manipulation, we developed a comprehensive system allowing users to both provoke and quantitatively measure VOR in mice.

This developed system consists of 1) a motor-driven turntable that can deliver rotational stimulus to the mouse vestibular system; 2) a binocular video oculography (VOG) system that records the mouse-eye movement; 3) a mouse holder that immobilizes the mouse

during measurement in the absence of anaesthetization; and 4) a customized image-processing software package capable of analyzing the mouse-eye movement by extracting and tracking the pupil from each frame of the recorded video. The whole system is enclosed in a chamber that provides dark environment preventing the ocular reflex from any visual input during VOR measurement. The illumination for video recording was implemented with near-infrared (NIR) LEDs inside the chamber. Cameras inside the chamber were monitored and controlled in real time through tablet computers outside the chamber when recording. Each pair of camera and tablet computer communicated with each other via Wi-Fi. The mouse holder was specially designed to immobilize the mouse without requirement of pre-surgery. As pre-surgery on the mouse head under anaesthesia was typically involved in previously reported VOR-measuring systems for installing mounting gadgets (*e.g.*, nuts, bolts) to immobilize the animal, our mouse holder allowing noninvasive animal immobilization serves as an advantage of our system over those surgery-required systems.

To verify the efficacy of our system, vestibular dysfunction in mice, which were induced by the administration (via intraperitoneal injection) of ototoxic 3,3';-iminodipropionitrile (IDPN) to the mice, was evaluated by measuring their VOR progression during a 7-day period. Significant decline in VOR amplitude was detected in IDPN-positive mice since the 4th day after administration, indicating that our system is able to evaluate vestibular function based on quantitative VOR measurement.

PS 263

Development of video-oculography using infrared Frenzel with high quality image camera.

Makoto Hashimoto; Takuo Ikeda; Yosuke Okinaka; Hironori Fujii; Kazuma Sugahara; Yoshinobu Hirose; Hiroshi Yamashita
Department of Otolaryngology, Yamaguchi University Graduate School of Medicine

Background

It is essential to use an infrared CCD camera in clinical examination of the vestibular system. Devices are currently available that can quite accurately record human eye movements, based on the principle of video-oculography (VOG). We devised an original VOG (HI-VOG) system using a commercialized infrared CCD camera, a personal computer and public domain software program (ImageJ) for data analysis. In the present study, we revised the VOG and image filing system for real-time 3D quantitative analysis of nystagmus, using infrared Frenzel with high quality image camera, yVOG-glass.

Methods

The video image from a infrared CMOS camera was captured at 60 frames per second at a resolution of 640*480 pixels. For analysis of the horizontal and vertical components, the X-Y center of the pupil was calculated. For analysis of torsional components, the whole iris pattern was overlaid with the same area of the next iris pattern, and the angle at which both iris patterns showed the greatest match was calculated.

Results

Accurate measurements of horizontal, vertical and torsional eye movement were taken while recording the video image in real-time. For quantitative analysis, the slow phase velocity of each occurrence of nystagmus and the average value of the slow phase velocity were analyzed automatically.

Conclusion

Using the revised yVOG system, it was possible to perform real-time quantitative 3D analysis of nystagmus from video images recorded with a infrared CMOS camera with high quality image camera.

PS 264

Comparison of suppression head impulse and conventional head impulse test protocols

Gi-Sung Nam; Eun Jin Son[1]; Kyung Jin Roh[2]; Ju Young Kim[1]; Min Seok Kang[1]
[1]Yonsei University College of Medicine; [2]Inje University College of Medicine

Purpose

The head impulse test paradigm (HIMP) assesses semicircular canal function by measuring compensatory saccades during head movements as an indication of an impaired vestibulo-ocular reflex (VOR). The recently introduced suppression head impulse test (SHIMP) protocol examines anti-compensatory saccades after head movements as a measure of intact VOR. Thus, HIMP measures a decrease in vestibular function, whereas SHIMP measures residual function. We evaluated the effectiveness of SHIMP, compared HIMP and SHIMP results in the same subjects, and examined the relationship between the two tests.

Materials and Methods

HIMP and SHIMP protocols were performed in 73 patients. The patients were instructed to maintain their gaze on a fixed target for the HIMP, or a moving target for the SHIMP during head impulses. The VOR gain and saccade parameters were compared.

Results

HIMP and SHIMP data were obtained for all ears except in three patients. The VOR gain with SHIMP was smaller than for HIMP, but showed significant correlation ($r = 0.8356$, $p < 0.001$) and substantial agreement (k = 0.79). However, neither the percentage of saccades (appearance of HIMP compensatory saccades and reduction of SHIMP anti-compensatory saccades) nor their amplitudes were correlated between the two tests.

Conclusions

The HIMP and SHIMP protocols are valuable tools to evaluate VOR during high-velocity head movements. Our results confirm their agreement as measures of VOR gain during head impulses, but also show that the relationship between compensatory and anti-compensatory saccades is not straightforward. Thus, care should be taken during clinical interpretation of either protocol.

PS 265

Increased Anxiety Symptoms of Veterans with PTSD is associated with reduced ability to suppress VOR during Suppression Head Impulse (SHIMP) Motor Learning Task.

Yaa Haber[1]; Michael C. Schubert[2]; Jorge Serrador[1]
[1]Rutgers University; [2]Johns Hopkins University

Recent evidence indicates that vertigo, disequilibrium and dizziness are common among veterans with Posttraumatic Stress Disorder (PTSD). Conventionally, symptoms of PTSD have been considered psychological in nature and attributed to the anxiety centers of the brain. However, several studies have shown a direct link between the anxiety centers of the brain and the balance centers of the brain. Impairments within the brain';s balance centers, namely the vestibular organs and the cerebellum have been shown to result in symptoms including vertigo, disequilibrium and avoidance in patients with vestibular disorders. Studies in our lab have shown that the time constant of the slow phase velocity (SPV) of horizontal eye movement is prolonged during rotation in veterans with PTSD. A key modulator of SPV is the cerebellum. The cerebellum modifies the vestibular ocular reflex (VOR) through a visual-vestibular interaction. Here we measure cerebellar adaptation of the vestibular ocular reflex using a Suppression Head Impulse Paradigm (SHIMP). For this motor learning task, 10 subjects (5 +PTSD: 5 -PTSD) were trained to perform active head impulses in the horizontal while visually tracking a head fixed target in complete darkness. There were a total of 3 suppression trials, 5 minutes long. Prior to each

trial, we measured both an active and passive Head Impulse VOR response. We anticipated that an impaired cerebellar function may contribute to reduced ability to adapt the VOR and expected limited suppression of VOR in the PTSD group. We analyzed this data using custom written software in Matlab (MATHWORKS). We excluded 2 of the participants with PTSD as they were unable to complete the motor learning task, leaving 3 participants with PTSD and 5 without PTSD. We performed a general linear model focusing on saccade latency, cumulative saccade amplitude, and saccade frequency. For the group without PTSD, VOR gain was reduced from 0.96 +/- 0.06 to 0.59 +/-0.05 by the 3rd trial whereas the group with PTSD reduced their gain from 0.89 +/- 0.07 to 0.76 +/- 0.07. Overall the group with PTSD only showed a 14% reduction whereas the group without PTSD showed a 38% reduction. Interestingly, the group with PTSD utilized a higher frequency of saccades during the third suppression trial (Mean 23 vs 15). In contrast there were no differences between the groups for saccade latency or amplitude. This data seems to suggest that impaired ability to adapt the VOR may contribute to symptoms of dizziness in PTSD.

PS 266

Human Otolith Accelerometer-Seismometer Predicted Response in VEMPs Testing

Wally Grant[1]; Ian S. Curthoys[2]
[1]VA Tech; [2]University of Sydney

Introduction
Vestibular otolithic organs are recognized as transducers of head acceleration and function as such up to their undamped natural frequency (UDNF). It is well recognized that these organs respond to frequencies above their UDNF, up to 2 to 3 kHz [Curthoys et al, 2016]. A mechanics model for transduction displacement of these organs was developed that predicts the response below the UDNF as an accelerometer and above that frequency as a seismometer [Grant and Curthoys, 2017]. The model transfer function for human response is utilized and applied to Vestibular Evoked Myogenic Potential (VEMP) testing with Bone Conducted Vibration (BCV).

Methods
Human anatomical and physiologic data were used to predict utricle UDNF = ω_n, where: $\omega_n^2 = k/m$, k = the gel layer (GL) shear stiffness, and m = otoconial layer (OL) mass. This result was then used to construct a transfer function for the mechanics model. Results from stimulus acceleration magnitudes in VEMPs testing were used to predict utricle displacement in its seismometer mode at 750 and 1000 Hz. This utricle displacement was compared to bundle displacement of a Type I hair cell model in the striolar region of the utricle.

Results
ω_n estimate for humans = 649 Hz, based on the following: stiffness k = 5.79 N/m and a mass m = 0.348 mg. These base on the following values: shear modulus G = 20 Pa, OL thickness = 35 mm, GL thickness = 14.5 mm, dorsal surface area = 4.2 mm^2, and OL density = 2368 kg/m^3. The transfer function magnitudes as a seismometer were: x/D = 0.64 μm/μm at 750 Hz, and x/D = 0.66 μm/μm at 1000 Hz; where: x = relative displacement between OL and Neuroepithelial Layer (NEL), and D = NEL displacement. Utilizing VEMPs mastoid acceleration stimulus magnitudes, the relative displacements were: x = 153 nm at 750 Hz, and x = 102 nm at 1000 Hz. Comparing these displacements to a Striolar Type I Hair Cell bundle model, these displacements put the 750 Hz and 1000 Hz stimuli at complete saturation of the Hair Cell.

Conclusions
Human VEMPs testing stimulus acceleration magnitudes easily exceed the estimated saturation displacement value for striolar Type I hair cell bundle deflection.

References
1. Curthoys, et al. (2016). Hearing Research 331:131-143.

2. Grant and Curthoys(2017). Hearing Research 353:26-35.

PS 267

Utricle Finite Element model; Implications at VEMPs Stimulation Frequencies

Zach Land[1]; Julian Davis[1]; Ian S. Curthoys[2]; **Wally Grant**[3]
[1]University of Southern Indiana; [2]University of Sydney; [3]VA Tech

Background
The mechanism of otolith transduction during high frequency (500 to 3000 Hz) stimulus has been an undiscovered. This high frequency stimulus is now used in Vestibular Evoked Myogenic Potential (VEMP) and is an established clinical test, however the mechanism for the high frequency stimulus is undiscovered. This investigation is one method of investigation for potential stimulus mechanisms for VEMPs.

A Finite Element Model of the utricle is utilized to discover the natural frequency of multiple vibratory modes (mode frequencies, MF) and motions of the various elastic parts and fractions of these parts or sections (mode shapes, MS). The overall system is treated as an elastic continuum model resting on a solid base. The 3 layers are: otoconial layer (OL), compact gel layer (CGL), and column filament layer (CFL), resting on the neural epithelial layer base (NEL).

Methods

Osmium enhanced micro-CT images of guinea pig inner ears were used to construct detailed utricle FEA model. Eleven cross sections of the utricle were outlined every 78 microns using AutoCAD. Split lines, dividing each layer were added to each cross-section to splitting each section into three layers each of the three elastic layers. Material properties of the three layers are as follows:

OL: Density=2400 kg/m^3, Poisson ration=0.45; Elastic Modulus= 6.6 MPa.

CGL: Density=1000 kg/m^3, Poisson ration=0.45; Elastic Modulus= 6600 Pa.

CFL: Density=1000 kg/m^3, Poisson ration=0.45; Elastic Modulus= 16 Pa.

Results

Modal analysis using this finite element model indicates the first five natural frequencies are 343 Hz and 537 Hz, 755 Hz, 828 Hz & 992 Hz. These first three modes of vibration induce a shearing of the hair bundle layer, either through a rigid body linear displacement of the OL, or by rigid body rotation of the OL over the plane of the epithelial surface. Vibrations modes 4 through 6 indicate oscillatory motion of the OL somewhat perpendicular to the epithelial surface.

Conclusion

The model clearly shows that the overall utricle can respond to stimulus frequencies utilized in VEMPs testing that utilize: 500, 750, and 1000 Hz. The various mode shape motions shown in the model illustrate that these motions are capable of hair cell bundle deflection and stimulation.

PS 268

Toward Optimizing cVEMP: 2000 Hz Tone Bursts Improve the Diagnostic Ability of cVEMP in SCD Patients

Kimberley S. Noij[1]; Barbara S. Herrmann[2]; John J. Guinan[1]; Steven D. Rauch[1]
[1]*Massachusetts Eye and Ear Infirmary; *[2]*Massachusetts Eye and Ear Infirmary, Harvard Medical School*

Background

The cervical vestibular evoked myogenic potential (cVEMP) is a test that measures saccular and inferior vestibular nerve function. It is mostly used for the evaluation of patients with Meniere';s disease and semicircular canal dehiscence (SCD). Patients with SCD syndrome suffer from a variety of auditory and vestibular symptoms caused by a bony defect in the superior semicircular canal (SSC). Acoustic stimulation of an ear with such a "third window" causes energy created by stapes footplate motion to shunt towards the dehiscence and away from the cochlear partition. As a result, the pressure difference across the basilar membrane decreases while energy transmission at the vestibular sense organs increases. This can lead to a low frequency air-bone gap (ABG) on audiometric testing, and lower thresholds and larger amplitudes on cVEMP testing, when compared to healthy controls. There is, however, overlap with the healthy population. The aim of this study was to optimize the applicability of cVEMP as a diagnostic tool in SCD patients. Multiple methods were compared, including the use of high frequency tone burst (2000 Hz) stimuli, calculating normalized peak-to-peak amplitude (VEMPn), VEMP inhibition depth (VEMPid; a metric that estimates the percentage reduction in spike rates of sternocleidomastoid muscle motoneurons during a cVEMP test), and a "third window indicator" (TWI) statistic, calculated by subtracting the audiometric ABG at 250Hz from the cVEMP threshold.

Methods

Nineteen patients with SCD and 23 age-matched healthy controls underwent cVEMP testing at 500, 750, 1000 and 2000 Hz. Sound level functions were obtained at all frequencies to acquire threshold and to calculate VEMPn and VEMPid. TWIs were calculated by subtracting the 250 Hz ABG from the ipsilateral cVEMP threshold at each frequency. Ears of SCD patients were divided into three groups based on CT imaging: dehiscent, thin or unaffected. The ears of healthy control subjects constitute a fourth group.

Results

Comparing metrics at all frequencies revealed that 2000 Hz stimuli were most effective at differentiating SCD from normal ears. ROC analysis indicated that for both 2000 Hz cVEMP threshold and for TWI, 100% specificity can be achieved with a sensitivity of 92%. For 2000 Hz VEMPn and VEMPid, 100% specificity can be achieved with a sensitivity of 95.5%.

Conclusion

The best diagnostic accuracy of cVEMP in SCD patients is achieved with 2000 Hz tone burst stimuli.

Audiometric and cVEMP Thresholds Show Little Correlation with Symptoms in SCD Patients

Kimberley S. Noij[1]; Kevin Wong[1]; Maria J. Duarte[1]; Salwa Masud[2]; Nicholas A. Dewyer[1]; Barbara S. Herrmann[3]; John J. Guinan[1]; Daniel J. Lee[4]; Steven D. Rauch[1]
[1]*Massachusetts Eye and Ear Infirmary;* [2]*Harvard Program in Speech and Hearing Bioscience and Technology;* [3]*Massachusetts Eye and Ear Infirmary, Harvard Medical School;* [4]*Eaton Peabody Lab, Massachusetts Eye and Ear Infirmary*

Background
Semicircular canal dehiscence (SCD) syndrome is a condition characterized by the presence of a bony defect in the superior semicircular canal which can lead to a variety of audiologic and vestibular symptoms. Tests to objectively assess the auditory and vestibular system in these patients include threshold audiometry and cervical vestibular evoked myogenic potentials (cVEMP). Patients with SCD often show low frequency air-bone gaps (ABG) and lower thresholds on cVEMP testing compared to non-SCD ears. However, how these metrics correspond with symptomatology remains unknown. In the present study we sought to test the hypotheses that SCD patients'; auditory symptoms are correlated with measureable abnormalities of auditory threshold, specifically a greater ABG, and that patients'; vestibular symptoms are correlated with lower cVEMP thresholds.

Methods
One hundred SCD patients with audiometric, cVEMP, CT imaging data and information about symptoms were included. Medical records and, if available, completed questionnaires, were used to tabulate reported symptoms, which included hearing loss, aural fullness, autophony, hyperacusis, tinnitus, vertigo, imbalance and sound-, pressure- and exercise-associated dizziness. Twenty-five patients also completed the hearing handicap inventory (HHI), dizziness handicap inventory (DHI), autophony index (AI) and the 36-item Short Form Survey (SF-36).

Results
Patients who subjectively reported hearing loss had significantly greater ABG at 250 Hz than patients without this symptom (p=0.001). The magnitude of the ABG at 250 Hz did not correlate with any other auditory symptoms. Patients reporting symptoms of hyperacusis and tinnitus had significantly lower cVEMP thresholds at 500 Hz (p=0.039 and p=0.049) than patients without these symptoms. There was no significant correlation of cVEMP threshold with any vestibular symptoms. Although HHI and AI scores increased with ABG at 250 Hz and

DHI scores increased with cVEMP threshold, these trends were not significant (r^2=0.128, p=0.079; r^2=0.052, p=0.273 and r^2=0.025, p=0.450 respectively). Likewise, neither audiometric nor cVEMP measures showed a significant correlation with SF-36 quality of life scores (r^2=0.01, p=0.634 and r^2=0.02, p=0.505 respectively).

Conclusion
Larger ABG at 250 Hz is correlated with symptomatic subjective hearing loss and lower 500 Hz cVEMP threshold is correlated with symptoms of hyperacusis and tinnitus in SCD patients. Neither the 250 Hz ABGs nor the cVEMP thresholds correlated significantly with auditory- and vestibular handicap scores or quality-of-life. While threshold audiometry and cVEMP are powerful tools to diagnose SCD, they do not correlate with patients'; subjective vestibular symptoms or with how much patients are affected by their symptoms.

Air-Conducted Vestibular Evoked Myogenic Potential Testing in Children and Young Adults: Threshold Responses, Frequency Tuning, and Effects on Sound Exposure

Amanda Rodriguez; Megan Thomas; Kristen Janky
Boys Town National Research Hospital

Objectives
Pediatric vestibular evaluations incorporate cervical and ocular vestibular evoked myogenic potential (c-and oVEMP, respectively) testing; however, characterization of VEMP threshold responses and frequency tuning are unknown. Additionally, unsafe sound exposure can occur because several trials are needed to obtain a VEMP threshold. Obtaining normative VEMP threshold responses at various frequencies in children provides insight on frequency tuning and how to limit excessive sound exposure. The objectives of this study were to (1) characterize c-and oVEMP threshold responses in children and young adults with normal hearing (CNH; ANH) using 500 Hz and 750 Hz tone burst (TB) stimuli, (2) compare frequency tuning of 500 Hz and 750 Hz, and (3) assess whether cochlear changes exist following VEMP threshold testing.

Design
10 younger CNH, 10 older CNH, and 10 ANH participated. All subjects received c-and oVEMP testing at maximum stimulation and threshold. To address frequency tuning, subjects received a 500 Hz TB stimulus in one ear and a 750 Hz TB stimulus in the other ear. Subjects completed tympanometry pre-VEMP, and audiometric threshold testing, distortion product otoacoustic emission (DPOAE) testing, and subjective questionnaire pre-

and post-VEMP to study the effect of VEMP exposure on cochlear function for each stimulus frequency.

Results
(1) c-and oVEMP thresholds were found below maximum stimulation levels for younger (cVEMP= 106 dB SPL; oVEMP= 111 dB SPL) and older (cVEMP= 107.5 dB SPL; oVEMP= 112.5 dB SPL) CNH and ANH (cVEMP= 111.5 dB SPL; oVEMP= 116 dB SPL). Similar threshold responses were found between groups except for younger CNH who had significantly lower thresholds compared to ANH. Additionally, equivalent ear canal volume (ECV) and VEMP threshold responses were linearly correlated. (2) There was no effect of stimulus frequency on VEMP response rates, latencies, peak-to-peak amplitudes, or threshold responses, suggesting similar frequency tuning for 500 Hz and 750 Hz. (3) There were no significant effects of VEMP threshold testing on cochlear function for either stimulus frequency.

Conclusions
CNH and ANH show VEMP threshold responses below high stimulation levels and similar frequency tuning between 500 Hz and 750 Hz. Use of 750 Hz could be regarded as the safer stimuli due to its shorter duration and thus reduced sound exposure. Children with smaller ECV had present responses at maximum stimulation and lower thresholds, suggesting that VEMP testing could be initiated at lower acoustic levels to minimize sound exposure and optimize testing.

PS 271

Ocular and Cervical Vestibular Evoked Myogenic Potentials Evoked with Airborne Low-Frequency Sound in Humans

Vivien Lücke[1]; Lutz Wiegrebe[1]; Torsten Marquardt[2]; **Markus Drexl**[3]
[1]*Ludwig-Maximilians-Universität München, Division of Neurobiology, Dept. Biologie II Ludwig-Maximilians-Universität München;* [2]*Ear Institute, University College London;* [3]*German Center for Vertigo and Balance Disorders, Ludwig-Maximilians Universität München, Munich, Germany*

Sound is not only detected by the cochlea, but also, at high intensities, by the vestibular system. Acoustic activation of the vestibular system can manifest itself in vestibular evoked myogenic potentials (VEMPs). VEMPs are typically recorded from the sternocleidomastoid muscle (cervical, or c, VEMPS) or from the extra-orbital muscles (ocular, or o, VEMPs) and are mainly driven by activation of the otolithic organs. In a clinical setting, VEMPs are usually evoked with rather high-frequency sound (500 Hz and higher), despite the low-pass properties of the otolithic membranes. Only a fraction of saccular and utricular hair cells, in the striolar region, is available for high-frequency stimulation, as they are not, or to a lesser extent, subject to low-pass filtering. Here, we recorded growth functions of oVEMPs and cVEMPs evoked with airborne sound in order to estimate VEMP thresholds at several low-frequency stimuli in 24 young, healthy participants. Sound stimuli were generated with a 10-inch aluminium cone loudspeaker, coupled to a 4.5- meter-long plastic tube, the tip of which was fed and sealed into the ear canal of the participants, resulting in a low-distortion, high-output system. Acoustic stimuli (40, 60, 80, 100 and 120 Hz) consisted of 128 single periods (Hanning-windowed), and were calibrated in-situ. Stimuli were presented with repetition rates between 3 and 6 Hz, and maximum levels did not exceed 140 dB pSPL. It was also ensured that the daily total sound energy exposure did not exceed 132 dB (the LAeq exposure specified by EU limits). cVEMPS and oVEMPs could be evoked with all tested frequencies. Thresholds showed simple high-pass characteristics, i.e. lower thresholds with higher frequencies, with a median minimum of 119 dB pSPL and 121 dB pSPL at 120 Hz, respectively. A-weighting the thresholds of cVEMPS and oVEMPs resulted in median thresholds for all frequencies between 103 and 104 dB (A), and 101 and 105 dB (A), respectively. Since A-weighting mostly reflects middle ear attenuation, it can be concluded that the observed characteristics are mainly due to middle ear properties. Latencies of N1 and P1 were frequency-independent when the stimulus period was taken into account. The response of the otholitic organs, as assessed with oVEMPS and cVEMPs, to low-frequency sound is uniform and not tuned when corrected for middle ear attenuation by A-weighting. This work was funded by a BMBF grant (01EO1401) to MD and LW, and TM was supported by EMPIR project 15HLT03 (EARS II).

PS 272

Development of a Cost Effective System for Measuring Vestibular Evoked Potentials

Yawen Yu[1]; Peter Agada[1]; Eric Anson[2]; Emily Keshner[1]
[1]*Temple University;* [2]*Johns Hopkins Medical Institutes*

Background
The overarching goal of the current project was to develop a cost-effective system measuring vestibular evoked potential (VEP) that can be synchronized to motion capture system and virtual environment. Such synchronization may allow looking into research questions about the connection of vestibular response to visual dependence, visual-induced vection, and motion sickness. Here, vestibular responses to acoustic stimuli were compared between a commercial system and our cost-effective system.

Methods

Six healthy young adults (age: 29.5 ± 6.3 years) without known neurological, otological, and ophthalmological disease/complaints participated in the study. All participants underwent testing procedures by both the commercial and the cost-effective systems to elicit both ocular and cervical vestibular evoked potentials (VEP) using tone burst stimuli (500Hz, 125dB SPL, repeats at 5Hz). The commercial system delivered the sound stimuli mono-aurally via foam eartips from the VIASYS healthcare (Madison, WI) and recorded the electromyographic (EMG) with the Carefusion Synergy system (Dublin, OH). The cost-effective system delivered the sound stimuli mono-aurally via Etymotic ER-3C audiometric insert earphone with foam eartips (Elk Grove Village, IL), and recorded the EMG using a circuit with 2-channel instrumentation amplifier and a customized LabVIEW program for communicating with the data acquisition board and integrating user interfaces. A total of 9 electrodes were placed on mid-point of the sternocleidomastoid muscles, the sternoclavicular junctions, the edge of the inferior oblique muscles, and 2 cm below IOs, and manubrium sterni as a shared ground. EMG signals were amplified 2500x and band-pass filtered (20-2000Hz for cervical and 3-500Hz for ocular evoke potentials). Subjects were tested in the supine position with trunk elevated 30° from horizontal, and were instructed to maintain a 20° upgaze during the procedure for ocular VEP. The latency and amplitude of p13, n23 of cervical VEP and n10, p16 of ocular VEP were recorded; asymmetry ratios (AR) were computed accordingly. Interclass correlation (ICC) with 2-way random effect, absolute agreement model was employed.

Results

Between the two systems, cervical VEP (p13, n23) latencies and AR had fair-to-good reliability (ICC>0.6). Ocular VEP (n10) latency and amplitude had fair-to-good reliability (ICC>0.5); ocular AR had excellent reliability (ICC>0.75).

Conclusions

Overall, our cost-effective system demonstrated similar VEP results as that gathered using a commercial system. Such a cost-effective system producing similar results as a commercial system will create more opportunities to pair with other experimental devices to answer broader research questions.

Human Aspects of Cochlear Synaptopathy

SYMP 01

Effects of noise exposure on young adults with normal audiometric hearing

Christopher J. Plack[1]; Garreth Prendergast[1]; Hannah Guest[1]; Karolina Kluk[1]; Rebecca E. Millman[1]; Rebecca S. Dewey[2]; Deborah A. Hall[3]; Kevin J. Munro[1]
[1]University of Manchester; [2]University of Nottingham; [3]National Institute for Health Research Nottingham Biomedical Research Centre

Results from rodent models show that noise exposure can cause loss of synapses between inner hair cells and auditory nerve fibers (cochlear synaptopathy) without affecting threshold sensitivity. However, in a series of studies involving humans aged 18 to 35 with normal audiograms and a wide range of lifetime noise exposures we have found no evidence for an effect of noise exposure on auditory brainstem response amplitude (including wave I), or envelope following response amplitude. We have also found no evidence for an effect of noise exposure on behavioral measures including frequency discrimination, intensity discrimination, interaural phase discrimination, modulation detection, sound localisation, musical harmony perception, and speech-in-noise identification. Considered in relation to other recent findings, it seems likely that humans are less susceptible to noise-induced synaptopathy than rodents. Noise-induced synaptopathy may only be a significant cause of hearing deficits in humans with extreme exposures, and may always occur in combination with a high-frequency audiometric loss.

SYMP 02

Evidence for age-related synaptopathy unrelated with supra-threshold speech-in-noise intelligibility deficits

Enrique A. Lopez-Poveda[1]; Peter T. Johannesen[1]; Byanka C. Buzo[1]; James M. Harte[2]; Niels H. Pontoppidan[3]
[1]University of Salamanca; [2]Interacoustics Research Unit; [3]Eriksholm Research Centre

Cochlear synaptopathy (or the loss of primary auditory synapses) remains a subclinical condition of uncertain prevalence in living humans. Here, we investigate (1) whether it occurs in humans, (2) whether it may be di-

agnosed using brief tone audiometry, and (3) whether it contributes to supra-threshold speech-in-noise intelligibility deficits. For 80 listeners with normal clinical audiograms (age range: 16-68 years, mean: 29 years), we measured click-evoked auditory brainstem responses (ABRs), self-reported noise exposure across the whole life, absolute detection thresholds for brief tones, and speech reception thresholds (SRTs) for sentences (at 65 dB SPL) and words (at 50, 65 and 80 dB SPL) in steady-state and fluctuating maskers. Based on findings in animals, we assumed that the shallower the rate of growth of ABR wave-I amplitude as a function of level, the higher the risk of suffering from synaptopathy. We found that wave-I growth rates decreased with increasing age but not with increasing noise exposure. In an attempt to account for the potential effect of high-frequency audiometric losses on the shallower growth rates, we identified 13 pairs of younger and older listeners with matched audiograms up to 12 kHz. The older group still had shallower wave-I growth rates, indicating that high frequency loss was not the only contributor to the negative effect of age on wave-I growth rate. Surprisingly, neither the audiometric thresholds for brief sounds or the SRTs were correlated with wave-I growth rate and they were statistically similar for the two paired groups. Altogether, the data are consistent with the existence of age-related but not noise-related synaptopathy. In addition, the data do not support the notion that synaptopathy causes supra-threshold speech-in-noise intelligibility deficits. [We thank Filip Rønne for his help at the project start, and the Oticon Foundation, MINECO (BFU2015-65376-P), and FEDER for financial support.]

SYMP 03

Hidden hearing loss in humans with normal audiometric thresholds

Stéphane F. Maison; Peizhe Wu; Leslie Liberman; M. Charles Liberman
Harvard Medical School

We are taking two approaches to the extension of our studies of cochlear synaptopathy and hidden hearing loss from animals to humans. In one ongoing study, we are quantifying survival of hair cells, cochlear nerve synapses and peripheral axons using confocal microscopy in human temporal bones obtained at autopsy. Our data from "normal-hearing" adult ears aged 30 - 90 yrs suggests that, as in aging mice, there is dramatic loss of cochlear neural elements before there is corresponding loss of inner hair cells. In a second set of studies, we are comparing a battery of physiological measures with performance on challenging word-recognition tasks in adults with normal audiometric thresholds but widely varying histories of ear abuse. Results to date suggest that performance deficits on difficult word-recognition

tasks are correlated with physiologic response deficits consistent with cochlear synaptopathy. Alternative approaches toward the diagnosis of this condition in humans will be discussed.

SYMP 04

Individualized assays of suprathreshold hearing deficits - translational challenges

Hari Bharadwaj; Alexandra Mai; Jennifer Simpson; Michael Heinz
Department of Speech, Language, and Hearing Sciences, Purdue University

Animal studies have robustly established that acoustic overexposure can cause cochlear synaptopathy without hair-cell degeneration or permanent audiometric threshold shifts. Separately, we have documented that even among listeners with normal audiometric thresholds, large individual differences exist in the ability to perceive temporal features of clearly audible sounds, and to selectively listen to target sounds amidst competition. Crucially, these differences correlate with non-invasive auditory nerve and brainstem measures, suggesting that they may arise from cochlear synaptopathy. However, studies on individuals at higher risk for synaptopathy using similar measurements have yielded inconsistent results. Indeed, the largest studies of individuals with normal thresholds do not show a link between estimated noise-exposure levels and non-invasive measures of auditory nerve integrity. While one possible interpretation of these null results is that synaptopathy does not occur to significant extent in humans, it is also possible that other sources of variability from measurement-related, physiological, and genetic factors obscure the effects of noise exposure. Here, we consider many such sources of variability, and describe how we have modified our experiment design and non-invasive battery for an ongoing study of noise-exposed individuals based on insight from recent literature.

SYMP 05

Model-based design of subcortical EEG methods that quantify the synaptopathy aspect of hearing loss.

Sarah Verhulst[1]; Viacheslav Vasilkov[2]; Markus Garrett[3]; Sarineh Keshishzadeh[1]
[1]Ghent University; [2]Oldenburg University; [3]Cluster of Excellence "Hearing4all" and Medizinische Physik, Dept. of Medical Physics and Acoustics, Oldenburg University, DE

Even though animal physiology studies have demonstrated that cochlear synaptopathy affects the amplitude of auditory brainstem responses (ABRs) and en-

velope-following responses (EFRs), the sensitivity of these subcortical EEG metrics in diagnosing synaptopathy in humans is unclear. Confounding factors include head size, gender and other forms of peripheral hearing loss (e.g., outer-hair-cell (OHC) loss) that may co-exist and affect subcortical EEG amplitudes as well. Although OHC loss can be quantified using otoacoustic emissions, it is worthwhile focusing on a single EEG metric that can quantify both aspects of peripheral hearing loss. EEG measurement accuracy can be improved by designing stimulation paradigms on the basis of model simulations that can simulate and disentangle how different forms of peripheral hearing loss impact EEG metrics.

In this work, we optimize subcortical EEG stimulation paradigms for synaptopathy using a computational model of the auditory periphery that simulates the broadband and level-dependent features of human ABR and EFRs. First, we focused on rendering EFR methods more frequency-specific by masking off-CF, and enhancing on-CF, contributions to the EFR. The optimized stimulation paradigms allow for an interpretation of EFR strength in terms of localized AN synapse differences. Secondly, we simulated how OHC loss or dysfunction impacts the sensitivity of ABR and EFR metrics of synaptopathy and show that: (i) a combination of the slope between the EFR fundamental and 1st harmonic together with the ABR/EFR amplitude ratio, or (ii) the ABR growth ratio that takes into account both the amplitude and latency growth of ABRs, can map listeners onto a OHC loss vs synaptopathy degree scale. We compared the simulations to recordings from listeners with normal and sloping high-frequency audiograms to evaluate the practical use of the proposed relative subcortical EEG metrics.

SYMP 06

Noise Exposure, Cochlear Synaptopathy and Listening Difficulties: EEG and Behavioural Measures

Elizabeth Beach[1]; Ingrid Yeend[2]; Joaquin Valderrama[3]; Mridula Sharma[4]; Harvey Dillon[1]
[1]National Acoustic Laboratories/HEARing CRC;
[2]National Acoustic Laboratories/Macquarie University/HEARing CRC; [3]National Acoustic Laboratories;
[4]Macquarie University/HEARing CRC

We investigated the relationship between noise exposure, cochlear synaptopathy, and listening difficulties in 122 adults aged 29 to 57 with normal or near-normal hearing. Participants undertook a large test battery that included audiometric testing, tasks that assessed attention and memory, speech-in noise tasks, and other measures of auditory perception. A subset of participants (n=74) completed additional electrophysiological testing which included responses from the auditory brainstem

and cortex. When auditory brainstem responses (ABR) were plotted against lifetime noise exposure, there was considerable variability across the sample. Nevertheless, we observed a significant (but weak) association between noise exposure and wave I ABR amplitudes to clicks presented at 75 dB nHL (-0.038 μV/log10Pa2h, p = 0.026). The significant trend revealed that those with more noise exposure produced smaller wave I ABR amplitudes than those with less noise exposure, although the result appeared to be driven by a small number of subjects whose data were consistent with the hypothesised pattern of results. Analysis of cortical auditory evoked potentials (in response to /da/ presented at (a) +10 dB, (b) +5dB and (c) 0dB SNR; and 'iterated ripple noise' obtained at (a) SNR=+60dB; (b) SNR=+60dB; (c) SNR=+15dB; (d) SNR=+5dB) revealed no association between noise exposure and any of the cortical responses. This suggests that any effects of noise exposure either dissipate at higher levels of the auditory pathway or are unable to be observed using our chosen measures. In the larger cohort, we found no relationship between noise exposure and performance on speech-in-noise or other auditory tasks. However, regression analysis showed that attention, working memory and extended high frequency hearing thresholds were significant factors that affected listening in noise. When taken together, our results suggest that listening difficulties arise from a constellation of factors, and although noise-related cochlear synaptopathy may be one of these, we need better methods for measuring it if we are to fully understand its role relative to other cognitive and auditory factors.

SYMP 07

Reduced ABR wave I amplitude in Veterans and firearm users suggests synaptopathy

Naomi Bramhall; Dawn Konrad-Martin; Garnett P. McMillan
VA RR&D NCRAR

ABR wave I amplitude reductions are associated with animal models of cochlear synaptopathy. As a proxy for synaptopathy in humans, wave I amplitude was measured in young people with normal pure tone thresholds. Veterans with high levels of military noise exposure and non-Veterans who reported using firearms demonstrated smaller wave I amplitudes at suprathreshold levels than participants with less noise exposure. Tinnitus was associated with the Veteran high exposure group and with reduced ABR wave I amplitude. These data suggest that synaptopathy may occur in response to noise exposure in humans and be associated with tinnitus.

Decision Making in Complex Statistical Environments: Neural Representation and its Correspondence with Principles of Decision Making

SYMP 08

Evidence accumulation mechanisms for sensory detection in the human brain

Simon Kelly[1]; Redmond O'Connell[2]
[1]University College Dublin; [2]Trinity College Dublin

Humans and animals often face situations where relevant sensory changes must be detected within streams of constant stimulation and immediately acted upon. When these events are intermittent and sometimes subtle, reliable detection is afforded by integrating evidence over protracted time scales, eventually gathering "enough" to commit to a decision to act. Using simple paradigm innovations, it has recently been demonstrated that such integrate-to-bound processes can be dynamically traced in noninvasively recorded electrophysiological signals on the human scalp (EEG). Similar to findings in monkeys and rodents, effector-selective motor preparation signals in EEG exhibit buildup dynamics at a rate that scales with evidence strength and reach a stereotyped level at the time of the response regardless of how long it took to initiate that response. These properties, which are hallmarks of the accumulation-to-bound processes posited in longstanding computational models of decision making, are also exhibited by a centro-parietal event-related potential component ("CPP") that represents cumulative evidence at an abstract, supramodal, and motor-independent level. In this talk I will describe a line of studies focusing on the dynamics of this process to gain insights into sensory detection mechanisms for various visual and auditory target detection paradigms. I will particularly focus on recent work providing evidence for 1) the adaptive adjustment of decision bounds across contexts with different expected sensory target strengths, in accordance with computational mechanisms of leaky integration, 2) the employment of low-level target detection mechanisms to facilitate evidence accumulation by signaling the time and location of evidence onset, and 3) the forging of multiple parallel evidence accumulation processes to detect targets in multisensory visual-auditory stimulus streams. The findings place evidence accumulation at the center of a multi-tiered neural architecture for accomplishing challenging sensory detection decisions.

SYMP 09

How the brain discovers structures in rapid sound sequences.

Maria Chait
University College London

I will present ongoing work in my lab using brain imaging (EEG, MEG and fMRI), behavioural and eye-tracking experimentation to reveal how human listeners discover patterns and statistical regularities in sound sequences. Sensitivity to patterns is fundamental to sensory processing, in particular in the auditory system, and a major component of the 'predictive coding' theory of brain function. However, a key element of this theory - the process through which the brain acquires this model, and its neural underpinnings - remains poorly understood. Our experiments focus on this missing link by measuring behavioural and time-locked brain responses to rapid tone-pip sequences governed by specifically controlled rules along a variety of feature dimensions.

SYMP 10

Texture Perception and Auditory Scene Analysis

Josh McDermott[1]; Richard McWalter[2]
[1]MIT; [2]Department of Brain and Cognitive Science

Sound textures, as produced by rain or crowd noise, are believed to be represented using time-averaged summary statistics. Textures often form the background to foreground sounds of interest, raising the question of how texture representations interact with auditory scene analysis. I will discuss evidence that the time-averaging underlying texture perception is selective, excluding foreground sounds that are not part of the texture. The results suggest that texture perception is a neglected but critical component of auditory scene analysis.

SYMP 11

Sensitivity to sound texture statistics in human cortex

Jens Hjortkjaer[1]; Richard McWalter[2]; Kristoffer Madsen[3]; Hartwig Siebner[3]; Torsten Dau[1]
[1]Hearing Systems group, Technical University of Denmark; [2]Department of Brain and Cognitive Science; [3]Danish Research Centre for Magnetic Resonance

Sounds in natural acoustic scenes exhibit statistical dependencies that are stable over long time scales. A central question is how such stimulus statistics might be represented in the auditory system. Here, we combined sound texture synthesis with human functional MRI to measure sensitivity to sound texture statistics at different stages of the auditory system. Sound texture stimuli were synthe-

sized using a biophysically plausible model of modulation processing in the auditory periphery, similar in structure to the one proposed by McDermott and Simoncelli (2011). Using this model, we analyzed recorded natural sounds and then imposed the measured statistics on a noise seed to synthesize texture stimuli. The statistics were cumulatively imposed in five parameter groups corresponding to: cochlear subband power, cochlear marginal statistics, correlation between cochlear subbands, modulation subband power, and correlation between modulation subbands. We found that responses across auditory cortex increased as these higher-order statistics were added to spectrally matched noise stimuli. Parametric increases in BOLD responses increased in a posterior direction from primary auditory fields into the planum temporale. Responses in the inferior colliculus, on the other hand, were equally strong for the different statistics and thus did not differentiate the statistical properties of the sounds. Our results indicate that neural sensitivity to the higher-order statistics that characterize texture sounds may emerge at the cortical level.

SYMP 12

Adaptive Time-Averaging for Texture Perception

Richard McWalter[1]; Josh McDermott[2]
[1]*Department of Brain and Cognitive Science; [2]MIT*

Sensory receptors measure signals over short time scales, but our perception of the natural world often entails integrating these measurements over much longer extents. Texture provides a paradigmatic example of such integration - it is believed to be represented by statistics that are time-averages of sensory measurements. We investigated the timescale of integration in human listeners for textures that underwent changes in statistics and temporal continuity. Our results revealed a multi-second integration process that appears to adapt itself to the temporal complexity of the texture, extending integration when it benefits statistical estimation of a variable signal.

SYMP 13

Multi-scale tracking of stimulus statistics from auditory cortices to frontal cortex

Jennifer Lawlor[1]; Célian Bimbard[2]; Bernhard Englitz[3]; Shihab Shamma[4]; Yves Boubenec[2]
[1]*Ecole Normale Supérieure; [2]Ecole Normale Supérieure, Paris, France; [3]Donders Institute for Brain Cognition and Behaviour, Radboud University; [4]Ecole Normale Supérieure, University of Maryland*

Complex, cluttered acoustic environment, such as a busy street, are characterized by their ever-changing dynamics. Despite their complexity, listeners can readily detect changes in continuous acoustic streams. However, the neural basis of the extraction of relevant information in complex streams during goal-directed behavior is currently not well understood. As a model for change detection in complex auditory environments, we designed spectrotemporally broad tone clouds whose statistics change at a random time. Ferrets were trained to detect these changes within continuous sound. Hence, they are faced with the dual-task of estimating the baseline statistics and detecting a potential change in those statistics at any moment, mimicking real-life challenges. To characterize the extraction of relevant sensory information performed between sensory cortices and frontal areas, we performed electrophysiological recordings in the primary auditory cortex (A1), secondary auditory cortex (PEG) and frontal cortex (FC) of the behaving ferret. A1 neurons exhibited strong onset responses and reduced change-related discharges specific to neuronal tuning. PEG population showed reduced onset-related responses, but enhanced and broader change-related modulations. Finally, FC neurons presented an enhanced response to all change-related events only during behavior, possibly reflecting accumulation of sensory evidence. In addition, PEG and FC population dynamics showed a time-dependent evolution within trials and before the change occurred, possibly reflecting an online estimation of the ongoing baseline statistics, a necessary process in this dual-estimation task. All together, these area-specific responses suggests a behavior-dependent mechanism of sensory extraction and amplification of task-relevant event.

SYMP 14

Modeling the neural representation of changes in stimulus statistics in audition

Bernhard Englitz[1]; Shihab Shamma[2]; Yves Boubenec[3]
[1]*Donders Institute for Brain Cognition and Behaviour, Radboud University; [2]Ecole Normale Supérieure, University of Maryland; [3]Ecole Normale Supérieure, Paris, France*

Change detection is commonly performed against the statistics of the stimulus environment. Only the conjunction between a new sound and the environmental statistics determines what constitutes a change. In realistic, continuous-time contexts, change detection requires an estimation process of the recent statistics in parallel with another process assessing whether the current stimuli are still consistent. We demonstrate that this dual-estimation can be achieved with a dual-time scale model, which performs similarly to humans on the same task. Further, a model of cortical processing accounts similarly well for the detection of statistical changes, thus building a bridge between principles and neural implementation.

Auditory Cortex: Anatomy, Physiology & Function I

PD 01

Auditory Cortex Drives Feedback-Dependant Vocal Control in Marmosets

Steven Eliades; Joji Tsunada
University of Pennsylvania

Individuals with hearing loss have difficulty in acquiring and maintaining normal speech. Even amongst those with normal hearing, self-monitoring of auditory feedback during vocal production plays an important role in the control of both speech and voice, and allows for rapid correction of errors in vocal output. Previous work in the auditory cortex of both humans and animals has demonstrated a suppression of neural activities during vocal production that acts to increase sensitivity to vocal feedback. However, the behavioral role played by the auditory cortex in the control of vocal production is unclear. We investigated the contribution of auditory cortical activity during feedback-dependant vocal control using marmoset monkeys. Combining real-time frequency-shifted feedback, chronic neural recordings, and electrical microstimulation of auditory cortex, we found that neuronal activity in the auditory cortex predictsfuture compensatory changes in vocalization acoustics. We further found that electrical stimulation of auditory cortex evokes rapid changes in vocal production, but only for stimulation of the right auditory cortex. Auditory cortical stimulation was also found to bias vocal compensation during frequency-shifted feedback. Together, these findings demonstrate the causal role of auditory cortex in vocal self-monitoring and feedback-dependant vocal control. These results have further implications for the understanding of the sensory-motor control of human speech. This work was supported by NIH/NIDCD Grant K08-DC014299.

PD 02

Separate representation of dry and reverberated natural stimuli in mouse auditory cortex

Tina Reuter[1]; Dominic Gonschorek[1]; **K. Jannis Hildebrandt**[2]
[1]University of Oldenburg, Cluster of Excellence Hearing4all; [2]Univesity of Oldenburg, Cluster of Excellence Hearing4all

Reverberation is a major source of noise in acoustic signals, masking both temporal and spectral features of acoustic signals. One solution for the invariant representation of such signals is a reverberation insensitive coding of acoustic signals within the same population of auditory neurons. Evidence for such a representation has been found in the mammalian auditory cortex and has been suggested to arise from dynamic inhibitory feedback[1]. An alternative strategy for the de-reverberation of acoustic signals would be an explicit representation of the reverb that could then be subtracted from a reverberation-containing representation in a feed-forward manner. We aimed to find evidence for either of these two strategies in the primary auditory cortex (ACx) of mice.

We recorded populations of neurons in ACx of awake mice in response to a set of animal vocalizations. We compared the neural representation of dry and reverberated stimuli in simultaneously recorded populations. To this end, we applied decoding analyzes of the temporal structure of the stimuli and stimulus reconstruction based on population responses. In order to further characterize the recorded units, we applied single tones and dynamic random chord (DRC) stimuli in addition to the vocalizations.

We observed that about 40% of the recorded units showed a significant response to the vocalizations. Single units responded specifically to different vocalizations and within the vocalization to different motives. Surprisingly, when comparing responses to dry and reverberated stimuli, up to a quarter of the responsive units in the population exclusive responded to either dry or reverberated stimuli. Stimulus reconstruction from theses two populations showed a representation of the original signal in either condition, supported by two distinct populations of cells. Further characterization of the two populations yielded clear difference both in response to pure tones and DRCs. Dry-exclusive units showed broad tuning and less-complex spectro-temporal receptive fields (STRFs). Reverb-exclusive units showed fine spectral tuning and specifically structured STRFs, featuring strong side-band inhibition and complex temporal structure. Linear filtering of reverberated stimuli with these receptive fields was able to recover most of the observed distinct responses.

Our results suggest an alternative strategy for the coding of reverberated acoustic signals in distinct populations of neurons using mostly linear processing. Such a strategy could preserve the information about the reverb within a suitable representation of the original signal.

[1]Mesgarani, N., David, S. V., Fritz, J. B., & Shamma, S. A. (2014). Mechanisms of noise robust representation of speech in primary auditory cortex. Proceedings of the National Academy of Sciences, 111(18), 6792–6797. http://doi.org/10.1073/pnas.1318017111

PD 03

Neuromodulation of behavioral responses to distress pup vocalizations

Ioana Carcea[1]; Naomi Lopez[2]; Rumi Oyama[2]; Robert C. Froemke[1]
[1]*NYU School of Medicine;* [2]*NYU Medical School*

Long-term plasticity in the cortex is thought to be important for learning and experience-dependent changes in behavior, but when do such changes occur during natural experience? Activation of subcortical neuromodulatory systems is often required to enable mechanisms of synaptic and spiking plasticity, and thus it is important to relate periods of heightened modulation to changes in cortical responses in a behavioral context. Social interactions such as forms of maternal care are likely to involve increases in activity particularly of the paraventricular nucleus (PVN) oxytocin neurons, but it has remained unclear when these neurons fire during maternal experience, and what behavioral episodes might drive experience-dependent maternal abilities.

Recently we examined how oxytocin acts in the mouse left auditory cortex to enhance responses to ultrasonic infant distress calls, promoting long-term synaptic plasticity and enabling maternal care towards pups in virgin females co-housed with an experienced mother and her litter (Marlin et al., Nature 2015). To understand when these changes might occur during days of natural maternal experience, we constructed a system for synchronously and continuously recording audio, video and neuronal responses before, during and after days to weeks of co-housing. Using this system, we documented episodes of interactions between the adult females and adults with the pups, while making tetrode recordings from PVN neurons and/or auditory cortical neurons in behaving mice. We found that in virgin mice, PVN neurons spiked more frequently during interactions with another female or with a pup, suggesting that the ongoing activity of this neurons would be higher during co-housing compared to single-housing conditions. PVN neurons in virgins also fired robustly when these mice observed a retrieving episode performed by the dam with which they were co-housed. We confirmed that PVN neurons also fire in mothers during the retrieval behavior. In the same system, we recorded bulk evoked calcium activity in left auditory cortex to identify changes in pup call representation over the course of learning retrieval behavior. This system therefore allows us to determine what environmental conditions or social interactions activate modulatory neurons, gating behaviorally-relevant cortical plasticity in real time.

PD 04

Absence of Early Hearing Experience Reduces Evoked Theta and Induced Alpha Activity in the Auditory Cortex

Prasandhya Astagiri Yusuf[1]; Peter Hubka[1]; Jochen Tillein[2]; **Andrej Kral**[1]
[1]*Institute of AudioNeuroTechnology (VIANNA), Hannover Medical School;* [2]*Department of Otorhinolaryngology, J.W. Goethe University*

Cochlear stimulation activates the auditory cortex through thalamic inputs, while the auditory cortical areas subsequently interact via corticocortical connections. These activations are reflected in local field potentials (LFPs) in the form of evoked (phase-locked) and induced (non-phased-locked) cortical responses, respectively. Here we investigated an effect of congenital deafness on evoked and induced responses in the primary auditory cortex (A1) and posterior auditory field (PAF). We evaluated bipolar derivation LFPs recorded simultaneously from A1 and PAF in hearing controls (HCs) and congenitally deaf cats (CDCs). Responses elicited by acoustic stimulation in HCs and cochlear implant electric stimulation in HCs and CDCs were compared to investigate the effect of stimulation mode (acoustic vs. electric) and developmental experience (hearing vs. deaf). To capture the highly dynamic cortical activities containing both oscillatory and transient components, a quadratic time-frequency transform called Matching Pursuit (MP) algorithm was used to decompose the signal and to reveal the evoked and induced responses. This method distributes the energy of the signal over the two independent variables time and frequency, including the low frequency components without compromising resolution in both domains (Mallat & Zhang, 1993, IEEE Trans Signal Process).

Similar to our previous observations using wavelet time-frequency decomposition (Yusuf et al., 2017, Brain), we observed reduced induced responses in CDCs. However, the MP algorithm additionally localized induced late activity decrease to the alpha band (7-15 Hz) in the deaf PAF. By the advantage of revealing low frequency components from this method, in the evoked response, we additionally revealed evoked theta band (4-7 Hz) oscillations, lasting until 400 ms post-stimulus time, both in A1 and PAF for all groups. Again, significantly weaker evoked theta was found in the CDCs. This evoked theta response likely represents the origin of the N1 component at latencies ~ 100 ms that is reduced in amplitude in EEG studies of late-implanted congenitally deaf children (Ponton et al, 2001, Hear Res). The findings are also in-line with sight restoration study from congenital blindness, which found weaker evoked theta response in comparison to controls (Bottari et al, 2016,

Sci Rep). This could indicate deficits in long-range synchronization of the auditory cortex with remote neural structures, including hippocampus.

PD 05

Dynamic conversion of sensory evidence to decision signal in ferret frontal cortex

Celian Bimbard[1]; Jennifer Lawlor[1]; Shihab Shamma[2]; Yves Boubenec[3]
[1]Ecole Normale Supérieure; [2]Ecole Normale Supérieure, University of Maryland; [3]Ecole Normale Supérieure, Paris, France

The frontal cortex is often associated with enhancement of relevant information for goal-directed behavior. In particular, frontal cortex (FC) neurons of the behaving ferret have been shown to respond selectively to target auditory stimuli during discrimination tasks (Fritz et al., 2010). However, in natural and cluttered environments, sounds are not necessarily presented in token-based sequences. Instead relevant events are embedded in continuous sound streams and their detection demands to dynamically update the representation of incoming stimuli (Lawlor et al., 2017). Here, we attempt at characterizing the extraction of relevant sensory information from complex continuous sounds performed at the level of frontal areas. To address this question, we trained ferrets on a change detection paradigm where animals have to constantly monitor a stochastic and continuous acoustic stream to detect subtle statistical changes. We then gathered electrophysiological data in the dorso-lateral FC of the behaving ferret. Because modulations in FC neurons' firing rate can be correlated with a large variety of (sometimes overlapping) task-relevant and irrelevant events, we used a Linear Non-Linear Poisson model to disentangle the contribution of different predictors (sound onset, change in stimulus statistics, decision, motor activity...) to those modulations. Our model allows us to orthogonalize the responses to each predictor and quantify their specific contribution to the firing rate of individual neuron. By focusing our study on the responses of the neurons at the single trial category level (hit vs. miss, small vs. big changes, etc.), we found that neurons encoded both stimulus changes in a stimulus-dependent manner and perceptual decisions in a categorical stimulus-independent fashion. A substantial fraction of the neurons (~25%) displayed a dual encoding of these two types of events, suggesting that conversion from sensory evidence towards a decision signal may take place in the FC.

PD 06

Assessing Temporal Dynamics of Auditory Processing Through Classification of Subcortical and Cortical Responses to Speech and Music Sounds

Blair Kaneshiro[1]; Steven Losorelli[1]; Gabriella Musacchia[2]; Nikolas Blevins[1]; Matthew Fitzgerald[1]
[1]Stanford University; [2]University of the Pacific

The ability to categorize sounds is foundational to speech perception. While normal hearing (NH) listeners perform this task with ease, hearing-impaired individuals can find it challenging. Populations receiving novel sensory input (e.g., cochlear implant users) may additionally have difficulty describing what is heard. Therefore, brain-based measures of sound perception can be useful for assessing and treating patient populations.

To address this issue, we classify cortical and subcortical EEG responses to speech and non-speech sounds. EEG classification has been used to study categorization of language, visual, and musical stimuli. Classifier confusion matrices can be visualized to display neural "representational spaces" of stimuli. This may allow us to determine whether a patient is capable of identifying a sound without providing a behavioral response. We employ a "searchlight" approach, classifying temporal subsets of responses to elucidate the time course of auditory processing.

We performed two pilot experiments. First, 8 NH participants heard six speech and music stimuli (length 135 msec, f0 100 Hz), while cABRs were recorded from Fz. Across participants, we obtained 94 trials for classification, each comprising the average of 500+/500- responses to a given stimulus. Next, 5 NH participants heard eight speech, music, click, and tone stimuli (length 120 msec, f0 180 Hz), while dense-array cortical EEG was recorded. We obtained 853 classification trials across participants, each comprising 10 trial-averaged responses to a given stimulus.

Cleaned data epochs were classified using Linear Discriminant Analysis. Brainstem responses were classified in nonoverlapping 8-msec windows from 0-136 msec post-stimulus onset with leave-one-out cross validation. Cortical responses were classified from -104-480 msec post-stimulus onset in 64-msec windows advancing in 40-msec increments with 10-fold cross validation. Confusion matrices were converted to distance matrices and visualized as dendrograms.

Brainstem accuracies reach statistical significance 8 msec post-stimulus onset and remain fairly consistent

thereafter. Dendrograms reveal consistent "ba"/"da" category clusters starting from 8 msec, possibly reflecting the transition from distinct consonant to identical vowel content. Cortical accuracies are statistically significant between 80-320 msec post-stimulus onset, peaking between 100-200 msec, possibly implicating N1/P2 components. Dendrograms show that acoustically similar stimulus pairs (e.g., "oo"/"ee", "da"/"ta") often form category clusters.

Taken together, these pilot results suggest that classification may objectively model sound processing in NH individuals, potentially providing means to study hearing loss and rehabilitation. We are now refining the experimental design with a consistent stimulus set, and considering alternative EEG features for classification.

PD 07

Natural Speech-Evoked Frontal Cortex Response Reflects Speech-In-Noise Understanding Difficulty

Subong Kim[1]; Adam Schwalje[2]; Phillip Gander[3]; Andrew S. Liu[4]; Timothy Griffiths[5]; Inyong Choi[6]
[1]University of Iowa; [2]University of Iowa Hospitals and Clinics; [3]Human Brain Research Laboratory, Department of Neurosurgery, The University of Iowa; [4]Human Brain Research Laboratory, Department of Otolaryngology-Head and Neck Surgery, University of Iowa Hospitals and Clinics; [5]Newcastle University; [6]The University of Iowa

Understanding speech in noise is a challenging task. Successful speech-in-noise (SiN) understanding depends on cognitive processing, such as lexical processing in frontal cortex, as well as accurate neural encoding of acoustic information in peripheral auditory system. However, the neural mechanism of SiN processing that involves both peripheral and central processing is not yet clear. Recent fMRI and electroencephalography (EEG) studies have shown engagement of higher-order processing for speech stimuli at frontal brain area. We hypothesized that the increase of energetic masking by background noise might more employ later frontal cortex activity, while decreasing activity at early auditory brain regions and that the cortical interplay between those regions might predict the wide variance in SiN understanding performance at the same amount of given noise. One challenge is that most studies investigating the cortical mechanism of SiN processing only use simple nonsense speech tokens. However, as the demand of ecologically valid experimental design has increased in the field of hearing science, we decided to use natural speech despite it not having yet been proven valid for event-related potential (ERP) analysis. We used one hundred consonant-vowel-consonant spoken words that are standardly used in clinic and heterogeneous across

different manner and place of articulation. The lists only contained 100 words so that any other factors that might affect the result, such as mental fatigue, would not be involved during simultaneous EEG recording. Given that the morphology of speech-evoked response is affected by the temporal envelope of words, k-means clustering was applied to partition the word lists into several clusters based on the temporal envelope. A word cluster with steepest attack curves followed by shortest decay contours that mostly included initial plosives was included for EEG analysis. We found that the harder condition, with lower signal-to-noise ratio (SNR), resulted in stronger late response (later than 600ms after the word onset) in the frontal area as well as weaker and delayed N1 response at the auditory region. Especially in the lower SNR condition, listeners with poor performance on the behavioral test showed stronger late frontal activity and weaker early temporal activity. Our results suggest that frontal cortical activity can predict SiN understanding difficulty when using a subset of the words for EEG analysis and can predict the performance of the entire group of words. This work will lead to a better understanding of cortical SiN processing by using ecologically valid and clinically useful collection of words.

PD 08

Altered Auditory Network at Resting-state in HIV Positive Individuals with Central Auditory Deficits

Yi Zhan[1]; Xiudong Shi[1]; Abigail Fellows[2]; Qiurong Yu[3]; Odile Clavier[4]; Sigfrid D. Soli[5]; Zhiyong Zhang[6]; Mingxia Fan[3]; Yuxin Shi[1]; Jay Buckey[2]
[1]Shanghai Public Health Clinical Center, Fudan Univerisity; [2]Space Medicine Innovations Laboratory, Geisel School of Medicine at Dartmouth, Hanover, NH, United States; [3]Shanghai Key Laboratory of Magnetic Resonance, East China Normal University; [4]Creare, LLC; [5]University of British Columbia; [6]Fudan University

Background
New research suggests that individuals with human immunodeficiency virus (HIV) have central auditory processing deficits, which may reflect central nervous system damage caused by HIV infection. The purpose of this study is to investigate the changes of functional connectivity of the auditory network (AN) in HIV positive individuals by using functional magnetic resonance imaging (Resting-state fMRI (RS-fMRI)).

Methods
A reduced ability to understand speech in noise despite otherwise normal hearing determined by audiometry was used as a marker of a central auditory deficit. We enrolled 10 HIV+ outpatients (8 male, 2 female, average age 46), with cognitive deficits (Montreal Cognitive Assessment (MoCA) scores <25) and speech-in-noise de-

tection deficits (composite speech reception threshold (SRT) > -6 dB)(HIV+/CAPD+ group) from the Shanghai Public Health Clinical Center in Shanghai, China. Their results where compared to 10 HIV- subjects (9 male, 1 female, average age 26) and 10 HIV+ subjects (10 male, average age 33) with normal MoCA and SRT scores (HIV-/CAPD- and HIV+/CAPD- groups respectively). All subjects had normal hearing determined by audiometry. The subjects underwent RS-fMRI, and the auditory network was identified via independent component analysis (ICA).

Results

Compared with the HIV+/CAPD- group, HIV+/CAPD+ subjects showed abnormal functional connectivity (FC) within the AN. Specially, FC of the AN significantly decreased in the left and right superior temporal gyrus (involving Brodmann areas 41 and 22) and the left precentral gyrus (Brodmann 4), (AlphaSim corrected, p<0.05) (Figure 1). Both the HIV+/CAPD+ and HIV+/CAPD- groups had reduced activity compared to controls (Figure 2). Within the HIV+ group, multiple linear regression of SRT as the response variable with AN FC and age as predictor variables showed a significant relationship of SRT with FC from Brodmann area 41 (p=0.04) and Brodmann area 22 (p=0.03) (Figure 3) that was independent of age (p>0.1). AN FC from Brodmann area 4 was significantly related to age (p=0.004), but not SRT (p>0.6).

Conclusions

These data show reduced activity in auditory relevant areas on RS-fMRI in HIV+ individuals with cognitive and central auditory deficits. AN activity was also reduced in the HIV+/CAPD- group compared to controls suggesting AN activity reductions may precede detectable speech-in-noise deficits. These data suggest that the central auditory findings in HIV+ have a functional correlate on neuroimaging, which supports the potential use of central auditory tests as a way to assess central nervous system effects of HIV.
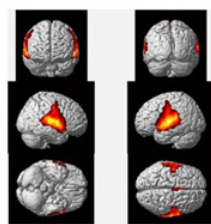
Figure.1A: Brain mapping of the Auditory network identified by ICA
(FDR corrected, P < 0.001, cluster size> 100)
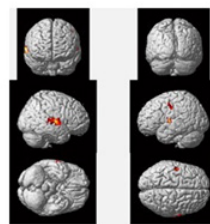
Figure.1B: Comparison of HIV+/CAPD- and HIV+/CAPD+ auditory network maps show HIV+/CAPD+ group decreased activity (red areas) (two-sample t-test, AlphaSim corrected, p<0.05)

Networks	Brain regions	Number of voxels	Brodmann Area (voxels)	t value	Peak location x	y	z
Auditory	Temporal_Sup_R	123	41 (21)	5.7	51	-21	6
			22 (19)	4.66	66	-9	6
	Temporal_Sup_L	24	41 (14)	3.39	-57	-9	6
			22 (11)	3.32	-54	-9	6
	Precentral_L	31	4 (5)	3.94	-48	-6	48

Table 1.Brain regions showing decreased auditory network activity in HIV+/CAPD+ group
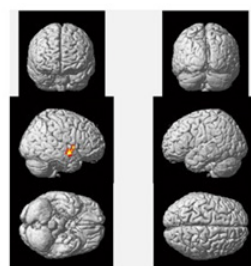
Figure.2A: Comparison of HIV- and HIV+/CAPD- auditory network maps show HIV+/CAPD- group decreased activity (red areas) (two-sample t-test, AlphaSim corrected, p<0.05)
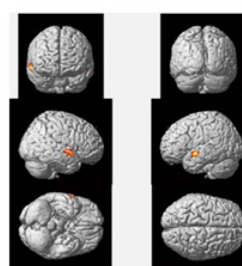
Figure.2B: Comparison of HIV- and HIV+/CAPD+ auditory network maps show HIV+/CAPD+ group decreased activity (red areas) (two-sample t-test, AlphaSim corrected, p<0.05)

	Networks	Brain regions	Number of voxels	t value	Peak location x	y	z
HIV- > HIV+/CAPD-	Auditory	Temporal_Sup_R	29	3.72	48	-3	-9
		Insula_R	18	3.44	48	6	3
HIV- > HIV+/CAPD+	Auditory	Temporal_Sup_L	28	3.95	-51	-3	-9
		Temporal_Sup_R	34	3.39	48	-6	-3
		Insula_R	26	3.94	42	-6	6

Table 2.Brain regions showing decreased auditory network activity in both HIV+/CAPD- group and HIV+/CAPD+ group, compared with HIV-

SRT B22 relationship
r2=0.599
p=0.030
Adjusted SRT
Adjusted B22
× Adjusted data
Fit: y=0.7306*x
95% conf. bounds

Development I
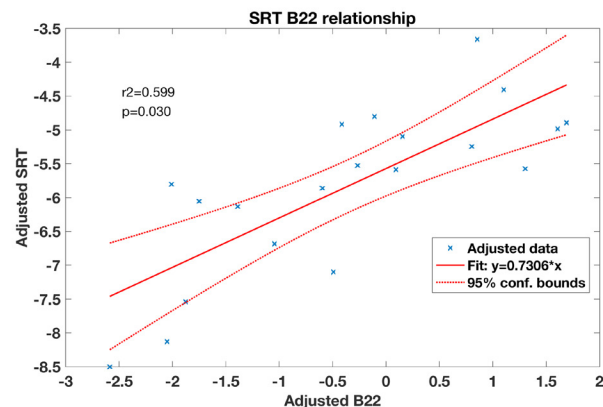
PD 09

Hippo/Yap signaling controls growth and regeneration of the inner ear sensory epithelia

Ksenia Gnedeva[1]; Mark Warchol[2]; Matthew Barton[3]; Neil Segil[1]
[1]Department of Stem Cell Biology and Regenerative Medicine, Keck School of Medicine of the University of Southern California; [2]Washington University School of Medicine; [3]Washington University in St. Louis

Background

Unlike non-mammalian vertebrates, adult mammals cannot replenish lost hair cells, resulting in permanent hearing impairment and balance disorders. This deficiency, in part, stems from the failure of mature supporting cells to proliferate in response to loss of hair cells. We hypothesize that an investigation of the mechanisms controlling sensory organ growth and proliferation during embryogenesis of the inner ear, will provide new approaches to manipulating the regenerative response in the mature inner ear. To this end, we are investigating the role of the Hippo pathway in regulating organ growth, progenitor cell proliferation, and cell cycle exit during cochlear and vestibular sensory development. Here our focus is on the transcriptional co-factor Yap—a direct downstream target of Hippo signaling.

Methods

We utilized a Pax2-Cre-driven conditional knockout of Yap to investigate its role in vestibular and hearing sensory organ development. By monitoring changes in cell proliferation, organ size, and architecture, we demonstrate that Yap signaling is crucial for normal inner ear sensory organ growth and morphogenesis. We have also employed viral loss and gain of function experiments to investigate the role of Yap during limited regeneration in the utricle *in vitro*.

Results

Our immunohistochemical analysis of Yap, MST1/2, and Nf2 expression during early vestibular and cochlear development (E12-E14.5) suggests that the Hippo/Yap signaling pathway regulates cellular proliferation in both vestibular and hearing sensory organs. Confirming this prediction, we found that loss of Yap during early development results in formation of significantly smaller sensory organs. Additionally, blocking Yap protein interaction with its transcription partners—the Tead genes—limits regenerative capacity in the neonatal utricle *in vitro.* In contrast, activation of the Yap/Tead signaling partly restores the ability of supporting cells to proliferate.

Conclusions

Our results suggest that the Hippo/Yap signaling pathway plays a major role during the development of the sensory organs of the inner ear, and that its activation is able to repress supporting cell proliferation. Further characterization of the role of Yap and other Hippo signaling pathway components in the developing ear will lead to a better understanding of both development and the failure of regeneration in the mammalian inner ear, and new approaches to overcoming hearing and balance impairment.

PD 10

Understanding insulin-like growth factor 1 actions in otic cells: activation of protein kinase B and reduction of autophagic flux

Blanca Cervantes[1]; Angela Garcia-Mato[1]; Lourdes Rodriguez-de la Rosa[1]; Carla Guillen-Pingarron[2]; **Isabel Varela-Nieto**[3]
[1]CSIC and CIBER; [2]CSIC and UAM; [3]Institute of Biomedical Research "Alberto Sols", Spanish National Research Council-Autonomous University of Madrid; Centre for Biomedical Network Research in Rare Diseases (CIBERER), Institute of Health Carlos III (ISCIII); Hospital La Paz Institute

Insulin-like growth factor 1 (IGF-1) deficiency causes sensorineural hearing loss in man and mice. To gain insight into the molecular targets of IGF-1 in otic cells, both sensory and neural, we have used the cell lines HEI-OC1 (derived from the auditory organ of the transgenic mouse Immortomouse™) and Neuro2a (a murine neuroblastoma). The expression of genes of the IGF system has been studied by RT-qPCR in both cell lines. We observed that *Igf1, Igf1r* and *Irs1* transcripts were more abundant in HEI-OC1 than in Neuro2a cells, whilst *Irs2* transcripts were highly expressed in Neuro2a. We also studied the actions and signaling of IGF-1 in both lines. Number of cells was determined using crystal violet staining method, apoptosis was studied by flow cytometry, location of IGF1R was determined by immunofluorescence and activation of target proteins was measured by Western Blotting. IGF-1 treatment increased the number of cells in both lines, and also protected against apoptosis blocking annexin V exposure and DNA strand breaks in HEI-OC1. IGF1R was translocated from the membrane to a perinuclear area after IGF-1 treatment in Neuro2a. Relative p-AKT^{Ser473} to total AKT levels increased and the autophagic flux decreased after IGF-1 treatment in both cell lines, whereas activated pERK1/2 increase was solely observed in Neuro2a cells. Therefore, both sensory cells and neurons express the IGF system elements and their survival is promoted by IGF-1. Consequences of blockade of the IGF system by both chemical and genetic methods will be discussed.

PD 11

The role of Id genes in mammalian developing cochlea

Susumu Sakamoto[1]; Tomoko Tateya[2]; Koichi Omori[1]; Ryoichiro Kageyama[2]
[1]*Department of Otolaryngology-Head and Neck Surgery, Graduate School of Medicine, Kyoto University;* [2]*Institute for Frontier Life and Medical Sciences, Kyoto University*

Background
The family of inhibitor of differentiation and DNA-binding (Id) proteins, including Id1 to Id4, is a group of evolutionarily conserved molecules, which plays important regulatory roles. Id proteins are small polypeptides harboring a helix-loop-helix (HLH) motif, which are known to mediate dimerization with other basic HLH proteins, primarily E proteins but Id proteins do not possess the basic amino acids adjacent to the HLH motif necessary for DNA binding. Id proteins can form heterodimers with other basic HLH proteins, but resulting complexes cannot bind DNA and are inactive. It has been reported that Id proteins have an inhibitory effect on Atoh1 proteins and function downstream of BMP4 signaling, however the roles and regulation of *Id* genes in the growth and differentiation of the cochlear epithelium during development are not fully elucidated.

The purpose of this study is to clarify the roles of these *Id*s in the development of cochlear sensory epithelium.

Methods
We performed both gain- and loss-of-function experiments in developing cochlear epithelium. To explore the deletion of *Id* genes in cochlear development, *Id1*^{-/-}, *Id2*^{-/-}, *Id3*[f/f] and *Emx2-cre* mice were bred to produce *Id* triple conditional knockout (CKO) mice. We examined *Id* CKO mice by immunohistochemistry and in situ hybridization. We also researched the effect of overexpressed *Id* genes on Atoh1 expression using Atoh1-EGFP fusion mice with electroporation method. To investigate the regulation of *Id*s and *Atoh1* expression by Bmp4 signaling, we examined expression levels of *Id*s and *Atoh1* in cochlear explants cultured with Bmp4, Noggin or LDN193189 (Bmp inhibitor).

Results
A reduction in *Id* gene dosage led to graded decrease of cochlear length. *Id* triple CKO mice had the shortest, hypoplastic cochlear duct where Sox2- and p27-positive prosensory domain was much smaller. CKO cochlear epithelium also showed disappearance of *p75* expression, decrease of *Atoh1* expression, and decreased and disorganized hair cells. Overexpressed *Id* genes did not induce nor inhibit *Atoh1* expression in prosensory cells before hair cell differentiation. Treatment of Bmp4 increased *Ids* but had no effect on *Atoh1* expression while Noggin and LDN193189 inhibited *Ids* and *Atoh1* expression.

Conclusions
These data indicate that Id has two roles. One is to regulate the size of the sensory progenitor population and the overall cochlear length. Another is to promote hair cell differentiation and to construct hair cell organization. Id genes are suggested to be downstream of BMP4 signaling, and necessary but not sufficient to induce Atoh1 expression.

PD 12

Helios - Shining a Light on Outer Hair Cell Functional Maturation via a Multi-Omic Approach

Maggie S. Matern[1]; Yoko Ogawa[2]; Michael C. Kelly[3]; Beatrice Milon[2]; Mark McMurray[1]; Allen Myers[1]; Lauren Chessum[4]; Yang Song[5]; Matthew W. Kelley[3]; Michael R. Bowl[4]; Ran Elkon[6]; Ronna Hertzano[7]
[1]*University of Maryland School of Medicine, Baltimore, MD;* [2]*University of Maryland School of Medicine, Baltimore, MD, USA;* [3]*NIDCD/NIH;* [4]*MRC Harwell Institute, Mammalian Genetics Unit, Harwell, Oxford;* [5]*University of Maryland School of Medicine, Baltimore MD, USA;* [6]*Department of Human Molecular Genetics and Biochemistry, Sackler School of Medicine, Tel Aviv University, Tel Aviv, Israel;* [7]*University of Maryland School of Medicine, Baltimore, MD USA*

To date, efforts to regenerate hair cells (HCs) either *in vivo* or *in vitro* result only in immature HC-like cells. In addition to ensuring correct placement and innervation of regenerated HCs, hearing restoration will rely on the ability to generate both mature inner HCs (IHCs) and outer HCs (OHCs). Molecular differences between mouse IHCs and OHCs are detectable as early as embryonic day 16; however, numerous IHC and OHC-specific markers are not uniquely segregated until early in the second postnatal week of life. Here we utilize OHC-RiboTag translatome sequencing, inner ear RNA-Seq, viral gene delivery and single-cell RNA-Seq (scRNA-Seq) to assess the complex temporal changes to OHC gene expression that occur postnatally, as well as identify key regulators of OHC functional maturation. Using Prestin-[CreERT2] and RiboTag mice, we performed a detailed

transcriptomic analysis of OHCs at 5 time points; P8, P14, P28, P42 and P70. A clustering analysis of gene expression in OHCs from P8 to P70 identifies 155 and 429 genes with a gradual activation or repression of expression, respectively. Using a regulatory motif prediction tool to analyze the promoter and enhancer regions of these genes, we then identify the Helios transcription factor as a candidate regulator of OHC gene expression. We previously showed that the *cello* mice, which have a mutation in the gene encoding Helios (*Ikzf2*), are deaf due to decreased OHC electromotility and show a gradual loss of OHCs with age, indicating the importance of this transcription factor in OHC function. Here we take a multi-pronged approach to identify genes regulated by Helios in OHCs. First, we compare the transcriptomes of wildtype and *cello* mutant P8 inner ears, and further validate these changes in gene expression in the mutant OHCs using *in-situ* hybridization and immunohistochemistry. Next, we utilize scRNA-Seq of *Ikzf2*/Helios virally transduced HCs to comprehensively assess the molecular program downstream of Helios. Through this, we identify a set of HCs with a hybrid IHC/OHC transcriptome, consistent with *Ikzf2* virally transduced IHCs that also express the Helios-directed transcriptional program.

Overall, the RiboTag-OHC expression dataset we describe represents a useful resource for the discovery of new OHC-specific genes, as well as for genes important for cell type specification and OHC functional maturation. Additionally, our analyses demonstrate the utility of *in vivo* HC viral gene transduction followed by scRNA-Seq as a novel method for elucidating downstream transcriptional cascades of transcription factors important for postnatal IHC and OHC specification.

PD 13

Epigenetic and Transcriptional Regulation of Hair Cell Differentiation from Lgr5-Positive Cochlear Progenitors

Danielle R. Lenz[1]; Albert Edge[2]
[1]*Eaton-Peabody laboratories, Massachusetts Eye and Ear; Department of Otolaryngology, Harvard Medical School; [2]Harvard Medical School*

Lgr5-positive cochlear progenitors (LCPs) can be harvested from mouse neonatal cochlea, expanded in vitro and differentiated into hair cells in large quantities. They represent a useful model for epigenetic and transcriptional analysis of hair cell differentiation, using large number of cells and enabling close inspection of the differentiation process. Chromatin accessibility and transcriptional analysis were performed using ATAC-sequencing and RNA-sequencing respectively to compare LCPs, early and late differentiated LCPs, and newborn supporting cells and hair cells isolated directly from the cochlea.

Cochleae from P2-P4 neonatal Atoh1-EGFP transgenic mice were used to generate LCPs. The GFP signal was utilized to detect differentiating hair cells. RNA-sequencing was performed in biological duplicates using Illumina NextSeq500 single-end 75 bp (SE75) and further analyzed using DeSeq2 for differential expression of hair cell genes. Principal component analysis demonstrated clear progression in differentiation from LCPs, through differentiation days 2, 4 and 10. Subsequent hierarchical clustering revealed that day 2 of differentiation segregated with expanded LCPs, while D4 segregated with D10. These results were supported by qPCR analysis showing gradual elevation of Atoh1 with a peak in expression between D3 and D4 that later decreased. This mimics the normal differentiation pattern, suggesting a transition of at least a portion of the cells between differentiation and maturation during this time frame.

ATAC-sequencing was performed on equivalent LCP samples in biological duplicates using paired-end 40 bp (PE40), and subsequent peak calling was conducted using MACS2. Preliminary analysis revealed that over 85% of the peaks from all samples overlapped with known DNAse hyper-sensitive sites that are highly active in the genome. Motif analysis using HOMER further identified the ubiquitously expressed heterotrimeric transcription factor NF-Y as the most significantly enriched binding motif in most samples. NF-Y binding is associated with highly permissive chromatin conformation both in stem cells and in early cell determination and differentiation, and it has been shown to bind together with Sox2 at major enhancer sites.

Integration of ATAC and RNA sequencing results sheds light both on the differentiation process of expanded Lgr5 cells as well native inner ear supporting cells and hair cells. It further specifies the extent of similarity between the in vitro LCP model and the native inner ear cells and establishes LCPs as a faithful model of hair cell differentiation and regeneration.

PD 14

Three-dimensional real-time imaging reveals the dynamics of hair cell specification and organization in developing cochlea.

Tomoko Tateya[1]; Susumu Sakamoto[2]; Fumiyoshi Ishidate[3]; Itaru Imayoshi[4]; Ryoichiro Kageyama[1]
[1]*Institute for Frontier Life and Medical Sciences, Kyoto University; [2]Department of Otolaryngology-Head and Neck Surgery, Graduate School of Medicine, Kyoto University; [3]World Premier International Research Initiative-Institute for Integrated Cell-Material Sciences (WPI-iCeMS), Kyoto University; [4]Graduate School of Biostudies, Kyoto University*

Background

During development, the prosensory domain is formed in the floor of the cochlear duct, and then hair cells (HCs) and supporting cells differentiate from common precursors in the prosensory domain. Atoh1 is a key player in the HC differentiation. Prior to Atoh1 role in the HC specification, it also functions as a proneural gene and is initially expressed in a relatively broad and diffuse stripe of prosensory cells. As development proceeds, Atoh1 expression becomes restricted to limited number of cells, which eventually give rise to one row of inner HCs and three rows of outer HCs. Thus, Atoh1 expression pattern dynamically changes in the prosensory domain during the period of a proneural factor to a commitment factor responsible for HC fate decision. This transition period is important because it is the exact process of HC specification and organization and occurs in approximately 1-2 days, too short to analyze accurately on fixed samples. To address this problem, we established two-color fluorescence three-dimensional real-time imaging system using the cochlear explants of the double transgenic mice.

Methods

We crossed two transgenic lines, Atoh1-EGFP, and mCherry reporter mice for the visualization of Dll1, Hes5 or nuclei. Overnight real-time imaging was performed on cochlear explants of the double transgenic mice. The fluorescence intensity and position of individual cells in prosensory domain were detected at each time frame, and labeled cells were tracked over time. The fluorescence intensity was enough to detect the initial weak Atoh1 expression in cochlear explants, accompanied with a specific trend of changes in fluorescence and migration among the Atoh1-positive cells.

Results

Weak, fluctuating Atoh1 expression was seen in prosensory cells before differentiation. HC specification processes were divided into three; first some prosensory cells showed a steep increase of Atoh1 expression, next migrated toward apical surface of the epithelium, and finally expressed Dll1 to differentiate HCs. HC induction initially occurred at the medial periphery of prosensory domain and thereafter at the lateral periphery. The area of outer HCs induction came to expand and outer HCs were produced in an outside-in manner. Cyclopamine administration altered the pattern of outer HC induction.

Conclusions

Three-dimensional cell tracking using the data obtained by real-time imaging revealed the dynamic changes of Atoh1 expression level and position of individual cells in developing cochlear epithelium. The location information and the timing regulated by hedgehog signaling are important for specification and organization of HCs.

PD 15

Transcriptional Dynamics of Hair-Bundle Morphogenesis Revealed with CellTrails

Daniel C. Ellwanger[1]; Mirko Scheibinger[1]; Rachel A. Dumont[2]; Peter G. Barr-Gillespie[2]; Stefan Heller[1]
[1]*Stanford | School of Medicine | Department of Otolaryngology - Head & Neck Surgery;* [2]*Oregon Health & Science University | Oregon Hearing Research Center and Vollum Institute*

Hair bundles are mechanosensitive organelles found on sensory hair cells, which mediate the mechanical-to-electrical transduction that is at the heart of hearing and balance. In this work, we describe the spatial and temporal expression of 183 key hair bundle transcripts using single cell analysis. The full spectrum of developing and mature cell types exists in a single snapshot of an asynchronous developing organ, such as the chick utricle at embryonic day 15. Bundle assembly and growth are dictated by sequential and overlapping cellular processes, which are concealed within gene expression profiles of individual cells. In addition to developmental differences among cells, the utricle also shows regional variation in cell organization and structure. Although type and developmental age of individual cells are not preserved during sampling, we hypothesized that their transcriptional profiles encode this information. We therefore devised a novel algorithm, CellTrails, to determine the topology and dynamically changing cellular states of a branching trajectory of utricle hair cells during bundle assembly. *In situ* hybridization and immunolabeling confirmed the predicted spatial information as well as temporal dynamics. Moreover, the precise temporal ordering of cells and accompanying expression changes in individual genes were robustly correlated with stereocilia elongation, which we utilized as an *in situ* ruler for developmental progression. CellTrails'; spatiotemporal mapping identified specific markers for type I and type II hair cells and provided evidence for two distinct classes of type II hair cells. We further established a strategy for the alignment of extracted linear trajectories (trails) that allows comparison of gene expression dynamics as different hair cell types develop. Examining genes involved in hair bundle development, including the processes of lengthening, widening, tapering, actin-crosslinking, transport, and transduction, we found that *CALB2* and *ATP2B2*, two genes involved in Ca^{2+} regulation, are dynamically regulated during stereocilia elongation in different hair cell types. Precise spatiotemporal control of $[Ca^{2+}]_i$ consequently appears to be an important component of hair bundle development. Our analysis provides insight into spatial, temporal, and cytomorphological aspects of hair bundle development at unprecedentedly high resolution.

CellTrails utilizes a new concept of uncovering and visualizing latent spatiotemporal information from single cell gene expression data; moreover, we show through additional analyses that it performs as well with RNA-Seq data as it does with single cell multiplex qRT-PCR data.

PD 16

Molecular characterization and prospective isolation of human fetal inner ear pro-sensory domain progenitor cells

Marta Roccio[1]; Michael Perny[2]; Megan Ealy[3]; Hans Ruedi Widmer[4]; Stefan Heller[5]; Pascal Senn[6]
[1]*Laboratory of Inner Ear Research, Department of Biomedical Research, University of Bern, Switzerland & Dept. of Otorhinolaryngology, Head & Neck Surgery, Inselspital Bern, Switzerland;* [2]*Laboratory of Inner Ear Research, Department of Biomedical Research, University of Bern and Neuroinfection Laboratory, Institute for Infectious Diseases, University of Bern, Switzerland;* [3]*Dept. of Biology, Drury University, Missouri, USA and Dept. of Otolaryngology, Head & Neck Surgery, Stanford University School of Medicine, CA.;* [4]*Dept. of Neurosurgery, Neurocenter and Regenerative Neuroscience Cluster, Inselspital Bern, Switzerland.;* [5]*Stanford | School of Medicine | Department of Otolaryngology - Head & Neck Surgery;* [6]*Department of Clinical Neuroscience, Service ORL and HNS, University hospital of Geneva, Switzerland*

Mechanosensitive hair cells located in the cochlea are the sensory cells essential for the detection of sound. Their loss is irreversible in humans and a major cause of permanent hearing loss. Unraveling the mechanisms of human inner ear development and hair cell specification might enable establishment of novel therapeutic directions such as the development of human cell-based assays for screening of otoprotective and otoregenerative compounds.

Hair cells occur in sensory epithelia that are derived from prosensory domains. Our current knowledge of the developmental mechanisms and timing leading to organ of Corti hair cell formation relies on molecular studies performed in mice.

Here we have carried out a systematic analysis of the fetal human inner ear, in a temporal window spanning from week 8 to week 12 postconception, i.e. the time period when cochlear hair cells become specified. We have analyzed gene and protein expression of the developing cochlear duct, spiral ganglion and utricle. In addition, 3D organoid culture methods have been developed for expansion of flow cytometrically sorted EPCAM+ human cochlear duct cells. Here we present data

showing that organoids conserve protein expression and localization typical of their in vivo counterparts, namely epithelial marker expression (CD49F, EPCAM, E-Cadherin, β-Catenin), apical basal polarity (ZO-1), cochlear duct markers (SOX9) and prosensory markers (SOX2; CD271), and can be induced to differentiate to hair cells expressing the markers MYO7A and apical hair bundles.

Importantly, we have identified a surface marker combination, based on the co-expression of the epithelial marker EPCAM and the neurotrophin receptor CD271 that can be used for isolation of prosensory hair cell progenitors. The human inner ear organoids derived from the EPCAM+/CD271+ population differentiate with high efficiency to MYO7A+ hair cells displaying apical F-actin-rich bundles, in contrast with the lack of hair cell differentiation from the remaining cochlear duct population (EPCAM+/CD271-).

Our data provides beyond state-of-the art insight into the development of the human cochlea with particular emphasis on new methods for selection and expansion of inner ear /hair cell progenitors in vitro.

Inner Ear Gallimaufry

PD 17

Cochlear Shape Variability from 987 Computed Tomography Images

Thomas Demarcy[1]; Clair Vandersteen[2]; Dan Gnansia[1]; Hervé Delingette[3]; Nicholas Ayache[3]; Charles Raffaelli[2]; Nicolas Guevara[2]
[1]*Oticon Medical;* [2]*Nice University Hospital;* [3]*Inria*

Obtaining detailed characterization of interindivual and intraindividual cochlear anatomy variability is key to the development of implantable hearing devices and to the optimal planning of cochlea surgeries. This study analyzed cochlear anatomic features in *in vivo* human temporal bones. The dataset consists of 987 clinical Computed Tomography (CT) images with a voxel size of 187.5x187.5x250 µm³.

Using a joint shape and appearance model-based segmentation method the scala tympani and the scala vestibuli can be precisely localized from CT images. Image isotropic resampling and rigid registration is first performed to orient the cochlea in the cochlear coordinate system centered on a smaller region of interest. The method is validated with manually segmented pairs of low-resolution CT and high-resolution µCT images (25 µm voxel size), the mean surface error of the automatic segmentation is equal to 0.12 mm, which is at least 33% lower than previous studies. The use of cochlear shape

fitting with a local appearance model allows subpixel accuracy segmentation.

Anatomic features such as the volume, the width, the length and the longitudinal profile of the cochlea are statistically studied with the large dataset. The cochlear shape parameters are mostly independent (since the parameters covariance matrix is diagonal dominant). The parameter modeling the longitudinal profile of the cochlea is bimodal (following a mixture of the two normal distributions) while most of the parameters follow roughly a normal distribution. The first mode (N = 306) generates a cochlear shape with a straight longitudinal course, while the second mode (N = 681) generates a cochlear shape with a pronounced "rollercoaster" longitudinal course. Finally the bilateral symmetry in cochlear anatomy is quantified: if the interpatient cochlear shape variability is greater than the intrapatient bilateral variability, the study shows that the symmetry is not obvious.

To the best of our knowledge, it is the first time that tridimensional cochlear shape reconstruction and variability study is reported on such a large dataset.

PD 18

Transduction-Dependent Remodeling: a Unique Maintenance Mechanism of the Mammalian Auditory Stereocilia or a Common Hair Cell Trait?

A. Catalina Velez-Ortega[1]; Patricia M. Quiñones[2]; Carolina Galeano-Naranjo[1]; Sebastiaan W. F. Meenderink[2]; Mike Grossheim[1]; Dolores Bozovic[3]; Gregory I. Frolenkov[1]
[1]*Department of Physiology, University of Kentucky;* [2]*Department of Physics and Astronomy, University of California, Los Angeles;* [3]*University of California, Los Angeles, Department of Physics & Astronomy*

Stereocilia are actin-filled projections of the inner ear hair cells. In the mammalian auditory hair cells, they are arranged in rows of precisely-determined increasing heights. This specific arrangement is maintained throughout the life of the organism via largely unknown mechanisms. We have recently discovered that the length of the shorter row stereocilia, which harbor mechanotransduction channels, is regulated by the resting mechanotransduction current, more specifically, by the influx of calcium ions through these channels (Velez-Ortega et al., 2017). However, the physiological significance of this phenomenon is unclear. The transduction-dependent regulation of the stereocilia actin cytoskeleton may represent a unique mechanism of stereocilia maintenance in the non-regenerating mammalian auditory hair cells. Alternatively, this regulation could represent a phenomenon common to all vertebrate hair cells.

Here, we studied the effects of mechanotransduction channel blockers on the remodeling of the stereocilia actin core in the bullfrog auditory and vestibular hair cells (which can regenerate), and in the mouse vestibular hair cells (which show limited potential for regeneration). If cultured in the presence of autologous serum, stereocilia bundles of bullfrog sacculus hair cells maintain their tip links and mechanotransduction currents after stereocilia shortening. Similar to our findings in young postnatal mouse and rat auditory hair cells, scanning electron micrographs show that the long-term (5-24 hours) blockage of mechanotransduction channels leads to abnormally-thin tips and eventual shortening of stereocilia in the hair cells of the adult frog sacculus and amphibian papilla. These data indicate: a common transduction-dependent mechanism of stereocilia regulation in hair cells of different species. To further explore the exact time course and hence the potential physiological relevance of this mechanism, we performed live-cell imaging of rat organ of Corti explants using hopping-probe ion conductance microscopy (Novak et al., 2009; Velez-Ortega and Frolenkov, 2016). We observed the presence of nanoscale changes to the morphology of the stereocilia tips within minutes after the blockage of mechanotransduction channels, which indicates that the transduction-dependent stereocilia remodeling may participate in the slow regulation of mechanotransduction. We conclude that the transduction-dependent stereocilia remodeling is a common phenomenon for hair cells of at least two different vertebrate classes. We hypothesize that this remodeling may adjust the resting tension of the mechanotransduction machinery.

PD 19

Stapes velocity and intracochlear pressure transfer functions for low-frequency, high-intensity sound are comparable beween chinchilla and human

John Peacock[1]; Mohamed Alhussaini[2]; Daniel J. Tollin[3]
[1]*University of Colorado School of Medicine;* [2]*University of Colorado;* [3]*Department of Physiology and Biophysics, University of Colorado School of Medicine*

Background
Exposure to high intensity (blast) sounds can result in both conductive and sensorineural damage to hearing. This includes rupture of the tympanic membrane and dislocation of the middle ear ossicles, as well as damage to the inner and outer hair cells in the cochlea. A clearer understanding of how the hearing system responds to blast could help us better prevent auditory trauma, and support those who have been exposed to such sounds.

Chinchillas are often used in studies of hearing due to the similarity between the chinchilla and human audiograms. The suitability of their use in research on auditory trauma from blast noise will depend on the extent to which cochlear pressures generated in chinchillas compare to those in humans.

Methods
In order to gain a more detailed understanding of the response of the ear to blast sounds, a custom built sound concentrating horn was used to expose chinchilla and human cadavers to a series of single frequency tones of varying pressure levels. Fibre optic pressure probes (FISO, Inc.) were simultaneously inserted into the scala vestibuli and scala tympani to measure the resulting intracochlear pressures, and a laser vibrometer was aimed at the stapes footplate to record displacement.

Results
In both species, intracochlear pressures increased with applied sound pressure, but begin to saturate as the stapes reaches its maximum displacement. The exact saturation point, and the saturation pressures showed a strong frequency dependence. Overall stapes displacement and resulting intracochlear pressures were remarkably similar between chinchilla and human specimens, although differences emerged at the highest sound pressures levels and at higher frequencies.

At the lowest frequencies, below 250 Hz, the chinchilla and human intracochlear pressure data mostly overlaps. However, above 250 HZ the pressures in the chinchilla cochlea begin to grow larger than those in the human cochlea for any given sound pressure level. Increasing the sound pressure level above 160 dB causes increasingly larger human cochlear pressures as compared to those in the chinchilla.

Conclusion
Intracochlear pressures measure in chinchilla and human temporal bones shows significant areas of overlap, but some differences are noticeable. Overall, our data suggests that the chinchilla is a good surrogate for studies of human auditory injury from blast exposure, which contain predominantly low-frequency energy, and studies with chinchillas can provide useful data to improve models of auditory hazard for humans.

PD 20

Modulation of lateral line afferent neuron activity during motor behaviors in larval zebrafish; insights from electrophysiology and optogenetic imaging

James Liao[1]; Elias Lunsford[1]; Katie Kindt[2]
[1]*University of Florida;* [2]*National Institutes of Deafness and Other Communication Disorders, National Institutes of Health*

During locomotion, cholinergic efferent hindbrain neurons of the lateral line system produce a motor copy command that serves to decrease sensitivity at the peripheral hair cells and afferent terminals. How this compensatory system scales across types and strengths of motor behaviors to ensure that animals remain attentive to biologically-relevant signals remains unknown. Here we perform simultaneous afferent neuron and ventral motor roots recordings to investigate the relationship between motor activity and the modulatory effect of efferents on spontaneous afferent neuron activity. To look at population-level afferent activity, we used optogenetics to image all afferent terminals at the site of specific neuromasts using *hsp70l: GCaMP6s-caax-sill1* zebrafish (*Danio rerio,* 4-6 dpf), which expresses a calcium indicator in afferent neurons. We quantified changes in fluorescence in afferent terminals in response to fluid-stimulated neuromasts during bouts of non-swimming activity and compared it to bouts of fictive swimming. This approach allowed us to monitor what portion of afferents are stimulated and if they are uniformly modulated by the efferent system. To understand whether efferents can gain down the sensitivity of hair cells directly, we conducted the same experiments using the *myo6b:G-CaMP6s-caax* line, which expresses a calcium indicator in hair cells. We found that when a neuromast was stimulated with a water jet, only a subset of the afferent terminals that innervated it were active. When the animal was swimming, this activity decreased, presumably by the activity of the cholinergic efferent system. Similarly, only a subset of hair cells was active when a neuromast was stimulated. However, no decrease in calcium flux was observed during locomotion, suggesting that the efferent system modulates the lateral line at the site of the afferent terminals and not directly through the hair cells.

PD 21

Probing the Role of Neuroligin-3 in Cochlear Synapses

Miguel Ramirez; Nopporn Jongkamonwiwat; Jeffrey Savas
Department of Neurology, Feinberg School of Medicine, Northwestern University, Chicago, IL

In a recent publication, we reported a draft of the cochlear proteome and identified a single synaptic adhesion protein, neuroligin-3(Nlgn3). Neuroligins have been shown to induce synapse formation and have synaptic organizing properties within the brain but have been unexplored within the cochlea. Given Nlgn3';s potential to physically link and organize the ribbon synapses we aim to determine if Nlgn3 contributes to hearing and increase our understanding of possible mechanisms underlying temporary hearing loss.

To confirm the specific cells expressing trans-synaptic adhesion proteins, RNA probes for Nlgn3, myosin7a and β-tubulin were synthesized and used for in situ hybridization experiments. Antibodies for Nlgn3 and ribbon synapse markers were used to verify localization patterns within the hair cells and spiral ganglion neurons. Our previous experiments aimed to explore the hair cell proteome were met with challenges due to the relatively small proportions of ribbon synapse proteins in the cochlea. To measure Nlgn3 levels within the cochlea without enrichment, a targeted mass spectrometry (MS) method was developed. An ion inclusion list was generated from the most abundant peptide masses from fully tryptic digests of Nlgn3. The tandem mass spectra were searched against UniProt mouse protein database and matched to sequences using the ProLuCID algorithm. Searches were filtered with DTASelect2 through Integrated Proteomics Pipeline with a protein false-discovery rate of 1%. Mice were exposed to thirty minutes of noise at 94 and 105db and used for immunofluorescence, qPCR, and targeted MS to determine if noise effects Nlgn3 levels.

In situ hybridization confirmed expression of Nlgn3 within spiral ganglion neurons and immunofluorescence verified that Nlgn3 specifically co-localizes with ribbon synapse markers. Noise-exposure resulted in the decoupling of presynaptic ribbons with postsynaptic AMPA receptors consistent with previous reports, in addition, Nlgn3 also became delocalized in its staining patterns demonstrating that noise effects localization of Nlgn3. Using targeted MS we have enhanced our detection of Nlgn3, and preliminary qPCR data demonstrated that increasing levels of noise exposure acutely increased Nlgn3 mRNA levels. The results of these experiments confirm that Nlgn3 localizes to ribbon synapses, is ex-pressed predominantly in spiral ganglion neurons and after noise exposure is delocalized and upregulated within the cochlea. Future experiments will explore how Nlgn3 may contribute to cochlear synaptogenesis, synaptic transmission, healthy hearing, and cochlear synaptopathy.

PD 22

Role of radixin in modulation of outer hair cell stereocilia function in inner ear

Sonal Prasad[1]; Anders Fridberger[2]
[1]*Linkoping University;* [2]*Linköping University*

Background
Previous data has shown that the axial stiffness of outer hair cell bundles are actively regulated, but the molecules that could underlie this stiffness modulation has not been determined. We hypothesize that Radixin (Rdx)could be involved in the modulation of stereocilia stiffness and length.Radixin is a cytoskeletal protein which binds actin filaments to the plasma membrane.It is found at a higher concentration at the base of stereocilia in guinea pigs. To test this hypothesis, we used the quinocarmycin analog DX-52-1 to prevent Rdx activation. DX-52-1 binds strongly and specifically to Rdx

Methods
Temporal bones were excised from young normal hearing guinea pigs, and a small opening was made at the cochlea';s base and at the apex. The basal opening was used to perfuse scala tympani with oxygenated tissue culture medium, whereas the apical opening provided an outlet for the perfusion solution and also allowed the organ of Corti to be observed using time-resolved confocal imaging. Special double-barreled electrodes were used for cochlear microphonic recording, electrical stimulation, staining of the bundle membrane with the membrane dye Di-3-ANEPPDHQ, and delivery of radixin inhibitor DX-52-1. In order tovisualize the sound-evoked motion of stereocilia, sequences of confocal images were acquired duringsound stimulation. Pixels acquired during the same phase of the stimulus were extracted using a Fourierseries technique, and arranged into movies showing the sound-evoked motion of the bundle. Imageacquisition triggered acoustic and electric stimulus. The extracellular potentials are tuned to a particularsound stimulus of 64 dB SPL frequency near 220 Hz to get maximum response. The acquired image sequences werelow-pass filtered and motion quantified through optical flow analysis using Matlab.Immunohistochemistry and surface preparation was performed on whole mount preparations of organ of Corti.

Results

Immunohistochemistry showed that Rdx was present mostly at the base in OHC stereocilia. When the radixin blocker was introduced, a pronounced change in the sound-evoked bundle deflections wasobserved with the motion both at the base and the tip of the bundle decreased. We observed an irreversible change in the amplitudes of the cochlear microphonic potential after the application of the blocker. Paradoxically, electrically evoked motility increased after the application of DX-52-1.

Conclusions

The regulatory mechanism of radixin in the hearing organ influences several aspects of hair cell function most importantly electromotility includingthe bundle movement. This change in hair cell functioncontributesstrongly to control of hearing sensitivity.

PD 23

The Effect of Gap Junctions on Active Cochlear Amplification Is Progressively Extended from High to Low Frequency Region with Ages and Has Difference in Low and High Frequency Regions

Liang Zong[1]; Jin Chen[1]; Yan Zhu[2]; **Hong-Bo Zhao**[3]
[1]*University of Kentucky Medical Center;* [2]*1.University of Kentucky Medical Center;* [3]*1. University of Kentucky Medical Center*

Background

Our recently studies demonstrate that alternation of gap junctional coupling between cochlear supporting cells or deletion of Cx26 in the cochlear supporting cells can change outer hair cell (OHC) electromotility and reduce active cochlear amplification, even though hair cells have no connexin expression and gap junctional coupling. We also found that this is a major deafness mechanism for Cx26 deficiency induced late-onset hearing loss. These previous studies demonstrate that Cx26 and gap junctional coupling between cochlear supporting cells play a critical role in the active cochlear amplification. In this study, we further investigate detailed information about the regulations of cochlear supporting cells' gap junctions on active cochlear amplification.

Methods

As described in our previous studies, we used Prox1-Cx26 conditional knockout (cKO) mice, in which the Cx26 expression in the OHCs' supporting cells, Deiters cells and outer pillar cells, were target-deleted. ABR threshold, DPOAE, and cochlear microphonics (CM) were recorded to assess cochlear and hearing function.

Results

Hearing loss and the reduction of active amplification in the Cx26 targeted-deletion mice are progressive, first occurring in the high frequency region and then extending to the middle and low frequency regions with mouse age increased. The speed of hearing loss extending was fast in the basal high frequency region and slow in the apical low frequency region, showing a logarithmic function with age. Before postnatal day 25, there were no significant hearing loss and the reduction of active cochlear amplification in the low frequency region. Hearing loss and the reduction of active cochlear amplification also appeared different at high and low frequency regions, severe and large in the high frequency regions.

Conclusions

These new data indicate that the effect of Cx26 deletion on active cochlear amplification is progressive but, consistent with our previous report, exists in both high and low frequency regions in adulthood. These new data also suggest that cochlear gap junctions may have an important role in age-related hearing loss.

PD 24

Cochlear mononuclear phagocytes in meningitis: a tale of two monocytes

Song-Zhe Li[1]; Richard Ransohoff[2]; **Keiko Hirose**[1]
[1]*Washington University in St. Louis;* [2]*Biogen*

Background

Pneumococcal meningitis is a life-threatening infection that leads to profound hearing loss in 25% of survivors. Bacteria from the spinal fluid enter the perilymph and massive cochlear inflammation follows. We hypothesized that the immune response to bacterial meningitis contributes to loss of hearing and neo ossification. The two chemokine receptors, CX3CR1 and CCR2, which distinguish the resident monocyte/macrophage population from the inflammatory monocyte population, are important determinants of final outcome in cochlear damage after meningitis, and their different roles in the pathophysiology of hearing loss after meningitis is presented.

Methods

Streptococcus pneumoniae bacteria were injected intrathecally in CCR2[RFP] CX3CR1[GFP] knockout and reporter mice at 6 weeks of age. Depletion studies using CX3CR1-DTR were also performed in mice with pneumococcal meningitis. ABR and anatomic/histologic analysis was performed using microCT and plastic embedded or

frozen cochlear sections at various time points after infection ranging from 2 weeks to 12 months post infection.

Results
CCR2 knockout mice suffered worse threshold shift, experienced more rapid and extensive cochlear ossification, and demonstrated a higher severity score of disease when compared to CCR2 expressing mice. Neither CX3CR1 knockout mice nor CX3CR1 depleted mice demonstrated significant differences in hearing loss or in structural changes in the inner ear or disease severity with pneumococcal meningitis.

Conclusions
CCR2 expressing monocytes and CX3CR1 monocytes and macrophages were abundant in the perilymph during acute pneumococcal meningitis. The result of CCR2 deletion demonstrated the importance of inflammatory monocytes in controlling disease and an overall beneficial effect in hearing preservation. Cochlear vulnerability to CCR2 deletion may result from impaired bacterial clearance in the KO mouse.

A Tribute to Barbara Bohne: Current Basic and Clinical Observations of Noise-Induced Hearing Loss

SYMP 15

Circadian control of the auditory function: implications for chronopharmacological strategies for treating hearing loss

Barbara Canlon
Karolinska Institutet

We identified a biological circadian clock in the cochlea that controls how auditory thresholds and synapses recover after noise trauma at different times of the day. The same noise exposure causes greater physiological and morphological consequences during nighttime compared to daytime. Consequently, a robust molecular circadian clock machinery including the circadian genes Per1, Per2, Bmal1, and Rev-Erba, was identified in the cochlea and was found to regulate this differential sensitivity to day or night noise exposure. Using RNAseq we recently identified 7211 genes in the cochlea that have circadian expression and a large proportion of them regulate cell signaling, hormone secretion and inflammation. Near ⅔ of these genes show maximal expression at nighttime, a finding which can only be captured when performing analyses around the clock. Moreover, from a therapeutic standpoint, our findings are relevant to the most common treatment of hearing disorders, namely the use of anti-inflammatory steroids such as dexamethasone. Unfortunately, the use of steroids for hearing disorders are well known to have mixed success in treatment outcome. This mixed outcome could likely be due to the protocol of administration, which usually includes several doses throughout the day. Time-dependent treatment strategies (chronopharmacology) have been highly successful in the treatment of cancer and inflammation. Interestingly, our findings show that dexamethasone treatment is effective in preventing noise-induced hearing loss only when administered during the daytime, and not at nighttime. Alternatively, pre-treating animals with a TrkB agonist before a night noise trauma was protective but not when administered during daytime. The idea of chronopharmacology needs to be considered in the auditory field both clinically and experimentally since circadian rhythms, and possibly inflammation, appear to control important physiological responses in the cochlea, including synaptic maintenance and repair. Finally, the large proportion of physiology regulated by the circadian clock suggests that the clock itself might present a possible pharmaceutical target to increase efficacy and reduce side effects. In order for such treatments to be effective, a more detailed knowledge will be required not only of how clocks control physiology, but also of how clocks in different organ systems contribute to different processes relevant to hearing disorders.

SYMP 16

Models of noise-induced hearing loss and hearing dysfunction: translation from rodents to humans

Colleen G. Le Prell
University of Texas at Dallas-Callier Center

Permanent noise-induced threshold shift cannot be systematically controlled and manipulated in human subjects for obvious ethical reasons. Therefore, most of what we know about permanent noise injury comes from systematic manipulation of noise exposure in animal models ranging from rodents to primates. Experimental data collected from human participants have largely been collected using temporary threshold shit (TTS) paradigms. The relatively more recent identification of noise-induced synaptopathy after noise exposures that resulted in TTS, but no permanent elevation in thresholds, has now raised questions about the safety of TTS studies in humans. The highly similar patterns of neural injuries in mice, guinea pigs, rats, and non-human primates suggest humans are also likely to be vulnerable to noise induced neural injury, but damage-risk criteria

that identify where risk begins, and how risk grow with increasing exposure, are not known. This presentation will briefly review the most common rodent models used in laboratory-based studies and contrast them with the design of studies enrolling human participants. The effects of noise on hearing dysfunction as derived using electrophysiological and psychophysical tools in these two populations (rodents, human participants) will be reviewed and the implications for damage-risk criteria discussed.

SYMP 17

Macrophages in the Cochlea

Keiko Hirose
Washington University in St. Louis

Macrophages in the inner ear have been observed in a variety of conditions including during development, after inner ear damage, in the setting of systemic inflammation, and in cochlear infection. One of the original observation of macrophages in the inner ear dates back to 1971 in Professor Bohne's dissertation entitled: Scar formation in the inner ear following acoustical injury: sequence of changes ranging from early signs of damage to healed lesion. In her thesis, she describes changes that occur in the sensory structures after acoustic injury, and she notes the presence of macrophages adjacent to the organ of Corti in the act of tissue clearance.

Since the initial observations of cochlear macrophages in plastic embedded sections by light and electron microscopy, further studies employing genetic reagents in mice, including fluorescent reporters of chemokine receptors, have provided more detailed information regarding the myeloid cell population in the inner ear and the roles they play during damage and repair. We will review the work that has followed the initial description of macrophages in the acoustically damaged ear to include studies of inner ear leukocytes in a variety of conditions with a focus on the mammalian cochlea.

SYMP 18

Synaptopathic Consequences of Noise Exposure

Sharon G Kujawa
Eaton-Peabody Laboratories, Massachusetts Eye and Ear Infirmary and Department of Otolarynology, Harvard Medical School, Boston, Massachusetts

Noise-induced hearing loss occurs when sound overexposure injures delicate inner ear tissues and compromises vulnerable inner ear functions. Threshold elevations after noise can be temporary or permanent and the underlying injury subtle or dramatic. Barbara Bohne and her colleagues have provided extensive documentation of noise-induced changes in structure and function in research spanning four decades. Experiments in our laboratories have extended these observations by revealing a more insidious, but common process that doesn't kill hair cells, but instead, permanently interrupts their communication with cochlear neurons. Subtotal inner hair cell (IHC) synapse loss is invisible in routine histopathological material and the threshold audiogram, the test most fundamental to the diagnosis of sensorineural hearing loss, is silent to its presence. We now know that noise exposure produces significant and widespread cochlear synaptopathy in all mammalian species studied thus far, including compelling preliminary data obtained from human temporal bone cases. It is present for a broad range of exposures, including many that would be considered benign based on threshold assays. We have documented the early appearance and gradual progression of IHC synapse loss with age, a decline that is exaggerated in ears with recovered thresholds after noise exposure. Accumulating evidence in animal models suggests that IHC synaptopathy may be a common finding in other forms of acquired sensorineural hearing loss as well. This talk will serve as a brief overview of key findings and potential public health significance for humans. Work supported by grants from the NIH/NIDCD, DoD and ONR.

SYMP 19

Searching for Evidence of Noise-Induced Cochlear Synaptopathy in Humans: Looking for a Needle in a Haystack

Tiffany A. Johnson[1]; Nikki Go[1]; Navin Viswanathan[2]
[1]University of Kansas Medical Center; [2]University of Kansas

There is emerging evidence from several labs that the cochlear synaptopathy that has been reported in animal models may also occur in noise-exposed, normal-hearing humans. These findings are intriguing because synaptopathy may provide an explanation for the clinical dilemma of noise-exposed, normal-hearing individuals who report difficulty hearing in noise. Unfortunately, substantial inter-subject variability in the group data makes it difficult to distinguish individuals with likely synaptopathy from those exhibiting normal variability, limiting the clinical translation of these findings. Recent work in our lab has focused on exploring the extent to which humans show physiologic and perceptual patterns consistent with cochlear synaptopathy. A particular focus has been on developing tools that are expected to be sensitive to synaptopathy but that would reduce random variability. Our recent findings call into question the extent to which general recreational and occupational exposures in normal-hearing, young adults produce symptoms of synaptopathy that can be measured with current tools.

SYMP 20

Alteration of Glutamatergic Synapses in the Cochlear Nucleus after noise-induced tinnitus and their restoration after brain circuit modulation.

Susan Shore
University of Michigan

Projections from somatosensory nuclei to the cochlear nucleus (CN) colabel with vesicular-glutamate transporter (VGLUT)2 while auditory nerve colabels with VGLUT1. After cochlear ablation, VGLUT2 in CN increases while VGLUT1 decreases. We asked what happens after noise exposure and tinnitus? Are the changes in VGLUT2 specific to tinnitus or a global change after noise damage.

To induce tinnitus, guinea pigs received mild (98 dB SPL; ¼ Octave band, 1.5 h), unilateral noise exposure that induced tinnitus in about half of the animals, as revealed by gap-prepulse inhibition of the acoustic startle. Following tinnitus induction, a subset of animals with tinnitus received bimodal, auditory-somatosensory stimulation designed to reverse dorsal cochlear nucleus circuit plasticity, previously shown to reduce tinnitus (Marks et al., Science Translational Medicine, 2017). The bimodal stimulation was performed for 20 min/day for one month.

Increases in VGLUT2 in the CNs ipsilateral to noise damage were confined to noise-exposed animals that developed tinnitus. After bimodal treatment, VGLUT levels were not significantly different from normal controls. VGLUT1, in contrast, showed tinnitus-specific decreases in the contralateral CN.

The tinnitus-specific increases in VGLUT2 were confined to regions that receive somatosensory projections and are therefore likely due to increased somatosensory projections to the CN in tinnitus. The decreased VGLUT1 in the contralateral CN may reflect altered auditory nerve activity in the contralateral ear, perhaps due to altered activity of later olivocochlear efferents. Reversal of VGLUT2 and VGLUT1 to normal levels after bimodal stimulation suggests that bimodal treatment effects involve somatosensory plasticity as well as LOC changes.

ARO 2017 short invited.docx

SYMP 21

Validating The Frequency Pattern of Noise-Induced Hearing Loss With A Unique DPOAE Protocol

Brenda Lonsbury-Martin[1]; Barden Stagner[2]; Glen Martin[3]
[1]*Loma Linda University Health;* [2]*Research Service, VA Loma Linda Healthcare System;* [3]*VA Loma Linda Healthcare System and Loma Linda University Health*

Distortion product otoacoustic emissions (DPOAEs) have not lived up to their promise of being the objective counterpart of the clinical audiogram. Current thinking attributes DPOAE generator sources as a mixture of distortion and reflection components. Recent studies using interference tones or onset-latency measures indicate that DPOAEs are generated considerably more basal along the basilar membrane than previously assumed. These findings explain a number of puzzling DPOAE phenomena including the inverted U-shaped f2/f1-ratio function. The influence of this new knowledge about the extended generation sites of DPOAEs may lead to an improved objective DP-gram that better complements the clinical audiogram.

Auditory Prostheses III

PD 25

Relating Vowel Confusions to Focused Thresholds in Pediatric Cochlear Implant Users

Kelly Jahn; Mishaela DiNino; Matthew Winn; Julie G. Arenberg
University of Washington

Speech perception is variable across cochlear implant (CI) users. Some of this variability may be due to differences in spectral resolution, as accurate speech identification requires the ability to resolve frequency components of a complex signal. In CI users, loss or distortion of spectral information may arise from suboptimal interfaces between CI electrodes and their target neurons, the extent of which can vary between individuals and across a single electrode array. Suboptimal interfaces are believed to arise from regions of low neural survival or poor electrode placement and may be identified by channels with elevated thresholds measured with spatially-focused electrode configurations. Because vowel identification is particularly sensitive to changes in spectral detail, focused thresholds may provide insight into a CI users'; specific vowel confusions. Thus, the goal of the present study was to relate vowel confusion patterns of pediatric CI users to their focused threshold profiles across the electrode array. Eight pediatric Advanced Bionics CI users (15 implanted ears) between the ages of 11-17 years participated. Vowel recognition in the

presence of a 4-talker babble (+10 dB signal-to-noise ratio) was assessed with a closed set of medial vowels. Focused thresholds were measured on electrodes 2-15 with a partial tripolar (pTP) electrode configuration (σ = 0.9). Patterns of vowel recognition were examined using a perceptual vowel space analysis, which models the direction of errors in terms of physical articulatory and acoustic space. In typical vowel space, the first formant generally varies as a function of vowel height, whereas the second formant varies with vowel advancement. Accordingly, the hypothesis was that higher focused thresholds on channels transmitting low frequency information would be associated with errors in vowel height, whereas higher focused thresholds on channels transmitting high frequency information would be related to errors in vowel advancement. Results from a linear mixed model analysis showed that average focused thresholds on the most basal electrodes (12-15) predicted perception of front vowels as more back. These errors are consistent with the idea that higher focused thresholds for basal channels indicate reduced sensitivity of higher-frequency energy that is characteristic of front vowels. These findings suggest that suboptimal electrode-neuron interfaces could affect perception of fundamental vowel characteristics that are extracted from global spectral properties of the signal.

PD 26

Effects of a Potassium Channel Modulator on Temporal Processing by Cochlear Implant Listeners: The QuicK+fire Study

Robert P. Carlyon[1]; John M. Deeks[1]; François Guérit[2]; Wiebke Lamping[3]; Alexander Billig[4]; Charles H. Large[5]
[1]*MRC Cognition and Brain Sciences Unit, University of Cambridge;* [2]*MRC Cognition & Brain Sciences Unit, University of Cambridge;* [3]*Hearing Systems group, Department of Electrical Engineering, Technical University of Denmark;* [4]*Brain and Mind Institute, The University of Western Ontario;* [5]*Autifony Therapeutics*

Temporal processing by cochlear implant (CI) listeners is degraded. When the pulse rate applied to a single electrode is increased, pitch increases only up to an upper limit of about 300-500 pps, and, even at lower pulse rates, the smallest detectable change is much larger than in normal hearing. Inferior Colliculus (IC) recordings from animals show that a physiological correlate of the upper limit is reduced by deprivation and increased by subsequent chronic stimulation. We have previously used psychophysical tests of the upper limit of pitch and of the discrimination of pulse-rate changes to demonstrate significant improvements over the first two months following implant activation. Here we use the same techniques to evaluate the effects of a pharmaceutical intervention on temporal processing by CI users.

The fast-acting Kv3.1 potassium channel is important for sustained temporally accurate firing and is susceptible to deprivation, the effects of which can be partially restored in animals by the molecule AUT00063. As part of a larger randomised placebo-controlled double-blind study, we investigated the effects of AUT00063 on the upper limit of temporal pitch, gap detection, and discrimination of low rates (centered on 120 pps) for monopolar pulse trains presented to an apical electrode. The upper limit was measured using the optimally efficient MidPoint Comparison (MPC) pitch-ranking procedure; thresholds were obtained for the other two measures using an adaptive procedure. Twelve CI users (MedEl and Cochlear) were tested before and after two 28-day periods of AUT00063 or placebo in a within-subject crossover study. No significant differences occurred between post-drug and post-placebo conditions. This absence of effect occurred despite high test-retest reliability for all three measures, obtained by comparing performance on the two baseline visits, and despite the demonstrated sensitivity of the measures to changes over the first two months post activation. Hence we have no evidence that AUT00063 improves temporal processing for the doses and patient population employed in the QuicK+fire study. Observations of our experience with this first-ever clinical trial of a drug aimed at improving hearing by CI users will be presented.

PD 27

Evaluation of Alternative Implementations of a Binaural Cochlear-Implant Sound Coding Strategy Inspired by the Medial Olivocochlear Reflex

Enrique A. Lopez-Poveda[1]; Almudena Eustaquio-Martín[1]; Milagros J. Fumero[1]; José M. Gorospe[2]; Rubén Polo López[3]; María Auxiliadora Gutiérrez Revilla[3]
[1]*University of Salamanca;* [2]*Hospital Universitario de Salamanca;* [3]*Hospital Ramón y Cajal*

The MOC strategy is a binaural sound coding strategy aimed at reinstating the unmasking benefits of the contralateral medial olivocochlear (MOC) reflex to the users of cochlear implants (CIs) (Lopez-Poveda, 2015, EU patent WO2015/169649 A1). Inspired by the inhibitory effect of the contralateral MOC reflex on basilar-membrane gain and compression, the MOC strategy involves using dynamic and contralaterally controlled acoustic-to-electrical compression functions in each frequency channel of processing. We have previously shown that bilateral CI users can show better speech recognition in noise with the MOC strategy than when using two independent audio processors with time-invariant compression, the current clinical standard (STD) (Lopez-Poveda

et al., 2016, Ear Hear. 37(3):e138-e148; Lopez-Poveda et al., 2017, Hear. Res. 348:134-137). The tests conducted so far, however, have been limited to an implementation of the MOC strategy with fast control of compression and with greater inhibition in the higher than in the lower frequency channels. Here, we investigate if bilateral CI users may show even better speech recognition in noise with a more realistic MOC implementation that involves slower control of compression, and slightly greater inhibition in the lower than in the higher frequency channels. Speech reception thresholds (SRTs) were measured with the STD, the fast (original) MOC, and the slower MOC strategies for single target and noise sources at azimuthal angles of (0, 0), (-15, +15), (-60, +60) and (-90, +90) degrees. The mean SRT was 1.0 dB SNR worse for the fast MOC than for the STD strategy for co-located target and noise sources, but was 1 to 2.5 dB SNR better for spatially separated sources. Mean SRTs were 1.5 to 2 dB better for the slower MOC than for STD strategy across all of the spatial configurations tested, including the co-located condition. Overall, the slow MOC strategy maintains the benefits of the fast MOC strategy for spatially separated target and maskers and extends them to other spatial configurations [Work funded by MED-EL, and MINECO (ref. BFU2015'65376'P)].

PD 28

Using Vibrotactile Stimulation to Improve Cochlear Implant Performance in Pitch-Related Listening Tasks

Stephanie Long; Kiana Gerard; Gabriella Isaac; Lauren Hayes; **Xin Luo**
Arizona State University

Introduction
Current cochlear implants (CIs) do not faithfully encode pitch cues due to the limited spectral and temporal resolutions. Poor pitch perception with CIs may partially account for the great challenges that CI users experience when listening in a competing talker background, perceiving music, and processing speech prosodic cues such as vocal emotions and lexical tones. A recent study (Huang et al., 2017) reported that tactile vibrations at the fundamental frequency (F0) of acoustic input significantly improved CI users'; speech recognition in noise. This study tested the extent to which vibrotactile stimulation may compensate for the limited access to pitch cues and improve CI performance in pitch-related listening tasks such as melodic contour identification and vocal emotion recognition.

Methods
10 normal-hearing listeners listened to acoustic CI simulations with 4 and 8 noise bands. A vibration motor (Precision Microdrives) was attached to the forearm top

of right hand to provide vibration at the F0 of acoustic input. Melodic contour identification and vocal emotion recognition were tested with acoustic stimulation alone, vibrotactile stimulation alone, and combined acoustic and vibrotactile stimulation. For melodic contour identification, musical notes were transposed to the frequency range from 55 to 220 Hz for presentation through the vibrotactile stimulation. Different device conditions and different spectral resolutions with CI simulations were tested in random order. In each condition, training with feedback was provided before testing without feedback. Vibration detection thresholds and vibration frequency discrimination thresholds were also measured.

Results
Data collection is still ongoing. Preliminary data showed variable sensitivity to vibrotactile stimulation across subjects. Frequency discrimination and melodic contour identification with vibrotactile stimulation alone were worse than those with normal hearing but similar to those with CI simulations alone. Training improved melodic contour identification and vocal emotion recognition in different conditions.

Conclusions
Training may play an important role in using vibrotactile stimulation to improve CI performance in pitch-related listening tasks.

PD 29

Effect of Envelope Modulations in Bilateral Cochlear-Implant Listeners

Matthew Goupell; Olga Stakhovskaya; Stephen Fong; Kristina Milvae
University of Maryland, College Park

Introduction
Relatively slow envelope modulations are thought to improve the salience of interaural time differences (ITDs) conveyed by high-rate carriers in normal-hearing (NH) listeners. Envelope modulation encoding and loudness growth functions, however, may be significantly interaurally asymmetric for bilateral cochlear-implant (CI) listeners, unlike the assumed symmetry of NH listeners. The purpose of this study was to determine if envelope modulations decrease ITD sensitivity for bilateral CI users.

Methods
Data from bilateral CI listeners were compared to a control group of NH listeners. The electrical stimuli were pulse trains presented using direct stimulation on single electrodes; the acoustic stimuli were bandlimited acoustic pulse trains presented over headphones. The three factors that were varied were pulse rate (100-400 pulses per second), place of stimulation, and envelope

amplitude modulation (unmodulated=Flat, modulated and binaurally correlated=Correlated, or modulated and binaurally uncorrelated=Uncorrelated). Modulations for the electrical stimuli were transformed by the typical compression function used in CI sound processing algorithms. The pulse trains were presented at comfortable levels. The listeners'; task was to detect a target in a three-interval, two-alternative forced-choice procedure. Target intervals had 180° interaurally out-of-phase pulse trains (non-zero ITD); non-targets had in-phase pulse trains (zero ITD). Listeners were presented 100 repetitions per condition and the percentage of correct responses was measured in a method of constant stimuli. To understand the symmetry of the ears, perceptual loudness growth functions (LGFs) were measured in both CI and NH listeners. Electrically evoked compound action potential amplitude growth functions (ECAP-AGFs) were also measured in the CI listeners.

Results
Preliminary data in six CI and three NH listeners suggest that overall ITD discrimination performance decreases with increasing rate and the rate limitation becomes more pronounced with advancing age of the listener. There was no systematic effect of place of stimulation. Data for the critical comparison across envelope types suggest a decrease in performance for the modulated envelope conditions (Correlated and Uncorrelated) compared to the Flat condition. A relationship between the difference in ITD discrimination in the Flat and Correlated conditions, and the interaural differences in LGFs and ECAP-AGFs will be investigated.

Discussion
Envelope modulations, intended to be interaurally correlated and to possibly improve ITD sensitivity, may become interaurally decorrelated by CI sound processing and/or interaurally asymmetric neural encoding. These sources of interaural decorrelation would be a limiting factor to greater binaural hearing benefits, such as good sound localization and speech understanding in noise performance.

PD 30

O-15 Water PET study of speech in noise processing in cochlear implant patients

Phillip Gander[1]; Laura Ponto[2]; Inyong Choi[2]; Bob McMurray[2]; Timothy Griffiths[3]
[1]Human Brain Research Laboratory, Department of Neurosurgery, The University of Iowa; [2]The University of Iowa; [3]Newcastle University

One of the most important issues in hearing impairment (HI) is difficulty with speech in noisy real-world environ-

ments. Recent research in normal hearing listeners indicates that auditory cortex is active while abstracting speech objects from noise and provides input to fronto-temporal networks for further perceptual, attentional, and semantic analysis. We sought to understand whether the neural mechanisms by which cochlear implant listeners detect speech in noisy environments are similar.

We measured [15O]Water positron emission tomography (PET) blood flow in a group of 9 cochlear implant patients while they listened to 2-min blocks of continuous sentences in noise or noise alone (matched on RMS sound level). On a given run for speech in noise (+7 dB), 30 unique sentence tokens (~2.5 sec length) were presented (1.5 sec inter stimulus interval). We acquired 12 scans (6 each condition, random order) to allow for single subject inference. PET data were analyzed in SPM12 using a flexible factorial model.

We found robust activations in single subjects for the contrast speech in noise vs noise in auditory cortex (lateral Heschl';s gyrus, planum polare, and planum temporale) and inferior frontal cortex (frontal operculum and inferior frontal gyrus) bilaterally (p

Ten age-matched normal hearing control subjects were scanned for comparison of neural substrate of the network and overall activity level. We found similar brain activations in auditory cortex, however inferior frontal activity was largely absent. Differences between the groups likely reflect signal audibility and effort.

Our results support a similar model for speech in noise processing in cochlear implant patients and normal hearing listeners. Differences in level of activation between the groups, in particular inferior frontal cortex, highlight key brain regions to target for improved cochlear implant performance.

PD 31

Speech Understanding of Cochlear Implant Listeners using a Mixed Rates Strategy

Thibaud Leclère[1]; Alan Kan[2]; Ruth Y. Litovsky[2]
[1]Waisman Center, University of Wisconsin Madison; [2]University of Wisconsin-Madison

Cochlear implant (CI) users demonstrate good speech recognition in quiet situations, but still encounter difficulties in noisy environments. With a second implant, CI users can benefit from the head shadow effect and demonstrate some spatial masking release which, however, remains less than that obtained by normal hearing (NH) listeners. Clinical CI processors typically discard temporal fine structure and encode speech cues by ap-

plying the envelope of the speech signal to a pulsatile high-rate (~1,000 Hz) carrier. At these high rates, CI users are insensitive to interaural time differences (ITDs), and thus have lower binaural unmasking, and poorer localization performance compared with NH listeners. To improve ITD sensitivity, pulse rates must be lowered to <300 Hz (for most CI users). However, there is a trade-off between needing high rates for speech understanding and low rates for spatial hearing. Previous work has shown that using low and high rates at the apex and base, respectively, can improve ITD sensitivity while maintaining reasonable speech understanding. However, recent work has shown that the previous rate/place configuration may be suboptimal for enabling ITD sensitivity. In the present study, we investigate the effect of different mixed-rate configurations on speech understanding in quiet, unilateral listening. Speech recognition tests were conducted in CI and NH listeners using research processors and 16-channel vocoder simulation, respectively. Three high- and low-rate configurations along the cochlear array were tested for the NH listeners, and five configurations were tested for CI listeners, including: all-high, all-low, interleaved high/low, apical low/basal high and basal low/apical high. The influence of the number of low-rate channels and the effect of "dead regions" were also investigated. Results from both listener groups showed that speech recognition scores were best when all electrodes operated at a high pulse rates, and worst when all electrodes operated at low pulse rates. Concerning the conditions in which pulse rates were mixed across the cochlear array, results showed that speech recognition scores were intermediate to the all-high or all-low rate conditions. When disabling the channels operating at low rates (simulating "dead regions"), speech recognition scores dropped significantly, suggesting that listeners did not completely ignore low-rate channels. These results provide a proof of concept demonstrating that low-rate channels can be combined with high-rate channels without a huge detriment to speech understanding. The next step in this work is to determine whether using mixed rate strategies could improve binaural unmasking in bilateral CI listeners.

PD 32

Benefits of cochlear implantation for single sided deafness: Data from the House Clinic-USC-UCLA FDA trial

John Galvin[1]; Qian-jie Fu[2]; Eric Wilkinson[3]; Dawna Mills[3]; Suzannah Hagan[3]; Eric Lupo[3]; Monica Padilla[4]; Robert Shannon[4]
[1]House Ear Institute; [2]SPAPL, Dept. of Head and Neck Surgery, DGSOM, UCLA; [3]House Clinic; [4]Keck School of Medicine, USC

We report data for 10 patients who participated in this FDA-approved study of cochlear implantation for SSD. Audiological thresholds, localization, speech perception in quiet and in noise, tinnitus severity, dizziness severity, and quality of life (QoL) were measured before implantation and during the six-month period after activation of the cochlear implant (CI). All patients were implanted with the Med-El Flex 28 device.

Pure-tone average (PTA) thresholds were calculated across 0.5, 1.0, and 2.0 kHz. Speech understanding in quiet was measured using CNC words and HINT sentences. Localization was measured in sound field using a 12-speaker array. Sentence recognition thresholds (SRTs), defined as the signal to noise ratio (SNR) needed to produce 50% correct word recognition for HINT sentences in noise, were adaptively measured for three spatial conditions: 1) speech and noise from the center (S0N0), 2) speech from center, noise to the CI ear (S0Nci), and 3) speech from the center, noise to the NH ear (S0Nnh). Tinnitus severity was measured using a visual analog scale (VAS) with the CI off or on, and using the Tinnitus Functional Index (TFI). Dizziness severity was measured using the Dizziness Handicap Inventory (DHI). QoL was measured using modified versions of the Glasgow Hearing Aid Benefit Profile (GHABP) and the Spatial, Speech, and Quality (SSQ) questionnaires.

Data reported is six months post-activation, relative to baseline. Mean PTA thresholds with the CI improved from 92 to 39 dBHL. Mean CNC and HINT performance with the CI improved by 50 and 83 percentage points, respectively. For localization, mean RMS error was reduced by 11°. Mean SRTs slightly worsened by 0.3 dB for the S0Nci condition, and improved by 2.1 and 2.2 dB for the S0N0 and S0Nnh conditions, respectively. The mean tinnitus VAS score was reduced by 1.9 points (scale: 0-10). The mean TFI score was reduced by 20 points (scale: 0-100). The mean DHI score was reduced by 4 points (scale: 0-100). For the GHABP, mean difficulty was reduced by 1.4 points with the CI on (scale: 0-5); patients generally found the CI to be helpful and were moderately satisfied with the CI. For the SSQ (scale: 0-10), mean scores improved by 2.0, 2.8, and 0.9 points for the speech, spatial, and quality categories, respectively.

These data suggest that cochlear implantation can improve SSD patients'; sound awareness, speech understanding in quiet and in noise, sound source localization, and QoL, while reducing tinnitus and dizziness severity.

PD 33

Potential Role of XIRP2 in the Maintenance and Repair of Hair Cell Stereocilia

Elizabeth L. Wagner; Tingting Du; Maura I. Nakahata; Jung-Bum Shin
University of Virginia

The auditory system is particularly sensitive to damage, as mature mammalian sensory hair cells are incapable of regeneration. Therefore, hair cell death can lead to irreparable hearing loss. Damage to hair bundles, the mechanosensitive organelles at the surface of hair cells, can also lead to decreased hearing function. However, in some cases, it is possible for minor hair bundle damage to be repaired. For example, tip links can be spontaneously regenerated after they are broken. Additionally, damage to the stereocilia core may also be reversible, as evidenced by the localization of γ-actin and other proteins important for F-actin elongation and nucleation to sites of breakage. Our preliminary studies suggest that XIRP2 (Xin Actin Binding Repeat Containing 2) may also be involved in stereocilia F-actin repair. We previously described XIRP2 as a novel hair cell protein enriched in the hair bundle, where it colocalizes with F-actin. Knockout of Xirp2 causes hearing loss in mice; moreover, heterozygous mutations in XIRP2 were identified in humans with age related hearing loss. While less severe than the hearing loss in the total Xirp2 KO mice, heterozygous Xirp2 mice also develop progressive hearing loss.

Two major isoforms of XIRP2 are expressed in the hair cell. The long isoform localizes to F-actin based structures including the cuticular plate and the pericuticular necklace. The short XIRP2 isoform colocalizes with the F-actin core of stereocilia in the hair bundle. We have observed an enrichment of short XIRP2 immunostaining at breaks in F-actin signal. We hypothesize that short XIRP2 is recruited to damaged stereocilia where it may stabilize and/or facilitate the repair of F-actin. To test this hypothesis, we will knock in GFP at the endogenous Xirp2 locus, enabling ex vivo live imaging of the response of short XIRP2 to mechanical stereocilia damage. Furthermore, we plan to investigate the role of short XIRP2 by identifying interacting proteins and by determining the effects of specific ablation of the short isoform.

In summary, this project proposes a novel mechanism for the maintenance and repair of hair cell stereocilia.

PD 34

Endocytosis and Transcytosis Mechanisms of the Outer Hair Cell

Csaba Harasztosi[1]; Entcho Klenske[1]; Susanne Badum[1]; Emese Harasztosi[1]; Anthony W. Gummer[2]
[1]*Section of Physiological Acoustics and Communication, University of Tübingen, Germany;*
[2]*University of Tübingen*

Background
Membrane particles are intensively endocytosed at the apical pole of outer hair cells (OHCs) and transcytosed to different locations, namely into the basolateral membrane and along a central strand down to the nucleus (Griesinger et al., 2004; Kaneko et al., 2006). Endocytic vesicles have been demonstrated in the infranuclear region of OHCs using electron microscopy (Nadol, 1983) and horseradish peroxidase staining (Siegel & Brownell, 1986). Here, the aim is to study endocytosis and transcytosis bidirectionally.

Methods
The styrylpyridinium dye FM1-43 was applied locally to investigate endocytic activity and vesicle traffic of OHCs isolated from the guinea-pig cochlea. The perfusion system was designed for dye application at either the apex or base of the cell. To reveal different modes of endocytosis, concanavalin-A, an inhibitor of clathrin-mediated endocytosis, or phenylarsine oxide, a blocker of pinocytosis and phagocytosis, was applied. Different types of transcytosis mechanisms were tested using monastrol, a blocker of the microtubular motor protein kinesin, or 2,4,6-triiodophenol, a blocker of the microfilament transport protein myosin VI. A fluorescence-threshold intensity of 20% of the saturated plasma-membrane signal was used to estimate the delay of intracellular vesicle transport relative to the onset of the plasma-membrane signal. Trafficking speed was determined from the slope of linear regression of fluorescence onset-delays at different intracellular locations.

Results
Average signal-onset delays in infracuticular and infranuclear regions relative to the plasma-membrane signals were 51±21 s (n=15) and 14±5 s (n=7), respectively. The endocytosis blockers increased the onset delays in both regions: concanavalin-A to 125±55 s (n=8) infracuticular and 97±51 s (n=7) infranuclear; phenylarsine oxide to 156±79 s (n=7) infracuticular and 301±109 s (n=6) infranuclear. Investigating apicobasal and basoapical trafficking, the slope parameter was found to be 0.129±0.007 μm/s (n=15) and 0.196±0.015 μm/s (n=7), respectively. In the case of apicobasal traffic, 2,4,6-triiodophenol significantly reduced the slope parameter (0.034±0.001 μm/s, n=4), but monastrol had no statistically significant

effect (0.119±0.004 µm/s, n=5). In the case of basoapical traffic, both monastrol (0.055±0.001 µm/s, n=8) and 2,4,6-triiodophenol (0.054±0.002 µm/s, n=7) significantly reduced the slope.

Conclusion

The data demonstrate more intense endocytic activity at the nuclear pole and larger vesicle traffic towards the apex of the OHC. Application of endocytosis inhibitors reveals the presence at both poles of both clathrin-mediated and non-clathrin-mediated processes. The data also imply myosin VI carrying vesicles in both apicobasal and basoapical directions, but that kinesin participates only in basoapical trafficking.

PD 35

Transmembrane Inner Ear protein (Tmie) regulates proper Tmc localization in zebrafish hair cells

Itallia Pacentine; Teresa Nicolson
OHSU

The transmembrane inner ear (TMIE) protein is required for the function of auditory and vestibular hair cells. Mutations in *TMIE* cause deafness in fish, mice, and humans; previous work suggests an unidentified role in mechanotransduction (MET). We generated twelve transgenes of zebrafish *tmie* that systematically delete or replace peptide segments, and then assayed for localization and functional rescue in a *tmie* mutant, *ru1000*. Results revealed that Tmie can function as a single-pass transmembrane protein. By testing FM labeling in these transgenic mutants, we also identified a new functional region of Tmie, the extracellular region and second transmembrane domain, which lack full rescue when mutated. Overexpression of full-length Tmie enhances bundle expression of a GFP-tagged transmembrane channel-like (Tmc2b-GFP), whereas transgenic Tmc1-GFP and Tmc2b-GFP are unable to traffic to the bundle in the absence of Tmie. Finally, transgenic *tmie* constructs that do not fully rescue the transduction defect in *ru1000* show reduced levels of bundle Tmc2b-GFP. In sum, our results suggest that Tmie's role in MET is to regulate Tmc bundle localization.

PD 36

A molecular basis for water motion detection by the mechanosensory lateral line of zebrafish

Shih-Wei Chou[1]; Zongwei Chen[1]; Shaoyuan Zhu[1]; Robin Davis[1]; Jiaqi Hu[1]; Li Liu[1]; Carol Fernando[1]; Kayla Kindig[1]; William Brown[1]; Ruben Stepanyan[2]; **Brian McDermott**[1]

[1]*Department of Otolaryngology, University Hospitals Cleveland Medical Center, Case Western Reserve University School of Medicine;* [2]*Dept. Physiology, Univ. Kentucky; Dept. Otolaryngology, Case Western Reserve University*

Detection of water motion by the lateral line relies on mechanotransduction complexes at stereocilia tips. This sensory system is comprised of neuromasts, patches of hair cells with stereociliary bundles arranged with morphological mirror symmetry that are mechanically responsive to two opposing directions. Here, we find that transmembrane channel-like 2b (Tmc2b) is differentially required for mechanotransduction in the zebrafish lateral line. Despite similarities in neuromast hair cell morphology, three classes of these cells can be distinguished by their Tmc2b reliance. We map mechanosensitivity along the lateral line using imaging and electrophysiology to determine that a hair cell';s Tmc2b dependence is governed by neuromast topologic position and hair bundle orientation. Overall, water flow is detected by molecular machinery that can vary between hair cells of different neuromasts. Moreover, hair cells within the same neuromast can break morphologic symmetry of the sensory organ at the stereocilia tips.

PD 37

Hair Bundle Stimulation by Fluid Jet Results in Complex Hair Bundle Movements that Modify the Manifestation of Adaptation

Anthony Peng[1]; Yanli Wang[2]; Alexandra Scharr[3]; Andrew Mecca[4]; Dailey Nettles[4]; Anthony J. Ricci[5]

[1]*Department of Physiology and Biophysics, University of Colorado Anschutz, Aurora, CO;* [2]*Mechanical Engineering Graduate Program, Stanford University, Stanford, CA, USA.;* [3]*Neurosciences Graduate Program, Stanford School of Medicine, Stanford, CA, USA.;* [4]*Neuroscience Program, University of Colorado Anschutz, Aurora, CO;* [5]*Department of Otolaryngology, Head and Neck Surgery, Stanford School of Medicine, Stanford, CA, USA.*

Hair cells convert sound vibrations into electrical signals through the process of mechanotransduction that occurs in the stereocilia hair bundle. A key mechanism of this process involves the cells ability to adapt to sus-

tained hair bundle deflections. Calcium has long been thought to drive this adaptation process, but we recently proposed a calcium independent form of adaptation (1) using displacement-controlled stimuli to hair bundles. However, others have subsequently claimed only calcium dependent adaptation in mammalian hair cells when using force-controlled stimulation (2–4). Using high speed video imaging of rat auditory outer hair cell hair bundles paired with electrophysiological recordings and a faster force-controlled stimulus rise time of 0.5 ms, we characterize the force-controlled stimulation of the hair bundle to reveal a complex motion with multiple rise-times and non-uniform displacement. The complex motion likely has contributions from fluid dynamics and hair bundle mechanics. The hair bundle movement kinetics are altered when changing the mechanical properties of the hair bundle with BAPTA treatment to break inter-stereocilia linkages or with paraformaldehyde fixation of the hair bundle. We find these complex movements mask fast adaptation in the current response, however, when providing a displacement-controlled step stimulation to the hair bundle with a fluid jet, we observe fast adaptation at both negative and positive potentials indicating a calcium independent form of adaptation. We also find that force-controlled fluid jet stimulation unmasks a slow component of adaptation that did not manifest as clearly with a displacement step from a stiff fiber. These data have implications as to how the hair cell receptor potential is shaped by the in vivo mode of hair bundle stimulation.

1. Peng AW, Effertz T, Ricci AJ (2013) Adaptation of Mammalian Auditory Hair Cell Mechanotransduction Is Independent of Calcium Entry. *Neuron* 80(4):960–972.
2. Corns LF, Johnson SL, Kros CJ, Marcotti W (2014) Calcium entry into stereocilia drives adaptation of the mechanoelectrical transducer current of mammalian cochlear hair cells. *Proc Natl Acad Sci U S A* 111(41):14918–23.
3. Corns LF, Johnson SL, Kros CJ, Marcotti W (2016) Tmc1 Point Mutation Affects Ca2+ Sensitivity and Block by Dihydrostreptomycin of the Mechanoelectrical Transducer Current of Mouse Outer Hair Cells. *J Neurosci* 36(2):336–349.
4. Beurg M, Goldring a. C, Fettiplace R (2015) The effects of Tmc1 Beethoven mutation on mechanotransducer channel function in cochlear hair cells. *J Gen Physiol* 146(3):233–243.

PD 38

Outer hair cell nonlinear capacitance mirrors prestin kinetics, but does not report on electromotility frequency response.

Joseph Santos-Sacchi[1]; Winston Tan[2]
[1]*Department of Surgery (Otolaryngology), Neuroscience, and Cellular and Molecular Physiology, Yale University School of Medicine, New Haven, Connecticut, USA;* [2]*Department of Surgery (Otolaryngology), Yale University School of Medicine, New Haven, Connecticut, USA*

The voltage-dependent protein SLC26a5 (prestin) underlies outer hair cell (OHC) electromotility (eM), known to be responsible for cochlear amplification (CA) in mammals. The electrical signature of eM is a bell-shaped nonlinear capacitance (NLC), which peaks at the membrane voltage (V_h). We recently determined that the apparent voltage dependencies of NLC and eM differ depending on interrogation frequency, revealing slow (multi-exponential) intermediate conformational transitions between required anion binding and voltage-driven prestin charge movements (Song and Santos-Sacchi, PNAS 110:3883-8, 2013). These results appear to challenge the concept of tight coupling between prestin sensor charge (Q_p) and eM, namely piezoelectric-like behavior of the protein. Indeed, we subsequently found phase differences between membrane voltage and eM (Santos-Sacchi and Song, Biophys J 107:126-33, 2014). Here we study simultaneous prestin electrical activity and eM across frequency to further assess electro-mechanical coupling.

Simultaneous electrical (either prestin displacement/gating currents or NLC) and mechanical activity of guinea pig OHCs were obtained under voltage clamp at frequencies up to 6.25 kHz, with induced eM measured by either photo diode or fast video (25000 fps) techniques. Analysis of fundamental and harmonic gating currents and corresponding eM responses showed complementary magnitude and phase measures, confirming tight coupling between the two. However, simultaneous measures of NLC and eM showed both similarities and differences. Since NLC is a ratio of changes in prestin charge and membrane voltage (dQ_p/dV_m), measures of NLC are impervious to voltage clamp time constant because our dual-sine C_m analysis technique solves for OHC admittance. The frequency dependent behavior of NLC thus derives from intrinsic kinetics of prestin transitions. On the other hand, since eM is tightly coupled to Q_p, as confirmed above, the mechanical response magnitude follows membrane voltage perturbation (the drive for Q_p movements) in frequency. Thus, while NLC is impervious, patch clamp time constant is linearly related to eM and Q_p cutoff frequency, with NLC itself contributing to the RC cutoff. In fact, eM and Q_p cutoff frequency can

be increased by series resistance compensation which increases voltage delivery bandwith, but is ultimately limited by NLC (prestin transition) kinetics.

These data indicate that NLC cannot be used to infer eM frequency response, and that NLC kinetics is rate limiting for eM and Qp. Furthermore, NLC contributes to a dynamic "RC time constant" in OHCs, which decreases on either side of V_h. Thus, the position of V_h vis-à-vis the OHC resting potential will set eM, and consequently, CA gain and bandwidth.

PD 39

TMC2 partially restores hair cell and auditory function in mice lacking TMC1

Yukako Asai[1]; Bifeng Pan[1]; Carl Nist-Lund[1]; Alice Galvin[1]; Andrei Lukashkin[2]; Victoria Lukashina[2]; Ian Russell[2]; Jeffrey R. Holt[3]; Gwenaelle Geleoc[1]
[1]Boston Children's Hospital, Harvard Medical School; [2]University of Brighton, UK; [3]Boston Children's Hospital, Harvard Medical School

Background
Sensory hair cells of the inner ear convert mechanical signals into electrical signals using a sensory transduction complex residing at stereocilia tips. Tmc genes, associated with dominant and recessive nonsyndromic sensorineural hearing loss (Kurima et al., 2002), encode for transmembrane channel like proteins which are components of the sensory transduction complex. In developing auditory hair cells, Tmc2 is expressed transiently and is followed by sustained Tmc1 expression beginning after postnatal day 3 (Kawashima et al., 2011). The rise of Tmc2 expression coincides with the developmental acquisition of hair cell transduction, while the rise of Tmc1 expression precedes the onset of auditory function. Analysis of transduction currents in cochlear outer hair cells of mice lacking Tmc1 or Tmc2 revealed nearly normal responses during the first postnatal week (Kawashima et al., 2011). Mice lacking both Tmc1 and Tmc2 had no sensory transduction in any hair cell from any region at any time point. Based on these observations we hypothesize that TMC1 and TMC2 proteins have redundant functions and that expression of either TMC1 or TMC2 may be sufficient for hair cell sensory transduction.

Methods
To explore the temporal requirements of Tmc2 gene expression and the functional redundancy between Tmc1 and Tmc2, we generated a knock-in mouse model allowing Cre-inducible expression of Tmc2 under the control of a CAG promoter. We assayed for changes in hair cell survival, sensory transduction and auditory function in developing and mature mice in which endogenous expression of Tmc1, Tmc2 or both was replaced with Cre-inducible expression of transgenic Tmc2 (Tmc2Tg). Results: We demonstrate that Tmc2Tg can partially, but not fully, compensate for the absence of Tmc1. We show that hair cells from mice lacking Tmc1 but expressing constitutive Tmc2Tg had enhanced survival. Tmc2Tg hair cells acquire sensory transduction at earlier stages and maintain expression for an extended period relative to Tmc1-null cells. Despite cellular recovery, minimal recovery of auditory brainstem responses was observed at the onset of hearing in the Tmc2Tg mice. ABR thresholds were absent at 6 weeks of age.

Conclusion
Our results show that Tmc2Tg can partially compensate for Tmc1 but cannot substitute long-term for the absence of Tmc1 expression. Since TMC2 was sufficient for restoration of sensory transduction, but insufficient for auditory function, we hypothesize that Tmc1 expression must provide some additional necessary function, not provided by Tmc2.

PD 40

Gating without swinging: a two-channel model of hair-cell mechanotransduction with membrane-mediated cooperativity.

Francesco Gianoli[1]; Thomas Risler[2]; **Andrei Kozlov**[1]
[1]Department of Bioengineering, Imperial College London; [2]Laboratoire Physico Chimie Curie, Institut Curie, PSL Research University, CNRS; Sorbonne Universités, UPMC Univ Paris 06, CNRS

Sound-induced vibrations of the inner ear stretch tip links between stereocilia of hair cells and open mechanotransduction ion channels. Channel opening relaxes the tip links, which reduces the hair-bundle stiffness and enhances the hair cells'; sensitivity. The classical explanation for this gating compliance has been that a conformational rearrangement of a single channel directly shortens the tip link, but that model requires an unrealistically large steric change for a single channel. Experimental evidence indicates, however, that each tip link is a dimeric molecule, associated on average with two channels at its lower end. It also indicates that the lipid bilayer bearing these channels modulates their gating, although it is not clear how. Here we will present a new model of mechanotransduction, with two channels per tip link, mobile within the membrane. Their states and positions are coupled by membrane-mediated elastic forces arising from the interaction between the channels'; hydrophobic cores and that of the lipid bilayer. The model quantitatively reproduces the main properties of hair-cell mechanotransduction using only realistic parameters. This work provides an insight into the funda-

mental role that membrane-mediated ion-channel cooperativity can play in sensory physiology.

Auditory Nerve Impairment, Preservation, and Repair: Implications for Cochlear Implants

SYMP 22

The auditory nerve in profoundly deaf ears

M. Charles Liberman
Harvard Medical School

This talk will summarize what is known from the study of animal models and human temporal bones about the time course and patterns of auditory nerve degeneration in ears with sensorineural hearing loss of different degrees, etiologies and durations. Although the cell body and central axons of auditory nerve fibers can survive for years after the onset of deafness, the speed and extent of degeneration depends on the nature of the damage to the organ of Corti, especially the extent to which supporting cells remain intact. Although the electrical thresholds and conduction velocities of the auditory nerve remain normal long after they have lost connections to their hair cell targets, there is evidence for changes in synaptic transmission at their central connections in the cochlear nucleus.

SYMP 23

ECAP measures of neural health in a guinea pig model

Dyan Ramekers[1]; Stefan B. Strahl[2]; Sjaak F. L. Klis[1]; Huib Versnel[1]
[1]University Medical Center Utrecht, Brain Center Rudolf Magnus, Utrecht University; [2]Research and Development, MED-EL Medical Electronics, Innsbruck, Austria

The electrically evoked compound action potential (ECAP) is a direct functional measure of the auditory nerve, and is therefore thought to contain valuable information with respect to the nerve's health. Often only the ECAP threshold is used for diagnostics, CI fitting and research purposes, thereby ignoring a wealth of additional possibly useful information about the condition of the auditory nerve. Additional suprathreshold measures derived from input-output functions, as well as other characteristics derived from ECAP morphology, may greatly improve its prognostic and diagnostic utility. Comparing such ECAP characteristics in healthy and pathological cochleae - in combination with detailed histological analysis - may reveal distinct functional consequences of specific cochlear pathology. We have shown that the effect size of pulse shape variation on various ECAP measures, such as the N1 latency and the slope of the

input-output function, is indicative of neural survival in deafened guinea pigs (Ramekers et al. 2014, J Assoc Res Otolaryngol 15: 187-202). Similarly, we have shown that the modulation depth of the alternating pattern in ECAP amplitude that emerges with high pulse rates is highly correlated with neural survival (Ramekers et al. 2015, Hear Res 321:12-24). These ECAP measures may be used to assess the functional effects of neuroprotective treatments (Ramekers et al. 2015, J Neurosci 35:12331-12345). In addition, these measures can be applied to estimate neural health in human cochlear implant patients.

SYMP 24

Clinical applications of neural-health measures

Kara C. Schvartz-Leyzac[1]; Christopher J. Buswinka[1]; Timothy A. Holden[2]; Aaron P. Hughes[1]; Deborah J. Colesa[1]; H. Alexander Arts[1]; Teresa Zwolan[3]; Jill B. Firszt[2]; Yehoash Raphael[4]; Bryan E. Pfingst[1]
[1]Department of Otolaryngology - Head and Neck Surgery, University of Michigan; [2]Department of Otolaryngology - Head and Neck Surgery, Washington University School of Medicine; [3]University of Michigan; [4]Kresge Hearing Research Institute, University of Michigan

Animal models have allowed for improved understanding of auditory nerve anatomy and function in hearing-impaired ears and have demonstrated relationships between neural status and simple measures of cochlear-implant function. For example, studies have shown that specific characteristics of the electrically-evoked compound action potential (ECAP) are related to neural status in electrically-stimulated guinea pig cochleae. Consequently, such measures can be used to estimate neural status in cochlear implanted humans. While previous studies using postmortem temporal bone methods have not provided strong evidence that speech recognition outcomes in humans are related to peripheral neural density, interpretation of these studies is complicated by the temporal separation between the functional and histological measures. Further, these studies often compare speech recognition across subjects with diverse central and cognitive processing abilities. We propose that ECAPS can be used to estimate neural status and thus allow comparison between auditory nerve function and speech understanding in humans during the same time period and using a within-subject design. From these studies, there is evidence that cochlear implant outcomes in humans are determined, in part, by properties of the stimulated auditory nerve. Results to date show that certain ECAP measures are affected to various degrees by extraneous non-neural factors such as distance from the electrode to presumed site of neural excitation; therefore, certain measures may be better

suited than others for estimation of neural status in humans. This talk will focus on the relationship between electrophysiological measures of neural health and cochlear implant performance in humans, and will discuss potential application and limitations of these measures to be used in a clinical setting.

SYMP 25

Closing the gap between the cochlear implant and the auditory nerve

Pascal Senn[1]; Marta Roccio[2]; Helge Rask-Andersen[3]; Marcus Mueller[4]; Hubert Loewenheim[5]
[1]Department of Clinical Neuroscience, Service ORL and HNS, University hospital of Geneva, Switzerland; [2]Laboratory of Inner Ear Research, Department of Biomedical Research, University of Bern, Switzerland & Dept. of Otorhinolaryngology, Head & Neck Surgery, Inselspital Bern, Switzerland; [3]University of Uppsala; [4]University of Tuebingen, Germany; [5]University ENT clinic, University of Tuebingen, Germany

Cochlear implants (CI) restore functional hearing in the majority of deaf patients. Despite the tremendous success of these devices, some limitations remain. The bottleneck for optimal electrical stimulation with CI is caused by the anatomical gap between the electrode array and the auditory neurons in the inner ear. As a consequence, current devices are limited through (i) low frequency resolution, hence sub-optimal sound quality and (ii), large stimulation currents, hence high energy consumption (responsible for significant battery costs and for impeding the development of fully implantable systems). A recently completed, multinational and interdisciplinary project called NANOCI aimed at overcoming current limitations by creating a gapless interface between auditory nerve fibers and the cochlear implant electrode array. This ambitious goal was achieved in vivo by neurotrophin-induced attraction of neurites through an intracochlear gel-nanomatrix onto a modified nanoCI electrode array located in the scala tympani of deafened guinea pigs. Functionally, the gapless interface led to lower stimulation thresholds and a larger dynamic range in vivo, and to reduced stimulation energy requirement (up to five-fold) in an in vitro model using auditory neurons cultured on multi-electrode arrays. In conclusion, the NANOCI project yielded proof of concept that a gapless interface between auditory neurons and cochlear implant electrode arrays is feasible. These findings may be of relevance for the development of future CI systems with better sound quality and performance and lower energy consumption. The present overview summarizes the NANOCI project history and achievements as well as applicability and conceptual limitations for future clinical cochlear implant systems.

Inner Ear: Mechanics & Modeling I

PD 41

Amplification in the Mammalian Cochlea Arises from Active Feedback to Hair Bundles

Daibhid O Maoileidigh
Department of Otolaryngology - Head and Neck Surgery, Stanford University School of Medicine

To amplify their responsiveness to sinusoidal and step stimuli, the auditory and vestibular hair bundles of non-mammalian vertebrates employ an active process. Active hair-bundle motility arises from nonlinearity inherent to the mechanotransduction channels, feedback from adaptation, and electrochemical energy sources. Although it is likely that mammalian predecessors possessed active hair-bundle motility, mammalian hair bundles have not been observed to exhibit active motions and outer hair cells possess somatic motility. It remains unclear how sensory systems based on active hair-bundle motility evolved to incorporate somatic motility.

To understand evolution of the cochlear amplifier, we compare the dynamics of active hair bundles to that of the cochlea as a whole. We construct a mathematical model of active hair-bundle motility based on calcium-dependent adaptation and a model of the cochlear amplifier that employs somatic motility. Despite differences in their components, we show that the dynamics of these systems is fundamentally similar. Active amplification in the mammalian cochlea can arise from somatic motility, mechanical coupling between the soma and bundles of outer hair cells, and energy extracted from the endocochlear potential and the resting potentials of outer hair cells. In other words, active feedback to a hair bundle can be achieved through calcium-dependent adaptation or through somatic motility coupled to electrical energy sources.

Although the cochlear model has multiple degrees of freedom, whereas the hair bundle is described by only two variables, the dynamics of both models is controlled by a hair bundle';s mechanical load. The response of either model to sinusoidal stimulation is large, sharply tuned, and nonlinear when they operate under similar conditions. Owing to somatic motility, however, the cochlear model can detect much higher-frequency input than the model describing a single hair bundle. Feedback from somatic motility provides negative damping to the hair bundle, allowing a bundle embedded in the cochlea to operate at high frequencies.

In summary, the common principle connecting amplification by hair bundles and amplification in the mammalian cochlea is active feedback to hair bundles. We pro-

pose that somatic motility evolved to supplement active hair-bundle motility, but now likely dominates feedback to hair bundles in the mammalian cochlea. Whether active hair-bundle motility is required for hearing in mammals is still an open question.

PD 42

Compression and suppression on the basilar membrane and inside the organ of Corti

Marcel van der Heijden; Nigel Cooper
Erasmus MC

Using Optical Coherent Tomography (OCT), we recorded the mechanical response of the basilar membrane (BM) and the Deiters cells (DC) region to multi-tone (zwuis) stimuli in the 16-30-kHz region of gerbil cochleae. We studied compression by simultaneously varying the sound intensity of all the components; suppression was studied by varying the intensity of a single component while keeping the others fixed. The BM responses exhibited the familiar combination of linear growth in the low-frequency tail and increasingly compressive growth for higher frequencies, starting from ~1/2 octave below the characteristic frequency (CF). The DC region showed compression over the entire range of frequencies tested, down to 6 octaves below CF. Near-CF components in the DC region showed hypercompression, with the response magnitude decreasing with increasing magnitude. Suppression showed a similar dichotomy between the BM and the DC region. On the BM, only near-CF components could be suppressed; whereas in the DC region, probes of any frequency could be suppressed by increasing the intensity of another component. In particular, it was possible to suppress low-frequency (<<CF) probes by near-CF suppressors.

PD 43

Analyzing and Visualizing the Onset of Distortion Product Generation Using a Computational Model

Thomas Bowling; Julien Meaud
G.W.W. School of Mechanical Engineering, Georgia Institute of Technology

Distortion products (DPs) are generated in the cochlea in response to stimulation by two primary tones (f1 and f2). Measuring DPs in the ear canal as distortion product otoacoustic emissions provides a noninvasive measure of the health and functionality of the ear that is used in both clinical and research applications. Due to the presence of the primary tones in the response, both experimental and modeling analyses of DPs are usually performed in the frequency domain. However, by systematically varying the phase of the two primaries and combining the measured waveforms through ensemble averaging, the primaries and all DPs except the DP of interest (e.g. 2f1-f2) are removed from the response. When used with a computational model, this enables visualization of the onset of DP generation within the cochlea. The present work uses a physiologically-based nonlinear computational model of the gerbil ear cochlea to study the onset of DP generation. The model includes a two-duct three-dimensional model of the intracochlear fluid and is formulated in the time domain. The stimulus to the model is a two-tone signal with a raised cosine envelope. Simulations of both the DP intracochlear fluid pressure and basilar membrane velocity responses are presented. Both the initial and steady-state DP response are examined to provide a fuller understanding of DP generation and propagation. Using a two-duct fluid model enables decomposition of the intracochlear fluid pressure into an antisymmetric component associated with the slow traveling wave and symmetric component associated with the fast traveling wave. Varying the primary phases and combining waveforms through ensemble averaging shows how these pressure components vary during the onset of DP generation and several animations are presented to aid in visualization.

PD 44

The Effect of Localized Organ of Corti Impedance Irregularities on Stimulus-Frequency Otoacoustic-Emission Generation: A Mouse-Cochlea Finite-Element Model Study

Hamid Mottalebzadeh[1]; Sunil Puria[2]
[1]*Eaton Peabody Lab, Massachusetts Eye and Ear Infirmary, Harvard Medical School;* [2]*Eaton-Peabody Laboratory, Massachusetts Eye and Ear; Department of Otolaryngology, Harvard Medical School; Speech and Hearing Bioscience and Technology, Harvard University Graduate School of Arts and Sciences*

Stimulus-Frequency Otoacoustic emissions (SFOAEs) are reflections of base-to-apex forward travelling waves due to impedance irregularities of the organ of Corti (OoC) structures that travel backwards and are measured in the ear canal. While it is known that the anatomical and material properties vary from base to apex, it remains to be determined which of the structures are most influential in the generation of SFOAEs. In addition, there is debate that the dominant region is from near the traveling-wave peak and/or from basal to the peak. In the present work, we study the contribution of the different structures and regions of the OoC in SFOAE generation by introducing random perturbations of the structural properties in a 3D finite-element model of the mouse cochlea. The model has been previously validated against experimental measurements at both the low-frequency apical and high-frequency basal regions to produce level dependent amplification and tun-

ing characteristics of the mouse cochlea (Motallebzadeh and Puria, ARO, 2017). We introduced random perturbations to the following model parameters: Young';s moduli of basilar membrane (BM), reticular lamina (RL), and outer hair cells (OHC); the thickness of the BM; and the OHC gain factor a (OHC force to stereocilia shear ratio). The results were calculated in the 20 to 30 kHz range with a frequency resolution of 100 Hz with 10% random perturbation from the baseline parameter values. The BM thickness and Young';s modulus and OHC gain a have the most significant effect on SFOAE. In addition, spatially selective and incremental addition of perturbations in the BM Young';s modulus indicates that SFOAEs are generated mainly in a region within about 20% of the cochlear length basal to the peak of the best frequency (BF). This observation is consistent with the coherent reflection filtering theory which states that the tall-and-broad peak regions of traveling waves are the dominant backscattering contributors to SFOAE generation (Shera and Zweig, 1995; Zweig and Shera, 1995). Similar incremental perturbations apical to BF suggests that the contributions of cochlear structure apical to BF are negligible. The spatial resolution of the structural perturbations was also studied and results show that when the spatial distance between perturbation increases from a fraction of inter-OHC spacing to up to 8 times the spacing, the SFOAE magnitudes generally increase.

PD 45

Spectral Ripples in Round-Window Cochlear Microphonics

Karolina K. Charaziak[1]; Jonathan Siegel[2]; Christopher Shera[3]
[1]Caruso Department of Otolaryngology, University of Southern California; [2]Hugh Knowles Center, Roxelyn and Richard Pepper Department of Communication Sciences and Disorders, Northwestern University; [3]Caruso Department of Otolaryngology and Department of Physics and Astronomy, University of Southern California

The cochlear microphonic (CM) results from the vector sum of transduction currents, primarily of outer hair cells (OHCs), excited by a sound stimulus. The common notion that the CM measured at the round window in response to pure tones is dominated by cellular sources located within the tail region of the basilar-membrane (BM) excitation pattern predicts that CM amplitude and phase vary little with stimulus frequency. We tested this prediction in chinchillas using low-level tones swept in fine steps over a wide range of frequencies. Contrary to expectations, the CM amplitude and phase demonstrate a striking, quasiperiodic pattern of spectral ripples, even at frequencies above 3 kHz where interference with delayed neurophonic responses appears unlikely. By analogy with mechanisms responsible for spectral ripples in distortion-product otoacoustic emission (DPOAE fine structure), we hypothesize that CM spectral ripples represent an interference pattern produced by CM components with different phase gradients: a short-latency component with a shallow phase gradient, and a long-latency component with a rapidly rotating phase. We explore this possibility using a model of CM generation in the chinchilla. In the model, the short-latency CM component arises from sources located in the tail region of the BM excitation pattern. In this region, unlike near the peak region, the BM moves nearly in phase and the OHC currents add constructively. Although sources within the peak region would normally tend to cancel, the long-latency CM component arises from this region through a mechanism analogous to "coherent reflection". When the spatial-frequency content of random spatial irregularities in the strength of local OHC currents includes components that match the wavelength of the traveling wave, potentials combine coherently, producing a significant long-latency contribution to the total CM. Spectra ripples in the model CM responses were observed only if both short- and long-latency components were included in the simulations. Suppression experiments in chinchillas also support the existence of long-latency CM components originating predominately near the peak. When a higher-level suppressor tone at a nearby frequency is presented concurrently with the stimulus, the amplitude of the spectral ripples is considerably reduced. The two-component CM source model captures well the trends observed in the data, such as the size and spacing of the ripples. Although alternative models (e.g., based on multiple internal reflection) also produce spectral ripples, our preliminary results suggest that the two-component source model best captures the trends observed in the data.

PD 46

Interaural Coupling and Synchronization of Two Active Ears

Christopher Bergevin[1]; Natasha Mhatre[2]; Jaina Negandhi[3]; Robert Harrison[3]
[1]York University; [2]University of Toronto, Scarborough; [3]The Hospital for Sick Children, Toronto, Ontario, Canada

To a first order, the vertebrate inner ear can be considered active and "self-contained" in that the key elements for auditory transduction are coupled together and mechanically isolated within the bony labyrinth of the inner ear. A salient manifestation is the idiosyncratic nature of human spontaneous otoacoustic emissions (SOAEs),

which effectively provide a unique acoustic "fingerprint" for a given ear. Aside from efferent innervation in tetrapods, non-mammalian classes exhibit acoustic interaural coupling (i.e., a contiguous internal airspace between tympanic membranes). Such is believed important in some species for improved azimuthal sound localization (e.g., Christensen-Dalsgaard, 2011) as the coupling allows for the two ears to effectively act as a "pressure difference receiver" (e.g., Fletcher & Thwaites, 1979). Unlike humans, SOAE activity from both ears of a lizard generally exhibit strikingly similar spectral features (e.g., comparable peak frequencies). Furthermore, recent results reporting temporal SOAE correlations between ears for the gecko (Roongthumskul & Hudspeth, 2017) suggest the two active ears mechanically synchronize with one another. We sought to further explore this provocative notion using a two-pronged empirical approach in a lizard model (Anolis carolinensis) that displays robust SOAE activity. First, we attempted to measure SOAE activity via the mouth. The hypothesis was that if acoustic crosstalk occurs between the two ears to drive synchronized SOAE activity, than such should be apparent in the oral cavity (which appears to be connected to the interaural airspace). We were readily able to observe "SOAEs" in the oral cavity, which shared highly similar spectral features with the spectra measured from each ear at the external meatus. Evoked emissions could also be readily detected orally. Second, to better characterize the acoustic pathway for crosstalk between ears, we examined middle ear morphology and the interaural space by means of both gross dissection and microCT. We found a clear airborne pathway between the two ears and with the oral cavity. Preliminary results indicate features of ossicular coupling between the tympanic membrane and oval window that may contribute to how inner-ear-generated sound appears in the interaural/oral space. Taken together, these data support the hypothesis that acoustic coupling can cause the two ears to effectively synchronize biomechanically. This notion may have profound implications for the role of "coupling" between active elements (e.g., determining more precisely the relevant forces acting upon a given hair cell) and functional features such as sound localization in non-mammalian tetrapods.

PD 47

The Missing Fundamental Found on the Reticular Lamina at the Base of the Gerbil Cochlea by Heterodyne Low-coherence Interferometry

Tianying Ren[1]; Wenxuan He[2]
[1]*Oregon Hearing Research Center, Oregon Health & Science University;* [2]*Oregon Hearing Research Center*

Background

While the mechanism underlying pitch perception of the missing fundamental remains to be determined, recent micromechanical measurements demonstrated that the outer hair cell-driven reticular lamina vibration is highly nonlinear and not frequency specific. It generates a variety of distortion products in response to different tone stimulations at frequency ranges broader than those of the basilar membrane vibration. We hypothesized that, like other distortion products, the perceived missing fundamental is generated by outer hair cells and manifests as the reticular lamina vibration at its generation location. This hypothesis was tested by measuring the reticular lamina vibration at the missing fundamental frequency using heterodyne low-coherence interferometry.

Methods

Young Mongolian gerbils with normal hearing were used in this study. Harmonic complex tones comprised of frequencies 2f0, 3f0, 4f0, and 5f0 (f0=500, 1,000, or 2,000 Hz) at different sound pressure levels were used to stimulate the cochlea. Displacements of the reticular lamina and basilar membrane vibration were measured through the round window from the base of the cochlea as a function of time using a custom-built heterodyne low-coherence interferometer. Spectra of the time waveform were obtained and used to show the missing fundamental. An external tone at frequencies close to f0 was used to suppress the missing fundamental on the reticular lamina.

Results

At intermediate sound pressure levels, the missing fundamental was found in magnitude spectra of the reticular lamina vibration but not in those of the basilar membrane vibration in sensitive cochleae. Although a tone at a frequency close to f0 at appropriate levels suppressed an external single tone-induced reticular lamina vibration completely at f0, it did not induce significant change in complex tone-evoked reticular lamina vibrations at the missing fundamental frequency.

Conclusion

The present data support the working hypothesis that the missing fundamental is generated by outer hair cells and displayed on the reticular lamina. The lack of suppression of the missing fundamental indicates that mechanical activities outside the travelling wave contribute to the cochlear processing of complex sounds. When the travelling wave at f0 is suppressed, the missing fundamental generated and detected at the high-frequency region is responsible for pitch perception.

Funding

PD 48

Wave interference and the electrically evoked organ of Corti response spectrum

Amir Nankali[1]; Karl Grosh[2]
[1]University of Michigan; [2]University of MIchigan

Input sounds to the mammalian ear produce waves that travel from the base to the apex of the cochlea. These traveling waves stimulate the microstructure of the organ of Corti (OoC) in the center of the cochlea. The interplay between the traveling wave and a distinct nonlinear amplification process boosts the cochlear responses and enables sound processing over a broad frequency and intensity ranges. In vivo intracochlear electrical stimulation also induces a mechanical response of the OoC. The frequency response of the electrically evoked motion of the BM shows an antiresonance notch slightly below the characteristic frequency (CF) of the measurement location [1,2]. In order to interpret the experimental data and identify the underlying mechanism, a comprehensive three-dimensional model of the cochlea is used. Our model predicts, as in the experiment [1], a notch at the frequency below the CF which is attributed to the interference of the multiple travelling waves along the cochlea. Electrical stimulation causes energy to be propagated basally to the stapes, setting up standing waves in the fluid between the excitation location and the base. It is found that the depth of the notch is sensitive to the BM boundary condition as well as the active process mediated by the OHC somatic force. Our model predicts similar notch for the reticular lamina (RL) motion as the BM while the RL displacement amplitudes are larger, as seen in the experiments [2].

K. Grosh, J. Zheng , Y. Zou, E. de Boer, A. Nuttall. High-frequency electromotile responses in the cochlea. Acoustical Society of America, 115(5):2178–2184, 2004.

T. Ren, W. He, P. Barr-Gillespie. Reverse transduction measured in the living cochlea by low-coherence heterodyne interferometry. Nature communications, 2016, 7, 10282-10282

Molecular Landscape of Hearing Loss I

PD 49

Hear-'n-SEQ: an international collaboration to discover unknown genetic etiologies of hearing loss in kids

Jun Shen[1]; Michael Cohen[1]; Anne Giersch[1]; Paula Goldenberg[1]; Margaret Kenna[1]; Andrea Oza[1]; Marcie Steeves[1]; David Sweetser[1]; Alexander O'Brien[2]; Arti Pandya[2]; Hatice Duzkale[3]; Nilnur Eyerci[4]; Ye Cao[5]; Richard Choy[5]; Youjin Li[6]; Yilai Shu[7]; Xue-Zhong Liu[8]; Mustafa Tekin[8]; Denise Yan[8]; Hela Azaiez[9]; Richard J. H. Smith[9]; Giorgia Girotto[10]; Anna Morgan[10]; Paolo Gasparini[10]; Cynthia Morton[1]
[1]Harvard Medical School Center for Hereditary Deafness; [2]University of North Carolina; [3]Cincinatti Children's Hospital Medical Center; [4]Kafkas University; [5]The Chinese University of Hong Kong; [6]Shanghai Children's Hospital Medical Center; [7]1. Department of Otolaryngology, Harvard Medical School, 2. Eaton-Peabody Laboratory, Massachusetts Eye and Ear Infirmary, 3. Department of Otolaryngology, Hearing Research Institute, Affiliated Eye and ENT Hospital of Fudan University; [8]University of Miami Miller School of Medicine, Department of Otolaryngology; [9]Molecular Otolaryngology and Renal Research Laboratories, Department of Otolaryngology—Head and Neck Surgery, Carver College of Medicine, University of Iowa; [10]IRCCS "Burlo Garofolo"

Hearing loss is one of the single most common birth defects with life-long impacts, because it affects a child';s

ability to develop speech, language, cognitive and social skills. The earlier a child with hearing loss starts receiving appropriate medical and educational services, the more likely they are to reach their full potential. More than half of early hearing loss is due to genetic factors. While the majority of prelingual hearing loss is nonsyndromic, over 400 syndromes have been described that have hearing impairment as a component. It is critical to identify the etiology of hearing loss for many reasons, as there may be important health surveillance implications particularly with syndromic causes and for family members. Although hundreds of genes have been associated with hearing loss, currently available clinical genetic testing for congenital hearing loss can only explain about a third of the cases, because: 1) the clinical significance cannot be determined for many genetic variants found in known hearing loss genes; 2) certain types of genetic variants affecting known hearing loss genes are not detectable by current testing methods; and 3) it is estimated that a large number of hearing loss genes are as yet unknown. We have organized an international consortium to overcome this hurdle. Through a collaborative project called Hear-'n-SEQ: Sequencing Kids First for Hearing, we leverage resources of the Gabriella Miller Kids First Pediatric Research Program supported by the National Institutes of Health Common Fund';s. The goal is to "seek-out" the genetic etiology of childhood hearing loss through comprehensive phenotypic and genomic analyses in an international cohort of hearing impaired patients. This international collaboration is positioned to produce a maximum yield of diverse genetic causes, as it has been well established that different populations segregate distinct concentrations of hearing loss alleles. We have identified and collected well-curated patient clinical information and DNA samples from children with hearing loss and their parents (trios) or carefully selected multiple affected individuals based on the pedigree structure. Affected children have been screened to exclude known genetic causes for hearing loss. To date, we have submitted 473 individuals in 151 families for whole genome sequencing (WGS) through the program. They represent samples from hearing impaired pediatric populations of parts of East Asia (Hong Kong and China), Europe (Italy), the Middle East (Turkey), and the US (individuals of European, African American, Central American and Caribbean descent). WGS interrogates the whole genome thus revealing variants in novel genes as well as noncoding and structural variants that are undetectable by standard testing. In addition to identifying novel etiologies for hearing loss, ultimately this work is designed to help create a pipeline for routinely integrating genomic sequencing into clinical diagnostics, generating more refined diagnostic capabilities, and eventually more targeted therapies or interventions for children with hearing loss. Furthermore, members of the Hear-'n-SEQ consortium have agreed to share both phenotypic and sequence data with the pediatric research community. We are working on integrating the data collectively into a shared harmonized data resource. We believe the collaborative effort will empower the greater research community to identify molecular mechanisms that underlie hearing loss. Hear-'n-SEQ will become more valuable, if more physicians and researchers know about it and join the force.

PD 50

The Deafness Variation Database: An Integrative Approach to Variant Classification for Deafness

Hela Azaiez[1]; Sean Ephraim[1]; Kevin Booth[2]; E Ann Black-Ziegelbein[3]; Bradley Crone[1]; Julie Wertz[4]; Andrea Hallier[5]; Eliot Shearer[6]; Christina Sloan-Heggen[7]; Diana Kolbe[1]; Carla Nishimura[1]; Thomas Casavant[5]; Michael Schnieders[8]; Terry Braun[8]; Richard J. H. Smith[1]

[1]Molecular Otolaryngology and Renal Research Laboratories, Department of Otolaryngology—Head and Neck Surgery, Carver College of Medicine, University of Iowa; [2]Molecular Otolaryngology and Renal Research Laboratories, Department of Otolaryngology—Head and Neck Surgery; Interdisciplinary Graduate Program in Molecular Medicine, Carver College of Medicine, University of Iowa; [3]Department of Otolaryngology-Head and Neck Surgery; [4]Iowa Institute of Human Genetics, University of Iowa; [5]Center for Bioinformatics and Computational Biology, Departments of Electrical and Computer Engineering and Biomedical Engineering, University of Iowa College of Engineering; [6]Department of Otolaryngology—Head and Neck Surgery, Carver College of Medicine, University of Iowa; [7]Medical Scientist Training program, Carver College of Medicine, University of Iowa; [8]Department of Biomedical Engineering

Comprehensive genetic testing using next-generation sequencing has evolved to become the most informative clinical test in the diagnostic evaluation of various diseases including deafness. However, the classification of genetic variants yielded by this approach represents a major challenge in the post-genome era because of both their extraordinary number and the complexity in elucidating their clinical significance. To address this challenge in the clinical evaluation of hearing loss, we have designed the Deafness Variation Database (DVD). The DVD is a deafness-specific, comprehensive, open-access resource that collates and summarizes all available data from major public databases to computationally provide a single classification in addition to expert curation of genetic variants in deafness-causing genes.

Data for the DVD are collected, combined, filtered and analyzed using a custom-built internal computational

pipeline. Available annotations including population-scale variant allele frequency, evolutionary conservation, deleteriousness scores and known disease genotype-phenotype associations are utilized to make an informed interpretation about the pathogenicity of each variant.

In its 8th version, the DVD reports 876,135 variants in 152 known deafness-causing genes. Of these variants, 7,474 (0.85%) are classified as pathogenic (P); 673 (0.08%) are likely pathogenic (LP); 15,285 (1.75%) are likely benign (LB); 156,971 (17.91%) are benign (B); and 695,732 (79.41%) are variants of uncertain significance (VUS). A systemic evaluation of these variants including expert review and curation identified over 300 medically significant discrepancies in 53 genes, which in the DVD are either upgraded to, or downgraded from a P/LP classification as compared to the classification in either ClinVar or the Human Gene Mutation Database. Of the top 20% of genes carrying the greatest number of medically significant discrepancies, six are associated with the diagnosis of Usher syndrome.

Of the known pathogenic variants, ~ 88% are exonic and 12% are splicing variants. Missense variants are the most common type representing nearly half of all reported pathogenic variants followed by frameshift indels, nonsense, splice-altering variants and inframe indels (22%, 13%, 12%, and 3% respectively). Novel and rare variants (Minor allele frequency (MAF) < 0.5%) represent 82% of all variants. Taken together, these findings highlight the complexity of distinguishing disease-causing variants from the "haystack" of VUSs.

In conclusion, the DVD integrates an automated genomic and bioinformatic pipeline, coupled with expert manual curation, to provide the most comprehensive deafness-specific variant interpretation available that will empower clinical decision making and provide an invaluable resource for scientists and clinicians. (Supported in part by NIDCD RO1s DC003544 and DC012049)

PD 51

Genetic defects in progressive hearing loss

Hannie Kremer[1]; Mieke Wesdorp[2]; Jeroen Smits[3]; Silvia Murillo-Cuesta[4]; Theo Peters[5]; Adelaida Celaya[6]; Margit Schraders[7]; Jaap Oostrik[1]; Martijn Huynen[8]; Pia de Koning-Gans[9]; Ignacio Del Castillo[10]; Pau Serra[11]; Ronald Admiraal[12]; Lies Hoefsloot[13]; Helger Yntema[14]; Isabel Varela-Nieto[15]; Ronald Pennings[12]

[1]Hearing & Genes Division, Department of Otorhinolaryngology, Radboud University Medical Center; [2]1Hearing & Genes Division, Dept. Otorhinolaryngology, Radboud University Medical Center; [3]1Hearing & Genes Division, Department of Otorhinolaryngology, Radboud University Medical Center; [4]Institute of Biomedical Research "Alberto Sols", Spanish National Research Council-Autonomous University of Madrid; Centre for Biomedical Network Research in Rare Diseases (CIBERER), Institute of Health Carlos III (ISCIII).; [5]Hearing & Genes Division, Dept Otorhinolaryngology, Radboud University Medical Center; [6]Institute of Biomedical Research "Alberto Sols", Spanish National Research Council-Autonomous University of Madrid; [7]Hearing & Genes Division, Dept. Human Genetics, Radboud University Medical Center; [8]5Centre for Molecular and Biomolecular Informatics, Radboud University Medical Center; [9]Dept Clinical Genetics, Leiden University Medical Center; [10]Servicio de Genetica, Hospital Universitario Ramon y Cajal, IRYCIS; [11]Institut D'Investigacions Biomèdiques August Pi i Sunyer (IDIBAPS); [12]Hearing & Genes Division, Dept. Otorhinolaryngology, Radboud University Medical Center; [13]Dept. Clinical Genetics, Erasmus Medical Centre; [14]Dept. Human Genetics, Radboud University Medical Center; [15]Institute of Biomedical Research "Alberto Sols", Spanish National Research Council-Autonomous University of Madrid; Centre for Biomedical Network Research in Rare Diseases (CIBERER), Institute of Health Carlos III (ISCIII); Hospital La Paz Institute

Unraveling the causes and pathomechanisms of progressive disorders is essential for development of therapeutic strategies. For a significant percentage of families with hereditary progressive hearing impairment (HI), a genetic diagnosis and thus mutation-based (genetic) counseling cannot be provided currently. We have analysed a series of families with progressive HI and either a dominant or recessive inheritance pattern by whole exome sequencing. In two families of Dutch origin with dominantly inherited HI, we identified heterozygous pathogenic missense variants of LMX1A. One of these variants occurred de novo and affected an amino acid of LMX1A's homeodomain, which is essential for DNA-binding. The second variant affected a zinc-binding residue of the second LIM domain that is

involved in protein-protein interactions. Although Lmx1a mouse mutants demonstrate neurological, skeletal, pigmentation and reproductive system abnormalities, no syndromic features were present in the participating subjects of either family. LMX1A has previously been suggested as a candidate gene for intellectual disability, but our data do not support this, as affected subjects displayed normal cognition. Phenotype characterization of the affected individuals revealed large variability in age of onset (congenital to 35 years), (a)symmetry, severity (mild to profound) and progression rate of HI. About half of the affected individuals displayed vestibular dysfunction and experienced symptoms thereof. We concluded that a single LMX1A wild-type copy is sufficient for normal development but insufficient for maintenance of cochleovestibular function and that genetic and/or environmental factors significantly affect the phenotypic outcome of the pathogenic variants. Currently, indications have been obtained for two additional genes to be associated with non-syndromic progressive HI and phenotypic characterization and analysis of further families and mouse models are ongoing to confirm disease association for these candidate genes.

PD 52

Analysis of candidate genes for age-related hearing loss from Genome-wide Association Studies

Neil Ingham[1]; Victoria Rook[2]; Annalisa Buniello[2]; Giorgia Girotto[3]; Paolo Gasparini[3]; Karen Steel[1]
[1]*King's College London and Wellcome Trust Sanger Institute;* [2]*King's College London;* [3]*IRCCS "Burlo Garofolo"*

A Genome-Wide Association Study (GWAS) of age-related hearing loss in a Southern European population indicated some candidate genes for involvement in the pathogenesis (Girotto et al 2011, J Med Genet 48: 369-374). Some showed specific expression patterns in the mouse cochlea, further supporting their candidacy (Girotto et al 2014, PLOS ONE 9:e85352). We investigated the potential role of several of these genes in hearing by generating the corresponding mouse mutants with severe or complete knockdown of each gene and analysing a wide range of auditory function, using the Auditory Brainstem Response (ABR), including threshold sensitivity, ABR waveform features, frequency tuning curves and temporal processing, in homozygous mutants and wildtype controls at 14 weeks old. Eleven genes analysed were A430005L-14Rik, Grm8, Slc16a16, Amz2, Ptprd, Evi5, Fzd6, Arsg, Tgm6, Sik3 & Dclk1, but only one (Dclk1) showed any functional abnormality at 14 weeks old. We studied Dclk1 mutant mice up to 12 months old and the small number of mutants available showed severe threshold elevations at frequencies of 12 kHz and higher.

There are several possible explanations for the scarcity of auditory phenotypes in these 11 mutant lines. Firstly, the mouse mutations produced either no gene expression or severely knocked-down expression, and it may be that any effects on hearing of variants in the human genes were mediated by abnormal protein function rather than a lack of protein. Secondly, although we generated alleles with severe effects on gene expression, it may be that any impact would only be seen at ages older than 14 weeks. Thirdly, we only tested two mutant lines for enhanced susceptibility to noise-induced damage, and maybe other genes would have shown such a genetic predisposition. Finally, the GWAS candidate genes may have been false positive findings or may have made only a very small contribution to the phenotypic variation. Recently a meta-analysis of published GWAS suggested that significant GWAS hits may explain such a small fraction of the total variance in the disease studied that the hits may be general fitness indicators rather than clues to disease-specific molecular pathways (Boyle et al 2017, Cell 169: 1177-1186). Our findings in this set of genes support this proposal and suggest that the genetic architecture of age-related hearing loss may be skewed towards many rare mutations each with a measurable impact on hearing rather than many common variants as detected by GWAS.

PD 53

The Impact of Next-Generation Sequencing on Genetic Diagnosis in the Israeli Jewish Deaf Population

Zippora Brownstein[1]; Suleyman Gulsuner[2]; Lara Kamal[3]; Ming Lee[2]; Noam Shomron[4]; Bella Davidov[5]; Lina Basel[5]; Moshe Frydman[6]; Michal Macarov[7]; Michal Sagi[7]; Tzippora Falik-Zaccai[8]; Tom Walsh[2]; Reuven Sharony[9]; Chana Vinkler[10]; Dorit Lev[11]; Hagit Baris-Feldman[12]; Moien Kanaan[3]; Stavit Allon-Shalev[13]; Mary-Claire King[2]; Karen B. Avraham[14]

[1]Department of Human Molecular Genetics & Biochemistry, Sackler Faculty of Medicine, Tel Aviv University, Tel Aviv, Israel; [2]Department of Medical Genetics, University of Washington, Seattle, WA, USA; [3]Department of Biological Sciences, Bethlehem University, Bethlehem, Palestine; [4]Department of Cell & Developmental Biology, Sackler Faculty of Medicine, Tel Aviv University, Tel Aviv, Israel; [5]Department of Medical Genetics, Rabin Medical Center, Petah Tikva, Israel; [6]Danek Gertner Institute of Human Genetics, Sheba Medical Center, Tel Hashomer, Israel; [7]Department of Human Genetics and Metabolic Diseases, Hadassah-Hebrew University Medical Center, Jerusalem; [8]Institute of Human Genetics, Western Galilee Medical Center, Nahariya, Israel; [9]Genetics Institute, Meir Medical Center, Kfar Saba and Sackler Faculty of Medicine, Tel Aviv University, Tel Aviv, Israel; [10]Wolfon's institute of genetics, Wolfson Medical Center, Holon, Israel; [11]Wolfon's institute of genetics, Wolfson Medical Center, Holon, Israel and Sackler Faculty of Medicine, Tel Aviv University, Tel Aviv, Israel; [12]Genetic Institute, Rambam Health Care Campus, Haifa, Israel and Rappaport Faculty of Medicine, Technion, Haifa, Israel; [13]Genetics Institute, Ha'Emek Medical Center, Afula, Israel; Rappaport Faculty of Medicine, Technion, Haifa, Israel; [14]Department of Human Molecular Genetics & Biochemistry, Sackler Faculty of Medicine and Sagol School of Neuroscience, Tel Aviv University, Tel Aviv 6997801, Israel

The complex structure of the ear and the many proteins involved in its function are responsible for clinical variability and genetic heterogeneity of hearing loss. One of our challenges has been to develop in this context an accurate and efficient approach to diagnosis of genetic hearing loss on behalf of Israeli families. In recent years, our application of next generation sequencing (NGS) to gene discovery in Israeli families with hearing loss has led to the realization that mutations in at least 22 different genes lead to hearing loss in Jewish Israeli families. We developed and deployed the HEar-Seq panel of 375 deafness genes, including protein-coding genes, micro-RNAs and human orthologues of mouse deafness genes, in order to characterize the distribution of hearing loss-associated mutations in our population and thereby develop a precise approach to their diagnosis in the clinic. Our study consisted of a cohort of 169 deaf individuals of various European and Sephardic Jewish ancestries, some from multiplex families and other with no family history. We evaluated a discovery series of 76 patients using the HEar-Seq panels, identifying the causal gene and mutation in 36 of them (46%). We then genotyped the remaining 93 subjects for all pathogenic variants from the discovery series by Sanger sequencing, identifying the causal mutation for 30 more subjects, giving a total of 66 subjects (39%) with their cause of deafness resolved. Pathogenic variants, including missense, indel, splice, nonsense, and copy number variants, were found in 22 different genes. Given that Israeli Jews have origins in in Europe, western Asia, and Northern Africa, in addition to the Middle East, it was not surprising to find so many different responsible genes and mutations in the hearing-impaired population. This study allowed us to make recommendations for specific founder mutations and genes that should be screened in patients based on their geographic origin, simplifying diagnostic testing in the clinic. For patients whose genetic hearing loss remains unresolved, the complete HEar-Seq panel is the most effective diagnostic tool.

PD 54

Enhanced cochlear transgene delivery with round window membrane inoculation combined with semi-circular canal fenestration in adult mice

Hidekane Yoshimura[1]; Seiji B. Shibata[1]; Paul T. Ranum[2]; Richard J. H. Smith[3]

[1]Department of Otolaryngology, Molecular Otolaryngology and Renal Research Laboratories, University of Iowa, Iowa, USA; [2]The University of Iowa; [3]Molecular Otolaryngology and Renal Research Laboratories, Department of Otolaryngology—Head and Neck Surgery, Carver College of Medicine, University of Iowa

Background

To date, there are several successful reports of auditory and/or balance restoration following intra-cochlear gene therapy in neonatal mouse models of genetic deafness. Differences in the rate of inner ear maturation, however, preclude translating these results to human hearing; transgene delivery to the mature murine ear is required but hampered by the bony labyrinth. Heretofore, round window membrane (RWM) injection has been utilized to deliver vectors to the inner ear of adult mice. Transduction efficiency via this approach is low, causes cochlear damage, and is limited to the basal turn. In this study, we sought to establish a cochlear delivery method that enabled apex-to-base transduction, was highly efficient, and caused minimal cochlear damage.

Methods

Two viral vectors were utilized in this study: rAAV2/9 (3.90×10^{13} vg/ml) and AAV2/Anc80L65 (1.40×10^{12} vg/ml), both expressing eGFP driven by the CMV promotor. One microliter of the viral vector was injected into the cochlea using two different techniques: RWM or RWM with semi-circular canal fenestration (RWM+CF). Mice were injected at either P15-16 or P56-60 mice. In all animals, auditory thresholds were assessed by ABR 2 weeks post injection. Cochlear and vestibular histology was evaluated to assess transduction efficiency.

Results

RWM injection with rAAV2/9 resulted in transduction of the basal turn with variable transduction efficiency in inner hair cells (IHCs): apex 1.9%, middle 20.8% and base 68.1%. Slight auditory threshold shifts (13 vg/ml) and AAV2/Anc80L65 (1.40×10^{12} vg/ml) performed identically.

Conclusions

RWM+CF is a safe and efficient method to transduce IHCs in the adult murine inner ear and should be broadly applicable to the investigation of gene therapy to correct hereditary hearing loss in mature murine models of human deafness.

PD 55

Dominant mutations in tubulin cause sensorineural disease with hearing loss and severe retinal dystrophy

Romain Luscan[1]; Sarbina Méchaussier[2]; Antoine Paul[3]; Guoling Tian[4]; Xavier Gérard[2]; Natalie Loundon[5]; Sabine Defoort-Dhellemmes[6]; Isabelle Audo[7]; Julien Dumont[8]; Nathalie Boddaert[9]; Stanislas Lyonnet[10]; Josseline Kaplan[11]; Nicholas J. Cowan[4]; Jean-Michel Rozet[12]; Isabelle Perrault[12]; Sandrine Marlin[13]
[1]*Necker Enfants Malades Hospital, Laboratory of Embryology and genetics of human malformation, INSERM UMR1163, Institute of Genetic Diseases, Imagine;* [2]*Laboratory of Genetics in Ophthalmology , INSERM UMR1163, Institute of Genetic Diseases, Imagine;* [3]*Laboratory of Embryology and genetics of human malformation, INSERM UMR1163, Institute of Genetic Diseases, Imagine;* [4]*Department of Biochemistry & Molecular Pharmacology, NYU Langone Medical Center;* [5]*Pediatric ENT department, Hôpital Necker-Enfants Malades, APHP, Paris, Descartes University;* [6]*CHRU de Lille - Hôpital Roger Salengro;* [7]*Centre Hospitalier National d'Ophtalmologie des Quinze-Vingts;* [8]*Cell Division and Reproduction. Institut Jacques Monod, CNRS, University Paris Diderot;* [9]*Department of Pediatric Radiology, Hôpital Necker-Enfants Malades, APHP, Paris, Descartes University;* [10]*1Laboratory of Embryology and genetics of human malformation, INSERM UMR1163, Institute of Genetic Diseases, Imagine, Paris Descartes University;* [11]*Laboratory of Genetics in Ophthalmology, INSERM UMR1163, Institute of Genetic Diseases, Imagine, Paris Descartes University;* [12]*Laboratory of Genetics in Ophthalmology , INSERM UMR1163, Institute of Genetic Diseases, Imagine, Paris Descartes University;* [13]*Necker Enfants Malade Hospital, APHP, Laboratory of Embryology and genetics of human malformation, INSERM UMR1163, Institute of Genetic Diseases, Imagine, Paris Descartes University*

Tubulins are the subunits of microtubules (MT), dynamic polymers which participate in a striking variety of essential cellular functions. Mutations in tubulin isotypes have been implicated in a wide and overlapping range of brain malformations collectively known as the tubulinopathies. We identified two dominant mutations in a gene encoding an isotype of beta-tubulin affecting the same aminoacid (Arg391), in four families with a previously unreported association between sensorineural hearing loss (SHL) and Leber congenital amaurosis (LCA), a early onset severe retinal dystrophy. Whole exome sequencing and deep sequencing suggest de novo events in two families. In contrast, mosaicism was detected in the asymptomatic mother's DNA of a third family (13%). In the last family, the index case and her mother were both affected, supporting a dominant transmission, and the maternal grandmother, who had isolated SHL, carried the change in 29% of the reads generated from her DNA. The alpha-beta tubulin heterodimers assemble together to form microtubule protofilaments. Inspection of the atomic structure of the microtubule (MT) protofilament reveals that the beta-tubulin Arg391 residue contributes to a binding pocket that interacts with alpha-tubulin contained in the longitudinally adjacent alpha-beta-heterodimer, consistent with a role in maintaining MT stability. We analyzed the products of coupled in vitro transcription/translation reactions driven by constructs encoding wild type and mutant forms. The wild-type and mutant proteins were transcribed and translated with the same efficiency. However, kinetic analysis of these reactions revealed some differences with respect to wild-type in the yield of de novo folded heterodimers. Functional analysis in cultured cells overexpressing FLAG-tagged wild-type or mutant protein and in patient skin-derived fibroblasts showed that the mutant tubulins were able to fold, form alpha-beta-heterodimers and co-assemble into the endogenous MT lattice. However, the dynamics of growing MTs were consistently altered, showing that the mutations have a significant dampening impact on normal MT growth. The MT polymerization anomaly in fibroblasts had no impact on cell proliferation, ciliogenesis and cilia trafficking. In summary, we present a previously unreported autosomal dominant syndrome manifesting as LCA and SHL.

Our data provide the first link between a sensorineural disease and anomalies in MT behavior.

PD 56

A SOX10 Gene Point Mutation Causes Autosomal Dominantly Inherited Mondini Inner Ear Malformation Phenotype in Pigs

Shiming Yang
Chinese PLA Medical School

Background

Mondini dysplasia is a frequent type of inner malformation and is associated with some syndromes and isolated hearing loss with complex inherited model and pathogenic mechanism. So far, no causative gene has been identified associated with Mondini dysplasia. In this study, we identified and characterized a novel ENU-mutagenized pig model with stably inherited phenotypes of Mondini inner ear malformation, profound bilateral hearing loss and pigmentary abnormalities by autosomal dominant inheritance.

Methods

A Genome-wide association analysis combined with sequencing candidate genes was performed to map the causative gene.

Results

We first identified and confirmed the causative gene and the mutant locus, c.325A>T mutation in SOX10 (SOX10 p.R109W), responsible for the inherited Mondini dysplasia. This changed amino acid is within the left of a highly conserved nuclear localisation signals (NLSs) of DNA-binding HMG (high-mobility group) domain (amino-acids107-175). A deleterious protein may be produced by the mutant nucleotide by analysis of molecular structure. Mutant SOX10 fusion protein expression located in both the nucleus and cytoplasm in mouse NIH3T3 cell line and porcine fibroblast cell. Targeted knock-in pig of SOX10 c.325A>T was generated by CRISPR/Cas9 and reproduced those phenotypes including Monidini malformation observed in the mutant pig family. Practically, 10 mutations including 5 novel mutations of SOX10 were identified in patients with inner malformation including Monidini dysplasia, which validated the pathogenicity of SOX10 mutant in human.

Conclusions

This established novel pig model of stably inherited Mondini dysplasia would provide invaluable large animal model for researches of pathogenesis, clinical treatment and evaluation of drug and medical devices of human hereditary hearing loss caused by Mondini dysplasia. The identified causative gene would provide invaluable clue for etiology and pathogenesis of Mondini dysplasia.

Age Related Changes & Treatments in Animal Models

PS 273

Evaluation of nicotinamide riboside on auditory structure and function in mouse models of Cockayne syndrome

Beatrice Mao[1]; Mustafa Okur[2]; Tracy S. Fitzgerald[3]; Scott J. Haraczy[1]; Kamren Edwards-Hollingsworth[1]; Vilhelm Bohr[2]; Matthew W. Kelley[4]
[1]*National Institute on Deafness and Communication Disorders, NIH;* [2]*National Institute on Aging, National Institutes of Health;* [3]*NIDCD, NIH;* [4]*NIDCD/NIH*

Cockayne syndrome (CS) is a rare genetic disorder caused by mutations in two genes, CSA and CSB, both of which are involved in DNA repair. Patients with CS exhibit impaired growth and neurological development, accelerated aging, photosensitivity, eye disorders, loss of hearing, and premature death. Csa knockout mice and a Csb mouse with the CS1AN mutation found in patients display many characteristics consistent with CS including progressive hearing loss and a concomitant decrease in the number of cochlear hair cells. As is common with many types of hearing loss, outer hair cells are more severely affected than inner hair cells, and hair cells located at the base of the cochlea show the greatest degree of sensitivity. A loss of spiral ganglion neurons has also been reported in Csa and Csb mutant mice. Recently, a high-fat diet and supplementation with nicotinamide riboside (NR), a precursor to NAD+ which contains vitamin B3, were shown to rescue some aspects of the phenotype in a CS mouse model. CS mice raised on the high-fat diet exhibited improved performance on a behavioral hearing test and possible rescue of some spiral ganglion neurons, compared to CS mice on a standard diet. However, the effect of NR on hearing in CS mouse models was not explored. To determine whether NR supplementation may help to preserve hearing in CS patients, we are examining the effects of NR on auditory structure and function. ABR and DPOAE assessments in Csa and Csb mutant mice indicate a rescue of hearing function at early time points. These results will be combined with anatomic assessments of hair cell number and health. The results of these studies should provide insights regarding the potential clinical impact of NR-treatment on hearing in CS patients.

The GABAA gamma 1 subunit is increased in GABAergic and glutamatergic cells throughout the inferior colliculus during aging.

Jeffrey G. Mellott; Lauren Robinson
Northeast Ohio Medical University

The subunit composition of $GABA_A$ receptors changes with age in the inferior colliculus (IC). The γ_1 subunit is not expressed at young ages but appears in older animals. Incorporation of a γ_1 subunit into the GABA receptor increases the conductance of the channel to chloride ions, increasing the efficacy of GABAergic transmission and presumably compensating, at least in part, for age-related losses of GABAergic input. It is unknown whether γ_1 upregulation is restricted to certain IC subdivisions or cell types (i.e. glutamatergic or GABAergic). To address these issues, we used immunohistochemistry for glutamate decarboxylase (GAD) and $GABA_A$ γ_1 in old (>26 months) Fisher Brown Norway rats. Animals were perfused with 4% paraformaldehyde. Brain sections (40 μm) were stained for GAD67 (Millipore; MAB5406) and anti-$GABA_A$ γ_1 (Alomone Labs; AGA-016). We classified cell bodies as expressing γ_1 based on the presence of any immunofluorescent γ_1 puncta along the membrane.

Cells that expressed γ_1 were observed in all IC subdivisions, with the highest number of cells in the central nucleus (ICc), fewer in lateral cortex (IClc) and fewest in dorsal cortex (ICd). Within the ICc, the γ_1-expressing cells appeared to be more numerous in the ventral region, where high frequency sounds are processed, than in the dorsal region, where low frequency sounds are processed.

IC cells are either GABAergic or glutamatergic. γ1 subunit expression occurred in GAD+ (presumptive GABAergic) and GAD-negative (presumptive glutamatergic) IC cells. The percentage of GAD+ cells that expressed γ1 varied very little across IC subdivisions: ICc-16%, IClc-14%, and ICd-15%. The percentage of GAD-negative cells that expressed γ1 was more varied: 24%, 8%, and 16% in the ICc, IClc and ICd, respectively.

Our data lead to three main conclusions regarding the expression of the γ1 subunit of the $GABA_A$R in aged animals. **First**, the γ1 subunit is expressed in a subset of cells in all major IC subdivisions. This implies that circuits throughout the IC are changing, presumably to compensate for age-related loss of GABAergic inputs. **Second**, in the ICc, cells that express γ1 are more common in the high frequency region than in the low frequency region. Such changes may be related to the greater deficits in high frequency hearing typically associated with age-related hearing loss. **Third**, in all IC subdivisions, increased expression of γ1 occurs in both inhibitory and excitatory cells. This latter point suggests that age-related changes in the IC are affecting both excitatory and inhibitory circuits.

Dysmyelination and Disruption of the Nodes of Ranvier in the Auditory Nerve

Clarisse H. Panganiban; Kelly C. Harris; Hainan Lang
Medical University of South Carolina

Hearing loss due to functional declines in the inner ear is a well-documented hallmark of aging. Loss of cochlear neurons and their processes have been seen in cochleas of aged animal and human ears. Myelin sheaths and nodes of Ranvier are necessary for rapid conduction of signals from the auditory nerve (AN) to the brain. Loss/dysfunction of nodal components, in addition to demyelination, have been associated with contributing to the neurological symptoms in diseases such as Guillain-Barré syndrome and multiple sclerosis. The relationship with aging and the myelinating glia and nodes of Ranvier in the ANs have yet to be elucidated. Here we test the hypothesis that pathophysiological alterations of myelin and nodes of Ranvier occur in aged ANs and these changes contribute to age-related auditory function declines.

CBA/CaJ mice were used in this study because of their "good hearing" and minimal age-related cochlear cell loss until approximately 1.5-2 years old. The aging group was between 2-3 years old and were compared to a young-adult control group between 1-3 months old. Histological comparisons of aged and young-adult of ANs were completed via electron microscopy and immunostaining. ANs from both groups were isolated for RNA-seq and expression profiles of node-related genes were queried in the RNA-seq datasets. Differences in AN function were assessed using a custom comprehensive multimetric compound action potential approach.

Ultrastructural analyses of aging ANs showed dysmyelination, as evidenced by myelin whorls and increased presence of non-compact lamellae and Schmidt-Lanterman incisures along AN fibers compared to control. Axo-glial connections in aged paranode regions were also disrupted, with terminal myelin loops detaching from the axolemma and increased assembly of large, electron-dense circular occlusions within the terminal loop heads. Node of Ranvier lengths significantly increased and widths decreased in aged ANs compared to young-adult. Differential expression analysis revealed that 23 out of 30 (77%) node-related genes, signifi-

cantly decreased with aging. Importantly, genes that decreased in expression included that of ion channels necessary for saltatory conduction. In addition, auditory brainstem response wave I thresholds were increased in aged mice compared to young-adults.

Our study revealed that dysmyelination and nodal structural aberrations are pervasive in aged mouse ANs. Studies to investigate the functional consequences of this dysmyelination in aged mice by analyzing specific components of the AN response are ongoing, in addition to the characterization of myelination and nodes of Ranvier in aged ANs of human temporal bones.

PS 276

Aldosterone-Mediated Age-Related Autophagic Changes in the Cochlea

Bo Ding[1]; Xiaoxia Zhu[2]; Mckenzie Watson[3]; Carlos Cruz[3]; Robert D. Frisina[1]
[1]Global Center for Hearing and Speech Research, University of South Florida- Tampa; [2]Global Center for Hearing & Speech Research, University of South Florida- Tampa; [3]University of South Florida- Tampa

Background

Aldosterone (ALD), a mineralocorticoid hormone, is essential for regulation of sodium and extracellular potassium concentrations. Also, ALD levels decrease with age, and we previously discovered that higher serum ALD levels are correlated with better hearing in aged humans. The precise role that aldosterone plays in age-related hearing loss (ARHL) is not completely known, but we recently reported that ALD rescues key features of ARHL via prevention of cochlear cell loss, and modulates the expression of NKCC1 and Na, K-ATPase, two cochlear ion channels. Since ALD has been shown to change autophagic activation, a key physiological process for removal of cell waste, this study was undertaken to determine how ALD affects cochlear autophagy processes.

Method

CBA/CaJ mice were divided into: ALD treatment, Chloroquine (CH), CH+ Arsenic trioxide (AST), and control groups. The animals underwent measurement of auditory brainstem responses (ABR) and distortion product otoacoustic emissions (DPOAEs). Dissected cochleae (in vivo) and SV-K1 cells (in vitro) were processed for autophagic analysis.

Results: For aging mice, ABR and DPOAE threshold improvements due to the ALD treatments were discovered at all frequencies, comparing the treated groups to the non-treated control group. The autophagic marker

LC3II was increased in the aged cochlea compared to young adult cochlea, similar to the results of our in vitro experiment with the autophagy inhibitor CH treatment. Combining the autophagy blocker CH with the agonist AST treatments resulted in the same effects as CH treatment alone, suggesting that an increased LC3II is not always indicative of autophagy induction or a blockade of autophagy. Therefore, we utilized P62 as a second autophagic marker. The increased accumulation of P62 was discovered in the aged cochlea; and for CH, or CH with AST treatments in the SV-K1 cell line. These results suggest that aging processes in the cochlea may modulate the autophagy pathway. Lastly, an autophagy turnover experiment in vivo was performed in old CBA mice. There was no LC3 II change observed for a CH treatment group compared with our non-treatment group, suggesting that autophagic suppression may occur in the autophagy pathway step involving fusion between autophagosomes and lysosomes. The observed pattern of LC3 for the ALD+CH treatment was identical to treatment with the autophagy activator AST, strongly suggesting that ALD is an autophagic agonist.

Conclusion

Aging suppresses autophagy cochlear processes, and ALD prevents presbycusis via inhibition of age-related autophagy suppression.

Supported by

PS 277

Inflammatory Cytokines are Associated with Aging Processes in the Cochlea

Tanika T. Williamson*; Parveen Bazard*; Robert D. Frisina; Bo Ding
Global Center for Hearing and Speech Research, University of South Florida- Tampa

Inflammation, a normal adaptive response that restores tissue functionality and homeostasis against stress conditions, such as infection and injury, may be associated with age-related hearing loss (ARHL); and clinical strategies aimed at reducing auditory dysfunction by preventing inflammation are under scrutiny. Our study evaluated the involvement of key inflammatory factors: nuclear factor-kappaB(NF-kB), interleukin-6(IL-6), and protein kinase B(AKT) in the aging cochlea using stria vascularis(SV) tissue (in vivo), as well as SVK-1 cells to mimic aging (in vitro).

Methods and Materials

Treatments, including H_2O_2 and cisplatin, were administered to SVK-1 cells to mimic inflammatory processes.

After 24 hours of treatment, the cells were washed and extracted. SV tissue was also obtained from the cochlea of young (Y, 5 months) and old (O, 32 months) CBA/CaJ mice to evaluate natural effects of aging. RT-PCR was performed to measure gene expression.

Results
We found that NF-kB, IL-6, and AKT were expressed for both in vivo and in vitro, for SV using RT-PCR. SVK-1 treated cells (relative to untreated control cells) and SV cells from the cochlea of old mice (relative to young adults) both displayed a lower gene expression of NF-κB. NF-κB is a family of structurally related inducible transcription factors. Since IL-6 is one of the most highly induced NF-κB-dependent cytokines and AKT is a downstream target of NF-κB, we checked both and found that they are increased in SV cells under inflammatory stimulation. Interestingly, in contrast, IL-6 gene expression also increased over the course of treatment with in vitro SVK-1 cells compared to controls, but we could not find any changes in AKT.

Conclusion
Our findings suggest that NF-kB becomes down-regulated in the aging cochlea due to inflammatory stress. In vitro findings for IL-6, a known inflammatory biomarker, coincided with previous reports of increased gene expression during aging. Interestingly, this gene can be either pro-inflammatory or anti-inflammatory, depending on the physiological conditions. In our study, changes of IL-6 and AKT were not related, suggesting that new variations of inflammatory cytokine expression may be involved in ARHL. Overall, our findings will help to elucidate the roles of inflammatory cytokines in ARHL; and ongoing goals include determination of whether nonsteroidal anti-inflammatory drugs (NSAIDs) can be used as therapeutic options to slow down the progression of presbycusis-ARHL.

PS 278

Inflammation Dysfunction in the Aging CBA/CaJ Mouse Cochlea

Xiaoxia Zhu[1]; Bo Ding[2]; Nate Watson[3]; Robert D. Frisina[2]
[1]*Global Center for Hearing & Speech Research, University of South Florida- Tampa;* [2]*Global Center for Hearing and Speech Research, University of South Florida- Tampa;* [3]*Duke University*

Background
Age related hearing loss (ARHL)—presbycusis, affects about 20 million people in the US, and tens of millions more worldwide. The biological mechanisms are not clearly understood, since multifactorial conditions with multiple pathways and underlying conditions are involved in cochlear aging processes. So, there are no medical interventions or drugs to prevent hearing loss, including ARHL. Inflammation has recently been reported as a possible mechanism, as several pro-inflammatory cytokines such as tumor necrosis factor alpha (TNF-α) and interleukins (IL) have been suggested. Our present study investigated TNF-α and downstream pathways involving nitric oxide synthases (NOSs) in the aging mouse cochlea.

Methods
Sixyoung adult (2-4 month [mon]) and six old (24-28 mon) CBA/CaJ mice (equal #s males and females) were used. After testing auditory brainstem responses (ABRs), distortion product otoacoustic emissions (DPOAE) amplitudes and thresholds, both cochleae were dissected; and one cochlea prepared for immunhistochemical (IHC) staining, the other one for reverse transcription (RT) PCR and western blot molecular analyses.

Results
As before,we observedABR threshold elevations, and DPOAE amplitude and threshold shifts with age in CBA/CaJ mice, confirming the presence of age-related hearing loss in this mouse model of presbycusis. TNF-α protein expression increased with age, with the expression appearing prominently in the hair cells, the cochlear lateral wall and in spiral ganglion neurons. The strongest TNF-α expression was located in the cochlear lateral wall. It is known that TNF-α increases when the mitochondrial electron transport chain is stressed and dismutated by H_2O_2. Additionally, we hypothesized that impaired nitric oxide (NO) bioavailability will contribute to age-linked cochlear oxidative stress. Interestingly, we could not find any change in the gene expression levels for inducible NOS (iNOS) and neuronal NOS (nNOS) in the cochlea, comparing young adults and aging mice. However, protein expression of iNOS was significantly increased in aging mice, suggesting that aging processes may exert themselves via post-transcriptional modification of mitochondrial oxidative stress pathways.

Conclusions
Inflammatory activation increases with age in the cochlea and impaired NO bioavailability may be involved through the regulation of iNOS but not nNOS, at post-transcriptional levels. Since iNOS, an inflammatory mediator, increases with age, this nitrosative stress may be a key inflammatory pathway of presbycusis. Future experiments will focus on further recognition and characterization of cochlear inflammatory mech-

anisms for ARHL-presbycusis and other types of acquired hearing impairment.

Supported by

PS 279

Age-associated alterations of immune and inflammatory responses in the aged mouse and human auditory nerve

LaShardai N. Brown; Ting Liu; Clarisse H. Panganiban; Jeremy L. Barth; Hainan Lang
Medical University of South Carolina

Background
Age-related hearing loss, or presbyacusis, is a leading chronic condition affecting older adults. Studies have shown that declines in auditory function seen in presbyacusis can result from loss of the peripheral auditory nerve and alterations of the cochlear microenvironment. Macrophages, immune cells of the inner ear, play a critical role in maintaining a healthy microenvironment by eliciting inflammatory responses and clearing apoptotic cells and cellular debris. Aging promotes chronic activation of the immune system and the proliferation of immune cells, such as macrophages, exacerbating the pathology of neurodegenerative disorders. Macrophages of the aged auditory nerve have not been well characterized. Furthermore, it is unknown whether macrophages are beneficial or detrimental to the health of the aged auditory nerve. In this study we used a combination of genomic and morphological assays to examine the inflammatory changes in the auditory nerve of the aged mice and human temporal bones from older donors.

Methods
Auditory sensitivities of a young adult (2-4 months) group and two aged adult groups (16-25 months and > 25 months) CBA/CaJ mice were compared using auditory brainstem response measurements. Microarray and RNAsequencing experiments were used to identify biological pathways and genes that are differentially expressed between young and aged auditory nerves. The ultrastructural alterations of neural cells and macrophages in the auditory nerve were examined in young and aged mice to investigate macrophage morphology and macrophage-related cell associations. Immunohistochemistry for a panel of macrophage-specific markers was conducted to characterize age-related phenotypical alterations of macrophages in the auditory nerves of mouse and human temporal bones.

Results
Our studies revealed that immune-related biological processes, such as complement activation, antigen presentation and macrophage activation, were enriched in auditory nerves of aged mice. Analysis of our genomic studies revealed that macrophage-associated genes and immune response regulator genes were increased in aged nerves, compared to young nerves. Ultrastructure of auditory nerves revealed that aged nerves possess more macrophages than young nerves. Aged macrophages surveyed normal cells and were in contact with degenerating axons and cells. Immunohistochemistry analysis of macrophages from young and aged mice revealed an age-related increase in macrophage numbers and an increase in the presentation of macrophage-associated activation markers.

Conclusions
Our results suggest that immune-related biological processes, including macrophage activation, are increased in the aged auditory nerve. Further studies of macrophages in the aging cochlea will provide insight into ways to use resident immune cells as therapeutic targets for presbyacusis.

PS 280

Accumulation of Mitochondrial DNA Deletions Accelerates Age-related Hearing Loss in Mice

Mi-Jung Kim[1]; Suraiya Haroon[2]; Karessa White[1]; Dalian Ding[3]; Hyo-Jin Park[1]; Chul Han[1]; Kevin Boyd[1]; Isabela Caicedo[1]; Kaitlyn Evans[1]; Richard Salvi[4]; Paul Linser[5]; Marc Vermulst[2]; Shinichi Someya[1]
[1]*University of Florida, Department of Aging and Geriatric Research;* [2]*University of Pennsylvania, Children's Hospital of Philadelphia;* [3]*University at Buffalo, USA;* [4]*Center for Hearing and Deafness; State University of New York at Buffalo;* [5]*University of Florida, Whitney Lab*

Background
Mitochondrial DNA (mtDNA) mutations are thought to have a causal role in age-related pathologies. mtDNA mutator mice (PolgD257A/D257A), expressing a proofreading-deficient version of the catalytic subunit of DNA polymerase gamma, accumulate mtDNA mutations and display features of accelerated aging. In the current study, we investigated the roles of mtDNA deletions and point mutations in the pathogenesis of age-related hearing loss (AHL) in wild-type (WT) and mtDNA mutator mice that were backcrossed onto the CBA/CaJ strain, a well-established model of late onset AHL.

Methods

To investigate whether accumulation of mtDNA point mutations or deletions accelerates AHL in mtDNA mutator mice, we performed auditory brainstem response (ABR) tests to measure ABR hearing thresholds, wave I amplitudes, and wave I latencies in 3-5-month-old and 14-19-month-old WT and PolgD257A/D257A mice that were backcrossed onto the CBA/CaJ strain for 5 generations (CBA/CaJ-PolgD257A/D257A mice). We also performed histological analyses to assess hair cell loss, spiral ganglion neuron density, and stria vascularis thickness in the cochlea of young and middle-aged WT and PolgD257A/D257A mice. Lastly, we performed random mutation capture (RMC) assay to measure mtDNA point mutation and deletion frequencies in the inner ear tissues of young and middle-aged WT and PolgD257A/D257A mice. Results: We found that middle-aged PolgD257A/D257A mice showed a 12-45 dB increase in ABR hearing threshold at 4, 8, 16, 32, 48, and 64 kHz compared to age-matched WT mice. In agreement with the hearing test results, middle-aged PolgD257A/D257A mice showed a 22-fold increase in inner hair cell loss and a 6-fold increase in outer hair cell loss, and a 45% decrease in spiral ganglion neuron density in the cochlea compared to age-matched WT mice. Furthermore, middle-aged PolgD257A/D257A mice showed a 5-fold increase in mtDNA deletion frequencies in the inner ear tissues compared to young PolgD257A/D257A mice, while there was no difference in mtDNA point mutation frequency in the inner ear tissues between young and middle-aged PolgD257A/D257A mice. Conclusions: Together, these results provide direct evidence that mtDNA deletions drives AHL in mice.

Funding

PS 281

Activation of MiR-34a Impairs Autophagic Flux and Promotes Cochlear Cell Death via Repressing ATG9A: Implications for Age-Related Hearing Loss

Hao Xiong[1]; Jiaqi Pang[2]; Yiqing Zheng[2]
[1]Medical University of South Carolina; [2]Sun Yat-sen Memorial Hospital, Sun Yat-sen University, China

Age-related hearing loss is a major unresolved public health problem. We have previously elucidated that the activation of cochlear miR-34a is correlated with age-related hearing loss in C57BL/6 mice. A growing body of evidence points that aberrant autophagy promotes cell death during the development of multiple age-related diseases. The aim of this study was to investigate the role of miR-34a-involved disorder of autophagy in the pathogenesis of age-related hearing loss. Our results showed that miR-34a expression was markedly up-regu-lated in the aging cochlea accompanied with impairment of autophagic flux. In the inner ear HEI-OC1 cell line, miR-34a overexpression resulted in an accumulation of phagophores and impaired autophagosome-lysosome fusion, and led to cell death subsequently. Notably, AT-G9A, an autophagy protein, was significantly decreased after miR-34a overexpression. Knockdown of ATG9A inhibited autophagy flux, which is similar to the effects of miR-34a overexpression. Moreover, ursodeoxycholic acid significantly rescued miR-34a-induced HEI-OC1 cell death by restoring autophagy activity. Collectively, these findings increase our understanding of the biological effects of miR-34a in the development of age-related hearing loss and highlight miR-34a as a promising therapeutic target for its treatment.

PS 282

Accelerated Age-related Degradation of the Tectorial Membrane in Ceacam16βgal/βgal Knockout Mice May Contribute to Presbycusis

Mary Ann Cheatham[1]; Richard Goodyear[2]; Souvik Naskar[3]; Yingjie Zhou[1]; Jing Zheng[4]; Guy P. Richardson[2]
[1]Department of Communication Sciences and Disorders, Northwestern University; [2]University of Sussex; [3]University of Warwick; [4]Northwestern University

Background

The tectorial membrane is an extracellular component of the cochlea required for normal hearing. It contains collagen fibrils imbedded in a laminated, striated-sheet matrix composed of TECTA, TECTB and CEACAM16. In Ceacam16βgal/βgal null mutant mice on a C57BL/6J background, the striated-sheet matrix fails to form correctly and the incidence of spontaneous otoacoustic emissions (SOAE) is greatly increased, but auditory brain-stem responses (ABR) and distortion production otoacoustic emissions (DPOAE) are initially near normal in young animals. Because a previous report (Kammerer et al., 2012) indicated that mice lacking Ceacam16 have a progressive hearing loss, we examined the anatomy and the physiology of these animals at older ages.

Methods

Both OAEs and ABRs were acquired to document changes in cochlear physiology. Anatomical evaluations included X-Gal staining of Ceacam16 driven -galacto-sidase expression, light and electron microscopy, anti-body labelling, Western blot analysis and construction of cochlear cytograms.

Results

An analysis of 6-7 and ~12-month-old Ceacam16βgal/βgal mice reveals a progressive loss of matrix from the central core of the tectorial membrane that involves the loss of TECTB followed by that of TECTA. These changes are more extensive in apical, low-frequency regions of the cochlea where Ceacam16 expression levels are relatively low in normal animals. Although an apically-biased loss of matrix from the core of the tectorial membrane is also observed in wild-type C57BL/6J mice, these changes occur at much later ages, i.e., after ~2 years of age. In Ceacam16βgal/βgal mice at 6-7 months, ABR thresholds are increased at high frequencies, the magnitude of the DPOAE at 2f1-f2 is decreased for f2 frequencies >10 kHz, and the incidence of SOAEs is considerably reduced relative to that observed in young mice. By ~12 months of age, SOAEs and DPOAEs are not detected in Ceacam16βgal/βgal mice and ABR thresholds are increased by 30-40 dB across the mouse audiogram, even in apical regions with a normal complement of hair cells. At more basal regions, cytograms show that loss of both inner and outer hair cells is similar in Ceacam16βgal/βgal mice and their controls. Interestingly, at ~12 months of age there is an increase in the incidence of SOAEs in the heterozygous Ceacam16+/βgal mice (63.6%) relative to that in controls (~7.7%) at the same age.

Conclusion

The loss of Ceacam16 expression accelerates age-related degeneration of the tectorial membrane, a process that may contribute to presbycusis. (Work supported by NIDCD (DC000089, DC011813) and The Wellcome Trust (087377).

PS 283

Early onset of age related hearing loss in LDHB knock out mouse.

Young Sun Kim[1]; Yeon Ju Kim[2]; Yun Yeong Lee[1]; Oaksung Choo[1]; Yun-Hoon Choung[1]
[1]*Department of Otolaryngology, Ajou University School of Medicine, Suwon, Republic of Korea; [2]Department of Otolaryngology, Ajou University School of Medicine*

Age related hearing loss (AHL) is a main feature of mammalian aging and is the most common sensory dysfunction in the elderly. AHL is associated with an age dependent loss of sensory hair cell, spiral ganglion neurons, and stria vascularis cell in the inner ear. Because hair cells and cochlear neuron cells are unable to regenerate, progressive loss of these cells eventually results in hearing loss. Mitochondria is the key of energy supply, cellular redox balance, signaling and regulation of intrinsic apoptosis in the inner ear, especially in the high energy demanding cells, such as hair cells and neuron cells.

Lactate dehydrogenates B is an important enzyme in maintaining high level of pyruvate which in the presence of oxygen will be further metabolized in the TCA cycle to produce NADH and FADH2 for oxidative phosphorylation in the mitochondria. This study aimed to observe the functional study of age-related hearing loss in LDHB knockout mice.

In this study, we investigated the molecular mechanism of hearing loss caused by LDHB deficiency by using in vitro hair cell UB-OC1. We found that differentiated UB-OC1 showed LDHB and increase of the mitochondrial function: mitochondrial respiratory subunits and MMP enhanced, which was also accompanied by increase of ATP and NAD+/NADH ratio. LDHB knock down decreased mitochondrial function in differentiated UB-OC1 cell, the decrease of NAD+ and increase of HIF1a which probably caused mitochondrial dysfunction. In vivo, hearing function of wild-type and LDHB-knockout mice at 2, 5, and 10 months of age were quantified with auditory brainstem response (ABR). Mice, both wild-type and LDHB-knockout, exhibited normal hearing thresholds at 8, 16 and 32 kHz frequencies at the age of 2 months. However, the hearing function of the 5-month-old LDHB-KO mice was equivalent to 10-month-old wild-type mice of the same genetic background. In response to deletion of LDHB gene in mouse caused early onset of age related hearing loss, as increase of high frequency threshold, hair cell death, neuron cell and lateral wall degradation, which are the typical features of age-related hearing loss.

In summary, LDHB knock down decreased NAD+ level and stabilized Hif1a which probably caused mitochondrial dysfunction in hair cell. The deficiency of LDHB gene causes early onset of age related hearing loss.

PS 284

Age-related Change in the Auditory Sensitivity of Adult zebrafish (Danio rerio)

Ruiyu Zeng[1]; Andrew D. Brown[2]; Joseph Sisneros[1]
[1]*University of Washington; [2]Department of Speech and Hearing Sciences, University of Washington*

Previous studies on the ontogeny of auditory sensitivity in zebrafish suggest that an age-related decrease in auditory sensitivity occurs in older adult zebrafish; however, in those studies the age of adult zebrafish was estimated based on standard body length. Because body size can be influenced during development by environmental factors such as rearing density and food availability, body length may not be the best correlate of age. Here, we examine how auditory sensitivity changes across known age groups of adult wild type (AB-WIK)

zebrafish using the auditory evoked potential (AEP) recording technique. AEPs were recorded from 12 and 24 month old adult zebrafish while sound was presented via an underwater speaker. AEP thresholds were determined for five frequencies from 115 Hz to 1850 Hz. Thresholds were defined as the lowest sound (tone) level that evoked a significant auditory potential at twice the stimulus frequency. Our preliminary results suggest that 24-month-old adult zebrafish were less sensitive to the lowest (115 Hz) and highest (1850 Hz) frequencies tested compared to 12-month-old adults. No differences in auditory thresholds were observed at frequencies from 650 to 1000 Hz between 12-month and 24-month old adults. Our results suggest that after 12 months of age adult zebrafish incur a reduction in auditory sensitivity at relatively low and high frequencies within their hearing range. Preliminary data thus suggest that zebrafish experience age-related hearing loss. The form of this hearing loss relative to that observed in other vertebrate taxa, including humans, is discussed.

PS 285

Are big brown bats (Eptesicus fuscus) resistant to age-related hearing loss?

Inga Kristaponyte; Hope Ball; Debin Lei; Jianxin Bao; Lisa Cooper; Alexander Galazyuk
Northeast Ohio Medical University (NEOMED)

Background

Mammals develop progressive, irreversible age-related hearing loss that tends to be more severe at higher frequencies. Echolocating bats may possess a uniquely resistant auditory system to delay or even prevent this high-frequency hearing decline however, as hearing is a dominant sensory input used to acquire food throughout their long lifespans. Bats live three to ten times longer than mammals of equivalent body size and have become a model for longevity research. This project aimed to compare the peripheral auditory system of young, middle-aged, and old bats. We hypothesized that bats exhibit a slower rate/lack of age-related hearing loss compared to reports from mice and humans.

Methods

We collected big brown bats (Eptesicus fuscus) of both sexes in the wild. Two different methods were used to determine their chronological ages: fecal metabolomics and postmortem counting of annual growth rings within the cementum of tooth roots. Auditory brainstem responses (ABR) and distortion product otoacoustic emissions (DPOAE) were recorded under isoflurane anesthesia.

Results

Both age assessment techniques provided congruent results. Our experimental group consisted of similar numbers of young, middle-aged and old Eptesicus. ABR thresholds and DPOAE amplitudes did not significantly differ between the animals of different ages, indicating no age-related changes in both inner and outer hair cell functioning.

Conclusions

Big brown bats might be an essential animal model for studying mechanisms underlying delay and prevention of age-related hearing loss. Understanding of the unique resistance to hearing loss in aging Eptesicus could ultimately lead to novel therapies in humans.

PS 286

Behavioral Evidence for the Treatment of Age-Related Hearing Loss via Modulation of the BK Channel with a Custom Peptide

Elliott Brecht[1]; Luisa Scott[2]; Joseph P. Walton[3]
[1]Department of Chemical and Biomedical Engineering, University of South Florida, Tampa, FL; [2]Section of Neurobiology, University of Texas-Austin, Austin, TX; [3]Department of Communication Sciences & Disorders, and Chemical and Biomedical Engineering, Global Center of hearing and Speech Research, University of South Florida, Tampa, FL

Background

Slow, Ca^{2+}-activated, BK-type-channels contribute to action-potential duration, firing frequency, and spike frequency adaptation. We've previously reported that blocking the BK-channel via local application of paxilline on the auditory midbrain affected not only temporal processing properties, but also decreased receptive field (RF) formation in young adult mice. In some respects, these results mimic the findings observed in aged mice. In contrast, we have also shown that a general BK-channel opener can increase excitatory drive within the RF and improve temporal processing in aged animals. We then investigated the electrophysiological effects of a custom-peptide BK-channel opener (using 0.1, 1, and 10-μM) applied to the surface of the IC. While all doses decreased sound evoked neural firing of high-frequency neurons, higher concentrations increased firing of low-frequency neurons, and in some cases de novo expression of RFs that were poorly defined emerged. Based on these findings, this study examined whether this peptide could alter behavioral sound perception in aged mice.

Methods

Pre-pulse inhibition of the acoustic startle response was conducted prior to and following systemic intraperitoneal

administration of the custom peptide (4.4mg/kg) in both young and aged mice. A second group served as sham and was administered saline. Low (8-kHz) and high frequency (32-kHz) 25-ms tone bursts were used as the pre-pulse, which was followed by a 50-ms 110-dB startle elicitor. The tone burst pre-pulses were randomly presented at intensities from 45-85 dB-SPL with an inter-trial interval between 15-30 sec. PPI was calculated as a percentage of the amplitude recorded from the startle elicitor with a pre-pulse over the amplitude for no pre-pulse.

Results/Conclusions
PPI of the ASR is a reliable method for assessing simple auditory perception in mice. Following systemic treatment with the BK channel-targeted peptide, both young and aged mice showed significant increases in salience of the low frequency pre-pulse. Young mice showed increased PPI for 8-kHz stimuli at all intensities, while aged animals only showed significant differences to mid-intensity PPs (55-65 dB). This indicates that functional improvement in sensitivity was intensity specific and complements the changes observed in the receptive fields. There was no significant effect on PPI to the 32-kHz pre-pulse for aged animals. In addition, sham treatment did not improve the salience of the response to either pre-pulse frequency. Our evidence that a BK-channel opener can improve the salience and responses to low-frequency sound in aged mice, not only electrophysiologically but also behaviorally, shows that this drug therapy may prove to be a potential treatment for aged-related hearing disorders.

PS 287

Estrogen replacement facilitates hearing restoration after acoustic overexposure in ovariectomized rat

Jae-Hun Lee[1]; Min-Tae Kim[2]; Eun Hee Kim[3]; So-Young Chang[3]; Nathaniel Carpena[2]; Ji-Eun Choi[2]; Min Young Lee[2]; Jae Yun Jung[2]
[1]Beckman Laser Institute Korea, Dankook University; [2]Dankook University College of Medicine; [3]Beckman Laser Institute Korea

Estrogen is the primary female sex hormone and its relationship with hearing function has been studied on humans and animals. Especially, estrogen supplementation is known to improve endothelial function in postmenopausal women. Since endothelial function is related with the homeostasis of the organ of Corti, vulnerability of the cochlea against external stress would change depending on the level of estrogen. Thus, we investigated the change of hearing vulnerability against noise exposure in the menopause stage of female rats by inducing menopause through ovariectomy. Sixteen female SD rats (6 weeks old) were included and were separated into four different groups (Sham surgery, ovariectomy only, ovariectomy with low and high dose estrogen). For both estrogen groups, 10 ug and 100 ug/kg of estradiol were injected through intra-peritoneal twice (before and 3 days after noise exposure). Hearing threshold was measured before and 1 day, 1 week and 2 weeks after noise exposure and the level of estrogen was also measured before and 1 day after noise exposure. After last the ABR measurement, we performed histological analysis using immunostaining. Hearing threshold was not significantly different between the sham surgery and ovariectomy only groups. However, both estrogen groups showed less threshold shift than ovariectomy only group, especially at the high frequency region. Immunostaining results showed that hair cell loss in 32 kHz was prominent in sham surgery and ovariectomy only group whereas no or little loss of hair cell in both estrogen groups. The result in this study suggests that estrogen replacement would decrease the vulnerability of hearing against noise exposure for women in menopause. This study was supported by a grant of the Ministry of Science, ICT and Future Planning grant funded by the Korea government (NRF-2012K1A4A3053142) and (NRF-2017R1D1A1B03033219).

PS 288

Autophagy Enhancer Rapamycin Ameliorate Age-related Hearing Loss in C57BL/6J Mice by Autophagy Activation

Hongyan Liu; Chunfu Dai
Department of Otolaryngology, Eye Ear Nose & Throat Hospital, Fudan University, Shanghai, China

Background
Age-related hearing loss (ARHL) is a frequent serious sensory deficit. So far, no effective treatment was available for this age-related disorder. We aimed to explore whether autophagy enhancer rapamycin could ameliorate ARHL and analyze the mechanism.

Methods
Sixty C57BL/6J mice (male, 12 weeks) were randomly divided into two groups. The first group (n=30) was given rapamycin in drink water (0.75 mg/kg per day) for 24 weeks; the second group (n=30) was given tap water without rapamycin and served as control. The auditory brainstem response (ABR) test was performed before and after treatment to detect the mice' hearing status. Western blot was used to analyze the expression levels of autophagy-related protein microtubule-associated protein light chain 3 (LC3), the adaptor protein p62/se-

questosome-1(p62, the substrate of LC3- II), and phosphorylated/ unphosphorylated p70 ribosomal protein S6 kinase (p70S6K, the mTOR downstream protein kinase). Immunohistochemical staining of LC3 was used to count the number of LC3-positive puncta/autophagosomes in spiral ganglion neurons.

Results

(1) There was no significant difference in the baseline hearing levels between these two groups (mice of 12 weeks old). The mean ABR thresholds of two groups were both 25dB. After rapamycin treatment for 24 weeks, the mean ABR threshold in study group was 55 dB, compared with 75 dB in control group (P<0.05). (2) Western blot analysis of LC3 demonstrated that the levels of LC3-II were lower in 36 weeks than in 12 weeks in both groups. Furthermore, the level of LC3-II and the ratio of LC3-II/I in rapamycin-treated mice were significantly higher than in control group at 36 weeks. Conversely, the expression of p62 protein was lower in rapamycin-treated group than in control group. The ratio of phosphorylated/ unphosphorylated p70S6K was much lower in rapamycin-treated mice than in control group. (3) In spiral ganglion neurons of control group, LC3 fluorescence was predominantly dispersed throughout the cytoplasm with only a few baseline autophagosomes present. In contrast, in spiral ganglion neurons of rapamycin-treated mice, the number of characteristic punctate fluorescent autophagosomes significantly increased development.

Conclusions

Rapamycin can ameliorate the hearing loss of aged mice through inhibit phosphorylation of mTOR downstream effectors and active autophagy. Our findings demonstrate a possible therapy for presbycusis using autophagy enhancer rapamycin.

PS 289

Otoprotective Effect of Selegiline in an Age-related Hearing Loss Model of Genetically Susceptible Mice

Judit Szepesy[1]; Viktória Humli[2]; Gábor Polony[3]; László Tamás[4]; Anita Gáborján[3]; Tibor Zelles[5]
[1]Department of Pharmacology and Pharmacotherapy and Department of Otorhinolaryngology, Head and Neck Surgery; Semmelweis Universiy; [2]Institute of Experimental Medicine, Hungarian Academy Of Sciences; Department of Pharmacology and Pharmacotherapy, Semmelweis Universiy; [3]Department of Otorhinolaryngology, Head and Neck Surgery; Semmelweis Universiy; [4]Department of Otorhinolaryngology, Head and Neck Surgery, Semmelweis University; [5]Department of Pharmacology and Pharmacotherapy, Semmelweis University; Institute Of Experimenal Medicine,Hungarian Academy Of Sciences

Sensorineural hearing losses (SNHLs) are among the most frequent sensory deficits affecting more than 360 million people worldwide. One of the most common form is age-related hearing loss (AHL) with increasing prevalence in the ageing population. Despite of their high social relevance, SNHLs - including AHL - have no efficient pharmacotherapy. We have investigated the otoprotective potential of selegiline [(-)-deprenyl] an irreversible monoamine oxidase-B (MAO-B) inhibitor used in the treatment of Parkinson disease and major depression. Selegiline has known anti-apoptotic and neuroprotective effects and also mitigates oxidative stress. These effects are all expected to be favorable in AHL, the pathomechanism of which involves oxidative stress, apoptosis and excitotoxicity in the organ of Corti and the primary auditory neurons.

We have tested the effect of selegiline on ageing male BALB/c mice. This strain carries an AHL-predisposing gene, having a homologue in humans. Hearing was assessed by auditory brainstem response (ABR) measurements using both click and tone burst (4 - 65 kHz) stimuli. The progression of hearing loss and the effect of selegiline on it were followed up monthly from the starting age (4 weeks) to the end of the experiment (49 weeks of age) in all four treatment groups (control plus three doses of selegiline). Selegiline was administered in the drinking water and the actual daily doses were calculated from the average fluid intake and the actual weight of the animals.

Hearing thresholds of BALB/c mice showed a continuous elevation with a significant acceleration at the age of 24 weeks. The highest dose of selegiline significantly alleviated the progressive elevation of hearing thresh-

olds at frequencies between 8 and 65 kHz from the age of 28 weeks.

In summary, we have set up a preclinical mouse model for testing the effect of drugs against AHL and used it successfully to show the otoprotective effect of selegiline. The complex, multifactorial pathomechanism of AHL, most likely requires drugs acting on multiple targets for effective therapy. The anti-apoptotic, neuroprotective and anti-oxidant action of selegiline is probably supplemented in the cochlea with its effect on the lateral olivocochlear (LOC) efferents. By inhibiting MAO, it increases the release of dopamine (DA) from the LOC efferents that provide endogenous protection against the excitotoxic damage of the primary auditory neurons. Selegiline, acting on multiple targets might be a good candidate for small-molecule-based pharmacotherapy in AHL.

PS 290

Expression Patterns Associated with Age-Related Hearing Loss Reveal Distinct Biological Processes and Potential Pharmaceutical Targets

Nick Schubert; Marcel van Tuinen; Kristof Joosten; Daniel Reijntjes; Sonja Pyott
University Medical Center Groningen

Background
Age-related hearing loss (ARHL) is a commonly occurring disease with enormous economic, societal and personal consequences. AHRL is also a complex disease with multiple underlying molecular processes associated with changes in the sensory, neural, metabolic, and conductive structures of the cochlea. The identification of these specific molecular pathways is necessary for the development of effective treatments of ARHL.

Methods
To identify the transcriptional changes and biological processes involved in specific functional structures of the cochlea, we micro-dissected the organ of Corti (including the spiral ganglion neurons (OC/SGNs) and stria vascularis (SV) separately from C57BL/6 mice aged six weeks and two years. The inner ear is fully developed at six weeks of age, whereas C57BL/6 mice at two years of age have significant hearing loss. The transcriptome of these different tissues was acquired using Lexogen RNA sequencing. Differential expression (DE) and gene ontology (GO) enrichment analyses were performed using R/Bioconductor software and DAVID v6.8. DE genes (DEGs) were crossed-referenced with DrugBank to identify existing drugs targeting these DEGs.

Results
*A*t 6 weeks and 2 years of age, the OC/SGN and SV share a similar set of expressed genes (92% in OC/SGN and 90% in SV at 6 weeks; 91% in OC/SGN and 89% in SV at 2 years). In contrast, the percentage of DEGs shared in response to aging was much smaller (32% in OC/SGN; 31% in SV). Examination of the biological processes associated with aging indicate both unique and shared processes between the OC/SGN and SV. Specifically, gene ontology analyses of DEGs indicates that ion transport and immune processes compared to signaling and immune processes are most differentially regulated with aging in the OC/SGN and SV, respectively. Cross referencing DEGs with DrugBank indicates that ion channels are the most druggable protein class in terms of total numbers of DEGs (97 and 93 in the OC/SGN and SV, respectively) with the percentage of DEGs with drug targets being 61% and 39%. The specific ion channels encoded by these DEGs are largely non-overlapping in the OC/SGN and SV (28%).

Conclusion
This study shows that different genes and biological processes are involved in the response to aging in particular structures of the cochlea. Although these results are not necessarily surprising given the different function of these structures they reveal that treatments for ARHL can be targeted to specific structures and functions of the cochlea.

Attention, Audiovisual Integration & Sound Localization

PS 291

Neural signatures of audio-visual binding in the "pip and pop" effect

Justin Fleming[1]; Alexander Hammerman[2]; Barbara Shinn-Cunningham[2]; Abigail Noyce[2]
[1]Harvard University; [2]Boston University

In many visual search tasks, reaction times (RTs) increase monotonically with the number of search items. In displays where the search items change (e.g., in color), and target changes are synchronized with a simple auditory tone, search time decreases, and RTs no longer increase with set size, indicating that the synchronous tones cause the visual target to "pop out" (Van der Burg et al., 2008). This "pip and pop" effect is reflected in both early and late components of the evoked response potential (ERP). Multisensory ERPs elicited by synchronous auditory and visual stimuli differ from the sum of their unisensory components as early as 50ms post-stimulus. Responses to AV targets and AV distractors (from catch trials where the tone is synchronized with non-target display items) diverge in later ERP components (Van der Burg et al., 2011).

Here, we tested the hypothesis that this "pip and pop" effect is driven by audio-visual binding. To this end, we manipulated two parameters that affect the likelihood of audio-visual binding: co-location and learned association. In Experiment 1, participants searched for a vertically or horizontally oriented bar among randomly oriented distractors. Similar to previous work, the target was located in one of two search displays on the left and right of the screen. Auditory tones were synchronized with target or distractor color changes (or neither). On separate trials, the tone was lateralized to be either on the same side (congruent trials) or the opposite side (incongruent trials) as the display containing the target. To test for the effect of learned associations, in Experiment 2 we presented two distinct tones, one that usually corresponded to vertical targets and the other to horizontal targets. Trials where the more common tone-orientation relationship holds were referred to as congruent, whereas on relatively uncommon incongruent trials, the tone-orientation combination was flipped.

The key hypotheses are that congruency in either location (Exp. 1) or association (Exp. 2) yields faster search, and that ERP components differ between congruent and incongruent AV target trials. Reliable differences between these two conditions argue in favor of a central role of audio-visual object formation in the pip and pop effect.

PS 292

Temporally Coherent Audiovisual Signals Enhance Auditory Target Processing

Sarah H. Baum[1]; Ross K. Maddox[2]; Eric Larson[1]; Adrian K.C. Lee[1]
[1]*University of Washington;* [2]*University of Rochester*

Background

Our environment is filled with a continuous stream of sensory information across multiple modalities. The ability to parse sensory information into objects promotes better attention to information of interest. Object-based attention theory states that when we attend to one element of an object, attention to other object features is also enhanced. Previous behavioral work has shown a perceptual benefit when the visual stream is temporally coherent with the target auditory stream, resulting in the formation of an audiovisual object . Here we used simultaneous magneto- and electroencephalography (M-EEG) to explore the neural correlates of this enhanced perceptual processing.

Methods

Auditory stimuli consisted of two tone streams with independent band-limited (< 7 Hz) amplitude modulations.

Participants were asked to selectively attend to the target auditory stream while ignoring a second masker stream. Simultaneously, subjects were asked to attend to a single visual stream, consisting of a white ring with luminance modulated at 10 Hz, and to press a button every time a frequency modulation 'blip'; in the target stream occurred at the same time as the visual target briefly changed color. Three conditions were tested: visual stream radius modulation coherent with the auditory stream amplitude modulation of (1) the auditory target (Match Target; MT), (2) the auditory masker (Match Masker; MM) and (3) neither of the auditory streams (Match Neither; MN). Simultaneous M-EEG was collected from n = 17 subjects while they performed this AV task and structurally constrained inverse imaging was used to analyze activity on the cortical surface.

Results

We analyzed the neural responses to the target 'blip'; in the MT and MM conditions to investigate the neural correlate of the behavioral benefit observed previously of better target detection when the visual stream is temporally coherent with the auditory target stream. We found that the evoked response to auditory targets was greater in the MT compared to the MM condition from 270-320 ms in the left auditory cortex, but not in the right auditory cortex.

Conclusions

Enhanced detection of auditory targets with temporally coherent audio-visual information seems to be reflected in an increase in the magnitude at around 300 ms, reminiscent of the P300 component. Because the visual information is irrelevant to the task, any improvement in performance can be interpreted as multisensory binding and object formation of the temporally coherent auditory and visual streams.

PS 293

Effects of Signal Reliability in Audiovisual Speech Integration for Cochlear Implant Users and Normal Hearing Listeners

Hannah Shatzer[1]; Aaron Moberly[1]; Mark Pitt[1]; Kara Vasil[1]; Jess Kerlin[2]; Antoine Shahin[2]
[1]*The Ohio State University;* [2]*University of California, Davis*

Much of human communication utilizes both auditory and visual speech signals. The Dynamic Reweighting Model (DRM; Bhat et al., 2015) makes predictions about the weighting of speech signal processing based on the

reliability of auditory and visual signals: If the auditory signal is degraded, a more reliable visual speech signal will suppress and overwrite early auditory cortex information, thus reweighting signal processing in favor of the more reliable visual linguistic information. Cochlear implant users, with an impoverished auditory signal, would therefore show stronger weighting of the more reliable visual signal and stronger suppression of early auditory cortex activity. The current study sought to test these predictions for both cochlear implant (CI) users and normal hearing (NH) listeners to assess the degree of visual influence with vary degrees of auditory and visual reliability.

Postlingually deafened CI users and age-matched NH controls participated in an audiovisual phoneme identification task with electroencephalography (EEG) recording. Auditory tokens (/aba/, /aga/, /awa/) were presented at a signal-to-noise ratio (SNR) above or below a participant';s predetermined threshold and paired with clear blurred videos of mouth movements that were either congruent or incongruent with the auditory token. Participants identified the consonant they heard with a button press.

Behavioral results showed that NH controls gave auditory-dominant responses in all conditions except when the auditory stimulus was presented below SNR and the visual stimulus was clear and therefore more reliable. CI users were generally more prone to reporting the visually presented consonant than NH controls, particularly when the visual stimulus was more reliable. Event-related potentials (ERP) time-locked to the acoustic onset show P1 suppression for both CI and NH participants in the clear relative to blurred conditions. NH participants also demonstrate N1 suppression for high SNR relative to low SNR audio when time-locked to the onset of noise, an effect that is absent for CI users.

Behavioral and ERP results suggest an early influence of reliable visual information on auditory cortex for both groups as predicted by the Dynamic Reweighting Model, though the effect is stronger for NH controls. The NH participants also show that intelligible auditory information suppresses early auditory activity, which is consistent with the DRM';s predictions. Variability in CI subjects' behavioral and neural performance likely contributes to weaker ERP suppression effects than predicted by the DRM; this variability as well as correlations between their performance and demographic characteristics will be discussed.

PS 294

Audiovisual Speech Enhancement Predicted by Cortical Neural Processing Speed

James W. Dias; Carolyn M. McClaskey; Kelly C. Harris
Medical University of South Carolina

Speech recognition benefits from multisensory auditory-visual input. Often, this benefit is greater than when unimodal auditory and visual recognition are summed together. This audiovisual speech enhancement can produce superadditive neurophysiological responses, greater than the summed responses measured when processing auditory and visual speech independently. However, the role of resting-state cortical neural processing speed in audiovisual speech enhancement has not been thoroughly investigated. Cortical oscillations in the alpha frequency range (8hz-14hz) have served as a stable metric for resting-state cortical neural processing speed. The frequency corresponding to the peak in amplitude within the alpha frequency range, known as the peak alpha frequency, can predict cognitive and motor processing speed and the processing of non-speech crossmodal auditory-visual information across time. We recently reported that peak alpha frequency can predict the degree to which auditory and visual syllables integrate to produce unified percepts (i.e., the McGurk Effect). Perceivers with faster peak alpha frequencies integrate auditory-visual syllables more often. The purpose of the current investigation is to determine whether the role of peak alpha frequency in auditory-visual syllable integration applies to spoken word recognition, and whether faster peak alpha frequencies predict greater audiovisual speech enhancement. Eleven normal hearing adults between the ages of 19 and 30 (7 female) participated in this study. These participants identified 288 words, balanced for lexical frequency and neighborhood density, spoken by a male speaker. These words were randomly presented auditorily, visually (lipread), and audiovisually in noise at -5dB, 0dB, and +5dB signal-to-noise ratios. Audiovisual enhancement was measured for each participant by subtracting the summed accuracies for auditory (AO) and visual (VO) trials from the accuracy for audiovisual (AV) trials, AV − (AO + VO). Peak alpha frequencies were determined from electroencephalographic (EEG) recordings taken during a period of quiet rest, eyes closed, as the frequency at which amplitude peaked between 8hz and 14hz. Participants with faster peak alpha frequencies were found to exhibit greater audiovisual speech enhancement. The relationship between peak alpha frequency and audiovisual speech are discussed with regard to the role of alpha as an indicator of cross-sensory and lexical processing. Peak alpha frequency, which has been found to be predicted by cortical white-matter microstructure, may service as an indicator of the connectivity between

auditory and visual processing areas. Faster alpha may indicate more efficient integration of information across sensory systems.

PS 295

Evidence for visually-mediated encoding of phonetic representations at the auditory cortex

Noelle Todd; Antoine Shahin
University of California, Davis

Audiovisual (AV) integration is essential to speech comprehension, especially in noisy situations. There are two theories that have been proposed to explain the neural mechanisms underlying AV integration. The prevailing theory posits that auditory and visual percepts fuse in a multi-sensory 'integrator';, mainly the posterior superior temporal sulcus/gyrus (pSTS/G). The second theory advocates that cross-modal influence occurs via one modality (e.g., visual cortex) acting upon the representations of a second modality (e.g. auditory cortex). In this study, we examine the viability of the second theory. We hypothesize that AV integration of speech occurs when the visual cortex influences the encoding of phonetic information at the auditory cortex and in certain situations alters the perception of acoustic information based on that encoded information. To test this hypothesis, we employed a play on the McGurk illusion experimental design. We recorded Auditory Evoked Potentials (AEPs) while participants watched videos of a speaker uttering the consonant vowel syllables /ba/ or /wa/ while the audio played /ba/ or /wa/ sounds. In the congruent condition, the auditory and visual inputs were the same (audio /ba/, visual /ba/; audio /wa/, visual /wa/); and in the incongruent condition, the auditory and visual inputs were different (audio /ba/, visual /wa/; audio /wa/, visual /ba/). AEP results for this study provided evidence in favor of phonetic encoding at the auditory cortex that is mediated by the visual cortex. The N1 AEP consistently shifted with perception of the auditory input towards that conveyed by the visual input. It increased in amplitude when they heard an illusory /ba/ (audio /wa/, video /ba/, heard as /ba/) and decreased in amplitude when they heard an illusory /wa/ (audio /ba/, video /wa/, heard as /wa/), mirroring the N1 amplitude distinction observed for congruent /ba/ and /wa/ CVs (N1 larger for /ba/ than /wa/). This bi-directional shift of auditory perception and N1 amplitude towards the direction of visual input provides evidence that AV perception, including that of the McGurk illusion, is not just an equal integration of information from the auditory and visual cortices in a multi-sensory 'integrator'; but rather it represents the phonetic encoding that begins at the visual cortex and feeds over to the auditory cortex.

PS 296

Brain oscillations to silent lip reading.

Ayden Malekjahani[1]; Varia Sajeniouk[2]; Antoine Shahin[3]; Joseph Chen[2]; **Andrew Dimitrijevic**[2]
[1]*University of Toronto;* [2]*Sunnybrook Hospital Otolaryngology Head and Neck Surgery, University of Toronto;* [3]*University of California, Davis*

Background
Typical face-to-face communication involves both auditory and visual cues. When a sensory modality is impoverished, plastic changes in the brain allow for a recalibration of perceptual weighting cues. For example, people with hearing loss may rely more on visual information to follow a conversation compared to normal hearing listeners. Neural plasticity is likely an important factor in successful outcome after cochlear implant (CI) surgery. Some studies have shown that auditory cortex is involved in visual processing in deaf people and is related to speech perception with a CI. A better understanding of the neural processing associated with watching lip movements during speech utterances will help characterize some of the variability of CI outcomes after surgery. This study examines neural processing associated lip reading in normal hearing and will serve as normative data for people with hearing loss and CIs.

Methods
High density EEGs (electroencephalogram) were recorded in normal hearing adults while they watched a silent movie clip of an actor saying a single syllable word. The task was to identify the spoken word.

Results
Watching the speech movie elicited robust alpha (8-12 Hz) and beta (13-19 Hz) event-related desynchronization. Using brain source analysis, the alpha rhythm was localized to central and parietal regions while the beta rhythm was localized to occipital cortex. More alpha desynchronization was observed on trials where participants made a mistake in word identification compared to correct identification. The opposite effect was seen with beta desynchronization, whereby more desynchronization was observed on correct trials versus incorrect trials.

Conclusions
The results of this study show that distinct oscillatory patterns emerge when watching lip movements during speech production. Alpha rhythms appear to index greater degrees of neural processing on incorrect trials perhaps related to extra cognitive processing of stimulus uncertainty. Beta rhythms appear to be related to stimulus encoding. These data may be useful for assessing neural plasticity associated with hearing loss and CI use.

PS 297

Attentive tracking in the presence of auditory and visual distractors

Daniel Bates[1]; Maria Chait[2]
[1]Mr; [2]University College London

WITHDRAWN

Listeners'; ability to s~~ ~~ly track a sound source through a busy scene ~~elab~~orates in the presence of distractor sounds ~~an eff~~ect, often termed 'informational masking';, ~~occurs~~ even when the target and distractors do not o~~verlap~~ spectrally and is thought to reflect a limit on percep~~tual att~~entional resources which are required in the process of attentional selection. Previous work in our lab using EEG has demonstrated that that attended streams are associated with enhanced power relative to non-attended streams and that the size of this effect depends on scene size. Additionally, we reveal a link between fluctuations in occipital alpha-band activity and responses to unattended sounds. In the current study we utilise EEG and eye-tracking to try and tease apart how attention shapes responses when attending to sounds with a mixture and how those responses are further changed when attention is directed elsewhere (be it in the auditory or visual domain). Acoustic scene are comprised of 4 streams, with one allocated as the attended stream. Each stream is a sequence of pure tones with a different rate (3, 7, 13, 23Hz) and carrier frequency (CF, between 200 and 4248Hz). The main track task has participants attend to and detect gaps one of the 4 streams whilst inhibiting responses to gaps appearing in the ignored streams. To allow us to estimate brain activity associated with a 'neutral'; state (i.e. scene components neither attended nor ignored), embedded within all scenes are visual and auditory secondary tasks. In the auditory neutral task, two or three 100ms pure tones with frequency substantially above that of the scene are presented. In the visual neutral task, overlaid on a disk of white noise are either two or three flashes of a higher luminance disk. On a proportion of the trials, listeners were instructed to respond to either the tones or visual luminance changes. This task allows for the extraction of neural responses to main task sequences when passively observed. Ongoing analysis suggest that differences exist in the strength of spectral responses to streams based on whether they have been actively ignored or passively observed within or across modalities.

PS 298

Mismatch negativity as an index of auditory spatial attention gradients

Edward Golob; **Jeffrey Mock**
University of Texas, San Antonio

A main benefit of spatial hearing is the ability to panoramically monitor the environment for unexpected sounds. In spatial attention tasks the current direction of attentional focus influences processing of nearby stimuli, but attention can also be drawn to stimuli at locations away from the attentional focus. Recent behavioral studies suggest a complex interplay between where subjects are voluntarily attending in space and how they respond to sounds at various distances from the attentional focus. Computational modeling suggests two processes: one that corresponds to a top-down, voluntary attentional focus, and the other a more automatic, bottom-up response that may be tuned away from the top-down focus. Here we studied young adults (n=13) using a spatial mismatch negativity paradigm to examine bottom-up responses to stimuli at a standard location (L→ R: -90°, 0°, +90°, separate blocks) and infrequent shifts to other locations in the frontal horizontal hemispace. Results showed three main peaks: the mismatch negativity (~120 ms), followed by a P3a (~200 ms) and subsequent negative peak (~300 ms). The far left and right standard locations had comparable MMN and P3a amplitudes within the ipsilateral hemispace, and became progressively larger at midline and contralateral space (p';s<.03). Amplitude of the third peak did not significantly vary over locations. The effect of location was not significant when the standard was at midline. The MMN and P3a results at lateral standard locations support the idea of a bottom-up gradient centered on an expected location, but this did not generalize to standards at midline.

Golob & Mock_ARO Abstract_09-22-17.docx

PS 299

Natural auditory spatial cues benefit spatial selective attention

Yuqi Deng[1]; Barbara Shinn-Cunningham[2]; **Robert Baumgartner**[3]
[1]Boston University, College of Engineering; [2]Boston University; [3]Psychoacoustics and Experimental Audiology, Austrian Academy of Science

Spatial separation between competing talkers is known to help listeners focus on a signal of interest; however, past studies came to conflicting conclusions about the relative importance of interaural differences in time (ITDs) and intensity (ILDs) for spatial release from masking (SRM). However, most past studies used non-individualized head-related transfer functions and presented stimuli differing in their semantic and linguistic predictability. Here we asked whether natural spatial cues lead to more robust SRM in a carefully controlled setting, using individualized spatial cues and unpredictable sequences of speech syllables. Six normal-hearing listeners were asked to report the content of one of two competing syllable streams (random sequences of /ba/, /da/, and /ga/) located at roughly +30° and -30° azimuth.

The competing streams consisted of syllables from two different-sex talkers. Spatialization was based on 1) a natural combination of spatial cues (individualized head-related transfer functions, HRTFs), 2) only broadband ITDs, or 3) only frequency-specific ILDs. We measured behavioral performance as well as electroencephalographic markers of selective attention. Behaviorally, target recall performance was similar across conditions. Neurally, spatial attention modulated N1 magnitudes significantly more strongly for natural auditory spatial cues compared to the conditions using ITDs or ILDs only. Consistent with this, parietal oscillatory power in neural responses in the alpha frequency band (8-14 Hz; associated with filtering out distracting events from unattended directions) shows significantly more attentional modulation with natural spatial cues than with ITDs or ILDs only. Specifically, the natural condition produced a larger and faster alpha modulation index (AMI). These neural results hint that natural spatial cues produced the same behavioral SRM with more attentional control. These findings show that hearing devices should maintain natural characteristics of auditory space in order to facilitate the attentional control needed to communicate in complex auditory scenes.

PS 300

Low Frequency Oscillations in Distortion Product Otoacoustic Emissions during Selective Attention to Visual Stimuli

Constantino D. Dragicevic[1]; Marcela Navarrete[2]; Bruno Marcenaro[3]; Paul H. Delano[4]
[1]Departamento de Neurociencia, Medicina, Universidad De Chile; [2]Programa de Magister en Ciencias Biológicas, mención Neurociencias, facultad de Ciencias, Universidad de Valparaíso; [3]Centro Interdisciplinario de Neurociencias, Medicina, Pontificia Universidad Católica De Chile; [4]Otolaryngology Department, Clinical Hospital of the University of Chile

Though evidence in animal and human studies shows that selective attention to visual stimuli modulates cochlear responses, the neural mechanisms that drive these cortico-olivocochlear modulations are completely unknown. Here, we explored this topic by continuous electroencephalogram (EEG, 32 channels, Tucker-Davis Technologies® EEG workstation) and distortion-product otoacoustic emissions (DPOAE, ER10-C, Etymotic Research®) recordings in 14 healthy subjects. Volunteers performed alternating visual and auditory attention tasks that switched immediately upon their responses. In this work, we present data from the visual task. By considering the auditory efferent system as part of the top-down

attentional networks that initiate and sustain modulations of cochlear sensitivity, we transformed the DPAOE raw signal into a virtual channel that contains the amplitudes of DPOAE with a time resolution of 256 Hz. The virtual DPOAE channel was analyzed in a similar manner to the other EEG channels. Results: Time averages of the EEG channels showed a robust evoked response after the onset the visual cue, but we did not find a significant change in the mean amplitude of DPOAE. On the other hand, analysis in the frequency domain revealed novel low frequency (1-7 Hz) oscillations of DPOAE amplitudes in 13 of the 14 subjects, induced only during the visual attentional period (visual cue period), and resembling EEG oscillatory activity in the same time-frequency region. These oscillations were explored further through measures such as phase-locking to the attentional cue and cross-channel synchrony between the DPOAE channel and the 32-EEG channels. In addition, we also incorporated the DPOAE channel into topographical projection maps of electroencephalographic activity mainly to illustrate the capabilities of our method. We end by speculating a yet to be demonstrated causal relation between electroencephalographic and DPOAE amplitude low frequency oscillations, based on the observation that on average, the amplitude peak of cochlear oscillations in delta and theta bands (1-7 Hz) follows the peaks in the same bands of EEG channels.

PS 301

A closed-loop platform for real-time attention control of simultaneous sound streams

Daniel D.E. Wong[1]; Jens Hjortkjaer[2]; Enea Ceolini[3]; Søren V. Nielsen[4]; Sergi R. Griful[5]; Søren A. Fuglsang[4]; Ilya Kiselev[3]; Maria Chait[6]; Thomas Lunner[5]; Torsten Dau[2]; Shih-Chii Liu[3]; Alain de Cheveigné[1]
[1]Equipe Audition, Departement d'Études Cognitives, Ecole Normale Supérieure; [2]Hearing Systems group, Technical University of Denmark; [3]Institute for Neuroinformatics, University of Zürich/ ETH Zürich; [4]Hearing Systems group, Department of Electrical Engineering, Technical University of Denmark; [5]Eriksholm Research Centre; [6]University College London

Robust single-trial EEG measures of selective attention have recently suggested the possibility of decoding in real-time who a listener is attending to in multi-talker situations. This poses potential BCI perspectives for 'cognitive control'; of hearing prostheses that selectively amplify the attended sound source. Yet, little is known about the dynamics of such a closed-loop scenario. Here we present a real-time implementation of a wireless plat-

form that allows closed-loop EEG-steering of speech sources recorded in real-time. The platform consists of a multi-microphone hardware device that separates simultaneous speech sources via beamforming. The amplitude envelope of each audio source is extracted and streamed to a software platform that synchronizes the audio with multi-channel EEG. The synchronized EEG and audio streams are then fed to a real-time decoding algorithm that classifies the attended talker based on correlations between the EEG and the audio envelopes. The classification output is fed back to the audio platform to control the relative level of each sound stream presented to the listener. We present data recorded with this platform in a two-talker situation and discuss the dynamics of this closed stimulus-response loop.

PS 302

Electrophysiologic Investigation of Spatial Release from Masking in Adults with Normal Hearing

Alireza Pourjavid[1]; Kailyn McFarlane[1]; Nicole Marrone[2]; Barbara Cone[1]
[1]*University of Arizona, Speech, Language and Hearing Sciences;* [2]*University of Arizona*

Human communication frequently takes place in noisy environments and an individual';s successful understanding of speech is facilitated by the ability to extract and use spatial cues for separating speech from noise. The main aim of this study was to measure the key neurophysiologic markers of speech-feature perception abilities in noise and spatial-release-from-masking (SRM) in adults with normal hearing. We hypothesized that cortical auditory evoked potential (CAEP) latency and amplitude would vary systematically with sensation level (SL), signal-to-noise ratio (SNR), and spatial location of the noise source relative to the signal.

We obtained CAEPs from 19 adults with normal hearing thresholds (250-8000 Hz) in response to speech tokens (/ta/ or /da/) presented in the sound field. Speech stimuli were presented in quiet at 15, 30, 45 and 60 dB SL. Masked conditions used 10-talker babble noise from the AzBIO sentence test. The babble was presented either co-located, at 0 degrees azimuth in 3 different SNRs (10, 0, -5) and at the same levels tested in quiet, or spatially-separated at 90 degrees. CAEP component latencies and amplitudes were evaluated as a function of stimulus (speech token), sensation level, SNR, and condition (Quiet, co-located, or spatially-separated noise).

CAEP component latencies and amplitudes demonstrated systematic shifts as a function of stimulus type, SL, SNR, and noise location. Latencies were shorter for /da/ versus /ta/, reflecting the neural encoding of voice onset time. Latencies decreased and amplitudes increased for the P1-N1-P2 response components as level increased. Latencies increased and amplitudes decreased as SNR was decreased. Latencies increased and amplitudes decreased in the co-located noise condition compared to quiet. As compared to co-located noise, there was a release from masking with latencies decreased and amplitudes increased significantly when noise was spatially-separated.

The slopes of the latency-level and amplitude-level functions in quiet were used to estimate the electrophysiologic advantage of spatially-separated noise. The latency and amplitude differences suggested a spatial benefit that could not be fully accounted for on the basis of ear canal acoustics alone, but rather on central auditory nervous system binaural mechanisms. This suggests that the central auditory system is able to squelch background noise via processing of spatial information, and that this capacity is enhanced in more challenging listening environments. Further study is warranted with combined electrophysiologic and behavioral measures to more fully understand the neural encoding and perceptual benefits of spatial release from masking.

PS 303

Exploring the Bilateral Interaction Using Cortical Auditory Evoked Responses in Cochlear Implant Users with Single-Sided Deafness

Lamiaa Abdelrehim[1]; abd-Elmateen Mossa[2]; Nadia Kamal[3]; Dalia Hassan[3]; Chelsea Blankenship[4]; Lisa Houston[1]; Theresa Hammer[1]; **Fawen Zhang**[1]
[1]*University of Cincinnati;* [2]*Sohag University;* [3]*Ain Shams University;* [4]*Cincinnati Children's Hospital and University of Cincinnati*

Background
Single-sided deafness (SSD) is a condition in which the patient has non-functional hearing on one ear and normal hearing on the contralateral side. Cochlear implantation (CI) in SSD patients is expected to enhance binaural hearing. Understanding of the neural substrates of binaural hearing in CI users with SSD is crucial for eventually improving CI outcomes and using objective neurophysiological measures to assess CI benefits. The goal of the study was to examine the binaural integration in CI users with SSD using the cortical auditory evoked potentials. The binaural interaction is manifested by the deviation in the cortical responses with true binaural stimulation (B) from the predicted response based on the digital sum of right and left monaural responses (R+L).

Methods
CI adults with SSD were recruited. Normal hearing

young listeners were also recruited to provide data of normal cortical binaural integration. Each CI user was asked to perform the following tests: 1) questionnaires including Speech, Spatial and Qualities of Hearing Scale (SSQ) and Hearing Handicap Inventory for Adults (HHIA); 2) speech tests (AzBio Quiet and Quick-SIN); and 3) electroencephalographic (EEG) recordings. For the EEG recordings, stimuli were tones of 250 Hz with 1-sec duration that contained upward frequency changes, which allow the examination of the onset cortical auditory evoked potential (CAEP) and the acoustic change complex (ACC). Subjects were asked to ignore the stimuli during EEG recordings. All behavioral and EEG tests were performed under 3 conditions: right (R), left (L), and binaural (B), respectively, in a random order. The stimuli were presented via a loudspeaker located 1 meter from the subject at zero azimuth. The non-test ear was blocked with an earplug. The peak-to-peak amplitudes were measured in the onset CAEP and ACC for the L, R, and B conditions. The percent of binaural interaction was calculated using [(L+R)-B]/(L+R) amplitude ratio, with a larger ratio representing more binaural integration.

Results

The data collecting is still ongoing to include more participants. The present preliminary data showed that the percent of binaural interaction was approximately 40-50% in NH listeners and it was smaller in CI users with SSD. More data will allow for the examination of the correlation between the percent of binaural interaction of the cortical responses and the binaural benefits assessed with behavioral tests and questionnaires.

Conclusions

The cortical auditory evoked potentials provide a tool to examine cortical binaural integration in CI users.

2018 ARO (SSD).docx

PS 304

Binaural Selectivity of Hemodynamic Responses in Human Auditory Cortex is Enhanced by Forward Suppression

Nathan C. Higgins; Sandra Da Costa; Monica L. Folkerts; G. Christopher Stecker
Vanderbilt University Medical Center

The mammalian auditory cortex (AC) plays a necessary role in sound localization (cf. Malhotra et al. 2004 J Neurophysiol 92:1625-43). That role is supported by binaural sensitivity (i.e. tuning to interaural time differences [ITD] and interaural level differences [ILD]) among the majority of AC neurons (Kitzes 2008 Hear Res 238:68-76). Most of these exhibit broad contralateral preferences in the form of hemifield or axial location tuning (Middlebrooks and Pettigrew 1981 J Neurosci 1:107–20). AC population responses are thus strongly biased toward contralateral locations (Stecker et al. 2005 PLoS Biol 3:e78), as are hemodynamic responses measured in human AC (Stecker et al. 2015 Neuroimage 120:456-66; Derey et al. 2016 Cereb Cortex 26:450-64). Surprisingly, functional magnetic resonance imaging (fMRI) reveals limited sensitivity to ITD compared to ILD or simulated azimuth (McLaughlin et al 2015 JARO 17:37-53; Higgins et al 2017 PNAS 114:E7602-11). In this study, we used a binaural phase-encoding paradigm to address two hypotheses: The first–that intense MRI scanner noise reduces binaural selectivity–was addressed by comparing hemodynamic responses recorded with fMRI and with functional near-infrared spectroscopy (fNIRS, an intrinsically silent approach). The second–that competing sounds enhance AC binaural selectivity via forward suppression (Middlebrooks and Bremen 2013 J Neurosci 33:10986-1001)–was addressed by interleaving target sounds with a spatially static competitor. The two imaging methods (fMRI and fNIRS) were tested with identical stimuli (amplitude-modulated inharmonic tone complexes) that periodically (30 s) traversed a range of ITD and/or ILD values spanning left to right or vice versa. Hemodynamic time-courses obtained via continuous imaging at 0.5 Hz (fMRI) or 10 Hz (fNIRS) were cross-correlated to the ITD/ILD time-course to obtain stimulus-response functions for regions of interest in each AC hemisphere. Consistent with previous studies, the results revealed broad contralateral tuning in left AC and clearer bilateral tuning in right AC. Forward suppression was observed in the form of reduced response to targets when located in vicinity of the competitor. Sensitivity to ITD remained weaker than to ILD, but increased dramatically with stimulus competition. Results were comparable between fMRI and fNIRS, suggesting no dramatic effect of eliminating scanner noise but also demonstrating the feasibility of fNIRS as an approach to measure binaural sensitivity in (presumably lateral) AC. Supported by NIH R01DC011548 (to G.C.S.) and HHF 2016 Emerging Research Grant (to N.C.H.).

PS 305

Using spatial release from masking to estimate the magnitude of the familiar-voice intelligibility benefit

Ysabel Domingo[1]; Emma Holmes[1]; Ingrid Johnsrude[2]
[1]*Brain and Mind Institute, University of Western Ontario;* [2]*Brain and Mind Institute, University of Western Ontario; School of Communication Sciences and Disorders, University of Western Ontario*

The ability to perceptually segregate a target talker from competing talkers is crucial for successful communication. Studies in our lab (Johnsrude et al., 2013; Domin-

go, Holmes, & Johnsrude, in preparation) have demonstrated a 10-20% intelligibility benefit for familiar compared to unfamiliar talkers in the presence of a competing talker. This benefit is commensurate with one of the largest benefits to speech intelligibility that is currently known—that gained by spatially separating two talkers. However, because of differences in methods of these previous studies, the relative benefits of spatial separation and voice familiarity are unclear. In this study, we aimed to directly compare the familiar-voice benefit and spatial release from masking, and examine how these effects add.

Participants were recruited in pairs who had known each other for 6 months or longer. Pairs completed a speech intelligibility task, in which they heard three sentences spoken simultaneously on each trial. The three sentences were selected from the Boston University Gerald (BUG; Kidd et al., 2008) corpus, which uses the structure "[Name] [verb] [number] [adjective] [noun] ". Participants had to report words from the target sentence, which began with a target Name ("Bob" or "Pat"). The target sentence was presented from a simulated azimuthal spatial location (using ITDs and ILDs) of 0 degrees (0 degrees elevation). The two masker sentences were either collocated with the target (i.e., simulated at 0 degrees) or were separated symmetrically about the target at 5, 10, 15, 25, 45, or 90 degrees. In the Familiar Target condition, the target sentence was spoken by the participant';s partner and the two masker sentences were spoken by an unfamiliar talker. In the Both Unfamiliar condition, the target sentence was spoken by an unfamiliar talker and the two masker sentences were spoken by a different unfamiliar talker. Three target-to-masker ratios (TMRs) were used: -3, 0, and 6 dB.

Consistent with previous results from our lab, most participants were able to report more words when their partner';s voice was the target, compared to unfamiliar voices. Very preliminary results show that the familiar-voice benefit to speech intelligibility is on average 9.4%, which is equivalent to the benefit gained from symmetrically separating the two masker talkers by 8.5 degrees on either side of the target.

PS 306

Behavioral Manifestations of Listening Effort: Head Rotations

Madhur Murli[1]; Christopher Bennett[2]; Michael Hoffer[3]; **Hillary Snapp**[4]
[1]Sonos; [2]University of Miami Department of Acoustical Engineering; [3]Department of Otolaryngology and Neurological Surgery, University of Miami; [4]University of Miami Department of Otolaryngology

Background
Listening is an active mechanism that involves effort. A number of internal and external factors effect listening effort including audibility of the target signal, competing signals, context, and attention. Research has demonstrated an increase in effort is required for those with hearing loss, with evidence suggesting an association with fatigue and stress. In addition to subjective report, behavioral metrics of listening effort focus on detecting changes in listening effort as a function of task and/or listening condition. Objective measures such as pupilometry have also been used as a marker for listening effort. Listeners use multiple cues to identify and process auditory stimulus. Head rotations and consequent head orientation are important factors that govern these cues and can be thought of as behavioral corrections that the body applies to improve listening conditions. There are no studies of the actual behaviors applied by listener';s in real world scenarios to reduce effort. This study aims to explore the effects of head rotations and orientation in listening effort.

Methods
12 normal hearing subjects were evaluated to assess perception of conversational speech as a function of talker location. Custom stimuli representing a 5-talker conversation were generated to simulate real world listening scenarios. Subjects were required to track these conversations in the presence of restaurant noise. Accuracy as a function of talker location was calculated for 2 experimental conditions: 1) restricted – no head rotations, subject maintains head oriented at 0° azimuth; and 2) unrestricted – subject free to rotate head to locate the talker. Head rotations and orientation were monitored using a gyroscope. Changes in listening effort were assessed using pupilometry.

Results and Conclusions
Preliminary findings suggest that head rotations contribute to improved accuracy. Specifically, when subjects were not able to orient themselves towards the talker, their ability to accurately track conversation decreased significantly. Objective measures of pupilometry also suggest that effort is decreased when head orientation is closer to the source. Changes in pupil dilation as a function of head-source orientation was observed, suggesting listeners employ behavioral compensatory strategies to reduce effort. Similarly, those subjects who subjectively reported increased listening effort under adverse listening conditions were also more likely to apply head rotations to compensate. These findings suggest that listeners use head rotations to improve accuracy and reduce effort in complex listening environments.

ARO Abstract 2018.docx

PS 307

Neural responses to concurrent speech reflect the emergence of an SNR-invariant representation of the attended talker

Lorenz Fiedler[1]; Malte Wöstmann[2]; Sophie Herbst[1]; Jonas Obleser[2]
[1]Department of Psychology, University of Lübeck, Lübeck, Germany; [2]Department of Psychology, University of Lübeck

Listening conditions in real-life scenarios are rarely constant but vary unpredictably. While the focus of auditory attention can be detected from EEG, varying acoustical conditions may involve different neural mechanisms responsible for amplification of the attended signal (here, a talker) and/or suppression of the ignored noise (here, another talker).

Here, we investigated the effect of varying signal-to-noise ratio (SNR) on the neural response to concurrent speech. Eighteen participants attended to one of two simultaneously presented, spatially non-segregated talkers, while we measured their EEG. The SNR was varied by stochastic variation in the sound intensity of both the signal (attended) and noise (ignored) such that changes of SNR occured unpredictably. Using a forward encoding-model approach, neural responses to the attended and ignored talker were estimated. We investigated the influence of SNR (i.e. bottom-up) and attentional (i.e. top-down) manipulations on both amplitude and phase of the neural response functions.

Across conditions, responses to the attended talker showed a P1-N1-P2 complex in all subjects, whereas the N1-P2 components to the ignored talker were largely suppressed. First, the magnitude of the P1 component solely depended on the SNR and tracked the louder talker. However, the P1 response to the ignored talker was phase-delayed, which suggests that the attended signal becomes prioritized relatively early. Second, the N1 to the attended (vs. the ignored) talker was larger in all SNR-levels, but this difference increased in magnitude with more favorable SNRs. Lastly, the P2 component clearly contrasted the attended from the ignored talker, but this contrast was constant across SNRs. Interestingly, a late negative, N2-like deflection occurred only in responses to the ignored talker and only under the worst SNR. This additional component localized to parietal regions (whereas all other effects localized to superior and middle temporal regions). This is likely a signature of fronto-parietal attention network activity actively suppressing the ignored talker in a top-down manner. This chain of the P1-N1-P2 complex as revealed by a forward-encoding model approach and their sensitivity to temporally unpredictable changes in SNR indicate that the neural representation of the attended talker gets successively isolated from the distractor. This was also reflected in enhanced classification accuracy in the P2 interval across conditions when utilizing a temporal generalization method to identify the attended talker. Our findings give insight into the spatio-temporal unfolding of the neural cortical response, and how an attentional set can help overcome acoustic challenges along the auditory pathways.

Auditory Cortex: Anatomy, Physiology & Function II

PS 308

Complementary Cell Type-Specific Shifts in AMPA and GABAA Receptor Transcripts Underlie Increased Central Gain in the Adult Auditory Cortex Following Single-Sided Deafness

Pooja Balaram[1]; Daniel B. Polley[2]
[1]Eaton-Peabody Laboratory, Massachusetts Eye and Ear Infirmary/ Department of Otolaryngology, Harvard Medical School; [2]Massachusetts Eye and Ear Infirmary, Harvard Medical School

Background

Cochlear deafferentation depresses sound-evoked activity at early stages of the auditory pathway, but causes a paradoxical increase in activity at the level of auditory cortex (ACtx). Increased "central gain" supports variable degrees of recovered cortical processing; some mice regain normal auditory thresholds while other mice show no recovery of auditory processing, despite equivalent damage to the inner ear. We hypothesized that homeostatic regulation of AMPA and $GABA_A$ postsynaptic receptors in auditory cortical neurons would contribute to central gain, and may explain variable levels of recovered auditory processing between individuals. Further, homeostatic regulation of postsynaptic receptors could differ between excitatory and inhibitory cortical neurons, and the opposing directions of receptor shifts between these two populations could work synergistically to maximally increase central gain.

Methods

We performed daily widefield and 2-photon calcium imaging in cortical pyramidal neurons through a cranial window implanted in awake, head-fixed adult mice. After several days of baseline imaging, we injected sterile water into the contralateral cochlear oval window, which eliminated all otoacoustic and brainstem markers of hearing without affecting the ipsilateral ear. We tracked daily increases in ipsilaterally evoked responses in ACtx over a 5-day period following hearing loss. We then used fluorescence in situ hybridization to quantify transcription levels of Gria2 mRNA, which encodes an AMPA receptor subunit, and Gabra1 mRNA, which en-

codes a subunit of the GABA$_A$ receptor. Levels of mRNA were quantified separately in genotyped excitatory and inhibitory neurons, as indexed by their expression of VGLUT1, VGLUT2, or VGAT mRNA.

Results
Within 24 hours of unilateral cochlear damage, sound-evoked GCaMP activity in the contralateral ACtx was significantly reduced relative to baseline hearing with the contralateral ear intact. Over the following 1-4 days, sound-evoked responses from the intact ipsilateral ear increased in all cortical fields. At 5 days post-injury, Gria2 and Gabra1 transcript levels were significantly shifted relative to controls, with complementary shifts between VGLUT-positive and VGAT-positive neurons.

Conclusions
Complementary transcriptional shifts in AMPA and GAB-AA receptor subunits in excitatory and inhibitory cortical neurons may reflect a network homeostatic process to increase the gain on reduced afferent inputs and recover normal levels of activity following sudden single-sided sensorineural hearing loss.

Balaram.ARO 2018 abstract.FINAL.docx

PS 309

Horizontal sound localization performance by a gleaning bat, Antrozous pallidus

Dustin Brewton[1]; Khaleel Razak[2]
[1]*University of California, Riverside; *[2]*UC, Riverside*

The auditory cortex is necessary for sound localization, but how the auditory cortex represents sound locations is unclear. The pallid bat hunts terrestrial prey by listening to prey-generated noise while reserving echolocation for obstacle avoidance. The auditory cortex of the pallid bat contains a region tuned between 5-35 kHz, selective for broad band noise that mimics prey-generated noise. This noise-selective region (NSR) is organized into two binaural clusters based on interaural level difference (ILD) selectivity. Cells within the peaked cluster respond best to midline stimuli generating ILD ~ 0 dB. Cells within the binaurally inhibited (EI) cluster respond best to contralateral stimuli. Previous studies of azimuth selectivity of these cells have suggested a testable hypothesis regarding how systematic changes in the extent of active cortex encodes azimuth. Here we present data that begins to test this hypothesis.

To determine contributions of these regions to localization behavior, we have characterized the horizontal sound localization ability of the pallid bat with controlled head position. Bats were trained to localize noise stimuli

for a food reward on an 'approach to stimulus'; task. The effect of sound location and bandwidth (low- and high-pass filtered at 15 and 20 kHz) on performance was measured. Average percent of correct trials and error measured in degrees are reported.

Results indicate that the pallid bat has one of the best azimuth localization abilities measured. Acuity in an open loop localization task with a 100 msec duration broadband (5-30 kHz) noise is ~4 degrees (N=7 bats). Both quantitative measures (percent correct and error) co-vary with location and bandwidth of the broadband stimulus (p<0.05). Pairwise comparisons suggest the bandwidth effect is restricted to low-pass stimuli, meaning frequencies between 20-30 kHz are sufficient for peak performance.

Peaked and EI type neurons have been identified in most mammalian brains examined, but the contributions they make to localization behavior remains speculative. The segregated representation of these neurons in the brain and the ability to measure localization accuracy facilitates examination of the contributions these neuron types make to localization. For reversible 'lesioning'; of these clusters, pyramidal cells within each cluster will be targeted by AAV injections carrying a chemogenetic repressor (AAV8-CaMKII-hM4Di) and inactivation by CNO injection. Here, we describe advances made towards reversible inactivation of the NSR with the DREADDs. These experiments contribute to the development of the pallid bat prey-localization behavior using passive listening as a neuroethological model to understand sound localization mechanisms.

PS 310

Synaptic and Spiking Responses to Infant Vocalizations in Mouse Paraventricular Hypothalamus In Vivo

Silvana Valtcheva; Robert C. Froemke
NYU School of Medicine

Experience-driven changes in neural circuits are believed to have important consequences for information processing and sensory perception. A fundamental question is how neural plasticity occurs under natural conditions, to promote the recognition of stimuli with behavioral significance. Motherhood is a dramatic natural experience (Dulac et al., 2014), but little is known about the underlying changes in neural circuits for parenting behavior. The neuropeptide oxytocin is synthesized by hypothalamic areas including the paraventricular nucleus (PVN), and is important for maternal behaviors including parturition, lactation, and parent-child bonding, perhaps in part by increasing salience of social information

(Insel & Young, 2001). Indeed, many women experience oxytocin release and milk ejection simply in response to infant cries (McNeilly et al., 1983). Recently, we showed that oxytocin can enable maternal behavior by balancing synaptic inhibition with excitation in the auditory cortex (Marlin et al., 2015; Mitre et al., 2016). Therefore, cortical modulation and plasticity produced by oxytocin signaling might enable long-lasting enhancements of social interactions and maternal care. However, beyond the necessity for lactation, mechanisms of oxytocin release in the brain leading to naturally-induced forms of plasticity are not well understood.

Here, we aimed at identifying how social stimuli activate PVN oxytocin neurons in vivo, and if these responses were gated or changed after maternal experience. We performed in vivo cell-attached and whole-cell recordings from PVN neurons in awake head-fixed mice. We examined PVN neuronal responses to ultrasonic vocalizations (pup isolation calls) and pure tones. PVN neurons did not display frequency selectivity in response to pure tones but they showed reliable responses to pup calls. However, in virgin females these responses remained predominantly subthreshold. Our results suggest that PVN neurons can receive information about acoustic input, reflecting projections from central auditory areas. In absence of maternal experience, however, these responses are unreliable and less coherent, keeping the synaptic responses subthreshold and preventing spurious action potential generation and subsequent oxytocin release in naïve animals.

PS 311

Persistent Encoding of Sound Categories in Primary Auditory Cortex

Rupesh Chillale[1]; Sophie Bagur[2]; Shihab Shamma[3]; Srdjan Ostojic[1]; Yves Boubenec[4]
[1]Ecole Normale Superieure; [2]ESPCI Paris Tech; [3]Ecole Normale Supérieure, University of Maryland; [4]Ecole Normale Supérieure, Paris, France

Categorizing sounds in task-relevant classes is a key process for assigning proper goal-directed behavioral responses to acoustic stimuli. Our previous study (Bagur et al., under revision) suggested that primary auditory cortex (A1) plays a highly flexible role in processing incoming stimuli and implement a first step in encoding a behavioral representation of stimuli at the population level during task engagement. Here we wanted to investigate how the encoding of sound behavioral meaning can be maintained during the delay period at the population level in categorization task. For this we trained ferrets to classify regular click trains in Go/NoGo categories (low and high rates) during an appetitive choice task. After training, we found that stimulus identity was asymmetrically represented at the population level when ferrets passively listened to stimuli. Consistent with our previous results, task-engagement enhanced this asymmetry, even after excluding all lick-related neuronal activity. Interestingly, task-engagement induced persistent representation of the sound category during the delay period preceding the response window. The encoding scheme of categories changed at the transition points between the different epochs of the trial (sound presentation, delay, response window). All together, these results suggest that training over a categorization task can form long-term encoding of stimulus behavioral meaning in the primary auditory cortex. Furthermore, the encoding scheme of sound categories dynamically evolves throughout the course of the trial during task-engagement, possibly reflecting feedforward- and feedback-driven representations of sounds in A1 during task-engagement.

PS 312

Spatial profile of input to Layer 2/3 auditory cortex in rats exposed to polychlorinated biphenyls

Christopher M. Lee[1]; Susan L. Schantz[2]; Daniel A. Llano[3]
[1]University of Illinois at Urbana-Champaign; [2]College of Veterinary Medicine, University of Illinois at Urbana-Champaign; [3]Department of Molecular and Integrative Physiology, University of Illinois at Urbana-Champaign

Developmental exposure to polychlorinated biphenyls (PCBs) is associated with reduced hearing sensitivity in humans and rats. PCBs, a family of synthetic compounds, were once used in the manufacture of industrial products, including capacitors, transformers, hydraulic fluids, and lubricants. Due to their toxicity and resistance to degradation, production of PCBs was banned in the 1970s. However, humans continue to be exposed, primarily through ingestion of contaminated food, and PCBs can be transferred to infants through the placenta or through breast milk.

Hearing loss induced by disruptions to the periphery may lead to compensatory changes in the central auditory system. We have previously demonstrated that developmental exposure to PCBs is associated with both an elevation of ABR thresholds and an increase in the frequency and amplitude of spontaneous and miniature IPSCs in Layer 2/3 cortical cells. Thus, the changes in inhibitory input to layer 2/3 of the cortex may reflect a homeostatic change that compensates for increased ascending input from the midbrain. In this study, we further investigate these findings by using laser scanning photostimulation (LSPS) to map the spatial profile of inputs to auditory cortical neurons in PCB-exposed and control rats. In addition, by simultaneously recording pairs

of neurons, we assessed the extent of common input to pairs of neurons in the cortex. Female breeding rats were dosed with 0 or 6 mg/kg/day of an environmental PCB mixture from 4 weeks prior to breeding until weaning on postnatal day 21. ABRs were recorded from adult offspring. Coronal brain slices were then prepared and auditory cortex layer 2/3 pyramidal neurons were recorded under whole-cell configuration. Excitatory and inhibitory synaptic input to individual neurons were mapped using LSPS. We compare the spatial profile of excitatory and inhibitory inputs in control and PCB-exposed rats.

PS 313

Characterization of termination patterns of layers 5 and 6 cortical neurons in the mouse inferior colliculus.

Georgiy Yudintsev[1]; Daniel A. Llano[2]
[1]Neuroscience Program, University of Illinois at Urbana-Champaign; [2]Department of Molecular and Integrative Physiology, University of Illinois at Urbana-Champaign

Top-down modulation is thought to be one mechanism by which the brain can disambiguate sensory signals, and descending projections are believed to be the substrate through which this modulation occurs. One of such projections - the corticocollicular (CC) projection - recently garnered much attention due to its potential to alter response properties in the inferior colliculus (IC). However, the anatomical organization of this pathway remains poorly understood.

Earlier, we demonstrated significant heterogeneity in the distributions of layer 5 and 6 CC neurons in the cortex, with layer 6 cells spanning across a broader area of the cortex than layer 5. However, the comparison of the termination patterns from layer 5 and layer 6 neurons is yet to be made. In the present study, we used two viral approaches in Rbp4-cre mouse line to differentially express fluorescent markers in layer 5 and layer 6 corticocollicular neurons in the same animal, and later compare the distributions of their axons in all subdivisions of the IC. Using confocal microscopy, we found that both layer 5 and layer 6 CC neurons heavily projected to lateral (LC) and dorsal cortices (DC) in the ipsilateral IC, with some terminals found in the contralateral DC and ipsilateral central nucleus (CN). Additionally, layer 6 CC axons and terminals tended to be thinner and smaller on average than axons and terminals from layer 5 CC cells. These findings further suggest different functions for layer 5 and 6 CC neurons and provide a foundation for further differential optogenetic manipulations of layer 5 and 6 corticocollicular projections.

PS 314

Cortical Map Plasticity as a Function of Vagus Nerve Stimulation Rate and Train Duration

Elizabeth Buell; Kris Loerwald; Michael Borland; John Buell; Corinne Kelly; Irfath Khan; Katherine Adcock; Collin Chandler; Jayant Kurvari; Michael Kilgard
UT Dallas

Background
Pairing a brief train of vagus nerve stimulation (VNS) with an external event can reorganize the sensory or motor cortex (Borland et al., 2016; Hays et al., 2014; Navzer D. Engineer et al., 2011; Porter et al., 2012). Repeatedly pairing a tone with sixteen VNS pulses presented at a frequency of 30 Hz significantly increases the number of neurons in primary auditory cortex (A1) that respond to tones near the paired tone frequency (Borland et al., 2016; Navzer D. Engineer et al., 2011). It is not known if changing VNS pulse rate or duration would increase or decrease the degree of cortical map plasticity.

Objective/Hypothesis
This project investigates the effects of VNS rate and train duration on cortical plasticity. We hypothesize that changing these parameters will affect the degree of driven plasticity.

Methods
Rats were assigned to groups receiving low (7.5 Hz), moderate (30 Hz), or high (120 Hz) VNS rates or short (125 ms), moderate (500 ms), or long (2000 ms) VNS train durations paired with 9 kHz tones 300 times per day over a 20 day period.

Results
The VNS moderate rate group exhibited significantly more A1 neurons that respond to the paired tone, as well as a significantly larger response strength to tones. Rats that received high or low rate VNS had significantly fewer neurons responding to frequencies near 9 kHz compared to rats in the moderate frequency group. Preliminary data shows that 125 ms and 500 ms train durations effectively drive plasticity while 2000 ms duration does not.

Conclusion
These results are consistent with the inverted-U effect on plasticity observed with VNS intensity and suggest that the magnitude of plasticity driven by VNS is sensitive to changes in multiple stimulation parameters.

PS 315

Tonotopic Neural Responses to Acoustic and Electric Stimuli in the Rat Primary Auditory Cortex

[1]**Jani S. Manring**, [2]Guangchen Ji, [2]Volker Neugebauer, & [1*]Yang-soo Yoon
[1]*Department of Speech, Language, & Hearing Sciences, Texas Tech University Health Sciences Center (TTUHSC), TX, USA*
[2]*Department of Pharmacology & Neuroscience, TTUHSC, TX, USA*

Despite improvements in performance gained from cochlear implants (CIs) and auditory brainstem implants (ABIs), patients continue to face considerable difficulty understanding speech in noise. Similarly, CIs and ABIs are not sufficient options for treating patients with injury or disease at or above the brainstem region. These auditory prostheses are unable to provide optimized spectral and temporal information due to the challenges of spectral mismatch, which is an incongruence between auditory information received from these auditory prostheses and neurons stimulated in the Organ of Corti. In order to (1) overcome the reduced benefit caused by spectral mismatch, and (2) provide salient auditory information to patients who are ineligible for current devices, a new device must be developed. The long-term goal of this project is to develop an auditory cortex implant that provides superior fidelity of spectro-temporal information to the primary auditory cortex (A1) by directly stimulating specific tonotopic points in the A1 region with electric signals processed by an external speech processor. The characterization of tonotopic organization within the A1 allows for more significant precision of electrode placement than CIs and ABIs, resulting in significant reduction of spectral mismatch; in essence, spectral and temporal transmission will be significantly enhanced. Electric and acoustic signals may be processed differently in a normal auditory system. However, electrical signal processing and tonotopic frequency distribution in the A1 region is unknown. Initially, we compared tonotopic maps created by recording neural responses to electric and acoustic stimulation in the A1 region in an intact animal auditory system. Baseline frequency mappings within A1 are an essential part of our study as we characterize the electrical tonotopic organization within the A1 area relative to existing frequency mapping of acoustic tonotopic organization. The full comparative frequency mapping, recorded by evoked action potential generation to electric and acoustic stimuli, will be presented.

*Corresponding and presenting Author

Jani Manring, M.A., M.Sc.
Doctoral student, Department of Speech, Language, & Hearing Sciences
Signal Processing and Communications Lab
Advisor: Dr. Yang-soo Yoon
Texas Tech University Health Sciences Center
3601 4th St Stop 6073, Lubbock, TX 79430 USA
Email: jani.manring@ttuhsc.edu
Phone: 806-690-2430
2018 ARO abstract JM YY.docx

PS 316

Emergence of selectivity and invariance in primary auditory cortex

Pilar Montes-Lourido; Shi Tong Liu; **Srivatsun Sadagopan**
University of Pittsburgh

Humans and vocal animals use vocalizations to communicate and interact with members of their species. Real-world environments add noises, echoes and other sounds to the intended message, degrading its acoustic content. However, we can maintain stable sound perception independent of listening conditions. We aim to determine the neural mechanisms by which stable sound perception can be achieved. To address this question in the context of natural behaviors, we use Guinea pig (GP) vocalizations as an experimental model. Previous studies in GPs have shown that at the level of the inferior colliculus and thalamus, few neurons show selective responses for individual vocalization categories. In primary and secondary cortical areas, more neurons become selective for particular vocalization categories. It is not known, however, at which stage of the auditory hierarchy this selectivity arises, and how it is preserved or changed in the presence of real-world distortions. Here, we first tested if GPs can perceive vocalizations presented in a wide range of noisy environments using pupillometry as a behavioral readout. This allowed us to determine the GP';s threshold for detecting a vocalization in noise. We then recorded single-unit activity in the medial geniculate body (MGB) and auditory cortex (A1) of awake GPs passively listening to vocalizations in different listening conditions. We discovered that neurons in MGB and thalamorecipient A1 layers (A1 L4) have low selectivity for vocalization categories and are more susceptible to acoustic distortions. In contrast, superficial layers of A1 (A1 L2/3) were highly selective for vocalizations and more invariant to distortion. These data demonstrate that both vocalization selectivity and invariance to listening conditions co-emerge in A1 L2/3. These results suggest that a dense representation of complex sounds in A1 L4 is transformed into an invariant and sparse representation in A1 L2/3.

PS 317

Tone-evoked Acoustic Change Complex (ACC) in an animal model

Alessandro Presacco; John C Middlebrooks
University of California, Irvine

Introduction The Auditory Change Complex (ACC) is a cortical evoked potential complex generated in response to changes (e.g. frequency, amplitude) within an auditory stimulus. The ACC is generally characterized in humans by a P1-N1-P2 complex that varies in amplitude with the capability of the brain to detect changes in the auditory stimulus. The ACC has been recorded in both normal-hearing human subjects and in cochlear implant users, suggesting that the ACC would be useful in clinical applications. Recent findings also show that presence of the ACC tends to correlate with psychoacoustic discrimination, thus suggesting that ACC might be used as a surrogate for time-consuming psychophysical studies. Despite the promising results in humans, it remains unknown whether the ACC can be recorded from animals. The purpose of the current study was to investigate the feasibility of recording ACC in response to frequency and level discrimination tasks in sedated cats. Methods Five purpose-bred domestic shorthaired cats were studied. No hearing deficits were evident. A light level of anesthesia was induced with an intramuscular injection of ketamine (20 mg/kg) and acepromazine (1 mg/kg). All the auditory stimuli were presented at an intensity of 75 dB SPL from an open-field speaker located near the right ear. Continuous tones alternated between high and low frequencies or levels in 500-ms blocks. Frequency and level steps were varied parametrically. Scalp potentials were recorded with needle electrodes (two active electrodes = one on each hemisphere, reference: mastoid ipsilateral to the stimulus, ground = back of the cat). Results ACC was successfully elicited in all cats by both frequency and level steps. As reported by previous studies conducted in humans, the ACC showed a clear asymmetry, in that amplitudes were greater for increasing than for decreasing or frequency or level steps. Interestingly, the detection thresholds measured were in good agreement with previous behavioral studies in which cats where trained to perform similar discriminations. Conclusions The results of this study confirm the feasibility of recording ACC in this animal model. Responses bore several similarities to human studies, making this animal model a good candidate for use in clinically-relevant applications, such as the objective measurement of the performance of innovative modes of invasive stimulation for hearing restoration.

PS 318

Exposure to Loud Sound Induces Cell-Specific Changes in the Intrinsic Properties of Auditory Cortical Projection Neurons: Implications for Tinnitus

Amanda Henton[1]; Laura Marinos[1]; Shanshan Xiong[1]; Wai Lok Tsang[2]; Thanos Tzounopoulos[3]
[1]Department of Otolaryngology, University of Pittsburgh; [2]Physician Scientist Training Program, University of Pittsburgh; [3]Department of Otolaryngology, University of Pittsburgh, Department of Neurobiology, University of Pittsburgh, Pittsburgh, PA 15261

Hearing loss, tinnitus, hyperacusis, and other auditory disorders are most commonly caused by exposure to loud sound. While some of the structural and biophysical mechanisms underlying plastic changes that occur in the auditory system are known, such as loss of ribbon synapses in hidden hearing loss and the hyperexcitability in the auditory brainstem in tinnitus, the biophysical mechanisms underlying noise-induced changes in the in the auditory cortex remain less understood. Here, we investigated noise-induced changes in the intrinsic properties of specific subpopulations of projection neurons in auditory cortex. Namely, we focused on pyramidal tract (PT) neurons, which project to the inferior colliculus and auditory brainstem, and intratelencephalic (IT) neurons which project to the contralateral cortex. After noise exposure, whereas no changes were found in the intrinsic properties of IT neurons, the resting membrane potential of PT neurons in auditory cortex was significantly lower than controls. These findings may reveal a novel cell-specific site of modulation in auditory cortex after noise exposure, and in pathological conditions such as tinnitus. Moreover, we recently developed an operant behavior model for the detection of tinnitus in mice. Our behavioral model utilizes the operant conditioning of mice to cross from one chamber to another, and to suppress that behavior in silent trials, thus in tinnitus, the suppression of crossing behavior would be reduced. In addition to investigating the changes in intrinsic properties after noise exposure, we aim to study the tinnitus-specific changes in intrinsic properties of auditory cortex.

Synaptic zinc shapes cortical frequency tuning in a neuron-specific fashion and improves sound frequency discrimination

Manoj Kumar[1]; Charles Anderson[1]; Shanshan Xiong[2]; Thanos Tzounopoulos[3]
[1]Department of Otolaryngology, University of Pittsburgh, Pittsburgh, PA 15261; [2]Department of Otolaryngology, University of Pittsburgh; [3]Department of Otolaryngology, University of Pittsburgh, Department of Neurobiology, University of Pittsburgh, Pittsburgh, PA 15261

Synaptic zinc modulates cortical responsiveness to sound in a neuron-specific fashion (Anderson et al., 2017). However, the role of synaptic zinc in shaping sound frequency tuning, a fundamental aspect of auditory processing, and auditory-driven behaviors remains unknown. Here, we used two-photon in vivo imaging in awake mice to investigate the effect synaptic zinc on the frequency tuning of auditory cortical neurons. Moreover, we employed behavioral techniques to assess the effect of zinc on sound frequency discrimination. We discovered that synaptic zinc sharpened the frequency tuning of CaMKII-expressing principal neurons, but it widened the tuning of somatostatin-expressing interneurons, without affecting the tuning of parvalbumin- and vasoactive intestinal polypeptide-expressing interneurons. In the absence of cortical synaptic zinc, mice showed reduced ability in detecting changes in sound frequencies. Synaptic zinc is a novel modulator of cortical frequency tuning that enhances acuity for sound frequency discrimination

Population coding of high frequency amplitude modulations in auditory cortex

Justin Yao; Dan Sanes
New York University

Background
Our goal is to understand how activity across a neural population encodes sensory information required for the perception of signals with rapid temporal information. Here, we examined how population-level activity in the gerbil auditory cortex (ACx) obtained during task performance encodes the detection of fast amplitude modulations (AM).

Methods
Freely-moving gerbils were tested on an appetitive Go-Nogo AM detection task while recordings were obtained telemetrically from a 16-channel array implanted in left ACx. "Go" stimuli consisted of AM signals (broadband noise carrier, AM rates: 64-512 Hz, modulation depths ≤100%). The "Nogo" stimulus consisted of unmodulated (0% modulation) broadband noise. We used a linear support vector machine (SVM) classifier to assess ACx sensitivity across a population of neurons. The SVM procedure identifies a linear hyperplane that best separates responses corresponding to separate stimulus conditions. This readout was obtained by training a linear classifier to learn the optimal representation for each stimulus condition. Classifiers were trained on 80% of trials pooled across a population of neurons, and were subsequently tested on the remaining 20% of trials, without replacement. This procedure was conducted across 250 iterations. We also used choice probability (CP) analysis to quantify the relationship between ACx spike firing and behavior choice on a trial-by-trial basis.

Results
Gerbils were capable of detecting AM rates up to 512 Hz, with thresholds declining at higher rates. Whereas the neural sensitivity of individual cortical units typically underestimated psychometric sensitivity, we found that encoding performance across a population of ACx neurons could account for psychometric performance. In contrast, CP values from our entire population of cortical units did not differ from chance (median CP: 0.50-0.53, p > 0.05, Wilcoxon rank-sum, Ho: median CP = 0.50), suggesting that cortical units did not represent the animal';s behavior choice during task performance.

Conclusion
Population-level ACx activity contains sufficient sensory information to detect AM at very high rates despite the absence of periodicity coding. In principle, the linear classifier output, which utilizes a linear-decision boundary to separate population activity between unmodulated and AM noise, could be transformed by downstream neurons as a thresholded sum of weighted synaptic inputs for appropriate decoding. This provides a prediction that can be tested in downstream decoding regions.

Funding

Effect of Attention on Neural Responses in the Ferret Auditory Cortex in a Cocktail Party Model

Neha Joshi[1]; Daniel Duque[1]; Jonathan Fritz[1]; Shihab Shamma[2]
[1]University of Maryland; [2]Ecole Normale Supérieure, University of Maryland

An auditory scene typically comprises of multiple speakers and an often-noisy environment. The ability to listen to the most relevant stream in a particular context depends primarily on the ability to selectively attend to a cue by parsing the scene into perceptually coherent representations, termed auditory streams. The auditory cortex in the brain does this with ease, which has been demonstrated previously in Mesgarani et al., 2012, O';Sullivan et al, 2015 and Akram et al, 2016 for ECoG, EEG and MEG signals respectively.

We use the ferret as an animal model to study speech representation in a multi-speaker environment. The ferret serves as an excellent model to study effects of human speech because the range of sounds frequencies heard by a ferret is similar to humans, their Auditory Cortex is complex enough to encode phoneme classes (Mesgarani et al., 2008) and they can be trained to differentiate syllable sequences (Bizley et al., 2015; Duque et al., 2016). To explore the role of attention in neural mechanisms of stream segregation, we developed a behavioral paradigm to study the role of selective attention to a target word at the neuronal level. We trained ferrets to discriminate tri-syllabic pseudo-words using a conditioned avoidance GO/NO-GO task. They are trained to attend to a target word (Eg. Fa-Be-Ku) by a female speaker while ignoring a simultaneous male background speaker. In order to analyze neural encoding in stream segregation, we performed single unit neurophysiological recordings in primary and secondary areas of the Auditory Cortex in head-fixed ferrets. We explored whether responses during the tasks showed adaptively enhanced representation of the attended female speaker.

Preliminary neurophysiological data indicate that neuronal responses to words in the male distractor voice in the cocktail party scenario showed specific suppression, enhancing relative representation of the attended female target word. This study shows that neurons in higher order Auditory Cortex can encode pseudo-words selectively in a multi-speaker scenario depending on the attentional context. These results will help us understand the neural basis for representation of complex sound sequences and yield deeper insight into neural mechanisms underlying initial stages in human speech processing of the cocktail party problem.

PS 322

Perineuronal net expression in the auditory cortex of mice

Sarah Reinhard; Maximiliano Abundez Toledo; Katherine Espinoza; Khaleel Razak
UC, Riverside

The auditory cortex of the mouse consists of four to six distinct regions. The auditory "core" region consists of primary auditory (A1) and anterior auditory (AAF) fields. In many ways these two fields are similar, each organized in a tonotopic arrangement of neurons and receiving inputs from the ventral MGB of the thalamus. These regions also exhibit distinct temporal properties, with the AAF showing faster latencies, better synchrony to fast amplitude modulations and stronger response and preference for fast frequency modulated sweep rates compared to A1 neurons. Studies performed in cats also suggest that AAF may be more susceptible to multimodal reorganization of auditory map "space" after peripheral sensory deprivation. These data suggest that the AAF may be more temporally 'precise'; and show more malleability with experience compared to A1. The cellular correlates of these differences are unclear.

Parvalbumin positive (PV) interneurons are thought to shape temporal firing patterns in the auditory cortex, particularly those involved in representing rapid changes in spectrotemporal shape of sounds. PV neurons are closely associated with an extracellular matrix component called perineuronal nets (PNN) that may provide protection against oxidative stress and play a role in maintaining excitability of these inhibitory interneurons. Changes in these two cellular structures are seen in models of abnormal auditory processing such as after noise induced and age-related hearing loss, and in neurodevelopmental disorders with hyperacusis such as the model of fragile X Syndrome. We characterized differences in PNN and PV cell expression in A1 and AAF of mouse auditory cortex in adult WT mice. The boundary between A1 and AAF was identified with electrophysiological mapping. IHC for PV and WFA labeling for PNNs reveal a larger number of PNNs and a higher co-localization of PV/PNN in AAF compared to A1. Layer specific analyses were performed. We further looked at the effect of developmental sound exposure to broadband noise on distribution of PNNs in A1 and AAF. Results represent a possible cellular correlate to observed differences in A1 AAF function and support the idea of these two regions have distinct roles in auditory processing.

PS 323

Exponentially decaying temporal integration in networks can explain much of the dependence of neural responses on stimulus history in primary auditory cortex.

Monzilur Rahman[1]; Benjamin D.B. Willmore[1]; Andrew J. King[2]; Nicol Harper[2]
[1]*Department of Physiology, Anatomy, and Genetics, University of Oxford;* [2]*University of Oxford*

Responses of neurons in the primary auditory cortex to sound stimuli are often characterized using a linear non-linear (LN) model. For the LN model to achieve a high level of performance (normalized correlation coefficient, CCnorm 0.71; Hsu et al. 2004, Network: Comput Neural Syst: 15; Schoppe et al. 2016, Front Comput Neurosci: 10) in predicting single unit neural responses to natural sounds in ferret primary auditory cortex, we found that it is necessary to include in the spectrotemporal receptive field (STRF) a large amount of stimulus history, going back up to about 200 ms in the past. Given this finding, we asked how much of this dependence on stimulus history can be explained by certain simple dynamical aspects of neurons. We constructed a neural-network-like model whose output is the weighted sum of the response of multiple units, each of which resembles an LN model in using an STRF and a nonlinearity. However, the response of each unit of the network model was modified in accord with a dynamic firing-rate equation. This low-pass filters the unit';s response (by convolving with an exponential decay impulse response) providing a simple exponentially decaying memory governed by a time constant individual to each unit. This integrative characteristic can be related to the capacitance and resistance of neural membranes, and the time-constant can be related to the membrane time constant of real neurons (Dayan & Abbott 2001, Theoretical Neuroscience). The results of our work show that this dynamic-network model, when fitted to the neural data using component STRFs that are of only 25 ms in duration, can achieve prediction performance on a held-out dataset (CCnorm 0.70) comparable to the best performing LN model. In other words, much of the dependence of auditory cortical neural responses on stimulus history beyond 25 ms can be modelled by exponentially-decaying temporal integration processes in networks. When the network model with 25 ms STRFs is fitted without the dynamic aspect, its predictive performance is substantially impaired. Also, when the units in the dynamic network that have long time constants are silenced, the predictive performance of the model is affected significantly. Moreover, long time constants are associated with network units that are inhibitory. These findings suggest that membrane time constants and/or other simple exponentially-decaying memory processes may underlie much of the dependence of the neural responses on stimulus history beyond 25 ms.

Sensorimotor Mismatch Signals for Learned Motor-Auditory Associations: A Two-Photon Imaging Study in Auditory Cortex of Behaving Mice

Samuel A. M. Picard[1]; Yves Weissenberger[1]; Andrew J. King[2]; Johannes C. Dahmen[1]
[1]Department of Physiology, Anatomy, and Genetics, University of Oxford; [2]University of Oxford

Predicting the sensory consequences of one';s actions is critical to perception and action in dynamically changing environments. In many cases, there is a fixed, general relationship between a given action and its sensory feedback, such as visual flow during locomotion (Fiser et al., 2004) or vocalization feedback (Eliades and Wang, 2008). More recently, neurons have been reported in primary visual cortices that signal mismatch between predicted and actual sensory feedback (Keller et al., 2012), and a circuit basis that could underlie such mismatch detection has been reported in the auditory system as well (Nelson and Mooney, 2016). However, it currently remains unclear whether cortical mismatch signals are specific to fixed sensorimotor contingencies or whether they may also arise with arbitrary, newly learned contingencies. We developed and validated a behavioural task that requires head-fixed mice to learn novel, arbitrary motor-auditory associations. Animals were trained to freely navigate through a one-dimensional, abstract auditory landscape (Aronov et al., 2017) composed of equally spaced pure tones, by licking either of two lick-ports. We show that mice are capable of using auditory feedback to adaptively guide behaviour, and are sensitive to unexpected feedback. Next, we used two-photon calcium imaging to investigate the functional properties of auditory cortical neurons in mice performing this task. Among the various acoustic tuning profiles encountered in layer 2/3 of auditory cortex, some otherwise sparsely active neurons were found to be particularly responsive following sounds that violated the learned sensorimotor contingency. This activity was dependent on whether or not the animal was actively engaged in the task. Taken together, these results suggest that a network of cortical neurons is engaged in predicting the sensory consequences of motor actions, even when the relation between motor action and sensory feedback is arbitrary and newly learned.

Aronov D, Nevers R, Tank DW (2017) Mapping of a non-spatial dimension by the hippocampal–entorhinal circuit. Nature 543:719–722.

Eliades SJ, Wang X (2008) Neural substrates of vocalization feedback monitoring in primate auditory cortex. Nature 453:1102–1106.

Fiser J, Chiu C, Weliky M (2004) Small modulation of ongoing cortical dynamics by sensory input during natural vision. Nature 431:573–578.

Keller GB, Bonhoeffer T, Hübener M (2012) Sensorimotor mismatch signals in primary visual cortex of the behaving mouse. Neuron 74:809–815.

Nelson A, Mooney R (2016) The Basal Forebrain and Motor Cortex Provide Convergent yet Distinct Movement-Related Inputs to the Auditory Cortex. Neuron:1–14.

PS 325

Encoding and decoding stimuli and behaviour in mouse auditory cortex over the course of learning

Yves Weissenberger[1]; Michael Lohse[1]; Peter Keating[2]; Andrew J. King[3]; Johannes C. Dahmen[1]
[1]*Department of Physiology, Anatomy, and Genetics, University of Oxford;* [2]*The Ear Institute;* [3]*University of Oxford*

Understanding the computational and circuit mechanisms by which animals learn is a fundamental problem in modern neuroscience. Furthermore, the contribution of sensory areas to learning processes and the enactment of operant behaviour is unclear. The auditory cortex has been implicated in the performance of various auditory tasks and activity therein has been shown to correlate with behavioural and cognitive variables. Here, we present chronic two-photon imaging data from the auditory cortex of head-fixed mice during learning. Mice were trained to perform a simple click-detection task and subsequently an attention-demanding version of the same task, where stimuli were presented at reduced levels. To better interpret these data, we developed novel model-based behavioural analyses that allow us to measure performance and directly decode the causes of the animals'; behaviour, with single trial resolution. Using these methods, we show that during learning and performance of these detection tasks, auditory cortical activity and functional connectivity correlates with both single-trial behavioural variables and ongoing strategies. Additionally, we present preliminary data showing that inactivation of the auditory cortex impairs performance in this task. Together this work highlights the role of auditory cortex in the performance of learned behaviours and further elucidates the neurophysiological changes that are associated with the process of learning.

PS 326

Auditory Temporal Processing Tests: Indicator for Central Pathology

Renata Filippini[1]; Frank Musiek[2]; **Bryan Wong**[2]
[1]*University of Sao Paulo;* [2]*University of Arizona*

Background
Performance on auditory temporal processing tests (ATP) has shown to be decreased in subjects with lesions affecting the CANS (Musiek & Pinheiro, 1987; Musiek et al., 1990; Musiek et al., 2005). The goal of this review is toevaluate and compare ATP performance for different populations with a variety of centrally mediated pathologies. The Gaps-In-Noise, Frequency Pattern and Duration Pattern tests were used.

Methods
A total of 15 studies on 329 people with Epilepsy (N=6), Stroke (N=3), Multiple Sclerosis (MS; N=1), Dyslexia (N=3) and blast exposure (N=2) were included.

Results
For all five conditions, the neuro-auditory groups performed below the norms, for all three tests, with significant poorer performance than their corresponding control groups. Moderate to large Effect Size were obtained for all studies and measures, with Cohen';s d ranging from 0.47 to 2.64. Conclusion:ATP test performance for all three measures seem to be negatively affected by a broad range of central pathologies. These tests have the capability to clinically evaluate CANS integrity for a wide range of central pathologies, and it is strongly encouraged that clinicians routinely apply them to fully assess hearing in neurological populations.

Auditory Pathways Brainstem II

PS 327

In vivo intracellular responses of octopus cells in the gerbil ventral cochlear nucleus

Hsin-Wei Lu[1]; Tom P. Franken[2]; Bertrand Fontaine[1]; Mark Sayles[3]; Philip H. Smith[4]; Philip X. Joris[5]
[1]*KU Leuven;* [2]*KU Leuven; The Salk Institute for Biological Studies;* [3]*Purdue University;* [4]*University of Wisconsin - Madison;* [5]*KU Leuven, University of Leuven*

Octopus cells in the mammalian ventral cochlear nucleus are projection neurons with distinctive morphological and physiological properties. Their dendrites span a wide frequency range of auditory nerve fiber (ANF) inputs. Their membrane resistance and time constant are remarkably low and short, causing small and rapid excitation from individual ANF. Sound-evoked spikes

of these cells are unique: a well-timed onset spike to high frequency tones and a series of spikes in-sync with click trains up to several hundred hertz. These findings suggest that octopus cells encode sounds by integrating synchronous ANF activity. However, direct evidence for such coincidence detection is lacking and requires measurements of its subthreshold responses to sound.

We conducted in vivo whole cell and sharp electrode recordings of octopus cells in anesthetized gerbils. Cells were filled with neurobiotin or biocytin through the recording pipette to confirm their identity. Only rarely did octopus cells fire spontaneously; however, they showed abundant (> 250 events/s), small (mostly 0.3 - 2 mV), and fast (decay tau ~ 0.4ms) spontaneous excitatory postsynaptic potentials (EPSPs). The size and frequency of the EPSPs increased significantly in response to ipsilateral but not contralateral wide band noise. Action potentials were small (~ 5 - 30 mV) and their sizes varied depending on stimuli. The most easily distinguished action potentials were observed during click train stimuli (> 15 mV in amplitude), with larger spikes found at higher sound levels. These spikes are perfectly timed (vector strength > 0.99) and could entrain up to ~400 Hz. In response to high frequency (> 4kHz) tones, octopus cells only fired one spike at the onset. Surprisingly, there are numerous large EPSPs (> 5 mV) with rise times < 1ms following the onset spike, suggesting near synchronous activation of multiple smaller ANF inputs during tone stimuli. These events and spike output were dominantly tuned to high frequencies (> 5kHz, average 13.4 kHz) and had high minimal thresholds (> 60 dB SPL on average). They also showed clear membrane depolarizations phase-locked to the sound envelope in response to amplitude-modulated tones.

In conclusion, our intracellular data confirm that octopus cells are particularly sensitive to stimulus transients, but the responses also suggest a sustained source of synchronous input which is not anticipated from knowledge available from in vitro recordings.

PS 328

Mechanistic and Structural Bases for Functional Diversity in MSO Neurons Across the Tonotopic Axis

David B. Haimes[1]; Brian J. Bondy[1]; Nace L. Golding[2]
[1]Department of Neuroscience and Center for Learning and Memory, University of Texas at Austin; [2]Department of Neuroscience, University of Texas at Austin

The Medial Superior Olive (MSO) is a mammalian brainstem nucleus that computes cues used for azimuthal sound localization (interaural time differences, ITDs). Despite evidence from the avian MSO highlighting differences in both synaptic inputs and electrical properties, mammalian models of ITD processing typically assume uniform properties. The evidence for tonotopic differences in MSO structure and function in mammals remains inconsistent and incomplete.

We used current clamp electrophysiology recordings from a large (>450) number of MSO neurons, anatomically labeled with biocytin, to quantify the pattern and shape of action potentials (APs) across the tonotopic axis in coronal slices taken from Mongolian Gerbils P17-80. Using immunohistochemistry and confocal microscopy, we labeled MSO neurons for the axon initial segment (AIS) marker, AnkyrinG, and imaged z-stacks to reconstruct and quantify AIS parameters in Neurolucida 360.

We found that MSO neurons exhibit three subclasses based on their firing patterns to depolarizing current steps: phasic, typically consisting of a single, small AP with fast membrane properties, oscillators, which fire large, high frequency trains of APs interrupted by pauses that contain large amplitude subthreshold membrane oscillations, and tonic, characterized by regular firing patterns of large APs with distinct after-hyperpolarizations. Both oscillator and tonic neurons'; APs exhibited ~2 fold larger maximum rates of rise compared to phasic neurons (417.9±23.6 and 423.9±28.1mV/ms vs. 172.9±14.1mV/ms respectively), and exhibited larger first AP amplitudes relative to threshold (48.6±2mV and 56.1±2.5mV vs.22.7±1.8mV). To investigate whether these differences in spiking reflect AIS morphological differences, we used immunolabeling to assess AIS morphology along the tonotopic axis. Tonic and oscillator neurons tend to be located at the ventral and dorsal fifths of the MSO. However, the morphological parameters of the AIS were uniform across the tonotopic axis for the AIS length and standard deviation (average 17.8±4.0 µm; n=288 axons from 3 gerbils) as well as the distance of the start of the AIS from its attachment point on the soma or proximal dendrite (~0.1 µm). Current experiments are investigating that the functional differences underlying

MSO neuron subclasses is reflected in the spatial distribution or properties of voltage-gated sodium channels.

Taken together, we find that the MSO clusters subclasses of neurons towards the tonotopic extremes, categorized by their AP firing patterns and properties. Strikingly, MSO neurons'; do not show tonotopic-dependent changes in AIS parameters, distinct from findings in the avian MSO, where changes in these parameters across the tonotopic axis alters excitability.

PS 329

A novel form of synaptic plasticity: rebound effect in inputs to the lateral superior olive

Elisa G. Krächan; Martin Fuhr; Jennifer Winkelhoff; Vanessa Augustin; Isabelle Römer; Eckhard Friauf
Department of Biology, University of Kaiserslautern

Sound source localization in the mammalian auditory brainstem is achieved by processing interaural time and level differences (ILD). Synapses involved in these tasks are capable of transmitting signals in a precise and reliable manner, even during sustained high-frequency activity. They are equipped with specific morphological features, e.g. inner hair cell ribbon synapses and endbulbs and calyces of Held. The lateral superior olive (LSO) is located in the center of the ILD pathway, integrating excitatory signals from the ipsilateral ear and inhibitory signals from the contralateral ear. Although LSO inputs appear to lack morphological specifications, they process binaural signals in the millisecond range over sustained periods of time. Here, we assessed the characteristics of inhibitory, glycinergic and excitatory, glutamatergic LSO inputs in response to continuous (60 s) high-frequency trains (50-200 Hz). For comparison, we offered bursts followed by gaps of silence, a more physiological pattern. We performed whole-cell voltage clamp recordings in juvenile (P11) and young adult (> P20) mice while electrically stimulating excitatory glutamatergic inputs from the cochlear nucleus (CN-LSO) or inhibitory inputs from the medial nucleus of the trapezoid body (MNTB-LSO). Evoked postsynaptic currents (ePSCs) of both input types showed frequency-dependent short-term depression (STD). Gaps reduced STD via within-gap replenishment of synaptic vesicles. When analyzing the first ePSC of each burst ($ePSC_1$) as readout of within-gap replenishment, we found an unexpected increase of amplitudes after initial STD, which we named rebound effect. The rebound effect was present at about 75 % of P11 MNTB-LSO synapses, yet only at frequencies >50 Hz. The gradual increase of $ePSC_1$ amplitudes began remarkably late (~20 s), reaching a maximum ~25 % higher than the maximal STD level. Furthermore, it lasted until the end of 60-s train. It is of presynaptic origin because the quantal size was con-

stant during the 60-s train, thus excluding postsynaptic receptor desensitization or saturation. The ratio of inputs displaying a rebound effect declined with age to ~50 % at P20, whereas the extent and timing remained unchanged. While $eIPSC_1$s increased, the subsequent ePSCs in each burst became reciprocally smaller, leading to an unchanged cumulative ePSC per burst and thus pointing to an increase in release probability (P_v). CN-LSO inputs displayed no rebound effect, although heterogeneous plasticity was found. Collectively, we describe a novel form of plasticity at inhibitory MNTB-LSO synapses. It converts tonic responses to onset responses and may thereby enable efficient computation of repetitively offered sound bursts.

PS 330

How robust and temporally precise is synaptic transmission in the auditory brainstem? A comparative analysis of inputs to the lateral superior olive and the inferior colliculus

Sina Brill; Katrin Janz; Eckhard Friauf
Department of Biology, University of Kaiserslautern

The mammalian auditory system processes exquisitely timed information, e.g. to compute interaural level differences during sound source localization. The latter process takes place in the lateral superior olive (LSO) by comparing binaural inputs from the cochlear nucleus (CN) and the medial nucleus of the trapezoid body (MNTB). The synaptic performance of MNTB-LSO synapses has previously been investigated (Krächan et al, 2017; J Physiol), revealing fast, temporally precise and reliable signal transmission even at >100 Hz. Less is known about the performance of CN-LSO synapses and synapses at higher auditory stations, such as the inferior colliculus, which is not involved in sound source localization in the sub-ms domain. We asked the following question: are robustness and precision general features of auditory brainstem synapses? To address the question, we analyzed the synaptic performance of CN-LSO and lateral lemniscus-IC (LL-IC) synapses, both being of excitatory nature. The analysis was followed by a meta-analytical comparison including MNTB-LSO synapses. Whole-cell patch-clamp recordings of LSO and IC neurons were performed in acute slices of mice (P11) while electrically stimulating the ventral acoustic stria and LL fibers, respectively, at 1-200 Hz each train lasting 60 s. Synaptic performance was assessed regarding several aspects (Table), e.g. release rate and latency jitter. IC neurons were categorized as onset, sustained, and adapting based on their intrinsic firing pattern in response to rectangular current injections. Their performance was cell-type independent, enabling us to pool sample data which were subsequently compared to MNTB-LSO and CN-LSO synapses (Table). Frequency-dependent depression differed between synapse

types. LL-IC synapses depressed completely when stimulated at >10 Hz. CN-LSO and MNTB-LSO synapses, however, released robustly even at >100 Hz, indicative of superior replenishment mechanisms. Concerning the temporal precision, LSO inputs displayed lower latency jitter than IC synapses, again demonstrating their superiority. The better performance of LSO inputs, particularly of MNTB-LSO synapses, is based on exceptional release properties (N_{RRP}, P_v) not present at LL-IC synapses. When comparing CN-LSO to MNTB-LSO inputs, the former were surprisingly inferior in several aspects. Collectively, we demonstrate homogeneity in the performance of excitatory inputs to various IC cell types. Their performance is less robust, precise and powerful than at CN-LSO and MNTB-LSO synapses. We conclude that robustness and precision are key features of early brainstem synapses but no longer eminent at higher auditory stations.

	Frequency [Hz]	**MNTB-LSO**	**CN-LSO**	**LL-IC**
Steady-state (last 10 ePSCs) release rate [vesicles/s]	10	140	23	16
	100	288	79	indeterminable
Steady-state latency jitter [ms]	10	0.15	0.14	0.45
	100	0.33	0.66	indeterminable
Vesicles in readily releasable pool N_{RRP}		202	59	18
Quantal size q [pA]		24	20	20
Release probability P_v [%]		16	11	33

PS 331

Synaptic mechanism underlying temporally precise information processing in the VNLL

Michael Rebhan[1]; Linda Fischer[2]; Felix Felmy[2]; Christian Leibold[3]
[1]*Division of Computational Neurobiology, Department Biology II, Ludwig-Maximilians-University München;* [2]*Institute for Zoology, Universtiy of Veterinary Medicine Hannover;* [3]*Bernstein Center for Computational Neuroscience Munich*

Within the ventral nucleus of the lateral lemniscus (VNLL) exists a population of cells that exhibits a precise onset response to pure tone stimuli. It is believed that these cells play an important role in information processing of amplitude modulated sounds, such as conspecific vocalisation. One major excitatory input to VNLL onset cells arises from the octopus cells of the posterior ventral cochlear nucleus (PVCN), and thus much of the VNLL onset behaviour is presumed to be inherited from octopus cells. We find that glutamatergic synapses at VNLL cells, that presumably convey octopus cell activity, have a double exponential conductance shape combining a fast (sub millisecond) AMPA component and a slow time component, which we attribute to NMDA receptor activation by pharmacological intervention.

It is unclear how such complex synaptic filtering would affect the processing of octopus cell inputs. To elucidate the effects of such synaptic filtering, we devised a model network with octopus cells feeding into VNLL neurons. Octopus cells are thereby described by a novel phenomenological model that only comprises few well-constrained free parameters and closely emulates the properties of the octopus cell responses to pure tones and amplitude modulated tones. In addition to simulated octopus cell responses the VNLL neuron also receives broadband inhibition, assumed to be originating from multiple neurons of the medial nucleus of the trapezoid body (MNTB).

To understand the role of VNLL onset responses in the processing of natural sounds, we used information theory to determine the optimal frequency range and stimulus features most efficiently driving VNLL responses. Preliminary testing with human speech stimuli suggests that the model favours certain phonemes over others depending on the centre frequency of the modelled octopus cells. Applying information theoretical tools to the processing of human speech, we find that most of the information transmission occurs for modulation frequencies below 200 Hz. This suggests that the fine structure of the stimulus is suppressed and only the low frequency amplitude modulations of complex sounds are *preserved.*

PS 332

Knock-Out of Astrocytic GlyT1b/c Interferes with proper MNTB-LSO Signaling

Julia Hammerich; Jonathan Stephan
Animal Physiology Group, Department of Biology, University of Kaiserslautern

The main inhibitory input to the lateral superior olive (LSO) arises from the medial nucleus of the trapezoid body (MNTB). Astrocytes in the LSO express different inhibitory neurotransmitter transporters, i.e. GlyT1, GAT-1, and GAT-3 (Stephan and Friauf; Functional analysis of the inhibitory neurotransmitter transporters GlyT1, GAT-1, and GAT-3 in astrocytes of the lateral superior olive, Glia, 2014, DOI: 10.1002/glia.22720). However, the contribution of astrocytic neurotransmitter transporters to MNTB-LSO signaling is so far unexplored. Therefore, we prepared acute brainstem slices of GlyT1b/c KO mice and wild-type littermates at P19-21 and performed whole-cell voltage-clamp recordings from identified LSO principal neurons. We analyzed inhibitory postsynaptic currents (IPSCs) that occurred spontaneously or were evoked by stimulation of MNTB-LSO fibers. In GlyT1b/c KO mice, the spontaneous activity of MNTB-LSO synapses was reduced while IPSC kinetics were not affected. In contrast, a higher stimulation frequency resulted in stronger depression of evoked IPSCs. Furthermore, the MNTB-LSO synapse exhibited a reduced fidelity. Taken together, our results demonstrate the requirement

of GlyT1b/c during high frequency synaptic transmission and its dispensability during spontaneous and low activity. GlyT1b/c absence did not affect IPSC kinetics, but increased depression and reduced fidelity. Accordingly we conclude that GlyT1b/c is not important for neurotransmitter clearance, but is necessary for replenishment to ensure efficient and sustained MNTB-LSO signaling.

PS 333

Glycinergic Synapses onto Medial Olivocochlear Neurons in the Ventral Nucleus of the Trapezoid Body

Lester Torres Cadenas; Matthew Fischl; Catherine Weisz
NIH / NIDCD Section on Neuronal Circuitry

Synaptic inputs onto medial olivocochlear (MOC) efferent neurons in the brainstem ventral nucleus of the trapezoid body (VNTB) are poorly understood. Excitatory, glutamatergic inputs originate in the cochlear nucleus, but the source, strength, or identity of neurotransmitters at putative inhibitory synaptic inputs have not been characterized. We performed whole-cell voltage-clamp electrophysiological recordings in MOC neurons to investigate inhibitory synaptic inputs. MOC neurons in the VNTB were identified for recordings in brainstem slices from P12-P23 mice using either a transgenic mouse line that labeled cholinergic neurons, via a retrograde neuronal tracer injected into the cochlea, or both techniques simultaneously. Neuronal morphology was determined in some experiments by filling the neuron with biocytin during the recording followed by DAB staining to confirm MOC identity. During recordings, spontaneous post-synaptic currents (sPSC) were partially sensitive to the AMPA type glutamate receptor blocker CNQX. The reversal potential of remaining sPSCs was about -30 mV, corresponding to the chloride reversal potential, indicating inhibitory synaptic currents. Application of strychnine further reduced PSC frequency, demonstrating the presence of glycinergic synaptic transmission. To determine the source of inhibitory synaptic inputs to MOC neurons, electrical stimulation delivered via a micropipette was used to evoke neurotransmitter release from subsets of pre-synaptic axons, while evoked (e)PSCs were measured in postsynaptic MOC neurons. Excitatory and inhibitory synaptic inputs were both evoked from axons originating primarily from the same ear. ePSCs in MOC neurons using 'paired pulse' stimulation at inter-stimulus intervals (ISI) from 10-500 ms suggests that there is a facilitation of inhibitory synaptic inputs at ISIs from 50-200 ms. Our work indicates that MOC neurons in the VNTB receive inhibitory inputs in addition to glutamatergic inputs. These inhibitory inputs were at least partially glycinergic and exhibited facilitation over a range of paired pulse intervals. Future work will confirm the neuronal source of inhibitory synaptic inputs to MOC neurons and further characterize the effect of inhibitory neurotransmission on MOC function.

PS 334

The role of Ca2+-permeable AMPA receptors at the calyx of Held synapse

Brendan Lujan; Andre Dagostin; Henrique von Gersdorff
Vollum Institute, Oregon Health and Science University

GluA2-lacking Ca^{2+}-permeable AMPARs (CP-AMPARs) have previously been identified to play integral roles in synaptic plasticity and mediate excitotoxic cellular signaling at a number of glutamatergic synapses throughout the brain. However, the role of CP-AMPARs in the maintenance of synaptic transmission at the calyx of Held synapse is still poorly understood. Here, we report functional evidence for CP-AMPARs at the calyx of Held synapse, in an in vitro slice preparation. Through a combination of electrophysiological and Ca^{2+} imaging approaches from the principal cells of the medial nucleus of the trapezoid body (MNTB), we show that stimulation of the afferent fibers near the midline activates these receptors and leads to robust Ca^{2+}-influx before the onset of hearing in mice from P8-10. Using a selective open channel blocker of CP-AMPARs, IEM 1460 (IEM), we estimate approximately 65% of the AMPAR population are permeable to Ca^{2+} at this age. However, after the onset of hearing in more mature synapses at P18-22 and P30-34, we discovered that Ca^{2+}-influx through these receptors was reduced. We estimate that CP-AMPARs only comprise 39% and 31% of the entire AMPAR population at P18-22 and P30-34, respectively. As the calyx of Held synapse matures, the presynaptic action potential becomes extremely short and fast. Since IEM is an open-channel blocker, we tested whether the observed reduction in functional CP-AMPARs was simply due to decreased efficacy of IEM at the more mature synapse. By pharmacologically manipulating the shape of the presynaptic action potential to a waveform that is more similar to P8-10, we show that the apparent reduction of CP-AMPARs was not due to speeding of the presynaptic action potential in functionally mature synapses. Finally, using synaptic depression trains to trigger the readily-releasable pool of synaptic vesicles, we show that inhibition of CP-AMPARs influences the short-term plasticity of the synapse. We conclude that CP-AMPARs play a major role in short-term plasticity and development at the brainstem calyx of Held synapse.

PS 335

Resurgent Sodium Current Promotes Action Potential Firing in the Avian Auditory Brainstem

Hui Hong[1]; Xiaoyu Wang[2]; Ting Lu[1]; Yuan Wang[2]; **Jason Tait Sanchez[1]**
[1]*Northwestern University;* [2]*Department of Biomedical Science, Program in Neuroscience, Florida State University College of Medicine*

Auditory brainstem neurons are functionally primed to fire action potentials (APs) at markedly high-rates in order to rapidly encode acoustic information of sound. This specialization is critical for survival and the comprehension of behaviorally relevant communication functions, including sound localization and signal discrimination. It is well established that high-voltage activated potassium channels are key players in regulating high-frequency firing ability. Here, we investigated Na_V channel mechanisms essential for high-rate AP firing in neurons of the chicken nucleus magnocellularis (NM) – the avian analog of bushy cells of the mammalian anteroventral cochlear nucleus. Whole-cell current-clamp recordings on late-developing (embryonic [E] days 19-21) NM neurons revealed their remarkable ability to follow square pulse trains up to 200 Hz with good fidelity. Consistently, voltage-clamp recordings using double-pulse protocols demonstrated that Na_V currents in NM neurons are able to fully recover within 5 ms. This observation raised an important question: what factor(s) contribute to facilitating Na_V channel recovery in NM neurons?

We observed robust generation of resurgent sodium current (I_{NaR}) in late-developing NM neurons, which showed similar properties with those reported in mammalian neurons. The unique mechanism of "open channel block", which induced I_{NaR} in NM neurons, facilitated the recovery and increased the availability of Na_V channels shortly after depolarization. Additionally, our preliminary experiment using the "AP clamp" method showed the presence of I_{NaR} immediately after an AP, which provides a small depolarizing drive to the membrane and thus likely promotes repetitive neuronal firing. Indeed, using a computational model of NM neurons, we demonstrated that removal of I_{NaR} reduced high-rate AP firing.

We also documented the development of I_{NaR} relative to hearing onset. Surprisingly, NM neurons at E14-16, which corresponds to the period of during hearing onset, presented with similar I_{NaR} properties with their late-developing counterparts. This suggests that E14-16 is a priming period during hearing development for establishing mature auditory functions. In contrast, NM neurons at E11-12 (i.e., a "prehearing" period), showed weak I_{NaR} with properties dramatically different from the older neurons. In line with these results, E14-16 NM neurons

displayed frequency-firing ability closely resembling late-developing neurons, while E11-12 neurons were only able to follow square pulse trains up to 70 Hz. Finally, we detected strong Na_V1.6 expression that clustered along the axon initial segment for mature neurons. This expression pattern became increasingly less distinct at hearing onset and prehearing periods, suggesting that multiple Na_V channel subtypes may differentially contribute to I_{NaR} during development.

PS 336

Control of Spike Timing via Membrane Potential Oscillation Frequencies: Role of Kv3.1 K+ Current Modulation

Timothy Olsen[1]; Alberto Capurro[1]; Nadia Pilati[2]; Charles H. Large[2]; Martine Hamann[1]
[1]*University of Leicester;* [2]*Autifony Therapeutics*

Our recent study shows that modulation of Kv3 K+ currents controls spike-timing of dorsal cochlear nucleus (DCN) fusiform cells via an effect on membrane potential fluctuations (1). Frequency components of membrane potential fluctuations have been shown to contribute to modulation of spike-timing at the cellular level (2 3). Here we tested whether membrane potential oscillations at different frequencies control spike timing in DCN fusiform cells, and we explored the role of Kv3.1 K+ current modulation on these oscillations. Patch clamp recording of dorsal cochlear nucleus fusiform cells were carried out on brain slices obtained from CBA mice (P14-P16). Spontaneous membrane voltage fluctuations were recorded at -65 mV, and deconstructed into major brainwave frequency components (delta: 3 Hz; theta: 6 Hz; alpha: 10 Hz; beta: 20 Hz; gamma: 40 Hz). Wavelet-filtered noise (from 4Hz to 40 Hz) was then injected back into the fusiform cell to test the effects on spike-timing. Wavelet-filtered noise decreased spike-timing precision in a frequency dependent manner (from 3 Hz 40 Hz). AUT1, a Kv3.1 K+ channel modulator, decreased the amplitude of membrane potential fluctuations oscillating from 10 to 40 Hz. When wavelet-filtered noise centred at those frequencies was injected in DCN fusiform cells, AUT1 was without further effect on spike-timing disrupted by the filtered noise. This suggests that AUT1 acts preferentially at a site distant from the recorded fusiform cell. In conclusion, our study shows that membrane voltage fluctuations (within the range of alpha to gamma oscillations) control spike timing in DCN fusiform cells. In addition, AUT1 decreases the amplitudes of membrane potential fluctuations at the frequencies most disruptive for spike timing.

(1) Olsen T. et al., Kv3 K+ currents maintains regular spike-timing of dorsal cochlear nucleus fusiform cells. Poster ARO meeting 2018

(2) Cohen M.X. Fluctuations in oscillation frequency control spike timing and coordinate neural networks. J Neurosci. (2014); 34(27): 8988-98.

(3) Ermentrout GB et al. Reliability, synchrony and noise. Trends Neurosci. (2008) 31(8):428-34.

PS 337

ZnT1-Dependent Zinc Inhibition of NMDA Receptors in the Dorsal Cochlear Nucleus

Rebecca Krall[1]; Aubin Moutal[2]; Rajesh Khanna[2]; Michal Hershfinkel[3]; Elias Aizenman[4]; Thanos Tzounopoulos[5]
[1]Departments of Neurobiology and Otolaryngology, University of Pittsburgh; [2]Departments of Pharmacology, Anesthesiology, and Graduate Interdisciplinary Program in Neuroscience, College of Medicine, University of Arizona; [3]Department of Physiology and Cell Biology, Ben-Gurion University of the Negev; [4]Department of Neurobiology, University of Pittsburgh; [5]Department of Otolaryngology, University of Pittsburgh, Department of Neurobiology, University of Pittsburgh, Pittsburgh, PA 15261

Synaptically released zinc modulates glutamatergic neurotransmission in many brain areas, including in the dorsal cochlear nucleus (DCN), an auditory brainstem nucleus, and the auditory cortex. Synaptic zinc is loaded into pre-synaptic vesicles by the transporter ZnT3 and released with activity. In the DCN, synaptic zinc inhibits NMDARs and AMPARs. Interestingly, ZnT3 knockout mice maintain part of the zinc-mediated inhibition of NMDARs indicating that other transporters, regulating extracellular zinc levels, may contribute to the zinc-mediated inhibition of NMDARs. Consistent with this hypothesis, it was recently shown that ZnT1 binds to the C-terminal domain of GluN2A-containing NMDARs. We hypothesized that through this association, ZnT1 regulates NMDAR inhibition by locally increasing zinc levels in the extracellular milieu surrounding NMDARs. To test this hypothesis, we developed a peptide that competitively interferes with ZnT1-GluN2A association. The peptide sequence was identified by using a far-Western screen to identify which sequence of the C-terminal domain of GluN2A has the highest affinity for ZnT1. We found that our interfering peptide, but not its scramble control, completely abolished zinc inhibition of NMDARs in rat cortical cultures (Kruskal-Wallis ANOVA, p = 0.0013). Furthermore, in slice preparations of the DCN, peptide treatment reduced zinc inhibition of NMDARs (Two-way ANOVA, p = 0.0002). These results indicate that ZnT1 localization critically contributes to zinc inhibition of NMDARs and consequent glutamatergic transmission and reveals a new ZnT1-dependent mechanism of synaptic zinc regulation.

PS 338

Plasticity of Synaptic Zinc Signaling in the Dorsal Cochlear Nucleus

Nathan W. Vogler[1]; Thanos Tzounopoulos[2]
[1]Department of Otolaryngology, University of Pittsburgh; [2]Department of Otolaryngology, University of Pittsburgh, Department of Neurobiology, University of Pittsburgh, Pittsburgh, PA 15261

In many excitatory synapses, mobile zinc is found within glutamatergic vesicles and is co-released with glutamate. Ex vivo studies established that synaptically released (synaptic) zinc inhibits excitatory neurotransmission at lower frequencies of synaptic activity, but enhances steady state synaptic responses during higher frequencies of activity (Mcallister & Dyck, 2017; Kalappa et al., 2017). Recent in vivo studies established that synaptic zinc modulates cortical auditory processing by enhancing the gain of sound-evoked responses in auditory cortical principal neurons and reducing the gain of cortical interneurons (Anderson et al., 2017). Zinc-mediated modulation of neurotransmission and presynaptic zinc levels are modulated by activity in many brain areas, such as somatosensory and visual cortex, the retina, and the dorsal cochlear nucleus (DCN), an auditory brainstem nucleus (Nakashima & Dyck, 2009; Li et al., 2017; Kalappa et al., 2015). However, the signaling mechanisms underlying this plasticity remain unknown. To study these mechanisms, we employed in vitro electrophysiological recordings in DCN brain slices. Application of the extracellular zinc chelator ZX1 (100μM) potentiates AMPAR and NMDAR EPSCs evoked by stimulation of parallel fibers, demonstrating AMPAR/NMDAR inhibition by synaptic zinc. High frequency stimulation (HFS, 3 x 100 Hz) of parallel fibers eliminates potentiation by ZX1, indicating activity-dependent plasticity of zinc-mediated inhibition (zinc plasticity). Zinc plasticity is blocked by the intracellular calcium buffer BAPTA (10mM), as well as the metabotropic glutamate receptor (mGluR) antagonist MCPG (500μM), and the Group 1-specific mGluR antagonists MPEP (4μM) and LY367385 (100μM). Furthermore, application of CPA (20μM), an inhibitor of SERCA ATPase which depletes calcium from intracellular stores, is sufficient to induce zinc plasticity. Application of the Group 1 mGluR agonist DHPG at a low concentration (5μM) also eliminates zinc-mediated inhibition; however, DHPG at a higher concentration (50μM) increases zinc-mediated inhibition. Our results demonstrate the activity-dependent plasticity of zinc-mediated inhibition at DCN parallel fiber synapses. Zinc plasticity involves activation of Group 1 mGluRs and release of calcium from intracellular stores. Furthermore, our results suggest a role for mGluR sig-

naling in the bidirectional modulation of zinc plasticity. Together, these results reveal a novel synaptic plasticity mechanism that modulates zinc-mediated inhibition of glutamatergic neurotransmission.

PS 339

Calretinin development in the chicken auditory brainstem: multiphase profile and cell-type specificity

Xiaoyu Wang[1]; Diego A. R. Zorio[2]; Yuan Wang[1]
[1]*Department of Biomedical Science, Program in Neuroscience, Florida State University College of Medicine;* [2]*Department of Biomedical Sciences, College of medicine, Florida State University*

Calretinin has an important role as a modulator of neuronal excitability at the basal level and during the induction of synaptic plasticity. In addition, calretinin functions in modifying the spatiotemporal aspects of calcium transients. In this study, we examine the developmental profile of calretinin in the chicken nucleus magnocellularis (NM) and nucleus laminaris (NL), the avian analogues of the mammalian anteroventral cochlear nucleus (AVCN) and medial superior olive (MSO). These auditory neurons are fast spiking and express high levels of calretinin in mature brains.

At embryonic day 9 (E9) when NM and NL can be identified as separate cell groups, calretinin immunoreactivity is not detectable in NM except at the rostral pole where cell bodies were lightly stained. Subsequently, the intensity of calretinin immunoreactivity increases gradually with age, starting in the rostromedial NM and progressing caudolaterally. By E19, NM neurons display strong calretinin immunostaining throughout the nucleus, except for a caudolateral region. A second phase of calretinin development takes place in this caudolateral NM. Starting from E19, the number of calretinin expressing neurons increases with age, instead of the level of calretinin per individual cells. At post-hatch day 14 (P14), this caudolateral NM can be divided into a calretinin-expressing and calretinin-negative subregions, corresponding to structurally and functionally distinct NMc1 and NMc2 identified in our previous studies.

NL displays a distinct development profile of calretinin as compared to NM. At E9, NL is characterized with strong somatic staining throughout the nucleus. Subsequently, the somatic staining decreases in intensity between E11 and E15 and increases again at E19. In contrast, neuropil staining is weak at E9 but becomes stronger at E11 and E15 and is maintained at high levels at E19 and P14. Double labeling studies further demonstrated that neuropil staining in NL are mostly axonal at E15 and both axonal and dendritic at E19.

Taken together, our findings demonstrate a tightly regulated developmental profile of calretinin in fast-spiking auditory neurons, in a way associated with the formation of functionally distinct subregions and the establishment of tonotopic axis.

PS 340
Lmx1a and b together define cochlear and cochlear nucleus projection and formation.

Victor Chizhikov; Igor Iskusynkh; **Bernd Fritzsch**
University of Iowa

Background
The central cochleotopic projection of the organ of Corti is the basis for tonotopic hearing. Lmx1a mutants are deaf. Their basal turn consist of a mix of vestibular and cochlear hair cells that blend into the saccule (Nichols et al., 2008). The aberrant basal turn has a tectorial membrane but lacks a spiral limbus and displays an unusual pattern of innervation by what seems to be spiral ganglion neurons. Whether theses basal turn innervating neurons project in a topological fashion exclusive to cochlear nuclei or also to vestibular nuclei has not been investigated. In the brainstem, Lmx1a and b are redundant and cooperate to regulate Atoh1 expression and thus cochlear nuclei formation (Mishima et al., 2009). If and how Lmx1a/b interact in ear development and affect neuronal projections to non-existing nuclei is unknown.

Methods
Mice with a missense mutation of Lmx1a (dreher) and null for Lmx1b were breed to homozygosity or various combinations of heterozygosity (Mishima et al., 2009). Mice were collected at various embryonic and neonatal stages, fixed in 4% PFA and their peripheral and central innervation was assessed using lipophilic dye tracing (Fritzsch et al., 2016). Brains and ears were mounted and imaged using Leica SP5 confocal microscopy.

Results
Lmx1a (dreher) mice have a clear segregation of basal turn and apex central projection that resembles that of control animals. However, the basal turn projection is to the vestibular nuclei immediately adjacent to cochlear nuclei in a pattern that is reminiscent of saccular projection. Moreover, the basal turn projection is restricted to what appears to be one rhombomere instead of expanding to all parts of the cochlear nucleus complex. Lmx1a/b double null mice have no organ of Corti in a sack like ventral expansion of a purely vestibular ear dominated

by a large saccule and posterior canal crista (Fig.1). A few basal spiral ganglion neurons seem to form (Fig.1). Lmx1a/b double null mutants have no cochlear nuclei and the remaining vestibular projection reach only r4 vestibular nuclei and show no rostro-caudal fibers to the medulla or the cerebellum

Conclusions

Lmx1a and b regulate Atoh1 expression and thus formation of an organ of Corti and cochlear nuclei. They also affect vestibular nuclei reducing the vestibular nucleus complex to a single rhombomere that receives input from a mostly saccular ear. Lmx1a mutants show cochleotopic projection that targets vestibular nuclei for basal turn fibers that innervate mostly vestibular hair cells.

Presentation1.pptx

PS 341

Mechanisms of changes in synaptic depression in response to different levels of activity at endbulbs of Held

Xiaowen Zhuang[1]; Wei Sun[2]; Matthew A. Xu-Friedman[3]
[1]*SUNY UNIVERSITY AT BUFFALO;* [2]*State University of New York at Buffalo;* [3]*University at Buffalo, Department of Biological Sciences*

Abnormal levels of auditory activity trigger an adaptation mechanism that changes the properties of endbulbs of Held, which are synapses formed by auditory nerve fibers onto bushy cells in the anteroventral cochlear nucleus. After exposure to an augmented acoustic environment, endbulbs of young mice reduce their synaptic depression, while after a week of ear occlusion, they show greater synaptic depression. It is important to understand the mechanisms underlying these changes, because abnormal auditory activity is associated with hearing problems including tinnitus and processing disorders. The most likely mechanism involves changes in presynaptic calcium, either changes in calcium influx, or in the efficacy of calcium driving neurotransmitter release. We tested these possibilities using voltage-clamp recordings of bushy cells in mouse brain slices. Bathapplication of the slow chelator EGTAAM blocked EPSCs more effectively in augmented endbulbs than in control endbulbs. This is consistent with decreased calcium influx or reduced coupling efficacy between calcium channels and the release apparatus, which could account for decreased synaptic depression. We also tested changes in coupling efficacy by quantifying the cooperativity following exposure to different sound environments and found no change. We are testing calcium influx using calcium imaging and preliminary results showed calcium influx increased after ear occlusion. Another question is whether activity adjusts endbulbs only during development. We found that mature endbulbs (>postnatal 50 days) showed activitydependent changes in synaptic depression similar to young endbulbs. This suggested there is no critical period for this phenomenon and endbulbs adjust their properties as auditory nerve activity changes throughout life. By understanding the mechanism of changes in synaptic depression, it may provide new ideas for treating disorders such as tinnitus and conductive hearing loss.

PS 342

Search for electrophysiological indices of Hidden Hearing Loss

Chandan Suresh; Ananthanarayan Krishnan
Purdue University

Recent studies in animals suggest that even moderate levels of noise exposure can damage synaptic ribbons between the inner hair cells and auditory nerve fibers without affecting audiometric thresholds, giving rise to the use of the term "hidden hearing loss" (HHL). Given the pervasive exposure to occupational and recreational noise in the general population, it is likely that individuals afflicted with HHL will go unidentified unless sensitive clinical measures are developed to diagnose this condition. To date, the studies employed to characterize HHL in humans have yielded confounding results. For example, Stamper & Johnson (2015) reported that the magnitude of wave I amplitude decrease is related to amount of noise exposure, and suggestive of fewer intact auditory nerve synapses; Liberman et al., (2016) reported enhanced summating potential to action potential ratio in individuals at risk for HHL; and Prendergast et al. (2017) found no differences in ABR or frequency following responses (FFR) in individuals with normal hearing and a wide range of noise exposure history. The objective of the project is to develop sensitive clinical electrophysiologic measures for early detection of HHL. We utilized specific stimulus manipulations that will likely produce a greater degradation of responses (recorded from different levels-inner ear, auditory nerve, and brainstem) in individuals at high risk for HHL compared to controls, due to loss of synapses and/or neurons. The specific stimulus manipulations include response measures across sound levels, two different adaptation paradigm (stimulus rate neural adaptation and adaptation recovery for click train paradigm), and changes in rate of frequency sweep. Consistent with previous studies, there were no differences between the low- and high-risk groups in audiometric thresholds or DPOAE amplitude. The high-risk group had significantly lower Wave I amplitude at high sound levels only; different pattern of amplitude recovery from adaptation; and greater disruption in encoding

of frequency change particularly at high rates. These results suggest that certain stimulus manipulations could potentially isolate individuals at risk for HHL.

Auditory Pathways: Midbrain II

PS 343

Noise Induced Hearing Loss Differentially Modulates Dimerized Dopamine Receptor Levels and NSF-1 Interaction in Auditory Related Brain Regions

Aaron K. Apawu[1]; *Angela Dixon*[2]; *Brittany Adams*[2]; *Bozena E. Fyk-Kolodziej*[2]; *Mirabela Hali*[2]; *Avril G. Holt*[3]
[1]*Wayne State University School of Medicine;* [2]*Wayne State University Medical School;* [3]*Wayne State University School of Medicine/ JD Dingell VAMC*

Noise induced hearing loss (NIHL) is linked to spatio-temporal changes in spontaneous neuronal activity (SNA) in auditory related pathways. While, the neurochemical basis for these changes remains unclear, studies from our lab and others suggest that dopaminergic signaling is affected by exposure to loud noise. Alterations in dopamine signaling occur within these very pathways following noise exposure (NE) during a time frame consistent with changes in SNA. To further our understanding of the role of dopamine (DA) signaling in hearing related pathways, two models of NIHL (temporary threshold shift -- TTS and permanent threshold shift -- PTS) were used to explore DA receptor (Drd) localization, dimerization, and trafficking.

Adult male Sprague Dawley rats (n=14) were divided into three groups: normal hearing (NH), TTS (16 kHz, 106 dB SPL, 1 hour), and PTS (10 kHz, 118 dB SPL, 1/3 octave band, 4 hours). Localization of Drds was examined in cryosections (40 μm) containing the inferior colliculus (IC), auditory cortex (AC), or the medial geniculate body (MGB). Protein isolated from these brain regions was used to compare levels of Drd1 and Drd2. (Western blotting 7 μg protein/lane) or Drd interactions with the trafficking protein NSF-1 (co-immunoprecipitation).

In the IC from the NH group, Drd1 labeling was primarily somatic, while Drd2 labeling was both somatic and dendritic. Somatic labeling for Drd1 increased in the PTS group compared to the NH group, while somatic but not dendritic labeling for Drd2, decreased. In the IC, AC, and MGB, Drd1 and Drd2 each exist as both monomers (~ 50 kDa) and dimers (~100 kDa). In the PTS group, dimerized Drd2 was significantly decreased in the AC, but not in the IC. In the MGB, while diminished Drd1 dimerization was observed only in the PTS group, dimerized levels of Drd2 diminished in both TTS and PTS groups. At a time when hearing thresholds had returned to normal in the TTS group (one week after NE), both the IC and AC showed calcium dependent Drd-NSF-1 complexes. Specifically, Drd1-NSF-1 increased in the IC, while both Drd1-NSF-1 and Drd2-NSF-1 increased in the AC.

Dopamine receptors exhibit differential spatio-temporal localization, dimerization, and trafficking following NIHL, suggesting modulation of inhibitory tone and SNA. Future work will explore Drd complex composition and post-translational modification. These results have implications for understanding mechanistic underpinnings, determining future risk, and ultimately providing treatment for conditions associated with exposure to loud noise such hearing loss and tinnitus.

PS 344

Frequency-specific effects of noise-induced hidden hearing loss on coding of speech sounds in gerbil midbrain neurons

Jessica M. Monaghan[1]; Jose Garcia-Lazaro[2]; Roland Schaette[2]; David McAlpine[1]
[1]*Macquarie University;* [2]*UCL Ear Institute*

It is increasingly recognized that individuals whose hearing thresholds are normal can also show unexpected difficulty understanding speech in noise. Recent evidence suggests that some of these difficulties arise from exposure to loud sounds that lead to permanent and selective damage to high-threshold auditory-nerve fibres (ANFs), damage that precedes the more commonly considered form of sensorineural deafness associated with damage to the sensory hair cells. The selective loss of high-threshold ANFs leads to 'hidden hearing loss (HHL)';—hidden because it is undetected by conventional tests such as audiometry. Here, we test whether noise exposure that generates HHL impacts more neural coding of sounds in the frequency range most at risk; i.e. within and above the band of damaging noise.

We used multi-electrode arrays to record neural responses from the inferior colliculus (IC) of gerbils one month after exposure to 2 hours of 105 dB SPL, band-pass (2-4 kHz) noise. Responses were recorded to vowel-consonant-vowel combinations (VCVs; e.g. AMA, ASA etc.) presented at moderate (60 dB SPL) and high (75 dB SPL) sound levels in quiet, and in 5 different levels of background noise, generating signal-to-noise ratios (SNRs) of +12, +6, 0, -6, and -12 dB for each level. VCV discrimination performance was measured using a template-matching procedure in which neurograms (summed responses of many neurons recorded across the tonotopic axis of the IC) to VCVs in background noise were compared to those generated by speech in quiet.

Discrimination performance was lower at the same SNR for the high, compared to the moderate, sound level, and fell with decreasing SNR. The effect of HHL was most evident at the higher sound level, with VCV discrimination at 75 dB SPL significantly lower in exposed compared to control animals. For consonant discrimination, protection was afforded by distance from the noise band. The VCVs ANA and AMA—nasal consonants with energy at frequencies well below the 2-4 kHz band of damaging noise—were relatively immune to noise exposure, whilst AFA and especially ASA—with energy at frequencies above the noise band—were most affected. For vowel discrimination (UTU vs. ATA, vs. ITI), ITI—with the second formant of its 'I'; sound lying within the band of damaging noise—was significantly less well discriminated than UTU and ATA; the second formants of the vowel sound in these VCVs reside well below the frequency of the damaging noise. Our data suggest that discrimination of speech sounds in HHL is influenced by the location of spectral energy relative to the frequency of the noise exposure, is potentially subject to the half-octave shift in maximum damage observed for noise damage that targets hair cells, and affects both consonant- and vowel-discrimination performance.

PS 345

Evaluating Hidden Hearing Loss in the Military: Objective and Physiologic Responses of Blast and Non-Blast Exposed Service Members

Kimberly Jenkins[1]; Sandeep Phatak[1]; Scott Bressler[2]; Barbara Shinn-Cunningham[2]; Kenneth Grant[1]
[1]*Walter Reed National Military Medical Center;* [2]*Boston University*

VA centers and military treatment facilities across the country are noting an increase in the number of service members (SMs) seeking care for perceived hearing difficulties, particularly in the presence of noise. However, diagnostic test batteries indicate that many of these individuals present with clinically normal or near-normal hearing and are not typical candidates for treatment methods such as hearing aids. Concerns regarding the prevalence of this phenomenon within the military population gave rise to a multi-site investigation of hearing difficulties in a non-clinical population of more than 3,500 active duty military personnel. SMs found to have normal to near-normal hearing thresholds were given a hearing screening battery that consisted of surveys (history of blast exposure, & Speech, Spatial, and Qualities of Hearing), a speech-in-noise test that contained speeded speech and speech in reverberation, and the Binaural Masking Level Difference test. It was found that 31% of listeners exposed to one or more blasts had abnormally low performance on binaural and speech tests. Moreover, experiencing blasts close enough to feel the heat

or pressure wave increased the prevalence of hearing deficits by a factor of 2.5 compared to a non-blast group. This study clearly indicates that blast exposure results in auditory dysfunction that may go undetected by traditional diagnostic hearing tests.

To better understand the effects of blast on hearing and communication, the current study compared differences between service members who have been exposed to blasts and those who have not on a test battery that included subjective surveys, hearing tests, and cognitive measures. This discussion will focus on comparisons of the objective, physiologic measures of both groups. The two groups underwent measures of distortion product otoacoustic emissions (DPOAEs), click-evoked auditory brainstem responses (ABRs), frequency following responses (FFRs) to speech and tonal stimuli, and EEG cortical potentials in response to a selected melody attention task. It was found that DPOAEs, ABR and FFR amplitudes were less robust for the blast-exposed group than the nonblast-exposed group. EEG responses to the selected attention task showed no differences between the two groups, consistent with other cognitive tests of attention. This leads us to believe that blast exposure preferentially affects primarily cochlear, auditory brainstem, and certain aspects of binaural processing as opposed to the central auditory system. This information will help improve the diagnostic test battery and guide more effective treatment options for those experiencing functional hearing deficits.

PS 346

Auditory and cognitive processes in children with word reading difficulty.

Rakshita Gokula[1]; Mridula Sharma[2]; Linda Cupples[1]; Joaquin T. Valderrama Valenzuela[3]
[1]*Macquarie University;* [2]*Macquarie University/HEARing CRC;* [3]*Macquarie University & National Acoustic Laboratories*

Previous literature has reported auditory processing deficits in children with word reading problems. Research using behavioral tasks have revealed deficits of speech perception in noise, frequency discrimination, attention, and working memory in children with reading disorders (Moore, Ferguson, Halliday, & Riley, 2008; Sharma, Purdy, & Kelly, 2009; Halliday & Bishop, 2006). Similarly, using electrophysiological tasks such as MMN, CAEPs, ASSR have also shown differences in children with reading disorders (Gilley, Sharma, & Purdy, 2016; Sharma, Purdy, Newall, Wheldall, & Beaman, 2007). In the current study, we looked at the behavioral and electrophysiological responses of children on several auditory processing skills. The cognitive skills of the children such as selective attention, working memory, and statistical

learning were also assessed. This presentation aims to report the differences across auditory skills such as pitch percept, amplitude modulation percept, among other auditory processing skills in the children with specific word and nonwords reading deficits. Data was collected from 27 children in the control group and 28 children with word reading difficulties. The children in the two groups were not significantly different in age, [f (1.53, 53) = 0.60, p = 0.44]. Children in the experimental group were significantly different from the controls in their performance on frequency discrimination. perception of sinusoidal amplitude modulation at 4Hz, and for percept of pitch tested electrophysiologically. Attention was significantly different between the groups: sustained attention [f (1, 53) = 10.15, p = 0.002], and attention switching [f (1, 53) = 36.34, p = 0.000]. With statistical learning, children with reading problems showed to have difficulties with learning of auditory stimuli (Mann-Whitney U = 86, Z = -2.775, p = <0.000), and visual stimuli (Mann-Whitney U = 85.5, Z = -3.504, p<0.000). Thus, the conclusion of the study is that children with word reading disorders should be assessed across both auditory and cognitive measures. The implications of these findings are that when planning the intervention for children with reading disorders, management must include specific auditory training for better outcomes.

PS 347

Localizing the Source of Context-Dependent Serotonin Release in the Inferior Colliculus of the Mouse

Alexander Koo[1]; Christopher Petersen[2]; Laura M. Hurley[2]
[1]Vassar College; [2]Indiana University

The neuromodulator serotonin (5-HT) is released in a context-dependent manner within the inferior colliculus (IC), in the auditory midbrain. While the majority of 5-HT in the IC comes from the dorsal raphe nucleus (DRN), it remains unknown whether functionally and anatomically discrete DRN sub-regions differentially innervate IC. The goal of this study was to localize the source of serotonergic projections to IC within the DRN. We performed stereotaxic surgeries in order to inject fluorescent Retrobeads into the IC of male CBA/J mice (Mus musculus). Five days post-surgery, mice were placed into either isolated, social (with a novel female), or restraint stress conditions, sacrificed, and their brains were processed for multi-fluorescence immunohistochemistry. Brains were labeled for tryptophan hydroxylase (TPH; the rate limiting enzyme in 5-HT prodution) as well as Fos, a marker for neural activation. Neurons immunoreactive (-ir) for TPH and Fos, as well as backfilled neurons (i.e., retrobead-positive; RB+) were visualized via confocal microscopy throughout the extent of DRN. Neurons that were TPH-ir/RB+ were localized primarily within the dorsolateral and dorsal subregions of the DRN. There were relatively few TPH-ir/RB+ neurons within the rostral, caudal, and dorsoventral DRN subregions. Our results suggest that the dorsal and lateral subregions of DRN may play a role in context-dependent release of 5-HT in IC. To test this hypothesis, we will quantify Fos-ir neurons within TPH-ir/RB+ neurons in DRN. We hypothesize that triple-labeled neurons (TPH-ir, Fos-ir, RB+) will be differentially distributed within DRN subregions between mice within the social and stress conditions. This finding would suggest that different DRN subgroups are responsible for serotonergic activity in the IC in divergent contexts.

PS 348

Optogenetic Induction of Endogenous Dopamine Release Alters Auditory Responses in the Inferior Colliculus

Jeffrey Hoyt[1]; Anthony Ziegenfuss[1]; David Perkel[2]; Christine Portfors[1]
[1]Washington State University Vancouver; [2]university of Washington

Background

The ability to understand speech relies on accurate auditory processing of communication sounds by the auditory system. Individuals with Parkinson';s disease suffer from speech perception deficits, suggesting that dopamine is involved in the encoding of complex sounds. The inferior colliculus (IC) is rich in both dopaminergic fibers and D2-like receptors, and recent studies from our lab demonstrated that application of exogenous dopamine has heterogeneous effects on the responses of many IC neurons in mice, although the strongest effect is to suppress neural activity. It is currently unknown, however, whether the observed effects reflect the effect of the endogenous dopamine system in the IC. In this study, we tested the effect of optogenetically induced dopamine release on auditory responses of individual IC neurons.

Methods

We crossed a Cre-dependent channelrhodopsin (ChR2) mouse with a dopamine transporter (DAT):Cre mouse to produce a DAT/ChR2 mouse line. Offspring were genotyped as Cre+/- or Cre-/- prior to weaning. We recorded extracellular responses of single IC neurons in adult mice that were awake and restrained. We compared the rate, timing, and fidelity of responses to tones and mouse vocalizations before and after stimulation with blue light pulses (75 ms, 6 Hz, 2 per repetition) through an optrode to evoke local dopamine release.

Results

Similar to the effects of exogenous dopamine application, blue light decreased spike rate evoked by tones while increasing spike latency in the majority (75%) of cells in mice expressing ChR2. In the same mice, blue light additionally decreased the frequency tuning areas of auditory neurons while increasing selectivity to mouse vocalizations. Blue light produced no effects on neuronal responses in wild type littermates.

Conclusion

We found that activation of the endogenous dopamine system in the IC suppresses responses of auditory neurons. Understanding how dopamine modulates auditory processing will ultimately inform therapies targeting mechanisms underlying auditory and communication disorders.

Funding

PS 349

Dopaminergic Modulation of Stimulus-Specific Adaptation in the Inferior Colliculus of the Rat

Catalina Valdés-Baizabal[1]; Manuel S. Malmierca[2]
[1]Auditory Neuroscience Laboratory. Institute of Neuroscience of Castilla y León (INCyL). Salamanca. Spain; [2]Auditory Neuroscience Laboratory. Institute of Neuroscience of Castilla y León (InCyL). Salamanca. Spain

Some neurons in the inferior colliculus (IC) display stimulus-specific adaptation (SSA) which is a rapid and pronounced decrement of neural responsiveness to trains of identical stimuli that recovers when a stimulus parameter is changed. This property has been considered the neuronal correlate of early indices of deviance detection. Since the IC receives dopaminergic inputs from the subparafascicular thalamic nucleus and IC neurons express D2-like dopamine receptors, the aim of this study was to address what role, if any dopamine plays in the modulation of SSA.

We recorded in vivo extracellular single unit responses in the IC of anesthetized young adult Long Evans rats. Neurons were recorded before, during and after the microiontophoretic application of 10 mM eticlopride (D2-like receptor antagonist) under the stimulation with an oddball paradigm, where two pure tones are presented with different probability of occurrence (90%, standard) and (10%, deviant). SSA was quantified by measuring the adaptation CSI index (CSI=[d(f2)+d(f2)-s(f1)-s(f2)]/[d(f2)+d(f2)+s(f1)+s(f2)]).

So far, we have recorded 37 single units from the IC under the oddball paradigm. Up to 65% of neurons recorded (24/37) showed a significant change in their firing rate with the eticlopride application. Eticlopride had heterogeneous effects on the CSI of IC neurons. A majority of neurons (15/24, 63%) neurons showed an increase of the CSI, changing from 0.23±0.08 to 0.38±0.09 (P < 0.001). This CSI change was due to a combination of effects with an increase of the firing rate of up to 16% in the response to deviant stimuli (P = 0.041) and to a decrease in response to standard stimuli by a 24%, (P = 0.013). By contrast, for the remaining 37% (9/24) of the neurons, the CSI decreased from 0.39±0.09 to 0.26±0.09 (P < 0.001). The decrease in their CSI (n = 9) was due to an increase in the response to both deviant and standard stimuli although these changes were not statistically significant. Furthermore, there were neither changes in the spontaneous firing rate nor in first spike latency. Interestingly, our preliminary data analysis suggest that eticlopride modulates neurons with low- and high CSI levels preferentially.

We conclude that the dopaminergic system plays a complex and active neuromodularory role on SSA in IC neurons.

PS 350

Activation of the gerbil's auditory pathway studied with 18F-FDG PET - effects of anesthesia

Mariella Kessler[1]; Martin Mamach[1]; Rainer Beutelmann[2]; Jens P. Bankstahl[3]; Tobias L. Ross[3]; Frank M. Bengel[3]; Georg M. Klump[4]; Georg Berding[1]
[1]Cluster of Excellence Hearing4all and Medical School Hannover; [2]Cluster of Excellence Hearing4all and Carl-von-Ossietzky University Oldenburg; [3]Medical School Hannover; [4]University of Oldenburg

Introduction

In this study, results of ^{18}F-fluorodeoxyglucose (^{18}F-FDG) positron emission tomography (PET) in the Mongolian gerbil are presented. As in most neurophysiological studies of auditory processing, anesthesia has to be applied in preclinical PET imaging. However, anesthesia may have diverse effects on measurements of auditory activation in PET and electrophysiology. Therefore, we examined the suitability of anesthetics frequently used in electrophysiology for auditory activation studies with FDG PET.

Methods

Neuronal activity in the brain was measured performing ^{18}F-FDGPET in 3 conditions: (i) awake state, (ii) ketamine/xylazine (KX) and (iii) fentanyl/midazolam/medetomidine (FMM) anesthesia. Two different acoustic free-field conditions were applied in a sound-shielded box: 30dB laboratory background noise (BG) and 90dB frequency modulated sounds (FM). For each scan, 18.2±2.1 MBq of ^{18}F-FDG were injected intraperitoneally, followed by 40 min uptake phase in the box. Thereafter, 30 min acquisition was performed using an Inveon PET/CT system (Siemens). Blood glucose levels were measured after the uptake phase before scanning. Standardized uptake values (SUVs) were normalized to mean pons activity. Anatomical locations were assigned after implementing a volume of interest (VOI) template based on high-resolution images of a stereotaxic brain atlas of the Mongolian gerbil (Radtke-Schuller et al. 2016, Brain Structure and Function 221, Suppl.: 1-272). Data were analyzed using PMOD v3.7. Mean SUVs were extracted using VOIs and additional voxel-wise analysis was carried out using SPM8 software.

Results

Comparing FM to BG stimulation revealed significantly higher activation (16%, p=0.0003) in the inferior colliculus (IC) during awake state. Likewise, a significant higher activation in IC was observed under FMM anesthesia (15%, p=0.0012). In contrast, no difference was observed with KX anesthesia. These results are also reflected in SPM analyses. Significant differences at the voxel level between FM and BG stimulation were detected in the ICs for the awake state (65% of IC voxels significantly more activated; p

Conclusions

In electrophysiological studies of auditory processing in gerbils successfully used KX and FMM (opioid-based) anesthesia. However, our present results suggest that only opioid-based anesthesia is suitable for ^{18}F-FDG PET measurements while KX fails to provide significant activation signals – possibly due to increased levels of "cold" glucose in the blood interfering with FDG uptake.

PS 351

Modulation of neural activity during locomotion in the mouse auditory midbrain

Yunseon Yang; Gunsoo Kim
CNIR-IBS

Behavioral states can powerfully impact sensory processing. This is highlighted by the recent evidence in the mouse visual and auditory cortex that locomotion modulates sensory responses. Neural activity in the visual and auditory thalamus is also modulated during locomotion, indicating subcortical auditory pathways are also impacted by behavioral states. However, the extent and nature of the subcortical modulation and its relationships with cortical modulation remain unclear. To address this question, we investigated neural activity of the inferior colliculus (IC) the major midbrain auditory integration center in awake mice.

We recorded spontaneous and sound-evoked neural activity of IC neurons in head-fixed mice (C57BL/6), free to run on a circular treadmill. Sound-evoked neural responses were obtained by presenting 5 different pure tones (4, 8, 16, 32, 64 kHz; 100 msec duration) at 70 dB sound pressure level. A unit';s response strength (RS) was defined as the average firing rate during the first 25 msec of tone presentation minus the baseline firing rate.

When mice were stationary, mean spontaneous firing rates of IC single units ranged 0.1 to 79 Hz with the median rate of 16 Hz. We found that in 43 of 56 units, spontaneous firing rate differed significantly during locomotion. The modulation of spontaneous activity was bidirectional in that the rate increased from 18±3 Hz to 34±4 Hz in 32 units during locomotion, while the rate decreased from 35±9 Hz to 28±9 Hz in 11 units.

To determine whether sound-evoked activity of the IC neurons is also modulated during locomotion, we compared RS, which measures the tone-evoked firing rate relative to the spontaneous rate, between the stationary and walking periods. Of the 42 units that showed excitatory response to tones, 32 units showed significant modulation in RS. In most units, the overall RS (RS summed over the tones that evoked response) decreased during locomotion on average from 182±41 Hz to 131±38 Hz (n=29). In 3 units, the RS increased from 13±10 Hz to 75±23 Hz (n=3). The suppression in RS often decreased spectral bandwidth such that fewer frequencies evoked response during locomotion (2.6±0.3 vs 1.7±0.3 frequencies; n=29).

By recording the neural activity of IC neurons in awake behaving mice, our results demonstrate that both spontaneous and sound-evoked activity of midbrain auditory neurons can be modulated during locomotion. Our results suggest that auditory midbrain neurons are informed of behavioral states, which may facilitate acoustically guided behavior.

PS 352

Recording ECochG via the Advanced Bionics Cochlear Implant System

Andreas Büchner[1]; Michael Bardt[2]; Sabine Haumann[1]; **Thomas Lenarz**[3]
[1]Department of Otolaryngology, Hannover Medical School, Germany; Cluster of Excellence; [2]Medical University Hannover; [3]Department of Otolaryngology, Hannover Medical School, Germany and DFG Cluster of Excellence Hearing4all

The process of inserting a cochlear implant (CI) electrode array leaves the surgeon quite blind as to what is happening inside the cochlea. Real time feedback can be obtained by recording ElectroCochleography (ECochG) elicited by acoustic stimulation while the electrode array is being inserted. Such feedback allows the surgeon to make adjustments to the insertion and may lead to improvements in surgical technique and reduced trauma to the cochlea

In this study, ECochG was recorded via the CI system using an intra-cochlear electrode contact. Recordings were made for 24 adult subjects during and following implantation of the Advanced Bionics HiRes90K implant. All subjects had at least one pre-operative threshold of better than 80 dBHL. During insertion of the electrode array, recordings were made for 50 ms acoustic tone burst stimulus. Following insertion, recordings were made, where possible, for 125, 250 and 500 Hz tone bursts. Typically 20 averages were used for each individual measurement. Subtraction of recordings, time-locked to phase reversed acoustic tone-burst stimuli, allowed extraction of the cochlear microphonic (CM) signal. Comparisons were made between an extrapolated CM threshold and behaviourally measured hearing thresholds. Analysis was also made of CM amplitude during insertion of the electrode array and correlated with the surgical report.

It was possible to record ECochG in all cases for at least one stimulus frequency. The average electrode insertion took approximately 25 seconds, with ECochG updated rapidly enough to give useful real-time surgical feedback. A significant correlation was found between ECochG and behavioural estimates of low-frequency hearing threshold. Changes in CM amplitude during electrode array insertion were very largely in line with surgical feedback and surgical video review. Correlations between ECochG and post-implant speech perception are currently being accumulated.

It appears practical to record ECochG both intra- and post-operatively using the standard Advanced Bionics CI system hardware. Recording speed is sufficient to give surgical feedback that allows the surgeon to make changes during electrode array insertion. A correlation exists between CM predicted and behavioural estimates of low-frequency hearing thresholds. Future ECochG research should focus on improving hearing preservation surgery and the programming of electro-acoustic stimulation.

PS 353

Individualized cochlea implantation using a predictive model

Thomas Lenarz[1]; Rolf Salcher[2]; Max Eike Timm[3]; Tobias Weller[4]; Andreas Büchner[5]
[1]Department of Otolaryngology, Hannover Medical School, Germany and DFG Cluster of Excellence Hearing4all; [2]Department of Otolaryngology, Hannover Medical School, Germany; [3]Department of Otolaryngology, Hannover Medical School; [4]Medizinische Hochschule Hannover; [5]Department of Otolaryngology, Hannover Medical School, Germany; Cluster of Excellence

Background
Individual Cochlear Implantation - meaning an individual selection of electrode insertion depth and stimulation modality (electric-acoustic stimulation (EAS) or electric stimulation (ES)) - aims for the best possible hearing outcome for every patient. Important factors to take into account for achieving optimal outcomes are hearing preservation - using adequate atraumatic electrode arrays - and optimal cochlear coverage for the electric stimulation up to the region of functional postoperative residual hearing.

Methods
More than n=500 Patients with different degrees of residual hearing were treated with atraumatic electrode arrays of different lengths ranging from short (16 mm) to long (28 mm). In addition, the concept of partial insertion was developed: atraumatic electrodes of 24 mm and 28 mm lengths are partially inserted to allow for future adaptation of electrical cochlear coverage to the progression of hearing loss. A previous study has shown that a reduced number of contacts is sufficient for providing the same speech perception results as a larger number of electrode contacts in patients with high frequency deafness.

Major parameters are investigated including cochlear anatomy with length and shape, residual hearing and patient history of hearing loss in order to develop a predictive model.

Results

At first activation the median hearing loss after cochlear implantation ranges from 12.0 dB for a 16 mm electrode (n=12) to 24.0 dB for a 28 mm electrode (n=40) showing that hearing preservation depends on electrode length and insertion depths. Hence, short electrodes would be preferable. However, if no function residual hearing can be used for EAS, patients with longer electrodes (28 mm) (n=31) and higher cochlear coverage (avg. 75%) achieve significantly better hearing results in noise with 42% (HSM 10 dB SNR) compared to patients with shorter electrodes (20 mm) (n=20) with 15% in ES. Partial insertion with the choice of a patient specific insertion depth and the option for its adaption could overcome this trade-off. With partial insertion excellent hearing preservation and speech outcomes in EAS are achieved. Based on the cochlear geometry and the preoperatively predicted degree and slope of postoperative hearing loss, the individual insertion depth according to Greenwood can be calculated for every patient.

Conclusion

The prediction model supports the surgeon with the individual selection of an optimal electrode insertion depth to achieve best individual outcomes in EAS or ES. Partial insertion allows for further, patient specific adaptation of the insertion depth if hearing is progressive over time.

PS 354

Evaluation of an Implantable Robotic-Assisted System for Cochlear Implant Insertion Control

Allan Henslee[1]; Christopher R. Kaufmann[2]; Marlan R. Hansen[3]
[1]iotaMotion, Inc.; [2]Department of Otolaryngology - Head & Neck Surgery, University of Iowa Hospitals and Clinics; [3]Department of Otolaryngology - Head & Neck Surgery, University of Iowa Hospitals and Clinics, Iowa City, IA

Background

Hearing preservation surgical techniques and cochlear implants (CIs) provide significant benefits to patients with residual hearing. However, additional functional acoustic hearing loss following surgery has been reported in some patients. Intracochlear trauma during electrode insertion is considered one possible contributing factor for this post-surgical hearing loss. We have developed an implantable robotic-assisted CI insertion system which aims to reduce electrode insertion trauma and enable post-surgical, remote electrode position adjustments. In this study, we evaluated the surgical feasibility of our system in a cadaveric model and characterized the electrode insertion forces in both synthetic and cadaveric cochleae.

Methods

Our implantable insertion system was utilized to perform insertions of standard electrodes (Slim Straight, Cochlear) into both 3D-printed synthetic and cadaveric cochleae at multiple insertions speed (0.1, 0.5, and 1 mm/sec). Insertions (n=3) were characterized with respect to the maximum insertion force (mN) and force variation (mN/sec) using a single axis force transducer and compared to manual insertions by-hand at corresponding insertion speeds. For proof of concept surgical evaluation, the insertion control unit was implanted in a human cadaver using a standard mastoidectomy with facial recess approach to assess both robotic-assisted system electrode insertion and remote advancement functionality. X-ray fluoroscopy and microCT imaging was used to assess the intracochlear electrode position.

Results

At an insertion velocity of 0.5 mm/sec into synthetic cochleae, results showed the system significantly reduced the average maximum insertion force from 169.4±66.2 to 41.9±3.9 mN and the force variation from 925.4±322.4 to 282.8±28.7 mN/sec, when compared to manual insertions respectively (Figure 1). Similarly, insertions into cadaveric cochleae resulted in a significantly reduced maximum insertion force from 139.3±57.0 to 83.5±12.2 mN and a reduced force variation from 561.1±270.6 to 181.1±31.0 mN/sec. The system was successfully implanted utilizing standard approaches with CI electrodes inserted and wirelessly advanced into the human cadaveric cochlea. MicroCT confirmed correct intrascala position and insertion.

Conclusions

The implantable robotic-assisted insertion system reduces maximum insertion forces and force variations compared to manual electrode insertions. Cadaveric evaluations support the surgical feasibility of the implantable system and compatibility with standard surgical approaches. Our system has the potential to improve hearing preservation CI surgery by both facilitating atraumatic electrode insertion and wirelessly optimizing intracochlear electrode position. Support

Figure_1_Henslee.pdf

PS 355

Electrode insertion force measurements in sheep temporal bones

Rolf Salcher[1]; Martina Nullmeier[2]; Thomas Lenarz[3]; Nick Pawsey[4]; Bernd Waldmann[2]; Omid Majdani[1]; Thomas Rau[1]

[1]*Department of Otolaryngology, Hannover Medical School, Germany; [2]Cochlear Deutschland GmbH & Co. KG; [3]Department of Otolaryngology, Hannover Medical School, Germany and DFG Cluster of Excellence Hearing4all; [4]Cochlear Limited*

Measuring insertion forces in a cochlea bench model is a standard procedure for estimating trauma of cochlear implant electrode arrays. These measurements are done either in bench models made of various materials, like PTFE, glass, acrylic, epoxy, etc. in combination with various lubricants, or in (fresh frozen) temporal bones.

In this study fresh never frozen sheep temporal bones were used. The sheep cochlea is similarly proportioned to the human, provides straightforward surgical access and is readily available. Based on DVT scans of the sheep temporal bones the insertion depth equivalent to a hearing preserving implantation in humans was determined. The temporal bone specimens were cut down and mounted on a single axis load cell for the insertion force measurements. A dummy electrode based on the Cochlear Slim Straight electrode was inserted in the sheep cochlea to a depth of approximately 15 mm or one turn. The measurements could be repeated in each bone.

We established the procedure to measure insertion forces in fresh sheep temporal bones in our lab. In the future we plan to use this data, together with insertion forces measured in a bench cochlea model matching the dimensions of the sheep cochlea obtained from DVT imaging, to verify the frictional properties of the material-lubricant combination of our bench model.

PS 356

Feasibility of a Simple, Safe, and High-Precision Approach to Minimally Invasive Cochlear Implantation

Samuel John[1]; Marcel Kluge[2]; Peter Erfurt[1]; Samuel Müller[3]; Jakob Lexow[1]; Lüder Kahrs[4]; Thomas Rau[1]; Tobias Ortmaier[3]; Omid Majdani[1]; Thomas Lenarz[5]

[1]*Department of Otolaryngology, Hannover Medical School, Germany; [2]HörSys GmbH; [3]Leibniz University Hannover; imes; [4]Leibniz Universtity Hannover; imes; [5]Department of Otolaryngology, Hannover Medical School, Germany and DFG Cluster of Excellence Hearing4all*

Introduction

Minimally invasive cochlear implantation, if available on the market, would certainly revolutionize the field. The de-facto standard treatment to severe to profound sensorineural hearing loss is a cochlea implant and the standard surgical procedure is a mastoidectomy with facial recess approach (MFRA) where the mastoid bone is successively removed and a passage through the facial recess is carefully identified by removing a larger volume. The benefit of this delicate procedure is that a straight insertion path, tangential to the basal turn of the cochlea is possible. Several groups are pursuing different concepts to reach this goal. Among those are impressively engineered custom-made navigated robotic setups as well as much simpler mini-stereotatic frames.

Methods

Our group is developing a high-precision mini-stereotatic solution (RoboJig™) that is also practical and it will be very cost effective. It is based on the concept of patient individual drilling jigs that will be customized to the planned drill path right in the OR. The jig is mounted on the bone anchored frame without any movable mechanic parts. In two recent full cadaver head experiments under realistic operating theater environment conditions, we evaluated the surgical handling and (in the second experiment) the overall system precision. Here, we share the preliminary results of an ongoing evaluation of the current system. Earlier temporal-bone evaluations with an older generation of our system showed a somewhat sufficient precision of around 0.5 mm. The new generation went through a complete system optimization and calibration.

Results

While we discovered areas where we have to make the system even more "surgeon safe" as we call it, the currently reached overall system precision (including image registration, marker detection, jig production, and drilling into the skull) was better than our post-operative DVT analysis could tell. Therefore, we estimate that the reached precision was better than or equal to 0.15 mm (half the DVT resolution).

Conclusion

While there has been a scientific competition to reach sufficiently low precision, other factors that make a system usable have perhaps gotten out of sight. Making minimally invasive implantation a reality requires not only the precision that other groups before and we have have shown now, but equally important, a successful medical product has to be simple, practical and be operated by available clinic staff around the world. This is a multi-objective optimization; only one – but a necessary condition – is the a sufficient precision.
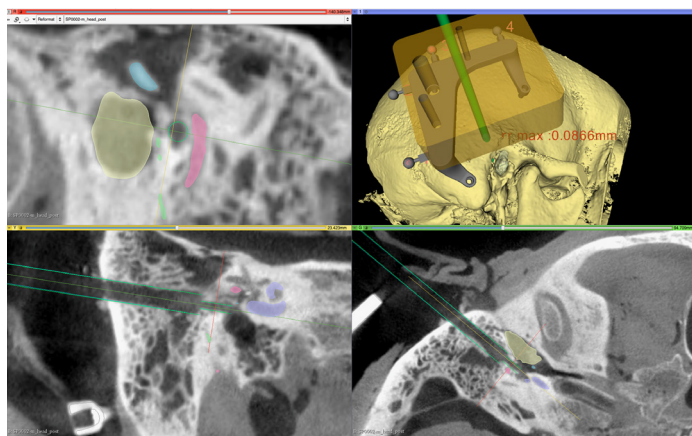
PS 357

Stem Cell Therapy Improves Cochlear Implant Performance on Animal Model

Wei Chen[1]; Weiwei Guo[2]; Liangwei Xu[1]; Lidong Zhao[1]; Tao Cong[1]; Wei Sun[3]; **Shiming Yang**[2]
[1]*Chinese PLA General Hospital;* [2]*Chinese PLA Medical School;* [3]*State University of New York at Buffalo*

Background

Stem cell therapy for regenerating or improving the function of spiral ganglion neurons (SGNs) has been explored to boost the performance of cochlear implants (CIs). However, as the SGNs are surrounded by a solid bone structure in the Rosenthal';s canal of the cochlea, stem cells transplanted into SGNs are limited. In addition, the trauma caused by conventional transplantation methods limits its clinical implication. Recently, several studies found that physiological electric fields can guide the migration of stem cells.

Methods

In the study, hiPS cells with a green fluorescent protein (GFP) reporter were surgically injected into the scala tympani (ST) through the round window of Rongchang pigs, a large animal model of genetic deafness featuring a MITF mutation. An electrode array was then inserted into the cochlea. A bipolar pulsed electric field (BPEF) was produced by the CI electrode array inside the cochlea at 3 hours, 3 and 7 days after CI surgery.

Results

The BPEF can provide guidance for transplanted hiPS cells and enhance their penetration into Rosenthal';s canal, and then the regeneration of SGNs induced a connection between the CI and the newly developed auditory nerve and improved the efficacy of the CI. Animals injected with hiPS cells without CI insertion and those injected with hiPS cells with CI insertion, but no BPEF stimulation, were used as control groups. No hiPS cell survival or SG neurite regeneration was found in Rosenthal';s canal in these control groups. However, 14 days after BPEF-mediated hiPS treatment, a high density of surviving hiPS cells and regenerated SG neurites were found in Rosenthal';s canal in the experimental group. The eABR threshold elicited from the cochlear implant was also significantly lower in the experimental group than in the control groups.

Conclusions

Our results provide the first evidence that electrical stimuli can guide hiPS cell migration and improve the function of cochlear implants. Therefore, BPEF could be used as a potential stem cell delivery tool, and CI-combined stem cell therapy may become a new therapeutic strategy for deafness.

PS 358

Long Term Implantation of Cochlear Implant Electrodes in Guinea Pigs

Erik Pierstorff[1]; Josef Miller[2]; Susan DeRemer[2]; Christopher Ellinger[2]; Diane Prieskorn[2]; William Slattery[1]
[1]*O--Ray Pharma;* [2]*University of Michigan*

Cochlear implants have restored hearing in thousands of patients over the past two decades. Because of the increasing benefits, reflecting new technologies and rehabilitation procedures, implantation has been offered to a larger population of hearing impaired, including those with significant residual hearing; and a positive relationship is being reported between extent of residual hearing and implant hearing benefits. However, in a significant percentage of patients residual hearing is damaged in the process of cochlear implantation, thus reducing hearing benefits in this population. Many patients with severe hearing loss and residual hearing that can benefit from cochlear implants are not currently implanted for fear of losing their residual hearing. For this reason, much research has been focused in the areas of development and delivery of pharmaceutical and biological agents to preserve residual hearing during the electrode implantation event. In order to effectively monitor the activity of potential therapies to preserve residual hearing, animal models need to be developed which closely reproduce the conditions of cochlear implant patients.

In this study, Cochlear Corporation H8 animal electrodes were wired to connectors which were mounted to the dorsal skull with electrode implantation into normal hearing guinea pig cochlea. Electrodes were chronically stimulated and electrode impedances and hearing, via acoustically- and electrically- evoked auditory brainstem responses, were recorded at set times following implantation. The initial goal was a six-month period study covering the time frame of most major hearing

loss events following implantation and the expected duration of many pharmaceutical interventions. However, due to technical challenges identified during preliminary implantation studies, the study was altered to complete after three months. Even in this reduced three-month period, a number of animals lost their head caps housing the electrode connectors, leading to device failure and trauma and requiring immediate euthanasia. Electrical stimulation was reduced for the last three weeks of the study in hopes of reducing the number of animals lost. Except for the issues with head caps, the results of this study showed very good tolerance of chronic stimulation over ~three months. Impedances and hearing assessments were successfully measured throughout the study with no adverse effects observed aside from the expected hearing damage from trauma and inflammation from electrode implantation. These results demonstrate that this guinea pig model can be an effective tool for assessing the activity of pharmaceutical and biological interventions for the preservation of residual hearing during and following a cochlear implant surgery.

PS 359

Long-term safety of focused multipolar stimulation

Andrew Wise[1]; Robert Shepherd[1]; Ya Lang Enke[2]; Paul Carter[2]; James Fallon[1]
[1]Bionics Institute; [2]Cochlear LTD

Cochlear Implants (CIs) have a limited number of independent stimulation channels due to the highly conductive nature of the fluid-filled cochlea. Focused multipolar (FMP) stimulation uses simultaneous stimulation via multiple current sources to reduce interaction between stimulating channels. FMP also allows the use of more complex stimuli, than conventional biphasic current pulses, that includes extended periods of stimulation before charge recovery is achieved, raising questions on whether chronic stimulation with this strategy is safe.

The present study evaluated the long-term safety of intracochlear stimulation using FMP in a preclinical animal model of profound deafness. Six cats were bilaterally implanted with scala tympani electrode arrays two months after deafening, and received continuous unilateral FMP stimulation at levels that evoked a behavioural response for periods of up to 182 days. Electrode impedance, electrically evoked compound action potentials (ECAPs) and auditory brainstem responses (EABRs) were monitored periodically over the course of the stimulation program from both the stimulated and contralateral unstimulated control cochleae. On completion of the stimulation program cochleae were examined histologically and the electrode arrays were evaluated for evidence of platinum (Pt) corrosion.

There was no significant difference between ECAP and EABR thresholds evoked from control or stimulated cochleae at either the onset of stimulation or at completion of the stimulation program. Chronic FMP stimulation had no effect on spiral ganglion neuron (SGN) survival when compared with unstimulated control cochleae. Long-term implantation typically evoked a mild foreign body reaction proximal to the electrode array. Interestingly, stimulated cochleae exhibited a small but statistically significant increase in the tissue response. However, there was no significant difference in electrode impedance between control and chronically stimulated electrodes following long-term FMP stimulation. Finally, there was no evidence of Pt corrosion following long-term FMP stimulation.

In summary, chronic intracochlear FMP stimulation at levels used in the present study did not adversely affect electrically-evoked neural thresholds or SGN survival but evoked a small, benign increase in inflammatory response compared to control ears. Moreover chronic FMP stimulation does not affect the surface of Pt electrodes at suprathreshold stimulus levels. These findings support the safe clinical application of an FMP stimulation strategy.

PS 360

Focused electrical stimulation using a single current source

Philipp Senn; Robert Shepherd; **James Fallon**
Bionics Institute

Objective

Cochlear implants are the only treatment available for severe to profound sensorineural hearing loss. While providing significant benefits to recipients, speech understanding and music appreciation remains limited due to broad neural activation. Focussed multipolar stimulation (FMP) is an advanced stimulation strategy that uses multiple current sources to produce highly focussed patterns of neural excitation in order to overcome these shortcomings.

Approach

This report presents single-source multipolar stimulation (SSMPs), a novel form of stimulation based on a single current source and a passive current divider. Compared to conventional FMP with multiple current sources, SSMPS can be implemented as a modular addition to conventional (i.e. single) current source stimulation systems facilitating charge balance within the cochlea. As with FMP, SSMPS requires the determination of a transimpedance matrix to allow focusing of the stimulation. The first part of this study therefore investigated

the effects of varying the probe stimulus (e.g. current level and pulse width) on the measurement of the transimpedance matrix. SSMPS was then studied using in vitro based measurements of voltages at non-stimulated electrodes along an electrode array in normal saline. The voltage reduction with reference to monopolar stimulation was compared to tripolar and common ground stimulation, two clinically established protocols. Finally, a proof of principle in vivo test of SSMPS in a feline model was performed.

Main Results
A probe stimulus of at least 40 nC is required to reliably measure the transimpedance matrix. In vitro stimulation using SSMPS resulted in a significantly greater voltage reduction compared to monopolar, tripolar and common ground stimulation. Focussing could be achieved when the transimpedance measurement was performed with varying measurement parameters. Interestingly, matching measurement and stimulation parameters did not lead to an improved focussing performance. Compared to monopolar stimulation, SSMPS resulted in reduced spread of neural activity in the inferior colliculus, albeit with increased thresholds.

Significance
The present study demonstrates that SSMPS successfully limits the broadening of the excitatory field along the electrode array and a subsequent reduction in neural excitation.

PS 361

Relation of Fibrous Tissue to Cochlear Implant Function

Aaron P. Hughes[1]; Donald L. Swiderski[2]; Deborah J. Colesa[1]; Christopher J. Buswinka[1]; Yehoash Raphael[2]; Bryan E. Pfingst[1]
[1]Department of Otolaryngology - Head and Neck Surgery, University of Michigan; [2]Kresge Hearing Research Institute, University of Michigan

Introduction
Fibrous tissue often forms in the scala tympani following cochlear implantation. The density of the tissue varies, depending in part on a variety of variables associated with implantation. Here we examine the relationships between density of tissue and some basic psychophysical and electrophysiological measures of implant function. In previous studies in guinea pigs we have found that roughly 50% of the variance across subjects in several psychophysical and electrophysiological measures of implant function can be accounted for by across-subject variance in nerve survival, specifically spiral ganglion neuron (SGN) density near the primary test electrodes.

The hypothesis motivating the current study was that fibrous tissue in the region of the implant affects these psychophysical and electrophysiological measures.

Methods
We examined cochleae of 47 guinea pigs that were implanted with banded cochlear implants. Variables associated with implantation included implantation in a hearing ear, deafening with neomycin, and deafening plus viral-mediated neurotrophin over-expression. After implantation psychophysical and electrophysiological measures of implant function were obtained over a period averaging nine months. The animals were then euthanized and prepared for histological examination. Psychophysical measures included detection thresholds for pulse trains and sinusoids, and multipulse integration (MPI) functions. Electrophysiological measures included electrically-evoked compound action potential (ECAP) amplitude growth functions and effects of interphase gap (IPG) on those functions. Nerve survival was quantified by counting healthy appearing SGNs and determining their density (cells/mm^2) near the stimulating electrode. Fibrous tissue found between the implant and the auditory neurons was ranked as low tissue density (low TD) or high tissue density (high TD).

Results and Conclusions
SGN density was significantly higher in the low TD group (mean= 727.4 cells/mm^2; n = 24) than the high TD group (mean= 260.7 cells/mm^2; n = 23); t-test, p < 0.0001. With the current data, we cannot say if this was a causal relationship (e.g., tissue density causing SGN loss) or if both SGN density and tissue density were the result of other common variables (deafening procedure, insertion trauma, treatment, etc.). However, within the deaf, neurotrophin-treated group, the treatment was more effective at preserving SGNs in the low TD group than in the high TD group. This suggests that tissue density interacted with neurotrophin treatment to affect SGN survival. There was no evidence in our data to suggest that fibrous tissue had an effect on the functional measures that could not be accounted for by SGN density.

Electrode Impedance and Tissue Growth in the Implanted Cochlea

Christopher J. Buswinka[1]; Deborah J. Colesa[1]; Donald L. Swiderski[2]; Yehoash Raphael[2]; Bryan E. Pfingst[1]
[1]*Department of Otolaryngology - Head and Neck Surgery, University of Michigan;* [2]*Kresge Hearing Research Institute, University of Michigan*

Electrode impedance and fibrous tissue in the implanted cochlea often increase following insertion of a cochlear implant, but the relationship between these two variables is poorly understood. To investigate these relationships, the following study was conducted.

Five adult male guinea pigs were inoculated with Ad.TGF-β1 to induce a rapid onset of fibrotic growth in the scala tympani, while five guinea pigs were left untreated as controls. Two-channel platinum-ball electrode arrays were implanted twenty minutes post inoculation for the Ad.TGF-β1 group, while the control animals were implanted in an otherwise untreated ear. Animals received twice-daily electrochemical impedance measurements and once-daily electrically-evoked compound action potential (ECAP) measurements immediately following the second impedance measurement. Impedances were recorded using 10μA constant current, sinusoidal electrical stimuli from 100Hz to 100 kHz. At fourteen days post implantation, animals were euthanized and perfused with paraformaldehyde. The animal heads were nanoCT scanned prior to explantation then the cochleae were removed. The explanted electrodes were then later viewed with environmental scanning electron microscopy (ESEM). The cochleae were decalcified and embedded in JB-4 resin and sectioned in the para-midmodiolar plane, centered at the location of the primary stimulating electrode. Fibrous tissue density in the region of the implant was assessed. From the raw nanoCT data electrode position was determined and various distance measurements were taken. When possible the electrode distance measurements were verified by the presence of a visible implant tract outlined by fibrotic tissue and visible in the histological sections. A circuit model was created and used to estimate physical or chemical components of recorded complex impedances.

At two weeks after implantation, the implant only group had significantly lower tissue growth and significantly higher magnitude of recorded electrode impedance when compared to the group treated with Ad.TGF-β1. The circuit model suggested that the impedance was dominated by the interfacial double layer capacitance, while the impedance due to the spreading resistance was small. The model results were supported by ESEM images that showed the presence of biological matter on electrodes with high impedances. There was a significant positive correlation between the severity of fibrosis in the scala tympani and the modeled spreading resistance, however none to the overall recorded impedance. Implant distance from Rosenthal';s canal showed minimal variation across animals and had no measureable effect on recorded impedance.

Otopathologic Changes and Audiometric Outcomes following Misplacement of Cochlear Implant Electrodes

Danielle R. Trakimas[1]; Iman Ghanad[1]; Reuven Ishai[2]; Elliott D. Kozin[1]; Barbara S. Herrmann[1]; Joseph B. Nadol[3]; Aaron K. Remenschneider[1]
[1]*Massachusetts Eye and Ear Infirmary, Harvard Medical School;* [2]*Massachusetts Eye and Ear Infirmary;* [3]*Department of Otolaryngology, Massachusetts Eye and Ear, Harvard Medical School, Boston, MA, USA*

Background
Newly designed, precurved electrodes provide perimodiolar placement within the cochlea, but risk foldover of electrode arrays, which can damage intracochlear structures. Studies have shown that traumatic insertions, overinsertion, and interscalar translocation lead to poorer audiometric outcomes, possibly from direct spiral ganglion neuron (SGN) damage or decreased stimulation efficiency. Long-term intracochlear changes, such as differential fibro-osseous tissue formation, likely affect post-implant outcomes in cases with suboptimal electrode placement. We hypothesize that buckling of electrode arrays represents a severe form of intracochlear damage, which may cause extensive fibro-osseous tissue formation, SGN death and poor outcomes.

Methods
Specimens from a human temporal bone repository having undergone cochlear implantation were evaluated. Inclusion criteria were: 1) comparable pre-implantation interaural hearing thresholds, word recognition scores (WRS), etiology and duration of hearing loss and 2) available post-operative WRS. Specimens with buckling of electrodes on histological analysis constituted study cases. Specimens with proper placement (electrode within the scala tympani) and minimal gross intracochlear damage (basilar membrane disruption, osseous spiral lamina or modiolar fracture) constituted controls. All

specimens were examined by light microscopy and histopathologically described. SGN counts (%age-matched controls) were analyzed as differences between the implanted ear of interest and contralateral ear within each patient. Pre- and postoperative WRS were compared.

Results

Four cases of array buckling and five controls were identified. While all specimens demonstrated new ossification at cochleostomy sites, buckled cases additionally showed near complete fibro-osseous obliteration of the scala tympani or entire cochlear lumen near sites of buckling. Buckled cases demonstrated a mean loss of total SGNs compared to the contralateral ear (-11.1±9.9%,p<0.01), while controls showed no change compared to the contralateral ear (1.3±4.7%,p=0.11). The greatest differences in intercochlear SGN survival between buckled and control specimens were observed in Segments I and II, near the locations of buckling, with significant losses seen in buckled cases (p<0.01,p<0.01) and no significant changes seen in controls (p=0.06,p=0.08). Audiometric data, from a mean follow-up time of 3.5±1.5yr (buckled cases) and 3.9±1.2yr (controls), showed that buckled cases tended to have lower post-implant improvements in mean WRS (CNC,NU-6) compared to controls (26±20% vs 45±31%), although this difference was not statistically significant.

Conclusions

Initial placement of cochlear implant electrodes is critical to preservation of intracochlear structures, as severe, atypical fibro-osseous changes and neuronal loss are observed in cases of electrode misplacement. Future studies are necessary to determine if immediate recognition and correction of misplacement can prevent long-term degenerative changes.

PS 364

The Effect of Extended Systemic Steroid Administration for the Hearing Preservation after Cochlear Implantation in Guinea Pig

Yoon Chan Rah[1]; Min Young Lee[2]; Hayden Eastwood[3]; Stephen O'Leary[3]; Jun-Ho Lee[4]
[1]*Korea University College of Medicine; [2]Dankook University College of Medicine; [3]Department of Otolaryngology, University of Melbourne, Royal Victorian Eye and Ear Hospital; [4]Seoul National University Hospital*

Background

Recently, glucocorticoid is frequently used to preserve residual hearing after cochlear implantation (CI). One of the principal mechanism is the suppression of inflammatory response elicited by the introduction of electrodes.

Local delivery has a substantial limitation in preserving low tone hearing for its inevitable concentration gradient from the base to the apex of cochlea and failed diffusion through round window membrane. Systemic delivery for a sufficient duration is required to suppress the second phase of inflammatory response and subsequent tissue remodeling which increased the impedance around the electrodes. This study was aim to evaluate the effectiveness of extended delivery of systemic steroids to achieve long term hearing preservation after CI in guinea pigs.

Methods

Dexamethasone (4 mg/ml) was delivered parenterally via a mini-osmotic pump for either 3- or 7- days. The control group underwent CI without steroid infusion. A dummy CI electrode was inserted via a cochleostomy approach in 8-week-old guinea pigs. Auditory thresholds were assessed from tone burst auditory brainstem responses (2, 8, 16, 24, and 32 kHz) at 1 day prior to CI and 1, 4, and 12 weeks after implantation. Histologic evaluation of the cochleae was carried out to determine the tissue remodeling after inflammation and the status of the inner ear microstructures.

Results

Preoperatively, no significant differences were found in hearing thresholds among groups. Significantly better hearing threshold was achieved at 8, 16, 24, and 32 kHz only in the 7-day infusion group compared with the control group at 1 week after CI. The same trend was also confirmed at 4 weeks (16, 24 kHz) and 12 weeks (16, 24, and 32 kHz). Histologic review of the 7-day infusion group revealed less loose connective tissue deposition, less fibrosis in the scala tympani and the preservation of more spiral ganglion cells, compared with the control group.

Conclusion

Seven-day administration of systemic steroids was more effective in preserving hearing for 12 weeks after cochlear implantation (CI) than a 3-day delivery.

PS 365

Laminin coated cochlear implant electrodes promote Schwann cells-mediated axonal outgrowth

Esperanza Bas[1]; Mir R Anwar[1]; Stefania Goncalves[1]; Juan A Chiossone[2]; Thomas R Van De Water[1]; Christine T. Dinh[3]
[1]*Department of Otolaryngology, University of Miami Miller School of Medicine; [2]Fundacion Venezolana de Otologia; [3]University of Miami Miller School of Medicine, Department of Otolaryngology*

The benefits of cochlear implant (CI) technology depend on the number of excitable neurons remaining and the

distance between the electrode and these neurons, located in the modioulus. Among new designs, perimodiolar electrodes aim to bring the electrode closer to the neuronal target allowing for a decrease in signal spread and power consumption. However, the perimodiolar electrode is not suitable for all patients and it may flick during the insertion causing mechanical trauma. A different approach would be to bring the axons of the auditory neurons closer to the electrode by infusing growth factors such as brain-derived neurotrophic factor (BDNF) and neurotrophin-3 (NT-3) into the cochlea. Some limitations for the use of growth factors include their low stability and the risk for tumor growth, for example schwannoma. Neuronal growth cone environments can be created by chemical gradients, topographic features, adhesive patterns and altering the stiffness of the matrix. In this study laminin coated electrodes are used to promote Schwann cells-mediated axonal outgrowth of the auditory neurons towards the electrode.

The in vitro part of this study using organ of Corti explants from neonatal rats shows that 1) Schwann cells and neurites are attracted towards laminin coated surfaces, 2) the neurite outgrowth was significantly larger in laminin coated compared to uncoated dishes (p<0.001), 3) the synthetic corticosteroid Dexamethasone used concomitantly with laminin did not affect the neurite guidance and outgrowth (p>0.05). These results were confirmed in an in vivo model of CI in adult rats. A higher number of S100, p75 (both Schwann cell markers) and beta-3 tubulin (neuronal marker) positive cells were found in contact to the laminin coated electrode analog compared to the uncoated (p<0.001).

These data suggest that Schwann cells are attracted to laminin coated CI-electrodes and promote axonal regrowth, guidance and myelination of the spiral ganglion neurons. Future studies will focus on optimizing laminin coated electrodes and electrophysiological responses in the implanted ears.

PS 366

Intracochlear Pressure Transients During Cochlear Implant Electrode Insertion: Effect of Micro-mechanical Control on Limiting Pressure Trauma

Renee M. Banakis Hartl[1]; Christopher R. Kaufmann[2]; Marlan R. Hansen[3]; Daniel J. Tollin[4]
[1]Department of Otolaryngology, University of Colorado School of Medicine; [2]Department of Otolaryngology - Head & Neck Surgery, University of Iowa Hospitals and Clinics; [3]Department of Otolaryngology - Head & Neck Surgery, University of Iowa Hospitals and Clinics, Iowa City, IA; [4]Department of Physiology and Biophysics, University of Colorado School of Medicine

Background
With increasing focus on hearing preservation during cochlear implant surgery, atraumatic electrode insertion is of the utmost importance. It has been established previously that large intracochlear pressure spikes can be generated during the insertion of implant electrodes[1-2]. Estimates of equivalent ear canal pressure suggest these peak pressures may be of sufficient intensity to cause trauma similar to that of an acoustic blast injury[1] and may be one source for postoperative loss of residual hearing. Here, we examine the effect of utilizing a micro-mechanical insertion control tool on intracochlear pressure trauma exposures during cochlear implantation. We hypothesize that the use of micro-mechanical control will result in reduced number and magnitude of pressure transients when compared with standard electrode insertion by hand.

Methods
Human cadaveric heads were surgically prepared with an extended facial recess. Electrodes from three manufacturers were placed both by utilizing a custom micro-mechanical control tool and by hand. Insertions were performed via a round window approach at three different rates: 0.2 mm/s, 1.2 mm/s, and 2 mm/s (n=20 each). Fiber-optic sensors measured intracochlear pressures in scala vestibuli and tympani. The effect of electrode type, insertion speed, and use of the device on pressure magnitude was calculated using an n-way ANOVA. Chi-squared analysis was used to assess the relative number of insertions with pressure transients with and without the micro-mechanical control system.

Results
CI electrode by-hand insertion produced a range of pressure transients in the cochlea (up to 174 dB SPL), consistent with results from previous studies. Average intracochlear pressure during transient events was significantly lower when utilizing the micro-mechanical control device when compared with standard insertion by hand (p<<0.001). No difference in pressure magnitude was noted across electrode type or speed. In addition, a significantly lower proportion of insertions contained pressure spikes when the control system was used (p<<0.001).

Conclusion
Our results confirm previous data that suggest cochlear implant electrode insertion can cause pressure transients with intensities similar to those elicited by high-level sounds. Results affirm the importance of atraumatic surgical techniques and suggest that the use of a micro-mechanical insertion control system may mitigate trauma from pressure events, both by reducing the amplitude and the number of pressure spikes resulting from

cochlear implant electrode insertion. 1. Greene NT, Mattingly JK, Banakis Hartl RM, Tollin DJ, Cass SP. Intracochlear Pressure Transients During Cochlear Implant Electrode Insertion. Otol Neurotol. 2016;37:1541-1548. 2. Mittmann P, Mittmann M, Ernst A, Todt I. Intracochlear Pressure Changes due to 2 Electrode Types. Otolaryngol Head Neck Surg. 2016 Dec 1:194599816684104.

Keywords
Intracochlear pressure, cochlear implant, electrode insertion, insertion tool

Support

PS 367

Bench and Bedside: Comparison of AMEI Output Level Predicted with Two Experimental Methods and Clinical Results

Hannes Maier[1]; Martin Großöhmichen[1]; Susan Busch[2]; Bernd Waldmann[3]; Thomas Lenarz[4]
[1]*Department of Otolaryngology, Hannover Medical School, Germany; Cluster of Excellence;* [2]*Dept. Otolaryngology, MHH;* [3]*Cochlear Deutschland GmbH & Co. KG;* [4]*Department of Otolaryngology, Hannover Medical School, Germany and DFG Cluster of Excellence Hearing4all*

Objectives
The ASTM F2504-05 standard describes a method to predict the output level of implantable middle ear hearing devices (IMEHD) from cadaver studies. Here we intended to validate intracochlear pressure difference (ICPD) as an alternative method to quantify the output level of IMEHDs experimentally in cadaver studies and to compare results to in vivo results from clinical data.

Methods
Clinical results were analyzed in a retrospective review of 24 recipients with a MET® Middle Ear Implant System (Otologics or Cochlear). From bone conduction thresholds and direct thresholds determined with the fitting software using the sound processor as a signal generator the actuator output level at a given driving voltage was determined. Cadaver experiments were performed with the same device (T2 actuator as used in the Cochlear MET and Cochlear Carina® Systems) in 10 human cadaveric temporal bones (TBs) compliant to the acceptance criteria (Rosowski et al., 2007) of ASTM F2504-05. The eardrum was stimulated acoustically and the incus body was stimulated mechanically by the IMEHD actuator at a controlled static contact force. In both stimulation modes, stapes footplate (SFP) vibration was measured by LDV (Polytec) and intracochlear pressures differences between scala tympani (ST) and scala vestibuli (SV) were measured using FISO FOP-M260 pressure sensors. Equivalent sound pressure levels (eq SPLs) generated by the actuator stimulation were calculated based on SFP vibration, ICPD and from clinical results.

Results
The mean MET output level measured in cadaveric TBs by ICPD was 100 to 120 eq dB SPLFF @1VRMS. The output levels calculated from SFP vibration as recommended by ASTM F2504-05 were similar. At 5mN contact force the output levels from ICPD in cadaver experiments were nearly identical to clinical results within approx. 3 dB.

Conclusion
In incus stimulation IMEHD actuator output levels calculated from ICPD were similar to output levels determined by SFP vibration (ASTM) and identical to clinical data. Based on our results, clinical output levels of IMEHDs stimulating the ossicles can be predicted by cadaver studies with a high precision. Furthermore both, SFP vibration and ICPD are reliable measures to predict expected output level preclinically in cadaver studies.

PS 368

Importance of Adhesiolysis in Revision Surgery for VIBRANT SOUNDBRIDGE Device Failures at the Short Incus Process

Young Joon Seo; Bo Yeon Lee; Kyu Rin Hwang; Hyun Mi Ju; Sun Hee Lee
Yonsei University Wonju College of Medicine

Objectives
To report a Vibrant Soundbridge (VSB) implant revision surgical method involving adhesiolysis at the short incus process under local anesthesia and demonstrate successful hearing performance after surgery.

Design
Three cases of VSB surgery, performed in 2015, were enrolled. All cases had diagnoses of device failure. This 'seven-incision line' exposed the floating mass transducer directly, after which the three steps (adhesiolysis, curettage, and hydrocortisone injection) were performed. Upon fitting the VSB, sound fields were evaluated immediately and at 3 months after the revision.

Results
During surgery, all patients achieved unexpected, immediate hearing gains and noticed differences in the outer devices with different amplifications. Satisfactory improvements in hearing thresholds and speech recog-

nition abilities were confirmed by improvements of 20-30 dB in hearing loss 3 months after revision surgery.

Conclusions

The VSB implant revision surgical method involving adhesiolysis is safe and efficient for patients who experience a VSB device failure. This method will reduce the requirement for surgery under general anesthesia, reduce the overall period of clinical therapy, and therefore, minimize patients' medical costs.

PS 369

Towards Decoding Speech Sound Source Direction from Single-Trial EEG Data in Cochlear Implant Users

Waldo Nogueira[1]; Irina Schierholz[1]; Andreas Büchner[2]; Stefan Debener[3]; Martin Bleichner[3]; Bojana Mirkovich[3]; Giulio Cosatti[1]
[1]Department of Otolaryngology, Hannover Medical School, Germany; Cluster of Excellence Hearing4all; [2]Department of Otolaryngology, Hannover Medical School, Germany; Cluster of Excellence; [3]Applied Neurocognitive Psychology, Carl-von-Ossietzky-University, Oldenburg, Germany; Cluster of Excellence Hearing4all

Single-trial EEG can be used to decode the direction of an attended speech source from single-trial EEG data in normal hearing listeners. The ability to detect the attended speech source from EEG may find applications to steer noise reduction algorithms (e.g. beamformers, blind source separation algorithms) and therefore improve the signal to noise ratio for a given target speaker talking from the attended direction. Speech intelligibility in noise is a major problem in cochlear implant (CI) users, and therefore there is great interest in investigating whether it is possible to detect selective attention in this population. However, the decreased spectral resolution and the electrical artifacts introduced by a CI may impair the possibility to decode selective attention for this population. The goal of this study is to investigate whether selective attention can be decoded in CI users. First, experiments in NH listeners were conducted to validate the experimental setup. Second, experiments in NH listeners using vocoded sounds were conducted to investigate whether spectral smearing decreases accuracy in detecting selective attention. Finally, experiments in a group of CI users were conducted to assess whether the artefact and/or reduced spectral resolution decreases selective attention accuracy.

12 normal hearing (NH) listeners and 12 bilateral CI users participated in the study. Speech from two audio books, one uttered by a male voice and one by a female voice, was presented through inner ear phones to the NH listeners and via direct audio cable to the CI users. Participants were instructed to attend to one out of the two concurrent speech streams presented and to keep their eyes fixed to the front while a 96-channel EEG was recorded. For NH listeners, the experiment was repeated using a noise-vocoder. The noise-vocoder causes spectral smearing and consequently a worse spectral resolution, simulating speech perception with a CI in NH listeners. Speech reconstruction from the single-trial EEG data was obtained by training decoders using a regularized least square estimation method. Reconstruction performance was evaluated by means of parametric correlations between the reconstructed signal and both, the envelope of the attended and the unattended speech stream. The attended speech stream was correctly identified when the correlation with the attended speech stream envelope was higher than the correlation with the unattended one. Decoding accuracy was defined as the percentage of accurately reconstructed trials for each subject.

Results have shown the feasibility to identify the direction of an attended sound source by means of single-trial EEG not only in NH with a vocoder simulation, but also in CI users whenever enough training data are used. It seems that the limitations in detecting selective attention in CI users are more influenced by the lack of spectral resolution than by the artifact caused by CI stimulation. Possible implications for further research and application are discussed.

Basic Psychoacoustics in Humans & Animals

PS 370

Absolute auditory threshold: testing the absolute

Peter Heil
Leibniz Institute for Neurobiology

The mechanisms underlying the detection of sounds in quiet, one of the simplest tasks for auditory systems, are debated. Several models proposed to explain the threshold for sounds in quiet and its dependence on sound parameters (e.g., duration) include a minimum sound intensity ('hard threshold'), below which sound has no effect on the ear. Also, many models are based on the assumption that threshold is mediated by integration of a neural response proportional to sound intensity. We tested these ideas. Using an adaptive forced choice procedure, we obtained thresholds of many normal-hearing human ears for tones in quiet. Tones differed in their temporal amplitude envelopes, with most tones being

composed of sequential high- and low-amplitude portions (composite stimuli). An effect of the low-amplitude portion can be inferred if the threshold for the composite stimulus is lower than that for a stimulus consisting only of the high-amplitude portion, i.e., from a decrease in threshold with an increase in the amplitude ratio of the two portions. Grand-mean thresholds and standard deviations were well described by a probabilistic model proposed earlier (Heil, Matysiak, Neubauer, Hearing Res 2017). According to this model sensory events are generated by a Poisson point process with a low rate in the absence, and higher, time-varying rates in the presence, of stimulation. The subject actively evaluates the process and bases the decision about the presence of a stimulus on the number of events observed. The sound-driven rate of events is proportional to the instantaneous amplitude of the envelope of the bandpass-filtered sound raised to an exponent. We find no evidence for a hard threshold: when the model is extended to include such a threshold, the fit does not improve. Furthermore, we find an exponent of 3, consistent with our previous studies and further challenging models that are based on the assumption of the integration of a neural response directly proportional to sound amplitude or intensity. Supported by the Deutsche

PS 371

Measurement of Spectral Ripple Discrimination in Infants Using an Observer-based Method of Constant Stimuli Procedure

Brian A. Walker[1]; Lynne A. Werner[2]; David L. Horn[3]
[1]University of Washington School of Medicine, Virginia Merrill Bloedel Hearing Research Center; [2]University of Washington Department of Speech and Hearing Sciences; [3]University of Washington Department of Otolaryngology, Virginia Merrill Bloedel Hearing Research Center

Psychoacoustic testing is intrinsically difficult in infants and toddlers due to immature attention, memory, and cognitive processing. Single-interval observer-based procedures have been widely used to investigate auditory development throughout infancy. While robust for measuring average differences across ages, these procedures have relatively high attrition rates and poor test-test reliabilty thereby limiting their utility for measuring individual infants'; thresholds. Moreover, given the limits of infant attention, it is often challenging to obtain more than one threshold from an individual infant. Previously we have measured spectral ripple discrimination thresholds in 3 and 7 month old infants using a procedure where ripple depth increased whenever the infant reached a particular response criterion (adaptive criterion method). In the present study we used a method of constant stimuli (MOCS) approach where the threshold

was computed from the psychometric function at 70% Pc. It was hypothesized that, when comparing the adaptive criterion and MOCS methods, 1) the threshold yield would be greater using the MOCS, 2) the number of trials needed to obtain a threshold would be fewer for MOCS, and 3) that mean thresholds would be similar between the two methods.

Our subjects were sixty-four 28 week old infants who passed OAEs bilaterally and did not have a personal or familial history of hearing loss. Method (MOCS or adaptive criterion) was between subjects and spectral ripple depth (10 or 20dB) was within subjects. Spectral ripple stimuli were 2s broadband noise with a phase inversion of the spectral envelope at 1s (signals) or a constant envelope (no-signal) presented in soundfield at 65dBA. Ripple density was varied to obtain the highest density (threshold) at which the infant could discriminate signal and no-signal trials.

Threshold yield was higher among those who completed testing via the adaptive method (84% vs 25% yield of both 10dB and 20dB thresholds and 95% vs 60% for one threshold). However, the total trials needed to obtain a threshold was significantly lower utilizing the MOCS. Thresholds obtained between the two methods were similar.

These findings suggest that the MOCS is a valid tool for psychoacoustic testing in infants, however it did not improve threshold yield. The reduced number of trials for MOCS, when a threshold was obtained, suggests that this method may be more efficient than the adaptive criterion method in listeners who have well defined psychometric functions. Further work using MOCS with older infants and toddlers is planned.

PS 372

Relationship between spectrotemporal modulation detection and music perception in normal-hearing, hearing-impaired, and cochlear implant listeners

Ji-Eun Choi[1]; Helena Seol[2]; Jong Ho Won[3]; Il Joon Moon[4]; Sung Hwa Hong[5]
[1]Dankook University College of Medicine; [2]Hearing Research Laboratory, Samsung Medical Center; [3]Division of Ophthalmic and Ear, Nose and Throat Devices, Office of Device Evaluation, Center for Devices and Radiological Health, US Food and Drug Administration; [4]4Department of Otorhinolaryngology - Head and Neck Surgery, Samsung Medical Center, Sungkyunkwan University School of Medicine; [5]Department of Otorhinolaryngology - Head and Neck Surgery, Samsung Changwon Hospital, Sungkyunkwan University School of Medicine

The objective of this study was to examine the relationship between spectrotemporal modulation (STM) sensitivity and the ability to perceive music. Ten normal-nearing (NH) listeners, ten hearing aid (HA) users with moderate hearing loss, and ten cochlear Implant (CI) users participated in this study. Three different types of psychoacoustic tests including spectral modulation detection (SMD), temporal modulation detection (TMD), and STM were administered. Performances on these psychoacoustic tests were compared to music perception abilities. In addition, psychoacoustic mechanisms involved in the improvement of music perception through HA were evaluated. Music perception abilities in unaided and aided conditions were measured for HA users. After that, HA benefit for music perception was correlated with aided psychoacoustic performance. STM detection study showed that a combination of spectral and temporal modulation cues were more strongly correlated with music perception abilities than spectral or temporal modulation cues measured separately. No correlation was found between music perception performance and SMD threshold or TMD threshold in each group. Also, HA benefits for melody and timbre identification were significantly correlated with a combination of spectral and temporal envelope cues though HA.

PS 373

The effects of ipsilateral, contralateral, and bilateral precursors on gain reduction across the frequency range

William Salloom; Elizabeth Strickland
Purdue University

Background
The medial olivocochlear reflex (MOCR) can modulate the gain of the cochlear amplifier when activated. There are both physiological and psychoacoustic methods that are thought to measure MOCR strength in humans. However, basic questions remain: are there differences between contralateral, ipsilateral, and bilateral MOCR strength, and how does MOCR strength vary across the frequency range? Physiological research using otoacoustic emissions (OAEs) has shown that bilateral and ipsilateral MOCR strength is greater than contralateral strength (Lilaonitkul and Guinan, 2012). OAE data also suggests that the effect of the MOCR is stronger at lower frequencies, but measuring OAEs at higher frequencies has been difficult. However, bilateral, ipsilateral, and contralateral elicitation of the MOCR and effects of signal frequency have not been compared in the same subjects using psychoacoustic techniques. In the current study, normal-hearing humans are tested using a psychoacoustic forward masking paradigm to measure gain reduction, which would be consistent with the MOCR.

Methods
Gain reduction was measured at 1-, 2-, and 4-kHz signal frequencies in normal-hearing humans using a psychoacoustic forward masking paradigm. For 2 and 4 kHz, threshold for a 10-ms signal was measured. The level of a 20-ms masker nearly an octave below the signal frequency was found which would just mask the signal. The masker was then fixed at this level, and signal threshold measured with and without a pink noise precursor. Since the masker should have a linear response at the signal frequency place, the difference in threshold was interpreted as gain reduction. At 1 kHz, the masker was replaced by 20 ms of silence, since an off-frequency masker cannot be assumed to be linear at the signal frequency place for this low frequency. Gain reduction was measured as a function of precursor level for ipsilateral, contralateral, and bilateral precursors.

Results/Conclusions
Gain reduction grew compressively as a function of precursor level in each condition. Bilateral and ipsilateral precursors produced gain reduction which was approximately equal for all signal frequencies tested. Contralateral precursors produced smaller amounts of gain reduction, which was greater at lower frequencies than at higher frequencies.

Acknowledgements

PS 374

Temporal Effects on Amplitude Modulation Detection in Cochlear-Implant Users: Evidence For Central Dynamic-Range Adaptation Mechanisms

Miriam I. Marrufo-Pérez; Almudena Eustaquio-Martín; Milagros J. Fumero; Enrique A. Lopez-Poveda
University of Salamanca

For listeners with normal hearing (NH), amplitude modulation (AM) detection thresholds are better when the AM probe is delayed 300 ms from the onset of an ipsilateral, contralateral, or bilateral noise (Marrufo-Pérez et al., 2017, ARO abstract #PS395) or when it is preceded by an ipsilateral precursor (Almishaal et al., 2017, J. Acoust. Soc. Am. 141:324-333). This temporal effect is unlikely due to the acoustic reflex or to overshoot in probe audibility and has been attributed to the linearization of basilar membrane responses by the medial olivocochlear (MOC) reflex. The effect, however, may be due to central dynamic-range adaptation (e.g., Dean et al., 2005, Nat. Neurosci. 8:1684-1689). Here,

we try to elucidate between these two mechanisms by measuring AM detection thresholds for bilateral cochlear implant (CI) users with an experimental sound processing strategy that lacked any form of dynamic processing. The probe was a 50-ms, 1.5 kHz tone modulated in amplitude at a rate of 40 Hz. AM detection thresholds were measured monaurally for the probes presented at the onset (early condition) of a 400-ms broadband (0.1-10 kHz) noise or delayed by 300 ms (late condition). The levels for the probe and the noise were fixed at -20 and -30 dB full scale (FS), respectively. The noise was presented ipsilaterally, contralaterally, and bilaterally to the test ear. On average, AM detection thresholds were 4 dB better in the late than in the early condition and the size of the temporal effect was similar for the three noise lateralities. The results were broadly consistent, both in trend and magnitude, with our previous results for NH listeners. Because CI users lack both acoustic and MOC reflexes and since we used a time-invariant sound processing strategy, the data suggest that the temporal effect on AM detection is due to central dynamic-range adaptation for both NH and CI listeners. [Work supported by the University of Salamanca, Banco Santander, MED-EL GmbH, and MINECO (BFU2015-65376-P).]

PS 375

Frequency modulation excursion and rate discrimination in normal-hearing and hearing-impaired listeners

Isabel Schindwolf[1]; Marianna Vatti[2]; **Sébastien Santurette**[1]
[1]Hearing Systems, Department of Electrical Engineering, Technical University of Denmark & Department of Otorhinolaryngology, Head and Neck Surgery, and Audiology, Copenhagen University Hospital; [2]Eriksholm Research Centre, Oticon A/S

Most natural sounds contain frequency fluctuations over time such as changes in their fundamental frequency, non-periodic speech formant transitions, or periodic fluctuations like musical vibrato. These are sometimes characterized as frequency modulation (FM) with a given excursion (FMe) and rate (FMr). Accurate processing of FM may play an important role in music and speech perception, especially in complex instrument or talker situations. While age and sensorineural hearing loss (SNHL) can affect FM detection thresholds, less is known about how they affect FMe and FMr discrimination. As discrimination tasks are closer to what listeners may use to segregate sound sources, this study investigated the effects of age and SNHL on FMe and FMr difference limens (DLs) for reference values typical of frequency fluctuations observed in speech and music signals.

FMeDLs and FMrDLs were measured in younger normal-hearing (NHy), older near-normal-hearing (NHo), and older hearing-impaired (HIo) listeners with moderate sloping SNHL, for pure tones at Fc=400 and Fc=1000 Hz to which sinusoidal FM was applied. Reference FMe values ranged from 2.1% to 18.1% of Fc. Reference FMr values were 2, 5, and 20 Hz. In a 3-alternative forced-choice adaptive procedure, listeners had to choose the interval with the highest FMe or FMr. As a measure of TFS processing ability, the highest frequency at which listeners could detect an interaural-phase-difference (IPD) of 180° was obtained.

The results were very similar for Fc=400 and Fc=1000 Hz. FMeDLs, expressed as the Weber fraction, decreased with increasing FMr and increasing FMe. Group differences were enhanced at large reference FMe values, with significantly elevated FMeDLs in HIo vs NHy listeners, and NHo listeners in between on average. For FMrDLs, the Weber fraction decreased with increasing FMe but did not vary consistently with FMr. Group differences were larger for the small reference FMe, with significantly elevated FMrDLs for NHo and HIo vs NHy listeners. IPD detection thresholds were significantly correlated with FMeDLs at slow rates and large excursions, consistent with an advantage of having access to TFS cues in these conditions.

Overall, SNHL affected the ability to discriminate changes in both FMe and FMr, while age mostly affected rate discrimination. The difficulties of HIo listeners with FMe discrimination were most pronounced at large excursions and slow rates, more related to the frequency changes present in speech formant transitions and musical vibrato. Therefore, impaired processing of FM may partly account for altered perception of such features.

PS 376

Individual Differences in Frequency Modulation Detection in Listeners with Sensorineural Hearing Loss

Kelly L. Whiteford; Heather A. Kreft; Andrew J. Oxenham
University of Minnesota

Background
In the peripheral auditory system, frequency may be represented by either the place of maximal excitation along the cochlea (place code), or by the precise, phase-locked firing of auditory nerve fibers, providing a pooled representation of the stimulus periodicity (temporal code). Whether pure-tone frequency modulation (FM) uses one or both of these mechanisms remains unclear. Studies in normal-hearing listeners have led to the hypothesis

that a temporal code is used for low-frequency carriers ($f_c < $ ~4-5 kHz) at slow rates ($f_m < $ ~10 Hz), whereas a place code, involving FM-to-AM conversion is used for low-frequency carriers at high rates and high-frequency carriers at all rates. The present study used individual differences in FM and AM detection in listeners with sensorineural hearing loss (SNHL) to address this question. The prediction from the hypothesis was that fast- but not slow-rate FM should correlate with the steepness of the cochlear filter slopes around the carrier frequency.

Methods

Forty listeners (46 ears) with mild to moderate SNHL at 1 kHz completed sinusoidal FM and AM detection for f_c = 1 kHz at slow (f_m = 1 Hz) and fast (f_m = 20 Hz) rates. Pure-tone forward masking patterns were assessed for a 500-ms, 1-kHz masker fixed in level at 8 signal frequencies (800, 860, 920, 980, 1020, 1080, 1140, and 1200 Hz).The sharpness of cochlear filtering was estimated by calculating two linear slopes between the four lowest and the four highest signal frequencies.

Results

Several tasks thought to use similar peripheral codes were significantly correlated, including slow and fast AM as well as fast FM and fast AM. However, there was a similarly strong correlation between slow- and fast-rate FM, two tasks thought to utilize different mechanisms. Most interestingly, both slow- and fast-rate FM significantly correlated with the overall steepness of the filter slopes, even after controlling for sensitivity to AM and absolute thresholds at 1 kHz.

Conclusion

Sensitivity to FM in SNHL appears to be partly related to the steepness of cochlear filter slopes, suggesting a role for place coding of FM, even for carrier frequencies within the limits of phase-locking at very slow rates.

Funding

Electrophysiological and Psychophysical Electric-Acoustic Forward Masking in EAS Users

Marina Imsiecke[1]; Benjamin Krüger[2]; Thomas Lenarz[3]; Andreas Büchner[2]; Waldo Nogueira[4]

[1]*Department of Otolaryngology, Hannover Medical School, Germany;* [2]*Department of Otolaryngology, Hannover Medical School, Germany; Cluster of Excellence;* [3]*Department of Otolaryngology, Hannover Medical School, Germany and DFG Cluster of Excellence Hearing4all;* [4]*Department of Otolaryngology, Hannover Medical School, Germany; Cluster of Excellence Hearing4all*

Introduction Cochlear implant users with ipsilateral residual hearing combine acoustic and electric stimulation in one ear both (EAS). In EAS users, forward masking can be shown for electric probes following acoustic maskers and vice versa. Masking effects in acoustic-on-acoustic stimulation are generally attributed to nonlinearities of the basilar membrane and hair cell adaptation effects. However, similar masking patterns are observed more centrally in electric-only stimulation. Consequently, the stage at which interaction between the two modalities takes place is so far unclear. Animal studies have shown that electric-acoustic forward masking can result in reduced spike rates in the cochlear nerve and the inferior colliculus. In CI users with residual hearing it is possible to record intracochlear potentials with a high spatial resolution via the implanted electrode array. An investigation of the electrophysiological effects during combined electric-acoustic stimulation in humans might be used to assess peripheral mechanisms of masking. Methods Nine MED-EL Flex electrode users with ipsilateral residual hearing participated in an electric-acoustic forward masking experiment. Psychoacoustic methods (a 3I-AFC paradigm) were used to measure the changes in thresholds due to the presence of maskers. Subjects were stimulated electrically with unmodulated pulse trains using a research interface and acoustically with pure tones delivered via headphones. Neural response telemetry was used to obtain electrically evoked compound action potentials (ECAP) and electrocochleography (ECochG) separately and for combined electric-acoustic presentation. Results Behavioral thresholds of probe tones, either electric or acoustic, were significantly elevated in the presence of acoustic or electric maskers, respectively. Six subjects showed significant elevation in acoustic-on-electric forward masking with an exponential fit revealing recovery constants of 200 ms. Electric-on-acoustic forward masking showed more pronounced but shorter masking effects in four subjects, with a recovery constant of 96 ms. So far intracochlear electrophysiological measurements could be obtained in one subject during combined electric-acoustic stim-

ulation. Preliminary analysis of these results shows a change in ECAP amplitude due to additional acoustic stimulation, depending on the phase of the acoustic stimulus. Additionally, the ECochG difference potential for 750 Hz showed a reduced spectral peak with additional electric stimulation. Conclusions From these results it can be concluded that both electric and acoustic stimulation mask each other when presented sequentially, with recovery constants ranging from 100 to 200 ms for electric and acoustic masking. Preliminary analysis of the electrophysiological pilot measurement indicates that masking effects are already to some extent present in the periphery. This work received funding from the DFG Cluster of Excellence 'Hearing4all' and MED-EL Medical Electronics.

PS 378

Discrimination of harmonic and inharmonic tone complexes based on temporal fine structure: a comparison of gerbils and humans

Henning Oetjen[1]; Georg M. Klump[2]
[1]Cluster of Excellence Hearing4all and Carl-von-Ossietzky University Oldenburg; [2]University of Oldenburg

Background
Bandlimited harmonic tone complexes and inharmonic tone complexes produced by shifting the tonal components of the harmonic tone complex by the same frequency difference can be discriminated by analyzing the temporal fine structure (TFS). This discrimination paradigm called TFS1-test has been applied in several human studies (e.g., [1]=Moore & Sek (2009), Int J Audiol 48: 161-171; [2]=Jackson & Moore (2014), J. Acoust. Soc. Am 135: 1356-1370). However, behavioral studies in mammalian animal models are missing that can provide for a better understanding of the mechanisms underlying the processing of TFS1-test stimuli. Here we investigate the behavioral sensitivity of Mongolian gerbils discriminating such stimuli and compare their performance with that of human subjects.

Methods
Young (<18 month) Mongolian gerbils were trained in a repeated background Go/No-Go procedure with food rewards to discriminate TFS1 stimuli. Hit rate and false alarm rate were measured to calculate the sensitivity d'; and discrimination threshold (criterion d';=1). A filter with a bandwidth that included 7 adjacent frequency components of the complex and slopes of 30 dB/octave was applied. Pink noise was added to mask distortion products. The component tone level was 60 dB SPL and the stimulus duration was 0.4 s including 25 ms Hanning ramps. Harmonic tone complexes with two fundamental frequencies F0 200 Hz and 400 Hz and three center frequencies Fcenter 1600 Hz, 3200 Hz and 4800 Hz were used. The inharmonic tone complexes had all frequencies shifted upwards. Components of both harmonic and inharmonic stimuli had the same random phase with different phase values in each trial.

Results and Conclusions
Preliminary data show that gerbils are able to perform the TFS1 test. If a gerbil uses temporal fine structure for discrimination, it has lower thresholds than human subjects ([1, 2]). This ability to rely on temporal fine structure is consistent with the gerbils being more sensitive than humans when detecting a mistuned component in a sine phase harmonic tone complex which also may rely on the analysis of temporal fine structure (Klinge & Klump (2009), J Acoust Soc Am 125: 304:314).

Fig. 1: Sensitivity for detecting a frequency shift of components in a harmonic tone complex. Filled symbols indicate the frequency shift at threshold (d'; = 1). Round symbols reflect the relation between frequency shift and sensitivity for detection (exemplary psychometric function). Human data from the studies of Refs ([1, 2]).
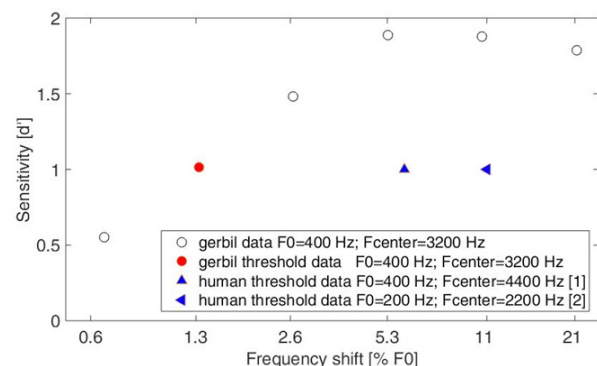
PS 379

Effect of Current Steering and Current Focusing on Spectral Resolution

Monica Padilla[1,2] and David M. Landsberger[1]
[1]New York University School of Medicine, New York, NY USA
[2]University of Southern California, Los Angeles, CA USA

Introduction
Spectral resolution has been thought to be a major limiting factor for performance with a cochlear implant. One method used to try to improve spectral representation is by using current steered virtual channels to increase the number of sites of stimulation. Another approach to trying to improve spectral resolution is current focusing

to reduce the interactions between adjacent channels. In this study, we investigate the effect of current steering and current focusing separately and collectively on a spectral resolution task.

Methods

Preliminary spectral resolution performance was measured using the SMRT task (Aronoff and Landsberger, 2013) in four Advanced Bionics cochlear implant users. Experimental maps using monopolar (MP; no steering and no focusing), monopolar virtual channels (MPVC; steering but no focusing), tripolar stimulation (TP+1; focusing but no steering) and virtual tripolar (VTP; both steering and focusing) stimulation were created using the BEPS+ research software on BTE research processors. Maps were loudness balanced to the subjects'; clinical maps so stimuli could be presented at a comfortable level. The average of four runs per map per subject were used as an estimate of spectral resolution.

Results and Conclusions

Preliminary results suggest that both steering and focusing can improve spectral resolution, although the benefit of each of these manipulations is inconsistent across subjects. However, there is no evidence of focusing or steering reducing spectral resolution. This suggests that steering and focusing may be beneficial for some but not all subjects. Further data needs to be collected in order to have a better understanding of the effects of steering and focusing.

PS 380

Efficient characterization of individual differences in compression ratio preference in hearing-impaired listeners

Lucas S. Baltzell; Jing Xia; Sridhar Kalluri
Starkey Hearing Technologies

While wide dynamic range compression (WDRC) is a standard feature of modern hearing aids designed to address limitations in dynamic range, it can be difficult to fit compression settings to individual hearing aid users. While standard prescription algorithms such as the NAL-NL2 prescribe compression settings based on the listener';s audiogram, it is not necessarily the case that listeners with similar audiograms would prefer the same compression settings. Furthermore, it is not necessarily the case that an individual listener prefers the same compression settings across different listening environments. Indeed, recent work has suggested that there are individual differences in the perceptual bene-

fits of compression, that these benefits can vary across listening conditions, and that these differences may be affected by attributes such as cognitive capacity (Lunner & Sundewall-Thoren, 2007) and residual cochlear compression (Johannesen et al., 2016). The goal of the current project was to develop a practical test to learn the preference of individual listeners for different compression ratio (CR) settings in different listening conditions (speech-in-quiet and speech-in-noise). While it is possible to exhaustively test different CR settings, such methods can take many hours to complete, making them impractical, especially for hearing impaired listeners. We used Bayesian optimization methods to find CR preferences in individual listeners in relatively short amount of time (between 15 and 45 minutes per listening condition). Using this practical preference learning test, we can examine individual differences in CR preference across a relatively wide range of CR settings in different listening conditions. In experiment 1, we verified the accuracy of our preference learning test in normal hearing listeners by showing that the results of the preference learning test did not significantly differ from the results of the exhaustive preference test. In experiment 2, we show that individual hearing impaired listeners differ in their CR preferences. We show that some listeners reliably prefer the CR setting identified by the preference learning test over linear gain, that others prefer this setting over the NAL-NL2 CR prescription, and that some prefer this setting over both linear gain and the NAL-NL2 prescription. We also show that some listeners prefer different CR settings in different listening conditions. Our results underscore the importance of fitting CR settings to individual listeners.

PS 381

Comparison of Speech Dynamic Range and LTASS Between ISTS and Korean Speech

Kyungju Lee[1]; Suyeon Shin[1]; In-Ki Jin[2]
[1]*Department of Speech Pathology and Audiology, Graduate school, Hallym University, Chuncheon, South Korea;* [2]*Research Institute of Audiology and Speech Pathology, Division of Speech Pathology and Audiology, Hallym University, Chuncheon, South Korea*

Background

The International Speech Test Signal (ISTS) is an internationally recognized test signal used in many countries to analyze technical evaluation of hearing instruments. Recordings in six different mother tongues (Arabic, English, Mandarin, Spanish, French, German) were created, with the speakers reading 'The north wind and the sun' in six different, natural, female voices. However, different languages have different acoustic and linguistic characteristics. Although the ISTS reflects 6 different languages' acoustic characteristics such as long-term

average speech spectrum (LTASS), it is unclear whether the ISTS reflects other languages that are not included in the ISTS, e.g., Korean.

Purpose

The purpose of this study was to compare LTASS and speech Dynamic Range (DR) between the ISTS and a Korean speech stimuli.

Methods

Fifty normal-hearing female talkers who are native Korean speakers participated in recording a Korean translation of 'The north wind and the sun.' The recorded Korean speech stimuli were concatenated to remove any pauses and were normalized as 65 dB SPL. Then, the DR was defined between 99% as a maximum level and 30% as a minimum level, which was the same as the ISTS. DR of 99% means that 99% of the speech signals are at or below the peak level. DR of 30% means that 30% of the speech signals fall at or below the minimum level. Then, the LTASS and the DR were compared between the ISTS and the Korean speech stimuli.

Results

LTASSs of the Korean stimuli were higher than the LTASSs of the ISTS in the frequency band below 1600 Hz. However, LTASSs of ISTS were higher than LTASSs of Korean stimuli in the frequency band above 1600 Hz. For the DR, the ISTS was higher than the Korean speech stimuli in most frequency bands.

Conclusion

The current results indicate that the ISTS does not reflect acoustic characteristics of Korean speech stimuli. Thus, a test signal based on Korean language may be more effective for accurately evaluating hearing aids and verifying effectiveness for Korean hearing aid (HA) users.

PS 382

Auditory hypersensitivity and temporal integration deficits in Fragile X rats

Kelly Radziwon[1]; Benjamin D. Auerbach[1]; Rohith Kolisetti[2]; Mary Beadle[2]; Richard Salvi[1]
[1]*Center for Hearing and Deafness; State University of New York at Buffalo;* [2]*University at Buffalo*

Hypersensitivity to sounds and auditory processing deficits are hallmarks of individuals with Fragile X (FX). Studies in the mouse model of FX (Fmr1 KO) have revealed several abnormalities consistent with auditory processing deficits, including an increased propensity for audiogenic seizures, disrupted prepulse inhibition, and enhanced cortical sound-evoked responses. However,

in depth examination of auditory processing in FX has been hindered by the limited repertoire of psychoacoustic testing that can be readily performed in mice. Recently, a Fmr1 KO rat has been developed which allows for greater flexibility in behavioral testing. Therefore, the purpose of this study is to measure loudness perception and assess auditory temporal integration in our rat model of FX using precise psychophysical techniques.

Four Fmr1 KO rats and four wildtype (WT) rats were trained to detect noise and tone bursts using a go/no-go operant conditioning procedure. To assess loudness perception in each rat, suprathreshold reaction times (RTs) were recorded from the onset of the noise/tone burst to the time the rat made a response. Given that auditory reaction time is a reliable measure of loudness perception in both humans and animals, we used this operant RT procedure to compare loudness sensitivity in Fmr1 KO to their WT littermates. In addition to suprathreshold RTs, we also obtained detection thresholds for each frequency (4, 8, 16, 20, and 26 kHz) across four stimulus durations (20-300 ms) to determine hearing threshold and temporal integration function in both the Fmr1 KO and WT rats.

We found that the Fmr1 KO had faster RTs for moderate and high level sounds than their WT counterparts. Since faster RTs are a measure of increased loudness sensitivity, it appears that, like humans with FX, the Fmr1 KO rats have enhanced loudness sensitivity. This sound hypersensitivity may also be related to the auditory perceptual disorder hyperacusis. In addition to altered loudness sensitivity, the Fmr1 KO had flatter than normal temporal integration functions compared to the WT which is indicative of impaired temporal processing.

FX is often behaviorally identified by sensory processing deficits and communication dysfunction. Therefore, characterizing the precise auditory and temporal processing abnormalities in Fmr1 KO rats provides an important behavioral model of FX and is the first step in determining the physiological and biological underpinnings of the disorder. Beyond FX, these results provide important foundational work for the broader study of autism spectrum disorders and, potentially, hyperacusis.

PS 383

Gap detection and temporal summation deficits in Chinchillas with selective inner hair cell loss

Celia Escabi; Jeffrey Martin; Edward Lobarinas
University of Texas at Dallas

The effect of selective inner hair cell loss on functional measures of hearing is not well understood. In previous experiments, we showed that selective inner hair cell loss had little to no effect on hearing thresholds in quiet. However, selective inner hair cell loss significantly impaired hearing in noise. In the present study, we evaluated the effects of selective inner hair cell loss on a gap detection task and a temporal summation task in chinchillas treated with carboplatin to assess whether temporal deficits correlated with poorer hearing in noise. Adult male and female chinchillas (1-3 yrs of age ,500-800 g) were trained to avoid a brief (2 sec) foot shock (0.5-1.5 mA) by rearing and breaking a photobeam when tone stimuli (500-12,000 Hz) of varying duration or a gap (3-128 ms) in an otherwise continuous broadband carrier noise (40-75 dB SPL) was presented. Prior to carboplatin treatment (50-75 mg/kg), gap detection thresholds ranged from 3-6 ms. Post-carboplatin (2-4 wks), gap thresholds increased to 7-16 ms. In contrast, temporal summation, assessed via threshold to tone durations ranging from 3-300 ms, did not show significant differences. These data suggest that poorer hearing in noise observed in carboplatin treated animals may not be the result of poorer temporal coding but could instead be mediated by changes in intensity coding or mechanisms essential for the detection of gap onset-offset cues.

PS 384

Effects of acoustic overstimulation on hearing loss in C57BL/6.CAST-Cdh23Ahl+ mice

Katja Bleckmann[1]; Georg M. Klump[2]
[1]*Cluster of Excellence Hearing4all and Carl-von-Ossietzky University Oldenburg; *[2]*University of Oldenburg*

This study illustrates the possible effects of a moderate acoustic overstimulation on the hearing performance of C57BL/6.CAST-Cdh23[Ahl+] mice. This strain carries a Cdh23 allele that results in little age-related hearing loss (ARHL). It is of interest for establishing this strain as a more general model of auditory processing deficits, to evaluate the hearing in noise and the susceptibility to acoustic trauma.

To demonstrate the effects of noise-induced hearing loss (NHIL) we compared auditory thresholds in silence and with a background noise (spectrum level 20 dB/Hz, frequency range 2-50 kHz)) before and two weeks after an acoustic overstimulation. Absolute and masked auditory thresholds were measured applying a reward-based operant conditioning Go/NoGo paradigm. Based on the hit and false alarm rates thresholds were obtained for sensitivity values d'; of 1.8. For eliciting a threshold shift, ketamine-anesthetized animals were exposed to an octave band of noise (8-16 kHz) for 2 h at 100 dB SPL for a temporary threshold shift (Kujawa & Libermann, 2009, J Neurosci 29: 14077-14085) or 115 dB SPL for permanent threshold shifts (Ehsraghi & Van de Water, 2006, Anat Rec A Discov Mol Cell Evol Biol 288: 473-481). A third unstimulated group served as a control. Auditory-evoked brainstem response (ABR) thresholds were measured before and two weeks after the noise exposure under ketamine anesthesia using pure tones of 5, 10, 20, 30 or 40 kHz with a duration of 0.5 ms. Amplitudes of ABR wave 1 and 4 were determined.

Fig. 1: (left) Exemplary psychometric function describing the absolute auditory thresholds at 10 kHz in silence and with background noise before undergoing acoustic trauma in a typical subject. (right) Auditory thresholds at 5, 10, 20, 30, 40 kHz (mean ± SD) in silence (n=4) and in background noise (n=4).

Preliminary results (fig. 1) show an increase of auditory thresholds in the presence of background noise for all frequencies compared to thresholds in silence. The size of the increase is slightly higher than expected from the critical masking ratio data obtained by Ehret (1976, Biol Cybernetics 24: 35-42) which may be related to our threshold criterion. Currently we are assessing the auditory performance of animals after being traumatized and are analyzing the ABR results for both time points. Our results so far show that C57BL/6.CAST-Cdh23[Ahl+] mice are a suitable animal model for investigating the effects of NIHL while avoiding possible effects of ARHL.

Figure_1_Abstract_Bleckmann_Klump.pdf

PS 385

Processing of Signals in Noise in Macaques with Noise Induced Hearing Loss: Effects of Spatially Separated and Amplitude-Modulated Noises

Jennifer McCrate[1]; Samantha Hauser[2]; Maureen Virts[2]; Jessica Feller[2]; Chase Mackey[2]; Ramnarayan Ramachandran[3]
[1]*Vanderbilt University; *[2]*Vanderbilt University Medical Center; *[3]*Department of Hearing and Speech Sciences, Vanderbilt University Medical Center*

Noise induced hearing loss (NIHL) is known to have significant consequences for the perception of signals in

noisy, natural environments. Our recent studies of NIHL in nonhuman primates showed that noise exposures that caused 40-60 dB permanent thresholds shifts resulted in widespread outer hair cell loss, variable inner hair cell loss and ribbon synaptopathy on inner hair cells basal to the region of the cochlea that corresponds to the exposure frequency. A companion study noted that these noise exposed subjects show frequency specific audiometric tone threshold elevations as well as a frequency specific reduction in threshold shifts with increasing masker levels compared to normal hearing subjects. Here we report on consequences of these NIHL on processing of signals in spatially disparate maskers and in sinusoidally amplitude modulated (SAM) maskers.

Five macaques (two Macaca mulatta and one Macaca radiata with normal hearing, one Macaca mulatta and one Macaca radiata with hearing loss induced by 4 hour exposure to 50 Hz bandwidth noise around 2 kHz) were used in studies of masked tone detection in which the temporal and spatial characteristics of the masker were manipulated. Normal hearing (NH) macaques showed lower tone detection thresholds in SAM broadband noise masker relative to steady (unmodulated) maskers. The threshold reductions were highest for low modulation frequencies and gradually decreased to match the threshold in unmodulated noise at higher noise modulation frequencies. NH macaques also showed lower masked tone thresholds when tone and masker were spatially separated compared to co-localized tone and masker (spatial release from masking, SRM). When similar studies were done with hearing impaired (HI) macaques, the spatial and temporal processing was different from NH macaques. When tone thresholds were assessed in SAM masker in HI macaques, threshold reductions were smaller than those for NH macaques; additionally, even at moderate modulation frequencies where significant threshold reductions were observed in NH macaques, HI macaques showed no threshold reduction. When steady masker was spatially separated from the tone signal, no threshold reduction was observed in HI macaques relative to co-localized tone and masker, indicating SRM was abolished after noise exposure. The indices of hearing changes in SAM masker were correlated with the audiometric threshold changes, but the changes in SRM were uncorrelated with the audiometric changes. These results suggest that temporal processing changes after NIHL may have a cochlear basis, but spatial processing changes reflect some higher order changes that occur after noise exposure.

PS 386

Perceptual Auditory Filters in Noise Exposed Macaque Monkeys with Permanent Hearing Loss

Jane Burton[1]; Ramnarayan Ramachandran[2]
[1]*Vanderbilt University;* [2]*Department of Hearing and Speech Sciences, Vanderbilt University Medical Center*

Sensorineural hearing loss (SNHL) is known to impair auditory processing, causing difficulties in many listening environments including speech in background noise. Loss of spectral resolution abilities has been associated with SNHL and is thought to contribute to these deficits. We previously established a nonhuman primate model of noise-induced SNHL, which was validated with physiological (auditory brainstem response), histological (inner/outer hair cell and ribbon synapse counts), and behavioral (tone detection in quiet, steady state noise, and modulated noise) measures. Building off additional prior work in our lab investigating perceptual auditory filters of normal hearing macaques, the aim of this study was to measure spectral resolution in macaque monkeys with noise-induced SNHL.

Two monkeys (one Macaca mulatta and one Macaca radiata) were trained in a Go/No-Go lever release task to detect pure tone signals (0.5-32 kHz) in quiet and in noise maskers. Spectral resolution was measured based on responses to noises that were spectrally notched around the tone frequency. Tone thresholds in quiet were used to construct an audiogram for each subject. Tone thresholds in notched-noise were used to derive perceptual auditory filters using the rounded exponential fit. Filter widths were characterized using the half power bandwidth (BW3dB), equivalent rectangular bandwidth (ERB), and a quality factor (qERB). Behavioral data were obtained at baseline and following exposure to a 50 Hz bandwidth of noise centered at 2 kHz of 141 or 146 dB SPL for four hours.

Compared to baseline, post-exposure tone alone thresholds were higher and auditory filters were broader for both subjects in a frequency-specific manner. Greater changes were observed i) at and above 2 kHz for both macaques and ii) overall for the 146-dB-exposed macaque. Filter broadening was similar to that reported for humans with similar degrees of SNHL. Ratios of post-exposure to baseline BW3dB, ERB, and qERB values correlated with changes in the audiogram. These findings are the basis for ongoing investigations of the neural correlates of SNHL-induced perceptual changes.

PS 387

The effects of cochlear synaptopathy on chinchilla amplitude-modulation detection thresholds

Amanda C. Maulden[1]; Michael K. Walls[1]; Vijaya P.K. Muthaiah[1]; Michael Heinz[2]
[1]*Purdue University;* [2]*Department of Speech, Language, and Hearing Sciences, Purdue University*

Recent animal studies suggest that moderate-level noise exposure can create permanent cochlear synaptopathy despite not permanently damaging hair cells or elevating hearing thresholds in quiet. This hidden hearing loss has been hypothesized to underlie the difficulties some listeners with normal audiograms have in noisy situations. However, it is difficult to test this hypothesis directly because of the inability to measure cochlear synaptopathy directly in humans and the fact that synaptopathy has mainly been shown in rodent models for which behavioral measures at speech frequencies are difficult. We recently established a relevant mammalian behavioral model by showing that chinchillas have corresponding neural and behavioral amplitude-modulation (AM) detection thresholds that are in line with human thresholds. Furthermore, we have shown that cochlear synaptopathy occurs at speech frequencies in chinchillas following moderate noise exposure. In the present study, behavioral AM-detection thresholds were measured in chinchillas, before and after noise exposure, using the method of constant stimuli. Animals were trained to discriminate a sinusoidal AM (SAM) tone from a pure tone, in the presence of a notched-noise masker designed to limit off-frequency listening. Successfully trained animals were tested at a range of AM depths (3-dB steps between -30 and 0 dB), for a range of modulation frequencies. Within a signal-detection-theoretic framework, psychometric AM-detection thresholds were computed as a function of modulation frequency. Behavioral thresholds before noise exposure were in the range of -15 to -26 dB, and were consistent across individual animals. Following synaptopathy-inducing noise exposure, amplitude-modulation detection for SAM tones was not significantly degraded. The low behavioral AM-detection thresholds found here contrast with previous work on other mammalian species (e.g., rabbits, gerbils). Our data are more in line with AM-detection thresholds found in avian species (e.g., budgerigars) and in humans. The lack of an observed deficit in performance in chinchillas with confirmed synaptopathy suggests that amplitude-modulation detection for high-level SAM tones in notched noise may not be sensitive enough for the diagnosis of cochlear synaptopathy. More complex tasks that provide a greater challenge to population neural coding are likely to be required.

PS 388

Relationship between speech intelligibility in noise, suprathreshold abilities and noise exposure in normal hearing listeners

Guillaume Andeol[1]; Clara Suied[2]; Elodie Vannson[3]; Fabrice Giraudet[4]; Annie Moulin[5]; Christian Lorenzi[6]; Christophe Micheyl[7]
[1]*Institut de Recherche Biomédicale des Armées;* [2]*Département Action et Cognition en Situation Opérationnelle, Institut de Recherche Biomédicale des Armées, Brétigny-sur-Orge, France;* [3]*Ecole du Val de Grace;* [4]*Université de Clermont Auvergne;* [5]*Centre de recherche en neurosciences de Lyon;* [6]*Laboratoire des systèmes perceptifs, Département d'études cognitives, École normale supérieure, PSL Research University, CNRS;* [7]*Starkey*

Background

Individual differences are large in speech in noise intelligibility even among young normal hearing listeners. Cochlear synaptopathy could explain a part of these individual differences. A previous study (Liberman et al, 2016) shows a relationship between word in noise performance at 0 and 5 dB SNR and history of noise exposure. The mean word in noise performance was lower among the population with a higher noise exposure based on questionnaires than among the population with a lower exposure. The present study aims to extend and explain those results by assessing word in noise performance, consonants identification in noise performance, frequency modulation detection thresholds and amplitude modulation detection thresholds.

Methods

Eighty two normal hearing listeners (< 45 years old) participated in the study. They varied widely in history of noise exposure.

Consonants identification scores were evaluated using 48 nonsense vowel-consonant-vowel-consonant-vowel (VCVCV) logatomes presented in quiet and against a steady-state speech-shaped noise (SSN) masker at +10, 5, 0, -5, -10 SNR. Word in noise performance was assessed by recognition scores of 5 lists of 50 one-syllable words presented in quiet and in a steady-state speech-shaped noise (SSN) maskers at +10, 5, 0, and -5 SNR. Frequency and amplitude modulation detection thresholds were assessed for a carrier frequency of 0.5 and 4 kHz, presented at 10 and 60 dB SL.

Multidimensional statistical analysis were used to identify subgroup of listeners according to their performance in the different psychoacoustics tests.

Results

Large individual differences was observed for each tests, confirming that normal hearing listeners can perform very differently, especially in speech in noise tasks. Preliminary results from multidimensional statistical analysis suggest that only major and relatively rare noise exposure would lead to appreciable lower scores in speech in noise tasks used in the present study.

Binaural & Spatial Hearing: Perception & Modeling

PS 389

A Model of the Auditory Pathway Applied to Solving the Cocktail Party Problem

Kenny Chou; Junzi Dong; H. Steven Colburn; Kamal Sen
Boston University

The brain';s ability to focus on a single acoustic stream within a complex auditory scene remains unmatched by machines, despite a long history of intensive research across various academic disciplines. At a cocktail party, humans can broadly monitor the entire acoustic scene to detect important cues, or selectively listen to a conversation partner. This impressive dual-mode listening of normal-hearing listeners stands in sharp contrast with the difficulty faced by hearing-impaired listeners, even with hearing-assistive devices, and machine-hearing algorithms. Recently, we developed a novel algorithm to model this behavior. The model processes binaural acoustic sounds through a cochlear filter-bank, a midbrain spatial-localization network, and a cortical network. In order to remain physiologically accurate, the midbrain and cortical models employed are based on the observations in the barn owl midbrain and the zebra finch auditory cortex, respectively. In addition, both midbrain and cortical models process the stimulus in the neural domain. The model output is decoded into the acoustic domain using a stimulus-reconstruction technique. Here, we show that the model displays dual-mode responses to spatially distributed natural sounds and can perform sound segregation as well as state-of-the-art engineering algorithms. This model may help improve the performance of hearing-assistive devices and speech-recognition technology, which are both currently challenged by cocktail-party-like settings. The model also helps make predictions in neuroscience studies, and can incorporate observations from the auditory cortex as they emerge.

PS 390

A Lateral Superior Olive Model with Bilateral Cochlear Implant Stimulation

Mathias Dietz[1]; Sebastian Ausili[2]
[1]*Western University;* [2]*Donders Institute, Radbound University*

Bilateral cochlear implant users are able to localize sound better than unilateral users but expectedly fall short of normal hearing listeners. Over the last 20 years a variety of reasons has been identified ranging from interaural cue distortion and omission of temporal fine-structure, to differences of neural processing between acoustic and electric stimulation. The latter has been investigated in many studies using carefully controlled direct stimulation with fixed-rate pulse trains presented to a single left-right electrode pair. Both human and animal studies indicate a close to normal sensitivity to interaural level differences (ILD) but an approximately one order or magnitude worse sensitivity to interaural time differences (ITD) with best detection thresholds near 100 μs. Furthermore, experimental studies consistently report an ITD rate limit in the range of 200 to 500 pps (pulses per second), much below the 1400 Hz fine-structure ITD limit in normal hearing listeners. Remarkably, both the rate limitation and the best thresholds are very similar to normal hearing sensitivity to ITDs applied to the envelopes of high-frequency sounds, which is generally thought to be processed primarily in the lateral superior olive (LSO) together with ILDs.

We thus hypothesize that LSO-type binaural processing is predominant under electric stimulation and that the medial superior olive (MSO)-type fast processing cannot be properly exploited. Therefore, we investigate how an "off the shelf" LSO model (Wang and Colburn, J Neurophysiol 111:164-181, 2014) behaves to electric pulse trains as a function of pulse rate, pulse amplitude, ITD, ILD, and neural parameters.

Results show that with the published "default" LSO parameters, ITD sensitivity drops from good at 200 pps to absent at 500 pps. The specific ITD dependence of the model LSO neuron for different pulse rates depends on the overall stimulation level and on the ILD. Model results will be related to the modelled auditory nerve input response rates but also to published physiologic data from the inferior colliculus, to model MSO data, and to published behavioral data. The similarities with behavioral data notwithstanding, the current study does not address the central question why faster MSO-like ITD processing appears to be absent with electric stimulation, even with apical electrodes.

PS 391

Modeling Adaptation to Emphasize Interaural Time Differences During Rising Amplitude

Andrew Brughera[1]; Jason Mikiel-Hunter[2]; H. Steven Colburn[1]; David McAlpine[2]
[1]Boston University; [2]Macquarie University

Correctly localizing a target sound in a background of competing sources is vital for survival in many species and important for human communication. Direct sound (emanating directly from a sound source to a listener';s ear) is useful for source segregation and localization. Reverberant sound reflecting from multiple surfaces in the environment can obscure direct sound, but during a sound amplitude minimum of sufficient duration both the direct sound and reverberation become small. Then during the subsequent increase in sound amplitude, direct sound is relatively stronger than reverberation because direct sound leads reverberation in time. Noting this acoustic emphasis of source location information during increasing sound amplitude, Dietz and colleagues (2013, 2014) applied the amplitude-modulated binaural beat (AMBB, in which sound amplitude and interaural-phase difference (IPD) are modulated with a fixed mutual relationship), and their investigations produced two key results: (1) the human auditory system uses interaural timing differences in the temporal fine structure of modulated sounds only during the rising portion of each modulation cycle, and (2) the IPD during the rising segment dominates the total response in 78% of MSO neurons (anesthetized gerbils) and 69% of IC neurons (anesthetized guinea pigs), with the remaining neurons predominantly encoding IPD near the modulation maximum. Comparing two phenomenological models, they concluded that emphasis on IPDs during the rising slope of the AM cycle depends on adaptation processes occurring before binaural interaction. This modeling effort continues in the present study with the exploration of adaptation in biophysical models that aim to emphasize the encoding of IPD during rising amplitudes. Here AMBB stimuli will drive inputs to existing model auditory nerve fibers (Zilany et al, 2014), which in turn drive our models for cochlear nucleus (CN) bushy cells and MSO neurons. While the realistic adaptation of model auditory nerve fibers does not appear sufficient to emphasize IPD during the rising amplitude envelope, synaptic depression of inputs to spherical bushy cells (Xu-Friedman and Regehr, 2008) will be modeled as an additional means of adaptation. A recent globular bushy cell model (Rudnicki and Hennert, 2017) that constrains this synaptic depression together with measured entrainment of CN-driven inputs to the MSO (Joris et al., 1994) will be leveraged where practical. Model MSO neurons with slow membranes and synapses will be explored in relation to the minority of neurons that encode IPD near the modulation maximum.

PS 392

Fully Cued versus ITD- and ILD-based Sound Localization

Maike Gerhard[1]; Hartmut Führ[1]; Patrick Schillberg[2]; Hermann Wagner[2]
[1]Lehrstuhl A für Mathematik, RWTH Aachen University; [2]Institute of Biology II, RWTH Aachen University

In a linear model of acoustic signal transfer, Head-Related Transfer Functions (HRTFs) completely describe the direction dependent acoustic filtering of sounds by the listener's torso, head and pinna. Thus HRTFs contain all binaural and monaural spatial cues available to determine the position of a sound source. The most important cues among these are Interaural Time Difference (ITD), Interaural Level Difference (ILD), and spectral notches in the high frequency domain. Previously we introduced the Acoustic Distance, a measure for the acoustic similarity of two sound source positions that can be computed explicitly and easily from the HRTFs associated with these positions. This measure makes full use of the available direction dependent information inherent in HRTF, and can be shown mathematically to be essentially optimal. The acoustic distance methodology also provides a localization algorithm that is easily implemented and essentially optimal. In this study we compare the acoustic distance-based localization algorithm with a more classical method based on ITD and ILD, where these cues are extracted from the incoming binaural signal, and optimally matched to ITDs and ILDs associated to the HRTFs. In order to test the methods on realistic data, we employed newly measured HRTF sets of six adult barn owls (Tyto furcata). Each set consists of 528 positions in space ranging in azimuth from -160 to 160 degree and in elevation from -70 to 80 degree in 10 degree steps, respectively.

PS 393

Is Monaural Spectral Localization the Phlogiston of Auditory Neuroscience? Almost Certainly

Mark Riggle
Causal Aspects LLC

Does monaural spectral localization (MSL) play any role in auditory localization? Despite 50 years of assuming otherwise, a deep analysis of both theory and data says no; while there are restricted special cases, in the general case, still no. For MSL, the mathematics and simulations are quite clear -- a solution is not possible in the general case because it is one equation (a single transfer function) while having two unknowns: the source spectra and the source location. The reasoning flaw that birthed MSL theory in the mid-1960s was assuming that interaural level difference

(ILD) could only localize in one dimension -- azimuth (formalized as the cone-of-confusion in 1939). Based on that ILD assumption, it was reasoned that the only other possible cue available for elevation was a monaural spectral cue caused by the pinna. Thus the origin of the two-step localization theory: first use ILD to determine a lateralization (a cone) and then use MSL to determine elevation (including front-back determination). This two-step theory has been accepted for 50 years despite no implementations that can compute localization with this method. The flaw is that ILD, when formulated correctly as a vector of ILD by frequency bins (referred to here as ILD-V), is a complete, single step localization method for azimuth and elevation (and even distance to some extent). Unfortunately, the ILD-V method was not understood until about 1995, or about 30 years too late to displace a theory believed to work well. We review the following areas: the mathematics and the computational studies showing ILD-V localization; the low dimensionality of the ILD-V localization problem; and its direct application to biological use. Second, by applying the mathematics of MSL and ILD-V, we review some studies that claim MSL does work in biology and also some studies that claim some form of ILD-V is not used biologically; for all those studies, we show the methodology or the interpretation flaws that lead to those erroneous conclusions. Finally and most importantly, we show how ILD-V is essential in separating multiple sound sources and then for streaming a particular source; these are tasks the two-step localization method remains silent on. Why the Phlogiston connection? Even though the genius Joseph Priestley discovered oxygen, at his death nearly 30 years later, he still believed oxygen to only be dephlogisicated air; this was well after combustion was understood.

PS 394

The Numerosity of Multiple Spatially Separated Sound Sources

M. Torben Pastore; **William A. Yost**
ASU

These studies address questions of sound source numerosity, e.g., how many sound sources can humans process at one time. Answers to such questions are theoretically relevant to how the brain processes multiple sound sources, in an instance and over time, and practically important to applications such as auditory virtual reality. We concatenate Constant-Vowel (CV) pairs spoken by a large number of male and female talkers to create stimuli of various lengths. These stimuli are either co-located at a single loudspeaker or played from spatially separated loudspeakers. We ask normal hearing listeners to determine which stimulus has more talkers than another, to estimate how many talkers there are

in a particular stimulus, and to discriminate differences in the spatial arrangement of presented sound sources. When CV stimuli are presented simultaneously, or nearly so, listeners only appear able to process a few sounds or sources (approximately five or fewer). For these stimuli, numerosity is low. Longer stimuli, made up of a larger number of concatenations, result in higher numerosity than shorter ones. Most of the time, spatial separation appears to increase numerosity, but so far, listeners appear relatively insensitive to changes in spatial separation of multiple, simultaneously presented sounds. These results imply that the auditory scene is relatively small and as such virtual auditory reality systems may not have to process or render large numbers of simultaneous sound sources to invoke a sensation of virtual auditory reality. (Research supported by grants from the NIDCD and Oculus VR, LLC)

PS 395

Differential Use of Absolute and Relative Distance Information in Auditory/Visual Distance Perception

Paul Anderson[1]; Pavel Zahorik[2]
[1]Murray State University; [2]Heuser Hearing Institute

Background
Compared to visual distance perception (VDP), auditory distance perception (ADP) is less accurate and more imprecise. ADP can be influenced by both acoustic cues to distance and a listener';s familiarity with the stimuli. The investigation of how repeated stimulus presentation shifts distance judgments is often framed in relation to relative vs. absolute distance cues, where systematic variation of judgments after repeated presentations indicate the use of relative distance cues. However, the manner in which distance judgments shift with experience of previous presentations has not been thoroughly investigated, particularly compared to VDP. In the present study, participants made distance judgments in either an auditory (A) or visual (V) condition, and judgments were analyzed to quantify how distance perception is influenced by experience with previous stimuli.

Methods
62 (41 female) normal-hearing listeners, ranging in age from 18 to 55.

Auditory Stimuli
Binaural room impulse responses (BRIRs) were measured from 11 logarithmically-spaced distances ranging from 0.3 to 9.75 m in a concert hall, with broadband T60 = 1.9 s, using a KEMAR manikin at a fixed location near the edge of the stage, facing away from audience seating. The sound source was moved on stage to manipulate distance. The source signal was a 100 ms sample of Gaussian noise.

Visual Stimuli

Wide-angle digital photographs of the measurement loudspeaker taken from the position of KEMAR, and displayed on a high-quality large-screen HDTV.

Procedure

Participants directly estimated egocentric distance to the sound source in each condition: A and V. Each condition contained 110 trials (11 distances x 10 replications) and was presented within its own block. The order of blocks was counterbalanced, and the order of trials within each block was randomized.

Results

A moving average analysis of distance judgments suggests distance judgments in A are pushed farther away with subsequent trial presentations, which corresponds to increasing inaccuracy. Distance judgments in V, however, remained constant across presentations. Variability in A judgments decreased with experience, while V judgments maintained a lower, constant level of variability.

Conclusions

ADP was found to become less accurate but also less variable as participants gained experience, while VDP had constant levels of accuracy and precision throughout the testing session. In ADP listeners tended to erroneously increase their judgments with more experience. This confirms that VDP is more reliable and stable than ADP, and suggests that ADP likely relies heavily on relative distance cue information, whereas VDP uses absolute distance information.

PS 396

A novel concept for dynamic adjustment of auditory space

Andrea Lingner[1]; Michael Pecka[1]; Christian Leibold[2]; Benedikt Grothe[1]

[1]Ludwig-Maximilians-Universitaet Munich; [2]Bernstein Center for Computational Neuroscience Munich

Traditionally, the auditory system is thought to serve reliable sound localization. Recent electrophysiological evidence however indicates that specific feed-back systems in the early binaural pathway cause the subjectively perceived location of sounds to be strongly influenced by preceding stimuli; contradicting the canonical concept of sound localization and raise questions about the functional significance these feed-back loops.

Here we combined human psychoacoustic testing and computer modeling of neuronal coding to study the nature of context-dependent spatial sensitivity and its underlying representation. In accordance with previous human psychophysical studies, we found pronounced shifts in the spatial perception of sounds away from a preceding adapter sound, corresponding to a substantial miss-judgment of absolute sound source positions in the range of tens of degrees of auditory space. For a strongly lateralized preceding adapter (ITD of +635 µs), theses shifts in perception were restricted to the hemisphere of the adapter location. Computer modeling showed that such hemispheric confinement of localization errors was incompatible with the traditional labeled-line and hemispheric-difference models of auditory space coding. We therefore developed a new decoding model incorporating recent electrophysiological findings in which sound location is initially computed in both brain hemispheres independently and combined to yield a hemispherically balanced code. This model closely captures the observed absolute localization errors caused by stimulus history, and furthermore predicts a selective dilation and compression of perceptual space relative to the adapter location. In accordance with this model prediction, human listeners reported a selective increase in spatial resolution near the adapter location on the expense of locations further away. Together, our findings indicate the need for a new concept for the coding of auditory space which is based on the assumption that spatial hearing in mammals facilitates focal sound source segregation at the expense of absolute sound localization, thus questioning existing concepts of spatial hearing in mammals.

PS 397

Threshold Interaural Time Differences Under Optimal Conditions

Sinthiya Thavam; Mathias Dietz
Western University

Background

Humans and other animals use their two ears to localize sounds from their surroundings. The sound';s location causes a specific interaural time difference (ITD) which can be exploited by specialized neural circuits in the brainstem to inform on the azimuthal sound arrival direction. Particular in the 1950s several studies have investigated human threshold ITDs with various stimuli and reported lowest thresholds to be near 10 µs. Despite the fact that these studies were partly preliminary reports and that they did not attempt to systematically find the smallest threshold ITD, they still serve as best available references.

Goal of the study

The goal of this study is to systematically determine the stimulus and the experimental paradigm that results in the smallest threshold ITD for well-trained normal hearing listeners and to provide an accurate reference value.

Methods

Reviewing the literature and conducting pilot experiments, resulted in seven stimulus and procedure parameters that may influence ITD sensitivity: stimulus waveform, stimulation level, stimulus duration, adaptive versus constant stimulus procedure, alternative-forced-choice (AFC) procedure, inter-stimulus pause duration, and complete waveform versus ongoing ITD. In part 1 of this study, threshold ITDs were measured in 8 normal hearing listeners using 11 stimulus waveforms, which were categorized into three different types of stimuli: pure tones, tone complexes and noise. The fixed procedure for part 1 was a two-interval two-AFC task with a three-down one-up staircase procedure, level of 70 dB SPL, inter-stimulus intervals of 0.3 s and interval durations of 0.5 s. For part 2 the two best stimulus waveforms from part 1were chosen and the other six parameters were varied to identify the optimal procedure and stimulus level for ITD sensitivity.

Results

The condition yielding the lowest threshold ITD was Gaussian noise band-pass filtered from 20-1400 Hz, presented at 70 dB SPL, with a short inter-stimulus pause of 50 ms, and an interval duration of 0.5 s. The average threshold ITD for this condition at the 79% correct level was 8.3 μs.

Conclusions

The threshold ITDs are of comparable magnitude as in previous studies. Compared to Klumpp and Eady (JASA 1956) the shorter inter-stimulus pause, shorter stimulus duration and extensive training are the most apparent factors that result in slightly lower thresholds in our study.

PS 398

Temporal Weighting Functions for Lateralization of Amplitude-Modulated Click Trains

G. Christopher Stecker
Vanderbilt University Medical Center

Many types of spatial judgments are dominated by binaural features of the sound onset. Onset dominance is particularly evident for pure tones and for rapid periodic stimuli such as click trains with interclick interval [ICI] less than 5 ms, but not for slower or aperiodic stimuli. Recent studies have extended our understanding of onset dominance to reveal the importance of rising slopes in other types of envelopes–such as periodic amplitude modulation (AM)–imposed on tonal and click-train carriers. Recently, Hu et al. (2017 JASA 141:1862-73) compared the effect of sinusoidal AM on binaural discrimination of click-train carriers at 200 and 600 Hz (5 and 1.67 ms ICI), reporting dominance of rising envelope slopes at 600 but not 200 Hz. That result is entirely consistent with the known rate-dependency of onset dominance (Hafter and Dye 1983; JASA 73:644-51) and its quantification via binaural temporal weighting functions (TWF; Saberi 1996 Percept. Psychophys. 58:1037-46; Stecker et al. 2013 JASA 134:1242-52). The current study adapted the procedure of Stecker et al. (2013) to measure TWF for lateralization of interaural time and level differences (ITD and ILD) in filtered click trains with 20-Hz sinusoidal AM similar to Hu et al. (2017). Consistent with previous findings, elevated weights were observed during the rising phase of the 20-Hz envelope when the ICI was short (2 ms). Lengthening the ICI to 5 ms reduced the weight on rising-phase clicks and increased the weight on later clicks occurring near the peak of the AM cycle. These differences were apparently greater for ILD than for ITD, consistent with listeners'; greater access to post-onset ILD cues (Brown and Stecker, 2010 JASA 128:332-41). Supported by NIH R01 DC011548.

TWF_AM2_meanTWF_short.pdf

PS 399

Rapidly varying interaural time difference cues within tonal and noise stimuli: Evidence that perceived lateralisation is weighted towards cues presented in the early/rising portions of sounds.

Nicholas Haywood; Jaime A. Undurraga; David McAlpine
Macquarie University

Rapid modulations to interaural time/phase differences (ITDs/IPDs) of a low-frequency sound suggest that lateralisation judgments are influenced predominantly by the ITD during the early portion of a stimuli (e.g., Dietz et al., 2013; Stecker & Bibee, 2014).

Here, the first pilot presented a modified amplitude-modulated (AM) binaural-beat stimulus (Dietz et al., 2013). Current stimuli comprised a tone with diotic 8 Hz AM. A 4 Hz binaural-beat was evoked from dichotic 498 Hz and 502 Hz carrier tones. Therefore, within one AM cycle, the carrier transitioned through a 180° IPD range. Carrier IPD was set to either +90°/-90° at onset, and ended at -90°/+90° respectively at offset. Beat direction was varied so that carrier IPD was always 0° at the AM peak. Subjects heard four AM cycles of identical IPD characteristics, and reported whether the stimuli were heard to the left/right (2AFC, n=8). Perceived lateralisation favoured strongly the side corresponding to the IPD of the initial half of the AM cycle (86% of responses). For beating stimuli with a predominantly flat amplitude envelope (125-ms duration, 20-ms onset/offset ramps), subjects again favoured the initial IPD direction (75%). How-

ever, for beating stimuli presented with a long rising envelope (105-ms) and abrupt offset (20-ms), subjects judged lateralisation towards the IPD of the final portion of the stimulus (84%). These results are consistent with Dietz et al. (2013), suggesting weighting based on both time-from-onset and envelope characteristics - specifically, IPDs during rising envelope portions may be given strongest perceptual weight.

The second pilot presented diotic band-pass filtered noise (300-700 Hz). An ITD was imposed on the noise during a 20-ms ITD-window';, whilst an 8 Hz AM envelope was held diotic. In an 2I-2AFC task, subjects heard stimuli with left-leading and right-leading ITD-windows of identical magnitude. Subjects identified the left-leading stimuli, and the size of the ITD-window was varied adaptively (two-up, one-down). The ITD-window was centred on either; the rising portion of the AM cycle (¼-point of the cycle), the peak (½-point), or the falling portion (¾-point). The mean minimum audible angle (MAA) was smallest for the rising-centred ITD-window (136-μs, n=6), and larger for the peak- or falling-centred ITD-windows (215/219-μs respectively). Those who showed the strongest lateralisation judgments in Pilot 1 had smaller MAAs (R2=0.733), suggesting both tasks assessed a common mechanism.

These pilot experiments will be expanded to further assess both individual variability in lateralisation performance, and the effects of envelope shape on ITD weighting.

PS 400

Does a lack of precisely timed input hamper envelope ITD sensitivity when presenting amplitude-modulated low-frequency (< 500hz) carriers?

Jason Mikiel-Hunter[1]; Andrew Brughera[2]; David McAlpine[1]
[1]Macquarie University; [2]Boston University

Sensitivity to interaural time differences conveyed in the temporal fine structure (TFS) of low-frequency sounds is most often assessed using unmodulated sound envelopes. Nevertheless, many natural sounds are modulated in amplitude, and a recent psychoacoustic study highlighted how sensitivity to ITDs conveyed in the TFS is weighted as a function of the location within the envelope modulation cycle (Hu et al., 2017). Whilst perception of ITDs is dominated by ITDs conveyed in the initial, rising phase of an amplitude-modulated 600Hz stimulus (consistent with psychoacoustic/physiological studies employing 500-Hz carriers (Dietz et al., 2013, 2014)), it resides in the middle portion of the modulation cycle

for a 200-Hz stimulus. This disparity in envelope ITD processing strategies is surprising: the 200-Hz carrier strategy more closely resembles an "integration of energy across the modulation cycle" approach observed for high-frequency (>1500Hz) carriers (Dietz et al., 2013; Remme et al., 2014).

The binaural computations underlying envelope ITD processing for such low-frequency carriers are typically ascribed to principal neurons in the MSO (Dietz et al., 2013, 2014). Their exquisite ability to detect fine structure ITDs arises from biophysical specializations seemingly ubiquitous across the MSO';s tonotopic axis (Svirskis et al., 2004; Scott, Mathews and Golding, 2005; Chirila et al., 2007; Mathews et al., 2010; Myoga et al., 2014; Remme et al., 2014). It is therefore more likely that the observed shift in envelope ITD sensitivity from rising phase to peak of modulation cycle for a 200Hz carrier is a result of the synaptic input generated in the rising amplitude envelope being more unreliable for a 200-Hz carrier compared to a 600-Hz carrier (i.e. fewer synaptic input cycles with increased jitter during the rising phase).

To test this hypothesis, we presented the amplitude-modulated stimuli employed by Hu et al. (2017) to an auditory nerve computational model (Zilany, Bruce and Carney, 2014) and harnessed its output to generate synaptic input for a linear MSO principal neuron model that included a threshold mechanism for spiking (Remme et al., 2014). Simulated neurometric functions (d primes) were thereby generated from the linear model';s suprathreshold responses to the various envelope ITD conditions (i.e. envelope ITDs in rising, middle and end phases). Initial results suggest that it is indeed possible to reproduce the psychoacoustic results within our model for both 200Hz and 600Hz carrier stimuli.

PS 401

The Relation between Source Width Perception and Speech Intelligibility with Virtual Sound Sources

Axel Ahrens[1]; Marton Marschall[1]; Torsten Dau[2]
[1]Hearing Systems group, Department of Electrical Engineering, Technical University of Denmark; [2]Hearing Systems group, Technical University of Denmark

Increases in the perceived width of sound sources have previously been found for hearing-impaired listeners (Whitmer et al., 2012). In addition, some types of hearing-instrument signal processing, such as wide dynamic range compression, may also degrade spatial perception for listeners, typically leading to a wider perceived source width (e.g. Cubick et al., 2017, Hassager et al., 2017). In this study, we investigated if changes in per-

ceived source width also lead to changes in a spatial speech intelligibility task presented in a virtual sound environment. It was hypothesized that a wider source-width percept leads to a reduced ability to separate target and interfering talkers, in particular when closely spaced. To generate sound sources with a varying source width percept, virtual sources were generated using a horizontal 24-loudspeaker array and higher-order ambisonics coding. The ambisonics order is directly related to the spatial spread of energy and was previously shown to affect the source width percept. In the first experiment, speech reception thresholds (SRTs) were measured with two interfering talkers co-located and symmetrically separated by 15°, in an anechoic and a simulated reverberant environment. The conditions were presented at various ambisonics orders. In the second experiment, listeners were asked to estimate the location and perceived width of a single sentence. The sentence was presented either from the front or from 15° left or right. The same ambisonics orders as in the first experiment were applied. Data showed that the perceived source width decreased with increasing ambisonics order. Speech intelligibility remained constant in the co-located condition and increased with ambisonics order in the separated condition, thus providing an increased spatial benefit with increasing ambisonics order. Thus, the spatial spread of energy was found to correlate with the percept of source width as well as with speech intelligibility with closely separated interferers. The speech intelligibility results were well accounted for by a better-ear glimpsing model, while a short time signal-to-noise ratio analysis of a single receiver did not show differences between the ambisonics orders. Also, a binaural masking level difference model could not predict the differences in SRT. The modeling reveals that the spatial spread of energy limits the available signal-to-interferer ratio at the ears, due to a spread of energy from the contra-lateral interferers. The auditory cues underlying changes in source-width perception for different ambisonics orders are, however, not yet clear.

Development II

PS 402

Mapping the cis-regulatory elements enhancing prosensory gene expression

Brent A. Wilkerson[1]; Leah S. VandenBosch[1]; Matthew Wilken[2]; Thomas Reh[1]; Olivia Bermingham-McDonogh[1]
[1]*University of Washington;* [2]*Altius Institute for Biomedical Sciences*

To elucidate transcriptional control mechanisms specifying the cochlear prosensory cells that generate the hair cells and support cells critical for hearing function, we are mapping the cis-regulatory elements such as promoters and enhancers that precisely orchestrate where, when and how genes are expressed. More specifically, we compare chromatin accessibility using ATAC-seq in sorted prosensory cells (Sox2-EGFP[+]) and non-sensory cells (Sox2-EGFP[-]) from isolated embryonic cochlear ducts. Our datasets reveal prosensory cell-specific open chromatin regions possibly related to prosensory specification (Sox2 and Jag1) and hair cell and support cell differentiation (Prox1, p27[Kip1] and Atoh1). Our working hypothesis is that many prosensory cell-specific open chromatin regions represent cis-regulatory modules enhancing prosensory cell-specific gene expression. Supporting this hypothesis, we find significantly more consensus binding sites for Sox2—a transcription factor that is both necessary and sufficient for prosensory specification early in development—in open chromatin regions of sorted prosensory cells than in those of sorted nonsensory cells. Moreover, in prosensory cells, we find more open chromatin regions having Sox2 sites near several genes known to be spatially restricted in expression to the prosensory (floor region of the cochlear duct) including Sox2 (e.g., 5 open regions in E14.5 Sox2^{+} vs. 0 in E14.5 Sox2^{-}), Jag1, Prox1, p27[Kip1], Atoh1, Dll1, Hey1, Eya1, Ntf3, Mycn and Fgf20. Currently, we are evaluating the enhancer activity of prosensory cell-specific open chromatin regions near these key regulatory genes. Our results so far reveal many potential interactions between regulatory gene expression, chromatin structure and transcription factor-binding across cochlear development and will direct further mechanistic investigation of the gene regulatory networks specifying the prosensory cells that generate the hair cells and support cells critical for hearing function.

PS 403

Gene regulatory networks governing mouse hair cell differentiation and maturation

Litao Tao[1]; Zlatka Stojanova[2]; Haoze Yu[3]; Talon Trecek[4]; Xizi Wang[4]; Juan Llamas[4]; Neil Segil[3]
[1]*University of Southern California, Caruso Dept. of Otolaryngology, Keck School of Medicine;* [2]*Xencor, Inc.;* [3]*Department of Stem Cell Biology and Regenerative Medicine, Keck School of Medicine of the University of Southern California;* [4]*University of Southern California*

Background
Sensory hair cells within the mammalian organ of Corti are highly derived evolutionarily, and their function depends on a precise and complex pattern of developmentally-regulated gene expression. In the mouse, hair cell differentiation starts at ~embryonic day13.5 (E13.5) under the influence of the bHLH transcription factor Atoh1; and during the following several weeks, hair cells mature with temporally and spatially regulated assembly of specialized functional apparatus, including ciliogenesis and

synaptogenesis. The gene regulatory networks (GRNs) that govern Atoh1-dependent differentiation, and subsequent emergence of salient characteristics of hair cells, are largely unknown. Using a combination of transcriptomic, epigenomic, and chromatin structure data collected longitudinally during embryonic and perinatal organ of Corti maturation, we took a computational approach to identify GRNs involved in hair cell differentiation and maturation.

Methods

Mouse inner ear prosensory progenitors (E13.5-p27-GFP+) and hair cells (E17.5-, P1- and P6-Atoh1-GFP+), were FACS-purified and used to obtain ATACseq, RNA-seq, and histone ChIPseq NextGen datasets. The resulting data was used to identify transcription factors that become active during early hair cell differentiation, based on temporal changes in average accessibility of genomic footprints, as well as the flanking regions of cognate binding motifs. The list of putatively active transcription factors was further curated based on expression data from RNAseq, and then their binding sites were imputed by digital footprint analysis combined with epigenetic data (H3K27ac). This approach allows us to infer transcriptional regulatory relationships between transcription factors and target genes. Finally, the software Cytoscape was used for network visualization.

Results

Using these inferred transcriptional relationships, we built preliminary GRNs that identify regulatory heirarchies responsible for the emergence of several characteristic hair cell functions. The GRNs predicted by this approach are consistent with previously reported, experimentally-derived regulatory relationships, and will be further validated using in vitro enhancer assays, gene knockouts, and transcription factor ChIPseq. Here we report on the GRN involved in the initiation of ciliogenesis in hair cells, and identified the previously described transcription factors Rfx3 and FoxJ1 in this process.

Conclusion

The use of NextGen sequencing data from ATACseq, RNAseq and ChIPseq provides a means of establishing putative GRNs with testable hypotheses. In this report, we describe our data collection and computational approach, as well as a resulting network that appears to be involved in ciliogenesis in the nascent hair cell. We also present preliminary validation of this approach through a variety of biological assays.

PS 404

Histone phosphorylation events during the development and maturation of the mouse inner ear

Kimberly Callahan[1]; Lauree Thomas[1]; **Bradley J. Walters**[2]
[1]*University of Mississippi Medical Center;* [2]*Department of Neurobiology and Anatomical Sciences, and Department of Otolaryngology and Communicative Sciences, University of Mississippi Medical Center*

Post-translational modifications of histone proteins play critical roles in the organization and accessibility of chromatin. While much attention has focused on the acetylation and methylation of histones and their resultant effects on transcriptional activity, histones are also phosphorylated at many residues. Indeed histone phosphorylation can regulate not just transcription, but replication, chromatin segregation, and DNA repair, as well as the acetylation and methylation of other residues on the histones themselves. Despite this, most of the existing literature concerning histone phosphorylation relegates these modifications to cell cycle control and DNA damage repair. Here, we investigated the spatiotemporal distribution of several phosphorylated histone variants during the development and maturation of the mouse inner ear. Antibodies specific to phosphorylated residues of histone proteins were used to immunostain mouse cochlear and vestibular tissues at embryonic days (E)14.5 and E16.5, and postnatal days (P)0, P14, and P30. The resulting patterns of expression for several phosphorylated histone variants suggest that cells within the mouse inner ear undergo a wide array of histone phosphorylation and dephosphorylation events during this critical period of cochlear and vestibular maturation. While several histone phosphorylation events were clearly correlated with stages of the cell cycle in nonsensory cells, we also noted robust immunoreactivity for several phosphorylated histone proteins in quiescent hair cells, supporting cells, and neurons. The widespread and persistent immunostaining in stable cell populations suggest that histones are phosphorylated not just in dying or dividing cells, but in normal, healthy cells in the inner ear. Furthermore, several of the phosphorylated histone variants inversely correlated with condensed heterochromatin, suggesting that certain histone phosphorylation sites may be important for DNA unpacking and transcriptional activation in post-mitotic cells. Combined, these findings suggest that phosphorylation of histone proteins in the developing and mature mouse inner ear is fairly prevalent, and may be important for the regulation of gene expression independent of cell cycle or DNA damage, suggesting possible roles in neurosensory function.

PS 405

The ATP-Dependent Chromatin Remodeler CHD7 is Critical for Proper Cochlear Length, Hair Cell Structure, and Auditory Nerve Connectivity

Vinodh Balendran[1]; Lisa A. Beyer[2]; Jennifer M. Skidmore[3]; Elizabeth Hurd[4]; Yehoash Raphael[5]; Donna M. Martin[6]
[1]Departments of Pediatrics and Human Genetics, University of Michigan, Ann Arbor, MI, USA.; [2]Kresge Hearing Research Institute University of Michigan, Ann Arbor, Michigan, USA; [3]Departments of Pediatrics and Communicable Diseases University of Michigan, Ann Arbor, MI, USA.; [4]CBS Deputy Director, University of Edinburgh; [5]Kresge Hearing Research Institute, University of Michigan; [6]Departments of Pediatrics and Human Genetics, University of Michigan, Ann Arbor, MI, USA

Epigenetic regulation of gene transcription by chromatin remodeling proteins has recently emerged as an important contributing factor in inner ear development. Pathogenic variants in CHD7, the gene encoding Chromodomain Helicase DNA binding protein 7, cause CHARGE syndrome, which presents with malformations in the developing mammalian ear. Germline deletion of Chd7 in mice is embryonic lethal, whereas heterozygous Chd7 loss-of-function mice display mild mixed sensorineural/conductive hearing loss. Chd7 is broadly expressed in the developing and mature mouse auditory epithelium as early as E13.5, yet the pathogenic effects of Chd7 loss in the cochlea have yet to be fully defined. Here we characterized cochlear and auditory epithelial phenotypes after Chd7 deletion in the otocyst and surrounding mesenchyme (using Foxg1Cre), in the otic mesenchyme (using TCre), in hair cells (using Atoh1Cre^{ERT2}), and in developing neuroblasts (using Ngn1Cre). Inner ears were examined using scanning electron microscopy, immunofluorescence for neurofilament, phalloidin staining, and paintfilling. Deletion of Chd7 in Foxg1Cre;Chd7$^{Gt/flox}$ mice resulted in disorganized, ectopic, and supernumerary rows of hair cells and disrupted innervation with excess axonal looping. Deletion of Chd7 in the mesenchyme by Tcre led to normal cochlear morphology at E14.5. Deletion of Chd7 in hair cells at E12.5 by Atoh1Cre^{ERT2} did not disrupt E17.5 hair cell organization. Deletion of Chd7 in developing neuroblasts by Ngn1Cre also did not preclude neuronal differentiation. Together, these observations suggest the presence of dosage-, tissue-, and time-sensitive roles for Chd7 in cochlear elongation, hair cell morphology, and cochlear neuron organization. Interestingly, the otocyst and maturing neurons appear uniquely sensitive to Chd7 deficiency, whereas the surrounding otic mesenchyme is not. These studies indicate that CHD7 acts to regulate cochlear size and epithelial and neuronal organization, providing novel information about roles for Chd7 in development of both auditory epithelia and neurons.

PS 406

Evaluation of Single Nucleus Isolation Methods for Single Cell Gene Expression Profiling of the Mammalian Inner Ear

Michael C. Kelly[1]; Joseph C. Mays[1]; Kaya Matson[2]; Ariel Levine[2]; Matthew W. Kelley[1]
[1]NIDCD/NIH; [2]NINDS/NIH

Cell type specific transcriptional analysis has provided valuable insight into the genes involved in the development and function of the mammalian auditory and vestibular sensory organs. The unprecedented resolution of single cell RNA-Seq has provided a comprehensive and unbiased survey of the transcriptional profiles of cell types at multiple developmental timepoints. However, several limitations remain for profiling complex inner ear tissues across all developmental timepoints and conditions. Importantly, whole-cell single cell genomic methods generally require the dissociation of live cells before downstream applications such as single cell RNA-Seq profiling. For tissues with extensive cell-cell adhesion and intercalation, the process of isolating single whole cells without contamination from neighboring cells while also maintaining high cell viability of target cell types can be difficult. Furthermore, in the case of transcriptional assays, the added time required for efficient dissociation raises concerns about potential transcriptional drift, unintended cellular responses to the dissociation process, and selective loss of cell types. One potential solution to some of these challenges is the isolation and analysis of nuclei instead of whole cells. Nuclei can be rapidly released from most cell types in diverse tissue contexts, and recent evidence suggests that mRNA transcripts sampled from a cell';s nucleus are largely representative of the mRNA content of the entire cell. Using neonatal mouse cochlear epithelial cells, we evaluate a fast-extraction single nucleus RNA-Seq method by comparing results to those obtained using our existing whole-cell single cell RNA-Seq method. We also explore methods to enrich for nuclei of specific cell types, which would further extend the utility and efficiency of single nuclei genomic profiling experiments. These methods hold promise in allowing the profiling of both gene expression and gene regulation mechanisms, such as chromatin status and transcription factor binding, at single cell resolution across all developmental timepoints.

PS 407

Characterization of the effects of HDAC inhibition during cochlear development using Single Cell RNA-Sequencing

Joseph C. Mays; Matthew W. Ke[...] [...]hael C. Kelly
NIDCD/NIH

The mammalian coch[...] comprised of diverse cell types that vary si[...]ly in structure and function. While conside[...] [...]rts have been made to identify the genetic [...]ing pathways that drive the development, d[...] [...]ation and maintenance of different cochlea[...] types, the role(s) of epigenetic mechanisms in these processes is comparatively poorly understood.

One of the most significant epigenetic mechanisms used to modulate gene expression is histone modification, which affects chromatin architecture and accessibility of DNA to transcriptional machinery. A particularly well characterized aspect of this histone modification is the dynamic acetylation and deacetylation of histones by histone acetyltransferase (HAT) and histone deacetylase (HDAC), respectively. Both processes can alter gene expression on a broad scale.

We have previously shown that Class I HDACs are required for the maintenance of cellular morphology in the neonatal cochlea, as inhibition of these enzymes in culture causes disorganization of cochlear patterning and flattening of the cochlear epithelium. This complex phenotype is likely to arise as a result of broad cell type-specific transcriptional changes that, if characterized, could provide insight into the specific roles of histone acetylation dynamics in the maintenance of cell identity. Furthermore, these analyses could also reveal possible mechanisms underlying the loss of cellular plasticity that occurs as the mammalian cochlea matures.

To accomplish this analysis, we employed droplet-based single-cell mRNA sequencing (scRNA-seq), to generate transcriptomic profiles for individual cells within control and HDAC inhibited cochlear explants. Differential gene expression analysis between analogous cell-types indicates a variety of transcriptional changes, both specific to cell populations and broadly across all cochlear cells, as well as changes in genes known to regulate critical developmental processes such as adhesion. Continued analysis of these results will provide valuable insights regarding the roles of histone acetylation in gene regulation and cochlear development at the single cell level.

PS 408

The role of β-catenin deletion in Sox2-specific cells in inner ear development and polarity regulation in mice

Xiao-Qing Qian; Cong Ning; Meng Zhao; Xiaoyu Yang; Yu Zheng; Fanglu Chi; **Dong-Dong Ren**
EYE & ENT Hospital of Fudan University

Background

Sensory hair cells are coordinately oriented within each inner ear organ, exhibiting a particular form of planar cell polarity (PCP) necessary for mechanotransduction. The coordinated orientation is vital for matured functions in hearing and balance. The cochlear PCP formation is mainly controlled by the non-canonical Wnt/PCP signal pathway, and the relative genes of Wnt are expressed in the procedure of inner ear development. However, the developmental events associated with establishing PCP in the vestibule are unclear to date. β-catenin is the core protein of canonical Wnt/β-catenin signaling. To further explore the canonical Wnt/β-catenin role in the development and polarity regulation of inner ear, our study was designed to explore the gross morphology changes of inner ear and the polarity transformation of HCs in the organ of Corti and the vestibular maculae.

Methods

β-catenin deletion was first induced at E11.5 and E12.5 in Sox2-CreERT;β-catenin$^{f/flox(exon2-6)}$ mice, and were dissected and analyzed at E18.5. Morphological changes of the inner ear were observed. The lengths of the otic vesicle and the organ of Corti, as well as the areas of utricular and saccular maculae were gauged and compared with the control group. Deletion of β-catenin was also induced at E15.5 and E16.5, the organ of Corti and the vestibule dissected, immunofluorescence stained and analyzed at P2.

Results

Compared with the control group, in earlier E11.5 and E12.5 days, knock-out of β-catenin in Sox2+ cells resulted in smaller otic vesicles, cochleae and vestibules and fewer HCs in vestibular sensory epithelium. In later E 15.5 and E16.5 stage, knock-out of β-catenin in Sox2+ cells resulted in patterning defects in the hair cell stereocilium, while a few kinocilia showed mis-orientation in the cochlea. In the vestibules, the line of polarity reverse could still be determined, but HCs scattered and misoriented in the maculae.

Conclusions

Knockout of β-catenin in precursor cells of the inner ear sensory epithelium results in inhibition of the development of inner ear and HCs, disturbance of the patterning

cell-cell arrangements in the cochlea, and disarray of the hair cell polarity in maculae of the vestibule. In summary, β-catenin is crucial for the inner ear development and HC polarity management in mice. The β-catenin-dependent canonical Wnt signaling is implicated in cochlear extension and PCP regulation of the inner ear.

PS 409

SOX2 is Sequentially Required for Non-sensory Formation Followed by Sensory Development in the Mammalian Inner Ear

Aleta Steevens[1]; Jenna C. Glatzer[2]; Peter Santi[3]; Amy Kiernan[2]
[1]*University of Rochester Medical Center; *[2]*University of Rochester; *[3]*University of Minnesota*

The transcription factorSOX2 is firmly established as a factor critical for the development of all the inner ear sensory progenitors. However, it is not known how early and specifically SOX2 marks the sensory areas, nor whether it is exclusively required for these regions. To address these questions and elucidate the mechanism of SOX2 function, we used a tamoxifen-inducible Cre recombinase system to simultaneously fate map and delete SOX2 throughout otocyst stages. Sox2-Cre[ERT2] mice were crossed with a Rosa26[CAGtdTomato]/Sox2^{+/fl} line and Cre recombination was induced at either embryonic day (E)8.5, E10.5, or E12.5. Embryos were harvested when cell types were identifiable (E18.5). Fate-mapping demonstrated that in the cochlea, early (E8.5 & E10.5) SOX2 primarily contributes to non-sensory tissue and does not contribute to the organ of Corti in all turns until later (E12.5). In the vestibule, early SOX2 is diffusely reported in both sensory and non-sensory cells, whereas later (E12.5) SOX2 is specific to the sensory regions. Timed-deletion experiments demonstrated that early SOX2 is important for non-sensory formation and inner ear morphogenesis, whereas deletion of SOX2 later (E12.5) produced morphologically normal inner ears lacking an organ of Corti. Because SOX2 is also a required factor for the formation of inner ear neurons, it was possible that some of the morphological defects were caused secondarily by a reduction of the cochleovestibular ganglia (CVG). To investigate this, we examined ears from NEUROG1-deficient mice (Neurog1^{-/-}),that completely lack the CVG. NEUROG1-deficient ears showed a much milder morphological inner ear phenotype, indicating that the defects in E8.5-deleted SOX2 mutants were not due to loss of the CVG, but rather loss of early non-sensory SOX2 expression. Short-term harvests (E10.5-E11.5) further demonstrated that SOX2 was initially (E8.5 & E9.5) localized to the dorsolateral portion of otocyst that mainly gives rise to the vestibule and non-sensory cochlear tissue. Around E10.75 we observed a dynamic switch in which a broad dorsolateral otic domain became largely negative for SOX2, while the ventromedial region became positive. Based on the later fate mapping results, these changes likely correspond to the switch in SOX2 expression from largely non-sensory regions, to the more exclusive expression in the sensory areas. Taken together, these results indicate that the morphological defects in SOX2 mutants are directly due to loss of SOX2, and do not occur secondarily due to loss of sensory or neuronal development, establishing an early and novel role for SOX2 in otic development.

SOX2Nonsensory_ARO_Abstract_2018__final.docx

PS 410

Six1 is essential for differentiation and patterning of the mammalian auditory sensory epithelium

Ting Zhang[1]; Jinshu Xu[1]; **Pin-Xian Xu**[2]
[1]*Icahn School of Medicine at Mount Sinai; *[2]*Icahn School of Medicine ay Mount Sinai*

The organ of Corti in the cochlea is a two-cell layered epithelium: one cell layer of mechanosensory hair cells that align into one row of inner and three rows of outer hair cells interdigitated with one cell layer of underlying supporting cells along the entire length of the cochlear spiral. These two types of epithelial cells are derived from common precursors in the four- to five-cell layered primordium and acquire functionally important shapes during terminal differentiation through the thinning process and convergent extension. Here, we have examined the role of Six1 in the establishment of the auditory sensory epithelium. Our data show that prior to terminal differentiation of the precursor cells, deletion of Six1 leads to formation of only a few hair cells and defective patterning of the sensory epithelium. Previous studies have suggested that downregulation of Sox2 expression in differentiating hair cells must occur after Atoh1 mRNA activation in order to allow Atoh1 protein accumulation due to antagonistic effects between Atoh1 and Sox2. Our analysis indicates that downregulation of Sox2 in the differentiating hair cells depends on Six1 activity. Furthermore, we found that Six1 is required for the maintenance of Fgf8 expression and dynamic distribution of N-cadherin and E-cadherin in the organ of Corti during differentiation. Together, our analyses uncover essential roles of Six1 in hair cell differentiation and formation of the organ of Corti in the mammalian cochlea.

PS 411

Translatome Analysis of Outer Hair Cells and Supporting Cells from Adult Mouse Inner Ears

Beatrice Milon[1]; Yoko Ogawa[1]; Yang Song[2]; Ran Elkon[3]; Ronna Hertzano[4]
[1]University of Maryland School of Medicine, Baltimore, MD, USA; [2]University of Maryland School of Medicine, Baltimore MD, USA; [3]Department of Human Molecular Genetics and Biochemistry, Sackler School of Medicine, Tel Aviv University, Tel Aviv, Israel; [4]University of Maryland School of Medicine, Baltimore, MD USA

While many studies have described the transcriptomes of the different cell types in the embryonic and perinatal mouse inner ear, cell-specific data for the adult inner ear are still largely missing. The lack of data could be in part due to the technical challenge of atraumatic dissociation of the mature inner ear. This gap in the knowledge is important as we consider candidate genes and pathways that may underlie acquired and age related hearing loss.

Here, we used the RiboTag approach to characterize gene expression profiles of outer hair cells (OHCs) and supporting cells (SCs) from 10-week old mice. The RiboTag mouse results in hemagglutinin- (HA) tagging of the 60S ribosomal subunit in the presence of Cre-recombinase, subsequently allowing immunoprecipitation (IP) of actively translated mRNA with an antibody for the HA tag. We generated RiboTag;PrestinCreERT2 and RiboTag;Sox2CreERT2 mice to enrich for OHC and SC actively translated transcripts, respectively. Cre recombination was induced at 2 weeks of age by tamoxifen injection.

Our results using a reporter mouse show that while prestinCreERT2 is specific for OHC, Sox2CreERT2 induces recombination in SC as well as in a subset of cells in the spiral ganglion which are consistent with glial cells. To identify OHC and SC-specific transcripts, a gene was labelled as specific for a cell-type if it was enriched at least two fold in its corresponding IP as compared to the input, and depleted at least two fold in the IP of the other cell types. We identified 410 transcripts specific for OHC and 282 transcripts specific for SC/glial cells. Fifty six of the OHC-specific transcripts and 37 of the SC/glial-specific transcripts mapped to genomic intervals of unresolved deafness loci. A gene ontology analysis (FunRich) showed that the OHC-specific transcripts are enriched for nuclear proteins, while SC-specific transcripts are enriched for genes that encode plasma membrane proteins. Finally, a cis-regulatory analysis using the iRegulon program predicted a major role for IKZF2 and GFI1 in regulating the OHC translatome, and SOX2 and REST in regulating the supporting cell/glial translatome.

In conclusion, the RiboTag approach combined with cell type-specific Cre-expressing mouse lines is a powerful method to identify cell-type specific expression profiles in the adult mouse cochlea.

PS 412

Characterizing a Novel vGlut3-P2A-iCreER Knock-in Mouse Strain in Cochlea

Chao Li[1]; Yilai Shu[2]; Guangqin Wang[1]; He Zhang[1]; Ying Lu[1]; **Zhiyong Liu**[1]
[1]Institute of Neuroscience, Chinese Academy of Sciences; [2]1. Department of Otolaryngology, Harvard Medical School, 2. Eaton-Peabody Laboratory, Massachusetts Eye and Ear Infirmary, 3. Department of Otolaryngology, Hearing Research Institute, Affiliated Eye and ENT Hospital of Fudan University

Precise mouse genetic studies rely on specific tools that can label specific cell type. In mouse cochlea, previous studies suggest that vesicular glutamate transporter 3 (vGlut3), also known as Slc17a8, is specifically expressed in inner hair cells (IHCs) and loss of vGlut3 causes deafness. To take advantage of its unique expression pattern, here we generate a novel vGlut3-P2A-iCreER mouse strain. The P2A-iCreER cassette is precisely inserted before the stop codon of vGlut3, by which the endogenous vGlut3 is intact and paired with iCreER as well. Approximately, 10.7 ± 0.8 % (n=3), 85.6 ± 8.1% (n=3), 41.8% ±9.9% (n=3) of IHCs are tdtomato+ when tamoxifen is given to vGlut3-P2A-iCreER/+; Rosa26-LSL-tdtomato/+ reporter strain at P2/3, P10/11 and P30/31, respectively. Tdtomato+ OHCs are never observed. Interestingly, besides IHCs, glia cells, but not spiral ganglion neurons (SGNs), are tdtomato+, which is evidenced by the presence of Sox10+/tdtomato+ and td-tomato+/Prox1(Gata3 or Tuj1)-negative cells. We further independently validate vGlut3 expression in SGN region by vGlut3 in situ hybridization and antibody staining. Furthermore, total number of tdtomato+ glia cells decreased gradually when tamoxifen is given from P2/3 to P30/31. Taken together, vGlut3-P2A-iCreER is an efficient genetic tool to specifically target IHCs for gene manipulation, which is complimentary to Prestin-CreER strain exclusively labelling cochlear outer hair cells (OHCs).

PS 413

Application of CRISPR-stop technology for high-throughput gene screening in mouse inner ear.

He Zhang[1]; Hong Pan[2]; Changyang Zhou[1]; Yifei Ren[3]; Yu Wei[3]; Wenqin Ying[1]; Hui Yang[1]; Zhiyong Liu[1]
[1]Institute of Neuroscience, Chinese Academy of Sciences; [2]Guangxi University; [3]Institute of Neuroscience, Chinese Academy of Sciences

Genetic manipulation greatly contributes to identification of critical genes during mouse inner ear development. Recently it is reported that CRISPR base editor (BE3) approach can create stop codon by directly converting single nucleotide C to T without causing double strand break, which is called "CRISPR-stop" approach. By microinjecting four Tyr sgRNAs into zygotes together with BE3, Tyr homozygous mutant F0 mice with white skin hair are produced effectively. Because hair cells (HCs) are completely absent in Atoh1 -/- mouse, we further mutate Atoh1 to test the efficiency of this approach in inner ear. Two, three and four Atoh1 gRNAs are injected together with BE3, 10/10, 7/8 and 10/10 F0 mice cochlea completely lose HCs, respectively. It suggests that two gRNAs are enough to achieve efficient homozygous mutagenesis. In the end, we simultaneously inject vGlut3 and prestin gRNAs together with BE3, and 10/10 F0 mice lose vGlut3 and prestin expression are generated. It makes possible multiple gene mutation at the same time. Taken together, CRISRP-stop is an efficient genetic approach to generate F0 homozygous mutants, which greatly reduces the burden of mouse breeding and is suitable to perform high-throughput gene screening in mouse inner ear.

PS 414

Interplay between Atoh1 and Neurod1 bHLH transcription factors during inner ear development

Iva Macova[1]; Martina Dvorakova[1]; Romana Bohuslavova[1]; Tetyana Chumak[2]; Josef Syka[3]; Bernd Fritzsch[4]; Gabriela Pavlinkova[1]
[1]Laboratory of Molecular Pathogenetics, Institute of Biotechnology CAS; [2]Institute of Experimental Medicine CAS; [3]Department of Auditory Neuroscience, Institute of Experimental Medicine of the Czech Academy of Sciences; [4]University of Iowa

Background
The basic Helix-Loop-Helix transcription factors (bHLH TFs) are indispensable for neuronal development in the central and peripheral nervous system. Several bHLH TFs are also indispensable for neurosensory development in the ear, where they form a not yet fully understood cross-regulatory network. In particular, Neurod1 plays a central role in the differentiation and survival of cochleovestibular neurons and Atoh1 in the differentiation of sensory epithelium. Neurod1 is also regulated by Atoh1 and in turn regulates Atoh1.

Methods
We used mouse model Islet1-Cre to delete Atoh1 or/and Neurod1 genes. The phenotypes of conditional deletion mutants were evaluated using immunohistochemistry, in situ hybridization, ABR and DPOAE analyses.

Results
After conditional deletion of Atoh1, neither hair cells nor supporting cells are found in the inner ear and as a consequence, nerve fibers are missing at P0. The loss of Neurod1 results in cochlear shortening and disorganization of hair cells in apex. The number of spiral ganglion neurons of Neurod1 deletion mutant is reduced compared to control. These morphological changes are associated with significant hearing impairment of adult Neurod1 mutant mice. Double deletion of Atoh1 and Neurod1 genes results in similar changes in sensory epithelium observed in mice with Atoh1 single conditional excision. However, inner ear innervation of double Atoh1/Neurod1 mutant forms a unique and yet undescribed pattern.

Conclusions
The transcription factor Islet1 plays a key role in the specification of neurosensory cells in the inner ear. Our results confirm necessity of Atoh1 for hair cell differentiation and Neurod1 for cochleovestibular ganglion formation. An ongoing challenge is to define the mechanistic contributions of the double deletion of Atoh1 and Neurod1 in neuronal fiber guidance.

PS 415

Hedgehog co-receptor Cdo negatively regulates inner ear hair cell specification

Elaine Y.M. Wong[1]; Helena Caro[2]; Yujien Liu[2]; Marcus Atlas[3]; Rodney Dilley[3]
[1]Ear Science Institute Australia, Nedlands, Australia; [2]School of Biomedical Sciences, The University of Hong Kong, Hong Kong SAR, China; [3]Ear Sciences Centre, The University of Western Australia, Nedlands, Australia

Hearing loss is one of the most common congenital disorder affecting over 360 million people globally, with approximately 1 in 800 children born with a serious permanent hearing impairment. Although genes involved in deafness have been reported, a large number of human deafness related genes remain to be identified. The development of the inner ear involves complex processes of patterning, morphogenesis and cell fate specification.

Cdo (Cell adhesion molecule-related, down-regulated by oncogenes) is novel receptors of the Hedgehog (Hh) pathway. Mutations in Cdo cause holoprosencephaly, a human congenital anomaly defined by forebrain midline defects prominently associated with diminished Hedgehog pathway activity. Cdo functions as both components and targets of the Hh signalling and feedback network. Cdo enhances Shh signalling by acting as co-receptors with Ptch1, or via regulation of Gli transcription factors. A proper balance of Gli repressor and activators is required to mediate Hh signalling druing inner ear morphogenesis.

Cdo homozygous knockout mice have profound hearing loss. However, the role of Cdo in inner ear development is still unknown. To understand the function of Cdo co-receptor in the modulation of Hh signaling in mammalian inner ear development, we present the differential expression pattern of Cdo in the developing mouse inner ear and analyse Cdo mouse mutant phenotypes. We found that the expression of Cdo at E12.5 marks the prospective organ of Corti, but by E16 Cdo is down-regulated in cells that will differentiate into hair cells and becomes restricted to supporting cells, suggest that Cdo may have distinct roles in molecular pathways that direct cells towards different cell fates in cochlea. Besides, the otic vesicle-derived inner ear structures are under-developed, with reduced proliferation and premature cell cycle exit during prosensory specification and ectopic hair cells formation in the Cdo mutants. It is possible that Cdo in Hh signaling are required for inhibiting cells from differentiating into hair cells and specifying progenitor cells to generate the distinctly fated cell populations in the inner ear.

PS 416

The Role of LIN28B and let-7 miRNAs in Cochlear Tonotopic Specialization

Meenakshi Prajapati; Angelika Doetzlhofer
The Solomon H. Snyder Department of Neuroscience and Center for Sensory Biology, Johns Hopkins University School of Medicine

The inner ear cochlea is the organ responsible for the detection of sound. Its spiral-shaped sensory epithelium contains mechano-sensory hair cells (HCs) that transduce sound waves into neuronal signals. This sensory epithelium is tonotopically organized such that it detects high frequency sounds at the base of the spiral and low frequency sounds at the apex. Features of this tonotopic specialization include graded differences in HC soma and stereocilia size as well as differences in HC-specific gene expression. Little is known of the mechanisms that produce tonotopic specialization in the mammalian cochlea. Here, we investigate the role of the RNA binding protein LIN28B and the let-7 family of miRNAs in co-

chlear tonotopic specialization. The mutual antagonistic LIN28B and let-7 miRNAs are post-transcriptional regulators that control the expression of large numbers of genes in a dose-dependent manner. Our lab has recently shown that opposing expression gradients of LIN28B and let-7s in the cochlea regulate the timing of cell cycle exit and HC differentiation (Golden at al., 2015). Interestingly, we found that these gradients persist during the maturation and tonotopic specialization of HCs, with let-7s being highest expressed in basal HCs, and LIN28B being highest expressed in apical HCs. To determine the role of LIN28B and let-7 miRNAs in the tonotopic specialization of HCs, we manipulated LIN28B/let-7 levels in maturing HCs using LIN28B or let-7g overexpressing transgenic mice. To determine if these manipulations disrupt frequency-specific HC function, we recorded Auditory Brainstem Responses (ABRs) from these mice. Our hypothesis predicts that LIN28B overexpression will result in a more 'apical' identity of HCs. This would disrupt the function of the basal (high frequency) region of the cochlea. Indeed, ABRs from these mice revealed a severe deficit specifically in high frequency hearing, compared to control littermates. Histological analyses confirmed that these deficits are not due to HC loss. Conversely, overexpression of let-7g would cause HCs to have a more 'basal' identity, and a deficit in transduction of low frequency sound. Consistent with this prediction, mice overexpressing let-7g during HC maturation show deficits specifically in low frequency hearing, compared to control littermates. These results suggest that the LIN28B/let-7 pathway plays a critical role in tonotopic specialization, with LIN28B activity conferring a more 'apical' identity to HCs, while let-7 miRNAs impart a more 'basal' identity. Funding: F31 DC016538 (MP) and David M. Rubenstein Fund for Hearing Research (AD)

PS 417

Short Stature Homeobox 2 in Zebrafish Otic Development

Alejandra Laureano[1]; Kathleen Flaherty[2]; Hatem Sabaawy[2]; Kelvin Kwan[1]
[1]Rutgers University; [2]Rutgers University-Cancer Institute of New Jersey

Introduction
The discovery and study of genetic factors that contribute to syndromic hearing loss allows advancement of early screening methods, diagnosis and treatment. Studying molecular factors that govern the development of the inner ear will lead to a better understanding of the etiology behind syndromic hearing loss. Using molecular biology and bioinformatics tools, the Short Stature Homeobox 2 gene (SHOX2)was identified as acandidate transcription factor involved in early auditory neuron development. To better understand and recapitulate

the role of SHOX2 in human inner ear development zebrafish was chosen as a model organism. Zebrafish, like humans possess both orthologues from the SHOX gene family, SHOX and SHOX2. Whereas mice only have the SHOX2 in their genome.

Results

Zebrafish shox2 has not been previously identified in the inner ear. Utilizing in situ hybridization, we showed that shox2 transcripts levels initially peaked at 18hpf (hpf) during otic development. shox2 is dynamically expressed throughout zebrafish development and continues to be present in otic cell types at 18, 24, and 48 hpf. Furthermore, expression of shox2 at 18hpf correlates with the known early otic vesicle marker pax2a. At 48hpf we observed expression of shox2 transcript in the vicinity of anterior maculae. To further assess the function of shox2 in the developing inner ear, antisense morpholinos were used to reduce shox2 transcript levels. At 72 hpf embryos were tested for abnormal behavior. The observed behaviors in shox2 morphants include circling, lack of avoidance behavior and spasms. These behaviors suggested inner ear and neurological deficits. Embryos with low shox2 levels correlated to abnormal behaviors. To further determine the role of shox2 in inner ear development, a shox2 null mutation was generated using CRISPR/Cas9.

Discussion

These results suggest the involvement of shox2 in early otic neurosensory development. We propose that shox2 is essential for determining hair cell and neuronal fate. Generation of shox2 reporter lines for cell lineage tracing will help determine the cell progeny that arise.

PS 418

The role of neuroligins and neurexins in mechanosensory hair cell synapse formation

John H. Oldroyd; Alek Graff; Mary Davis; Arminda Suli
Brigham Young University

Emerging evidence suggests that assembly of neurocircuits and establishment of synapses relies on concerted actions of cell adhesion molecules (CAM). Neurexins (nrxns) and neuroligins (nlgns) are two families of CAMs that, when expressed in heterologous cells, promote adhesion between these cells in a Ca 2+ dependent manner. In co-culture experiments, expression of nlgns in fibroblast cells can induce the formation of pre-synaptic terminals in the axons of neurons touching these non-neuronal cells. The pre-synaptic terminals show all the hallmarks of regular synapses including synaptic vesicles, electron-dense material at the plasma membrane as well as known pre-synaptic proteins. In

an in vivo setting, knocking out nrxns or nlgns in mice show dramatic functional impairments, including perinatal death. However, no significant defects in synaptogenesis were observed. Therefore, it is thought that nrxns and nlgns are not required for the initiation of synaptogenesis, but rather needed to organize synaptic molecules and promote synapse maturation. We found that nlgn2a and nlgn2b are expressed in the afferent neurons innervating the mechanosensory hair cells (HC) in the lateral line system of zebrafish larvae, which are similar to the auditory and vestibular HCs. Furthermore, looking at the BioVU patient sample set from the Vanderbilt University Medical Center, we found a significant correlation of hearing loss with SNPs in the nrx2 gene, which codes for nrx2 protein, the binding partner of nlgn2 protein. This suggested that nlgn2a, nlgn2b and their nrxn2 binding partners might be involved in the development of HC synapses. We are in the process of determining the role of these proteins in HC synapse development by knocking these genes using the CRISPR/Cas9 technology and analyzing synapse formation in HCs and behavioral impacts in the mutant larvae.

PS 419

The Notch Ligand Jagged1 is Required for the Survival of Supporting Cells in the Mouse Cochlea

Elena Chrysostomou[1]; Luyi Zhou[2]; Kaley Graves[2]; Yuanzhao Darcy[2]; Michelle Randle[2]; Angelika Doetzlhofer[1]; Brandon C. Cox[3]
[1]The Solomon H. Snyder Department of Neuroscience and Center for Sensory Biology, Johns Hopkins University School of Medicine; [2]Department of Pharmacology, Southern Illinois University School of Medicine; [3]Department of Pharmacology and Department of Surgery, Division of Otolaryngology, Southern Illinois University School of Medicine

The highly organized, mosaic pattern of hair cells (HCs) and supporting cells (SCs) in the mammalian cochlea is thought to be the result of Notch-mediated lateral inhibition which occurs during embryonic development. Progenitor cells destined to become HCs express Notch ligands which bind to the Notch receptor expressed on neighboring cells to inhibit a HC fate and promote a SC fate. In addition to this HC repressive function, a recent study by Campbell et al., suggests that Notch signaling may play an instructive role in SC development and survival. A potential candidate for mediating this function is the Notch ligand, Jagged 1 (Jag1). In the differentiating cochlea Jag1 is expressed by SCs. While other Notch ligands are downregulated during the first postnatal week, SC-specific Jag1 expression continues throughout adulthood where its function is unknown. To investigate the role of Jag1 in differentiating SCs, we gen-

erated Sox2-CreER/+::Jag1loxP/loxP mice which received tamoxifen at embryonic day (E) 14.5 and E15.5 and were analyzed at E18.5. Controls included Cre-negative littermates, as well as Sox2-CreER/+::Jag1loxP/loxP and Sox2-CreER/+ mice thatdid not receive tamoxifen to control for Sox2 haploinsufficiency. In the absence of Jag1, we found that the density of SCs that surround outer HCs, particularly the Deiters'; cells and Hensen cells, was significantly reduced compared to controls. Similar changes were also observed in the postnatal cochlea, when Jag1 was deleted from HCs, pillar, and Deiters'; cells using Fgfr3-iCreER::Jag1loxP/loxP mice that received tamoxifen at postnatal day (P) 0 and P1. In the samples with P0 deletion of Jag1, we observed a loss of Hensen cells at P7, and in contrast to embryonic deletion of Jag1, Deiters'; cells remained intact. However, loss of Jag1 did not alter HC density in either model, suggesting that the reduction in SCs was not due to SC-to-HC conversion, but likely due to defects in SC formation and survival. At P30, mice lacking Jag1 expression exhibited hearing loss at 4 kHz and besides the loss of Hensen cells, there were no further morphological changes. To identify pathways/genes that may be deregulated in the absence of Jag1, we conducted a series of microarray experiments using Sox2-CreER/+::-Jag1loxP/loxP mice with tamoxifen given at E14.5/15.5. These experiments revealed mitochondrial dysfunction as a potential mechanism for the observed defects in SC formation/survival. Taken together, our preliminary data suggests that Jag1 is required for the survival/formation of SCs and that loss of these cells leads to hearing loss. Funding: NIH/NIDCD R01DC011571 (AD and EC) and DOD CDMRP W81XWH-15-1-0475 (BC)

PS 420

Multi-scale analysis of the interplay between cell morphology and cell-cell signaling

Liat Amir Zilberstein[1]; Roei Cohen[1]; Dmitri Rivkin[1]; Micha Hersch[2]; David Sprinzak[1]
[1]Tel Aviv University; [2]University of Lausanne and Swiss Institute of Bioinformatics

Multi-scale analysis of the interplay between cell morphology and cell-cell signaling

During its development, the organ of Corti undergoes a transition from an undifferentiated disordered tissue to the precisely patterned rows of intercalated hair and supporting cells. This transition involves spatially coordinated differentiation of cells as well as dramatic changes in the morphology of the whole tissue and of the individual cells. While some of the regulatory processes involved has been elucidated, we still lack a systems level understanding of how differentiation processes and cellular mechanics coordinate this transition.

To study the interplay between cell morphology and Notch signaling in the developing mammalian cochlea, we established an assay that allows tracking of tissue dynamics as well as the differentiation state of the cells in the organ of Corti. To do that we generated a double transgenic line expressing both a green fluorescent membrane tag (ROSA26-ZO1GFP) and Atoh1-GFP, which is a marker for hair cell precursors. This setup enables tracking of both the cell boundaries and the cellular differentiation states over time. Our preliminary results show that the local organization of cells in the organ of Corti is quite dynamic, exhibiting significant changes in cell morphology as well as rearrangements over periods of tens of minutes. We are developing automated image analysis code to extract quantitative data both on cellular morphology and on dynamics of regulatory processes.

On the modeling side, we develop a hybrid modeling approach combining regulatory circuits, such as lateral inhibition, with mechanical models describing the position and shape of each cell. We show how a combination of cellular reorganization and differentiation circuits can give rise to precise and robust patterning. Taken together, our results suggest a unified picture of the patterning of the organ of Corti.

PS 421

Development of vestibular organ cultures of utricle, saccule and crista ampullaris in which hair cells are attached to the superior and inferior vestibular ganglia

Haiyan Jiang[1]; Dalian Ding[2]; Jianhui Zhang[3]; Richard Salvi[4]
[1]Staet University of New York at Buffalo; [2]University at Buffalo, USA; [3]State University of New York at Buffalo; [4]Center for Hearing and Deafness; State University of New York at Buffalo

Background
Vestibular organotypic cultures have been used to study hair cell function, vestibular organ developments and the processes involved in hair cell degeneration and regeneration. We previously developed organotypic cultures of the utricle containing the hair cells, but are unaware of organotypic cultures in which the utricle, saccule or crista ampullaris were cultured along with their vestibular nerve fibers. To address these issues, we developed vestibular dissection techniques in which the vestibular end organs remain connected with the vestibular nerve fibers and neurons.

Methods
Vestibular organotypic cultures were derived from post-

natal day 3 (P3) rat pups. The macula of utricle and the crista ampullaris of the lateral and superior semicircular canal together with the superior vestibular ganglion neurons and superior vestibular nerve trunk were carefully micro-dissected out in Hanks solution. The macula of saccule and crista ampullaris of the posterior semicircular canal along with the inferior vestibular ganglion neurons and nerve trunk were also micro-dissected out separately. The vestibular end organs together with their connecting vestibular ganglion neurons were placed on a drop of collagen gel in serum free medium and cultured several days. After the fixation, the sensory hair cells of vestibular explants were stained with Alexa Fluor 555-conjugated phalloidin and the vestibular ganglion neurons and their nerve fibers and terminals were immunolabeled with tubulin and Alexa Fluor-488-conjugated secondary antibody.

Results
Using confocal fluorescence microscopy, two types of vestibular hair cells, type I and type I and their connecting vestibular peripheral ganglion neurons could be clearly identified. The red-fluorescently-labeled hair cells had well-organized stereocilia bundles with a kinocillium. The green fluorescently labeled vestibular ganglion neurons gave off peripheral nerve fibers that formed nerve terminals beneath the type I and type II hair cells.

Conclusion
The development of vestibular organ culture of the utricle, saccule and crista ampullaris connected to the superior and inferior vestibular ganglia will provide researchers with a useful in vitro model for studying vestibular development, the toxic effect of drugs on both hair cells and neurons and the electrophysiological properties of the type I and II hair cells and neurons.

Haiyan Vestibular culture V2.docx

PS 422

ATP Activated Ca2+ Signalling in the Deiters' cells of the Mature Organ of Corti in Mouse Hemicochlea Preparation

Eszter Berekméri[1]; Ádám Fekete[2]; László Köles[1]; Beáta Sperlágh[3]; Tibor Zelles[4]
[1]Department of Pharmacology and Pharmacotherapy, Semmelweis University; [2]The Hospital for Sick Children; [3]Institute of Experimental Medicine, Hungarian Academy of Sciences; [4]Department of Pharmacology and Pharmacotherapy, Semmelweis University; Institute Of Experimenal Medicine, Hungarian Academy Of Sciences

The supporting cells of the organ of Corti and their ATP activated Ca^{2+} signalling are studied extensively in cochlear explants of newborn mice and the fundamental role of the ATP-dependent spontaneous activity in cochlear development has been shown. However, information on purinergic Ca^{2+} signalling in the mature cochlea are much sparse.

We have investigated the ATP-evoked Ca^{2+} signals in Deiters'; cells in the hemicochlea preparation of hearing mice (>P15).

Single-cell electroporation of Deiters';cell with Ca^{2+} sensitive dyes and their fluorescent imaging showed that the ATP-induced Ca^{2+} elevation in the process preceded the one in the soma by several seconds. The phenomenon was present in different mouse strains and was independent from the direction of ATP perfusion. The adenosine receptor antagonist 8-(p-sulfophenyl)-theophylline did not inhibit the ATP response and perfusion of adenosine had no effect on the concentration of intracellular Ca^{2+}. The omission of the Ca^{2+} from the extracellular solution and inhibition of L-type voltage-gated Ca^{2+} channels (L-VGCCs) by nifedipine reduced the time delay between the process and the soma response and decreased the amplitudes of the Ca^{2+} transients in both compartments of the Deiters'; cells. In contrast, the sarco/endoplasmic reticulum Ca^{2+}-ATPase inhibitor cyclopiazonic acid, which empties intracellular Ca^{2+} stores by preventing their refilling, increased the time delay, whilst the amplitudes were decreased in both compartments.

Our results show that adenosine receptors are not, but extracellular Ca^{2+} dependent P2X and intracellular Ca^{2+} store dependent P2Y receptors are involved in the ATP-evoked Ca^{2+} transients. Influx of Ca^{2+} through L-VGCCs was required for the proper Ca^{2+} dynamics. The time delay between the transient in the phalangeal process and the soma of Deiters'; cells might be caused by the different subcellular distribution of the ionotropic and metabotropic ATP receptors. Subcellular differences in ATP-evoked intracellular Ca^{2+} dynamics might reflect the active role Deiters'; cells play in mature hearing, i.e., participation in cochlear amplification and protection against excessive noise exposure.

PS 423

Effect of Everyday Listening Conditions on Preferred Listening Levels

Gibbeum Kim[1]; Ji Hun Shin[2]; Woojae Han[3]; Changgeun Song[4]; Chanbeom Kwak[5]
[1]Department of Speech Pathology and Audiology, Graduate School, Hallym University; [2]Department of Convergence Software, Graduate School, Hallym University; [3]Division of Speech Pathology and Audiology, College of Natural Science, Hallym University; [4]Department of Convergence Software, College of Information and Electronic Engineering, Hallym University; [5]Division of Speech Pathology and Audiology, College of Natural Sciences, Hallym University

Purpose

Personal listening devices (PLD), such as MP3 players, are conveniently used to listen to music through simple earphones. More recently, the MP3 function of the newest smartphones enables everyone to listen to music without additional PLD. However, in noisy environments, the user often raises the volume to louder than usual. The purpose of the current study was to investigate the influence of listening environments on users' preferred listening levels while applying a newly developed smartphone application.

Methods

Fifty-one young listeners (26 male and 25 female) with normal hearing participated in the study. They were asked to listen to four genres of music (K-ballad, K-dance, Pop songs, New Age) in five different listening environments (library, on-campus, off-campus, cafeteria, gym) at a preferred listening volume level. At the same time, their smartphone installed the application to measure background noise levels through an external microphone and their preferred volume level through an internal microphone while music was playing. Data was analyzed by mean levels of the background noises and volume levels in terms of sound pressure level in decibels (dB SPL).

Results

The results showed that there was a significant difference in results among background noise levels and genres of music. Use of devices at the gym and library showed the highest (70.14 dB SPL) and the lowest volume levels (61.47 dB SPL), respectively. That is, the participants demonstrated higher preferred listening levels in noisy environments as compared to quiet environments. Also, among the music genres studied, K-dance and New Age showed the highest (70.98 dB SPL) and the lowest preferred listening levels (59.32 dB SPL), respectively. As we expected, subjects' preferred listening levels were significantly increased as a function of the four music genres among the different background noise levels.

Conclusion

In summary, depending on levels of background noise, subjects' listening levels could be increased unconsciously. Moreover, as environmental noise increases, listening volume levels will increase, which suggests that public education and more concrete criteria to keep the users' healthy hearing are needed to prevent potential noise-induced hearing loss and/or tinnitus.

PS 424

Effects of Developmental Conductive Hearing Loss on Cochlear Tuning

Yi Ye[1]; Antje Ihlefeld[2]; Merri J. Rosen[3]
[1]Hearing Research Group, Dept. Anatomy&Neurobiology, Northeast Ohio Medical University; [2]New Jersey Institute of Technology; [3]Hearing Research Group, Dept. Anatomy & Neurobiology, Northeast Ohio Medical University

Conductive hearing loss (CHL) is frequently experienced during childhood as a result of otitis media, an illness correlated with later problems in speech processing (Whitton & Polley, JARO 2011). An extensive literature demonstrates that bilateral CHL induces neural changes across the entire auditory system. Bilateral malleus removal induced early in development is often used as a model for childhood otitis media. A premise of this model is that malleus removal attenuates acoustic transmission without altering peripheral tuning. However, there is conflicting evidence in the literature. In animals with adult-induced CHL, normal bone conduction thresholds suggest an absence of peripheral sensorineural damage (Tucci et al., Laryngoscope 1999). Nevertheless, reduced inner hair cell synaptic counts can emerge over time, at higher frequencies (Liberman et al., PLoS One 2015). No study has explicitly tested whether extended CHL alters peripheral tuning, nor have long-lasting tuning effects as a result of developmental CHL been examined. Here in Mongolian gerbils, we tested the effect of early bilateral malleus displacement on peripheral tuning, as assessed in adulthood with compound action potential (CAP) measurements from the round window. CHL was induced at P11, prior to ear opening, by bilateral malleus dislocation. Cochlear CAPs were measured from the round window of the right ear at ages ranging from P100 to P200 using free field stimulation from a calibrated speaker. Outer and middle ear dissection verified malleus dislocation. Animals with middle ear infections were excluded. Measured by CAPs, malleus dislocation created on average a 25-35dB threshold shift across frequencies from 1-16kHz. Cochlear tuning was then measured using forward masking of tone bursts at

1, 2, 4, 8, and 16kHz, with the center tone presented at 20dB above threshold, and flanking maskers presented at 1/10 octave increments. The tuning curve sharpness parameters Q10 and Q20 were calculated and compared between CHLs and controls. Overall, early CHL induced by malleus dislocation created shallower tuning curves across frequencies in adulthood. However, the magnitude of the tuning differences was small, and was most pronounced in the tails of the tuning curves, as opposed to the peaks. The implications of these data will be discussed in the context of relevance for auditory perception. Work supported by NIH-NIDCD (R01 DC013314 to MJR and R03 DC014008 to AI).

PS 425

Identification of Cellular Lineage Trajectories in the Mouse Cochlea.

Kevin Shengyang Yu[1]; Stacey M. Frumm[1]; Lauren E. Byrnes[1]; Daniel D.E. Wong[2]; Angie Koo[1]; Heydi Malave[1]; Julie B. Sneddon[1]; Aaron D. Tward[1]
[1]*University of California, San Francisco;* [2]*Equipe Audition, Departement d'Études Cognitives, Ecole Normale Supérieure*

Background
Cochlear development is a poorly understood process that requires complex interactions of multiple cell types throughout key developmental time points. The identities of these cell types and the cell states through which they pass remain mostly uncharacterized. Advances in single-cell RNA-sequencing (scRNA-seq) technology permit us to elucidate the heterogeneity of developmental systems with a far greater resolution than previously possible through improved measurements on gene expression profiles for cellular differentiation, signaling processes, cellular heterogeneity and cell identity.

Aim
To identify and characterize all cell types in the developing and adult cochlea via gene expression profiles and build a developmental trajectory for the cochlea.

Methods
We dissected and dissociated mouse cochlea from 6 time points (E12.5, E14.5, E16.5, E18.5, P2 and Adult) and performed scRNA-seq using the 10x Genomics platform. Using a graph-based clustering framework, we developed an algorithm to categorize and validate all cells into unique groups based on significant and differentially expressed genes. This method allowed us to define genes that are representative of each group, correlate these groups to previously characterized or unknown cells identities and then correlating these relationship throughout our different time points to develop lineage trees. Furthermore, we mapped known deafness genes and previously characterized cochlear markers to anchor and further our developmental atlas.

Results
Across developmental time, there is an expansion of the number of identified cell types within the cochlea that peaks around E18.5 after which there is a progressive maturation of the gene expression profiles of the different cells. There are 12 groups at E12.5 and 88 groups at P2 and cell cycling gene expression has ceased within all lineages by E18.5. We identified multiple novel subtypes of cells within the Organ of Corti, melanocytes, and mesenchymal cells of the cochlea while gaining a higher resolution expression profile for known groups. Using in situ hybridization, we validated many of the predicted and previously unknown cell types. In addition, the map of deafness genes onto this lineage tree provided many insights on the cellular mechanism by which they cause deafness.

Conclusions
The cochlea possesses a previously unappreciated diversity of cell types, with specification completed by E18.5 and a process of cellular maturation that terminates in adulthood. This work also forms the basis of a developmental atlas of cells within the cochlea with utility in developmental biology, genetics, and regenerative medicine.

ARO_figure.pdf

Hidden Hearing Loss

PS 426

A sustained-exposure formulation of the neurotrophic factor BDNF protects against noise-induced cochlear synaptopathy in young adult and aged rats

Fabrice Piu; Natalia Tsivkovskaia; Rayne Fernandez; Xiaobo Wang; Anne Harrop-Jones; Tiffany Altmann; Jennifer Hou; Martha Pastuszka; Cintia Vasquez; Raylyn DeGuzman; Dragos Dherase; Bonnie Jacques
Otonomy Inc

Background
Cochlear synaptopathy has been recently identified as the primary pathology of various otic insults, in particular noise exposure and age-related hearing loss. It is characterized by the loss of synaptic connection between inner hair cells (IHCs) and type I spiral ganglion neurons (SGNs) with low spontaneous rates and high thresholds. Evidence of cochlear synaptopathy in humans has been demonstrated on the basis of cross-sectional observa-

tions from temporal bone studies, and has been direct-ly implicated in "hidden hearing loss" and the "cocktail party syndrome". Brain-Derived Neurotrophic Factor (BDNF) is a member of the neurotrophic factor family, a class of biomolecules involved in neuronal differenti-ation, maintenance and survival. In particular, BDNF is required for normal development and innervation of co-chlear hair cells, and its administration to the otic com-partment has been proposed to offer protection against noise insults. A thermosensitive, sustained-exposure formulation of BDNF was developed for round window delivery. Its pharmacokinetic and pharmacological activ-ity in a model of noise-induced cochlear synaptopathy were characterized in young adults and aged rats.

Methods

Male and female Sprague Dawley rats (ranging from 5 to 11 months old) received a single intratympanic ad-ministration targeting the round window membrane (IT-RWM) of the BDNF formulation at different doses. BDNF levels in the inner ear compartment were deter-mined at different time points by ELISA. For evaluation of noise-induced cochlear synaptopathy, several func-tional (ABR, Wave 1 amplitude) and histological (cochle-ar nerve synapse count, hair cell viability) parameters were monitored.

Results

The round-window delivery of a BDNF formulation pro-vided significant and sustained-exposure to the inner ear compartment for several weeks, depending on the dose. Following noise-exposure, BDNF statistically im-proved all measures of cochlear synaptopathy (ABR, Wave 1 amplitude, synaptic punctae counts) throughout the one-month duration of the study. BDNF treatment improved cochlear synaptopathy in both young and old rats, albeit to a different extent.

Conclusions

A sustained-exposure formulation of BDNF was effec-tive in alleviating noise-induced cochlear synaptopathy and demonstrated a suitable pharmacokinetic profile, therefore constituting an attractive and novel therapeu-tic approach for the treatment of cochlear synaptopathy associated disorders.

PS 427

Proteome Biology of Noise Induced Cochlear Synaptopathy

Nopporn Jongkamonwiwat[1]; Miguel Ramirez[1]; Kwang Pak[2]; Allen Ryan[3]; Jeffrey Savas[1]
[1]Department of Neurology, Feinberg School of Medicine, Northwestern University, Chicago, IL; [2]UCSD; [3]Departments of Surgery & Neuroscience, University of California San Diego and Veterans Administration Medical Center, La Jolla, CA

The World Health Organization reported that one third of hearing loss cases are caused by noise exposure. Recent evidence has shown that hearing deficits are commonly undetected due to reduced sensitivity with-in normal thresholds. Our research aims to ameliorate noise-induced cochlear synaptopathy by identifying sig-nificant proteins and pathways that affected from acous-tic overstimulation. We used ABR & DPOAE recordings to define the level of noise exposure to produce tem-porary or permanent threshold shifts (TTS, PTS). We found an exposure to 94 dB and 105 dB levels for 30 minutes elicits TTS and PTS, respectively. We have es-tablished several quantitative proteomic analysis work flows that have revealed the effect of noise on the co-chlear proteome. Cochleae were extracted immediate-ly after noise exposure to capture acute noise-induced protein perturbations. Liquid chromatography with tan-dem mass spectrometry (MS) was used to analyze co-chlea extracts at TTS and PTS of noise-exposed levels. To obtain accurate quantitation, we use cochleas from nitrogen-15 stable-isotope-labeled mice as an internal standard to quantitate a wide range of changes in pro-tein levels. Unlabeled and labeled cochleae were ho-mogenized and mixed 1:1, followed by protein precip-itation, trypsin digestion and MS analysis. Attractively, isobaric peptide labeling with 10plex TMT tags was used to unbiasedly quantitate the level of protein changes across the different levels of noise exposure. Acquired mass spectra were searched with ProLuCID/DTASe-lect2, and quantified with Census and QuantCompare. We successfully quantitated 4,376 cochlear proteins in the 105 dB noise exposure condition and identified small collection with significantly altered abundances follow-ing varying levels of noise exposure. Many upregulated proteins were associated with the SNARE component binding protein (Stxbp), proteins associated with ribbon synapse (Ctbp1, Ctbp2) also, inhibitory post-synaptic cytoskeleton protein Gephyrin, indicating strong alter-ation of synaptic proteins following cochlear insulted by noise. Abundances of several myelin associated pro-teins (Mbp, Prx and Mpz) were also widely increased, suggesting noise increase many proteins abundance. Interestingly, Cochlin a protein found in spindle-shaped cells located along nerve fibers between auditory gan-

glion and sensory epithelium, was found to be upregulated as a result of noise trauma. This protein plays a role in neurite extension to innervate hair cells. Moreover, we found several myosins were decreased from temporary to permanent damaging sound levels which confirm deterioration of hair cells structure. Overall, our MS based coverage of the noise-damaged cochlear proteome provides multiple protein targets. Currently, we are following up on these candidate proteins with biochemical assays, histological analysis, and preclinical animal models.

PS 428

Blast-induced cochlear synaptopathy in chinchillas

Tyler Hickman[1]; Christopher Smalt[2]; Johanna Babrow[2]; Thomas Quatieri[2]; M. Charles Liberman[3]
[1]Eaton Peabody Labs, Massachusetts Eye and Ear Infirmary, Harvard Medical School; [2]Bioengineering Systems and Technologies, MIT Lincoln Laboratory; [3]Harvard Medical School

Exposure to intense sound can destroy hair cells (HCs), and cause permanent threshold shift (PTS), but recent research shows that cochlear neurons are more vulnerable than HCs to acoustic overstimulation. Thus, exposures to continuous noise causing only temporary threshold shifts (TTS), and no permanent hair cell damage has, nevertheless, been shown to destroy ribbon synapses and permanently silence the spiral ganglion neurons that were connected to them. While cochlear thresholds return to normal, this synaptopathy reduces suprathreshold amplitudes of auditory brainstem responses (ABRs) and compound action potentials (CAPs). Synaptopathy may also cause difficulties hearing in noise and may be an important elicitor of tinnitus. Since blast injuries do not always cause PTS, but often cause tinnitus, we hypothesized that blasts producing large TTS and minimal PTS, as with continuous noise, may cause synaptopathy without HC loss.

To test this hypothesis, we exposed anesthetized chinchillas bilaterally to individual blasts, or trains of 5 - 10 blasts at intensities from 165 – 175 dB SPL peak. To create the insult, we used a compressed-air shock tube to generate Friedlander pressure waveforms similar to explosive blasts. Our aim was to create a large TTS, with minimal PTS, while minimizing damage to the middle ear. Cochlear function was assessed by CAPs and distortion product otoacoustic emissions (DPOAEs). Cochlear histopathology was assessed in cochlear wholemounts, immunostained to reveal hair cells (MyoVIIa), pre-synaptic ribbons (CtBP2) and post-synaptic glutamate receptors (GluA2).

Multiple exposures at 175 dB ruptured the eardrum, whereas exposures at 165 dB SPL did not. The 165 dB exposures caused a high-frequency TTS of 40 dB, at 2-5 hrs post-exposure. At 2 wks post exposure, animals exposed to 10 blasts at 165 dB showed minimal PTS (< 5 dB). Histological analysis showed virtually no loss of inner hair cells (IHCs), and only sporadic, localized loss of outer hair cells (OHCs). Significant IHC synaptopathy, i.e. 20 – 45% loss, was seen in many, but not all, exposed animals. There was no obvious correlation between loci of OHC damage and loci of synaptopathy. In contrast to the regionally diffuse synaptopathy seen after continuous noise exposures, blast-induced synaptopathy was highly localized, most commonly occurring in the 2 kHz and 8-16 kHz regions.

The apparent vulnerability of the 2 kHz region may be related to the ear-canal resonance near that frequency. The localized nature of blast-induced synaptopathy may be important in the generation of narrow-band tinnitus.

PS 429

Hidden Hearing Loss? Effects of Recreational Noise on Auditory Function and Evoked Potential Amplitude

Sarah K. Grinn; Kathryn B. Wiseman; Jason A. Baker; Colleen G. Le Prell
University of Texas at Dallas-Callier Center

Background
There is significant speculation about the extent to which common recreational activities, which can result in temporary threshold shift (TTS), may be hazardous. This study therefore tested hypothesized relationships between noise exposure and auditory function. First, baseline audiometric data was measured and potential associations with noise exposure history were assessed. Second, participants were followed prospectively to assess potential effects of new recreational sound exposure on auditory function.

Methods
Participants included 32 young adults (13M, 19F, ages 21-27) with thresholds of 25-dB HL or better from 250 to 8000 Hz, and plans to attend a loud recreational event. The study design included 3 pre- and post-exposure sessions. Otoscopy, tympanometry, pure-tone audiom-

etry (250 to 8000 Hz), distortion product otoacoustic emissions (DPOAEs) (f2 frequencies of 1000 to 8000 Hz), Words-in-Noise (WIN) test, and electrocochleography (eCochG) measurements at 70, 80, and 90-dB nHL (click and 2000 to 4000 Hz tone-bursts) were collected at each test session. Baseline data was collected at the first session. The second session occurred the day after a loud recreational event; this test time was selected to be consistent with previous animal studies. The third session was scheduled 1-week later to allow the recovery of any deficits to be assessed. A total of 26 participants completed all 3 sessions.

Results
The retrospective analyses revealed no statistically significant relationships between recreational noise history and auditory test metrics at baseline. After acute event exposures, there was a statistically significant relationship between recreational noise dose and deficits on the word-in-noise test. However, sound-evoked Wave I neural response amplitude was unchanged. Final tests one week later showed recovery of function on the WIN test.

Conclusions
There was no evidence of auditory deficits as a function of previous noise exposure history. In addition, there were no permanent changes in any study outcome measures after new recreational noise exposure. Although there were temporary deficits on the WIN test, we did not observe any evidence of changes in evoked potential amplitude even in the small number of participants with measurable TTS the day after recreational exposure. The observed pattern of small TTS deficits suggests little risk of synaptopathy from common recreational noise exposures experienced by these participants, and for this reason it is not surprising that there were no observed changes in evoked potentials. The current data did not support hypotheses that common, recreational noise exposure is likely to result in "hidden hearing loss".

PS 430

Ciliary Neurotrophic Factor Promotes Synapse Regeneration after Noise-Induced Cochlear Synaptopathy

Sepand Bafti[1]; Steven H. Green[2]
[1]University of Iowa; [2]The University of Iowa

Background
Noise exposure destroys cochlear afferent synapses between inner hair cells (IHCs) and spiral ganglion neurons (SGNs), even in the absence of hair cell loss or permanent threshold shift. This cochlear "synaptopathy" is a result of excess release of the neurotransmitter glutamate from IHCs and consequent glutamate excito-toxicity. Noise induced cochlear synaptopathy in animal models can be detected as a reduction in the number of synapses on the IHCs. Few, if any, synapses normally regenerate but application of neurotrophic factors such as BDNF or NT-3 promotes regeneration. NT-3 is normally expressed in the organ of Corti (OC) and appears necessary for regeneration. Ciliary Neurotrophic Factor (CNTF) is also normally expressed in the OC (Bailey & Green, 2014) and we ask here whether CNTF can promote cochlear synapse regeneration after synaptopathy resulting from excitotoxic trauma.

Methods
Cochlear explant cultures from postnatal day 5 rat pups were prepared as described by Wang et.al, 2011. These cultures maintain intact a portion of the organ of Corti, associated SGNs, and synaptic connections. Synaptopathy is caused by addition of the glutamate agonist kainic acid (KA) for 2 hours (equivalent to the duration of noise exposure used in vivo). Exposure was to 0.5 mM or 0.03 mM KA that, respectively, cause nearly complete synapse loss or synapse loss comparable to that seen after noise exposure in vivo. The cultures were then incubated for three days after KA exposure, with CNTF and/or NT-3 or no neurotrophic factors. Labeling was with anti-Ribeye (presynaptic ribbons), anti-PSD95 (postsynaptic densities) and anti-Myosin 6 (IHCs). Synapse counts were compared among experimental conditions and controls. To facilitate the process of quantifying synapse loss/regeneration in confocal image stacks we are developing software that automates it, rapidly and accurately counting synapses. Dose response experiments were performed using the culture method in order to identify what the optimum concentration for recovery is for in vivo experiments.

Results
Following exposure to 0.5 mM KA, which leaves 1-2 synapses/IHC, regeneration of cochlear synapses is significantly enhanced by CNTF, nearly as well as by NT-3; the difference between CNTF and NT-3 is not significant. Nearly half of the synapses were restored.

Conclusions
Our data shows that CNTF has the ability to promote synapse regeneration after excitotoxic trauma and may be useful for synapse regeneration after noise exposure in vivo.

Development of rodent models of cochlear synaptopathy and auditory neuropathy

Jeremy Barden[1]; Natalia Tsivkovskaia[2]; Xiaobo Wang[2]; Fabrice Piu[2]; Bonnie Jacques[2]
[1]*Otonomy; [2]Otonomy Inc*

Background

Rodent models of noise-induced hearing loss (NIHL) are commonly used to mimic human hearing loss and to evaluate the efficacy of potential therapeutic agents for hearing protection and restoration. In "hidden hearing loss", the primary pathology is synaptopathy, characterized by the loss of synaptic connections between inner hair cells and Type I spiral ganglion neurons (SGNs), which functionally translates into reduced ABR wave I amplitudes. More severe manifestations of cochlear synaptopathy as well as auditory neuropathy are characterized by permanent ABR threshold shifts, synaptic loss and ABR wave I amplitude reduction. To better understand these therapeutic targets, the development of additional models for evaluating hearing loss/restoration would be beneficial. Several models of chemical-induced hearing loss have been described in which animals are locally exposed to either kainic acid or ouabain. Kainic acid is a glutamate receptor agonist, a major effector of excitotoxicity and subsequent synaptic damage. Ouabain is a neurotoxin which inhibits the Na^+/K^+-ATPase pump resulting in neuronal cell death. Here we sought to characterize these models in comparison to the more traditional NIHL paradigm.

Methods

Male Sprague-Dawley rats were used for all experiments. Prior to any treatment, all animals were baseline tested for ABR and wave I amplitude. For NIHL, animals were bilaterally exposed to noise (8-16 kHz, 105 dB) for 1 hour under anesthesia. For chemical-induced hearing loss, animals were anesthetized and unilaterally dosed intratympanically with either kainic acid or ouabain at concentrations ranging from 0-100 mM. Functional and histological assessments included ABR, wave I amplitude, cochlear synapse counts and SGN morphology.

Results

Exposure to kainic acid resulted in dose-dependent hearing impairment; while ABR thresholds showed almost complete recovery by day 7, wave I deficits were still present at day 14 post-exposure. Hearing deficits resulting from kainic acid exposure were similar to those resulting from noise. In contrast, exposure to ouabain resulted in significant hearing impairment with no recovery of ABR thresholds up to day 14 at high doses, with some recovery at lower doses; wave I amplitudes could not be measured due to the severity of hearing loss.

Conclusions

Intratympanic delivery of kainic acid or ouabain resulted in different functional hearing deficits. Kainic acid exposure appears to closely mimic noise-induced models of hidden hearing loss, whereas ouabain exposure is more related to severe auditory neuropathy. Thus, chemically-induced models of hearing loss may be valuable additions to NIHL models for the evaluation of therapeutic approaches.

Identifying the Molecular Markers Associated with Hidden Hearing Loss

Yingying Chen[1]; Pezhman Salehi[1]; Debin Lei[2]; Charlie Nelson[1]; Jianxin Bao[2]
[1]*NEOMED; [2]Northeast Ohio Medical University (NEOMED)*

Background

Sensorineural hearing loss (SNHL) has been the most frequently diagnosed form of hearing loss. Historically, the principal cause of SNHL was thought to be loss of hair cells and spiral ganglion neurons (SGNs). Recently, researchers found that loss of synapses between inner hair cells (IHCs) and SGNs is the primary pathology, even withintact hair cell populations and normal audiograms. This form of SNHL is referred to as cochlear synaptopathy, or hidden hearing loss. Glutamate excitotoxicity is reported to be a causal factor, and the entry of excess calcium ions may underlie cochlear synaptopathy. Our group found that blockers for T-type calcium channels protect both hair cells and synapses between IHCs and SGNs. Thus, this study is designed to determine possible changes in expression levels of T-type calcium channel isoforms in a noise-induced hidden hearing loss model.

Methods

Forty-eight 4-month-old CBA/CaJ mice (female and male) were divided into a control group and two noise-exposed groups. In the latter two groups, mice were exposed to an octave band of noise (8-16 kHz) for 2-hour at either 91 dB or 96 dB SPL. Auditory brainstem response (ABR) and distortion product otoacoustic emissions (DPOAE) were determined 2-day before noise exposure as well as 1-day and 2-week after noise exposure. CTBP2, GluA2 and myosin VIIA immunostaing was used to count the numbers of synapses and hair cells. Real-time quantitative PCR (RT-qPCR) and single-molecule fluorescence in situ hybridization (smFISH) methods were used to analyze the gene expression for three T-type calcium channel subtypes—cacna1g, cacna1h and cacna1i—and their splicing isoforms.

Results

For both noise-exposed groups, ABR thresholds and DPOAE amplitudes were recovered at 2-week post–noise exposure. However, ABR wave I amplitude decreased from 10 kHz to 40kHz in the 96 dB group while no changes occurred in both the control and 91 dB group. Consistent with the results of the ABR wave I measurement, the synaptic ribbon count decreased at 20kHz to 40kHz in the 96 dB noise-exposed group. RT-qPCR and smFISH measurement revealed up-regulation of cacna1h and cacna1i in both noise-exposed groups, while there was no change in cacna1g after noise exposure.

Conclusion

T-type calcium channel subtypes exhibit different patterns of expression in a hidden hearing loss model. Detailed investigation of the calcium channel isoforms can reveal possible changes of SGN neural activities following noise exposure, and help pinpoint the molecular markers associated with noise-induced hidden hearing loss.

PS 433

Impaired Speech Perception in Noise with a Normal Audiogram: No Evidence for Cochlear Synaptopathy and No Relation to Lifetime Noise Exposure

Hannah Guest[1]; **Rebecca E. Millman**[2]; Kevin J. Munro[2]; Christopher J. Plack[2]
[1]*Manchester Centre for Audiology and Deafness, University of Manchester;* [2]*University of Manchester*

Introduction

Some individuals experience difficulties with speech perception in noise (SPiN) despite normal pure-tone audiometric thresholds. Possible etiologies include mild dysfunction of the middle ear or cochlea, impaired auditory processing, deficits of cognition (language, attention, and memory), and psychological factors.

Recently, it has been suggested that SPiN impairment with a normal audiogram might result from "cochlear synaptopathy": destruction of synapses between inner hair cells and auditory nerve fibers. In rodents, noise-induced synaptopathy can occur without widespread hair cell loss or permanent threshold elevation, but is associated with reduced brainstem response amplitudes at medium-to-high sound levels. Hence, it has been suggested that this pathophysiology might explain why SPiN ability varies so widely among audiometrically normal humans. The present study set out to test for evidence of cochlear synaptopathy in humans with impaired SPiN despite normal pure-tone audiograms.

Methods

All participants (aged 18-40 years) exhibited normal middle ear function and pure-tone audiometric thresholds ≤20 dB HL up to 8 kHz. SPiN performance was assessed using a task incorporating high sound levels, multiple talkers, and spatial cues. Auditory brainstem responses (ABRs) and envelope-following responses (EFRs) were recorded at high stimulus levels, yielding amplitude measures and within-subject difference measures. A detailed measure of lifetime noise exposure, based on the equal energy hypothesis, was obtained via structured interview.

In the main analysis, 16 individuals with both self-reported and lab-confirmed SPiN impairment were compared with 16 controls matched for age, sex, and audiometric thresholds up to 14 kHz. Additionally, one supplementary analysis compared the SPiN-impaired group with controls matched only for age and sex, to rule out audiometric over-matching. A second supplementary analysis defined SPiN impairment solely by self-report (n = 32 in each group).

Results

Impaired SPiN was not associated with ABR wave I amplitude, ABR wave I/V amplitude ratio, EFR amplitude, nor growth of EFR amplitude with modulation depth, despite small standard errors. Nor did lifetime noise exposure differ significantly between impaired-SPiN and control groups. These null results persisted regardless of whether SPiN difficulties were merely self-reported or confirmed by laboratory measurements, and were evident in analyses both with and without audiometric matching.

Conclusions

The results do not support the contention that synaptopathy is a significant etiology of SPiN impairment with normal audiometric thresholds.

Funding

PS 434

Brainstem correlates of cochlear nonlinearity measured via frequency-following responses (FFRs): A neural marker of "hidden hearing loss" or individual variation in central auditory processing?

Gavin M. Bidelman; Jessany Knapp; Victoria Heitzmann; Shaum Bhagat
University of Memphis

Scalp-recorded frequency-following responses (FFRs) are EEG-based potentials used to characterize the pre-attentive, subcortical encoding of complex sounds. In the present study, we aimed to determine if FFRs carry information regarding cochlear health (nonlinearities) and putative diagnostic information on "hidden hearing loss" (HHL) that has heretofore remained elusive to measure in humans. Based on the premise that normal (healthy) cochlear transduction is characterized rectification and compression, we reasoned that these nonlinearities would create measurable harmonic distortion in the FFR spectrum in response to pure tone input. In normal hearing individuals, we compared conventional indices of cochlear nonlinearity, via distortion product otoacoustic emission (DPOAE) I/O function, to the total harmonic distortion measured from their FFRs (FFR_{THD}). FFR_{THD} quantifies the relative amplitude of response at harmonic (cochlear generated) distortion components to that at the stimulus frequency; HHL was predicted to produce a more linearized response resulting in FFRs at only the stimulus frequency and thus weaker FFR_{THD}. Physiologic measures were then compared to QuickSIN scores as poorer speech-in-noise perception in the presence of a normal audiogram has been suggested as an indicator of preclinical neurodegeneration and HHL. Analysis of DPOAE I/O functions and the FFR_{THD} revealed listeners with higher cochlear compression thresholds had lower neural distortion, (i.e., more linearized responses), thus linking cochlear and brainstem correlates of auditory nonlinearity. Importantly, FFR_{THD} was negatively correlated with QuickSIN scores whereby listeners with more nonlinear FFRs (higher FFR_{THD}) were better at perceiving speech in noise (i.e., lower QuickSIN scores). We infer that individual differences in SIN and FFR nonlinearity even in normal hearing individuals may reflect early HHL not captured by normal audiometric evaluation. Nevertheless, future studies in hearing impaired individuals and animal models are necessary to confirm diagnostic utility of FFR_{THD} and its relation to neural degeneration/synaptopathy in human listeners.

PS 435

The Effect of Chronic Noise and Restraint Stress on Cognitive Behavioral Function in Rats

Hyo Jeong Yu[1]; Dong Won Yang[2]; Min Jung Kim[3]; Jung Mee Park[4]; So Young Park[5]; Dong-Kee Kim[6]; Shi Nae Park[7]

Purpose

Noise exposure has been well characterized as an environmental stressor with auditory and non-auditory effects. Restraint stress induces negative outcomes on feeding behavior conditions as well as neurogenesis in rats due to physiological changes. The purpose of this study was to establish chronic dual stress rat models using noise and restraint, and to investigate the changes in cognitive function after stress.

Methods

Male Wistar rats were divided into two age-matched groups: experimental group exposed to dual stress of noise and restraint and control group. The experimental group was exposed to double stress stimuli of noise and restraint; 110dB SPL white band noise for 3 hours every day up to 7 days and restraint in cylindrical plastic films, DecapiCones, with rubber bands fixed at the tails. Hearing tests of ABR and DPOAE were performed before and after stress exposure. Behavior assessment was also performed by novel object recognition (NOR) test. The changes in body weight and the mortality rate after dual stress were also investigated.

Results

Cognitive function measured by NOR test significantly decreased in the dual stress model group compared to the control group (p < 0.05). Hearing levels and the body weight also significantly decreased after the dual stress. The mortality rate of 6-week-old rats with 3 hours of restraint with 6 times of ventilation was up to 17%..

Conclusion

Dual stress in rat models caused cognitive dysfunction as well as significant decrease in body weight. The study investigating relevant mechanisms of these phenomena is ongoing in our laboratory.

!_editedJMPARK_SNPark_SYPARK_20170921_PSN's Cx final.docx

Human Development

PS 436

A Longitudinal Study of Auditory and Visual Development in Children with Cochlear Implants

Kristina C. Backer[1]; Andrew S. Kessler[2]; Sharon Coffey-Corina[1]; Laurel A. Lawyer[1]; Lee M. Miller[1]; David P. Corina[1]
[1]University of California, Davis; [2]University of Washington, Seattle

Although cochlear implant (CI) technology has significantly improved over the last thirty years and has facilitated the acquisition of spoken language skills in deaf children, individual language outcomes remain highly variable. One potential explanation is that neural resources available for auditory processing are limited by an expansion of resources dedicated to visual processing as a result of cross-modal reorganization of auditory cortex. The overarching goal of the present longitu-

dinal study is to systematically test this hypothesis. To reach this goal, we use a novel electroencephalography (EEG) paradigm that enables us to quickly and simultaneously measure auditory and visual evoked potentials in children. Results from the first year of EEG data collection will be presented. We obtained usable EEG data from 30 normal hearing (NH) children and 24 children with bilateral CIs, ranging in age from 21 months to 8 years. Cluster-based permutation tests were used to analyze the EEG data; results were thresholded at p < 0.05. As expected, the NH children exhibited larger auditory evoked potentials than the children with CIs. We also observed differences in visual onset responses, such that the visual evoked potential (P1) was larger and more widespread in the NH children, a response pattern inconsistent with a cross-modal account. In a separate analysis, we examined visual activity in the time-frequency domain, using inter-trial phase coherence, which is a measure of the consistency in the timing of neural activity. This revealed that relative to NH children, children with CIs had greater phase-locking of neural activity following the onset and at the offset of the visual stimulus, even over frontal sites. However, phase-locking strength in frontal channels did not correlate with receptive or expressive language scores in the CI group. Our data provide indications that NH and CI children engage the auditory cortex to a different extent during auditory and visual processing. However, the present results revealed no significant relationship between neural measures of visual activity and spoken language abilities in children with CIs.

PS 437

The Development of Hierarchical Beat Perception: Effects of Age on Perception of Musical Meter

Jessica Nave-Blodgett[1]; *Joel S. Snyder*[2]*; Erin Hannon*[2]
[1]University of Nevada, Las Vegas; [2]University of Nevada Las Vegas

When we listen to music and participate in musical activities such as performance or dance, we are confronted with rich, multimodal temporal patterns. In Western cultures, the temporal structure of music, or musical meter, is hierarchical, with recurring patterns of stronger (downbeat) and weaker (upbeat) events. While perceiving the beat alone is often enough to synchronize simple movements to music, such as clapping or head bobbing, perception of multiple levels of this metrical hierarchy can facilitate solo and group synchronization to music, such as complex partner dances.

Although prior research suggests listeners of various ages are sensitive to the beat in music, it is unclear how sensitive younger children are to the beat, and how or when listeners begin to perceive multiple hierarchical levels of musical meter. To investigate, we created a modified version of the Beat Alignment Task (BAT; Iversen & Patel, 2008) with commercially-performed ballroom dance music. We paired the music with metronomes that matched or mismatched the beat and the measure of the music, creating zero, one, or two levels of matching between the music and the metronome. Children (5-10 years), adolescents (11-17 years), and young adults (18+ years) listened to the music and metronome pairs and rated how well the metronomes matched the human-performed music.

The patterns of ratings of fit from different age groups suggests a prolonged period of development and refinement of perception of hierarchical beat patterns. Children and adolescents were sensitive to the fit of the metronome to the music at the beat level, rating beat-matching metronomes as better fitting than beat-mismatching metronomes. However, even the oldest adolescent age group did not distinguish in their ratings of fit between metronomes that matched or mismatched at the measure level of the musical meter. Furthermore, there was a strong developmental trend in the sensitivity of children and adolescents to beat-level matching between metronomes and music: children in older age groups gave progressively more nuanced ratings of fit for beat-matching and beat-mismatching metronomes compared to younger children. It was not until adulthood (18+ years) that listeners consistently rated auditory metronomes that matched the music at the beat and measure levels as fitting the music better than metronomes that matched only the beat of the music. The ability to perceive multiple levels of hierarchical temporal structures in music (i.e. musical meter) may not emerge until relatively late in adolescence or early adulthood.

PS 438

Infants benefit from onset asynchrony in an auditory scene analysis task

Monika-Maria Oster[1]; Lynne A. Werner[2]
[1]University of Washington; [2]University of Washington Department of Speech and Hearing Sciences

Infants increasingly acquire language in noisy environments. Although previous research has demonstrated that infants have greater difficulty than adults separating competing sounds, the reasons are not clear. Adults use spectral, temporal and spatial location cues to accomplish this task. To date only few studies have systematically investigated how infants use such cues to separate sounds. Notably infants'; use of onset asynchrony cues, which are strong cues for adults, has not been investigated.

To investigate this question, 7-month-old infants and adults are tested using a modified double-vowel paradigm. In each vowel pair, one female and one male natural production of an American-English vowel are superimposed. Using the seven vowels /iː/, /uː/, /ʊ/, /æ/, /ɛ/, / ɔː/ and /ɪ/, different vowels are paired in all possible combinations, resulting in 42 vowel pairs. A continuous sequence of vowel pairs is presented with an interval of 1200 ms between pairs. In the baseline condition, the vowels have simultaneous onset. In the cue condition, the target vowel onset is delayed by 100 or 200 ms. The vowels in a pair always have simultaneous offset. Target-to-nontarget ratios are chosen to equate infant and adult performance in the baseline condition. For infants, the target-to-nontarget ratio is +12dB; for adults the target-to-nontarget ratio is -20dB. All subjects are tested in the baseline condition and in one cue condition. For half of the subjects the target vowel is a male /iː/; for half the subjects the male /uː/ is the target. Using the observer based procedure, subjects are trained to respond to a target vowel when it occurs in any vowel pair and to withhold a response when the target vowel does not occur. After reaching an 80% correct training criterion, subjects complete 15 target and 15 nontarget trials in each condition, with condition order counterbalanced across subjects. The measure of performance is d', and cue benefit is defined as the difference in d' between baseline and cue conditions.

Preliminary results indicate that both 7-month-old infants and adults receive a cue benefit from onset asynchrony. However, while adults, receive a larger benefit at 200ms asynchrony than at 100 ms asynchrony, infants appear to receive the same cue benefit from the 100ms and 200ms onset asynchrony. Thus, although infants benefit from onset asynchrony, their benefit appears less dependent on asynchrony duration than adults';. The reasons for this age-related difference are not clear.

PS 439

Listening Difficulties in Children: Influence of High Frequency Hearing Loss and PE Tubes

David R. Moore[1]; Allison Bradley[1]; Audrey Perdew[1]; Nicholette Sloat[1]; Chelsea Blankenship[2]; Lisa L. Hunter[2]
[1]*Cincinnati Children's Hospital;* [2]*Cincinnati Children's Hospital and University of Cincinnati*

Children with listening difficulties (LiD) but 'normal'; audiometry may have a sub-clinical hearing loss. We previously reported extended high frequency (8-16 kHz) hearing loss in some of these children (ARO, 2017). In completion of the first stage of a longitudinal study, we compare here measures of hearing speech in noise (LiSN-S; BKB SIN), cognitive function (NIH Tool box), 'auditory processing'; (SCAN), and parent report (ECLiPS) across a broad sample of children (n=154) aged 6-12 years, on the basis of audiometry and history of otitis media. Children were mainly recruited from clinical services of Cincinnati Children';s (CCH) and from advertisements on the CCH website. Each child participated in a wide range of physiological and behavioral tests, many in 2-day summer camps. Parents completed questionnaires on their children';s listening and communication abilities and on their medical and related history. About half the children had LiD, associated along a continuum with higher likelihood of high frequency hearing loss (LiD: 37%, TD: 19%), impaired speech perception (LiSN-S; Talker Advantage p < 0.001, Spatial Advantage p < 0.02), and poorer cognitive function (p < .0001). These children with LiD also had more doctor visits, a higher rate of medical consultations for hearing, and greater, earlier life prevalence of pressure equalization (PE) tubes for otitis media. Hearing loss was associated with more PE tubes across the frequency range, but particularly for frequencies > 8 kHz. PE tubes were associated in both TD and LiD groups with reduced performance on the highly demanding LiSN-S Low cue (Lc) condition (same speaker, same position), but no other LiSN-S measure, including Spatial Advantage (c.f. Cameron et al, Int J Audiol, 2014). Children with LiD were disproportionately disadvantaged by tube history. Among children with a tube history, all 17 in the LiD group had Lc < 0, whereas half of those in the TD (10/19) had Lc < 0 (Lc difference between groups: p = 0.007; Kruskal Wallis). Although children with LiD generally had lower cognitive ability than TD children, PE tube-related hearing loss was not associated with additional cognitive impairment. We conclude that sub-clinical hearing loss associated with earlier PE tubes contributes to LiD in school age children.

PS 440

Peripheral auditory function in children with listening difficulties: Extended high frequency hearing and otoacoustic emissions

Lisa L. Hunter[1]; Chelsea Blankenship[1]; Allison Bradley[2]; Nicholette Sloat[2]; Audrey Perdew[2]; David R. Moore[2]
[1]*Cincinnati Children's Hospital and University of Cincinnati;* [2]*Cincinnati Children's Hospital*

"Auditory processing disorder" is a poorly understood condition in which children with otherwise normal hearing present with generalized listening difficulties (LiD). One hallmark of APD in position statements by professional organizations is particular difficulty understanding speech in noisy environments, such as in classrooms. Despite this auditory concern, the contribution of peripheral auditory impairment to LiD has not been studied

systematically. We recently reported poorer extended high frequency hearing in children with LiD (aka 'suspected APD') that was related to poor speech-in-noise performance, and to a history of otitis media treated with tubes (Hunter et al., ARO, 2017). As part of a longitudinal study, we are exploring mechanisms for LiD. To assess peripheral factors, we measured standard and extended high frequency pure tone thresholds, DPOAE, extended high frequency TEOAE (Keefe et al., 2017), wideband middle ear reflectance and wideband acoustic reflex thresholds. Children with LiD (n=64, ages 6-15 yrs) and age-matched typically developing (TD) children (n=56, ages 6-14), were tested with a range of behavioral and physiologic measures of hearing. Hearing thresholds were significantly poorer in the cases with tube history (n=31 tube history, n= 88 no tubes) between 0.5-16 kHz, with larger differences in the higher frequencies. DPOAE signal to noise ratios were significantly lower from 2 to 10 kHz frequency in the tube history group and were lower at 5-6 kHz in the LiD group compared to the TD group. Wideband reflectance measures and broadband noise acoustic reflex thresholds were not significantly different based on tube history or listening difficulties. A history of PE tubes was related to peripheral auditory dysfunction (extended high frequency thresholds and DPOAEs), but not to middle ear reflectance or acoustic reflexes. Thus, these differences are most likely cochlear in nature. Such effects have been hypothesized to relate to basal damage as a consequence of previous chronic OM. In the LiD group with tube history, speech in noise performance was poorer for low-cue condition in the Listening in Spatialized Noise test, supporting the hypothesis that LiD is related to auditory factors in children with histories of otitis media treated with PE tubes.

PS 441

Exploration of speech-evoked brainstem responses to assess indicators of neurotoxicity in at-risk newborns.

Gabriella Musacchia[1]; Jiong Hu[1]; Vinod K. Bhutani[2]; Ronald J. Wong[3]; Meiling Tong[4]; Matthew Fitzgerald[5]
[1]*Department of Audiology, University of the Pacific;* [2]*Stanford University School of Medicine;* [3]*Stanford University Medical School;* [4]*Obstetrics and Gynecology Hospital Affiliated to Nanjing University;* [5]*Stanford University*

Bilirubin-induced neurologic dysfunction (BIND) is a spectrum of central nervous system (CNS) disorders that frequently impacts auditory system development in premature infants. Abnormal development of the auditory system can have a profound effect on hearing and language outcomes. However, the incidence, severity, and time course of central auditory system abnormalities (inclusive of bilirubin binding status, co-morbidities, etc.) in premature infants is not known. In addition, there are currently no reliable methods of assessing CNS dysfunction in preterm infants. If signs of dysfunction could be reliably and validly assessed, brain damage prevention or treatment could be undertaken. The automatic auditory brainstem response (AABR), used for universal hearing screening, is routinely used in neonatal intensive care units (NICUs) and used to assess peripheral auditory function. The AABR, however, is not designed to detect central auditory processing abnormalities. A potentially more useful measure is the complex ABR (cABR) which is similar to the AABR, but uses a speech stimulus that can capture more subtle aspects of central auditory system neuromaturation and injury. Previous cABR data confirm observable differences in normal developing infants as they age and children with language impairments, dyslexia, autism, or poor reading skills. To test whether bilirubin levels were related to cABR measures in preterm infants, we compared the magnitude of speech-evoked brainstem responses to total bilirubin (TB) levels in 23 NICU infants. Our results show a negative correlation between TB levels and measures of the cABR, such that lower TB levels are associated with more robust speech encoding. These data advance our understanding of neurologic deficits associated with preterm birth and exposure to high TB levels.

PS 442

Auditory neurophysiological development of children ages 3-8: a growth curve modeling approach

Elaine C. Thompson; Stephanie Huang; Spencer B. Smith; Jennifer Krizman; Travis White-Schwoch; Nina Kraus
Northwestern University

Childhood is a period of marked sensory development, yet investigations into human auditory maturation have tended to focus exclusively on inner ear physiology or cortical evoked potentials. As a result, maturation at the level of the midbrain has often been overlooked. One large cross-sectional study from our lab examined auditory brainstem function across the lifespan, revealing plasticity in midbrain processing well past the age of 2. The present investigation is an extension of that work, yet evaluates auditory neurophysiology with greater granularity in childhood through a longitudinal dataset of over 450 data points. Here, we examine auditory neurophysiology in children, ages 3-8 years, by collecting Frequency Following Responses (FFR). The FFR reflects encoding from large populations of neurons in the auditory brainstem and is sensitive to distinct aspects of speech processing (e.g., latency, frequency encoding, response consistency, nonstimulus activity). By assessing the FFR longitudinally, we are poised to de-

tect subtle but meaningful changes in a dataset that, for the first time, is sufficiently large to examine changes using growth curve analysis. Preliminary findings reveal distinct developmental trajectories across the various FFR parameters: while frequency encoding is stable during this age range, processing of timing information is dynamic. These results demonstrate the development of speech encoding at the auditory midbrain continues into late childhood, and corroborates our lab';s previous work that FFR parameters are independent at these earlier stages of life as well.

Inner Ear: Disease and Injury Models

PS 443

Expression of advanced glycation end-product in the cochlea of metabolic syndrome model mice

Kazuma Sugahara; Yoshinobu Hirose; Makoto Hashimoto; Yosuke Takemoto; Shunsuke Tarumoto; Hiroshi Yamashita
Department of Otolaryngology, Yamaguchi University Graduate School of Medicine

Introduction

The metabolic syndrome is characterized by obesity concomitant with other metabolic abnormalities such as hypertriglyceridemia, hyperlipidemia, elevated blood pressure and diabetes. It is known that the prevalence of hearing loss is high in the patients with diabetes. TSOD (Tsumura-Suzuki-Obese-Diabetes) male mouse presented metabolic abnormality such as obesity and hyperlipidemia, high blood pressure, diabetes with aging.

Advanced glycation end products (AGEs) are proteins or lipids that become glycated after exposure to sugars. AGEs are prevalent in the diabetic vasculature and contribute to the development of atherosclerosis. In the last meeting, we reported that the mice showed the age-related hearing loss related with the angiostenosis in the inner ear. In the present study, we evaluated the expression of advanced glycation end-product in the cochlea of metabolic syndrome model mice. In addition, the effect of pyridoxamine on the production of AGEs in the cochleae.

Materials and Methods

TSOD male mice used in study were derived from the Tsumura Research Institute. Animals were divided into two groups (control group, pyridoxamine group). Pyridoxamine, the inhibitor of AGEs production was administrated in the water (2 mg/ml) in pyridoxamine group. We evaluated the ABR thresholds, the weight and blood glucose level. In addition, the histological examination was performed in the end of experiments.

Results

There was no difference between 2 group in the 6 months aged TSOD mice. The elevation of ABR thresholds were observed in 6 months aged TSOD mice. in each group. However, the thresholds of 12 months aged were more in control groups than in pyridoxamine group. The expression of AGEs was enhanced in vessels in the TSOD mice. The administration of pyridoxamine could suppress the expression of AGEs.

Conclusion

The result suggested that pyridoxamine could prevent the hearing loss in the animal model of metabolic *syndrome.*

PS 444

A Model for Comparative Study of Inner Ear Synaptic Loss & Repair Mechanisms using Excitotoxic Injury

Pierrick Bordiga[1]; Raphaelle CASSEL[2]; Yves Cazals[3]; Alain Tonetto[4]; Axel Assie[2]; Isabelle Watabé[2]; David Péricat[5]; Jonas Dyhrfjeld-Johnsen[6]; Christian Chabbert[5]
[1]*CNRS/Sensorion;* [2]*Aix-Marseille University;* [3]*INSERM;* [4]*Aix-Marseille university;* [5]*CNRS;* [6]*Sensorion*

Hearing and balance disorders constitute a growing and major health problem. Indeed, vestibular disorders represent 5% of hospital emergencies, whereas hearing loss affects more than 10% of the adult population in France. Current therapeutic solutions lack specificity and efficiency. This unsatisfactory situation can be attributed to a lack of knowledge of hearing and vestibular pathophysiological mechanisms. A large proportion of these pathologies is attributed to direct inner ear damage, with acute deafferentation increasingly thought to play an important role in a number of auditory and vestibular syndromes such as noise-induced and sudden hearing loss, labyrinthitis, vestibular neuritis, vertigo of ischemic origin and Menière';s disease. Using rodent models of excitotoxically-induced inner ear synaptic damage, an endogenous process of at least partial synaptic repair has been demonstrated in the mammalian inner ear. This process may, at least in part, support the spontaneous functional recovery of hearing and balance.

In order to compare the synaptic repair processes between cochlear and vestibular endorgans following an excitotoxic injury, we implemented a mouse model of excitotoxically-induced inner ear deficits and explored the various steps of functional recovery that occurs over days and weeks after the acute synaptic insult. Induction of inner ear deficits was achieved through unilateral transtympanic infusion of the glutamate-receptor agonist kainic acid. Hearing and vestibular deficits were evalu-

ated using audiometry (Auditory Brainstem Response -ABR-, Distortion Product of Oto-Acoustic Emission -DPOAE- recordings), a set of behavioral assessments of the gait and balance and immunohistochemistry analyses. Based on the combination of these different methods, functional and cellular changes may be tracked and described over time. Using vestibular behavioral analyses, we report that there are at least two distinct phases observed following an acute excitotoxic injury: An acute phase of behavioral symptoms during which all the vestibular deficits achieve their peak magnitude followed by a second phase, during which balance deficits progressively recover over time. In the same way, ABR recordings show a transient peak increase of auditory thresholds followed by a full threshold recovery over the following weeks. Ongoing work focuses on comparing cochlear and vestibular synaptic plasticity mechanisms using immunohistochemical approaches. Our latest results in this model of isolated synaptic deafferentation and repair will be compared and discussed at the ARO meeting.

PS 445

Visualizing Wnt Activation Patterns in the Cochlea upon Hair Cell Injury

Hao Chiang[1]; Niliksha Gunewardene[2]; Albert Edge[3]
[1]*Massachusetts Eye and Ear Infirmary Harvard University;* [2]*1 Department of Otolaryngology, Harvard Medical School, Boston, MA, USA 2 Eaton-Peabody laboratories, Massachusetts Eye a;* [3]*Harvard Medical School*

Activation of the canonical Wnt signaling pathway induces supporting cell proliferation and hair cell generation in the postnatal cochlea. To dissect Wnt activity in the postnatal cochlea under naïve and hair cell-injured conditions, we used a Tcf/Lef:H2B/GFP reporter mouse carrying 6 copies of Tcf/Lef1 DNA binding sites followed by a nuclear localized GFP. In the P1 cochlea, Hensen';s cells, inner phalangeal cells, and greater epithelial ridge, as well as some hair cells, were GFP-positive, indicating active Wnt signaling. The P1 cochlea responded to Wnt activation based on increased nuclear Wnt reporter activation in Deiters'; cells after incubation with GSK3β inhibitor, CHIR99021, for 13 hr. Incubation with CHIR99021 for 48 hr induced supporting cell proliferation based on EdU incorporation. Significant reporter activation was induced in Deiters'; cells 3 days after intracochlear neomycin delivery at P1-P2 to remove hair cells. Wnt activity was also seen during spontaneous hair cell regeneration in diphtheria toxin (DT)-induced hair cell ablation in Wnt reporter mice crossbred with Pou4f3[DTR] knock-in mice with DT receptor sequence inserted into the Pou4f3 locus. In addition, we have profiled the expression of ligands, receptors and regulators in the canonical Wnt pathway upon DT treatment in Gfi1-cre driven inducible DTR transgenic mice. We localized genes with significantly altered expression with RNAscope and are investigating potential relationships of Wnt receptors and Lgr proteins to Wnt pathway changes. Wnt activation occurred also in adult cochlea in Hensen';s cells, Claudius cells and some inner hair cells. Activation was seen 1 day and 1 week after noise exposure with increased GFP expression in residual inner and outer hair cells and in the mesenchymal cell region. This increase in GFP expression had abated 1 month after noise exposure. The current study identifies the supporting cell populations that activate Wnt signaling after damage and may act as a regenerative pool in the sensory epithelium after release of Wnts from adjacent cells. The altered regulators in the Wnt signaling pathway upon hair cell damage provide potential targets for Wnt pathway manipulation for hair cell regeneration.

PS 446

Cochlear Pericyte Depletion Leads to Hearing Loss

Xiaohan Wang[1]; Han Jiang[2]; Xiaorui Shi[3]
[1]*Oregon Hearing Research Center;* [2]*Oregon Hearing Research Center, Oregon Health & Science University;* [3]*Oregon Hearing Research Center, Oregon Health & Sciences University.*

Mural cells stabilize and regulate integrity and tone of vessels in different organs, especially at the tissue-blood barrier. In the cochlea, pericytes are the mural cells supporting the blood-labyrinth barrier which are critically involved in cochlear homeostasis. In this study, we crossed mice expressing Cre-recombinase under a FoxD1 promotor to Rosa26-loxP-STOP-loxP-iDTR mice and generated a transgenic mouse model in which FoxD1-derived cells heritably express the diphtheria toxin receptor and are sensitive to diphtheria toxin (DT). At 6-8 weeks, FoxD1-Cre, Rs26-iDTR, and control mice received daily intraperitoneal injections of DT at 10 ng/g body weight for 4 consecutive days. Hearing threshold shift was measured by auditory brainstem response (ABR) following each DT injection. We found that depletion of pericytes leads to a threshold shift, particularly at high frequencies (24 KHz, and 32 KHz). Hearing threshold was elevated immediately after the first injection, continued to progressively elevate after the second and third injection, and plateaued at the fourth injection. The elevated hearing threshold persisted for 2 weeks. The control mice receiving the same dose and schedule of DT maintained normal hearing. We also examined capillaries in the stria vascularis after this treatment regime. Enlarged vessels were observed in the region of pericyte damage. The ratio of the area of the blood vessel to vessel length was measured to assess vessel enlargement. In the control group this ratio was 11.2 ± 2.1. In

the DT-treated group, the ratio was 25.4 ± 4.8. Outer hair cells were lost in regions corresponding to 24 KHz, and 32 KHz. Our results underscore that normal vascular function is essential for hearing and pericytes play a critical role in vascular stability. This work was supported by the National Institutes of Health grants NIH NIDCD R01-DC010844 (X Shi), R01-DC015781 (X Shi), R21 DC016157 (X Shi), P30-DC005983 (Peter Barr-Gillespie), and Medical Research Foundation (MRF) of Oregon Health and Science University (X.Shi).

PS 447

Development of Animal Models With Stress-induced Hearing Loss

Yeong Cheol Kim[1]; Jong Ju Lee[2]; Young Sun Kim[2]; Yeon Ju Kim[1]; Yun Yeong Lee[2]; Oak-sung Choo[2]; Beomyong Shin[1]; Mi-Jin Choi[2]; Jeong Hun Jang[2]; Yun-Hoon Choung[2]
[1]*Department of Otolaryngology, Ajou University School of Medicine;* [2]*Department of Otolaryngology, Ajou University School of Medicine, Suwon, Republic of Korea*

Background

Stress is one of the causes for sensorineural hearing loss (SNHL). however, there is no particular animal model for this condition. Thus, it is rather difficult to identify the mechanism, and discover drug targets for therapeutic intervention. The purposes of this study were to develop a stress induced SNHL animal model, and to evaluate the effect of dexamethasone that may reduce hearing loss in response to stress.

Methods

Eight-week-old male Sprague-Dawley (SD) rats was exposed to stress for 6 days. The protocol for stress included swimming, overcrowding, shaking, shaking with heating and cold stimuli. Swimming procedure was performed in water at 22°C for 1 hour, and overcrowding procedure was cared out in a narrow case environment for 22 hours with starvation. Shaking procedure was performed for 1 hour at 250 RPM and maintained at 40°C when heating was included. During cold stimuli procedure, SD rats were kept in an environment at 4°C for 4 hours. With the stress protocol, hearing status was measured by auditory brainstem response (ABR) test. For the final step, the SD rats were treated with dexamethasone in different injection methods. They were divided into 4 groups   according to dexamethasone- injection method: (1) control group, (2) intraperitoneal injection for 1 week (IP group), (3) intratympanic injection, every other day for 1 week (4 times in total) (IT group), and (4) IT+IP group.

Results

Before stress exposure, hearing thresholds were 10 dB at 16 kHz, and 10 dB at 32 kHz. Six days after stress procedure, hearing loss was observed in 29 (74%) out of 39 SD rats by ABR test. The hearing thresholds were 46 dB at 16 kHz, and 43 dB at 32 kHz, and this threshold shift was maintained for more than 2 weeks. The results of dexamethasone injection showed that the IP group were able to restore hearing by 13 dB. However, control, IT and IP+IT group did not show any effect on hearing loss.

Conclusion

We developed an animal model design for stress-induced SNHL, and expect this model to be useful in finding a efficient therapeutic intervention. In addition, systemic dexamethasone (IP group) seems to be a definite treatment method for stress-induced SNHL compared to other administration methods of dexamethasone. Future studies with longer periods of experiments will be needed to confirm the results of our study.

PS 448

A role of kinase inhibitor in hair-cell death of the zebrafish lateral line.

Yosuke Tekemoto; Yoshinobu Hirose; Kazuma Sugahara; Makoto Hashimoto; Hiroshi Yamashita
Department of Otolaryngology, Yamaguchi University Graduate School of Medicine

Introduction

The lateral line which detects a stream exists in the body surface of a zebrafish, and it is consist of neuromasts which have a hair cell. Hair cells can be easily labeled and imaged in vivo with fluorescence microscopy. Zebrafish lateral-line hair cells have been used in several previous studies to investigate the efficacy of various agents against aminoglycoside-induced damage. We have reported the hair-cell protection effect, using a zebrafish about antioxidants, such as a quercetin, an astaxanthin, and a kanpo-preparation.

We observed about the role of kinase in hair-cell death this time. A kinase phosphorylates a protein, and it has been reported that a part of kinase have an important role for hair-cell death. Then, we considered the relevance of kinase inhibitor and a hair-cell death as a collaboration with Cancer Research Institute of Kanazawa University. We report that some kinase inhibitor protect hair cells against neomycin.

Materials and Methods

Zebrafish embryos were used in this study. Zebrafish larvae were exposed to kinase inhibitor (0.1-10 ug/ml) for 1 hour before 100 uM neomycin to induce hair cell

death for 1 hour. We also created the group which does not prescribe a neomycin for the zebrafish. After that, they were fixed in 4% paraformaldehyde, incubated with anti-parvalbumin, Alexa 488, and hair cell damage was assessed.

Results and Conclusion

We identified the pharmacon which cause a hair-cell death or protect from neomycin. We examined the relevant of kinase and hair-cell death this time using the larvae of a zebrafish. Among them, the protein kinase C inhibitor have strong hair cell protective effect. We also examined the mechanism. We were able to screen kinase inhibitor and were able to identify the pharmacon with which a relevance with hair-cell death is suggested. We will repeat the further investigation, we would like to reveal about the role of kinase in a cell death.

PS 449

Homeless hair cells: anoikis in the cochlea

Dalian Ding[1]; Jianhui Zhang[2]; Haiyan Jiang[3]; Richard Salvi[4]
[1]University at Buffalo, USA; [2]State University of New York at Buffalo; [3]Staet University of New York at Buffalo; [4]Center for Hearing and Deafness; State University of New York at Buffalo

Background

The growth, differentiation and survival of anchorage-dependent cells are tightly regulated by signals derived from adjacent cells and the surrounding extracellular matrix (ECM). When the cells become detached from one another by loss of normal cell-matrix interactions, they undergo programmed cell death by a process known as anoikis. The role of anoikis in cochlear cell death is currently poorly understood. To address this issue, we treated cochlear organotypic cultures with a variety of ototoxic drugs to determine if any induced anchorage-dependent hair cell death (anoikis).

Methods

Cochlear organotypic cultures were prepared from postnatal day 3 (P3) Sprague-Dawley rats. After 24 h in culture, the explants were treated with different dose and duration of paraquat, gentamicin, cisplatin, mefloquine, or cadmium. Myosin VI immunolabeling and/or phalloidin were used to label cochlear hair cells, and a sox2 antibody was used to label supporting cells. Antibodies against β-catenin and E-cadherin were used to label the ECM. Cell death was also monitored by a fluorogenic probe for initiator caspase-8, caspase-9, and executioner caspase-3.

Results

The pattern of supporting cell vs. hair cell death varied with the type of ototoxic agent. Paraquat, a robust superoxide generator, initially destroyed the Deiters and other support cells resulting in loss of contact with the intact hair cells. Approximately 12-24 h later, the hair cells began to degenerate suggesting that their death was mediated in part by anoikis. In contrast, the aminoglycoside antibiotic, gentamicin, initially damaged the hair cells; nearby supporting cells remained intact. Cisplatin, an antineoplastic agent, simultaneously destroyed hair cells and surrounding supporting cells. Cadmium, a neurotoxic heavy metal, also simultaneously destroyed cochlear hair cells and supporting cells. Mefloquine, a widely used antimalarial, destroyed supporting cells first leading to the loss of cell-matrix interactions and subsequent hair cell death, likely mediated by anoikis.

Conclusion

Paraquat and mefloquine initially kill cochlear supporting cells; this disrupts the ECM, which likely leads to anchorage-dependent hair cell death (anoikis). Gentamicin initially kills hair cells whereas cisplatin and cadmium simultaneously kill hair cells and supports cells most likely by apoptosis or necrosis.

Dalian Ototoxic chemicals anoikis V3.docx

PS 450

Live Cell Imaging of Neurite Length and Cell Death in Cultures of Dissociated Neurons from Scarpa's Ganglion

*F*abien Loustalot; Mickaël Deage; **Montserrat Bosch-Grau**; Jonas Dyhrfjeld-Johnsen
Sensorion

The loss of synaptic connections and delayed neurodegeneration in inner ear pathologies are receiving increasing attention in both preclinical and clinical research. While in vivo models of synapse loss, neurite retraction and delayed cell death exist, screening for potential drug targets and candidates would be more ethically and efficaciously achieved in vitro. We here present live-cell imaging data quantifying dose-dependent effects of oxidative stress and ototoxic insult in phenotypic cultures of dissociated neurons from Scarpa';s ganglion on neurite length and neuronal death.

Cultured of primary peripheral vestibular neurons from Scarpa';s ganglion of P5 Wistar rat pups 48 well culture and treated with antimitotics for 48 hours, then transfected with a lentivirus for expression of red fluorescent protein using a synapsin promoter and live-cell imaging started (scan every 6h for 1 week). Four days after

transfection, groups of cultures (n=4) were exposed to either control medium, hydrogen peroxide (16.6/50/150 µM, 6h) or cisplatin (16.6/50/150 µM, 72h). Neurite lengths and cell body cluster counts were normalized to the group mean at baseline (last scan before insult).

Both peroxide (6h) and cisplatin (48h) exposure dose-dependently induced loss of neurites and reduction in cell body cluster counts. Peroxide exposure induced rapid and strong reduction of both neurite length (33-48%) and cell body clusters (38-57%) within the first 12h of application, with neurite growth subsequently resuming at a lower rate (0.172– 0.240 mm/h*mm^2) than for controls (0.324 mm/h*mm^2) within 6-12h for the 16.6 and 50 µM concentrations. Cisplatin exposure induced slower, but continued reduction in neurite length for all concentrations until 168h (37-95%), with reduction in cell body clusters (85%) only appearing within 30h for 150 µM cisplatin, while delayed and ongoing lower cell body loss (after ~30h) was apparent for both 16.6 and 50 µM conditions until 168h (20-51%).

These preliminary data demonstrate the feasibility of a High Content Screening approach to quantifying dynamics of neurite length reduction and regrowth, as well as cell death in cultures of dissociated peripheral vestibular neurons from Scarpa';s ganglion. Furthermore, the experimental paradigm was capable of quantifying differences between both doses and types of insult (hydrogen peroxide vs cisplatin), suggesting a both robust and sensitive tracking of neurodegeneration through live-cell imaging. We believe this approach is relevant and applicable to the screening for drug targets and candidates targeting neuroprotection and repair in the inner ear.

PS 451

Paraquat-induced cochlear anoikis

Jianhui Zhang[1]; Dalian Ding[2]; Hong Sun[3]; Richard Salvi[4]
[1]State University of New York at Buffalo; [2]University at Buffalo, USA; [3]Central South University; [4]Center for Hearing and Deafness; State University of New York at Buffalo

Background
Paraquat, one of the most widely used herbicides, exerts its cellular toxic effects by generating the superoxide radical, resulting in lipid peroxidation, mitochondrial degeneration and DNA damage. Previous in vitro studies in our lab using cochlear organotypic cultures showed that paraquat damaged hair cells in a dose dependent manner. Interestingly, prior to dying, we observed significant dislocation of the normally well-organized rows of inner and outer hair cells. We hypothesized that hair cell row dislocation could be due to damage to the surrounding support cells and extracellular matrix (ECM) that anchor the hair cells in the proper orientation and location within the sensory epithelium. To test this hypothesis, we treated cochlear organotypic cultures with paraquat and evaluated the time course of supporting cell loss and hair cell loss and disruption of the ECM.

Method
Postnatal day 3 (P3) rat cochlear organotypic cultures were treated with paraquat doses ranging from 0 to 500 µM for 24 h. Hair cell loss and dislocation were evaluated by immunolabeling hair cells with myosin VI or fluorescently conjugated phalloidin. Supporting cell loss and dislocation were detected by immunolabeling support cells with sox-2. Programmed cell death was assessed using a flurogenic probe that detects executioner caspase-3. Superoxide was evaluated using dihydroethidium. Antibodies against β-catenin and E-cadherin were also used to detect disruption and loss of the ECM.

Results
Paraquat-induced hair cell loss began in the basal turn and progressed towards the apex and outer hair cell loss (OHC) was greater than inner hair cell (IHC) loss. Interestingly, dislocation and derangement of the hair cell row occurred prior to hair cell loss. Paraquat-induced damage first occurred in the supporting cells resulting in the loss ECM staining and collapse of the supporting structures that hold the hair cells in place within the organ of Corti. This was followed by loss of OHC and IHC.

Conclusion
When the cells become detached from one another due to loss of the ECM, they undergo a specific form of anchorage dependent programmed cell death referred to as anoikis. Our results suggest that the superoxide radical generated by paraquat initially damages cochlear supporting cells and the ECM; their detachment results in hair cell row dislocation and derangement. Taken together, our results suggest that hair cell loss results from a combination of anoikis, disruption of the ECM and oxidative stress.

Paraquat-induced cochlear anoikis V2.docx

PS 452

Cell death map in drug-induced hearing loss: apoptosis, autophagy, and necroptosis

Mi-Jin Choi[1]; Young Sun Kim[1]; Yeon Ju Kim[2]; Yun Yeong Lee[1]; Oak-sung Choo[1]; Beomyong Shin[2]; Yeong Cheol Kim[2]; Chi-Kyou Lee[3]; Kye Hoon Park[3]; Seong Jun Choi[3]; Yun-Hoon Choung[1]

[1]Department of Otolaryngology, Ajou University School of Medicine, Suwon, Republic of Korea; [2]Department of Otolaryngology, Ajou University School of Medicine; [3]Department of Otolaryngology-HNS, Soonchunhyang University Cheonan Hospital

Introduction

Gentamicin (GM) and cisplatin (CDDP) show various side effects such as sensorineural hearing loss and dizziness in which the mechanisms have not been identified. The purpose of the study is to analyze the difference among drug type-induced auditory cell death mechanisms including apoptosis, autophagy and necroptosis.

Methods

HEI-OC1 auditory cells were cultured and treated with various doses of GM (0, 2.5, 5, and 7.5 mM) or CDDP (0, 3.25, 7.5, and 15 µM), and then analyzed by western blot. To analyze apoptotic effects by GM- and CDDP-induced ototoxicity, cleaved PARP and cleaved caspase-3 bands were analyzed in Western blot. RIP1 and RIP3 were used as the markers for necroptotic effect. For autophagy markers, Beclin1, p62, and LC3 were used. In vivo study, healthy 6~8-week-old male Sprague-Dawley rats (200–350 g) were used. Auditory brainstem responses (ABRs; 8, 16 and 32 kHz) were measured at the time of pre-injection and post-injection, and hearing threshold shifts were analyzed. Each doses of GM (270 mg/kg) or CDDP (16 mg/kg) were intraperitoneally injected, and then analyzed by H&E staining, TUNEL, and immunofluorescence for the morphologic study.

Results

On the 6 weeks after GM injection, hearing loss was detected, with thresholds increasing to 26.3 ± 20.0 dB, 23.8 ± 18.9 dB and 27.5 ± 21.9 dB at 8, 16 and 32 kHz, respectively. 4 days after cisplatin injection, ABR thresholds also increased to 24.4 ± 14.2 dB, 29.7 ± 16.8 dB and 30.8 ± 18.7 dB at 8, 16 and 32 kHz, compare to control (11.7 ± 4.0 dB). In H&E stain, we found the change of nuclear morphology, such as breakdown and shrinkage, and the decreased number of spiral ganglion cells treated with GM and CDDP. In immunofluorescence, LC3B and TUNEL staining were much more highly expressed than RIP1 and RIP3 in spiral ganglions and lateral ligaments in GM-induced ototoxicity. Reversely, RIP1 and RIP3 was much higher expressed than LC3B and TUNEL staining in spiral ganglions and lateral ligaments under CDDP.

Conclusion

GM and CDDP seem to have different ototoxic mechanisms; apoptosis or autophagy in GM and necroptosis in CDDP.

Middle Ear Physiology

PS 453

High-speed holographic shape and transient response measurements of mammalian tympanic membrane

Payam Razavi[1]; Hami Tang[1]; Nima Maftoon[2]; Michael E. Ravicz[3]; John J. Rosowski[2]; Cosme Furlong[1]; Jeffrey T. Cheng[4]

[1]Center for Holographic Studies and Laser micro-mechaTronics, Mechanical Engineering Department, Worcester Polytechnic Institute; [2]Eaton Peabody Lab, Massachusetts Eye and Ear Infirmary, Harvard Medical School; [3]Eaton-Peabody Laboratory, Massachusetts Eye and Ear Infirmary/ Department of Otolaryngology, Harvard Medical School; [4]Eaton Peabody Laboratory, Massachusetts Eye and Ear Infirmary; Department of Otolaryngology, Harvard Medical School

Background

We are developing a High-speed Digital Holographic (HDH) system to measure acoustically induced transient displacements of live mammalian Tympanic Membrane (TM) for research and clinical applications. To date, the HDH can make one-dimensional displacement along the laser illumination direction. Because of the TM';s tent-like shape and angled orientation inside the ear canal, these 1-D measurements need to be combined with measurements of the shape and orientation of the TM to determine the true surface normal (out-of-plane) TM displacements. Shape information enables displacement measurement independent of the direction of observation, which helps correlate the results of measurements made after changes in specimen orientation or location. In addition, shape parameters such as curvature, depth of cone etc., can be used to better understand the TM mechanics. These parameters can also be as part of a quantitative diagnostic assessment.

Method

The novel HDH shape measurement enhancements can make up to 100 shape measurements per seconds with varied shape resolution range. The enhancements require minimal hardware modifications, using the same imaging optics for HDH displacement measurements. Interferograms gathered with continuous high-speed optical phase sampling while altering the wavelength of a tunable laser allow reconstruction of the TM shape. This rapid acquisition of shape data reduces the sensitivity of our measurements to small motions induced by breath-

ing and heartbeat, making this technology suitable for in vivo measurements.

Results

We present preliminary measurements on post-mortem human and chinchilla TMs with outer ear canal partially removed. The shape measuring resolution is ~120 μm in full-field of view and at >100,000 points. The shape determination is followed by the transient displacement measurements in response to broadband acoustic clicks with temporal resolutions of >67.2 kHz and spatial resolution < 20 μm. Both shape and displacement measurements can be made within less than 150 ms. Because in-plane TM motion is insignificant, surface normal displacements can be calculated from the shape and one-dimensional displacement measurements in order to derive the out-of-plane displacements.

Conclusion

High-spatial resolution measurements of TM shape and its displacement along one dimension allow accurate determinations of out-of-plane TM motions. This capability allows investigations of acoustic-to-solid interaction on the TM surface, better modal and finite element analyses of TM models, and better quantification of the TM transient response. The shape measurements can also provide significant clinically relevant information.

Funding

PS 454

The Effect of Ossicular Joint Fusion on the Human Middle Ear Frequency Response

Yona Visbuch[1]; Peter Gottlieb[2]; Sunil Puria[3]
[1]STANFORD UNIVERSITY; [2]Stanford University Department of Mechanical Engineering; [3]Eaton-Peabody Laboratory, Massachusetts Eye and Ear; Department of Otolaryngology, Harvard Medical School; Speech and Hearing Bioscience and Technology, Harvard University Graduate School of Arts and Sciences

Introduction

There are different clinical scenarios in which the middle ear ossicular chain is either disrupted, partially absent or fused, which necessitates ossicular chain reconstruction (OCR) with partial or total prosthesis (PORP or TORP). This reconstruction bypasses the middle ear joints. The literature is divided regarding the relative effectiveness of these two methods[1,2] . Clinical outcomes of ossicular chain reconstruction with PORP or TORP are much less favorable than the excellent results after Stapedotomy procedures using a piston prosthesis. We present a frequency response comparison of the effects of fusing the incusstapes joint (ISJ), incus-malleus joint (IMJ) and both and relate this to the above mentioned clinical scenarios.

Material and Methods

The 3D velocity of the stapes was first measured in unaltered cadaveric human cadaver temporal bones (N=9), stimulated with pure tones (100Hz-20kHz), using a Polytec CLV-3D laser Doppler vibrometer. The measurements were then repeated after fusing one or both of the ossicular joints.The sound source was used to play a wide range of frequencies, and the pressure at the TM was measured using the TM microphone.

Results

Fusing the incudo-malleolar joint cuased a gain in the high frequencies. Fusing the incudo-stapedial joint caused a mild loss at the very low frequencies and a mild gain along the rest of the frequencies. Fusing both joints caused low frequency loss along side with mid and high frequencies gain.

Disscution

In order to shed light on the effect of ossicular joint bypass clinical scenarios, we examined the effect of synovial joints fusion. By fusing the incus-malleus joint we simulate a PORP connecting the tympanic membrane to the stapes super structure. Fusing both joints mimics a TORP which connects the tympanic membrane to the footplate in a columella like manner, and by fusing only the incus-stapes joint we mimic the piston stapedotomy prosthesis which connects the long process of the incus to the stapes footplate while bypassing the joint. When comparing the 3 fusion cases it';s clear that the IMJ fusion created the most prominent effects, with not a big difference from both joint fused state, which implies that when compering the PORP to the TORP reconstruction the difference in the clinical outcomes is not derived solely by the anatomical change. Fusing the ISJ did not have a major impact on the response which corresponds to the excellent clinical outcomes that are reported following stapedotomy surgery. In the future we are planning to compare the different axis of stapedial motion.

References

1 Puria S, Kunda LD, Roberson JB Jr, Perkins RC. Malleus-to-footplate ossicular reconstruction prosthesis positioning: cochleovestibular pressure optimization. Otol Neurotol. 2005 May;26(3):368-79

2 Murugasu E, Puria S, Roberson JB Jr. Malleus-to-footplate versus malleus-to-stapes-head ossicular recon-

struction prostheses: temporal bone pressure gain measurements and clinical audiological data. Otol Neurotol. 2005 Jul;26(4):572-82.

ARO FIG.doc

PS 455

Middle Ear Response to high intensity sound with normal and perforated Tympanic Membrane

Jeffrey T. Cheng[1]; Iman Ghanad[2]; Aaron K. Remenschneider[2]; John J. Rosowski[3]
[1]Eaton Peabody Laboratory, Massachusetts Eye and Ear Infirmary; Department of Otolaryngology, Harvard Medical School; [2]Massachusetts Eye and Ear Infirmary, Harvard Medical School; [3]Eaton Peabody Lab, Massachusetts Eye and Ear Infirmary, Harvard Medical School

Background

In the absence of a working middle-ear muscle reflex, the human middle ear is generally considered a linear system as it conducts environmental sound to the cochlea. However, the response of the middle ear to high intensity impulsive sounds, like those from blast, can be expected to be nonlinear. It is speculated that rupture of the tympanic membrane (TM) by high intensity sound provides a protective mechanism that reduces further damage to the middle and inner ear by decreasing the sound energy imparted to the ossicular chain and cochlea; however this hypothesis has not been rigorously tested.

Methods

We use cadaveric human ears with closed middle-ear cavities to characterize middle ear responses to high intensity sounds. Tones between 200 and 10000 Hz with levels between 80 and 160 dB SPL are generated by a compression driver and delivered to the ear canal. Sound pressure levels near both the lateral and medial surfaces of the TM are monitored by calibrated microphones. Simultaneously, Laser Doppler Vibrometry is used to record sound induced vibrations of the umbo and the stapes. Measurements are performed both with the TM intact and after controlled TM perforation. Growth functions of the umbo and stapes displacements with respect to the ear canal sound pressure levels are studied.

Results

The displacement of the umbo and stapes shows different nonlinear responses to high intensity sounds: The umbo displacement grows faster than stimulus level (an expansive nonlinearity) at low frequencies, while the stapes exhibits compressive growth (grows less than the stimulus level) over a wide frequency range. The sound pressure level threshold that induces nonlinearity is frequency dependent, and is lower at the stapes than at the umbo. This behavior is consistent with a nonlinear action of the stapes annular ligament that is separated from the umbo by the ossicular joints. Descriptions of the effect of TM perforations with variable sizes on the middle ear response to high intensity sounds are in progress.

Conclusions

The human TM and ossicular system exhibits nonlinear behavior at ear-canal sound pressure levels as low as 110 dB SPL, and the umbo and the stapes show different nonlinear behaviors.

PS 456

Quantifying the effects of the external-ear bone-conduction source in chinchilla

Peter N. Bowers[1]; Michael E. Ravicz[2]; John J. Rosowski[3]
[1]Harvard University; Eaton Peabody Lab, Massachusetts Eye and Ear Infirmary; [2]Eaton-Peabody Laboratory, Massachusetts Eye and Ear Infirmary/ Department of Otolaryngology, Harvard Medical School; [3]Eaton Peabody Lab, Massachusetts Eye and Ear Infirmary, Harvard Medical School

Introduction

Bone conduction (BC) hearing results from vibrations of the skull that are perceived as sound. Although this phenomenon is used in the clinic for diagnosis and treatment of middle-ear disease, its mechanisms are not fully understood, as skull vibrations travel through multiple pathways to the inner ear. Here we examine one BC pathway, the external-ear component of BC hearing that is related to sound pressure produced in the ear canal by the vibratory stimuli. The magnitude and phase of this effect are estimated using existing and model impedance data and new ear-canal sound pressure measurements.

Methods

Ear canal sound pressure (ECSP) was measured in live, anesthetized chinchillas and cadaveric chinchilla heads. Measurements were made in several conditions—normal, incudostapedial joint (ISJ) interruption, and incus fixed to the cochlear bone. In each condition, ECSP measurements were made while the ear was open and blocked to quantify the 'occlusion effect';, an increase in ECSP after EC occlusion that is used in the diagnosis of middle-ear disease. We estimated the magnitude and phase of the hypothetical vibration-driven external ear BC (EEBC) source using the ECSP measurements

along with existing impedance data of the middle ear and the reverse ear-canal input impedance, and impedance models of the occluded ear canal and middle ear in the manipulated states.

The contribution of the EEBC source to hearing in chinchilla was also directly quantified via measurements of the compound action potential (CAP) thresholds in response to BC stimulation by comparing the threshold between the normal state and after removing the contribution of EEBC to hearing via interruption of the ISJ.

Results and Conclusions
The output of the EEBC source, quantified as a volume velocity normalized by skull vibration, is relatively flat in magnitude and phase over the frequency range where the BC stimulator operates most effectively—0.4 to 4kHz.

The CAP threshold produced by BC stimulation is increased below 3 kHz when the occluded normal ear is unoccluded and when the ISJ is interrupted, consistent with a significant EEBC effect on BC hearing after occlusion in this frequency range. The magnitude of increase in CAP after occlusion is similar to the change in ECSP after occlusion. The similarity of BC thresholds when the ear canal is unoccluded and the ISJ is interrupted suggests little effect of ECSP when the ear canal is unoccluded.

PS 457

Effects of Tympanic-Membrane Perforation in Gerbil on Distortion Product Otoacoustic Emissions: Middle-Ear Transmission in Forward and Reverse Directions

Wei Dong[1]; Glenna Stomackin[2]; Timothy Jung[3]; Glen Martin[4]
[1]*VA Loma Linda Health Care System and Otolaryngology, Loma Linda University;* [2]*VA loma Linda Healthcare System;* [3]*Loma Linda University Health;* [4]*VA Loma Linda Healthcare System and Loma Linda University Health*

Distortion product otoacoustic emissions (DPOAEs) evoked by a pair of tones carry information about the mechanisms that generate and shape them, and therefore hold promise for providing powerful noninvasive diagnostics of cochlear operations and impairments. DPOAEs are sensitive to middle-ear (ME) function, because they have been shaped by ME transmission twice--primaries in the forward and DPOAEs in the reverse direction. However, the effects of ME injuries to DPOAEs have not been systematically characterized. The current study focused on how perforated tympanic membranes (TMs) influence gerbil DPOAEs by systematically characterizing ME transmission in both forward and reverse directions.

This study systematically explored variations in DPOAEs and ME transmission in forward and reverse directions under several TM-perforation (pars tensa) conditions. The care and use of animals were approved by the IACUC of the VA Loma Linda facility. Two equilevel ($L_1=L_2$) primary tones at f_1 and f_2, with a fixed f_2/f_1 ratio (1.25) were generated and responses acquired using Tucker-Davis Technologies (TDT) System III, and programed using MATLAB and the TDT visual-design studio. Pressure responses at the TM near the umbo (P_{TM}) and in scala vestibuli (P_{SV}) near the stapes, along with the velocity of the umbo (V_{umbo}), were simultaneously measured using a Sokolich ultrasound probe-tube microphone, a micro-pressure sensor, and a laser Doppler vibrometer. Measurements were made following mechanically-induced TM perforations ranging from miniscule to complete removal of the TM leaving only the ossicular chain intact. ME transmission in both forward and reverse directions under these conditions was illustrated by the variation of P_{TM}, V_{umbo}, and P_{SV} at either primary or DPOAE frequencies.

Results indicated that $2f_1$-f_2 DPOAEs were measurable up to ~40% TM perforation. DPOAE reductions increased with increasing size of the TM perforation--DPOAE reduction mainly occurred at higher frequencies when the TM was perforated <20%. With more than 20% perforation, DPOAEs decreased dramatically at all frequencies. Variations of ME-pressure gain in the forward and ME pressure loss in the reverse direction were mainly associated with the loss of the efficiency of sound transmission between the TM and umbo, which appeared to account for DPOAE reductions.

Since human TM perforations are usually caused by either trauma or infection, our results contribute towards providing insight into understanding ME transmission under pathological conditions as well as promoting the application of DPOAEs in the evaluation and diagnosis of deficits in ME transmission.

PS 458

Role of Suspensory Attachments in the Gerbil Middle Ear

Eileen Y. Brister[1]; Claus-Peter Richter[2]; Nikita Kumar[3]; Xiaodong Tan[4]; Robert H. Withnell[1]
[1]Department of Speech and Hearing Sciences, Indiana University; [2]Department of Otolaryngology-Head and Neck Surgery, Feinberg School of Medicine, Northwestern University & Resonance Medical, LLC, Chicago; [3]Indiana University; [4]Department of Otolaryngology-Head and Neck Surgery, Feinberg School of Medicine, Northwestern University

Background
The middle-ear ossicles are held in place through several ligaments/attachments. The impact of these attachments on the motion of the ossicles is not fully understood. This study investigates the mechanics of attachments in the gerbil middle ear through systematic detachment of the ligaments and measurement of the impact on both auditory evoked potentials and ossicle position.

Methods
Auditory evoked potentials were measured in anesthetized gerbils with an open middle ear cavity and an intact ossicular chain. Measurements were repeated after detaching the posterior incudal ligament and/or the anterior malleal attachment. In addition, gerbil temporal bones were scanned at beamline 2-BM at the Advanced Photon Source, Argonne National Laboratory (Argonne, IL, USA) using microtomography with monochromatic photon energy near 27 keV. All scans were completed with an open middle ear cavity and an intact ossicular chain then repeated after detaching the posterior incudal ligament and/or the anterior malleal attachment. Change in angle and position of the ossicles was quantified.

Results
Detachment of ligaments and attachments in the gerbil middle ear caused increased auditory evoked potential thresholds. This was accompanied by a change in ossicular position. Imaging data suggested a difference in composition between the anterior malleal attachment and the posterior incudal ligament in the gerbil middle ear, with the anterior malleal attachment more closely resembling bony structures.

Conclusion
Elimination of the attachments of the middle ear impacts the suspension of the ossicles, causing a change in the middle ear transfer function. The ligaments and attachments play an essential role in the mechanics of the ossicular system. [This research used resources of the Advanced Photon Source, a U.S. Department of Energy (DOE) Office of Science User Facility operated for the DOE Office of Science by Argonne National Laboratory under Contract No. DE-AC02-06CH11357.]

PS 459

Symmetry of Angles of Axes of Incudes

Jessica Specht; N Wendell Todd
Emory

Background
Phylogenetic relationships of mammals can be inferred from the auditory ossicles. For incudes, one difference used is the angles of axes: the angle between "short process axis" and the "long process axis". Humans show a more open angle (mean 64.0 degrees) between the axes than do chimpanzees (mean 55.7 degrees). Objective

To check if the angles of the axes of incudi exhibit bilateral symmetry – which is expected if the axes are genetically determined.

Methods
Post-mortem material-analysis prevalence study of incudes from 41 modern adult crania with clinically normal temporal bones. Angles of axes were determined on rectilinear digital photographs of incudes in standard lateral orientation. Two observers independently drew the axes and measured the axes.

Results
Observer agreement was within 4 degrees for the 24 of 34 left-sided incudes, and for 27 of 35 right-sided incudes. The mean of the two observer';s angle determinations were used. Left incudes median 67 degrees, range 60 -73; right 67.5, range 58.5-77. Bilateral symmetry of angles of axes was found: Spearman';s correlation coefficient 0.50, 95% confidence interval .17 to 72, N=31.

Discussion
We found the range of angles of axes of incudes similar to pooled left-and-right values reported by Quam et al.(2014).

Conclusions
Despite concerns about inter-observer agreement and physiologic/evolutionary advantage, angles of axes of incudes are probably genetically determined features.

Middle-ear anatomy and hinge-like rotational motion of the malleus-incus complex in sheep and human

Jae Hoon Sim[1]; Ivo Dobrev[2]; Dominik Péus[1]; Flurin Pfiffner[2]; Merlin Schär[1]; Lukas Prochazka[2]; Christof Röösli[2]; Alexander Huber[2]
[1]*University Hospital Zurich;* [2]*University of Zurich, University Hospital Zurich, Department of Otorhinolaryngology, Head and Neck Surgery, Switzerland*

Background
The middle ear in mammals converts acoustic waves in air to vibration of cochlear fluid. It has been known that the fluid pressure in the cochlea is amplified in comparison to the air pressure in the ear canal. However, anatomy of the middle ear in mammals significantly differs with species, and such a large anatomical variation across species is not clearly explained from the aspect of middle ear sound transmission and hearing perception.

Methods
In order to describe the relation between the middle-ear anatomy and hinge-like rotational motion of the malleus-incus complex (MIC), 1) characterization of the middle-ear anatomy, 2) measurement of impedance for the hinge-like rotational motion, and 3) analysis of hinge-like rotational motion using a simple-lever model of the middle ear were performed for human and sheep cadaveric ears. Relevant anatomical features of the middle ear, of both species, were characterized using micro-CT imaging, and the middle-ear impedance was measured using a 3-axis PalpEar force sensor (Sensoptic) for both the intact middle-ear ossicular chain and isolated stapes.

Results
Anatomy of the sheep middle ear provides a relatively small impedance and a relatively large lever ratio for the hinge-like rotational motion of the MIC compared to anatomy of the human middle ear. The inertial distribution of the middle-ear ossicles and anatomy of the incudo-stapedial joint suggest that the rocking-like motion of the stapes footplate can occur more easily in the human middle ear. The impedance measurements showed that relative contribution of the stapes to the middle-ear impedance is smaller in human than the corresponding contribution in sheep. The model simulation with such anatomical features and measured impedance revealed that restriction of the hinge-like motion by the tensor tympani tendon can be made more easily in the human middle ear.

Conclusions
Considering the findings of this study, it is presumed that the sheep middle ear is more optimal for hinge-like rotational motion of the malleus-incus complex and the rocking-like motion of the stapes footplate along its short axis is prevented. The human middle ear is presumed to achieve protection of the inner ear against stimulation of high intensity levels and/or adaptation of middle-ear sound transmission to changes of conditions surrounding the middle ear, by sacrificing some amounts of efficiency in the middle-ear sound transmission.

PS 461

Understanding the consequences of anatomically extreme single-ossicle middle-ear systems in extinct reptiles

James Nassif; Lawrence Witmer
Ohio University

The middle ear is thought to have evolved to decrease the loss of energy as sound waves pass from the environment to the inner ear. Though absolute frequency sensitivity is not strongly correlated with middle ear function, critical functions including sound localization and inner-ear damage mitigation have been tied to middle-ear morphology across diverse species. Whereas mammals are often the focus of middle-ear anatomical research, the evolution and dynamics of the independently-evolved hearing systems of other vertebrates have received less attention. In living reptiles and birds, the middle-ear conduction pathway is comprised of a single rod-like ossicle (the columella), typically connected to a tympanic membrane by cartilage. Birds and non-avian dinosaurs present an opportunity to explore both the physical and developmental constraints of the ear across many different magnitudes of size. Because the hearing apparatus of extinct reptiles is poorly understood, basic anatomical investigation is necessary to explore any functional consequences of morphology. Though the columella is the only middle-ear structure known to fossilize, preliminary investigation suggests that the anatomy of the middle ear in extinct species may be constrained through identifying osteological correlates in extant taxa of both key soft-tissue structures and unpreserved hard tissues. Cadaveric specimens representing ecologically and taxonomically diverse birds and several species of crocodilian were μCT scanned, and ear structures including columellae were digitally reconstructed using Avizo. Specimens were also dissected to visualize the anatomy and identify the attachments of middle-ear structures to hard tissues. Fossil specimens were also scanned and photographed. Using data from dissections and scanned specimens, tentative osteological correlates of soft tissue structures were identified and compared to the osteology of extinct taxa, consistent with estab-

lished methods of phylogenetic bracketing. Additionally, the shape and size of incompletely preserved columellae were constrained by the anatomy of the braincase. Though the columellae of some ornithischian dinosaurs are dimensionally similar to those of extant reptiles, the columellae of large theropods such as Tyrannosaurus are exceptionally long and thin. Other groups show morphologies that may be consistent with atympanic middle ears. Preliminary mechanical analyses suggest these extreme morphologies have functional consequences for the transmission of sound. These results are compared to previous studies of archosaurian ear morphology. Beyond evolutionary implications, any insights into the functional morphology of a single-ossicle middle ear have potential applications in the design of prosthetic implants for humans that are better able to meet the challenges of an active life.

PS 462

Optical Coherence Tomography of the Tympanic Membrane and Middle Ear: A Review

Hsern Ern Tan[1]; Philip Wijesinghe[2]; Brendan Kennedy[2]; Ben Allardyce[3]; Rob Eikelboom[4]; Marcus Atlas[5]; Rodney Dilley[5]
[1]*Ear Science Institute Australia;* [2]*BRITElab, The University of Western Australia;* [3]*Institute for Frontier Materials, Deakin University;* [4]*Ear Sciences Centre, School of Surgery, The University of Western Australia;* [5]*Ear Sciences Centre, The University of Western Australia, Nedlands, Australia*

Objective

To review the current literature and predict future trends of tympanic membrane and middle ear imaging using optical coherence tomography (OCT), for the purpose of tympanic membrane and middle ear diagnostics and reconstructive tympanoplasty planning.

Review Methods

A comprehensive literature search of the PubMed, EMBASE, Google Scholar, Scopus and Web of Science databases from Janurary 1950 to August 2017 with the keywords tympanic membrane, imaging, and optical coherence tomography was performed. Articles were screened and reviewed based upon predefined inclusion and exclusion criteria. Articles were restricted to the English language.

Results

Of 728 abstracts, 34 articles using OCT to visualize the tympanic membrane and middle ear were identified. 15 articles used OCT exclusively ex-vivo, and 19 articles demonstrated OCT use in-vivo to characterize the human tympanic membrane and middle ear structures for improved diagnostics, middle ear biomechanical modelling, and surgical planning.

Conclusion

Conventional imaging techniques cannot adequately resolve the micro-features of the fine tympanic membrane and middle ear structures, sometimes necessitating exploratory surgery in diagnostically challenging otological pathology. As a high-resolution, non-invasive imaging technique, OCT can act as an diagnostic aid for several otologic conditions including otitis media, retraction pocket, cholesteatoma and myringitis. OCT vibrometry can quantify ossicular chain dysfunction and tympanic membrane nanoscale vibration in conductive hearing loss and otosclerosis. 3D volumetric reconstruction of the tympanic membrane with OCT is crucial for reconstructive tympanoplasty planning. OCT imaging has limited field of view through the narrow, angled external auditory canal and is easily distorted from patient motion artefact. Future imaging devices must overcome the optical signal attenuation caused by the tympanic membrane and improve focal depth to image past the tympanic membrane into the middle and inner ear.

PS 463

Human Tympanic Membrane Shape and Thickness Map Measured with Optical Coherence Tomography (OCT)

Nam Hyun Cho[1]; Xiying Guan[2]; Michael E. Ravicz[3]; Nima Maftoon[4]; Sunil Puria[5]
[1]*Eaton-Peabody Lab., Mass. Eye & Ear; Department of Otolaryngology, Harvard Medical School;* [2]*Eaton-Peabody Laboratory, Massachusetts Eye and Ear; Department of Otolaryngology, Harvard Medical School;* [3]*Eaton-Peabody Laboratory, Massachusetts Eye and Ear Infirmary/ Department of Otolaryngology, Harvard Medical School;* [4]*Eaton Peabody Lab, Massachusetts Eye and Ear Infirmary, Harvard Medical School;* [5]*Eaton-Peabody Laboratory, Massachusetts Eye and Ear; Department of Otolaryngology, Harvard Medical School; Speech and Hearing Bioscience and Technology, Harvard University Graduate School of Arts and Sciences*

The shape and the spatial thickness distribution 'thickness map'; of the human tympanic membrane (TM) varies with location, between ears, and with middle-ear disease. The normal morphology of the TM among healthy human ears is not well characterized, as existing studies have used histological methods known to change its shape and thickness. Due to the density differences between air and soft tissue, Micro-CT has been used to obtain the shape of the TM, but it overestimates the thickness by more than a factor of two. More recently, OCT measurement techniques are being used but typically

on middle ears prepared with fixatives or dyes that can distort its soft tissue structures. In addition, most studies to date have used custom OCT equipment, which is costly and typically has a long development time.

In the present study, TM shape and thickness were measured in unfixed human cadaver temporal bones using a ThorLabs Ganymede III, 905 nm wavelength, High Resolution OCT system. The axial resolution (normal to the tympanic annulus plane) was 1.9 um; the lateral resolution varied with field width but was typically on the order of 10 um. The ear canal was dissected to visualize the TM. A three-dimensional (3D) volume scan was acquired using our in-house VibOCT software. The depth of field is limited to about 1.9 mm; thus, two or more volume scans were acquired at different focal depths. The volume scans were denoised and segmented using ImageJ thresholding and image processing routines. After processing, the multiple TM volumes were "stitched together" to obtain a full TM scan. The thickness map was constructed using the ImageJ sphere-filling algorithm.

In addition to measurements of the TM shape and thickness, the VibOCT software allows measurements of vibration response to sound stimulation of the TM and of the malleus and incus through the TM in the same specimen and with the same registration frame as the morphometry measurements. Combined measurements of TM shape, thickness map, and vibrations are important for understanding the effects of anatomical variations on middle ear function. These morphometry and vibrometry measurements are also being used to develop detailed finite-element models of individual ears. Supported in part by grant R01 DC05960 from the NIDCD of NIH.

Otoacoustic Emissions I

PS 464

Identifying the Origins of Cochlear Action Potentials, Transient Evoked Otoacoustic Emissions, and Stimulus Frequency Otoacoustic Emissions

Choongheon Lee[1]; Shawn Goodman[2]; John J. Guinan[3]; Jeffery Lichtenhan[1]
[1]*Washington University School of Medicine in St Louis;* [2]*University of Iowa;* [3]*Massachusetts Eye and Ear Infirmary*

Background
Objective measures are widely used in the laboratory and clinic to understand how the ear works and to differentially diagnose hearing disorders. However, most objective measures are incompletely understood. If their origins were better understood, their usefulness would be advanced. Our work addresses the origins along the cochlea of compound action potentials (CAPs), transient evoked otoacoustic emissions (TEOAEs), and stimulus frequency otoacoustic emissions (SFOAEs).

Methods
Our approach uses calibrated injections of solutions into the fourth turn of the guinea pig cochlea. Solutions are slowly driven from the apex to the cochlear aqueduct in the base, sequentially manipulating cochlear properties starting from the lowest-frequency region. Apical injections allow the short-wave region of the traveling wave to be manipulated without affecting of the long-wave region. Previous pharmaceutical, acoustic-trauma, and acoustic-suppression manipulations of the short-wave region also affected the long-wave region.

Results & Conclusions
For CAPs evoked by a variety of tone burst frequencies and levels, we quantified the injection time when solutions (e.g. kainic acid) reduced CAP amplitudes by various percentages. The abolition time courses indicate that low-level tone-burst CAPs originate from the cochlear region tuned to the tone frequency (as expected), but surprisingly, for moderate- and high-level tone bursts, a substantial fraction (e.g. 50%) of the CAP originates from the most sensitive audiometric region regardless of the tone-burst frequency.

The effects of solutions (e.g., KCl) on TEOAEs from clicks of various levels allow us to determine if short-latency TEOAE components originate from the cochlear frequency place tuned to the component';s frequency, or from cochlear frequency places tuned to higher frequencies associated with shorter latencies.

The effects of solutions (e.g., KCl) on SFOAEs were studied by presenting a probe tone throughout an injection. SFOAEs were extracted as the difference between the ear-canal sound pressure from the probe tone (SFOAE and probe-tone sound pressures combined) and the probe-tone sound pressure alone measured in one of two ways: (1) by adding a second tone to suppress the SFOAE (but through cochlear nonlinearity may also generate a new SFOAE source), and (2) from subtracting the probe-tone sound pressure at the end of the injection when the solution had removed all active processes. Preliminary results with high-frequency probe tones show almost identical results from the two methods and that the SFOAE is almost completely abolished when the solution is just past the probe-tone';s cochlear frequency place. Data from low-frequency probe tones are being analyzed.

PS 465

Temporal Interactions in Basilar-membrane and Otoacoustic-emission Responses to Pairs of Clicks

Karolina K. Charaziak[1]; Wei Dong[2]; Christopher Shera[3]

[1]Caruso Department of Otolaryngology, University of Southern California; [2]VA Loma Linda Health Care System and Otolaryngology, Loma Linda University; [3]Caruso Department of Otolaryngology and Department of Physics and Astronomy, University of Southern California

Click-evoked otoacoustic emissions (CEOAEs) can change when another click stimulus precedes or follows the evoking click. This change in the CEOAE response is believed to arise through temporal interactions between the mechanical vibrations produced by the two clicks on the basilar membrane (BM). Thus, noninvasive measurements of CEOAE responses to click pairs may reveal temporal properties of BM vibration. We test this idea in gerbils by performing parallel measurements of CEOAEs and BM velocity (laser Doppler vibrometry) in response to pairs of clicks separated by varying time intervals. Physiologically vulnerable nonlinear interactions in the paired-click responses were observed in both CEOAE and BM recordings. As expected, nonlinear interactions in BM motion at the characteristic-frequency (CF) place were detected only if the time separation, Δt, between the two clicks was shorter than the duration of the BM click response. The BM response to the evoking click was maximally reduced in amplitude (suppressed) when the other click preceded the evoking click by Δt corresponding to ~1 period of the CF. Furthermore, the amount of suppression varied periodically with Δt as the varying phase-shift between the BM responses to the two clicks produced a pattern of alternating constructive and destructive interference. CEOAE responses at the frequency corresponding to the CF of the BM preparation showed a similar pattern of temporal interaction. In particular, the interactions diminished as Δt increased beyond the BM click response duration, and a periodic modulation in the strength of the CEOAE interactions was detected. When the evoking click was preceded by another click, the CEOAE response was suppressed, as observed in the BM vibrations; however, the maximum CEOAE suppression occurred at longer values of Δt (~2 periods of the CF). Interestingly, when the evoking click was followed by another click, the CEOAE response was augmented rather than suppressed. Augmentation was not observed in the BM vibrations at the CF. Thus, although important aspects of the temporal interactions seen in CEOAE responses, such as their time course and periodic modulation, match the temporal properties seen in BM responses, single-frequency CEOAE components do not always faithfully mimic the BM vibrations at the CF. Perhaps the distributed nature of emission generation limits the ability of CEOAEs to match BM responses measured at a single location. Alternatively, CEOAEs may correlate better with the vibratory patterns of other structures within the organ of Corti (e.g., the reticular lamina) than they do with the BM.

PS 466

Suppression of Spontaneous Otoacoustic Emissions in the Barn Owl (Tyto alba)

Sina Engler[1]; Pim van Dijk[2]; Geoffrey A. Manley[3]; Emile de Kleine[2]; Christine Koeppl[4]

[1]Department of Otorhinolaryngology, University Medical Center Groningen, Netherlands; [2]Department of Otorhinolaryngology, University Medical Center Groningen, The Netherlands; [3]Cluster of Excellence Hearing4all, Department of Neuroscience, Carl von Ossietzky University Oldenburg, Germany; [4]Carl von Ossietzky University Oldenburg

Background

Spontaneous otoacoustic emissions (SOAEs) have been observed in a variety of different vertebrates, including humans and barn owls (Tyto alba). The underlying mechanism producing the SOAEs and the meaning of their characteristics regarding the frequency sensitivity of an individual and species is, however, still under debate. The avian basilar papilla is homologous to the mammalian cochlea and the hearing range of barn owls is similar to that of humans. Moreover, behavioral tests showed that birds and mammals perform similarly when discriminating frequency or intensity. Barn owls'; short hair cells lack an afferent innervation, but also show functional similarities to mammalian outer hair cells. Therefore, understanding the SOAE properties of owls might help elucidate their source.

Methods

In the present study, we suppressed SOAE amplitudes by presenting pure tones at different frequencies and intensities to lightly-anesthetized barn owls. Suppression effects were quantified by deriving suppression tuning curves (STC) with a criterion of 2 dB suppression. These STCs were then compared to published frequency-threshold curves of auditory-nerve fibers.

Results

SOAEs were found in 100 % of ears (n=14). On average, 13 SOAEs were detected per ear, with a median distance between neighboring SOAEs of 417 Hz. The center frequencies of the SOAEs ranged from 3.1 to 10.5 kHz, with a median of 6.9 kHz. The majority of SOAEs were recorded at frequencies that fall within the barn owl';s "auditory fovea" (5 -10 kHz). The 3 dB bandwidth

correlated negatively with the emission amplitude. For SOAEs whose amplitude was sufficient for measuring an STC (n=89), the 3 dB bandwidth ranged between 15 and 300 Hz, with a median of 116 Hz. The STCs were V-shaped and sharply tuned, similar to human STCs. Between 5.3 and 10.7 kHz, the median Q10 dB value of STC was 5, and thus similar to that of single-unit neural data. There was no evidence for secondary suppression side lobes as seen in humans. The best thresholds of the STCs varied from 13 to 61 dB SPL and showed a clear correlation with SOAE amplitude, such that smaller SOAEs required a higher sound level to be suppressed.

Conclusions

The frequency-threshold curves of auditory-nerve fibers and STCs of SOAEs are very similar in their tuning characteristics. Thus, these data show that SOAE suppression tuning in the barn owl reflects neural tuning in primary auditory nerve fibers.

PS 467

Carbamazepine shifts Spontaneous Otoacoustic Emission Frequencies Upward

Emile de Kleine[1]; Bert Maat[1]; Jan D.M. Metzemaekers[2]; Pim van Dijk[1]
[1]*Department of Otorhinolaryngology, University Medical Center Groningen, The Netherlands;* [2]*Department of Neurosurgery, University Medical Center Groningen, The Netherlands*

Carbamazepine (CBZ) is a medical drug that is applied against epilepsy and trigeminal neuralgia. A known side-effect of CBZ is that it produces a down-shift in pitch of about one semitone (100 cents) at 500 Hz (Braun & Chaloupka, 2005). This shift is only noticable by people who have absolute pitch perception, so most patients taking the drug will not notice a change in their auditory perception. It has been suggested that the pitch shift is due to the effect of the drug on central auditory function. Alternatively, CBZ might affect cochlear processing. We investigated the possible cochlear changes due to CBZ, by measuring spontaneous otoacoustic emissions (SOAEs) in patients using CBZ.

We measured SOAEs in three patients who were using CBZ for trigeminal neuralgia. The daily dosage across our subjects differed between 800 and 1200 mg per day, respectively. SOAEs were recorded during and after the drug was used. SOAEs were identified in five out of six ears.

In all ears, CBZ caused a consistent upward shift in SOAE frequency of 30-111 Hz, at frequencies ranging from 1.3 to 2.4 kHz. This corresponds to a shift between 2.3 and 4.9%, or between 39 and 82 cents. The magnitude of the frequency shift proportionally increased with increasing frequency. In one patient, we were able to measure that an increased CBZ dosage gives an increased frequency shift.

Carbamazepine produced an upward shift in SOAEs (this work) and a downward shift in perceived pitch (Braun & Chaloupka, 2005). This suggests that CBZ alters the mechanics of the inner ear, by increasing resonance frequencies along the basilar membrane. Then, the excitation pattern of a music tone will shift towards the apex. Hence, the tone will stimulate neurons that were excited by lower-pitched sounds prior to CBZ administration. This may account for a downward shift of the pitch percept. Other manipulations of OAEs, like contralateral acoustic stimulation and changes of body posture and ear canal pressure, typically show frequency shifts on the order of 10 Hz. These emission changes are much smaller and can probably be accounted for by changes in middle ear stiffness.

We conclude that a shift in the basilar membrane resonance properties does at least partially account for the CBZ-induced pitch shift described by musicians with absolute pitch perception.

Reference: Braun, M., & Chaloupka, V. (2005). Carbamazepine induced pitch shift and octave space representation. Hearing Research, 210(1–2), 85–92. http://doi.org/10.1016/j.heares.2005.05.015

PS 468

Effects of Overstimulation on Otoacoustic Emissions Generated by the Basilar Papilla

Ariadna Cobo-Cuan; Peter M. Narins
University of California Los Angeles

Introduction

The two auditory organs in the amphibian ear, the amphibian and basilar papillae, differ not only in sensitivity and frequency tuning but also in their physiological vulnerability. Distortion-product otoacoustic emissions (DPOAEs) generated from the amphibian papilla (AP) are more susceptible to physiological insult than are those from the basilar papilla (BP). Similar differences are expected in DPOAE responses following acoustic overstimulation. In the bullfrog, DPOAE responses from the AP were temporarily silenced after loud noise exposure (Simmons et al. 2014). This study aims to evaluate DPOAE shifts arising after high-level stimulation in the BP. The susceptibility of this auditory end-organ to high-intensity noise stimulation is analyzed.

Methods

DPOAE audiograms were evaluated in Rana pipiens with a fixed-frequency ratio $f_2/f_1=1.1$ and stimulus levels $L_1=L_2=60$ dB SPL. The frequency $2f_1-f_2$ of highest emission level was identified in the spectral range corresponding to the BP response to design the acoustic overstimulation paradigm. High-level stimuli (100 dB SPL) were delivered for two hours via a closed acoustic system using either pure tones or 1/3-octave band noise. We also measured input–output curves from the BP. Stimulus levels were increased in 2-dB steps from 30 to 80 dB SPL. DPOAE measurements were taken immediately before noise exposure and 15 min, 1, 2 and 24 h post-noise exposure.

Results

In all frogs investigated, DPOAE-audiograms exhibited a bimodal shape with low- and high-frequency peaks representing DPOAEs generated within the AP and the BP, respectively. After 2 hours of high-level stimulation, BP-DPOAEs dropped to or near noise floor levels in nearly all ears. Minor shifts were observed in AP-DPOAEs. As expected, DPOAE changes were more variable following pure-tone exposure. Input–output curves revealed drastic changes in BP sensitivity. In some individuals, evidence of recovery was observed 1 h following acoustic trauma, but DPOAE shifts typically returned to pre-exposure levels after 24 h.

Conclusions

Short-term acoustic overstimulation in the BP produces maximal DPOAE shifts. The time required for complete recovery suggests there was no damage to the sensory epithelium. DPOAEs from the BP are not thought to involve an active process, but metabolic alterations following acoustic trauma could affect the generation of this passive nonlinear response.

PS 469

Stimulus Frequency Otoacoustic Emissions Evoked without Suppressor Tones and Analyzed with a Time-Varying Parametric Model Reveal Additional Finestructure: Is this Evidence for Incomplete Suppression?

Joshua J. Hajicek[1]; Ivan W. Selesnick[2]; Simon Henin[1]; Carrick L. Talmadge[3]; Glenis Long[1]
[1]The Graduate Center, City University of New York;
[2]Tandon School of Engineering New York University;
[3]National Center for Physical Acoustics, The University of Mississippi

Introduction

Stimulus frequency otoacoustic emissions (SFOAEs) were measured with- and without-suppressor tones.

Significant differences between these paradigms were not expected since the chosen suppressor parameters are commonly used. Differences were revealed only after applying a variation of the least squares (LS) fitting analysis that allowed the amplitude and phase to change in a time-varying (TV) manner. When a traditional LS fit was used, differences were small. In theory, the TV-LS approach better models the dynamic time-frequency fluctuations that occur locally over a given data segment. Using this tool, we present evidence that valid SFOAE responses may be obtained without the use of suppressor tones.

Methods

SFOAEs were measured from 19 human ears. The probe and suppressor tones, were continuously swept in frequency. In the without-suppressor condition, the probe tone was swept alone, from 1-8 kHz at 35 dB SPL. Probe tone amplitudes of, 25-40 dB SPL, in 5 dB steps, were measured in a subset of 7 ears. In the with-suppressor condition, a suppressor tone was presented in alternate trials. The suppressor tone was 50 Hz, and 20 dB SPL above the probe tone. A SFOAE$_{residual}$ was produced by subtracting the averages of the with- and without-suppressor responses. Signal components present in each condition were estimated using a LS parametric model on ½ second of Blackman windowed data. Time-varying-LS parametric models were also applied to each condition.

Results

When the LS fits were non-TV, SFOAE responses between the with- and without-suppressor conditions were similar. Interestingly, when the time varying LS fit was applied to the SFOAE$_{residual}$ and without-suppressor conditions significant differences were observed. Specifically, applying TV basis functions to the without-suppressor condition led to increased fine-structure, increased amplitude, and changes in phase slope. However, when the TV basis functions were used to estimate SFOAEs from the residual, little change was observed. SFOAE responses were also detected in the presence of suppressor tones, especially at low frequencies. Results were compares with SFOAEs generated by a time-domain, traveling-wave cochlear model.

Conclusions

The use of commonly accepted high-side suppressor paradigms may incompletely suppress SFOAEs or only suppress a subset of SFOAE generators.

ARO Figure Hajicek et al..pdf

Evaluation of the Coherent-reflection Component from Extracted Distortion-product Otoacoustic Source Components

Anthony W. Gummer; Dennis Zelle; Ernst Dalhoff
University of Tübingen

Introduction

Distortion product otoacoustic emissions (DPOAEs) emerge in the healthy cochlea in response to two simultaneously presented stimulus tones of frequencies f1 and f2. DPOAEs are assumed to consist mainly of two components, a nonlinear-distortion component and a coherent-reflection component. Recently, it was shown that using short stimulus pulses instead of conventional, continuous stimulation enables the extraction of the two DPOAE components in the time domain from the averaged microphone signal by solving a least-square optimization problem (Zelle et al., 2013). Due to their distinct generation mechanisms, the two types of DPOAE components may be used to analyze different cochlear properties (Abdala and Kaluri, 2017). Here, the short-pulse acquisition paradigm is used to evaluate the coherent-reflection component from six normal-hearing subjects.

Methods

Short-pulse DPOAEs were recorded unilaterally in a frequency range of f2 = 1 to 4 kHz (f2/f1 = 1.2) in 20-Hz steps for L2 = 45 dB SPL. The stimulus level of the f1-tone was chosen to be a function of f2 and ranged between L1 = 58 and 66 dB SPL. After averaging and band-pass filtering, the DPOAE short-pulse responses were fitted with a mathematical model to extract the amplitudes and phases of the nonlinear-distortion and coherent-reflection components. For the sake of comparison, DPOAEs were also recorded with continuous stimulus tones, yielding a superposition of the two DPOAE components.

Results

The extracted DPOAE components show fundamental differences in their amplitudes and phases. The coherent-reflection component exhibits a pronounced fluctuation in amplitude, whereas the amplitude of the nonlinear-distortion component varies smoothly with frequency. The phase of the coherent-reflection component rotates rapidly with an average phase shift of -14.0±2.1 periods between f2 = 1 and 4 kHz. In contrast, the phase of the nonlinear-distortion component exhibits only a minor shift (-1.5±0.3 periods). The phasor sum of the extracted DPOAE components matches the continuous DPOAE data closely (r2 = 0.75±0.08), indicating accurate extraction of the DPOAE components. In general, the amplitude of the coherent-reflection component decreases slightly with increasing frequency and is positively correlated (r2 = 0.94, p < 0.01) with the occurrence of spontaneous otoacoustic emissions.

Conclusion

Short-pulse DPOAEs enable accurate extraction of the DPOAE components in the time domain, allowing the evaluation of nonlinear distortion and coherent reflection from a single recording. The results suggest that coherent reflection is more pronounced at moderate frequencies and in cochleae with a large number of spontaneous emissions.

Comparing generator DP I/O estimates from different methods

Michal Fereczkowski[1]; Konstantinos Anyfantakis[2]; Ewen MacDonald[1]; Bastian Epp[1]
[1]*Hearing Systems group, Department of Electrical Engineering, Technical University of Denmark;*
[2]*Technical University of Denmark*

Background Otoacoustic emissions provide a non-invasive, yet objective tool for investigating cochlear state. Distortion-product otoacoustic emissions are currently modelled as the sum of a distortion component (arising from the overlap area of the two primary tone traveling waves) and a delayed reflection component. While the former is believed to reflect the state of the outer hair-cells in the overlap region, the latter arises due to micro-mechanical irregularities along the cochlea. The interference of these two components leads to high variability of the emissions recorded in the ear canal, which limits the applicability of the method to investigate frequency-specific I/O functions. Several techniques have been proposed to separate the generator component and thus reduce the variability in the recorded emission. This study compares two separation techniques based on least-squares fitting and on averaging of the fine structure in normal-hearing listeners. Method Distortion-product otoacoustic emissions were recorded for three octave-wide primary sweeps and two primary-level paradigms (scissors and equal level), for four levels of the second primary, L2 (input). The values were uniformly distributed between 35-80 dB SPL. Forward pressure level calibration was applied to control the primaries' presentation levels at the eardrum and to reduce the variability of the OAE levels due to probe placement. The recorded DPOAEs were then processed by a) a least-squares fit (LSF) method and b) averaging the DPOAE fine structure across five points around each DPOAE target frequency. The processed DPOAEs were used to estimate the generator-related cochlear response (output) at 29 frequencies. The comparison of the resulting I/O functions obtained from the two methods was performed on

data obtained from 10 normal-hearing listeners. Results Correlation analysis was performed on the DPOAE responses and I/O function estimates obtained with the two methods and the unprocessed DPOAE responses. The results showed that the responses and compression ratios estimated with the averaging method were highly correlated to the estimates obtained from the LSF method. Moreover, the averaging-method estimates could explain significantly more variance in the corresponding LSF-method estimates than the unprocessed-data estimates could. Additionally, the test-retest variability of the estimated compression ratios was similar between the averaging and LSF methods, and lower than in the unprocessed case. Conclusions The results suggest that the averaging method provides a viable approximation to source-unmixing, at least when estimating I/O functions in normal-hearing listeners.

PS 472

Analysis of DPOAE level maps using random field theory

Chris Brooks[1]; Odile Clavier[1]; Lindsay Allen[1]; Catherine Rieke[2]; Abigail Fellows[2]; Jay Buckey[3]
[1]Creare, LLC; [2]Space Medicine Innovations Laboratory, Geisel School of Medicine at Dartmouth, Hanover, NH, United States; [3]Geisel School of Medicine at Dartmouth

Background

DPOAE level maps are obtained by varying both the f2 frequency and the f2/f1 ratio (2346 frequency-ratio pairs in this study) to collect a more comprehensive picture of cochlear function than standard DP-grams. This may offer more sensitive detection of cochlear damage, but new analysis techniques are needed to derive the full value from the complex dataset. DPOAE maps are usually represented as a two-dimensional image where the DPOAE levels in color are mapped over a grid of ratio versus DPOAE frequency (Figure 1 top). This representation provides an opportunity to analyze the map using imaging analysis techniques such as Random Field Theory (RFT). RFT fits a statistical model to the image, and then uses the model parameters to determine whether changes between two images (or maps) are significant. We hypothesized this would help distinguish actual cochlear damage from random variation and measurement noise.

Methods

To provide the RFT model with data on normal variability, we measured a minimum of 3 DPOAE maps over no more than 10 weeks on 29 audiometrically-normal subjects with no known exposure to ototoxins or noise. For each individual ear, the model consists of a baseline with "systemic" and "local" changes at each trial as well as measurement errors. We used the repeated maps

to establish the baseline, measurement noise, and "normal" systemic variability. We then measured DPOAE maps on noise-exposed subjects who attended a loud musical event with exposures greater than 90 dBA. For each noise-exposed subject, we measured three baselines prior to the noisy event, and then measured their DPOAE maps immediately after exposure (night of the event), the next day, and one week later (Figure 1, top). We used our model to produce plots of the distribution of changes within the map (Figure 1, bottom).

Results

Assuming that cochlear changes measured by DPOAEs tend to occur around the f2 and DP frequencies, we used a 2-D Gaussian ("smoothing") filter to disentangle significant cochlear changes from measurement noise and normal variability. The separation of the map analysis into measurement noise and distributed changes provided a sharp delineation between pre- and post-noise exposure maps in those with significant exposures. Work is ongoing to use the technique with lower level exposures.

Conclusion

Random Field Theory is a novel approach to the analysis of DPOAE level maps which may provide a sensitive tool to detect pre-clinical cochlear changes caused by noise or ototoxins.

Figure 1. Top images show the maps collected before (maps 1-3) and after (maps 4-7) loud music exposure. Changes are apparent in the original maps (top), but the changes are much more readily seen (bottom) after removing measurement noise using the smoothing filter and focusing on the 3 kHz - 4 kHz frequency band.

Plasticity, Learning & Adaptation to Hearing Impairment I
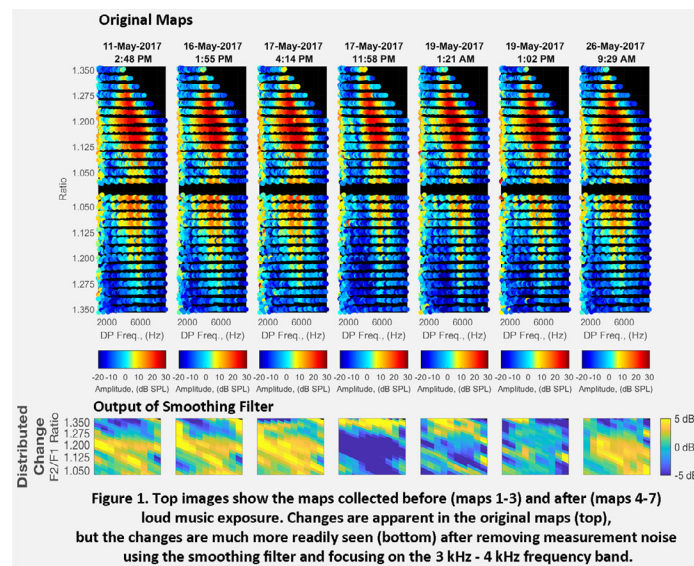
PS 473

Enriched or traumatic sound differentially drive transcript-specific BDNF expression and memory acquisition

Philipp Eckert[1]; Wibke Singer[1]; Lucas Matt[2]; Rama Panford-Walsh[3]; Anne Bausch[2]; Marie Manthey[3]; Enrico Tongiorgi[4]; Carlos Duarte[5]; Csaba Harasztosi[6]; Peter Ruth[2]; Thomas Ott[7]; Lukas Rüttiger[3]; Thomas Schimmang[8]; Knipper Marlies[3]

[1]Department of Otolaryngology, Tübingen Hearing Research Centre (THRC), Molecular Physiology of Hearing, University of Tübingen; [2]Institute of Pharmacy, Department of Pharmacology, Toxicology and Clinical Pharmacy, University of Tübingen, Auf der Morgenstelle 8, 72076 Tübingen, Germany; [3]Department of Otolaryngology, Tübingen Hearing Research Centre (THRC), Molecular Physiology of Hearing, University of Tübingen, Elfriede-Aulhorn-Straße 5, 72076 Tübingen, Germany; [4]B.R.A.I.N. Centre for Neuroscience, Department of Life Sciences, University of Trieste, Via L. Giorgieri, 34127 Trieste, Italy; [5]Centre for Neuroscience and Cell Biology (CNC) and Department of Life Sciences, University of Coimbra, 3004-504 Coimbra, Portugal; [6]Section of Physiological Acoustics and Communication, University of Tübingen, Germany; [7]Transgenic Facility Tübingen, University of Tübingen, Otfried-Müller-Straße 27, 72076 Tübingen, Germany; [8]Instituto de Biologíay Genética Molecular, Universidad de Valladolid y Consejo Superior de Investigaciones Científicas, E-47003 Valladolid, Spain

Brain derived neurotrophic factor (BDNF) is a key modulator of synaptic plasticity. It remains unclear how the different transcripts of the complex BDNF gene contribute to its multifaceted functions. We generated the BLEV (BDNF-live-exon-visualization) reporter mouse which visualizes BDNF expression following promoter-specific usage of exon-IV and exon-VI by translating CFP and YFP simultaneously to BDNF protein in characteristic neuronal, glial, and vascular locations in the hippocampus. Animals exposed to acoustic enrichment showed increased Schaffer collateral LTP together with improved acquisition in the Morris-Water-Maze. In parallel, usage of BDNF promoters IV and VI was altered together with the expression of parvalbumin in the hippocampus and along the auditory axis. Altered BDNF promoter usage and increased hippocampal synaptic plasticity were not observed following acoustic trauma. Enriched sensory experience may thus synchronize BDNF promotor usage in different cell types linked to improved stimulus coding through associated learning, a feature that fails upon traumatic acoustic events.

PS 474

How impaired SGN axon bifurcation affects sound processing in the auditory brainstem of the mouse

Lukas Rüttiger[1]; Steffen Wolter[2]; Dorit Möhrle[2]; Peter Pilz[2]; Dennis Zelle[2]; Hannes Schmidt[2]; Knipper Marlies[1]
[1]Department of Otolaryngology, Tübingen Hearing Research Centre (THRC), Molecular Physiology of Hearing, University of Tübingen, Elfriede-Aulhorn-Straße 5, 72076 Tübingen, Germany; [2]University of Tübingen

Research Background

cGMP signaling triggered by the binding of C-type natriuretic peptide (CNP) to its receptor guanylyl cyclase B (GC-B; Npr2) has been linked by genetic evidence to a remarkable variety of physiological functions like skeletal bone growth, female fertility, cardiac growth, fat metabolism and gastrointestinal function. For the nervous system it has been recently demonstrated that the CNP/GCB/ cGMP/cGMP-dependent protein kinase type I (cGKI) signaling pathway is essential for sensory axon branching. Lack of Npr2 leads to blurred tonotopic organization [1] and to failure of axon bifurcation at the dorsal root entry zone of the spinal cord during embryonic development [2]. Also auditory nerve fibers (ANF) - that differ in their discharge rate and sound sensitivity - bifurcate at the border of the embryonic hindbrain and consequently extend daughter branches that finally innervate the anteroventral, posteroventral, and dorsal cochlear nuclei.

Methods

We studied the functional consequences of ANF bifurcation loss on hearing and central plasticity in a mouse model with a global deletion of the gene for the particulate guanyly cyclase type B (Npr2). In these adult GC-B KO mice, we describe the hearing function of adult GC-B knockout mice and their wildtype littermates in detail, using evoked auditory brainstem response (ABR), distortion product otoacoustic emission (DPOAE) and auditory steady state response (ASSR). Histological correlates of the auditory phenotype were verified by applying immunohistochemistry on sections of cochlea and high-resolution fluorescence microscopy.

Results

In the cochlea, GC-B is not expressed in the Organ of Corti, but in SGNs. Our GC-B deficient mouse model shows mildly increased hearing thresholds with no indication of a conductive hearing loss. Cochlear synaptic phenotype and expression of specific molecular hair cell markers and neuronal markers will be described. Stimulus-evoked activity in the auditory nerve and neuronal activation of the early auditory brainstem (SOC) was analysed in view of reduced efferent synapse activity and OHC function (MOC).

Conclusions

The GC-B-cGMP signaling pathway plays an important role during development. Strikingly, the resulting anatomical peculiarities are reflected also in the post-developmental performance upon very specific auditory tasks.

[1] Lu CC, Cao XJ, Wright S, Ma L, Oertel D, Goodrich LV. Mutation of Npr2 leads to blurred tonotopic organization of central auditory circuits in mice. PLoS Genet. 2014 Dec 4;10(12)

[2] Ter-Avetisyan G, Rathjen FG, Schmidt H. Bifurcation of axons from cranial sensory neurons is disabled in the absence of Npr2-induced cGMP signaling. J Neurosci. 2014 Jan 15;34(3):737-47

PS 475

Cochlear Impairments and Central Neural Plasticity in Low-Level Noise Environments

Xiaopeng Liu[1]; Benjamin D. Auerbach[2]; **Guang-Di Chen**[3]; Richard Salvi[2]
[1]Xiaopeng Liu; [2]Center for Hearing and Deafness; State University of New York at Buffalo; [3]Guang-Di Chen

Background

In cats, prolonged exposure to sounds up to 80 dB SPL failed to induce an ABR threshold shift (TS), nevertheless depressed sound-evoked activity in the auditory cortex (AC) at frequencies within the band but enhanced response at the edges. In contrast, prolonged exposure to a low-level narrowband noise at 75 dB SPL decreased the cochlear compound action potential (CAP) in rats, but paradoxically increased sound evoked activity in the inferior colliculus in the noise band. These discrepancies could be due to differences in the recording sites, species or peripheral impairment. To clarify these issues, we measured CAP and AC-responses in rats exposed to the noise presented at different levels.

Methods

Rats were exposed to a narrowband noise (18-24 kHz) for 6 weeks at intensities from 45 to 85 dB SPL. CAP and multiunit clusters from the AC anterior auditory field (AAF) were recorded 3-12 hours post-noise. The AAF was vertically divided into 4 sub-divisions and 24 recordings in each sub-division in each animal were averaged as one subset of a population response.

Results

At the cochlea, the exposure reduced CAP amplitudes at low stimulus levels resulting in TSs at frequencies within the noise band whereas it mainly reduced CAP amplitudes at high stimulus levels at frequencies above the noise band. No changes were noted in the CAP at frequencies below the noise band. In the AAF, TS was absent or less than CAP TS. Despite significant reductions in CAP amplitudes at frequencies within and above the noise band, AAF-responses remained at the control levels, evidence of central compensation. At low frequencies where there was no CAP-changes, AAF responses were significantly enhanced especially at moderate stimulation levels. Inspection of individual subsets of population responses revealed frequency profiles with "in-band suppression but edge-enhancement" as previously observed in cats; these changes were noise level dependent. The remaining responses showed smooth change across frequency with low-frequency-enhancement and a progressive decline in responses in high-frequency regions.

Summary

Our results show that long term, low-level noise exposures significantly reduce CAP amplitudes and cause mild TS. These peripheral deficits give rise to robust central compensation in AAF that partially or totally compensate for the CAP TS. The magnitude of the cochlear changes and AAF compensation varied in a complex manner that depended on the intensity of the noise exposure and frequency and intensity of the stimulus used to elicit the response.

PS 476

Cross-modal Interactions of auditory and pain sensory inputs: a possible model of pain hyperacusis

Senthilvelan Manohar[1]; Caitlyn Potter[2]; Henry Adler[2]; Kelly Radziwon[3]; Manjit Kaur[2]; Richard Salvi[3]
[1]University at Buffalo, USA; [2]University at Buffalo; [3]Center for Hearing and Deafness; State University of New York at Buffalo

Introduction

Some individuals with partial hearing loss perceive moderate-intensity sounds as extremely loud, a condition known as hyperacusis. A subpopulation of hyperacusis patients also experience moderate-intensity sounds as painful, a condition referred to as pain hyperacusis. Pain hyperacusis is defined as a manifestation of a more complex sensory hypersensitivity disorder affecting visual, vestibular, and somatic pain pathways associated with migraines, fibromyalgia and autism. Prima facie interactions between auditory and pain pathways are evident in normal subjects who experience sounds as painfully loud at high intensities, e.g., 140 dB SPL. These results suggest that pain hyperacusis might arise from heighted cross-modal interactions between central auditory and pain pathways. To test this hypothesis, we developed the Auditory Nociception Task (ANT), a novel behavioral paradigm

which assesses thermal pain sensitivity in the absence and presence of auditory stimulation.

Method
ANT is based on the thermal tail-flick latency test, which is used to assess a rodent's pain perception by dipping the rat's tail (1-2 cm) into the 52oC water. The latency to remove the tail from the warm water is proportional to the level of nociception. To test the effect of auditory stimulation on pain sensitivity, we measured tail-flick latencies in the absence or presence of broadband noise presented at 70, 80, 90, 100 or 115 dB SPL. The noise was presented for 60 seconds, the last 15 seconds during which the rat's tail was submerged in the water. Tail-flick latency was measured for each condition and stimulus order was randomized.

Results
In Quiet, mean thermal tail-flick latencies were ~9 sec. Moderate-intensity noise increased tail-flick latencies, which were interpreted as sound-induced hypoalgesia. We then increased the noise intensity to 115 dB SPL, and found that tail-flick latencies shortened at higher intensities (e.g., 4 seconds, more than twice as fast relative to Quiet). The shorter tail-flick latency is interpreted as evidence for sound-induced hyperalgesia or central pain sensitization.

Conclusion
Our results confirmed previous studies that moderate intensity sound can induce thermal hypoalgesia. The current study also extends these findings by showing that louder sounds (>100 dB) can induce thermal hyperalgesia. Our data suggest that the auditory system could modulate thermal pain sensitivity via cross-modal interactions between central auditory and pain pathways. Moderate intensity sound reduces pain sensitivity whereas high intensity sound increases pain sensitivity. In conclusion, ANT may provide the first behavioral model to investigate pain hyperacusis. Supported by NIH (R01DC014452, R01DC014693) and HHF (78121).

PS 477

Postnatal Exposure to an Acoustically Enriched Environment Influences the Morphology of Neurons in the Adult Rat Auditory System.

Jana Svobodova Burianova; Josef Syka
Department of Auditory Neuroscience, Institute of Experimental Medicine of the Czech Academy of Sciences

Evidence has accumulated that various kinds of acoustic exposures during the critical postnatal period of development can modify the morphology of the central auditory system. In our previous study (Ouda et al., 2014), we demonstrated that an early postnatal short noise exposure (8 min, 125 dB, postnatal day 14) resulted, in rats, in a remodeling of the neuronal trees in the inferior colliculus (IC), medial geniculate body and auditory cortex (AC), including changes in the numerical density of spines on the dendrites of pyramidal neurons in the AC. In the present study, we analyzed, using the Golgi-Cox method, the morphology of neurons in the IC and AC of 4-month-old Long-Evans rats exposed to an acoustically enriched environment (AEE), during the third and fourth weeks of life. The AEE consisted of a spectrally and temporally modulated sound reinforced by an active behavioral paradigm with positive feedback. In AEE exposed rats, the mean neuronal volume, total length of the neuronal tree, and the area of the perikaryon were found to be greater than in control animals in the external cortex and the central nucleus of the IC, but not in the dorsal IC cortex. In the AC, AEE exposed rats exhibited longer basal and apical dendritic segments of pyramidal neurons, as well as greater spine density in the basal but not apical dendrites. These findings demonstrate that an AEE exposure during the critical postnatal period can induce permanent changes in the structure of neurons in the central auditory system, which apparently represent morphological correlates of the functional plasticity.

PS 478

Neuronal Plasticity in auditory cortex and brainstem after auditory deafferentation

Jae Joon Han[1]; **Ye Ji Shim**[2]; Ho Sun Lee[3]; Seung Ha Oh[4]; Min-Hyun Park[2]
[1]Seoul National University Hospital; [2]Seoul National University, Boramae Medical Center; [3]Seoul National University Boramae Medical Center; [4]Seoul National University Hospital

Auditory deafferentation induces plastic changes in many brain regions, including the auditory pathway. The change of neocortical activity and recruitment by the other sensory systems is a well-known neurological phenomenon which is occurred by intra- and cross- modal plasticity after sensory deprivation. Unilateral hearing loss was also affects the auditory system, and could evoke plastic changes, however, it was not evaluated yet fully. Here, we evaluate plastic change of neuron in inferior colliculus (IC) and auditory cortex (AC) after unilateral and bilateral deafness using an animal model.

The structural changes of neuron after deafness were evaluated with dynamic change of non-phosphorylated neurofilament heavy change (NEFH), which was immunoreacted with SMI-32 monoclonal antibody, by western blot analysis. The mRNA expression level of NEFH was evaluated with RT-PCR in AC and IC, and by cell count of SMI-32-immunoreactive (-ir) neuronal population in IC. Deafness was induced by cochlear ablation bilaterally (BD) or unilaterally at right side (RD), and the brain tissues were harvested at 4 and 12 weeks after deafness. In AC, SMI-32 mRNA expression and SMI-32-ir protein levels were increased in the BD group. In particular, SMI-32-ir protein levels increased significantly 6 and 12 weeks after deafness was induced. In contrast, no significant changes were detected in the right or left auditory cortices at any time point in the UD group. In IC, the mRNA expression level of NEFH was not changed in BD and UD groups until 12 weeks after deafness at both side. However, in BD group, the ratio of SMI-32-ir neuron was increased at 4 weeks after deafness and western blot supported this finding. The ratio was return to normal level at 12 weeks after deafness. In UD group, no significant changes were identified. Bilateral auditory deafferentation induces plastic change in AC and IC.

PS 479

Enhanced Activation of Layer 1 Interneurons by Thalamic and Neuromodulatory Input to Auditory Cortex during a Developmental Critical Period

Anne E. Takesian[1]; Ana C. Castro[2]; Emma He[2]; Takao K. Hensch[1]
[1]Boston Children's Hospital and Harvard University; [2]Harvard University

Sound frequency (tonotopic) maps in primary auditory cortex (A1) are refined during a developmental critical period to best represent the surrounding acoustic environment. How and why this robust plasticity is restricted to early life remains unclear. We recently identified an inhibitory cell type within layer 1 (L1) whose activity gates A1 map plasticity in mice. This L1 subclass expresses ionotropic serotonergic receptors (5-HT$_{3A}$R) but not vasoactive intestinal peptide (VIP). Here, we reveal these interneurons to be robustly activated by thalamic and modulatory cholinergic inputs that change during transitions into and out of the critical period. First, expressing an anterograde viral tracer in cells within auditory thalamus (medial geniculate body; MGB) to visualize their projections into A1 revealed a robust innervation of L1. MGB axons preferentially surrounded non-VIP, 5-HT$_{3A}$R-expressing cells, forming putative contacts that co-localized with the vesicular glutamate transporter 2 (vGluT2), a marker of thalamocortical boutons. Using in situ hybridization to localize neuromodulatory receptor transcripts, we found that these interneurons also pref-

erentially expressed nicotinic acetylcholine receptors (nAChRs) containing the α4 subunit. Finally, in a series of developmental studies, both thalamic and modulatory inputs to these L1 interneurons were enhanced during the critical period for tonotopic plasticity (postnatal day, P12-15). vGluT2 expression in L1 was increased in critical period-aged mice (P14) as compared to juveniles (P20) or adults (>P60). An analysis of gene expression in the 5-HT$_{3A}$R-expressing L1 interneurons after fluorescence-activated cell sorting (FACS) further indicated 5-HT$_{3A}$R and nAChR signaling to be augmented early in life as well. Indeed, functional studies using voltage-sensitive dye imaging (VSDI) in auditory thalamocortical slices revealed heightened L1 responses during the critical period to both MGB stimulation and drugs targeting 5-HT$_{3A}$ and nACh receptors. Taken together, our results suggest that the interneuron circuits in L1 that gate cortical plasticity are strongly engaged by both thalamic and neuromodulatory inputs during a transient developmental period. Understanding how these L1 interneurons can be activated may yield novel strategies to engage cortical plasticity and recovery of auditory function following hearing loss across the lifespan.

PS 480

Neural Correlation between Frequency-Layers in the Inferior Colliculus of Rats after Salicylate Administration

Xiaopeng Liu[1]; Guang-Di Chen[2]; Richard Salvi[3]
[1]Xiaopeng Liu; [2]Guang-Di Chen; [3]Center for Hearing and Deafness; State University of New York at Buffalo

Background
High doses of salicylate reliably induce tinnitus in the rat model in ~10-20 kHz frequency range. Salicylate has therefore been an invaluable tool for studying the mechanisms of tinnitus. Elevated spontaneous activity, reorganization of frequency representation, and increased synchrony between neurons in the central auditory system all may be associated with the phantom auditory perception of tinnitus. Salicylate-induced increases in spontaneous activity in the inferior colliculus (IC) of rats are observed selectively in the neurons related to tinnitus frequency. Salicylate administration also induces tonotopic reorganization in the IC and higher auditory centers, with both low- and high-frequency neurons shifting their tuning towards the tinnitus frequency range However, the frequency-dependency of tinnitus-related changes in neural synchrony remains unclear. To address this, correlation coefficients between multiunit activities recorded simultaneously from different frequency-layers in the IC were compared pre- and post-salicylate administration.

Methods

Rats were anesthetized with ketamine (50 mg/kg) and xylazine (6 mg/kg). A linear electrode array with 16 channels spaced 100 µm apart was inserted along the dorsal-ventral axis of the IC (across frequency-layers). Multiunit activity in response to tone-bursts at different frequencies and intensity levels were recorded to obtain frequency receptive fields. Spontaneous activity was recorded for the inter-channel correlation analysis. The rats received an injection of sodium salicylate (300 mg/kg, i.p.) and post-salicylate data were compared to the pre-salicylate baseline activity.

Results

Salicylate administration induced an increase in the inter-channel correlation with significant changes observed selectively in the mid-frequency region. Preliminary data also suggests a similar increase in correlation after intense noise exposure. Interestingly, the increase in inter-channel correlation appeared to be suppressed by a moderate-level broadband background noise.

Discussions

The frequency-specific increase in neural correlation in the mid-frequency region of the IC may be related to salicylate-induced tinnitus perception. Increased connectivity between the mid-frequency neurons and their neighboring low- and high-frequency neurons may cause low- and high-frequency regions of the IC to respond more to mid-frequency sounds, which could account for the tonotopic reorganization observed with salicylate. Although suppression of inhibitory activity has been proposed to mediate many of the plastic changes observed in the central auditory system following salicylate administration, further studies are needed to determine the mechanisms underlying these frequency-dependent changes in neural synchrony. Suppression of inter-channel correlation by the background noise may be consistent with the clinical use of background noise for tinnitus suppression.

PS 481

Norepinephrine and Auditory Plasticity in Cochlear Implant Learning

Erin Glennon; Ina Shehu; Ioana Carcea; Mario Svirsky; Robert C. Froemke
NYU School of Medicine

Cochlear implants are neuroprosthetic devices that can provide hearing to deaf patients. However, the learning rates and peak performances of speech perception with cochlear implant use are highly variable across patient populations (Blamey et al. Audiol Neurotol 2013). Adaptation to use the electrical signals provided by cochle-

ar implants is believed to require neuroplasticity within the central auditory system, and Individual differences in plasticity are thought to be an important source of outcome variability (Fallon et al. J Neural Eng 2009). However, the mechanisms by which behavioral training enables plasticity and improves outcomes are poorly understood. Here we investigate the hypothesis that neural mechanisms that promote plasticity in the rodent auditory system are key to optimizing cochlear implant usage, and might be especially helpful in cases of poor performance. In particular, we focus on noradrenergic modulation of the auditory thalamus and cortex by the locus coeruleus, which can enable robust and long-lasting neural and behavioral changes (Manunta and Edeline J Neurophysiol 2004; Martins and Froemke, Nat Neurosci 2015; Sara, Curr Opin Neurobiol 2015)

Recently we developed a new surgical approach for cochlear implantation in adult rats (King et al. J Neurophysiol 2016). Our approach optimizes insertion depth of a multi-channel electrode array (with eight separate channels) and allows animals to freely behave while using the cochlear implant to perform auditory-based behavioral tasks. Normal hearing rats are trained on an auditory recognition go/no-go task, and self-initiate trials to respond for a food reward to a target tone and withhold responses to non-target foil tones. Previously we have shown that this task requires auditory cortex activity, performance on the task affects auditory cortical responses to target and foil tones, and that this task is sensitive to cortical neuromodulation and receptive field plasticity (Carcea et al., Nat Commun 2017; Froemke et al., Nat Neurosci 2013; Kuchibhotla et al. Nat Neurosci 2017; Martins and Froemke, Nat Neurosci 2015). Thus we reasoned that cortical neuromodulation and plasticity might also be important for learning to recognize the behavioral meaning of cochlear implant stimulation.

Here we tested if changes in locus coeruleus activity could affect or improve auditory perceptual learning in normal hearing and cochlear-implanted rats. Normal hearing animals were first trained and tested as before (King et al., J Neurophysiol 2016). Prior to each daily behavioral training session with the cochlear implant, rats underwent a 5-10 min locus coeruleus pairing session, with optogenetic stimulation delivered at the onset of acoustic stimulation of the target cochlear implant channel. We also examined how locus coeruleus stimulation might affect task performance in normal hearing rats, when a new sound became the target. The new target tone (a previous foil tone) was paired with locus coeruleus stimulation as for cochlear-implanted animals. Some animals were wild-type rats, and other animals were transgenic TH-Cre rats used to restrict expression of ChETA channelrhodopsin-2 to noradrenergic locus

coeruleus neurons. Locus coeruleus stimulation accelerated the rate at which deafened animals learned with the cochlear implant and normal hearing animals learned the reversal task. We also used fiber photometry to monitor neural activity of noradrenergic locus coeruleus neurons. Together, these studies indicate that neuromodulation might play a powerful role in shaping outcomes with cochlear implant use and training.

PS 482

Binaural Interactions in the Inferior Colliculus following Unilateral Noise-Induced Hearing Loss

Joan Nguyen[1]; John Morley[2]; Carl Parsons[2]
[1]School of Medicine, Western Sydney Univeristy;
[2]School of Medicine, Western Sydney University

The auditory system is a bilateral system normally receiving input from two ears. Information from both ears is integrated and utilized to subserve seminal auditory functions such as sound localisaton and location of signals within noisy environments. The binaural functioning of the auditory pathway implies a balance of excitation and inhibition between inputs from either ear. Disruption to this balance, as may occur following unilateral noise-induced hearing loss, may profoundly affect the normal functioning of the auditory system. Consequences of unilateral noise-induced hearing loss include, global presentation of hyperactivity and increased spontaneous activity. There is a growing consensus that the imbalance of excitation and inhibition that may occur due to hearing loss may manifest in tinnitus. Therefore, understanding the neuronal alterations following noise-induced hearing loss may aid us in understanding the neural basis of tinnitus. In this study, we investigate the consequences of unilateral, noise-induced hearing loss on binaurally driven responses in the inferior colliculus (IC). Almost all ascending and descending auditory projections synapse within the IC. Moreover, neurons in the IC are predominately binaural and are dominated by excitatory-inhibitory (EI) responses. Thus, when an IC neuron is presented with sounds from both ears, there is a lower yield of driven neuronal activity. We hypothesize that due to unilateral, noise-induced hearing loss, the proportion of binaural neurons with an EI response will decrease. Adult male Wistar rats (n = seven) were unilaterally exposed to a 115 dB SPL 16 kHz for 1-hour. Seven normal hearing animals were used as controls. After a minimum recovery period of 3 months, post ABRs confirmed permanent threshold shifts in the noise-exposed animals. Using 32-channel, single shank electrodes, we simultaneously recorded from left and right ICs under monaural and binaural conditions (0-85db, 1-44khz), with combinations of left and right ear presentations delivered stochastically. Contralateral recording in the IC showed frequency

tuning curves that bordered the spectral range of the noise-trauma stimulus. Ipsilateral stimulation of normal hearing animals typically yields a low proportion of neurons displaying driven activity. In contrast, in animals with hearing loss, ipsilateral stimulation of the intact hearing ear resulted in an increased proportion of excitation in the ipsilateral IC, suggesting a release of inhibition. This is reflected in higher proportion of EE binaural neurons in this group.

PS 483

Distinct stages of perceptual learning revealed by the time course of anterograde interference on interaural-level-difference discrimination

Robert B. Baudo[1]; Beverly A. Wright[2]
[1]Department of Communication Sciences and Disorders, Northwestern University; [2]Department of Communication Sciences and Disorders, Knowles Hearing Center, Northwestern University Institute for Neuroscience, Northwestern University

Listeners improve on perceptual tasks with practice, providing a means to enhance normal perceptual abilities and treat perceptual disorders. However, this improvement can be disrupted by training on a second perceptual task. In retrograde interference, learning on one task is disrupted by subsequent training on another. The time over which this interference occurs is thought to indicate the time necessary to stabilize newly acquired information in long-term memory (consolidation). In contrast, in anterograde interference learning on one task is disrupted by preceding training on another. Anterograde interference can occur without retrograde interference, suggesting that anterograde interference may disrupt an earlier stage of learning: acquisition. By this view, the time frame over which anterograde interference occurs would indicate the time it takes for the initially trained task to complete the entire acquisition process. With this idea in mind, we investigated the time course of anterograde interference between two interaural-discrimination tasks.

We examined the influence of three different two-day training regimens on performance on interaural-level-difference discrimination (ILD). On day 1, training on ILD at 4 kHz occurred either in isolation (L-only regimen; n=13), or immediately (TL regimen; n=11) or 30 minutes after (T30L regimen, n=7) training on interaural-time-difference discrimination (ITD) at 500 Hz. On day 2, all listeners were tested on ILD immediately after ITD. All conditions were performed at midline.

For the L-only regimen, ILD thresholds on day 2 were lower than on day 1, documenting improvement on

ILD discrimination. In contrast, for the TL regimen, ILD thresholds on day 2 did not differ from day 1, demonstrating anterograde interference. However, for the T30L regimen, ILD thresholds on day 2 were lower than those for the TL regimen and similar to the L-only regimen, showing that anterograde interference from training on ITD did not last for 30 minutes. Finally, day 1 ILD thresholds were lower for the T30L regimen compared to the TL regimen, indicating that training on ITD benefitted performance on ILD when the two tasks were separated by 30 minutes.

These outcomes suggest that the acquisition processes associated with training on ITD were complete less than 30 minutes after training, and differed fundamentally from subsequent learning processes. These data add to other behavioral evidence of a clear distinction between the acquisition and consolidation phases of learning. A greater understanding of the stages of learning could lead to more optimal training strategies and improved diagnosis of learning disorders.

PS 484

Biosonar Performance of Big Brown Bats Recovers Rapidly After Exposure to Intense Band-limited Sound

Andrea Simmons[1]; Kelsey Hom[2]; Alexandra Ertman[1]; James Simmons[1]
[1]Brown University; [2]City University of New York

Echolocating bats fly, orient, and forage in a cluttered acoustic environment where they are exposed to their own biosonar pulses, to the pulses of other bats, and to echoes from multiple surrounding objects. Aggregate sound pressure levels recorded from flying bats range from 110 dB to 130 dB SPL, but these animals experience no difficulty hunting or orienting in these noisy conditions. We reported previously that intense broadband noise exposure does not affect biosonar performance of big brown bats flying in dense acoustic clutter in the laboratory. Here, we extend these results by quantifying flight performance and parameters of pulses emitted by bats navigating through an acoustically-cluttered corridor 2 min after exposure to intense band-limited noise or FM sweeps (mean level 116 dB SPL rms, sound exposure level 152 dB). Navigation errors increased after exposure to some stimuli, but with considerable individual variability between bats and with rapid recovery. Numbers, amplitude, and temporal patterning of pulses in successful flights varied between bats but were not affected systematically by prior noise exposure. Navigation errors may reflect a change in motivation rather than a decline in hearing sensitivity or in the ability to process biosonar signals. Alternatively, big brown bats may experience temporary threshold shifts after noise exposure but recover quickly.

PS 485

Hearing Loss and Social Support in Rural and Urban Alabama

Marcia Hay-McCutcheon; Adriana Hyams; Xin Yang; Jason Parton
The University of Alabama

A large body of evidence has suggested that social support has a significant impact on health outcomes. Recently, there has been increased interest in how perceived social support affects the clinical and rehabilitative management of those with hearing loss. Social support is related to how an individual's social network provides both psychological and material resources to cope with stressful situations. For this study, a traditional measure of hearing handicap, the Hearing Handicap Inventory for Adults (HHIA), was used to assess emotional and social consequences of hearing loss. Additionally, a social support questionnaire, the Medical Outcomes Study (MOS) Social Support Survey, was used to evaluate how social support impacts adults with and without hearing loss living in rural or urban geographical regions of Alabama. Data were analyzed from 82 study participants with hearing loss (43 females, 39 males) and from 121 adults with normal hearing (82 females, 39 males). It was that found the degree of hearing loss and the social and emotional consequences of hearing loss as assessed using the HHIA did not differ between adults who lived in rural or urban settings. It was found, however, that specific types of social support differed for adults with and without hearing loss who lived in the two different residency settings. For adults with hearing loss, tangible support or having access to people who provide behavioral support or material aid, was poorer for those who lived in rural settings compared to those with hearing loss who lived in urban settings. This trend was not observed for adults with normal hearing. For adults with normal hearing, residency was not associated with tangible support but it was associated with other types of social support including informational support, emotional support and positive social interaction. Our findings suggest that for adults with hearing loss, those who lived in rural areas had the perception of poor tangible support, and consequently, the provision of support to address a hearing loss, both professional and non-professional, could be poorer for these adults compared to adults who lived in urban settings. These findings have consequences for the clinical management of adults with hearing loss who live in rural areas of the country.

PS 486

Rapid Auditory Learning: A Detriment to Speech in Noise Perception in Older Adults?

Hanin Karawani[1]; Limor Lavie[2]; **Karen Banai**[2]
[1]*Department of Hearing and Speech Sciences, University of Maryland;* [2]*University of Haifa*

Background

Why speech perception in noise declines with aging remains under substantial debate. One hypothesis is that older adults adapt to perceptually-difficult listening conditions to a lesser extent than younger adults, and this, in turn, contributes to their difficulties. To test this hypothesis, we are conducting an ongoing study on the association between speech perception and perceptual learning. Here we compared the rapid learning of speech in noise between normal-hearing older and younger adults.

Methods

Younger and older adults with age-normal hearing completed 40 minutes of training during which they listened to auditory passages embedded in adaptively-changing babble noise and answered content questions. To assess learning and transfer, participants were tested on the trained task and on two untrained tasks (pseudoword discrimination and sentence verification) before and after training. Starting SNRs of all tasks were adjusted to account for the known age differences in task performance.

Results

Both groups showed improvements over the course of the training session with no age effect. Pre- to post-test improvements were observed on the trained task but not on either of the untrained ones, again with no age effect. In older adults only, the amount of learning on the trained task accounted for significant amounts of variance on the untrained tasks (30% of the variance in pseudoword discrimination and 47% of the variance in sentence verification), even after controlling for the correlations between different indices of speech perception in noise. Conclusions: Under the conditions of the present study short-term perceptual learning of speech in noise was well preserved in older adults. The strong correlations found between the amount of improvement during training and baseline performance on the untrained tasks in older adults is consistent with the idea that in this group, poor rapid learning might limit the perception of speech in noise.

PS 487

Hearing aid use may improve working memory

Hanin Karawani[1]; Samira Anderson[2]
[1]*Department of Hearing and Speech Sciences, University of Maryland;* [2]*University of Maryland*

Objective

Age-related hearing loss (ARHL) is one of the most prevalent chronic health conditions among the elderly and its incidence is expected to increase with the aging of the population. Hearing loss is independently associated with accelerated cognitive decline. Specifically, working memory performance declines with age, and the decline is accelerated with hearing loss. What remains unknown is the mechanistic basis of the association between hearing loss and decreased cognitive function and the potential for offsetting cognitive decline through hearing rehabilitation. We asked whether hearing aid use would improve or offset working memory decline and whether there would be associated changes in auditory neural function.

Methods

32 older adults with age-related sensorineural hearing loss between the ages of 62-82 with no prior history of hearing aid use were fit with hearing aids. The experimental group (n = 18) wore the hearing aids for a period of six months and the control group (n = 14) did not use their fitted hearing aids during this period of time. All participants were tested with the same pre-test measures and were seen again for an identical post-test session after six months. Outcome measures included working memory assessments and electrophysiological cortical recordings to the speech sound /ga/ in quiet condition and noise conditions. Recordings were conducted in aided and unaided conditions.

Results and Conclusion

The use of hearing aids enhanced working memory performance and increased cortical evoked response amplitudes. Neurophysiologic changes correlated with working memory changes, suggesting a mechanism for the association between hearing loss and decreased cognitive function. These results underscore the importance of providing auditory rehabilitation for individuals with age-related hearing loss as a means for improving cognitive and neural function.

Pitch discrimination in normal-hearing and hearing-impaired listeners with and without musical training: behavioral data and modeling

Federica Bianchi[1]; Sébastien Santurette[2]; Torsten Bianchi[1]; Laurel H. Carney[3]
[1]*Hearing Systems Group, Department of Electrical Engineering, Technical University of Denmark;* [2]*Hearing Systems, Department of Electrical Engineering, Technical University of Denmark & Department of Otorhinolaryngology, Head and Neck Surgery, and Audiology, Copenhagen University Hospital;* [3]*Departments of Biomedical Engineering, and Neurobiology & Anatomy, University of Rochester , Rochester*

Hearing-impaired (HI) listeners typically have a reduced ability to discriminate the pitch of complex tones as compared to normal-hearing (NH) listeners. This perceptual deficit may be ascribed to a variety of factors, including reduced frequency selectivity and temporal fine structure cues. However, HI listeners perform as well as NH listeners when the complex tone only contains high-numbered harmonics. Thus, while fine spectro-temporal cues are disrupted, temporal envelope cues may be relatively more robust in HI listeners. Hence, the relative importance of spectral and envelope cues for pitch processing may be altered. The aim of this study was, on one hand, to clarify how the complex-tone pitch representation is altered by hearing loss in the auditory periphery and, on the other hand, to clarify whether musical training could help restoring the relative importance of pitch cues in HI listeners.

Fundamental frequency (F0) discrimination limens (F0DLs) were obtained for harmonic complex tones with an F0 of 125 Hz and varying harmonic content. Five conditions were tested: a resolved condition (RES, harmonics: 3-9), an intermediate condition (INT, harmonics: 10-16), two unresolved conditions (UN1, harmonics: 17-23; UN2, harmonics: 17-36) and a broadband condition (ALL, harmonics: 3-36). Fourteen young NH listeners (seven musicians) and ten HI listeners (five musicians) participated in this study. Phenomelogical models of the auditory periphery (Zilany et al., 2014) and midbrain (Mao et al., 2013) were used to examine the effects of hearing loss on the complex-tone representations at the level of the auditory nerve and inferior colliculus.

The F0DLs of the HI listeners were, on average, significantly larger (worse) than those of the NH listeners for the RES, INT and ALL conditions but were similar to NH listeners for the UN conditions. In both groups of listeners, the musicians'; performance for the RES and ALL conditions was enhanced relative to non-musicians, despite being limited by hearing loss. Although the model predictions were, on average, lower (better) than the data averaged across musicians and non-musicians, they could account for the difference in performance across conditions for both NH (Pearsons'; correlation to the data: r = 0.87, p <0.001; Mean Absolute Error, MAE: 3.1%) and HI listeners (Pearsons'; correlation: r = 0.90, p <0.001; MAE: 3.8%).

The behavioral findings of this study showed that musical training could partially restore the importance of low-numbered harmonics in HI listeners. The model predictions were fairly accurate and could account for about 80% of the variance.

Behavioral Evidence of Brain Plasticity by Musical Experience

Keonseok Yoon[1]; Jessica Yoo[2]; Hyesoo Ryu[1]; Hyunsook Jang[1]
[1]*Hallym University;* [2]*Mempis Univ.*

Research background The human brain's susceptibility to structural or functional changes by experience or training is widely studied. Temporal processing and dichotic listening tasks are behavioral paradigms for observing auditory processing abilities in hemispheric and inter-hemispheric regions. One of the most widely used ways to assess temporal processing skills is by using frequency pattern test (FPT) (Emanuel, 2002). FPT assesses areas of frequency discrimination, temporal ordering, and linguistic labels and is sensitive to cortical lesions and inter-hemispheric transfer. One of the tests that observes dichotic paradigm is the Dichotic Digits Test (DDT) (Musiek, 1983), which measures binaural integration in the cortical levels. This study aims to examine the effect of musical experience on brain plasticity by increasing stimulus complexity through the two behavioral paradigms. Methods FPT and DDT were tested on 15 normal hearing adults with at least 5 years of musical experience and 15 normal hearing adults without any musical experience. FPT is composed of 2 tones (high frequency- 1,122 Hz, low frequency- 880 Hz) and were presented in 3-, 4-, 5-, or 6-tones for stimulus complexity. Conditions in tone, response (humming and labeling), and ear (right and left ear) were tested and the performance was observed according to the musical experience of the two groups. In DDT, stimulus complexity was increased from 2-digit to 3-digit condition, and the performances in conditions in number of digits (2 or 3) and ear (right or left) were observed. Results In FPT, the individuals with musical experience showed an increase in performance as stimulus complexity increased from 3-tones to 6-tones and also showed a significantly high performance in 6-tone humming and 3~6 labeling condi-

tions. Similar high performance in humming and labeling conditions for the individuals with musical experience indicated almost no difference in left-to-right and right-to-left transmission in the hemispheric region, indicating the enhancement in both verbal and tonal sounds. The effective interhemispheric transfer is clearly shown for the musician group. This can be explained through acquired experience coded into the hemispheres, which enables individuals to have more effective control over the incoming stimulus. In DDT, the individuals with musical experience showed a significantly high performance in 2- and 3-digit conditions compared to the individuals without musical experience. Thus, musical experience showed to have a significant effect on faster transmission of auditory information and speech processing between the hemispheres. Conclusion High performance in temporal and dichotic listening with increased stimulus complexity indicates the effect of musical experience not only on temporal processing and transmission abilities in cerebral hemisphere, but also supports the existing theory on brain plasticity. This study demonstrates that the absence and presence of musical experience needs to be considered in central auditory processing tests and suggests the importance of musical experience on auditory training.

Regeneration II

PS 490

Magnetic Targeting of Stem Cell Therapy to The Inner Ear

Trung Le[1]; Louise Straatman[2]; Anat Yanai[3]; Ronak Rahmanian[3]; Cathie Garnis[3]; Urs Hafeli[3]; Tashana Poblete[3]; Brian Westerberg[3]; Kevin Gregory-Evans[3]
[1]University of Toronto; [2]UMC Utrecht; [3]University of British Columbia

Background
Severe-to-profound sensorineural hearing loss is accompanied by a reduced population of auditory neurons presumed to be the result of gradual neural degeneration following injury to the cochlear epithelium and hair cell loss. Cochlear implant function depends on a healthy complement of neurons and their preservation and/or regeneration to achieve optimal results. We develop a technique to localize mesenchymal stem cells (MSCs) to a deafened rat cochlea, and determine the neuroprotective effect of systematically delivered MSCs on the survival of spiral ganglion neurons (SGNs) and their auditory function.

Methods
MSCs were labeled with superparamagnetic nanoparticles, injected via the systemic circulation, and magnetically targeted to the deafened cochleae using a magne-tized permalloy implant and an external magnet. Neurotrophic factor concentrations, survival of SGNs, and auditory function were assessed at 1 week and 4 weeks after treatments and compared against multiple control groups.

Results
Significant numbers of magnetically targeted MSCs (>30 MSCs/section) were present in the cochlea with accompanied elevation of brain-derived neurotrophic factor and glial cell-derived neurotrophic factor levels (p<0.001), and maintenance of SGN survival (100%) at 1 week. Hearing threshold levels in magnetically targeted rats were found to be significantly better than those of control rats (p<0.05). These results indicate that magnetic targeting of MSCs to the cochlea can be accomplished with a magnetized cochlear permalloy implant and an external magnet. The targeted stem cells release neurotrophic factors which results in improved SGN survival and hearing recovery.

Conclusion
Magnetic targeting can localize significant numbers of systemically injected MSCs to the inner ear and produce therapeutically useful histological and biochemical changes in the target tissue. In addition, improved hearing threshold levels, which correlate with improved SGN survival would suggest a valuable role for this approach in cochlear implant surgery.

PS 491

Transplantation of human pluripotent stem cell-derived cells into the selectively ablated mouse organ of Corti

Hiroki Takeda; Anna Dondzillo; Jessica Randall; Samuel Gubbels
University of Colorado, Department of Otolaryngology

Most cases of hearing loss are caused by degeneration of cochlear hair cells followed by auditory neurons. One of the potential therapeutic options for regeneration of cochlear function is a pluripotent stem cell-based strategy. The development of this therapy requires development of reliable and robust methods for differentiating pluripotent stem cells to cochlear hair cells or neurons in vitro, as well as methods of transplantation that allow for engraftment and differentiation to functional hair cells in vivo. Here we report on in vitro differentiation of human embryonic stem cells to an otic fate followed by transplantation of these cells to the murine cochlea. First, we differentiated human pluripotent stem cells (hPSCs) to the preplacodal ectoderm-like cells using a previously reported method (Leung, et al. 2013). We then transplanted these partially differentiated cells through the

round window into the neonatal mice cochlea in which the hair cells had been selectively ablated. We then evaluated the localization of the transplanted cells within the cochlea at several time points after grafting. We found that hPSCs were differentiated into preplacodal ectoderm-like progenitors as identified by their expression of EYA1, SIX1 and other placodal markers for 6-8 days in vitro. Furthermore, some of the transplanted cells at day 7 of differentiation could engraft in the lesioned organ of Corti at 4 and 11 days after grafting. Our future studies will focus on characterizing whether the transplanted and engrafted cells terminally differentiated into mature hair and/or supporting cells and how to enrich the survival and differentiation of grafted cells.

PS 492

Transcriptome Analysis of Native and Stem Cell-Derived Murine Otic Vesicles

Stacy A. Schaefer; Liqian Liu; **Robert K. Duncan**
University of Michigan

The generation of inner ear organoids from embryonic stem cells (ESCs) follows sequential developmental milestones, including formation of non-neural ectoderm, otic placode, otic vesicles, and sensory epithelia. While this technique is opening avenues for stem cell-based disease modeling and regenerative medicine, several barriers remain. Differentiation efficiency decreases with each milestone such that only a portion of ESC-derived vesicles produce organoids. Moreover, sensory hair cell fate appears restricted to immature vestibular phenotypes. To address limited efficiency and fate specification, we sought to compare molecular phenotypes of ESC-derived and native otic vesicles using RNASeq. Native vesicles were dissected from C57BL6 mouse embryos at embryonic day 10.5. Derived vesicles came from R1/E mouse ESCs differentiated as 3-dimensional aggregates (protocol modified from Koehler and Hashino, 2014). We examined derived vesicles from aggregates cultured with or without the TGFβ inhibitor SB431542 on culture day 3; these groups are referred to as BSFL and BFL, respectively. We observed that TGFβ inhibition is not required for vesicle formation but is required for organoid production. On culture day 12, aggregates were enzymatically disrupted and vesicles manually harvested. RNASeq was performed on 3-4 biological repeats per experimental group using TruSeq RNA Library prep kits and single-end, 50 bp sequencing of mRNA. After adapter sequences were trimmed, reads were aligned to the mouse genome using HISAT2 and gene level counts obtained with HTSeq-Count. Differential gene expression was analyzed with DESeq2, and gene networks were analyzed with iPathwayGuide. Principle component analysis showed clear delineation of the three experimental groups with the two ESC-derived groups separated along one axis and the derived vs native groups separated along the orthogonal axis. Hmx2/3 expression was >40-fold lower in BFL vesicles than BSFL, providing a possible explanation for the loss of dorsolateral signals and arrested maturation of vestibular sensory epithelia. In contrast, BSFL vesicles showed similar levels of key dorsal patterning genes (Dlx5/6 and Hmx2/3) compared to native but lower levels of ventral markers (Otx1 and Lfng), consistent with the generation of dorsal, vestibular hair cells in BSFL organoids. Notably, Tbx1 expression was >60-fold lower in BSFL vesicles than in native. This transcription factor is essential to inner ear organogenesis following the formation of otic vesicles. Genes involved in retinoic acid (RA) signaling were higher in BSFL vesicles than in native, consistent with known reciprocal repression between Tbx1 and RA pathways. Therefore, aberrant RA signaling may present a barrier to organoid differentiation and maturation.

PS 493

Effects of Vestibular Cell-conditioned Medium on Differentiation of Embryonic Stem Cells into Inner Ear Vestibular Hair Cells

Masaharu Sakagami[1]; Yukiteru Ouji[2]; Norikazu Kawai[2]; Tadashi Kitahara[1]; Masahide Yoshikawa[2]
[1]*Department of Otolaryngology - Head and Neck Surgery, Nara Medical University;* [2]*Department of Pathogen, Infection and Immunity, Nara Medical University*

Background and Aim

The vestibular system in the inner ear is essential for maintaining spatial orientation and balance. Current options for treating vestibular disorders are limited and include vestibular rehabilitation, medication, and surgery. However, to fully restore vestibular function, the only method presently available is vestibular hair cell (V-HC) regeneration and subsequent nerve innervation. Embryonic stem (ES) cells are a candidate source for cell therapy as treatment for a range of organs because of their potential for self-renewal and pluripotency. Recently, we developed a simple and efficient technique, termed the HIST2 method, to obtain ES-derived HC-like cells within a relatively short period of cultivation, for which only conditioned medium from cultured ST2 stromal cells is used. In the present study, we investigated differentiation of ES cells into inner ear V-HCs using the differentiation-inducing activity of supernatant obtained from cultures of vestibular cells isolated from the inner ear of adult mice.

Methods

We utilized the mouse ES cell line EB5 and subline Math1-GFP ES cells carrying the GFP gene driven by

the Math1 promoter. Mouse vestibular cells (VCs) were isolated from inner ear utricles and cultured, then the resultant conditioned medium (V-CM) was collected. Embryoid bodies (EBs) were prepared for 4 days using a hanging drop method, then cultured for 14 days in V-CM. GFP expression was examined using FACS and fluorescence microscopy. Furthermore, expressions of HC-related markers including those of V-HCs were examined by real time RT-PCR and immunocytochemistry.

Results
The number of GFP-positive cells was increased in EB outgrowths cultured in V-CM, whereas few cells were detected in its absence. Moreover, expressions of HC-related markers including some V-HC-related markers were increased in those cultured in V-CM.

Conclusion
The differentiation-inducing activity of V-CM was effective to induce differentiation of ES cells into HC-like cells including V-HCs.

PS 494

Making Tool for Analysis of TRIOBP Function Using Induced Pluripotent Stem Cells

Hiroe Ohnishi[1]; Shin-ichiro Kitajiri[2]; Xiangxin Lou[3]; Akiko Taura[4]; Mirei Taniguchi[1]; Fumi Ebisu[5]; Tatsunori Sakamoto[6]; Norio Yamamoto[7]; Juichi Ito[8]; Koichi Omori[9]; Takayuki Nakagawa[10]
[1]Department of Otlaryngology, Head and Neck Surgery, Graduate School of Medicine, Kyoto University; [2]Department of Hearing Implant Sciences, Shinshu University School of Medicine; [3]Department of Bioengineering, Donghua University; [4]National Hospital Organization Kyoto Medical Center; [5]Institute for Protein Research, Osaka University; [6]Tazuke Kofukai Medical Research Institute, Kitano Hospital, Department of Otolaryngology, Head & Neck Surgery; [7]Department of Otolaryngology, Head and Neck Surgery, Graduate School of Medicine, Kyoto University; [8]Shiga Medical Center Research Institute; [9]Department of Otolaryngology-Head and Neck Surgery, Graduate School of Medicine, Kyoto University; [10]Department of Otolaryngology - Head and Neck Surgery, Graduate School of Medicine, Kyoto University

Background
TRIOBP is identified as responsible gene of human hereditary deafness DFNB28. Stereocilia of inner ear hair cells are composed of actin bundles which have rootlets extending into the cytoplasm and TRIOBP is localized in the stereocilia rootlets. TRIOBP is an actin bundler and Triobp KO mice lack stereocilia rootlet and cause pro-

gressive degeneration of stereocilia. Triobp KO mouse were established and cochlea explant cultures of this KO mouse were used as functional analysis tool until now. However, gene transfer efficiency in cochlea explant cultures is not sufficient for functional analysis of TRIOBP. In this study, to establish the TRIOBP KO in vitro model for the analysis of TRIOBP function by cell biological approaches with gene transfer, hair cell induction was performed using Triobp KO mouse-derived induced pluripotent stem (iPS) cells.

Methods
Triobp KO mouse iPS cells were generated from mouse embryonic fibroblasts (MEFs) using retrovirus vector and the embryonic stem (ES) cell-like cell lines were selected. Then characterization of these ES cell-like cells were performed by examination of pluripotent stem cell marker expression and differentiation potency into three germ layer cells, genotyping and transgene silencing. Then, the hair cell induction of Triobp KO mouse-derived iPS cells was examined using the published methods.

Results
Several lines of ES cell-like cells were obtained. These cells were regarded as Triobp KO mouse MEF-derived iPS cells (TRIOBP KO iPS cells) by pluripotent marker expression, differentiation potency into three germ layer cells, transgene silencing and Triobp KO mouse genotype. In addition, otic progenitor-like cells were observed in hair cell induction experiment using TRIOBP KO iPS cells.

Conclusion
TRIOBP KO iPS cells were generated and differentiated into otic progenitor-like cells, which express otic progenitor marker. This technique would make it possible to reveal stereocilia degeneration mechanism, including cell biological analysis by gene transfer, in vitro.

PS 495

Creating a Stem Cell Niche with Spheroids and Hydrogel Microspheres Using Human Stem Cell Derived Otic Neural Progenitors

Kyle Coots[1]; Shun Kobayashi[2]; Duncan Chadly[3]; Kevin Nella[4]; Charles Miller[1]; Alexandra Edelbrock[5]; Samuel Stupp[6]; John Kessler[1]; Akihiro Matsuoka[7]
[1]Feinberg School of Medicine at Northwestern; [2]University of Texas Austin; [3]California Instituite of Technology; [4]University of Miami; [5]Northwestern University Department of Biomedical Engineering; [6]Northwestern University Simpson Querrey Institute; [7]Northwestern University Feinberg School of Medicine

Background

The clinical application of stem cell replacement therapy has been hindered by the effectiveness of neuronal differentiation from human pluripotent stem cells (hPSCs) and the post-operative survival of single suspended cells. To help overcome these hurdles, we have proposed two unique vehicles for cell delivery: otic neural progenitor (ONP) spheroids and hydrogel microspheres. The overall goal is to increase cell-to-cell interactions and signaling to mimic in vivo conditions.

Methods

Frozen hESC-derived ONPs were cultured in an ONP maintenance medium (ONPMM) previously established by our lab. Microspheres were created with a laminar flow patterning device and a self-assembling peptide amphiphile. Mid-stage ONPs were seeded into the microspheres and subsequently differentiated into late-stage ONPs. A fluorescent live cell assay specific to neuronal cells was used to image the cells following differentiation. Mid-stage ONPs were also differentiated to late-stage ONPs in a hydrogel bonded with the bioactive peptide sequence IKVAV to determine the effects on neural differentiation. A low adhesion EZSPHERE plate (Nacalai USA) that utilizes self-assembly allowed for the growth of isolated spheroids in 3-D culture. After one week in culture, spheroids were characterized using immunocytochemistry, flow cytometry, apoptosis assay, and RT-PCR.

Results

The laminar flow patterning device was able to successfully create microspheres of uniform size and shape. Cells grown within the IKVAV hydrogel showed a higher number of neurite-bearing cells than those grown in traditional culture or in a hydrogel with a scrambled peptide sequence. Immunocytochemistry shows that our spheroids are positive for the ONP markers Nestin and Pax8. Preliminary flow cytometry data indicates a significant increase in Nestin and Pax8 expression in spheroids when compared to ONPs grown in 2-D culture.

Conclusion

Microspheres provide a viable option for encapsulating single cell suspensions. Microspheres can be used to co-culture ONPs alongside other cell types, such as Schwann cells, which secrete neurotrophic factors like BDNF that help improve the growth of ONPs. These microspheres can be further customized to help enhance the growth and survival of a variety of cell types. Cell spheroids can be formed that closely resemble ONPs. The spheroids are small and durable enough to be transplanted into mouse cochlea. Further studies are needed to assess the ability of the spheroids to further differentiate into spiral ganglion neurons within the cochlea.

PS 496

Controlled Delivery of Human Pluripotent Stem Cell (hPSC) Derived Otic Neural Progenitors to the Cochleae of Rodent Models

Cong Ran[1]; Charles Miller[1]; Kyle Coots[1]; Andrew Oleksijew[1]; Duncan Chadly[2]; Shun Kobayashi[3]; Kevin Nella[4]; John Kessler[1]; Akihiro Matsuoka[5]
[1]Feinberg School of Medicine at Northwestern; [2]California Instituite of Technology; [3]University of Texas Austin; [4]University of Miami; [5]Northwestern University Feinberg School of Medicine

Background

Sensorineural deafness is a condition that is thought to result from loss of sensory hair cells and the associated spiral ganglion neurons. The use of stem-cell replacement though introduced a promising future for the therapy of this disease, it presents several challenges for clinical translation. Maintaining cellular viability and function post-transplantation is a highly active area of research, since limited success has been demonstrated when single cell suspension of stem cells were transplanted. This has led to the more recent thought of transplanting encapsulated stem cell or progenitor cells in 3D structures such as spheres. We present recent progress in our laboratory toward the goal of positioning hPSC-derived aggregates into the scala tympani of rodent cochleae, with first demonstrating two feasible models to do so.

Methods

The transplantation recipients include: (1) mice from a diphtheria-induced hair-cell loss related deafening (DTR) mouse model described by Tong et al; (2) gerbils from the ototoxic drug induced auditory neuropathy model. The transplanted cells are hPSC-derived otic neural progenitor cells (ONP) grown in unique microsphere environment. The ONP aggregates are delivered to the round window after a standard surgical exposure using two different approaches : (1) delivery using a constant-pressure system (analogous to cell immobilization used in in vitro egg fertilization) and (2) fluid displacement provided by a controlled microsyringe pump. The successfully transplanted animals underwent ABR studies and subsequently sacrificed for histology analysis of transplanted aggregate after 3-5 days.

Results

Our study demonstrated the feasibility of using the two different and controlled delivery methods to transplant ONP aggregates in vivo. We were also able to demonstrate preliminarily that the transplanted stem cells are viable by demonstrating human ONP signature expressing cells within scala tympani of transplanted animal. The ONP aggregate transplanted animals demonstrated

improve auditory-evoked response thresholds, suggesting therapeutic benefit of this type of cell replacement methods.

Conclusions
Controlled delivery of cellular aggregate of ONP into rodent scala tympani significant reduces the variability between animals receiving transplantation. In our preliminary study, it is demonstrated that this method of delivery using ONP spheres can produce viable and functional cells that enhance auditory evoked response thresholds.

PS 497

NEUROG1 Regulates CDK2 to Promote Proliferation in Otic Progenitors

Zhichao Song[1]; Azadeh Jadali[2]; Bernd Fritzsch[3]; Kelvin Kwan[2]
[1]Rutgers University-New Brunswick; [2]Rutgers University; [3]University of Iowa

Loss of spiral ganglion neurons (SGNs) significantly contributes to hearing loss. Otic progenitor cell transplantation is a potential strategy to replace lost SGNs. Understanding how key transcription factors promote SGN differentiation in otic progenitors accelerates efforts for replacement therapies. A pro-neural transcription factor, Neurogenin1 (Neurog1), is essential for SGN development. Using an immortalized multipotent otic progenitor (iMOP) cell line that can self-renew and differentiate into otic neurons, NEUROG1 was enriched at the promoter of cyclin dependent kinase 2 (Cdk2) and neurogenic differentiation 1 (NeuroD1) genes. Changes in H3K9ac and H3K9me3 deposition at the Cdk2 and NeuroD1 promoters suggested epigenetic regulation during iMOP proliferation and differentiation. In self-renewing iMOP cells, overexpression of NEUROG1 increased CDK2 to drive proliferation while knockdown of NEUROG1 decreased CDK2 andreduced proliferation. In iMOP-derived neurons, overexpression of NEUROG1 accelerated acquisition of neuronal morphology, while knockdown of NEUROG1 prevented differentiation. Our findings suggest that NEUROG1 can promote proliferation or neuronal differentiation.

PS 498

Rebuild the Auditory Circuit from the Cochlea to Central Nervous System via Stem Cell-based Approaches

Zhenjie Liu; Yiyun Jiang; Xiaoyang Li; Zhengqing Hu
Wayne State University School of Medicine

Background
In the auditory system, spiral ganglion neurons (SGNs) transfer auditory signals to the cochlear nucleus (CN) located in the brainstem. These neural components are usually damaged in hearing loss, a major health problem affecting 10% of the population. Embryonic stem (ES) cell-based replacement has been proposed to regenerate degenerated auditory pathway. However, how to stimulate integration of ES cell-derived neurons (ESNs) into the native auditory system remains a challenge. In this research, a novel co-culture system was developed to understand whether mouse ESNs synapse with wild-type mouse CN neurons.

Methods
An in vitro Cre-Loxp system was used to generated GFP-ESNs, which were co-cultured with CN neurons in the presence or absence of thrombospodin-1 (TSP1). Immunofluorescence using neuronal and synaptic specific antibodies was used to evaluate neural connections between ESNs and CN neurons. Antagonist, gain- and loss-of function studies were applied to determine whether the α2δ1 receptor played important roles in TSP1-induced synaptogenic effects. FM-based synaptic vesicle recycling and pair recording excitatory postsynaptic current (EPSC) electrophysiology were used to evaluate the function of new synapses.

Results
GFP-ESNs expressed SGN-like genes and proteins including TUJ1, NeuN, neurofilament, TrkB, TrkC, and NeuroD1. Quantitative study revealed that 65.95%±3.72% and 78.22%±4.96% of TUJ1 positive cells were also VGluT1 and Gata3 positive respectively. ESNs were labeled by sodium channel protein Na-V and exhibited neuronal activities similar to SGNs. In co-cultures, TUJ1-expressing neurites were observed between ESNs and CN neurons, which was stimulated in the presence of TSP1. Quantitative study suggests that 10 nM TSP1 may be the best concentration to promote SV2 expression along ESN-CN connections. Antagonist and loss- of function studies indicate that TSP1 stimulated ESN-CN synaptogenesis via the α2δ1 receptor. Newly-generated ESN-CN connections were labeled by pre- and post-synaptic proteins, as well as glutamatergic marker VGluT1. Synaptic vesicle recycling and pair recording electrophysiology suggest functional synaptic vesicles and trans-synaptic activities.

Conclusions
ES-derived ESNs can form synapses with native CN neurons, which is a critical step for integration of ESNs into the native auditory system to rebuild the auditory circuit. These discoveries may suggest the possibility of developing novel strategy to utilize stem cell-derived neurons to replace damaged SGNs to reconnect to the CN neurons for the treatment of a variety of auditory disorders.

PS 499

Effects of Genetic Correction on the Differentiation of Hair Cell-like Cells from IPSCs with Deafness-associated MYO15A Mutations

Jia-Rong Chen; Min-Xin Guan
Zhejiang University

Deafness or hearing loss is a major global public health problem. Inner ear hair cells are the main hearing sensory receptors. Defects in hair cells are one of the major reasons causing deafness. A combination of induced pluripotent stem cell (iPSC) technology with CRISPR/Cas9 technology may be a promising cell-based strategy to regenerate hair cells and treat hereditary deafness in human beings. Here, we report the generation of iPSCs from members of a Chinese family carrying MYO15A c.4642G>A and c.8374G>A mutations and the induction of hair cell-like cells from those iPSCs. The compound heterozygous mutations of MYO15A resulted in abnormal morphology and dysfunction of the derived hair cell-like cells. Finally, we genetically corrected the MYO15A mutation in the iPSCs and rescued the morphology and function of the derived hair cell-like cells. Our data demonstrate the feasibility of generating inner ear hair cells from human iPSCs and the functional rescue of gene mutation-based deafness by using genetic correction.

PS 500

Differential Effects of TGFβ Pathway Inhibitors Applied at an Early Stage in Formation of Inner Ear Organoids from Mouse Embryonic Stem Cells

Stacy A. Schaefer; Liqian Liu; **Robert K. Duncan**
University of Michigan

Deriving mature tissues from stem cells is a multi-step process, and the efficiency of each step impacts the ultimate yield. Recently, a method of producing inner ear sensory tissue in 3-dimensional aggregates of embryonic stem cells (ESCs) was established, but its yield remains limited (Koehler and Hashino, 2014; Koehler et al., 2013). One of the earliest steps in the method is inhibition of TGFβ signaling to promote differentiation of ectoderm, the germ layer from which otic vesicles develop. This inhibition is achieved through addition of the small molecule SB431542 (SB). SB targets ALK4, ALK5, and ALK7, the TGFβ-family type I receptors for ligands activin, TGFβ, and nodal (Inman et al., 2002). Other inhibitors with unique mechanisms are available including SIS3, which specifically targets the downstream effector Smad3 (Jinnin et al., 2005), and RepSox, a potent inhibitor ALK5 (Ichida et al., 2009). In this study, we examined the impact of these alternative mechanisms

of TGFβ signaling inhibition on the yield of derived otic tissue. Aggregates of R1/E mouse ESCs were differentiated according to the published inner ear organoid protocol (Koehler and Hashino, 2014). On day 3, SB (1 μM) was applied, omitted (no treatment control), or substituted with SIS3 (3 μM) or RepSox (1 μM). Application of SB resulted in otic vesicle-like structures that ultimately developed into organoids, with hair cells revealed by immunofluorescence staining for Myo7a and F-actin. Control aggregates produced structures analogous to otic vesicles both in morphology and expression of key markers (ECAD, Pax2, Six1, and Sox2); however, these did not develop into organoids. SIS3 and RepSox were effective substitutes for SB in generating vesicles and organoids. Vesicle production was quantified by disrupting a standard number of aggregates on day 12 and counting vesicles manually harvested within 20 minutes. By this measure, SIS3- and RepSox-treated aggregates produced vesicles more efficiently than SB-treated or control aggregates. Organoid production was quantified by scoring aggregates as positive or negative on day 20 by visualization of their distinct cystic morphology under light microscopy. SIS3 and RepSox resulted in more organoid-positive aggregates than SB did on average, but the difference was not statistically significant. Cultures treated with RepSox were least variable in otic vesicle and organoid formation, an advantage for future applications. We are currently examining differences in TGFβ inhibitor-treated and untreated cultures by RNASeq to elucidate which features of derived otic vesicles are necessary for hair cell fate.

PS 501

An Adult Mouse Thyroid Side Population Cell Line can be incorporated as part of follicles in mouse injection models

Yoshinori Takizawa[1]; Manabu Iwadate[2]; Tsubasa Murata[3]; Hiroshi Nakanishi[4]; Shioko Kimura[5]
[1]Seirei Mikatahara General Hospital; [2]Fukushima Medical University Hospital; [3]Tomakomai City Hospital; [4]NIDCD, NIH; [5]NCI, NIH

Background
Studies of thyroid stem/progenitor cells have been hampered due to the small organ size and lack of tissue, which limits the yield of these cells. A continuous source that allows the study and characterization of thyroid stem/progenitor cells is desired to push the field forward.

Method
A cell line was established from Hoechst-resistant side population cells derived from mouse thyroid that were previously shown to contain stem/progenitor-like cells. Characterization of these cells were carried out by using in vitro two- and three-dimensional cultures and in vivo

reconstitution of mice after orthotopic or intravenous injection, in conjunction with quantitative reverse transcription polymerase chain reaction, Western blotting, and immunohisto(cyto)chemistry/immunofluorescence analysis.

Results

These cells were named SPTL (side population cell-derived thyroid cell line). Under low serum culturing conditions, SPTL cells expressed the thyroid differentiation marker NKX2-1, a transcription factor critical for thyroid differentiation and function, while no expression of other thyroid differentiation marker genes were observed. SPTL cells formed follicle-like structures in Matrigel cultures, which did not express thyroid differentiation marker genes. In mouse models of orthotopic and intravenous injection, the latter following partial thyroidectomy, a few SPTL cells were found in part of the follicles, most of which expressed NKX2-1.

Conclusion

These results demonstrate that SPTL cells have the capacity to differentiate into thyroid to a limited degree. SPTL cells may provide an excellent tool to study stem cells of the thyroid.

PS 502

Utilizing Tumor Suppressor Knock Out Mice to Characterize Spiral Ganglion Regeneration in Response to Ototoxicity

Jonathan D. Jones[1]; Bradley J. Walters[2]
[1]*University of South Alabama;* [2]*Department of Neurobiology and Anatomical Sciences, and Department of Otolaryngology and Communicative Sciences, University of Mississippi Medical Center*

Intro

There is an inverse correlation of patient age and successful outcome of cochlear implantation. Implants are less efficacious in adult populations due to decreased CNS plasticity, but also because the loss of neurons and/or synapses in the 8th cranial nerve is overly common. Indeed, spiral ganglion neurons (SGNs) are lost subsequent to cochlear hair cell damage (i.e. sensorineural hearing loss), and synaptic connections are frequently lost even in the absence of hair cell damage (i.e. cochlear synaptopathy or so-called hidden hearing loss).

In order for cochlear implants to be a viable option for adult patients with SGN loss or cochlear synaptopathy, the nerve cells would need to be regenerated or their plasticity enhanced. Here we have investigated the genetic deletion of the INK4A/ARF locus as a method for enhancing SGN regeneration.

Methods

Mice were bred to isolate wild type and homozygous deletions of the tumor suppressor INK/ARF gene locus. Male and female mice were used. Two cohorts were analyzed for each genotype, one that, at 4 weeks of age, had been treated with kanamycin at a dose sufficient to cause near complete outer hair cell loss (1g/kg), and one that was untreated. Cochleae were dissected at 6 weeks of age.

Sectioned cochleae were then simultaneously immunostained using an antibody against proliferating cell nuclear antigen (PCNA) and either a glial marker (S100), a neuronal marker (beta III tubulin a.k.a. TUJ1), or a pan-macrophage marker (CD68). The sections were imaged using confocal microscopy. Counts of proliferative cells and co-labeled cells within the spiral ganglia were normalized for volume of tissue analyzed to yield rates of proliferation of the three cell types experimental vs. control groups.

Results/Discussion

The majority of PCNA positive cells in both wild type and INK4A/ARF null mice co-labeled with CD68, though PCNA, S100 double positive cells were also observed in both genotypes suggesting that macrophages and glia-like cells in the SG are proliferative. While no PCNA positive neurons were seen in wild type samples, we did observe a couple of TUJ1, PCNA double positive cells in some of the INK4A/ARF samples. We also found that kanamycin induced a significant increase in cell proliferation in the spiral ganglion.

While these preliminary findings are encouraging, further studies are required to fully elucidate the role of INK4A/ARF inhibition on PNS regeneration.

PS 503

Manipulating Neurite Growth of Human Embryonic Stem Cell-Derived Spiral Ganglion Neuron-Like Cells through Neurotrophic Factor Gradients in a Microfluidic Device

Kevin Nella[1]; Kyle Coots[2]; Jose Fernandez[3]; Duncan Chadly[4]; Shun Kobayashi[5]; Andrew Oleksijew[2]; John Kessler[2]; Akihiro Matsuoka[6]
[1]*University of Miami;* [2]*Feinberg School of Medicine at Northwestern;* [3]*Northwestern Dept. of Chemical Engineering;* [4]*California Instituite of Technology;* [5]*University of Texas Austin;* [6]*Northwestern University Feinberg School of Medicine*

Background

The neuroprotective effects of neurotrophic factors (i.e. brain-derived neurotrophic factor) on spiral ganglion

neurons (SGNs) has been widely studied. However, many studies have shown that the eventual depletion of neurotrophic factors (NTFs) leads to an accelerated decline in neuronal survival. Additionally, the role of stem cells in otolaryngology is expanding, and there is a need for more research studying the effects of NTFs on stem-cell derived neurons. Furthermore, most of the in vitro studies in this realm have been conducted in conventional laboratory plates (i.e. 6 well plates, etc.) and do not accurately represent the microenvironments in which the cells exist. In this study, we set out to investigate the effects of various sustainable BDNF sources on stem-cell derived SGNs in a microfluidic culture system.

Methods

The microfluidic culture system used to establish an appropriate microenvironment is the SND-450 by XONA Microfluidics LLC. The microfluidic device consists of 2 main chambers that are connected by hundreds of microgrooves across a length of 450 microns. The grooves are small enough in size that the soma of the SGN-like cells cannot migrate across. The hESC-derived SGN-like cells were derived from human embryonic stem cells (hESCs) (H1, H7, and H9) through a protocol developed by our laboratory, published in Stem Cells Translational Medicine in 2016. The sustainable BDNF sources studied were PODS by Cell Guidance Systems, a BDNF-mimetic amphiphile gels and, primary Schwann cells. Three-dimensional diffusion was modeled graphically prior to experimentation to optimize initial PODS concentrations. Immunocytochemistry was used to stain and visualize the SGN-like cells after experimentation.

Results

Preliminary result demonstrated that neurites were growing towards the BDNF PODs crystals. It appeared that the length of neurite was proportional to the number of PODS crystals. We will compare the length of neurites from hESC-derived SGN-like cells across PODS, a BDNF- BNDF mimetic amphiphile gels and, primary Schwann cells.

Conclusions

Three-dimensional diffusion of long-term BDNF diffusion may help differentiate hESC-derived ONPs into an SGN lineage. The application of this technology needs to be tested in an animal model as a next step.

PS 504

Finite Element Model for Assessing the Mass Transport Phenomena of Brain Derived Neurotrophic Factor

Jose Fernandez[1]; Shreyas Bharadwaj[2]; Charles Miller[2]; Duncan Chadly[3]; Shun Kobayashi[4]; Kevin Nella[5]; Kyle Coots[2]; Andrew Oleksijew[2]; Claus-Peter Richter[6]; John Kessler[2]; Akihiro Matsuoka[7]
[1]Northwestern Dept. of Chemical Engineering; [2]Feinberg School of Medicine at Northwestern; [3]California Instituite of Technology; [4]University of Texas Austin; [5]University of Miami; [6]Department of Otolaryngology-Head and Neck Surgery, Feinberg School of Medicine, Northwestern University & Resonance Medical, LLC, Chicago; [7]Northwestern University Feinberg School of Medicine

Background

Sensorineural hearing loss can be overcome by reestablishing synaptic connections between extant Spiral Ganglion Neurons (SGNs) and transplanted human stem-cell derived SGNs. To achieve this goal, it is necessary to direct the growth of both of SGN neurites towards each other. We have developed a computational model that utilizes finite element analysis to evaluate the mass transport of Brain Derived Neurotrophic Factor (BDNF) inside a XONA Microfluidics SND450 device and also inside a 3D model of a gerbil cochlea reconstructed from micro-computed tomography images. The goal of this study was to obtain estimates of the parameters required to obtain the desired experimental conditions in vivo to study SGN neurite growth.

Methods

Reaction kinetics of the release of BDNF from Polyhedrin Delivery System (PODS, provided by Cell Guidance Systems) and its subsequent degradation was approximated from release and degradation data of PODS containing Leukemia Inducing Factor. MATLAB was used to fit the concentration-time data and obtain kinetic constants. Diffusivity coefficient of BDNF was approximated by the diffusivity of b-Lactoglobulin, another globular protein of similar size. The XONA SND450 device was recreated to scale using Autodesk Inventor and transferred to MATLAB platform. The differential mass transport equation was solved with MATLAB Partial Differential Equation Toolbox. Gerbil cochlea tissue samples were scanned at Advanced Photon Source (Argonne National Laboratory, Argonne, IL). The stack of images was uploaded to Fiji imaging software, converted to binary and subsequently cleaned of noise. The processed image stack was used to construct a 3D surface which was then exported to Autodesk Inventor for modifications. The differential mass transport equation was similarly solved.

Results

The model predicts that PODS must be added in the order of tens of millions of individual PODS crystals to maintain a constant supply of BDNF. The model found that a noticeable BDNF gradient is obtained by introducing PODS crystals at a single source, and that a uniform concentration of BDNF throughout the device is achieved. Our initial result on the 3D reconstruction model was able to delineate detailed structure of the scala tympani. The finite element model will be developed and data will be presented.

Conclusion

Our computational models can provide a viable starting point to predict the optimal initial parameters to achieve desired experimental conditions in vivo. It is possible to achieve a BDNF gradient across the microfluidic device, which will be useful to test which BNDF concentration is optimal/necessary for neurite extension.

PS 505

Laminar sequestering microfluidic device for directed neurite growth of human embryonic stem cell derived otic neuronal progenitors

Andrew Oleksijew[1]; Duncan Chadly[2]; Kyle Coots[1]; Shun Kobayashi[3]; Kevin Nella[4]; Charles Miller[1]; Alexandra Edelbrock[5]; Samuel Stupp[6]; John Kessler[1]; Akihiro Matsuoka[7]
[1]*Feinberg School of Medicine at Northwestern;* [2]*California Instituite of Technology;* [3]*University of Texas Austin;* [4]*University of Miami;* [5]*Northwestern University Department of Biomedical Engineering;* [6]*Northwestern University Simpson Querrey Institute;* [7]*Northwestern University Feinberg School of Medicine*

Background

The widespread loss of peripheral dendrites of the spiral ganglion neurons is an intrinsic limitation of a cochlear implant. Stem-cell replacement therapies are a promising route for the restoration of peripheral dendritic processes. The regeneration of the human spiral ganglion neurons (SGNs) using hESCs (human embryonic stem cells) requires techniques to promote survival after implantation as well as direct neurite growth and synaptic connection with extant SGNs. We present a novel microfluidic test bed that utilizes laminar flow of peptide amphiphile (PA) gels to prevent cell migration while evaluating neurotropic factors for neurite extension and neurite-neurite synapsing.

Methods

Microfluidic devices are often fabricated using photolithography to produce a silicon wafer mold on which polydimethylsiloxane (PDMS) is casted. This process is labor intensive, requires cleanroom facility and can be cost prohibitive for researchers. Our device is instead casted in a mold that is 3D printed, a cost-effective method to produce many devices at low cost by comparison. Two experiments were performed. First, hESC-derived Schwann cells and SGNs suspended in backbone E2 PA-gels were perfused next to gelling solutions. Flow was halted and gel assembled via diffusive mixing with the gelling solution, leaving layers in between to perfuse media and allow neurite extension. Second, layers of hESC-derived SGNs and extant SGNs were perfused opposite to a layer which contained various neurotrophic source. Cells were characterized using immunocytochemistry.

Results

Laminar sequestering in the device was observed and retained after flow had stopped. Media was successfully perfused next to gel layers and no cell migration was observed. Preliminary studies have demonstrated neurite extension towards sources of neurotrophic factors.

Conclusions

Regeneration of dendritic processes of extant human SGNs may be possible without the migration of transplanted hESC-derived neuronal progenitor using PA-gels and concentrated BDNF expression. Future experiments would involve application of these techniques to new forms of cochlear implants to then be testing in animal models.

PS 506

HPN-07 Treatment Induces Cochlear Neuritogenesis In Vitro and Synaptogenesis In Vivo

Wei Li[1]; Matthew West[1]; Jianzhong Lu[1]; Qunfeng Cai[2]; Donald Ewert[1]; Xiaoping Du[1]; Robert Floyd[3]; Richard Kopke[4]
[1]*Hough Ear Institute;* [2]*Hough Ear Institute and Otologic Pharmaceutics Inc;* [3]*Oklahoma Medical Research Foundation;* [4]*Hough Ear Institute, Oklahoma Medical Research Foundationand, Departments of Physiology and Otolaryngology, University of Oklahoma Health Sciences Center, Otologic Pharmaceutics Inc*

It has been known for a long time that some people with normal hearing still have difficulty understanding speech in a noisy environment. However, the underlying physiological mechanism for this phenomenon was, until recently, unclear. Recent published studies have demonstrated that cochlear synaptopathy can occur as a primary excitotoxic outcome under conditions in which IHCs and normal auditory function are preserved. This pathophysiological response results in reduced peripheral auditory signaling to the brain, which

has etiological ramifications for auditory disorders, such as presbycusis, tinnitus, and hyperacusis. As a result, therapeutic intervention strategies targeting the restoration of cochlear ribbon synapses hold great potential for addressing these auditory disorders. Currently the treatment options reported in the literature for cochlear synaptopathy are limited and often invasive, minimally involving middle ear injections. Here we have developed an alternative, systemic approach to pharmacologically treat cochlear synaptopathy, using a small-molecule nitrone-based spin trap agent, HPN-07 (2,4-disulfonyl α-phenyl tertiary butyl nitrone), with pro-neuritogenic properties, whose safety has been well-established in clinical trials for the treatment of stroke. In vitro experiments conducted among three tissue culture models (PC12 cells, SGN explants, and SGN/HC explants) provided proof-of-concept support for HPN-07';s intrinsic neuritogenic properties and, furthermore, demonstrated potentiation of neurite outgrowth induced by canonical neurotrophic factors, such as Brain-Derived Neurotrophic Factor (BDNF). Quantitative histological evaluations revealed that HPN-07 treatment significantly enhanced neurite densities within SGN organotypic cultures and differentiated PC12 cells via mechanisms that involve canonical pro-neuritogenic programs, such as upregulation of growth associated protein 43 (GAP-43) expression. In vitro models of noise-induced excitotoxic trauma conducted using SGN/HC explants demonstrated that HPN-07 treatment was able to also promote significant reinnervation of deafferented IHCs following exposure to high levels of the glutamate receptor agonist, kainic acid (KA), consistent with a pro-synaptogenic response. Using high-resolution immunohistological techniques and an in vivo model of mild acoustic trauma that induced a slight threshold elevation, preservation of IHCs, and pervasive ribbon synapse loss, we found that delayed intervention with systemic (intraperitoneal) HPN-07 (formulated with N-acetylcysteine) administration significantly restored SGN/IHC pre- and post-synapse densities to levels that approached those observed in undamaged controls. These results suggest that HPN-07 may represent a safe pharmacological means to regenerate lost ribbon synapses in the inner ear, providing a promising non-invasive alternative for treating cochlear synaptopathy and its associated clinical manifestations.

PS 507

Deriving the Auditory Neuron: A Microfluidic Platform for Optimizing Human Stem Cell Differentiation

Duncan Chadly[1]; Andrew Oleksijew[2]; Jose Fernandez[3]; Shun Kobayashi[4]; Charles Miller[2]; Kevin Nella[5]; Kyle Coots[2]; John Kessler[2]; Akihiro Matsuoka[6]
[1]*California Instituite of Technology;* [2]*Feinberg School of Medicine at Northwestern;* [3]*Northwestern Dept. of Chemical Engineering;* [4]*University of Texas Austin;* [5]*University of Miami;* [6]*Northwestern University Feinberg School of Medicine*

Human pluripotent stem cells (hPSCs) are promising therapeutic tools for inner-ear regeneration. Development of cell-replacement therapies for sensorineural hearing loss will require the ability to generate high-quality spiral ganglion neurons rapidly and at high yield, potentially using different differentiation conditions for each hPSC line used. We present a versatile microfluidic platform capable of efficiently optimizing hPSC differentiation conditions. Our devices have three main advantages: minimization of manual labor by passive, on-chip dilution and mixing; a large surface area to volume ratio in on-chip culture wells, permitting study of auto/paracrine signaling; and ease of manufacture. Wells are kept isolated from diffusive contact, allowing for controlled culture with or without continuous perfusion. Although process optimization is most efficiently achieved through iterative factorial design, the number of experimental conditions that must be setup can be limiting. To address this problem and improve reproducibility, the device automatically performs combinatorial mixing, dilutions, and distribution for 3- and 4-factor full-factorial experimental designs. Notably, this is accomplished passively by the device without the need for pneumatic control. Using multiple devices in parallel, the number of experimental factors can be increased and include variables such as time spent in differentiation medium or, indirectly, endogenous factor accumulation through medium exchange frequency. Accumulation of endogenous factors has been shown to significantly affect cell survival and differentiation efficiency, especially in ectoderm and neuronal lineages. However, relevant concentrations are largely unattainable in traditional culture plates and flasks. Microfluidic devices are typically created using photolithography to produce a silicon wafer mold on which to cast polydimethylsiloxane (PDMS), a labor-intensive process requiring a cleanroom facility that creates a cost barrier for researchers not associated with a dedicated microfluidics group. By designing a mold that can be 3D printed, we bypass the need for special facilities and incur dramatic cost savings. We apply these devices to optimizing differentiation medium composition for a recently published protocol for the differentiation of hPSCs toward auditory neurons, and demonstrate in situ

immunocytochemistry after culture. In addition, our device has the potential to be used for rapid optimization of other processes including antibody concentration in immunocytochemistry, reagent concentration for lipofection protocols, siRNA delivery protocols, in vitro testing for combination drug effects, and more.

PS 508

Tuning Biochemical and Topographical Features to Investigate Hierarchical Guidance of Neurites from Spiral Ganglion Neurons

Kristy Truong[1]; Braden Leigh[2]; Mark Ramirez[3]; Reid Bartholomew[4]; Allan Guymon[2]; Marlan R. Hansen[5]
[1]Department of Otolaryngology - Head & Neck Surgery, Univeristy of Iowa Hospitals and Clinics; [2]University of Iowa, Department of Engineering; [3]Department of Anesthesiology, Michigan Medicine; [4]University of Iowa Hospitals and Clinics; [5]Department of Otolaryngology - Head & Neck Surgery, University of Iowa Hospitals and Clinics, Iowa City, IA

Introduction
Directed regeneration of spiral ganglion neuron (SGN) afferent fibers towards electrode arrays may allow for improved neural stimulation and outcomes. The interaction of both biochemical and topographical physical cues determine the ultimate trajectory of neurite growth. Engineering materials that will allow us to understand the hierarchal relationships of biochemical and topographic cues on SGN neurite pathfinding will provide vital information for regenerative therapies.

Methods
Physical microgrooves are fabricated using a photomask of specified periodicities in a single process step. Biochemical patterns are generated by adsorbing laminin, a cell adhesion protein, onto acrylate polymer surfaces followed by irradiation through a photomask with UV light to deactivate protein in exposed areas and generate parallel biochemical patterns. By first creating topographical micropatterns and then rotating the photomask 90 degrees, we created competing biochemical and physical patterns. The relative guiding strength of physical cues was varied by independently changing both the amplitude by controlling light exposure and periodicity, by varying the line spacing of the photomask of the microgrooves. Dissociated rat SGN alignment cultured on the competition assay was measured as a distribution of angles relative to the horizontal plane of 10 μm neurite segments.

Results
Photopolymerization and photodeactivation of laminin enabled rapid and precise patterning of topographical and biochemical neurite guidance cues, respectively. Laminin deactivation was shown to increase as a function of UV light exposure while remaining adsorbed to the polymer surface. On surfaces with laminin stripes perpendicular to the physical micropatterns, SGN neurites aligned to laminin patterns with lower physical pattern amplitude and higher periodicity and thus weaker cues. Alignment of SGNs shifted toward the physical pattern with higher amplitude and lower periodicity which represent stronger topographical cues.

Conclusions
We investigated the effects of competitive photogenerated topographical and biochemical guidance cues using a novel technique creating laminin stripes perpendicular to topographical micropatterns with varying periodicity or amplitude through a combined photopolymerization and photodeactivation process. These findings demonstrate that physical and/or biochemical cues can be used to align neurites and that neurites can even overcome conflicting cues. Modulating alignment of inner ear neurites even in the presence of competing cues lays the groundwork for next general cochlear implants and other neural prosthetic devices.

PS 509

The exploration of the mechanism of facial nerve regeneration around the injured facial nerve.

Takashi Sato[1]; Naoki Matsushiro[2]; Ryusuke Imai[1]; Hidenori Inohara[3]
[1]Department of Otorhinolaryngology-Head and Neck Surgery, Osaka University Graduate School of Medicine; [2]Osaka Police Hospital, Department of Otolaryngology Facial Nerve disorder, Ear and Skull Base Surgery and Hearing Loss Center; [3]Department of Otorhinolaryngology-Head and Neck Surgery, Graduate School of Medicine, Osaka University

Background
Bell palsy or idiopathic facial paralysis has a lifetime risk of 1 in 60. Most of patients generally carry a good prognosis. The remainder have persistent moderate to severe weakness, facial contracture, or synkinesis. When electroneuronography testing score is below 10%, patients will be sure to have incomplete recovery. In our clinic, those patient are able to take surgical decompression. Despite decompression surgery, some of patients have a good recovery and others do not recover. The recovery of facial nerve paralysis is mainly depend on the severity of injury. We consider that the environment around the facial nerve in the healing process make the influence on recovery.

Methods

The sheath of facial nerve were obtained from 32 patients who received surgical decompression in our clinic. We selected 6 samples and divided two groups (each of 3 samples). At over 10 months following the onset of paralysis, in one non-recovery group, facial nerve score (Yanagihara score) was below half of total score. In another recovery group, Yanagihara score was beyond ninety percent of total score. The gene expression profiles of each of groups were examined and compared to each other by the complementary DNA microarray technique.

Results

85 genes were found to be expressed in recovery group more than two fold statistically more than in non-recovery group. Among of 85 genes, for each sample in recovery group, 3 genes were two fold increase compared to all individual samples in non-recovery group.

Conclusions

Microarry data suggested that three increasing genes have some influence on the facial nerve regeneration.

PS 510

Spiral Ganglion Neurite Outgrowth on Electrospun Nanofibrous Piezoelectric Scaffolds and Nanofibrous Piezoelectric Carbon Nanotube Composites

Hassan A. Zabalawi[1]; Mohamed Jomaa[2]; Wenhui Song[2]; Xaio Liu[3]; Thomas Maltby[4]; Antonio Vilches[4]; Jonathan Gale[1]
[1]UCL Ear Institute; [2]UCL Centre for Nanotechnology and Regenerative Medicine; [3]Department of Electronic and Electrical Engineering, University College London; [4]Electrical and Electronic Engineering, London South Bank University

One of the most critical factors for cochlear implant functionality is the number and excitability of surviving spiral ganglion neurons (SGNs). Progressive degeneration of SGN peripheral processes raises the thresholds needed for electrical stimulation, necessitating higher currents reducing battery life. Stimulating SGN regeneration has the potential to improve the efficacy of future cochlear implants, but if we are to achieve functional SGN regeneration proper spatial separation and alignment of SGN peripheral neurites is required. We took a multidisciplinary approach to promote and direct regrowth of auditory neurons using electrospun nanofibres, that could be used to improve CI functionality and feasibility.

We examined the viability of oligosilsesquioxane–poly(ε-caprolactone) (POSS–PCL), polyhedral oligomeric silsesquioxane poly(carbonate-urea) urethane (POSS-PCU) and Polyvinylidene Trifluoroethylene (PVDF-TrFE) for SGN adhesion and survival. The effects of the scaffolds on the length and orientation of re-growing SGN neurites and glia were tested in vitro using primary cultures from C57BL/6 P5 mice. Two methods of SGN preparation were compared; SGN explants and dissociated SGN cultures, both maintained on the scaffolds for 72 hours. After fixation and immunostaining, neural and glial cells were counted, and the lengths and directions of the regrown neurites were measured and analyzed.

Due to its biocompatibility and piezoelectric properties, PVDF-TrFE was chosen to add directional growth cues through electrospinning aligned nanofibre scaffolds. After testing, primary SGNs showed preferential affinity to PVDF-TrFE nanofibers and were found to promote SGN neurite regrowth and induce alignment, compared to glass cover slips. Accordingly, PVDF-TrFE – carbon nanotube (CNT) nanocomposite electrospun scaffolds were fabricated and tested. The CNT addition was found to be biocompatible with primary SGNs, and the PVDF-TrFE neurite promotion withholds in the presence of CNTs. The nanocomposite allows the nanofibers to transfer electrical current, which renders it suitable for testing electrical induction regenerative protocols in vitro. In both primary SGN dissociated cultures and explants cultures, the regrown neurites follow the pattern of the scaffold's fibrous surface.

We aim to induce regeneration and control alignment of SGN neurites in order to maintain SGN tonotopy while bridging the gap between SGNs and CI electrodes. The nanofibrous piezoelectric electroactive nanocomposite scaffold, combined with a specific protocol of electrical induction in the first weeks of implantation, could significantly improve cochlear implantation results, frequency selectivity and minimize power demands. In addition, the scaffolds could be further biofunctionalized with neuron modulating drugs to further sustain the effect after implantation.

PS 511

Stereotaxic delivery of neural progenitors for cochlear reinnervation in mouse

Judith S. Kempfle[1]; Mingjie Tong[2]; Ngoc-Nhi Luu[2]; Albert Edge[3]
[1]1, Department of Otolaryngology, Massachusetts Eye and Ear, Boston, MA, USA. 2, Department of Otology and Laryngology, Harvard Medical School, Boston, MA, USA. 3, Department of Otolaryngology, University Tübingen Medical Center, Germany; [2]massachusetts Eye and Ear Infirmary; [3]Harvard Medical School

Background

Sensorineural hearing loss (SNHL) is caused by irreversible loss of auditory neurons and/ or hair cells, and is increasing in prevalence. Auditory neurons do not regenerate after damage, and cellular therapies such as transplantation of stem cell derived neural progenitors may offer a therapeutic approach, but surgical access to the cochlea is challenging. Minimally invasive stereotaxic surgery has long been used in the brain for successful delivery of drugs or cells in humans and mouse models and may offer a viable approach for the cell-based therapies to the cochlear nerve.

Methods

Tau-GFP expressing mES cells were subjected to a neural induction protocol to derive neural progenitors that expressed peripheral sensory neuron markers. The auditory nerve was accessed via a stereotaxic approach in a mouse model of auditory neuropathy. Progenitors were transplanted into the denervated auditory nerve trunk 1 week after damage. Successful engraftment was confirmed by immunohistochemistry 10 days, 4 weeks or 3 months after transplantation. Functional response was measured by auditory brainstem evoked responses (ABRs) before and after auditory nerve ablation and transplantation.

Results

Sensory neural progenitors derived from mES cells were successfully transplanted using standardized stereotaxic coordinates. Progenitor cells survived and exhibited neurite outgrowth within the first 10 days of transplantation. Four weeks after transplantation, neural progenitors continued to express GFP and co-labeled with neuronal marker TuJ. Graft integration with outgrowth of peripheral and central neurites was observed. After 3 months, neurites were found at the level of the organ of Corti, and functional testing revealed improvement of ABR at frequencies corresponding to basal and mid-basal cochlear regions.

Conclusion

Stereotaxic transplantation of mES cell derived neural progenitors allows for minimally invasive access to the mouse auditory nerve. Progenitor cells integrate into the adult peripheral and central auditory pathway and improve cochlear function in mice. This study represents a first step toward future cell based regeneration strategies for hearing loss in the human.

Thalamus and Primary Auditory Cortex

PS 512

Influence of deafness on the development of early cortical circuits

Xiangying Meng; Patrick Kanold
University of Maryland

Sensory experience, esp. sensory deprivation, has a profound influence on cortical development. Subplate neurons (SPNs), the earliest generated neuronal population in the cerebral cortex, play a critical role on the development of brain circuitries. They provide a transient excitatory relay of thalamic information to layer 4 and lesions of SPNs can alter cortical development.

Since SPNs are the first cells to receive sensory activity, we speculated that sensory deprivations could alter SPN function. To test whether sensory experience, esp. at very early ages influences SPNs we utilize genetic deafness models which allow us to investigate changes due to sound deprivation even before ear opening. To investigate synaptic circuits onto SPNs we use laser-scanning photostimulation (LSPS) in thalamocortical slices of ACX from mice at postnatal days 6-14. We compare mice deficient in sound transduction such as TMC1 and TMC2 double knock-out (TMC DKO) mice as well as those deficient in synaptic transmission from hair cells such as Otoferlin knock-out mice (OTOF KO).

In TMC DKO mice we find that compared to normal control mice SPNs show hyper-connectivity from cortical layers at ages before ear opening (P6-P9) and that these circuit changes remain after ear opening (P11-P14). OTOF KO mice also show altered SPN circuits. However, the detailed spatial patterns of the changes vary between these deafness models.

Our analysis suggests that deafness alters the earliest cortical circuits, suggesting that early sound experience as well as peripheral spontaneous activity before the onset of thalamocortical transmission to layer 4 can sculpt intracortical circuits. Because mice are altricial, the changes we observe are likely to be present in congenitally deaf humans in utero. Thus, restoration of hearing after birth has to take these altered circuits into account.

PS 513

Model of developing auditory cortex shows low probability stimuli as drivers of cortical organisation.

Adarsh Mukesh[1]; Muneshwar Mehra[2]; Sharba Bandyopadhyay[3]
[1]Dept. of Biotechnology, IIT Kharagpur; [2]Advanced Technology Development Centre, IIT Kharagpur; [3]Department of Electronics and Electrical Communication Engineering, IIT Kharagpur

Low probability stimuli are usually salient and important for carrying meaningful information about the external world. In this study we examine the role of low probability sounds in development of the auditory cortex (ACX). In order to develop the network model we include thalamic inputs, projecting to subplate neurons (SPNs), a transient layer of neurons present only during development, and thalamo-recipient Layer IV neurons (L4). Based on recorded single unit responses in developing ACX of the mouse, of SPNs and L4 during development we model response properties of the SPNs and L4 neurons using depressing synapses. Overall the model captures the context dependence in responses present in L4 and SPNs and show stimulus specific adaptation. By including plasticity in the synapses based on spike times (STDP) the network model is made to adapt to different developmental stimulus experiences. First we use a simplified two inputs (two stimuli) network and show that low probability stimuli, due to high deviant selectivity of SPNs and L4 early on development shows over representation of low probability stimuli. We then extend the simplified network to an array of inputs representing a gradual change in a stimulus parameter along the array (for example tone frequency). Using a standard-deviant (high and low probability) stimulus exposure during the development we show that the L4 neurons'; tuning shift towards the deviant low probability stimulus. A critical aspect of this plasticity is the time scales at which the stimulus is presented or it changes. Aspects of the importance of time scales of standard-deviant stimulus are investigated by a variety of stimulus exposure paradigms in the development model showing the importance of low probability stimuli in auditory cortical development. Such plasticity in the thalamo-recipient layer (L4) could underlie the observed heterogeneity in auditory cortical tuning organization based on natural stimulus frequency content statistics and the time scales of change in natural stimuli.

PS 514

Layer-specific representation of interaural time and level differences in the auditory cortex of normally hearing and congenitally deaf cats

Monique Hajduk[1]; Jochen Tillein[2]; Andrej Kral[1]; **Peter Hubka**[1]
[1]Institute of AudioNeuroTechnology (VIANNA), Hannover Medical School; [2]Department of Otorhinolaryngology, J.W. Goethe University

Binaural cues, interaural time and level differences (ITD and ILD, respectively), are crucial for auditory orientation in the horizontal plane. Their cortical depth distribution and its dependence on experience was not studied in details yet. The present study is aimed to map layer distribution of ITD and ILD responses in the normally hearing and the congenitally deaf cats evoked by intracochlear electric pulse train stimulation.

Cortical multiunit activities from nine hearing controls and nine congenitally deaf cats (CDC) were recorded in A1 from all cortical layers simultaneously by means of the 16 channel microelectrode arrays in light general anesthesia (isoflurane, 0.8-1.5%). All animals were electrically stimulated with cochlear implants. Binaural responses were evoked by pulse trains (500 Hz, 3 pulses) at intensities of 0-12 dB above auditory brainstem response (ABR) thresholds. Time delays between the binaural stimulation was systematically shifted in time (from -600 to 600 μs; 100 μs step) and intensity (relative current levels from -12 dB to +12dB; step 2dB; averaged binaural level was kept constant at 6dB above ABR threshold) in order to record ITD and ILD functions, respectively. Multiunit responses were evaluated for latencies 0-15 ms (early response) and 16-30 ms (late response).

In the hearing controls, the differences in depth distributions between ITD and ILD representations within primary auditory cortex were found. In the infragranular layers, ITD and ILD activations were stronger, latencies were shorter and the modulation depth was smaller when compared with the responses in supragranular layers. The tuning of binaural hearing cues differed in the two analyzed time windows: early responses were contralaterally tuned for both cues; later response of ILD remained contralaterally tuned whereas ITD response showed ipsilateral preference. In the CDC, the basic tuning properties of single ITD and ILD functions was similar to the hearing controls. However, modulation depth of both ITD and ILD functions was smaller and the ITD and ILD responses were observed in supragranular layers, but responsiveness was reduced in infragranular layers.

The present results demonstrate differences in the representation of ITD and ILD along cortical depth in the primary auditory cortex of both studied groups. This indicate a diverse role of supra- and infragranular layers in the processing of binaural cues. Strong bias of ITD and ILD activation to the supragranular layers in CDC confirms that developmental experience is necessary for recruiting and integrating infragranular layers into the one complex cortical processing unit.

PS 515

Cortically independent subcortical auditory contrast gain control

Michael Lohse[1]; Benjamin D.B. Willmore[1]; Victoria Bajo[1]; Andrew J. King[2]
[1]Department of Physiology, Anatomy, and Genetics, University of Oxford; [2]University of Oxford

Contrast gain control has been identified in the visual, auditory and somatosensory systems. Gain control may be beneficial because the statistics of the sensory environment are constantly changing, meaning that neurons may not be able to accurately represent the range of stimulus values that occur at any moment unless they adapt their dynamic ranges accordingly. Furthermore, adaptation to sound contrast is also a mechanism that may be useful in generating noise-tolerant neural representations of complex sounds.

It is currently unknown whether the robust contrast gain control previously described in cortex is a local cortical computation or a subcortical process inherited by cortex. To determine whether contrast gain control is exhibited by subcortical structures in the mouse auditory system, we recorded, using multi-electrode arrays (4 x 8 or 2 x 32 sites), from auditory thalamus (16 mice: 14 C57BL/6J + 2 Gad2-IRES-Cre) or inferior colliculus (2 Gad2-IRES-Cre) in ketamine/medetomidine anaesthetised mice. We presented dynamic random chord stimuli (25 ms chords) at two different contrasts (± 10 and ± 20 dB) and similar mean sound levels (40 dB SPL). We fitted the neuronal responses with a linear spectro-temporal receptive field and a sigmoidal output nonlinearity, which was used to estimate the gain of each unit.

We found that the lemniscal auditory thalamus (ventral division of the medial geniculate body (MGB)) and the central nucleus of the inferior colliculus both exhibit contrast gain control, which is similar in strength to the contrast gain control previously found in ferret and mouse auditory cortex, while the non-lemniscal pathway (dorsal and medial divisions of the MGB) show less contrast gain control relative to the lemniscal pathway.

We also silenced auditory cortex by optogenetically (AAV5-DIO-hChR2(H134R)-YFP) activating GAD2 positive cells (40 Hz light train) while measuring the strength of contrast gain control in the subcortical structures. Preliminary results suggest that inactivation of auditory cortex does not affect contrast gain control in either thalamus or midbrain. Together, these results suggest that contrast gain control operates subcortically without dependence on descending cortical input.

PS 516

Increasing the Complexity of Sinusoidal Amplitude Modulated Stimuli Boosts Sequential Preference in Rat Auditory Thalamic Neurons

Srinivasa prasad Kommajosyula[1]; Rui Cai[2]; Donald Caspary[1]
[1]SIU School of Medicine; [2]SIU School of Medicne

Background
Older adults are shown to have difficulties in speech understanding in noise. Top-down projections are implicated in compensation for deficits in older adults. In a recent study, medial geniculate (MG) units recorded in older rats showed increased preference for sequential (SEQ) over randomly (RAN) presented Sinusoidal Amplitude Modulated (SAM) stimuli (Cai et al., 2016). We hypothesized that the degraded up-stream signal in aged MG units resulted in anticipation of the repeated acoustic signal, in SEQ preference, suggesting increased use of cognitive resources. The present study hypothesized that decreasing the salience of a SAM stimulus by increasing its complexity would increase SEQ preference in MG units recorded from young awake rats.

Methods
Tetrode microdrives or tungsten microelectrodes were implanted/inserted into MG of young adult (4-6mos) Fischer Brown Norway rats. SAM stimuli were generated and delivered as in Cai et al. (2016). Complex SAM stimuli were generated by decreasing modulation depths (MD) or adding a low-pass filtered (1000Hz) noise to the SAM envelope (Noisy SAM), which effectively jittered the envelope decreasing SAM salience. Total energy differed by < 2 dB across all stimuli. The sequence preferring ratio was calculated from 80 trials of SAM stimuli presented either RAN or SEQ-ly. The total number of spikes were compared between simple SAM and complex SAM stimuli using a Chi-Square test.

Results
Fifty-nine single units (31 awake; 28 anesthetized)

were recorded from rat MG. In recordings from awake MG units, over two-thirds (67.7 %) preferred RAN, while only 6.45 % preferred SEQ in response to simple 100% MD SAM stimuli. As the complexity of the SAM stimulus increased, a significant (p<0.01) increase in SEQ preference neurons was observed at 25% MD (38.7%) and NOISY (41.3%) SAM in awake, but not anesthetized rats. Conversely, there was a significant (p<0.01) decrease in RAN preference for 25% MD (45.1%) or NOISY (51.72%) SAM in awake, but not in anesthetized rats.

Conclusions

The present findings support the contention that an increase in stimulus complexity will further engage top-down resources as shown by increased MGB unit responses to SEQ over RAN stimuli. This was true for units from awake MGB, but not in anesthetized rats. Rate and temporal modulation functions parsed across different modulation frequencies will be analyzed in future. This study may provide insight into training approaches to improve speech recognition in the elderly. Funding: NIH grant DC000151 to Donald M. Caspary.

PS 517

Neuronal responses to vocoded communication sounds in the thalamo-cortical auditory system: Robust discrimination based on temporal envelope cues?

Samira Souffi[1]; Christian Lorenzi[2]; Jean-Marc Edeline[1]; Chloé Huetz[1]
[1]*NeuroPSI UMR CNRS 9197; [2]Laboratoire des systèmes perceptifs, Département d'études cognitives, École normale supérieure, PSL Research University, CNRS*

Cochlear implants are neuroprosthetic devices that directly stimulate auditory-nerve fibers to restore hearing in the case of severe to profound deafness. The "speech processor" operates as a "vocoder" that splits the input signals into a limited number of frequency bands and extracts temporal-envelope fluctuations from the narrow-band stimuli. A vast literature describes the perceptive abilities of human subjects to correctly identify speech (or words) as a function of the number of frequency bands used by the vocoder. However, very few studies have tried to determine whether the discrimination between communication sounds by auditory neurons is impacted by the vocoding process. Also, how the neuronal discrimination of acoustic stimuli is impacted by the vocoding when progressing in the auditory system hierarchy remains unknown.

Four guinea pig vocalizations (Whistle) were processed by a tone vocoder using several levels of spectral reso-
lution (10, 20 and 38 frequency bands). The original and vocoded vocalizations were presented either in quiet or in noisy conditions using two types of noise: a "chorus" noise mimicking a cocktail party effect, and a wide-band unmodulated noise those spectrum matched the one of the chorus noise. Three signal-to-noise ratios (SNR) were tested: +10, 0 and -10 dB. We recorded responses from auditory thalamus (MGB), primary (A1) and non-primary (VRB) auditory cortices and compared responses to original and vocoded vocalizations in anesthetized guinea pigs.

In AI, the evoked firing rate (FR) and the temporal reliability (CorrCoef) of cortical responses were slightly and progressively reduced by the vocoding process as the spectral resolution decreased. Neuronal discrimination (quantified by the Mutual Information, MI, carried by the temporal spike patterns) significantly decreased when the number of frequency bands was reduced from 38 to 10. These three parameters were much weaker in the area VRB when the vocalizations were vocoded. Both with original and vocoded vocalizations, MI was higher in MGB than in auditory cortex, but MGB responses were more attenuated by the vocoding process. However, the effects of the two types of noise were similar for normal and vocoded vocalizations and were similar in AI, VRB and MGB: The lower the SNR, the higher the reduction in FR and MI.

These data indicate that a robust discrimination between vocoded vocalizations, probably based upon temporal-envelope cues, is present in primary and non primary auditory cortex but is even more prominent in thalamus.

PS 518

Spectral Contrast Selectivity of Excitatory and Inhibitory Neurons in the Mouse Auditory Cortex

Muneshwar Mehra[1]; Sharba Bandyopadhyay[2]
[1]*Advanced Technology Development Centre, IIT Kharagpur; [2]Department of Electronics and Electrical Communication Engineering, IIT Kharagpur*

Spectral contrast is an important feature of auditory stimuli that may allow recognition of sound objects in different situations for example in background noise. Further, spectral contrast plays a role in the coding of complex stimuli with wideband characteristics and in presence of multiple sound sources. Such stimuli and situations are more naturalistic as opposed to the use of tonal sound stimuli, used generally to study tuning and coding properties of auditory cortical neurons. In this study spectral coding by excitatory and different classes of inhibitory (parvalbumin positive, PV+ and somatostatin-positive, SOM+) neurons (EXNs and INNs) in the mouse auditory

cortex (ACX; primary ACX, AI and anterior auditory field, AAF) are studied using random spectral shape (RSS) stimuli of varying spectral contrast. The stimuli have a steady spectral shape throughout its duration and each stimulus have random spectral content (frequency resolution 1/8th octave) drawn from a Gaussian distribution of different standard deviations, which defines the spectral contrast of the stimulus set. Two-photon Ca^{2+} imaging was performed in the following mice: Thy1-GCamp6f, PV-cre X td-Tomato and SOM-cre X td-Tomato with AAV-syn-GCamp6s injected, and PV-cre and SOM-cre with AAV-flex-GCamp6s injected. Virus injections were made in multiple locations to allow imaging over multiple regions in the ACX. Ca^{2+} based fluorescence responses from EXNs and/or INNs (PV+ or SOM+) to sets of RSS stimuli were collected either simultaneously or exclusively depending on the type of mouse line and virus injections used. Responses were parsed into two parts – onset and offset and their spectral selectivity was determined. It was found that PV+ neurons had a higher preference for low contrast stimuli and in essence provides broadband inhibition in layer II/III. SOM+ neurons were more selective for high contrast stimuli and hence provide narrowband inhibition and further, they responded sparsely. EXNs could be both selective for high and/or low contrast stimuli. Local circuits based on the above responses provide an understanding of cortical micro-circuits in Layer II/III of the mouse auditory cortex and show differential processing of low and high spectral contrast stimuli by different classes of neurons.

PS 519

Predicting Error and Repetition Suppression in the Auditory Thalamocortical System in a Rat Model of Schizophrenia

Gloria G. Parras[1]; Javier Nieto-Diego[1]; Manuel S. Malmierca[2]
[1]Auditory Neurophysiology Laboratory. Institute of Neuroscience of Castilla y León (InCyL). Salamanca. Spain; [2]Auditory Neuroscience Laboratory. Institute of Neuroscience of Castilla y León (InCyL). Salamanca. Spain

MMN is a memory-based change-detection brain response to any discriminable change in a stream of auditory stimulation (Näätänen et al. 2014). MMN is obtained by subtracting responses to deviant stimuli minus standard stimuli in an oddball paradigm. In the predictive coding framework, MMN can be decomposed by two different concepts, the error signal elicited by a violation of a pattern regularity (predicting error) and the memory trace form by a repetition of a standard stimuli (repetition suppression).

Schizophrenia studies have consistently reported atten-uated MMN amplitudes compared to normal controls, raising the possibility that sensory memory is critically dependent on NMDA receptor activation (Javitt et al. 1993). Animal models using NMDA receptor hypofunction such MK-801, have demonstrated analogous symptoms to these observed in schizophrenic patients. But currently it is unknown where in the auditory pathway these changes emerge and how these processes are affected in schizophrenia.

We have recorded single units from AC and MGB in MK-801-systemic-treated rats and from control rats. Targets sounds were selected from each neuron';s frequency response area. Recordings were made after stimulation with an oddball paradigm and a control cascade paradigm. Responses to the same frequency were compared when presented as deviant (DEV), standard (STD) and control (CAS). Three indexes were computed resulting from the relation between the normalized response to Deviant-Standard (Mismatch: iMM); Cascade-Standard (Repetition_Supression: iRS) and Deviant-Cascade (Predicting_Error: iPE).

Results show that neurons recorded in the MK-801-treated rats display significant changes in the firing rate such that responses to STD stimuli in all AC and MGB subdivisions decrease and a those to DEV stimuli increase only for non-lemniscal AC fields. Moreover, neurons recorded in the MK-801-treated group shows higher iRS in all MGB subdivisions, while only the non-lemniscal AC neurons show lower iRS than in the control group. All AC subdivisions and lemniscal MGB neurons show high iPE values than in the control group, while only non-lemniscal MGB neuronsbecome negative compared with the control group.

The results demonstrate that failures in processing auditory information occurs both at the thalamic and cortical levels in schizophrenia. Neurons in the MK-801 rat model of schizophrenia maintain higher levels of adaptation than normal rat, showing decreased responses to regular context. These results support the notion that the sensory memory-based mechanism is altered in schizophrenia.

Tinnitus II

PS 520

Effects of Suppressive Spectrum on the Tinnitus Frequency and Intensity

Ming Zhang[1]; Alysia Jeske[2]; Sarah Young[2]
[1]LSU Health Sci Ctr; [2]University of Alberta

It is well known that the tinnitus can affect sufferer';s emotion, attention, cognition and working memory, as well as cause anxiety, depression, hyperacusis, insomnia and hearing impairment, resulting in a decrease in quality of life. While a variety of therapies may provide some relief and reduce symptoms, no cure has been identified from existing approaches according to the American Tinnitus Association. To explore some new approach, in general, we designed an approach that was expected to be able to change the tinnitus intensity as well as tinnitus frequencies. The approach involved a special spectrum pattern formulated according to a suppression mechanism, while the carrier for this spectrum is noise, which is to be shaped and modulated with the spectrum. So, we called this approach as the suppressive noise spectrum. In addition, this spectrum was customized with the tinnitus spectrum, such as in tinnitus frequencies and intensities. We hypothesized that this approach would improve the tinnitus, such as change the tinnitus intensity as well as tinnitus frequencies. To our knowledge, no proposal has been identified in the literature including such an approach with such a hypothesis. We also tried the suppressive noise spectrum in treating the tinnitus patients and found that this approach did change the tinnitus frequency and intensity, which is another point that has not been identified in the literature to our knowledge. In specific, single-subject design was adopted, with fifteen ears suffering from tonal tinnitus to be recruited to undergo the intervention. Patient received the treatment through listening to the suppressive noise spectrum. The results related to their tinnitus were measured over time. After 3 months of experience being exposed to the customized suppressive noise spectrum therapy, the measured results showed a shift in tinnitus frequency in addition to a significant decrease in tinnitus intensity based on a comparison of the measurements between the pre-treatment and post-treatment condition (p<0.05). Typically, improvement was gradual based on a comparison between 3 sets of data which were collected at baseline before treatment, 1.5 months and 3 months after treatment. As a conclusion, applying the suppressive noise spectrum on treating the tinnitus is novel. Based on our findings, using a customized suppressive noise spectrum is effective in shifting the frequency, reducing the intensity of subjective tonal tinnitus, and improving the handicap based on THQ test. From this seminal report, factors related to maximizing its effectiveness (e.g., length of listening time, level of hearing impairment, and application for alternative tinnitus types) may be considered for future research.

PS 521

Early Age Low Level Noise Exposure is a Risk Factor for Hyperacusis

Anaam Alkharabsheh[1]; Senthilvelan Manohar[2]; Richard Salvi[3]; Wei Sun[4]
[1]University at Buffalo; [2]University at Buffalo, USA; [3]Center for Hearing and Deafness; State University of New York at Buffalo; [4]State University of New York at Buffalo

Background

The normal development of the central auditory system is critically dependent on sensory input from the cochlea. Early age low-level noise (LLN) exposure, even if it does not cause severe hearing loss, can disrupt development of the central auditory system, impairs auditory learning, sound localization and temporal processing. As early age hearing loss has been linked to hyperacusis, we speculated that early LLN might induce hyperacusis. To test this hypothesis, we exposed young rats to LLN to determine if it would induce hyperacusis. Because LLN is often used to treat hyperacusis, we also hypothesized that prolonged low-level noise exposure might alleviate the hyperacusis related to early noise induced hearing loss (eNIHL).

Methods

Three groups of postnatal day 16 rats were used for this study. The eNIHL+LLN group was exposed to narrow band noise (12 kHz, 115 dB SPL, 4 h/d for two days) in an effort to induce hyperacusis and subsequently subjected to continuous LLN (10-20 kHz, 78 dB SPL) for three weeks in an effort to suppress hyperacusis. The LLN group was only treated with low-level noise for three weeks. The Control group was raised under normal conditions without noise exposure. At 45 days of age, all groups underwent behavioral training for loudness test. Reaction time and loudness response functions were evaluated using narrow band noise bursts centered at 2, 4, and 12 kHz (40-110 dB SPL, 10 dB step). The auditory brainstem response (ABR) was used to monitor hearing threshold.

Results

ABR test shows that ABR thresholds in the LLN and Control groups were similar. However, the LLN group showed significantly reduced reaction times compared to the Control group, behavioral evidence of hyperacusis. Rats in the eNIHL+LLN group showed about 10-20 dB hearing loss at 12 kHz and above, but not at low

frequencies. Their reaction times were also significantly shorter than the Control group at moderate to high intensities, behavior consistent with hyperacusis.

Conclusion
Our preliminary results show that prolonged LLN at an early age, which does not cause a permanent hearing loss, leads to shorter than normal reaction times at moderate to high intensities, behavior indicative of hyperacusis. Similar results were seen in the eNIHL+LLN group. Our results suggest that early LLN exposure (

PS 522

Association between stress and tinnitus: an experimental study in a rat model of stress-induced tinnitus

Min Jung Kim[1]; So Young Park[2]; Ilyong Park[3]; Hyo Jeong Yu[4]; Jung Mee Park[5]; Shi Nae Park[6]

Background
Gap-prepulse inhibition of the acoustic startle reflex (GPIAS) has been used in rats and mice for tinnitus screening and assessment. The proper function of neurons in many brain areas depends on the physiological homeostasis maintained and regulated by glutamate and GABA, which create the opposite excitatory/inhibitory forces in the brain. This animal study has been performed to evaluate the association between stress and tinnitus and to observe the changes of excitatory and inhibitory responses in the brain tissue in the rats with stress induced tinnitus.

Methods
Male Wistar rats aged 1 month were used and sub-grouped according to the single or double stimuli of noise and stress. Noise-induced tinnitus (NIT) was induced by 110dB SPL, 16kHz narrow band noise for 1hr and restraint-induced acute stress (RIAS) was induced by restraining rats with taped plastic film envelopes for 1hr. ABR thresholds and DPOAEs were recorded before and after the induction of noise and stress. Tinnitus was assessed by GPIAS by obtaining GN ratios. Stress hormones and relevant neurotransmitter receptors, NMDA and GABA receptors were observed in the cochlea and the brain hippocampal tissue.

Results
Increased hearing thresholds and decreased DPOAE responses were observed after 1 hr noise stimuli. RIAS group showed the increased GN ratio compared to the control group (p<0.05), which indicates that stress alone can cause tinnitus. Double stimuli with noise and stress developed more significantly increased GN ratios regardless of their induction order (p<0.005). In western

blotting and immunofluorescence staining of hippocampus, expression of NMDA receptor (NMDAr)in the experimental groups, especially RIAS groups, was decreased compared to the control group (p<0.05).

Conclusion
Tinnitus induced by RIAS and noise as well as its aggravation by double stress stimuli were distinctly observed in our study. Reduced NMDAr in the hippocampus seems to be related to the relevant mechanisms on tinnitus development and its association with stress. This novel animal study results support the strong association among noise, stress and tinnitus.

[!2018 ARO abstract- Tinnitus and Stress_ MJKIM_20170920_PSN Cx final.docx](#)

PS 523

Neural correlates of tinnitus in the guinea pig ventral cochlear nucleus

David T. Martel[1]; Susan Shore[2]
[1]University of Michigan, Ann Arbor; [2]University of Michigan

Introduction
Previous studies have shown that noise exposure can elicit increased spontaneous firing rates (SFR) and cross-unit spontaneous synchrony in tonotopically-restricted groups of dorsal cochlear nucleus (DCN) fusiform cells, which correlate with behavioral measures of tinnitus (Wu et al., J Neurosci 2016). Recent studies have shown that the same noise exposure can produce increases in SFR in bushy cells of the ventral cochlear nucleus (VCN; Martel et al, ARO 2016). Bushy cells exhibit high onset firing rates and highly synchronous primary-like responses (Winter and Palmer, 1990), potentially providing a significant contribution to the auditory brainstem response (ABR; Melcher et al, 1996). Studies of humans with tinnitus suggest that enhanced later ABR wave amplitudes (Schaette and McAlpine, J Neurosci 2011; Gu et al., J Neurophys 2012) might be a tinnitus correlate. ABR waves II-V arise predominantly from the bushy cell pathway (Melcher et al, 1996), suggesting that bushy cells may play a role in tinnitus in addition to the documented fusiform cell role. Here we examined the role of the bushy cell pathway in tinnitus generation by recording ABRs and neural activity from bushy cells in animals with behaviorally-verified tinnitus.

Methods
Guinea pigs were exposed to unilateral narrow band noise (1/2 octave, centered at 7 kHz, 97 dB SPL) for two hours to induce temporary threshold shifts. Tinnitus was assessed using gap/prepulse-inhibition of acoustic

startle (GPIAS; Turner et al., Behav Neurosci 2006), and quantified using distribution differences between pre- and post-exposure GPIAS values (Tinnitus Index, TI). Once chronic tinnitus was established (p<0.05; Student's t-test; 8 weeks after noise-exposure), the animals were anesthetized with ketamine/xylazine, ABRs measured, and 16-channel probes stereotaxically inserted into the VCN. Individual ABR wave 11-V amplitudes were manually identified and normalized by the corresponding wave I amplitude. Spontaneous and tone-evoked activity were recorded from VCN units, identified as bushy cells by their location in CN and peristimulus-time histogram pattern (Winter and Palmer, J Acoust Soc Am 1990).

Results
ABR wave amplitude ratios correlate with frequency-matched tinnitus indices. Bushy cells in tinnitus animals show higher spontaneous firing rates, higher onset firing rates, and lower first spike latency variance than non-tinnitus and control animals. Further, SFR and onset firing rates correlate with frequency-matched tinnitus indices.

Conclusions
Our results demonstrate that, in addition to DCN fusiform cells, tinnitus-related alterations to bushy cell firing patterns may underlie enhanced ABR wave amplitude ratios and potentially tinnitus pathology. Future studies are necessary to reconcile tinnitus-related activity in DCN and VCN. Funding:R01-DC004825(SES),T32-DC00011(DTM)

PS 524

Salicylate alters stimulus timing dependent plasticity and increases spontaneous firing rates in guinea pig dorsal cochlear nucleus fusiform cells

David T. Martel[1]; Thibaut Pardo[1]; Susan Shore[2]
[1]University of Michigan, Ann Arbor; [2]University of Michigan

Introduction
Following noise exposure and tinnitus-induction, fusiform cells of the dorsal cochlear nucleus (DCN) show increased spontaneous firing rates (SFR), increased spontaneous synchronization and altered stimulus-timing dependent plasticity (STDP) (Wu et al, J Neurosci 2016; Koehler and Shore, J Neurosci 2013), which correlate with behavioral measures of tinnitus. Sodium salicylate, commonly used to induce tinnitus, increases spontaneous activity in the ascending auditory pathway (Basta et al, Hear Res 2008) and activates NMDA receptors in the cochlea (Guitton et al, J Neurosci 2003). NMDA receptor activation is essential to mediate STDP in many brain regions. Blocking NMDA receptors in DCN

fusiform cells can alter STDP timing rules and decrease synchronization (Stefanescu and Shore, Front Neural Circuit 2015). Thus, systemic activation of NMDA receptors with sodium salicylate could elicit changes to STDP as well as increases in SFR and synchrony that underlie tinnitus. Here we examined the role of salicylate in tinnitus generation in vivo by measuring tinnitus behavior with two tests and performing single unit recordings from DCN fusiform cells pre- and post-salicylate administration.

Methods
Guinea pigs were injected with sodium salicylate (i.p. 350 mg/kg) to induce tinnitus. Tinnitus behavior was assessed using two methods: 1) gap-prepulse inhibition of acoustic startle paradigm (Wu et al, J Neurosci 2016; Turner et al, Behav Neurosci 2006) and 2) an operant conditioning technique (Yang et al, PNAS 2011) in which guinea pigs were trained to cross a box when hearing a sound; during silence trials, the guinea pigs with tinnitus hear a phantom sound and increase their crossing rates. Single unit recordings were obtained using Silicon-substrate electrodes (NeuroNexus) placed into the DCN fusiform cell layer after ketamine/xylazine anesthesia. Fusiform cells were identified by electrode position within the DCN and sound-evoked responses 20 dB above unit threshold at best-frequency (BF) (Stabler et al, J Neurophys. 1996). Responses from neurons with BFs ranging from 6 kHz to 18 kHz were analyzed. STDP timing rules were measured as the percent change in firing rate as a function of bimodal stimulation interval (+/-20 ms, +/-10 ms, +/-5 ms, or unimodal) and a stimulus paradigm consisting of somatosensory stimuli (via transdermal stimulating electrodes placed on C2; square-wave electrical pulses at the sub-contraction threshold, 1 kHz rate, 100 us/phase), and 40 dB SL acoustic stimuli at the most common unit best frequency for each animal.

Results
Guinea pig administered salicylate showed impaired gap detection not attributable to hearing loss and increased crossing rates during silence compared to baseline, consistent with tinnitus induction. After salicylate administration, fusiform cell SFR was significantly increased, and STDP timing rules were shifted towards long-term potentiation compared to baseline.

Conclusions
These results suggest salicylate-induced tinnitus may have a similar pathophysiology in DCN to that shown after noise damage (Koehler and Shore, J Neurosci 2013; Wu et al, ARO 2016). Further studies are necessary to understand precisely how salicylate influences multisensory plasticity to induce tinnitus. Funding:R01-DC004825(SES),T32-DC00011(CW,DTM)

PS 525

Nitric oxide as a modulator in the ventral cochlear nucleus: a potential tinnitus generation mechanism.

Adam Hockley[1]; Joel Berger[1]; Paul Smith[2]; Alan Palmer[1]; Mark Wallace[1]
[1]MRC Institute of Hearing Research; [2]University of Nottingham

Tinnitus chronically affects an estimated 10-15% of adults and is characterised by the perception of sound independent of external stimuli. Nitric oxide synthase (NOS) expression has been studied in guinea pig ventral cochlear nucleus (VCN) where it is located in a sub-population of each cell type. Following unilateral acoustic over-exposure, a within-animal asymmetry of NOS expression was found exclusively in animals that developed tinnitus (Coomber et al., 2015). The decrease in NOS expression in the contralateral VCN was observed as soon as 1 day after acoustic-over exposure, and the asymmetry in NOS expression was strongest at eight weeks after noise exposure. This provided evidence for a role of nitric oxide (NO) in tinnitus, and not simply as a biomarker for hearing loss.

Here, we describe the use of iontophoresis to apply the NOS inhibitor L-N^G-Nitroarginine methyl ester (L-NAME) and the NO donor 3-Morpholinosydnonimine hydrochloride (SIN-1) to units within the VCN of the anaesthetised guinea pig. Upon isolation and characterisation of a single unit, hour-long, pure tone pulse-trains were presented at the characteristic frequency (200 ms tone pip, 800 ms silence, 3600 repeats). Spontaneous and auditory-driven spike rates were recorded over the hour while drugs were applied iontophoretically.

In response to the NO donor SIN-1, there was an increase in both the proportion of units increasing and decreasing their spontaneous firing rate (0% to 22%, and 4% to 14% respectively) following noise exposure. This suggests that noise exposure may increase the sensitivity of units in the VCN to NO. When blocking NO production with L-NAME, changes correlated with behavioural evidence of tinnitus. The proportion of neurons decreasing their firing rate in the control group, noise exposed non-tinnitus and noise exposed tinnitus groups following L-NAME appication were 9%, 5% and 37% respectively. Therefore, in tinnitus animals endogenous NO may be increasing excitability in a larger proportion of neurons, potentially producing an increase in transmission through the auditory system with potential to contribute to the 'increased central gain'; thought to be present in tinnitus.

PS 526

Tinnitus or Hearing Loss? Relationship between GPIAS Deficits and ABR Thresholds after Repeated Salicylate Administration in Rats

Christophe Tran Van Ba[1]; Mathieu Petremann[1]; Cindy Gueguen[1]; Charlotte Romanet[1]; Vincent Descossy[1]; Pauline Liaudet[1]; Christopher R. Cederroth[2]; Jonas Dyhrfjeld-Johnsen[1]
[1]Sensorion; [2]Karolinska Institutet

The use of the gap-prepulse inhibition of acoustic startle (GPIAS) paradigm in preclinical models of tinnitus using salicylate is attractive due to the rapid induction of tinnitus-like behavior and absence of animal training. However, recent work highlighted the potential confound of hearing loss in this model, while suggesting using an operant conditioning paradigm, that this could be compensated by sufficiently high intensity noise carriers (Radziwon et al., 2015). We here show a strong relationship between salicylate-induced hearing loss and gap-detection deficits for narrow-band (1 kHz bandwidth) noise-carriers using the GPIAS paradigm.

Following 3 consecutive days of 200 mg/kg sodium salicylate (SS) administration twice daily, male Sprague-Dawley rats developed GPIAS deficits relative to baseline, which increased from 1h to 5h after the last administration and remained relatively stable up to 7h post administration (65 dB SPL background carrier level, 50 msec silent gaps, interstimulus interval 100 ms). Deficits were greatest at 16, 24 and 32 kHz (~66.2-75.8% reduction of inhibition) but relatively small at 8 kHz (~28.3%). Audiometric characterization of a second cohort of rats showed ABR threshold shifts of ~20-30 dB after repeated sodium salicylate administration across all frequencies tested. Using a higher background carrier level of 75 dB SPL, post-SS GPIAS deficits were only observed at 32 kHz (~40.8%), and none were found using a carrier level of 85 dB SPL.

The results on salicylate-induced hearing loss and GPIAS deficits in this model show a dependence on the the the carrier level, whereby GPIAS deficits are no longer seen when the difference between frequency specific ABR thresholds and background carrier level (the sensation level, SL) exceeds ~15 dB. Consistent with this notion, the largest salicylate-induced GPIAS deficits were detected at 16 and 32 kHz where the greatest post-salicylate ABR threshold shifts. Contrary to this Yu et al. (2017) recently reported persistent GPIAS deficits using carrier levels of increasing intensity in mice following 3-day administration of 300 mg/kg/day SS, suggesting potential species differences.

Since a large number of neural correlates of tinnitus have been reported after salicylate administration in paradigms not requiring auditory stimulation, these data do not necessary question the ability of salicylate to induce tinnitus. They however question the broad applicability of the GPIAS paradigm to assess tonal tinnitus in animal models with bilateral hearing impairment, and emphasize the need for consistent reporting of audiometric data along with GPIAS deficits.

PS 527

Improving the Reliability of Tinnitus Testing in Laboratory Mice

James Engel; Brad May
Johns Hopkins School of Medicine

When we encountered difficulties with tinnitus screening during our neurophysiological studies of laboratory rats (Ropp et al. 2016), we were able to improve test reliability by placing a new emphasis on stimulus generalization paradigms (Jones and May 2017). In the context of tinnitus screening, the objective of a generalization paradigm is to get animals to group the "sound" of tinnitus with actual sounds that share similar perceptual features. We achieve that goal by training animals to drink from a spout during silent trial intervals (when tinnitus is most obvious) and to suppress drinking in the presence of broadband noise. When trained animals are subsequently presented with ambiguous stimulus probes (neither silence nor broadband noise), they display a natural tendency to drink in the presence of certain probes which are assumed to convey a tinnitus-like percept. These selective responses not only confirm a positive status, they also reveal properties of the animal';s subjective tinnitus experience (e.g.; pitch, loudness). This poster will describe how we are currently revising our generalization paradigm to accommodate another important tinnitus model, laboratory mice. We will begin by discussing considerations for the selection of strain, age, and sex, as well as the best practices for creating a safe state of water deprivation prior to training. We will describe how to optimize training efficiency so that most mice achieve criterial performance in less than two weeks. We will suggest changes in the sound-exposure procedures that are typically used to induce tinnitus. Of particular concern from the perspective of mouse models, is the timing of the exposure, the risk of anesthesia, and the potential effects of environment on the induction process. We will introduce new metrics for the analysis of conditioned suppression and identify multiple performance measures that can serve as behavioral indications of tinnitus. For non-behavioral laboratories that might find these procedures impractical, we will conclude by offering suggestions on how the basic principles of stimulus generalization can be adapted to alternate testing methods.

PS 528

Towards human validation of gap detection for objective tinnitus measurement: Estimating acoustical properties of tinnitus and recording gap-evoked potentials in tinnitus-like sounds

Brandon Paul; Marc Schoenwiesner; Sylvie Hébert
University of Montreal

The rationale behind the gap pre-pulse inhibition of the acoustic startle (GPIAS) procedure to screen for tinnitus in an animal is that tinnitus "fills in" silent temporal gaps in a background sound prior to a startle elicitor. However efforts to validate this procedure in humans with tinnitus have failed. Here, in lieu of startle responses, we propose to measure auditory cortical potentials evoked by gaps in sounds engineered to match a person';s tinnitus. If tinnitus masks these gaps, we expect responses to be attenuated or absent. We will present two pilot studies supporting this effort.

First, background sounds containing gaps must be closely matched to the tinnitus perception if tinnitus is expected to mask gaps. To achieve this, we used a psychophysical procedure requiring participants to indicate which of two candidate sounds is more similar to their tinnitus. Bandwidths and center frequencies of candidate tinnitus sounds were sampled from initial measurements of the tinnitus likeness spectrum, and sampling was directed by a Monte Carlo Markov Chain (MCMC) procedure lasting 200 trials. The most probable tinnitus frequency and bandwidth was taken from the peak of the probability distributions estimated from all participant-chosen responses. These estimates were verified using a follow-up 2AFC task in which 85% accuracy was required. Preliminary results suggest the MCMC task can accurately estimate a person';s tinnitus.

Second, tinnitus is commonly of high frequency (< 4 kHz) and low sensation level (<30 dB SL). It is unknown if potentials evoked by such weak acoustic properties are measureable by EEG. Twelve non-tinnitus participants (M = 24.5 years old, 8 F) were presented with either a 5 kHz or 10 kHz narrowband noise of 5 s duration at stimulus levels of 5, 15, or 30 dB SL. Interspersed in each NBN stimulus were six 20 ms silent gaps (2 ms onset and offset) at random locations. To detect the presence of gap-evoked responses, N1 global field power (GFP) was computed for the 64 channel EEG. Bootstrapped estimates of N1 GFP were computed for subsamples of single trials which were compared to bootstrapped estimates of the pre-stimulus baseline. If the 99% confidence interval of the N1 GFP estimates exceeded that

of the baseline, the N1 GFP was deemed present. N1 responses were detected for all but 4 stimulus conditions for 3 individuals. The results suggest that this measurement approach is suitable to use in tinnitus cases. (Sponsored by American Tinnitus Association).

PS 529

Hippocampal Remodeling after Noise Exposure and Tinnitus in the Guinea Pig

Liqin Zhang[1]; Calvin Wu[2]; David T. Martel[1]; Michael West[2]; Michael Sutton[1]; Susan Shore[3]
[1]University of Michigan, Ann Arbor; [2]University of Michigan Ann Arbor; [3]University of Michigan

Introduction
Noise exposure can lead to damage to the auditory pathway resulting in hearing loss and tinnitus. The underlying mechanisms by which people develop these deficits have received much attention. Previous research in humans showed tinnitus related changes in the hippocampus (Vanneste et al., Neuroscience 2011; Ueyama et al., PLoS One 2013), a brain region that plays an important role in learning and memory. Here, we investigate whether hippocampal neural circuitry in the guinea pig is altered by noise-exposure and tinnitus.

Methods
Two groups of guinea pigs were exposed to unilateral narrow band noise for two hours. Auditory brainstem threshold (ABR) was measured immediately before and after noise exposure. To assess the effects of noise exposure prior to chronic tinnitus onset, animals were sacrificed two weeks after noise exposure. To assess the effects of chronic tinnitus, a second noise exposure was performed two weeks after the first one, followed by Gap-Prepulse Inhibition of the Acoustic Startle (GPIAS) tinnitus assessments 8-12 weeks later. Immunohistochemistry was performed to examine vesicular acetylcholine transporter (vAChT), and vesicular GABA transporter (VGAT) expression on 30um-thick coronal hippocampal sections. VAChT and VGAT puncta density and intensity in dentate gyrus (DG) and areas CA3 and CA1 was assessed. Images were captured using a fluorescent microscope equipped with the appropriate filter for Alexa 555 (Leica, DM).

Results
ABR thresholds were elevated immediately after noise exposure for both the early noise-exposure and the chronic tinnitus groups, but returned to normal a few days after exposure. In the two-week noise-exposure group, both vAChT and VGAT staining showed a similar decrement compared to control animals. In the chronic tinnitus group, animals with tinnitus had higher intensity and puncta counts for vAChT and VGAT staining than animals exposed but without tinnitus. There was no significant difference between the ipsilateral and contralateral sides within both the two-week and chronic tinnitus group.

Conclusions
Our results demonstrate that two weeks after noise exposure, vAChT and VGAT levels decreased in DG, CA3, and CA1 on both sides of the hippocampus suggesting early onset of neural circuitry changes in hippocampus after noise exposure. The differences between animals with and without tinnitus in the chronic exposure group suggest that tinnitus-specific changes occur at a later time after noise exposure. Further studies are necessary to assess the effect of noise exposure to hippocampal inhibitory neuron populations as well as the basal forebrain, the primary source of cholinergic innervation to the hippocampus.

PS 530

Investigating Tinnitus in Nonhuman Primates

Lars Rogenmoser; Paweł Kuśmierek; Denis Archakov; Josef Rauschecker
Laboratory of Integrative Neuroscience and Cognition, Department of Neuroscience, Georgetown University Medical Center

Tinnitus, the most common hearing disorder characterized by a phantom perception of sound (i.e. constant sensation of ringing), impairs the quality of life of millions, making it a current concern for Public Health. Animal models are necessary for a better understanding of its pathophysiology and ultimately for the development of evidence-based therapy. Currently, studies are increasingly criticizing validity of existing animal models used in tinnitus research, especially with regard to their transferability to human tinnitus patients. Rodents are commonly used as animal models; however, they hardly exhibit prefrontal structures (i.e., ventromedial prefrontal cortex, vmPFC). Our previous studies in three independent cohorts of human tinnitus patients revealed that the vmPFC plays a crucial role and undergoes significant volume loss in tinnitus patients. We assume that the morphological changes in the vmPFC disable top-down inhibition from this structure to auditory centers, thus preventing normally available suppression of the tinnitus signal. Given that the vmPFC is highly developed in nonhuman primates, we aimed to establish a tinnitus model in rhesus monkeys (Macaca mulatta).

Tinnitus was determined by using a non-acoustic startle paradigm. Eye blinks were monitored by recording electromyographic (EMG) activity in response to air-puffs as

startle stimuli, preceded by short auditory stimuli varying in frequency and intensity. The tones were adjusted according to the animals'; hearing thresholds, which were determined by frequency-specific Auditory Brainstem Response (ABR) recordings. In this pilot study, one monkey was tested at its baseline, at a reversible tinnitus level (after administration of salicylate, 150 mg/kg), and at a follow-up level. In order to ensure translation of the results to humans, a sample of human tinnitus patients and of matched control subjects without tinnitus underwent the same testing paradigm.

Preliminary results suggest that the preceding tone facilitates the eye blink response as long as it is reliably perceived. A larger sample of animals and patients will reveal whether the tinnitus frequency is reflected by a lack of eye blink facilitation at the condition of the specific preceding tone, thus mimicking the tinnitus. The use of a non-acoustic startle stimulus is advantageous since it is free from acoustic interference and is less aversive (especially for patients with hearing issues like tinnitus and hyperacusis).

PS 531

Development and characterization of a MRI capable, targeted nanoparticle platform for receptor mediated transcytosis over an in vitro blood-brain-barrier model

Stephanie M. Curley[1]; Anthony Cacace[2]; James Castracane[1]; Avril G. Holt[3]; Nathaniel Cady[1]
[1]*SUNY Polytechnic Institute, Colleges of Nanoscale Science and Engineering;* [2]*Wayne State University;* [3]*Wayne State University School of Medicine/ JD Dingell VAMC*

Tinnitus affects over 50 million people in the United States, and is currently the most compensated disability for military veterans. This condition has been linked with spatial and temporal brain hyperactivity even after a single exposure to a noise that results in a temporary hearing loss. These regions of high brain activity have been shown to correspond to an upregulation of the NMDA receptor 2D subunit (NMDAR2D) in the brains of rats with tinnitus-like symptoms. Targeting these brain regions via delivery of theranostic nanoparticle (NP) agents could facilitate diagnostics and delivery of drugs to reduce neuronal activity and help alleviate symptoms of tinnitus.

Fundamental challenges remain to deliver functional nanoparticles to brain regions that demonstrate hyper-

activity following tinnitus onset. A multifunctional NP system is needed that 1) can be loaded with functional molecules, 2) transport across the BBB, and 3) localize to hyperactive regions in the brain. In this work, we have developed a delivery system based on the MS2 bacteriophage capsid. Angiopep-2 (AP2) is a 3kDa synthetic peptide capable of receptor-mediated transcytosis over the BBB. We will use this targeting moiety, along with an antibody against NMDAR2D, to specifically target these overactive regions of the brain.

Both targeting moieties were conjugated to the surface of MS2 using the heterobifuntional reagent SMCC (succinimidyl-4-(N-maleimidomethyl)cyclohexane-1-carboxylate). Additional reaction of Traut's Reagent with IgG was necessary before conjugation to the MS2 capsid surface was possible. The dually functionalized NP constructs were tested for the presence of the two targeting moieties using a dot blot. The particles were also tested for their ability to recognize NMDAR2D receptors in brain cell lysate using a Western blot. Confluent 2D monolayers of primary rat brain microvascular endothelial cells (RBMECs) on Transwell inserts were used to evaluate the ability of these particles to cross an in vitro BBB model. Nanoparticle transport over the BBB model was monitored over 24 hours using real-time reverse transcriptase PCR. Samples were taken from the bottom compartment and amplified using probe sequences for MS2 RNA.

Preliminary results show that both AP2 and anti-NMDAR2D IgG were successfully conjugated to the MS2 capsid surface and that the antibody is functional after reaction. Studies are currently ongoing to determine the ability of BBB-targeted MS2 NPs to cross the in vitro BBB system and the potential for using PCR in MS2 NP detection.

PS 532

Combined Blast and Impact Induced Tinnitus and Related mTBI

Edward Pace[1]; Bin Liu[1]; Hao Luo[1]; Dalian Ding[2]; Bo Pang[1]; Norair Adjamian[1]; Lauren Kassa[1]; Srinivas Kallakuri[1]; Ayeshah Sarfaraz[1]; Richard Salvi[3]; Jinsheng Zhang[1]
[1]*Wayne State University;* [2]*University at Buffalo, USA;* [3]*Center for Hearing and Deafness; State University of New York at Buffalo*

Blast is known as a major cause of tinnitus, hearing loss and related mild traumatic brain injury (mTBI) in military personnel. However, blast often co-occurs with secondary concussive impact from shock-wave-propelled debris or shrapnel. The contributions of combined blast

and impact to the induced tinnitus, hearing loss and related mTBI, as well as the underlying mechanisms, remain unclear. To elucidate this issue, we subjected rats to a unique blast-plus-impact or impact alone procedure. Our data showed that blast-plus-impact induced long-term noise-type and tonal tinnitus and hearing loss, which were accompanied by severe inner and outer cochlear hair cell loss, and increased microglial activity in the dorsal cochlear nucleus (DCN), inferior colliculus (IC), and auditory cortex (AC). Animals exposed to impact alone, however, did not develop long-term tinnitus. Electrophysiologically, both noise-type and tonal tinnitus groups showed decreased spontaneous firing rate (SFR), bursting, and within-structure synchrony for the IC, but increased synchrony within the DCN and increased between-structure synchrony for the AC and IC. For rats with noise-type tinnitus, decreased SFR and bursting, and increased synchrony were also seen within the AC, along with increased bursting within the DCN. For rats with tonal tinnitus, increased synchrony was observed between the AC and DCN, and between the IC and DCN. Overall, these results suggest that both hypoactivity, and increased or decreased synchrony within and between central auditory structures, can play an important role in tinnitus perception. The additive effect of concussive impact to blast and its induced, robust neuroinflammation throughout the central auditory system may contribute to this hypoactivity and general lack of hyperactivity. The fact that persistent tinnitus occurs following combined blast and impact suggests that the lasting, overall increase in neurosynchrony or neuro-interconnectivity may be vital in the etiology of tinnitus.

Vestibular: Genes to Behavior

PS 533

Characterization of the transcriptomes of the striolar and extrastriolar supporting cells in the mouse utricle

Shan Sun[1]; Dan You[1]; Wenyan Li[2]; Renjie Chai[3]; Huawei Li[4]

[1]*Eye and ENT Hospital, Fudan University;* [2]*1. Department of Otolaryngology, Harvard Medical School, 2. Eaton-Peabody Laboratory, Massachusetts Eye and Ear Infirmary, 3. Department of Otolaryngology, Hearing Research Institute, Affiliated Eye and ENT Hospital of Fudan University;* [3]*Southeast University;* [4]*Department of Otolaryngology, Hearing Research Institute, Affiliated Eye and ENT Hospital of Fudan University*

It has been reported that the supporting cells(SCs) in striolar region could response to the hair cell(HC) loss and activate the Wnt target gene Lgr5, serve as the resource of HC regeneration in neonatal mouse utricle.It is important to understand the difference between the SCs in striolar region and extrastriolar region, which may provide clues for the HC regeneration purpose. Here, we used Lgr5-EGFP-CreERT2 and Plp1-tdTomato+ mice to isolate the striolar and extrastriolar SCs after HC damage by flow cytometry. As expected, we found Lgr5+ striolar SCs had higher proliferation and HC regeneration ability compared with Plp1+ extrastriolar SCs after the hair cell damage, Wnt signaling activation and Notch signaling inhibition. Next, we performed RNA-Seq to determine the transcriptome expression profiles of these two types of SCs. We conducted analysis of the enriched and differentially expressed genes; and focused on the cell cycle genes, transcription factors, and Wnt and Notch signaling pathway genes. We found 13 cell cycle genes, 102 transcription factors, and 19 cell signaling pathway genes that were differentially expressed in Lgr5+ striolar SCs or Plp1+ extrastriolar SCs. Lastly, we made a protein-protein interaction network to further analyze the role of these differentially expressed genes.

PS 534

The Role of Pou4f3 in Regulating Survival of Vestibular Hair Cells

Nnenna Ezeilo[1]; Brandon C. Cox[2]
[1]*Southern Illinois University School of Medicine;* [2]*Department of Pharmacology and Department of Surgery, Division of Otolaryngology, Southern Illinois University School of Medicine*

While much is known about the regulation of hair cell [HC] survival during embryonic development, the pathways that promote survival of HCs after differentiation remain under investigation. Similar to the cochlea, vestibular organs have neuroepithelia with specialized HCs that receive and transduce perception of head movements to mediate balance. Vestibular HC loss occurs with aging and after exposure to vestibulotoxic agents, which results in balance dysfunction. Previous studies have shown that the transcription factor Pou4f3 is critical for HC maturation and survival during development. Pou4f3 is also expressed in vestibular HCs during postnatal and adult ages. Mice with germline deletion of Pou4f3 form abnormal HCs with most cells only surviving for a few days. However, the role of Pou4f3 in regulating vestibular HC survival in postnatal mice has not been studied. To investigate the role of Pou4f3 in regulating vestibular HC survival, we used the CreER/loxP system to delete Pou4f3 from vestibular HCs at postnatal ages. Specifically, Atoh1-CreER[TM/+]:Pou4f3[loxP/loxP] mice and Cre-negative littermate controls were injected with tamoxifen at either postnatal day (P) 0 and P1 (neonatal) or at P13 and P14 (juvenile). Temporal bones were collected at 2 and 4 weeks after tamoxifen injection. Using immunofluorescence and confocal microscopy, we quantified

the number of HCs present in striolar and extrastriolar regions of the utricle, noting the presence or absence of Pou4f3. Two weeks after tamoxifen injections at neonatal ages, ~50% of striolar HCs and ~70% of extrastriolar HCs were Pou4f3-negative in experimental mice; this decreased to ~15% of striolar HCs and ~25% of extrastriolar HCs when tamoxifen was injected in juvenile mice, which likely reflects decreased number of Cre-positive cells. Additionally, there was ~35% HC loss when tamoxifen was injected at neonatal ages, while the samples that received tamoxifen at juvenile ages experienced less HC loss (~10%), compared to Cre-negative controls. In contrast to a similar study performed in the cochlea, there was a significant number of vestibular HCs that survived, yet did not express Pou4f3 in both neonatal and juvenile mice at 2 weeks post-tamoxifen. We are currently working on additional samples to confirm these findings at the 2 week post-tamoxifen period and investigating samples from the 4 week post-tamoxifen timepoint. Our preliminary data suggest that Pou4f3 may not be required for vestibular HC survival after HCs have differentiated or that it takes more than 2 weeks for Pou4f3-negative HCs to die. We are currently investigating these two hypotheses.

PS 535

Murine congenital Cytomegalovirus infection leads to vestibular dysfunction.

Pranav D. Mathur[1]; Ali Almishaal[2]; Sarath Vijayakumar[3]; Timothy A. Jones[4]; Jun Yang[2]; Matthew Firpo[2]; Albert Park[2]
[1]Otonomy Inc.; [2]University of Utah; [3]University of Nebraska-Lincoln; [4]University of Nebraska, Lincoln

Background
Cytomegalovirus (CMV) infection is the most common infectious cause of hearing loss and neurological disorders in pediatric population. Globally approximately 0.5% of newborns are affected with CMV. About 15% of the children affected with congenital CMV have hearing loss. For those with hearing loss. More than 50% will develop future progressive loss. Human studies on CMV seropositive children have reported that a majority of children with sensorineuronal hearing loss due to CMV infection also have some degree of vestibular impairment. Despite many studies related to hearing loss, CMV related vestibular impairment is not well studied. In this study, we tested the vestibular anatomy and function in a murine CMV model.

Methods

We have previously shown that Balb/c neonates injected with 2000pfu of murine-CMV develop moderate to severe hearing loss by 28 days post injection. In this study, we used behavioral tests like Rotarod and swimming tests to estimate balance function. In addition, we studied linear vestibular sensory evoked potentials (VsEPs) to understand the physiology of vestibular function in mCMV infected mice. To determine the morphological basis of the vestibular dysfunction, we studied histology of vestibular tissues by phalloidin staining and scanning electron microscopy.

Results
We found that mCMV infected mice had worse swimming behavior, but spent similar time on rotarod when compared to uninfected controls. VsEPs of mCMV infected mice had higher thresholds and lower amplitudes (numerically) compared to uninfected controls. The peripheral peak latency in the CMV infected animals was also significantly prolonged when compared to the uninfected controls. This finding suggests that CMV infection significantly impairs the vestibular function in mice. In addition, whole mount Phalloidin immunostaining and Scanning Electron Microscopy showed missing patches of hair cells in the cristae and otolith organs of the mCMV infected mice.

Conclusions
To our knowledge, this study is the first to report vestibular abnormalities in mCMV infected mice. This study will serve as benchmark for future studies to understand the pathogenesis of CMV induced vestibular dysfunction and for testing the effect of various therapeutic agents.

PS 536

The pathology of the vestibular apparatus of the Lassa Fever model mice

Tomoharu Suzuki[1]; Junki Maruyama[2]; Paessler Slobodan[2]; Tomoko Makishima[1]
[1]Department of Otolaryngology, University of Texas Medical Branch; [2]Department of Pathology, University of Texas Medical Branch

Lassa fever (LF) is a viral hemorrhagic fever endemic to West African countries. LF has a fatality rate of 1 - 15%, with many humans infected with the Lassa virus (LASV) unknowingly overcome the disease with only mild symptoms. However, approximately one-third of Lassa virus (LASV) infected patients develop sudden onset sensorineural hearing loss after surviving the acute phase of the disease or later in the convalescence phase. In addition to the hearing loss, vestibular symptoms such as dizziness, vertigo and ataxia have been reported in LF patients. The mechanism of inner ear injury caused

by LASV infection is unknown. Our LF model mice are valuable resources to study the pathology underlying these symptoms, as the phenotype in these mice highly mimic that of human LF patients. We recently reported severe destruction of the spiral ganglion cells and cochlear nerve while cochlear hair cells remain intact in mice with severe hearing loss caused by LASV infection. In some of these mice, we observed behaviors indicative of vestibular dysfunction such as head bobbing and shaking. Our goal was to depict the pathology of the vestibular apparatus in mice infected with LASV. Thin section temporal bones of LASV infected mice were processed for H&E staining, LASV antibody labeling or CD3 antibody labeling. We observed hemorrhagic changes around the stroma underlying the sensory epithelia, the utricular and saccular macula and crista of the semicircular canals. In contrast, the vestibular hair cells or supporting cells were intact. LASV antigen as well as lymphocytes positive for CD3 were present mainly near the same area of the hemorrhagic changes. Systemic hemorrhagic changes including the central nervous system was also observed. Based on the observation in the LF model mice, we speculate that the injury to the inner ear by LASV was caused either directly via hemorrhagic injury, or indirectly via a virus induced immunological injury, affecting both the auditory and vestibular system. The vestibular symptoms may also be aggravated by infection and inflammation in the central nervous system.

PS 537

α−DTX-sensitive Kv Currents in Type II Hair Cells of the Mouse Utricle

Vicente Lumbreras[1]; Anna Lysakowski[2]; Ruth Anne Eatock[1]
[1]University of Chicago; [2]University of Illinois at Chicago

Type II hair cells of vestibular epithelia, like other hair cells, have large outwardly rectifying K^+ conductances that activate near or positive to resting potential and shape the receptor potential. Expression data show significant expression of Kv1 subunits by mouse utricular hair cells (Scheffer et al., J Neurosci 35:6366, 2015). We have used the Kv1-selective blocker, α-dendrotoxin (αDTX), to investigate Kv1 contributions to the outwardly rectifying current.

Whole-cell currents were recorded from identified type II hair cells in semi-intact preparations of the utricle in immature mice (P5-P7). The tissue was bathed with L-15 medium at room temperature. Recording pipettes were filled with KCl-based internal solution and a fluorescent dye. Cell capacitances were 4.9±0.1 pF and input resistances were 1.0±0.1 GΩ (SEM; 36 cells). Following a de-inactivating prepulse to 124 mV, depolarizing voltage steps evoked outwardly rectifying currents with steady-

state activation as previously reported (for tail currents at 40 mV, the midpoint was 30±2 mV and G_{max} was 29±3 nS; 9 cells). All cells had an inactivating current component, I_A (peak minus steady-state current). For steps to −4 mV, I_A was 34±3% of the total peak current (36 cells), with no significant differences detected across epithelial zones: striola (8 cells), lateral extrastriola (11) and medial extrastriola (11).

αDTX differentially affected the inactivating and sustained current components. For steps from −124 mV to −4 mV, 10 nM αDTX blocked total peak current by 26±10%, steady-state current by 8±5%, and I_A by 49±18% (6 cells). 100 nM αDTX blocked peak current by 40±6%, steady-state current by 24±7% and I_A by 76±6% (8 cells). Similar αDTX-sensitivity was observed for voltage commands to +16 and +36 mV. The IC50 for I_A (~10 nM) but not the steady-state current (>100 nM) is in the range of K_D';s for aDTX-sensitive Kv1 subunits (1-25 nM). The αDTX-blocked current either was purely inactivating with a double-exponential decay (time constants of 32±5 ms and 246±67 ms at −4 mV, 6 cells), or included a steady-state component and an inactivating component with a single-exponential decay (184±22 ms, 6 cells), or did not inactivate (1 cell).

Based on the combination of inactivation and αDTX-sensitivity, hair cell expression data (Scheffer et al. 2015), and the literature on neuronal channels (Rudy et al., Encyclopedia of Neuroscience, 10:397-425, 2009), we suggest that I_A may flow through heteromeric channels comprising Kv1.1 and 1.4 α subunits and Kvβ1 subunits.

PS 538

Pharmacological Characterization of the tetrakis-Quaternary Ammonium Compound ZZ204G as an Alpha9 Nicotinic Acetylcholine Receptor Antagonist in the Vestibular Periphery

Anqi Wan[1]; Peter Crooks[1]; Allison Morningstar[2]; **Joseph C. Holt**[2]
[1]University of Arkansas for Medical Sciences;
[2]University of Rochester

Nicotinic acetylcholine receptors containing the alpha9 subunit (α9nAChRs) are credited with playing an important role at the interface of the CNS with the inner ear. Inner ear efferents, innervating the cochlea and vestibular end organs, are known to activate α9nAChRs on outer hair cells and type II vestibular hair cells, respectively. During efferent stimulation, activation of α9nAChRs invariably results in a subsequent calcium influx that activates nearby calcium-dependent, small-conductance

potassium channels (SK), thereby hyperpolarizing postsynaptic hair cells. While some functional roles for α9nAChRs in both the auditory and vestibular systems have been identified in α9nAChR-subunit knockout animals, what is lacking is a panel of potent, selective α9nAChRs antagonists that can be used to probe function in normal mammalian models. The peptides α-bungarotoxin and α-conotoxins RgIA are considered potent inhibitors of α9nAChRs, but the large and bulky nature of these molecules may limit their access into the inner ear when used to probe efferent function or behavior in vivo. Recent developments have led to the discovery of several nonpeptide, small-molecule α9nAChR antagonists, including the tetrakis-quaternary ammonium compound ZZ204G, which has renewed our interest in using such compounds to interrogate the role of α9nAChRs in the peripheral vestibular system. To first assess whether ZZ204G is effective at blocking α9nAChRs in the vestibular periphery, we have characterized its potency and selectivity in a turtle vestibular preparation where cholinergic efferent synaptic mechanisms governing afferent responses to efferent stimulation have been well-characterized.

For this study, sharp electrodes were used to extracellular spike activity from afferents innervating the turtle posterior crista during electrical stimulation of vestibular efferents and pharmacological interrogation with ZZ204G. In the turtle posterior crista, afferent responses to efferent stimulation are quite heterogeneous. Efferent-mediated afferent inhibition is attributed to the activation of α9nAChRs/SK in type II hair cells while efferent-mediated afferent excitation requires the direct activation of α4α6β2-nAChRs and/or muscarinic ACh receptors on afferent terminals. We have demonstrated that ZZ204G, at concentrations as low as 10 nM, reversibly blocks efferent-mediated afferent inhibition without impacting efferent-mediated afferent excitation indicating that it is a potent and selective antagonist of α9nAChRs on turtle type II hair cells. We are now comparing these results with two other nonpeptide compounds also known to block α9nAChRs. These new pharmacological tools may ultimately prove useful for probing efferent vestibular function.

PS 539

Synaptic Ribbons in Vestibular Hair Cells of the Human Macula Utricle

Michele Gandolfi[1]; Gail Ishiyama[2]; Larry F. Hoffman[3]; Akira Ishiyama[4]; Ivan Lopez[5]
[1]House Clinic; [2]UCLA Department of Neurology; [3]UCLA Department of Head and Neck Surgery; [4]David Geffen School of Medicine, University of California, Los Angeles; [5]Department of Head & Neck Surgery, Geffen School of Medicine at UCLA

Background

Synaptic ribbons (SRs) are presynaptic electro-dense structures surrounded by neurotransmitter filled vesicles found in hair cells and photoreceptor cells specialized for graded synaptic transmission. The localization and physiological role of synaptic ribbons (SRs) in vestibular hair cells is well documented in animal models, however the identification of SRs in the human vestibular periphery remains elusive. For this purpose, we aim to identify at the cellular and ultrastructural level SRs in the human macula utricle

Methods

Formalin fixed macula utricles (n=3) obtained from ablative surgery from patients diagnosed with intractable stage IV Meniere';s disease and from autopsy (n=3) (no vestibular disorders) were used. Each whole utricle was cut into two halves. One half was post fixed in glutaraldehyde, osmicated, dehydrated and further processed for transmission electron microscope (TEM) observations. Ultrathin sections (80-100 nm) were observed with a T20 (FEI) TEM at low 5000 and high 25000 magnification. The second half of the utricle was cryoprotected with sucrose and 20-micron thick cryostat sections were obtained. These sections were immunofluorescence stained with affinity purified antibodies against human C- terminal-binding protein 2 (CTBP2), a marker for synaptic ribbons, and choline acetyltransferase (ChAT), a marker for cholinergic terminals. They were also stained with Myosin 7a antibodies to identified hair cells, and glial fibrillary acidic protein (GFAP) antibodies to identify supporting cells. Laser confocal microscopy analysis was performed on the immunofluorescence stained slides.

Results

Ultrastructural analysis of the macula utricle from normal and Meniere';s specimens showed the presence of synaptic ribbons (simple and double) rod type in the basal portion of type I vestibular hair cells (presynaptic), with mitochondria seen close to the SRs. Calyx-like terminals (post synapsis) were also present. Well-preserved efferent-like terminals (filled with numerous synaptic vesicles) were seen intermingling in the basal portion of hair cells. Using double labelling immunofluorescence and confocal microscopy, CTBP2 punctate immunoreaction was seen mainly at the basal portion of myosin 7a positive vestibular hair cells. ChAT immunofluorescence was seen at the basolateral portion of hair cells.

Conclusions

The presence of SRs in vestibular hair cells, afferent and efferent nerve terminals in the macula utricle sensory epithelia from patients diagnosed with Meniere';s disease suggest that the remaining hair cells may be func-

tional and able to cause spells of vestibular dysfunction.

PS 540

Cellular Features of the Mammalian Utricular Stiola Dependent Upon Head Movement-Driven Activity

Terry J. Prins[1]; Felix Schweizer[2]; Hoffman Larry[3]
[1]Department of Integrative Biology and Physiology; UCLA; [2]Department of Neurobiology; Geffen School of Medicine at UCLA; [3]Geffen School of Medicine at UCLA

Our laboratory is exploring the cellular features of mammalian vestibular epithelia that are dependent upon modulation of hair cell activity due to natural head movement behaviors using models in which this modulation is altered upon exposure to novel environments (Sultemeier et al. J. Neurophysiol. 117:2163-2178, 2017) or those in which it is genetically modified. The otoferlin-null (Otof-/-) mouse is one such genetic model, as the absence of otoferlin has been shown to drastically alter depolarization-evoked neurotransmitter exocytosis in some type I hair cells of the utricular striola. Type II hair cells of Otof-/- utricles exhibit modified relationships between depolarization-evoked inward calcium conductance and exocytosis. In this investigation, we tested the hypothesis that the distribution of calretinin-positive (CALB2+) calyces and oncomodulin-positive (OCM+) hair cells, reliable indices of striolar cellular organization, are similar in utricles from Otof-/- and wild-type (WT) mice. Rejection of this hypothesis would be indicative of striolar cellular components that are dependent upon activity driven by natural head movement stimuli.

Methods
Vestibular epithelia from Otof-/-, Otof+/-, and WT adult mice were harvested following decapitation in deeply anesthetized animals. Fixation was achieved by rapid infusion of 4% paraformaldehyde (in 0.1M phosphate buffer) directly into the vestibule, and temporal bone specimens were immersed into this fixative for 2 hrs. Microdissected utricles and semicircular canal cristae were then immunohistochemically processed under standard methods using primary antibodies to CALB2, OCM, and beta-3-tubulin, and fluorophore-conjugated secondary antibodies. Fluorophore-conjugated phalloidin was also used to label stereocilia for hair cell counts and elucidation of hair cell morphologic polarization. Confocal imaging was conducted on whole-mounted specimens.

Results
The distributions of CALB2+ calyces and OCM+ hair cells in Otof+/- specimens were similar to those found in WT vestibular epithelia. However, the distribution of CALB2+ calyces in utricles from Otof-/- exhibited striking differences from age-matched WT specimens, whereby the number of CALB2+ calyces was diminished primarily in the caudal striola. The distribution of OCM+ hair cells in these specimens was similar to that found in Otof+/- and WT specimens. Curiously, the distribution of CALB2+ hair cells in Otof-/- cristae did not exhibit parallel diminished numbers.

Summary
These results indicate that CALB2 expression in afferent neurons, a defining characteristic of the mammalian utricular striola, is labile to head movement driven activity modulation from type I hair cells. These data provide critical insight into underlying factors shaping the cellular organization of adult vestibular epithelia.

PS 541

Heterogeneity of Na+ Channel Subunits in Vestibular Afferent Terminals

Frances Meredith[1]; Annika Divakar[2]; Katherine Rennie[2]
[1]University of Colorado AMC; [2]University of Colorado School of Medicine

Introduction
The vestibular system relays information about head position via afferent nerve fibers to the brain in the form of action potentials. Voltage-gated sodium channels drive the initiation and propagation of action potentials. Regional differences in the immunolocalisation of channel α subunits (Nav1.1-1.9) within vestibular afferent calyx terminals have been described. However, their electrophysiological expression during development and their underlying contributions to firing in mature afferent populations are unknown. Electrophysiological and immunohistochemical techniques were used to determine sodium channel types in vestibular calyx-bearing afferents in different zones of the crista at different developmental stages.

Methods
Whole-cell voltage clamp recordings were made from calyx afferent terminals in gerbil cristae in 2 age groups: postnatal days (P)8-14 when calyces have formed but electrophysiological properties of hair cells and associated afferents are immature and P20-30 when electrophysiological properties are mature. Recordings were made from isolated calyces still attached to their type I hair cells, and from thin slices, which allowed identification of central zone (CZ) and peripheral zone (PZ) calyces. Fluorescent dye (Alexa 488) was included in the patch electrode solution in some experiments to dis-

tinguish calyx-only and dimorphic afferents. Potassium currents were minimized with appropriate blockers and removal of external potassium ions. Nav channel blockers were applied by extracellular perfusion.

Results
Tetrodotoxin (TTX, 200–300 nM) completely blocked sodium current (I_{Na}) in PZ (n=5) and CZ (n=3) calyces at P21-29. At these concentrations, TTX blocks TTX-sensitive channels without affecting TTX-insensitive (Nav1.5) and TTX-resistant (Nav1.8 and 1.9) channels. At P8-11, approximately 5% of peak I_{Na} remained in 200 nM TTX (n=6) suggesting that Nav1.5, 1.8 and/or 1.9 may be present during postnatal development. Application of 1 μM TTX, which should block Nav1.5 channels, but not Nav1.8 or 1.9, completely abolished I_{Na} in immature calyces (n=3). In the presence of 4,9-anhydrotetrodotoxin (which blocks Nav1.6 channels), I_{Na} was reduced by 24% in P11-14 calyces (n=4), by 28% in mature PZ calyces (n=11), but by less than 5% in mature CZ terminals (n=4). I_{Na} showed significantly slower inactivation kinetics in mature calyx-only afferents compared to dimorphic afferent calyx endings.

Conclusions
TTX-insensitive I_{Na} is present in calyx terminals during the second postnatal week, but is no longer present by P21. Nav1.6 contributes to TTX-sensitive I_{Na} in both age groups, but may be more prevalent in mature dimorphic calyx terminals than calyx-only terminals. Faster inactivation of I_{Na} in dimorphic afferents could promote rapid and tonic firing.

PS 542

Vestibular Afferent Discharge in Otoferlin-null Mice

Hoffman Larry[1]; Terry J. Prins[2]; Michael Paulin[3]; Felix Schweizer[4]
[1]*Geffen School of Medicine at UCLA;* [2]*Department of Integrative Biology and Physiology; UCLA;* [3]*Department of Zoology; University of Otago;* [4]*Department of Neurobiology; Geffen School of Medicine at UCLA*

Otoferlin is a component of the presynaptic molecular assembly in inner ear hair cells that is critical to the linear relationship between depolarization-induced calcium influx and transmitter exocytosis. Mutations of the otoferlin gene in humans result in a form of hereditary deafness (DFNB9). Within the vestibular epithelia, type I hair cells within the utricular striola of otoferlin-null (Otof-/-) mice were shown to be incapable of depolarization-induced exocytosis, while in extrastriola hair cells it appears that the linear relationship between depolarization-induced local calcium and exocytosis is modified. Despite this loss and/or modification of crucial presynaptic mecha-

nisms for stimulus-induced exocytosis, spontaneous discharge in afferent neurons was intact, while vestibular evoked potentials exhibited higher thresholds and lower amplitudes when compared to WT and heterozygous (Otof+/-) animals. This model offers the opportunity, therefore, to investigate modifications in the hair cell and afferent local circuit within vestibular epithelia due to partial dysfunction resulting from altered presynaptic mechanisms. In this investigation we probed the hair cell/afferent circuit through recording spontaneous and evoked discharge characteristics from individual primary afferent neurons projecting to the semicircular canal cristae, and compared these metrics to WT and Otof+/- animals. In the data collected thus far we have found little evidence of modifications in spontaneous discharge recorded from afferents in Otof-/- compared to WT or Otof+/-. Furthermore, in confirmed semicircular canal afferents (e.g. those responding to rotational stimuli) afferent response dynamics from Otof-/- preparations were similar to those of WT and Otof+/- for stimuli up to 1 Hz. We are exploring the responses to higher stimulus frequencies and velocities. We are also probing the discharge of afferents that are unresponsive to rotation in Otof-/- animals; in our preparatons such afferents could reflect the absence of stimulus-evoked exocytosis in canal afferents, or they may represent utricular afferents that retain sensory functionality (e.g. project from extrastriolar utricular regions) despite the lack of otoferlin.

PS 543

Influence of the hyperpolarization-activated mixed cationic current on spike-timing regularity in vestibular ganglion neurons

Christopher M. Ventura[1]; Radha Kalluri[2]
[1]*University of Southern California, Otolaryngology;*
[2]*University of Southern California*

Variability in spike-timing regularity is a hallmark feature used to classify vestibular ganglion neurons (VGN). Differences in regularity reflect the type of information encoded by these neurons, yet the origins of regularity are not fully understood. We previously suggested that neurons containing low-voltage-gated potassium currents (I_{KL}) are likely to produce 'irregularly-spaced firing'; and those lacking I_{KL} are likely to produce more 'regularly-spaced firing';. However, firing patterns in these in vitro studies were less regular than those reported in vivo. Recent recordings from the terminals of vestibular neurons suggest that another current, hyperpolarization-activated mixed-cationic current (I_H), may be needed for highly regular firing. Although I_H was present in the ganglion neurons of our previous study, it did not drive regular firing. This could be because previous studies were conducted at an age (P0-14) when I_H had not reached mature expression. Moreover, because the

activation properties of the I_H current are susceptible to modulation by intracellular concentrations of cAMP, its activation range may have been too negative in the perforated patch recording configuration to allow it to influence spike-timing. Therefore, we hypothesized that the recording conditions of our previous study were not favorable for activating I_H.

To test this hypothesis, we recorded from isolated VGN from rats (post-natal day 9 through 25). We characterized the activation properties of I_H in responses in perforated-patch configuration and to various concentrations of cAMP [10,100,200,500 µM cAMP] and 500 µM db-cAMP, a time-stable analogue of cAMP. The half-activation of I_H in perforated-patch recordings was -96 mV, confirming our hypothesis that the current was unlikely to be adequately activated to influence spike timing. The half-activation voltage of I_H shifted from -98 mV in 10 µM cAMP to -84 mV in 500 µM db-cAMP. As a consequence of this shift, more I_H current was available near sub-threshold voltages and this had a notable effect on spike timing. Firing rates were faster (40-70 spikes/sec vs 15-30 spikes/sec), after-hyperpolarization trajectories were steeper, and the action potentials reached their peaks more rapidly in the 500 µM db-cAMP condition than in the 100 µM condition. However, these effects were not sufficient to produce highly regular firing in vitro. We hypothesize that a developmental up-regulation in I_{KL} counteracted the influence of I_H. We plan to study the interaction between I_{KL} and I_H using a conductance-based model.

PS 544

Suppression of the Vestibular Short Latency Evoked Potential with Electrical Stimulation of the Central Vestibular System

Christopher Pastras[1]; Ian S. Curthoys[1]; Daniel Brown[2]
[1]University of Sydney; [2]Meniere's Laboratory, University of Sydney

Background
Currently the functional role of the Efferent Vestibular System (EVS) is unknown. The EVS has both fast (10-100ms) and slow (5-20s) kinetics, and is thought to be involved in the modification of peripheral vestibular gain and homeostasis. Electrical stimulation (ES) of the mammalian EVS results in modest increases in background afferent firing, in vivo. Although efferent mediated effects on spontaneous vestibular activity have been characterized, the same cannot be said about dynamic vestibular activity. To view the effects of the EVS on peripheral dynamic vestibular function we have monitored the Vestibular short-latency Evoked Potential (VsEP) evoked by Bone-Conducted Vibration (BCV) during electrical stimulation of the EVS in anaesthetized guinea pigs.

Methods
The VsEP was recorded from a facial nerve canal electrode. A posterior craniotomy was undertaken to expose the floor of the fourth ventricle for EVS stimulation. A bipolar stimulating electrode pair was placed in the area of the EVS cell bodies using stereotaxic map coordinates and functional responses. Cochlear responses following ES at the midline were also recorded as a reliable measure of peripheral efferent activity. After ablating the cochlea, VsEPs were evoked shortly after ES of the EVS, with a variety of stimulation protocols used to characterize the changes.

Results
ES of the EVS resulted in a suppression of the VsEP in all animals, at a threshold of approximately 80µA. The suppression occurred with ES localized to a small region at the ipsilateral floor of the fourth ventricle, lateral of the facial nerve genu and was abolished following electrolytic lesion. VsEP suppression occurred following a single ES pulse, and the level of suppression varied with current strength and shock delay. The VsEP amplitude was suppressed by more than 50% when the delay between the ES and the VsEP was less than 3ms, but there was little suppression with delays greater than 10ms. The VsEP threshold and latency did not change during ES, irrespective of rate or level. Strychnine and DMPP treatment failed to block the VsEP suppression, despite blocking CAP suppression with midline stimulation. Finally, ES produced a nerve response (ECAP) immediately following the ES artefact, whose amplitude correlated closely with the VsEP suppression.

Conclusion
Ultimately, we suggest the observed VsEP suppression results from antidromic stimulation of the afferent neurons, causing neural blockade of the afferent response (VsEP). All other attempts to induce effects using ES in the brainstem failed to produce any changes in the VsEP.

PS 545

The Role of Corticotropin-Releasing Hormone Receptor 1 (CRFR1) in Mouse Vestibular Afferent Activity and Vestibulo-Ocular Reflex (VOR)

Jun Huang; Kathleen T. Yee; Yue Yu; Youguo Xu; Robby Tianwen Chen; Yiji Tu; Yang Ou; Douglas E. Vetter; Wu Zhou; **Hong Zhu**
University of Mississippi Medical Center

Introduction
Corticotropin-releasing factor (CRF) signaling has been shown to play an integral role in cochlear homeostatic balance and protection against noise-induced hearing

loss (Graham and Vetter, 2011; Graham et al., 2010). We recently presented evidence that vestibular peripheral end organs also express corticotropin-releasing hormone receptor 1 (CRFR1) as well as its ligand CRF (Yee et al, 2016). However, we know little about CRF signaling in the vestibular function. The goal of the present study was to examine the role of CRFR1 in vestibular physiology by recording single unit activity of vestibular afferents in loss-of-function (CRFR1 knockout) mice and measuring the vestibulo-ocular reflex (VOR) responses before and after administration of antalarmin, a CRFR1 antagonist, to wild type mice.

Methods
Single unit recordings of vestibular afferents of the CRFR1 knockout and wild type mice were performed under ketamine/xylazine anesthesia as previously described (Zhu et al., 2011, 2014). Spontaneous firing rates and sensitivity to sinusoidal head rotations were measured. Using an infrared eye tracking system, rotational and translational VOR responses were recorded before and after administration of antalarmin hydrochloride (20mg/kg, i.p.).

Results
A total of total of 71 vestibular afferents were recorded from the superior vestibular nerve, which contains afferents innervating the horizontal (HC) and anterior (AC) canals and both of the otoliths (SO). In comparison to the wild type mice, the regular and irregular HC and SO afferents of the CRFR1 knockout mice exhibited higher spontaneous firing rates. The wild type mice and CRFR1 knockout mice exhibited similar sensitivities to head rotation. Preliminary results further showed that administration of the CRFR1 antagonist antalarmin to wild type mice decreased VOR gains to sinusoidal and step head rotations.

Conclusions
The results provide evidence for a role of CRF signaling in the vestibular function. Our early studies have demonstrated that high intensity noise exposure induces peripheral vestibular damage (Stewart et al., 2016). Ongoing studies will further investigate whether the CRF plays a role in protection of noise-induced vestibular deficits. R01DC012060 (HZ), R01DC014930 (WZ), R21EY025550 (WZ), R21DC015124 (DEV)

The Biophysical Origins of Tullio Phenomenon
Marta Iversen[1]; Hong Zhu[2]; Wu Zhou[2]; Charles C. Della Santina[3]; John Carey[4]; Richard D. Rabbitt[1]
[1]University of Utah; [2]University of Mississippi Medical Center; [3]Johns Hopkins University; [4]Johns Hopkins University School of Medicine

Introduction
Tullio phenomenon is characterized by sensitivity of the semicircular canals (SSC) to sound, often leading to symptoms of sound-induced vertigo and nystagmus. It is most commonly caused by superior canal dehiscence syndrome (SCDS), but why this causes SSC afferent responses remains unclear. Recordings in an animal model of SCDS show afferent neurons can phase lock to auditory stimuli and/or respond with sustained changes in firing rate [1]. Phase-locked responses are well described by hair bundle vibration caused by acoustic stimulus, but origins of sustained responses are uncertain. It has been suggested that nonlinear acoustic streaming or Liebau impedance pumping might be responsible, but neither can describe the direction or frequency dependence of sustained sound-evoked responses. Here, we recorded SSC afferent responses and endolymph pumping in an animal model of SCDS to identify the origin of sustained responses. We further developed a mathematical model based on first principles to explain how auditory stimuli lead to endolymph pumping. Results explain origins of the Tullio phenomenon, including frequency dependence of the direction and magnitude of afferent responses and corresponding slow phase eye movements.

Methods
Fluorescent beads were introduced into the endolymph of the oyster toadfish horizontal canal in vivo, and the canal was stimulated with auditory frequency stimuli. Particle image velocimetry (PIV) was performed to analyze endolymph movement by tracking fluorescent bead motion. Single-unit afferents were recorded in separate experiments using the same stimulus conditions. Further, first principles were applied to model non-linear interaction between the deformable membranous labyrinth and surrounding fluids to explain and interpret results.

Results
PIV revealed that auditory stimuli evoke steady endolymph pumping in the canal with frequency-dependent direction and magnitude. Sustained afferent responses to auditory stimuli were consistent with the time course and frequency dependence of endolymph pumping. Phase-locked afferent responses were also observed, consistent with cupula vibration at the stimulus frequen-

cy superimposed on slow displacement caused by non-linear endolymph pumping. Results are consistent with a wave model of nonlinear interaction between the deformable membranous labyrinth and inner ear fluids.

Conclusion

Results demonstrate endolymph pumping in the SSC of an animal model of SCDS (or perilymphatic fistula), thus explaining sustained afferent responses and eye movements in patients. Analysis based on first principles explains sustained responses in terms of nonlinear interactions between inner ear fluids and the deformable membranous labyrinth that leads to frequency-dependent wave pumping.

Funding

References

[1]JP Carey, et al., Otol Neurotol (2004)25,345-52.

PS 547

Dynamic Response and Sensitivity of the Utricular Macula, Measured in vivo Using Laser Doppler Vibrometry in Guinea Pigs.

Christopher Pastras[1]; Ian S. Curthoys[1]; Daniel Brown[2]
[1]University of Sydney; [2]Meniere's Laboratory, University of Sydney

Background

Single unit recordings from irregular otolith neurons have demonstrated that otolith receptors are sensitive to bone-conducted vibration (BCV) and air-conducted sound (ACS) up to several kilohertz (Curthoys et al., 2016). Attempts have been made to characterize otolith sensitivity, however previous studies have relied on indirect measurements such as cranial acceleration or ear-canal sound pressure levels that do not directly reflect the mechanics of the macula. Here we have used Laser Doppler Vibrometry to measure the dynamic response of the utricular macula, with simultaneous measurement of the Vestibular Microphonic (VM) and Vestibular short-latency potential (VsEP) to BCV and ACS, in vivo.

Methods

Experiments were performed on anaesthetized guinea pigs using a ventral surgical approach allowing direct access to the utricle. Following cochlea ablation, reflective beads were placed onto the basal surface of the utricular macula and on the bone within the vestibule. Macula and bone velocity was measured with a Laser

Doppler Vibrometer during stimulation with continuous BCV or ACS stimuli between 100 to 2000 Hz. The level of the stimulus was adjusted to maintain a relatively constant level of macula velocity. VMs were simultaneously recorded with a glass micropipette placed on the basal surface of the utricular macula, and were used as an indicator of macula sensitivity. Additionally, the VsEP in response to BCV or ACS was recorded from the facial nerve canal, with simultaneous measurement of macula vibration.

Results

The dynamic response of the utricular macula differed to that of the nearby bone. The macula only responded to ACS with sufficient fluid in the vestibule to couple the stapes footplate to the utricular macula, and wicking the fluid away reduced the sensitivity by an order of magnitude, evident in both vibrometry measurements and VM measurements. The VM was most sensitive to low frequency (100 to 200Hz) BCV and ACS. At certain frequencies, there was a large decrease in the sensitivity of the macula to BCV, which appeared to be mostly due to distortion of the macula';s vibration, or due to complex resonances in our experimental setup, rather than arising from a reduction in the sensitivity of the utricular macula to BCV.

Conclusion

Utricular macula velocity differs to that of nearby bone at higher frequencies. The VM is most sensitive to low frequency BCV and ACS, and activation of otolithic receptors using ACS involves fluid coupling. Displacement of the macula alters vestibular sensitivity by mechanically dampening the utricular macula.

PS 548

Localization of Vestibulo-Sympathetic Reflex-related Central Vestibular Neurons Activated by Pulsed, Focused Infrared Stimulation of Individual Semicircular Canal or Otolith End Organs

Gay R. Holstein[1]; Darrian Lee Rice[2]; Weitao Jiang[2]; Suhrud Rajguru[3]; Giorgio P. Martinelli[1]
[1]Icahn School of Medicine at Mount Sinai; [2]University of Miami; [3]Department of Biomedical Engineering and Otolaryngology, University of Miami

Background

The vestibulo-sympathetic reflex (VSR) mediates direct and rapid modulation of blood pressure (BP) at the onset of movement or postural adjustments in order to assure consistent cerebral perfusion. The VSR pathway conveys signals from vestibular end organs to areas of the caudal vestibular nuclei (VNc) that, in turn, project to key pre-sympathetic sites for integration of cardiovascu-

lar signals. We previously demonstrated that there are direct projections from VNc neurons to these regions, and that neurons in these pathways are activated by sinusoidal galvanic vestibular stimulation (sGVS). However, sGVS is a global vestibular stimulus that activates the entire vestibular nerve. The present study compared the locations of vestibular neurons activated by pulsed infrared neural stimulation (INS) focused on the posterior semicircular canal or the utricle, in the context of the VSR.

Methods

Experiments were approved by the Institutional Animal Care and Use Committees at University of Miami and/or Mount Sinai Medical Center. The subjects were adult male Long-Evans rats. For INS, a head post was cemented to the skull of the anesthetized rats and attached to a stereotaxic frame. BP and heart rate were measured using a tailcuff system or an implanted telemetric sensor, while frequency modulated stimuli (1863nm, 200us, 100-250pps, varied radiant exposure) were delivered to vestibular end organs using 200 or 400 µm optical fibers.

Results

To localize the central VNc neurons activated by INS, cFos protein was visualized by immunolabeling of brainstem sections from rats euthanized by cardiac perfusion with aldehydes 90 min after the cessation of INS. Labeled cells in VNc were counted in skip-serial sections separated by at least 100 µm. The distribution of cFos-positive cells in each stimulated rat was mapped onto atlas templates of 16 representative rostro-caudal levels through the region. Cell counts for each rat were divided into 7 equal bins, represented as a heat map.

Conclusions

We show that pulsed, focused, INS directed at individual peripheral end organs can be used to activate the VSR pathway and alter BP. The specific end organs stimulated by the radiation can be assessed using eye movement recordings and micro-CT analysis post-stimulation, and the distributions of activated VNc neurons following INS of individual end organs reflects the high spatial resolution of the focused INS stimulation. Future work will continue to examine the differential effects of posterior canal and utricular stimulation on BP and the VSR.

PS 549

Differential Effects of Pulsed, Focused Infrared Stimulation of Individual Semicircular Canal or Otolith End Organs on Vestibulo-Sympathetic Reflex Responses

Darrian Lee Rice[1]; Weitao Jiang[1]; Giorgio P. Martinelli[2]; Gay R. Holstein[2]; Suhrud Rajguru[3]
[1]University of Miami; [2]Icahn School of Medicine at Mount Sinai; [3]Department of Biomedical Engineering and Otolaryngology, University of Miami

Background

The vestibulo-sympathetic reflex (VSR) is responsible for the rapid modulation of heart rate (HR) and blood pressure (BP) with changes in posture and head position ensuring consistent cerebral perfusion. Previous studies have demonstrated cardiovascular changes with physiological stimuli and galvanic stimulation (GVS) of vestibular endorgans. However, these contemporary stimuli cannot effectively highlight the contributions of individual endorgans, limiting our understanding of the pathway and its importance in clinical conditions. The present study investigated changes in HR, BP, and sympathetic nerve activity evoked by focused, infrared nerve stimulation (INS) of the posterior canal (PC) or utricle in a rat model.

Methods

The University of Miami and/or Mount Sinai Medical Center Institutional Animal Care and Use Committee approved all procedures. Changes in HR and BP were studied in adult male and female Long-Evans rats (300-500g), anesthetized with ketamine (44mg/kg) and xylazine (2.5 mg/kg) throughout the experiments. A head post was cemented to the skull of each rat and attached to a custom-designed stereotaxic frame to restrict movement during stimulation. Frequency modulated INS (1863nm, 200us, 250pps, varied radiant exposure and frequencies) was delivered to the PC or utricle using 200 or 400 mm optical fibers. Mean BP and HR were measured with implantable, telemetric sensors (DSI) inserted into the femoral artery prior to stimulation or a non-invasive tail cuff-based BP system (CODA, Kent Scientific). Eye movements were simultaneously recorded using a custom-modified video-oculography system (ISCAN Inc.). Following the measurements, the fiber was fixed in place and the orientation and distance of the typical optical fiber placement relative to vestibular structures were determined using micro-CT.

Results

Sinusoidal INS directed at the PC induced significant oscillations in HR and BP. In several trials, an initial increase or reduction in BP was observed followed by sinusoidal modulation and return to baseline. The chang-

es were accompanied by physiological eye movements. With INS directed at otolith organs, significant eye movements but little change in HR or BP was observed. MicroCT analysis highlighted the spatial selectivity of optical INS.

Conclusions
Frequency modulated INS-evoked cardiovascular responses compared well with previous observations. Clarifying the role of vertical canal activation in SNA and how it potentiates change in BP resulting from otolith activation alone will lay the groundwork for understanding VSR';s role in maintaining physiological function and in pathology.

PS 550

Activation of Vestibulo-ocular Reflex by Focused, Pulsed Infrared Stimulation of Individual Semicircular Canal or Otolith End Organs

Weitao Jiang[1]; Suhrud Rajguru[2]
[1]University of Miami; [2]Department of Biomedical Engineering and Otolaryngology, University of Miami
Activation of Vestibulo-ocular Reflex by Focused, Pulsed Infrared Stimulation of Individual Semicircular Canal or Otolith End Organs

Background
Light at infrared wavelengths has been demonstrated to modulate the pattern of neural signals transmitted from the angular motion sensing semicircular canals of the vestibular system to the brain. In the present study, we have characterized physiological eye movements evoked by focused, pulsed infrared radiation (IR) stimuli directed at individual semicircular canal or otolith end organs in a mammalian model. Pulsed IR (1863nm) was directed to vestibular endorgans using custom optical fibers and evoked bilateral eye movements were measured using a custom-modified videoculography system.

Method
All procedures were approved by the University of Miami Institutional Animal Care and Use Committee. Bilateral eye movements were recorded in Long-Evans rats anesthetized with ketamine (44 mg/kg) and xylazine (2.5 mg/kg). A head post secured the animal to a modified stereotaxic system during stimulation and recording procedures. Eye movements were recorded using a video-based eye tracking system (ISCAN inc, Woburn, MA) and analyzed with custom MATLAB program. For utricular stimulation, IR (1863nm, 200μs, 250pps, different radiant exposures) was delivered through the oval window by coagulating stapedial artery and gentle removal of stapes. For anterior canal stimulation, frequency modulated IR (0.05-1Hz) was directed medial to oval window after carefully removing the footplate and annual ligament. Following the measurements, the distance of the fiber from target structures and orientation of the beam relative to vestibular structures were determined using micro-computed tomography.

Results
The activation of vestibulo-ocular motor pathways by frequency modulated pulsed IR evoked significant, characteristic bilateral eye movements. When single anterior semicircular canals were stimulated with IR pulse trains, the resulting eye movements were disconjugate with the ipsilateral eye moving primarily upwards and rotational contralateral eye movement. IR directed at the utricular macula evoked upward-torsional movements of ipsilateral eye with a downward, clockwise rotation of the contralateral eye. The eye movements were stable through several hours of repeated stimulation and could be maintained with 30+ minutes of continuous, frequency-modulated IR stimulation. Micro-CT reconstruction images confirmed the posterior canal ampullary region or utricular macula to be the target of infrared beam path.

Conclusions
Results form the basis for future applications of optical neural stimulation to control of neural activity in the inner ear, study the role of vestibular labyrinth in maintaining physiological functions and in pathology, and the development of potential therapeutic applications, including bionic vestibular neuroprostheses.

Funding

ARO2018_INS eye movements (1).docx

PS 551

Effect of intratympanic vasopressin on vestibular function in normal guinea pigs

Minbum Kim
Catholic Kwandong University International St. Mary's Hospital

Objectives
The purpose of this study was to evaluate vestibular function change after intratympanic injection of vasopressin.

Methods
A total of 11 guinea pigs were used. Through a small trans-mastoid bony hole, 0.2cc of desmopressin (([de-

amino-Cys1,D-Arg8]-vasopressin acetate salt hydrate) was injected to the middle ear (IT-VP). Bidirectional sinusoidal harmonic acceleration (SHA) test with an animal rotator were performed before, 1h and 3h after IT-VP, respectively. Histologic sections parallel to the modiolar axis were made for observing changes in the Reissners membrane and endolymphatic hydrops. Results: One hour after IT-VP, symmetry score on bidirectional SHA tests increased from 5.85 ± 3.88 to 22.45± 8.73% (p=0.003). However, symmetry score decreased to the initial score 3h after IT-VP (9.24± 9.10%, p=0.477). Two different types of vestibular response ,irritative response (n=4) and paralytic response (n=7), were observed after IT-VP, however, symmetry score of two groups were not significantly different (22.46± 8.36 vs. 22.44± 9.60%). Histologically, slight distension of Reissners membrane was observed. In two animals, significant saccular hydrops was shown.

Conclusion

IT-VP can transiently induce asymmetric vestibular dysfunction without the ablation of endolymphatic sac, which can be irritative or paralytic. This model can be applied to the study of acute endolymphatic hydrops and initial stage of Menieres disease.

PS 552

Bilirubin Aggravates the Excitotoxicity of MVN Neurons through Potentiating the Activity of Acid-Sensing Ion Channels 1a/2a Heteromers

Ke Lai[1]; Hao-song Shi[1]; Hai-bo Shi[1]; Lu-yang Wang[2]; Shan-kai Yin[1]
[1]*Department of Otorhinolaryngology Head & Neck surgery, Shanghai Jiao Tong University Affiliated Sixth People's Hospital;* [2]*Program in Neurosciences & Mental Health, SickKids Research Institute and Department of Physiology, University of Toronto*

Purpose

To investigate the effect of bilirubin on ASICs (Acid-Sensing Ion Channels) in neurons from MVN (medial vestibular nucleus) in hyperbilirubinemia complicated with acidosis.

Methods and Materials

Brainstem slices containing MVN were made using a microtome and the MVN region was located using a dissecting microscope. The MVN neurons were triturated using a mechanical device incorporating a fire-polished glass pipette. The brain slices were used to assess the cell death due to excitotoxicity by exposing to the fluorescent dye calcein-AM and PI, the MVN region was isolated for cell injury assay-LDH measurement. Acute associated neurons were used to electrophysiology and

Ca^{2+}-imaging. ASICs were activated by a "Y-tube" and a multi-channel perfusion system.

Results

The activation of ASICs in MVN neurons is positively modulated by perfusion bilirubin at micromolar concentrations. We characterize the pharmacological effects of bilirubin on ASICs in MVN neurons. The proton-induced currents potentiated by bilirubin are large extent from heteromeric ASIC2a/1a channels, which is confirmed by blockers for different subunits of ASICs. With 20 mM BAPTA loaded into these neurons, an underlying mechanism of intracellular signal transduction involved in bilirubin potentiation may be fast Ca^{2+}-dependent. Bilirubin aggravates the cell death through ASICs showed by calcein-PI co-staining, the relative release of LDH also demonstrates the acidosis-induced injury potentiated by bilirubin. The fura-3 AM fluorescent Ca^{2+}-imaging technique shows that application of bilirubin with even a mild pH drop leads to the [Ca^{2+}]$_i$ overloaded, which is partly responsible for the cell death.

Conclusion

Our studies suggest that bilirubin may play an important role in potentiation of ASICs, leading to a synergistic effect for the increased neuronal excitability and neurotoxicity in pathological conditions.

Fig3_慢性灌流胆红素.pdf

Fig5_不同阻滞剂的作用.pdf

Fig7_胆红素对酸诱发动作电位的作用.pdf

Fig8_钙成像.pdf

Fig10_LDH释放检测细胞凋亡.pdf

Ion Channels in the Inner Ear

SYMP 26

Precise positioning of ion channels in post-hearing auditory neurons and their distinct anatomical structure determine the speed of impulses to the brain.

Ebenezer Yamoah
University of Nevada Reno

The auditory system is renowned for the precise timing and speed of information processing. However, the spiral ganglion neurons (SGNs) have structural features (bipolar morphology) that can impede the speed of electrical conduction. To define the distinct features of the auditory system, multidisciplinary approaches in-

cluding physiological and imaging analyses combined with computational studies were used. Specifically, we determine the structural properties and the constellation of voltage-gated ion channels/currents in SGNs that allow auditory neurons to overcome their intrinsic structural impedance. We demonstrate that there is a distinct map of voltage-gated ion channels along the length of the primary auditory neuron with precise localization of individual subtypes of channels that is paramount to the remarkable physical qualities of SGNs. Specifically; 1) The distribution of the nodes of Ranvier are distinctly heterogenous along the axis of SGN axons. 2) SGN axons have a sparse distribution of nodes at the proximal terminal. However, the density of the nodes increases as the axon approaches the cell body. 3) Similarly, there is an uneven distribution of a multitude of ion channels along SGN axons including, Na+, K+ and Na+/K+ conductances. We demonstrate that the distribution patterns of the ion channels along SGN axons and the structural features are required to ensure the speed of conduction of auditory information.

SYMP 27

Regional Variations in Ion Channels in Vestibular Calyx Terminals

Katie Rennie; Frances Meredith
University of Colorado AMC

Semicircular canal hair cells respond to head accelerations and convey information to the central nervous system via specialized afferent nerve fibers. Spiking patterns in afferent fibers range from regular to irregular and vary with the morphology of nerve terminals which can be calyx, dimorphic or bouton endings. The most irregular firing patterns are observed in pure calyx afferents in central regions of the crista, whereas highly regular firing patterns are associated with peripherally located nerve endings. Our research addresses the hypothesis that specific groups of ion channels in calyx endings influence action potential firing characteristics in vestibular afferents. Voltage-dependent Na+ and K+ currents were recorded in whole cell voltage clamp from calyx terminals in thin slices of gerbil cristae and action potentials were recorded in current clamp. Slice recordings allowed identification of calyx type in central or peripheral zones of the crista and pharmacological blockers were applied to identify ion channel sub-types. Channel expression was also probed with immunohistochemistry performed on wholemounts or crista slices. Non-inactivating dendrotoxin-sensitive Kv1 currents were more prevalent in mature calyces in central crista regions, whereas inactivating margatoxin-sensitive Kv1 currents were more prominent in peripheral calyces. Blocking Kv1 channels increased action potential firing frequency in both zones. KCNQ currents, sensitive to

XE991, were found in all calyces studied and mediated slowly activating and sustained currents in both zones. Calyx Na+ currents (INa) were completely blocked by tetrodotoxin (TTX, 200-300 nM) in both zones of the mature crista. However at ages younger than 2 weeks, a small residual INa remained in 200 nM TTX that was completely blocked by 1 uM TTX. This TTX-insensitive INa may be mediated by Nav1.5 channels, since Nav1.5 immunoreactivity was observed on the inner face of calyx terminals. Staining for Nav1.6 channels was found in calyx terminals and their axons in both zones of the crista. 4,9-Anhydrotetrodotoxin (100-200 nM), a selective blocker of Nav1.6 channels, reduced INa to a greater extent in peripheral zone compared to central zone calyces. In conclusion K+ and Na+ channel expression varies with epithelial location in calyx-containing vestibular afferents. These variations may contribute to differences in firing patterns and coding of vestibular signals. Modulation of identified ion channel sub-types has the therapeutic potential to regulate excitability in vestibular afferents.

SYMP 28

The roles of multifunctional alpha2delta subunits of voltage-gated Ca2+ channels in inner hair cells and spiral ganglion neurons

Jutta Engel; Barbara Fell; Friederike Stephani; Stephanie Eckrich; Kerstin Blum
Center for Integrative Physiology and Molecular Medicine (CIPMM) and Department of Biophysics, Saarland University, Homburg, Germany

Voltage-gated calcium channels (VGCCs) are composed of an α1 pore-forming subunit and auxiliary subunits β and α2δ. The largely extracellular α2δ proteins 1-4 modulate Ca2+ current properties but the reasons for their partial redundancy/specificity are enigmatic. In the auditory system, the most important function of VGCCs is synaptic transmission. We have shown that α2δ2 together with β2 and Cav1.3 forms the Ca2+ channel complexes at mature inner hair cell (IHC) presynapses essential for transmitter release. In addition to increasing and modulating the Ca2+ current, α2δ2 contributes to trans-synaptic coupling of Ca2+ channels with GluA4 receptors. An α2δ2 null mutant showed moderate hearing impairment and increased latencies of ABR wave I. In contrast to IHCs, spiral ganglion neurons (SGN) express all three neuronal α2δ subunits 1,2, and 3 plus 6 pore-forming subunits. Lack of α2δ specifically reduced Cav2.1 currents, the dominating VGCCs in mature cultured spiral ganglion neurons of 3-week-old mice, by 60%. Lack of α2δ3 led to malformed and smaller endbulbs of Held in mice aged three weeks. Surprisingly, at P5, when P/Q (Cav2.1) channels in SGN were not yet expressed, α2δ3 was nevertheless required for normal endbulb of Held

synapses. This indicates a specific function for α2δ3 in synapse development independent of the P/Q Ca2+ channel. Taken together, the extracellular proteins α2δ2 and α2δ3 not only determine VGCC current sizes and properties, but in addition mediate extracellular functions in trans-synaptic coupling and in synaptic maturation. Supported by DFG SFB894 and DFG PP1608

SYMP 29

Hair Cell & Afferent Channels Modulate Quantal Transmission by Ion Accumulation in the Synaptic Cleft

Donatella Contini; Jonathan J. Art
University of Illinois College of Medicine

Fast neurotransmitters often act in conjunction with slower modulatory effectors that may accumulate in restricted, femtoliter, spaces found at giant synapses such as the calyceal endings in the auditory and vestibular systems. The synaptic cleft is a dynamic environment where ongoing hair cell transduction currents, and synaptic vesicle fusion, may dramatically alter the Ca2+, H+, and K+ concentrations in the space, as compared to their values in bulk solution. We have used dual patch-clamp recordings from turtle vestibular hair cells and their afferent neurons to examine how ion accumulation can modulate membrane potentials of both hair cell and afferent, and thus extend the range and fidelity of quantal transmission. Viewed from the presynaptic side, transduction currents entering the apex of a type I hair cell, exit as a potassium efflux through large basolateral potassium conductances. These large conductances, when combined with the hair cell capacitance, would minimize the membrane time constant of type I hair cells, a result that is ideal for high fidelity quantal transmission. These large basolateral conductances, however, would raise the concern that transduction currents alone might not be large enough to depolarize the hair cell to potentials required for calcium influx and subsequent vesicle fusion implicated in quantal transmission. In the context of the restricted volume between hair cell and afferent calyx, the K+ efflux into the cleft, and the resulting elevated [K]cleft would be sufficient to shift the hair cell potassium equilibrium potential, and bootstrap the hair cell to more depolarized potentials sufficient for calcium influx, and quantal transmission. This process is in contrast to that observed at type II hair cells with conventional bouton endings, where the transduction currents exit through modest basolateral conductances, and the current flow across this higher impedance is sufficient to directly depolarize the hair cell to potentials necessary for quantal transmission. Similarly, on the postsynaptic side, the calyceal afferent endings have both potassium channels as well as potassium- and proton-sensitive Hyperpolarization-activated Cyclic Nucleotide-gated (HCN) channels facing the cleft. Elevation of [K]cleft is sufficient to shift not only the equilibrium potential for afferent potassium channels facing the cleft, but it will also increase an inward current through the HCN channels. In combination, this results in a potassium-evoked depolarization of the afferent towards the threshold for action potential generation, and raises the possibility that large, single quanta will be sufficient to trigger afferent action potentials.

SYMP 30

KV channels, synaptic transmission and spiking in afferent terminals of the mouse utricular epithelium

Omar López Ramírez[1]; Antonia González Garrido[1]; Koh Koizumi[2]; Anna Lysakowski[3]; Ruth Anne Eatock[1]
[1]*University of Chicago;* [2]*Department of Otorhinolaryngology-Head and Neck Surgery, Akita University, Japan;* [3]*University of Illinois at Chicago*

The striolar and extrastriolar zones of the mammalian utricular epithelium supply afferents with different spike regularity and response dynamics. In both zones, the afferents form calyceal synapses on type I hair cells and bouton synapses on type II hair cells, but zonal differences in more subtle aspects of terminal morphology likely contribute to the physiological differences. Here we focus on the contributions of voltage-gated K (KV) channels in hair cells and afferent terminals to afferent transmission and spiking. Type I hair cells transmit to calyces via both synaptic vesicles (quanta) and a unique non-quantal mechanism resulting from current flow through hair cell and afferent ion channels. The two transmission modes shape the transmitted signal differently. The hair cell channels required for non-quantal transmission are low-voltage-activated K channels (gK,L). In the postsynaptic calyx membrane, large numbers of low-voltage-activated Kv7 and Kv1 channels influence spike regularity. Supported by NIDCD

SYMP 31

The morphology and biophysics of developing auditory neurons

Radha Kalluri
University of Southern California

The cell bodies of auditory afferents are heterogeneous in their ion channel composition. Such heterogeneity has been proposed to be important for shaping the threshold sensitivity of Type I auditory afferents, but, clear associations between the ion channel properties of spiral ganglion neurons (SGN) and functionally or morphologically distinct subgroups of Type I afferents has not been demonstrated. We are testing this idea using in vitro patch-clamp recordings combined with reconstructions of fiber morphology in semi-intact cochlear preparations

from rats ranging in age between P1 and P16. We characterized the gross electrophysiological properties of SGN by measuring the size of net inward-flowing and outward-flowing whole-cell currents and firing patterns in response to simple step stimuli. Following recordings, biocytin was loaded into each neuron to subsequently visualize the peripheral processes of SGN and their connections with hair cells. The contacts between the peripheral processes of SGN and inner hair cells were imaged by high resolution confocal scans. 3-D reconstructions from the images allowed us to extract morphological features such as fiber diameter, number of peripheral branches and position of contact with the inner hair cell. We combined the morphology and physiology data in a multivariate analysis to test for sub-groups within the larger group of Type I SGN. Our analysis suggests that there are co-varying spatial gradients in the electrophysiological and morphological properties of SGNs. Whether these differences eventually disappear in mature neurons or stabilize into electro-physiologically different neuronal sub-groups remains to be determined. I will discuss these results as well as the merits and limitations of extending this approach to older ages.

SYMP 32

Implications of Auditory Nerve Fiber Ion Channel Types and Characteristics for Cochlear Implants

Ian C. Bruce[1]; Jason Boulet[2]
[1]*McMaster University; [2]NA*

Accurate models of how auditory nerve fibers (ANFs) respond to electrical stimulation can assist in developing improved sound coding strategies for cochlear implants (CIs). While much progress has been made over several decades in determining what model structures and parameters can best explain some aspects of in vivo electrophysiological data for CI stimulation, many physiological details remain unknown or uncertain, and optimization of parameters can be problematic if there are mistakes in the basic model structure.

Historically, variants on the Hodgkin-Huxley equations have been used to model ANFs, but the included ion channels were not based directly on characterizations of mammalian ANF channels. In this talk, we will review how recent investigations of voltage-gated ion channels in ANFs are contributing to computational models with improved predictions of a wider range of physiological data. In particular, hyperpolarization-activated cation channels and low-threshold potassium channels appear to impart significant temporal interactions in the response properties of electrically-stimulated ANFs, including suprathreshold and subthreshold adaptation that can produce profound reductions in the spiking responses to high-rate stimulation from a CI. Additionally, heterogeneity in these

ion channels can explain a large amount of the variability in strength of adaptation observed across ANFs. Furthermore, simulation results for a multi-compartment model of an entire ANF indicate that the spatial location of these different ion channels can have substantial effects on the response properties as a function of the CI electrode location relative to the ANF. In particular, hyperpolarization-activated cation channels located at the peripheral terminal and around the soma are likely to regulate spike timing in an intact ANF. With progressive ANF degeneration, which tends to affect the peripheral process first, spike initiation may move to the central processes (which do not contain hyperpolarization-activated cation channels), having consequences for neural circuits in the auditory brainstem that are sensitive to ANF spike timing.

Linking Theoretical and Experimental Approaches to Understand Auditory Cortical Processing

SYMP 33

Fifty Years of Interplay between Theory and Experiments in Auditory Cortical Studies

Christoph Schreiner; Craig Atencio; Brian Malone
UCSF

Over the last few decades, studies of auditory cortical physiology have benefitted from linking theoretical and computational considerations with experimental approaches. We will provide a brief overview illustrating several lines of theoretical influences that have advanced auditory cortical studies. Thoroughly characterized statistical properties of natural sounds have been used to show their influences on cortical processing. Artificial sounds appropriately designed for a more rigorous systems analysis have further advanced our experimental approaches leading to mathematically more accessible descriptors like spectro-temporal receptive fields and their higher dimensional expansions. Principles of information theory and modeling of the behavior of neurons and networks of neurons have provided further cues for advancing our approach to and understanding of auditory cortical processes.

SYMP 34

Auditory Model Development Via Deep Learning

Josh McDermott
MIT

Auditory models are traditionally derived from engineering principles and biological observations. Recent machine learning advances have enabled an alternative

approach: model development via task optimization. I will discuss new models of audition obtained by training deep neural networks on audio classification tasks, and three ways in which they yield insight. First, unlike traditional ideal observer models, deep network models can be derived for real-world audio signals, allowing tests of normative principles in new domains. Second, model representation stages can be compared to brain data, revealing hierarchical organization. Third, network architecture optimization for multiple tasks can generate hypotheses about functional segregation.

SYMP 35

Neurocomputational analysis of statistical inference in the brain

Benjamin Skerritt-Davis; **Mounya Elhilali**
Johns Hopkins University

The brain's ability to extract statistical regularities from sound is an important tool in auditory scene analysis, necessary for object detection and recognition, structural learning (in speech or music), or texture perception. Traditionally, the study of statistical structure of sound patterns has focused on first-order regularities; particularly mean and variance which can be easily assessed using physiological measures. In this talk, we will examine insights from EEG recordings using complex sound patterns and present an integrated neuro-computational analysis of statistical tracking in the brain.

SYMP 36

Unsupervised methods reveal a new functional organization of human auditory cortex

Liberty Hamilton
University of Texas at Austin

A fundamental goal in the neurobiology of language is to understand how acoustic information in speech is transformed into meaningful linguistic content. To achieve this goal, researchers have employed model-based methods to determine how acoustic, phonetic, or higher order linguistic cues map onto neural representations. However, such approaches are limited in that they require a priori knowledge of the features to be modeled. In this talk, I show how we employed data-driven computational methods on an extensive set of high-density intracranial recordings from 27 patients to reveal the existence of a spatially-localized region of the pSTG that specifically parses acoustic onsets. By combining unsupervised methods with model-based approaches, we relate these results to previous work on phonetic feature and spectrotemporal representations. Our findings demonstrate a fundamental organizational property of the human auditory cortex that has been previously unrecognized.

SYMP 37

The state space for top-down control of auditory processing

Stephen V. David[1]; Zachary P. Schwartz[2]; Daniela Saderi[3]; Charles Heller[1]
[1]Oregon Health and Science University; [2]Neuroscience Graduate Program, Oregon Health and Science University; [3]Oregon Health & Science University

It is well-established that changing behavior state has diverse effects on auditory cortical activity, but these findings have yet to be integrated into a coherent theory of how internal state influences sensory encoding. We developed a paradigm to isolate the effects of multiple contextual variables—task engagement, arousal, selective attention and behavioral effort—during a simple tone detection task. We recorded single-unit activity in primary auditory cortex of ferrets performing these behaviors and observed a dissociation in the neural subpopulations affected by different variables, as well as how the variables modulated neural selectivity. Ongoing studies are applying state space analysis to simultaneously recorded neural populations to characterize interactions of these variables at the network level.

SYMP 38

Distinct sensory and extra-sensory processing in two types of deep layer auditory cortex projection neurons

Ross S. Williamson; Daniel B. Polley
Massachusetts Eye and Ear Infirmary, Harvard Medical School

Neurons in layers (L) 5 and 6 of the auditory cortex (ACtx) give rise to a massive subcortical projection that innervates all levels of the central auditory pathway as well as non-auditory areas including the amygdala and striatum. L5 and L6 neurons feature distinct morphology, connection patterns, intrinsic membrane and synaptic properties, yet little is known about how these differences relate to sensory selectivity in vivo. In this talk, I will describe quantitative theoretical and experimental tools that can be used to record activity from ensembles of deep-layer projection neurons, to characterize their sensory selectivity, and to understand their functional connectivity within local ACtx circuits. Our studies show that each class of deep-layer projection neuron performs distinct operations on internal and external signals, which likely impart distinct effects on their subcortical targets.

A Soxist Guide to Neurosensory Development and Repair of the Ear

SYMP 39

Sox2 function in Neural Stem Cells

Alexey Terskikh
Neuroscience and Aging Research Center, Development, Aging and Regeneration Program

Newborn granule neurons from neural progenitor cells (NPCs) in the adult hippocampus play a key role in spatial learning and pattern separation. Here, we report a novel function for SOX2 in regulating the epigenetic landscape of poised genes activated during neuronal differentiation. We found that SOX2 binds bivalently marked promoters of proneural and neurogenic genes where it maintains the bivalent chromatin state. Conditional ablation of SOX2 in hippocampal NPCs impaired activation of these genes, resulting in neuroblast death and aberrant neurons. We propose that SOX2 sets a permissive epigenetic state in NPCs, enabling proper activation of the neuronal differentiation program.

SYMP 40

The shifting sands of Sox2 sensory selection

Rogers Brown[1]; Amy Kiernan[2]; Martin L. Basch[3]; Rende Gu[1]; **Andy Groves**[1]
[1]Baylor College of Medicine; [2]University of Rochester; [3]Case Western Reserve University School of Medicine

Sox2 is both necessary and sufficient for the formation of prosensory tissue in the inner ear. However, its early expression in the ear is extremely broad and dynamic, implying that many non-sensory regions of the ear initially express Sox2. This is confirmed by fate-mapping of Sox2-expressing progenitors: early Sox2-expressing cells contribute to non-sensory regions of each sensory organ as well as the semicircular canals, but later Sox2-expressing cells contribute exclusively to sensory organs. These dynamic changes also seen with components of the Notch signaling pathway such as Jag1. They suggest that Notch signaling may not be required for the induction of Sox2 and prosensory regions during early otic development, but rather to stabilize the prosensory nature of these regions as development proceeds. These results are confirmed by conditional ear-specific mutants of the canonical Notch co-activator, Rbpj, in which prosensory patches begin to form but then disappear as the otocyst matures and are replaced by non-sensory tissue. Our results suggest that Sox2 may be a competence factor for prosensory fates at early stages and is later required to maintain Jag1-Notch signaling in prosensory regions of the ear.

SYMP 41

SoxC transcription factors are essential for development of the inner ear

Ksenia Gnedeva[1]; Haoze Yu[1]; Litao Tao[2]; Yassan Abdolazimi[3]; A. James Hudspeth[4]; Neil Segil[1]
[1]Department of Stem Cell Biology and Regenerative Medicine, Keck School of Medicine of the University of Southern California; [2]University of Southern California, Caruso Dept. of Otolaryngology, Keck School of Medicine; [3]Stanford University; [4]Howard Hughes Medical Institute and Laboratory of Sensory Neuroscience, The Rockefeller University

The capacity to produce hair cells is lost in the adult sensory organs of the mammalian inner ear. To investigate the molecular basis of this deficiency, we explored the role of two members of SoxC gene family—Sox4 and Sox11—transiently expressed in the embryonic sensory epithelia. SoxC genes are known to be critical regulators of cell proliferation, survival, and differentiation in many types of progenitor cells. We found that during development of the vestibular and hearing sensory organs, SoxC expression is limited to proliferating progenitor cells, and persists as these cells differentiate into hair cells. SoxC expression is subsequently lost perinatally, around the same time that supporting cells lose the ability to divide and differentiate into sensory receptors. Functionally, we demonstrate that heterozygous knockout of both Sox4 and Sox11 genes results in partial hair cell loss and reduction in the overall sensory organ size, leading to vestibular ataxia and hearing deficiency. Homozygous knockout of both Sox4 and Sox11 yields stunted vestibular and hearing sensory organs that lack hair cells. Further, we demonstrate that reactivation of SoxC expression in the mature utricle and in cochlear sensory progenitor cells can induce hair cell production. Through analysis of ATAC-seq and RNA-seq data we will analyze the gene network(s) regulated by SoxC during normal development. Together these results support roles for SoxC in sensory development and mitogenic control during inner ear development.

SYMP 42

Sox2 Regulates the Expression of Atoh1 during Differentiation of Cochlear Hair Cells

Albert Edge
Harvard Medical School

HMG domain transcription factor, Sox2, is a critical gene for the development of cochlear hair cells. Here, we show that Sox2 played a role in initiating progenitor cell differentiation to hair cells. Sox2 activated Atoh1 through an interaction with the 3' enhancer of Atoh1, and the extent of enhancer binding correlated to the extent

of activation. Atoh1 activation by Sox2 was necessary for embryonic hair cell development: deletion of Sox2 in an inducible mutant, even after progenitor cells were fully established, halted development of hair cells, and silencing also inhibited postnatal differentiation of hair cells induced by inhibition of Notch signaling.

SYMP 43

Sox2 differentially regulates Cdkn1b to promote neuronal differentiation

Alejandra Laureano[1]; Alexis Tam[2]; Azadeh Jadali[1]; Kathryn Cheah[2]; **Kelvin Kwan**[1]
[1]Rutgers University; [2]University of Hong Kong

Sox2 is a transcription factor essential for neurosensory development of the inner ear. The lack of Sox2 during inner ear development results in the improper development of cochlear hair cells, supporting cells and spiral ganglion neurons (SGNs). Sox2 hypomorphic mice show a defect in proliferation of neuroblasts that contribute to the future cochlear vestibular neurons. To delineate the molecular role of Sox2 in otic neuronal differentiation, immortalized multipotent otic progenitor (iMOP) cells were used. In differentiating iMOP cells, genome-wide binding sites of Sox2 were identified by ChIP-seq to reveal a large number of targets involved in cell cycle regulation. These targets include the cyclin dependent kinase inhibitor 1B (Cdkn1b), a key gene involved in preventing cell cycle progression. During neuronal differentiation, Sox2 dependent expression of Cdkn1b increases. We propose that Sox2 differentially regulates Cdkn1b expression to maintain a post-mitotic state during neuronal differentiation.

SYMP 44

Sox Gene Manipulations Verify Neurosensory Origin in the Ear.

Bernd Fritzsch; Karen L. Elliott-Thompson
University of Iowa

Background
The otic placode generates the inner ear with all its neurosensory cells according to most investigators. However, certain data generated after placodal manipulations or in transgenic mice suggest that a variable number of neurosensory cells derive from neural crest and are secondarily incorporated into the developing ear or lateral line neurosensory system contrasting to the majority of studies. We have reinvestigated the ability of crafted cells to integrate into the migratory lateral line and confirm this possibility can occur. We also re-investigated the possible contribution of neural crest to the developing mouse ear and found no reduction in hair cells or neurons as should be expected.

Methods
We assessed the possibility that e-GFP labeled crafted cells form donor ears can incorporate into the migrating lateral line of host frogs using ear transplantations. We generated Wnt1-cre mediated deletion of Sox10, an essential gene for neural crest derived Schwann cells and neurons, to eliminate all neural crest derived cells around the developing ears. Presence of hair cells was assessed using My7a immunocytochemistry, and the distribution of neurons and the patterning of the inner ear innervation was assessed using lipophilic tracers and immunocytochemistry.

Results
Our frog data suggest that occasionally GFP positive cells from transplanted ears and skin of the donor can be incorporated into the migratory lateral line. Immunocytochemistry with Myo VI reveals that some of the e-GFP positive cells can differentiate into hair cells, confirming that indeed some occasional contribution of foreign cells to migratory lateral line placodes can occur under certain experimental circumstances. Our data on Wnt1-cre mediated Sox10 deletion completely eliminated all Schwann cells to the peripheral nervous system as well as nearly all sensory neurons of the PNS except those derived from various placodes. Despite this loss of neural crest derived neurons and Schwann cells there was no obvious reduction in hair cells allegedly derived by a variable proportion from Pax3 positive neural crest cells (Freyer 2011)

Conclusions
While some contribution to developing ears/lateral line is possible under certain experimental conditions, indicating a surprising level of flexibility, there is little hard evidence that this flexibility is in wide use during development. Our data and those of most others strongly support the notion that in normal development all neurosensory cells of the ear derive from the developing ear with neural crest contributing important cells such as Schwann cells and pigment cells necessary to induce proper endolymph formation.

SYMP 45

SOX2 in the Sensory and Neuronal Lineages of the Inner Ear

Aleta Steevens[1]; **Amy Kiernan**[2]
[1]University of Rochester Medical Center; [2]University of Rochester

SOX2 is required for multiple critical progenitor cell lineages in the inner ear, including the sensory and neuronal progenitor lineages. In the neuronal lineage, deletion of SOX2 leads to a dramatic decrease in the

cochleovestibular (CVG) ganglion volume, indicating SOX2 is required for the majority of otic neurons. Analysis of early proneural markers, including NEUROG1 and NEUROD1, showed a near absence of these markers in the developing SOX2 mutant otocyst. These results demonstrate that SOX2 is required for proneural expression in the CVG progenitors. Previous studies have also demonstrated that SOX2 is required for all sensory development in the inner ear and marks the sensory areas by E12.5. Using a fate-mapping and timed deletion approach, we investigated whether SOX2 specifically marks the sensory progenitors prior to E12.5, as well as the timing of expression required for normal otic development. Interestingly, fate mapping revealed that between E8.5 and E10.5 SOX2 does not specifically mark the early sensory progenitors and labels several non-sensory populations. Further, timed deletion analysis revealed that early expression of SOX2 is important for the morphogenesis of the inner ear, whereas later expression is specifically required for sensory development in the cochlea. These results indicate that at early otocyst stages SOX2 may have a role in directing non-sensory development. Thus, our results indicate that SOX2 has critical roles in three progenitor populations in the early otocyst: neuronal, sensory and non-sensory. A challenge for future studies is to determine how a single factor can act to promote these different progenitor lineages in the developing inner ear.

Central Gain Control in Auditory Processing and Hearing Loss

SYMP 46

Contrast gain control in the auditory system

Andrew J. King[1]; James Cooke[2]; Michael Lohse[1]; Neil Rabinowitz[1]; Nicol Harper[1]; Jan Schnupp[3]; Benjamin DB Willmore[1]
[1]University of Oxford; [2]University College London; [3]City University of Hong Kong

Adaptation to changes in the statistics of the acoustic environment, such as the mean level or contrast of recently heard stimuli, has been demonstrated at various levels of the auditory pathway. This fundamental property allows the nervous system to operate over the wide range of intensities and contrasts found in the natural world. For example, neurons in auditory cortex continuously adjust their gain (their sensitivity to change in sound level) to compensate for the contrast between a sound and its background, helping to construct neural representations of complex sounds that are robust to the presence of noise. Furthermore, incorporating a nonlinear pre-processing stage that mimics such adaptation improves the predictive capacity of models of the spectrotemporal receptive field properties of cortical neurons. Recent work has focused on where contrast gain control emerges in the auditory pathway, demonstrating that this property is also found in both the thalamus and midbrain, and on the role of local cortical circuits as well as the interplay between cortical and subcortical processing in mediating these adaptive changes in sensitivity.

SYMP 47

Homeostatic modifications of cortical compensation after auditory nerve damage

Jennifer Resnik[1]; Daniel B. Polley[2]
[1]Massachusetts Eye and Ear Infirmary Harvard Medical School; [2]Massachusetts Eye and Ear Infirmary, Harvard Medical School

Cortical neurons remap their receptive fields and rescale sensitivity to spared peripheral inputs following sensory nerve damage. Cortical reorganization is thought to reflect homeostatic mechanisms that normalize spiking within the denervated cortical zone by rapidly reducing local inhibitory tone and scaling up sensitivity to weak excitatory inputs. Deafferented central auditory neurons become hyperexcitable, exhibiting elevated spontaneous firing rates and increased central gain. We will discuss how these distinct biomarkers of cortical reorganization following injury are coordinated over the days and weeks following sensory nerve injury, and whether these plasticity processes are correlated to homeostatic regulation of intracortical inhibition.

SYMP 48

Adaptation deficits through hidden hearing loss reveal interplay between threshold and gain adaptation

Warren Bakay[1]; Lucy Anderson[2]; Jose Garcia-Lazaro[2]; David McAlpine[3]; Roland Schaette[2]
[1]University of Manchester; [2]UCL Ear Institute; [3]Macquarie University

The dynamic range of hearing greatly exceeds the dynamic range of individual auditory nerve fibres (ANFs) and neurons in the central auditory system. Auditory neurons must thus adapt their responses to changes in the prevailing acoustic environment, to enable the detection and decoding of sounds in quiet as well as loud environments. Here, we investigated the ability of neurons in the inferior colliculus (IC) of the mouse to adapt their responses to repeated switches between relatively quiet and relatively loud sound environments, and how this adaptation was impaired through noise-induced "hidden hearing loss", i.e. through noise exposure that causes a loss of, or damage to, synaptic contacts between cochlear hair cells and auditory nerve fibres (cochlear synaptopathy), without affecting hearing thresholds.

Compared to control mice, noise-exposed mice with evidence of cochlear synaptopathy showed significant impairment in neural adaptation to loud environments, where neural thresholds adapted less, supra-threshold firing rates were lower, and responses were less informative about the intensity distribution. A detailed comparison of the adaptation behaviour of neurons from control and exposed mice revealed two specific mechanisms underlying adaptive coding in the IC - threshold adaptation and gain adaptation, which, combined, generated a stable long-term firing rate regardless of the overall sound intensities in the environment. Only threshold adaptation was directly impaired by noise exposure, whereas gain adaptation remained fully functional. Surprisingly, the normal function of gain adaptation in noise-exposed mice actually aggravated deficits for loud stimuli, where thresholds were mal-adapted, by reducing neural responses substantially in order to stabilize long-term firing rates. The resulting reductions in gain significantly reduced neural information about variations in sound level for loud environments. These findings reveal a cascade of adaptation mechanisms, with gain adaptation downstream of threshold adaptation, and show that central adaptation mechanisms might not only not be able to compensate for deficits caused by damage to the periphery, but can even aggravate them.

SYMP 49

Maladaptive central gain enhancement and aberrant loudness perception following acoustic trauma

Benjamin D. Auerbach; Kelly Radziwon; Guang-Di Chen; Richard Salvi
Center for Hearing and Deafness; State University of New York at Buffalo

The central auditory system displays a remarkable ability to adapt its response properties to changes in sound level. This includes compensatory increases in neuronal gain that can partially restore sound detection following long-term hearing loss. A price of this plasticity, however, is the potential for maladaptive sound encoding in response to abrupt or extreme changes in auditory input. To explore this issue, we examined the relationship between central auditory gain changes and behavioral measures of loudness following acoustic trauma. Simultaneous recordings from multiple levels of the central auditory system demonstrated that noise-induced gain enhancement gradually emerged along the ascending auditory pathway, culminating in excessive amplification of sound-evoked activity in the auditory cortex. In chronic recordings from behaviorally-trained animals, we found this cortical hyperactivity to be strikingly correlated with changes in loudness perception. These results indicate that loss of afferent drive decouples cortical re-sponses from subcortical auditory input, leading to mal-adaptive sound intensity coding and aberrant loudness perception. These changes have particular relevance to hyperacusis, a common auditory perceptual disorder associated with hearing loss where moderate, everyday sounds are perceived as intolerably loud or painful.

SYMP 50

The role of the attention system in hearing loss and tinnitus: evidence from brain imaging studies

Fatima Husain
Dept. of Speech and Hearing Science, the Neuroscience Program and the Beckman Institute for Advanced Science and Technology, University of Illinois at Urbana-Champaign

Chronic tinnitus can alter how the attention system interacts with auditory and emotion processing, even when controlling for comorbid hearing loss. Recent brain imaging studies using resting state and task based fMRI of emotional processing in patients with tinnitus and their controls suggest that the attention system may regulate the engagement of the emotion processing network. Further, the effect of tinnitus on attention systems (possibly mediated by maladaptive gain) appears to be modality specific on sensory and short-term memory tasks, with tinnitus patients exhibiting lower engagement of the attention network when performing auditory tasks compared to visual tasks.

Clinical Otolaryngology & Pathology II

PD 57

Infant hearing assessed using the Pupil Dilation Response

Avinash D S. Bala; Clifford H. Keller; Terry Takahashi
University of Oregon

We used a simple, no contact hearing assay based on the pupillary dilation response (PDR) to probe auditory detection in infants. Six to 14 month old children were seated in a car seat, facing a monitor. An age appropriate animation served to attract the infant';s gaze towards the monitor, and also oriented them towards a camera and speaker, located in line with the center of the monitor and just below it. Pupil size was recorded during 4-s intervals which either included a sound presentation (⅓ octave narrowband noise, centered at 2 kHz), or served as catch trials. We found that infants display a clear and robust sound-elicited dilation, the magnitude of which varies with sound level. The infant PDR habituates rapidly at higher sound levels, suggesting that the PDR can be used to test discrimination as well as auditory detection.

PD 58

Speech in noise in the basic audiologic test battery: effects of auditory pathology, hearing asymmetries, and the relation to perceived communication handicap

Matthew Fitzgerald; Austin Swanson; Steven Losorelli
Stanford University

Word-recognition in quiet has been a staple of the audiologic test battery for over 60 years, despite having little relationship with the real-world communication abilities of individual patients. Moreover, word-recognition in quiet is likely to be insensitive to subtle auditory deficits which may be associated with noise exposure, increasing age, or other auditory processing disorders. As a result, there is increasing awareness that the audiologic test battery needs to be revised to include speech in noise (SIN) assessment on a consistent basis.

To address these issues, we have added speech in noise assessments to our standard test battery, with the intent of making SIN the default test of speech perception in clinical audiology. Thus, in addition to our basic audiometric testing, we have added two additional features: a) monaural and binaural speech-in-noise testing via the QuickSIN, and b) the SSQ12 (Speech Spatial Questionnaire 12). To date we have SIN data on nearly 3000 adults, which we are using to predict 1) instances in which word-recognition in quiet is likely to be excellent and thus could be skipped entirely, and 2) when word-recognition in quiet is likely to be suboptimal, and therefore have diagnostic significance. While these data are highly promising, there are several additional areas which must be addressed before SIN testing could completely replace word-recognition in quiet in everyday practice. For example, the relationship between perceived communication difficulty and clinical SIN measures needs to be better defined. Perhaps more important, the influence of auditory pathology on SIN outcomes needs to be fully understood as well. Finally, the effect of asymmetries in hearing or SIN performance also needs to be outlined. This work is ongoing, but our preliminary results suggest the following:

SIN performance relates more closely to perceive patient handicap than word-recognition in quiet, although this relationship is not linear.

SIN performance appears to be more sensitive to auditory pathology than word-recognition in quiet

Asymmetries in performance appear to be more common with SIN testing than in quiet.

Taken together, these results continue to suggest that SIN assessment can replace word-recognition in quiet in most instances in the conventional audiologic test battery. Making this subtle, but fundamental shift in the audiologic test battery is likely to have both research and clinical implications, allowing for better diagnosis and management of individuals with hearing loss.

PD 59

The Impact of Flat Panel CT-Guided Pitch-Place Mapping on Speech & Pitch Perception in Cochlear Implant Users

Nicole Jiam[1]; Melanie Gilbert[1]; Patpong Jiradejvong[2]; Josh Stohl[3]; Daniel Cooke[1]; Karen Chan. Barrett[2]; Meredith Caldwell[4]; Charles Limb[5]
[1]University of California - San Francisco; [2]Sound & Music Perception Lab, Department of Otolaryngology-Head & Neck Surgery, University of California - San Francisco, San Francisco, CA; [3]MED EL; [4]Johns Hopkins University School of Nursing; [5]Sound & Music Perception Lab, Department of Otolaryngology-Head & Neck Surgery, University of California - San Francisco, San Francisco, CA

Music remains the single most challenging sound for cochlear implant (CI) users, for whom accurate representation of pitch is severely limited. This difficulty with CI-mediated pitch perception may in part be due to the pitch-place mismatch that occurs with intra-operative variability with insertion, anatomical variations between individuals, and a "one-size-fits-all" approach that often occurs with post-implantation programming. Over the past ten years, flat panel computed tomography (FPCT) has emerged as a unique CT technology capable of high-spatial resolution volumetric imaging and dynamic imaging. In a prior study, we demonstrated FPCT';s superiority, relative to standard multislice CT, in identifying individual electrode channels in vivo. Our findings revealed significant pitch-place mismatch between the actual maps being used by CI users and the theoretical maps based on post-implantation FPCT findings. To assess whether this pitch-place mismatch may account for poor pitch perception among CI users, we evaluated the impact of using an individualized, image-guided approach towards CI programming on speech and music perception performance. We enrolled 17 cochlear implant users who underwent FPCT imaging between June 2016 and May 2017. To create theoretical pitch-place maps for each CI participant, we used secondary reconstructions of the FPCT images, three-dimensional curved planar reformation software, and standardized programming parameters. The allotted acclimation period for the pitch-place maps was 30 minutes. Each research subject participated in speech perception tasks (e.g. CNC; BKB-SIN; vowel identification) and a pitch

scaling task while using the image-guided pitch-place map (intervention) versus their actual pitch-place map (modified control). We observed a statistically significant median increase in pitch scaling accuracy when using the image-based map compared to the modified-control map. Specifically, there was a decrease in the number of major pitch reversals (a pitch reversal between two notes greater than 1.65 semitones apart from one another) when using an image-based approach to CI programming versus the modified control map. While there was no observable improvement in speech perception while using an image-based map, we found it interesting that large, acute changes in frequency allocation and electrode channel deactivations with the image-guided map did not worsen CNC and BKB-SIN speech perception performance relative to the clinical map. These findings suggest that an image-based approach to CI mapping may improve pitch perception outcomes by reducing pitch-place mismatch. Future studies employing a longer acclimation period with chronic stimulation over several months are needed to assess the full range of potential benefits of personalized image-guided CI mapping.

PD 60

Clinical Assessment of Superior Canal Dehiscence Repair Outcomes using Power Reflectance

Raphaelle Chemtob; Salwa Masud; Inge Knudson; Daniel J. Lee; Hideko Nakajima
Department of Otology and Laryngology, Massachusetts Eye and Ear, Harvard Medical School, Boston, MA, USA

Background
Superior canal dehiscence (SCD) syndrome is caused by a bony defect of the superior semicircular canal and can cause a variety of auditory and/or vestibular symptoms. Patient outcomes following surgical repair can be difficult to quantify and are often estimated by analysis of subjective symptoms. Power reflectance (PR) is a non-invasive measure of the macro-mechanics of the ear. Our group has shown that in ears with SCD, there is a characteristic decrease in PR (notch) near 1 kHz. In this study, we aim to determine if PR can be used to detect mechanical changes following surgical SCD repair, and if so, whether these changes are associated with symptom improvement.

Methods
We have an ongoing prospective study at the Massachusetts Eye and Ear examining outcomes following SCD repair. For the following analysis, we examined MEE patients from 2001-2017 who underwent surgical SCD repair. From our database of 306 SCD patients, 133 surgical repairs were performed. Inclusion criteria include the completion of SCD symptom questionnaires (including measure of hearing and dizziness handicap) and PR measurements both preoperatively and 3 months postoperatively.

Results
For the study period of 2001-2017, we identified 306 patients diagnosed with SCD. Of these cases, 27 patients fulfilled our inclusion criteria. A notch near 1 kHz was detected in 21 patients (78%) preoperatively. Following SCD repair, 3 patients (11%) continued to have a 1 kHz notch. Improvement of chief complaint such as auditory and/or vestibular symptoms was detected in most patients. However, for improvement in auditory or vestibular symptoms, no statistical significance was seen between patients with a normalized PR compared to those with a persistent notch.

Conclusion
Our preliminary findings show that most SCD patients with a preoperative 1 kHz notch in PR did not continue to have a notch following surgical repair. The majority of SCD patients with PR notch changes postoperatively also had improvement in auditory and/or vestibular symptoms. Analyses of perioperative PR measurements and prospectively collected objective and subjective outcome data in a larger cohort of patients will determine if PR changes predict symptom improvement following SCD repair.

PD 61

Few adverse effects from simulated wind turbine emissions

Meredith E. Adams[1]; Andrew J. Byrne[2]; Michael J. Sullivan[2]; Peggy B. Nelson[3]
[1]University of Minnesota Medical School and Center for Applied and Translational Sensory Science; [2]University of Minnesota, Center for Applied and Translational Sensory Science; [3]University of Minnesota

Introduction
There is a need for additional scientific evidence to determine whether wind turbine emissions cause adverse health effects. Herein we describe our initial assessment of the perceptual effects of simulated wind turbine emissions on healthy volunteers.

Methods
Fifty healthy adult subjects ages 21-73 years attended to audible and infrasound signals generated from a wind turbine, recorded at 300 meters and re-created in a laboratory. Stimuli consisted of modulated and unmodulated audible turbine sound at 50 dB SPL, as well as natural and peak-enhanced turbine infrasound at an overall

level of approximately 85 dB SPL (peaks up to 100dB SPL). Participants were tested for their postural stability on a force plate and detection and ratings of audible and infrasound emissions from turbines. They also completed pre- and post-testing surveys for general and otologic symptoms.

Results
No significant adverse effects among healthy adults have been noted to date. We observed no evidence of any change in postural sway over baseline in the presence of infrasound in the group tested. All combinations of the audible and infrasound were rated as neutral on a positive to negative slider scale. As a group, participants detected something other than the audible stimulus in approximately half of the trials that contained an infrasound stimulus. Participants detected something other than the audible stimulus for a fifth of the trials that did not contain an infrasound stimulus. Some individuals reliably detected the infrasound stimuli. Using a scale from 0 to 3 (0=not at all, 1=mild, 2=moderate, 3=severe) approximately 40% of participants reported 0 for all symptoms. No participants have reported motion sickness. Three symptoms – general discomfort, fatigue, and fullness of head/ears – were reported as mild by 25% of participants and as moderate by 1 to 4 participants each. Four symptoms – eyestrain, difficulty focusing, stomach awareness, and dizziness (with eyes closed) – were reported as mild by up to 10% of participants and as moderate by 1 participant each. Symptoms rarely or not reported were dizziness (with eyes open), vertigo, nausea, sweating, headache, increased salivation, blurred vision, burping). No symptoms were rated as severe.

Conclusions
Simulated wind turbine emissions did not induce changes in postural sway or reports of motion sickness. Future investigations will include electrophysiological assessments of inner ear function during turbine emission exposure among symptomatic and non-symptomatic individuals.

Funding

PD 62

Human Vestibular Schwannoma Reduces Density of Auditory Nerve Fibers in the Osseous Spiral Lamina

Maura C. Eggink[1]; Johan H. Frijns[2]; Jessica E. Sagers[3]; M. Charles Liberman[4]; Konstantina M. Stankovic[5]; Jennifer T. O'Malley[6]
[1]Massachusetts Eye and Ear, Harvard Medical School,; [2]Leiden University Medical Center, The Leiden Institute for Brain and Cognition; [3]Department of Otolaryngology, Eaton Peabody Laboratories, Massachusetts Eye and Ear, Program in Speech and Hearing Bioscience and Technology, Harvard Medical School; [4]Harvard Medical School; [5]Department of Otolaryngology, Massachusetts Eye and Ear; [6]Massachusetts Eye and Ear Infirmary

Objective
Hearing loss in patients with vestibular schwannoma (VS) is commonly attributed to mechanical compression of the auditory nerve, though recent studies suggest that this retrocochlear pathology may be augmented by a cochlear mechanism. Although VS-associated damage of inner hair cells, outer hair cells, and spiral ganglion cells has been reported, it is unclear to what extent peripheral auditory nerve fibers (ANFs) are damaged in VS patients. Understanding the extent of damage VSs cause to ANFs will prove crucial for accurately modeling clinical outcomes of cochlear implantation, which is a therapeutic option to rehabilitate hearing in VS-affected ears.

Materials and Methods
A retrospective analysis of human temporal bone histopathology was performed on archival specimens from the Massachusetts Eye and Ear collection. Seven patients met our inclusion criteria based on the presence of sporadic, unilateral, untreated VS. Tangential sections of five regions of the cochlea were stained with hematoxylin and eosin, and adjacent sections were stained to visualize the plasma membrane (with CellMask) and efferent fibers (with an antibody against choline acetyltransferase). Following confocal microscopy, peripheral ANFs within the osseous spiral lamina were quantified manually and by using a novel "pixel-counting" method.

Results
The density of peripheral ANFs was substantially reduced on the VS side compared to the unaffected contralateral side. The greatest difference between the two sides was found in the upper basal turn, corresponding to the region tuned to 1000 Hz. This observation provides histological insight into the clinical observation that asymmetrical sensorineural hearing loss at the 3000 Hz region is most predictive of a VS. The total number of peripheral ANFs was linearly correlated with

the total number of spiral ganglion cells. Our novel pixel-counting method was validated against manual ANF counts.

Conclusion
We present the first quantitative analysis of peripheral ANFs in patients with VS. The pixel-counting method we developed for quantification of ANFs in the osseous spiral lamina is applicable to other sensorineural hearing loss pathologies. Future research is needed to classify ANFs into morphological categories, accurately predict their electrical properties, and use this knowledge to inform optimal cochlear implant programming strategies.

Grant Support

Author list Abstract ARO.docx

PD 63

Spatial Release from Masking is Diminished Among Individuals with Poorly Controlled Diabetes

Frederick Gallun[1]; Sarah Theodoroff[1]; Nirmal Srinivasan[2]; Dawn Konrad-Martin[1]
[1]VA RR&D NCRAR; [2]Towson University

Background
Diabetes mellitus (DM) is a metabolic disease that affects roughly 1 in 10 people in the U.S. and is well known to impair vascular and nervous system function. Hearing is increasingly being shown to be at risk as well.

Methods
Participants were tested on a measure of spatial release from speech-on-speech masking using the Coordinate Response Measure (CRM) corpus. The task involved reporting two keywords (a color and a number) from a target sentence presented over headphones in the presence of two masking sentences also from the CRM corpus. An auditory virtual spatial array was used to simulate over headphones either a reverberant or an anechoic environment in which all three sentences were presented either in a "colocated" condition (same location for all three) or a "separated" condition, where the target was in front of the listener and the maskers to the left and right by either 8 or 30 degrees. Primary outcomes examined were the estimated target to masker ratio (TMR) associated with criterion performance, and the difference in TMR between the separated and colocated conditions, referred to as "spatial release from masking" (SRM).

Participants were categorized based on clinical diagnoses of type 2 DM and their glycated hemoglobin (HbA1c) levels. Of the 200 tested, 74 had no DM (no clinical diagnosis and HbA1C<5.7%) and 77 were defined as having uncontrolled DM (DM diagnosis and HbA1c=<7%). The remainder were prediabetic (n=16; HbA1c>5.7%) or had controlled DM (n=33; HbA1c<7%). For this preliminary analysis, only the two extreme groups were examined statistically (n=151), and the group effect was estimated in relation to age and the average bilateral pure-tone hearing thresholds (0.5, 1, 2, and 4 kHz).

Results
All participants performed similarly in the colocated condition. Smaller separations and the presence of reverberation reduced SRM for all participants. Increased age and bilateral hearing thresholds were associated with reduced performance, but even controlling for these, DM status had a significant effect on SRM in the anechoic condition. Preliminary SRM data are shown in the supplementary graph for the no DM group (black bars) and uncontrolled DM group (grey bars).

Conclusion
These results show that uncontrolled DM is associated with a reduction in the ability to make use of binaural cues present in the environment. Future work will involve longitudinal tracking of test-retest performance of these participants over time. [Support provided by VA RR&D and NIH/NIDCD].

SRM Figure.pdf

PD 64

Auditory neurophysiology of HIV infection suggests a central nervous system origin for listening difficulties

Travis White-Schwoch[1]; Albert Magohe[2]; Abigail Fellows[3]; Catherine Rieke[3]; Brandon Vilarello[1]; Trent Nicol[4]; Enica Massawe[2]; Ndeserua Moshi[2]; Nina Kraus[4]; Jay Buckey[3]
[1]Auditory Neuroscience Laboratory, Department of Communication Sciences, Northwestern University, Evanston, IL, United States; [2]Muhimbili University of Health and Allied Sciences, Dar es Salaam, Tanzania; [3]Space Medicine Innovations Laboratory, Geisel School of Medicine at Dartmouth, Hanover, NH, United States; [4]Northwestern University

Although there are frequent anecdotal reports of hearing difficulties associated with human immunodeficiency virus (HIV) infection, recent work suggests that there is no greater incidence of sensorineural hearing loss among HIV patients compared to controls (e.g., Maro et al.,

2014, Ear Hear; Ibid. 2016). HIV+ individuals, however, report greater difficulty understanding speech in noise, have higher gap detection thresholds, and perform more poorly on sentence-in-noise perception tests than HIV-controls (Maro et al., 2014, Ear Hear; Zhan et al., 2016, ARO Abs). We hypothesize that hearing complaints in HIV positive individuals originate in the central nervous system. To test this hypothesis we evaluated auditory-neurophysiological responses (auditory brainstem responses, ABRs, and frequency-following responses, FFRs) in HIV+ individuals in Tanzania. The first experiment compared ABRs, FFRs, and listening skills in matched groups of HIV+ and HIV- adults (total N = 38, ages 20-52 yr). ABR amplitude and latency were identical between groups, suggesting the early synapses between the ear and brain are healthy. However, the HIV+ group had diminished FFRs to the pitch and formant cues in multiple speech sounds, suggesting degraded coding of behaviorally-salient spectral cues in speech. In a second experiment we evaluated ABRs and FFRs in a convenience sample of 63 HIV+ women ages 30-50 yr in Tanzania. FFRs to pitch and formant cues in speech were correlated with HIV+ women';s sentence-in-noise perception, suggesting this degraded neural coding underlies the aforementioned listening difficulties associated with HIV. Moreover, FFRs correlated with CD4 and CD8 t-cell counts in the bloodstream, suggesting a link between disease severity and auditory CNS health. Together, these findings support the idea that HIV disrupts listening skills through central neural mechanisms. The neural coding of spectral centers-of-gravity that provide crucial information about sound';s identities and locations are specifically disrupted by HIV. More broadly, this work suggests that auditory-neurophysiological responses might provide proxies to quantify HIV effects in the CNS, which could assist in the clinical management of HIV';s neurological sequelae.

Vestibular Susceptibility to Insult: What's Lost and How Do We Assess It?

SYMP 51

The vestibular inner ear: Sensory processing and sites of vulnerability

Ruth Anne Eatock[1]; Omar López Ramírez[1]; Antonia González Garrido[1]; Anna Lysakowski[2]; Jennifer Stone[3]
[1]University of Chicago; [2]University of Illinois at Chicago; [3]University of Washington

Vestibular epithelia provide uniquely fast information about head motions, allowing real-time stabilization of gaze, posture and heading as we move. In mammals, the epithelia share key features: two types of hair cell (I and II) and afferent terminal (calyceal and bouton) have distinct modes of synaptic transmission, and central and peripheral zones differ markedly in afferent response dynamics and spike patterns, reflecting different terminal morphologies and ion channel expression. Characterization of the ion channels may inform the development of pharmaceutical and prosthetic therapies. The calyceal synapse, which employs a unique form of synaptic transmission involving current flow through pre- and post-synaptic ion channels, is particularly sensitive to injury. In mammalian vestibular epithelia, unlike the cochlea, limited hair cell regeneration is possible, and changes in ion channel expression in regenerating hair cells reveal the extent to which they mature functionally.

SYMP 52

Insult and Dysfunction With Only Modest Hair Cell Loss: A Condition of 3 Lesions

Larry F. Hoffman[1]; David Sultemeier[2]; Ivan Lopez[2]
[1]Department of Head & Neck Surgry, Geffen School of Medicine at UCLA; [2]Department of Head & Neck Surgery, Geffen School of Medicine at UCLA

Over the past several years the concept of a vestibular insult has taken on new importance, due largely to the recognition that partial dysfunction may result from a variety of etiologies, including ototoxicity, acoustic trauma, and aging. In this Symposium segment the cellular targets of vestibular insults will be addressed by presenting recent findings from investigations in which partial ototoxic lesions in the peripheral vestibular epithelia were induced, and as such may provide insight into more general pathophysiologic mechanisms. These experiments were made possible through the development of an animal model of direct intraperilymphatic gentamicin administration, which provided firm control over the small quantities of the lesioning agent administered. Three primary targets were identified, including partial hair cell loss, severe attenuation in stimulus-evoked afferent discharge, and retraction of the afferent calyx. Hair cell loss was very modest, and therefore unmasked the other two other targets of the treatment which were far more widespread. These findings suggest an action of gentamicin on a subcellular target(s) within hair cells that severely compromises stimulus-evoked transmitter exocytosis. In addition, they are indicative of direct action on calyces that result in their structural collapse. Subsequent preliminary experiments in which lower gentamicin doses were administered indicated very subtle functional changes in afferent response dynamics. These findings provide insights upon which a generalizable model of the cellular bases of vestibular insults may be built.

SYMP 53

Assessment of noise induced damage in rats

Courtney E. Stewart
University of Michigan

Although noise overexposure is commonly implicated as a cause of acquired hearing loss, the possibility of concomitant vestibular damage is less accepted. Because the sacculus is located directly behind the oval window, it is exposed to considerable force from the footplate of the stapes. Sound-sensitive type-I hair cells are innervated by medium- to large-diameter afferents that are known to terminate in calyceal endings and carry information related to abrupt acceleration and loud sound stimulation via the eighth nerve to the brainstem. An emerging test of peripheral vestibular function, the vestibular short-latency evoked potential (VsEP), uses linear acceleration to produce an evoked potential produced by activation of the otolith organs. Previous studies suggest that afferents terminating in calyx endings could be primary sources of the VsEP. These afferents can be further divided into two groups: afferents with calyx-only endings and dimorphic afferents with calyceal and bouton endings. We hypothesize noise exposure causes pathological changes in calyceal synapses that disrupt signal transmission. Consistent with this hypothesis, the VsEP is profoundly attenuated by intense, low-frequency noise up to 3 days post noise exposure and then partially recovers in some animals over a time course of several weeks.

SYMP 54

Using Manganese Enhanced Magnetic Resonance Imaging (MEMRI) to Assess Calcium Dependent Activity in Linear Acceleration Detection Pathways following Otolith Stimulation

Avril G. Holt[1]; Anthony Cacace[2]; Aaron K. Apawu[3]; Mirabela Hali[3]; Rodney Braun[3]
[1]Wayne State University School of Medicine/ JD Dingell VAMC; [2]Wayne State University; [3]Wayne State University School of Medicine

Manganese enhanced magnetic resonance imaging (MEMRI) is a powerful imaging paradigm that has been used both in vitro and in vivo for mapping neuronal pathways and objectively evaluating spatial and temporal dynamics of neuronal activity. Manganese is a paramagnetic contrast agent that acts as a calcium surrogate and accumulates in active neurons, primarily through voltage-gated calcium channels. Therefore, MEMRI can be used to appraise calcium channel function and quantify neuronal activity. While auditory, visual, and olfactory systems have begun to be evaluated with MEMRI, studies of the vestibular and balance pathways have been limited. Using short bursts of linear acceleration (jerks) known to stimulate otolith organs and produce short latency vestibular evoked potentials (VsEPs), we assess manganese uptake in central vestibular nuclei (lateral, medial, superior, and spinal vestibular nuclei) as well as related cerebellar nuclei in adult Sprague Dawley rats. The current MEMRI data reveal significant manganese uptake in central vestibular nuclei 24 hours after administration, which has returned to baseline levels within two weeks. In addition, there is differential manganese uptake in rats with jerk stimulation compared to those without. These results may provide important clues regarding mono and disynaptic excitatory and inhibitory inputs to central vestibular neurons and help to clarify contributions of central neurons to VsEP waveforms. In the future MEMRI can be used in longitudinal experimental designs to evaluate models of vestibular dysfunction.

SYMP 55

Vestibular consequences of noise exposure in humans

Faith Akin; Owen Murnane; Jennifer Sears
Mountain Home VA Medical Center

Evidence for the impact of pressure waves on vestibular function has been demonstrated in humans. Studies in humans using tests of horizontal semicircular canal/VOR function were inconclusive; however, the cervical vestibular evoked myogenic potential (cVEMP) has been used more recently to examine the impact of noise, blast exposure, and traumatic brain injury on the vestibular system. Emerging data suggest that the saccule may be particularly susceptible to noise or blast-related injury. In a study examining veterans with asymmetric noise-induced hearing loss (NIHL) and age-matched controls, we observed abnormalities in 33% of the participants with hearing loss, and none of the controls. Furthermore, cVEMPs were more likely to be absent in individuals with more severe NIHL than in individuals with less severe NIHL. These findings not only provide indirect evidence that pressure waves may affect otolith function but are consistent with recent studies in animals and humans that suggest the otolith organs may be particularly susceptible to noise-related damage.

SYMP 56

Age-related vestibular loss

Yuri Agrawal
Johns Hopkins School of Medicine

Age-related vestibular loss has been described as a "partial, progressive bilateral vestibulopathy," and represents the cumulative exposure of the vestibular system to toxic, metabolic, infectious, ischemic, and inflam-

matory insults that accrue with age. Age-related vestibular loss does not present with acute rotatory vertigo but rather with progressive disequilibrium and gait instability, and as such can be considered another cause of hidden vestibular loss. In this talk, we will review the specific elements of the vestibular system that decline as a function of aging, and discuss the different rates of decline observed across different vestibular structures. We will then review the clinical tests that can be used to detect age-related vestibular loss. We will discuss the strengths and shortcomings of these clinical tests and explore new tests that could augment the diagnosis of age-related vestibular loss and its clinical and functional impacts.

Regeneration III

PD 65

Examining Functionally Distinct Hair Cell Progenitor Populations in the Zebrafish Lateral Line

Eric Thomas; David W. Raible
University of Washington

Mechanosensory hair cells of the zebrafish lateral line regenerate rapidly and completely following drug-induced damage. These renewed hair cells have been shown to arise from the proliferation of the surrounding support cells, which undergo symmetric division to produce two hair cell daughters. Support cells are assumed also have the ability to replenish themselves, thus ensuring the regenerative capacity of the neuromast. Whether the ability to generate new hair cells is shared by all support cells or limited to a specific population within the neuromast remains unknown. Using an EdU incorporation assay, we have shown that support cell proliferation is temporally and spatially restricted, and that support cells replenished after one round of regeneration are capable of generating hair cells and other support cells after a second ototoxic insult. These data indicate that support cells are capable of transitioning through different progenitor identities. Whether these different identities represent distinct, defined populations of cells within the neuromast remain unknown. To test this idea, we have utilized the CRISPR/Cas9 knock-in method to generate transgenic lines (sfrp1a, tnfsf10l3, hopx, and sost) in which the photoconvertible protein Eos is expressed in a subset of support cells. Eos-expressing cells can be converted from green to red fluorescence following brief exposure to ultraviolet light, allowing us to track these cells over time. Following photoconversion and hair cell death, only the sfrp1a population was unable to generate new hair cells. However, the sost population had a much higher regenerative capacity than the tnfsf10l3 and hopx populations, generating sixty percent of all regenerated hair cells. These results provide evidence for functionally distinct progenitor populations within the neuromast. The extent to which these populations may overlap with one another, as well as their necessity for hair cell regeneration, remains to be determined. Overall, this approach allows us to correlate hair cell progenitor identity with specific molecular markers, gaining a greater understanding of the mechanisms regulating hair cell regeneration in the lateral line.

PD 66

Single cell gene expression analysis identifies hair cell progenitors/stem cells in zebrafish

Daniel Diaz; Nina Koenecke; Helena Boldt; Madeleine St. Peter; **Tatjana Piotrowski**
Stowers Institute for Medical Research

Hearing loss in mammals can often be attributed to damage or destruction of sensory hair cells located within the inner ear. While some other sensory epithelial structures can regenerate in eff adults, sensory hair cells lack such regenerative capacity in mammalian systems. Non-mammalian vertebrates, however, routinely regenerate sensory hair cells during homeostasis and following injury. The zebrafish lateral line has emerged as an excellent model system for studying sensory hair cell regeneration, particularly because the morphology and developmental mechanisms of hair cells are highly conserved between the major vertebrate lineages. Previous studies have shown that sensory hair cell regeneration in the zebrafish lateral line is spatially and temporally regulated by interactions between Wnt and Notch signaling, but a unique molecular signature for a candidate stem cell population has yet to be determined. To further characterize the molecular underpinnings of hair cell regeneration, we performed single cell RNA-Seq of zebrafish neuromasts, the principal organs of the lateral line containing sensory hair cells. Using low and high throughput methods, our expression analyses revealed the existence of approximately eight8 different cell populations in homeostatic neuromasts, including hair cell progenitors and stem cells. Subsequent analyses using pseudotime aligned these cell populations along a trajectory according to their differentiation status, thereby identifying new genes required for hair cell differentiation. Importantly, we also performed single cell RNA-Seq analysis at 5 different time points after hair cell death. Notch and Fgf signaling are immediately downregulated after hair cell death and analysis of a fgf3 mutant revealed that Fgf3 negatively regulates proliferation during homeostasis. Our results show that single cell RNA-Seq is a powerful tool to gain mechanistic insight into hair cell regenration at unprecedented, cellular detail.

PD 67

Overexpression of a YAP1 Mutant Drives Cell Cycle Re-Entry in Mature Mouse Utricles

Anna Andreeva[1]; **Mark Rudolf**[2]; Mikolaj Kozlowski[2]; Robin Singleton[2]; Christina Kim[2]; Jeffrey Corwin[2]
[1]Nazarbayev University; [2]University of Virginia

Background

Mammalian supporting cells exhibit sharp declines in regenerative proliferation during early maturation. Concurrently, they develop reinforced apical junctions with F-actin "belts" of exceptional thickness and stability relative to other epithelia, including the readily regenerative supporting cells of non-mammals. Gnedeva et al. (2017) demonstrated that a signaling axis of mechanical force, YAP1, and TEAD transcription factors regulates proliferation in the perinatal mammalian utricle, yet it was unknown whether mature supporting cells remain responsive. Although the reinforced junctions impede the transmission of mechanical tension in mature maculae of mammalian utricles, we hypothesized that supporting cells might remain susceptible to downstream manipulations in the mechanical tension-YAP1-TEAD axis.

Methods

To test the hypothesis, we transduced utricles of one-month-old mice with adenovirus type 5 to cause overexpression of one of three constructs: (1) Wild-type YAP1, (2) YAP1-5SA, which has five serine-to-alanine mutations that prevent inhibitory phosphorylation by LATS, and (3) YAP1-5SA/S94A, which has an additional mutation that disrupts binding to TEAD. We cultured the utricles with BrdU for three days and measured subcellular distribution of YAP1 protein.

Results

Despite expectations, overexpression of wild-type YAP1 in mature mouse utricles did not significantly increase S-phase entry over mCherry controls (1±1 vs zero BrdU+ cells/utricle, mean±SD). However, overexpression of LATS-insensitive YAP1-5SA resulted in significant S-phase entry (108±36), which was abolished in the YAP1-5SA/S94A variant that does not bind TEAD (2±2). Supporting cells transduced with YAP1-5SA and YAP1-5SA/S94A exhibited significantly higher nuclear:cytoplasmic ratios of the protein compared to cells expressing wild-type YAP1 (0.85±0.12 and 0.97±0.09 vs 0.66±0.07). A phospho-serine-127-specific antibody labeled cells that overexpressed wild-type YAP1, but not YAP1-5SA. These data suggest wild-type YAP1 is phosphorylated by LATS and retained in the cytoplasm, while YAP1-5SA enters the nucleus and spurs cell cycle re-entry with TEAD.

Conclusions

Our results show that mature supporting cells express functional levels of a TEAD transcription factor and can be induced to re-enter the cell cycle by manipulating the mechanosensitive YAP1-TEAD signaling axis, which controls organ size in embryonic development. They also raise the possibility that LATS activity is elevated in mature mammalian supporting cells and could collaborate with stiffened junctions in maintaining their quiescence.

PD 68

Sox2 Haploinsufficiency Primes Regeneration and Wnt-responsiveness in the Neonatal Mouse Cochlea

Yaodong Dong[1]; Patrick J. Atkinson[1]; Shuping Gu[1]; Wenwen Liu[1]; Tomokatsu Udagawa[1]; Alan G. Cheng[2]
[1]Department of Otolaryngology-HNS, Stanford University; [2]Department of Otolaryngology-Head and Neck Surgery, Stanford University

Background Sox2 (SRY (sex determining region Y)-box 2) is a SoxB1 HMG-domain transcription factor, which plays essential roles in cell division and differentiation in multiple developing organs. Limited data have shown that activation of Sox2 in somatic stem cells is needed for tissue homeostasis and regeneration. In the developing mouse cochlea, Sox2 expression marks the prosensory region, which harbors cells primed to give rise to mechanosensory hair cells and non-sensory supporting cells of the organ of Corti. Yet, its roles in cochlear hair cell regeneration after damage remain to be determined. Here, we employed combinations of transgenic mouse models to reveal that Sox2 haploinsufficiency, rather than impairs, increases cochlear regeneration in vivo. Methods Three transgenic mice lines (Sox2CreERT2/+, Sox2GFP/+, Sox2fl/+) were used to examine Sox2 haploinsufficiency. Hair cells were ablated via diphtheria toxin injection to Pou4f3DTR/+ mice. EdU was administered to monitor proliferation and tamoxifen to induce Cre recombination. Cochleae from multiple combination of transgenic mice lines (Sox2CreERT2/+; Pou4f3DTR/+, Pou4f3DTR/+; Fgfr3-iCre; Ctnnb1fl(ex3)/+, Pou4f3DTR/+; Sox2CreERT2/+; Ctnnb1fl(ex3)/+) were collected and immunostained to determine the effects of Sox2 haploinsufficiency and ß-catenin stabilization on both proliferation and hair cell regeneration after hair cell ablation. Fgfr3-iCre; Ctnnb1fl(ex3)/+, Sox2CreERT2/+; Ctnnb1fl(ex3)/+ and Fgfr3-iCre; Ctnnb1fl(ex3)/+; Sox2fl/+ mice were also used to determine the interaction between Sox2 and Wnt signaling. Sox2, and Wnt and Notch target genes were measured via qPCR. Results Sox2 haploinsufficient cochleae displayed delayed terminal mitosis and ectopic hair cells. Damage in the neonatal Pou4f3DTR/+ cochlea stimulated proliferation

and Atoh1+ transitional cell formation. Both effects were amplified by Sox2 haploinsufficiency. Wnt activation via ß-catenin stabilization alone failed to induce proliferation or transitional cell formation. In contrast, ß-catenin stabilization enhanced proliferation when either Sox2 haploinsufficiency or damage was present. An increase in transitional cell formation by ß-catenin stabilization was observed when both damage and Sox2 haploinsufficiency were present. Mechanistically, Sox2 haploinsufficiency and damaged neonatal cochleae displayed lower levels of Sox2 and the Notch target gene Hes5. Conclusion Sox2 and damage act as permissive signals for ß-catenin-induced proliferation and transitional cell formation in the neonatal mouse cochlea. Our study unveils a previously unknown interplay between Sox2 and Wnt in priming tissue regeneration.

PD 69

ErbB2 Signaling is Sufficient to Drive Proliferation and Supernumerary Hair Cell Formation in Neonatal Mouse Cochlear Supporting Cells

Jingyuan Zhang[1]; Quan Wang[2]; Dunai Abdul-Aziz[2]; Jonelle Mattiacio[3]; Albert Edge[4]; **Patricia White**[5]
[1]Department of Biology, University of Rochester School of Arts and Science; [2]Department of Otolaryngology, Harvard Medical School; [3]Department of Biology, St. John's Fisher College; [4]Harvard Medical School; [5]Dept. of Neuroscience, University of Rochester School of Medicine

Introduction
In mammals, cochlear hair cells are not regenerated once they are lost, leading to permanent hearing deficits. In other vertebrates, such as birds, fish and amphibians, some adjacent supporting cells act as a stem cell compartment for hair cells. These supporting cells may proliferate and/or differentiate into auditory hair cells, restoring hearing. There is considerable interest in identifying strategies to promote hair cell regeneration in mammals, particularly of outer hair cells whose function is crucial for auditory thresholds. In this report we describe the effects of activating a candidate signaling pathway, ERBB, in neonatal mouse cochlear supporting cells. ERBB signaling and some of its downstream effectors have been implicated in proliferation of both avian and mouse supporting cells. However, its sufficiency for driving regeneration-like activities in intact mouse cochleae in vivo has not been described.

Methods
We used three independent strategies to activate ERBB2 signaling in neonatal mouse cochlear supporting cells. First, we constructed adenoviruses that drive expression of either a constitutively active or inert human ERBB2 protein (CA-ERBB2 or I-ERBB2, respectively) in conjunction with GFP. Viruses were used on neonatal mouse cochleae in vitro. Second, we used a Tet-On expression system to drive a similar transgenic rat-derived CA-ERBB2 protein in supporting cells in vivo. Expression of the rtTA transcription factor from the ROSA locus was controlled by Fgfr3-iCRE activation to limit expression of the transgene. Finally, two small molecules previously reported to activate signaling downstream from ERBB3 were also tested on neonatal mouse cochleae in vitro. Western blots were used to validate the new reagents, and EdU incorporation and immunofluorescence were used to assay proliferation and hair cell differentiation.

Results
We found significant proliferation of supporting cells in vitro after viral transduction. Proliferating supporting cells were adjacent to infected supporting cells, strongly implicating a short-range second signal. Moreover, proliferating supporting cells down-regulated SOX2. In vivo, proliferation was observed, but was limited in scope. Strikingly, supernumerary outer hair cells were observed throughout transgenic cochleae when CA-ERBB2 was activated in supporting cells in vivo, also in a non-cell autonomous fashion. Both proliferation and supernumerary hair cells were observed with small molecule activation in vitro. These data are consistent with a role for ERBB2 receptors in a signaling cascade, in which ERBB stimulated cells relay a short-range damage signal to endogenous stem cells to initiate regeneration.

PD 70

Regeneration of cochlear hair cells in adult mice by direct trans-differentiation of rejuvenated cochlear epithelial cells

Wenyan Li[1]; Yi-Zhou Quan[2]; Mingqian Huang[3]; Yilai Shu[1]; Yong Tao[4]; Xuezhong Liu[5]; Zhengmin Wang[6]; Huawei Li[6]; Zheng-Yi Chen[7]
[1]1. Department of Otolaryngology, Harvard Medical School, 2. Eaton-Peabody Laboratory, Massachusetts Eye and Ear Infirmary, 3. Department of Otolaryngology, Hearing Research Institute, Affiliated Eye and ENT Hospital of Fudan University; [2]1. Department of Otolaryngology, Harvard Medical School; 2. Eaton-Peabody Laboratory, Massachusetts Eye and Ear Infirmary; [3]1. Department of Otolaryngology, Harvard Medical School, 2. Eaton-Peabody Laboratory, Massachusetts Eye and Ear Infirmary; [4]Eaton Peabody Laboratory, Massachusetts Eye and Ear Infirmary; [5]Department of Otolaryngology, University of Miami Miller School of Medicine; [6]Department of Otolaryngology, Hearing Research Institute, Affiliated Eye and ENT Hospital of Fudan University; [7]1. Department of Otolaryngology, Harvard Medical School, 2. Eaton Peabody Laboratory, Massachusetts Eye and Ear Infirmary

Background

Mouse cochlear hair cells can be regenerated by Atoh1 overexpression in neonatal mice. However, The lack of regenerative capacity in the adult mammalian cochlea is the major hurdle to the development of treatment for permanent hearing loss. We have recently shown that MYC and Notch signals are sufficient to reprogram cells in adult mouse cochleae to induce proliferation. We hypothesize that those reprogrammed cells can regain the potential reminiscent of young cochlea, with the capacity to respond to hair cell induction signal

Methods

Using doxycycline (Dox)-inducible rtTA/tet-Myc/tet-NICD transgenic mice, we transiently activated MYC/Notch signals by adding Dox in adult cochleae culture medium or by placing gelfoam soaked with Dox in the round window niche in vivo. Atoh1 was subsequently over-expressed with viral delivery in adult cochlear organ culture or by cochleostomy in vivo. Active blockade of Notch signaling upon Dox withdrawal was performed with Notch inhibitors. Lineage tracing was used to study the origin of regenerated hair cells. Hair cells were further characterized by specific markers, for the presence of transduction channels and the ability to connect with adult neurons.

Results

Robust regeneration of new MYO7A+ hair cells was observed after forced Atoh1 overexpression in reprogrammed adult cochlear epithelia in vitro and in vivo. Multiple cochlear cell subtypes were transdifferentiated to hair cells with differed transdifferentiation efficiency. Both dividing and non-dividing reprogrammed adult cochlear cells were capable of transdifferentiating to hair cells, indicating hair cell transdifferentiation does not depend on quiescence of reprogrammed cells. New hair cells are labeled with hair cell markers including VGLUT3 for inner hair cells and SLC26A5 (prestin) for outer hair cells. FM1-43 uptake study supports the presence of transduction channels. New hair cells formed direct connections with adult ganglion neurons in vitro and in vivo. Notch inhibition after MYC/NICD down-regulation leads to the production of new hair cells.

Conclusion

We have identified a new mechanism by which transient MYC/NOTCH activation leads to reprogramming of fully mature adult cochlea. Reprogrammed mature cochlear cells are able to respond to hair cell signals (Atoh1 expression or Notch inhibition) to efficiently transdifferentiate to hair cells that are highly differentiated in vitro and in vivo. The ability of reprogrammed adult cochlear cells to transdifferentiate to hair cells will enable further study of the underlying mechanism and open up a new avenue of potential treatment for deafness

PD 71

Alsterpaullone, 2-cyanoethyl, a p27Kip1 inhibitor, promotes new hair cell regeneration from Atoh1-expressing supporting cells in adult mouse cochleae

Shiyong Diao[1]; Jie Fang[1]; Jian Zuo[2]
[1]*St. Jude Children's Research Hospital; [2]Department of Developmental Neurobiology, St. Jude Children's Research Hospital, Memphis, Tennessee, USA*

Over 5% of the world';s population 360 million people has disabling hearing loss. Despite significant progress in neonatal regeneration of cochlear hair cells (HCs), such regeneration in adults has been proved extremely difficult. While gamma secretase inhibitors have shown some promise in regenerating noise-damaged auditory HCs in adult mice, no drugs have been proven effective for functional hearing recovery in adult mammals, including humans to date. Remarkably, we recently observed new HC formation in adult mouse cochleae when p27Kip1 was inactivated combined with Atoh1 ectopic expression was simultaneously induced in supporting cells (SCs) in our generic model, although manipulation of the individual genes had no effect. Therefore, our promising results lead us to investigate the druggability of small-molecule inhibitors of p27Kip1 in converting Atoh1-expressing SCs to new HCs in adult mouse cochleae. In our previous study, we have completed a high-throughput screen of ~8,000 FDA-approved bioactive compounds, in which small-molecule inhibitors of p27Kip1 transcription were detected by using the p27Kip1 promoter to drive luciferase expression in transiently transfected HeLa cells. We identified 9 lead compounds that inhibit p27Kip1 transcription at sub-micromolar IC50 in three different mouse and human cell lines, without affecting cell survival. Alsterpaullone, 2-Cyanoethyl (A2CE), our lead compound which we are focusing on now, is able to repress p27Kip1 mRNA in neonatal mouse cochlear explants, both p27Kip1 mRNA and protein expression in Hela cells. Further in vivo validation shows that local delivery of A2CE can induce 60% mRNA reduction of p27Kip1 in mouse Organ of Corti via transtympanic injection. In current study, we observed that local administration of A2CE (5mM, 5µl) with single transtympanic injection can significantly promote the new hair cell regeneration comparing to the DMSO control group in Fgfr3-iCreER; Atoh1-HA+; p27flox/wt generic model (55.5±31.8 VS 6±2.8 per cochleae) which was induced by tamoxifen at P28 and harvested cochleae at ~P49. No new regenerated HCs were detected in the Fgfr3-iCreER; Atoh1-HA+; p27wt/wt model with or without A2CE administration after tamoxifen induction,

which is consistent with our previous reports that Atoh1 alone can';t convert supporting cells to hair cells in the adult cochleae. Our future studies will be focusing on the optimization of drug administration of A2CE or combination with other available compounds to obtain more new hair cells in the Fgfr3-iCreER; Atoh1-HA+; p27flox/wt and Fgfr3-iCreER; Atoh1-HA+; p27wt/wt models or wild type mice for the clinical usage.

PD 72

Lin28 Promotes Proliferation of Cochlear Neural Progenitor Cells

Ngoc-Nhi C. Luu[1]; Judith S. Kempfle[2]; Marco Petrillo[1]; Albert Edge[3]

[1]Eaton-Peabody Laboratories, Massachusetts Eye and Ear; Department of Otolaryngology, Harvard Medical School; [2]1, Department of Otolaryngology, Massachusetts Eye and Ear, Boston, MA, USA. 2, Department of Otology and Laryngology, Harvard Medical School, Boston, MA, USA. 3, Department of Otolaryngology, University Tübingen Medical Center, Germany; [3]Harvard Medical School

Background

Sensorineural hearing loss is irreversible and can be caused by loss of inner ear neurons or hair cells. Regeneration of these cell types from remaining endogenous cells offers a future alternative to implantable hearing devices. Lin28, a highly conserved RNA-binding protein plays a role in post-transcriptional regulation of mRNA. The transcription factor Sox2 is crucial for proliferation of progenitor cells and neurogenesis and interacts with Lin28 in human neural precursors to maintain optimal levels of Lin28. In the postnatal inner ear Sox2 has previously been associated with expansion of sensory progenitors that develop into hair cells. We found that proteolipid protein 1 (Plp1), a marker for glial cells that can act as progenitor cells for neurons in the CNS, is coexpressed with Sox2 in peripheral glia of the inner ear. Further Plp1-expressing progenitor cells were dependent on Sox2 and Lin28 for stem cell activity.

Methods

Spiral ganglion stem cells were isolated from the cochlea of postnatal Plp-Cre-ER;Lin28[flox/flox];Rosa26[tdTomato] mice or from Plp-CreER;Lin28[TetO/+];Rosa26[tdTomato] mice. Single cell suspensions of spiral ganglion tissue were cultured with growth factors to obtain proliferative spheres. After 12 days in vitro and 2 passages, neurospheres were obtained and quantified by immunohistochemistry. After 12 days in differentiation-promoting culture conditions, neural progenitor cells, glia and neurons in the neurospheres were quantified based on marker expression and quantitative RT-PCR. Lineage tracing of Plp-expressing neural progenitor cells was performed by immunohistochemical colocalization with tdTomato. We overexpressed Lin28 in adult Plp-CreER;Lin28[TetO/+];Rosa26[tdTomato] mice after inducing auditory neuropathy where Type I spiral ganglion neurons were destroyed with Ouabain and analyzed gene expression in the spiral ganglion by quantitative RT-PCR.

Results

Plp1-positive glial cells from the spiral ganglion maintain proliferation in the presence of Lin28 and Sox2. Downregulation of Lin28 in Plp1-positive neurospheres showed reduced proliferation in vitro but differentiated to neurons, suggesting a role for Lin28 during early stages of progenitor differentiation. Overexpression of Lin28 increased the number of Plp1-positive progenitors that differentiated into neural progenitors and subsequently into neurons in vitro. In an adult model of auditory neuropathy, upregulation of Lin28 in Plp-positive glial cells led to increase of proneural genes.

Conclusion

Lin28 interacts with Sox2 in cochlear neural progenitors to promote proliferation and to drive them towards a neural fate in the inner ear.

Tinnitus: Human & Animal Studies

PD 73

International Consensus on Core Outcome Domains for Early-Phase Clinical Trials of Sound-, Psychology-, and Pharmacology-Based Interventions to Manage Chronic Subjective Tinnitus in Adults: The COMIT'ID Study

Deborah A. Hall

National Institute for Health Research Nottingham Biomedical Research Centre

Background

The reporting of outcomes in clinical trials of subjective tinnitus indicates that many different tinnitus-related complaints are of interest to investigators, from the perceptual attributes of tinnitus (e.g. loudness) to psychosocial impacts (e.g. quality of life). Even when considering one type of intervention strategy for subjective tinnitus, there is no agreement about what is critically important

for deciding whether a treatment is effective. The main purpose of this observational study is therefore to develop Core Outcome Domain Sets for the three different intervention strategies (sound, psychological, and pharmacological) for adults with chronic subjective tinnitus that should be measured and reported in every clinical trial of these interventions (even if they are not one of the primary outcomes).

Methods

The 'Core Outcome Measures in Tinnitus: International Delphi'; (COMIT';ID) study used a mixed methods approach for achieving consensus, designed with input from healthcare users, clinical experts and a trialist. Healthcare users, healthcare practitioners, clinical researchers, commercial representatives and funders all participated in online Delphi surveys (over 650 participants, from over 30 countries) and face-to-face meetings (over 55 participants). For transparency, our methods have been published ahead of the analysis (Fackrell et al., 2017).

Results

Findings will be reported for three independent studies; one for each intervention. In each case, the Delphi surveys reduced a long list of over 60 candidate outcome domains to those 20 or so considered by all stakeholder groups to be important and critical. The subsequent meetings reduced these down to a maximum of 6. Some were common to more than one intervention strategy (e.g. 'tinnitus intrusiveness';), others were deemed to be specific to just one intervention strategy (e.g. 'negative thoughts and beliefs';).

Discussion

This COMIT';ID study seeks to improve future tinnitus research by creating an evidence-based consensus about minimum reporting standards for outcomes in clinical trials of a tinnitus intervention. The output will be a core set of important and critical outcomes to be measured and reported in all clinical trials. Wide dissemination will be crucial for promoting uptake across the community.

Reference

Fackrell K, Smith H, Colley V, Thacker B, Horobin A, Haider HF, Londero A, Mazurek B, Hall DA (2017) Core Outcome Domains for early phase clinical trials of sound, psychology-, and pharmacology-based interventions to manage chronic subjective tinnitus in adults: the COMIT';ID study protocol for using a Delphi process and face-to-face meetings to establish consensus. Trials 18(1): 388.

PD 74

Characteristic molecular and functional biomarkers for tinnitus in humans

Knipper Marlies[1]; Benedikt Hofmeier[2]; Ebrahim Saad Aldamer[2]; Moritz Walter[2]; Ulrike Ernemann[3]; John Thiericke[4]; Lukas Rüttiger[1]; Stephan Wolpert[5]; Uwe Klose[3]

[1]*Department of Otolaryngology, Tübingen Hearing Research Centre (THRC), Molecular Physiology of Hearing, University of Tübingen, Elfriede-Aulhorn-Straße 5, 72076 Tübingen, Germany;* [2]*Tübingen Hearing Research Centre (THRC);* [3]*Department of Neuroradiology;* [4]*Department of Otolaryngology, ENT Clinic Tübingen;* [5]*Department of Otolaryngology Tübingen ENT Clinic*

Tinnitus is a widespread auditory disorder affecting approximately 10-15% of the population, often with debilitating consequences. The exact neurophysiological basis of chronic tinnitus remains unknown and in various aspects highly controversial. While some studies link a pathological increase in central responsiveness subsequent to cochlear damage with tinnitus other suggest that hearing loss is not necessarily causally involved in tinnitus and a failure to generate central hyperactivity is rather associated with tinnitus. We here present the results from preclinical pilot studies that aimed to investigate characteristic functional and molecular biomarkers in homogenous matched hearing impaired human subjects with and without tinnitus. Using a combination of investigations from biomarkers in body fluids, from audiometry fine structure analysis and resting or evoked fMRI in distinguished patient and control groups we present new characteristic features for the tinnitus group. We will discuss the findings in the context of urgent needs for using objective biomarkers for future therapeutic interventions in tinnitus patients.

PD 75

Hidden Hearing Loss in Tinnitus Patients with Normal Audiograms

Binbin Xiong[1]; Xiaoming Zhao[1]; Wei Sun[2]
[1]*Zhuhai Hospital Affiliated with Jinan University;* [2]*State University of New York at Buffalo*

Object

Tinnitus is highly related with hearing loss. However, it is not uncommon to see tinnitus patients with normal audiograms on conventional pure-tone tests. The aim of this study is to detect the potential cochlear lesion in

these tinnitus patients who showed normal audiograms (0.25 to 8 kHz in one-octave step).

Methods
Hearing threshold in 106 tinnitus patients who showed normal PTA were tested using a small frequency step (1/24 octave step), referred as precision PTA (P-PTA), at ±1/3 octave band centered at their tinnitus frequency. Tinnitus pitch, loudness and residual inhibition were re-evaluated based on P-PTA. DPOAE was also tested to measure the outer hair cell function.

Results
Using the P-PTA test, we found 49% (52 out of 106) of tinnitus patients with normal audiograms did show notch hearing loss at their tinnitus frequencies. In a control group without tinnitus, only 8 out of 82 ears showed notch in their audiograms (9.76%). Using a small frequency step (1/24 octave) for tinnitus pitch match, the rate of tinnitus pitch match increased from 50.9% to 95.3% (Fisher';s test, P < 0.0001, n = 106). The tinnitus loudness and residual inhibition was retested based on the pitch of tinnitus. We found that the number of tinnitus patients whose tinnitus loudness was less than 5 dB SL increased from 25.9% to 55.1% (n = 106, Chi-Square test, P=0.015) and the positive residual inhibition rate increased from 30.7% to 53.9% (Fisher';s test, P=0.014). DPOAE tests revealed a significant reduced amplitude in about 2/3 of these patients, suggesting the lesion of outer hair cells may contribute to their notch hearing loss.

Conclusions
Our study confirmed cochlear impairment in tinnitus patients with normal audiograms in conventional pure-tone test. P-PTA can help to identify cochlear lesion hidden from the conventional PTA. P-PTA also improved the precision of tinnitus assessments

PD 76

Replicability and robustness of fMRI biomarkers of tinnitus in military and civilian populations

Fatima Husain[1]; Sara Schmidt[2]; Benjamin Zimmerman[2]; Yihsin Tai[2]; Rafay Khan[2]; Charla Levy[3]; Paul Sherman[4]; Carlos Esquivel[3]
[1]*Dept. of Speech and Hearing Science, the Neuroscience Program and the Beckman Institute for Advanced Science and Technology, University of Illinois at Urbana-Champaign;* [2]*Unviersity of Illinois at Urbana-Champaign;* [3]*Hearing Center for Excellence;* [4]*Neuroimaging Center*

Tinnitus is a subjective hearing disorder, where the presence of tinnitus and the degree of severity of its associated symptoms are estimated entirely via self-report. Our lab and others have used brain imaging measures to better understand the neural mechanisms of tinnitus and find objective correlates for the condition and its related severity. In this study, we assessed the replicability of objective brain imaging biomarkers of tinnitus in military and civilian groups. Patients and controls (all civilians) were scanned using resting state functional MRI at University of Illinois at Urbana-Champaign (UIUC). Smaller numbers of Active Duty Service Members and Veterans (patients and controls) were scanned at Wilford Hall Ambulatory and Surgical Center (WHASC) and Hearing Center for Excellence. Each participant was scanned twice, using identical protocols of 10 mins resting state fMRI, a week apart. At UIUC, the pure tone average (PTA) in control participants were 10.66 ± 7.51, while tinnitus participants had PTAs of 21.36 ± 15.23. At WHASC, the PTA for controls was 11.53 ± 5.48, and for tinnitus participants, it was 14.88 ± 6.52. More control participants are currently being collected at both sites to better match hearing thresholds across groups. At UIUC, tinnitus severity scores assessed via the Tinnitus Functional Index (TFI) ranged from 3.6 to 58.8, with an average of 25.79 ± 14.91 at the first scan and 22.42±17.03 at the second. Similarly, at WHASC, TFI scores ranged from 11.2 to 48.4, with an average of 26.65±13.21 at the first visit and 24.57 ±9.37 at the second. We examined the default mode, dorsal attention, and auditory resting state networks. Standard resting state functional connectivity analysis did not reveal noteworthy differences between tinnitus and control groups at either visit, either at UIUC or at WHASC. We tested for replicability in those same networks and found them to be replicable, with no notable differences across visit for either control participants or, more importantly, the tinnitus participants, despite the small differences in severity scores between visits. Our results show that resting state fMRI measures are replicable and reliable objective biomarkers of a subjective condition. This paves the way for using resting state fMRI to measure the efficacy of interventions and to propose better management options.

PD 77

Neural Correlates of Tinnitus: Spontaneous Local Synchrony within Rat Auditory Cortex

Naoki Wake[1]; Tomoyo I. Shiramatsu[2]; Hirokazu Takahashi[2]
[1]*Department of Mechano-Informatics Graduate School of Information Science and Technology, The University of Tokyo;* [2]*Research Center for Advanced Science and Technology, The University of Tokyo*

Background
Tinnitus is likely caused by maladaptation of hearing loss, where cortical activities in a sensory deprived to-

notopic area are complemented by activities in other areas. Here, we hypothesized that the auditory cortex of tinnitus subjects exhibits an elevated neural synchrony between the sensory affected frequency area and a tinnitus frequency area in the tonotopic map. To verify this hypothesis, we examined synchrony patterns in the auditory cortex of an animal model of tinnitus.

Methods

We exposed a high-intensity pure tone to the left ear of Wistar rats for 60 minutes (10kHz, 125 dB SPL) to induce lateral acoustic trauma. Before and 28 days after the acoustic trauma, pre-pulse and gap inhibition tests examined behavioral sign of hearing loss and tinnitus with varied frequency tones (4, 8, 16, 32 kHz, and broadband noise, 60 dB SPL). Neural signals were recorded using a microelectrode array with a grid of 10×10 recording sites (ICS-96 Array; Blackrock Microsystems Inc., Salt Lake City, UT). Spontaneous local field potentials in layer IV of right auditory cortex were obtained under anesthesia in the tone-exposed groups and non-exposed controls. At each recording site, the frequency response area (FRA) was estimated from multiunit firing activities in response to binaural tone bursts. Cross-correlation coefficient between signals quantified local synchrony within the auditory cortex.

Results

The exposed group exhibited a decreased inhibition of startle reflex response in 32 kHz background noise in the gap inhibition test without affecting the pre-pulse inhibition, suggesting the onset of tinnitus around 32 kHz. The neural synchrony in spontaneous activities between 10 kHz and 22–45 kHz tonotopic regions increased in the exposed group. This synchrony was significantly positively correlated with tinnitus scores in the gap inhibition test, whereas no such relationship was found in the controls.

Conclusion

Thus, local field potential synchrony within the tonotopic map in the auditory cortex is a potential neural correlate of tinnitus. The neural correlate of tinnitus may lead to future therapeutic and diagnostic applications.

PD 78

Enhanced olivocochlear feedback after cochlear synaptopathy may contribute to tinnitus suppression

Calvin Wu[1]; David T. Martel[2]; Leslie Liberman[3]; M. Charles Liberman[3]; Susan Shore[4]
[1]University of Michigan Ann Arbor; [2]University of Michigan, Ann Arbor; [3]Harvard Medical School; [4]University of Michigan

While tinnitus is closely associated with sensorineural hearing loss, ~10-15% of tinnitus sufferers do not have clinically measurable threshold deficits, and only 60% of cases with hearing loss report tinnitus comorbidity. The apparent loose association is likely due to many factors including: 1) that cochlear synaptopathy may be key to tinnitus generation, yet is undetected by threshold audiometry, and 2) that modulation of response gain in auditory central pathways, including cochlear feedback loops, is important in tinnitus suppression.

To test the role of cochlear synaptopathy and cochlear feedback gain in tinnitus generation, we induced temporary threshold shifts using mild noise exposures in guinea pigs and assessed tinnitus using gap-prepulse inhibition of acoustic startle. Tinnitus was confirmed in 16 of 27 (~60%) guinea pigs. While all noise-exposed guinea pigs showed suprathreshold ABR wave I decrements and cochlear ribbon-synapse losses compared to controls, no difference in the degree of synaptopathy was observed between the exposed-tinnitus (ET) and exposed-no-tinnitus (ENT) subgroups. Despite equivalent synapse loss, the ENT subgroup showed an increased density of lateral olivocochlear efferent innervation, as revealed by immunostaining of cochlear whole mounts for choline acetyltransferase (ChAT), and as quantified by measurement of silhouette area in maximum projections of confocal z-stacks from the ChAT channel.

Together, these results suggest 1) that synaptopathy alone is insufficient to cause tinnitus after noise exposure, and 2) that increased feedback from the cholinergic lateral efferents may be involved in central mechanisms working to stabilize spontaneous activity in the ascending auditory pathways.

PD 79

Comparison of salicylate-induced and noise-induced tinnitus rat models

Sylvie Cosnier-Pucheu[1]; Veronique Baudoux[1]; Philippe Larroze-Chicot[1]; Aurore Marie[1]; Maida Cardoso[2]; Amandine Laboulais[2]; Yves Cazals[3]; Arnaud Noreña[4]; Cristophe Goze-Bac[2]; Sergio Gonzalez-Gonzalez[1]
[1]Cilcare, Montpellier, France; [2]BionanoNMRI, CNRS, University of Montpellier, France; [3]INSERM; [4]Université d'Aix-Marseille, Centre national de la recherche scientifique (CNRS)

Tinnitus, the perception of a "phantom" sound in the absence of external stimulation, is a common conse-

quence of damage to the auditory periphery. It affects around 15% of the population and may induce intolerable discomfort. Whereas some drug candidates are in the process of being developed, nowadays no effective treatment exists to cure tinnitus. Because it remains very difficult to detect tinnitus objectively in animal models, carry out new quantitative methods become the key step to develop new compounds involved in tinnitus treatment.

Aim

The objective of this study is to compare the salicylate-induced and the noise-induced tinnitus rat models using three robust and validated experimental in vivo techniques: behavioral tests, auditory cortex electrophysiology and brain in vivo imaging.ß

Material and Methods

For salicylate-induced tinnitus model, salicylate is administered by intraperitoneal injection at 300mg/kg/day. For acoustic trauma-induced tinnitus model, animals are exposed to a unilateral acoustic trauma of 116 to 118dB SPL of two octaves (8-24KHz) band noise centered at 16 kHz during 1h. Two hours after salicylate administration or 30 days after acoustic trauma the presence of tinnitus is determined using gap prepulse inhibition test, unicellular electrophysiology of primary auditory cortex and in vivo manganese enhanced MRI.

Conclusion

ßThe combination of behavioral test, electrophysiology recording and in vivo imaging allows to measure putative signs of tinnitus in both rat models. Similar results were observed in electrophysiology and MEMRI imaging read-outs for salicylate and noise induced tinnitus model. However, using gap prepulse inhibition test, we observed that salicylate induced tinnitus at the broadband noise (bbn) whereas the acoustic trauma induced tinnitus at 12, 16 and 24 kHz but not at the bbn. Taken together, these data open the door for screening and characterization of new drug efficacy on tinnitus disorder.

PD 80

A new method for assessing masking and residual inhibition of tinnitus

Philippe Fournier[1]; Anne-Flore Cuvillier[1]; Stéphane Gallego[2]; Alain Londero[3]; Arnaud Noreña[1]
[1]Université d'Aix-Marseille, Centre national de la recherche scientifique (CNRS); [2]Institut des Sciences et Techniques de la Réadaptation, Lyon, France; [3]Hôpital Européen Georges-Pompidou, France

Purpose

While masking and residual inhibition (RI) may provide diagnostic and prognostic valuable information, these measures are rarely performed in clinics, as they are not adapted to clinical constraints. In this context, we devised a new method to assess these measures. The main goal of the present study was to validate this new method.

Methods

The new method used an acoustic sequence made of pulsed acoustic stimulation of fixed duration and inter-stimulus interval. Firstly, the level of the stimulus was raised until the tinnitus was masked during the stimulus presentation (measurement of the minimum masking level - MML). Secondly, the level of the stimulus was raised further (from the MML) until tinnitus is suppressed during the silence interval between the acoustic pulses. A total of 68 participants with continuous tinnitus (either unilateral or bilateral) including large variety of hearing loss configurations were tested in two different sites with two different teams: Marseille (n=34) and Lyon (n=34). Different parameters such as the stimulation duration (1 sec, 3 sec and 5 sec) and frequency of the center noise were tested.

Results

Overall, tinnitus masking was obtained in at least one condition for all of the 64 tinnitus patients tested except one (98.5%) and some level of residual inhibition was obtained for 59 participants (86.7%). In terms of stimulation durations, the 3 and 5 seconds stimulations provided both, optimal masking and inhibition, compared to the 1 sec stimulation. The RI was found stronger (lower MRIL from this new approach) within the frequency region close to the tinnitus frequency. Conclusions: Our study confirms that, from this new approach, MML and MRIL can be easily, quickly and reliably obtained from a wide variety of patients displaying different hearing loss configurations such as presbyacusis, flat hearing loss and even normal hearing. More so, this approach allows the categorization of tinnitus patients into different sub-groups based on the properties of their MRIL. Thus, MRIL may provide crucial prognostic information on clinical approaches based on acoustic stimulation and could even be used as a treatment approach.

PS 553

Long-term changes in neural firing rates in primary auditory and rostral belt cortices following noise exposure and bimodal stimulation are tinnitus and cholinergic dependent.

Gregory Basura[1]; David T. Martel[2]; Rasha Jawad[1]; Juan San Juan[1]; Susan Shore[1]
[1]*University of Michigan; [2]University of Michigan, Ann Arbor*

Background
We previously demonstrated that bimodal stimulation (spinal trigeminal nucleus [Sp5] paired with best frequency tones) could induce long-term alterations in tone-evoked and spontaneous firing rates (SFRs) in primary auditory cortex (A1) and the associative rostral belt (RB) cortex (Basura et al., 2015; Takacs et al., 2017) in guinea pigs with and without noise-induced tinnitus. Since the cholinergic system can influence neural plasticity in numerous cortical areas, the rationale for the present study was to determine if long-term bimodal plasticity in A1 and RB is influenced by cholinergic inputs to play a role in tinnitus.

Methods
Artificial cerebrospinal fluid (ACSF) or muscarinic receptor blocker, atropine (ATR) was infused into A1 using drug-delivery silicon probes (Neuronexus). Guinea pigs were divided into sham (S) and unilateral (left ear) temporary threshold shift noise-exposure groups with (ET) and without evidence of tinnitus (ENT) per gap-induced pre-pulse inhibition of the acoustic startle. Simultaneous extra-cellular single-unit responses were recorded from the contralateral A1 and RB before (at time of drug delivery) and after bimodal stimulation (pairing interval of 0 ms). Tone-evoked responses and SFRs were compared to baseline (after drug delivery, before bimodal stimulation) 15, 60 and 120 min minutes after bimodal stimulation in the presence of ACSF or ATR.

Results
Significant increases in A1 tone-evoked and SFRs were observed after noise exposure only in ET animals. ATR suppressed both tone-evoked and SFRs prior to bimodal stimulation in A1. Bimodal stimulation suppressed A1 tone-evoked firing rates below pre-drug levels for 2 hours; an effect independent of ATR. In contrast, ATR blocked the effects of bimodal stimulation in ENT animals. SFRs in A1 were only suppressed 2 hours after stimulation compared to pre-drug levels. In ET animals, ATR reversed bimodal stimulation on SFRs at 15 and 60 min. In RB, ATR applied to A1 increased tone-evoked and SFRs prior to bimodal stimulation in S and ENT animals but decreased firing rates in ET. Bimodal stimulation reversed the effects of ATR in S animals out to 2 hours and decreased tone-evoked and SFRs at 60 and 120 min in ET; an effect that was heightened by ATR.

Conclusions
The findings demonstrate that the observed neural changes in A1 may contribute to tinnitus etiology. Furthermore, muscarinic receptor blockade differentially affects tone-evoked and SFRs in A1 and the RB, a finding that may give clues as to underlying mechanisms contributing to tinnitus perception.

PS 554

Localizing vocalizations in space with high precision to study social interactions

Jesse Heckman; Reinder Dorman; Minty Vissers; **Bernhard Englitz**
Donders Institute for Brain Cognition and Behaviour, Radboud University

Mice display a wide repertoire of vocalizations that varies with age, sex, and context. Especially during courtship, mice emit ultrasonic vocalizations (USVs) of high complexity, whose detailed structure is poorly understood. As animals of both sexes vocalize, the study of social vocalizations requires attributing single USVs to individuals.

The state-of-the-art in sound localization for USVs in 2D allows spatial localization at centimeter resolution. However, animals interact at closer ranges, involving tactile, snout-snout exploration. Hence, improved algorithms are required to reliably assign USVs. We have developed a general solution to this problem using a minimal number of microphones for localizations in 1D, 2D and 3D. The algorithm combines an analytic correction for relative microphone height, an improved generalized cross-correlation and a probabilistic combination of microphone estimates. The reliability of the algorithm is verified on artificial sounds and real interactions of multiple animals on a free running platform. We achieve a median precision of ~10mm for typical vocalizations, allowing a safe assignment of the vast majority of vocalizations to individual animals. The algorithm internally estimates its certainty for each localization, thus further improving the reliability of assignment.

In conclusion, the improved attribution of vocalizations to their emitters in 1D, 2D, and 3D lays the basis for a deeper understanding of social vocalizations, in particular sequences of USVs.

PS 555

Selective auditory attention to a single sound stream suppresses responses to temporally non-coherent sounds in ferret auditory cortex

Kelsey Dutta[1]; Kai Lu[1]; Wanyi Liu[1]; Jonathan Fritz[1]; Shihab Shamma[2]
[1]*University of Maryland;* [2]*Ecole Normale Supérieure, University of Maryland*

Background
Most natural acoustic stimuli are complex sounds that have many spectral components as well as temporal feature dimensions such as intensity, pitch contour, timbre, amplitude and frequency modulation rates. The ability to "bind" many frequency components of the auditory environment into few perceptual "streams," and to selectively attend to a single stream, is a fundamental function in listening and attention whose mechanisms are unresolved. The present study explores the neural correlates and mechanism of auditory stream binding and segregation.

Methods
Ferrets were trained on Go vs. Nogo selective attention task to detect an amplitude change in a narrowband noise stream. The stimulus included an alternating tone sequence with one tone temporally coherent with the noise stream. In half the trails, the frequencies of the coherent and incoherent tones were reversed. This paradigm provides insight into the "binding hypothesis" that responses to tones synchronous with the attended noise would be enhanced, whereas responses to asynchronous tones would be suppressed.

Results
Neurons in multiple areas of auditory cortex exhibited a significant correlation between the temporal coherence effect and the tuning properties. Neurons responding to tone sequences asynchronous with the noise stream were significantly suppressed. The effects are mostly seen during behavioral engagement.

Conclusion
Sound components which are asynchronous with the attended stream are suppressed in multiple areas of auditory cortex. Temporal coherence is a driver for perceptual binding of frequency components in attended sound streams.

PS 556

Feature selectivity and vocalization processing across auditory cortex of the common marmoset

Xiao-Ping Liu; Xiaoqin Wang
Department of Biomedical Engineering, Johns Hopkins University

In the visual system, a general understanding has emerged regarding the nature of basic visual features and their hierarchical and parallel composition through identified anatomical structures to process complex natural stimuli, such as faces. A similar level of understanding of the auditory system has yet to emerge. Marmosets are highly vocal non-human primates whose auditory cortices have been extensively mapped. Although a number of studies in non-human primates have looked at cortical processing of natural sounds such as conspecific vocalizations, there is a lack of a systematic exploration of the receptive fields and selectivities underlying vocalization-selective responses. Secondly, the anatomical organization of processing remains unclear. Some possible processing schemes have been proposed, for example, a core-to-belt hierarchy, posteriorly-directed "where" versus anteriorly-directed "what" pathways, a combination of both, or other models entirely. We performed single-unit extracellular recordings along the full extent of auditory cortex in awake marmoset to characterize a set of receptive field properties followed by responses to pre-recorded and synthetic marmoset vocalizations. This approach allowed us to dissect the feature selectivity underlying vocalization selectivity and look for differences in processing between auditory cortical fields that may point to hierarchical or parallel streams of processing. We found that many neurons preferred one to a few vocalization types, and in a number of cases, this selectivity could be understood by property tuning to simpler stimuli, such as bandwidth preference or linear FM direction selectivity. Some neurons seemed to better convey temporal information, while others better conveyed spectral information, consistent with proposed notions of spectrotemporal trade-off. Neurons in the lateral belt did not appear to show greater selectivity for call type than those in the auditory core. These preliminary results begin to identify features useful in the processing of vocalizations and will help us better understand the anatomical organization of auditory cortical processing.

PS 557

Responses of auditory cortex neurons in mutant mice lacking of the two-pore channels: is there a deficit in processing communication sounds?

Juliette Royer; Florian Occelli; Chloé Huetz; Jose-Manuel Cancela; Jean-Marc Edeline
NeuroPSI UMR CNRS 9197

The responses of auditory cortex (ACx) neurons to communication sounds are influenced by a myriad of physiological factors, and among them, the concentration of neuromodulators and neurohormones can exert a powerful control on the strength and the temporal reliability of cortical responses (Edeline 2012).

Over the last years, our team has been working on mutant mice lacking two-pore channels (TPC1 and TPC2). Two-pore channels (TPCs) are important members of the voltage-gated ion channel family: they mediate Ca(2+) signals through the Ca(2+)-mobilizing messenger nicotinic acid adenine dinucleotide phosphate (NAADP) to control a range of Ca(2+)-dependent events, such as the release of numerous neuromodulators and neurohormones. Compared with WT mice, TPC KO mice show a deficit in maternal behavior. As (i) the pups of TPC KO mice loudly vocalize and (ii) these mice present ABRs similar to WT mice (tested < 4 months), we evaluated whether the cortical processing of vocalizations were similar in WT and TPC KO mice.

Responses from ACx neurons were tested under Ketamine/Xylazine anesthesia using both adult and pups calls and also heterospecific vocalizations. With pure tones, the receptive fields of ACx neurons slightly differed: they were of shorter duration and spectrally narrower in TPC KO mice than in WT mice. Also, the BF distribution was slightly shifted toward lower frequencies in TPC mice. When tested with communication sounds, the firing rate (FR) evoked by pups and adult vocalizations was lower in TPC mice than in WT mice. The temporal reliability of the responses, indexed by the CorrCoef index, was lower in TPC mice than in WT mice. Finally, the neurons discriminative ability, indexed by mutual information, was also lower in TPC mice than in WT mice. Altogether, these results suggested that, despite normal audiograms (from ABR), the processing of communication sounds is less efficient in ACx of TPC mice. Obviously, there are potentially many physiological differences between WT and TPC mice. Recently, it was shown that, in virgin mice, Ocytocine (OT) injections facilitate ACx responses to pup calls (Marlin et al 2015). Therefore, plasmatic concentrations of different neurohormones (OT, vasopressine) and/or intracerebral concentrations in neuromodulators have to be measured. Future experiments will also be performed in natural situations such as in WT dams (where OT concentration is higher) to evaluate the contribution of OT.

PS 558

Auditory cortex interneuron development requires cadherins operating hair-cell mechanoelectrical transduction

Baptiste Libé-Philippot[1]; Vincent Michel[1]; Jacques Boutet de Monvel[1]; Sébastien Le Gal[1]; Typhaine Dupont[1]; **Monica Dias Morais**[1]; Mathilde Gagliardini[1]; Paul Avan[2]; Christine Métin[3]; Nicolas Michalski[1]; Christine Petit[4]
[1]Institut Pasteur, INSERM UMRS 1120, Université Pierre et Marie Curie; [2]Centre Jean Perrin, Université Clermont Auvergne, INSERM UMR 1107; [3]Institut du Fer à Moulin, INSERM UMRS 839; [4]Institut Pasteur, INSERM UMRS1120, Université Pierre et Marie Curie, Institut de la Vision, Collège de France

Many genetic forms of congenital deafness affect the sound reception antenna of cochlear sensory cells, the hair bundle. The resulting sensory deprivation jeopardizes auditory cortex (AC) maturation. Early prosthetic intervention should revive this process. Nevertheless, this view assumes that no intrinsic AC deficits coexist with the cochlear ones, a possibility as yet unexplored. We show here that many GABAergic interneurons, from their generation in the medial ganglionic eminence up to their settlement in the AC, express two cadherin-related (cdhr) proteins, cdhr23 and cdhr15, that form the hair bundle tip links gating the mechanoelectrical transduction channels. Mutant mice lacking either protein showed a major decrease in the number of parvalbumin interneurons specifically in the AC, and displayed audiogenic reflex seizures. Cdhr15- and Cdhr23-expressing interneuron precursors in Cdhr23$^{-/-}$ and Cdhr15$^{-/-}$ mouse embryos, respectively, failed to enter the embryonic cortex and were scattered throughout the subpallium, consistent with the cell polarity abnormalities we observed in vitro. In the absence of adhesion G protein-coupled receptor V1 (adgrv1), another hair bundle link protein, the entry of Cdhr23- and Cdhr15-expressing interneuron precursors into the embryonic cortex was also impaired. Our results demonstrate that a population of newborn interneurons is endowed with specific cdhr proteins necessary for these cells to reach the developing AC. We suggest that an "early adhesion code" targets populations of interneuron precursors to restricted neocortical regions belonging to the same functional area. These findings open up new perspectives for auditory rehabilitation and cortical therapies in patients.

PS 559

A new electrophysiological technique to determine gap detection thresholds as a measure of central auditory processing in a rat model

Emre Ocak[1]; Jorge Bohorquez[2]; Rahul Mittal[1]; Jeenu Mittal[1]; Adrien Eshraghi[1]
[1]*Hearing Research Laboratory, Department of Otolaryngology, University of Miami Miller School of Medicine, Miami, FL 33136, USA;* [2]*Department of Biomedical Engineering, College of Engineering, University of Miami*

Background

Gaps embedded in noise (GIN) have been used as acoustic stimulus to evaluate the auditory temporal processing of different study populations such as in subjects with central auditory processing disorders (CAPD). Since GIN are very short as miliseconds (ms), they have been used to evaluate temporal resolution which is defined as the ability to detect small changes in sound over time, or slight discontinuities in ongoing stimuli. Poor temporal resolution has been shown to correlate with speech recognition difficulties. The gap detection threshold (GDT) is defined as the shortest gap that can be perceived in an otherwise continuous background stimulus. Electrophysiological assessment of GIN has focused mainly on Late Latency Responses requiring awake alert subjects (humans or animals). As rat models are commonly employed to understand the molecular mechanisms underlying auditory disorders, there is a need to develop techniques to determine CAP in experimental animal models. The aim of this study was to develop an electrophysiological technique that can be used as an objective measure of CAP in anesthetized rat model.

Methods

We developed method to find the Objective Gap Detection Threshold (OGDT) in rats. QSSR elicited by noise modulated by 40Hz gaps of different durations were analyzed in time and frequency domains. The detection was performed in frequency domain, by applying the Hotelling';s T2 test to the 40Hz complex fundamental frequency component. The OGDT is estimated by analyzing the confidence ellipses of the 40Hz spectral component.

Results

When the confidence ellipses (p=0.05) contain the origin of the complex plane, we can state that the subject is not significantly detecting the noise gap. We observed that the rats were detecting noise gaps of 12, 10 and 8ms and not detecting the 6ms gap. We also observed the "vanishing" of response into the background noise when a 4ms noise gap is applied. The 5ms OGDT result was verified by the statistical T2 test and is consistent with the previous animal studies with awake rats.

Conclusions

We have developed an electrophysiological method to determine GDT as a measure of CAPD in anesthetized rat model. This technique eliminates the need for being alert and awake during the test bringing a new dimension especially in animal experiments regarding central auditory evaluation. Studies are in progress in our laboratory to validate this technique employing animal models of neurological disorders and cochlear implant where CAPD is commonly observed. A better understanding about CAPD will help in developing novel interventions.

PS 560

Stability of Frequency Tuning and Acoustic Threshold of Auditory Cortical Neurons Across Arousal States

Zachary P. Schwartz[1]; Stephen V. David[2]
[1]*Neuroscience Graduate Program, Oregon Health and Science University;* [2]*Oregon Health and Science University*

Recent research indicates that luminance-independent fluctuations in pupil size predict variability in spontaneous and sound-evoked activity of single neurons in auditory cortex (McGinley, David, and McCormick Neuron 2015). These findings suggest that pupil is an indicator of large-scale changes in brain state that, in turn, affect sensory cortical function. However, it remains unclear whether pupil-related state influences the selectivity of auditory neurons. We recorded pupil size and single-unit spiking activity in the primary auditory cortex (A1) of non-anesthetized ferrets during presentation of tone-pip sequences sampling a range of frequencies and sound levels. We then characterized neural selectivity by measuring the average response to each distinct sound. Pupil size predicted changes in baseline activity and the gain of sensory responses to tone-pips, consistent with earlier findings on the variability of responses to natural sounds (Schwartz and David ARO 2017). In the majority of neurons, pupil-related modulations consisted of a shift and/or scaling of the frequency-response area without changes to its shape. In most neurons, parametric measures of tuning including acoustic threshold, tuning bandwidth, and best frequency similarly remained stable across large changes in pupil size. These findings suggest that the arousal state indexed by pupil size predominantly modulates the overall excitability of A1 neurons rather than their sensory selectivity.

PS 561

Cutting for Medial Olivocochlear Bundle Increases Susceptibility of the Auditory Cortex to Noise Overexposure in Mice

Lian Fang; Jiamin Zhou; Yue Zhang
The First Affiliated Hospital of Wenzhou Medical University

Introduction

It has previously been shown that noise-induced hearing loss is associated with apoptosis-related physiological and anatomical changes within the central auditory pathway. The auditory center provides an efferent innervation to the cochlea through medial olivocochlear(MOC) axons. The MOC function is to protect cochlea from acoustic overstimulation through suppressing cochlear response and regulating cochlear afferent signaling. However, little is known about the protective effect of medial olivocochlear system(MOCS) for auditory cortex. To determine the role of MOCS in noise-induced cellular apoptosis of auditory cortex, we cut crossing or uncrossing MOC bundle to clarify the role of MOC efferent nerve on the auditory center. Then, p27 and caspase3 were both detected to suggest apoptotic cells in the auditory cortex following noise overstimulation.

Methods

In this study, we used noise exposure to induce cell apoptosis of auditory cortex after cutting MOC bundle. We divided C57 mice into 3 groups, Group 1: control; Group 2: cutting for crossing MOC bundle; Group 3: cutting for crossing and uncrossing MOC bundle. Mice were noise-exposed (4h, white noise) at 98 dB SPL for four days and investigated immediately at 1d, 1w, 2w, and 4weeks after the noise exposure. We examined all samples for the expressions of p27 and caspase3 with immunohistochemical method and analyzed the time course changes of their expressions for the auditory cortex.

Results

In the present work, we found that p27 and caspase3-positive cells were elevated at 2 and 4 weeks after noise exposure in three groups. However, there was a statistically significant difference between groups in the expressions of p27 and caspase3 after 2 weeks, except for Group2 and 3. Moreover, Group3 showed a significant decrease in cell number at 4 weeks after noise exposure compared to the other groups.

Discussion

These data indicate that cutting for crossing or uncrossing MOC bundle will both increase apoptotic cells of auditory cortex following noise exposure. Moreover, cutting for the whole MOC bundle may increase susceptibility to noise-induced hearing loss and facilitate the apoptosis-related cell loss in auditory cortex. MOCS proved to be potentially effective in the prevention for cell apoptosis of auditory cortex after noise exposure in C57 mice. Thus, an increased MOC function may contribute to the protection of the auditory center from noise trauma.

PS 562

The use of wavelets during image reconstruction in mouse X-ray tomography

Claus-Peter Richter[1]; Christoph Rau[2]
[1]*Department of Otolaryngology-Head and Neck Surgery, Feinberg School of Medicine, Northwestern University & Resonance Medical, LLC, Chicago;*
[2]*Diamond Light Source*

Background

It has been demonstrated previously that cochlear soft tissue structures can be imaged without opening the cochlea. The method uses synchrotron radiation and relies on inline phase contrast imaging. For our first successful efforts to image the soft tissue structures of a cochlea, we decalcified the specimen before scanning. We were able to image soft tissue structure at a resolution that allows the identification of single outer hair cells and spiral ganglion neurons. The reconstructed images could also be used for quantitative analysis. Hair cells and spiral ganglion neurons can be counted manually. Likewise the numbers can be obtained automatically using custom written software. In a recent effort we have furthered the method and are now able to visualize soft tissue structures without decalcifying the specimen. One of the methods includes the pre-processing each of the projections captured during the scanning.

Methods

Calcified and decalcified mouse cochleae were scanned at Diamond Light Source (UK) and were subsequently reconstructed. The resulting images were examined for cochlear bony and for soft tissue structures. To improve the reconstructions, we applied a wavelet transform to each of the images. Two approaches were selected, a line-by-line analysis and reconstruction of the image and a 2D approach. Testing the majority of available mother wavelets for the analysis, it appears that the morel mother wavelet is a good choice. The coefficient vector resulting from the wavelet transform were manipulated accordingly and a reverse wavelet transform was applied. The resulting images were than used for the reconstruction of the samples.

Results

We used the discrete wavelet transform up to level 10

with the 'morel'; mother wavelet. In particular levels above level 6 were reduced in amplitude. The results demonstrate that contributions by strongly absorbing materials can be reduced. The latter helps in the reconstruction of the projections, which are used for the tomographic reconstructions of the samples.

Conclusions: Improvements of the reconstruction methods are necessary to enable identification of cochlear soft tissue structure in vivo.

PS 563

Network-Level Control of Frequency Tuning in Auditory Cortex

Hiroyuki K. Kato[1]; Samuel K. Asinof[2]; Jeffry S. Isaacson[2]
[1]*University of North Carolina at Chapel Hill;* [2]*University of California, San Diego*

Lateral inhibition is a fundamental circuit operation that sharpens the tuning properties of cortical neurons. This operation is classically attributed to an increase in GABAergic synaptic input triggered by non-preferred stimuli. Here we use in vivo whole-cell recording and two-photon Ca2+ imaging in awake mice to show that lateral inhibition shapes frequency tuning in primary auditory cortex via an unconventional mechanism: non-preferred tones suppress both excitatory and inhibitory synaptic inputs onto layer 2/3 cells ("network suppression"). Moreover, optogenetic inactivation of inhibitory interneurons elicits a paradoxical increase in inhibitory synaptic input. These results indicate that GABAergic interneurons regulate cortical activity indirectly via the suppression of recurrent excitation. Furthermore, the network suppression underlying lateral inhibition was blocked by inactivation of somatostatin-expressing interneurons (SOM cells), but not parvalbumin-expressing interneurons (PV cells). Together, these findings reveal that SOM cells govern lateral inhibition and control cortical frequency tuning through the regulation of reverberating recurrent circuits.

PS 564

Effects of inhaled particulate matter on perineuronal nets in the mouse primary auditory cortex

So Young Kim[1]; Moo Kyun Park[2]
[1]*CHA Bundang Medical Center;* [2]*Seoul National University Hospital*

Objective
The adverse effects of particulate matter on airway and cardiovascular system are well known. However, there is still a lack of research on the effects of particulate matter exposure to the central nervous system, including the auditory cortex. Perineuronal nets are specialized extracellular matrix that commonly enwraps cortical parvalbumin (PV) containing GABAnergic interneurons. Whether changes to cortical PNNs follow exposure to particulate matter (PM) remains unclear. The aim of the present study was to examine how PM impacts on oxidative stress and inflammatory processes in the brain cortex. In addition, this study examines PV/PNN expression in primary auditory cortex following PM exposure.

Methods
C57/BL6 mice were exposed for four and eight weeks to PM (100ug/m3). Different brain regions (olfactory bulb, frontal cortex, striatum, and primary auditory cortex) were harvested from the mice following exposure to PM. Prooxidant (HO-1 and SOD-2), inflammatory marker (TNFa), proliferative markers (neurotropin-3 and BDNF) and unfolded protein response markers (XBP-1S and BiP) were measured using real-time PCR and western blot. Sections containing A1 were imaged using a confocal microscope at 20X. The numbers of PV and PNN cells were counted using PV and WFA staining. Results: The expressions of HO-1, SOD-2, and TNFa were elevated in accordance to the exposure to PM. On the other hands, neurotropin-3 and BDNF were decreased after exposure to PM. The 8 week PM exposure group showed more augmented changes of markers than those of 4 week PM exposure group. The impacts of PM were different according to brain regions. In the primary auditory cortex, WFA were increased in overall. However, the number of PV only and PV+WFA co-staining cells were decreased after PM exposure.

Conclusion
PM activated oxidative stress and inflammation in various brain cortical areas with different amounts. The chronic exposure to PM induced decreased number of interneuron and unwrapped with PNNs, which might contribute to PM-related central auditory dysfunction, such as cognition.

PS 565

Cortical robustness to real-world background noise differentiates primary from non-primary auditory cortex

Alexander J. E. Kell[1]; Erica N. Shook[1]; Josh H. McDermott[2]

[1]Department of Brain and Cognitive Sciences, MIT; Center for Brains, Minds, and Machines, MIT; [2]Department of Brain and Cognitive Sciences, MIT; Center for Brains, Minds, and Machines, MIT; Program in Speech and Hearing Biosciences and Technology, Harvard

In everyday listening, sounds of interest are often embedded in background noise. The brain must be robust to the effects of such noise in order to recognize sound sources. Previous work has primarily studied robustness to unnatural, synthetic sounds, such as spectrally-shaped noise. Here we examined robustness to real-world noise sources. We measured fMRI responses in human auditory cortex to a set of thirty natural sounds, presented in quiet as well as embedded in thirty different everyday background noises (bacon frying, rain hitting pavement, etc.). We quantified the robustness of neural responses to background noise by correlating each voxel';s response to the natural sounds in isolation with its response to the natural sounds mixed with background noise. This measure quantifies the extent to which a voxel';s response is the same when sounds are presented in quiet and when they are embedded in noise. Responses in anatomically-defined primary areas (TE 1.1 and 1.0) were substantially affected by background noise (r2 ~ 0.40). However, voxel noise-robustness was substantially higher in non-primary areas, in some cases being hardly affected by the background noises (r2 ~ 0.80). Mean responses in primary and non-primary regions were both only slightly lower in the presence of background noise, indicating that the difference in robustness between regions was not due to background noise differentially suppressing responses in primary areas. The results were replicated in a follow up experiment in which speech and music were excluded from the sound set, indicating that the robust responses in non-primary areas were not merely due to previously-reported selectivity for speech and music. Additionally, to compare our results with previous work, we ran an experiment in which we replaced the real-world backgrounds with Gaussian noise whose spectrum was matched to a real-world background. We found that primary auditory cortex was substantially more robust to these synthetic backgrounds, and nearly as robust as non-primary areas. The results begin to illustrate the neural underpinnings of everyday noise robustness, and suggest that a key physiological signature that differentiates primary and non-primary auditory cortex is robustness to real-world background sounds.

PS 566

Is the Auditory P1-N1-P2 Response a Biomarker for Deprivation-Related Cortical Plasticity?

Kate McClannahan[1]; Kristina C. Backer[2]; Kelly Tremblay[3]

[1]Washington University in St. Louis; [2]University of California, Davis; [3]University of Washington

There is currently a push to identify cortical auditory evoked potentials (CAEPs) sensitive to sound deprivation related changes in the brain. Recent studies propose CAEPs, specifically the P1-N1-P2, as candidate responses, showing differences between those with and without hearing loss. However, most studies have not accounted for differences in stimulus audibility or, moreover, separated those who do vs. do not receive daily auditory stimulation through the use of hearing aids. Subsequently, differences in evoked neural response patterns may be driven by one or a combination of: 1) stimulus presentation level artifacts, 2) deprivation-related changes in cortical function, or 3) stimulation-related neural plasticity. In this study, we hypothesized that stimulus audibility contributed to cortical evoked activity differences previously reported in the literature. We tested this hypothesis, as well as determined the effect of hearing aid use on the brain, by comparing CAEPs to a synthetic speech syllable (/ba/) across 3 age-matched groups of older adults with different hearing abilities, (normal hearing (NH), untreated age-related hearing loss (u-HL), and treated age-related hearing loss (t-HL), under two stimulus level conditions (equal sound pressure level (SPL) and equal sensation level (SL)). Cluster-corrected permutation tests revealed significant differences in the P1-N1-P2 response between groups. Specifically, there were increased latencies for both HL groups, when compared to NH, at time-points consistent with the P1 and N1-P2 transition, but only when the sound was played at the same physical level for all participants in the equal SPL stimulus condition (i.e. equal SPL across groups). There were no significant differences between NH and u-HL or between u-HL and t-HL when sounds were modified to account for hearing thresholds in the SL condition. However, differences emerged during the N1 component window when comparing NH to t-HL. Our results suggest that 1) group differences in neural responses previously described may be driven by stimulus audibility and not evidence of experience-related changes in the brain previously attributed to auditory deprivation; and 2) there are differences in cortical response patterns between NH and t-HL that are not found in non-hearing aid users, once hearing thresholds are taken into account. Funded by NIH NIDCD F30 DC010297, T32-DC005361 and AAA Student Investigator Research Grant.

PS 567

Task-relevant modulation of neuronal phase-locking in primary auditory cortex

Manuel Beiran[1]; Martin Averseng[1]; Shihab Shamma[2]; Yves Boubenec[3]
[1]Ecole Normale Supérieure; [2]Ecole Normale Supérieure, University of Maryland; [3]Ecole Normale Supérieure, Paris, France

Studying changes in neuronal responses induced by task-engagement is crucial to understanding how the brain processes inputs to match behavioral demands in a changing environment. These behavior-dependent plastic changes in neuronal responses have already been reported in auditory primary cortex (A1) (Fritz et al. 2003), with responses to sounds near the target tone frequency enhanced compared to other frequencies. However, the dynamics of such plastic changes along the course of stimulus presentation have not yet been investigated. In this study, we investigated how task engagement modulates A1 phase-locked neuronal responses in a task-relevant manner.

We analyzed A1 extracellular recordings from two adult ferrets trained to perform a discrimination task , in which they had to distinguish between Go (Reference) and No-Go (Target) stimuli corresponding to click trains of different rates. The activity of the same neural population was recorded when the animals were engaged in the task, and when they passively listened to the same stimuli. We applied linear reconstruction techniques at the single-trial level, providing an estimate of stimulus temporal information as it is encoded by each neuron. We assessed changes in neuronal encoding using reconstructed data from the passive and active conditions.

As suggested by previous studies (Bagur et al, submitted), we found that the global quality of phase-locked encoding was substantially degraded for all stimuli during task engagement, due to an increase in spontaneous firing rate. However, we observed that reconstruction accuracy was larger for target click trains than for reference stimuli during behavior. Furthermore, the encoding accuracy of click timings increased along the presentation of target stimuli, while it decreased for reference stimuli, suggesting a modulation of click-evoked phase-locked responses over the course of stimulus presentation. These effects were not observed in passive sessions recorded before and after the active sessions, indicative that this task-relevant modulation of neuronal phase-locking is a rapid process. Overall, we demonstrated that A1 neuronal phase-locking can be rapidly modulated not only by behavioral states, as previously shown, but also to match behavioral requirements.

PS 568

Inter-Hemispheric and Inter-Regional Comparisons of Click Train Responses in Parabelt Auditory Cortex

Deborah Ross[1]; Yoshinao Kajikawa[1]; Troy Hackett[2]; Charles Schroeder[3]
[1]Nathan Kline Institute; [2]Vanderbilt University, Medical Center; [3]Columbia University

The auditory cortex of primates contains three major regions (core, belt, parabelt) arranged in a processing hierarchy. The highest known stage is the parabelt (PB), which occupies a large region located on the superior temporal gyrus (STG). Ongoing studies in our laboratory are aimed at understanding the nature of the auditory processing in this region. The current study highlights a subset of that work aimed at revealing potential hemispheric differences in processing. Studies in humans suggest that the left and right hemispheres are specialized for the processing of temporal and spectral information, or fast and slow temporal information, respectively. Further, the progression of functional asymmetry from the core to higher areas, such as the PB, are also suggested. In this study, we compared responses to click trains in the PB between hemispheres and with the core. One monkey had 3 recording chambers, two over the PB region in both hemispheres, and one targeting the core region on the right side. Another monkey was implanted with a recording chamber on the left STG. We delivered 640 ms click trains (inter-click intervals: logarithmic steps from 320 to 5 ms via free field speakers, and recorded MUA responses using linear-array microelectrodes. Responses during the second half (320 ms) of click trains were used to construct periodograms and derive vector strength (VS), best synchronous frequency (BMF) and synchronization boundary frequency (Bound-F). Comparisons were made between left PB, right PB and right core using Kruskal-Wallis tests. Preliminary results showed that all sites in the core responded to clicks, and synchronously to trains up to 200 Hz. In PB, many sites lacked responses to clicks or responded with suppression at repetition rates at >25 Hz. All 3 measures of synchrony (VS, BMF, and Bound-F) showed the trend of Core > left PB > right PB. The results are suggestive of the difference in temporal processing between hemispheres, in favor of greater temporal precision in the left hemisphere than the right, concordant with findings in humans.

PS 569

Effect of Hearing on Cognitive Impairment and Alzheimer's Disease

Dami Kim; Munyoung Choi; Alphonse Umugire; Hyong-Ho Cho; **Sungsu Lee**
Chonnam National University Hospital

Introduction Both hearing loss(HL) and Alzheimer's disease(AD) are steeply rising due to population aging. It is already clinically reported that hearing loss accelerates cognitive decline and dementia. There has been some suggestion that glutamate receptor genes are both working in age-related HL and AD. Others proposed that progressive mitochondrial dysfunction are noted in HL and AD. However, due to the lack of proper model and method, it was not thoroughly studied in vivo. Herein, we wanted to establish an in vivo model to investigate the effect of HL to cognition. Methods Several transgenic mice that over-expressed amyloid precursor protein and presenillin were used for Alzheimer model (Tg2576, 5xFAD, 3xAD). To induce HL, kanamycin(900mg/kg) and furosemide(200mg/kg) were administrated to 4 week-old mouse. One day after injection, destruction of the tympanic membrane were done additionally to make a complete deaf. Behavioral tests conducted were as follows; Rota-rod, open field test, Novel object, Y-maze, Morris water maze, Radial water maze, Elevated plus maze, Passive avoidance. ABR and middle latency response (MLR) were checked to evaluate hearing level and auditory pathway. Long term potentiation (LTP) was measured with brain slice to see the synaptic plasticity. PET-CT was taken to evaluate the activity of the brain. Results Behavioral test was done at age 40-50 weeks. Novel object and Y-maze test showed decreased response in AD mouse which were more lowered in HL group. Radial water maze revealed that HL group spent longer time to finish the task. In elevated plus maze, AD stayed more on the open arm, and HL group extended this time more. These all reveal that HL aggravates cognitive impairment. LTP was decreased in Tg2576 HL group. We could also see that LTP was lowered in HL group compared to normal hearing even in wild type mouse. For MLR, 5xFAD mouse demonstrated Na-Pa interlatency elongation and interamplitude decrement. We used 7 month-old 3xAD mouse for PET-CT. Transgenic mouse showed hypermetabolism on PET which was accelerated in HL group. Interestingly, HL group was hyperactive compared to normal group at this age. Conclusion HL accelerated cognitive dysfunction in both normal and AD prone conditions. Tg2576, 5xFAD, 3xAD mice were efficient model to test the effect of hearing to cognition and dementia. Hearing preservation or recovery may reduce the incidence of Alzheimer's disease.

PS 570

Streaming of spectro-temporal regularity in core and belt auditory cortex

Daniela Saderi[1]; Brad N. Buran[2]; Stephen V. David[3]
[1]*Oregon Health & Science University;* [2]*Oregon Hearing Research Center, Oregon Health and Science University;* [3]*Oregon Health and Science University*

Spetro-temporal patterns in natural sounds facilitate segregation of distinct auditory objects, or streams. Repetition is one cue that drives stream segregation. Here, we test whether ferrets can also detect these spectro-temporal regularities and assess whether evidence for streaming can be observed in the activity of neurons in core (A1) and/or belt (PEG) regions of the auditory cortex.

Stimuli were generated by summing two streams of samples randomly chosen from a set of twenty naturalistic (1/f) noise stimuli. After a random number of samples, the sample in one of the two streams began to repeat. In humans, this repetition produces stream segregation, in which the repeating samples are perceived as a distinct, foreground object against a background of the random samples.

We tested the prediction that auditory cortex neurons facilitate stream segregation by either 1) enhancing their response to all stimuli or 2) selectively enhancing their response to the repeating stream. Neural responses to the set of stimuli were fit with a linear model in which the strength of the neural response was scaled by a global repetition gain (i.e., both streams scaled equally) or stream-specific repetition gain (e.g., one stream';s response may be suppressed while the other is enhanced).

On average, we found a strong reduction in global response gain during the repeating phase relative to the random phase, and the gain decrease was stronger in PEG than in A1. This decrease is reminiscent of stimulus-specific adaptation and may compete with enhancement of responses to the foreground stream. When we measured stream-specific changes in response gain, the responses of a subpopulation of neurons to the repeating stream were either enhanced or less strongly suppressed than responses to the background stream. This stream-specific enhancement was also significantly larger in PEG than A1. We conclude that, while overall auditory responses were reduced during the repeating phase, a selective enhancement of responses to the repeating stream provides evidence for stream segregation that emerges in A1 and is refined in PEG.

PS 571

Hearing Outcomes in a Phase Ib Clinical Trial Evaluating the Safety, Pharmacokinetics, and Exploratory Pharmacodynamics of AUT00206 in Patients with Schizophrenia

Victoria A. Sanchez[1]; Anil Sajjala[2]; Alice Sharman[2]; John Hutchison[2]; Charles H. Large[2]
[1]*University of South Florida;* [2]*Autifony Therapeutics*

Patients currently treated with antipsychotics for Schizophrenia receive relief from positive symptoms (e.g., hallucinations, delusions), but still often complain of cognitive and negative symptoms including sensory processing impairments. There is an urgent need for novel therapies with improved efficacy across all symptom domains, and which have a better safety profile compared to existing drugs. AUT00206 is a novel and selective small molecule modulator of Kv3.1 and Kv3.2 voltage-gated potassium channels, which are expressed on fast-spiking (FS), parvalbumin-positive (PV+), GABA-ergic interneurons, in corticolimbic brain circuits and principal neurons of the auditory brainstem. Tests in relevant animal models suggest that AUT00206 could be an effective oral treatment for cognitive and sensory symptoms of schizophrenia. PV+ interneurons play a key role in the synchronization of cortical circuits, and in the generation of rhythms that underpin attention, sensory processing, and cognition. Thus, activation of Kv3 channels, which allow FS interneurons to fire accurately at high frequency, helps to synchronize the activity of cortical networks. There is reduced expression of Kv3.1 in the cortex of patients with schizophrenia, which may contribute to PV+ interneuron dysfunction, reduced gamma activity, and deficits in connectivity and cognition. Furthermore, patients with schizophrenia also show an impairment in central auditory processing, which we speculate could also be linked to reduced Kv3 channel function. AUT00206 is currently being evaluated in a randomized, double-blind, placebo-controlled Phase IIa clinical trial (clincaltrial.gov ID# NCT03164876) to assess the pharmacokinetics, safety and tolerability of repeated doses of AUT00206, for 28 days, as adjunctive therapy in male patients with a stable diagnosis of schizophrenia and taking stable doses of 1 or 2 antipsychotic drugs. The secondary and exploratory objectives will evaluate the effects of AUT00206 on auditory-evoked Mismatch Negativity (MMN) and additional hearing-related outcomes. It is well known that the auditory-evoked MMN is reduced in patients with Schizophrenia, but unknown if the site of lesion for the reduction in cortical activity starts lower at the brainstem or even within the auditory peripheral system. Therefore, tests selected are known to be sensitive at detecting abnormities at the level of the cortex (dichotic digits), brainstem (masking level difference), and the peripheral structures and functions (pure-tone audi-ometry, speech-in-noise, and contra-lateral suppression otoacoustic emission). Here we report the layout of the trial design, methodology and the rationale behind the selected hearing-related outcome measures and the potential of these hearing measures as biomarkers for the present and future pharmaceutical studies.

PS 572

Hearing in noise ability correlates with one back test performance in normal hearing HIV positive adults

Albert Magohe[1]; Abigail Fellows[2]; Catherine Rieke[2]; Enica Massawe[3]; Ndeserua Moshi[3]; Michael Boivin[4]; Jay Buckey[5]
[1]*Muhimbili University of Health and Allied Sciences, Dar es Salaam, Tanzania;* [2]*Space Medicine Innovations Laboratory, Geisel School of Medicine at Dartmouth, Hanover, NH, United States;* [3]*Muhimbili University for Health and Allied Sciences;* [4]*Michigan State University College of Human Medicine;* [5]*Geisel School of Medicine at Dartmouth*

Background

Individuals with HIV infection can have diffuse central nervous system (CNS) damage with cognitive slowing manifest as deficits in attention and working memory. Since understanding speech-in-noise is a neurologically demanding task, we hypothesized that central auditory processing would also be affected in HIV. To test this hypothesis we measured attention and working memory using the one-back test (OBT) and speech-in-noise interpretation ability (as a marker of central auditory capability) using the triple digit test (TDT) in HIV+, normal hearing adults in Tanzania. We expected that hearing in noise performance would correlate significantly with performance on the one-back test.

Methods

181, normal-hearing HIV+ adults (142 women, 39 men, average age 43) were tested at the Dar Dar project Infectious Disease Clinic in Dar es Salaam, Tanzania. The signal to noise ratio (SNR) on the triple digit test was correlated to OBT speed and accuracy using multiple linear regression with the SNR as the outcome variable and age, OBT results, and pure-tone averages on the right and left as predictor variables.

Results

Subjects had no middle ear disease and audiometric thresholds at 500, 1000, 2000, 4000 Hz < 20 dB HL bilaterally. Lower speech recognition SNRs were significantly correlated individually with slower speed (p=0.003, Figure 1) and accuracy (p<0.04) on the OBT. The multiple linear regression analysis showed that only

OBT speed, and not OBT accuracy, age or pure-tone thresholds contributed significantly to the SNR results.

Conclusions
OBT performance correlated with TDT results, and this was independent of age. Although the OBT and TDT use different sensory modalities (vision vs. audition) both seem to detect the underlying cognitive slowing associated with HIV infection. Assessing speech in noise perception, and perhaps other central auditory tests, may offer an additional way to detect HIV-related central nervous damage.

OBT speed v triple digit
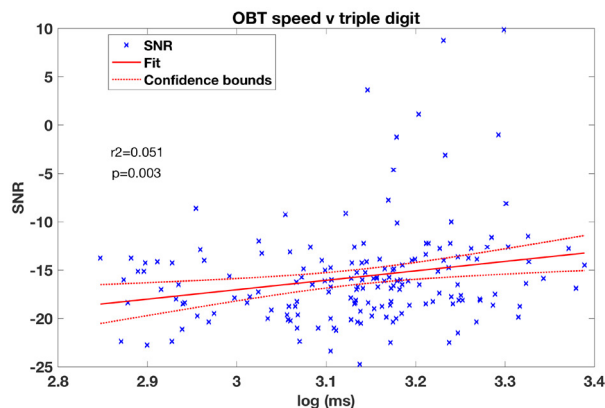
Auditory Nerve II

PS 573

Effect of iNSC transplantation in ouabain-induced auditory neuropathy gerbil

So-Young Chang[1]; Jae Yun Jung[2]; Hosup Shim[3]; Jae-Hun Lee[4]; Ji-Eun Choi[2]; Phil-Sang Chung[5]; Min Young Lee[2]

[1]*Beckman Laser Institute Korea;* [2]*Dankook University College of Medicine;* [3]*Department of Nanobiotechnology, College of Pharmacy Department of Nanobiomedical Science and BK21 PLUS NBM Global Research Center for Regenerative Medicine, Dankook University;* [4]*Beckman Laser Institute Korea, Dankook University;* [5]*Beckman Laser Institute Korea, Department of Otolaryngology-Head & Neck Surgery, College of Medicine,*

Background and Objective
One of the challenges for stem cell therapy is acquiring the cell capable of differentiate into the specific cell. Recently these limitation has been minimized by adopting the new technique that induces the pluripotent cells from the fully differentiated cells from the body. Auditory neuropathy (AN) can be caused by degeneration of spiral ganglion neuron cells (SGNs). Currently no treatment option is available for this specific disease, they show intact hair cell function but there hearing gradually de-

creases. Therefore, we tried to use the induced neural stem cell which is derived from the differentiated fibroblast for treatment of the AN animal model. This aim of study is to assess the survival and localization of iNSC after transplantation into the scala tympani and to analyze its effect on hearing function.

Materials and Methods
Five μL of ouabain (1 mM) soaked in gelfoam was placed on the round window for 1 hour to induce the neuropathy then hearing function was evaluated using Mongolian gerbils. Three μL of iNSC (2×10^4 cells/μL) was injected into scala tympani 2 weeks after ouabain application. To check the hearing function, ABR was evaluated before and after ouabain and iNSCs treatment to the gerbils. The survival and location of iNSC were assessed 1 and 2 weeks after iNSC transplantation.

Results
Ouabain application increased the ABR threshold. At 1 week after the surgery, we could observe the GFP positive cells which are thought to be the surviving transplanted iNSCs. At 1 and 2 weeks after transplantation of iNSC, SGNs were increased in apical, middle and basal turn of the cochlea compared to contralateral and this result was statistically significant at 2 weeks after surgery. Despite higher density of SGNs in the ipsilesional side, functional hearing (ABR) was not improved after the surgery.

Conclusion
This study demonstrated that transplanted iNSCs in the scala tympani can survive in the cochlea especially in the spiral ganglion replacing the damaged SGNs in the denervated inner ear. This study was supported by grants of the Ministry of Science, ICT and Future Planning grant funded by the Korea government (NRF-2016R1D-1A1B03932624 and NRF-2017R1A6A3A11031784).

PS 574

Gas Anesthesia Impairs Auditory Sensitivity in Barn Owls (Tyto alba)

Nadine Thiele; Christine Koeppl
Carl von Ossietzky University Oldenburg

Background
Gas anesthesia is commonly recommended as the preferred state-of-the-art in veterinary science. However, in several mammalian species it has been shown to have detrimental effects on hearing sensitivity. We initially noticed a systematic difference between thresholds measured under two different anesthetic protocols in young barn owls. This was followed by a dedicated ABR study on adult barn owls, comparing different anesthetics in the same individuals.

Methods

CAP- and auditory-nerve single-unit recordings were carried out on 21 young barn owls, aged post-hatch days 11 to 86. The anesthetic protocol was changed during this developmental study, from initially a ketamine/xylazine injection to isoflurane in 100% oxygen, delivered by artificial respiration (tracheotomy plus air sac opening). In a subsequent experimental series, monoaural ABR was recorded in four adult barn owls. Each bird was tested under three different anesthesia protocols, using ketamine/xylazine, isoflurane, or sevoflurane in carbogen, with one week recovery between treatments. Finally, in terminal experiments, the ABR was repeated under the different protocols, using invasive artificial respiration and different dosages of isoflurane. Stimuli were tone bursts, delivered through a closed, calibrated system. Anesthetic dosage was generally adjusted near the minimum required to keep the animal anesthetized. EKG recordings aided in this judgement.

Results

We consistently observed poorer sensitivity under the influence of gas anesthetics than under ketamine/xylazine injection anesthesia. For the adult individuals, ABR thresholds were significantly higher under isoflurane and sevoflurane, on average by 7 and 15 dB, compared to ketamine/xylazine. In addition, there was a significant effect of dosage: increasing Isoflurane from 1% to 2% reversibly raised ABR thresholds further. Delivering the gas anesthetics by artificial respiration for prolonged times also appeared to compound the detrimental effect on auditory sensitivity. Thresholds for the two groups of young owls were between 17 and 26 dB higher in the isoflurane group (with artificial respiration) than in the ketamine group (without artificial respiration). Similar deterioration was observed in the terminal ABR experiments using artificial respiration in adults after several hours.

Conclusions

Our results indicate that different anesthetic protocols can differentially affect auditory sensitivity and that gas anesthetics are less preferable. These observations are consistent with mammalian (Cederholm et al., 2012, Hear Res 292:71-79; Ruebhausen et al., 2012, Hear Res 287:25-29) and reptilian data (Dodd, Capranica, 1992, Hear Res 62:173-180). Importantly, we observed impaired thresholds even when the anesthetics were carefully dosed at the minimum required level.

PS 575

Multi-dimensional Stimulus Encoding in the Auditory Nerve of the Barn Owl

Brian Fischer[1]; Jacob Wydick[2]; Christine Koeppl[3]; Jose Pena[4]
[1]Seattle University; [2]Seattle UniversityJacob Wydick; [3]Carl von Ossietzky University Oldenburg; [4]Albert Einstein College of Medicine

Stimulus encoding in the auditory nerve depends on interactions between responses to multiple frequencies, which may be nonlinear. Most encoding models include a pre-defined number of filters and input-output nonlinearity, and fit model parameters to data. We used a spike-triggered covariance (STC) analysis of auditory nerve responses in the barn owl to determine the number of filters and the form of the input-output nonlinearity that describes how filter outputs interact to produce responses. We found that auditory nerve responses depend on multiple stimulus dimensions (median number of significant filters = 3). The most significant filter was the spike triggered average, excitatory for each neuron. The second most significant filter could be either suppressive or excitatory. Whether the second filter was suppressive or excitatory varied with best frequency (BF). Neurons with BFs below and above 4 kHz tend to have suppressive and excitatory second filters, respectively. The center frequencies of the second and third filters could be either above or below the center frequency of the first filter. We then estimated the nonlinear function that maps the filter outputs to a spiking probability. Most neurons had an expansive nonlinearity along excitatory dimensions. Interestingly, in several high-frequency neurons the nonlinearity approximates a squaring function. Moreover, the first and second filters are excitatory at the same center frequency and differ only by a phase shift difference of pi/2. This type of model approximates an energy model and introduces a phase-invariant component to the spiking probability, which is consistent with diminished phase locking in high frequency neurons. We evaluated the resulting models by predicting the response to repeated frozen noise stimulus not used to fit the model. The model prediction accuracy was negatively correlated with the BF of the neuron and consistent with a BF-dependent variability of the neural responses. To provide a reference for prediction accuracy, we split the data for each neuron into two sets consisting of the odd and even trials. The correlation between the model prediction and the data was similar to, and often exceeded the correlation between the PSTHs from the two data sets, thus supporting the model. This analysis shows that encoding in the auditory nerve of the barn owl is multidimensional and exhibits diverse patterns over the population. This suggests that parametric models with fixed numbers of filters and relationships between filters may be insufficient to describe how sound is initially encoded in the auditory system.

PS 576

The red-shifted opsin f-Chrimson mediates spiral ganglion neurons firing at high rates and temporal precision in vivo

David L. de la Morena[1]; Thomas Mager[2]; Christian Wrobel[3]; Sangyong Jung[4]; Kai Bodensiek[5]; Vladan Rankovic[5]; Lorcan Browne[6]; Antoine Huet[7]; Ernst Bamberg[2]; Tobias Moser[5]

[1]*Institute for Auditory Neuroscience - University Medical Center Göttingen;* [2]*Department of Biophysical Chemistry;* [3]*Department of Otorhinolaryngology;* [4]*InnerEarLab, Institute for Auditory Neurosciences, University Medical Center Goettingen, Germany;* [5]*Institute for Auditory Neuroscience;* [6]*UCL Ear Institute;* [7]*Institute for Auditory Neuroscience Göttingen and The Institute for Neurosciences of Montpellier (Inserm U1051)*

In recent years, optogenetic stimulation of the auditory nerve has become a promising alternative to restore hearing. Unlike electrical current, light can be conveniently confined causing less spread of excitation and thus, the optical cochlear implant (oCI), is expected to surpass the frequency resolution of state-of-the-art electrical CIs. However, the slow deactivation of channelrhodopsin-2 (ChR-2) limited the temporal fidelity of optogenetic stimulation of spiral ganglion neurons (SGNs).

Here we scrutinized the capability of a fast-gating variant of the red-shifted ChR Chrimson (f-Chrimson) to stimulate SGNs with high temporal fidelity. To render SGNs responsive to light, we delivered adeno-associated virus carrying the f-Chrimson-YFP transgene under control of the human synapsin promoter using postnatal injections via the round window into the scala tympani of p3-p5 C57BL6/J mice.

Confocal imaging of YFP and parvalbumin immunofluorescence revealed high opsin expression levels (near 80% in all cochlear turns in the injected ear and less than 5% in the non-injected ear) and unaffected SGN survival, indicating efficient and rather specific transduction of SGNs 8-14 weeks post-injection.

We then used 9 months-old mice as a model of age-related hearing loss to test the potential of f-Chrimson in restoring auditory activity. To analyze opsin functionality, we inserted a 50 μm optical fiber through the round window to project the light of a 594 nm continuous wave laser and to elicit optically-evoked auditory brainstem responses (oABR). Light intensities as low as 0.5 mW and short stimuli down to 40 μs were able to evoke oABR that showed increasing amplitudes and shorter latencies as light intensity rose giving an output dynamic range

exceeds that of current CIs, >20 dB while amplitudes decreased when shortening stimulus duration or speeding pulse rates up to 250 Hz.

Extracellular recordings from single auditory nerve fibers showed that individual SGNs fired with high temporal precision at stimulus rates of up to hundreds of Hz, nearly mimicking sound-evoked activity. Over 900 ms-long light-pulse trains (100 ms inter-train interval, 20 trials), vector strength and spike probability peaked at stimulation frequencies 50-200 Hz, declining as rates increased up to 1 kHz. Temporal jitter (standard deviation of spike latency across trials) was usually below 1 ms and tended to decrease from 400 Hz upwards.

We have thus established postnatal transduction of SGNs with f-Chrimson, which enables red-shifted optogenetic stimulation of SGN firing with low light intensities at near physiological rates, while avoiding blue-light phototoxicity.

PS 577

In Vitro Characterization of Cochlear Optogenetics

Carlos J. Duque Afonso[1]; Daniel Keppeler[1]; Kai Bodensiek[1]; Vladan Rankovic[1]; Lorcan Browne[2]; Katie Smith[2]; Dan Jagger[2]; Tobias Moser[1]
[1]*Institute for Auditory Neuroscience;* [2]*UCL Ear Institute*

Activation of the auditory pathway by cochlear optogenetics has been shown to be feasible. Given the fact that light can be better confined than electric current, its application to cochlear prosthetics provides a alternative to currently employed electrical cochlear implants with a greater number of independent stimulation channels. In addition, cochlear optogenetics can be used as a research tool to answer fundamental questions in auditory research, bypassing cochlear micromechanics and its changes with stimulus level. The plethora of light-sensitive channels that are currently available offers different possibilities - not only regarding their biophysical properties, but also in terms of excitation wavelength which implies different light propagation profiles. We aim to build a computational model that combines the light distribution profile from our emitter through the cochlear tissues with electrophysiological responses of light-activated spiral ganglion neurons (SGN). To study the light propagation, we have conducted Monte Carlo ray tracing simulations using structurally realistic data from X-ray tomography, optical parameters obtained from literature and the emission profile of our emitters. In preparation for a biophysical constrained SGN model, we are using the whole-cell patch clamp technique to characterize the properties of various opsins with different spectral properties in postnatally AAV-transduced SGNs in vitro. Fi-

nally, this model will enable us to test and study different strategies in silico that will finally assist in the development of future optogenetic cochlear implants.

PS 578

The biophysical properties of morphologically identified spiral ganglion neurons

Alexander Markowitz; Radha Kalluri
University of Southern California

Patch-clamp recordings have shown that the ion channel properties of spiral ganglion neurons (SGN) are heterogeneous, leading to the suggestion that such variance in the intrinsic biophysical properties of SGN contributes to their functional diversity. In vivo, SGN differ in their response thresholds, spontaneous firing rate (SR), and dynamic range, which are properties that underlie the neurons'; ability to encode different sound intensities. Whether differences in ion channel expression contribute to the functional heterogeneity of SGN remains unknown and untested.

To bridge this gap in knowledge, we are using an acute semi-intact preparation of the cochlea in which we simultaneously record and label SGN somata and its peripheral process using patch-clamp electrodes. Because we maintain the in situ organization of SGN with their pre-synaptic partners, we are able to classify neurons as being either "modiolar-contacting" or "pillar-contacting" based on the spatial position of their peripheral terminal around the base of the inner hair cell. This bi-modal classification was motivated by previous studies observing that the modiolar-pillar axis is roughly correlated with the intensity-coding classification of in vivo responses. Recent observations in developing rodents show that pre-synaptic morphology and physiology also vary along this modiolar-pillar axis.

We have performed this experiment on rats from post-natal day (P)1-P16. This age range encompasses an important period for synaptic maturation. We found that the number of terminal branches made by SGN decreased as a function of age with the modiolar-contacting neurons having fewer branches than the pillar-contacting neurons. We quantified the electrophysiological phenotype of each SGN by measuring whole-cell currents and action potential features. Next, we used the morphological and electrophysiological data to apply a multivariate statistical technique to test if the intrinsic properties of modiolar- and pillar-contacting neurons were statistically different. Our preliminary analysis shows that modiolar- and pillar-contacting SGN are discriminable by their electrophysiological properties and that these differences emerge during the course of development. By the second postnatal week, modiolar-contacting SGN have larger steady-state outward currents than pillar-contacting SGN. Our results suggest that modiolar-contacting SGN are developing faster than pillar-contacting SGN. Whether these developmental trajectories persist to make functional distinct neurons remains untested.

PS 579

Correlation of ABR wave I level-growth and amplitude modulation discrimination in listeners with poor word recognition in noise

Bastian Epp; **Pernille Holtegaard**
Hearing Systems group, Department of Electrical Engineering, Technical University of Denmark

Numerous studies have exhibited physiological evidence of noise-induced synaptopathy and neural degeneration prior to outer hair cell (OHC) loss in small rodents. Efforts have been made to investigate deficits supporting the presence of similar effects in human listeners with a history of noise-exposure, using both behavioural and physiological measures. The results are, however, inconclusive. One reason could be that susceptibility to noise-induced auditory damage differs across listeners, while animal models represent a more homogeneous population. This heterogeneity in the human listeners could obscure the correlation between the reported exposure and the outcomes of physiological and behavioral measures.

In the present study, young adult normal hearing listeners (pure-tone thresholds ≤ 20 dB HL between 0.25 - 8 kHz) were recruited and grouped based on their word discrimination score in noise. The aim of the present study was to investigate if normal hearing listeners with reduced speech discrimination score in noise would show signs of synaptic and neural degeneration in audiological and electrophysiological measures. The hypotheses were that a) listeners with poorer speech discrimination show reduced level-growth of ABR wave I, b) ABR wave-I level-growth is a predictor of speech discrimination score, c) listeners with poorer speech discrimination have poorer amplitude discrimination especially when tested at higher levels (80 dB SPL) and high frequencies (4 and 8 kHz) and, d) amplitude discrimination thresholds are a predictor of speech discrimination performance). Cochlear and auditory nerve function was assessed using auditory brainstem response (ABR) measured with 4 kHz-tone bursts and with clicks. Sensitivity was assessed using clinical audiometry, word-recognition in noise and amplitude modulation discrimination using a stimulus level of 45 dB SPL at 1 and 4 kHz and a stimulus level of 80 dB SPL at 1, 4 and 8 kHz. The data indicate a correlation between reduced ABR wave I level-growth and poorer word discrimination score in noise. Amplitude modulation

discrimination thresholds were, however not significantly lower in listeners with poorer speech discrimination. Furthermore, no correlation was found between amplitude modulation discrimination threshold and word discrimination or ABR wave I level-growth. While the correlation between ABR wave-I level growth and word discrimination in noise suggest that poorer speech discrimination in noise, in listeners with normal sensitivity, could be related to synaptic and neural degeneration, the results for amplitude modulation discrimination thresholds do not support the initial hypothesis.

PS 580

Effects of noise exposure history on Low-Sound-Level Auditory Processing

Warren M H. Bakay[1]; Christopher J. Plack[2]; Michael A. Stone[2]
[1]University of Manchester (ManCAD); [2]University of Manchester

Introduction

Sub-clinical hearing loss appearing only at low-sound-levels has been reported in humans either without any change in absolute thresholds (Stone, Moore, & Greenish, 2008), and with small but sub-clinical changes in thresholds (Vinay & Moore, 2010). Because these deficits occur at low-sound-levels, they do not fit with the suspected mechanism of Hidden Hearing Loss (HHL): cochlear synaptopathy of high-threshold fibres (Kujawa & Liberman, 2009; Furman et al., 2013; Hesse & Bakay et al., 2016). People so far identified with low-level sub-clinical hearing deficits have a history of exposure to high-level noises, such as from recreational noise (clubbing, live music events, motorsport, shooting). People with traditional hearing losses have a compressed hearing range, and this low-sound-level impairment should occupy a larger portion of their reduced range.

Goal

To quantify low-sound-level deficits and determine their correlation to sound exposure history, and to determine whether they affect speech comprehension in people with sub-clinical hearing loss.

Methods

Participants were recruited between the ages of 30 and 65 with no previous experience of wearing hearing aids, and underwent a screening session of standard clinical measures: Pure Tone Audiometry (PTA), Tympanometry, Threshold Equalising Noise (TEN) tests, Bekesy Audiometric Tracking, and Interaural Timing Difference (ITD) threshold testing). Participants were divided into different noise exposure groups (high and low) using the NESI (Noise Exposure Structured Interview).

Thresholds were determined at three different levels of TEN noise: 0dB (unmasked, 12dB SL and 24dB SL. Preliminary results suggest a difference in TEN test thresholds between the 12dB and 24dB masking levels.

Subjects with elevated PTA at 4kHz but not at 1kHz were invited for electrophysiological testing, comprising the Auditory Brainstem Response (ABR) and Auditory Steady State Response (ASSR). These were recorded using Biosemi electrodes from multiple sites, including in the ear canal using tiptrodes.

Octave band chirp stimuli to induce ABRs were presented in two different frequency bands (750-1500Hz, and 2.5–5 kHz) and three different intensity levels (100dB SPL, 30dB SL, and 15dB SL). ASSR stimuli were presented in two different complexes (2 carriers, 2 modulators, with 2 octaves between carriers, at 750Hz/3kHz, and 1kHz/4kHz)

PS 581

Both inner and outer hair-cell dysfunction degrade neural coding of perceptually relevant complex sounds

David R. Axe[1]; Vijaya P.K. Muthaiah[1]; Michael Heinz[2]
[1]Purdue University; [2]Department of Speech, Language, and Hearing Sciences, Purdue University

Sensorineural hearing loss (SNHL) disrupts the quality of life of millions of people around the world. The clinical category of SNHL is a catchall that includes several types of cochlear damage that can result from different causes (e.g., noise overexposure, chemical ototoxicity, aging). Two patients with similar degrees and configurations of SNHL (i.e., audiograms) can have significantly different speech intelligibility. This common clinical outcome illustrates the need for additional diagnostic measures, which will require a more detailed understanding of the variety of mechanistic changes that can occur following SNHL.

The goal of this work was to investigate several underlying mechanisms of SNHL by selectively perturbing individual components of the peripheral auditory system, specifically the inner (IHCs) and outer hair cells (OHCs). This was accomplished by measuring both invasive single-unit and non-invasive evoked neural responses in chinchillas that were administered ototoxic drugs chosen for their hair-cell specificity (gentamicin – OHCs;

carboplatin – IHCs). Single auditory-nerve-fiber (ANF) responses were measured to stimuli ranging from simple tones to more complex sounds, including amplitude- and frequency-modulated tones and broadband noise, which represent fundamental acoustic features of speech and music in real-world environments. This experimental approach made it possible to measure the isolated effects of damage to each cell type on peripheral neural processing (i.e., without confounding interactions of damage to other peripheral components that often occur with noise over-exposure or age). Light microscopy was used to quantify IHC and OHC loss and scanning electron microscopy illustrated that remaining IHCs can have disrupted stereocilia that appear to limit their functional efficiency.

Changes in distortion-product otoacoustic emissions were predictive of several well-known physiological effects of OHC dysfunction, including loss of peripheral frequency selectivity. Physiologically, IHC dysfunction produced subtle or no effects on common threshold measurements, but perceptually relevant effects were predicted from neural responses to suprathreshold sounds. Our results suggest that frequency-modulated tones may be effective stimuli for IHC diagnostics.

While IHC damage has long been viewed primarily in terms of cochlear dead regions (i.e., missing IHCs), our physiological and anatomical evidence suggests that even remaining functional IHCs may produce degraded ANF responses that provide less neural information for the perception of complex sounds, but do not affect thresholds in a major way. Thus, IHC dysfunction appears to be an important factor to consider in cases of hidden (or mild) hearing loss.

PS 582

Peak-Splitting in the Auditory Nerve of Chinchilla

Eric Verschooten; Philip X. Joris
KU Leuven, University of Leuven

Cat auditory nerve fibers stimulated with low-frequency tones can show complex phase-locking behavior, generally referred to as "peak-splitting" (Kiang and Moxon, 1972; Kiang, 1984, 1990). Over a small range of SPLs, multiple modes are observed per stimulus cycle, and at that range of SPLs there can be a reduction in discharge rate causing a non-monotonicity ("Nelson';s notch") in the rate-intensity curve. At still higher levels, phase-locking can return to unimodal behavior, but at a different phase than at low levels. The origin of this behavior is unclear but several possible mechanisms have been proposed (Liberman and Kiang,1984; Kiang,1990; Ruggero et al.,1995; Cody and Mountain, 1989;Dallos and Cheatham,1989) ranging from micromechanical models to models incorporating electrical interactions between inner and outer hair cells. In this study we map the phenomenon in the auditory nerve of chinchilla.

Spiking activity of single auditory nerve fiber (AN-fibers) was recorded with sharp glass microelectrodes in normal hearing chinchillas under general anesthesia. The characteristic frequency (CF) of AN-fibers was obtained with a threshold tuning curve in response of pip-tones. AN-fibers were excited with tones at various levels and frequencies (

Peak-splitting was observed in all animals studied. Most high-CF AN-fibers showed peak-splitting or abrupt phase shifts when stimulated in their low frequency tail at high levels (typically >70 dBSPL). AN-fibers with Low CF also exhibit peak-splitting at frequencies below CF and, more rarely, at CF. The rate reductions associated with phase transitions were typically small, and never reached spontaneous activity as they do in cat (McGee et al.,1981,1982;Kiang and Moxon,1972;Kiang,1984). Peak-splitting occurred in various complex forms with phase shifts at multiple stimulus levels, as low as 50 dB-SPL, and sometimes resulting in more than two modes per stimulus cycle. Phase transitions can shift back to the original phase; they can be gradual over an extended SPL range or very abrupt over a small range, as small as 1 dB. The peaks of peak-splitting responses in single AN-fibers measured over a frequency range between 400-500Hz showed no relative phase dependence with frequency.

'Peak splitting'; in the AN in chinchilla is similar to that in cat, but with some differences such as the occurrence of peak-splitting at low levels, small associated rate reductions and erratic combinations of multiple modes and phase transitions.

PS 583

Co-modulation Masking Release Begins in the Auditory Periphery

Mark Sayles
Purdue University

Coherent across-frequency amplitude modulation can be exploited by humans and other animals to improve signal detection in noisy listening environments. This has been quantified behaviorally as "co-modulation masking release" (CMR). Neurophysiological studies

have identified neural correlates of CMR in a variety of brainstem and cortical circuits. The common theme across these studies is the interaction of narrowband excitation with broadband inhibition. However, the potential contribution of cochlear suppressive non-linearities in mediating CMR have not been investigated. Here we test the hypothesis that frequency-dependent suppressive interactions in the cochlea result in a neural correlate of CMR in the auditory nerve. Spike trains were recorded using standard techniques from isolated single auditory nerve fibers (ANFs) in the anesthetized normal-hearing chinchilla (Chinchilla lanigera). For each fiber, we quantified frequency tuning using an automated threshold-tracking algorithm. From this we estimated characteristic frequency (CF). For some fibers, we also gathered data on the threshold for two-tone suppression using a similar tracking algorithm. To study CMR, we presented a CF signal tone (S) at 20-dB SL in the presence of a narrowband masker which consisted of a sinusoidal amplitude-modulated tone with fc at CF, and fm of 10-Hz. The signal, S, was gated on and off in the amplitude minima of the modulated masker. This basic condition is referred to as the reference condition (RF). Two further conditions included an additional out of band 10-Hz amplitude-modulated noise masker. This noise masker was either modulated in-phase with the narrowband masker (co-modulated condition; CM), or in anti-phase with the narrowband masker (co-deviant condition; CD). The noise masker was either a notched noise, with a 4ERB-wide notch centered on CF, or only the corresponding high- or low-pass segments of this. All stimuli were 500-ms duration, repeated every 900-ms, for typically 25 repetitions. Data were obtained from 120 ANFs. We quantified firing rate in response to the signal tone, S, in the three stimulus conditions (RF, CM, CD) as a function of the sound level of S. For low spontaneous rate fibers, the response to the signal tone grew much faster in the CM condition compared to RF. Additionally, the response to the signal grew more slowly in the CD condition compared to RF. High spontaneous rate fibers responses showed similar trends on average, but of much smaller magnitude. Comparing the effects of high-side vs. low-side noise maskers, we found stronger influences of the low-side out-of-band noise on the firing rate in response to the signal. In the anesthetized chinchilla, responses of ANFs (especially the low-SR variety) support the hypothesis that across-frequency suppressive interactions in the cochlea results in a neural correlate of CMR. How that representation is further processed or enhanced by brainstem circuits including broadband inhibition is unknown. Weakened suppressive non-linearities in hearing-impaired animals could negatively impact the establishment of CMR effects in the auditory periphery, making listening in noisy places more difficult.

PS 584

Single-unit Responses from Gerbil Auditory Nerve to Schroeder-phase Stimuli

Friederike Steenken[1]; Laurel H. Carney[2]; Rainer Beutelmann[3]; Lichun Zhang[1]; Christine Koeppl[1]
[1]*Carl von Ossietzky University Oldenburg;*
[2]*Departments of Biomedical Engineering, and Neurobiology & Anatomy, University of Rochester , Rochester;* [3]*Cluster of Excellence Hearing4all and Carl-von-Ossietzky University Oldenburg*

Background

Inverse signed multiphasic harmonic sweeps, so called Schroeder-phase Stimuli (SCHR-stimuli), differ in their fast fluctuations, but not in their wideband envelopes. SCHR-stimuli have previously been used in psycho-acoustic discrimination (Drennan et al., 2008, JARO 9: 138-149) and masking studies (Lentz and Leek, 2001, JARO 02: 408-422). It has been suggested that the ability to discriminate positive (downward sweeping) and negative SCHR-stimuli might largely rest on the neural coding of temporal fine structure (TFS) information. We compare the discriminability of positive and negative SCHR-stimuli in auditory-nerve responses to behavioral discrimination scores obtained in the same species, the gerbil. TFS coding requires phase locking and is therefore carried by auditory-nerve fibers with best frequencies below 4-5 kHz. However, the impulse response of cochlear filters presumably alters the envelope of positive and negative SCHR-stimuli. Here, we investigate how the auditory nerve codes SCHR-stimuli.

Methods

Recordings from the auditory nerve were carried out in Mongolian gerbils (Meriones unguiculatus). Positive and negative SCHR-stimuli with fundamental frequencies (F0) of 50, 100, 200, and 400 Hz, components from F0 to 5 kHz, and phase factors of 0.25, 0.5, 0.75, and 1 were presented monaurally at a fixed sound level of 60 dB SPL per component. These parameters matched those used in a companion behavioral study. Data were analyzed with a custom MATLAB script, and two different metrics were derived: d'; based on mean discharge rates, and percent-correct-classification of positive and negative SCHR-stimuli, based on the van-Rossum spike-distance metric (van Rossum, 2001, Neural Comput 13: 751-763) with different time constants.

Results

Values of d'; were mostly less than 1 (i.e. sub-threshold). The percent-correct-classification showed the overall highest values when a time constant of about 1ms was used for the van-Rossum analysis. The phase factor did not affect the percent-correct-classification; the lowest percent-correct values, however, were obtained for

spike trains in response to SCHR-stimuli with an F0 of 400 Hz, and those were significantly different from all other percent-correct values for the other F0s.

Conclusion

Mean discharge rates did not differ significantly in response to positive and negative SCHR-stimuli across F0s and phase factors, suggesting no discrimination based on auditory-nerve mean discharge rates. The highest percent-correct values were obtained with a rather short time constant of analysis, suggesting that discrimination more likely relies on timing. The percent-correct values were lowest for an F0 of 400 Hz, which is consistent with behavioral performance (abstract #199, ARO 2017).

PS 585

Spatial Distribution of Numbers and Volumes of Cochlear Ribbon Synapses on Inner Hair Cells of Young Adult Gerbils

Lichun Zhang[1]; Sina Engler[2]; Lena Koepcke[1]; Friederike Steenken[1]; Christine Koeppl[1]
[1]Carl von Ossietzky University Oldenburg; [2]Department of Otorhinolaryngology, University Medical Center Groningen, Netherlands

Background

Classic data from cats showed that afferent nerve fibers projecting to the pillar side of inner hair cells (IHC), closer to the outer hair cells, have higher spontaneous discharge rates and lower thresholds to acoustic stimulation, and terminals that face smaller presynaptic ribbons, compared to fibers contacting the modiolar side of IHC (Merchan-Perez and Liberman, 1996, J Comp Neurol 371:208-221). More recent studies in mice suggested that, in addition, they have larger postsynaptic GluR patches (Liberman et al., 2011, J Neuroci 31:801-808). The Mongolian gerbil is a well-established animal model in auditory research. As a prerequisite for studying age-related changes, we quantify here, for young adult gerbils, volumes of presynaptic ribbons and postsynaptic GluR patches, using immunohistochemistry.

Methods

Five cochleae from 4 Mongolian gerbils (Meriones unguiculatus), aged 80 to 219 days, were triple-labeled with antibodies against CtBP2, GluR2 and MyosinVIIa. Confocal images of log-spaced tonotopic locations between 0.5 and 32 kHz were evaluated using image analysis software custom-written in MATLAB. Spatial coordinates of synaptic elements were referred to all 3 axes of the individual IHC. Pre- and postsynaptic volumes were normalized to their respective median in each confocal stack. Colocalization of pre- and postsynaptic elements, i.e. functional synapses, was defined by a maximal-distance criterion.

Results

In total, 1973 functional synapses, distributed nearly equally to the modiolar and pillar sides of their IHCs, were evaluated. Both presynaptic ribbons and postsynaptic GluR2 patches were significantly larger on the modiolar side. However, the difference was small: median normalized volumes for presynaptic ribbons were 1.04 for modiolar and 0.98 for pillar locations; for postsynaptic GluR2 patches, the median normalized volumes were 1.10 and 0.90, respectively. Similarly, at the level of individual synapses and independent of spatial location, presynaptic ribbon and postsynaptic GluR2 patch volumes were clearly positively correlated.

Conclusion

In young gerbils, a modiolar-pillar gradient of decreasing presynaptic ribbon volume, similar to that reported in mice, cats and guinea pigs, was present. However, the volumes of postsynaptic GluR2 patches showed the same increasing modiolar-pillar gradient - which is the reverse of that reported in mice - as well as an overall positive correlation with ribbon volume. Thus, in the gerbil, there were no opposing gradients in the volumes of pre- and postsynaptic elements. Furthermore, the spatial gradients in the gerbil were less pronounced than in the mouse.

PS 586

Refractory properties of auditory-nerve fibers inferred from the recovery of spike amplitude under natural excitation conditions

Adam J. Peterson[1]; Antoine Huet[2]; Jérôme Bourien[3]; Jean-Luc Puel[3]; Peter Heil[1]
[1]Leibniz Institute for Neurobiology; [2]Institute for Auditory Neuroscience Göttingen and The Institute for Neurosciences of Montpellier (Inserm U1051); [3]The Institute for Neurosciences of Montpellier (Inserm U1051) and University of Montpellier

The refractory properties of mammalian primary auditory afferents (auditory-nerve fibers, ANFs) impact the timing of spikes during both spontaneous and sound-driven activity. Direct electrical stimulation of ANFs has been used previously to characterize refractory periods, with the finding that refractoriness tends to be short (1-2 ms) and is well described by an absolute refractory period followed by a short single-exponential relative refractory period. It is conceivable, however, that refractory properties inferred from electrical stimulation might differ from those present under more natural excitation conditions. In addition, some modeling work has included the assumption that relative refractoriness contains both short and long exponential components. Furthermore, it has been proposed that relative refractory periods decrease with increasing spike rate.

Here, we estimate refractory properties from the recovery of spike amplitude as a function of the time since the previous spike. Data were recorded extracellularly from ANFs in anesthetized gerbils during spontaneous and sound-driven activity. We find that the recovery of spike amplitude (and, presumably, neuronal excitability) following a brief absolute refractory period is well characterized by a single exponential component with a short time constant < 1 ms. We find no evidence for a long relative refractory component and no evidence that the relative refractory period depends inversely on the spike rate. These results are consistent with the refractory properties inferred from electrical stimulation. They also support the assumption of brief refractoriness in, for example, the inner-hair-cell-to-ANF synapse model of Peterson and Heil (2017).

PS 587

Recovery from Kainate Excitotoxicity in Gerbil Cochlea

Jérôme Bourien[1]; Martin Nedelec[2]; Gilles Desmadryl[2]; Sharon G. Kujawa[3]; Jean-Luc Puel[1]
[1]*The Institute for Neurosciences of Montpellier (Inserm U1051) and University of Montpellier;* [2]*Institute for Neurosciences of Montpellier (Inserm U1051) and University of Montpellier;* [3]*Eaton-Peabody Laboratories, Massachusetts Eye and Ear Infirmary and Department of Otolarynology, Harvard Medical School, Boston, Massachusetts*

Background
Prior work from our labs has documented inner hair cell (IHC) synaptic damage resulting from exposures to exogenously-applied glutamate agonists and to noise, which stimulates excessive endogenous release. Although there are important similarities in the response to the two insults, there appear to be key differences that may serve to clarify mechanisms and address observed differences in long-term neural status after agonist vs. noise exposure. The present experiments are part of a larger series aiming to clarify the nature of these differences by carefully examining the time course of injury, the involvement of pre- and post-synaptic structures and the potential for recovery after agonist- vs. noise-induced injury. Here, we examine the acute response to, and recovery from glutamate agonist (kainate)-induced excitotoxicity in a gerbil model.

Methods
Young adult Mongolian gerbils were treated unilateral-ly, via round-window application, with kainate (~20 μl of 25 mM drug in artificial perilymph; AP) or an equal volume of vehicle alone. Animals were recovered and outer hair cell-based distortion product otoacoustic emissions (DPOAE) and neural-based auditory brainstem responses (ABR) were recorded (2-32 kHz, 0-80 dB SPL) immediately before and 1, 3, 7 and 14 days after treatment. Tissues were recovered for study from subsets of animals at the terminal test, 14 days after treatment.

Results
One day after the drug application, a significant ABR threshold shift (+35 dB) associated with a 50% reduction of the ABR amplitude was observed at all tested frequencies. No effect was observed in the control group treated with AP alone. By 7 days post-kainate, DPOAE and ABR wave 1 thresholds and suprathreshold amplitudes were not different from AP-treated control or contralateral ear values. Histologic analysis is ongoing.

Conclusion
Unlike our findings in noise-exposed ears, ABR wave 1 amplitude recovery post kainate suggests no persistent synaptic or neural loss, to be verified in ongoing histologic examination of these tissues. If confirmed, results suggest different, and/or additional factors contributing to persistent neural response declines after noise.

PS 588

Neurophysiological Evaluation of Speech Masking Release Based on the Envelope Power Spectrum Model

Satyabrata Parida[1]; Michael Heinz[2]
[1]*Purdue University;* [2]*Department of Speech, Language, and Hearing Sciences, Purdue University*

Perceptual studies have shown that speech intelligibility (SI) in normal-hearing listeners is better in the presence of a fluctuating masker compared to a stationary masker. This difference has been suggested to be due to the ability of normal-hearing listeners to use speech information in the dips of fluctuating noise. However, the underlying neural basis for the reduced ability of listeners with cochlear hearing loss remains unknown. Here we present a multi-resolution speech envelope power spectrum model (mr-sEPSM[neural]) based on auditory-nerve spike trains to predict SI in the presence of fluctuating and stationary maskers. We apply correlogram and wavelet analyses to estimate a signal-to-noise neural envelope power ratio (SNR_{env}^{neural}) by computing envelope power in response to noisy speech and to that

of noise alone. The advantage of our model is two-fold. First, the model is based on neural information and incorporates important neural mechanisms for complex sounds, such as adaptation and suppression. Second, the health of outer and inner hair cells can be manipulated separately in both phenomenological models and in animal models. It is important because patients with similar audiograms often have variable perceptual performance, which could be attributed to differences in outer and inner hair cell health. Simulation results were pooled across fibers of different characteristic frequencies and spontaneous rates for multiple sentences using responses from a phenomenological model. Higher SNR_{env}^{neural} was predicted in the presence of a fluctuating masker. However, there was a high degree of variability in SNR_{env}^{neural} when estimated from individual fibers. Simulation results for low, medium and high spontaneous rate fibers show different trends, and thus may have implications for cochlear synaptopathy (hidden hearing loss) where low-spontaneous-rate fibers appear to be preferentially lost. Additionally, this glimpsing model allows us to estimate the predicted contribution dynamics arising from different temporal segments of the stimulus. Results based on spike trains collected from anesthetized chinchilla auditory-nerve fibers will be presented and linked to simulation results. In the future, we will validate the SI model by collecting neural data across various conditions of cochlear hearing loss.

PS 589

Auditory Nerve Preservation following Clinically Applicable Neurotrophic Treatment in Deafened Guinea Pigs

Henk A. Vink; Dyan Ramekers; Hans G.X.M. Thomeer; Sjaak F. L. Klis; **Huib Versnel**
University Medical Center Utrecht, Brain Center Rudolf Magnus, Utrecht University

There is growing evidence that in cochlear implant (CI) recipients the health of the auditory nerve may be compromised, which may negatively impact CI effectiveness. In animal studies, it has been established that spiral ganglion cells (SGCs) progressively degenerate in the absence of cochlear hair cells - most likely because neurotrophic support from the organ of Corti is lost, since numerous studies have shown enhanced survival with neurotrophic treatment. Here we examine neurotrophic factor treatment strategies for clinical application in CI users. We have compared the effects of several neurotrophic compounds on SGC survival in ototoxically deafened guinea pigs. The used compounds include brain-derived neurotrophic factor (BDNF), neu-

rotrophin-3 (NT-3) and 7,8,3'-trihydroxyflavone (THF), a small-molecule BDNF mimetic. Gelfoam containing these compounds was placed on the round window membrane, which is a clinically feasible delivery method (Havenith et al., 2015, Otol Neurotol 36:705-713). Histological analysis of the SGCs was complemented using advanced stimuluation paradigms of electrically evoked compound action potentials (eCAPs; among others varying the inter-phase gap) shown to be indicative of neural health (Ramekers et al., 2015, J Neurosci 35:12331-12345). Treatment with BDNF resulted in substantial SGC preservation, which was limited to the basal turn of the cochlea, consistent with previous findings. The THF-treated animals showed less SGC survival than BDNF. The IPG variation-induced eCAP measures showed a positive correlation with cell survival. Although prevention of SGC loss was limited with this clinically applicable delivery method, auditory nerve responsiveness was nonetheless improved, suggesting that clinical application is worth considering. Finally, while theoretically superior to BDNF, the small molecule THF seemed less effective.

PS 590

Hyperpolarization-activated and Cyclic Nucleotide-Gated Channels in the Mammalian Inner Ear

Maria Luque Calvo[1]; Anneliese Schrott-Fischer[1]; Wei Liu[2]; Helge Rask-Andersen[3]; Elisabeth Pechriggl[4]; Erich Brenner[4]; Heval Benav[5]; Rudolf Glueckert[1]
[1]*Department of Otolaryngology, Medical University of Innsbruck , Austria;* [2]*Department of surgical sceinces, Uppsala university, Uppsala, Sweden;* [3]*University of Uppsala;* [4]*Department of Anatomy, Medical University of Innsbruck , Austria;* [5]*MedEl*

Hyperpolarization-activated and cyclic-nucleotide-gated (HCN) channels are voltage-gated dependent cationic channels. Unlike other voltage-gated channels that open following membrane depolarization HCN channels do so following hyperpolarization, cyclic nucleotides such as cAMP facilitate activation. HCN channels play a prominent role in setting the pace of biological oscillations and are therefore termed "pacemaker" channels. HCN-mediated lowering of activation thresholds contributes to the peripheral pain sensation. In primary auditory neurons a hyperpolarisation activated current (I_h) may shorten excitatory postsynaptic potentials (EPSPs) keeping these signals brief and prevent temporal summation. There are four different subunits (HCN1-4) arranged to form homo- or heterotetramers with different biophysical characteristics. Little is known about function and cellular location in the mammalian inner ear, especially in human. We describe the expression pattern and semi-quantitative distribution of HCN isoforms with immunohistochemical techniques in hu-

man, three inbred mouse strains and cat inner ear tissue. HCN2 localizes in the afferent and efferent innervation of the inner and outer hair cells as well as an intense membrane staining around the soma of spiral ganglion neurons (SGNs). Likewise HCN1 was present in the spiral plexus underneath the inner hair cells and peri-somatic SGN membrane. HCN4 protein resided in the organ of Corti and in the SGNs soma membrane, with an intense staining in neuron cell clusters. HCN3 was not detected in human or any other mammalian cochleae. HCN1 was more expressed in SGNs of the basal turn than in the apex. It is the fastest channel in terms of activation kinetics. Opposing results were detected for HCN4 which is the channel with the slowest activation kinetics. HCN2 and HCN4 showed an age-dependent change in protein expression level. HCN channels were not restricted to excitable cells-HCN1 showed membrane staining in sensory epithelium supporting cells. HCN2 may help setting firing properties due to its high level of expression in neurons and innervation in the organ of Corti. HCN4 could be the most important channel in SGN clusters with a modulating function between the neurons and controlling temporal information important for binaural sound localisation with lower frequencies. Fastest kinetics, low modulation effect by cAMP or tyrosine phosphorylation qualifies HCN1 for preserving temporal information and amplitudes in high frequency neurons. Formation of various hetero-tetramers may open possibilities to finetune timing information of EPSPs in SGNs with different spontaneous spiking rates and modulate information of sound signals at the level of the soma and axon initial segment.

PS 591

Masking Noise Partitions the Spike-time and Spike-rate Modes to Encode Behavioral Auditory Threshold

Antoine Huet[1]; Gilles Desmadryl[2]; Thomas Justal[3]; Régis Nouvian[4]; Jean-Luc Puel[4]; **Jérôme Bourien**[4]
[1]Institute for Auditory Neuroscience Göttingen and The Institute for Neurosciences of Montpellier (Inserm U1051); [2]Institute for Neurosciences of Montpellier (Inserm U1051) and University of Montpellier; [3]Institute for Neurosciences of Montpellier, Inserm U1051; [4]The Institute for Neurosciences of Montpellier (Inserm U1051) and University of Montpellier

The auditory nerve fibers (ANFs) encode sound through two modes of coding, spike-time or spike-rate depending of the sound stimulation frequency. In response to low-frequency tone, the ANF firing is phase locked to the acoustic stimulus. Because temporal coding vanishes with increasing frequency, high-frequency sound coding relies on the spike-rate of the ANFs. Because adding a background noise elevates the discharge rate, the ANFs having low threshold/high-spontaneous rate (SR), become saturated making them unable to encode tone-in-noise. Thus, the ANFs, having an elevated threshold/low-spontaneous rate, mostly contribute for behavioral threshold detection in noise. However, the capability of ANFs to encode threshold through spike-time, independently of their spontaneous rate in noisy environment have never been investigated so far. Using single-fiber recordings from the auditory nerve of gerbils, we show that high-SR ANFs use spike-time, even if their discharge rate is saturated, thus demonstrating a robustness of spike-time in noise for low-frequency sound stimulation. Moreover, increasing the spike discharge rate with the background noise makes the low-SR fibers able to encode the threshold in a temporal mode, in contrast to tone-in-quiet, in which the threshold was encoded in rate. For high-frequency sound stimulation, all the ANFs use spike-rate to encode threshold. By comparing behavioral thresholds with single unit recordings, the interplay of these two encoding modes in the auditory nerve able the cochlea to challenge noise over a large range of frequencies (0.4 - 40 kHz). Taking into account the frequency range of hearing in gerbils, it is thus tempting to expect that a similar mechanism operates in humans.

PS 592

Effect of CGRP and acetylcholine on type 1 spiral ganglion neuron synapses.

Sriram Hemachandran; Steven H. Green
The University of Iowa

Introduction
Cochlear inner hair cells transmit sound stimuli by releasing glutamate at its synapse with the type 1 spiral ganglion neurons (SGNs). SGNs have AMPA receptors on their post synaptic surface, which is the major receptor involved in calcium influx during sound perception. Loud stimuli cause excessive glutamate release leading to increased influx of Ca^{2+} in the SGN postsynaptic bouton, excitotoxic trauma and the destruction of the synapse.

The lateral olivocochlear (LOC) efferents innervate the SGNs axoaxonic synapses. Multiple neurotransmitters are used by the LOC to modulate the SGN activity. Among these are calcitonin gene related peptide (CGRP) and acetylcholine. Here we ask whether these neurotransmitters affect the extent of glutamate excitotoxicity.

Hypothesis
These LOC neurotransmitters, CGRP and acetylcholine (ACh) will exacerbate glutamate excitotoxicity. Because

of the mechanism of CGRP signal transduction, CGRP will be exerting its effect via cyclic adenosine monophiosphate (cAMP) signaling.

Methods

The oOrganotypic cochlear explant cultures was prepared as explained in Wang et al, 2011contain a portion of the organ of Corti, typically middle turn of a neonatal rat, with the corresponding portion of the spiral ganglion and all synaptic connections intact. Synapses were visualized by immunofluorescent labeling The of the presynaptic ribbon protein, CtBP-2ribeye (CtBP2) and postsynaptic density scaffold protein (PSD-95.) were labelled. The cColocalization of CtBP-2 and PSD-95 was termedis our operational criterion for a morphological synapse as a 'synapse';.

To determine whether ACh or CGRP exacerbate excitotoxicity, explants were treated for 2 hr with a low concentration (0.01 mM) of the excitotoxic agent kainate, which by itself causes nearly undetectable synapse loss, in combination with neurotransmitters. Neurotransmitter treatments used included 10 nM CGRP or 10 µM ACh with 100 µM neostigmine. To determine whether CGRP exerts its effects via cAMP signaling, 20 µM H-89 was used to inhibit cAMP-dependent protein kinase (PKA), 1 mM cpt-cAMP was used as a cAMP agonist.

Results & Conclusions

While 0.5 mM kainate typically results in destruction of most synapses, a 2 hr exposure to 0.01 mM kainate results in destruction of ACh the number of synapses lost in 0.01 mM kainate was significantly increased. Treatment with CGRP and cAMP also showed significant loss of synapses. This exacerbation was not prevented by H-89 treatment, showing that cAMP acts through an alternative pathway that does not involve PKA. The principal alternative pathway is via exchange protein activated by cAMP (EPAC), the future experiment will be to look for synapse loss after treatment with EPAC specific activator, 8-pCPT-2';-O-Me-cAMP.

Auditory Prostheses V

PS 593

Unique Ear Pathology in the Deafened DTR Mouse Makes It a Promising Model for Chronic Cochlear Implant Research

Deborah J. Colesa[1]; Bryan E. Pfingst[1]; Yehoash Raphael[2]
[1]Department of Otolaryngology - Head and Neck Surgery, University of Michigan; [2]Kresge Hearing Research Institute, University of Michigan

Introduction

Because cochlear implants (CIs) function by stimulating the auditory nerve (AN), it is assumed that the condition of the neurons plays an important role in perception of the electrical stimuli. Animal models are needed to test ways to improve the condition of the nerve and to test its effects on CI function. However, a limitation of many animal models is that the condition of the AN is closely tied to hair cell (HC) survival, so it is difficult to determine which of these elements contributes directly to the functional responses to electrical stimulation. We adopted the diphtheria toxin receptor (DTR) mouse as a novel candidate for CI research and developed a chronically-implanted DTR mouse model. Following diphtheria toxin (DT) injection, these mice exhibit robust AN survival despite complete HC depletion.

Methods

DTR mice treated with DT and wild type (WT) mice were implanted with a single platinum/iridium ball electrode in the scala tympani and tested for up to 70 days. Electrically-evoked auditory brainstem responses (EABRs) and ensemble spontaneous activity (ESA) levels recorded under anesthesia were obtained to assess differences in evoked neural activity and changes over time after implantation. To determine whether the mouse would be a feasible alternative for CI research, we compared it to a long-term stable chronic CI guinea pig model.

Results

EABR amplitude growth functions (neural response magnitude vs stimulus current level) for DT deafened DTR mice and WT mice were similar to those reported for CI guinea pigs with moderate to good AN survival. ESA levels for DT deafened DTR mice and WT mice were between levels for hearing and deaf CI guinea pigs, but the distinct peak at 900Hz seen in CI guinea pigs with hair cells was not as distinct in the mice. Histology will evaluate the condition of the HCs and ANs for correlation to electrophysiological results.

Conclusions

Further testing is needed to determine reliability of similarities or differences between groups and species. The absence of functional differences between WT and DT deafened DTR mice would suggest that HCs are not contributing to the functional measures. Based on results to date, the chronically implanted DTR mouse is a promising model for investigating the effects of HC and AN survival on CI function.

Acknowledgements

PS 594

Neuronal Activation Pattern of Auditory Nerve Fibres due to Cochlear Implant Stimulation: A Modeling Study

Joerg Encke; Siwei Bai; Werner Hemmert
Technical University of Munich

Cochlear Implants (CI) are able to restore hearing to a level where patients are able to reach impressive speech recognition scores while still lagging in other areas like music perception or sound localization. One limiting limiting factor is the small number of frequency channels that can be provided by today';s CIs. One constraint for the number of independent channels within the cochlea is the current spread within the cochlea, which leads to an overlap of the excited neuronal populations. Current spread also plays an important role when trying to recover directional hearing in CI users by including fine structure cues into the coding strategy. Any fine structure cue presented on one channel can be disturbed by the stimulation of a neighboring electrode if the overlapping neural population is too large. So far, many studies tried to estimate the influence of current spread by looking at the decay of the electrical potentials along the length of the cochlea while neglecting the potential distribution along the auditory nerve fibres. In this study we used a finite element approach on a detailed reconstruction of an CI-implanted human cochlea to calculate the electrical potentials inside the whole cochlea and not only the cochlear ducts. Using a novel reconstruction method (detailed in the abstract of Bai et al.) enabled us to reconstruct realistic trajectories for 480 auditory nerve fibres. This approach allowed us to calculate the external electrical potential along each of these neurons for arbitrary stimulation paradigmas. Combining the results from the finite element simulation with cable models of the ANFs enabled us to model the response of each individual fibre to the stimulation. We use this combined model as well as the concept of activating functions to evaluate the influence of different stimulation paradigmas on the spacial and temporal activation pattern of the neuron population.

PS 595

Measurement of Acoustic and Electric Biasing of Electrophonic Response in the Guinea-pig Inferior Colliculus

Attila Fráter[1]; Søren K. Riis[2]; Patrick Maas[2]; Torsten Marquardt[1]
[1]*Ear Institute, University College London;* [2]*Oticon Medical*

Recent improvements in surgical techniques and electrode array design of cochlear implants (CI) offer the possibility to patients to benefit from low-frequency residual hearing when using combined electric and acoustic stimulation (EAS). Electric stimulation of outer hair cells is known to result in electromotility that leads to mechanical movements of the Basilar Membrane and electrically evoked otoacoustic emissions (EEOAE) (Nuttall & Ren., 1995). CI stimulation of the healthy cochlea is also shown to produce a separate, acoustic-like neural response, the electrophonic response (Sato et al, 2016). The current study attempts to demonstrate a common generator of EEOAEs and electrophonic responses by applying various biasing techniques.

Neural recordings using a 32-channel probe inserted along the tonotopic axis of the Inferior Colliculus (IC) of guinea-pigs are conducted in-vivo. EEOAE recording is done by an otoacoustic emission probe that also provided the acoustic stimulus. Electric sinusoid stimuli of 8ms are delivered in a bipolar mode at the tip electrodes of a cochlear implant inserted into the Scala Tympany via a cochleostomy. In one experiment, 100ms long acoustic biasing tones with various levels and frequencies corresponding to the characteristic frequency of the direct electric stimulation place are presented simultaneously with the electric sinusoids. In a second experiment 100ms long biasing DC current signals with positive and negative polarities and various levels are delivered via the stimulation electrode in addition to the electric sinusoids. In a third experiment, we intend to show that OHC motility in the vicinity of the electric stimulation underlies the generation of both EEOAE and electrophonic response.

Acoustic biasing had no effect on the electrophonic response and resulted in distortion products in the EEOAE signal. Positive DC polarity suppressed and negative DC polarity increased the neural response strength to direct electric stimulus, but had no effect on the electrophonic response and EEOAE.

Although unsuccessful so far, simultaneous change in electrophonic IC responses and EEOAE to biasing stimuli could be the first indication that EEOAEs might be useful non-invasive clinical tool to assess the presence of electrophonic hearing in EAS patients. Ongoing work explores the feasibility of EEOAE measurements in CI patients.

Nuttall, A. & Ren, T. 1995. Electromotile hearing: evidence from basilar membrane motion and otoacoustic emissions. Hearing Research, 92(1995), 170-177

Sato, M., Baumhoff, P & Kral, A. 2016. Cochlear implant stimulation of a hearing ear generates separate electrophonic and electroneural responses. The Journal of Neuroscience, 36(1), 54-64

PS 596

A High-Resolution Cochlear Model with Reconstructed Cochlear Nerve Fibres

Siwei Bai[1]; Joerg Encke[1]; Robin Weiß[1]; Friederike Schäfer[1]; Frank Böhnke[1]; Katharina Braun[2]; Werner Hemmert[1]
[1]Technical University of Munich; [2]Eberhard Karls University Tübingen

Most existing computer models of the cochlea in the literature are only able to roughly represent the shape of the cochlea. Here, we developed a finite element (FE) cochlear model with an anatomically-accurate geometry and high-resolution detail of the auditory nerve, and we then used this model to investigate the effects of the cochlear implant (CI) electrode array position.

The structural scans of a human cadaveric temporal bone were acquired using X-ray microtomography (µCT) at a spatial resolution of 5.9 µm. The temporal bone, cochlear canal, and cochlear nerve were segmented from the µCT scans and then smoothed. This composite was then embedded within the temporal bone of a reconstructed head model. The tetrahedral elements of the volumetric mesh were later constructed from the composite to create the FE model. In addition, 485 cochlear nerve fibres were reconstructed inside the FE cochlear nerve model. Each individual nerve fibre ran from the distal end of a dendrite (located within the osseous spiral lamina) through the Rosenthal';s canal to the distal end of an axon, based on Dijkstra';s shortest path algorithm. An additional constraint of a 45-degree spiral pathway around the modiolus axis was included to realistically reflect the spiral feature of the auditory nerve fibre bundles. Our three-dimensional cochlear model with individual cochlear nerve fibres provides a clear visualisation of the anatomical details in the cochlea: the locations of the cochlear ganglion cells are well-represented in the reconstructed model; and the convergences of the dendrites of cochlear ganglion cells are also clearly visible.

Subsequently, we investigated the effects of CI electrode array position by including several CI electrode arrays inside the cochlear canal of the FE model. They were positioned differently relative to the end of the nerve fibre sheet that is located within the osseous spiral lamina. The electrical potential distribution in the cochlea and the modiolus was calculated as a result of stimulating current delivered from the CI electrodes. The electrical potential along the reconstructed nerve fibres was interpolated from the potential distribution in the FE cochlear nerve model. The pattern of neuronal activation elicited by the CI electrode was then predicted based on the interpolated potential along the fibres (as detailed in the abstract of Encke et al).

PS 597

Correlation between Extra- and Intracochlear Electrocochleography during Cochlear Implantation

Adrian Dalbert; Flurin Pfiffner; Christof Röösli; Alexander Huber
University of Zurich, University Hospital Zurich, Department of Otorhinolaryngology, Head and Neck Surgery, Switzerland

Background
In human cochlear implant (CI) recipients, electrocochleography (ECoG) have been attempted from extra- as well as intracochlear sites during cochlear implantation. Both approaches seem to be able to detect electrophysiological changes. However, in intracochlear ECoG recordings the recording electrode together with the CI electrode array moves along the cochlea during insertion. This itself causes a change of the ECoG signal as the relative placement towards the generators of the ECoG signals shifts and makes the interpretation of changes of the ECoG signal difficult. Therefore, the correlation between extra- and intracochlear ECoG findings could allow a more adequate interpretation of intracochlear ECoG recordings.

Methods
ECoG responses to tone bursts at 500 and 750 Hz were recorded. For extracochlear ECoG, a recording electrode was placed on the promontory and left in an unchanged position for all recordings. Extracochlear ECoG recordings were performed after opening the cochlea and after full insertion of the CI electrode array. For intracochlear ECoG recordings, the most apical contact of the CI electrode array was used as recording electrode. Intracochlear ECoG recordings were obtained continuously during insertion.

Results
ECoG signals could be recorded from extra- as well as intracochlear sites. Extracochlear ECoG recordings after full insertion showed either no change in amplitude or a decrease. Intracochlear ECoG responses either continuously increased until full insertion or a decrease appeared at some point during insertion after an initial increase.

Conclusion
Intracochlear ECoG using the CI electrode itself as recording electrode is a promising method to monitor electrophysiological changes and thereby cochlear trauma during cochlear implantation. However, changes of intracochlear ECoG signals during insertion of the CI electrode are difficult to interpret. The correlation of ex-

tra- and intracochlear ECoG could help to elucidate the implications of such intraoperative findings.

PS 598

Can Electrocochleography in Cochlear Implant Recipients Estimate Residual Hearing?

William J. Riggs[1]; Jourdan T. Holder[2]; Robert Dwyer[2]; Amanda Ortmann[3]; Michael S. Harris[1]; Brendan O'Connell[2]; Robert F. Labadie[2]; Craig A. Buchman[3]; Oliver F. Adunka[1]; Leonid Litvak[4]; Kanthaiah Koka[4]
[1]The Ohio State University; [2]Vanderbilt University; [3]Washington University School of Medicine; [4]Advanced Bionics

Introduction

In cochlear implant (CI) patients with preserved residual hearing, intra-cochlear electrode/s from the implant array can be used to measure electrocochleography (ECochG) threshold in response to an acoustic pure tone stimulus. The goal of the present multi-center study was to determine if thresholds estimated based on cochlear microphonic magnitude ("CM thresholds") can be used to predict pure tone audiometric thresholds in CI recipients with residual hearing.

Methods

Seventy (mean age = 52 years, SD = 14) adult Advanced Bionics patients with HiRes90k cochlear implant and a HiFocus mid-scala electrode array participated in this study. Behavioral pure-tone thresholds for warble tones were measured using insert ear phones over the frequency range from 125 to 4000 Hz. ECochG waveforms were recorded on the most apical electrode of the implant array in response to calibrated pure tones and were used to estimate the CM thresholds. The frequencies with behavioral "No Responses" were replaced with 5 dB above audiometric tested stimulus levels.

Results

CM thresholds and behavioral audiometric thresholds could be measured for 63 subjects (266 test frequencies) have shown behavioral and ECochG responses and 7 subjects have shown no behavioral and ECochG responses. A strong correlation ($r2 = 0.85$, $p < 0.001$) was obtained between CM thresholds and the behavioral audiometric thresholds. The mean absolute difference between the ECochG responses and audiometric thresholds was 9 (STD=10.0) dB.

Conclusion

CM thresholds can be used to routinely measure and monitor residual hearing in CI recipients.

Audiogram vs ECochG Thresholds (All)
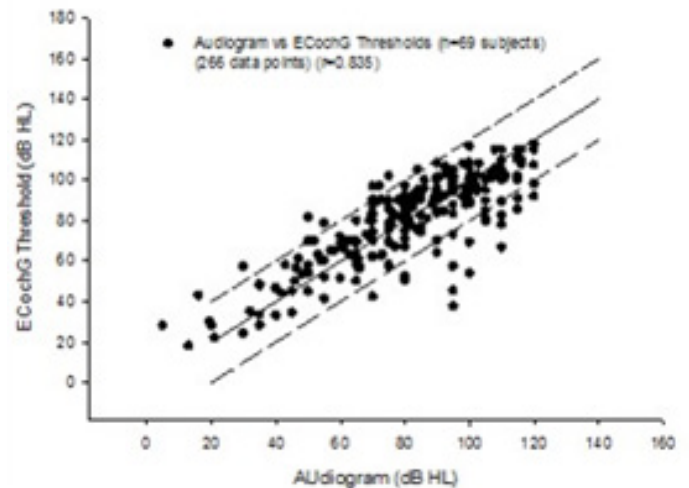
PS 599

Characteristics of electrically-evoked compound action potentials in a large clinical database

Erik Larsen[1]; Leonid Litvak[2]
[1]Decibel Therapeutics; [2]Advanced Bionics

There is an increasing level of interest in characterizing spiral ganglion neuron (SGN) survival and function in cochlear implant (CI) users to help predict or monitor outcomes and to inform potential therapeutic strategies. The electrically-evoked compound action potential (ECAP) provides a possible approach for such characterization, because animal research has indicated that the ECAP growth function slope (amplitude vs. stimulation level) correlates with SGN survival. In vivo measurement of SGN function in humans is possible using telemetry capabilities of CIs.

We conducted a retrospective analysis on ECAPs from a de-identified clinical database of approximately 10,000 Advanced Bionics CIs, which had approximately 170,000 ECAP growth functions measured on subsets of electrodes across one or more time points, in some cases up to 5+ years post-implantation. An ECAP growth function model with a non-linear fitting procedure allowed accurate estimation of noise floor, ECAP threshold, and ECAP growth function slope for approx. 75% of the data. Because no medical history or outcome measures were available, findings from this analysis were mainly observational with limited interpretation.

We found three clear patterns in the behavior of the median ECAP slopes across the database sample:

1) ECAP slopes decreased from apex to base

2) ECAP slopes depended on age at implantation: slopes increased as a function of age in children (0-20 years), but decreased as a function of age in adults (20-80+ years)

3) ECAP slopes increased as a function of duration of use of the CI in children for up to 5 years post-implantation, above and beyond the age-related effect mentioned above. In contrast, ECAP slopes did not change as function of duration of use in adult CI users

This analysis also suggests that the prospective use of ECAP growth functions in individual cochlear implant recipients to monitor changes in cochlear physiology over time is feasible, and may provide insight into the possible relationships of ECAPs with hearing outcomes.

PS 600

Towards Predicting Room Acoustical Effects on Sound-Field ASSR from Stimulus Modulation Power

Valentina Zapata-Rodriguez[1]; Søren Laugesen[1]; Cheol-Ho Jeong[2]; Jonas Brunskog[2]; James M. Harte[1]
[1]*Interacoustics Research Unit; *[2]*Acoustic Technology group, Department of Electrical Engineering, Technical University of Denmark*

One of the most important goals in early intervention of hearing loss is to ensure the childs access to speech. This can enable hearing impaired infants to develop language skills to a level comparable to normal-hearing infants. Hearing-aid fitting validation is important to ensure an appropriate amplification. However, this becomes challenging in pre-lingual infants because they do not respond to behavioral tests. For this reason, there is a growing interest in using objective electrophysiological measures for hearing-aid validation. Here, an approach based on the auditory steady-state response (ASSR) is considered. Instead of using insert earphones to deliver the stimuli, as is customary, the auditory signals are reproduced from a loudspeaker placed in front of the subject, so as to include the hearing aid in the transmission path. Loudspeaker presentation of the stimulus can lower its effective modulation depth due to reverberation and background noise in the measurement room. This could be critical for the quality of the measurement as ASSR magnitude is dependent on the amount of modulation in the stimulus. Previous studies have shown a reduction in the response magnitude as the modulation depth decreases, indicating a slope of about s = 0.8 between response magnitude and modulation depth both in dB (Boettcher et al., 2001; Rønne, 2012; Bharadwaj et al., 2015). However, the relation between observed sound-field ASSR magnitude and changes to stimulus modulation brought about by the acoustical properties of the measurement room has not been considered. The present work explores the relation between the stimulus modulation power and the ASSR amplitude in a simulated sound-field ASSR data set with varying reverberation time. Three rooms were simulated using the Greens function approach, and the impulse responses were convolved with narrow-band (NB) CE-Chirps centered at the octave-bands of 0.5, 1.0, 2.0 and 4.0 kHz. Fifteen normal-hearing adults were presented with the auralized stimuli, as well as an unmodified dry version using insert earphones. The modulation power analysis is done based on the physiological input/output curves previously mentioned. This study discusses to what extend this modulation-growth function can be used as a prediction model to determine the changes in the ASSR amplitude based on the stimulus modulation in the room.

PS 601

Mono- and Multipolar Electrical Stimulation of the Inferior Colliculus Asymmetrically Excite the Auditory Cortex

Gunnar L. Quaß[1]; Andrej Kral[2]
[1]*Dpt. of AudioNeuroTechnology (VIANNA), Hannover Medical School; *[2]*Institute of AudioNeuroTechnology (VIANNA), Hannover Medical School*

The Auditory Midbrain Implant (AMI) has been developed to directly stimulate the inferior colliculus (IC). Reducing the spread of excitation could improve speech understanding in AMI users. In CIs, multipolar stimulation is used to focus the electric field. We systematically investigated the effects of monopolar (MP), bipolar (BP), and tripolar (TP) stimulation of the IC on the cortical response strength and the spread of excitation.

We stimulated the IC of 10 young adult mice using a 1x16 multi-electrode array oriented along the tonotopic axis in MP, BP, and TP mode. The return currents were delivered to an electrode in the scruff (MP), to an electrode on the array immediately dorsal to the source electrode (BP), or split between two neighboring electrodes (TP). We used charge-balanced, biphasic single pulses of 200 µs / phase with alternating lead phases and currents ranging from 10 126 µA, and simultaneously recorded multi-unit activity from primary auditory cortical areas using a 4x8 multi-electrode array. The characteristic frequencies (CF) of all recorded and stimulated units were determined and the cortical responses were grouped with respect to CF-difference to the stimulated IC unit.

The median response thresholds were 70.8 - 79.5 µA peak current and not different between configurations.

The number of evoked spikes per stimulus at 2 dB above threshold was not different in median and around 1.5, and the evoked latencies were between 5 6 ms. Increasing the stimulation current led to stronger responses, and the dynamic ranges were about 14 dB for all configurations. Cortical responses differed in different cortical layers, with some indication of antidromic stimulation in infragranular layers.

All configurations elicited responses in the AC, but we could not find a significant current focusing effect. The spread of excitation was approximately +/- 1 octave in all conditions. We consistently found higher spike rates, lower thresholds, and a higher proportion of responses in regions tuned to frequencies up to one octave higher. In contrast, regions tuned to lower frequencies were less likely to respond and generally had higher electrical thresholds. Our study additionally provides evidence that current focusing in the case of direct contact with neural tissue is not effective in reducing current spread.

PS 602

Auditory brainstem response and compound action potential evoked by electrical stimulation of the guinea pig cochlea

Marcus Mueller[1]; Masaaki Ishikawa[2]; Monika Kwiatkowska[2]; Hubert Loewenheim[3]
[1]University of Tuebingen, Germany; [2]University Tübingen; [3]University ENT clinic, University of Tuebingen, Germany

The electrically evoked auditory brainstem response (eABR) and compound action potential (eCAP) reflect responses of the auditory nerve. We compare eABR and eCAP outcome variables calculated from input-output functions in normal hearing and deafened animals implanted with a 4 channel cochlear implant (provided by MedEl). Guinea pigs deafened using a local application of a kanamycin/furosemide mixture. One week later, a cochleostomy was performed and the scala tympani was filled with a hydrogel mixed with BDNF before insertion of the electrode array. Measurements were performed up to 42 days after implantation. Threshold, maximum amplitude, slope, dynamic range and noise were calculated from input-output functions o. In both eCAP and eABR changes in maximum amplitude, slope dynamic range were found during the observation time. The correlation of thresholds between eCAP and eABR was strong. The findings indicated that eCAP response is less influenced by post-operative time course and inter-electrode contact separation than eABR. Application

of the BDNF-gel resulted in improved physiological responses and, in rare cases, neurite outgrowth onto the cochlear implant. The post-operative effects on eCAP outcome variables were less pronounced than on eABR, indicating plasticity of the eABR response. Both, eCAP and eABR, can provide the identical information regarding the threshold of the AN. The eABR might be more sensitive for predicting the extent of functionalized auditory nerve in deafened cochleae.

PS 603

Does the Pulse Shape of Cochlear Implant Stimulations Influence the Strength and Spread of Neuronal Responses in the Guinea Pig Primary Auditory Cortex?

Victor Adenis[1]; Pierre Stahl[2]; Dan Gnansia[3]; Jean-Marc Edeline[4]
[1]Neuro-PSI, CNRS UMR 9197; [2]OTICON MEDICAL; [3]Oticon Medical; [4]NeuroPSI UMR CNRS 9197

A vast research area is still working on improving the coding strategies of cochlear implants (CI). It shows that the stimulation mode, the pulse shape and grounding schemes can exert either moderate or drastic consequences on the response strength, spread of excitation, electrode discriminability and nerve excitability. Several strategies are currently used to implement sound loudness such as increasing the pulse amplitude, or the pulse duration or the pulse rate. Here, we compared responses from auditory cortex neurons to stimulations delivered through a CI for which several parameters were modified such as the pulse amplitude, the pulse duration and the pulse shape.

Experiments were performed in urethane anesthetized guinea pigs (6-18months old). The tonotopic gradient of the primary auditory cortex (AI) was first established by inserting an array of 16 cortical electrodes (2 rows of 8 electrodes separated by 1mm and 350μm within a row). A dedicated stimulation array (300μm) was then inserted in the cochlea (4 electrodes inserted in the 1st basal turn) and its connector was secured on the skull. The cortical electrodes were placed back in auditory cortex at the exact same location as before the CI insertion. The eight nerve fibers were then stimulated with 20 levels of pulse amplitudes or 20 levels of pulse duration generating similar charges through a dedicated stimulation platform. Asymmetrical pulse shapes were tested for a given level of injected charge. The ratio between the pulses phases increased from 1/1 to 1/10 where one

of the pulse phase amplitude is one tenth of the second phase. The pulse shape was also modified from a current square shape to a current ramp shape.

The firing rate evoked by the pulse duration and pulse amplitude strategies was similar to the one evoked by pure tones and were often of shorter duration than the acoustic responses. The rate-level functions of cortical neurons differed between the acoustic and electric stimuli and can also differ between pulse duration and pulse amplitude strategy. These data suggest that equivalent cortical activation can be achieved by coding sound loudness either with pulse amplitude or with pulse duration. Analyzing the effect of asymmetrical pulses indicates that evoked activities and spatial activation tend to decrease as the ratio increased. Preliminary results on cortical activation by ramped pulses will be presented.

PS 604

Auditory Nerve Degeneration in Cochlear Implant Users Assessed with Electrically Evoked Compound Action Potentials

Ruben H.M. van Eijl; Dyan Ramekers; Sjaak F. L. Klis; **Huib Versnel**
University Medical Center Utrecht, Brain Center Rudolf Magnus, Utrecht University

It is well known from animal studies that the auditory nerve progressively degenerates following severe cochlear hair cell loss. Variability in auditory nerve degeneration is thought to be partly responsible for variability in speech perception among CI users (Seyyedi et al., 2014, Otol Neurotol 35:1446-1450; Kamakura and Nadol, 2016, Hear Res 339:132-141). We have previously shown in guinea pigs that several characteristics of the electrically evoked compound action potential (eCAP) recorded with varying inter-phase gap (IPG) are highly correlated with quantified histological measures of the auditory nerve (Ramekers et al., 2014, J Assoc Res Otolaryngol 15:187-202; Ramekers et al., 2015, Hear Res 321:12-24). In the present study we used the same IPG-mediated difference measures in CI users. We recorded eCAP amplitude growth functions in CI users from three different electrodes (basal, middle, and apical) with two IPGs (2.1 and 30 µs) per- and postoperatively. In addition, we measured speech perception in noise, using digit triplets and the consonant-vowel-consonant words. Overall, we were able to record eCAPs with varying IPG in CI users per- and postoperatively. With increasing IPG the latency of the N1 peak and the slope of the amplitude growth function increased. The effect size of varying IPG on the eCAPs in CI users agrees with observations in guinea pigs.

PS 605

Electrical Stimulation of the Dorsal Cochlear Nucleus: Effects of Dorsal Acoustic Stria Cuts

Stephen McInturff[1]; Osama Tarabichi[2]; Vivek V. Kanumuri[3]; Nicolas Vachicouras[4]; Stéphanie Lacour[4]; Daniel J. Lee[3]; M. Christian Brown[3]
[1]Mass Eye and Ear; [2]Massachusetts eye and ear Infirmary; [3]Eaton Peabody Lab, Massachusetts Eye and Ear Infirmary; [4]ÉCOLE POLYTECHNIQUE FÉDÉRALE DE LAUSANNE

Introduction

Electrical stimulation of the cochlear nucleus (CN) is provided by the auditory brainstem implant (ABI), a hearing prosthesis used by human subjects with absent or damaged auditory nerves. The ABI stimulates CN neurons that project to the inferior colliculus (IC) through the CN';s three acoustic striae, which are the dorsal (DAS), intermediate (IAS) and the ventral (VAS) acoustic striae. Here, in a mouse model of the ABI, we determine how IC responses are altered by cuts to the DAS.

Methods

Surgical exposure of dorsal CN (DCN) and IC were performed in anesthetized CBA/CaJ mice using a posterior craniotomy approach. A 3-channel conformable stimulating array microfabricated at the École Polytechnique Fédérale de Lausanne(EPFL) was placed on the DCN to provide monopolar electrical stimulation. Electrically evoked auditory brainstem responses (eABRs) were recorded with needle electrodes in the skin, and multi-unit activity was recorded with a 16-channel recording probe (NeuroNexus) placed in the IC central nucleus. Cuts were confirmed in Nissl-stained transverse sections. Histology indicated that both the DAS and IAS were cut but for simplification we will call this a "DAS cut".

Results/Conclusion

Before cuts, IC responses to electric stimulation formed a broad peak with latencies between 1.5 and 10 ms (avg = 3.97 ms). In 6 mice, comparison of responses pre/post DAS cut reveals that spiking activity with latencies 5 ms may increase slightly following DAS cut, however this does not appear to be significant (p=0.071). eABRs appear to be unaffected by DAS cut.

These results suggest that the earliest IC responses to DCN electrical stimulation are mediated by DCN pyramidal/fusiform cells (whose axons exit the cochlear nucleus via the DAS). However, other DCN cells or cells projecting out the IAS may also contribute to these responses. In contrast, the later IC responses are mediated by cell types whose axons project out the uncut VAS. These cells could include VCN multipolar or bushy cells.

It is likely that these VCN cells also play a role in the generation of eABRs.

PS 606

Evaluation of Optogenetic Midbrain Implants - a Setup for the Training of Mice in Listening Tasks

Meike M. Rogalla[1]; Lasse Osterhagen[1]; Niklas Lengner[1]; K. Jannis Hildebrandt[2]
[1]University of Oldenburg, Cluster of Excellence Hearing4all; [2]Univesity of Oldenburg, Cluster of Excellence Hearing4all

Behavioral experiments with freely-moving rodents tethered to cables or optical fibers typically need to be conducted in open setups. In hearing research, open-platform setups without walls are often placed in reverberation-free, sound attenuated chambers. This is contrasted with the fact that rodents tend to stay near vertical surfaces and usually dislike and avoid open spaces. Whereas partially enclosed setups lacking parallel surfaces (like wire cages) provide a strategy for the avoidance of escaping behavior and the improvement of experimental outcome in auditory listening tasks, these setups are impractical for the usage in optogenetic experiments with implanted and tethered animals. In this study we conducted behavioral listening tasks in mice within three different setups (enclosed, partially enclosed and open) to investigate how the design of the setup influences training procedure, experimental outcome and hearing thresholds. We show how our enclosed go/no-go setup improves performance during training procedure and how it can be used in experiments with mixed auditory and optogenetic stimulation.

Animals were first trained in either frequency discrimination or the detection of tone pips and clicks. After successful training, animals were transferred to the experimental stage, which consisted of either a frequency discrimination task or the detection of sound (clicks and tone pips) and optogenetic stimulation of an optogenetic midbrain implant placed in the inferior colliculus.

Training of animals in the enclosed chamber reduced time for the training procedure, compared with the partially enclosed and open setups. While in the closed setup mice were successfully trained with as little as five sessions, training in the open setup did not show any success after 10 consecutive sessions. Additionally, training within the enclosed setup had a positive influence on performance in experiments on the open setup later on. Our preliminary results indicate that thresholds obtained at the experimental stage did not differ largely between setups, both for frequency discrimination and the optogenetic detection task.

In conclusion, the enclosed setup made training significantly less time consuming. After successful training, the implanted and tethered animals can then be tested in open setups for tasks involving optogenetic stimulation or electrophysiological recordings without degrading behavioral performance.

PS 607

Hybrid Opto-electrical Neural Stimulation in Cochleae of Deaf White Cats

Zhiping Cao[1]; Yingyue Xu[1]; Naofumi Suematsu[1]; Xiaodong Tan[1]; Hunter Young[1]; Claus-Peter Richter[2]
[1]Department of Otolaryngology-Head and Neck Surgery, Feinberg School of Medicine, Northwestern University; [2]Department of Otolaryngology-Head and Neck Surgery, Feinberg School of Medicine, Northwestern University & Resonance Medical, LLC, Chicago

Background
It has been shown for the rat sciatic nerve that combined optical and electrical stimulation reduces the radiant energy required for INS. Decreasing the energy for INS also reduces the risk of laser-induced thermal damage. We postulate that combined opto-electrical stimulation can also be used in the cochlea to reduce the radiant energy required for optical stimulation. In this study, deaf white cats have been used to explore opto-electrical stimulation.

Methods
Eight cochleae of deaf white cats of either sex were used. Auditory brainstem responses (ABRs) and compound action potentials (CAPs) were measured in response to acoustic, optical, electrical, and the hybrid (opto-electrical) stimulation. Acoustic stimuli consisted of clicks and tone bursts at 2, 4, 8, 16, 32 kHz. Sound levels decreased from a maximum of 107 dB SPL (re 20 µPa) in step of 5 dB. CAPs evoked by opto-electrical stimulation were recorded while the radiant energy, the current amplitude and the time between the optical and electrical pulse delivery were manipulated. At the conclusion of the experiments, all cochleae were harvested and imaged with hard X-rays. The reconstructed images were used to quantify the number of the hair cells and the spiral ganglion neurons (SGNs). The results were confirmed using classical histology.

Results
No ABRs or CAPs could be evoked by acoustical stimuli in any of the deaf white cats. Optical and electrical stimuli were able to evoke ABR responses when delivered alone. Combined optical and electrical stimulation revealed excitatory and inhibitory effects. The timing

between the optical and electrical stimulus and the amplitude of the optical stimulus determined whether the interaction led to an excitatory or inhibitory response. Inhibitory effects were seen for large radiant energies and optical stimulus delivered before the electrical one.

Conclusion
Hybrid electro-optical stimulation of cochleae in deaf white cats showed an interaction between the modes of stimulation. Depending on the selected parameters, delivery of the pulses and timing synergistic and inhibitory effects were seen.

PS 608

Mouse Cochlear Implant Model: Exploring the Limits of Non-Stimulated versus Chronically Stimulated Outcomes

Rene Vielman Quevedo[1]; Alexander D. Claussen[1]; Jonathon R. Kirk[2]; Wolfram F. Dueck[2]; Brian Mostaert[1]; Marlan R. Hansen[1]
[1]Department of Otolaryngology - Head & Neck Surgery, University of Iowa Hospitals and Clinics, Iowa City, IA; [2]Cochlear Americas

Introduction
Cochlear implants (CI) are increasingly used to treat hearing loss, especially with recent advances that extend the candidate population to include patients with residual hearing. It is becoming more pertinent to address issues that hamper their efficacy, including loss of residual hearing after CI (Kopelovich et al., 2014; Kamakura & Nadol, 2016). A mouse CI model would have great utility in investigating mechanisms of cochlear responses to chronic implantation and stimulation given the well-developed genetic and molecular techniques established in mice. Here we present an update on our mouse CI model demonstrating the feasibility of chronic stimulation.

Methods
10 week-old CBA/CaJ adult mice were unilaterally implanted with a 3 electrode CI (Cochlear, Australia). A tethered, chronic stimulation group (n=6) was stimulated 4 hours per day starting 1 week post-operatively and underwent weekly impedance measures and Neural Response Telemetry (NRT). An untethered, non-stimulated group (n=6) served as controls. The pre-determined experimental endpoint was met when animals reached a minimum of 21 days post-operatively and had three consecutive impedance measurements in all electrodes over 35 kOhms (system exceeds programmable lev-

els). Impedance testing and NRT were performed with Custom Sound EP 4.2 (Cochlear, Australia) software. At sacrifice, X-ray imaging and 3D X-ray microscopy (Zeiss X-Radia) assessed implant positioning and integrity. Cochleae were then extracted and 3D X-ray images are obtained with the implant in situ to assess tissue response; histology is later performed to confirm these findings.

Results
Consistent, repeatable impedance and NRT measurements were achieved in both groups at least until 21 days post-operatively, with a longer duration in the unstimulated group. Behavioral responses at levels similar to NRT threshold were demonstrated using manual stimulation from Custom Sound EP 4.2. In situ 3D x-ray microscopy assessment revealed the common occurrence of fractures within the electrode array lead wires near the bullostomy.

Conclusion
We demonstrate the feasibility of a mouse CI model with chronic stimulation. Failure of the lead wires was a common finding, occurring sooner in the tethered, stimulated group. We hypothesize this is due to mouse behavior (scratching, contact with caging), and external forces on the implant caused by the tethering. However, at least 2 weeks of daily, chronic stimulation was achieved. Thus, we demonstrate a model capable of investigating pertinent clinical questions, including the relevance of post-implantation tissue response and mechanism of post-implantation hearing loss.

PS 609

Paired stimulation of the cochlea and the vagus nerve fails to induce cortical map plasticity in the Mongolian gerbil

Maike Vollmer[1]; Thomas Dietrich[2]; Armin Wiegner[2]
[1]Otolaryngology-HNS, University Hospital Magdeburg; [2]Comprehensive Hearing Center, University Hospital Würzburg

Degraded spectral selectivity of neural responses following cochlear trauma or deafness can cause increased channel interaction that negatively affects pitch and speech discrimination in multichannel cochlear implant (CI) users. In hearing rats, acoustic stimulation of the cochlea paired with electric stimulation of the vagus nerve (VNS) has been successfully used to restore normal cortical frequency tuning following noise-induced pathological expansion of receptive fields (Engineer et al., Nature 470, 2011). Thus, pairing acoustic stimulation with VNS appeared to be a promising approach for directing stimulus-specific cortical map plasticity through the release of neuromodulators.

Here we explored whether pairing electric stimulation of the cochlea with VNS (CI/VNS) is effective in reversing deafness-induced degradations in CI-channel selectivity. To investigate spectral interactions with CI stimulation, we developed a multichannel CI for tonotopically selective activation in the central auditory system in freely moving Mongolian gerbils (Wiegner et al., J Neurosci Methods 273, 2016). To test the effects of paired CI/VNS on spectral signal processing, gerbils were bilaterally deafened and implanted with a CI and a cuff electrode around the ipsilateral (left) cervical vagus nerve. Analogous to the prior pairings of pure tones with VNS (Engineer et al., 2011), single channel CI stimulation was repeatedly paired with brief pulses of VNS for several weeks. Acutely deafened gerbils and deafened gerbils with CI-only stimulation served as comparison groups. Standard microelectrode mapping techniques were used to construct spectral cortical maps for multichannel CI stimulation in anesthetized animals.

In deaf gerbils, paired CI/VNS had no effect on spectral selectivity in the auditory cortex. To exclude species-specific (rat vs. gerbil) and stimulus-specific (acoustic vs. electric) differences between the two studies as potential causes underlying the lack of VNS-induced plasticity, we also paired VNS with tones (see Engineer et al., 2011) in hearing gerbils. In these hearing animals, no changes were observed in the cortical representation of the VNS-paired acoustic signal.

In summary, pairing electric or acoustic stimulation of the auditory nerve with VNS failed to induce cortical map plasticity in either deaf or hearing gerbils. These findings contrast with prior results obtained in hearing rats. Our results suggest that the potential for paired VNS to direct cortical receptive field plasticity may be species specific. Additional factors that might have prevented replication of the results by Engineer and colleagues (2011) will be discussed.

Binaural Hearing & Sound Localization in Clinical Populations

PS 610

Speech Perception and Sound Localization in Unilateral Aural Canal Atresia

Malin Siegbahn[1]; Filip Asp[2]; Cecilia Engmér-Berglin[1]; Malou Hultcrantz[1]

[1]ENT-clinic, Karolinska University Hospital and Department of Clinical Science, Intervention and Technology, Karolinska Institutet, Stockholm, Sweden; [2]Department of ENT diseases, Section of Cochlear Implants, Karolinska University Hospital, Stockholm, Sweden; Department of Clinical Science, Intervention and Technology, Karolinska Institutet, Stockholm, Sweden

Background
Spatial hearing may be severely affected by unilateral hearing loss. However, not all individuals demonstrate poor performance. The aim of this study was to compare the performance of sound localization and recognition of speech in competing speech, in adults with congenital unilateral aural atresia and normal hearing adults.

Method
Adults with congenital unilateral aural canal atresia (atresic group, AG, n=13) along with normal hearing adults (NH, n=8) were tested with pure tone audiometry (PTA), speech in competing speech (SCS) and horizontal sound localization accuracy (SLA). The NH group was also tested with unilateral plug and muff, to experimentally induce unilateral hearing loss (EHL group). SLA was tested using eye tracking and results reported as error index (EI) where 0 is perfect and 1 is chance. SCS was measured using an adaptive procedure (fixed competing speech level of 63 dB SPLCeq), aiming at 40% speech recognition.

Results
13 AG subjects were tested with SCS test, and 8 subjects went through SLA test. One subject was excluded due to childhood canaloplasty. The average PTA (0.5, 1, 2 and 4 kHz) in the atresic ear was 66 dB HL, and 3 dB HL in the unimpaired ear. Average PTA in EHL ear was 43 dB HL. Significantly worse levels of speech recognition were observed in the atresic group (mean speech recognition threshold = -10.9 dB) compared to the NH group (-15.1 dB) (p

Conclusion
Adults with congenital unilateral aural atresia show significantly impaired horizontal sound localization accuracy and recognition of speech in competing speech, as compared to adults with normal binaural hearing.

The hearing thresholds in the atresic ear seem to predict horizontal sound localization accuracy, with better performance as a function of lower hearing threshold. There was a tendency towards better localization in congenitally atresic subjects as compared to experimentally induced unilateral conductive hearing impairment. This might be a result of other strategies used for localization, developing as a consequence of experience.

PS 611

Sound Localization Accuracy in Children with Single Sided Conductive Hearing Loss Due to Unilateral Aural Atresia Using a New Method

Hanna Josefsson; Malin Siegbahn; Cecilia Engmér-Berglin; Malou Hultcrantz
ENT-clinic, Karolinska University Hospital and Department of Clinical Science, Intervention and Technology, Karolinska Institutet, Stockholm, Sweden

Background
Children with congenital unilateral aural atresia and associated conductive hearing loss yield lower school results and need remedial education to a higher extent compared to their normal hearing peers. These children furthermore show difficulties with sound localization accuracy in conventional testing of horizontal sound localization. In Sweden, rehabilitation with bone-anchored hearing aids is available to these children from an early age. In this study, directional hearing in children with unilateral aural atresia is examined using a new method developed at Karolinska University Hospital.

Method
Children aged 5-7 with monaural canal atresia and conductive hearing loss were recruited. Directional hearing was tested using the Corneal- Reflection Eye- Tracking Technique, both aided using bone-anchored hearing aids and unaided. The children were placed in a sound isolated room facing 12 speakers paired with a screen. The pairs were situated in the frontal horizontal plane with 10-degree distance in a 110-degree arch. Combined auditory and visual stimulus were presented at 63 dB shifting between speakers at random. The visual stimulus was intermittently withdrawn and reintroduced while sound from the speaker was still playing. A laser measured the pupil positions in relation to the origin of stimulus allowing calculation of horizontal sound localization accuracy. The error index calculated for this group was compared to a control group of normal hearing children.

Results
Error index was calculated and differences estimated between aided and unaided measurements as well as between trial subjects and normal hearing controls. Collection of data is ongoing.

Conclusion
This method for testing horizontal sound localization has not previously been applied to children with unilateral conductive hearing loss. Further results will be discussed.

PS 612

Does a simulated unilateral hearing loss affect sound localization latency?

Martin Eklöf[1]; Filip Asp[1]; Erik Berninger[2]
[1]*Department of ENT diseases, Section of Cochlear Implants, Karolinska University Hospital, Stockholm, Sweden; Department of Clinical Science, Intervention and Technology, Karolinska Institutet, Stockholm, Sweden;* [2]*Department of Audiology, Karolinska University Hospital, Stockholm, Sweden; Department of Clinical Science, Intervention and Technology, Karolinska Institutet, Stockholm, Sweden*

Background
Eye gaze is an innate response to auditory events. Sound localization latency (SLL) of responses may be studied using gaze as a measure of sound localization behavior. The aim was to study the effect of simulated unilateral hearing loss (UHL) on SLL in normal hearing listeners.

Methods
Eight healthy and normal-hearing adults (aged 18 to 40 years) participated in this study as part of another study (1). An array of twelve loudspeaker/display-pairs spanning ± 55 degrees azimuth in the frontal horizontal plane was used for measuring sound localization responses. An ongoing auditory-visual stimulus presented at 63 dB SPL(A) was shifted to randomly assigned loudspeakers with 1.6 sec pauses of the visual stimulus, beginning at each azimuthal shift. The subjects'; saccades towards target was modeled by fitting an arctangent-function to the gaze samples after each shift. The time from an azimuthal shift of the sound to the 50%-point of the arctangent-function was defined as the single SLL. The median across the test (24 shifts) was calculated as a measure of individual performance.

SLL was assessed in normal-hearing condition and in two conditions with simulated UHL. One was achieved by an earplug (UHL1) and one by the combination of an earplug and a circum-aural hearing protector (UHL2), resulting in a mean threshold of 30 dB HL and 43 dB HL (average of 0.5, 1, 2, and 4 kHz).

Results

In the NH condition the average across subjects'; median SLL was 260 msec (SD=35). The intra-individual variation measured as an inter-quartile-range (IQR) was 90 msec on average. One-way repeated measures ANOVA showed a significant effect of listening condition on SLL for the three conditions [$F(21)=16.7$, $p<.000001$]. Post hoc comparisons using the Tukey HSD test and Bonferroni correction demonstrated that the mean SLL increased significantly in the UHL1 condition (mean SLL±sd: 330±60) and in the UHL2 condition (490±120).

Linear regression analysis showed a significant effect of attenuation (ΔUHL in dB, range: 15-45) on SLL prolongation. (ΔSLL=-160+11·ΔUHL, R^2_{adj}=0.62, $p<0.001$, n=8).

Conclusions

Sound Localization Latency assessed by arctangent least-fit of gaze samples showed an increase after a simulated UHL. The SLL prolongation as a function of the unilateral attenuation was 11 msec/dB, showing that increasing hearing thresholds in one ear is associated with prolonged SLL.

References

1. Asp F, Olofsson Å, Berninger E. Corneal-Reflection Eye-Tracking Technique for the Assessment of Horizontal Sound Localization Accuracy from 6 Months of Age: Ear Hear. 2016;37(2):e10418.

PS 613

Cortical reorganization after cochlear implant activation for adults with single-sided deafness

Legris Elsa[1]; Roux Sylvie[2]; Galvin John[3]; Aoustin Jean Marie[4]; Robier Mathieu[4]; Gomot Marie[2]; Marx Mathieu[5]; Bakhos David[1]

[1]*Université François-Rabelais de Tours, CHRU de Tours, UMR-S930, Tours, France; ENT department, Tours, France;* [2]*Université François-Rabelais de Tours, CHRU de Tours, UMR-S930, Tours, France;* [3]*House Ear Institute, Los Angeles, CA, USA;* [4]*ENT department, Tours, France;* [5]*ENT department, Toulouse, France*

Background

Adults with single sided deafness (SSD) experience a loss of binaural function, which is associated with difficulties in sound source localization, poorer speech understanding in noise, and a reduction in quality of life. For SSD patients, restoration of bilateral auditory input is possible only with a cochlear implant (CI). The aim of this study was to investigate cortical reorganization over time after cochlear implantation in order to better understand the effects of restored binaural function.

Method

Nine right-handed adult SSD CI patients participated in the study. Cortical auditory evoked potentials (CAEPs) were recorded before cochlear implantation, and then at 6 and 12 months post-implantation. CAEPs were elicited using speech stimuli (/ba/) delivered in sound field at 70 dBA. The latencies and amplitudes of components P1, N1, P2 and N2 were measured at the central electrode; T-complex waves Na, Ta and Tb in the temporal and mastoid scalp electrodes were also analyzed. Behavioral measures (sentence recognition in quiet and in noise, with and without spatial cues) were collected at the same intervals as for the CAEPs.

Results

At 6 and 12 months post-implantation, a significant increase in the T-complex was observed at the mastoid and temporal sites contralateral to the CI ($p<0.05$). Scalp maps potentials showed contralateral activation on the temporal side of the ear implanted. The increase in T-complex amplitude was correlated with duration of deafness (M2: $r^2 = -0.75$, $p = 0.026$; P8: $r^2 = -0.81$, $p = 0.011$). In the fronto-central electrodes, no significant change was observed for amplitude or latency for P1, N1 and P2 waves. However, there was a significant change in N2 amplitude and latency at 12 months ($p<0.05$). A significant improvement for speech understanding in noise was observed at 12 months when speech was presented to the CI ear and noise to the normal-hearing ear ($p=0.02$).

Conclusion

After cochlear implantation, speech understanding significantly improved when speech and noise were spatially separated. The correlation between T-complex amplitude and duration of deafness highlights the importance of early implantation for SSD patients. The absence and then restoration of the T-complex and N2 wave before and after cochlear implantation may reflect cortical reorganization and restoration of binaural function in SSD CI patients.

ARO 2018 abstract.docx

PS 614

Variability of binaural-phase sensitivity measurements in hearing-impaired listeners with similar audiograms

Olaf Strelcyk[1]; Pavel Zahorik[2]; Chhayakant Patro[2]; Peter Derleth[3]

[1]*Sonova US;* [2]*Heuser Hearing Institute;* [3]*Sonova AG*

Background

Interaural phase difference (IPD) detection has been

considered as a candidate measure for assessing supra-threshold deficits that may characterize individual hearing impairment (HI) beyond the audiogram. Low-frequency IPD sensitivity has been found to decrease with age, and some studies have found weak associations with hearing thresholds while others did not. The upper frequency limit up to which tone IPDs can be detected has previously been measured using adaptive staircase methods. Here, we use a Bayesian procedure instead, which has advantages in terms of efficiency and the ability to detect chance performances.

Methods

IPD detection limit frequencies were measured using a 2-interval, 2-alternative forced-choice task. Measurements were repeated with two different stimuli, amplitude-modulated (AM) tones (AM rate of 2.5 Hz) and gated tones of 1.6-s and 1-s durations, respectively. Tones were presented diotically in the reference interval while the IPD alternated between 0° and 180° in the target interval, with a presentation level of 30 dB above the individual';s pure-tone thresholds. Bayesian procedures were used to sample and estimate psychometric functions (IPD detection as a function of carrier frequency). Participants were of ages 56+ years and had similar, symmetric, sloping hearing losses with low-frequency pure-tone thresholds (average of 125 to 1500 Hz) ranging from 38 to 52 dB HL.

Results

Testing with AM tones versus gated tones yielded similar results. However, the measured IPD detection limits varied widely across listeners despite very similar audiograms. While some listeners showed performances at levels comparable to normal-hearing listeners, four out of thirteen listeners were not able to detect IPDs at any frequency down to 125 Hz, even after task-specific training. Furthermore, two listeners showed large test-retest variability.

Conclusions

Given the observed large across-listener variability, the IPD detection limits may reflect supra-threshold deficits not reflected by the audiogram. However, it needs to be clarified to what extent performances may have been limited by task demands and whether this could explain the observed cases of large test-retest variability.

PS 615

Binaural Aspects of Perceived Reverberation Strength in Normal-hearing and Hearing-impaired Listeners

Gregory Ellis[1]; Pavel Zahorik[2]
[1]*University of Louisville; [2]Heuser Hearing Institute*

Background

Previous research has shown that normal-hearing listeners report changes in perceived reverberation strength only when physical reverberation level is manipulated in both ears together, but not when manipulated in one ear alone. This suggests that perceived reverberation strength depends on binaural aspects of reverberant sound level. The purpose of this study is to further explore the impact of hearing loss on this phenomenon.

Methods

Stimuli were presented over headphones using virtual auditory space techniques. Binaural room impulse responses (BRIRs) were generated for a source 90-degrees to the listener';s right in a reverberant room (T_{60} = 1.8s). Reverberation level was scaled in the BRIR channel ipsilateral to the source or in both channels (3 dB steps from 0 to -21 dB). The direct-path was not changed. The source signal was 5 s of English spoken by a female talker.

55 NH and 9 HI listeners performed a magnitude estimation task with a standard (un-manipulated BRIR). HI listeners had symmetric, mild-to-moderate sloping high-frequency hearing loss profiles. To ensure stimulus audibility comparable to the NH listeners, linear amplification using the NAL-R prescription was implemented for the HI subjects. Listeners reported the amount of perceived reverberation in the test stimulus relative to the standard using a ratio scale. Listeners made five ratings per stimulus. Stimulus presentation order was randomized.

Results

Consistent with previous results, NH listeners reported changes in perceived reverberation strength when physical reverberation level was varied equally in both ears, but not when varied in one ear alone. This pattern of results may be explained by assuming that perceived reverberation strength depends on a summation of physical reverberation level at the two ears. Results from HI listeners were generally similar, but with increased intra-subject variability. This variability does not appear to be related to the audiogram, however.

Conclusions

HI and NH listeners scale perceived reverberation consistently when reverberation is reduced in both ears.

Reducing the amount of reverberation in the ear nearest the source has little to no effect on ratings of perceived reverberation in the conditions tested (source at +90 degrees) for HI and NH listeners.

HI listeners show considerably more variability than NH listeners.

A Rabbit Model of Sensorineural Hearing Loss for Sound Localization Research

Hariprakash Haragopal; Ryan Dorkoski; Mitchell L. Day
Ohio University

Human listeners with sensorineural hearing loss (SNHL) have impaired ability to localize sound sources. However, the neural correlates of this behavioral impairment remain unknown. Our aim is to investigate the effects of SNHL on neural coding of sound source location. Here, we create a rabbit model of SNHL—a species which 1) has a hearing range that overlaps with humans, 2) uses both interaural time and level differences to localize sound, 3) is easy to work with during awake, head-fixed neural recordings, and 4) has been used previously in sound localization research. To produce an SNHL, we presented loud, octave-band noises centered at 750 Hz to anesthetized Dutch-belted rabbits from two free-field speakers—one directed at each ear. Noise waveforms from each speaker were independent and uncorrelated with each other in order to produce the perception of a spatially diffuse source. Hearing loss was quantified as the difference in threshold levels between auditory brainstem responses (ABRs) measured prior to and 2 weeks after acoustic trauma (using clicks and tones from 0.5 to 16 kHz in octave steps). We tested exposure levels from 122 to 135 dB SPL and exposure duration from 15 to 90 min. An exposure of 133 dB SPL for 60 min produced, on average, an approximately 20-dB increase in pure-tone thresholds at all frequencies and a 15-dB increase in click thresholds. Exposure levels below 133 dB SPL failed to produce threshold shifts while those above 133 dB SPL produced profound deafness. Threshold shifts could be progressively increased by increasing the exposure duration at 133 dB SPL.

Head Motion Resolves Front-Back Confusions in Cochlear Implant Patients

M. Torben Pastore; Sarah J. Natale; Michael F. Dorman; William A. Yost
ASU

In real-world scenarios, listeners and sound sources are in motion much of the time. To distinguish the relative motion of surrounding sound sources from changes in auditory spatial cues resulting from listeners' own movements, listeners must integrate information from various sensory modalities, motor feedback, and cognitive processes. This disambiguation is essential to localizing sound sources in the context of a listener's local environment. Yet much of what we currently understand about audition in normal hearing (NH) and hearing impaired (HI) populations is based on experimental conditions that hold listeners and sound sources stationary. For sounds with sufficient high-frequency information, NH listeners can use spectral pinna cues to resolve front-back confusions, which they cannot do for low-frequency stimuli. However, for low-frequency stimuli, NH listeners can exploit their own motion, often using head-rotation, to resolve front-back ambiguities by comparing their own motion with the resulting changes in binaural difference cues. Most bilaterally implanted cochlear implant (CI) patients localize relatively poorly at low frequencies and have little or no access to high-frequency pinna cues, because of reduced spectral resolution and the location of the implant microphones on the head instead of in the concha. It can therefore be expected that they are likely to experience front-back confusions for high frequency stimuli at a rate that equals or surpasses NH listeners for low-frequency stimuli when they keep their head stationary. It is not known whether CI patients, with their reduced auditory spatial acuity, can resolve front-back confusions using a head-turning strategy similar to ones used by NH listeners for low-frequency stimuli. We will present results for listeners bilaterally implanted with Med-El cochlear implants who were presented with noise stimuli from six loudspeakers surrounding them in the azimuth plane. Results show that all listeners (1) exhibited a high incidence of front-back confusions when they did not move their head, (2) were able to use moderate head movements to substantially improve their reliability in distinguishing sound sources located in front from those behind them, and (3) were unable to realize this improvement when one implants was turned off. These results suggest that bilaterally-implanted CI listeners may, at least to some extent, be able to improve their localization performance by using their own motion to compensate for localization deficiencies observed under the static conditions commonly tested in laboratory settings. (Research supported by a grant from the NIDCD)

The choice of stimulation strategy might be of importance for the access to inter-aural time differences in children tested with their clinical processors

Martin Eklöf[1]; Bo Tideholm[2]
[1]Department of ENT diseases, Section of Cochlear Implants, Karolinska University Hospital, Stockholm, Sweden; Department of Clinical Science, Intervention and Technology, Karolinska Institutet, Stockholm, Sweden; [2]Department of ENT, Karolinska University Hospital, Stockholm, Sweden; Department of Clinical Science, Intervention and Technology, Karolinska Institutet, Stockholm, Sweden

Background

Bilateral cochlear implantation (CI) has been proven beneficial for treating severe hearing loss in children. The availability of binaural effects found so far has been limited to head shadow effect in communication and interaural level differences (ILD) in localization. Efforts have been made to make interaural time differences (ITD) available by introducing stimulation strategies that take the momentary phase of the soundwave into account, denoted fine structure (FS) strategies.

The aim of this study was to investigate:

- if the ITD ability is dependent of stimulation strategy.

- if there is a correlation between ITD, ILD and the ability to localize different stimuli.

Method

30 subjects aged 8-13 who was implanted bilaterally before the age of 3 were included in the study. 20 of the subjects used a FS strategy in their processors on both sides, denoted the FS group. 10 subjects used a non-FS strategy in their processor(s) one or both sides, denoted the non-FS group.

Psychophysical tests assessed their ITD and ILD just noticeable difference (JND) of a 250 Hz pure tone using their everyday stimulation strategy.

Furthermore, their ability to accurately localize sound in the horizontal plane were measured using a corneal reflection eye tracking technique described in Asp et al. (1). Two different stimuli were used; a broadband (BB) stimulus and a low-pass filtered (LP) stimulus (500 Hz cut-off frequency).

Results

10 of the 20 subjects in the FS-group obtained a physiologically legitimate threshold (

Conclusions

The ability to lateralize 250 Hz pure tones using only ITD was possible when the stimulation strategies had FS information. This ability did not influence the localization ability of the low frequency stimulus used in this study, but was associated with better localization ability of the broad band stimulus. The results also suggest that a low ILD is necessary to improve the localization ability.

References

1. Asp F, Olofsson Å, Berninger E. Corneal-Reflection Eye-Tracking Technique for the Assessment of Horizontal Sound Localization Accuracy from 6 Months of Age: Ear Hear. 2016;37(2):e10418.

PS 619

Perturbation of interaural level differences in bilateral cochlear implants

Sebastian Ausili[1]; Mathias Dietz[2]
[1]Donders Institute, Radbound University; [2]Western University

Several studies demonstrated the advantage of bilateral cochlear implantation over unilateral implantation. Free-field sound localization studies have shown that a typical bilateral cochlear implant (BICI) user has a binary left-right lateralization pattern but little or no systematic target-response relation on either side. On the contrary, studies investigating interaural level difference (ILD) perception in BICI users have shown that BICI users have a close to normal sensitivity to ILD. Differences may be due to the signal processing in the cochlear implant which is mostly bypassed in the ILD experiments but which perturbs ILDs in the free-field localization task.

The present study aims to investigate the device-related issues of a left-right pair of typical CIs in a clinical configuration and analyse the output to HRTF-filtered stimuli at the level of the electrode arrays. Specifically two stages have been identified to significantly corrupt ILDs: The front-end automatic gain control (AGC) and the n-of-m selection. Simulations were performed with each stage switch off, clinical setting, and with a binaurally coordinated setting.

In line with other studies AGC is shown to alter ILDs significantly. Especially for broadband stimuli we show that output levels at apical electrodes may be larger in the contralateral ear causing a blurred spatial representation. Similar effects are caused by n-of-m selection which for broadband noise tends to select basal channels at the ipsilateral side but apical channels at the contralateral side due to the lower head shadow. Under extreme circumstances even the overall stimulation current can be larger at the contralateral side, when both AGC and n-of-m are switched on.

In conclusion this study shows that bilaterally un-coordinated devices provide heavily distorted ILDs and the step-by-step analysis helps to better interpret the spatial hearing abilities of BICI users.

Development III

PS 620

Ion Channel Expression in the Developing Human Inner Ear

Rikki K. Quinn; Hannah R. Drury; Melissa A. Tadros; Robert J. Callister; Alan M. Brichta; **Rebecca Lim**
The University of Newcastle

Background

Sound and head movements are detected by hair cells (HCs) of the inner ear. To generate their electrochemical output HCs express important ion channels in their basolateral membranes. However, little information is known about when these ion channels are first expressed during human HC development, and our understanding of when HCs become functional is even more limited. The vast majority of studies investigating inner ear development have focussed on rodent models with little information available on human inner ear development. Therefore, the aim of the current study was to determine the expression patterns of ion channels, such as potassium and calcium channels, in the utricle, cristae, and cochlea of the human developing inner ear.

Methods

Inner ears from human products of conception ranging from fetal age 9 to 17 weeks gestation were dissected to isolate vestibular (utricle and cristae) and cochlea (apex, middle and base) regions. Tissue was homogenised and RNA isolated using QIAGEN miRNeasy Mini Kits. RNA was reverse transcribed into cDNA using Superscript III Reverse Transcriptase and qPCR run to assess ion channel expression in the inner ear.

Results

Expression of ion channels were significantly different between regions of the inner ear. In particular, expression of potassium (KCNQ4) and calcium (CACNA1C) channels were significantly higher in the middle region of the cochlea than other regions. Moreover, KCNQ4 showed significantly lower expression in the cristae than utricle or cochlea regions. KCNQ4 expression, however, increases with gestational age in most regions of the inner ear. In contrast, CACNA1C expression seems to diverge in the two regions of the inner ear. CACNA1C expression decreases in the vestibular organs, but increases in the cochlea with gestational age.

Conclusion

Our results show that ion channel expression in developing human fetus varies with gestational age and across inner ear regions. For example, the pattern of CACNA1C expression indicates that development of calcium signalling likely occurs earlier in vestibular organ development, compared to the cochlea. KCNQ4 shows significantly higher expression in the utricle and middle portion of the cochlea compared to other regions. Although the reason for these regional differences is unclear, it suggests a greater role for this ion channel subtype within these specific regions. Identifying key ion channels involved in functional development of HCs and their spatial expression may allow us to promote regenerative HC growth from pluripotent stem cells. This in turn, may lead to the potential targeted treatment of deafness and balance disorders of the inner ear.

PS 621

Position- and ATP-dependent signaling activity in mouse developing inner hair cells

Anne-Gabrielle Harrus; Jean-Charles Ceccato; Gaston Sendin; Jérôme Bourien; Jean-Luc Puel; Régis Nouvian
The Institute for Neurosciences of Montpellier (Inserm U1051) and University of Montpellier

During development, the sensory cells of the cochlea, the inner hair cells (IHCs), fire spontaneous calcium action potentials. This spontaneous spiking activity at the pre-hearing stage allows the IHCs to automatically excite the auditory nerve fibers and hence, represents a valuable mechanism to shape the tonotopic organization along the ascending auditory pathway. Spontaneous spiking pattern may depend to the IHCs position along the base to apex gradient of the cochlea (the tonotopic axis) and rely on the ATP secretion from neighboring supporting cells. Here, we used calcium imaging in the immature neuro-sensory epithelium of the cochlea, the Kölliker´s organ, to gain insights in the IHCs spiking activity. After loading the Kölliker´s organ with the calcium dye fura-2 AM, propagation of spontaneous calcium waves were readily observed across supporting and sensory cells. Both basal and apical IHCs were characterized by similar spontaneous calcium transients interspaced with silent periods, reminiscent of bursts of action potential recorded in patch-clamp. In addition, neighboring cells show a strong degree of synchronous activity. Incubation with apyrase, which hydrolyzes ATP, prevents the spontaneous calcium increase that propagates across the supporting cells within the Kölliker's organ, but leaves the spontaneous calcium transients in IHCs mostly unaffected. These findings support the hypothesis that the tonotopic map refinement in higher auditory centers arises coordinated activity of neighboring sensory cells, which seems to be independent of ATP.

PS 622

Sema5b controls cochlear sensory domain patterning and may control SGN branching patterns

Kaidi Zhang[1]; Johnny Jung[1]; Maeher Grewal[1]; Mark McMurray[2]; Ronna Hertzano[3]; Thomas M. Coate[4]
[1]*Georgetown University;* [2]*University of Maryland School of Medicine, Baltimore, MD;* [3]*University of Maryland School of Medicine, Baltimore, MD USA;* [4]*Department of Biology, Georgetown University*

Semaphorins (Semas) and their Plexin (Plxna) receptors constitute a large family of axon guidance factors. Many Semas and Plxnas are known to be expressed in the mammalian inner ear during development, but their precise functions remain unclear. Here we show that cells of the cochlear prosensory domain express Sema5b before hair and supporting cells are specified. As development proceeds, Sema5b expression becomes limited to inner and outer hair cells and is also apparent in spiral ganglion neurons (SGNs). Compared to WT control littermates, mice lacking Sema5b show significantly more extra outer hair cells clustered with additional supporting cells. We are currently investigating the possibility that Sema5b normally restricts the spatial limits of the prosensory domain. During cochlear wiring, the SGNs express PlexinA1 and PlexinA3 (two known receptors for Sema5b) and thus we hypothesized that Sema5b acts as a mediator of SGN guidance decisions. In cultured cochleae, exogenous Sema5b-Fc restricts SGN filopodial extension, suggesting that Sema5b normally acts in a repulsive role. Using standard antibody markers, Sema5b null mice do not show conspicuous alterations in cochlear wiring and synapse formation and we are currently employing a sparse genetic labeling approach to more carefully examine SGN morphology in these mutants. In addition, we are currently determining the extent to which the loss of Sema5b leads to hearing impairment by analyzing auditory brainstem responses.

PS 623

Morphogenesis of Type I Spiral Ganglion Neurons and a potential role for Sema3a/Nrp1 signaling

Homero Cantu[1]; Thomas M. Coate[2]
[1]*George Town University Medical Center;* [2]*Department of Biology, Georgetown University*

Proper connectivity of spiral ganglion neurons (SGNs) and hair cells is necessary for conveying sound information to the brain. The majority of SGNs are composed of type I fibers that innervate inner hair cells (IHCs) in the organ of Corti and transmit the vast majority of sound input. However, very little is known about the molecular mechanisms that mediate type I SGN innervation patterns on IHCs. Classic studies in the cat auditory nerve (by Liberman et al) have suggested two distinct morphological and functional populations of type I SGNs: thin SGNs with low rates of spontaneous discharge tend to innervate the modiolar side of the IHCs, and thicker SGNs with higher rates of spontaneous discharge tend to innervate the pillar cell side of IHCs. Using genetic SGN sparse labeling, confocal imaging, and morphometric analyses, we have begun to characterize the developmental time course of type I SGN innervation of mouse IHCs. Interestingly, at early stages, the average diameter of fibers contacting the modiolar side of the IHC is significantly lower than the diameter of fibers contacting the pillar side of the IHC. But, at P8 these differences are not apparent. Our data show that, around the onset of hearing and through P30 that type I SGNs on the modiolar side of the IHC become thicker compared to those on the pillar cell side of the IHC. Using genetic models, we are attempting to identify signaling factors that may play a role in this pattern of innervation. We have found that Semaphorin 3a (Sema3A) and its main receptor Neuropilin 1 (Nrp1) may be part of this organization. Sema3A is a diffusible member of the semaphorin family known to act as a chemorepellent leading to the collapse of growth cones. Via in situ hybridization, we identified the expression of Sema3a around IHCs in the developing cochlea suggesting a potential role in the innervation pattern of type I SGNs. Nrp1 protein is detectable on SGN processes and enriched in fibers projecting toward the pillar cell. We are currently examining several Nrp1 and Sema3a mutant models to determine if Sema3a/Nrp1 interactions control type I SGN synaptic organization at the IHC.

PS 624

Birthdates of ventral cochlear nucleus neurons correlate to their tonotopic locations

Austin Shepard; Wei-Ming Yu
Department of Biology, Loyola University Chicago

Tonotopy is a key anatomical feature of the vertebrate auditory system. However, little is known about the mechanisms that are responsible for the development of this feature. In the cochlea, spiral ganglion neurons are born in a basal to apical progression along the length of the cochlea, with neurons in the base responding to high frequency sounds born early around mouse embryonic day (E) 9.5 and those in the apex responding to low frequency sounds born late around E12.5 to 13.5. It is not clear whether cochlear nucleus neurons are also born in a similar fashion. Using nucleotide analog incorporation assay, we examine whether cochlear nucleus neurons are born in a regional gradient according to their birthdates. Most cochlear nucleus neurons are born between E10 to E13, with a peak at E12.5. No regional gradient

was observed in the dorsal cochlear nucleus. However, some neuronal clusters can be found in the ventral cochlear nucleus and these neurons are born in a dorsal to ventral gradient, which correlates with their tonotopic locations. Currently, we are analyzing whether these cell clusters are formed by the same cell type, the bushy cell, and whether the birthdates of ventral cochlear nucleus neurons also correlate with the tonotopic connections from the spiral ganglion neurons.

PS 625

Inhibitory synapses in the auditory brainstem develop a fast and Ca2+-dependent vesicle replenishment after hearing onset

Dennis J. Weingarten[1]; Nicolas Müller[2]; Eckhard Friauf[2]; Henrique von Gersdorff[3]
[1]*Animal Physiology Group, Department of Biology, University of Kaiserslautern;* [2]*Department of Biology, University of Kaiserslautern;* [3]*Vollum Institute, Oregon Health and Science University*

Mammals have evolved the ability to accurately pinpoint the location of high frequency sounds in the horizontal plane. This requires a system that can distinguish sound signals that differ by minute amounts of intensity. Indeed, reliable synaptic transmission is a hallmark of the ascending auditory pathway where highly specialized excitatory synapses allow the processing of auditory information with exquisite temporal precision. However, less is known about how inhibitory synapses shape the processing of sound signals after hearing onset. Here, we investigated the inhibitory synapses converging from the medial nucleus of the trapezoid body (MNTB) to the lateral superior olive (LSO) in the mouse auditory brainstem. An acceleration of evoked excitatory and inhibitory postsynaptic currents (EPSCs & IPSCs) has been observed in the LSO during postnatal development. Yet, changes in presynaptic parameters remain unclear. Using whole-cell patch clamp recordings in acute brainstem slices we characterized inputs from the MNTB and the cochlear nucleus (CN) to principle neurons of the LSO (MNTB-LSO and CN-LSO synapses) via electrical stimulation of the respective axons. Recordings were done at 36±1°C from pre-hearing mice at postnatal day P10-12 and young adults at P28-34. Evoked IPSCs of MNTB-LSO synapses showed a 2-fold acceleration of their kinetics from P10-12 to P28-34. Accordingly, miniature IPSCs (mIPSCs) showed a 2-fold speeding of their kinetics between both age groups, whereas mIPSC amplitudes remained unchanged at around 25 pA. The mIPSC frequency increased from 3 to 6 Hz. Furthermore, IPSC onset latency was reduced from ~1 ms to below 500 µs (P10-12: n=9, P28-34: n=14). Via application of high-frequency stimulation trains (50 pulses of 50, 100, and 200 Hz) we estimated the readily re-

leasable pool (RRP) and the delay and extent of vesicular replenishment in both ages. Surprisingly, a strong reduction of RRP vesicles from 600 to 200 vesicles was observed (P10-12:n=14, P28-34:n=14), whereas, the vesicular release probability doubled after hearing onset from 6 to 12%. To cope with this accelerated emptying of the RRP, MNTB-LSO synapses stimulated at 100 Hz showed a faster onset of replenishment, which shifted from 80 ms to 40 ms (P10-12:n=14, P28-34:n=14). In both age groups this onset became shorter with higher stimulation frequencies, hinting at a Ca^{2+}-dependent mechanism. Introducing gaps of different lengths (10-5000 ms) in between stimulation trains revealed an increased Ca^{2+}-dependent RRP replenishment in P28-34. In summary, mature MNTB-LSO synapses have remarkably fast and resilient presynaptic machinery for replenishing synaptic vesicle pools.

PS 626

Ears on Rears: Transplantation of Ears Reveals Afferent Pathfinding Properties in Spinal Cord and Peripheral Nerves

Clayton Gordy; Karen L. Elliott-Thompson; Bernd Fritzsch
University of Iowa

Background
Afferents develop from the inner ear to establish precise connections between hair cells and central nuclei. How the topology of central connections (vestibular fibers to vestibular nuclei, cochlear fibers to cochlear nuclei) are established is unknown. Transplantation of a third ear immediately rostral to the native ear demonstrated that afferents of transplanted ears project with native afferents into the vestibular nucleus of the hindbrain, suggesting molecular pathfinding (Elliott et al., 2015). More recently, Wnt signaling was identified as a possible diffusible organizer for these projections (Yang et al., 2017). Since Wnt expression is continuous between the hindbrain and spinal cord, we transplant a third ear caudally adjacent to the spinal cord to investigate peripheral and central navigational properties of afferents.

Methods
Otic placodes or vesicles were transplanted to the spinal cord or ventral heart region of same stage Xenopus laevis embryos (St 24-36). To reveal generality of our conclusions, we also transplanted otic vesicles next to the spinal cord of chicken embryos. Axonal projections were revealed with lipophilic dye at stage 46-47 using confocal microscopy.

Results
Ears transplanted to the spinal cord at stage 24-30 show

fibers projecting dorsally within the spinal cord. Co-labeling of dorsal root ganglia revealed that most ear afferents were dorsomedial to native spinal cord afferents. Many fibers elongate along the dorsal funiculus to reach the hindbrain where they reroute to the vestibular nucleus. Later transplanted ears received lateral line afferents and projected into the lateral line nerve. This may have occurred because lateral line placode migration was spatially close to the ear transplantation, attracting afferents to reach unusual targets (lateral line to inner ear, inner ear along lateral line fibers). Alternatively, ear afferents could prefer to grow along placodally-derived neurites. To check for this, we transplanted ears next to the heart and found ear afferents projecting along vagal nerves to the hindbrain.

Conclusions

Consistent with Atoh1 knockout mice that show topologically correct hindbrain projections in the absence of cochlear nuclei, we show here topologically correct projection to the spinal cord using presumably the same molecular guidance. Here we show that inner ear afferents are opportunistic in their ability to navigate along existing nerves. Upon reaching the CNS, afferents are guided to dorsal spinal cord regions and the vestibular nucleus of the hindbrain. We are investigating the roles of dorsally expressed diffusible molecules in axon guidance using molecular knockdown of Wnt signals and receptors.

PS 627

Postnatal development of vestibular nerve afferents and hair cells in mouse utricles

Roxanna Massoodnia[1]; Brandon C. Cox[2]; Remy Pujol[3]; Mark Warchol[4]; Jennifer Stone[5]
[1]*University of Washington, Speech and Hearing Sciences Department;* [2]*Department of Pharmacology and Department of Surgery, Division of Otolaryngology, Southern Illinois University School of Medicine;* [3]*University of Montpellier;* [4]*Washington University School of Medicine;* [5]*University of Washington*

The vestibular epithelia of mature rodents contain type I and type II hair cells (HCs), which are distinguishable by their morphology, molecular properties, and vestibular nerve contacts. Type I and II HCs are interspersed throughout the epithelia, and HC nuclei are organized in discrete laminae, particularly in peripheral zones. Vestibular HCs develop during embryogenesis and the first postnatal week. In the mouse utricle, approximately half of the HCs are formed during the first postnatal week (Burns et al., 2012). However, little is known about the types of HCs that are produced or how HCs become innervated during this postnatal period. Here, we explored these two aspects of vestibular development in mouse utricles.

To identify HCs formed postnatally, we fate-mapped neonatal supporting cells (SCs) by injecting Plp-CreER^{T2}::Rosa26^{tdTomato} mice at postnatal day 2 (P) 2 and 3 with tamoxifen, which induces expression of the fluorescent protein tdTomato (Tom) in 81% of SCs and a small number of HCs. At P9 (7 days post-tamoxifen) and at P30 (28 days post-tamoxifen), we dissected utricles and classified Tom-positive HCs as type I or II using cell-specific antibodies. At 7 days post-tamoxifen, the macula was poorly laminated and there were 308 HCs Tom-positive HCs per utricle that were immature and not classifiable as either type I or II HCs. By contrast, at 28 days post-tamoxifen, the macula was well laminated and mature-appearing. There were 604 Tom-positive HCs per utricle, which was 2x that recorded at 7 days post-tamoxifen. The vast majority (95%) of Tom-positive HCs were type II.

To further explore postnatal development of vestibular HCs, we labeled utricles from mice between P0 and P21 with an antibody to Sox2, which is expressed by type II, but not type I,HCs. We also labeled utricles with neuronal markers to reveal calyx nerve terminals of type I HCs. We found that between P3 and P10, there was a significant reduction in the percentage of HCs that were Sox2-positive (~ 80% at P3 and ~60% at P10). Numbers of calyx nerve terminals increased dramatically during this same period. Cell-by-cell analysis indicated that type I HCs lose Sox2 immunoreactivity as calyces are forming, but type II HCs retain Sox2 expression as they mature.

These findings demonstrate that most HCs produced during the postnatal period become type II HCs, and many HCs formed prior to P2 downregulate Sox2 and acquire the type I phenotype during this period.

PS 628

Determining the Role of Bassoon in Ribbon Development

Brendon Warner; Sarah Cox; Skyler Young; E. Jacob Ivey; Benjamin Merrill; Jonathan K. Alder; Arminda Suli
Brigham Young University

Hearing loss can result from improper development of the sound-detecting mechanosensory hair cells (HC), incorrect innervation of the HCs, or faulty synapse formation. Our goal is to better understand the mechanisms by which synapses in HCs are formed. Ribbons, the specialized structures that tether synaptic vesicles at HC synapses are thought to be anchored by the cytomatrix protein bassoon. In bassoon mutants, ribbons are found floating and not attached at the active zone. Furthermore, they show reduced vesicle exocytosis, re-

duced reliability of spiking at the auditory stimulus onset and abnormal auditory brain responses. Recently, bassoon was implicated in having an additional function at ribbon synapses: that of trafficking ribbons to the active zone of photoreceptor cells, another cell type that uses ribbons at their synapses. This function is consistent with that in conventional synapses, in which bassoon aids in transporting other cytomatrix proteins, such as piccolo, ELKS2/CAST, to the active zone. In conventional synapses, bassoon is also thought to cluster synaptic vesicles and speed synaptic vesicle reloading at release sites. Because the "floating" ribbon phenotype in ribbon synapses could simply be due to failure to be transported at the active zone, we would like to test the possibility that bassoon is not needed for ribbon tethering. For this purpose, we would like to remove bassoon in a conditional manner during ribbon localization and after mature synapses are formed. Using the CRISPR/Cas9 system, we can tag the endogenous bassoon gene for conditional degradation in the zebrafish model system. This work will allow us to determine if bassoon is required for tethering ribbons at HC synapses and open the possibility to test additional functions of bassoon at ribbon synapses, which could be similar to those in conventional synapses.

PS 629

Astrocytes exhibit correlated bursts of activity in the mouse inferior colliculus prior to hearing onset

Vered Kellner; Travis Babola; Dwight E. Bergles
Johns Hopkins University

Neurons in the developing auditory system fire highly correlated bursts of action potentials prior to hearing onset. This activity originates within the cochlea when supporting cells release ATP, which triggers a cascade of events that ultimately leads to excitation of groups of inner hair cells near sites of ATP release. The subsequent excitation of SGNs induces correlated firing of tonotopically aligned neurons, as activity propagates through auditory circuits. This form of spontaneous activity ceases after hearing onset, suggesting that it may promote initial refinement of synapses in auditory centers, reinforcing connections that carry activity from similar frequency domains within the cochlea. However, the role of this spontaneous activity in the development of precise tonotopic maps is still unclear. Like neurons, astrocytes undergo dramatic morphological and physiological changes during the first two postnatal weeks, suggesting that they may be affected by the bursts of activity carried by neurons during this period. Recent studies indicate astrocytes promote functional maturation of synapses in nascent circuits by secreting molecules such as thrombospondins, suggesting that reciprocal signaling between neurons and astrocytes may be crucial to circuit development. To determine if astrocytes are activated by spontaneous neural activity in auditory centers prior to hearing onset, we monitored astrocyte calcium levels in the inferior colliculus (IC) of awake GLAST-CreER;R26-lsl-GCaMP3 mice aged postnatal day 7-9. Time lapse fluorescence imaging using a wide field stereo microscope revealed that astrocytes in IC exhibit periodic increases in calcium at this age. Astrocyte activity was synchronized across wide bands, aligned to the tonotopic organization of the IC. Although the activity of astrocytes was similar to that exhibited by IC neurons at this age, responses from astrocytes were smaller in amplitude and longer in duration. Unilateral ablation of the cochlea dramatically reduced astrocyte activity in the contralateral IC, indicating that calcium signaling in IC astrocytes is similarly dependent on input from the cochlea. Systemic administration of an mGluR5 antagonist abolished astrocyte activity, suggesting that astrocytes are responding to glutamate released by incoming afferents within the IC. Together, these results indicate that neurons and astrocytes exhibit correlated activity in the developing IC. This periodic excitation of astrocytes may enable reciprocal signaling to promote the maturation of neurons and astrocytes, and shape the initial refinement of auditory circuits.

PS 630

Neurotrophic receptors and transcription factor expression in the differentiation of hair cells and supporting cells in the fetal human inner ear

Lejo Johnson Chacko[1]; Michael J F. Blumer[1]; Helge Rask-Andersen[2]; Elisabeth Pechriggl[3]; Alexander Haim[1]; Helga Fritsch[1]; Rudolf Glueckert[4]; Jozsef Dudas[1]; Anneliese Schrott-Fischer[4]
[1]Medical University of Innsbruck; [2]University of Uppsala; [3]Department of Anatomy, Medical University of Innsbruck , Austria; [4]Department of Otolaryngology, Medical University of Innsbruck , Austria

The expression patterns of the neurotrophin receptors and transcription factors in the developing human fetal inner ear between the gestational weeks (GW) 9 to 12 were examined via immunohistochemistry. Expression of neurotrophin receptors like p75NTR, TrkB and TrkC were upregulated towards GW12. p75NTR immunostaining was most prominent in the nerve fibers which penetrate into the sensory epithelia of the cochlea, the utricle and the saccule as gestational age progresses. TrkB and TrkC expression intensified towards GW 12. TrkA expression was limited to fiber subpopulations of the facial nerve at GW 10.

GATA-binding protein 3 (GATA3) a transcription factor which plays a role in inner ear morphogenesis and neurosensory development was identified for the first time

in the developing human inner ear. Previous research using knock out model of mice lacking GATA3 has been found to result in incomplete inner ear development. Expression of the SOX2 transcription factor previously identified to play a role in cochlear hair cell differentiation was identified by us in the developing vestibular hair cells. Expression of Transforming growth factor-β-activated kinase-1 (TAK1) previously identified as a marker for murine inner ear supporting cells was also identified in the developing and adult human inner ear supporting cells. Expression of Leucine-rich repeat-containing G-protein coupled receptor 5 (Lgr5), a stem cell marker was identified at the earliest gestational week examined. Faint immunoreactivity was present in supporting cells underlying utricular hair cells and cochlear ganglia. The expression of Lgr5 positive cells is indicative of the regenerative capacity of the fetal utriculus at this stage. All the data obtained would be compared to pre-existing murine developmental models.

We could demonstrate the highly specific staining patterns of neurotrophic receptors over a developmental period in which multiple hearing disorders are manifested. Our findings also suggest that hair cell markers are simultaneously expressed during the early stages of human inner ear development.

PS 631

Molecular, Anatomical and Physiological Characteristics of Inner Ear Organoids: Comparisons to Human Fetal Inner Ear derived from Human Pluripotent Stem Cells

Bryony A. Nayagam[1]; Cristiana Mattei[1]; Hannah R. Drury[2]; Babak Nasr[1]; Rachael Chatterton[3]; Tejal Kulkarni[1]; Pegah Jamshidi[1]; Giovanna D'Abaco[1]; Mirella Dottori[4]; Rebecca Lim[2]
[1]The University of Melbourne; [2]The University of Newcastle; [3]The Florey Institute of Neuroscience and Mental Health; [4]The University of Wollongong

Introduction
Mammalian hair cells exist in relatively low numbers and lose their capacity to regenerate early in development. As such, the derivation of inner ear tissue from human pluripotent stem cells (hPSC) sources offers an opportunity to study human inner ear development and provides a platform for drug screening and disease modelling.

Methods
We employed a dynamic three dimensional rotary cell culture system for deriving inner ear organoids from H9 human PSCs over a time course of 16 weeks in vitro. Analyses of differentiation and mechanosensitiviy of hPSCs-derived organoids were performed using a combination of qPCR, immunofluorescent histology and AM-144 staining. High resolution helium microscopy and path-clamp electrophysiology were employed to compare the anatomical and physiological characteristics of inner ear organoids to the developing human inner ear. K-Gluconate internal solution was used to record whole cell voltage activated currents from hPSC-derived inner ear organoids in Liebovitz';s L15 cell culture media between 13-16 weeks in vitro.

Results
Inner ear organoids show temporal expression of key developmental hair cell markers including Pax2, Athoh1, MyosinVIIa and CtBP2 by immunohistology and qPCR. Mechanosensitive progeny took up AM144 and showed outward currents consistent with those observed in developing human type II vestibular hair cells aged between 12-16 weeks gestation. These currents ranged in amplitude from 350pA to 5nA in response to a voltage step to +20mV (n = 8). Like developing human hair cells, some H9 cells also showed evidence of sodium currents. Moreover, striking morphological similarities were detected between inner ear organoids and developing inner ear using helium microscopy.

Conclusion
Here, we describe a novel three dimensional system for modelling human inner ear development using rotary cell culture. Our preliminary data suggest that this system is capable of generating a population of inner ear hair cells which resemble an early vestibular phenotype.

PS 632

Requirements for perinatal FGFR2b ligands in Muenke syndrome model and normal mouse hearing

Suzanne L. Mansour; Xiaofen Wang; Chaoying Li
University of Utah

Mice modeling Muenke syndrome ($Fgfr3^{P244R/+}$) have moderate hearing loss associated with supporting cell (SC) fate transformations of two Deiters'; cells to two pillar cells that develop sequentially between E17.5 and P3. Removing one copy of FGF10, which does not normally interact with FGFR3, but which is strongly expressed near these developing SCs, restores both SC fates and hearing. This occurs because the mutation changes the FGFR3 binding specificity, allowing it to be activated by FGF10. However, removing the Fgf10 allele does not block the SC fate change, which occurs on schedule in $Fgfr3^{P244R/+};Fgf10^{-/+}$ mice, but rather, it allows subsequent reversion of incorrect fates back to normal.

Therefore, to block <u>initiation</u> of Fgfr3$^{P244R/+}$ SC fate changes we endeavored to completely block FGF10 function. Since FGF10 is required for otocyst morphogenesis, we used doxycycline (DOX)-induced expression of a secreted dominant-negative FGFR2b ligand-binding ectodomain (DN-FGFR2b), which rapidly sequesters all FGFR2b ligands (FGFs 3,7,10 and 22), to block signaling through all endogenous receptors for those ligands (FGFR1b, FGFR2b and FGFR3b) starting just before the first Fgfr3$^{P244R/+}$ SC fate change.

None of the E16.5-P3 DOX exposures had any effect on SC fates in control pups and in those expressing ubiquitous DN-FGFR2b only (both were normal), or in Muenke-only pups (always transformed). Several DOX exposures, including E16.5-P0, E17.5-P0, E17.5-P3 and E18.5-P3, blocked SC fate transformations in P3 Fgfr3$^{P244R/+}$/DN-FGFR2b pups. Other DOX exposures, including E16.5-E18.5 and E18.5-P0, were partially effective, resulting in blockage of one SC fate transformation, and still others, the most transient, had no effect.

To determine whether such transient DN-FGFR2b expression restores hearing to Fgfr3$^{P244R/+}$ mice, we measured ABR thresholds following the DN-FGFR2b inductions that blocked SC fate transformations. Surprisingly, and in contrast to the normal hearing of most Fgfr3$^{P244R/+}$;Fgf10$^{-/+}$ mice, none of the DOX-exposed Fgfr3$^{P244R/+}$/DN-FGFR2b mice could hear normally. Even more surprisingly, there was significant hearing loss in most mice carrying DN-FGFR2b only. Thus, inducing ubiquitous DN-FGFR2b during the perinatal period in otherwise wild type mice causes variably penetrant hearing loss.This suggests that one or more FGFR2b ligands are required during the perinatal period for normal hearing.

To localize the requirement for FGFR2b ligands in normal hearing <u>and</u> to determine whether this requirement is separable from that needed to block Muenke model SC fate transformations and restore hearing, we have employed several different Cre drivers to limit the domain of DN-FGFR2b induction. Our most current results will be presented.

PS 633

Role of Daple in fine-tuning of the inner ear morphogenesis

Yoshiyuki Ozono[1]; Atsusi Tamura[2]; Elisa Herawati[3]; Shogo Nakayama[2]; Maki Takagishi[4]; Masahide Takahashi[4]; Hidenori Inohara[1]; Sachiko Tsukita[2]
[1]Department of Otorhinolaryngology-Head and Neck Surgery, Graduate School of Medicine, Osaka University; [2]Laboratory of Biological Science, Graduate School of Frontier Biosciences and Graduate School of Medicine, Osaka University; [3]Department of Biology, Faculty of Mathematics and Natural Science, Universitas Sebelas Maret; [4]Department of Pathology, Graduate School of Medicine, Nagoya University

Stereocilia, forming a bundle of hair-like processes, protrude from the apical end of each cochlear hair cell, which are essential for auditory transduction. During cochlear development, inner ear hair cells and supporting cells are aligned and the length of the cochlear duct increases, and all V-shaped stereocilia bundles on inner hair cells are oriented in the same direction following the movement of kinocilia located at the vertex. The cochlear developments are regulated by the planar cell polarity (PCP) pathway with the organization of cytoskeleton and apical surface. However, the PCP mechanisms of inner ear hair cells remain unclear.

Daple (Dishevelled-associating protein with a high frequency of leucine residues) was first reported as one of the Dishevelled-associating proteins. Dishevelled is the core protein of the canonical or non-canonical Wnt pathway (including Wnt/PCP pathway). Through the activation of Dishevelled, Daple controls embryonic development, tissue maintenance, and cancer progression. Additionally, analysis of Daple knockout (Daple KO) mice revealed that Daple regulated microtubule dynamics in the apex of multiciliated cells, ependymal cells, and induced the defect of PCP of motile cilia.

Recently, we analyzed the auditory function in Daple KO mice. The ABR thresholds were significantly higher beyond 24 kHz in the Daple KO mouse. By morphological examination, we found the miss-shaped pattern of the stereocilia bundle, whose phenotype is more marked in more basal areas of cochlea duct. Interestingly, the cochlea duct was not shortened, being different from the cochlear duct of some PCP-related protein-defect mice (e.g, Dishevelled, Vangl2, and Rac1).

To further understand the Daple function in cochlear development, we are examining the cytoskeletal organization of cochlea hair cells in the Daple KO mouse.

PS 634

Role of Itga8-Pcdh15 Proteins in Olfactory Cilia Development

Marisa Zallocchi; Linda Goodman
Boys Town National Research Hospital

Cilia formation and maintenance include basal body docking, assembly of the transition zone and axoneme and the directional transport of ciliary proteins. In recent years significant progress has been made in the identification of components involved in vesicular trafficking necessary for ciliogenesis. Among the proteins identified, Rab8, a member of the Rab family of small GTPases plays a critical function. To promote cilia biogenesis Rab8 needs to be activated by its guanine nucleotide exchange factor, Rabin8, which is targeted to the base of the cilia by GTP-Rab11-positive vesicles. In the olfactory organ, olfactory sensory neurons (OSNs) have multiple non-motile cilia responsible for perception of smell. The basal bodies and transition zones are located at the dendritic knob from which the cilia extend. Recently, a role for ciliary integrins in the regulation of primary cilia function has been suggested for bone tissue. Here, we are presenting novel data showing integrin alpha 8 (Itga8) ciliary localization in the olfactory sensory organ and the involvement of this integrin and protocadherin-15 (Pcdh15) in olfactory cilia formation. Zebrafish morphants/mutants were used to analyze olfactory cilia development in the absence of Itga8 or Pcdh15. Distribution of these proteins as well as vesicular markers involved in cilia formation was also evaluated in mutant mouse lines. A retinal pigmented epithelial (RPE) cell line and an OSN-derived cell line were employed to address the direct effect of Itga8 and Pcdh15 in ciliogenesis. Statistical significance was evaluated by Student's t test or one-way ANOVA followed by Dunnett's multiple comparisons test accordingly. We observed ciliary expression of both proteins in olfactory sensory neurons. Absence of Itga8 results in re-distribution of Rab8a from the axoneme to the base of the cilia, suggesting Itga8 is regulating Rab8a ciliary entrance. Knock down of Itga8 or Pcdh15a results in defects in ciliogenesis in the OSN-derived cell line, resulting in shorter cilia. Conversely, expression of both proteins in RPE cells results in longer cilia compared to control cells. Overall, the results support a role for Itga8 and Pcdh15 in cilia formation in OSNs. Since Rab8a cannot access the ciliary compartment when Itga8 is not present, this suggests a key role for Itga8 in Rab8a activation. This work was supported in part by the National Institutes of Health grant 5P20RR018788, the Tobacco Settlement Fund from the State of Nebraska.

PS 635

Role of the I-BAR Protein BAIAP2I2 during Stereocilia Development

Paroma Chatterjee[1]; Matthew Avenarius[2]; Michael Bateschell[1]; Peter G. Barr-Gillespie[3]
[1]OHSU; [2]Nationwide Children's Hospital, Columbus, Ohio; [3]Oregon Health & Science University | Oregon Hearing Research Center and Vollum Institute

Introduction

Mechanosensory hair cells possess actin-rich stereocilia at their apical surfaces. Precise mechanosensation by the hair bundles relies on information of the correct height and width of stereocilia during morphogenesis [1]. Although mechanisms that control stereocilia length have been extensively studied, the mechanism by which bundles widen is obscure. One of the key steps of bundle widening is reorganization of the stereocilia plasma membrane in co-ordination with the underlying actin cytoskeleton. From both in vivo and in vitro studies, it has become evident that membrane-deforming Bin-Amphiphysin-Rvs (BAR) superfamily proteins, which bear an intrinsically curved BAR module, can induce membrane curvature by imposing their curved shapes onto membranes [2]. Moreover, BAR proteins can also regulate cytoskeletal actin dynamics [2]. Whether BAR-domain proteins play a role in hair-bundle development has not been investigated. In a recent hair-cell regeneration study using RNA-seq in chicken utricle showed that Baiap2l2 transcripts disappeared when hair cells were ablated with antibiotics; transcripts were subsequently upregulated during hair-cell regeneration [3]. Another RNA-seq study examining gene expression changes using FACS-sorted mouse cochlear and utricular hair cells showed that both Baiap2l1 and Baiap2l2 expression levels increased during hair cell development [4]. Additionally, International Mouse Phenotyping Consortium indicated that Baiap2l2 global-knockout (KO) mice are profoundly deaf and exhibit abnormal ABRs. With the above findings indicating a connection between BAIAP2L2 expression and hair-cell development, in our study we have attempted to characterize the role of BAIAP2L2 in hair bundle development.

Methods

The expression profile of BAIAP2L2 at different stages during hair-bundle development was determined using immunofluorescence and high-resolution imaging techniques. We generated a Baiap2l2 mutant mouse line using a CRISPR-Cas9 KO approach. ABRs were run on the Baiap2l2 wild-type (WT) and homozygote KO mice.

Results

Our immunofluorescence data shows that there is robust expression of BAIAP2L2 in the postnatal (P) day

1 cochlear hair bundles, which disappears by P15. BAIAP2L2 antibodies strongly label the tips of stereocilia, where the membrane undergoes strong negative curvature. In the utricle, the BAIAP2L2 signal in the hair bundles was much weaker than that in cochlear bundles. ABR tests on Baiap2l2$^{\Delta/\Delta}$ homozygotes show that the homozygotes are profoundly deaf, with no response at the highest stimulus (90 dB), while WT mice hear normally.

Conclusion
The above results indicate that BAIAP2L2 protein is localized appropriately for controlling stereocilia curvature and that its function is essential for the auditory system, as loss of the protein results in complete hearing loss.

References
1) Dror AA, Avraham KB. 2009. Hearing loss: mechanisms revealed by genetics and cell biology. Annual review of genetics 43:411-437

2) Zhao H, Pykalainen A, Lappalainen P. 2011. I-BAR domain proteins: linking actin and plasma membrane dynamics. Current opinion in cell biology 23:14-21.

3) Ku YC, Renaud NA, Veile RA, Helms C, Voelker CC, Warchol ME, Lovett M. 2014. The transcriptome of utricle hair cell regeneration in the avian inner ear. The Journal of neuroscience 34:3523-3535.

4) Shen J, Scheffer DI, Kwan KY, Corey DP. 2015. SHIELD: an integrative gene expression database for inner ear research. Database : the journal of biological databases and curation 2015:bav071

ARO abstract 2018.doc

PS 636

Clonal analysis reveals differential Wnt-activated cell behavior in epithelial and mesenchymal tissues in the embryonic cochlea

Sara Billings[1]; Nina Myers[1]; Lee Quiruz[1]; Elvis Huarcaya Najarro[1]; Alan G. Cheng[2]
[1]*Stanford University;* [2]*Department of Otolaryngology-Head and Neck Surgery, Stanford University*

Background
The Wnt/beta-catenin pathway is essential for a wide range of functions during tissue development, including proliferation, differentiation and cell migration. In the developing cochlea, overactivation of the Wnt pathway via stabilization of the canonical mediator, beta-catenin, causes ectopic hair cell formation, downregulation of the epithelial marker E-cadherin and proliferation in the organ of Corti. However, cochlear cells are highly heterogeneous and whether individual cell types respond differently to Wnt pathway overactivation is not well understood. Here we assessed and compared the effects of beta-catenin stabilization on epithelial and mesenchymal tissues in the embryonic cochlea.

Methods
We used a transgenic approach, employing the following mouse strains: Axin2-CreERT2, Lgr5-CreERT2, Rosa26R-tdTomato, Ctnnb1-fl(ex3), Rosa26R-Rainbow. For Cre induction, tamoxifen was given at E12.5. Immunohistochemistry on whole-mounts and cross-sections was performed to assess cochlear morphology and the expression of markers of proliferation, and epithelial and mesenchymal cells. EdU was also given to assess proliferation.

Results
Fate-mapping experiments showed that Axin2-tdTomato cells resided in the cochlear duct and periotic mesenchyme, while Lgr5-tdTomato cells were restricted to the cochlear duct. We found that stabilizing beta-catenin in the cochlear duct resulted in the formation of cell clusters (foci), primarily in the pillar cell region. Similarly, stabilizing beta-catenin in the periotic mesenchyme led to foci formation in the modiolus, spiral ligament and interscalar septum. However, epithelial foci were proliferative while mesenchymal foci showed a reduced level of proliferation compared to controls. Clonal analysis with Rainbow fate-mapping experiments showed that epithelial foci are multiclonal whereas mesenchymal foci consisted of cell aggregates.

In the cochlear duct, expression of differentiation markers including Sox2, Prox1, Myo7a and Atoh1 was decreased. In addition, there was a loss of epithelial markers like E-cadherin and Keratin 8 and upregulation of the some mesenchymal markers such as Vimentin and LEF1. On the other hand, foci in the periotic mesenchymal downregulate markers like Sox9 and Brn4, while E-cadherin was ectopically expressed in all mesenchymal foci.

Conclusions
Activation of Wnt/beta-catenin signaling via B-catenin stabilization differentially affects cochlear epithelial and mesenchymal cells to proliferate and undergo an epithelial-mesenchymal transition.

PS 637

Targets of FGF Signaling in Mouse Inner Ear Morphogenesis

Huy Doan[1]; Xiaofen Wang[1]; Ree Lu[2]; Edgar Gutierrez[3]; Lisa D. Urness[1]; **Suzanne L. Mansour**[1]
[1]University of Utah; [2]Harvard College; [3]University of California, Davis

Signaling by FGFR2b ligands is required for many aspects of otic development. Periotic Fgf3 and Fgf10 are required together for otic placode induction. Hindbrain-expressed Fgf3 is subsequently required to initiate endolymphatic duct outgrowth from the otocyst, and epithelial Fgf10 is required for vestibular and cochlear morphogenesis, as well as for specification of two cochlear non-sensory domains; Reissner';s membrane and part of the outer sulcus. However, continuous and partially overlapping expression of both genes within the otocyst suggests additional combinatorial roles during morphogenesis.

To address redundant post-induction roles for FGFR2b ligands in otic development, we either conditionally inactivated Fgf3 and Fgf10 using Tg-Pax2Cre, or used doxycycline to induce a soluble (dominant-negative) ectodomain of their receptor, FGFR2b, at various times. Tg-Pax2Cre-mediated conditional deletion of both Fgf3 and Fgf10 did not affect otic induction, but blocked subsequent otic neurogenesis and both vestibular and cochlear morphogenesis. In contrast, conditional mutants with one normal Fgf allele remaining had distinctly different phenotypes depending on which allele it was, with Fgf3 null;Fgf10 het conditional mutants being much less severely affected than Fgf3 het;Fgf10 null conditional mutants, which had semicircular canal agenesis and a very short and narrow cochlea. Together, our morphologic and gene expression studies show that both Fgfs are required in the Pax2Cre lineage after placode induction for both vestibular and cochlear development.

Induction of the dnFGFR2b ligand "sink" throughout otic placode induction stages phenocopied global Fgf3/Fgf10 double null mutants. Transient DOX exposures permitted rapid and reversible quenching of FGFR2b signaling. Induction of dnFGFR2b for different intervals between E8.5 and E13.5 revealed highly penetrant and specific morphogenetic defects, showing that FGF3 and FGF10 are required together to initiate both cochlear and vestibular outgrowth from the otocyst and are required continuously during otic morphogenesis.

To identify proximal targets of FGF3 and FGF10 signals at the initiation of otocyst morphogenesis, we induced dnFGFR2b for three different overlapping intervals between E9.25-11.25. RNAs isolated from microdissected control and inhibited otocysts were profiled using RNA-Seq. In addition to expected targets, several new targets of FGF signaling were identified and validated, including transcription factors, signaling regulators and proteins associated with SHH, BMP and Notch signaling, suggesting crosstalk between different signaling systems that coordinate otic morphogenesis. Importantly, many of these targets were differentially regulated in all three RNA-Seq comparisons, suggesting that they represent an FGF-induced morphogenetic response dataset and should be functionally evaluated.

PS 638

Monitoring Auditory Development Using Whole Animal Hearing Tests

Noor-E-Seher Ali; Autefeh Sajjadi; Anthony J. Ricci
Department of Otolaryngology, Head and Neck Surgery, Stanford School of Medicine, Stanford, CA, USA.

Background
Development of the auditory system in rodents has been studied at many levels. Auditory brainstem responses (ABRs) are a non-invasive hearing test used to physiologically assess the auditory pathway and peripheral function. Distortion product otoacoustic emissions (DPOAE) also serve as a noninvasive monitor of cochlear amplification. In order to evaluate development of the auditory circuit on the whole animal level, we monitored two strains of mice as well as rat from the onset of hearing until full maturity.

Methods
Two different strains of mice were selected. CBA/CaJ mice served as controls since they maintain normal hearing for approximately two years of age. CD-1 is a known model of age related hearing loss. CD-1s have hearing loss at three weeks of age. ABR and DPOAE measurements were performed at various intervals starting from P13. Through the ABRs, the following characteristics of wave one were quantified: threshold, amplitude, full width at half maximum, and latency.

Results
We found that the CBA/CaJ mice had elevated hearing thresholds at the time of auditory canal opening (~P13). Hearing thresholds rapidly matured and were stabilized by P21. Interestingly, the high frequency region stabilized later than the low frequency region by about two days. DPOAEs matured over a similar time period. CD1 mice matured at a slightly earlier age but showed early

and progressive high frequency hearing loss that manifested in both ABR and DPOAE measurements. Rat showed a slightly earlier maturation time with normal thresholds by P15. In rat, threshold levels stabilized over the same time course as synapse morphology. In general, for all three sets of animals, the amplitude corresponded to changes in threshold of ABRs across all frequencies. The latency on the other hand seem to improve with age except for the high frequencies in CD1 strain of mice. In each case full width at half maximum and latency matured about 2 days after maturation of threshold levels.

Conclusion

Field potential measurements can be used to identify the time window for maturation of audition. Results can be difficult to interpret at the cellular level though because of multiple processes occurring. In all three models maturation occurred first in the apex and progressed to the base. Similarly maturation appears quite fast, reaching maturation within several days of ABR measurements appearing and the opening of the ear canal.

PS 639

Examination of Lgr5+ Cochlear Progenitor Cell Fate Determinants and Plasticity

Craig Hanna[1]; Danielle Lenz[2]; Albert Edge[3]; David Kaplan[4]
[1]*Tufts University School of Medicine; Tufts University Sackler School of Biomedical Sciences; Eaton-Peabody Laboratories, Massachusetts Eye and Ear Infirmary;* [2]*Eaton-Peabody Laboratories, Massachusetts Eye and Ear Infirmary;* [3]*Harvard Medical School;* [4]*Department of Biomedical Engineering, Tufts University*

Sensorineural hearing loss (SNHL) commonly involves damage to cochlear hair cells (HCs), and since mammalian HCs are incapable of regeneration, most forms of SNHL are permanent. Recent work has demonstrated the ability to isolate, clonally expand, and differentiate neonatal murine Lgr5+ cochlear progenitors (LCPs) in high yield. These LCPs are found in both the medial and lateral compartments of the cochlea, surrounding inner hair cells (IHCs) and outer hair cells (OHCs). Currently, it is not known what drives LCPs within clonally derived organoids toward IHC or OHC fate.

Sensory epithelial tissue from P3-P5 transgenic reporter mouse pups was harvested, expanded in 3D culture, and differentiated. Immunostaining and qPCR analysis was used to examine the role of LCP compartmental origin in determining HC fate following differentiation. Additionally, LCPs were differentiated in the presence of either

Wnt3a or Bmp4 in order to assess the effect of these morphogens on HC fate. Finally, silk fibroin protein films doped with bidirectional gradients of Wnt3a and Bmp4 were manufactured to investigate the importance of gradated signaling in specifying IHC and OHC fate.

Co-immunostaining for Myosin 7a, Prestin, and vGlut3 revealed that organoids derived from the clonal expansion of single LCPs contain cells expressing either IHC or OHC markers, but both HC markers are never found within the same organoid. Additionally, LCPs differentiated on silk fibroin protein films exhibit Myosin 7a and Atoh1 expression similar to those differentiated in 3D culture. ELISA protein assays demonstrate the ability to successfully dope silk fibroin protein films with Wnt3a and Bmp4.

These preliminary results provide insight into potentially important HC fate determinants. Future work includes in vitro lineage tracing to further investigate the relationship between compartmental origin and HC fate determination. Following successful optimization of morphogen doped silk fibroin protein film manufacture, LCPs will be cultured on these films to elucidate the importance of gradated signaling patterns in determining HC fate.

PS 640

Fluid Secretion in the Developing Inner Ear

Sung Huhn Kim; Philine Wangemann
Kansas State University

Background

Fluid secretion and fluid absorption need to be well balanced during inner ear development to prevent swelling of the membranous labyrinth which results in hearing loss, vestibular dysfunction and an enlarged vestibular aqueduct (EVA). The most common cause of EVA are mutations of SLC26A4. Studies in mouse models have localized fluid absorption to the endolymphatic sac and fluid secretion to the vestibular labyrinth (Kim et al 2010). Mitochondria-rich cells in the endolymphatic sac have been identified as the major site of fluid absorption and a molecular mechanism for fluid absorption during inner ear development has been proposed (Honda et al 2017). Fluid secretion during inner ear development, however, is much less well understood. The goal of the present study was to determine the location of fluid secretion in the developing vestibular labyrinth.

Methods

Vestibular labyrinths were isolated from E16.5 and E18.5 Slc26a4$^{\Delta/+}$ and Slc26a4$^{\Delta/\Delta}$ 129S6 mice and fractionated into different preparations: (1) an isolated utricle preparation with attached lateral and anterior ampul-

lae, (2) an isolated preparation of the anterior, lateral or posterior semicircular canal, (3) an isolated preparation of the common crus and (4) an isolated preparation of the saccule. Each preparation was manually sealed and maintained 24 hrs in organ culture in the absence or presence of inhibitors. The rate of fluid secretion was quantified based on volume measurements obtained by geometric approximation based on images acquired by laser-scanning microscopy. Immunocytochemistry of ATP1A1, a subunit of Na$^+$/K$^+$ ATPase, was used to identify epithelial cells that are potentially engaged in fluid secretion.

Results

All four preparations obtained from E16.5 Slc26a4$^{\Delta/+}$ mice engaged in fluid secretion. Rates of fluid secretion were higher in utricle and common crus preparations compared to preparations of semicircular canals or saccule. Rates of fluid secretion were similar for utricle preparations from E16.5 Slc26a4$^{\Delta/+}$ and Slc26a4$^{\Delta/\Delta}$ mice. Fluid secretion in utricle preparations from E16.5 Slc26a4$^{\Delta/+}$ mice was inhibited by ouabain, an inhibitor of the Na$^+$/K$^+$ ATPase but not by bumetanide, an inhibitor of the Na$^+$/2Cl$^-$/K$^+$ cotransporter. However, fluid secretion in utricle preparations from E18.5 Slc26a4$^{\Delta/+}$ mice was inhibited by bumetanide. Strong staining for ATP1A1 was found in vestibular dark cells, transitional cells, roof cells of the saccule and in sensory epithelia of the cristae and maculae.

Conclusion

These observations demonstrate that cells in different regions of the developing vestibular labyrinth are engaged in fluid secretion and that fluid secretion depends on Na$^+$/K$^+$ ATPase activity. The data suggest that fluid secretion is independent of the Na$^+$/2Cl$^-$/K$^+$ cotransporter until E16.5 and dependent on the Na$^+$/2Cl$^-$/K$^+$ cotransporter after E18.5. Mechanisms of fluid secretion are a potential therapeutic target for a non-invasive treatment strategy to prevent hearing loss associated with mutations of SLC26A4.

PS 641

Defining the relationship between maternal care behavior and hearing development in Wistar rats

Jingyun Qiu[1]; Preethi Singh[1]; Annalisa De Paolis[1]; Luis Cardoso[1]; Frances Champagne[2]; Adrian Rodriguez-Contreras[1]
[1]City University of New York, City College; [2]University of Texas at Austin

Previous studies in rodents have demonstrated the profound effects that the acoustic environment plays during the postnatal development of the auditory system. How-

ever, much less is known about how early sensory experience affects hearing onset. Recently, we found that handling rat pups during a postnatal sensitive period accelerates hearing development (Adise et al., 2014). We hypothesized that accelerated hearing development results from changes in maternal care behavior. However, the relationship between maternal care behavior and timing of hearing onset is unknown. To address this issue, we used a selection model in which natural variations in maternal care are identified in a large cohort of dams by measuring the frequency of different behaviors including licking and grooming (LG; Champagne et al., 2003). In a first selection experiment (n=36 dams), we tracked startle responses and eye opening in four low-LG (50 pups, mean LG score=7.1) and five high-LG (46 pups, mean LG score=15.8) litters. We found that the age at which 50% of pups showed a startle response (A_{50} in days after birth, mean ± sem) was 11.5 ± 0.4 and 13.1 ± 0.3 for low- vs high-LG litters, respectively. The A_{50} for eye opening was 13.8 ± 0.2 and 15.3 ± 0.5 for low- vs high-LG litters, respectively. To get a more quantitative measurement of the structural and functional changes at the auditory periphery we performed a second selection experiment (n=36 dams). We measured auditory brainstem responses to clicks from two low-LG litters (26 pups, mean LG score = 8.0), two high-LG litters (31 pups, mean LG score=11.9), and micro-CT scans from one low-LG litter (12 pups, LG score = 5.9) and a high-LG litter (12 pups, LG score=11.7). We found that the A_{50} for wave 1 onset was 12.2 ± 0.7 and 12.5 ± 0.6 for low- vs high-LG litters, respectively. Image segmentation analysis of micro-CT scans showed that middle-ear cavitation starts as tiny air pockets that increase in size in older animals. The A_{50} for middle and external ear cavitation was 13.3 ± 0.1 and 12.7 ± 0.1 for low- vs high-LG litters, respectively. Our preliminary results suggest that pups reared by dams with LG scores >14 have a delayed hearing onset compared to pups reared by dams with LG scores <14. Understanding the mechanisms by which maternal behavior influences hearing onset may provide new insight into the development of hearing in health and disease.

PS 642

GPI Anchorage of Tecta Regulates the Formation and Maturation of the Tectorial Membrane in the Cochlea

Dong-Kyu Kim; Ali Almishaal; Sungjin Park
University of Utah

The tectorial membrane (TM) is an extracellular matrix (ECM) structure in the inner ear and plays roles in frequency selection, propagation, and amplification of sound waves. The TM displays a defined shape and characteristic ultrastructure, and malformation of the TM

results in hearing deficits. However, the mechanism by which the TM is formed and matured in the extracellular space is unknown. The TM is initially formed on the apical surface of supporting cells, then thickens up to 50 microns, and is ultimately detached from the producing cells except in the spiral limbus prior to the onset of hearing. This progression suggests that surface anchorage and release of a structural organizer is tightly controlled. The TM is composed of both secreted proteins such as collagen and glycosylphosphatidylinositol-anchored proteins (GPI-APs), such as alpha-tectorin (Tecta) and beta-tectorin (Tectb). Tecta in particular is uniquely expressed in TM-producing supporting cells and functions as a molecular cross-linker of collagen fibers and other components. Since GPI-APs play versatile roles depending on cellular localization, we hypothesize that (1) Surface localization of Tecta by the GPI-anchorage is required to prevent the diffusion of secreted molecules and for the formation of the TM network on the apical surface at early developmental stages. 2) Release of Tecta networks from the cell surface is then required for the TM growth and detachment. When expressed in HEK293T cells, Tecta is released into the medium by bacterial phosphatidylinositol-phospholipase C (PI-PLC), which cleaves a GPI-anchor moiety. The released Tecta is pull-downed by alpha toxin, a bacterial toxin that strongly binds to GPI-anchor, showing that Tecta is GPI-anchored. To determine roles of the GPI-anchorage of Tecta in TM formation and function, we generated a mouse line, where GPI-anchored Tecta is converted into a constitutively secreted form by introducing a premature stop codon before C-terminal GPI-anchoring signal using the CRISPR/Cas9 genome editing (Tectasec knock-in). Tectasec mice show complete loss of the TM and significantly elevated thresholds in distortion product otoacoustic emissions (DPOAE) and auditory brainstem response (ABR), indicating that GPI-anchorage of Tecta is required for TM formation and auditory function. Notably, super-resolution imaging of the developing cochlea shows that Tecta forms filamentous structures stemming from the specific location of the apical surface to the body of the TM, further suggesting that release of Tecta complex is spatially controlled and plays a role in the formation of TM ultrastructure. Overall, the present study reveals a novel mechanism for the development of complex ECM structure wherein the regulated distribution of a GPI-anchored protein, Tecta, is critical for TM formation and maturation.

PS 643

Proliferation and Maturation of Resident Macrophage in the Mouse Cochlea

Ippei Kishimoto; Takayuki Okano; Koichi Omori
Department of Otolaryngology-Head and Neck Surgery, Graduate School of Medicine, Kyoto University

Background
The inner ear was once believed to be "immune-privileged", but recent studies have demonstrated presence of immune-competent cells in the specific parts of the inner ear such as the spiral ganglion (SG) and the spiral ligament (SL), which is referred to as resident macrophages in the cochlea. However, the role of cochlear macrophages and the mechanisms of macrophage migration into the cochlea still remain largely unknown. We showed that the resident macrophages which might be originated from hematopoietic progenitors in the yolk sac appeared around the cochlea at embryonic day (E) 10.5 (ARO 40th Annual MidWinter Meeting 2017). This time, we show the result of the further study about macrophage in the cochlea including quantitative analysis of macrophage distribution in the cochlea in various developing stages and the assessment about the functional aspects of macrophage in the cochlea.

Methods
The temporal bones of mice, between E 9.5 and postnatal day (P) 3, were dissected out, and the specimens were perfused with 4% paraformaldehyde in phosphate buffer overnight and cryoprotected with 30% sucrose. Specimens were prepared for cryostat sections (10 µm in thickness) and the midmodiolar sections were provided for the fluorescent immunohistochemistry. In this study, we used anti Iba-1 antibody as surface marker of macrophage. We performed 1) quantitative analysis of macrophage distribution in the cochlea, 2) assessment of tissue-specific alteration in macrophage density as cochlear development and 3) assessment of in situ proliferation activity by anti Ki67 and Phospho-Histone H3 antibody.

Results
The cell density of macrophage in the SL was not significantly different among E17.5, P0 and P3 mice, while in the SG it was higher at P3 than at E17.5 and P0. On the other hand, the macrophages in the stria vascularis (SV) were found only at P3 rather than E 17.5 and P3 (Figure. 1). The shape of macrophage in the cochlea was spherical at early stage such as E10.5, while it was dendritic at later stage such as P3 (Figure. 2). The macrophages positive for Ki67 and Phospho-Histone H3 were found in up to 1% of macrophages in the cochlea from E10.5 to P3 (Figure. 3).

Conclusion
The resident macrophages which might be originated from hematopoietic progenitors in the yolk sac have in situ proliferation potential. The macrophages appears to become matured during embryonic and early postnatal development while changing their cell shapes and distribution.

PS 644

Mechanism of FGF signaling in regulating mouse cochlear progenitor proliferation

Sung-Ho Huh[1]; **Michael Ebeid**[2]
[1]University of Nebraska Medical Center; [2]Univeristy of Nebraska Medical Center

Introduction

Mammalian inner ear lacks the capability to regenerate after injury resulting in irreversible hearing loss. A common approach to attempt regeneration is to reactivate developmental processes and one key process is sensory progenitor proliferation. Recent work has shown an emerging role of fibroblast growth factor (FGF) signaling in regulating sensory progenitor proliferation. Epithelial FGF9 and FGF20 activate mesenchymal FGF receptor1 (FGFR1) and FGFR2 to induce sensory progenitor proliferation and subsequent cochlear growth. The molecular events following receptor activation are not yet identified. The aim of this work is to identify genes and pathways functioning downstream of FGF signaling for regulating sensory progenitor development.

Methods

Fgf9/20 double mutant embryos are collected at E11.5 and E12.5 along with heterozygous controls. The mesenchyme tissues of the sensory side of the cochlear duct are isolated using Laser capture microdissection and total RNA is extracted. RNA library is prepared using Low Input DNA Library Prep Kit and RNA sequencing is performed on NextSeq Illumina sequencer. Data analysis is performed using the BaseSpace Sequence Hub and Ingenuity Pathway Analysis (IPA) is used to perform pathway analysis. A subset of differentially expressed genes is validated by in situ hybridization and immunohistochemistry. To assess the necessity of Etv4/5, which show downregulation in double mutants, the length of cochlea and hair cell number/density are analyzed from the P0 Etv4/5 compound mutants.

Results

RNA sequencing revealed 32 upregulated and 16 downregulated genes at E11.5, and 109 upregulated and 95 downregulated at E12.5 (Log2 fold change>0.6, adjusted p-value<0.05). Six genes were commonly downregulated and five genes were commonly upregulated. Three Ets transcription factors (Etv1, Etv4 and Etv5) and two secreted proteins (Fam19a4 and Tgfbi) showed downregulation in double mutants versus control at both time points. IPA identified upregulation of 2 bone morphogenic protein (BMP) signaling inhibitors (Sostdc1 and noggin) in double mutant mesenchyme at E11.5. In situ hybridization and immunostaining confirmed gene changes. Analysis of P0 Etv4/5 compound mutants showed shortened cochlea with reduced total hair cell number with no density change.

Conclusion

This work identifies genes operating downstream FGF epithelial mesenchymal reciprocal signaling during sensory progenitor proliferation. Etv4/5 double mutants partially recapitulate Fgf9/20 double mutant phenotype indicating that other factors might be operating downstream FGF signaling and contributing to the short cochlear phenotype. Further analysis of progenitor proliferation in Etv4/5 double mutants is required. Contribution of Etv1 will be assessed by generating Etv1/4/5 triple mutants.

PS 645

Effect of spontaneous mutation causes elimination of MITF-M expression on cochlear development

Weiwei Guo; Fei Ji; Jianan Li; Shiming Yang
Chinese PLA Medical School

Waardenburg syndrome (WS) causes hereditary sensorineural hearing loss due to gene mutation. To study the cochlear histopathology in WS, we examined cochlear morphology caused by MITF-M mutation (MITF-/-) in a porcine model. Morphology of cochleae were examined at embryonic and postnatal staged under light and electron microscopes. We found that the stria vascularis transformed into a complex tri-laminar tissue at embryonic 85 days (E85) in normal pigs, but not in the MITF-/- pigs. As the neural crest (NC) of cochlea was derived by melanocytes. MITF mutation caused failure of development of melanocytes which caused a subsequent collapse of cochlear duct and deficits of the epithelium after E100. Furthermore, the spiral ganglion neurons of cochlea in the MITF -/- pigs began to degenerate at postnatal 30 days (P30). Thus, our histopathological results indicated that the malformation of the stria vascularis was a primary defect in MITF -/- induced WT pigs which was resulted from the loss of NC-derived melanocytes. Subsequently, the cochleae underwent secondary degeneration of the vestibular organs. As the degeneration of spiral ganglion neurons happened after P30, it suggests that WS patients should be considered as candidates for cochlear implant. Our porcine model of MITF-M mutation may provide a crucial animal model for cochlear implant, gene therapy in patients with congenital hereditary hearing loss.

PS 646

CRISPR/Cas9-mediated knockout of Lim-domain only 4 retards organ of Corti cell growth

Rita Rosati[1]; Rajamani Rathinam[2]; **Samson Jamesdaniel**[2]
[1]*Wayne State University, Detroit, MI;* [2]*Wayne State University, Detroit, MI*

Lim-domain only 4 (LMO4), a transcriptional regulator that regulates cell survival and cell death signaling, is heavily expressed in epithelial cells including the sensory receptor cells of the inner ear. Recent findings indicate that it plays a critical role in mediating the ototoxic side-effects of cisplatin, a highly effective anti-cancer drug. However, the signaling mechanism by which cochlear LMO4 mediates otopathology is yet to be fully understood. Knockout cell culture models are useful tools for investigating the functional roles of novel genes and delineating associated signaling pathways. Therefore, LMO4 knockout organ of Corti cells were generated by using the CRISPR (clustered regularly interspersed short palindromic repeats)/Cas9 (CRISPR-associated protein 9) system. Successful knockout of LMO4 in UB/OC1 cells was verified by the absence of LMO4 protein bands in immunoblots and by a 6 base pair deletion in the target locus. Though the Knockout of LMO4 retarded the growth rate and the migratory potential of the cells it did not inhibit their long-term viability as the LMO4 knockout UB/OC1 cells were able to survive, proliferate, and form colonies. In addition, the knockout of LMO4 did not alter the expression of myosin VIIa, a biomarker of hair cells, suggesting that the knockout cells retain important characteristic features of cochlear sensory receptor cells. More importantly, Knockout of LMO4 enhanced the susceptibility of UB/OC1 cells to cisplatin-induced ototoxicity as treatment of LMO4 knockout UB/OC1 cells with 5 μm cisplatin significantly decreased the number of viable cells when compared to both wild-type and control cells ($P < 0.05$, n=3). Thus, the findings of this study indicate that CRISPR/Cas9 system is a simple and versatile method for knocking out genes of interest in organ of Corti cells and that LMO4 knockout UB/OC1 cells are viable experimental models for studying the functional role of LMO4 in ototoxicity. This study was supported by WSU faculty start-up funds and NIEHS P30 Grant (P30 ES020957).

Hair Cells IV

PS 647

Conformational switch of harmonin, a submembrane scaffold protein of the hair cell mechanoelectrical transduction machinery.

Amel Bahloul[1]; Sylvie Nouaille[1]; Aziz El-Amraoui[2]; Jean-Pierre Hardelin[1]; Dominique Durand[3]; Christine Petit[4]
[1]*Unité de Génétique et Physiologie de l'Audition, Institut Pasteur and UMRS 1120, Institut National de la Santé et de la Recherche Médicale;* [2]*Pasteur Institute;* [3]*CEA, CNRS, Université Paris-Sud, Université Paris-Saclay, Gif-sur-Yvette, France.;* [4]*Institut Pasteur, INSERM UMRS1120, Université Pierre et Marie Curie, Institut de la Vision, Collège de France*

Mutations in the gene encoding harmonin, a multi-PDZ domain-containing submembrane protein, cause Usher syndrome type 1 (congenital deafness and balance disorder, and early-onset sight loss). The structure of the protein and biological activities of its three different classes of splice isoforms (a, b, and c) remain poorly understood. Combining biochemical and biophysical analyses, we show that harmonin-a1 can switch between open and closed conformations through intramolecular binding of its C-terminal PDZ-binding motif to its N-terminal supramodule NTD-PDZ1 and through a flexible PDZ2-PDZ3 linker. This conformational switch presumably extends to most harmonin isoforms, and it is expected to have an impact on the interaction with some binding partners, as shown here for cadherin-related 23, another component of the hair cell mechanoelectrical transduction machinery.

Bahloul et al. Abstract ID 383050.docx

PS 648

Optimization of Adeno-associated Virus Transduction Rates in Mouse Cochleae

Graham Casey[1]; Mark Brimble[2]; Andrew Davidoff[2]; Bradley J. Walters[3]
[1]University of Mississippi Medical Center; [2]St. Jude Children's Research Hospital; [3]Department of Neurobiology and Anatomical Sciences, and Department of Otolaryngology and Communicative Sciences, University of Mississippi Medical Center

Worldwide, sensorineural hearing loss is one of the most prevalent disabilities and can arise from many sources. Such prevalence necessitates effective tools for studying the molecular machinery of the cells responsible for sensory transduction. Currently, one of the most popular means of expressing genes of interest in research models is adeno-associated viruses, or AAVs. While there are numerous AAV serotypes, their efficacy varies greatly and variability is even observed with the same serotype across reports. This inconsistency could be due to a number of factors as gene delivery via AAVs occurs through a number of steps. First, the viral particle must bind to the surface receptor of the cell and be internalized. After this, the viral particles must avoid degradation by the cell and translocate to the nucleus to achieve gene expression. Finally, a complimentary strand of the viral DNA must be synthesized by the cell so that transcription of the delivered gene can occur. Here we test 3 different hypotheses: (1) liposomal packaging of viral particles can increase cellular uptake and subsequently induce expression of our gene of interest (GOI) (2) pharmacological or thermal inhibition of degradation mechanisms can enhance GOI expression (3) self-complimentary viral DNA can bypass second strand synthesis to increase GOI expression. To assess the efficacy of these different conditions we produced AAV constructs to express GFP through the CMV promoter. We then explanted cochleae form neonatal mice and cultured them for 24 hours before applying the virus either with (1) no additional treatment (2) viral particles packaged in liposomes (3) treatment by heat shock to inhibit viral protein degradation (4) or in the presence of small molecule inhibitors of proteasomal degradation. We used several different viruses for this series of experiments: self-complimentary AAVAnc80L65-scCMV_GFP (Anc80), AAV3b-scCMV_GFP (3b), and single-stranded AAVAnc80L65-ssCMV_GFP (Anc80ss). Broadly, we found that liposomal packaging of the viral particles modestly increased GFP transduction rates suggesting that variability in efficacy may be due to limited viral particle penetrance rather than proteasomal degradation.

PS 649

Identification of Binding Partners of the Stereocilia Proteins GRXCR1 and GRXCR2

Pamela Song; Kristina L. Hunker; **David C. Kohrman**
University of Michigan Medical School, Department of Otolaryngology, Kresge Hearing Research Institute

Loss of function mutations in the Grxcr1 (glutaredoxin cysteine-rich 1) and Grxcr2 genes result in hearing loss in mouse and human and are associated with alterations in stereocilia maturation, including defects in dimension, orientation and organization of the bundle [1-4]. Sequence features suggest that GRXCR proteins act as molecular adaptors that may be required for the localization and function of other key proteins essential for normal bundle maturation. We have initiated a search for GRXCR interacting proteins by screening a yeast two-hybrid prey library with full-length GRXCR1 as bait. Inserts for the prey library were generated from the RNA of mouse cochlear sensory epithelia from mice aged P1 to P4. We have identified a total of 38 clones expressing both GRXCR1 and prey hybrid proteins that passed at least three levels of interaction selection. Several of these candidate interacting proteins are enriched in stereocilia bundles of chick basilar papilla or mouse utricles based on previously published proteomic data [5, 6]. These candidates include: GNB2L1, a scaffold protein for receptor signaling complexes; TMEM256, a transmembrane protein of unknown function; and PPP1CA, the catalytic alpha subunit of protein phosphatase 1, a serine-threonine phosphatase known to impact the phosphorylation state of a broad range of target proteins in many tissues and cell types [7]. PP1 catalytic subunits, while expressed ubiquitously, rely on interactions with a large number of distinct binding proteins for spatial and temporal regulation of the phosphorylation state of target proteins [8]. A GRXCR1-PPP1CA interaction has been previously identified in a large-scale screen for proteins with canonical PP1 docking sites [9]. Using a variety of approaches, including pull-down assays, co-localization in cells, and analysis of genetic mutants, we are currently verifying candidate-GRXCR interactions and evaluating their functional significance.

1. Odeh, H., et al., American J Human Genetics 86:148-60, 2010.
2. Avenarius, M.R., et al., 2017, in revision.
3. Schraders, M., et al., American J Human Genetics 86:138-147, 2010.
4. Imtiaz, A., et al., Hum Mutat 35:618-24, 2014.
5. Shin, J.B., et al., Nat Neurosci 16:365-74, 2013.
6. Ebrahim, S., et al., Nature Communications 7:10833, 2016.
7. Ceulemans, H. and M. Bollen, Physiol Rev 84:1-39,

2004.
8. Virshup, D.M. and S. Shenolikar, Mol Cell 33:537-45, 2009.
9. Hendrickx, A., et al., Chem Biol 16:365-71, 2009.

PS 650

Evolving Heterogeneity in Cells of the Postnatal Mouse Cochlea Revealed by Single Cell RNA Seq

Na Xue[1]; Lei Song[1]; Joseph Santos-Sacchi[2]; Hao Wu[3]; Dhasakumar Navaratnam[4]

[1]Department of Otolaryngology - Head & Neck Surgery, Shanghai Ninth People's Hospital; Ear Institute, Shanghai JiaoTong University School of Medicine; Shanghai Key Laboratory of Translational Medicine on Ear and Nose diseases, Shanghai, China; [2]Department of Surgery (Otolaryngology), Neuroscience, and Cellular and Molecular Physiology, Yale University School of Medicine, New Haven, Connecticut, USA; [3]Department of Otolaryngology Head & Neck Surgery, The Ninth People's Hospital, Shanghai Jiao Tong University School of Medicine, Shanghai, China. Ear Institute, School of Medicine, Shanghai Jiao Tong University, Shanghai, China. Shanghai Key Laborato; [4]Department of Neurology and Neuroscience, Yale University School of Medicine, New Haven, Connecticut, USA

Early postnatal cochlea show significant changes in morphology and physiology. To determine the branch points and molecular events that underlie these phenotypic changes we isolated single cells from the Organ of Corti at P0, P5 and P10, and performed single cell RNA seq. Single cell RNA seq provides a granular landscape of single cells as they transition into different cell types.

Methods
C57 mice of P0,5 and 10 days were obtained from Jackson Laboratory. The Organ of Corti was dissected and single cells isolated after treatment with trypsin. RNA seq was performed using the 10X genomics platform after determining cell viability in excess of 90%.

Results
Single cell RNA data was processed using a number of analysis packages in R. We used tSNE unsupervised cell clustering in the Seurat package to identify groups of cells at these developmental time points. Many of these unsupervised clusters contained genes exclusive to known phenotypic markers of cell types in the cochlea. Among the cell type clusters identified with known gene markers, there was considerable heterogeneity in gene expression. The degree of heterogeneity was also dependent on maturity based on the stage of profiling. However, even at the more advanced stages of profiling, there remained heterogeneity within cell populations including those in more differentiated states. Using Monocle we were able to assign a pseudo-time based evolution of cell ordering.

PS 651

Association of accessory subunits of the voltage gated Ca channel CAV 1.3 with BK channels in hair cells of the chick

Omolara Lawal[1]; Joseph Santos-Sacchi[2]; Dhasakumar Navaratnam[3]

[1]Department of Neurology, Yale University School of Medicine, New Haven, Connecticut, USA; [2]Department of Surgery (Otolaryngology), Neuroscience, and Cellular and Molecular Physiology, Yale University School of Medicine, New Haven, Connecticut, USA; [3]Department of Neurology and Neuroscience, Yale University School of Medicine, New Haven, Connecticut, USA

Large conductance K channels play many roles in hair cells. In non-mammalian vertebrates these channels play a key role in electrical resonance, a mechanism of frequency tuning. BK channels are closely associated with Cav 1.3 channels at the basolateral surface of hair cells. While the alpha subunits of BK channels have been shown to directly interact with the voltage gated Ca channels 1.2 and 2.1, a similar interaction with Cav 1.3 has yet to be determined.

Using immune localization we identify several auxiliary subunits of the Cav 1.3 channel to co-localize with BK channels in hair cells of the chick. Thus, we determine sharp co-localization with both Cacnb2 and Cacna2d3 subunits with BK channels in these cells. Similarly, we determine sharp co-localization between AKAP75/150, a protein that associates protein kinase A with its substrates that has also been shown to act as a scaffolding protein in interactions with voltage gated Ca channels (VGCC).

Providing further evidence of a direct interaction between the VGCC subunits and BK channels we determine that these subunits affect the relaxation times of Slo, the alpha subunit of BK channels. At physiologically relevant 5 micromolar Ca2+ concentration both Cacnb2 and Cacna2d3 prolong relaxation times of Slo.

Together these data raise the possibility that BK channel –VGCC interactions are more complex than hitherto envisaged based on prior proteomic data.

PS 652

Conditional Deletion of Pou4f3 in Outer Hair Cells Causes Cell Death in the Postnatal Mouse Cochlea

Jarnail Singh[1]; Stacie Gregory[2]; Bradley J. Walters[3]; Brandon C. Cox[4]

[1]Department of Pharmacology ,Southern Illinois University, School of Medicine; [2]Department of Surgery, Division of Otolaryngology, Southern Illinois University, School of Medicine; [3]Department of Neurobiology and Anatomical Sciences, and Department of Otolaryngology and Communicative Sciences, University of Mississippi Medical Center; [4]Department of Pharmacology and Department of Surgery, Division of Otolaryngology, Southern Illinois University School of Medicine

Auditory hair cells (HCs) in humans and other mammals are susceptible to damage and, unlike non-mammalian vertebrates, do not spontaneously regenerate at adult ages. Several transcription factors are thought to be involved in regulating HC survival directly or indirectly. Germline knockout and mutation studies have previously demonstrated the critical role of the transcription factor Pou4f3 in HC survival during embryonic development. However, the role of Pou4f3 in HC survival after HC differentiation is complete, is unknown. To investigate this question, we used the CreER-loxP system (Prestin[CreERT2]:Pou4f3[loxP/loxP]) to delete Pou4f3 in outer hair cells (OHCs). Prestin[CreERT2] is a knock-in mouse line which specifically targets the majority of OHCs after postnatal tamoxifen induction. Here, we injected tamoxifen on two consecutive days, in juvenile mice at postnatal day (P) 12 and P13, and in adult mice with mature hearing at 4 weeks age. Auditory Brainstem Response (ABR) was performed in adult mice at 1, 2, and 4 weeks post-tamoxifen induction, followed by collection of temporal bones. Prestin[CreERT2]:Pou4f3[loxP/loxP] mice displayed elevated ABR thresholds at all sound frequencies tested and at all timepoints tested in comparison to their Cre-negative control littermates. HCs were manually quantified from confocal images of whole mount cochlear turns immunostained with anti-myosin VIIa and anti-Pou4f3 antibodies. In Cre-negative control samples, OHCs and inner HCs were intact and expressed Pou4f3. However in Prestin[CreERT2]:Pou4f3[loxP/loxP] mice, there was a significant loss of OHCs after tamoxifen injections at both postnatal ages and at all time points analyzed. When the HC counts were separated by cochlear turn, we observed significantly more OHC loss in the middle (~20%) and basal turns (~88%) of the cochlea as compared to the apex (~12%) at 1 week post-tamoxifen given at P12/P13, with increased OHC loss observed at the 2 week post-tamoxifen timepoint. Similarly, in samples that were given tamoxifen at adult ages, there was more OHC loss in middle (~49%) and basal turns (~76%) than apex

(~12%) at 2 weeks post-tamoxifen with increased OHC loss observed at the 4 week post-tamoxifen timepoint. Further, the remaining OHCs in all experimental samples did not express Pou4f3. Current studies will confirm these preliminary results and investigate deletion of Pou4f3 at neonatal and reproductively mature ages (8 weeks).

PS 653

Investing the Impact of Hair Cell Activity on Ribbon Synapse Formation and Stabilization in the Zebrafish Lateral Line

Czarina Ramos; Sunita Warrier; Katie Kindt
National Institutes of Deafness and Other Communication Disorders, National Institutes of Health

In order to transmit high-fidelity auditory and vestibular information to the nervous system, hair cells must encode stimuli in a rapid and temporally precise manner. To accomplish such a task, hair cells rely on the ribbon synapse, a structure thought to enable rapid and sustained neurotransmission to the afferent neuron. Proper development and maintenance of a stable synapse is therefore essential for hearing and balance. Previous research has indicated that mutants with impaired presynaptic activity in the hair cell fail to maintain synaptic integrity throughout development. Our work aims to characterize how distinct aspect of hair cell activity shape the formation and stabilization of mature, functional ribbon synapses.

Using neuromasts in the zebrafish lateral line, we systematically examined ribbon synapses in Pcdh15, CaV1.3, Vglut3 and Otoferlin mutants. Respectively, these proteins have been shown to impact distinct aspects of hair cell activity: mechanotransduction, presynaptic calcium influx, glutamate transmission and vesicle fusion. To assess both ribbon synapse structure and function in these mutants, we employ immunohistochemistry, and in vivo electrophysiology along with functional imaging to examine ribbon synapse development and maintenance.

In all mutants, we observed normal synapse formation occurring during development. However we found that after hair cell formation, CaV1.3 and Otof mutants displayed a decrease in pre- and post-synapse juxtaposition. In contrast, ribbons in Pcdh15 and Vglut3 mutant hair cells remain juxtaposed to post-synaptic densities despite the absence of mechanotransduction and glutamate transmission. Functional analysis of these mutants confirm that mechanotransduction, presynaptic calcium influx, and glutamate transmission are not required for

ribbon synapse maintenance. Rather, vesicle fusion, either evoked or spontaneous fusion is sufficient to maintain synapses. In support of this, we found that both CaV1.3 and Otof mutants exhibit a dramatic reduction in spontaneous and evoked activity in the afferent neuron. Conversely, Pcdh15 and Vglut3 mutants are able to maintain vesicle fusion and their synapses.

We conclude that while mechanotransduction, presynaptic calcium influx, glutamatergic transmission and vesicle fusion are all required for ribbon synapse function, only vesicle fusion is necessary to maintain intact ribbon synapses.

PS 654

Optimising the Immunostaining of Guinea Pig synapses on Slide Section

Ichiro Furuta[1]; Norio Yamamoto[2]; Tomoko Kita[1]; Kohei Yamahara[3]; Takayuki Nakagawa[4]; Koichi Omori[5]
[1]*Department of Otolaryngology, Head and Neck Surgery, Kyoto University Graduate School of Medicine;* [2]*Department of Otolaryngology, Head and Neck Surgery, Graduate School of Medicine, Kyoto University;* [3]*Department of Otlaryngology, Head and Neck Surgery, Graduate School of Medicine, Kyoto University;* [4]*Department of Otolaryngology - Head and Neck Surgery, Graduate School of Medicine, Kyoto University;* [5]*Department of Otolaryngology-Head and Neck Surgery, Graduate School of Medicine, Kyoto University*

Compared with the mouse, the guinea pig has more accessible inner ears and it is easier to analyze morphologically and is frequently used as a model of hearing research. Also, the examination of synapse-related to hair cells has become intriguing after the discovery of hidden deafness. However, only a few reports described the protocol to stain guinea pig synapses, especially on the slice section. The immunohistochemistry on the slice section is very useful because the analysis of double or triple staining is easy and co-staining status and localization of the target are easily confirmed compared with whole mount staining. The issues for the staining of the glutamate receptor type 2 (GluR2), which is a characteristic AMPA receptor localized in hair cell synapse, is it requires a reaction at 37 degrees for a long time (more than overnight), resulting in the dry-up of the slice section. To avoid this situation, we decided to use a slide mailer during primary antibody reaction. Slide mailer is the small polypropylene box, has high airtightness, and it can contain ten pieces of slides at a time and save primary antibodies. Using slide mailers, we performed immunohistochemistry with rabbit anti-myosinVIIa to label hair cells, chicken anti-neurofilament-H to label the spiral ganglion soma and afferent dendrites, mouse

monoclonal IgG1 anti-CtBP2 to label pre-synaptic ribbons, and mouse (IgG2a) anti-GluR2 to label post-synaptic densities. We filled the slide mailer with primary antibodies and slides with guinea pig cochlear sections and performed the reaction overnight at 37 degrees. Secondary antibodies were Alexa Fluor 488-conjugated goat anti-mouse (IgG2a), Alexa Fluor 568-conjugated goat anti-mouse (IgG1), Alexa Fluor 350-conjugated goat anti-rabbit, or Alexa Fluor 647-conjugated goat anti-chicken. We confirmed that the pre-synaptic ribbons and the postsynaptic density were well visualized although background was a little bit high. Re-use of the primary antibodies is possible with this method because their recovery from slide mailers is easy.

PS 655

Hair cell death and synaptic changes in the zebrafish lateral line following noise-induced damage

Kristy Lawton; Phillip Uribe; Beija Robbins; Allison B. Coffin
Washington State University Vancouver

Noise-induced hearing loss is a prevalent issue in modern human society, with few therapeutic options to prevent or treat damage following excessive noise exposure. Larval zebrafish are a tractable model for studying acoustic trauma in vivo, due in part to their externally located lateral line system. The zebrafish lateral line is comprised of discrete clusters of hair cells which are both experimentally accessible and share cellular homology with mammalian systems. Previous work in our lab successfully used this system to identify potential otoprotective drug targets for pharmacologically-induced ototoxicity. We now extend the utility of this model system to understand the mechanisms of noise-induced hearing loss, via an acoustic trauma system developed in our lab. To induce acoustic trauma, an ultrasonic generator causes cavitation of microbubbles, creating broadband underwater shockwaves that damage the lateral line hair cells. Following development of this method, we sought to characterize the timing and extent of noise-induced hair cell damage. For the present experiments, larval fish were exposed to noise stimulus parameters that induced partial hair cell loss in both the anterior and posterior lateral line. Noise-induced hair cell death was assessed via direct counts of surviving hair cells at several time points post-noise exposure. After 24 hours, hair cell survival was comparable to controls, but by 48 hours, noise-damaged fish showed a 40% reduction in hair cell number. As an initial step towards understanding intracellular signaling cascades underlying noise-induced cell death, we wished to identify the timing of initiation of key cell death events. For this we used TUNEL staining of apoptotic cells to reveal the time window of max-

imum hair cell death following noise exposure. In mammals, noise-induced auditory damage is also known to occur at the level of the synapse, even in the absence of hair cell death, so we examined if this also occurs in zebrafish lateral line. We assessed synaptic integrity between hair cells and their afferent fibers at several different timepoints following noise exposure, by localizing the hair cell ribbon synapse protein RibeyeB and the post-synaptic density protein MAGUK. Future work will also explore mechanisms of noise-induced damage by examining transcriptional changes in hair cells following noise exposure. This research can inform how noise induces damage at the level of hair cells and their afferent synapses in an in vivo model, which may ultimately lead to potential targets for otoprotective drug development.

PS 656

Acquisition of Prestin Kinetics During Early OHC Maturation in the Mouse

Jun-Ping Bai[1]; Dhasakumar Navaratnam[2]; Joseph Santos-Sacchi[3]
[1]Department of Neurology, Yale University School of Medicine, New Haven, Connecticut, USA; [2]Department of Neurology and Neuroscience, Yale University School of Medicine, New Haven, Connecticut, USA; [3]Department of Surgery (Otolaryngology), Neuroscience, and Cellular and Molecular Physiology, Yale University School of Medicine, New Haven, Connecticut, USA

Prestin drives OHC electromotility (eM), known to be responsible for cochlear amplification (CA) in mammals. The electrical signature of eM is a bell-shaped nonlinear capacitance (NLC), the first derivative of prestin sensor charge vs. membrane voltage (dQp/Vm). NLC peaks at the characteristic membrane voltage (Vh). We have previously studied the development of NLC in OHCs of the mouse. Those studies demonstrated that increases in prestin charge (Qmax) continued after stabilization of linear capacitance (at p10), which corresponds to total membrane surface area (sum of membrane and embedded prestin surface area). Thus, though the number of prestin molecules appeared to stabilize, additional changes in NLC characteristics ensued, indication some sort of maturational events. Here we study, in developing OHCs, the maturation of prestin kinetics, which has recently been shown to be possess low pass characteristics in adult guinea pig OHCs.

C57/B6 pups aged postnatal days 5-18 were used for this experiment. Apical turns of the organ of Corti were dissected out and recorded with ionic current blocking solutions. Whole cell voltage clamp recordings were performed from all rows of outer hair cells (OHCs) of whole mount organ of Corti. OHCs were recorded with 140 mM chloride intracellular solutions at room temperature using jClamp software and an Axopatch 200B amplifier. Data were digitized at 100 kHz and low pass filtered at 10 KHz with Digidata 1320A. Chirp voltage stimuli were delivered and Cm across frequency (48-5000 Hz) was extracted, using dual-sine analysis of harmonic components of currents.

The frequency response of NLC altered during development, showing an accumulating low pass characteristic from p6 to p18, with the mature responses being similar to those observed in adult guinea pigs. Cm was fit across frequency with a two state Boltzmann, including Csa (that Cm component associated with membrane area/thickness change at hyperpolarizing voltage). Both Qmax and Csa increased during development, but whereas Qmax, showed developing frequency dependence, Csa did not. We are currently investigating the chloride influence on these biophysical parameters.

Hair Cells V

PS 657

Characterization of Aminoglycoside Hair Cell Toxicity Profiles in the Zebrafish Lateral Line and Efficacy of Small Molecule Protectant, ORC-13661

Patricia Wu[1]; Roberto Ogelman[1]; Julian Simon[2]; David W. Raible[1]; Edwin W. Rubel[3]
[1]University of Washington; [2]Fred Hutchinson Cancer Research Center; [3]Department of Otolaryngology, Bloedel Hearing Research Center, University of Washington

The zebrafish lateral line, made up of neuromasts containing clusters of mechanosensory hair cells that resemble those in the inner ear, has proven to be an effective model system for studying hair cell toxicity and for discovering genes and drugs that modulate toxicity. A high-throughput screen yielded PROTO-1, a drug-like small molecule that provides robust protection against neomycin-induced toxicity of zebrafish hair cells. An iterative, medicinal chemistry program enhanced the efficacy and pharmacokinetic properties of PROTO-1, yielding a new drug, ORC-13661. ORC-13661 provides robust protection against amikacin-induced hearing loss in mature rats and has completed preclinical development. The goals of the studies presented here are to: a) further explore the toxicity profiles of zebrafish lateral line hair cells across a broad range of aminoglycosides (AGs) and exposure periods; and b) determine the patterns of ORC-13661 hair cell protection against different aminoglycoside exposure conditions.

We examined short-term (1h) and long-term (24h) profiles for aminoglycoside-induced lateral line hair cell toxicity for amikacin, gentamicin, tobramycin, dihydrostreptomycin, hygromycin, and apramycin. Three distinct profiles emerged. Short-term exposures of neomycin and apramycin kill hair cells in a dose-dependent manner within one hour. The other aminoglycosides extend the time-course of dose-dependent hair cell toxicity over the 24-hour range tested. Overall sensitivity differs dramatically between aminoglycosides, with gentamicin and hygromycin being most toxic and amikacin as least toxic over 24 hours.

A pulse-chase AG treatment paradigm was developed to separate temporally distinct mechanisms of hair cell death. Hair cell toxicity after one hour of AG exposure is compared to toxicity after one hour followed by 23-hour incubation in embryo medium without AG. Gentamicin pulse-chase treatment produces similar dose-dependent toxicity as continuous exposure for the 24-hour period, while dihydrostreptomycin pulse-chase hair cell toxicity is minimal, similar to that seen with only short-term dihydrostreptomycin treatment. Dihydrostreptomycin toxicity appears to require continuous exposure. The third type of response to the pulse-chase paradigm is a dose-dependent hair cell loss that falls between short-term and long-term dose response functions. Timelines of hair cell toxicity from gentamicin long-term and pulse-chase exposures are also characterized.

We then address the requirement and efficacy of ORC-13661 presence before, during, and following gentamicin, amikacin, and hygromycin exposures. We show that ORC-13661 must be present during the initiation of aminoglycoside hair cell treatment in order to confer protection for any of the three proposed mechanisms of toxicity. ORC-13661 treatment is ineffective if added after aminoglycoside exposure.

PS 658

Purification of SLC26A6 for Cryo-EM as a pilot study for prestin structure determination

Alexei Surguchev[1]; Alberto Rivetta[2]; Frederick Sigworth[2]; Dhasakumar Navaratnam[3]; Joseph Santos-Sacchi[4]
[1]Department of Surgery (Otolaryngology), Yale University School of Medicine, New Haven, Connecticut, USA; [2]Yale Physiology; [3]Department of Neurology and Neuroscience, Yale University School of Medicine, New Haven, Connecticut, USA; [4]Department of Surgery (Otolaryngology), Neuroscience, and Cellular and Molecular Physiology, Yale University School of Medicine, New Haven, Connecticut, USA

Prestin, a member of the SLC26 family of anion transporters, is responsible for motility of outer hair cells. It is believed to function by responding to membrane voltage changes producing intra-molecule charge movements, resulting in conformational changes transmitted to the OHC lateral membrane. However the molecular mechanism governing these events is still unclear. Solving its 3D-structure on a molecular level would undoubtedly clarify the mode of action of this important membrane protein. Previously, we have attempted to purify gerbil prestin for crystallization studies. However we faced many experimental challenges including low expression yields, poor purity, and low monodispersity. With recent advances in Cryo-EM single particle technology including considerably improved resolution, and decreased size requirements, we decided to explore this approach as a viable option. Additionally, Cryo-EM has less stringent requirements for protein yields and somewhat for purity. Considering all the challenges in prestin expression and purification, we decided to carry a pilot project to test the feasibility of such an approach. We chose human SLC26A6 (A6) as a non-electromotile membrane protein which shares 40% identity with Prestin. A6 is membrane anion-exchanger that plays a major role as a component of the pH buffering system for maintaining acid-base homeostasis in the kidneys. Insect cells were used to express A6 with a construct engineered with a TEV-GFP-8x-HIS tag at the C-terminus. Cell membranes were solubilized with DDM, a non-ionic detergent, and proteins were partially purified by affinity chromatography, yielding about 2 mg of A6/liter of culture. We used size exclusion chromatography (SEC) to further purify A6. The resulting protein mainly eluted as a dimer with symmetrical peak, and over 90% purity. Currently we are planning the reconstitution procedures for purified A6 in lipid nanodisc for Cryo-EM structural studies. If proven successful this method would provide not only valuable technical information in attempts to express and purify prestin, but also insights into the structure and mode of action of A6. (Supported by NIH-NIDCD R01 DC000273, R01 DC016318 and R01 DC008130).

Activity-Dependent Phosphorylation by CaMKIId Alters the Ca2+ Affinity of the Multi-C2-domain Protein Otoferlin

Sandra Meese[1]; **Andreia P. Cepeda**[2]; Felix Gahlen[3]; Christopher M. Adams[4]; Ralf Ficner[1]; Anthony J. Ricci[5]; Stefan Heller[6]; Ellen Reisinger[2]; Meike Herget[5]
[1]*Department of Molecular Structural Biology, Institute for Microbiology and Genetics, and Collaborative Research Center 889, University of Göttingen, Göttingen, Germany.; [2]Molecular Biology of Cochlear Neurotransmission Group, Department of Otorhinolaryngology, University Medical Center Gottingen, Germany, and Collaborative Research Center 889, University of Göttingen, Göttingen, Germany.; [3]Department of Otorhinolaryngology, Head and Neck Surgery, Ruhr-University Bochum, D-44787 Bochum, Germany.; [4]Stanford University Mass Spectrometry, Stanford University, Stanford, CA, USA; [5]Department of Otolaryngology, Head and Neck Surgery, Stanford School of Medicine, Stanford, CA, USA.; [6]Stanford | School of Medicine | Department of Otolaryngology - Head & Neck Surgery*

Otoferlin is essential for fast Ca^{2+}-triggered transmitter release from auditory inner hair cells (IHCs), playing key roles in synaptic vesicle release, replenishment and retrieval. Dysfunction of otoferlin results in profound prelingual deafness. Despite its crucial role in cochlear synaptic processes, mechanisms regulating otoferlin activity have not been studied to date. We aim to study post-translational modifications of otoferlin and analyze their physiological significance. Further, we aim to identify novel functional interaction partners of otoferlin.

We identified Ca^{2+}/calmodulin-dependent serine/threonine kinase II delta (CaMKIId) as an otoferlin binding partner by pull-downs from chicken utricles. A direct interaction was supported by a co-immunoprecipitation with heterologously expressed CaMKIId and otoferlin proteins in HEK cells. The expression of CaMKIId in rodent IHCs was confirmed by immunohistochemistry and real-time PCR. An immunohistochemistry based proximity ligation assay (PLA) on acute explants of organs of Corti indicates close proximity (In vitro phosphorylation of otoferlin by CaMKIId revealed ten phosphorylation sites, five of which are located within C_2-domains. Exchange of serines/threonines at phosphorylated sites into phosphomimetic aspartates reduces the Ca^{2+} affinity of the recombinant C_2F domain 10-fold, and increases the Ca^{2+} affinity of the C_2C domain. Concordantly, phosphorylation of otoferlin and/or its interaction partners are enhanced upon hair cell depolarization and blocked by pharmacological CaMKII inhibition.

We propose that otoferlin activity is regulated by CaMKIId in IHCs. Upon hair cell stimulation, Ca2+ entering the IHCs activates CaMKIId which phosphorylates otoferlin. We hypothesize that this phosphorylation renders the C2F domain of otoferlin Ca2+ insensitive under physiological conditions, which might regulate the kinetics of exocytosis, vesicle replenishment and/or endocytosis.

Ribbon Development under Wnt9a Overexpression in Chicken Basilar-Papilla Hair Cells

M. Queralt Caus Capdevila; Ulrike Sienknecht; Christine Koeppl
Carl von Ossietzky University Oldenburg

Background

The molecular mechanisms responsible for extreme temporal precision in high-frequency phase locking are not completely understood. We aim to study the correlation between the number of ribbons and the temporal precision of the associated afferent. For this purpose, we generated Wnt9a transgenic chickens with a permanent overexpression in the basilar papilla of the gene Wnt9a, a developmental gene involved in cell proliferation and regulation of cell patterning. In the basilar papilla, overexpression of Wnt9a disrupts the development of a normal short-hair-cell phenotype and leads to both an increase in tall hair cells and an increase in synaptic ribbons (Munnamalai et al., 2017, J Neurosci, 37, 8975-8988). Here, we present a more detailed analysis of ribbon numbers and volumes during development of these Wn9a transgenic ears.

Methods

A retrovirus carrying Wnt9a was injected unilaterally into the right otocyst of chicken embryos at E3. In-situ hybridization to evaluate Wnt9a expression, and immunostaining of hair cells (HC) and ribbons was performed on sections and whole mounts. Three different developmental stages, E12, E14 and E16, were analyzed, comparing the normal embryonic development of the control ears with the Wnt9a injected ears. The number and volume of ribbons was quantified at two positions along the length (10 and 50% from the base) and three positions across the width of the papilla (neural, central and abneural).

Results

In control ears, neurally located tall HC showed the expected (Whitehead and Morest, 1985, Neurosci, 14:277-300) increase in ribbon numbers at E14. This then reduced toward E16, concurrent with an increase in ribbon volume. Ribbon volumes were initially higher in abneural HC in E12 and E14 control ears, and then reduced towards E16, while the number of ribbons remained stable

at this position. In Wnt9a injected ears, an abnormal increase of ribbon numbers occurred in abneurally located HC at E16, concurrent with an abnormal increase in ribbon volume.

Conclusions

The simultaneous decrease in the number of ribbons and their increase in size in neural tall HC in control ears suggests fusion of ribbons during normal maturation in tall HC. At the same time, in abneural short HC, ribbons decreased in size without any change in number, suggesting that here, reduction of ribbon volume might rather be a sign of synapse maturation. A similar maturation was not observed in Wnt9a ears. Instead, abneural HC showed an unusual, mixed ribbon phenotype with a synchronous increase of both number and volume.

PS 661

Gamma-Aminobutyric Acid Signaling in the Zebrafish Lateral Line

Austin Ramsay; Jackson O'Keefe; Megan Schwehr; Connell Crabtree; Tenzin Yangchen; **Cecilia P. Toro**
Linfield College

Decades of research have provided ample evidence that the inhibitory neurotransmitter gamma-aminobutyric acid (GABA) plays a role in inner ear circuitry. GABA binds to two types of receptors (GABARs): heteropentameric ionotropic $GABA_AR$s and heterodimeric G protein coupled $GABA_BR$s. Many GABAR subunits have been localized to both cochlear and vestibular labyrinth tissues, and it has been shown that early in development, GABA is an autoinhibitory transmitter released from cholinergic cochlear efferents. Additionally, in many species, hair cells of the vestibular labyrinth, but not the cochlea, synthesize GABA themselves. The role of this local source of GABA within the periphery is incompletely understood. While a number of $GABA_AR$ subunit isoforms have been localized to vestibular afferent terminals, $GABA_BR$ modulators have been shown to affect some peripheral vestibular activity. We seek to use the zebrafish lateral line to model and further understand peripheral vestibular GABA signaling. The zebrafish lateral line is an established model organ for mammalian hair cell physiology, and lateral line hair cells are most closely related to Type II vestibular hair cells. Little is known about the role of GABA in the lateral line. We have used immunohistochemistry, RT-PCR, and in situ hybridization to identify and locate key players in GABA circuitry, namely GABA, glutamate decarboxylase (GAD), and GABAR subunits. We have localized both GABA and GAD to lateral line hair cells. This suggests that, like some vestibular hair cells, lateral line hair cells synthesize GABA and are therefore a good model with which to further understand the role of this neurotrans-

mitter in the vestibular periphery. Using RT-PCR, we amplified 25 out of 26 GABA-related transcripts from larval tissue, and we have identified 13 as candidate lateral line genes. We have begun to locate candidate genes using in situ hybridization, and thus far have found that gabbr1a, which codes for $GABA_BR$ subunit B1a, is expressed by cells of the posterior and anterior lateral line ganglia, suggesting possible postsynaptic afferent $GABA_BR$ expression, and modulation of afferent activity by hair cell GABA release. Finally, we have begun to assay the effects of GABAR modulators on the lateral-line dependent rheotaxis behavior. We have found that GABAR antagonists increase the sensitivity of larvae to modest but not strong water currents. Together our results suggest that GABA may be released from lateral line hair cells and may function to dampen sensory responses to moderate stimuli while allowing strong stimuli to elicit robust behavioral responses.

PS 662

A possible role for Gαi and planar polarity in the position-dependent regulation of synapse properties in inner hair cells

Philippe Jean[1]; Basile Tarchini[2]; Tobias Moser[1]
[1]*Institute for Auditory Neuroscience;* [2]*The Jackson Laboratory*

The wide dynamic range of sound encoding in the mammalian cochlea is thought to be fractionated through functionally diverse spiral ganglion neurons (SGNs) at each tonotopic position. While the full range of sound levels is represented in the receptor potential of the inner hair cell, each of the 2-3 different SGN classes only cover part of this range. Each SGN is driven by a separate single inner hair cell active zone. It has been demonstrated that these active zones present distinct properties according to their position, to some extent forming a gradient between the modiolar (facing the spiral ganglia) and the pillar side (facing the outer hair cells). This active zone heterogeneity is a candidate mechanism for causing the functional diversity of SGNs. In this study, we are investigating whether the mechanisms known to influence cell-intrinsic planar polarity at the apical surface influence presynaptic heterogeneity. Specifically, we are testing the role of Gαi proteins that have been shown to be a marker for hair cell asymmetry, and to be required for proper orientation of cochlear hair bundles in the tissue, which is essential for hearing. Combining confocal / STED super resolution immunofluorescence microscopy and live calcium imaging experiments, we demonstrate that disruption of Gαi proteins affects the active zone heterogeneity in inner hair cells.

PS 663

Regulation of the localization of molecules in hair cell stereocilia by TRIOBP

Tomoko Kita[1]; Raj K. Ladher[1]; Shin-ichi Usami[2]; **Shin-ichiro Kitajiri**[3]
[1]*Department of Otolaryngology, Head and Neck Surgery, Kyoto University Graduate School of Medicine;* [2]*Department of Otorhinolaryngology, Shinshu University School of Medicine;* [3]*Department of Hearing Implant Sciences, Shinshu University School of Medicine*

Background

TRIOBP was identified as responsible gene for human hereditary deafness DFNB28. There are three major isoforms, TROBP-1, TRIOBP-4 and TRIOBP-5 in the inner ear. The human mutations disrupt two of them, TRIOBP-4 and TRIOBP-5, simultaneously. Mouse model that mimic human patients was generated, by targeting the common exon between TRIOBP-4 and TRIOBP-5 (Triobp KO mouse). All three major TRIOBP isoforms localized at stereocilia rootlets, and TRIOBP-4 turned out to be the actin bundler. In this KO mouse, rootlet structure was lost, with stereocilia becoming flaccid followed by progressive hair cell loss. In this study, we investigated the localization of each isoform in stereocilia and used immunoprecipitation (IP) was to discover TRIOBP-interacting molecules.

Methods

Immunohistochemical analysis was performed in Triobp KO mice to determine the localization of key molecules involved in stereocilia, and compared with control mice. Stained molecules are grouped by those involved in: stereocilia links, the ankle complex, actin regulation, and myosin. Using IP-mass spectrometry (IP-MS) methods, we identified potential interactors with the C-terminal of TRIOBPs from cochlear lysate of postnatal mice. The expression and localization in the inner ear was then conformed.

Results

In the absence of a rootlet in the KO mice, tip-link proteins such as Pcdh-15 and Fgfr1, are no longer localized at the tip of stereocilia. A few molecules for either ankle complex and actin regulation proteins, showed diffuse staining and aberrant localization in KO mice. Myosin localization in cochlear hair cells was not altered in both control and KO mice. By IP-MS method, several proteins were detected and some were localized in the stereocilia; TRIO, UACA and myosin phosphatase target subunit (MYPT).

Conclusion

The regulation of the localization of cilia molecules has been complicated and still unclear. TRIOBP binds TRIO and the small GTPase, Rho. Further study is needed to determine how TRIOBPs localize molecules to cochlear stereocilia.

PS 664

Murine Fam65B forms ring-like structures at the base of stereocilia critical for mechanosensory hair cell function

Bo Zhao[1]; Zizhen Wu[2]; Ulrich Mueller[2]
[1]*Indiana University, School of Medicine;* [2]*Johns Hopkins University*

Cochlear hair cells convert sound-induced vibration into electrical signals. FAM65B mutations cause hearing loss by an unknown mechanism. Using biochemistry and stochastic optical reconstruction microscopy (STORM), we show here that Fam65b oligomers form a circumferential ring near the basal taper of the mechanically sensitive stereocilia of murine hair cells. Taperin, a second protein near the taper, forms a dense-core-like structure that is disrupted in the absence of Fam65b. Stereocilia of Fam65b-deficient murine hair cells start to develop, but mechanotransduction is affected and stereocilia deteriorate. Yeast-two-hybrid screens identify RhoC as a Fam65b binding partner. RhoC co-localizes with Fam65b in stereocilia and regulates Fam65b oligomerization. Binding to RhoC and oligomerization are critical for Fam65b function. Our findings thus reveal a highly organized compartment near the base of stereocilia that is critical for hair cell function and affected in disease.

PS 665

Functional and histopathologic changes of cochlear after noise trauma in diabetic mice

Sun-Ae Shin[1]; Ah-Ra Lyu[1]; Dong-Sik Shin[2]; Yong-Ho Park[1]
[1]*Chungnam National University;* [2]*Chungnam National University Hospital*

The aim of study was to investigate the functional and histopathologic changes of cochlear in diabetic mice and also compare the susceptiblity after noise trauma in diabetic mice. The functional differences were evaluated with auditory brainstem response, cochlear blood flow and histopathologic changes were investigated with various molecularbiologic studies. Diabetic mice showed declining hearing and reduced vascularity on the lateral wall of cochlea with aging and synaptopathy with mitochondrial dysfunction was observed and it was more vulnerable to noise trauma compared with control mice and these results were thought due to increased inflam-

matory markers and reactive oxygen species. Hearing loss associated with diabetic mice is due to synaptic loss and changes of stria vascularis than hair cell loss and diabetic mice is more suspectible to noise trauma.

PS 666

The Physiological Properties of the Zebrafish Lateral Line during Regeneration of Hair Cells in vivo

Katherine Hardy[1]; Walter Marcotti[2]
[1]The University of Sheffield; [2]University of Sheffield

Background

The hair cells of the zebrafish posterior lateral line (pll) are clustered together in neuromasts and are used to detect hydrodynamic stimuli. These cells can be damaged by ototoxic agents such as copper. Unlike the hair cells of the mammalian inner ear, zebrafish hair cells are able to regenerate, allowing the zebrafish to continue to perform necessary behaviours that are largely reliant on the pll, such as schooling. Spontaneous activity (SA) is present in the afferent fibre that contacts the hair cells of the pll due to spontaneous release of glutamate from the hair cells in absence of external stimulation (Trapani & Nicolson 2011 J Neurosci. 31:5). However, how the SA is shaped during regeneration of hair cells is unclear.

Method

An outcrossed zebrafish line (Tg(myo6b:R-GECO)xT-g(NeuroD:EGPF)) was used for visualisation of the hair cells and afferent fibres respectively. Hair cells were ablated at 3 days post fertilisation (dpf) by incubating zebrafish in 10 µM copper sulphate ($CuSO_4$) in E3 medium for 2 hours. Hair cell loss was confirmed by fixing zebrafish in 4% paraformaldehyde and mounting for confocal microscopy. Extracellular loose-patch recordings of SA after hair cell ablation were obtained from the afferent fibres in the pll ganglion as previously described (Olt et al. 2016 Methods Cell Biol 133:253), and then fixed and mounted for hair cell counting. Recordings were obtained between 0-48 hours post treatment (hpt) in zebrafish aged between 3-5.2 dpf.

Results & Conclusions

10 µM $CuSO_4$ in E3 for 2 hours was sufficient to fully ablate all hair cells of the pll, whilst not damaging the afferent fibres to cause physical retraction or swelling. Our preliminary results show that following ablation, the first regenerated hair cells were present before 24 hpt and by 48 hpt the number of hair cells per neuromast was similar to that of age-matched controls. SA was present in the afferent fibres before 24 hpt, suggesting that very few hair cells are sufficient to trigger this activity. The mean range of frequencies of SA from recordings of treated fish was similar to that of age-matched controls despite the largely reduced hair cell number in treated zebrafish.

This work exemplifies how dynamic the system is and gives insight into the functionality of the pll during hair cell regeneration following $CuSO_4$ exposure and its ability to rapidly regain normal SA despite reduced hair cell numbers.

Inner Ear Drug Delivery I

PS 667

Perilymph Pharmacokinetics Compared for Dexamethasone-Phosphate, Dexamethasone and Triamcinolone with Local Applications.

Alec Salt[1]; Jared Hartsock[1]; Fabrice Piu[2]; Jennifer Hou[2]
[1]Washington University Medical School; [2]Otonomy Inc

Background

Perilymph concentrations of three steroids were compared with two local application methods in guinea pigs. Previous studies have shown that other substances applied to the round window (RW) niche enter perilymph through both the RW membrane and the stapes. Entry at the two sites has never been quantified for steroids. Some of the factors influencing perilymph levels of steroid were considered.

Methods

Fifty microliters of solution containing dexamethasone-phosphate (Dex-P; 0.4% solution), dexamethasone (Dex; 4.5 % suspension) or triamcinolone acetonide (TA; 6% suspension) were applied to the RW niche of guinea pigs as a liquid or in 17 % Poloxamer 407 gel. The applied volume covered the RW membrane and stapes footplate. After 1 hr, 10 x 2 µL samples of perilymph were collected by a sequential sampling technique from the lateral semi-circular canal (LSCC). Samples were diluted in methanol/water and assayed by HPLC/mass spectrometry. In other experiments, TA elimination was assessed by injecting diluted TA solution into the LSCC followed by perilymph sampling either immediately or after a delay of 2 hours. Similar data are already available for Dex-P and Dex.

Results

All three steroids were present in the initial perilymph samples (originating from the vestibule) and in later samples (originating from scala tympani), confirming that intratympanically-applied solutions / suspensions

enter the ear through both the stapes and the RW membrane. Normalized for the applied concentration, perilymph levels, calculated by averaging all 10 samples from each experiment, were highest for TA (2.4% of applied concentration), followed by Dex (2.3%) and substantially lower for Dex-P (0.13%). Larger differences were present when steroids were formulated in Poloxamer gel with normalized concentrations reaching 2.9% (TA), 1.4% (Dex) and 0.036% (Dex-P).

Discussion
The relative permeability of drugs through the lipid boundaries of epithelia and endothelia can be estimated from calculated molecular properties of the drug, including WLOPGP (an estimate of lipid partition coefficient) and $TPSA/A^2$ (topological polar surface area; an estimate of size and charge distribution on the molecule). Tools to calculate these parameters are available online (http://www.swissadme.ch). The lower entry of Dex-P found in this study is consistent with the more-polar properties of the molecule reducing the passage through the membranous boundaries into the ear, relative to Dex and TA. These considerations provide a rational basis for comparing drug entry, elimination and distribution in the ear and can be applied to most small molecules.

PS 668

Pathways for Drug Transfer Between the Two Ears.

Alec Salt[1]; Jared Hartsock[1]; Ruth Gill[1]; Stefan Plontke[2]
[1]Washington University Medical School; [2]Martin Luther University Halle-Wittenberg

Background
In studies where drugs are locally applied to the ear, the opposite ear is often used as an untreated control. Some studies, however, have suggested the applied substance can sometimes reach the opposite ear, a phenomenon that has been called the "Schreiner effect". In the present study, we have quantified transfer between the ears for two markers, and assessed the route by which transfer occurred.

Methods
Markers solutions containing fluorescein (FITC) or fluorescein-labeled dextran (FITC-dextran) were applied either by injection into the basal turn of scala tympani (ST) or by local application to the round window (RW) niche. Perilymph of the contralateral ear was subsequently collected by sequential sampling from the cochlear apex, allowing gradients along ST to be quantified. In addition, cerebrospinal fluid (CSF) was sampled from the cisterna magna and blood was collected from the jugular vein. Results were interpreted quantitatively using computer simulations of the experiments.

Results and Discussion
For either FITC or FITC-dextran injected into ST perilymph, fluorescence was readily detected in CSF at 5 - 75x lower concentration than applied and in perilymph of the opposite ear as basal-apical gradients of variable amounts. Computer modelling showed the findings were consistent with direct injections into perilymph causing outflow through the cochlear aqueduct, driving the marker into CSF. CSF entry and fluid exchange at the cochlear aqueduct of the contralateral ear subsequently allowed marker to enter perilymph of that ear.

FITC applied to the RW niche was found in the ipsilateral ear at 250x lower and in the contralateral ear 10^6x lower than the applied concentration. CSF averaged 794,000x lower and plasma 79,000x lower than the applied concentration. The amount and absence of gradients in perilymph were consistent with FITC entering the contralateral ear from the vasculature rather than from CSF following RW applications.

FITC-dextran applied to the RW niche was found in the ipsilateral ear at 31,000x lower and in plasma at 398,000x lower concentration than applied. Dextran was below the limit of quantification in CSF and in perilymph of the contralateral ear, corresponding to concentrations more than 10^7x lower than the applied concentration.

Transfer of substances between the ears after local delivery was confirmed and quantified in this study. The transferred amount depended on both the application method and on the permeability properties of the substance applied.

PS 669

Delivery of inner ear gene therapy using the dual-AAV system

Kevin Isgrig[1]; Hong Jun Wang[1]; Inna Belyantseva[1]; Thomas B. Friedman[2]; Shannon Boye[3]; Wade Chien[1]
[1]NIDCD/NIH; [2]Laboratory of Molecular Genetics, National Institute on Deafness and Other Communication Disorders (NIDCD), Bethesda, MD, USA; [3]University of Florida

Background
Adeno-associated virus (AAV) is a common viral vector used in inner ear gene delivery. A drawback of AAV is its limited gene carrying capacity (Myo7a (~7.2 Kb)) into the inner ear of the dominant headbanger (Hdb/+) mouse

model of hearing loss. The headbanger mouse has an ENU induced A>T transversion in an exon of Myo7a resulting in a phenylalanine substitution of isoleucine in the motor domain, which is associated with significant hearing loss as well as vestibular dysfunction (head bobbing and hyperactivity).

Methods
We used neonatal (P0-P5) headbanger mice. Dual AAV2 carrying the Myo7a cDNA (dual-AAV-Myo7a) was delivered through the posterior semicircular canal. Infection efficiency and stereocilia morphology were assessed using immunohistochemistry after auditory function was assessed by measuring auditory brainstem response (ABR) at 1 month.

Results
Dual-AAV-Myo7a successfully infected the cochlear and vestibular hair cells when delivered through the posterior semicircular canal. However, the infection efficiency was low (

Conclusions
Dual-AAV-Myo7a infected the cochlear and vestibular hair cells at low rate. Improvement in auditory function was not seen in treated headbanger mice compared to non-treated controls. Injection of dual-AAV-Myo7a caused ABR threshold elevation in wild-type mice, suggesting possible inner ear toxicity.

PS 670

Nano-based AAV vector for Inner ear gene delivery

Mohammad N. Kayyali; Qiang Song; Andrew R. Ramsey; Daqing Li
University of Pennsylvania

Over the last decade, a lot of advances in the application of AAV based gene therapy have been made. The discovery of the genetic defects behind many hearing disorders has significantly enriched our knowledge and allowed us to explore potential treatments for inner ear diseases. However, the treatment options for these defects are limited by the lack of an effective transgene delivery system for the inner ear. Consequently, it is essential to develop a safe and efficient system to noninvasively deliver genetic materials into the inner ear, and to effectively transfer therapeutic genes to the targeted cell populations.

The present study investigates whether Nano-based AAV vectors can be safely used for inner ear gene delivery and whether they can achieve therapeutic effects in a mouse model. A lipid coated AAV system was constructed and delivered to the inner ear using our nov-el nanohydrogel delivery approach. Our animal study demonstrates that the lipid coated AAV system can successfully pass through the round window membrane and transfect the targeted inner ear cell populations. Our study further indicates that the lipid coated AAV system result in greater transfection efficiency as compared to uncoated AAV system.

Our study suggests that the lipid coated AAV system may achieve a better therapeutic outcome when incorporating a therapeutic gene because of great features of noninvasively passing through the round window membrane and transfecting the targeted cell populations.

PS 671

Biosensors Delivery into the Cochlea Using Adeno-Associated Viral Vectors

Sara Talaei[1]; Anthony J. Ricci[2]
1Stanford University, Otolaryngology, Head and Neck Surgery; 2Department of Otolaryngology, Head and Neck Surgery, Stanford School of Medicine, Stanford, CA, USA.

Current available technologies, limit intra-cellular recordings from hair cells and spiral ganglion neurons (SGNs) in the cochlea to in-vitro experiments. Furthermore, simultaneous intra-cellular recording from multiple cells is an extremely difficult task. We are investigating the feasibility of delivering genetically encoded fluorescent biosensors into the cochlea, to take advantage of advanced molecular sensors and microscopic technologies for monitoring the electrical and chemical activity in multiple hair cells and neural fibers simultaneously with single cell resolution. We use adeno-associated virus (AAV) for delivering genes into the cochlea that will encode fluorescent biosensor proteins in the hair cells and SGNs. AAV vectors are reported as useful tools for transducing cochlear cells. However, gene delivery into the cochlea without affecting the hearing, and transducing most cochlear cells, especially OHCs has been challenging. Recently, three papers have shown some success with a newly developed AAV (Anc80L65) in infecting most cell types in the cochlea[1-3].

We have developed a surgical method for effective gene delivery into the cochlea. Our method is based on injecting 1 µl of the virus at 300 nl/min into the cochlea through the posterior canal of the vestibular system in neonatal mice (i.e. P0-1). We have studied the efficiency of AAV DJ by evaluating the extent of hrGFP and mCherry gene expressions with CMV and synapsin promoters respectively, at different times post infection. Using this method, no hearing loss was observed in the animals injected with methylene blue dye or PBS. While injecting AAV DJ

with CMV promoter expressing GFP did not affect the ABR or DPOAE thresholds, injecting AAV DJ with synapsin promoter for expression of mCherry selectively in the nerves caused a slight increase in the ABR threshold. The average percentage of infected IHCs was increased from 60% at two weeks after injection to 89% at 5 weeks after injection. We have also compared the gene expression patterns in the cochlea of two different strains of mouse, CD1 and C57/BL6. By replacing the GFP gene with two different voltage sensors, we were able to express two different voltage sensors (i.e. ASAP and Ace2N-mNeon) in the hair cells and SGNs. We conclude that this delivery method should be effective for investigations at older ages in-vivo or in-vitro.

References

[1]Suzuki et al., Scientific Reports, 2017

[2]Pan et al., Nature Biotechnology, 2017

[3]Landegger et al., Nature Biotechnology, 2017

Funding

PS 672

Transduction efficiency of novel AAVs in mammalian inner ear

Kevin Isgrig; Hong Jun Wang; Wade Chien
NIDCD/NIH

Background

Inner ear gene therapy is a promising treatment for hearing loss and dizziness. One of the major challenges of inner ear gene therapy is identifying a viral vector which can infect target cells with high specificity and efficiency. In this study, we examined several novel AAVs'; ability to infect various cell types in the mouse inner ear.

Methods

Neonatal (P0-P5) CBA/J mice were used in this study. Several novel AAV-GFPs were injected into mouse inner ear using the posterior semicircular canal approach. Immunohistochemistry was used to assess the infection efficiency. ABR was used to assess auditory function.

Results

Different AAV-GFPs have varying inner ear hair cell infection efficiencies. Some AAVs infected supporting cells, while others also infected the spiral ganglions. The same strain of AAV-GFP from different sources also have different hair cell infection efficiencies, indicating the importance of the viral vector preparation process.

Conclusions

Several novel AAV strains were tested in this study. We found that some were able to infect hair cells with high efficiency. The method of viral vector production may also play a role in infection efficiency.

PS 673

Restoration of Inherited Hearing Loss by In Vivo Gene Delivery

Lian Liu[1]; Wei Xiong[2]
[1]*School of Life Science, Tsinghus University;* [2]*School of Life Science, Tsinghua University*

Hearing loss and/or deafness is one of the most devastating sensory disorders, which is largely resulted from genetic insults. Till now, many deafness genes have been characterized with critical roles in hair cells and mainly contribute to auditory transduction. Their functions are from mechanotransduction, to neurotransmission, and to metabolism, and so on. Loss-of-function of these genes causes hair cell deterioration. However, there is no translational application so far to alleviate it yet. The known barriers are predominantly due to inaccessibility of hair cells in vivo, complexity of spatiotemporal gene expression pattern, and super sensitive labyrinth compartments in the inner ear. Here we proposed to acquire a feasible methodology to perform efficient and effective gene therapy on congenital hearing loss. Firstly, we evaluated the tropisms and gene transfer efficiencies of major adeno-associated virus (AAV) serotypes, together with specific delivery approaches for inner ear. One of the tested serotypes could target IHCs and OHCs at efficiencies of 89.1% and 53.7%, respectively. Secondly, we further validated our gene transfer by pathogenic gene cDNA delivery towards deafness animal models. Lhfpl5 protein has been identified as a key component of hair cell mechanotransduction and Lhfpl5 null mice showed severe hearing loss and circling behavior. After virus-mediated cDNA delivery back into inner ears, the Lhfpl5 knock-out mice gained obvious balance restoration at 2-month age. In summary, we had established an efficient and effective viral delivery platform, which paved a way for us to further tackle the potential of genome editing to restore inherited inner ear disorders.

PS 674

Local gene therapy durably restores vestibular function in a mouse model of Usher syndrome type 1G

Ghizlene Lahlou[1]; Alice Emptoz[2]; Vincent Michel[3]; Andrea Lelli[2]; Omar Akil[4]; Jacques Boutet de Monvel[3]; Anaïs Meyer[2]; Typhaine Dupont[3]; Sylvie Nouaille[5]; Mathieu Beraneck[6]; Filipa Franca de Barros[6]; Didier Dulon[7]; Jean-Pierre Hardelin[5]; Lawrence R. Lustig[8]; Paul Avan[9]; Christine Petit[10]; Saaid Safieddine[11]

[1]Institut Pasteur, Paris; [2]Institut Pasteur; [3]Institut Pasteur, INSERM UMRS 1120, Université Pierre et Marie Curie; [4]University of California San Francisco, Epstein Lab, Dept Otolaryngology-HNS; [5]Unité de Génétique et Physiologie de l'Audition, Institut Pasteur and UMRS 1120, Institut National de la Santé et de la Recherche Médicale; [6]Centre de Neurophysique, Physiologie, et Pathologie, Centre National de la Recherche Scientifique UMR 8119, Université Paris-Descartes, Paris, France; [7]INSERM and University of Bordeaux; [8]Dept Otolaryngology-HNS, Columbia University, New York; [9]Centre Jean Perrin, Université Clermont Auvergne, INSERM UMR 1107; [10]Institut Pasteur, INSERM UMRS1120, Université Pierre et Marie Curie, Institut de la Vision, Collège de France; [11]Unité de Génétique et Physiologie de l'Audition, Institut Pasteur, UMRS 1120 Inserm

Abstract

Our understanding of the mechanisms underlying inherited forms of inner ear deficits has considerably improved during the last twenty years, but we are still far from curative treatments. We investigated gene replacement as a strategy for restoring inner ear functions in a mouse model of Usher syndrome type 1G (USH1G), characterized by congenital profound deafness and balance disorders. These mice lack the scaffold protein sans, which is involved both in the morphogenesis of the stereociliary bundle, the sensory antenna of inner ear hair cells, and in the mechanoelectrical transduction process. We show that a single delivery of the sans cDNA by the adeno-associated virus AAV8 to the inner ear of newborn mutant mice reestablishes the expression and targeting of the protein to the tips of stereocilia. The therapeutic gene restores the architecture and mechanosensitivity of stereociliary bundles, improves hearing thresholds, and durably rescues these mice from the balance defects. Our results open up new perspectives for efficient gene therapy of cochlear and vestibular disorders by showing that even severe dysmorphogenesis of stereociliary bundles can be corrected.

Acknowledgments

PS 675

Cochlear Pharmacokinetic Parameter Estimation - Impact of Localized 3D Image Registration and Reconstruction Noise

Sanketh S. Moudgalya[1]; Kevin Wilson[1]; Xiaoxia Zhu[2]; Mikalai M Budzevich[3]; Gary V Martinez[3]; Robert D. Frisina[4]; Joseph P. Walton[5]; Nathan D. Cahill[6]; David A. Borkholder[7]

[1]Rochester Institute of Technology; [2]Global Center for Hearing & Speech Research, University of South Florida- Tampa; [3]Moffitt Cancer Center; [4]Global Center for Hearing and Speech Research, University of South Florida- Tampa; [5]Department of Communication Sciences & Disorders, and Chemical and Biomedical Engineering, Global Center of hearing and Speech Research, University of South Florida, Tampa, FL; [6]Associate Dean for Industrial Partnerships in the College of Science at RIT; [7]Bausch and Lomb Professor of Microsystems Engineering

Prominent methods in cochlear fluid pharmacokinetics rely on 1D and 3D models to simulate drug transport in the inner ear, and are parameterized by drug half times and transfer coefficients across the scalae respectively. Our work focuses on determining the transfer coefficients along the length of different cochlea scalae viz. scala tympani (ST), scala vestibuli (SV), and scala media (SM), by leveraging micro Computed Tomography (μCT) scans of the murine cochlea taken during delivery of contrast agent (ioversol or gold nanoparticles) at multiple consecutive time instances. The spatio-temporal concentration profile is quantified within each scala by performing 3D image registration to a previously published mouse cochlear atlas and transferring the segmented regions in the atlas to the μCT scan. An inverse model of pharmacokinetics is used to estimate transfer coefficients along the length of each scala. The accuracy of the regional extracted concentration profiles can be compromised by both local registration problems and reconstruction noise. Registration problems can emerge because the cochlear atlas was built from the scan of a single mouse and is unable to accommodate significant variability in the shape and size of the scalae of dif-

ferent mice. This was overcome with a novel two-stage approach to registration, where the first stage uses a similarity metric that is applied globally; then, the second stage applies the similarity metric locally in order to minimize registration errors specific to certain regions in the scalae. The final improvement in registration is quantified using the global similarity metric. To determine the effect of reconstruction noise on transfer coefficient estimates, Gaussian noise across a range of standard deviations was added to the extracted concentration profiles prior to solving the inverse problem that estimates the transfer coefficients. Iterative processing yields a noise-dependent confidence interval for each calculated transfer coefficient, providing insight into acceptable noise in extracted concentrations. Inherent scan noise defines a lower bound on the number of voxels required for averaging to achieve robust estimates of cochlear transport parameters. These analyses are conducted on different sets of scans with ioversol and gold nanoparticles as contrast agents that are delivered via cochleostomy and at the round window membrane, respectively. The resulting spatially dependent transport parameters are used in a forward model of cochlear pharmocokinetics to predict intracochlear concentrations. The approach can be replicated on larger rodent models enabling optimization of clinical drug infusion profiles in the future.

PS 676

A Novel Bisphosphonate - Small Molecule Neurotrophic Factor Hybrid Compound for the Treatment of Cochlear Synaptic Degeneration

Christine M. Hamadani[1]; Judith S. Kempfle[2]; Nicholas Koen[3]; Kim Nguyen[4]; Boris A. Kashemirov[4]; Charles E. McKenna[4]; Albert Edge[3]; David H. Jung[5]
[1]Department of Otolaryngology, Harvard Medical School; [2]1, Department of Otolaryngology, Massachusetts Eye and Ear, Boston, MA, USA. 2, Department of Otology and Laryngology, Harvard Medical School, Boston, MA, USA. 3, Department of Otolaryngology, University Tübingen Medical Center, Germany; [3]Harvard Medical School; [4]University of Southern California; [5]Eaton-Peabody Laboratories, Massachusetts Eye and Ear; Department of Otolaryngology, Harvard Medical School

Neurotrophic factors in the cochlea may promote both survival of Spiral Ganglion Neurons (SGNs) and re-wiring of hair cells by surviving SGNs. 7,8-dihydroxyflavone (DHF) is a small molecule shown to have similar activity to brain-derived neurotrophic factor (BDNF), one of two primary neurotrophins expressed in the cochlea. By synthesizing a bisphosphonate-DHF hybrid molecule, we aim to assess the ability of bisphosphonates to an-

chor small neurotrophic molecules within cochlear bone, providing long term, sustained delivery to the inner ear to promote synaptic regeneration.

Methods
A carboxyl group was first added to the para position of 7, 8-Dihydroxyflavone (DHF)';s phenyl ring. This generated a DHF intermediate product, available to react with the nitrogen-containing pyridine of the bisphosphonate Risedronate via coupling reagents to form hybrid molecule Ris-DHF.

To measure Ris-DHF';s effect on neurite outgrowth, SGNs were dissected in vitro from p4 mouse cochleae and treated with Risedronate, DHF, Ris-DHF hybrid, or media control. The samples were then fixed, immunostained, and visualized with confocal microscopy.

To assess Ris-DHF';s ability to stimulate synaptic regeneration, Organ of Corti (OC) explants were dissected in vitro with attached SGNs. The explants were then treated with Kainic Acid (KA), thought to mimic excitotoxic damage to ribbon synapses. Following KA treatment, explants were treated with Risedronate, Ris-DHF, or DHF. Synapses were visualized using immunohistochemistry and confocal microscopy. Juxtaposed synapses were quantified with Amira 3D software.

To evaluate Ris-DHF';s functional ability following pre-binding to bone matrix in vitro, the SGN explant assay protocol was performed after pre-binding of Risedronate, Ris-DHF, and DHF to hydroxyapatite (HA) pellets. Neurite outgrowth was visualized via immunohistochemistry and confocal microscopy and quantified using Fiji/ImageJ software.

Results
Ris-DHF stimulated a significantly higher relative ratio of neurite outgrowth than untreated control and Risedronate alone, albeit at slightly lower levels than native DHF. Moreover, Ris-DHF, like DHF, promoted significant synaptic regeneration in our KA explant assay. Finally, Ris-DHF drove the highest levels of neurite outgrowth after pre-binding to hydroxyapatite pellets.

Conclusions
The hybrid Risedronate-DHF molecule retains neurotrophic properties in treatments pre-bound to hydroxyapatite as well as in media, indicated by neurite outgrowth length. Ris-DHF can drive synaptic regeneration in vitro. Taken together, these findings suggest bisphosphonate hybrid molecules may represent a viable system for cochlear drug delivery, and that Ris-DHF may represent a novel drug for treating cochlear synaptopathy.

PS 677

BDNF-Producing Stem Cells as Drug Delivery System in Cochlear Implanted Guinea Pigs

Verena Scheper[1]; Annika Hamm[2]; Thomas Lenarz[3]; Andrea Hoffmann[2]; Jana Schwieger[4]
[1]Department of Otolaryngology, Hannover Medical School, Germany; Cluster of Excellence; [2]Dep. of Orthopaedic surgery, Hannover Medical School, Germany; [3]Department of Otolaryngology, Hannover Medical School, Germany and DFG Cluster of Excellence Hearing4all; [4]Department of Otolaryngology, Hannover Medical School, Germany

The cochlear implant (CI) is the standard therapy for sensory hearing loss. It stimulates the neurons of the primary auditory pathway, the spiral ganglion neurons (SGN), and thus elicits a sound sensation in the patient. Amongst others, the success of a CI depends on the number and the excitability of the available SGN. BDNF (brain-derived neurotrophic factor) has a protective effect on SGN and can potentially help to increase the success of a CI. A long-term application of BDNF is desirable to establish a clinically relevant chronic growth factor therapy. Long-term administration of BDNF can be achieved by genetically modified mesenchymal stem cells (MSCs), but the MSCs must be protected from immune responses of the recipient organism and an uncontrolled proliferation and migration of the cells must be avoided. Alginate may serve as a matrix for the factor-producing cells, so that the requirements described above can be fulfilled. Methods: BDNF-producing MSCs were encapsulated in alginate. Four experimental groups were investigated using guinea pigs as animal model: Groups A, B and C were systemically deafened receiving A) a CI, B) an alginate-MSC-coated CI and C) an injection of alginate-embedded MSCs into the scala tympani followed by CI insertion and alginate polymerisation. Group D was normal hearing with a CI-insertion in both ears and a unilateral injection of alginate-MSCs. Hearing thresholds were measured before surgeries and before sacrificing the animals performing acoustically evoked auditory brainstem response measurements. Electrode impedances were measured weekly. Four weeks after implantation animals were sacrificed, temporal bones were harvested with the implant in situ, decalcified, immunhistochemically stained and cleared. The SGN density and fibrosis was analyses by confocal laser scanning microscopy. Results: Preliminary data poof that the MSCs survive being implanted for 4 weeks in vivo. Neither the alginate-MSC-injection nor the coat-ing does affect the impedances compared to the control group. Injecting the alginate-MSCs does not negatively affect the acoustically evoked hearing threshold. The histological analysis is ongoing. Therefore no data are available on neuronal survival and fibrosis up to now. Conclusion: The BDNF-producing MSCs encapsulated in alginate survive being implanted into guinea pig inner ears for four weeks. They do not seem to have any negative effect on postoperative residual hearing or impedance development. The histological data are pending and will give information on the neuroprotective effects of this novel drug delivery strategy. This study is supported by the German Research Foundation, grant SCHE 1636/2-1.

PS 678

Direct delivery of antisense oligonucleotides to the middle and inner ear improves hearing and balance in Usher mice

Jennifer J. Lentz[1]; Bifeng Pan[2]; Christopher Tran[3]; Carl Nist-Lund[4]; Abhilash Ponnath[3]; Alice Galvin[4]; Francine M. Jodelka[5]; Hamilton Farris[3]; Frank Rigo[6]; Michelle L. Hastings[5]; Gwenaelle Geleoc[2]
[1]Louisiana State University Health Sciences University; [2]Boston Children's Hospital, Harvard Medical School; [3]LSUHSC; [4]Boston Children's Hospital, Harvard Medical School; [5]Rosalind Franklin University of Med; [6]Ionis Pharmaceuticals

Usher syndrome (Usher) is the most common cause of concurrent hearing and vision impairment. Type 1 Usher syndrome (USH1) is characterized by congenital profound sensorineural hearing impairment and vestibular areflexia, with adolescent-onset retinitis pigmentosa. 2.5% of Usher cases are caused by mutations in the USH1C gene, which encodes harmonin, a protein essential for normal hair cell development and function. We previously described a mouse model containing the USH1C c.216G>A (216A) mutation responsible for nearly all USH1 cases in the Acadian population in Louisiana, USA and Canada. The 216A mutation creates a cryptic splice site that results in a truncated mRNA and harmonin protein. Systemic treatment with antisense oligonucleotides (ASOs) targeting the 216A mutation rescues hearing and vestibular function in Ush1c 216AA mice. In this study, we explored the feasibility of delivering 216A-targeted ASOs locally to the ear to treat USH1C. Three ASO delivery strategies in Ush1c c.216AA neonatal mice were investigated: round window membrane (RWM) injection, trans-tympanic membrane (trans-TM) injection, and topical-tympanic membrane (topical-TM) application of ASO-impregnated gel foam into the external auditory canal. Hearing and vestibular function were assessed by auditory-evoked brainstem response (ABR) and circling behavior, respectively. Functional hair cell

transduction currents were assessed by evoked stiff-probe deflections of cochlear IHCs. Ush1c gene expression and splicing was assessed by reverse-transcription PCR analysis of RNA isolated from the inner ear. Correct Ush1c gene transcript splicing, was observed in inner ear tissue after RWM injections and topical-TM administration of ASO-Ush. P1 injections of 30 mg ASO through the RWM of Ush1c c.216AA mutant mice also successfully rescued hearing in the low (5.6 kHz) to mid-frequency (22 kHz) with thresholds as low as 30 dB. Low thresholds were maintained in rescued mice by 3 months of age. RWM treatment with ASO-Ush at P1 also partially rescued cochlear hair cell transduction currents and reduced circling behavior. Although mice younger than 7 days have a particularly underdeveloped middle ear, topical-TM delivery of ASOs in Ush1c c.216AA mice at postnatal day 4-6 partially rescued hearing at low-mid frequencies (8 and 16 kHz) and significantly reduced circling behavior. Trans-TM treatment of older mice at P10-20 did not improve hearing, however a significant reduction in circling behavior was observed. We conclude that local delivery of ASOs to the middle and inner ear in neonatal Ush1c mice can improve hearing and balance, and suggest therapeutic potential of ASOs in Usher syndrome and other hereditary hearing impairments.

PS 679

Biocompatible Magnetic Nanocomposite Microcapsules as Highly Customizable Microfluidic One-way Diffusion Blocking Valves with Integrated Flow Sensing

Meng-Chun Hsu; Ahmed Alfadhel; Farzad Forouzandeh; David Borkholder
Rochester Institute of Technology

Implantable drug delivery systems are an important component of site-directed therapies addressing prevalent medical conditions, such as auditory and vestibular dysfunction. However long-term use is impeded by backflow and diffusion of body fluids that contaminate the drug contained within the microfluidic pumping system. Although several passive valve concepts have been proposed in the literature attempting to achieve flow rectification power efficiently, the state-of-the-art passive valves with good flow rectifying efficiencies are typically complex micromachined structures, failing to provide a simple solution for interconnecting channel systems. Moreover, these passive valves suffer from high opening pressure and significant diffusion at low backpressure, making them unsuitable for low flow rate drug delivery systems.

In this work, a one-of-a-kind biocompatible magnetic nanocomposite microcapsule is developed as an in-line passive valve that can be integrated with micropumps and microfluidic systems. These magnetic nanocomposites act as the core for building a valve that utilizes magnetic force attraction for sealing the microfluidic channels. The nanocomposites, molded with commercial microtubings, are prepared by incorporating Fe_3O_4 nanoparticles into polyethylene-glycol (PEG). Parylene-C provides a flexible, biocompatible shell and moisture barrier for the microcapsule that enables deformation and sealing to the microfluidic channel wall. The highly customizable valve design offers easy scalability, and simplicity for integration into microfluidic systems. After the microcapsule is placed in the microchannel and steered to the desired location, it is locked in place with a ring static magnetic field gradient source at one end of the capsule, and heated above the phase change temperature of PEG to break down the molecular chains and maintain the capsule in a liquid state. The microcapsule expands and the magnetic particles are attracted to the magnetic field source, sealing the valve at one edge while keeping the other end loose to realize flow rectification. This magnetically-responsive microcapsule demonstrates reliable performance as a passive one-way valve that exhibits unique features and capabilities including effective flow-rectification with steady flows, i.e., 76:1 forward/backward flow ratio at 14 kPa, extremely low leakage flows from backpressures at a rate of 4.7 nL/min kPa^{-1}, blocking 99.96% of diffusion, and ultra-low forward-flow opening pressure of 2.1 kPa. Approaches to integrate flow sensing capability with the valve are explored, with scalability to a broad range of microfluidic channels and systems. Our new, innovative valves provide an important microsystem capability for inner ear drug delivery therapies addressing auditory and vestibular dysfunction.

PS 680

Effects of dexamethasone on intracochlear inflammation and residual hearing after cochleostomy : A comparison of administration routes

Ah-Ra Lyu[1]; Sun-Ae Shin[1]; Dong-Sik Shin[2]; Yong-Ho Park[1]
[1]*Chungnam National University;* [2]*Chungnam National University Hospital*

Preservation of residual hearing after cochlear implant is an important issue with regards to hearing performance. Various methods of steroid administration have been widely used in clinical practice to reduce inflammation and preserve residual hearing. Here we compare the effect of different routes of dexamethasone administration on intracochlear inflammation and residual hearing in guinea pig ears. Dexamethasone was delivered into

the guinea pigs either through intracochlear, intratympanic or systemic route. The intracochlear concentration of dexamethasone, residual hearing, inflammatory cytokines and histopathologic changes were evaluated over time. A higher intracochlear dexamethasone concentration was observed after intracochlear administration than through the other routes. Residual hearing was better preserved with local dexamethasone administration as was supported by the reduced inflammatory cytokines, more hair cell survival and less severe intracochlear fibrosis and ossification concurrently seen in the local delivery group than in the systemic group. The results demonstrate that local dexamethasone delivery can reduce intracochlear inflammation and preserve residual hearing better than in systemically administered dexamethasone.

PS 681

In vivo imaging of central auditory neurons following acute pharmacological manipulation of the cochlea

Travis Babola[1]; Sally Li[1]; Stephanie Szobota[2]; Scott Coleman[2]; Alan C. Foster[2]; Dwight E. Bergles[1]
[1]Johns Hopkins University; [2]Otonomy Inc

Background
Changes in cochlear output influence the development of central auditory pathways and precipitate pathological changes in these circuits after traumatic injury to the inner ear. Obtaining mechanistic information about key events leading to these changes has remained challenging, due to the inability to acutely interrogate the involvement of discrete molecular components in the cochlea while assessing network activity in auditory centers in vivo. To define the patterns of activity that occur in auditory circuits and to investigate the signaling pathways that generate this activity, we developed an in vivo method for imaging synchronized neuronal activity in combination with targeted drug delivery to the inner ear through the round window membrane (RWM).

Methods
In prehearing mice, spontaneous activity was visualized in the intact inferior colliculus (IC) using the genetically encoded calcium indicator GCaMP6s, expressed under the pan-neuronal SNAP25 promoter. Wide-field epifluorescence and high resolution two-photon imaging revealed that groups of neurons in IC exhibit periodic increases in calcium before hearing onset (P7-9). To assess whether glutamatergic synaptic transmission between inner hair cells and spiral ganglion neurons is required for this activity, Gelfoam saturated with the AMPA receptor antagonist, NBQX, was acutely applied to the RWM prior to imaging. To assess whether this approach can also be used to manipulate signaling pathways in

hearing animals over multiple days, we applied NBQX in poloxamer hydrogel to the round window niche of adult animals (P60), and the auditory brainstem response was measured periodically after this treatment.

Results
Following application of NBQX in gelfoam, activity in the contralateral IC was selectively suppressed, mimicking unilateral cochlear ablation, indicating that hair cell – spiral ganglion neuron synaptic transmission is required and that permeation through the RWM is sufficient to enable pharmacological manipulation of the cochlea. Immediately after treatment with NBQX in poloxamer, responses to 24kHz tones were suppressed, followed by suppression of 16kHz tones one day later. Responses gradually recovered within a week, indicating that acute delivery of pharmacological agents in poloxamer can achieve sustained inhibition of cochlear targets in vivo.

Conclusions
This method provides a complementary approach to genetic manipulations, which often trigger compensatory changes that complicate interpretation, allowing pharmacological dissection of the pathways involved in generating spontaneous activity prior to hearing onset, as well as aberrant activity after traumatic noise injury. In addition to AMPA receptor inhibition, analysis of the effects of purinergic and NMDA receptor modulation will be presented.

PS 682

Functional Characterization of OTO-311, a sustained-exposure formulation of the NMDA receptor antagonist gacyclidine, in clinical development for the treatment of tinnitus

Natalia Tsivkovskaia; Rayne Fernandez; Stephanie Szobota; Xiaobo Wang; Jennifer Hou; Alan C. Foster; Fabrice Piu
Otonomy Inc

Background
Tinnitus (or ringing of the ears) is a debilitating condition characterized by the perception of noise in the absence of an objective external auditory stimulus. Its prevalence is significant, with over 50 million adults having reported tinnitus in the US alone, including 16 million individuals reporting having tinnitus in their past year. The etiology of tinnitus is complex and multi-factorial, but evidence suggests that NMDA receptor-mediated aberrant excitation of the auditory nerve and loss of spiral ganglion neuron afferent contacts with inner hair cells (ribbon synapses) in the cochlea may play a role. OTO-311 is a thermosensitive, sustained-exposure formulation of the potent non-competitive NMDA receptor antagonist ga-

cyclidine, which is currently in clinical development for the treatment of tinnitus. Using a variety of molecular biology, electrophysiology, and in-vivo techniques, the profile of gacyclidine (OTO-311) was characterized and compared to that of other known NMDA receptor antagonists.

Methods
Receptor binding and selectivity profiling of gacyclidine and other NMDA receptor antagonists was conducted against a panel of over 80 targets, including ion channels, transporters, GPCRs, nuclear receptors, tyrosine kinase receptors, and enzymes. Neonatal rat neurons, harvested either from the hippocampus or the cochlea, were cultured on multi-electrode arrays. Spontaneous neuronal activity was measured in the presence of NMDA receptor antagonists.The inner ear pharmacokinetic profile of gacyclidine, administered intratympanically as OTO-311, was conducted in Sprague Dawley rats. Gacyclidine levels were quantified at different time points using a liquid chromatography mass spectrometry method.

Results
Gacyclidine is a potent and selective NMDA receptor antagonist having low nM affinity, and a relatively rapid on-rate and slow off-rate, compared to other NMDA antagonists. Incultured neurons, saturating doses of gacyclidine almost completely blocked the NMDA receptor-sensitive spontaneous activity. The administration of OTO-311 provided significant and sustained-exposure to the inner ear compartment, while other NMDA receptors antagonists yielded limited duration of exposure (< 24 hours).

Conclusions
Gacyclidine is an attractive NMDA receptor antagonist with an excellent potency and selectivity profile. Formulated as OTO-311, its otic pharmacokinetic properties are adequate to ensure sustained inner ear exposure.

PS 683

Second Generation of CDK2 inhibitors as Otoprotectants against Cisplatin-induced Ototoxicity

Robert Hazlitt[1]; Tal Teitz[2]; Jaeki Min[3]; Justine Bonga[2]; Currier Duane[3]; Taosheng Chen[3]; Zoran Rankovic[3]; **Jian Zuo**[4]

[1]Departments of Developmental Neurobiology and Chemical Biology and Therapeutics, St. Jude Children's Research Hospital; [2]Department of Developmental Neurobiology, St. Jude Children's Research Hospital; [3]Chemical Biology and Therapeutics Department, St. Jude Children's Research Hospital; [4]Department of Developmental Neurobiology, St. Jude Children's Research Hospital, Memphis, Tennessee, USA

Cisplatin has become a cornerstone in chemotherapeutic regimens since its approval by the FDA in 1978. However its therapeutic benefits are often coupled with potentially debilitating ototoxicity, with some degree of hearing loss occurring in about 63% of patients. Despite the high incidence and the enormous social and economic consequences of the ototoxic side effects, no FDA approved therapies for cisplatin-induced hearing loss have been developed. We have identified kenpaullone, a potent CDK2 inhibitor, as a top hit for protection against cisplatin-induced toxicity from a high throughput screen of bioactive library in a cell line derived from neonatal mouse cochlea (HEI-OC1), using Caspase-glo and Cell-Titer-glo assays as read outs. We performed a follow up screen on a focused library that included known CDK and GSK3β inhibitors and discovered two known CDK2 inhibitors, AT7519 and AZD5438, as top hits. In addition, both AT7519 and AZD5438 are exceptionally potent in cochlear explant cultures, where AT7519 exhibited an EC50 of 15 nM and AZD5438 exhibited an EC50 of 5 nM. Furthermore, we have demonstrated in vivo efficacy of AZD5438 in cisplatin-induced ototoxicity in P30 FVB mice by using transtympanic injection to deliver the compound. In our study, AZD5438 significantly protected against cisplatin-induced ototoxicity, with the most pronounced protection at 32 kHz, where the group treated with cisplatin and AZD5438 was not significantly different from the untreated control group in auditory brainstem response (ABR) measurements, while the group that received cisplatin alone exhibited an 18 dB threshold shift. In our hit-to-lead process, we have acquired a total of 38 analogs of AT7519 from either in-house synthesis or from commercial sources. In addition, we have acquired 10 analogs of AZD5438 from commercial sources. Of the analogs, 8 display good to outstanding potency in our HEI-OC1 cell assay, with the top analog belonging to the AT7519 series. Preliminary testing in cochlear explants revealed that the top analog provides exceptional protection against cisplatin-induced toxicity.

In conclusion, we have identified AT7519 and AZD5438, as well as several analogs thereof that display promising potential as preclinical candidates for the prevention of cisplatin-induced ototoxicity.

PS 684

Attenuation of experimental sepsis-enhanced cochlear uptake of aminoglycosides in mice lacking TLR4

William Meier; Farshid Taghizadeh; Yuan Zhang; Allan Kachelmeier; meiyan Jiang; Peter Steyger
Oregon Hearing Research Center

Background

Aminoglycoside antibiotics such as gentamicin are critical for treating numerous gram-negative bacterial infections (sepsis) that induce host-mediated inflammatory responses. However, aminoglycoside therapy is coupled with the risk of severe side effects, such as permanent hearing loss (cochleotoxicity). Cochlear uptake of aminoglycosides across the blood-labyrinth barrier is potentiated by bacteriogenic-induced host-mediated inflammatory responses. Intravenous administration of lipopolysaccharide (LPS) is an experimental bacteriogenic model of sepsis in mice. LPS binds to Toll-like Receptor 4 (TLR4), triggering important signaling cascades that upregulate the expression of serum and cochlear pro-inflammatory cytokines and chemokines. Mutant mice with hypofunctional TLR4 express significantly less pro-inflammatory markers following exposure to LPS (Koo et al., 2015).

Aim

We hypothesized that mice lacking TLR4 (TLR4$^{-/-}$) have attenuated expression of pro-inflammatory markers and reduced cochlear uptake of gentamicin (compared to wildtype mice) following LPS exposure over time.

Methods

C57/BL6 wild type and TLR4$^{-/-}$ mice were each split into two groups: (i) one receiving 1 mg/kg LPS intravenously (i.v.), and (ii) another receiving neutral saline i.v., with 3 recovery time-points following injection: 3, 24 and 96 hours. Additionally the 96 hour group received 700 mg/kg kanamycin twice daily. At designated time-points, plasma and cochleae were harvested for determination of pro-inflammatory cytokines and chemokines using quantitative PCR and ELISA techniques. At each designated time-points, mice received 2 mg/kg GTTR, or 20 mg/kg gentamicin intraperitoneally, for 1 hour prior to cardiac-perfusion and processing for either (a) confocal microscopy of cochlear lateral walls, or (b) ELISA analysis, to (semi-)quantify cochlear uptake of GTTR or gentamicin, prior to comparative statistical analysis between the 4 groups at each timepoint.

Results

LPS upregulated the expression of plasma and cochlear pro-inflammatory cytokines and chemokines in wildtype, but not in TLR4$^{-/-}$, mice. LPS-also potentiated cochlear uptake of GTTR and native gentamicin in wildtype, but not in TLR4$^{-/-}$, cochleae using ELISA. Preliminary data indicated that LPS-potentiated cochlear uptake of GTTR in wildtype, but not in TLR4$^{-/-}$, cochlear lateral walls using confocal microscopy.

Conclusion

TLR4 signaling is required to upregulate the expression of pro-inflammatory markers in plasma and cochlear tissues, and also for experimental sepsis-enhanced cochlear uptake of aminoglycosides.

PS 685

Circadian vulnerability to cisplatin in GLAST deficient mice.

Evangelia Tserga; Rocio Paublete; Barbara Canlon; Christopher R. Cederroth
Karolinska Institutet

In humans, 75-100% of people who are treated with the chemotherapeutic agent cisplatin present hearing deficits. Cisplatin exposure is usually accompanied by outer hair cell loss (OHC) through apoptosis. Whether inner hair cell (IHC) function can be affected by cisplatin remains poorly understood. Our laboratory recently reported that mice deficient for the glutamate aspartate transporter GLAST exhibited 20-25 dB greater loss of hearing in comparison to WT mice when treated with salicylate, in spite of equally affected OHC function. These findings indicate that ototoxic agents may target the IHC/afferent synapse when defective in its glutamate buffering capacity. To test this hypothesis, we treated GLAST WT and KO mice with cisplatin (4 mg/kg per day for 4 consecutive days), during daytime (9am) or nighttime (9pm), at a dose that caused a moderate but permanent shift in auditory thresholds without affecting OHC function. Auditory brainstem responses (ABRs) and distortion products of otoacoustic emissions (DPOAEs) were collected 24h and 2 weeks after the last administration, and cochleae were sampled for histology and quantification of hair cell loss and synaptic ribbons. Whereas no gender effects could be detected, we found that night administration of cisplatin was more damaging than day administration and caused 25-30 dB threshold shifts at 8 and 24 kHz in KO mice when compared to WT mice, something not observed after day administration. Interestingly, this change in hearing thresholds was unrelated to effects at

the OHCs since DPOAEs remained unaffected. Consistent with the auditory measures, the number of synaptic ribbons was significantly decreased in GLAST KO treated at nighttime, but not when treated during daytime. These findings indicate that cisplatin targets the afferent synapse under the influence of circadian rhythms and could contribute to drug-induced auditory synaptopathy. Notably, our findings support a potential role of the glutamate transporter GLAST in shielding the IHC/afferent synapse to ototoxic insults.

PS 686

Tumor-targeted nanoparticles for delivery of siRNA to vestibular schwannomas

Yin Ren[1]; Jessica E. Sagers[2]; Lukas D. Landegger[1]; Sangeeta Bhatia[3]; Konstantina M. Stankovic[1]
[1]*Department of Otolaryngology, Massachusetts Eye and Ear;* [2]*Department of Otolaryngology, Eaton Peabody Laboratories, Massachusetts Eye and Ear, Program in Speech and Hearing Bioscience and Technology, Harvard Medical School;* [3]*Massachusetts Institute of Technology*

Vestibular schwannoma (VS) is the most common tumor of the cerebellopontine angle, and it typically presents with sensorineural hearing loss (SNHL). The genomic landscape of schwannoma is complex and many of the molecules implicated in VS pathogenesis represent targets not amenable to antibody-based or small molecule therapeutics. Tumor-targeted delivery of small interfering RNA (siRNA) therapeutics provides a direct and effective means to interrogate targets while minimizing off-target effects. To establish a preclinical model for therapeutic inhibition of putative targets in VS, archived tumor specimens, fresh tumor cells derived from patients with sporadic VS, and an established schwannoma cell line were screened. Nanoparticles directed by the tumor-homing peptide iRGD (internalizing RGD, CRGDR/KGPDC) were selectively taken up by primary VS cultures in vitro via interactions with avb3/b5 integrins and neuropilin-1 (NRP-1). Cellular uptake was inhibited by a neutralizing antibody against av integrin in a dose-dependent manner. When applied to primary VS cultures, iRGD-targeted nanoparticles delivered siRNA directed against tumor nerosis factor alpha (TNFa) in a receptor-specific fashion to potently silence gene expression and protein secretion. Taken together, our results provide a proof of principle for tumor-targeted, nanoparticle-mediated delivery of siRNA to VS and establish a novel platform for the development and pre-clinical screening of molecular therapeutics against VS.

Inner Ear: Mechanics & Modeling II

PS 687

On the zero-crossing invariance property of different 1-d transmission line cochlear models

Renata Sisto[1]; Arturo Moleti[2]
[1]*INAIL Research Department of Occupational and Environmental Medicine, Epidemiology and Hygiene;* [2]*University of Rome Tor Vergata, Department of Physiscs*

In a nonlinear cochlea, the zero-crossing invariance of the impulsive response as the stimulus level is varied in a wide dynamical range requires that the local resonance frequency is insensitive to changes of the system gain and damping. Indeed, increasing the stimulus level causes a decrease of both gain and tuning, due to an increase of the effective damping of the system. The described behavior of the oscillators constituting the cochlea transmission line is quite different from the behavior of a standard harmonic oscillator for which it is well-known that damping variations affect the resonance frequency. To enforce the zero-crossing property into a 1-d transmission line model, Zweig (1991) proposed a double-pole model for the harmonic oscillators associated with the local line transverse impedance. The three parameters characterizing the delayed stiffness transmission line, δ, ρ and μ are set in order to respect the resonance frequency invariance as the effective tuning is changed. The resonance frequency invariance could have a crucial role in the process of signal coding in the auditory system, so it seems very important for a reasonable cochlear model to respect this requirement. On the other hand, the Zweig and Shera impedance function would need a more physiological basis. Different 1-d transmission line models of the cochlea are studied from the point of view of the zero-crossing invariance and the correspondent admittance poles position in the complex frequency plane. The zero-crossing property, as well as other crucial properties of the response phase can effectively help identifying models capable of fully representing essential features of the cochlear function. A deeper insight into both the physiological nature and the response mathematical properties of the active mechanism is still required to fully understand how the cochlea works.

Zweig, G. Finding the impedance of the organ of Corti. Journal of the Acoustical Society of America, 89, 1229–1254 (1991)

Lim, K. M. and Steele, C. R. A three-dimensional nonlinear active cochlear model analyzed by the WKB-numeric method. Hearing Research, 170, 190–205 (2002)

PS 688

Inner and outer hair cell stereocilia bundle stimulation in a passive cochlear model

Nima Maftoon[1]; Hamid Mottalebzadeh[1]; John J. Guinan[2]; Sunil Puria[3]
[1]Eaton Peabody Lab, Massachusetts Eye and Ear Infirmary, Harvard Medical School; [2]Massachusetts Eye and Ear Infirmary; [3]Eaton-Peabody Laboratory, Massachusetts Eye and Ear; Department of Otolaryngology, Harvard Medical School; Speech and Hearing Bioscience and Technology, Harvard University Graduate School of Arts and Sciences

For over a century the shear motion between the reticular lamina (RL) and tectorial membrane (TM) has been thought to be responsible for the mechanical stimulation of inner-hair-cell (IHC) and outer-hair-cell (OHC) stereocilia bundles. This hypothesis is not always consistent with recent cochlear motion measurements. We continue to develop a fluid-structure-interaction, finite-element model of a radial cross section of the organ of Corti (OoC) of the gerbil cochlear apex to explore this question. This 3-D (24 µm thick) slice model was constructed using anatomical measurements from the gerbil apical turn (Edge et al., Hear. Res. 1998), supplemented with mouse cytoarchitecture measurements (Soons et al., JARO 2015). The model includes the arcuate and pectinate zones of the basilar membrane (BM), OHCs, Deiters cells with OHC and phalangeal process attachments, RL, TM and IHCs. These are surrounded by fluid in the inner sulcus, the sub-tectorial space (STS), and the scala media. New from our previous model formulations is representation of OHC and IHC stereocilia as bundles instead of as a single cilium. The model was driven by applying a uniform sinusoidally-varying pressure on the BM. Linearized Navier-Stokes equations coupled with linear-elastic equations discretized with tetrahedral elements were solved in the frequency domain. Our model results concur with recent OoC gerbil-apex measurements from the literature. We found that, in addition to the classic shear mechanism, an oscillatory radial flow resulting from changes in the STS gap height also contributed to IHC bundle stimulation. We also found that the OHC bundle deflections were not always in phase with each other. We studied the sensitivity of these results to changes in the material properties of the structures, for 0.1 to 10 kHz pressure drives. This work was supported in part by grant R01 DC07910 from the NIDCD of NIH.

PS 689

Dynamics of Cochlear Nonlinearities: Automatic Gain Control or Instantaneous Damping?

Alessandro Altoè[1]; Karolina K. Charaziak[2]; **Christopher A. Shera**[3]
[1]Department of Signal Processing and Acoustics, Aalto University; [2]Caruso Department of Otolaryngology, University of Southern California; [3]Auditory Research Center, Caruso Department of Otolaryngology, University of Southern California

Recent recordings from the gerbil basilar membrane [Cooper and van der Heijden. Physiology, Psychoacoustics, and Cognition in Normal and Impaired Hearing. Springer International Publishing, 2016. 267-273] show that the compressive nonlinearity of cochlear mechanical responses cannot be thought as a purely instantaneous phenomenon. For this reason, the cochlea has been thought to incorporate a type of automatic gain control (AGC) mechanism characterized by a finite reaction time.

Here, we study the effect of instantaneous nonlinear damping on the responses of oscillatory systems. The principal results are that: (i) instantaneous nonlinear damping produces a non-instantaneous gain control that differs markedly from typical AGC strategies; (ii) the kinetics of compressive nonlinearity implied by the finite reaction time of an AGC system appear inconsistent with the nonlinear dynamics measured on the gerbil basilar membrane; and (iii) conversely, those nonlinear dynamics can be reproduced using an harmonic oscillator with instantaneous nonlinear damping. Thus, an AGC system with finite reaction time appears neither necessary nor sufficient to explain nonlinear gain control in the cochlea.

PS 690

Vibration patterns of the organ of Corti due to acoustic and electrical stimulations

Jessica Huhunke; Talat Jabeen; Jonathan Becker; Jong-Hoon Nam
University of Rochester

According to recent observations, the organ of Corti (OoC) complex vibrates differently depending the existence of outer hair cell motility. The OoC micro structures vibrate roughly in-phase when passive. In contrast, when active, they vibrate out-of-phase when outer hair cell motility contributes to the vibrations. It is unclear

how this difference in OoC vibration modes is related to the cochlear function such as sound amplification or tuning. We used isolated cochlear turns to investigate the vibration patterns of the OoC due to mechanical and electrical stimulations.

Fresh cochleas were harvested from young gerbil (15-20 days old). To expose a targeted section of the OoC, the bones and tissues of the cochlea were removed until approximately a single turn of the cochlear coil left. The cochlear turn was attached to a custom-designed micro-chamber. The micro-chamber has two ports for fluid circulation and two ports for pressure application and release (analogous to oval and round windows in the cochlea). It also has a slit on which the cochlear turn is attached. Gold-coated micro-beads were spread on the top and bottom surfaces of the OoC complex. While acoustical pressures and electrical currents were delivered, the vibration amplitudes of the OoC complex were measured along the transverse and radial directions using a laser velocity meter and a dual-photodiode sensor. The measurement data was compared with computer model simulations of the OoC complex.

At the measurement location (approx. 8 mm from the basal end), the vibration amplitudes were greater at the tectorial membrane than at the basilar membrane for both stimulation methods. Within our measurement precision, there was no difference between the best responding frequencies of the tectorial and basilar membranes. Under electrical stimulation, the radial displacement of the reticular lamina lagged the radial displacement of the tectorial membrane by 180° above the best responding frequency. In contrast, these vibrations were in-phase for acoustical stimulations. Computer model analyses showed similar trends. Our observations, albeit preliminary, are consistent with the existing observations that outer hair cell motility is responsible for the out-of-phase vibrations among the OoC structures.

PS 691

Reticular Lamina and Basilar Membrane Responses to Clicks at the Base of the Gerbil Cochlea

Wenxuan He[1]; Tianying Ren[2]
[1]Oregon Hearing Research Center; [2]Oregon Hearing Research Center, Oregon Health & Science University

Background
Heterodyne low-coherence interferometry recently demonstrated that reticular lamina responses to tones are greater than basilar membrane vibrations not only at the best frequency but also at low frequencies. The phase of the reticular lamina vibration leads the basilar membrane phase by up to 180 degrees at low frequencies; and this phase lead decreases with frequency, approaching zero near the best frequency. These data suggest a global hydromechanical mechanism for cochlear amplification. This mechanism was tested in this preliminary study by measuring and comparing click-evoked reticular lamina responses to basilar membrane vibrations.

Methods
Young Mongolian gerbils of either sex with normal hearing were used. Reticular lamina and basilar membrane responses to clicks were measured from the base of gerbil cochleae through the round window using a custom-built heterodyne low-coherence interferometer. The data was collected at different sound levels under sensitive and insensitive conditions. Time waveforms of reticular lamina vibrations were compared to those of basilar membrane responses.

Results
In sensitive cochleae, the threshold of the click-induced reticular lamina response was lower than that of the basilar membrane. The reticular lamina displacement was greater and increased with the sound level at a slower rate than those of the basilar membrane. Reticular lamina responses started later and lasted longer than the basilar membrane vibration. The two vibrations were out of phase at the beginning of responses and gradually became in phase with time. This phase change coexisted with an increase of instantaneous frequency to the best frequency. Differences between the reticular lamina and basilar membrane response largely vanished under the postmortem condition.

Conclusion
Physiologically vulnerable time and amplitude differences between reticular lamina and basilar membrane responses to clicks indicate that the reticular lamina and basilar membrane vibrate in opposite directions at the cochlear base and in the same direction at the best-frequency location. These collaborative differential motions interact through the cochlear fluid to enhance the vibration at the best frequency location.

Funding

PS 692

Independent fluid structure coupling in the organ of Corti

Aritra Sasmal[1]; Karl Grosh[2]
[1]University of Michigan; [2]University of MIchigan

The cochlea owes its frequency selectivity to the tonotopic gradient of the electrical, chemical and mechanical properties of its sub-structures from the base to the apex. The organ of Corti (OoC) is positioned between the basilar membrane (BM) and the tectorial membrane (TM), and is responsible for transducing the vibration of the cochlear partition into neural signals. The scala media (SM) fluid is not only coupled to the BM but also to the TM. Recent in vivo experiments have shown that the OoC exhibits complex dynamics concomitant with multiple internal degrees of freedom, and the amplitude of the reticular lamina (RL) displacement is larger than that of the BM. This has necessitated the analysis of more detailed models with independent coupling of the TM and BM to the scalae fluid.

In this study, we have examined the effect of coupling both the TM and the BM to the SM fluid in a physiological non-linear model of the guinea pig cochlea. We found that the OoC can support a transverse traveling wave on the TM-RL complex, in line with previous linear models of Lamb and Chadwick (2011) and Cormack et al. (2015). The place-frequency map of the TM-RL traveling wave may differ significantly from that of the BM, and depends on the uncoupled resonance frequency of the complex and the strength of the mechanical coupling between the BM and the RL. We hypothesize that the Dieter cell processes, apart from its feed forward effect, may also serve to couple the RL and the BM. Kale and Olson (2015) have shown that the SM and ST pressures exhibit a notch close to the characteristic frequency of that place, which they have attributed to the interaction between the slow and fast waves in the fluid. Our model suggests that interactions between the different transverse modes of the slow fluid pressure wave are also important. These modes are non-linear and localized close to the best place, and may play a major role in the symmetric as well as the antisymmetric pressure forcing on the cochlear partition.

PS 693

Signal Envelope Processing In the Apex of the Guinea Pig Cochlea Recorded by Optical Coherence Tomography Vibrometry

George Burwood[1]; Anders Fridberger[2]; Ruikang Wang[3]; Alfred L Nuttall[1]
[1]Oregon Health & Science University; [2]Linköping University; [3]University of Washington

The structure and function of the mammalian cochlea permits the perception of speech and music via the envelope of the otherwise complex acoustic signal. Much of this ability is clearly due to post-sensory processing, as cochlear implant users may understand speech with sparse frequency coding provided by their electrode ar-

rays. Moreover, the understanding of signal encoding for low frequencies is complicated by the absence of bandpass frequency tuning of the apical organ of Corti in guinea pigs. Therefore, the organ of Corti is likely to possess the ability to relay envelope information, which is not necessarily reflected in the tuning of the Basilar Membrane.

Using Optical Coherence Tomography vibrometry in the intact apical turn of the guinea pig, we measured the response of the Reticular Lamina and the Basilar Membrane corresponding to the applied signal envelope of a three tone complex at several stimulus intensities. Each tone complex possessed an f1 of 200, 350 or 500Hz respectively, and each contained an f2 and f3 subsequently separated by 50Hz, producing a quadratic difference tone of 50Hz. Varying the phase of the f2 had the effect of reducing the amplitude of the envelope component, and this effect was less pronounced at higher stimulus intensities. In experiments with more than one recording location, the envelope signal was diminished or absent at the Reticular Lamina for regions closer to the helicotrema.

Based upon these observations, it is likely that envelope information is produced by cellular mechanosensory pathways that introduce distortion due to their non-linear nature. Such tissue displacement non-linearities could feasibly permit envelope information to be transduced by the auditory nerve, enabling the interpretation of complex acoustic signals.

PS 694

Suppression Side Lobes in a Nonlinear and Active Model of the Cochlea

Bastian Epp[1]; Geoff Manley[2]; Pim van Dijk[3]
[1]Hearing Systems group, Department of Electrical Engineering, Technical University of Denmark; [2]University of Oldenburg; [3]Department of Otorhinolaryngology, University Medical Center Groningen, The Netherlands

Oscillations at one tonotopic location of the cochlea can be suppressed by the presence of another remote oscillation. This suppression effect is a consequence of the nonlinear and coupled nature of the oscillatory structures in the inner ear. Suppression has been observed in various types of otoacoustic emissions and has also been linked to perceptual masking phenomena.

The amount of suppression depends on the spectral distance and the relative level between suppressor and

suppressee. Evaluated for frequency ratios between suppressor and suppressee close to 1, suppression leads to a V-shaped curve. Suppression tuning curves of spontaneous otoacoustic emissions (SOAEs) in lizards, Macaques and in human listeners can show multiple side lobes. Recently, Epp et al. (Mechanics of Hearing 2017) showed that such side lobes align with the nodes and antinodes of the standing wave pattern observed in a nonlinear and active transmission line model of the cochlea capable of simulating SOAEs. This finding is explained by differences in the modulation of the gain at tonotopic locations corresponding to nodes and antinodes of the standing wave between the cochlear base and the tonotopic place of the SOAE. However, in principle, a side-lobe suppression pattern does not require standing waves, but is a phenomenon that is inherent to nonlinear, driven oscillators.

We investigated whether the side lobes are in fact due to a standing wave pattern or to inherent properties of the model as a chain of coupled, nonlinear oscillators. If the suppression sidelobes are based on a modulation of the basal gain, similar effects should play a role in the interaction between two external stimuli. A two-tone suppression experiment was simulated by stimulation of the model by a low-intensity probe tone (suppressee) and an additional tone (suppressor) over a broad range of frequency and level, and in the absence of SOAEs (eliminated by removing the roughness in the place-frequency mapping). The comparison between the SOAE suppression tuning curves and the two-tone suppression tuning curves showed similarities in the presence of side bands. The width, the magnitude and the spacing of the side lobes was dependent on the level difference between suppressor and suppressee. Thus, a frequency-specific modulation of the gain does not require a standing wave on the basilar membrane. Consequently, interactions between the external stimuli and SOAE-related standing waves do not seem to be the sole mechanism underlying the SOAE suppression data.

PS 695

Sound-evoked vibration patterns of Reissner's membrane near the apex of the chinchilla cochlea

Wei Dong[1]; Nigel Cooper[2]
[1]*VA Loma Linda Health Care System and Otolaryngology, Loma Linda University; *[2]*Erasmus MC*

Vibration of the stapes creates a pressure difference between the scala vestibuli and scala tympani, which displaces the cochlear partition transversally, causing a transversal displacement wave to propagate longitudinally along the cochlea, known as the traveling wave. The traveling wave propagates more slowly than a sound wave propagating in water because it depends on interactions between the fluids and the mechanical elements of the cochlear partition. Traveling waves have been characterized in scala tympani and scala media, however, due to difficulties in accessing each chamber, the picture of wave propagation in the cochlea is not complete. Reissner';s membrane (RM), composed of two cell layers, epithelial and mesothelium, functionally separates the scala media (endolymph) from the scala vestibuli (perilymph). Characterization of sound induced vibration of RM provides insights into wave propagation in the cochlea';s fluids, especially at the interface between scala media and scala vestibuli.

Laser velocitometry was used to measure sound-evoked vibrations from RM in the apical turn of the living chinchilla cochlea. Access to the scala vestibule was provided by cutting a small hole near the apex of the cochlea, and lightweight silver-coated micro-spheres were used to enhance the reflectivity of the RM. The hole was then covered with a glass coverslip, but the cochlea was not resealed. Single tone sweeps and clicks were generated and responses acquired by commercial hardware and software (i.e., System III, Tucker-Davis Technologies (TDT), and MATLAB and the TDT visual-design studio). Distortion product otoacoustic emissions were recorded at key points during the experiment as a monitor of cochlear condition. Middle ear responses at the umbo were also measured. The care and use of animals were approved by the Institutional Animal Care and Use Committee (IACUC) of our VA facility.

Responses from eleven animals provided several consistent findings: RM responses exhibited compressive nonlinearity at frequencies above ~500 Hz. The nonlinearity was physiologically vulnerable, and disappeared post mortem. RM tuning characteristics, derived from either impulse (click) responses or from the variations in vibration amplitude as a function of stimulus frequency (for pure tones), had low-pass filter characteristics with a corner frequency of ~800 Hz. Phase accumulation was almost linear across this bandwidth, and amounted to ~2 cycles, consistent with the presence of an apically-propagating 'slow'; traveling wave. At frequencies beyond the slow traveling wave';s cutoff, i.e. > ~1 kHz, responses exhibited prominent phase and amplitude plateaus, confirming the existence of a 'fast'; compression wave that also propagated towards the cochlear apex.

PS 696

Outer Hair Cell and Basilar Membrane Responses to Zwuis Tone Complexes

Elika Fallah; C. Elliott Strimbu; Elizabeth S. Olson
Columbia University

Although the sound around us is in general a broadband signal consisting of many frequencies, most studies of cochlear mechanics use single or two tones as acoustic stimuli. There also have been studies that used noise or broad-band acoustic click stimuli, with the objective of making the stimulus more similar to the broadband environmental sounds. Zwuis tone complexes are a relatively novel stimulus paradigm that has two main advantages: 1) many distinct stimulus frequencies are sent to the ear at the same time, 2) there is no overlap between these frequencies up to third order distortion products, so distortion products are separable in the results. This technique was introduced by Van der Heijden and Joris (2003), who recorded auditory nerve responses to seven component Zwuis tones. Later, Van der Heijden and Versteegh (2012) used Zwuis stimuli in measurements of basilar membrane (BM) motion using a single point laser Doppler vibrometer, and compared the BM responses to single tone stimulation in gerbil. Recently, Cooper and Van der Heijden (2017) used the Zwuis with optical coherence tomography (OCT)-based motion measurements. We initially adopted the Zwuis tone stimulus for measurements with OCT, as it was an efficient stimulation that helps compensate for the long OCT processing time. In the work presented here, we used the dual pressure/voltage sensor developed in our lab to measure the pressure at the BM and the extracellular potentials generated by outer hair cells, in response to a Zwuis stimulus composed of 40 frequencies. Combining the dual sensors and wideband Zwuis tone stimuli gives us a deeper view into cochlear mechanics.

PS 697

Do Vibrations Measured Inside the Organ of Corti Reflect OAE Suppression Better than the Basilar Membrane?

Jonathan Siegel
Hugh Knowles Center, Roxelyn and Richard Pepper Department of Communication Sciences and Disorders, Northwestern University

Introduction

Stimulus frequency otoacoustic emissions (SFOAEs) appear to originate primarily in the cochlear region of the CF place of the evoking probe tone. It is commonly believed that SFOAE generation is a byproduct of the cochlear amplifier that enhances basilar membrane vibrations near the characteristic frequency place. However nonlinear interaction between the probe tone by suppressor tones more than an octave above that of the probe tone suggests that some structure(s) within the organ of Corti exhibit nonlinearity extending basal to the region thought to contribute to mechanical amplification (Charaziak and Siegel, JARO 16:317-329, 2015; Charaziak and Siegel, 12th MoH Workshop, AIP Conf. Proc. 1703:090006, 2015). This finding complicates the interpretation of the SFOAE phenomenon, because this basal region shows no evidence of nonlinear suppression in studies of basilar membrane vibrations. Recent reports from the Ren and Oghalai labs demonstrate nonlinear and vulnerable gain in the reticular lamina and other structures, when the basilar membrane appears passive and linear, at locations basal to the peak. Suppression studies in our lab of the ear canal sound pressure show broad frequency ranges of nonlinearity for single tones, intermodulation distortion evoked by pairs of tones and tone pips in several species including humans.

Methods

Methods for generating acoustic stimuli and measuring otoacoustic emissions are as described previously. The basic paradigm was to fix the frequency of a probe tone (SFOAE), tone pair (DPOAE) or tone pip (TEOAE) and to measure the residual using a suppressor tone stepped in frequency above the probe.

Results

Suppression patterns demonstrating residuals for all three stimulus classes mentioned above are presented. Broad nonlinear suppression is a consistent feature.

Conclusions

Should two-tone suppression be demonstrated in the mechanics of structures within the organ of Corti, then this suppression paradigm could be applied to these mechanical measurements to examine whether there is a more direct relationship to the acoustic suppression than evident in the basilar membrane. Focused attention on whether the recent intra-organ mechanical measurements support an active model would then apply directly to interpreting the ear canal suppression phenomenon. Resolving this question may also establish whether suppressor tones more than an octave above the frequency of the probe tone remove an SFOAE signal or act via passive nonlinearity (Berenzia-Greene and Guinan, J. Assoc. Res. Otolaryngol. 16:679–694, 2015).

Funding

PS 698

Investigation of the 2f1-f2 and 2f2-f1 tone distortion products using a rough 3D computational model of the gerbil ear

Haiqi Wen[1]; Thomas Bowling[2]; Charlsie Lemons[1]; Julien Meaud[2]
[1]Georgia Institute of Technology; [2]G.W.W. School of Mechanical Engineering, Georgia Institute of Technology

Distortion product otoacoustic emissions (DPOAEs), sounds measured in the ear canal induced by the cochlea nonlinearity, have been intensively studied due to their noninvasive advantage. Among two tone DPOAEs, the cubic difference tones (2f1-f2 and 2f2-f1) are of the most interest.

In this work, a 3D physiologically-based computational model of the gerbil ear was used to investigate the propagation of the 2f1-f2 and 2f2-f1 distortion products (DPs) inside the cochlea and the corresponding DPOAEs in the ear canal. The model includes a physiologically-based nonlinear time-domain model of the cochlea and a transmission line model of the middle ear. In addition, the model includes cochlear roughness to account for the inhomogeneity of the outer hair cells such that DPOAEs are generated both by a distortion mechanism and by a reflection mechanism. The model was used to simulate the generation of DPOAE for various input stimulus levels (L1=L2=60, 80 and 100dB) and primary frequency ratios (f2/f1 =1.05, 1.2 and 1.35). To further analyze DP propagation and DPOAE generation mechanisms, the total emissions are decomposed into distortion source and reflection source components. Numerical simulations are compared to available measurements of DPOAEs in the gerbil. The results show that the 2f1-f2 DPOAEs are mostly dominated by the distortion emissions from the f2 best place region, although ripples and fine structure are observed in the total DPOAEs due to interference between the reflection source and distortion source emissions. The 2f2-f1 DPOAEs are more affected by the reflection emission because the 2f2-f1 DP best place is basal to the region of distortion source generation, resulting in a smaller distortion source component. Furthermore, for both the 2f1-f2 and 2f2-f1 DPOAEs, the distortion emissions are approximately proportional to the primary stimulus level while the dependence of the reflection emissions on the primary input levels turns out to be more complicated. More fine structure is observed for low primary frequency ratios because of the closer best place of DP and primary tones, indicating a more complex interference between two waves originating at different locations on the basilar membrane. Because these simulations allow to observe both emission components in the ear canal and on the basilar, the model provides considerable insights into DPOAE generation in the presence of two sources.

PS 699

Basilar Membrane Impedance Measurements in Fresh Human Temporal Bones

Stefan Raufer[1]; Hideko Nakajima[2]
[1]Harvard University; [2]Department of Otology and Laryngology, Massachusetts Eye and Ear, Harvard Medical School, Boston, MA, USA

The cochlea is a mechanical frequency analyzer, owing its characteristics to the impedance of the basilar membrane (BM). In humans, the acoustic impedance of the BM has never been measured and the stiffness (or elasticity) of the human BM has not been revised since von Bekesy';s experiments. Current estimates of the BM stiffness in the cochlear base range over two orders of magnitude. We measured intracochlear pressures in scala vestibuli and velocities of the BM 1.2 mm from the base of the cochlea in six fresh human cadaveric specimens. By taking the ratio of the pressure and velocity measurements, the specific acoustic impedance can be calculated, i.e. $Z = p/v$. At low frequencies, where the BM impedance is stiffness-dominated, the stiffness can be extracted by multiplying the imaginary part of Z by the angular frequency. The specific acoustic impedance is decreasing by 6 dB per octave at frequencies between 100–10,000 Hz, with a phase close to -90 degrees. The real part of the impedance is positive and slightly increasing at low frequencies. The imaginary part is negative and dominating the Z at low frequencies; the imaginary part is indirectly proportional to the frequency. At frequencies one octave below the characteristic frequency (CF = 14 kHz at the measurement location), the impedance of the BM is stiffness-dominated. The specific acoustic stiffness at the measurement location amounts to 1.2 GPa/m ±0.5 GPa/m. The human BM in the hook region is a factor of five less stiff than the gerbil BM, which is not surprising given its larger width and lower resonant frequency. Compared to von Bekesy';s estimates of the static stiffness, our estimate of the dynamic stiffness is one order of magnitude higher. Thus, current model assumptions may be revised.

PS 700

Using a fluctuation analysis of limit cycle oscillations in inner ear hair bundles as a new test of low dimensional dynamical models

Janaki Sheth[1]; Dolores Bozovic[2]; Alexander Levine[1]
[1]University of California, Los Angeles, Department of Physics and Astronomy; [2]University of California, Los Angeles, Department of Physics & Astronomy

The transduction of pressure waves into electrical signals in the inner ear is an active (energy consuming) process involving the complex interplay of elastic elements, molecular motors, and mechanically sensitive ion channels. One dramatic manifestation of the active process in inner ear hair cells is the occurrence of spontaneous bundle oscillation, which has been observed in vitro in a number of species. Several systems of nonlinear differential equations have been proposed as models of this limit cycle oscillation, including the simple two-dimensional Hopf oscillator and more complex variants that attempt to explicitly incorporate physiological variables such as membrane potential, bundle deflection, and molecular motor activity. All such models that admit spontaneous oscillation exhibit a stable limit cycle in some parameter regime. Additionally, all of these lower dimensional models include stochastic noise in one or more variables representing implicitly the effect of other degrees of freedom. Examples include ion channel noise, Brownian motion of the bundle, and stochastic molecular motor activity.

We study the effects of noise on these stable limit cycle dynamics using both analytic calculations and numerical simulations. We show that d-dimensional noisy limit cycle oscillators generically display phase diffusion at long time scales and (d-1) degrees of freedom that behave roughly as overdamped oscillators with characteristic Lorentzian power spectra. On shorter time scales, deviations from these dynamics provide new information about the limit cycle, which can be used to probe the validity of each of these nonlinear models of inner ear dynamics. In particular, we show that noise in the dependent variables that are typically hidden from measurement, e.g., molecular motor activity, are coupled back to the observable variables in ways that allow one to use noise measurements to access otherwise unobservable features of the system. We then compare our theoretical results to data from Rana catesbeiana hair cells, showing that the physiological system indeed displays evidence of the nonlinear coupling of the fluctuations predicted by the proposed models. We also address the fundamental question of how experiments observing only a subset of the dynamical variables may use a fluctuation-based analysis to extract the maximal information regarding these remaining "hidden variables."

PS 701

Measurements of Mechanical Point Stiffness in the Basilar Membrane of Chinchilla and Comparisons to Other Species

Aleksandrs Zosuls[1]; Darlene R. Ketten[2]; H. Steven Colburn[1]
[1]Boston University; [2]Harvard Medical Boston University Woods Hole Oceanographic

When measured at physiologically relevant static displacements (1μm), there is evidence that the transverse stiffness of the basilar membrane plays a significant role in the frequency place tuning of the cochlea. When there is a large (> 5 μm) static basilar membrane displacement used during measurement, stiffness values increase. This suggests the cochlear partition becomes distorted and tension builds as more structures are recruited to contribute to the total stiffness. There is mounting evidence that the unusual arched pectinate region in the basilar membrane in gerbil (Meriones unguiculatis) buckles during large measurement displacements thus leading to underestimated stiffness values. In this study, new stiffness measurements were made in chinchilla (Chinchilla chinchilla) and compared to gerbil and other species. The pectinate region in chinchilla is a more typical mammalian basilar membrane in that it does not have the large arch found in gerbil.

In the current study measurements were made less than one hour post mortem in the base of the cochlea of adult chinchillas. A piezoelectric force probe was used to measure stiffness of the basilar membrane through a window in the scala tympani. The measuring tip on the force probe was a pulled glass pipette blunted to 20um in diameter. The same methods and probe were used to measure stiffness in the base of gerbil. Preliminary data indicates that the stiffness in the base of chinchilla is approximately (0.3 N/m) which is less than in the base of gerbil (0.6 N/m). The width of the basilar membrane at the measurement location was 200 μm in chinchilla and 160 μm in gerbil. Once the probe was in full contact with the tissue the loading curve of static displacement vs. stiffness was more linear and had less growth than in gerbil. The lower stiffness in the base of the chinchilla is consistent with audiogram data that indicates it has a lower high frequency hearing range than gerbil (30 kHz vs. 50 kHz).

PS 702

Variations in OHC-generated Voltage and DPOAEs with low EP

Yi Wang; Elika Fallah; Elizabeth S. Olson
Columbia University

Endocochlear potential (EP) is essential for cochlear amplification, by providing the voltage drop needed to drive outer hair cell (OHC) transducer current, which leads to OHC electromechanical force. An early study using furosemide to reversibly reduce EP showed that distortion product oto-acoustic emissions (DPOAEs) recovered before EP. This indicated that cochlear amplification may be able to adjust to a new, lower EP. To investigate the mechanism of this adjustment, EP, DPOAE and locally-measured OHC-generated voltage were measured simultaneously in gerbil with furosemide injection to reversibly reduce EP. Intraperitoneal (IP) and intravascular (IV) injection of 120 and 100 mg/kg furosemide was applied respectively. With IP injection, a slow variance was observed, showing that OHC-generated voltage and DPOAE started recovering before EP starts to recover. Both manipulations showed DPOAE and the second harmonics of OHC-generated voltage were able to get fully recovery even before the fundamental recovered to its level before furosemide injection. Those observations supported that the OHC response to low EP seems to include an operating point shift that boosts nonlinear distortion.

Inner Ear: Neural Anatomy & Physiology

PS 703

Age-related cochlear histopathologies in Old-World vs. New-World primates: the rhesus macaque (Macaca mulatta) and the common marmoset (Callithrix jacchus)

M. Charles Liberman[1]; Corinna Ross[2]; Suzette Tardif[3]; Gregg Recanzone[4]; Troy Hackett[5]; Ramnarayan Ramachandran[6]; Tara Moore[7]; **Michelle D. Valero**[8]
[1]*Harvard Medical School; [2]Department of Science and Mathematics, Texas A&M University San Antonio; [3]Southwest National Primate Research Center; [4]Center for Neuroscience and Department of Neurobiology, Physiology and Behavior, University of California at Davis.; [5]Vanderbilt University, Medical Center; [6]Department of Hearing and Speech Sciences, Vanderbilt University Medical Center; [7]Department of Anatomy & Neurobiology, Boston University School of Medicine; [8]Department of Otology and Laryngology, Harvard Medical School, Boston, MA, United States of America, Eaton-Peabody Laboratory, Massachusetts Eye & Ear Infirmary*

Recent data suggest that cochlear synapses are more vulnerable than hair cells in aging rodents (e.g., Sergeyenko et al., 2013) and humans (Viana et al., 2015). There are several therapies under development that aim to prevent, reduce, or reverse age-related cochlear pathologies, and a non-human primate model may be an important translational model system for such therapies. Here, we describe normal aging phenotypes in two primate species, the Old-World rhesus macaque (Macaca mulatta), which has a maximum lifespan of 40 years, and the New-World common marmoset (Callithrix jacchus), which has a maximum lifespan of 22 years.

Rhesus ears were from 5 young (mean(SD) = 7.6(1.5) yrs), 4 middle-aged (13.3(1.8) yrs), and 5 old (24.5(4.7) yrs) macaques from colonies at Vanderbilt University, Boston University, and U.C. Davis. Marmoset ears were from 8 young (3(0.5) yrs) and 10 old (16(2.3) yrs) monkeys from the colony at the Southwest National Primate Research Center in San Antonio, TX. Monkeys were euthanized as an end-point for other aging-related projects, and cochleas were harvested for histopathology. Specifically, we evaluated normal innervation patterns in young monkeys and quantified the effects of aging on the survival of hair cells and afferent cochlear synapses.

Aging macaques were missing up to 36% of their outer hair cells (OHCs) in high-frequency regions, while less than 15% of inner hair-cells (IHCs) were lost. However, up to 50% fewer synapses (re young) remained in surviving IHCs. Some aging marmoset cochleas had significant hair-cell loss, missing up to 85% in high frequency regions. Additionally, as many as 60% of afferent synapses were lost on surviving IHCs of aged marmoset cochleas. In both primate species, there were synaptopathic regions with little or no OHC loss. These data provide further evidence that synapses are the most vulnerable element in the aging primate cochlea and are therefore an important target for intervention strategies.

PS 704

The Acoustic Environment Modulates Tyrosine Hydroxylase Expression in Cholinergic Lateral Olivocochlear Intrinsic Neurons

Jingjing Sherry Wu[1]; Hamad A. Javaid[2]; Amanda M. Lauer[2]; Elisabeth Glowatzki[1]
[1]*Johns Hopkins School of Medicine, Department of Otolaryngology - Head and Neck Surgery; [2]Johns Hopkins University School of Medicine, Department of Otolaryngology - Head and Neck Surgery, Center for Hearing and Balance*

Lateral olivocochlear (LOC) neurons provide descending input from the brainstem to auditory nerve fiber (ANF)

endings underneath inner hair cells (IHCs). This input most likely modulates ANF activity and thereby affects coding of the sound signal. Two separate cytochemical groups of LOC neurons have been shown in mice: cholinergic LOC intrinsic neurons and dopaminergic LOC shell neurons (Darrow et al. 2006). Increased expression of tyrosine hydroxylase (TH), an enzyme responsible for the synthesis of dopamine, has been shown in the guinea pig cochlea after sound conditioning (Niu et al., 2004). The study here further investigates properties of dopaminergic LOC inputs to the cochlea.

Immunostaining of whole-mount cochlear preparations from 1-3-month-old C57BL/6J mice showed patches of TH[+] terminal boutons along the base of the IHCs (similar to Darrow et al., 2006), separated by regions containing only TH[+] fiber bundles. Cross-comparison among cochleas obtained from different mice raised in an uncontrolled acoustic environment showed that these TH[+] 'terminal patches'; varied in length, number and location along the cochlear coil, with a slight preference towards the base. Several lines of evidence suggest that in addition to dopaminergic LOC shell neurons, a subset of the cholinergic LOC intrinsic neurons express TH, forming the terminal patches in the cochlea.

We hypothesized that differences in the sound environment contribute to the variability of the TH[+] LOC innervation pattern in individual mouse cochleas. To test this hypothesis, mice were raised in a low-noise vivarium, and noise exposed at 7-8 weeks of age (1-octave band centered at 12 kHz, ~110 dB, 2-hour exposure). The TH expression was assessed 7-10 days after the noise exposure. Compared to control littermates, mice after noise exposure showed an increased coverage by TH[+] LOC terminals in the cochlea, as well as an increased number of TH[+] LOC intrinsic neurons in the brainstem. Furthermore, a less damaging sound paradigm (1-octave band centered at 12 kHz, ~90 dB, 12-hour exposure for 5 days) also caused an increase in TH expression in the LOC intrinsic neurons one week post-exposure, which returns to control levels three weeks post-exposure.

In summary, TH expression in LOC intrinsic neurons can be dynamically regulated by acoustic experience in mice. These data suggest that upon noise exposure, dopamine is released from cholinergic LOC terminals in the cochlea, possibly to protect against excessive activity induced neuropathy. In vitro electrophysiology experiments are currently underway to characterize the effects of LOC neurotransmitters on ANF activity.

PS 705

Presynaptic voltage-gated Ca2+ channels differentially contribute to transmitter release at the mouse medial olivocochlear-outer hair cell synapse at two postnatal stages.

Lucas Vattino[1]; Ana Belén Elgoyhen[2]; Eleonora Katz[3]
[1]Instituto de Investigaciones en Ingeniería Genética y Biología Molecular (INGEBI-CONICET); [2]Instituto de Investigaciones en Ingeniería Genética y Biología Molecular (INGEBI-CONICET)/ Universidad de Buenos Aires, Facultad de Medicina, Instituto de Farmacología; [3]Instituto de Investigaciones en Ingeniería Genética y Biología Molecular (INGEBI-CONICET)/Universidad de Buenos Aires, Facultad de Ciencias Exactas y Naturales, Departamento de Fisiología, Biología Molecular y Celular

In mammals, outer hair cells (OHCs) of the organ of Corti undergo voltage-dependent changes in length and stiffness, a process known as electromotility. This amplifies movement of the basilar membrane, increasing the gain and tuning of acoustic inputs. OHC electromotility is regulated by descending medial olivocochlear (MOC) fibers. The MOC-OHC synapse is cholinergic and inhibitory and is mediated by the α9α10 cholinergic nicotinic receptor coupled to the activation of Ca2+-activated K+ channels that hyperpolarize the OHCs. During development, before reaching the OHCs, MOC fibers transiently innervate the inner hair cells (IHCs) (from birth to hearing onset, postnatal day (P)12 in mice). The ion channels coupled to transmitter release at the MOC-IHC synapse have been previously described (Zorrilla de San Martin et al., 2010), however, ion channels coupled to this process at the MOC-OHC synapse are unknown. By using whole-cell voltage-clamp recordings in OHCs while electrically stimulating the efferent axons in acutely isolated mouse cochleas we show that ACh release is mediated by both P/Q and R-type voltage-gated Ca2+ channels (VGCC) at P11-13 and by P/Q- and N-type VGCCs at P20-22. In addition, we show that at P11-13, large conductance Ca2+-activated K+ channels (BK) are functionally expressed at the MOC-OHC synapse as block by iberiotoxin (200 nM) significantly increases release (control 0.16±0.02; Ibtx 0.30±0.05, n=7; p<0.01). Interestingly, both the L-type VGCC antagonist nifedipine (3 μM) and the agonist BayK (10 μM) significantly increased release (control 0.19±0.06; Nife 0.30±0.07, n=6; p<0.05; Control 0.32±0.10; BayK 0.66±0.25, n=6, p<0.05). Occlusion experiments with iberiotoxin and BayK indicate that Ca2+ flowing in through L-type VGCC is both activating BK channels and partially supporting ACh release at P11-13. In addition, after loading the efferent terminals with EGTA-AM the contribution of L-type VGCC to release was completely abolished. At P20-22, however, BayK decreased release (control

0.47±0.16; BayK 0.22±0.07, n=6, p<0.05), indicating that Ca2+ influx through L-type VGCC is only activating BK channels at this stage. These results show that the VGCCs coupled to ACh release at the MOC-OHC synapse at P11-13 are the same as those at the MOC-IHC synapse at early stages (P4 to 7; Kearney et al., ARO Abstracts 2014), while at P20-22, they resemble those of the MOC-IHC synapse at P9-11 (Zorrilla de San Martin et al., 2010). These results suggest that the MOC-OHC synapse is still immature at the onset of hearing. Support: UBA& ANPCyT to EK and ABE

PS 706

Enhanced Hair Cell Postsynaptic Responses Alter Release from Presynaptic Efferent Neurons to Prolong Inhibition of the Cochlea

Carolina Wedemeyer[1]; Lucas Vattino[2]; Jimena Ballestero[1]; Stéphane F. Maison[3]; Mariano N. Di Guilmi[1]; Julian Taranda[1]; M. Charles Liberman[3]; Paul A. Fuchs[4]; Eleonora Katz[5]; Ana Belén Elgoyhen[6]
[1]*Instituto de Investigaciones en Ingeniería Genética y Biología Molecular (INGEBI/CONICET);* [2]*Instituto de Investigaciones en Ingeniería Genética y Biología Molecular (INGEBI-CONICET);* [3]*Harvard Medical School;* [4]*Department of Otolaryngology-Head and Neck Surgery, the Center for Hearing and Balance and the Center for Sensory Biology, Institute for Basic Biomedical Sciences;* [5]*Instituto de Investigaciones en Ingeniería Genética y Biología Molecular (INGEBI-CONICET)/Universidad de Buenos Aires, Facultad de Ciencias Exactas y Naturales, Departamento de Fisiología, Biología Molecular y Celular;* [6]*Instituto de Investigaciones en Ingeniería Genética y Biología Molecular (INGEBI-CONICET)/ Universidad de Buenos Aires, Facultad de Medicina, Instituto de Farmacología*

Gain control of the auditory system operates at multiple levels. Cholinergic medial olivocochlear (MOC) fibers that originate in the brainstem and make direct synaptic contacts at the base of the outer hair cells (OHCs) are the final targets of several feedback loops from both the periphery and higher processing centers. Efferent activation inhibits somatic electromotility of OHCs, an active amplification system within the mammalian cochlea. This is mediated by the activation of a calcium permeable α9α10 ionotropic cholinergic nicotinic receptor (nAChR) functionally coupled to calcium activated SK potassium channels. The strength of cochlear inhibition is driven by the rate of MOC activity and short term facilitation at the MOC-OHC synapse (Ballestero et al., 2011).The present work shows that a knockin mouse with a mutation in the α9α10 nAChR (L9';T) with increased channel gating (Taranda et al., 2009) greatly prolongs hair cell evoked inhibitory postsynaptic currents (IPSCs). Long-term presynaptic

compensatory mechanisms lead to reduced quantum content (IHC wt =1.29 ± 0.21; L9';T= 0.83 ± 0.12, n=5-6. OHC wt =0.23 ± 0.04, L9';T = 0.14 ± 0.02, n=12-15). However, upon high frequency stimulation of MOC-OHC synapses, L9';T mice exhibited more facilitation leading to greatly prolonged synaptic responses ($S_2/S_{1-\,40Hz}$: wt = 1.37 ± 0.16, L9';T = 3.47 ± 0.44, n = 6-8, p< 0.05). At the cochlear physiology level, these synaptic changes were matched by a longer time course of efferent MOC suppression of DPOAEs. Thus, the maximal suppressive effect of electrical shocks (70-s, 200 Hz) at the base of the IVth ventricle was doubled both at 16 (p < 0.01) and 22 kHz (p < 0.05), reached much more slowly (16 kHz: wt = 5.3 ± 1.0 s, L9';T = 30.8 ± 4.1 s; 22 kHz: wt = 1.5 ± 0.4 s, L9';T = 44.1 ± 3.1 s) and persisted for a longer time after the shocks for both 16 and 22 kHz in L9';T mice (> 5 min) as compared to their wt littermates (≤1 s). These results indicate that the properties of the MOC-OHC synapse directly determine the efficacy of the MOC feedback to the cochlea being a main player in the "gain control" of the auditory periphery.

PS 707

Immunohistochemical Identification of Human Spiral Ganglia Neurons: Implications in Sensorineural Hearing Loss and Cochlear Implantation

Janice E. Chang[1]; Ivan Lopez[2]; Seiji Hosokawa[3]; Kumiko Hosokawa[3]; Gail Ishiyama[4]; Fred Linthicum[1]; Akira Ishiyama[5]
[1]*UCLA Department of Head & Neck Surgery;* [2]*Department of Head & Neck Surgery, Geffen School of Medicine at UCLA;* [3]*Hamamatsu University Department of Otorhinolaryngology - Head & Neck Surgery;* [4]*UCLA Department of Neurology;* [5]*David Geffen School of Medicine, University of California, Los Angeles*

Background

Human spiral ganglia neurons (hSGNs) persist in the human cochlea after hair cell loss, in contrast to SGNs in the cochlea of animal models. We hypothesize that the persistent immunolocalization of structural and functional proteins in hSGNs suggest that they may be active, even in the absence of hair cells. Here we investigate the immunolocalization of three specific structural and functional proteins in hSGNs in normal aging and inner ear pathologies, and in patients who have undergone cochlear implantation.

Methods

Temporal bones from 38 patients (age: 8-89 years; n=11 normal hearing, n=27 hearing loss, n=7 received cochlear implants) were identified. Celloidin-embedded human cochleas were immunostained using mouse monoclonal antibodies against pan-neurofilaments, acetylated-tubu-

lin, and calbindin. Qualitative immunohistologic analysis was performed.

Results
Neurofilaments (NF) and acetylated tubulin (AT) were present in the hSGNs of normal aging and inner ear pathologies, and were persistent in both implanted and non-implanted ears despite the loss of hair cells. NF and AT were detected in the cytoplasm of the hSGNs, but not in satellite cells. NF and AT distribution was similar throughout the basal, middle, and apical turns of the cochlea including the organ of Corti. NF and AT were found in the hSGN in patients with several degrees of hearing loss and older age individuals. Calbindin staining in these specimens corroborated the above findings.

Conclusions
The persistence of NF, AT, and calbindin immunostaining in these hSGNs including implanted versus non-implanted ears suggests that they may be functional despite the absence of hair cells, supporting an important role in inner ear function. Immunoreactive patterns of these proteins in the human cochlea paralleled those in animal models. hSGNs immunoreactivity persisted in remaining spiral ganglia neurons despite cochlear implantation: the degree of hSGN survival was not clearly predictable from implanted versus non-implanted ears. The consistent and reliable detection of these neural markers in human temporal bone specimens implicate their use in investigating normal inner ear cytoarchitecure, and their changes with age, disease and cochlear implantation.

Support

PS 708

Characterization of Transgenic Mouse Models for Labeling Type I and Type II Afferent Neurons

Pankhuri Vyas[1]; Jingjing Sherry Wu[2]; Adrian Jiminez[3]; Elisabeth Glowatzki[2]; Paul A. Fuchs[4]
[1]*Johns Hopkins University School of Medicine, Department of Otolaryngology - Head and Neck Surgery;* [2]*Johns Hopkins School of Medicine, Department of Otolaryngology - Head and Neck Surgery;* [3]*Johns Hopkins University School of Medicine, Otolaryngology, Head and Neck Surgery;* [4]*Department of Otolaryngology-Head and Neck Surgery, the Center for Hearing and Balance and the Center for Sensory Biology, Institute for Basic Biomedical Sciences*

Background
The cochlea is innervated by type I and type II primary afferent neurons. Type I afferents are myelinated, larger diameter neurons that make a single dendritic synapse on one inner hair cell, whereas unmyelinated type II afferents are fewer in number and receive input from many outer hair cells. This strikingly differentiated innervation pattern strongly suggests specialized functions. However, lack of specific genetic markers for type I and type II fibers has been a roadblock in labeling and manipulating one without significantly affecting the other. In this study we sought to characterize and compare three mouse models and test if they can be used to label either type I or type II cochlear afferents to facilitate experimental studies of innervation, synaptogenesis and development of sensory innervation in the cochlea.

Methods
Whole-mount cochlear preparations were analyzed from recombinant mouse lines Slc6a4-GFP (a BAC transgenic mouse line expressing GFP under the SERT/ serotonin transporter promoter), Drd2-Cre (a BAC transgenic mouse expressing Cre under D2 dopamine receptor promoter); Rosa26$^{LSL-EYFP}$ (Ai3) and nNOS^{CreER} (neuronal nitric oxide synthase); Rosa26-$^{LSL-tdTomato-WPRE}$ (Ai9) at postnatal days 7, 15 and 30. Labeled spiral ganglion neurons (SGNs) were quantified and plotted along the cochlear length.

Results
Drd2-Cre; Ai3 mouse showed reporter (EYFP) expression in type II afferent neurons and a few apical medial olivocochlear (MOC) efferent fibers. Slc6a4-GFP mice labeled type II fibers. Double labeling with α3 Na/K ATPase, a molecular marker for type I afferents and medial efferents, confirmed that the labeled SGNs in these two mouse lines were type II and not type I afferent neurons. nNOS^{CreER}; Ai9 (tdTomato) mice labeled afferents fibers that form terminal boutons on inner hair cells only and provide robust labeling when induced with tamoxifen postnatally. Quantification of SGNs expressing fluorescent reporter proteins in these mouse models showed that Slc6a4- GFP is expressed preferentially in the apical SGNs. In contrast, SGNs labeled by Drd2-Cre; Ai3 are found most abundant at the cochlear base and abruptly end at the middle turn of the cochlea. nNOS^{CreER}; Ai9 mice robustly labeled type I afferents throughout the cochlear spiral.

Conclusions
In conjunction with the TH$^{2A-CreER}$ and CGRPα-EGFP lines reported previously, the mouse lines reported here contribute to a growing toolset for genetic manipulations of type I and type II cochlear afferent fibers.

Neural Contributions to the Summating Potential: Spiking and Dendritic Components

Brendan T. Lutz; Kendall A. Hutson; Stephen H. Pulver; Douglas C. Fitzpatrick
University of North Carolina

The summating potential (SP) is a major component of the cochlear response to sound measured at the round window (RW). To tones, the SP is a baseline shift reflecting the stimulus envelope. Contributions to SP from hair cells (both inner and outer) and from the auditory nerve have been described. To further dissect the neural contribution into those arising from action potentials vs. summed excitatory post-synaptic currents (EPSCs) across auditory nerve dendrites, we did a series of three recordings in each gerbil; first recordings were taken at the RW, then repeated after application of tetrodotoxin (TTX) and again after application of kainic acid (KA) to the RW. TTX blocks only the spiking component of the auditory nerve contribution, leaving the dendritic components active. Subsequent application of KA deactivates the entire nerve terminal. Subtracting these responses allowed each neural contribution to be determined. Two groups of gerbils were used: one had normal hearing (NH) at the start of the experiment, the other had outer hair cells selectively destroyed using IP injections of furosemide and kanamycin (FK). Cochleas were excised, dissected and imaged to count hair cells for determining the effectiveness of the FK. The spiking nerve component contributes to the SP with a positive polarity, while the contribution from the dendritic component was negative and highly adapting. Comparisons between NH and KF animals showed that the outer hair cells contribution was generally negative while that from inner hair cells was either positive or less negative than from the outers, depending on the frequency and/or intensity of the tone. Thus, there are four distinct contributions to a tone generated SP as recorded at the RW: two from hair cells, including both inner and outer, and two from the auditory nerve, including separate contributions from action potentials and EPSCs.

The Anatomical Organization and Maturation of the African Naked Mole-Rat (Heterocephalus glaber) Inner Ear

Catherine Barone[1]; Thomas Park[2]; Sonja Pyott[3]
[1]University of Illinois at Chicago; [2]Department of Biological Sciences, University of Illinois at Chicago, Chicago, IL, 60607, USA; [3]University Medical Center Groningen

Background
African naked mole-rats (Heterocephalus glaber) are eusocial rodents that live underground in narrow burrows. Although, naked mole-rats (NMRs) are functionally blind, they rely highly on acoustic communication. Nevertheless, likely because of their unique subterranean environment, NMRs have poor high frequency hearing and limited ability to localize sound compared to other rodents. We examined the maturation of the molecular and anatomical organization of the peripheral auditory system to investigate factors that contribute to their poor high frequency hearing and sound localization ability. This investigation comprised the quantification of IHC and OHC afferent ribbons, the polarization in the number of afferent ribbons per IHCs versus OHCs compared to other rodents as well as the expression of markers of auditory maturation.

Methods
Mid-apical turns of the organ of Corti were isolated from naked mole-rat cochleae and immunostained for confocal microscopy and image analysis using previously established methodology.

Results
Our anatomical and developmental characterization demonstrates that NMR inner and outer hair cells undergo a delayed peripheral maturation. NMR inner hair cells and outer hair cells undergo synaptic reorganization consistent with the developmental maturation patterns observed in other rodents including: pruning of supernumerary afferent ribbons and retraction of efferent terminals to the IHCs, although at older ages. Additionally, NMRs have comparatively fewer inner hair cell afferent ribbons and more outer hair cell afferent ribbons compared to other rodents. Moreover, at one year of age, NMRs fail to express ion channels associated with the fast and synchronous firing of auditory neurons. The lack of final maturation in the NMR inner ear may contribute to the reportedly poor high frequency hearing and sound localization ability.

Conclusion
Our findings provide essential comparative insight into the peripheral mechanisms required for high frequency hearing and sound localization.

Immunocytochemical, Electrophysiological and Electron Microscopical Comparison of Native and 3D-Cultured Cochlear Fibrocytes.

Anya H. Osborn; Douglas Caruana; Michael Evans; David Furness; Shanthini Mahendrasingam
Keele University

Fibrocyte degeneration in the cochlear lateral wall is one possible pathology of age-related metabolic hearing loss (presbyacusis). Fibrocytes play a role in potassium recycling and maintenance of the endocochlear potential. It has been proposed that a cell replacement therapy could prevent fibrocyte degeneration in the CD/1 mouse model of hearing loss (Mahendrasingam et al., 2011). One source of replacement cells is cultured spiral ligament fibrocytes as they do not require significant differentiation or development so may integrate into the cochlea better than stem cells. Fibrocytes cultured as monolayers or on 3-D collagen I gels were compared with fibrocytes in cochlear slices or micro-dissected spiral ligament from ~P7 cochlea of CD/1 mice using immunocytochemistry, electrophysiology, and electron microscopy. Fibrocytes successfully grown for short periods on a 3D collagen I matrix resembled the native appearance, having rounded cell bodies with processes extending from them, compared to a flatter morphology when grown in a monolayer. Immunofluorescence showed expression of aquaporin 1 (AQP1) which, in the cochlea, is confined to type III fibrocytes, and to a lesser extent for S-100 found in several fibrocyte types. The cells also expressed the inwardly-rectifying potassium channel Kir5.1, known to be present in native fibrocytes, the large conductance calcium activated potassium channel BK, as well as labelling for the gap junction proteins connexin 26 and 31. Finally, whole-cell voltage clamp recordings in both the cultured and putative native fibrocytes revealed outwardly- rectifying potassium currents on depolarisation from -50mV, and inward rectification on hyperpolarisation. There was also a large group of linear response recordings, and a subset showing both inward and outward-rectification. There was no significant difference in the resting membrane potentials between the native and cultured cells in any of the characteristic group recordings. Thus 3-D cultured fibrocytes show native-like morphology and appear to possess functional potassium channels. Further characterisation of this potassium current using targeted blockers and immunogold labelling of protein expression will performed. If successful this would provide evidence that these cells are suitable for transplantation into the lateral wall of the cochlea in a cell therapy to treat metabolic presbyacusis.

Mahendrasingam et al (2011).pdf

PS 712

Neurovascular Unit in the Cochlear Peripheral Nervous System

Han Jiang[1]; Xiaohan Wang[2]; Xiaorui Shi[3]
[1]Oregon Hearing Research Center, Oregon Health & Science University; [2]Oregon Hearing Research Center; [3]Oregon Hearing Research Center, Oregon Health & Sciences University.

Sound stimulation of the inner ear imposes an energy demand that requires rapid delivery of oxygen and glucose. A well-regulated cochlear blood flow is needed to meet this demand. In this study we employ transgenic fluorescence reporter mice (age range, postnatal day 7, 4 weeks, and 12 weeks) to investigate neurovascular structures in the cochlea. These structures in the regions of the spiral lamina and spiral ganglions were meticulously dissected. Under confocal fluorescence microscopy, we noticed that microvessels structurally interact with the spiral ganglion neuron (SGN) and their nerve fibers, forming a specialized 'Co-Neuro-Vas-Unit'. The Co-Neuro-Vas-Unit comprises perivascular resident macrophages (PVMs), mural vascular smooth muscle cells, pericytes (PCs), endothelial cells (ECs), PVMs, and neurons. The structural morphology of the unit is different in young and adult mice. A relatively dense and branched vascular network is seen in postnatal day 7 mice. Relatively less branching is seen in microvessels of adult mice (4 weeks and 120 weeks old). Most notably, PVMs undergo drastic changes in morphology. In younger animals, most PVMs exhibit a spherical or nodular shape, and some of them can be caught in the act of transmigrating from the circulation. In adult mice the majority of PVMs is elongated and display orientation parallel to the vessels. In addition, PCs display regional and functional heterogeneity. Vascular permeability had regional difference. Taken as a whole, the data indicate the Co-Neuro-Vas-Unit may be an intrinsic regulating mechanism for controlling blood flow to correspond with neuronal activity. The difference in the cellular structure within the Co-Neuro-Vas-Unit in young and old mice may correspond with hearing activity.

PS 713

Effects of Noise on Olivocochlear Innervation of the Cochlea

Dillan F. Villavisanis[1]; Katrina M. Schrode[1]; Omobalade Odedoyin[1]; Hamad A. Javaid[1]; Matthew A. Xu-Friedman[2]; Amanda M. Lauer[1]
[1]Johns Hopkins University School of Medicine, Department of Otolaryngology - Head and Neck Surgery, Center for Hearing and Balance; [2]University at Buffalo, Department of Biological Sciences

Background
Hair cells and afferent neurons in the organ of Corti are contacted by a network of efferent neurons that send information from the brain back to the cochlea to modulate afferent activity. The efferent (olivocochlear) system is comprised of the medial olivocochlear system (MOCS),

which innervates the outer hair cells (OHCs), and the lateral olivocochlear system (LOCS), which innervates the auditory nerve fibers contacting the inner hair cells (IHCs). We investigated the effects of exposure to acute loud noise and chronic environmental noise on olivocochlear synapses using an antibody to label synaptic vesicle protein 2 (sv2).

Methods
Mice were housed in moderate environmental acoustic conditions or under normal acoustic conditions. A subset of the latter group was exposed to damaging noise for two hours. Mouse cochleae were dissected into five or six flat half-turns and standard immunohistochemistry protocols were used to visualize hair cells (rabbit anti-myo6 and Alexa Fluor 568 Goat anti-Rabbit) and sv2-labeled synaptic vesicles (mouse anti-sv2 and Alexa Fluor 488 Goat anti-Mouse). Images of cochlear half-turns were taken at 10x magnification to identify frequency specific points at half-octave intervals using the Measure Line ImageJ plugin. Confocal images at specific frequencies were taken at 63x magnification by creating maximum intensity projections from z-stacks. Density of sv2 labeling from confocal images was quantified for each hair cell by counting each type of hair cell (IHCs and OHCs) and dividing by the total associated area of sv2 labeling. We also dissected and imaged cochleae from mice genetically labeled for choline acetyltransferase (ChAT), which is present in efferent neurons.

Results
There was no statistically significant difference between sv2 density for the MOCS between mice housed in moderate acoustic conditions and those housed in standard housing. However, a statistically significant increase was found in the mice housed under moderate acoustic conditions for the LOCS at high frequency regions. Mice exposed to damaging noise showed small increases in sv2 labeling at some frequencies for the MOCS and LOCS, and innervation by ChAT-labeled fibers was generally sparser.

Conclusions
The increase of sv2 density in LOC neurons in mice exposed to moderate noise compared to mice exposed to standard housing conditions suggests a protective upregulation of the efferent system against moderate, chronic noise exposure. The increase of sv2 density and decrease in ChAT fibers in the group exposed to damaging noise may demonstrate that the efferent system is susceptible to loud acoustic conditions.

PS 714

Impaired Recovery from Noise-induced Hearing Loss in a Type 2 Diabetes Animal Model

Alberto Arteaga[1]; David S. Sandlin[1]; Laura L. Beneke[1]; Kathleen T. Yee[1]; Douglas E. Vetter[1]; Fan Fan[2]; Richard J. Roman[2]; Wu Zhou[1]; Hong Zhu[1]
[1]University of Mississippi Medical Center; [2]The University of Mississippi Medical Center

Introduction
Approximately 29. 1 million Americans, 9. 3% of the population, have diabetes (CDC 2014), and approximately ten million Americans have noise-related hearing loss. A recent comprehensive report (Agrawal et al. 2009) indicates that diabetes is a risk factor for hearing loss in US adults. Several clinical studies have investigated the interaction between diabetes and NIHL, but conflicting findings have been reported (Ishii et al. 1992; Hodgson et al. 1987). In the present study, we examined the susceptibility and recovery to NIHL of T2DN rats, a new diabetic model that mimics human Type 2 diabetes mellitus. This normotensive model develops spontaneous diabetes with progressive diabetic nephropathy similar to humans.

Methods
Five 9-month-old T2DN rats and three age-matched Wistar control rats were involved in the study. Unrestrained, awake rats were placed in a subdivided cage on a rotatory floor directly below the horn of a calibrated speaker in a reverberant chamber. Octave band noise (8-16 kHz) at 103 dB SPL was continuously delivered for 2 hours. Under ketamine and xylazine anesthesia, auditory brainstem responses (ABR) were measured at 5. 6, 8, 11.3, 22.6, 32 and 45.25 kHz, at 3 different time points: pre-noise, 24 hours and 7 days following noise exposure. ABR thresholds were defined as the lowest intensity at which tone bursts generated a well-defined and reproducible wave I.

Results
ABR thresholds of T2DN and Wistar rats were significantly increased 24 hours after noise exposure at 11. 3, 22. 6, 32 and 45. 25 kHz. The thresholds of Wistar rats returned to pre-noise levels 7 days after the noise exposure in all frequencies except for 45. 25 kHz. ABR thresholds of T2DN rats remained significantly elevated 7 days after noise exposure at 11. 3, 22. 6 and 45. 25 kHz when compared to pre-noise thresholds values. The thresholds of T2DN rats remained elevated at 32 kHz after 7 days, but the difference did not reach statistically significant values when compared to pre-noise thresholds.

Conclusions

The results suggest that T2DN rats are more susceptible to NIHL compared to Wistar rats. Recovery from noise-induced temporary hearing loss appears to be impaired in T2DN rats. Ongoing studies, including assessment of distortion product otoacustic emissions, ABR wave I amplitude and afferent synaptopathy, will further elucidate the underlying mechanisms.

PS 715
Alterations of inner hair cell ribbon synapses in noise-induced hearing loss

Huihui Liu[1]; Jiawen Lu[1]; Xu Ding[1]; Lei Song[2]; Genglin Li[3]; Hao Wu[1]

[1]Department of Otolaryngology Head & Neck Surgery, The Ninth People's Hospital, Shanghai Jiao Tong University School of Medicine, Shanghai, China. Ear Institute, School of Medicine, Shanghai Jiao Tong University, Shanghai, China. Shanghai Key Laborato; [2]Department of Otolaryngology - Head & Neck Surgery, Shanghai Ninth People's Hospital; Ear Institute, Shanghai JiaoTong University School of Medicine; Shanghai Key Laboratory of Translational Medicine on Ear and Nose diseases, Shanghai, China; [3]Department of Otolaryngology Head & Neck Surgery, The Ninth People's Hospital, Shanghai Jiao Tong University School of Medicine, Shanghai, China. Ear Institute, School of Medicine, Shanghai Jiao Tong University.

Aim

Noise exposure is the most common cause of sensorineural hearing loss. The aim of this study was to characterize changes of ribbon synapses in inner hair cells following noise exposure.

Methods

The CBA/Ca mice were exposed to 2-20 kHz noise band at 98 dB sound pressure level for 2 h. Auditory brainstem response (ABR) was used to determine the hearing threshold in pre-exposure, 1d, 3d, 7d and 14d post-exposure animals. Whole-mount cochlea immunofluorescence staining was carried out to exam changes of ribbon synapses in inner hair cells.

Results

The hearing threshold rose one day after noise exposure and recovered fully fourteen days later. The Wave I amplitude of ABR was also reduced following noise exposure but did not recover. Confocal analysis of the whole-mount cochleae revealed that the number of inner hair cell remained unchanged but the number of ribbon synapses per hair cell was reduced.

Conclusion

These results suggest that the loss of ribbon synapses in inner hair cells may contribute to noise-induced hearing loss.

notch-based metrics, called bulge depths A and B and the notch index, were found in the literature. The fourth metric, called the slope adjusted notch depth (SAND), was a new notch-based metric that, unlike the previous three metrics, is unaffected by the bandwidth of the hearing loss within the noise-sensitive frequency region. This modification made the SAND more similar to commonly used discrete notch definitions than other continuous indicators. The moderation of age and hearing loss by noise was evaluated in 2627 participants from the 2011/2012 cycle of the National Health and Nutrition Examination Survey. All participants were categorized into three occupational exposure groups: 1) no exposure, 2) loud noise exposure, and 3) very loud noise exposure. We ran one moderation analyses per metric. T-values for the standardized differences among noise groups were also measured to compare the metrics. The overall models were significant (p < 0.05 with a Bonferroni correction) for five of the six metrics; bulge depth B was not significant. Noise groups significantly moderated the effect of age on hearing loss for the models with the same five metrics; therefore, age must be considered when evaluating the effects noise on hearing loss using one of these five metrics. T-values for the standardized differences between noise groups were highest for the SAND when groups 1 and 2 were compared across the lifespan, but not groups 1 and 3. From these results, we conclude that threshold and notch-based continuous metrics may be a useful metric for estimating the contribution of noise to hearing loss. More research is needed to determine if the SAND is more useful for estimating the effects of noise on hearing in individuals with low levels of exposure compared to previously used metrics of noise-induced hearing loss.

PS 716

Moderation of Age and Six Continuous Metrics of Hearing Loss by Noise Exposure

Charles Pudrith[1]; Jeffrey Labban[2]; Susan Phillips[2]; Vincent Henrich[2]
[1]*Northern Illinois University;* [2]*University of North Carolina at Greensboro*

Approximately 16% of the world';s hearing loss is caused by noise exposure. It is difficult to measure hearing loss specifically caused by noise in individuals, but improving efforts to estimate this loss will enhance clinical research in this area. The purpose of this study was to measure the moderation of age and hearing loss by noise exposure with audiograms analyzed with six different metrics of noise-induced hearing loss. Two of these metrics implemented simple threshold measurements while the other four used notch-based measurements to compare hearing loss within and outside of noise-sensitive frequency regions. Three of the four

PS 717

Mitochondrial Calcium Transporters Mediate Sensitivity to Noise-induced Hearing Loss and Cochlear Synapopathy

Suhua Sa; Hao Xiong; Haishan Long; Kayla Hill; **Su-Hua Sha**
Medical University of South Carolina

Research Background

Mitochondrial calcium has been postulated to regulate a wide range of processes involved in noise-induced hearing loss (NIHL), including bioenergetics and cell death. The mitochondrial calcium uniporter (MCU) is a major specific calcium channel for calcium uptake. Conversely, extrusion of calcium from mitochondria is mediated primarily by a mitochondrial sodium calcium exchanger, encoded by the NCLX gene. Both MCU and NCLX are localized in the mitochondrial inner membrane, where they regulate the mitochondrial calcium concentration and modulates intracellular calcium signaling. In this

study, we investigated mitochondrial regulation of cellular calcium via MCU and NCLX in noise-induced loss of hair cells and synaptic ribbons, and NIHL.

Methods
CBA/J mice at 12 weeks of age were exposed to an octave band noise with a frequency spectrum from 8 to 16 kHz for 2 h at 101 dB sound pressure level (SPL) to induce permanent threshold shifts (PTS) with loss of inner hair cell synaptic ribbons and outer hair cells or 108 dB SPL to induce more severe PTS with loss of both types of sensory hair cells assessed 2 weeks after the exposure. Auditory thresholds were measured by auditory brainstem response. Outer hair cell loss was quantified from surface preparations labeled with myosin VII and then stained with DAB. Cochlear surface preparations, cryosections, silencing techniques, and specific inhibitors were utilized in the study.

Results
Our results show that immunoreactivity of MCU increased in cochlear sensory hair cells, including outer and inner hair cells, some of spiral ganglion cells, and fibrocytes of spiral ligaments, while immunoreaction of NCLX decreased in sensory hair cells in a time-dependent and exposure-dependent manner after noise exposure. Inhibition of voltage-gated calcium channels via treatment with verapamil reversed noise-induced changes in CaMKKβ, MCU and NCLX in sensory hair cells and attenuated NIHL. Furthermore, inhibition of MCU activity via MCU siRNA silencing or the specific pharmacological inhibitor Ru360 attenuated noise-induced loss of sensory hair cells and synaptic ribbons, wave I amplitudes, and NIHL. This protection was afforded, at least in part, through reduced cleavage of caspase 9.

Conclusions
These results suggest that cellular calcium influx during noise exposure leads to mitochondrial calcium overload via MCU and NCLX. Mitochondrial calcium overload, in turn, initiates cell death pathways and subsequent loss of hair cells and synaptic connections resulting in NIHL.

Acknowledgements

PEGF-BB Signaling Promotes Cochlear Pericyte Protrusion and Migration in Response to Acoustic Trauma

Zhiqiang Hou[1]; **Xiaohan Wang**[2]; Cai Jing[3]; Jinghui Zhang[4]; Xiaorui Shi[5]
[1]Oregon Hearing Research Center, Department of Otolaryngology/Head & Neck Surgery, Oregon Health & Science University; [2]Oregon Hearing Research Center; [3]Oregon Hearing Research Center, Oregon Health & Science University; [4]Oregon Hearing Research Center, Oregon Health & Sciences University; [5]Oregon Hearing Research Center, Oregon Health & Sciences University.

Loud sound damages auditory sensory cells and has marked effects on microvasculature in the inner ear. Pericytes (PCs) in the stria vascularis are particularly vulnerable and sensitive to acoustic trauma. Exposure of mice to loud sound at a level of 120 dB for 3 hours per day for 2 consecutive days caused PCs to protrude and migrate from vessel walls. The PC migration was associated with increased expression of platelet-derived growth factor beta (PDGF-BB). Blockade of PDGF-BB signaling with either imatinib, a potent PDGF-BB receptor inhibitor, or APB5, a specific PDGFRβ blocker, significantly attenuated PC migration. The PDGF-BB-mediated PC protrusion and migration was further confirmed in multiple experimental models, including in an in vitro cell migration assay, ex vivo strial capillary-network model, and in vivo animal model. PC migration took one of two different forms, here denoted type I or type II. Type I migration is characterized by PCs with a prominent triangular shape and fine strand at the top, frequently connected to a neighboring vessel. Type II migration is characterized by PC detachment from vessels. We also found the event of PC migration was preferentially in the neighborhood of the activated macrophages and the sites of PC migration highly associated with regions of vascular leakage. The data suggests that targeting PC migration by blocking increased PDGF-BB activity could prevent edema and restore homeostasis in the acoustic traumatized ear.

Noise-induced Dysregulation of Quaking RNA Binding Proteins Contributes to Auditory Nerve Demyelination and Hearing Loss

Clarisse H. Panganiban[1]; Jeremy L. Barth[1]; Lama Darbelli[2]; Yazhi Xing[1]; Jianning Zhang[1]; Hui Li[1]; Kenyaria V. Noble[1]; Ting Liu[1]; LaShardai N. Brown[1]; Bradley A. Schulte[3]; Stephane Richard[2]; Hainan Lang[1]
[1]Medical University of South Carolina; [2]McGill University; [3]The Medical University of South Carolina

Background
Noise exposure can lead to auditory nerve (AN) degeneration and hearing deficiency, though the molecular mechanisms responsible for these biological consequences are not entirely understood. Most AN fibers and spiral ganglion neurons are ensheathed by myelinating glia that provide insulation and facilitate rapid transmission of nerve impulses from the cochlea to the brain. Here we show that noise exposure causes glial dysfunction leading to myelin abnormality and altered expression of numerous genes in the auditory nerve, including quaking (QKI), a gene implicated in regulating myelination.

Methods
Young-adult CBA/CaJ mice of either sex were exposed to 8-16 kHz octave-band noise at either 106 or 112dB SPL for 2 hours, and were paired with non-exposed controls. Auditory brainstem response tests were performed before, immediately after, and 1-, 3-, 7-, and 14- day(s) post-noise. Along with immunohistochemical and ultrastructural analyses, qPCR and microarray studies were performed on AN samples from these noise-exposed mice, as well as on AN samples from various age groups of postnatal CBA/CaJ mice. Lists of myelin-related and putative-QKI target genes to query on microarray datasets via dCHIP were compiled using the gene ontology database and previous publications. To analyze the effects of QKI deficiency on the AN structure and hearing function, young-adult QKI$^{FL/FL;PLPCreERT}$ mice were used with QKI$^{FL/FL;-}$ littermate controls.

Results
Noise-exposed ANs compared to controls showed increased demyelination and loss of node of Ranvier structural integrity, which contributed to significantly increased ABR wave I threshold and latency responses and decreased amplitudes. Microarray analyses with qPCR validation in noise-exposed ANs showed widespread expression changes in myelin-related genes, including the RNA splicing regulator QKI and numerous QKI target genes. Expression profiling of these myelin-related, QKI target genes responsive to noise showed that changes in their expression patterns post-noise largely did not recapitulate changes in their expression patterns during postnatal development. In QKI$^{FL/FL;PLPCreERT}$ mice, protein expression of QKI isoforms were ablated in AN glia, and extensive dysmyelination, disruption of paranodal structures, and hearing loss were seen compared to control mice.

Conclusions
Noise exposure rapidly affected myelinating glial cells, causing abnormal molecular and cellular consequences. Aberrations in myelin and declines in hearing function in QKI deficient auditory glia cells support QKI';s importance in normal ANs. Our findings implicate that QKI dysregulation is a critical early component in noise trauma, influencing cochlear glia function that leads to AN demyelination and, ultimately, hearing deficiency.

Comparison of Levels for Noise-Induced Hearing Loss in CBA Mice

Reza Amanipour[1]; Xiaoxia Zhu[2]; Guillaume Duvey[3]; Sylvain Celanire[3]; Joseph P. Walton[4]; Robert D. Frisina[1]
[1]Global Center for Hearing and Speech Research, University of South Florida- Tampa; [2]Global Center for Hearing & Speech Research, University of South Florida- Tampa; [3]Pragma Therapeutics; [4]Department of Communication Sciences & Disorders, and Chemical and Biomedical Engineering, Global Center of hearing and Speech Research, University of South Florida, Tampa, FL

Overexposure to intense sound can cause temporary or permanent threshold shift (TTS, PTS). In this study we investigated the functional changes occurring in the normal hearing ear following exposure to two different noise traumas. Mice were exposed for 45 minutes to an 8-16 kHz octave band of noise at the two levels: 116 dB SPL (N=4) and 110 dB SPL (N=8). Auditory brainstem responses (ABRs) from 6 to 36 kHz were recorded, and measured pre, and 1 day, 2, and 4 weeks post exposure, to measure TTS and PTS. Outer hair cell function was assessed using closed-system distortion product otoacoustic emissions (DPOAEs) which acquired both DP grams and DP thresholds. In addition, a gap-in-noise ABR paradigm (60 dB SPL markers with gap durations of 1-64 ms) was used to assess auditory temporal processing.

Significant threshold shifts of 40-65 dB were seen 1 day post-noise exposure (110 or 116 dB SPL). At 2 weeks post trauma, PTS for the 116 dB group exceeded the 110 dB mice, as this group made almost a full recovery at 4 weeks post exposure. ABR threshold shifts when evaluated at 24 hours, 2 weeks, and 4 weeks post ex-

posure in 110 and 116 dB SPL groups were, respectively: 45 and 65 dB (24h), 20 and 55 dB (2 weeks) and 15 and 60 dB (4 weeks). DPOAE amplitudes measured 2 weeks post-exposure showed recovery within 10 dB of the baseline in the 110 dB group at all frequencies, however the 116 dB exposure resulted in an average 30 dB threshold shift. At 4 weeks, DPOAE thresholds returned to baseline levels in the 110 dB group, whereas the 116 dB group still showed shifts of 30 dB. For Gap ABRs, there was a significant decrease in both noise burst 1 (NB1) and noise burst 2 (NB2) amplitudes for peaks 1 and 4, and an increase in NB1 and NB2';s P1 and P4 latencies in the 116 dB group relative to the 110 dB group. These results indicate that a 6 dB increase in noise intensity results in a significant increased ototrauma in both the peripheral and central auditory systems. Our increased understanding of the nature and extent of noise-induced hearing loss in different environments is critical for testing new medical interventions targeted to otoprotection from acoustic overexposure .

PS 721

Trial of Noise Induced Hearing Loss Model of Common Marmosets (Callithrix jacchus)

Tomohiko Yoshida[1]; Masato Fujioka[2]; Sho Kurihara[1]; Makoto Hosoya[2]; Hirotaka James Okano[3]; Kaoru Ogawa[4]; Hiromi Kojima[1]
[1]*Department of Otorhinolaryngology, Jikei University School of Medicine;* [2]*Department of Otolaryngology, Head and Neck Surgery, School of Medicine, Keio University;* [3]*Division of Regenerative Medicine, Jikei University School of Medicine;* [4]*Department of Otolaryngology, Head and Neck Surgery, Keio University School of Medicine*

Introduction
Common marmosets (Callithrix jacchus) is a New World monkey which is often used for behavioral analyses due to its verbal communication, and, in the auditory field, for investigating central pathway. In this study, we are trying to establish a well reproducible noise induced hearing loss model of common marmosets for future translational researches.

Methods
Three marmosets with normal hearing (2 to 9 years old, Japan CLEA) were used. Noise exposure experiments were performed under general anesthesia. For induction, the monkey inhaled isoflurane (3-5 %) and injected mixed anesthesia (medetomedine 0.04 mg/kg, midazol-

am 0.4 mg/kg, butorphanol 0.40 mg/kg). Afterward the marmosets were intubated and respiratory state was maintained by a ventilator. The animals were set into a soundproofed box with the noise exposure apparatus, RION AA-67N for sound generator, XLS1502 power-amp and PDBT35 (Pile Driver) speaker, providing 8 kHz- centered octave band noise. Heart rate, SpO2, rectal temperature, EtCO2 and isoflurane concentration in expiration were monitored. Two conditions were tried. First protocol: 124 dBSPL noise with a single speaker on the forehead for 3 hrs. Second protocol: 130 dBSPL noise with double speakers from both ears for 3 hrs.

ABR and DPOAE were measured before and after noise exposure. After sacrifice, we counted the number of hair cells by immunohistochemistry under confocal microscopy. Changes in verbal communication were also assessed by counting and classifying their speech. All experiments were approved by an institutional animal committee (2015-099) in accordance with NIH guideline.

Results
With the first protocol, one animal suffered permanently thresholds shift (PTS) in ABR until 1 month after exposure, whereas the other animal suffered temporal shifts. With the second protocol, animals suffered PTS in ABR with decrease in DPOAE level. No differences were observed between left and right ears. In the animal, the number of hair cells were reduced in noise exposed animals. Hair cell losses were observed in both IHCs and OHCs. Damages were larger in basal turn than in apical. Verbal communication was significantly decreased in the noise-exposed marmosets.

Conclusion
The second protocol, noise exposure with double speakers to each ear enables to induce more stable and profound permanent hearing loss than with a single from forehead. The damaged area was tonotopically corresponded to the deafned frequency defined by ABR and DPOAE. Furthermore, deafened marmoset was likely to be silent. Statistical analyses will be presented at the meeting.

PS 722

Ecologically Valid Blast Tube for Rodent Mild Traumatic Brain Injury Evaluation

Jackson Rossborough[1]; **James Parrish**[2]; Jianzhong Liu[3]; Laura Gomezllanos[4]; Curtis King[5]; Suhrud Rajguru[6]; Michael Hoffer[7]
[1]Department of Biomedical Engineering, University of Miami; [2]Department of Otolaryngology, University of Miami; [3]Depatment of Otolaryngology; [4]Department of Otolaryngology; [5]Lucent Medical Systems; [6]Department of Biomedical Engineering and Otolaryngology, University of Miami; [7]Department of Otolaryngology and Neurological Surgery, University of Miami

Background

Mild traumatic brain injury (mTBI) is a significant public health risk with an incidence of over 3 Million Cases per year in the United States alone. The disorder is associated with acute neurosensory sequelae as well as long-term consequences. In order to effectively study the neuropathology underlying these sequelae, as well as studying optimal treatment modalities, it is critically important that we have the availably of small rodent models that mirror the pathology and disorders seen in humans. In the present study, we discuss development and characterization of a blast tube and present preliminary results with novel therapeutic interventions to prevent or reduce the primary neurosensory sequelae of mTBI and mitigate potential chronic effects.

Methods

The tube design followed (Courtney 2012) with two coupled tubes. The driver section, which holds stoichiometric oxyacetylene fuel, is 26.7cm long with 16mm ID and 22 mm OD. The driver has an inlet port for the fuel along with an electric igniter coupled to one end. The driven section was 183cm long with 27mm ID and 34mm OD and has ports for pressure sensors that allow characterization of the impulse. A medical grade plastic film was used as a seal covering the open end of the driver section. The anesthetized animal is held in a wire cage at the long end driven section. A signal conditioner and data acquisition board along with two pressure sensors (PCB Piezoelectronics) controlled using custom LabView program were used to collect the data.

Results

Profiles of the blast wave were characterized at the opening of the tube and near the animal';s head. Using this data we were able to produce a traumatic brain injury in rats. The magnitude of this mild injury was evaluated with electrophysiolgic tests of hearing and balance function as well as behavior and cognitive effects.

Conclusions

A primary challenge in mTBI research remains the inherent disadvantages of the commonly used small rodent injury models. We present results from an ecologically valid blast tube to produce injuries that can account for the clinical features and complexity of human TBI. Preliminary results suggest the possibility of establishing preclinical efficacy of a novel treatment.

References

Courtney et al. Rev Sci Instrum. 2012 Apr;83(4):045111.

PS 723

The Noise Exposure Structure Interview (NESI): a Comprehensive Self-Report Measure of Cumulative Lifetime Noise Exposure

Hannah Guest[1]; Christopher J. Plack[2]; Kevin J. Munro[2]; **Deborah A. Hall**[3]; Rebecca S. Dewey[4]
[1]Manchester Centre for Audiology and Deafness, University of Manchester; [2]University of Manchester; [3]National Institute for Health Research Nottingham Biomedical Research Centre; [4]University of Nottingham

Background and Purpose

Research into noise-induced hearing damage has proliferated in recent years, much of it relying on retrospective self-report measures of noise exposure. Such measures employ a variety of self-report procedures, many of which may not be well-equipped to elicit full and accurate reporting of noise exposure over the lifespan. Existing questionnaires tend to impose constraints on the types of noise exposures considered and on the reporting of changing exposure patterns over time. Methods for consistently estimating sound level and attenuation by hearing protective equipment also tend to be lacking.

The Noise Exposure Structured Interview (NESI) is intended to provide a relatively comprehensive measure of cumulative lifetime noise exposure. Its procedures are designed to be clear, easy to learn, and not unduly time-consuming for the practitioner.

Concept

The output of the interview is an estimate of the energy of total lifetime exposure to high sound levels, based on exposure duration, sound level, and use of hearing protection. Since noise exposure habits are unique to each individual and vary across the lifespan, the NESI adopts a flexible, mnemonic approach, breaking down an individual';s history into multiple exposure activities and life periods. Within each life period, standardised methods are applied in the estimation of sound level, duration, and usage and attenuation of hearing protection.

Methods

The interview procedure is characterized by the following key components: (a) identification of exposure activities; (b) segmentation of the lifespan; (c) estimation of exposure duration; (d) estimation of exposure level; (e) consideration of hearing protection; (f) quantification of firearm noise exposure; and (g) calculation of noise units.

Rationales for the above methods are outlined, along with practical information such as typical duration of interview and interviewer training needs.

Evaluation

Piloting of the NESI and closely related measures has provided useful indications regarding potential benefits and pitfalls, evident in the characteristics of the pilot data and in feedback from pilot users. Validation data are available for one key component of the NESI – a method for estimating sound level – and we propose means by which more extensive validation might be conducted.

Funding

PS 724

Fate of Cochlear Macrophages After Acute Inflammatory Response to Acoustic Stress

Bo Hua Hu; Celia Zhang; Mitchell Frye
University at Buffalo

Background

The inflammatory response is a major stress response of the cochlea that has been linked to diverse cochlear pathological conditions. Acute inflammatory activity is characterized by massive infiltration of circulating monocytes into the cochlea. These cells transform into macrophages and participate in the inflammatory response to stress. At the present, it is not clear how inflammatory immune cells are eliminated from the cochlea during the resolution phase of inflammation. Here, we report apoptotic death as a route of macrophage removal from the cochlea.

Methods

An intense broadband noise at 120 dB SPL for 1 hour was used to provoke the infiltration of monocytes into the cochlea in young C57BL/6J mice. Cochleae were collected at multiple time points after acoustic overstimulation to define macrophage dynamics. Macrophages were identified with a combination of two macrophage specific markers (F4/80 and Iba1) and one leukocyte marker (CD45). Cell death was determined based on the integrity of the cell membrane assessed by Trypan blue and propidium iodide ex vivo staining, the nuclear and cell body morphology examined by confocal and scanning electron microscopy, and the activation of death signaling including caspase-3 activation and Bax expression. Finally, the clearance of macrophage debris was assessed.

Results

Acoustic overstimulation provoked a massive infiltration of macrophages, starting at 1 day, culminating at 4 days, and then decreasing at 10 days, after noise exposure. Examining macrophages at 6 and 8 days after noise exposure revealed degenerative phenotypes, which included a decrease in the expression of macrophage marker proteins, cell body disintegration, and nuclear fragmentation. These degenerative macrophages were found in multiple cochlear partitions including the spiral ligament, scala tympani and neural regions, all of which are the major sites of monocyte infiltration. At the early stage, these cells maintained their membrane integrity. However, an increase in caspase-3 activity and Bax immunoreactivity was found, suggesting the involvement of the apoptotic pathway. At the final stage of cell death, macrophage debris were formed. While macrophage engulfment of these debris was found, many of the debris were scattered in places and no macrophages were found in the immediacy vicinity, suggesting that macrophage phagocytosis is not sufficient for a timely clearance of macrophage debris.

Conclusions

Local death is a biological mechanism for macrophage removal during the resolution phage of inflammation. This process leads to the formation of cell debris that could cause additional stress to the cochlea after acute damage.

PS 725

Preconditioning Noise Alters Immune Reaction to Subsequent Acoustic Overstimulation in the Cochlea

Celia Zhang[1]; Mitchell Frye[1]; Wei Sun[2]; Bo Hua Hu[1]
[1]University at Buffalo; [2]State University of New York at Buffalo

Introduction

Acoustic overstimulation is a common cause of hearing loss. Individuals who suffer from one episode of acoustic trauma are likely to sustain another episode of stress. The initial noise induces pathophysiological changes that are known to affect cochlear responses to subsequent stress. However, the biological details of such in-

fluence is not clear. We previously demonstrated that acoustic overstimulation alters cochlear immune environment. Here, we report that such change can exert a prolonged influence on immune cell response to subsequent damage.

Methods

A broadband noise at 120 dB SPL for 1 h was used to induce initial and repeated damage to C57BL/6J mice. Cochleae for the noise-control group were collected at 2 or 20 days after the initial noise treatment. Cochleae for the preconditioned group, which received a second noise exposure 20 days after the initial noise treatment, were collected 2 days after the 2nd noise. Cochlear macrophages were identified with immunolabeling of macrophage marker proteins, and macrophage numbers and sizes were quantified. Immunostaining of MHC II and Ccl2 was performed to examine the immune activity of macrophages. Scanning electron microscopy (SEM) was used to determine macrophage surface morphology. Transcriptional expression of a group of immune molecules with different functions were examined to determine the inflammatory activity of the cochleae.

Results

Exposure to the intense noise caused threshold shifts and sensory cell loss. This noise induced a marked increase in the number and size of basilar membrane macrophages as well as in the macrophage expression of pro-inflammatory molecules. At 20 days after initial damage, the number of macrophages reduced, but did not returned to the pre-noise level. A portion of macrophages maintained their enlarged morphology and MHC-II positive cells increased. These results suggest the persistence of immune activities. The repeated noise again caused an increase in the number and size of macrophages at 2 days post-noise. The level of the number increase was significantly higher than that observed after the initial damage. However, the numbers of monocytes, which reflect the level of newly-infiltrating cells, did not differ between the two groups, which was confirmed morphologically by SEM. Surprisingly, cochlear expression of inflammatory molecules was either lower or remained the same as compared with that observed after exposure to the initial noise.

Conclusions

A prior history of acoustic injury enhances macrophage reaction to subsequent acoustic overstimulation, but does not potentiate the production of inflammatory molecules in the cochlea.

PS 726

Progressive Hearing Damage after Exposure to Multiple Blasts in Chinchillas

Tao Chen; Kyle Smith; Rong Z. Gan
University of Oklahoma

Introduction

Hearing damage caused by blast waves is a frequent and common injury for Service members. A significant fraction of veterans suffers from long-term hearing disabilities. However, the extent of hearing loss or permanent hearing damage in relation to the number of blasts and the time interval between each blast has not been investigated. In this paper, we report our recent study in chinchillas to evaluate the middle ear function, hearing threshold, and cochlear response during the time course of hearing damage. Our goal is to determine whether multiple exposures to blast waves is the cause of progressive hearing damage and to evaluate the protective mechanism of hearing protection devices (e.g. earplug) for multiple exposures.

Methods

Two groups of chinchillas (N=10 each) were used in this study. One ear was left open and another ear was protected with an earplug. Animals in Group 1 and 2 were tested at low blast overpressure (3-5 psi) and the mild blast overpressure (12-15 psi), respectively. The animals were blasted twice on Day 1 with one hour interval between blasts. Before the first and after each blast, the cochlea and middle ear functions were measured using ABR, DPOAE, and wideband tympanometry. Animals recovered until Day 7, and their hearing functions were measured on Day 4 and Day 7, respectively.

Results and Discussion

In Group 1, for open ears, hearing damage accumulated after the first and second blast was observed by the ABR and DPOAE shifts. For protected ears, hearing damage after each blast was still accumulated, but at a much low level. On Day 4, there was some improvement in both ears. On Day 7 the protected ears fully recovered and the open ears almost recovered. In Group 2, the hearing damage after each blast was greater than that of Group 1. On Day 4 there was slight improvement in hearing and on Day 7 the hearing was further improved.

Conclusion

Multiple blast exposures can aggravate hearing loss. ABR thresholds were significantly elevated and DPOAE levels were largely reduced after the first and second blast. The ABR threshold and DPOAE level shift values were reduced in protected ears, especially at low frequencies. The difference of the hearing level restored in

the protected ears from that of the open ears shows the significance of hearing protection and recovery process. (Supported by DOD W81XWH-14-1-0228)

PS 727

SEM Imaging of Cochlear Hair Cell Damage Caused by Blast Exposure

Marcus Brown; Tao Chen; Rong Z. Gan
University of Oklahoma

Introduction

Exposure to blast overpressure (BOP) causes hearing loss by applying intense sound pressure to the ear, which can rupture the tympanic membrane and reduce the number of viable cochlear hair cells. While damaged hair cells can self-repair, studies have shown that stereocilia of mammalian hair cells do not easily self-repair or regenerate after experiencing acoustic trauma, which can lead to prolonged hearing loss (S. Jia et al., 2009). Scanning electron microscopy (SEM) has been used as a powerful tool to image hair cell damage induced by noise exposure. However, there is a lack of reports on the hair cell damage caused at different BOP levels, and how the BOP exposure relates to the damage variation from the basal turn to the apex of the cochlea. In this study, we utilized SEM to observe the damage to chinchilla';s hair cell stereocilia after the animal was exposed to one of three BOP levels ranging from below mild traumatic brain injury (TBI), mild and moderate TBI levels. We aim to understand the extent of auditory injury at different TBI levels and the resulting degree of cochlear hair cell damage.

Materials and Methods

Four groups of chinchillas (two for each) were used in this study with one group as control and three groups being exposed to blast (one ear plugged) at three BOP levels: 1.2–3.6 psi, 6–9 psi, and 22–35 psi. The animal was euthanized after the exposure and the cochlea was immediately harvested. The cochlea sample was then fixated overnight in 4% paraformaldehyde with 0.1M phosphate buffer saline (PBS) solution containing 5% sucrose, decalcified with 0.5M ethylenediaminetetraacetic acid in PBS for seven days, and microdissected for a post-fixation with 1% OsO_4 for 30 min. Samples were then dehydrated in ethanol, critical point dried with CO_2, sputter coated with gold/palladium, and examined with an electron microscope.

Results and Discussion

Results from SEM images showed that stereocilia of the outer hair cells were significantly damaged from the blast waves experienced. Most of the damage was observed in the basal turn of the cochlea. Higher BOP levels showed an increased disruption and damage to the stereocilia (Figure 1). The damage observed in cochlear hair cells was in agreement with the hearing function tests in chinchillas that were exposed to the same BOP levels. (Supported by DOD W81XWH-14-1-0228)
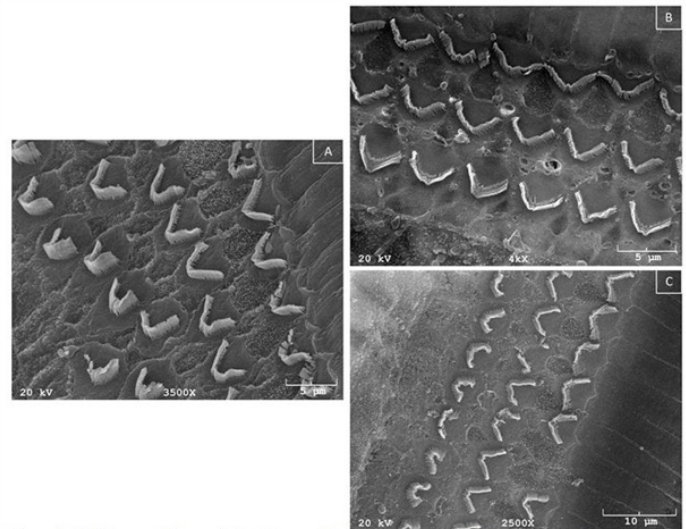
Figure 1: SEM images of the outer hair cells' stereocilia in the basal turn after blast exposure. The lowest pressure range of 1.8–3.6 psi (A) exhibited the least amount of damage and disturbance to the stereocilia bundles. The middle pressure range of 6–9 psi (B) showed an increase of damage while the highest pressure range of 22–35 psi (C) had the highest amount of damage to the stereocilia.

PS 728

Calpastatin Overexpression Ameliorates Permanent Noise-Induced Hearing Loss

Mary J. Freeman[1]; Mike Grossheim[1]; A. Catalina Velez-Ortega[1]; Kathryn E. Saatman[2]; Gregory I. Frolenkov[1]
[1]*Department of Physiology, University of Kentucky;*
[2]*Spinal Cord and Brain Injury Research Center, University of Kentucky*

Substantial damage to the actin core of stereocilia in auditory hair cells is a known feature of permanent hearing loss following acoustic trauma (Liberman 1987). Though the mechanisms of this disassembly of the actin core are unknown, elevated intracellular Ca2+ after acoustic stimulation may activate calpains, calcium-dependent cysteine proteases known to be involved in considerable cytoskeletal reorganization in many pathological conditions. Therefore, in this study, we explored calpain inhibition as a potential method to lessen the progression of actin core damage and protect against permanent noise-induced hearing loss. Given conventional calpains are endogenously inhibited by the protein calpastatin, we used a novel transgenic mouse that expresses human calpastatin (hCAST) under the ubiquitously expressed mouse prion protein promoter (Schoch et al. 2013) to explore the effects of calpastatin overexpression on susceptibility to noise-induced hearing loss. We utilized auditory brainstem responses to measure the hearing thresholds of hCAST/+ transgenic mice and their wild type littermates before and after ex-

posure to damaging noise (wide band 100 dB SPL for 30 minutes). We found that hCAST overexpression did not influence baseline hearing sensitivity or the noise-induced temporary threshold shift. However, the progression to permanent threshold shift was significantly attenuated in hCAST/+ mice as compared to their wild type littermates. These results suggest that calpain inhibition by endogenous calpastatin may be a viable approach to encourage stereocilia repair and provide protection against permanent noise-induced hearing loss. Supported by NIH (R01DC014658 to G.I.F.)

Middle Ear Modeling & Diagnostics

PS 729

Quasi-static and dynamic modelling of the incudostapedial joint

Majid Soleimani[1]; W. Robert J. Funnell[2]; Willem F. Decraemer[3]
[1]Department of BioMedical Engineering, McGill University; [2]Departments of BioMedical Engineering and Otolaryngology - Head & Neck Surgery, McGill University; [3]Department of Biomedical Physics, University of Antwerp

The mechanical properties and the geometries of the articulations of the ossicles are always simplified when modelling middle-ear mechanics. This can lead to inaccurate results, perhaps especially at high values of either acoustical pressure or static pressure. We have previously presented finite-element models of the incudostapedial joint with (1) a very simple geometry to compare the flexibility of the pedicle and the incudostapedial joint (2005); and (2) geometries based on histological serial sections and X-ray microCT scans, with plausible estimates for material-property parameters (2015). Preliminary simulations were compared with experimental tension and compression measurements. Later (2016 & 2017) we presented an analytical model of the joint with a simplified geometry using the theory of large deformations of elastic membranes to model the joint capsule. Results indicated that the mechanical behaviour of the incudostapedial joint may be influenced by mechanical instabilities of the joint capsule. We have also presented (2017) an improved finite-element model that includes the synovial fluid, capsule, cartilage layers and bones. We performed a sensitivity analysis to determine the effects of varying capsule length, thickness and curvature; synovial-fluid volume; and joint cross-sectional shape. In this work, we modify our model to fit the non-linear stress-strain simulations, with and without consideration of inertial and viscoelastic effects, to experimental data from the literature. We also simulate a relaxation test and show agreement with the experimental data. The results are beneficial in understanding the experimental

observations and in analyzing the effects of inertia and viscoelasticity on the mechanics of the ossicular chain.

PS 730

A comprehensive biomechanical model of the human stapes with 3D cochlear input impedance

Ivo Dobrev[1]; Merlin Schär[2]; Flurin Pfiffner[1]; Lukas Prochazka[1]; Christof Röösli[1]; Alexander Huber[1]; **Jae Hoon Sim**[2]
[1]University of Zurich, University Hospital Zurich, Department of Otorhinolaryngology, Head and Neck Surgery, Switzerland; [2]University Hospital Zurich

Background

The stapes, as the last part of the middle ear, transfers mechanical vibration of the middle-ear ossicular chain to the cochlea. In surgical reconstructions, such as ossiculoplasty and direct stimulation on the stapes using a floating mass transducer, the stapes interfaces to a prosthesis. Therefore, an exact and comprehensive model of the human stapes is desirable to predict the surgical outcomes in the reconstructed ears as well as effective stimuli to the cochlea in normal ears.

Methods

The inertial properties and dimensions/shape of the human stapes were obtained from its micro-CT images. The variation of the thickness (thickness map) of the annular ligament along the footplate boundary was obtained from the micro-CT images as well. The stapes was modeled as a rigid body with the obtained inertial properties and dimensions/shape, and the annular ligament was modeled as distribution of 120 beams with the thickness map considered. The mechanical properties of the annular ligament was obtained from measurements with quasi-static excitation on the isolated stapes. The inner-ear loads on the stapes footplate were added for the two rocking-like motions (along the long and short axes of the footplate) as well as the piston-like motion of the stapes footplate. To obtain the inner-ear loads on its spatial motions, the stapes was mechanically driven such that a specific motion component is emphasized, and fluid pressure change in the Scala Vestibule of the cochlea, at a distance of 1-2 mm medially from the footplate, was measured using a custom-made hydrophone.

Results

Without the inner-ear load, motion of the stapes footplate in the model simulation has smaller rocking-like components than physiological motion of the stapes footplate in literatures. The inner-ear load for the piston-like motion was generally larger than the inner-ear loads for the rocking-like motions, but the inner-ear loads for the rocking-like motions, which have been neglected in many

mechanical models of the stapes, were not negligible. The inner-ear loads tended to increase with frequency, resulting in large inner loads for the piston-like motion at high frequencies.

Conclusions

A comprehensive biomechanical model of human stapes was established based on exact anatomy and measurement of three-dimensional cochlear input impedance. The complex spatial motion of the stapes at high frequencies is presumed to be due to the increased inner-ear loads in combination with asymmetric features of the stapes. The model is expected to be used to predict functional outcomes of surgical middle-ear reconstruction.

PS 731

Modeling the Middle Ear Dynamics that Results from Exposure to High Intensity Impulsive Noise

Tim Walilko[1]; Jim Easter[2]; John Peacock[3]; Ted Walilko[1]; Daniel J. Tollin[4]
[1]Applied Research Associates, Inc; [2]Cochlear Boulder LLC; [3]University of Colorado School of Medicine; [4]Department of Physiology and Biophysics, University of Colorado School of Medicine

Background

In a combat environment, damage to the auditory system is typically a result of exposure to high intensity impulsive pressure waves generated by an explosive device, shoulder launched rocket, mortar round, and/or weapons fire. Numerical models have been developed to predict the potential for hearing damage, but the models have typically only been validated for exposure levels less than 140 decibels (dB) sound pressure level (SPL) using animal surrogate and/or limited human volunteer data. The objective of this paper is to quantify the motion of the stapes at high intensity noise levels (blast overpressure > 170 dB SPL) to improve a model';s performance at high intensity levels typically observed in the military combat and training environments.

Methods

To extend and validate the performance of hearing protection in the Auditory Hazard Assessment Algorithm for Humans (AHAAH) at high intensity blast levels, biological response data were collected from ten sets of instrumented post mortem human temporal bones. The experimental data collected were used to adjust the AHAAH middle ear elements, modifying the linear elements to include a nonlinear stapedial annular ligament element (SAL). The result of this addition was better prediction of stapes response to blast overpressure and energy transmission from the free field to the sensitive hair cells within the cochlea.

Results

The existing AHAAH model assumes a maximum stapes displacement of approximately 20 µm. Experimental data collected show that the actual displacement is on the order of 200 µm for acoustic pressures of approximately 170 dB SPL. Additionally, experimental results show that the scala vestibuli pressures varied nonlinearly with stapes displacements and cochlear impedance changed with frequency. These observed characteristics of the SAL have been built into the model, improving injury predictions of the model at these high SPLs. These changes to AHAAH have extended the accurate prediction of stapes displacement to SPLs greater than 140 dB SPL.

Conclusion

The measured displacement of the stapes has been used to improve the capability of the AHAAH model to predict human auditory system injury. This effort improves auditory hazard models for blast intensities to better assess auditory protective systems for the military environment and to inform the development of improved therapeutic strategies.

PS 732

Modeling and Analysis of the Human Middle Ear Dynamics using Multi-body Simulations

Diego Calero; Lucas Lobato; Lucas Bonomo; Stephan Paul; **Julio A. Cordioli**
Federal University of Santa Catarina - UFSC

The dynamics of the human middle ear has been studied in the past using several computational and experimental approaches in order to observe the effect on the hearing of different conditions, such as conductive diseases, corrective surgeries or implantation of middle ear prosthesis. Although finite element (FE) models have been widely used, they may imply large computational costs or require a high level of details. On the other hand, typical lumped parameter (LP) models are a usually a rather coarse representation and only 1-D vibration is analyzed. As alternative, multi-body (MB) models combine the analysis of flexible structures with rigid body dynamics, involving fewer degrees of freedom than FE models but with a more detail description of the system dynamics. This study describes the reduction of a FE model of the human middle ear to a multi-body model and compares the results obtained considering different levels of model simplification. The following sequence of MB models is considered: (i) all elements as flexible; (ii) ossicles assumed as rigid; (iii) ligaments and tendons described as lumped spring-damper elements; (iv) joints represented as kinematic joints with limited degrees-of-freedom (DOF); and (v) all simplifications implemented together. All models are compared by means

of the frequency response of stapes velocity vs. sound pressure at the tympanic membrane. By applying the elastic MB formulation, a difference of 2 dB mainly up to 1 kHz is observed when compared with the FE model. Comparing the results for flexible and the partially rigid MB models a similar discrepancy is also also observed, but the first two modal shapes are preserved. The representation of ligaments and tendons as lumped parameter allow the direct analysis of the impact of these elements dynamic properties, in special their stiffness. In this sense, the increase of stiffness in most of the ligaments and tendons involves a decay in response until 2 kHz. The stiffening of the annular ligament of the stapes footplate has a much larger reduction in response in a 1 - 10 kHz range. If only the piston-like motion is considered for the staples footplate (a typical assumption in LP models), the response is reduced in almost 6 dB until 2 kHz, also modifying the vibrational modes. This indicates that the rotational DOF around the axes within the plane of the stapes footplate must be considered. Flexibility in the translational and rotational DOF in the incudomalleolar and the incudostapedial joints have to be studied, because they adapt the complex motion of the tympanic membrane to the ossicles towards a larger motion of the stapes in the piston-like direction.
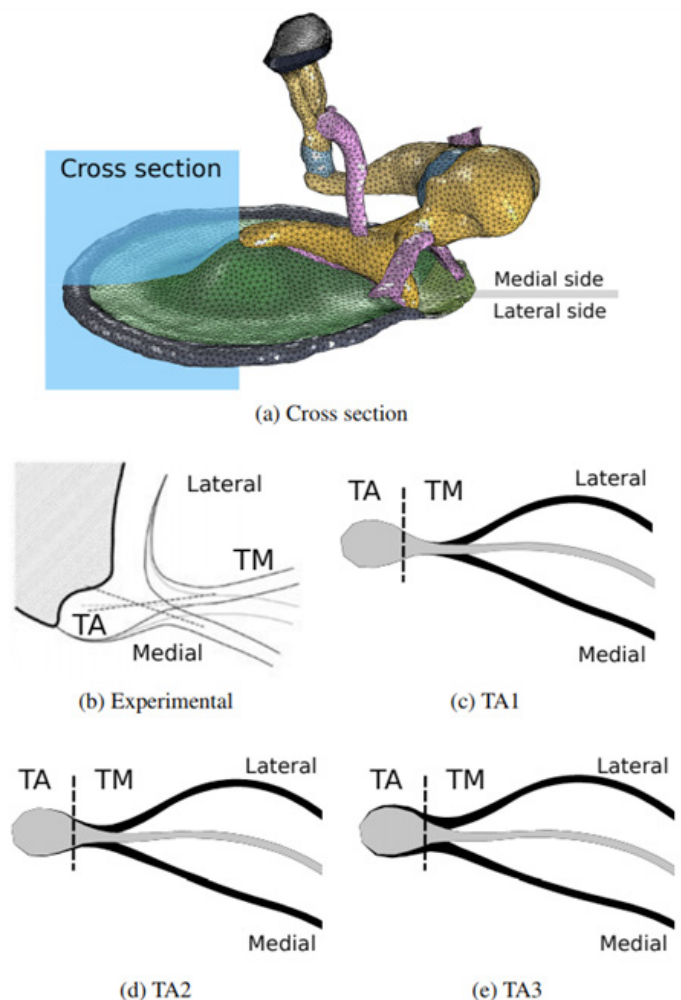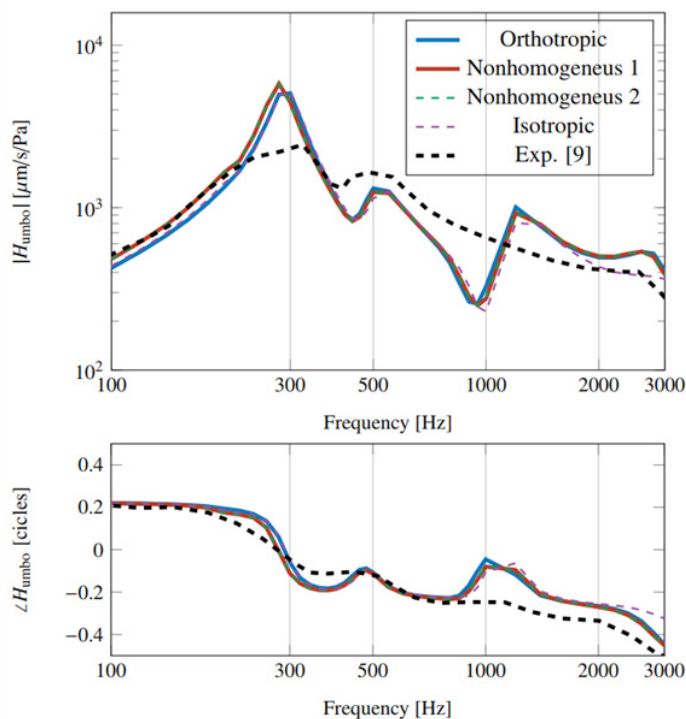
PS 733

On Material Models and Boundary Conditions in Finite Element Modeling of the Human Tympanic Membrane

Lucas Lobato; Stephan Paul; **Julio A. Cordioli**
Federal University of Santa Catarina - UFSC

The human tympanic membrane is known to be a complex tissue made of different collagen fiber layers, and it is attached to a bony sulcus in the ear canal wall by means of the tympanic annulus. Numerical models of the tympanic membrane dynamics are still an important research topic as experimental data on mechanical properties of the tympanic membrane are quite sparse. In this work, an assessment of variations in the outcome of tympanic membrane Finite Element (FE) models is done in the light of different mathematical models for material properties and different boundary conditions. The influence of three distinct boundary conditions is evaluated under static loads, comparing the numerical results for static deformation of the tympanic membrane edge to experimental data. Results show that a non-fully clamped condition of the tympanic annulus better reproduces the experimental result. Regarding mathematical models for certain material characteristics, four different models were evaluated: isotropic, orthotropic and two orthotropic nonhomogeneous models. In addition, elastic and viscoelastic models of the tympanic membrane were also analyzed, being the latter one backed by experimental data. Comparisons were based on the Frequency response function (FRF) that relates umbo velocity and sound pressure at the tympanic membrane surface, and no considerable different were found in magnitude or phase regarding the assumption of isotropy and homogeneity within the FE models. However, differences in magnitude and phase between numerical results and experimental data were found and described. The differences observed in the FRF are clearly caused by underestimating the internal damping of the system. Furthermore, within the dynamic analysis, those four FE models were also compared by means of the displacement field within the tympanic membrane surface at a single frequency. As already seen for the frequency responses, no relevant differences among the FE models were found for the displacement field when considering isotropic and orthotropic models or homogeneous and nonhomogeneous tympanic membrane models. On the other hand, linear elastic and viscoelastic models of the tympanic membrane resulted in considerable differences, both in frequency response and tympanic membrane displacement.

(a) Cross section

(b) Experimental

(c) TA1

(d) TA2

(e) TA3

ded sample was performed before slicing it by a hole saw. The thickness of the slices (98) was 30 μm with a distance of 340 μm between the slices. The slices were stained with methylene blue and alizarin red for optimal tissue differentiation, followed by digitization, and segmentation of the epithelial lining of ET lumen, cartilage, muscle, bone, and fat. As a last step the slices and segmentations were stacked based on the cannulas positions, yielding histologic 3D-models of the ET using 3DSlicer. These were fused with the DICOM-dataset of the CBCT.

Results
The histologic and radiologic 3D-datasets were successfully fused and reinforced. With the segmented compartments, a quantitative analysis of the distinctive topographic microanatomy regarding relational aspects and functional interactions was determined. Amongst other findings was a spiraled conformation of the long medial crura of ET cartilage in combination with the oblique orientation of the levator veli palatine muscle.

Conclusion
A method was established that enables the generation of a high resolution 3D-model of the ET, confirmed by fusion with a CBCT scan data. This model provides a wide spectrum of image information from the microscopic cellular level, to the functional anatomy of the ET and offers additional insight into the mechanism of ET opening.

PS 734

3D-Modelling of the Eustachian Tube - Elemental Functional Aspects

Robert Schuon[1]; Josef Schwarzensteiner[1]; Thomas Lenarz[2]; Gerrit Paasche[3]; Samuel John[1]
[1]*Department of Otolaryngology, Hannover Medical School, Germany;* [2]*Department of Otolaryngology, Hannover Medical School, Germany and DFG Cluster of Excellence Hearing4all;* [3]*Department of Otolaryngology, Hannover Medical School, Germany; Cluster of Excellence*

PS 735

Dimension and Position of the Eustachian Tube within Patients

Ida Janzen-Senn[1]; Robert Schuon[1]; Frank Tavassol[2]; Thomas Lenarz[3]; **Gerrit Paasche**[4]
[1]*Department of Otolaryngology, Hannover Medical School, Germany;* [2]*Cranio-Maxillo-Facial Surgery - Hannover Medical School;* [3]*Department of Otolaryngology, Hannover Medical School, Germany and DFG Cluster of Excellence Hearing4all;* [4]*Department of Otolaryngology, Hannover Medical School, Germany; Cluster of Excellence*

Introduction
Balloon catheter dilatation of the ET (BET) is an established procedure. There is evidence of a positive effect, but the underlying mechanism of ET dysfunction remains poorly understood except for an obvious genesis such as nasopharyngeal tumor or cleft palate. The extent of dysfunction is relevant for understanding the pathogenesis of secondary otological diseases such as acute or chronic otitis media. 3D-modelling based on high resolution images like histologic slices offers options for an improved understanding of the physiological valve mechanism and subsequent development of diagnostic and interventional tools. We chose blackface sheep as a proven animal model due to the close similarity to the human ET.

Methods
An ET of a blackface sheep was marked with three cannulas in the soft tissue approximately parallel to the axis of the ET and embedded in methylmetacrylate after formalin fixation. Cone beam CT (CBCT) of the embed-

Introduction
Eustachian tube (ET) dysfunction is one of the reasons that lead to chronic otitis media. Amongst current treatment options are Valsalva maneuver, tympanostomy tubes, and as more recent option balloon dilatation of the Eustachian tube (BET). All of them can provide benefits for the patient, but do not provide general success. In order to develop new therapies for Eustachian tube dysfunctions such as stents to facilitate middle ear ventilation, a general knowledge on dimensions and positions of the ET in humans is necessary.

Methods

Retrospectively, we investigated dimensions and positions of Eustachian tubes in cone beam CT scans from patients aged between 4 and 94. Parameters such as lengths of the cartilaginous and bony parts, diameters of the bony part, angle between pharyngeal opening and sagittal and horizontal planes as well as distance of the ostium from the nasal conchae were determined.

Results

Independent of any other possible medical indication, scans of 143 patients (77 male) were evaluated with 96 patients being 18y and older. For adult patients the length of the cartilaginous part was between 20.8 and 36.2 mm and that of the bony part was between 6.4 and 19.1 mm. The total length was between 32.6 and 47.2 mm. The average deviation of the left ostium from the horizontal plane was 35° (range: 3.7° to 56.1°) and from the sagittal plane 41.4° (range: 29° to 54.8°) and for the pharyngeal opening on the right side 34° (range: 18.6° to 55.3°) and 41.7° (range: 27.3° to 51.4°), respectively.

Conclusion

These measurements provide necessary information to develop stents for human application and tools for safe positioning of the stents inside the tube. A DVT scan of the patients can provide information for the individual patient regarding type and application of the stent.

PS 736

Establishment of a large animal model for eustachian tube functional study with miniature pigs

An Feng Wei
Chinese PLA General Hospital

Objectives/Hypothesis

The aim of the present study was to investigate whether miniature pig could be a valid animal model of ET.

Study Design

Descriptive study.

Methods

Sixteen Chinese experimental miniature pigs, aged more than 6 mouthes, provided the material for this investigation. The ten samples were used for the study of imaging and anatomy.Three samples were used for the study of morphology. Three samples were used for the feasibility study of balloon dilation of the eustachian tube (BDET).

Results

Three-dimensional (3D) reconstruction have revealed the full course of ET and much information about the length,diameter,curvature and inclination of the ET.Anatomic study present the location of pharyngeal orifice and tympanic orifice,and the structure ofLongitudinal section of ET lumen.Morphologic study shows the fine structure of the cross section of miniature pig ET in different levels.The experiment of BDET verify that miniature pig model enable repeat clinical operation.

Conclusions

The ET of miniature pig match very well the cartilaginous part of the human ET. Miniature pig enable repeat clinical operation. Therefore , we conclude that the miniature pig is a valid animal model of ET.

fig.1.docx

fig.3.docx

fig.5.docx

fig.6.docx

fig.7.docx

PS 737

A method of detecting frequency dependence in middle ear muscle contractions during task engagement

Nathaniel Greene[1]; Heath Jones[2]; Greg Flamme[3]; Stephen Tasko[3]; Kristy Deiters[3]; William Ahroon[2]
[1]US Army Aeromedical Research Laboratory; [2]U.S. Army Aeromedical Research Laboratory; [3]SASRAC

Middle ear muscle contractions (MEMCs) may be elicited by intense sounds, and could offer protection if engaged during a loud sound exposure. In order to detect MEMCs during task-related activity, we use a approach modified from one previously presented by Keefe et al. (2010), wherein a band-limited click stimulus is used as a probe, and the total reflected energy in the ear canal is measured with an in-ear microphone. An ongoing train of these clicks (presented with a 50 ms inter-click interval) is presented to the probe ear before, during, and after presentation of an MEMC-eliciting stimulus. Ongoing changes in middle ear status are assessed by taking the difference between each click relative to the average of clicks presented during a baseline period. Here, we compute the differences in the frequency domain between the ongoing and baseline clicks, allowing for the assessment of any frequency-dependent changes in both magnitude and phase of incoming signals during an MEMC, and present preliminary results for both acoustic and non-acoustic MEMC elicitors using this approach. An Et-

ymōtic ER-10X extended bandwidth probe system was used both to present the acoustic probe and to measure the ear canal sound pressure level. The acoustic elicitor was delivered using an ER-4PT insert earphone to the ear ipsilateral to the ER-10X probe system. Additionally, the activity of several muscles on the face and upper body were measured via a Bagnoli electromyography system, in order to investigate potential correlations in activity between these muscles and MEMCs. Such analyses informed whether multiple systems were activated within the same time frame as an MEMC was occurring. The ear canal microphone signal reveals changes occur with varying time-courses and frequency-dependences, and suggest multiple mechanisms may contribute to the change in the signal associated with the MEMC elicitor presentation. Overall, results suggest that this method is suitable for the assessment of MEMCs during conditions involving both passive and active engagement by the subject.

PS 738

Incorporating Evanescent Modes and Flow Losses into Reference Impedances in Acoustic Thévenin Calibration

Kren Rahbek Nørgaard[1]; Efren Fernandez-Grande[1]; Søren Laugesen[2]
[1]*Technical University of Denmark;* [2]*Interacoustics Research Unit*

The calibration of acoustic probes to obtain the Thévenin source parameters facilitates the measurement of middle ear acoustic impedance and reflectance. A frequently used, existing methodology derives the source parameters from the measured probe pressures in a number of short waveguides by solving an over-determined system of equations. Higher-order, evanescent modes occur at geometrical discontinuities between waveguides, and introduce errors into the Thévenin source parameters if not properly accounted for. An alternative calibration methodology is presented that models evanescent modes and flow losses in the transition between the probe tube and calibration waveguides. This is achieved by positioning the probe tube, without an ear tip, flush with the input plane in waveguides of well-defined dimensions. The known, physical lengths are used for calculating the analytical, plane-wave reference impedances and evanescent modes are included in the model by adding an acoustic inertance. The size of the inertance for each waveguide is iteratively adjusted to minimize the calibration error. Flow losses resulting from fluid motion tangential to the input plane are similarly accounted for by adding a resistive term, proportional to the square root of frequency. It is shown that the proposed methodology can reduce the calibration error across a wide range of frequencies and leads to an independence of the source

parameters on the calibration waveguide radius. However, subsequent impedance measurements are still affected by evanescent modes. The methodology could thus provide a step forward in increasing the precision of measurements of middle ear acoustic impedance and reflectance, and calibrating stimulus levels in-situ.

PS 739

Interacoustics Research Platform: a user-configurable hearing research instrument based on the Titan.

Lasse J. Villadsen[1]; James M. Harte[2]
[1]*Interacoustics A/S;* [2]*Interacoustics Research Unit*

This poster introduces the Interacoustics Research Platform, designed to make the Titan a more flexible system for conducting research on e.g. wide-band tympanometry (WBT), middle ear muscle reflex (MEMR) and otoacoustic emissions (OAE). The Titan is a commercial modular platform for performing a range of physiological audiometric tests and is widely used for screening, diagnostic and clinical applications. It has featured in many clinical and basic research publications due to its modular nature and configurability. However, for the broader hearing research community the Titan has a number of drawbacks. It is currently difficult to rapidly prototype new tests, and the post-processing of measured responses cannot be easily user defined, due in part to there being no access to the raw physiological data.

The Interacoustics Research Platform allows the Titan to act as a configurable soundcard controlled through MATLAB (Mathworks, Inc.), making it a flexible hearing research instrument. A user-defined application, written as a MATLAB script/GUI, communicates through a library interface which controls the USB communication to the Titan. In this way the user can completely control the calibration procedure, and flexibly program tests such as wide-band tympanometry (WBT), wide-band middle ear muscle reflex (WB-MEMR) & OAE applications. All of the raw data is streamed to the PC, so user specified processing pipelines can be written.

This poster describes the technical specification of the system, user available inputs (microphone, 1-channel EEG, and manometer) and outputs (2-channel audio via Titan probe or insert phones, and the pump for pressurisation). Additionally an example application implementing a WB-MEMR test is shown.

PS 740

Wide-band tympanometry in two Representations

Christof Stieger; Ferdinand Gygli; Flurin Honegger
University of Basel Hospital

Tympanometry at 226 Hz is an established clinical examination for diagnosis of the middle ear status. With the introduction of Wide-band tympanometry (WBT) the frequency range is enlarged from 226–8000 Hz. We introduced WBT in in our institution in 2014 using a commercial device (Titan, Interacoustics, Denmark). For our standard clinical procedure, we perform a conventional tympanogram followed by a WBT and an absorbance measurement at 0 daPa. However the additional information of WBT and absorbance is poorly considered. Therefore we investigate in different representations of WBT for better clinical acceptance.

For data analysis we exported WBT data via an XML-file into a Matlab. Data was resampled along the pressure in 2 daPa steps to equidistant points by cubic spline interpolation in a pressure range between -200 to 160 daPa and at fixed frequency steps from 226 -8000 Hz given by the system. Normative data was retrospectively calculated based on 33 ears (15 left/18 right) from patients who range from 6 to 64 years. We used a bootstep procedure with 1000 resamples and calculated mean-, 5%- and 95% surfaces of the WBT. Hereafter we compared this normative data with exemplary clinical type A, B, C tympanograms representing a normal middle ear, a fluid filed middle ear and a negative pressure in the middle ear [1,2] and otosclerosis [3]. Two types of representations where initially evaluated. First we used a 3D plot containing the normative data as a surface with a pressure, frequency and magnitude axes. The exemplary measurements where superposed in the same graph with different transparencies and viewing angles. We could not define a viewing angle and transparency which allowed identification and differentiation of our exemplary measurements. In the second representation we plotted a matrix of 3x3 2D plots where the rows included the top view, side view and front view of the WBT. The columns include the 5%, 95% values of the normative data and the exemplary data. With this second representation we could differentiate our exemplary data. 2D-projections of WBT might therefore be better suitable for clinical practice than 3D-representation for clinical practice.

References

[1] Lidén G. Impedance audiometry. Ann Otol Rhinol Laryngol Suppl. 1980 Sep-Oct;89(5 Pt 2):53-8.

[2] Jerger J. Clinical experience with impedance audiometry. Arch Otolaryngol. 1970 Oct;92(4):311-24.

[3] Nakajima HH et al. Assessment of ear disorders using power reflectance. Ear Hear. 2013 Jul;34 Suppl 1:48S-53S.

PS 741

Absorbance Levels in Preterm Infants Based on OAE Outcomes

Kerry Walker; Beth Prieve; Linda Hood; Devon Pacheco
Syracuse University

Background

Wideband absorbance (A) measures are excellent at identifying conductive pathologies of the outer/middle ear in humans. Their use is particularly important in newborns and infants because they can be measured without applying external pressure to the ear canal. Absorbance is higher in term newborns or mixed groups of preterm/term who pass otoacoustic emission (OAE) screenings than in those who do not, suggesting that outer/middle ear issues contributed to screening outcomes. There is little information whether the relationship between A and OAEs holds in preterm newborns. The purpose of the current study was to determine typical changes in absorbance level (A_L) for preterm infants tested at four ages. In addition, A_L was assessed based on OAE presence/absence and the relationship between A_L and ABR latencies were examined.

Methods

183 preterm infants are enrolled in the BabyEARS longitudinal study to date. Newborns were tested at 33 and 35 weeks gestational age (GA) in the neonatal intensive care unit and in a sound treated or quiet room at 48-52 and 62-66 weeks GA. The Mimosa Acoustics HearID was used to collect OAEs at 2 kHz and 4 kHz and A to 70 dB SPL chirps. Acceptable probe-fit for A testing was based on impedance phase criteria and repeatable impedance phase and absorbance. The Intelligent Hearing Systems SmartEP was used to collect click-evoked ABR recordings at 40 and 70 dB nHL.

Results

In preterm newborns aged 33 and 35 weeks GA, A is highest, or peaks, over a range of frequencies. Preterm infants aged 48-66 weeks GA, have peaks over several frequency ranges, a single peak, or have high A over a broad range of frequencies. In terms of A_L, preterm infants with present OAEs have high A_L for frequencies between 1.0-2.5 kHz, whereas those with absent OAEs have lower A_L across this frequency region, and often an A peak at 3 kHz or higher. ABR wave latencies were longer for preterm infants who had low A in the 1.0-2.5 kHz range. Collectively, low A, absent OAEs and long

ABR latencies are suggestive of a peripheral sound conduction dysfunction.

Conclusions
Absorbance level is different in preterm infants who do and do not have OAEs as young as 33 weeks GA. Expected OAE and ABR differences typical of ears with conductive pathology were also observed in preterm newborns and infants, suggesting A_L is sensitive to outer/middle ear dysfunction in preterm infants. [Funding: NIH-NIDCD R01DC011777]

Molecular Landscape of Hearing Loss II

PS 742

Disease modelling of GJB2 related hearing loss with induced pluripotent stem cell

Ichiro Fukunaga[1]; Kaori Hatakeyama[1]; Ayumi Fujimoto[1]; Osamu Minowa[2]; Katsuhisa Ikeda[1]; **Kazusaku Kamiya[1]**
[1]Department of Otorhinolaryngology, Juntendo University Faculty of Medicine; [2]BioResource Center, RIKEN

Mutation of the Gap Junction Beta 2 gene (GJB2) is the most frequent cause of hereditary deafness worldwide and accounts for up to 50% of non-syndromic sensorineural hearing loss cases in some populations. GJB2 encodes connexin (CX) 26, a component in cochlear gap junction. We have demonstrated that the drastic disruption of gap junction plaque (GJP) macromolecular complex composed of CX26 and CX30 are critical pathogenesis starting before hearing onset (Kamiya, J Clin Invest, 124(4):1598–1607, 2014). Therefore, cochlear CX26-gap junction plaque (GJP)-forming cells such as cochlear supporting cells are thought to be the most important therapeutic target for the treatment of hereditary deafness. The differentiation of pluripotent stem cells such as induced pluripotent stem (iPS) cells into cochlear CX26-GJP-forming cells had not been reported. To develop the effective therapy for GJB2 associated hearing loss, restoration of GJP macromolecular complex using iPS cell based drag screenings or regenerative therapy are expected to rescue the hearing function of GJB2 related hearing loss.

In this study, we developed a novel strategy to differentiate induced pluripotent stem cells into functional CX26-GJP-forming cells that exhibit spontaneous ATP- and hemichannel-mediated Ca2+ transients typical of the developing cochlea. Furthermore, these cells from CX26-deficient mice recapitulated the drastic disruption of GJPs, the primary pathology of GJB2-related hearing loss (Fukunaga, Stem Cell Reports, 7(6), 1023-1036, 2016). Human iPS cells were also developed form the

patients with common GJB2 mutations in east Asian population.

These in vitro models should be useful for establishing inner-ear cell therapies and drug screening that target GJB2-related hearing loss.

PS 743

Social health insurance-based comprehensive genetic testing clarified the molecular epidemiology of deafness

Shin-ichi Usami; Shin-ya Nishio; Hideaki Moteki; Maiko Miyagawa; Kentaro Mori
Department of Otorhinolaryngology, Shinshu University School of Medicine

Background
Targeted exon resequencing using Massively Parallel DNA Sequencing (MPS) is a powerful new strategy for identifying causative genes in rare Mendelian disorders such as deafness. We previously developed an advanced screening strategy (Invader assay) focusing on frequently recurring mutations (46 known mutations in 13 known deafness genes) that are most likely to be encountered in a clinical setting that can identify the causative gene in approximately 30% of deafness patients (Usami et al., 2012).This indicates that -30% of patients have deafness due to commonly found mutations, such as those in GJB2 or SLC26A4. In Japan, genetic testing using the Invader assay for deafness has been covered by social health insurance since 2012. For the remainder of patients with hearing loss of unknown etiology, we have applied MPS of 63 target candidate genes to identify rare causative genes. From August 2015 genetic testing using MPS for deafness was included in the social health insurance-based genetic testing.

Methods
Comprehensive screening for 63 deafness genes using Ion AmpliSeq™ and Ion PGM™ was employed for 4,692 randomly selected Japanese deafness patients. Appropriate filters were then used to select the responsible gene.

Results
Various rare genes responsible for hearing loss in the individual patients were identified using the MPS technology followed by an appropriate filtering algorithm. Approximately 50% of the patients could be diagnosed using the current platform, and GJB2 SLC26A4, CDH23, and mitochondrial genes are commonly found in deafness patients in Japan.

Conclusion

Our data suggests that targeted exon sequencing of selected genes using the MPS technology is able to identify rare responsible genes including new candidate genes for individual patients with deafness and improve the molecular diagnosis in a clinical setting (Miyagawa et al., 2013, Nishio et al., 2015, Mori et al., 2016). In addition, the present study, based on a large patient population, clarified the molecular epidemiology of deafness in Japanese. GJB2 is the most prevalent causative gene, and the major (commonly found) mutations in SLC26A4, CDH23, and mitochondrial genesare responsible for hearing loss in 30% of cases, with the remainder being the result of various rare genes/mutations that have been difficult to diagnose using the conventional one-by-one approach. In conclusion, targeted exon resequencing using MPS technology is a suitable method for identifying both common and rare causative genes for a highly heterogeneous monogenic disease such as hearing loss.

PS 744

Identification of OTOA, the "DFNB22 Gene" as a Cause of Deafness in Koreans and detection of the most upstream truncation variant of OTOA

Bong Jik Kim[1]; Jin-Hee Han[1]; Ah-Reum Kim[1]; Chung Lee[2]; Nayoung Kim[2]; Hye-Rim Park[1]; Min Young Kim[1]; Woong-Yang Park[2]; Doo Yi Oh[1]; Seungmin Lee[1]; Sungjik Park[3]; Byung Yoon Choi[1]
[1]Seoul National University Bundang Hospital;
[2]Samsung Genome Institute; [3]University of Utah

Background

OTOA encodesotoancorin which is required for limbal attachment of the tectorial membrane and is assumed to play a role in the stimulation of inner hair cells. Based on large deletions encompassing most of the OTOA genomic region in Palestinian, Turkish and Qatari families and three missense variants in Pakistani and Algerian families, OTOA is considered the gene underlying AR nonsyndromic hearing loss (DFNB22). Interestingly, a variant, p.E787X that leads to truncation of a substantial portion of C-terminal sequence of OTOA was frequently detected among normal controls, rendering us to think that a crucial function of this gene could be mainly from the N-terminal part. However, the minimal N-terminal extent required for proper functioning of otoancorin has never been elucidated yet. Further, a convincing variant of this gene has never been reported outside of Southwest Asia and Northern Africa. This study aimed to address aforementioned issues.

Methods

A 21-month-old boy visited clinic for genetic diagnosis of deafness. His pedigree showed an AR inheritance pattern and audiogram demonstrated a moderate degree hearing loss.

For genetic diagnosis, WES was used to narrow down the candidate variants. Thenfiltering steps including compatibility with inheritance pattern and audiogram pattern, in silico study, control and segregation study were done to finalize the diagnosis.

Results

WES identified two variants of OTOA in a trans configuration in the proband (Table 1). Minigene splicing assay supported the pathogenic potential of our splice site variant based on the presence of entrapped intron in a substantial portion of transcripts (Figure 1) and the fact that our truncation variant was located upstream to the previously reported missense variant, p.Pro627Ser, increased the pathogenic potential of our truncation variant. Additionally, we checked the indels and CNVs of OTOA in two Korean control groups: in-house data (n=1000) and Korean Variant Archive (n=944) respectively. There was no significant indel and only 2 CNVs of OTOA were detected among 944 Korean controls, raising the contribution of the OTOA variants to Korean deaf population.

Conclusions

Here, we report the first splice site variant of OTOA associated with DFNB22, and our results suggest that important functions of otoancorin can be accomplished only by N-terminal 589 amino acids given the location of our truncation variant. In addition, considering the first detection of OTOA variant outside the Southwest Asia and Northern Africa, our study implies that OTOA might play a globally significant role in the field of hereditary deafness.

Table1_OTOA_ARO.docx

Figure1_OTOA_ARO.docx

PS 745

Investigating the Genetic Basis of Otosclerosis through Whole-Exome and Targeted Sequencing Analysis

Michael Crompton[1]; Joanna L. Ziff[1]; Andrew J. Mowat[1]; University of Washington Center for Mendelian Genomics[2]; Jeremy A. Lavy[3]; Shakeel R. Saeed[1]; Sally Dawson[1]
[1]University College London; [2]University of Washington Center for Mendelian Genomics; [3]Royal National Throat Nose and Ear Hospital

Otosclerosis is the most common cause of progressive deafness in young adults, characterised by abnormal

bone remodelling in the otic capsule, leading to fixation of the stapedial footplate and an associated conductive hearing loss. Otosclerosis is a heterogeneous disorder, however one that in up to 50% of cases occurs with a strong familial inheritance pattern consistent with an autosomal dominant mutation that exhibits variable penetrance. Although familial linkage analysis, candidate gene and genome-wide association studies have been performed in recent years to identify disease-causing genes, little progress has been made in identifying the genes underlying the condition. Recently, our laboratory used a combination of whole-exome sequencing, transcriptome data and functional analysis to identify SERPINF1 as the first disease-causing gene in otosclerosis (Ziff et al., 2016). Our results demonstrated the power of an exome sequencing approach over linkage analysis in familial cases of a relatively common disorder, even in the presence of variable penetrance and heterogeneity. Here, we have expanded our approach with the aim of identifying further genetic causes of otosclerosis. Whole-exome sequencing was performed on 19 probands from families that exhibited a dominant monogenic inheritance of otosclerosis. A step-wise variant filtering process was designed to remove known common variants and prioritise those most likely to be involved in disease pathogenesis. We filtered variants based on allele frequency, functional impact and in silico predictions, with a focus on variants that were identified in multiple probands. After filtering, remaining variants were annotated and 186 variants across 70 genes were prioritised for follow-up. Prioritisation was based on a number of factors including expression in otosclerotic stapes, relevant phenotype in mutant mice and known biological function. Segregation analysis using Sanger sequencing in family members reduced the list of candidates to 61 genes. Sanger sequencing-based approaches in this number of candidates can be labour-intensive and relatively expensive. Therefore, we applied a next-generation sequencing-based approach to further investigate our candidate genes in a secondary cohort of 160 familial otosclerosis cases using a custom SureSelect Target Enrichment panel. The presence of any of the variants in additional cases of familial otosclerosis will provide strong evidence for a role of these genes in the disease pathology of otosclerosis and will be further investigated using functional analysis to determine how they contribute to the pathology of otosclerosis.

PS 746
Human and mouse CDC14A phosphatase activity is essential for hearing and male fertility

Ayesha Imtiaz[1]; Inna A. Belyantseva[1]; Alisha Beirl[1]; Cristina Fenollar-Ferrer[2]; Rasheeda Bashir[3]; Ihtisham Bukhari[3]; Amal Bouzid[4]; Uzma Shaukat[5]; Hela Azaiez[6]; Kevin Booth[7]; Hossein Najmabadi[8]; Atteeq Rehman[1]; Michael Hoa[1]; Lijin Dong[9]; Richard J. H. Smith[6]; Sheikh Riazuddin[5]; Saber Masmoudi[10]; Katie Kindt[11]; Sadaf Naz[3]; Thomas B. Friedman[12]

[1]NIDCD/NIH; [2]Laboratory of Molecular and Cellular Neurobiology, Section on Molecular and Cellular Signaling, National Institute of Mental Health, NIH, Bethesda, Maryland, USA; [3]School of Biological Sciences, University of the Punjab, Lahore, Pakistan; [4]Laboratoire Procédés de Criblage Moléculaire et Cellulaire, Centre de Biotechnologie de Sfax, Université de Sfax, Sfax, Tunisia.; [5]Center of Excellence in Molecular Biology, University of the Punjab, Lahore, Pakistan; [6]Molecular Otolaryngology and Renal Research Laboratories, Department of Otolaryngology—Head and Neck Surgery, Carver College of Medicine, University of Iowa; [7]Molecular Otolaryngology and Renal Research Laboratories, Department of Otolaryngology—Head and Neck Surgery; Interdisciplinary Graduate Program in Molecular Medicine, Carver College of Medicine, University of Iowa; [8]University of Social Welfare and Rehabilitation Sciences, Tehran Iran.; [9]Genetic Engineering Core, National Eye Institute, NIH, Bethesda, Maryland, USA; [10]Laboratory of Molecular and Cellular Screening Processes, Center of Biotechnology of Sfax; [11]National Institutes of Deafness and Other Communication Disorders, National Institutes of Health; [12]Laboratory of Molecular Genetics, National Institute on Deafness and Other Communication Disorders (NIDCD), Bethesda, MD, USA

Background

The interplay of phosphatases and kinases regulate many cell functions. Kinases essential for hearing have been reported, however, their counter-acting phosphatases are understudied. In yeast, cdc14 phosphatase is essential to reverse cdk-mediated phosphorylation in order to exit mitosis. Human CDC14A can rescue yeast from the lethal loss of cdc14. Using cultured human cancer cells, numerous disparate functions of over-expressed CDC14A have been published based on the premise that that human CDC14A is also involved in mitosis. More recently, morpholino knockdown studies reported a role for zebrafish cdc14aa in ciliogenesis. The published studies of vertebrate CDC14A lack mutant germ-line models to identify the in vivo functions and pathways for this phosphatase.

Methods

By whole exome sequencing we identified mutant alleles of CDC14A in eight human families segregating deafness linked to markers for the DFNB32 locus on chromosome 1p. Using computational structural models, we predict how missense variants of CDC14A impair phosphatase activity. LacZ-reporter, commercial and custom antibodies against CDC14A and gene-gun transfections of EGFP-CDC14A were utilized to study localization in mouse and zebrafish. Three targeted mutant alleles of mouse Cdc14a and CRISPR/Cas9 edited phosphatase dead mutants of zebrafish and mice were engineered. Histopathology of the inner ear and male reproductive system were evaluated by confocal and electron microscopies.

Results and Conclusions

We identified four previously unreported protein truncating and three missense alleles of CDC14A in eight human families segregating progressive, moderate-to-profound deafness. In five of these families, deaf males are infertile. Our computational molecular modeling predicts that CDC14A folds into a N-terminal catalytically inactive Dual specificity (DSPn) and catalytically active core phosphatase domain (DSPc). Three missense variants alter conserved residues essential for catalysis or folding of the protein. Several recessive mutations of mouse Cdc14a, including a CRISPR/Cas9-edited phosphatase-dead p.C278S substitution, result in substantial perinatal lethality, but surviving mice recapitulate the human phenotype of deafness and males are infertile. CDC14A protein localizes to inner ear hair cell kinocilia, basal bodies and stereocilia. Auditory hair cells of postnatal Cdc14a mutants develop normally, but subsequently degenerate causing deafness. Kinocilia of germ-line mutants of mouse and zebrafish have normal lengths, which does not recapitulate the published cdc14aa knockdown morphant phenotype of shortened kinocilia. These findings define a new monogenic syndrome of deafness and male infertility, revealing in vivo an absolute requirement of vertebrate CDC14A phosphatase activity for hearing and spermatogenesis. Other authors: K.Kahrizi, A.Maqsood, E.A.Wilson, T.S.Fitzgerald, A.Tlili, R.Olszewski, M.Lund, T.Chaudhry, M.F.Starost, A.Waryah and R.J.Morell

ARO_Abstract.docx

PS 747

Haplotype Reconstruction Provides Insights into the Contributions of known Deafness-Causing Genes to Age-Related Hearing Loss

E Ann Black-Ziegelbein[1]; Hela Azaiez[2]; Elisa Rubinato[3]; Kai Wang[4]; Anna Morgan[3]; Kevin Booth[5]; Marco Brumat[3]; Dragana Vuckovic[3]; Mariapina Concas[6]; Ginevra Biino[6]; Simona Vaccargiu[7]; Mario Pirastu[7]; Giorgia Girotto[8]; Paolo Gasparini[8]; Richard J. H. Smith[2]

[1]Department of Otolaryngology-Head and Neck Surgery; [2]Molecular Otolaryngology and Renal Research Laboratories, Department of Otolaryngology—Head and Neck Surgery, Carver College of Medicine, University of Iowa; [3]Department of Medical, Surgical and Health Sciences, University of Trieste; [4]Molecular Otolaryngology and Renal Research Laboratories, Department of Otolaryngology-Head and Neck Surgery, University of Iowa Hospitals and Clinics; [5]Molecular Otolaryngology and Renal Research Laboratories, Department of Otolaryngology—Head and Neck Surgery; Interdisciplinary Graduate Program in Molecular Medicine, Carver College of Medicine, University of Iowa; [6]Institute of Molecular Genetics, National Research Council of Italy; [7]Institute of Population Genetics, National Research Council of Italy; [8]IRCCS "Burlo Garofolo"

Age Related Hearing Loss (ARHL) or presbycusis is a broadly impacting complex disease that affects nearly one in three aging adults. Both environmental and genetic factors are implicated in its physiopathology. To illuminate genetic contributions, several association studies have been performed, which have suggested the involvement of different single nucleotide variants (SNVs) in several genes, although replication studies have been unsuccessful. We hypothesized that haplotype-based approaches, which detect the combinatorial impact of multiple SNVs within a locus, would be more powerful than single SNV analysis for uncovering susceptibility genes that contribute to ARHL.

To determine whether specific haplotypes in common deafness-causing genes contribute to susceptibility to ARHL we used targeted genomic enrichment (TGE) and massively parallel sequencing (MPS) to screen the coding regions of 87 known deafness-causing genes in an ARHL cohort (n=263) and matched controls (n=227) from a founder population in Sardinia. Haplotype phasing was performed with the ShapeIt2 program via the public Oxford Statistics Phasing Server, which employs both statistical and read-aware phasing algorithms leveraging the Haplotype Reference Consortium (HRC) reference panel of 64,976 haplotypes. Statistical analyses to test for association were performed using Fisher

Exact test on contingency matrices constructed at the gene and haplotype levels.

We demonstrate that for large genes such as CDH23 and PDCH15, the inclusion of all phased genotypes generates an overwhelming haplotype diversity (1000s of haplotypes) with rare haplotypes (allele frequency < 0.05) being most prevalent. To reduce the number of distinct haplotypes to an actionable number, we developed filtering criteria based on biological relevance, and considered allele frequency, CADD C-score (a measure of deleteriousness) and protein consequence as annotated with Variant Ensembl Predictor.

This study is the first to harness the power of next-generation haplotype reconstruction to analyze allelic association in an isolated population to investigate ARHL.

PS 748

A nonsense mutation in OTOG causes sporadic mild hearing loss at an early age

Hye Ji Choi[1]; Jee Eun Yoo[1]; Hyun Jae Lee[1]; Hak Jun Lee[1]; Hyun Jin Lee[2]; Yohan Lim[2]; Byung Soo Choi[1]; Jinsei Jung[1]
[1]Yonsei University College of Medicine; [2]Department of Otorhinolaryngology, College of Medicine, Yonsei University

Congenital hearing loss is genetically heterogeneous, and is mostly severe to profound. On the other hand, mild hearing loss in newborns and young children is believed to be much more common than diagnosed, although hard to detect. Here, we tried to find genetic variation that associated with mild hearing loss identified in young age. We performed whole-exome sequencing to find a causative novel mutation in a child with mild hearing loss. The mutation is a homozygous truncation (c.330C>G; p.Tyr110*) in OTOG, a gene linked to DFNB18 and encodes otogelin, a glycoprotein in the acellular membrane of the inner ear that facilitates mechanotransduction. The mutation essentially produces a null allele since the truncated protein contains no functional domains. While defects in otogelin were previously reported to result in both hearing loss and vestibular dysfunction, the latter was not noted in the patient. Since mild hearing loss is not easily detected in early life, OTOG mutations may be more prevalent than reported. In conclusion, genetic analysis of OTOG is recommended for children with mild hearing loss.

PS 749

OTOF mutation analysis with massively parallel DNA sequencing in 2135 Japanese sensorineural hearing loss patients

Yoh-ichiro Iwasa; Shin-ya Nishio; Shin-ichi Usami
Department of Otorhinolaryngology, Shinshu University School of Medicine

Background
The OTOF gene (DFNB9), encoding otoferlin, is reported to be one of the major causes of non-syndromic recessive sensorineural hearing loss, and is also reported to be most common cause of non-syndromic recessive auditory neuropathy spectrum disorder (ANSD). In the present study, we performed OTOF mutation analysis using massively parallel DNA sequencing (MPS). The purpose of this study was to reveal the frequency and precise genetic and clinical background of OTOF-related hearing loss in a large number of patients.

Methods
A total of 2135 Japanese sensorineural hearing loss (SNHL) patients compatible with autosomal recessive inheritance (including sporadic cases) from 67 ENT departments nationwide participated in this study. The mutation analysis of 68 genes, including the OTOF gene, reported to cause non-syndromic hearing loss was performed using MPS.

Results and Conclusions
We found 20 mutations in the OTOF gene in this study, with 13 of them novel mutations. Forty of the 2135 patients (1.87%) carried homozygous or compound heterozygous mutations in the OTOF gene. Twenty-seven patients (1.26%) carried only heterozygous mutations. It is assumed that the frequency of hearing loss associated with OTOF mutations is about 1.87-3.13% of autosomal recessive or sporadic SNHL cases. Hearing level information was available for 32 of 40 patients with biallelic OTOF mutations; 24 of them (75.0%) showed profound hearing loss, 7 (21.9%) showed severe hearing loss and 1 (3.1%) showed mild hearing loss. The hearing level of patients with biallelic OTOF mutations in this study was mostly severe to profound, which is consistent with the results of past reports.

Ten of the 40 patients with biallelic OTOF mutations had been diagnosed with ANSD. The genetic diagnosis of OTOF mutations has significant benefits in terms of clinical decision-making. Patients with OTOF mutations would be good candidates for cochlear implantation; therefore, the detection of OTOF mutations is quite beneficial for the patients, especially for those with ANSD.

PS 750

Synaptojanin2 mutation causes progressive high frequency hearing loss in mice

Elisa Martelletti[1]; Neil Ingham[2]; Johannna Pass[3]; Jing Chen[3]; Oliver Houston[4]; Walter Marcotti[4]; Karen Steel[2]
[1]*King's College London;* [2]*King's College London and Wellcome Trust Sanger Institute;* [3]*King's College London and Wellcome Trust Sanger Institute;* [4]*University of Sheffield*

Synaptojanin 2 (Synj2) is a phosphatidylinositol phosphatase that removes the 5-position phosphates from phosphoinositides, such as PIP2 and PIP3. In 2011 a point mutation of the Synj2 gene was reported to cause progressive hearing impairment in Mozart mice (Manji et al., 2011). We were interested in exploring whether a larger deletion within this gene has similar or different hearing phenotype in comparison with the Mozart mice.

Synj2^{tm1a} mutant mice were generated as part of the Sanger Institute';s Mouse Genetics Project and they showed normal ABR thresholds, which might be due to incomplete inactivation of transcription in the tm1a allele. Therefore, the Synj2^{tm1a} mutant mice were crossed to CMV-Cre mice in order to delete the critical exons of the Synj2 gene and generate the Synj2^{tm1b} mutant allele. The Synj2^{tm1b} mutant mice had normal auditory sensitivity at 2 and 3 weeks old, however the ABR thresholds of the high frequencies gradually increased starting at 4 weeks. The DPOAE thresholds were raised at 6 weeks at high frequencies, suggesting a functional defect of outer hair cells (OHCs). At the same age, the endocochlear potential was measured and no difference was found between mutant and littermate controls. Moreover, the intragenic deletion of Synj2 does not affect the synaptic transmission nor the general basolateral membrane properties of adult inner hair cells (IHCs). X-gal staining on sections of inner ear revealed that Synj2 is expressed in the IHCs and OHCs, spiral ganglion and supporting cells. At 6 weeks old, the gross morphology of nerve fibres, synapses and hair bundles were examined by confocal microscopy and scanning electron microscopy, showing no major defects, except some loss and fusion of OHC stereocilia only at the extreme base of the cochlea.

Overall, the Synj2^{tm1b} mutant mice showed progressive high frequency hearing loss revealed by increased ABR thresholds associated with impaired DPOAEs, suggesting that OHCs might contribute to the mechanism behind this phenotype. However, this mutation does not affect the development of the hearing system in the inner ear.

PS 751

No Evidence of an Association between Variation in RELN and Otosclerosis in a United Kingdom Cohort

Andrew J. Mowat[1]; Michael Crompton[1]; Joanna L. Ziff[1]; Christopher Aldren[2]; Jeremy A. Lavy[3]; Shakeel R. Saeed[1]; Sally Dawson[1]
[1]*University College London;* [2]*Windsor ENT Department;* [3]*Royal National Throat Nose and Ear Hospital*

Otosclerosis is a common form of conductive hearing loss which typically presents in young adults. The disease has a complex aetiology thought to involve both genetic and environmental factors. 50 % of patients have a strong family history of the disease, consistent with a monogenic autosomal dominant inheritance of reduced penetrance. Understanding of the genetics of the disease has progressed slowly due to an absence of large well characterised patient cohorts from which meaningful results can be obtained. Previous genetic studies involving linkage analysis in families or candidate gene association studies have not definitively identified the genes involved. Variation in the RELN gene was found to be associated with otosclerosis in a genome wide association study performed in a European population (Schrauwen et al., 2009). However, replication of this association has been variable dependent on the study population. Follow up replication studies have displayed conflicting results. An association has been established in other European and Tunisian populations. However, similar studies in Italian and Indian populations failed to detect an association. RELN codes for the protein reelin known to be involved in neuronal migration. It is unclear how the biological function of the protein would play a role in otosclerosis pathogenesis. The aim of this study is to test whether variation in RELN or other previously linked gene variants were associated with otosclerosis in a large UK case control cohort. We investigated eight candidate variants in the following six genes: RELN, BMP2, FGF2, COL1A1, TGFB1, and PPP2R5B, following a comprehensive review of previous genetic studies. Individuals with a confirmed diagnosis of otosclerosis were recruited from six different UK surgical centres. 374 otosclerosis cases were compared with 374 control cases who have had the disease excluded by audio-

gram. The study was approved by the London Bloomsbury NRES Ethics committee (11/LO/0489) and patients were recruited by informed consent. Genotyping was performed using TaqMan Allelic Discrimination Assays on an Applied Biosystems 7500 Real Time PCR System. No statistically significant association was identified between any of the three single nucleotide polymorphisms within RELN and otosclerosis. A weak association was detected between variation in TGFB1 and otosclerosis. This study adds to the conflicting evidence linking RELN variation to the pathology of otosclerosis.

PS 752

Investigating the Role of Peroxisome Defects in Hearing Impairment

Rafael M. Kochaj[1]; Neil Ingham[2]; Karen Steel[2]
[1]*King's College London;* [2]*King's College London and Wellcome Trust Sanger Institute*

Peroxisomes are highly dynamic and metabolically active organelles that play an important role in cellular functions, including lipid metabolism. Defects in peroxisome biogenesis cause disorders such as Zellweger syndrome. Pex3 is a peroxisomal membrane protein required for the formation of peroxisomes. The aim of this project is to establish how peroxisome defects can result in hearing loss, using a mouse with a mutation affecting the Pex3 protein.

The Pex3[tm1a(EUCOMM)Wtsi] mutant mice were generated and screened as part of the Sanger Institute Mouse Genetics Project and quantitative real-time PCR showed Pex3 knockdown to 16% of the normal level in brain tissue of homozygous mutants. Auditory Brainstem Response (ABR) measurements in response to click stimuli and tone pips ranging from 3-42kHz were recorded from anaesthetised mice at P17, P21, P28, P56 and P98. ABR recordings showed a progressive increase in thresholds at high frequencies at all the ages tested.

LacZ staining revealed Pex3 to be expressed ubiquitously in the cochlea. Since Pex3 was strongly expressed in the spiral ganglion and hair cells, cochlear whole mounts were labelled for the inner hair cell presynaptic ribbon marker Ribeye and the afferent neuron postsynaptic density marker GluR2 and imaged by confocal microscopy at locations corresponding to 12, 18, 24, 30 and 36kHz, using the physiological place-frequency map to determine the best frequency region. The labelling at P28 showed reduced overlap between ribbons and the postsynaptic marker in mutant inner hair cells compared to controls at higher frequencies. The ribbon synapses were misplaced in relation to the postsynaptic density. We therefore conclude that Pex3 is crucial for normal

hearing and malfunction in synaptic transmission may contribute to the hearing loss.

We examined whether there are differences in the number of peroxisomes in mutant hair cells compared to controls using catalase - a peroxisomal marker. The number of peroxisomes in the outer hair cells was the same in both mutants and controls. However, a reduction in peroxisome numbers was observed in the inner hair cells of mutants. These peroxisomal changes are also likely to contribute to the hearing impairment seen in Pex3 mutant mice.

Our results suggest that synaptic and peroxisome defects in inner hair cells may contribute to the progressive high frequency hearing loss observed in Pex3 mutant mice. Pex3 is a novel deafness gene and understanding the processes causing the hearing impairment, specifically the effects on peroxisomes and lipids, may ultimately reveal new drug targets.

PS 753

Rapid Functional Characterization of Pendrin Mutants

Koichiro Wasano[1]; Satoe Takahashi[2]; Jing Zheng[2]; Kaoru Ogawa[3]; Kazuaki Homma[2]
[1]*Department of Otolaryngology Head and Neck Surgery, Keio University School of Medicine;* [2]*Northwestern University;* [3]*Department of Otolaryngology, Head and Neck Surgery, Keio University School of Medicine*

Background
Pendrin (SLC26A4) is a member of the solute carrier 26 gene family, and its anion transport function is essential for normal hearing. Thanks to the advent of the next generation DNA sequencing technology and its prevalence, many novel mutations in the pendrin gene are being identified. In order to experimentally define the functional consequences of the large number of mutations found in pendrin, we develop a plate reader-based method that allows rapid functional characterization of many pendrin mutations.

Method
We generated stable cell lines that express wild-type or mutated pendrin proteins in a doxycycline inducible manner using the sleeping beauty system. A fluorescent pH indicator (SNARF-5F) or iodide-sensitive fluorescent protein (mVenus H148Q/I152L) was loaded or heterologously expressed in these cell lines so that the anion

transport activities of pendrin and its mutants are monitored fluorometrically. Time-dependent changes in fluorescence associated with bicarbonate/chloride or iodide/chloride antiport activity were monitored in a 96-well plate format. Then, we determined the transport rates by curve fitting analyses.

Results

We systematically determined both bicarbonate/chloride and iodide/chloride antiport rates for wild-type and mutated pendrin proteins using this high-throughput method. We found that the pendrin mutations can be classified into three major groups based on their functional effects on the anion transport functions - those affect neither bicarbonate/chloride nor iodide/chloride antiport activity (group 1), those severely affect either bicarbonate/chloride or iodide/chloride antiport activity (group 2), and those severely affect both bicarbonate/chloride and iodide/chloride antiport activities (group 3).

Conclusions

Since the fluorescence signals can be collected from a large number of cells at once, our method is statistically very powerful and highly reproducible. We expect that this high-throughput method allows systematic functional characterization of disease-associated mutations found in pendrin at an unprecedented rate, which will greatly facilitate efforts in defining the pathogenicity of numerous mutations found in this protein. We believe that our effort in classifying the pendrin mutants based on their functional phenotypes is important for understanding why some pendrin mutations are associated with DFNB4 while others are associated with Pendred syndrome.

PS 754

Novel Variants in EDNRB Gene in Waardenburg Syndrome Type II and SOX10 Gene in PCWH Syndrome.

Ivica Masindova[1]; Lukas Varga[2]; Daniel Danis[1]; Martina Skopkova[1]; Lucia Demesova[2]; Jakub Drsata[3]; Viktor Chrobok[3]; Daniela Gasperikova[1]; Milan Profant[2]
[1]Biomedical Research Center, Slovak Academy of Sciences; [2]Department of Otorhinolaryngology—Head and Neck Surgery, Faculty of Medicine and University Hospital, Comenius University; [3]Department of Otorhinolaryngology and Head and Neck Surgery, University Hospital Hradec Kralove, Charles University, Faculty of Medicine in Hradec Kralove

Background

Waardenburg syndrome (WS) is a phenotypically and genetically variable genetic disorder with four distinct clinical types and several subtypes. Here we present two Caucasian families with WS type II and PCWH (Peripheral demyelinating neuropathy, Central dysmyelination, Waardenburg syndrome, and Hirschprung disease) syndrome respectively who were referred to our laboratory for molecular-genetic testing. In both families, only the proband was presenting clinical symptoms, suggesting possibility of de novo mutation.

Methods

Proband of the family 1 (clinically WS type II) was analyzed by whole exome sequencing (WES) method. Identified candidate variant in EDNRB gene was confirmed in the proband and family members by Sanger sequencing. Proband of the family 2 (clinically PCWH syndrome) and his parents were tested directly for SOX10 gene (4 exons) by Sanger sequencing.

Results

In both families we identified novel candidate variants, which were not found in public available databases (ExAC, dbSNP). In family 1 a novel heterozygous variant c.521G>A was detected in EDNRB gene. The clinical phenotype of the proband is relatively mild and corresponds to WS type II (heterochromia irides and sensorineural hearing loss without dystopia canthorum or gastrointestinal abnormalities). Other three family members were carriers of this variant, however, they were apparently asymptomatic. Variant c.521G>A causes substitution of highly conserved cysteine by tyrosine (p.C174Y), which leads to loss of disulfide bridge between extracellular segments of the protein. A 3D model showed that c.521G>A disturbed the tertiary protein structure. In family 2, we identified a novel heterozygous variant c.900C>A in SOX10 gene in a 3 years-old proband with fully developed PCWH syndrome, including severe inner ear malformation (cochlear hypoplasia, aplasia of semicircular canals, hypoplasia of vestibulocochlear nerve). This variant was not found in his unaffected parents giving an evidence that the c.900C>A substitution occurred de novo in the proband. The c.900C>A results in premature termination (p.Tyr300*) of the SOX protein. Consistent with the literature, this novel truncating variant localised in the last coding exon of the protein is associated with PCWH disease phenotype.

Conclusion

Until recently, EDNRB mutations were only known to be associated with severe phenotypes of WS (type IV). In contrast, our investigated family demonstrated mild WS type II phenotype with extremely low penetrance. The novel de novo variant in SOX10 gene leads to onset of severe, life threatening symptoms early after birth. Our results contribute to the knowledge on genotype and phenotype diversity of WS.

Copy Number Variants in Genetic Diagnosis of Syndromic and Non-Syndromic Hearing Loss

Diana Kolbe[1]; Hela Azaiez[1]; Kathy Frees[1]; Donghong Wang[1]; Iman Kashmola[1]; Kevin Booth[2]; Carla Nishimura[1]; Richard J. H. Smith[1]
[1]Molecular Otolaryngology and Renal Research Laboratories, Department of Otolaryngology—Head and Neck Surgery, Carver College of Medicine, University of Iowa; [2]Molecular Otolaryngology and Renal Research Laboratories, Department of Otolaryngology—Head and Neck Surgery; Interdisciplinary Graduate Program in Molecular Medicine, Carver College of Medicine, University of Iowa

We have previously established that copy number variants (CNVs) are a significant contributing cause to non-syndromic hearing loss (NSHL), and should be included in comprehensive genetic testing. Here, we update frequencies of causative CNVs in a larger patient cohort and with an expanded testing panel covering more genes. We also include analysis of select hearing loss syndromes where clinical findings may initially mimic NSHL, such as Usher, Waardenburg and Branchio-Oto-Renal syndromes.

We used target capture and next generation sequencing to screen all coding regions of known deafness-causing genes for NSHL and NSHL mimics on OtoSCOPE panel versions 5, 6, or 7 (87, 116, or 133 genes, respectively). All genes were assessed for single nucleotide variants, indels and CNVs using a customized bioinformatics pipeline. 1693 patients with hearing loss were included in the study based on sequential arrival and including only probands.

Data analysis showed that CNVs represent a significant portion of disease burden in several Deafness syndromes. Their size ranged from a single exon to contiguous gene deletion. Deletions and conversions in STRC remain the most common findings, accounting for more than half of all CNVs discovered. The STRC locus has multiple pathogenic CNV alleles in our cohort at appreciable carrier frequencies, along with duplications that are likely benign. The next most common genes are OTOA, USH2A, and CDH23, but the tail of findings is long with more than 40 genes having at least one CNV discovered in our patient population.

These findings stress the need for a screening methodology that robustly detects novel deletion and duplication events in all tested genes rather than testing only for previously reported CNV events.

The Molecular Etiology of Deafness and Cochlear Implantation Performances in the Postlingually Deafened Cochlear Implantees

Ye Ji Shim[1]; Deuk Tae Cho[2]; Jin-Hee Han[2]; Ah-Reum Kim[2]; Hye-Rim Park[2]; Min Young Kim[2]; Jun-Ho Lee[3]; Jae-Jin Song[2]; Ja-Won Koo[2]; Seung Ha Oh[3]; Seungmin Lee[2]; Doo-Yi Oh[2]; Byung Yoon Choi[2]
[1]Seoul National University, Boramae Medical Center; [2]Seoul National University Bundang Hospital; [3]Seoul National University Hospital

Objectives
To investigate the molecular etiology of deafness and CI performances in the postlingually deafened cochlear implantees.

Design
74 postlingually deafened patients who had undergone CI between January 2010 and March 2017 at two tertiary hospital were included. Among them, 39 were consented to genetic testing(GT). Genetic etiologies were assessed by Sanger sequencing, panel sequencing or whole exome sequencing. Patients underwent GT were allocated to the following groups; Genetically diagnosed(GD),Genetically undiagnosed(GUD). Patients who did not undergo MGT were identified as controls. Speech performance was assessed using K-CID sentence score.

Results
Among the thirty-nine postlingually deafened cochlear implantees who underwent MGT, 20 patients (51%) turned out to have a conclusive Mendelian genetic etiology, leaving the other 19 patients (49%) undiagnosed. Such an extreme molecular etiologic heterogeneity as to involve 13 deafness genes was noted for this cohort. To interest, about half of the postlingually deafened genetic cases were due to autosomal recessive variants which were previously thought to causes mainly prelingual deafness. The most frequent causative gene was TMC1 (DFNA36) (3 cases), followed by the next tier of genes (2 cases each) (ACTG1, CDH23, COCH, SLC26A4, TMPRSS3) and the genes that were detected only once (ATP1A3, GJB2, ILDR1, MYO7A, NF2, OTOR and SERPNB6). All of these genes are expressed in membranous labyrinth(ML), except TMPRSS3 which is expressed abundantly in spiral ganglion neurons(SGN). The median ages of the GD, GUD and control groups were all younger than 55 years and the median deaf durations of the GD, GUD and control groups were all shorter than 5 years. Post-operative Spondee, PB word score and K-CID scores at 3months, 6months and 12months of the three groups overall did not show statistically significant differences, all reaching about at least 70% for K-CID

scores at 1 year. Rising trends in Spondee word scores and KCID scores of GD group at 3 months after CI tend to show slightly heavier, albeit statistically insignificant, than those of GUD group. Among the GD groups, there was no significant difference of speech perception performance between the groups of genes expressing in the SGN and genes expressed in the ML. Although most of the genetically diagnosed cases showed relatively good speech perception performances, two patients who had ACTG1 mutation and each one of the patients who had SLC26A4, CDH23, TMC1, TMPRSS3 and OTOR mutations had post-operative K-CID scores below interquartile range of control group. Among them, two patients with ACTG1 mutation and one of the patients with TMC1 mutation who had deaf durations over 10 years showed K-CID scores under 50% a year after CI.

Conclusions
Our genetic diagnosis rate was 51% in postlingually deafened cochlear implantees and a wide variety of causative genes have been found. Cochlear implantees who were genetically diagnosed showed speech perception performances comparable to the control group, even in the genes expressed in SGN. However, even with the same causative mutation, those with significantly longer deaf duration are associated with relatively worse performance, mandating prompt implantation, if indicated.

PS 757

Haplotype Analysis of GJB2 Mutations: founder effect or mutational hot-spot?

Jun Shinagawa[1]; Shin-ya Nishio[2]; Shin-ichi Usami[2]
[1]Shinshu University School of Medicine, Department of Otorhinolaryngology; [2]Department of Otorhinolaryngology, Shinshu University School of Medicine

Background
Congenital hearing loss is the most common sensory disorder with one out of 500 to 700 newborns experiencing bilateral hearing loss. The most frequent cause of congenital hearing loss is genetic etiology, and over 100 genes have been reported to be responsible for hereditary hearing loss. Among these genes, GJB2 is the most frequent causative gene worldwide. However, quite different types of GJB2 mutations have been identified among different ethnic populations. Recently, haplotype analysis using single nucleotide polymorphisms (SNPs) has enabled us to reveal that the commonly identified variants in many ethnic populations are caused by a common ancestor (viz., founder effect) or a mutational hotspot. We therefore performed haplotype analysis of some GJB2 mutations to investigate whether each mutation occurred via a founder effect or a hot spot muta-

tion. In addition, we estimated the time at which each GJB2 mutations occurred.

Methods
We enrolled 5,563 hearing loss patients with sensorineural hearing loss, and extracted patients with homozygous GJB2 mutations frequently identified in the Japanese population (i.e., c.235delC, p.V37I, p.[G45E, Y136X], p.R143W, c.176_191del, and c.299_300delAT). We performed SNP genotype analysis of the Tag SNPs inside of GJB2 gene and its peripheral 1M base region. We then analyzed the haplotype of each mutation, determined the presumed linkage disequilibrium region length, and then estimated the time at which each mutation occurred.

Results
A total of 273 patients with homozygous GJB2 mutations were identified among 5,563 patients (c.235delC: 192 cases, p.V37I: 39 cases, p.Y136X: 22 cases, p.R143W: 10 cases, c.176_191del: 2 cases, and c.299_300delAT: 8 cases). We performed haplotype analysis for 20 cases, Results showed that most patients with each mutation carried identical haplotypes in the peripheral region of the GJB2 gene. This result indicates that those mutations were caused by a founder effect, and each GJB2 mutation was estimated to originate about 8,000-12,000 years ago.

Conclusion
We performed haplotype analysis of commonly observed GJB2 mutations in the Japanese population and revealed that most of the GJB2 mutations occurred by a founder effect. We are now planning a haplotype analysis of GJB2 mutations commonly observed among different ethnic populations.

PS 758

A duplication mutation in HOXA2 causes autosomal dominant nonsyndromic mixed hearing loss and middle ear anomaly

Yoshihiro Noguchi[1]; Shin-ya Nishio[2]; Koichiro Wasano[3]; Taro Fujikawa[4]; Akinori Kimura[5]; Shin-ichi Usami[2]
[1]Department of Otorhinolaryngology-Head and Neck Surgery, International University of Health and Welfare School of Medicine; [2]Department of Otorhinolaryngology, Shinshu University School of Medicine; [3]Department of Otolaryngology Head and Neck Surgery, Keio University School of Medicine; [4]Department of Otolaryngology, Tokyo Medical and Dental University School of Medicine; [5]Department of Molecular Pathogenesis, Medical Research Institute, Tokyo Medical and Dental University

Middle ear anomaly can occur as a part of syndromic disorders, or as isolated defects. In the syndromic disorders, mutations in a variety of genes, including EYA1, SIX1, TCOF1, and NOG, have been reported to associate with middle ear anomalies. However, no causative gene for nonsyndromic hereditary middle ear anomalies had been reported. In this study, whole exome sequencing was performed for a Japanese family with autosomal dominant nonsyndromic mixed hearing loss and middle ear anomaly without apparent microtia. Seven potential causative variants, including a duplication variant in HOXA2, a deletion variant in MYCT1, and five non-synonymous missense variants were detected. Direct sequencing confirmed that all the seven variants were segregated with hearing loss. However, the five missense variants were predicted as "tolerated" in bioinformatics tools. Furthermore, MYCT1 was not likely to be a candidate causative gene, because it is thought to be a candidate tumor suppressor gene. Therefore, we considered HOXA2 to be the most potential candidate causative gene. Direct sequencing was carried out to screen HOXA2 mutations for other 19 patients with middle ear anomaly or microtia, but no mutation was detected. HOXA2 mutations were reported to cause autosomal recessive or dominant microtia in three families, but hearing loss was less constantly recognized in the families. Our findings suggested that a HOXA2 mutation caused autosomal dominant nonsyndromic mixed hearing loss, and middle ear anomaly but not apparent microtia.

Otoacoustic Emissions II

PS 759

Application of Otoacoustic Emissions to Spaceflight Fluid Shift Studies

David T. Kemp[1]; Douglas Ebert[2]; Rozela Melgoza[3]; Tyler Caldwell[4]; Richard Danielson[5]; Michael Stenger[6]; Alan Hargens[7]; Scot Dulchavsky[8]
[1]*Ear Institute, University College London;* [2]*KBRWyle Science;* [3]*Arizona State University;* [4]*University of Texas-Dallas;* [5]*Baylor College of Medicine;* [6]*NASA Johnson Space Center;* [7]*University of California;* [8]*Henry Ford Hospital*

Otoacoustic emissions (OAEs) have been recorded from International Space Station (ISS) crewmembers before during and after flight as part of NASA';s Fluid Shifts study. That study aimed to investigate the cause of the visual impairment associated with long-duration spaceflights in the microgravity environment, and its possible relation to raised intracranial pressure (ICP). OAE phase and amplitude are sensitive to posture change and ICP. They can be self-recorded using a handheld device and so were considered potentially useful as a noninvasive ICP monitor. Recordings were made using the Otoport Advance, clinical instrument (Otodynamics, UK).

During OAE recording audio frequency vibrations travel from the cochlea to the oval window and through the middle ear to the ear drum. This creates sound in the closed ear canal which is recorded by a microphone probe. Any change in ICP is quickly communicated to cochlea fluids, changing tension in the oval window and modifying the transmission of vibrations to the ear canal.

TEOAEs were recorded in response to 90dBSPLpe clicks using the 'QuickScreen'; protocol widely employed in newborn hearing screening. Ground-based measurements before and after the mission were made in three positions to alter ICP: seated, supine and 15^0 head down tilt (HDT). Preflight only, the 15^0 HDT recording was repeated with compensating lower body negative pressure (LBNP) applied . Inflight recordings in the microgravity of the ISS were made with and without LBNP. Data were collected from the right ears of 10 crewmembers.

Post recording data analysis was optimized to extract frequency specific phase changes from TEOAE waveforms. In most subjects the ground based data demonstrated systematic phase changes with posture between 800 and 1600Hz. Individual sensitivity to posture differed. Most subjects showed excellent long term repeatability. Compared to the seated baseline the phase changes averaged 15º for supine and 37º for HDT, reducing to 20º with LBNP applied. This pattern is consistent with expected ICP changes. The inflight TEOAE waveforms obtained under microgravity correlated strongly with the ground-based seated control data, with phase differences of only -10 to +10º in all but a few crewmembers. This led to the conclusion that pressure changes resulting from the microgravity environment were minimal in most crew members.

We are exercising caution before concluding that the exceptions seen to this pattern indicate ICP changes in individuals possibly more susceptible to the microgravity environment.The mechanics of OAE generation and transmission are complex. Factors other than ICP such as middle ear pressure, stapedial and tensor tympani muscle tone, acoustic coupling between probe and ear canal can affect OAE phase and amplitude. Wideband recordings of the ear canal acoustic response served as a control for some of these factors. We summarize experiments conducted to evaluate confounding factors and explain anomalous results.

PS 760

Phase characteristics of low-frequency distortion-product otoacoustic emissions in humans

Anders T. Christensen[1]; Carolina Abdala[2]; Christopher A. Shera[2]
[1]Keck School of Medicine, USC; [2]Auditory Research Center, Caruso Department of Otolaryngology, University of Southern California

Low-frequency distortion-product otoacoustic emissions (DPOAEs) indicate by non-invasive means the state and function of nonlinear mechanisms operating the apical half of the cochlea. Two stimulus frequencies, f_1 and f_2, evoke a prominent DPOAE component at the $2f_1$-f_2 frequency. In its phase measured with the ratio f_2/f_1 fixed across frequency, previous studies find a bend that is thought to mark a transition between apical and basal cochlear mechanics: At frequencies mapping to the base, the DPOAE phase is roughly invariant, consistent with the idea that the relative phase of the evoking stimulus waves scales with frequency. At frequencies mapping to the apex, the phase acquires a slope of approximately -1 cycle/octave for a typical stimulus ratio of 1.22. We previously reported a detailed account of the phase bend as a function of both frequency and f_2/f_1 ratio in 20 young, normal-hearing human subjects (Mechanics of Hearing Workshop, 2017). By extending the measurements 1-2 octaves below the standard frequency range we found that the bend does not occur in isolation---rather, it appears in our data to be the upper end of a sigmoidal-shaped phase-vs-frequency function that steepens towards narrow ratios and flattens towards wide ratios. Regardless of the ratio, however, the sigmoid is about 1.8 octaves wide, centered around 1.4 kHz. The present study extends this work and reports more measurements in select subjects at low frequencies and narrow ratios where noise and methodology are most confounding. In particular, poor signal-to-noise ratios near the low-frequency end of the sigmoid in some subjects made us uncertain of its prevalence. Measurements with improved SNR will enable us to determine whether the apical-basal transition is as abrupt as single phase breaks in the literature suggest, or whether a single break tells only half the story of a transition that happens over roughly 2 octaves as suggested by our sigmoidal-shaped curves. We discuss possible origins of the sloping phase, which include both passive transmission and active generation mechanisms.

PS 761

Examining the relationship between human cochlear tuning and distortion product otoacoustic emission amplitudes as a function of f2/f1 ratio

Uzma S. Wilson[1]; Sriram Boothalingam[2]; Jenna Browning-Kamins[1]; Alessandra Durante[3]; Sumitrajit Dhar[1]
[1]Northwestern University; [2]University of Wisconsin-Madison; [3]FCMSCSP

Background

Distortion product otoacoustic emissions (DPOAEs) recorded in the human ear canal are a mixture of two components: 1) nonlinear distortion generated within the overlap of the two stimulus tones f_1 and f_2, and 2) reflections from the $2f_1$-f_2 characteristic place. DPOAEs, when measured as a function of f_2/f_1 ratio show a band-pass shape resembling a filter. This bandpass property of DPOAEs could provide a non-invasive and objective estimate of human cochlear tuning. Here we report estimates of tuning (Q_{erb}) derived from the amplitude ratio function of the DPOAE distortion component ($DPOAE_{gen}$) for f_2 up to 16 kHz and examine their level dependence.

Methods

DPOAEs were recorded from seven normal-hearing participants (age 16-22 years) for fixed f_2 between 0.75-16 kHz using two sets of primary levels (L_1/L_2= 65/55 dB FPL and 55/40 dB FPL). Stimuli were calibrated in terms of forward pressure level (FPL) at the eardrum. F_1 was swept over a range of f_2/f_1 ratios from 1.05 to 1.5 for each f_2 frequency. Composite DPOAE levels were estimated using the least squares fit method, and DPOAE components were separated using an inverse-FFT method. Sharpness of tuning (Q_{erb}) was determined by dividing the best DPOAE frequency by the bandwidth of a rectangular filter that passes the same total power as the $DPOAE_{gen}$ filter. Linear regression analyses were performed to examine frequency and level effects on Q_{erb}.

Results

Our findings demonstrate that Q_{erb} derived from $DPOAE_{gen}$ filters increased as a function of f_2 frequency and decreased as a function of stimulus levels, except at 0.75 kHz, where a higher value of Q_{erb} was observed compared to 1kHz. Our findings also confirm that Q_{erb} is significantly correlated with the optimal f_2/f_1 ratio yielding the maximum DPOAE (r(9)=-0.94, p <.001).

Conclusions

The frequency- and level-dependence of tuning estimates from $DPOAE_{gen}$ filters are consistent with the mechanical tuning properties of the cochlea. The deviation from expected Q_{erb} at 0.75 kHz could be due to the basal

to apical differences in scaling symmetry. Lastly, we conclude based on the strong correlation between optimal f_2/f_1 ratio and Q_{erb} that human tuning estimates may be derived from the optimal f_2/f_1 ratio of DPOAEs. However, additional studies using this approach could provide useful insights on normal human cochlear processing and how it may be affected by aging or ototoxicity.

PS 762

Human Olivocochlear Efferent Activity Elicited by Dynamic Versus Static Noise

Ian B. Mertes; Kristin M. Johnson; Zoë A. Dinger
University of Illinois at Urbana-Champaign

Background
The medial olivocochlear reflex (MOCR) reduces outer hair cell electromotility to improve encoding of signals in noise. Human MOCR activity has been widely studied using contralateral suppression of otoacoustic emissions. Contralateral suppression elicited with static white noise has been well characterized. However, research on contralateral suppression elicited with dynamic, temporally-complex noise has yielded conflicting results. Some studies have shown that dynamic noises evoke greater MOCR activity than static noises (Maison et al. 1997, 1999), while others have found either no difference (Boothalingam et al. 2014) or that static noises activate greater MOCR activity (Kalaiah et al. 2017). The purpose of the current study was to compare the magnitude of contralateral suppression evoked by dynamic versus static noises with the same spectral content as a step toward determining how the MOCR responds to dynamic noise similar to that encountered in real-world listening situations.

Methods
Adults ages 18 to 40 with normal hearing and normal middle ear function participated. Transient-evoked otoacoustic emissions (TEOAEs) were measured using 65 dB pSPL clicks at a rate of 19.5/s. The MOCR was activated using three noise elicitors, referred to collectively as contralateral acoustic stimulation (CAS): 1) static white noise; 2) 100-Hz AM white noise; 3) white noise modulated by the envelope of a four-talker babble noise. All noises had the same spectral content. To examine the effect of CAS level on contralateral suppression, each noise elicitor was presented separately at 50 and 60 dB(A) SPL. Contralateral suppression was quantified for each noise elicitor as the decibel difference in TEOAE magnitude averaged across 1000-2000 Hz obtained without versus with CAS. Middle-ear muscle reflex (MEMR) activation was assessed using methods described in Mertes and Leek (2016).

Results
Preliminary results obtained from 12 subjects without MEMR activation showed a range of contralateral suppression values across subjects, consistent with previous reports. Contralateral suppression grew in magnitude with increasing CAS level for all noise elicitors, as expected. Mean contralateral suppression magnitude and growth functions were qualitatively similar between the three noise elicitors. Statistical comparisons will be conducted after data from a larger number of subjects are obtained.

Conclusions
The MOCR is responsive to both dynamic and static noise elicitors presented at levels of 50 and 60 dB SPL. Results will be discussed in terms of the potential functional relevance of the MOCR for listening in background noise that is dynamic in nature.

PS 763

The Relationship between Auditory Neural Response and Cochlear Tuning in Children Suspected with Auditory Processing Disorder

Sriram Boothalingam[1]; Sangamanatha Ankmnal Veeranna[2]; Chris Allan[2]; David Purcell[3]; Prudence Allen[2]
[1]*University of Wisconsin-Madison;* [2]*Western University;* [3]*Associate Professor*

Auditory processing disorder (APD) is characterized by poor speech perception in noise despite clinically normal audiograms. The test battery typically used for the diagnosis of APD is highly heterogeneous, with an emphasis on the central auditory nervous system. As such, the peripheral auditory system is typically only screened for the presence of an overt hearing loss. Our previous work suggested that children suspected of APD (sAPD) have atypically sharp cochlear tuning. We speculated that processing aberrations at the periphery could cause a cumulative detrimental effect on auditory neural responses. In the present work, we extend on our previous findings and test the hypothesis that cochlear tuning influences auditory brainstem response (ABR) latencies. Our hypothesis is based on filter theory, which suggests that a sharper filter will take longer to build-up and ring longer. We predict that sharper cochlear filters in sAPD should result in delayed ABR wave latencies compared to typically developing children. Cochlear tuning was derived from stimulus frequency otoacoustic emission (SFOAE) group delay around the 1 kHz region. SFOAEs were elicited using the suppression method with 40 dB SPL tones at discrete frequencies between 928 and 1248 Hz at 16 Hz intervals. ABR was measured using clicks presented at 80 dB nHL. ABR peak I latency was used for correlation with SFOAE group delay.

Preliminary data from 16 sAPD and 6 typically developing children show positive correlations between cochlear tuning and ABR peak I latency. Cochlear tuning also explains a significant proportion of the variance in ABR peak I latency (R2 = 0.25). Our preliminary findings suggest that cochlear tuning, objectively measured using SFOAE group delay, could be a valuable predictor of neural processing delays. As such, it appears that irregularities in cochlear processing might play a precursive role for neural problems higher-up in the auditory system. Therefore, including tests of cochlear function, such as tuning, will greatly enhance the diagnostic validity of APD test batteries.

PS 764

Swept-tone Stimulus-Frequency OAEs in Human Newborns

Carolina Abdala; Ping Luo; Yeini Guardia
Auditory Research Center, Caruso Department of Otolaryngology, University of Southern California

Otoacoustic emissions (OAEs) are a sensitive gauge of inner ear health and a remote metric of cochlear mechanics. For this reason, they are ideal for assessing hearing status in newborns and for probing maturation of cochlear function. The stimulus-frequency OAE (SFOAE), a reflection-source emission, has not been examined for its clinical utility although it is thought to be sensitive to mild disruptions in cochlear sensitivity and tuning. In a previous study, we reported on SFOAEs measured in a small number of newborns for a very narrow range of frequencies to show feasibility of SFOAE measurement in this population. However, the SFOAE has not been optimized for or fully characterized in newborns. Because the SFOAE is a low-level response, the averaging required to obtain a robust response with adequate SNR is challenging, in particular in newborns who have an elevated noise floor.

Here, we applied rapid swept-tone methodology to characterize SFOAEs in a group of newborns (n = 28) at 40 dB SPL across a four-octave frequency range. We swept the stimulus (using concurrent, stacked frequency segments) hundreds of times at a rate of 2 octaves per second from 0.5 to 8 kHz and used the interleaved suppression method to extract SFOAEs. Of the 28 newborns tested, 17 (60%) had a measurable SFOAE as per our definition: SNR ≥ 6 dB for at least 50% of analyzed frequency bands. Average SFOAE levels measured at spectral maxima ranged from 2 to 10 dB SPL over most of the frequency range; the highest SFOAE levels were in the low-to-mid-frequency bands (1-2 kHz) while the response dropped to negative values at the highest frequencies. Previously published work from our lab report adult SFOAEs that are roughly 4-5 dB lower than the newborn data measured here (though protocols/analyses techniques differed between studies). Phase vs. frequency functions were steep in newborns, and SFOAE phase accumulated nearly 40 cycles across the frequency range; likewise, the SFOAE delay (normalized by frequency and expressed in periods) was longer in newborns compared to published adult SFOAE delays. We consider the source of these age differences and discuss technical challenges to SFOAE recording in newborns, such as probe fit and stability (using the new ER10X probe), calibration methods (FPL vs SPL), noise immunity, and optimal recording and analysis strategies.

PS 765

Extended high frequency hearing, chirp-evoked otoacoustic emissions and speech-in-noise deficits reveal ototoxicity in children with cystic fibrosis

Lisa L. Hunter[1]; Chelsea Blankenship[1]; Douglas Keefe[2]; Patrick Feeney[3]
[1]Cincinnati Children's Hospital and University of Cincinnati; [2]Boys Town National Research Hospital; [3]Veteran's Administration National Research Center and Oregon Health Sciences University

Aminoglycoside drugs (tobramycin, amikacin) are frequently used to treat drug-resistant chronic lung infections in patients with cystic fibrosis (CF). These lifesaving drugs unfortunately cause hearing loss due to ototoxicity, the effects of which progress from the base to the apex of the basilar membrane. Therefore, in order to detect ototoxicity sooner, the frequency region above 8 kHz is critically important. Physiological measurements to detect ototoxicity at frequencies above 8 kHz are clinically important for children with CF who may be difficult to test with behavioral measures. This study reports extended high frequency audiometric thresholds (0.25-16 kHz) with transient evoked otoacoustic emissions (TEOAEs) to diagnose ototoxic hearing loss in CF patients (N=103 ears, ages 6-19 y.) and age-matched controls (64 ears, no CF). TEOAEs were measured using chirp stimuli at frequencies from 0.7-14.7 kHz with constant incident pressure level across frequency. Reflectance and ipsilateral acoustic reflexes were measured prospectively up to 8 kHz. Hearing thresholds were significantly poorer in the CF group than the control group at all frequencies, but particularly from 8-16 kHz, with thresholds in the CF group ranging up to 80 dB HL. Speech-in-noise performance using the BKB-SIN test was significantly poorer for the CF group compared to controls and age norms, and was related to high frequency hearing loss. TEOAE signal to noise ratios were significantly poorer in the CF group with significant hearing loss in the 8-10 kHz frequency regions, compared to control ears without hearing loss. Broadband noise acoustic reflex thresholds were also higher in the CF ears with hearing

loss. Wideband reflectance measures were not significantly different among groups, which was evidence for the absence of conductive hearing loss. The area under the receiver operating characteristic curve (AUC) for prediction of hearing loss in the CF compared to the control group was largest at 8 and 10 kHz for TEOAE SNR (AUC=0.78 and 0.76). This is the first report of chirp TEOAE measures in the extended high frequency range, and demonstrates the utility of these measures for detection of cochlear impacts of ototoxicity. Elevation of acoustic reflexes and poor speech-in-noise in the absence of middle-ear dysfunction provides additional physiologic evidence of cochlear, and possibly neural deficits.

PS 766

Using transient-evoked otoacoustic emissions for personal identification: What Ménières disease data suggest

Chun-Chi Wang[1]; Ya-Hui Chen[2]; Tzu-Chi Liu[1]; Hau-Tieng Wu[3]; Pa-Chun Wang[4]; **Yi-Wen Liu**[1]
[1]National Tsing Hua University; [2]Cathay General Hospital; [3]Duke University; [4]Cathay General University

Research Background

Otoacoustic emission (OAE) indicates the functional status of cochlea and can be used for hearing diagnostic purposes. Some previous research showed that OAE could also be used as a biometric identifier because it reflects the characteristic of a cochlea and is difficult to mock. However, it is not clear if features of the OAE stay invariant when a person';s hearing condition changes. In this study, click-evoked otoacoustic emission (CEOAE) was measured longitudinally from normal hearing and Ménière disease (MD) subjects to investigate the potentials and limitation of using CEOAE for biometric identification.

Methods

Acoustic impulses were delivered to the ear canal at 10 clicks per second using the ER-10C system. The peak sound pressure level was 74 dB. For each ear, up to 3000 responses to the clicks were averaged and analyzed further. So far, the data have been obtained from both ears of 10 normal hearing (NH) subjects and 9 MD patients. Each subject was measured at least 3 times; for MD subjects particularly, the data include the first time they visit the clinic after symptoms occurred and subsequent visits up to 6 months later while they received treatment. This research was approved by the IRB of Cathay General Hospital in Taipei, Taiwan.

Results

Post-stimulus responses from 5.0 to 13.0 ms were analyzed. After artifact rejection and mean removal, root mean square (RMS) distances between the signals were calculated. For the data from MD affected ears, we found that distribution of the RMS distance is similar when comparing within the same ear vs. across different ears (p=0.36). For the data obtained from the other ear of MD subjects (not affected by MD), the distance distribution of same-ear vs. across-ear is significantly different (p<0.01). For NH ears, the CEOAE from each ear apparently remained unique and stable so that the ear identity can be correctly found with >90% accuracy using a nearest-neighbor algorithm.

Conclusions

We conclude that the Euclidean distance-based comparison has good potentials for identifying a person by CEOAE if the hearing is normal. The identification would fail when a person suffers from fluctuating cochlear hearing loss. However, even though the CEOAE waveform changes while MD patients receive treatment, we speculate that perhaps some hidden invariant features could still be found. Further research is warranted.
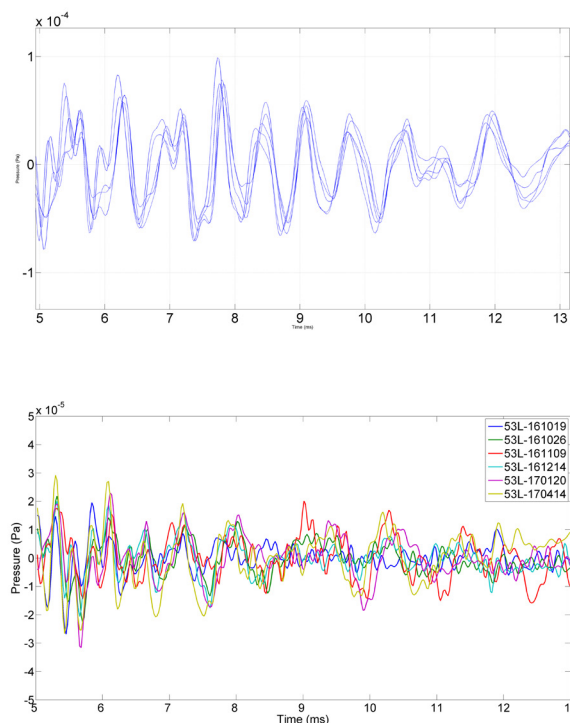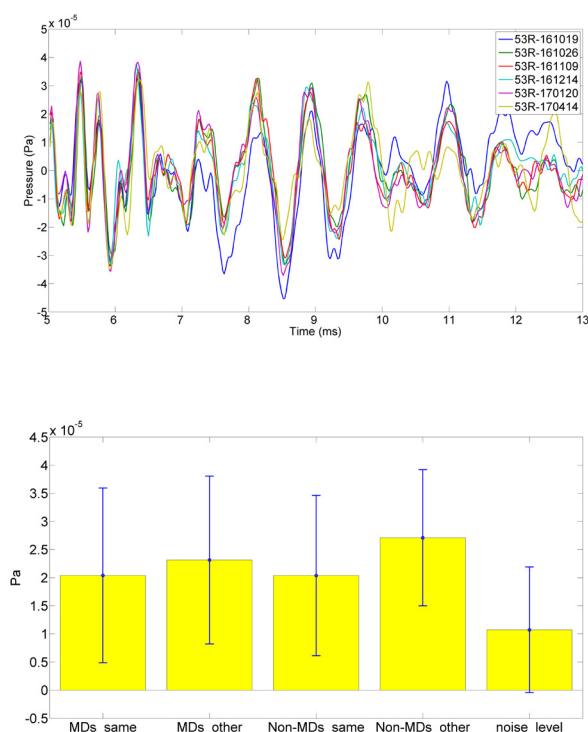
Ototherapeutics I

PS 767

Release of secretory exosomes as a mechanism of protection against hair cell death

Lindsey May[1]; Andrew M. Breglio[2]; Nora Welsh[1]; Lisa Cunningham[3]
[1]Section on Sensory Cell Biology, National Institute on Deafness and Other Communication Disorders, National Institutes of Health; [2]National Institute on Deafness and Other Communication Disorders & University of Oxford; [3]National Institute on Deafness and Other Communication Disorders

Background
We showed previously that supporting cells act as mediators of hair cell survival by secreting HSP70. Here we have examined the mechanisms of HSP70 secretion. HSP70 is released from a variety of cell types via exosomes, a type of endosomally-derived extracellular vesicle. This project investigates the roles of secretory exosomes as mediators of pro-survival signaling in the inner ear.

Methods
Exosomes from heat shocked and control utricles were visualized and quantified using nanoparticle tracking analysis (NTA), which tracks particles as they undergo Brownian motion. Exosome release was blocked using 0.5µM spiroepoxide, an inhibitor of neutral sphingomyelinase (nSMASE). To determine if exosomes are sufficient to protect hair cells against neomycin-induced death, we purified exosomes using ultracentrifugation and applied the exosomal (pellet) fraction or the non-exosomal (supernatant) fraction to naïve utricles. Hair cells were labeled and counted using myosin 7a immunoreactivity.

Results
Our data using NTA indicate that control utricles exhibit baseline exosome release, and heat shock results in ~4-fold increase in exosome release. Inhibition of nSMASe using spiroepoxide inhibited heat-shock induced release of exosomes. Inhibition of exosome release abolished the protective effect of heat shock. When applied to naïve utricles, isolated exosomes provided significant protection against neomycin-induced hair cell death; however the non-exosomal (soluble) fraction was not protective.

Conclusions
Our data using spiroepoxide indicate that exosome release is required for the protective effect of heat shock. Our data using isolated exosomes indicate that exosomes are sufficient to confer significant protection against neomycin-induced hair cell death. Together these data suggest that exosome release may constitute an important intercellular signaling event that can promote survival of sensory hair cells under stress.

Funding

PS 768

The antioxidant N-acetyl-L-cysteine (NAC) as a pharmacological candidate for age-related hearing loss

Sylvie Cosnier-Pucheu; Aurore Marie; Susanna Malmstrom; Sergio Gonzalez-Gonzalez
Cilcare, Montpellier, France

Introduction: Age-related hearing loss (ARHL) is the most common sensory disorder in the elderly population. The senescence-accelerated prone strain 8 (SAMP8) mouse model present accelerated senescence and have been identified as a model of gerontological research. SAMP8 displays sequential degeneration of cochlear hair cells, spiral ganglion neuron and stria vascularis which mimic human ARHL. The molecular mechanisms associated with SAMP8 senescence involve oxidative stress and altered levels of antioxidant enzymes leading to chronic inflammation and apoptosis. Here, we studied the

effect of NAC, an antioxidant, on SAMP8 hearing loss to determine the potential interest of this model in the study of new therapies. Material & Methods: To characterize hearing loss in SAMP8, we added NAC in the drinking water at 61 mM and we measured the auditory brainstem response (ABR) and the distortion product otoacoustic emissions (DPOAEs), two auditory parameters, every two weeks during two months. Results: we observed a strong decrease of ABR thresholds at all frequencies and a significant increase of DPOAE amplitude in NAC treated group compared to vehicle. Conclusion: NAC reduces the accelerated senescence process by decreasing ABR thresholds and protecting cochlear hair cells, strongly suggesting that antioxidants could be a pharmacological target for ARHL.

PS 769

The Effect of Atorvastatin on Hearing Impairment in Diabetic Mice

Yun Yeong Lee; Oak-sung Choo; Mi-Jin Choi; Yun-Hoon Choung
Department of Otolaryngology, Ajou University School of Medicine, Suwon, Republic of Korea

Research Background
It is known that high-fat with fructose diet (HF/F-diet) causes diabetes mellitus (DM). DM related hearing impairment is associated with hyperglycemia and hyperlipidemia which affects the microcirculation of the inner ear. Atorvastatin, a synthetic HMG-CoA reductase inhibitor used for the treatment of hyperlipidemia, significantly lowers plasma cholesterol and low-density lipoprotein cholesterol. The action of atorvastatin in hearing loss is still under debate. Up to date, atorvastatin has been reported to prevent noise-induced hearing loss and delay the deterioration of inner ear function in aging. Opposing theories have also been proposed such as the cause for irreversible hearing loss and increase in blood glucose. Thus, the aim of this study was to investigate the effect of atorvastatin in HF/F-diet-induced diabetes-associated hearing impairment using c57BL/6 mice.

Methods
C57BL/6J (7-week-old) mice were randomly assigned to normal and diabetic group. They were then divided into the following subgroups: (normal, n = 10; HF/F-diet with saline vehicle, n = 15; atorvastatin with HF/F-diet, n = 15). We established a diabetic model at 12 weeks followed by statistically significant difference in blood glucose, intraperitoneal glucose (IPGTT), insulin tolerance (IPITT), and serum lipid level. Vehicle or atorvastatin (20 mg/kg) were injected via intraperitoneal injection (IP) every other day from week 12 to 16. We analyzed 1) body weight, food/water intake, 2) Blood glucose, IPGTT and IPITT, 3) ABR measurement at 16, 32 kHz pre and post-16 weeks. Mice were sacrificed at week 17, and 4) serum lipid, 5) histology, and 6) Immunohistochemistry (IHC) were analyzed.

Results
The pre-medication ABR results showed normal hearing in all mice. After 16 weeks, increase in ABR threshold (22dB ± 1.5 shift) were noted in the HF/F diet with vehicle, and hearing preservation were noticed in the atorvastatin group. Moreover, increased body weight, blood glucose, serum lipid, fat storage, IPGTT, and IPITT were all improved by atorvastatin. From histological analysis, nuclear alterations of spiral ganglion neuron and swelling of stria vascularis were preserved by atorvastatin. Also, immunofluorescence analysis showed that atorvastatin was able to decrease the DHE fluorescence at inner, outer and supporting cells, and the Tunnel fluorescence at spiral ganglion neuronal and stria vascularis.

Conclusions
Atorvastatin could be a major mediator for prevention of DM mediated hearing impairment by decreasing ROS in hair and supporting cells along with inhibiting cell death in stria vasculais and spiral ganglion neurons through lowering of body weight, serum lipid, glucose and liver steatosis.

Acknowledgments

PS 770

AAV-Mediated Neurotrophin Gene Therapy Elicits Improved Survival of Cochlear Spiral Ganglion Neurons in Neonatally Deafened Cats

Patricia Leake[1]; Stephen Rebscher[1]; Chantale Dore'[1]; Christian Fahlman[1]; Lawrence R. Lustig[2]; Bas Blits[3]; Omar Akil[1]
[1]*University of California San Francisco, Epstein Lab, Dept Otolaryngology-HNS; *[2]*Dept Otolaryngology-HNS, Columbia University, New York; *[3]*uniQure biopharma B.V., Amsterdam, The Netherlands*

Cochlear implant (CI) efficacy depends partly upon the survival and health of the spiral ganglion (SG) neurons, which degenerate progressively following deafness. In early-deafened cats, intracochlear infusion of brain-derived neurotrophic factor (BDNF) from an osmotic pump improves neural survival. However, high concentrations of BDNF also elicit disorganized, ectopic sprouting of radial nerve fibers that could be detrimental to CI func-

tion due to loss of precise tonotopicity. Further, osmotic pumps are impractical for clinical application. This study explores the potential for using adeno-associated viral vectors (AAV) to elicit targeted neurotrophic factor expression and thereby promote improved SG survival in the deafened cochlea. Kittens were deafened prior to hearing onset by systemic injections of neomycin sulfate. ABRs showed profound hearing loss by 16-18 days postnatal. At ~4 weeks of age, AAV2-GFP (green fluorescent protein), AAV5-GFP, AAV2-BDNF, or AAV5-GDNF (glial-derived neurotrophic factor) was injected (10ul) through the round window into the left scala tympani. Four weeks following AAV2-GFP injections, immunohistochemistry showed strong expression of the GFP reporter gene in residual inner and outer hair cells, inner pillar cells, and some SG neurons. AAV5-GFP elicited robust transduction of IHCs and some SG neurons, but few OHCs or supporting cells. Animals examined 10 weeks after injections of AAV5-GDNF or AAV2-BDNF showed modest neurotrophic effects, with 5-6% increases in SG survival vs contralateral deafened ears. However, AAV5-GDNF also elicited undesirable disorganized ectopic sprouting of radial nerve fibers, which did not occur with AAV2-BDNF. Thus, long-term efficacy was assessed only for AAV2-BDNF. Cochleae examined ~6 months after AAV2-BDNF injections showed highly significant neurotrophic effects, with SG density averaging ~53% of normal vs. 39% contralateral and greatly improved radial nerve fiber survival (47% of normal vs. 24%). Importantly, the gene therapy approach also avoids deleterious side effects seen with high BDNF concentrations from osmotic pumps (ectopic fiber sprouting, angiogenesis, fibrosis). In summary, cochlear gene therapy with AAV2-BDNF promoted improved SG and radial nerve fiber survival in a cat model of congenital deafness. This research ultimately could benefit CI recipients by providing a clinical therapy to forestall auditory nerve degeneration and support optimized CI function. Moreover, recent studies have shown that primary loss of SG neurons in human cochleae may underlie hearing loss with aging or noise damage. Thus, the findings that AAV2-BDNF therapy can promote SG and radial nerve fiber survival could be an important first step toward a therapy to halt hearing loss or even restore hearing by reconnecting radial nerve fibers to hair cells.

Translational Development of the Clinical Stage Oral Otoprotectant SENS-401 for Sensorineural Hearing Loss

Jonas Dyhrfjeld-Johnsen; Mathieu Petremann; Christophe Tran Van Ba; Charlotte Romanet; Pierre Attali
Sensorion

Sensorineural hearing loss can be severely debilitating, leading to communication and learning problems, social isolation and cognitive decline. Currently no approved pharmaceutical treatment exists, underscoring the imperative for developing innovative treatments to serve this currently unmet medical need. Successful translational drug development hinges on reliable preclinical proof of concept in validated, pathologically relevant models, determination of required drug exposures and the confirmation that such exposures can be safely achieved and tolerated in man.

SENS-401 is small molecule, clinical stage drug candidate with orphan drug designation for the treatment of sudden sensorineural hearing loss and prevention of platinum-induced ototoxicity in pediatric patients.

Oral doses of 6.6, 13.2 and 26.4 mg/kg SENS-401 were tested versus placebo in models of severe noise-induced hearing loss (NIHL: 120 dB octave band noise 8-16 kHz for 2 hrs, mean acute hearing loss of 55+ dB) and cisplatin-induced ototoxicity (CIO: 8 mg/kg iv, 30 min infusion, hearing loss of 30-50 dB at D14). In the NIHL model, SENS-401 treatment was effective when initiated up to 48 hours after acoustic trauma, with significant and clinically relevant improvement of ABR threshold recovery (~130-430% enhancement) and DPOAE amplitude recovery (~230-630% enhancement) from 24h post-trauma to D14. Twice daily administration of 6.6 and 13.2 mg/kg were as effective as once daily 26.4 mg/kg SENS-401 for 28 days. In the CIO model, all three doses given orally once daily starting 15 min before cisplatin reduced ABR threshold shifts (up to ~79%) and DPOAE amplitude losses (up to ~78%) depending on frequency. In both models, SENS-401 demonstrated significant enhancement of outer hair cell survival.

The pharmacokinetics and local exposure of the tested SENS-401 doses demonstrated dose-dependent increases in blood plasma content, with relative concentrations in perilymph and inner ear tissue of respectively 25-30% and 35-50%.

In a recently finished double blind, placebo controlled phase 1 clinical trial, healthy volunteers received oral

SENS-401 twice daily for 7 days at increasing doses. SENS-401 was well tolerated with mild to moderate adverse events comparable to placebo, and the highest tested dose achieved a Cmax of 1.6-fold and AUC of 4-fold the minimal effective dose in the preclinical models.

Together, the preclinical pharmacodynamic and pharmacokinetic data along with healthy volunteer safety and pharmacokinetic data support the feasibility of significant and clinically relevant treatment effects for patients in SSNHL or CIO.

Clinical trial planning and regulatory interactions are ongoing targeting phase 2/3 clinical trials in 2018.

PS 772

CDK2 Inhibitors as Candidate Therapeutics for Cisplatin- and Noise- Induced Hearing Loss - Preclinical In Vivo Studies

Tal Teitz[1]; Jie Fang[2]; Justine Bonga[1]; Shiyong Diao[2]; Robert Hazlitt[3]; Jian Zuo[4]
[1]Department of Developmental Neurobiology, St. Jude Children's Research Hospital; [2]St. Jude Children's Research Hospital; [3]Departments of Developmental Neurobiology and Chemical Biology and Therapeutics, St. Jude Children's Research Hospital; [4]Department of Developmental Neurobiology, St. Jude Children's Research Hospital, Memphis, Tennessee, USA

There are currently no FDA approved drugs to treat cisplatin- and noise-induced ototoxicity. Our previously described high-throughput cell based screens identified CDK2 inhibitors as potential protective agents against cisplatin-induced damage to the cochlear cells. Here we compared our top CDK2 inhibitor, kenpaullone, with four well-known protective benchmark compounds and found that kenpaullone is more potent (lower cisplatin IC50) in ex-vivo mouse cochlear explant essays. In vivo we compared CDK2 knockout (KO) and wild-type (WT) littermate mice for noise- and cisplatin- sensitivities. For cisplatin ototoxicity, we utilized a multiple low dose cisplatin administration regimen that mimics the cisplatin treatment regimen in human cancer patients (Roy et al, JCI 2013): three rounds of cisplatin treatments, each consisting of four intraperitoneal (IP) injections of cisplatin (4 mg/kg), followed by recovery periods (10-15 days) and ABR measurement recording after the last treatment (47 days total). In this mouse model we observed complete protection at all frequencies in the KO CDK2 mice and significantly lower ABR threshold shifts (11.6 dB) than the WT littermates at 32 kHz (15-16 mice tested from each group). When the mice were exposed to 100 dB SPL, 8-16 kHz octave band of noise for 2 hours, we recorded in the CDK2-deficient mice an 8 dB

average lower ABR threshold shifts and enhancement of wave 1 amplitude at 8 kHz frequency, 14 days post noise (11-14 mice tested from each genotype). Finally, our top CDK2 inhibitor, kenpaullone, was tested in a well-established outbred Wistar rat model, which in comparison to our mouse models, provided greater threshold shifts after cisplatin treatment. In each rat, we delivered either kenpaullone (310 µM, 30 µl) or carrier 0.5% DMSO/PBS control by intra-tympanic injection one hour before cisplatin treatment. ABR thresholds were measured at pre- and post-day 4 of cisplatin administration. Kenpaullone provided full protection against cisplatin when administered at 13 and 16 mg/kg, with the magnitude of protection reaching approximately 40 dB, when compared to that in carrier DMSO/PBS-treated rats at 4-22 kHz frequencies (8-10 rats tested from each group). Rats injected intra-tympanically with kenpaullone alone had no statistically significant threshold shifts compared to rats injected with kenpaullone and treated with cisplatin at all frequencies tested. Based on these promising in vivo results in two animal models we will next determine the PK/PD properties and optimize the formulation and delivery of kenpaullone to the ear for best protection against cisplatin- and noise- induced hearing loss.

PS 773

Otoprotectant UoS 13143 (Linopirdine) Prevents Gentamicin-Induced Stimulation of Mitochondrial Respiration (State 4)

Molly O'Reilly; Luke Young; Anthony Moore; Guy P. Richardson; Corné J. Kros
University of Sussex

Background
The aminoglycosides are broad-spectrum antibiotics prescribed to treat life-threatening bacterial infections such as septicaemia. Whilst highly efficacious, they are also ototoxic. The antibiotics enter the sensory cells of the inner ear through their mechano-electrical transducer channels. They are thought to trigger mitochondrial dysfunction, thereby initiating apoptosis. Consistent with this, gentamicin has been shown to inhibit state 3 respiration in renal mitochondria (Simmons et al 1980 J Pharmacol Exp Ther 214:709-715). We screened a Tocris Ion Channel Library of 160 compounds and identified 13 that provide protection against gentamicin-induced hair-cell death in mouse cochlear cultures. Here we investigate whether the most effective otoprotectants (UoS 13097, 13142 and 13143) may provide protection by preventing the effects of gentamicin on mitochondrial respiration.

Methods
Oxygen consumption of isolated rat liver mitochondria was measured using an Oroboros oxygen electrode. Uncoupled state 3 respiration was investigated in the

presence of carbonyl cyanide-p-trifluoromethoxyphenyl-hydrazone (FCCP) (1 μM). State 4 respiration was determined following the addition of succinate (10 mM). Mitochondria were pre-incubated for 10 minutes either with 5 mM gentamicin or gentamicin plus the otoprotective compound.

Results
We confirm that gentamicin inhibits mitochondrial state 3 respiration and furthermore show that it significantly stimulates state 4. Ten minutes pre-incubation with 5 mM gentamicin followed by succinate resulted in a 2.1 fold increase in the O_2 consumption rate (117 and 55 nmolsmin^{-1}mg^{-1} respectively) (p = 0.0008). In the absence of gentamicin, FCCP increased succinate-dependent state 4 O_2 consumption 3.4 fold (186 nmolsmin^{-1}mg^{-1}) (p < 0.0001). However in the gentamicin-treated condition, uncoupled respiration was only 105 nmolsmin^{-1}mg^{-1}, suggesting that gentamicin inhibits state 3U respiration, possibly through substrate depletion. The respiratory control ratio in the control was 4.0 and in the gentamicin-treated condition 0.96. One of the three lead Tocris compounds (UoS 13143) significantly prevented gentamicin-induced stimulation of state 4 respiration, whereas the remaining two (UoS 13097 and 13142) did not. None of the compounds tested prevented gentamicin-induced inhibition of state 3U respiration.

Conclusions
Gentamicin inhibits state 3 and stimulates state 4 respiration in isolated rat liver mitochondria. The latter is prevented by one of the most effective otoprotective compounds identified in the Tocris library. Blocking the stimulation of state 4 mitochondrial respiration may therefore be an effective approach for combating aminoglycoside-induced ototoxicity. Further experiments will investigate effects of gentamicin on mitochondrial membrane potential, production of reactive oxygen species, and on mitochondria from different tissues.

PS 774

D-methionine Significantly Rescues Steady-State-Noise-Induced Hearing Loss at Time Delays Up toand Including 36 hours Across a Wide Dosing Range in the Chinchilla

Kathleen CM. Campbell[1]; Nicole Cosenza[1]; Shari Randall[1]; Stephen Verhulst[1]; Jun Qin[2]; Leonard Rybak[1]; Robert Meech[1]
[1]*Southern Illinois University School of Medicine;*
[2]*Southern Illinois University*

Background
Hearing loss is the third most common chronic condition in the United States (Centers for Disease Control and Prevention). D-methionine, the optimal isomer of the essential amino acid L-methionine, was discovered as an otoprotective agent against cisplatin-induced hearing loss in 1996 (Campbell et al. 1996). Since then, D-methionine has been continuously studied as an otoprotective agent against both drug- and noise induced-hearing loss. The aim of this study is to optimize D-methionine rescue dosing in steady state noise-induced hearing loss investigating dose-response curves at varying time delays knowing that future patients may not always access treatment immediately after noise exposure.

Methods
Twelve groups of male chinchillas underwent a baseline auditory brainstem response (ABR) test, and then exposed to 105 dB SPL broad band noise for 6 hours. Subjects were divided into one of three different rescue time groups: 1 hour, 24 hours, or 36 hours after noise exposure and further divided into one of four dosing groups per rescue time: saline control, 50 mg/kg/dose, 100 mg/kg/dose, 200 mg/kg/dose. D-methionine was administered every twelve hours IP for a total of five injections. Then 21 days after noise exposure, animals were given a second ABR to measure permanent ABR threshold shift from baseline.

Results
The saline control group at all three rescue time points showed the greatest ABR threshold shifts, with mean threshold shifts across all frequencies and time delays ranging from 19 dB to 34 dB. D-met treated groups showed significant (p ≤ 0.01) otoprotection at all rescue time delays, dosing levels, and stimulus frequencies tested relative to the noise-exposed control groups. Overall, no significant difference existed between dosing levels, with a few exceptions for isolated frequencies by ear, however protection was significant for both ears for all frequencies at all dosing levels relative to the controls.

Conclusions
D-methionine protects against steady-state noise-induced hearing loss across a wide range of dosing levels and rescue time periods up to and including 36 hour delay for initial administration.. These results can be critical for eventual clinical use, which aims to provide patients with the lowest maximally effective dosage of therapeutic agents over a range of time delays to treatment.

Campbell K, Rybak L, Meech R, Hughes L. 1996. D-methionine provides excellent protection from cisplatin ototoxicity in the rat. Hearing Research 102: 90-98.

Centers for Disease Control and Prevention website. Accessed Sept 20, 2017. http://www.cdc.gov/features/worker-hearing-loss/

PS 775

Combined administration of P7C3-A20 and ibuprofen protects rat spiral ganglion neurons after aminoglycoside deafening

Muhammad Rahman[1]; Bo Peng[2]; Catherine Kane[2]; Benjamin Gansemer[2]; Andrew A Pieper[3]; Steven H. Green[4]
[1]Interdisciplinary Graduate Program in Human Toxicology, The University of Iowa; [2]Department of Biology, The University of Iowa; [3]Department of Psychiatry, The University of Iowa; [4]The University of Iowa

Background

Spiral ganglion neurons (SGNs) gradually die after destruction of hair cells, their sole afferent input. During SGN degeneration, the ganglion exhibits both inflammation and upregulation of the major NAD catabolizing enzyme, CD38, an activation marker for inflammatory cells. The novel P7C3 series of neuroprotective compounds helps stabilize neurons in times of energetic stress by activating the rate-limiting enzyme NAMPT in the NAD salvage pathway. Here, we assessed the individual and combined abilities of P7C3A20, a highly active analog of P7C3, and the non-steroidal antiinflammatory agent, Ibuprofen to protect SGNs from death in a preclinical model of kanamycin-induced deafening by hair cell destruction.

Methods

Sprague Dawley rats were deafened by daily intraperitoneal injection of kanamycin, postnatal day 8 (P8)-P16. Rats showing an ABR for stimuli

Results

Kanamycin injection resulted in loss of inner hair cells throughout most of the cochlea. By P70, SGN density in kanamycin-injected rats was significantly reduced by ~70% in the basal region. The magnitude of SGN loss Either P7C3 or Ibuprofen improved the survival of SGNs after in the basal region was significantly (P, from ~30% to ~50% whereas a combination of these two agents improved it to ~ 60% reduced by injection of P7C3 or of Ibuprofen . Combined administration of these two agents further augmented protection of SGNs . We conclude that P7C3, Ibuprofen or a combination of these

two is protective against SGN death in basal cochlea after aminoglycoside deafening. This further suggests that dysregulation of NAD+ metabolism in both hair cells and inflammatory cells in the spiral ganglion may play a role in SGN death after deafening, and provide a basis for new therapeutic treatments for patients.

PS 776

Otoprotective Effect of a Propargylamine Derivative and its Analogue in Aminoglycoside-Induced Hearing Loss Model in Mice

Viktória Humli[1]; Judit Szepesy[2]; Szilárd I. Szabó[3]; Gábor Polony[4]; Anita Gáborján[4]; László Tamás[5]; Péter Mátyus[6]; György B. Halmos[7]; Balázs Lendvai[8]; E. Szilveszter Vizi[3]; Tibor Zelles[9]
[1]Institute of Experimental Medicine, Hungarian Academy Of Sciences; Department of Pharmacology and Pharmacotherapy, Semmelweis Universiy; [2]Department of Pharmacology and Pharmacotherapy and Department of Otorhinolaryngology, Head and Neck Surgery; Semmelweis Universiy; [3]Institute of Experimental Medicine Hungarian Academy of Sciences, Laboratory of Drug Research; [4]Department of Otorhinolaryngology, Head and Neck Surgery; Semmelweis Universiy; [5]Department of Otorhinolaryngology, Head and Neck Surgery, Semmelweis University; [6]Semmelweis University; Faculty of Pharmacology, Department of Organic Chemistry; [7]University Medical Center Groningen; Department of Otorhinolaryngology/Head & Neck Surgery; [8]Gedeon Richter Plc.; Pharmacology and Drug Safety Research; [9]Department of Pharmacology and Pharmacotherapy, Semmelweis University; Institute Of Experimenal Medicine,Hungarian Academy Of Sciences

Hearing impairment is the most frequent sensory deficit, affecting more than 360 million people worldwide. Despite the high prevalence, the sensorineural forms (SNHLs, e.g. presbycusis, noise- or aminoglycoside antibiotics induced hearing loss) have no effective pharmacotherapy. In this study, we tested the effect of selegiline [(-)-deprenyl] and one of its analogue in aminoglycoside antibiotic (AG) induced hearing loss. AGs are still indispensable in certain serious gram-negative infections like neonatal sepsis, intraabdominal infections or osteomyelitis, but can induce irreversible hearing loss. This side effect is primarily due to the generation of reactive oxygen species (ROS) and excitotoxicity resulting in the damage of hair cells, ribbon synapses, and auditory neurons. Selegiline is an irreversible monoamine oxidase-B (MAO-B) inhibitor used in the treatment of Parkinson disease and major depression. It has known neuroprotective and anti-oxidative stress effects. Furthermore, as an enhancer of dopaminergic (DAergic)

neurotransmission it may also potentiate the release of DA from the lateral olivocochlear (LOC) efferents, which is considered to be a protective feedback pathway of the cochlea by reducing the excitotoxic damage of the primary auditory neurons.

The release of DA from the LOC efferents in the isolated mouse cochlea was measured in a perfusion system with tritium-labeled DA. The otoprotective effect of the compounds was tested in vivo in four weeks old male BALB/c mice. The AG kanamycin (800 mg/kg, s.c.) was administered twice daily in the first two weeks while the test compounds were injected subcutaneously once every day during the three weeks long experimental procedure. The hearing thresholds were measured at the beginning and three weeks later by auditory brainstem response (ABR). Click and burst (4, 8, 16, 32 and 65 kHz) stimuli were used.

We showed that selegiline potentiated the action potential-evoked DA release from the LOC efferents in the mouse cochlea in a dose-dependent manner. Its analogue was also effective. The kanamycin-induced threshold shifts of hearing were alleviated by both compounds at all three doses used (0.5, 3 and 6 mg/kg) in a dose-dependent manner. The most prominent effects appeared at frequencies of 8- 65 kHz.

The complex, multifactorial pathomechanism of SNHLs, like AG-induced hearing loss, most likely requires drugs acting on multiple targets for effective therapy. Selegiline and its derivative, by their effects of enhancing the release of the protective DA from LOC terminals, inhibiting oxidative stress and exerting neuroprotection might be a good candidate for small-molecule-based otoprotective pharmacotherapy.

PS 777

ORC-13661 is a Permeant Blocker of the Hair-Cell's MET Channels and Protects Mouse Outer Hair Cells from Gentamicin and Cisplatin

Sian R. Kitcher[1]; Esra D. Camci[2]; David W. Raible[2]; Edwin W. Rubel[3]; Guy P. Richardson[1]; Corné J. Kros[1]
[1]*University of Sussex;* [2]*University of Washington;* [3]*Department of Otolaryngology, Bloedel Hearing Research Center, University of Washington*

Background
ORC-13661, a derivative of PROTO-1, provides robust protection of larval zebrafish lateral line hair cells across a broad range of aminoglycoside antibiotics and exposure conditions, and protects hearing when rats are exposed in vivo to prolonged courses of amikacin treatment. Previous studies have shown that aminogly-

cosides reversibly block the mechano-electrical transducer (MET) currents in hair cells and can enter these cells via their MET channels. Furthermore, hair cells with non-functional MET channels are protected from cell death induced by both the aminoglycosides and the cancer chemotherapeutic cisplatin. The objectives of the current study were to determine if ORC-13661 (i) interacts with the hair cell';s MET channel, and (ii) protects basal-coil outer hair cells (OHCs) in mouse cochlear cultures from gentamicin and/or cisplatin.

Methods
Organotypic cochlear cultures were prepared from CD-1 mice at postnatal day 2. After 1-2 days in vitro, MET currents were recorded from OHCs before and during exposure to ORC-13661 (0.01-10 μM, provided by Oricula Therapeutics, LLC) using the whole-cell configuration of the patch clamp technique at membrane potentials ranging from -164 mV to +96 mV. Bundle stimulation was achieved using a fluid jet driven by a piezoelectric disc. To determine protective properties, 1-day-old cultures were treated with 5 mM of either gentamicin or cisplatin in the presence of vehicle or ORC-13661 (3-30 μM) for a further 48 h prior to fixation, staining and evaluation of hair cell numbers.

Results
Electrophysiological recordings reveal that ORC-13661 is a permeant blocker of the MET channel, with a half-blocking concentration of 180 nM in the presence of 1.3 mM Ca^{2+} at -104 mV. Maximum block was observed at intermediate membrane potentials, with release of the block at depolarized but also extreme hyperpolarized potentials, the latter indicative of permeant block. Survival of OHCs in cultures treated with 5 μM gentamicin or cisplatin in the presence of 20-30 μM ORC13661 was significantly increased relative to that observed in cultures treated with 5 μM gentamicin or cisplatin alone. At 10 μM, ORC-13661 provided partial protection, whereas below 10 μM no protection was seen.

Conclusions
This study demonstrates that ORC-13661 (i) is a relatively high-affinity, permeant blocker of the hair cell';s MET channel and (ii) protects mammalian OHCs from the damaging side effects of both gentamicin and cisplatin.

PS 778

Protective Effect of Anti-oxidant Avenanthramide-C on Ototoxicity

Munyoung Choi; Alphonse Umugire; Dami Kim; Sungsu Lee; **Hyong-Ho Cho**
Chonnam National University Hospital

Introduction Sensorineural hearing loss has no adequate chemicals to prevent or treat so far. Noise exposure instigates various physical damages and cellular changes within the cochlear hair cells that result in hearing loss. ROS found in the cochlea orchestrates cascade reactions with different molecules within the cochlea and disrupt normal physiological mechanisms, and results in hair cell death. Avenanthramide (AVN) extracted from oat possesses antioxidant properties and exert protection on various cell types. In this present study, we wanted to investigate whether AVN-C can protect auditory hair cell and preserve hearing from ototoxicity. Methods Wild type C57BL/6 mouse was randomly used in 6 to 12 per individual study. Mouse tissue fluid samples were analyzed using Liquid Chromatography-mass spectrophotometry to detect AVN-C in mouse tissue fluids. Mice were subjected under noise stimuli centered at 100 dB, 8 kHz for 6 hours once a day for 7 days with or without pre-treatment of 10 mg/kg of AVN-C. ABR thresholds measurement were done. Outer hair cells were visualized by immunohistochemistry using confocal microscope. HEI-OC cells were treated with AVN-C and gentamicin in vitro; flow cytometry and RT-qPCR were conducted. Results AVN-C reached its climax into mouse serum after 1 hour post I.P. injection and decreased with time, to be washed out within 6 hours. Furthermore, AVN-C crossed blood brain barrier and peaked within 2 hours. The permeability of AVN-C towards blood labyrinth barrier was outlined by its presence into perilymph and noise exposure enhanced its clearance. Pre-treatment of AVN-C 24 hours contributed to preserve hearing to temporary threshold shift noise. Moreover, in Permanent threshold shift with 100 dB for 7 days, AVN-C proved to procure prominent protection to noise overstimulated subjects, one month post noise exposure. Cochlea histological analysis demonstrated loss of outer hair cells (OHCs) in noise induced only group, and preservation of OHCs in AVN-C pre-treated subjects confirming the noteworthy protective effect provided by AVN-C over noise overexposure. AVN-C exhibited protective effect, and thwarted the toxicity caused by Gentamicin when treated to HEI-OC cell culture 24 hours in advance to Gentamicin. Several apoptotic and reactive oxygen species (ROS) genes were downregulated by AVN-C. Conclusion AVN-C provided a significant protective effect over ototoxicity in noise overexposed wild type subjects, and revealed to be a good candidate molecule for future therapy on sensorineural hearing loss.

Physiology & Neurophysiology of Binaural & Spatial Hearing

PS 779

Role of the saccule and lagena in near-field sound source localization by the plainfin midshipman fish

Nicholas R. Lozier[1]; Paul M. Forlano[2]; Robert A. Mohr[1]; Jonathan T. Perelmuter[2]; Andrew D. Brown[3]; Joseph Sisneros[1]
[1]*University of Washington;* [2]*Brooklyn College;*
[3]*Department of Speech and Hearing Sciences, University of Washington*

Sound source localization has been widely studied in mammals, birds, reptiles, and amphibians, however, the neural mechanisms for sound source localization in fishes are still largely unknown. The purpose of this study was to delineate the role of the inner ear auditory end organs (saccule and lagena) in sound source localization by plainfin midshipman fish (Porichthys notatus). The plainfin midshipman is an ideal species for studying sound source localization because reproductive females exhibit robust unconditioned phonotaxis toward natural or simulated male advertisement calls. This study sought to test the hypothesis that binaural input from the saccule and lagena is required for successful sound source localization. The auditory end organs were either unilaterally or bilaterally removed in reproductive females that were tested in a sound source localization assay. Sound source localization behavior was video recorded and later processed and analyzed in Image-J. Positive phonotaxic responses were observed under the following conditions: control (sham), bilateral saccule, unilateral lagena, and bilateral lagena removals. Preliminary analysis suggests that control treated midshipman had significantly lower latency response time (s) for sound source localization compared to midshipman that underwent bilateral saccule, unilateral lagena, and bilateral lagena removals. Also, orientation error to the sound source was greatest for fish with bilateral and unilateral lagena removals compared to fish in the control and bilateral saccule removal treatment groups. Preliminary results suggest that bilateral saccule input is not required for successful sound source localization, and that the lagena plays a more important role than previously thought in sound source localization by the plainfin midshipman.

PS 780

Evidence that presynaptic protein synthesis is necessary to maintain high frequency synaptic transmission at the calyx of Held nerve terminal

Matthew Scarnati; **Kenneth Paradiso**
Rutgers University

High frequency firing of neurons for prolonged periods of time increases metabolic activity and can trigger protein synthesis. Using electrophysiological recordings and fluorescent imaging at the Calyx of Held, a large synapse in the mammalian auditory brainstem that fires at high frequencies, we tested if protein synthesis is necessary to maintain prolonged high frequency firing. We find that blocking protein synthesis by bath application of translational inhibitors produces an apparent elevation in responses during high frequency (200 Hz) trains of activity. After inhibiting protein synthesis, we also find changes in the frequency of spontaneous events, with no change in the amplitude of spontaneous events. These results are consistent with a presynaptic effect, and could indicate the need for newly synthesized proteins in the presynaptic terminal to maintain synaptic transmission. In agreement with this, we find evidence that ribosomes and RNA are present in the presynaptic terminal. To determine if ribosomes are active, we used puromycin to block active ribosomes then labelled puromycin incorporation into peptides. Active ribosomes, indicated by puromycin labelling, were colocalized with a presynaptic marker. In addition, inhibiting translation also eliminated puromycin labelling, demonstrating the specificity of this assay for labelling active ribosomes. The finding that presynaptic elements of synaptic transmission require protein synthesis to maintain normal activity levels, and that newly synthesized proteins and ribosomal components can be found in the presynaptic terminal indicate that local protein synthesis occurs at this nerve terminal and plays a role in synaptic transmission. This finding raises the possibility that local presynaptic protein synthesis could play a similar role at other auditory synapses that can fire at high frequencies.

PS 781

Microsecond precise post-inhibitory facilitation for control of action potential generation in the auditory brainstem

Barbara Beiderbeck[1]; Michael Myoga[2]; Nicolas Müller[3]; Alexander R. Callan[4]; Eckhard Friauf[3]; Benedikt Grothe[5]; Michael Pecka[5]
[1]Graduate School of Systemic Neurosciences, Ludwig-Maximilians-Universität, Munich; [2]Max Planck Institute of Neurobiology; [3]Department of Biology, University of Kaiserslautern; [4]Graduate School of Systemic Neurosciences, Ludwig-Maximilians-Universität Munich; [5]Ludwig-Maximilians-Universitaet Munich

The temporal integration of excitatory and inhibitory synaptic inputs constitutes a basic principle of sensory processing in neuronal circuits. Typically, inhibition not only lowers neuronal excitability, but differences in its arrival time relative to excitatory inputs also establish a time window for action potential (AP) generation. In most sensory circuits, inhibitory inputs are considered to be the limiting factor for temporal resolution of this integration process due to slower time courses compared to excitatory inputs. In the auditory sound localization system, however, the time course of both excitatory and inhibitory inputs has been demonstrated to be exceptionally short. Yet, the functional role of inhibition for the temporal processing and its resolution in these brainstem circuits is unclear. To examine these questions, we studied the temporal integration of inhibition and excitation in the lateral superior olive (LSO) of the Mongolian gerbil in vitro and in vivo. Neurons in the LSO gauge differences in sound amplitudes between the two ears by integrating glutamatergic excitatory and glycinergic inhibitory inputs from the ipsi- and contralateral ear, respectively. To determine the temporal resolution of this integration process, we presented click-train stimuli of varying inter-click-intervals (ICI) and assessed changes in action potential (AP) rate and AP timing. By modulating the relative onset times of the stimuli between the two ears (interaural time difference, ITD), we show microsecond precise sensitivity which remains functionally resolved for ICIs > 1 ms. Moreover, AP times shifted considerably as a function of ITD. Surprisingly, at specific ITDs with inhibition leading excitation, we observed a significant facilitation of AP rates compared to stimulation without inhibition. In vitro conductance clamp LSO recordings established that a reduction in the voltage threshold for spike initiation due to a prior hyperpolarization results in post-inhibitory facilitation of otherwise subthreshold synaptic events. We explain that this post-inhibitory facilitation can promote spatial separability of faint sounds during the processing of interaural level differences (ILDs) in the LSO. Thus, microsecond precise differences in the arrival of inhibition relative to excitation can facilitate spiking to promote sound localization precision.

PS 782

Selective Auditory Fear Conditioning Enhances the Neural Segregation of Concurrent Sounds Represented in the Inferior Colliculus of Awake Rats

Lu Luo; Liang Li
School of Psychological and Cognitive Sciences, Peking University

Background

In an echoic environment, both human listeners and animals are able to integrate the direct leading sound signal and its lagging reflections to form a fused sound image that is perceived as coming from the location of the sound source. This phenomenon, known as "precedence effect", can cause perceived spatial separation between concurrent sounds from various sources. Previous studies have shown that perceived spatial separation helps the listener better direct selective attention to the signal of interest, thereby improving the detection/identification of the target sound signals. However, whether the attentional modulation also modifies the neural representation of concurrent sounds in auditory subcortical areas remains unclear.

Methods

To simulate an echoic auditory scene with competing sounds, two narrowband noises (NBNs) with different central frequencies (1200 and 2800 Hz) and overlapping envelope spectra (0-200 Hz) were presented concurrently through two loudspeakers. The inter-loudspeaker delay for each NBN was manipulated separately to create different perceived spatial configurations. Awake rats with stainless steel electrodes implanted in the bilateral central nucleus of inferior colliculus (IC) underwent auditory fear conditioning (AFC). The conditioned stimulus (CS) was a 1200-Hz pure tone. Frequency following responses (FFRs) to the concurrent NBNs were recorded before and after the conditioning procedure. The accuracy of the neural representation of individual noise sounds were measured using linear coherence analyses.

Results

Before the AFC, IC neurons were able to take advantage of the precedence-effect-induced perceived spatial separation between the two NBNs: comparing with "perceived-co-location" conditions, enhanced response-stimulus coherence (RS coherence) was observed for the envelope component of the NBN with the contralateral loudspeaker (relative to the recorded IC) being the leading sound source, but not for that of the NBN whose fused "image" would be perceived as coming from the ipsilateral loudspeaker. After the AFC, FFRs to the NBN with the conditioned frequency band (i.e.

around 1200 Hz) further benefited from the perceived spatial separation, showing enhanced RS coherence with the envelope component of the conditioned NBN, regardless of whether the leading loudspeaker was the contralateral or the ipsilateral one.

Conclusions

The precedence-effect-induced perceived spatial segregation of concurrent sounds starts in the auditory brainstem, and the subcortical representation of the spatially separated sounds can be further facilitated by auditory fear conditioning of a target sound, probably due to the enhanced selective attention to the conditioned target sound that becomes ecologically significant.

PS 783

Individual Inferior Colliculus Neurons Encode Sound Location Over a Wide Range of Stimulus Frequencies

Ryan Dorkoski; **Mitchell L. Day**
Ohio University

A hallmark of the central auditory system is the topographic representation of the cochlear basilar membrane in each auditory brain area. From the base of the basilar membrane to the apex, there is an orderly progression of spectral sensitivity from high to low frequencies. In auditory brain areas, the characteristic frequencies of neurons (CF: the frequency that evokes a response at the lowest level) follow a similar topographic progression. Tuning to frequency in neurons at the level of the inferior colliculus (IC) and below is relatively narrow about the CF at low sound levels. Therefore, signal processing of complex sound features—including sound source location—is often described as occurring through an array of relatively narrow frequency channels. On the other hand, at high sound levels, frequency tuning (in response to tones) can be quite wide. To determine the dependence of sound location coding on both stimulus spectrum and level, we measured azimuth tuning curves (firing rate vs. azimuth) of IC neurons in awake rabbits for each of 4 bandpass noises (2/3-oct) centered at different frequencies, and at either a moderately high (70 dB SPL) or low (35 dB SPL) sound level. We quantified the azimuthal information encoded by a neuron as the mutual information (MI) between firing rate and azimuth. We found that at the low sound level, IC neurons have a large amount of MI for stimuli near the CF, while at the high sound level, they can have a large amount of MI for stimuli up to 3 oct away from the CF. Therefore, individual IC neurons can provide azimuthal information over a wide range of stimulus frequencies at high sound levels, and over a narrower range of stimulus frequencies at low sound levels, consistent with level-dependent changes in frequency tuning width. This suggests that a

large portion of the IC provides information about sound source location for moderately high-level sounds, even for sounds with narrow spectral content.

PS 784

Are neurons in the optic tectum tuned to interaural time and interaural level differences or to acoustic space?

Patrick Schillberg; Roland Ferger; Hermann Wagner
Institute of Biology II, RWTH Aachen University

Introduction
The American barn owl (Tyto furcata pratincola) has developed an excellent hearing capacity to catch its prey. Sound localization requires the localization of a certain position in acoustic space. This position maybe specified by acoustic parameters (interaural time difference (ITD), broadband interaural level difference (ILD), further parameters). Thus, the question arises whether the barn owl can represent a position in space directly or only via the acoustic parameters. We call the first possibility "space representation" and the second "parameter representation".

Objectives
We ask whether neurons in the optic tectum, a nucleus that is closely related to precise sound localization in these birds, represent acoustic space or acoustic parameters.

Material & Methods
We recorded head-related transfer functions (HRTFs) for 528 spatial positions from individual owls and calculated broadband ITD and ILD. We then checked for positions in space at which the ITD and ILD were equal (smaller difference than the localization precision of the barn owl in ITD and ILD). By filtering broadband noise with the specific HRTFs for each animal, we created virtual acoustic space stimuli. In a next step we adjusted the sound level so that the level at each position tested was equal. Two barn owls were used for standard extracellular electrophysiological experiments. So far we recorded data from 29 single units in the optic tectum.

Results
We first observed that the tuning to azimuth could well be predicted by the tuning to ITD, if the azimuthal axis was multiplied by a factor of 2.5. This conversion factor is equivalent to earlier reports (Campenhausen and Wagner, J comp Physiol A192: 1073-1082 (2006)). This suggests that the neurons might represent the parameter ITD. In a further step, we identified pairs of positions that were characterized by the same ITD and ILD. In owl 1 we identified 7 such pairs, while in owl 2 we identified 13 such pairs. When we recorded the responses with level corrected virtual auditory stimuli at these positions, we observed that in 20 cases the responses were statistically significantly different. This difference indicated that the responses of these neurons cannot not solely be characterized by their tuning to ITD and ILD, in other words these neurons represent space and not parameters. More data and a more in depth analysis is necessary to find out to what extent the neurons in the optic tectum represent space and to what extent they represent parameters.

PS 785

Effect of entrainment by the sound envelope on the coding of source location in the owl auditory system

Michael Beckert[1]; Brian Fischer[2]; Jose Pena[3]
[1]*Department of Neuroscience, Albert Einstein College of Medicine;* [2]*Seattle University;* [3]*Albert Einstein College of Medicine*

The spiking of neurons throughout the auditory system is entrained by the amplitude modulation of the sound, known as the envelope. Sensitivity to the envelope is linked to the neuron';s spectrotemporal tuning. In the brainstem of the barn owl (Tyto furcata), the tuning to binaural spatial cues (interaural time [ITD] and level difference [ILD]) and the spectrotemporal tuning are interdependent. Additionally, evidence that nearby neurons in the midbrain map of auditory space display similar spectral and spatial tuning as well as share inputs suggests entrainment by the sound envelope would affect population level firing, i.e. synchronous spiking, and the decoding of this population. Here we tested this hypothesis in the first nucleus where ITD and ILD information converge, the lateral shell of the inferior colliculus (ICls), as well as in the downstream map of space, the optic tectum (OT).

We performed extracellular recordings of single neurons in ICls and assessed the reproducibility of spike trains across repeated presentations of identical broadband noise at varying positions in space or varying binaural cues using headphones. Neurons in ICls displayed rate-dependent reproducibility for varying sound location such that the spike trains were most reproducible at their preferred location, the same trend was also observed with headphone stimulation. To test the hypothesis that this rate-dependent reproducibility influenced spike timing of populations of neurons in the downstream OT, we performed tetrode recordings of multiple single units simultaneously. OT neurons also displayed rate-dependent reproducibility. Additionally, nearby OT neurons displayed rate-dependent synchronous spiking, attributable to reproducible spiking. We tested whether

rate-dependent synchrony could affect the decoding of the OT population using a computational model. A modeled output population displayed narrower tuning curves when synchrony was rate-dependent as opposed to when synchrony was held constant. Thus rate-dependent synchrony can affect coding of sound location.

This work provides evidence that spiking entrainment by the sound envelope, a response parameter traditionally associated with coding of sound identity, can affect coding to sound location.

PS 786

Neural and Behavioral Correlates of ITD Reliability in Human Sound Localization

Rodrigo Pavao[1]; Elyse Sussman[1]; Brian Fischer[2]; Jose Pena[1]
[1]Albert Einstein College of Medicine; [2]Seattle University

Localizing sound in the horizontal plane requires detection of interaural differences in time (ITD) and level (ILD). We computed ITD statistics across frequency and azimuth from human head-related transfer functions (HRTFs). Mean ITD varied with azimuth following a sigmoid relationship consistent across frequency; whereas ITD variability over time depended on frequency and azimuth. For all frequencies, ITD is more variable in the periphery than in the front; i.e., the front is more reliable. We tested the hypothesis that these natural ITD statistics are hardwired in the human brain, as was shown for barn owls, driving detection of spatial deviants and perceptual estimation of sound location. Towards this end, we obtained neurophysiological and behavioral data that indicated whether ITD variability influenced novelty detection and sound localization performance in human volunteers. Neurophysiological effects were assessed with EEG signals recorded using an oddball paradigm, in which a series of repetitive ("standard") stimuli were embedded with sporadic ("deviant") stimuli. The mismatch negativity (MMN) EEG field potential was used to index discriminability between the standard and deviant stimuli. We presented tones shifted in time through inserted earphones, which had zero variability across time and locations. We selected pairs of tones having the same frequency and lying within reliable and unreliable ranges. We found smaller MMNs were elicited by standards in the periphery. Overall, adjusting ITD by the natural variability of the standard stimulus was the best predictor of the novelty EEG signals, indicating that novelty EEG signals are weighted by natural sensory reliability. To assess behavioral effects of sensory reliability on sound localization performance, tones of varying ITD were played through headphones and subjects were instructed to click on the virtual position that best matched the perceived sound location. They also reported a confidence rating for their responses. As previously reported, azimuth estimation as a function of ITD saturated in the periphery. Interestingly, the responses to frontal ITDs were more variable, displayed longer reaction times and yielded lower confidence scores than in the periphery. This seemingly counterintuitive result may be explained by more methodical estimations in the center, while more automatic and stereotyped in the periphery where ITD information is less reliable. In sum, our results showing a difference in novelty signals and sound localization performance between center and periphery are consistent with the hypothesis of a hardwired representation of ITD reliability in humans.

PS 787

Influence of Interaural Frequency Mismatch on the Binaural Interaction Component of the Auditory Brainstem Response

Andrew D. Brown[1]; Jesse I. Gilmer[2]; Kelsey L. Anbuhl[3]; Daniel J. Tollin[4]
[1]Department of Speech and Hearing Sciences, University of Washington; [2]Neuroscience Training Program, University of Colorado School of Medicine; [3]Center for Neural Science, New York University; [4]Department of Physiology and Biophysics, University of Colorado School of Medicine

The auditory brainstem response (ABR) is an evoked potential elicited via presentation of brief sounds and measured non-invasively via electrodes placed on the scalp. Over the past several decades, a derived component of the ABR, known as the binaural interaction component (BIC), has generated interest for its possible use a biomarker of binaural hearing. While a reliable biomarker could improve clinical detection of binaural dysfunction, the BIC has proven difficult to reliably measure even in normal-hearing adults, leading to skepticism concerning its potential clinical use. The small amplitude of acoustically elicited human BIC (compared to a relatively large BIC evident in many other mammals) may be attributable to the regressed size of a likely neural generator, the lateral superior olive (LSO), or to other factors (e.g., the geometry of the human head, which places electrode contacts relatively far from the lower brainstem). Nonetheless, recently, a rather different application of the BIC, as an objective index of interaural electrode matching in users of bilateral cochlear implants, has generated renewed interest in the potential. Specifically, it has been shown that the amplitude of the electrically elicited BIC (eBIC), which may be measured more readily than the acoustic BIC, is largest for electrode pairs that yield the best binaural behavioral performance. Interestingly, while amplitudes decrease for "spectrally mismatched" electrodes that also yield poorer behavioral performance, tuning functions are rather

broad, spanning several electrodes (and thus hundreds to thousands of hertz). It is unclear whether broad tuning is the result of device factors (e.g., current spread), or intrinsically broad tuning of the BIC itself (e.g., high tolerance to interaural spectral mismatch). Here we explore this matter by measuring the frequency-by-amplitude existence region of the acoustically elicited BIC using narrowband clicks in an animal model that is audiometrically comparable to humans, the chinchilla. Data show that the BIC is relatively broadly tuned, a result that is recapitulated using a simple model of binaural interaction in the LSO with biologically plausible frequency mismatching of excitatory and inhibitory inputs. These findings yield some new insights on basic properties (and candidate mechanisms) of the BIC, and may also prove useful toward improvement of eBIC measurement protocols.

PS 788

Neural representation of interaural time differences in the human brain

Jaime A. Undurraga; Lindsey N. Van Yper; David McAlpine
Macquarie University

Background
Humans use interaural time-differences (ITDs) between the two ears to localize low-frequency (below 1500 Hz) sound sources in the horizontal plane. Two main models have been proposed to explain the neural representation of ITDs: the straightness weighting model and the pi-limit model. The straightness weighting model postulates that ITDs are coded by neurons tuned to specific ITDs, and predicts that when a sound leads in time at one ear, neural activation at some level of brain processing is maximum at the opposite hemisphere, i.e. opposite to the lateralized image at any ITD size, and consistent across ITDs lateralized to the same side. In contrast, the pi-limit model postulates that ITD neurons are absent beyond half the period of their best frequency (the pi-limit) and predicts that ITDs lateralized to the same side perceptually may activate maximally opposite brain hemispheres in a manner dependent on the interaural phase difference of the centre-frequency of the sound, rather than its ITD. Here, using EEG, we test the hypothesis that the neural representation of interaural delays in the human brain is in terms of IPD rather than ITD.

Methods
EEG recordings were obtained from nine normal-hearing listeners. Responses were elicited by abruptly modulating the ITD periodically at a rate of 6.7 Hz – the interaural time modulation following-response (ITM-FR). We hypothesized that ITM-FRs should be larger when different neural populations result activated at each ITM. In contrast, if overlapping neural populations result excited at each ITM, responses should decrease due to neural adaptation. To test this, we measured ITM-FRs using band limited filtered noise (300-700Hz; centered at 500 Hz). ITM-FRs were obtained for the following ITMs: -500/500 us; 1500/500us; 1500/-500us; -1500/1500us. These conditions correspond to ITMs within and beyond the pi-limit (1 ms, for a 500 Hz centered signal). In addition, we investigated if ITM-FRs depended on the ITD size by including the following ITMs: 0/500us; 0/1500us; 0/2000us; 0/3000us; 0/4000us.

Results
Analysis of variance indicated that ITM-FRs were significantly smaller for 1500/-500 us and -1500/1500us conditions, than they were for -500/500us and 1500/500us. These results suggest that ITDs at 1500us activate similar neural populations cortically as ITDs at -500 us and -1500 us ITD, but not 500 us, where the ITD perceived to originate from the same side. When comparing ITMs centered at zero, responses were similar across all ITDs, suggesting that neurons respond similarly at different ITDs.

Conclusions
Results demonstrate that ITMs comparing phase-related ITDs within and beyond the pi-limit (-500/1500us) generate maximum adaptation of the ITM-FR, consistent with the predictions of the pi-limit model. Long ITMs beyond the pi-limit (-1500/1500us) also share some form of neural representation, consistent with them having identical values of interaural coherence. Moreover, responses were not reduced for ITMs centered at zero ITD (within and beyond the pi-limit), indicating that reduced responses were due to adaptation of overlapping neural *populations.*

PS 789

The interaural phase modulation following response as an objective measure of envelope ITD processing

Lindsey N. Van Yper; Jaime A. Undurraga; David McAlpine
Macquarie University

Background
The ability to process interaural time differences (ITDs)

is essential to effective listening in complex acoustic environments. Despite its importance, however, the neural mechanisms underlying ITD processing in humans remain poorly understood. To gain insight into specific neural mechanisms, we developed an objective measure of ITD sensitivity – the interaural-phase modulation following-response (IPM-FR; Haywood et al. 2015, Undurraga et al. 2016) – an EEG-response evoked by periodic transitions of interaural phase differences (IPDs). These IPM-FRs were evoked by IPDs in the temporal fine-structure of low-frequency sounds. However, ITDs are also available in the envelope of amplitude-modulated high-frequency sounds. Here, we assess IPM-FRs to periodic transitions of envelope IPDs.

Methods

IPDs were conveyed in the envelope of band-filtered click trains. IPMs switched between 0° to 180° IPD, at a rate of 7.1 Hz. To assess whether frequency mismatches affect the IPM-FR, the cutoff frequencies of the filter were varied in the left ear (3-4, 4-5, or 5-6 kHz band-pass filter), while kept constant in the right ear (4-5 kHz). So far, eight normal hearing listeners have been included.

Results

IPM-FRs were obtained in five out of eight participants. In these five subjects, response amplitude ranged from 0.2 to 0.4 µV. Response amplitude significantly decreased when an interaural offset in the carrier frequency was introduced (general linear mixed models, $F_{(2, 6.88)}=4.93$, $p<0.05$).

Conclusions

IPM-FRs can be elicited by ITDs in the envelope of high-frequency sounds, albeit highly variable between subjects. This inter-subject variability is consistent with psychoacoustic findings on envelope ITD sensitivity. The data suggest that the IPM-FR deteriorates when an interaural frequency mismatch is introduced. This finding may have repercussions for bilateral cochlear implant users, as it suggests that interaural electrode mismatches may be detrimental for spatial hearing in these patients.

PS 790

Effects of Perceived Separation and Selective Attention on the Cortical Representation of Speech Signals Against Informational Masking

Changxin Zhang[1]; Liang Li[2]
[1]*East China Normal University;* [2]*School of Psychological and Cognitive Sciences, Peking University*

To recognize speech in a noisy and reverberant auditory scene, listeners need to perceptually segregate the target talker';s voice from other competing sounds. A number of studies have suggested that precedence-effect-induced perceived spatial separation between the target speech and the maskers can facilitate the recognition of the target speech. To investigate both the effects of perceived separation on the cortical representation of the target speech and the attentional modulation on these effects, event-related potentials (ERPs) were recorded to a syllable (/bi/) masked by competing speech under active listening conditions. The results showed that the ERP N1 component to the target syllable was significantly enhanced when the target and the masker were perceptually separated than when perceived co-located regardless of whther the participants'; selective attention were directed to the target or not. However, the ERP P2 component was significantly enhanced when the target and the masker were perceptually separate than perceived collocated only when the participants attended to the target. Thus, the N1 component to the target speech was increased by perceived separation between target and masker, and independent of the direction of participants'; selective attention. On contrast, the effect of perceived separation between target and masker on the P2 component was dependent on the direction of participants'; selective attention.

Pitch Perception: Mechanisms & Learning

PS 791

The function of F0-based pitch

Malinda J. McPherson[1]; Josh H. McDermott[2]
[1]*Department of Brain and Cognitive Sciences, MIT; Program in Speech and Hearing Biosciences and Technology, Harvard;* [2]*Department of Brain and Cognitive Sciences, MIT; Center for Brains, Minds, and Machines, MIT; Program in Speech and Hearing Biosciences and Technology, Harvard*

Pitch is traditionally defined as the perceptual correlate of the fundamental frequency (F0) of a sound. The importance of F0-based pitch is often attributed to the need to compare the F0s of sounds with different spectra, such as successive syllables or different musical instruments. However, F0 could also provide a compressed representation of a sound for storage across a delay. To clarify the function of F0-based pitch, we tested its importance for making comparisons between sounds with different spectra, and sounds separated by delays. The reliance on F0-based pitch was assessed by comparing performance for harmonic and inharmonic sounds. If F0-based pitch is necessary for a task, performance for inharmonic stimuli (that lack an F0) should be worse than performance for harmonic stimuli. We first examined the effect of naturally occurring spectral variation using re-

corded notes from different instruments, and excerpts of speech. When participants were asked to discriminate the pitch of these sounds, we observed no advantage for harmonic over inharmonic sounds in either case. An advantage for harmonic sounds was evident only for extreme spectral variation (when successive tones had non-overlapping spectra). By contrast, deficits occurred for inharmonic tones when modest (5-10s) delays were introduced between comparison tones, suggesting that F0-based pitch aided storage across the delay. The results suggest that the spectral variation found in many natural pitched sounds does not on its own necessitate F0 estimation. Instead, F0-based pitch may primarily serve to facilitate compression of sounds for memory storage.

PS 792

Deep Neural Networks Replicate Properties of Human Pitch Perception

Ray Gonzalez[1]; Josh H. McDermott[2]
[1]*Department of Brain and Cognitive Sciences, MIT;*
[2]*Department of Brain and Cognitive Sciences, MIT; Center for Brains, Minds, and Machines, MIT; Program in Speech and Hearing Biosciences and Technology, Harvard*

Pitch perception exhibits well-established dependencies on stimulus characteristics. In human listeners, pitch is predominantly determined by low-numbered harmonics that are believed to be resolved by the cochlea, but is also conveyed to a lesser extent by high-numbered harmonics that are not individually resolved. Moreover, the relative phases of harmonics influence pitch perception only when the stimulus consists of high-numbered (unresolved) harmonics. To assess whether these dependencies reflect information constraints on the problem of extracting pitch from peripheral auditory representations, we trained a deep convolutional neural network to estimate the fundamental frequency (F0) of tones in noise from a simulated cochlear representation. The tones were generated with a source-filter model and replicated basic spectral properties of natural sounds. The resulting neural network model was tested on complex tones that varied in harmonic composition and phase (as in classic psychoacoustic experiments). The network qualitatively replicated features of human pitch perception, including better performance for tones containing low-numbered harmonics and worse performance when the phases of high-numbered (presumably unresolved) harmonics were randomized. Further, the network associated pure tones with the correct F0 even though such tones were not explicitly present in the training data. We obtained different results when the same network was instead trained on the psychophysical test stimuli. In this case performance was unaffected by harmonic number, suggesting that effects of harmonic number do not reflect intrinsic difficulty and instead depend on the properties of the sounds for which pitch perception is adapted. Together, the results are consistent with the notion that human pitch perception exhibits near-optimal performance characteristics for the task of estimating F0 from peripheral auditory representations, in that optimizing for performance of this task is sufficient to reproduce human performance characteristics.

PS 793

Effect of the number of components on perceptual integration for pitch at high frequencies

Anahita H. Mehta; Andrew J. Oxenham
University of Minnesota

Background
The two primary theories of pitch coding involve auditory-nerve spike timing (time code) and frequency-to-place mapping that occurs in the cochlea (place code). It was recently shown that pitch discrimination at very high frequencies improves dramatically for harmonic complex tones relative to discrimination of the individual frequency components (Lau, Mehta, Oxenham, 2017, J. Neurosci. 37:9013-21). Observed fundamental frequency difference limens (F0DLs) for these harmonic complex tones are better than predicted by optimal integration of information, assuming performance is limited by noise at the peripheral level, and are comparable to predictions based on more central sources of noise. This result suggests that performance at high frequencies is not constrained by the upper frequency limit of auditory-nerve phase-locking. The aim of the current study is to determine whether there is a minimum number of harmonic components needed to observe these super-optimal integration effects.

Methods
F0DLs and frequency DLs (FDLs) were measured for harmonics 6 to 10 of a 1.4-kHz F0 in twenty normal-hearing participants. The DLs were measured for each individual harmonic, and for combinations of two through five consecutive harmonics. The tones were all presented in random phase, which in combination with the high fundamental frequency (F0), background noise, and level roving helped rule out potential cues envelope repetition rate, distortion, or loudness changes.

Results
Preliminary results indicate that the F0DLs for the harmonic complex tones incrementally improve as the number of harmonics increases. Moreover, the observed F0DLs are in line with predictions based on more central limitations to performance and generally exceed the per-

formance predicted by optimal integration of information based on a peripheral noise source, thereby replicating the previously observed super-optimal integration effects.

Conclusions

The results indicate that harmonic pitch perception is possible at very high frequencies, even when all the components are above the limits of phase locking. We find that pitch discrimination improves dramatically when very high frequency tones combine to form a single harmonic complex, even when the complex contains only two harmonics. The results of consistent with the activation of central, harmonic-template neurons that are activated only when two or more harmonic components are presented.

PS 794

Multiple mechanisms in pitch perception revealed by individual differences

Malinda J. McPherson[1]; Josh H. McDermott[2]
[1]*Department of Brain and Cognitive Sciences, MIT; Program in Speech and Hearing Biosciences and Technology, Harvard; [2]Department of Brain and Cognitive Sciences, MIT; Center for Brains, Minds, and Machines, MIT; Program in Speech and Hearing Biosciences and Technology, Harvard*

Pitch perception has traditionally been equated with F0 estimation. However, recent results from our lab indicate that disrupting F0 does not always impair tasks thought to rely on pitch. Although some pitch-related tasks become more difficult when participants are tested with inharmonic sounds (that lack a clear F0), many other tasks are unaffected. To test whether these effects reflect the existence of more than one pitch mechanism, we examined individual differences among large groups of participants tested online using Amazon Mechanical Turk. We measured performance on two-tone up-down discrimination for pairs of harmonic tones, inharmonic tones, harmonic tones with non-overlapping spectra (which forced listeners to rely on F0-based pitch), and tones with fixed harmonics that varied in spectral centroid. Performance on tasks that rely on a common mechanism should be correlated across participants. The highest observed correlation was between the harmonic and inharmonic conditions. Both of these conditions were only weakly correlated with the non-overlapping harmonic condition. This result indicates that the same mechanism is used to detect up-down changes for harmonic and inharmonic tones, and that this mechanism is distinct from F0-based pitch estimation. We also

found only weak correlations between spectral centroid discrimination and both harmonic and inharmonic up-down discrimination. This latter result suggests distinct mechanisms for detecting shifts in fine and coarse spectral structure. Overall, these findings suggest an additional pitch mechanism that tracks shifts in the spectrum, rather than estimating F0.

PS 795

Cross-cultural similarities and differences in musical pitch representations

Nori Jacoby[1]; Eduardo A. Undurraga[2]; Ricardo Godoy[3]; Josh H. McDermott[4]
[1]*Columbia University; [2]P. Universidad Catolica de Chile; [3]Brandeis University; [4]Department of Brain and Cognitive Sciences, MIT; Center for Brains, Minds, and Machines, MIT; Program in Speech and Hearing Biosciences and Technology, Harvard*

The use of pitch in Western music is marked by three defining characteristics. First, pitch intervals expressed on a logarithmic scale are heard as equivalent irrespective of the register. Second, individual pitches separated by octaves are heard as musically equivalent. Third, music is composed of pitches from a finite range, beyond which pitch abilities deteriorate. Because pitch representations have not been studied in nonwestern cultures, it has remained unclear whether these aspects of pitch perception inevitably result from nonmusical constraints (e.g. acoustics and the biology of the auditory system), and/or whether they depend on experience with Western music. We tested members of a small-scale society from the Bolivian Amazon (the Tsimane';), who live in relative isolation from Western culture and music (McDermott et al. 2016). We developed a new paradigm to probe pitch representations that can be efficiently used across cultures: participants were asked to sing back a melody comprised of two pure tones. We manipulated the pitch register of the tones and the interval between them, and measured the reproduced interval. Reproduced intervals of both Amazonian and USA participants approximately replicated the heard intervals in semitones, even for tones well beyond the singing range. Moreover, Amazonian reproductions showed the same dependence on frequency evident in USA listeners, breaking down in accuracy for very high frequency tones. However, whereas USA participants sung back pitches that reproduced the chroma of the heard tones, Amazonians did not, ignoring the chroma class of the tones. The findings are consistent with the cross-cultural presence of a logarithmic scale for pitch, and with biological constraints on the upper limit of pitch, but suggest that octave equivalence is culturally contingent, potentially resulting from experience with musical harmony.

PS 796

Relationship of within-ear frequency tuning to binaural pitch fusion

Yonghee Oh; Lina A. J. Reiss
Oregon Health & Science University

Background
Recent studies suggest that hearing-impaired listeners differ from normal-hearing (NH) listeners in how they integrate sound between the two ears. In hearing-impaired listeners, binaural pitch fusion is often increased so that sounds that differ greatly in pitch between the two ears are still heard as a single percept (Reiss et al., 2014, 2017). Broad fusion leads to averaging of pitch between ears (Oh and Reiss, 2017), and can cause binaural interference for vowel perception (Reiss et al., 2016). The goal of this study was to investigate potential mechanisms underlying binaural pitch fusion using experimental and modeling approaches, with a focus on whether within-ear auditory sensitivity can explain broad binaural pitch fusion.

Methods
Twelve NH listeners and fourteen bilateral hearing-aid (HA) users were tested on psychophysical measures of within-ear frequency tuning, including audiograms and psychoacoustical tuning curves (PTCs). Individual PTCs were obtained by using the fast PTC measurement technique (Sęk et al., 2005) at various reference frequencies (0.5, 1, 2, 3, and 4 kHz) for both ears. The bandwidth of the auditory filter was derived by fitting the measured PTC data to the asymmetric roex filter (Oxenham and Shera, 2003). For simulating individual peripheral auditory processing, both the pure tone thresholds and filter bandwidths were characterized as model parameters for the auditory-periphery model (dynamic gammachirp filterbank model, Irino and Patterson, 2006). The amount of overlap of two monaural auditory filter outputs was compared with binaural pitch fusion results.

Results
Average estimated auditory filters for NH listeners were similar in bandwidth to the published equivalent rectangular bandwidths. HA users had substantially broader auditory filters than NH listeners, with greater inter-subject variability. In HA users, the width of the within-ear auditory filters was positively correlated with the frequency range of binaural pitch fusion. Overall, the overlap model output predicted the variation in individual binaural fusion ranges in both subject groups. This model also predicted asymmetric fusion function shapes observed in some HA subjects when the fusion testing was conducted with both ears as the reference.

Conclusions
The findings suggest that broadened monaural frequency tuning, which may reflect peripheral sensitivity, could be a potential factor in broad binaural pitch fusion in hearing-impaired listeners. Model-based interpretation could help indicate the relative importance of peripheral and central substrates in degraded benefits of binaural processing. Funding: Supported by NIH-NIDCD grant R01 DC013307, P30 DC005983, and F32 DC016193.

PS 797

Rabbits can discriminate harmonic complex tones with missing fundamentals

Bertrand Delgutte; Alice Gelman; Yoojin Chung
Massachusetts Eye and Ear

The pitch of harmonic complex tones is important for auditory scene analysis and the perception of speech and music, but the neural mechanisms for pitch extraction are poorly understood. Rabbits are an attractive animal model for neurophysiological studies in awake preparations, but nothing is known about pitch perception in rabbit. Here we tested rabbit discrimination of fundamental frequency (F0) for harmonic complexes with missing fundamentals.

Two rabbits were trained with food rewards to use auditory cues to approach a virtual target whose location within a 1.65x1.05m room was selected at random on each trial. The cue was a harmonic complex whose missing F0 varied in inverse relationship to the rabbit';s distance from the target over one octave (356-712 Hz). All harmonics were of equal amplitude and covered the range 0.8-16 kHz. Once the rabbits learned the task for this "wide-band" stimulus, they were tested with three additional stimuli having the same F0 variations but differing in spectral composition: (1) a "low harmonics" tone containing low-frequency, resolved harmonics (0.8-5 kHz); (2) a "high harmonics" tone containing high-frequency, unresolved harmonics (6.4-16 kHz); (3) a pure tone at F0. All stimuli were presented in threshold-equalizing noise to mask cochlear distortion products at F0. Performance was quantified by the fraction of trials in which the rabbit successfully reached the target within 45s. Chance performance was assessed using catch trials in which F0 was selected at random and did not vary with the rabbit';s distance to the target.

Both rabbits showed significantly better performance for the wide-band stimulus than for catch trials, showing they were able to utilize information in the F0 variations to find the target. Both rabbits also performed better than chance for the low harmonics stimuli, but only one rabbit did better than chance with the pure tone and

high harmonics stimuli. Performance of both rabbits was significantly better for the wide-band and low harmonics stimuli than for the high-harmonics stimulus.

Both rabbits were able to discriminate the F0 of harmonic complex tones with missing fundamentals, and performed better with stimuli containing resolved harmonics than with stimuli consisting of unresolved harmonics. This pattern of performance is qualitatively similar to human performance, but differs from patterns observed in other species (chinchilla, ferret, marmoset) which seem to rely more on temporal cues present in unresolved harmonics. Future studies will test whether the pattern holds for different ranges of F0.

PS 798

Temporal Course of the Benefits of Musical Experience on Frequency and Temporal-Interval Discrimination

Alex E. Clain[1]; David F. Little[2]; Beverly A. Wright[3]
[1]*Northwestern University;* [2]*University of Nevada Las Vegas;* [3]*Department of Communication Sciences and Disorders, Knowles Hearing Center, Northwestern University Institute for Neuroscience, Northwestern University*

Introduction
Musicians have been reported to be better than non-musicians at frequency and temporal-interval discrimination. However, these differences typically have been documented between non-musicians (greater than 1 year of musical experience) and professional musicians. Thus, little is known about how much musical experience is needed before these differences emerge.

Methods
To begin to address this issue, we tested 75 listeners (primarily university students) on all or a subset of six conditions: two tasks, frequency and temporal-interval discrimination, with 3 standard stimuli each (1kHz 50ms, 1kHz 100ms, 4kHz 100ms) presented as two brief tones separated by their respective time intervals. Listeners were divided into four bins based on their years of musical experience: 0-3 years, 4-6 years, 7-10 years, and 11-15 years.

Results
Preliminary analyses show better task performance with increasing years of musical experience on all six conditions. For frequency discrimination at 1kHz (regardless of temporal interval), thresholds were lower at 4-6 years of experience compared to 0-3 years, and were

no different between 4-6 and 11-15 years. For frequency discrimination at 4kHz, thresholds were again lower at 4-6 compared to 0-3 years, but were also lower at 11-15 compared to 4-6 years. For temporal-interval discrimination at 100ms (regardless of frequency), thresholds were lower at 7-10 compared to 0-3 years, and were no different between 7-10 and 11-15 years. For temporal-interval discrimination at 50ms, thresholds were only lower at 11-15 compared to 0-3 years.

Conclusions
These results suggest that the benefits of musical experience appear earlier for frequency discrimination (4-6 years) than for temporal-interval discrimination (7-10 years), and plateau earlier at lower (1kHz) compared to higher (4kHz) frequencies for the frequency task, and at longer (100ms) compared to shorter (50ms) intervals for the temporal-interval task. Thus, benefits of musical experience on fine grained discrimination tasks can be observed after only a few years of musical experience, and appear to arise from enhancements of task-and-stimulus specific processes.

PS 799

Retrograde interference of perceptual learning on a musical-interval discrimination task

Ruijing Ning[1]; Henry Cheng[1]; David F. Little[2]; Beverly A. Wright[3]
[1]*Department of Communication Sciences and Disorders, Northwestern University;* [2]*University of Nevada Las Vegas;* [3]*Department of Communication Sciences and Disorders, Knowles Hearing Center, Northwestern University Institute for Neuroscience, Northwestern University*

Introduction
Perceptual skills improve with practice, providing a means to treat perceptual disorders and to enhance normal perceptual abilities. However, learning on one perceptual task can be disrupted by subsequent training on another. Such retrograde interference suggests that processes important for learning continue after the training period is over. To date, retrograde interference in perceptual learning has only been documented for fine-grained discrimination tasks. Here we extend this demonstration to a task of practical importance that requires discrimination between stimulus categories: musical-interval discrimination.

Method
Listeners with no prior ear training performed a two-interval-forced-choice task in which they chose between random examples of a perfect 4th (target interval) and of a major 3rd, perfect 5th, or major 6th (foil intervals).

Different listener groups were trained on the 4th only (n=8), or on the 4th first and then on a major 7th (foils: perfect 5th, major 6th, and octave) either 0 or 6 hours later (both n=7). For all groups, periods of task practice alternated with periods of exposure to the soundtrack of earlier practice each for a total of 180 trials per interval per day for 3 days.

Results

Training on only the 4th yielded a ~17% improvement in discrimination performance on that interval, while training on the 4th followed immediately by training on the 7th yielded essentially no improvement on the 4th. Delaying the training on the 7th by 6 hours only partially restored the learning on the 4th. The magnitude of learning disruption was equal at both 0 and 6 hours for the 4th vs. the 3rd and the 4th vs. the 5th, but decreased as the time gap increased for the 4th vs. the 6th.

Conclusions

These data indicate that learning on a musical-interval discrimination task with one target interval can be disrupted by subsequent training with a different target interval, that such disruption can occur even when the two training periods are separated by 6 hours, and that such disruption decreases at different rates for different stimuli. These results imply that retrograde interference in perceptual learning occurs for the discrimination of stimulus categories as well as for fine-grained discrimination, that the process of solidifying perceptual memories continues for hours after training, and that the solidification occurs separately for different stimuli. Knowledge of such constraints on learning is necessary to optimize perceptual training regimens.

Psychoacoustics: Theoretical Frameworks & Models

PS 800

Incorporating absolute threshold and cochlear noise floor into the GammaChirp model of masking

Toshio Irino[1]; Kenji Yokota[1]; Toshie Matsui[1]; Roy D. Patterson[2]
[1]*Faculty of Systems Engineering, Wakayama University;* [2]*Department of Physiology, Development and Neuroscience, University of Cambridge*

In the early notched-noise (NN) filter-shape papers, it was noted that there was a low-level limit on tone-in-NN threshold that was well above absolute threshold [e.g. Glasberg et al., JASA, 76, 419-427, 1984]. It was suggested that this limit, P_0, might represent a cochlear noise floor but the hypothesis was not pursued. This paper reports a NN experiment with a large proportion of low-level, wide-notch conditions designed to confirm the noise floor hypothesis and, thereby, integrate absolute threshold into the power spectrum model of masking. The experiment included five NN spectrum levels (38, 28, 18, 8, and -2 dB) and six NN widths from 0.0 to 0.8 times the signal frequency, 2000 Hz. The NN thresholds and absolute thresholds of 8 normal-hearing (NH) listeners were averaged and fitted by a modified GammaChirp (GC) model of masking (Eqs 1 – 6) that included a term, N_{cch}, for the presumed cochlear noise floor. NN threshold, $\hat{P}_s$, is calculated (Eq. 1) from the sum of the external NN, $\hat{P}_{ext}$ (Eq. 3) and the internal, cochlear noise, $\hat{P}_{int}$ (Eq. 4) which was assumed to be constant along the ERB_N axis (Eq.5). Absolute threshold, $\hat{P}_{abs}$, was estimated from $\hat{P}_{int}$ (Eq. 2). The rms error was used to optimize the fit (Eq. 6).

The proposed model with noise-floor N_{cch}, was compared to the conventional model with threshold-limit, P_0, for three sets of thresholds, the Full 30 conditions, the Upper 18 conditions (38, 28, 18 dB), and the overlapping, Lower 18 conditions (18, 8, -2 dB). The fit was performed ten times with randomized initial coefficients. The minimum rms values were 1.7, 1.2 and 1.8 dB for the Full30, Upper18, and Lower18 sets, for both the N_{cch} and P_0 models. The minimum rms error for absolute threshold was invariably less than 0.4 dB, and the estimated value of N_{cch} at 1 kHz was between -17.0 and -17.5 dB. The filter shapes for the fits were essentially the same. The main advantage of the N_{cch} model was that the means and standard deviations of the sets of ten fits were much smaller for the N_{cch} model than the P_0 model; specifically, the standard deviations were reduced by factors of 8, 2.5 and 2 for the Full30, Upper18, and Lower18 sets, respectively. Thus, the new GC model that incorporates absolute threshold and estimates the noise floor level also finds the optimal fit quicker and more reliably.

$$\hat{P}_s = K + 10\log_{10}\{10^{\hat{P}_{ext}/10} + 10^{\hat{P}_{int}/10}\} \quad (1)$$

$$\hat{P}_{abs} = K + \hat{P}_{int} \quad (2)$$

$$\hat{P}_{ext} = N_0 + 10\log_{10}\left[\int_{fl_{min}}^{fl_{max}}|T(f)G_{cc}(f)|^2 df + \int_{fu_{min}}^{fu_{max}}|T(f)G_{cc}(f)|^2 df\right] \quad (3)$$

$$\hat{P}_{int} = 10\log_{10}\left[\int_0^{f_{max}}|N_{cch}(f)G_{cc}(f)|^2 df\right] \quad (4)$$

$G_{cc}(f)$: gammachirp; $T(f)$: transfer function from field to cochlea

$$N_{cch}(f) := N_{c1}\sqrt{ERB_N(1\text{kHz})/ERB_N(f)} : \text{uniform cochlear noise} \quad (5)$$

$$\mathbf{c}_{cgc} = \arg\min_{\mathbf{c}_{cgc}}\{\frac{1}{N}\sum_{i=1}^{N}(P_{s_i} - \hat{P}_{s_i})^2 + (P_{abs} - \hat{P}_{abs})^2\} \quad (6)$$

$$\text{where } \mathbf{c}_{cgc} := \{b_1, c_1, f_{rat}^{(0)}, f_{rat}^{(1)}, b_2, c_2, K, N_{c1}\}$$

PS 801

The Role of Offset Sensitivity in Consonant Discrimination in Noise

Fatima Ali[1]; Doris E. Bamiou[2]; Stuart Rosen[3]; Jennifer F. Linden[1]
[1]UCL Ear Institute; [2]The Royal National Throat, Nose and Ear Hospital; [3]Department of Speech, Hearing & Phonetic Sciences, UCL

Sound offsets are important cues for recognising, distinguishing and grouping sounds, but the neural mechanisms and perceptual roles of sound-offset sensitivity remain poorly understood. In particular, while it is known that troughs in amplitude modulation are essential to consonant perception, there is a gap in the literature relating physiological studies of sound-offset responses in the auditory brain to the psychophysics of speech perception.

Recent studies in a mouse model of developmental disorder have reported the discovery of an auditory deficit specific to the processing of sound offsets (Anderson & Linden, 2016). This finding raises the possibility that deficits in sound-offset sensitivity might contribute to listening difficulties associated with developmental disorders. Difficulty perceiving speech in noise is the characteristic feature of central auditory processing disorder, and is also associated with other developmental or language disorders (Ferguson et al, 2011).

Here, we used mathematical modelling to investigate how sound-offset sensitivity relates to discrimination of vowel-consonant-vowel (VCV) stimuli in multi-talker babble noise. We used a phenomenological model introduced by Anderson and Linden (2016), based on the assumption that auditory brain activity arises from a sum of inputs from independently weighted onset-sensitive and offset-sensitive channels. By reducing the weighting of the offset-sensitive channel, we simulated reduced offset sensitivity and assessed its influence on the discriminability of model outputs for 48 non-sense vowel-consonant-vowel (VCV) speech stimuli in varying levels of multi-talker babble noise (-12, -6, 0, 6, 12 dB SNR). We show that offset salience in noise can be used to categorise phonetic consonants into three groups of high, moderate and low salience, and we identify particular consonants for which discrimination in noise is more strongly or more weakly affected by offset sensitivity. We also report the results of an ongoing psychophysical study of offset sensitivity and VCV perception in normal healthy subjects aged 18-60, comparing ratios of sound-onset to sound-offset reaction times with thresholds for gap-in-noise detection and VCV discrimination in noise. Consistent with model predictions, our preliminary results show that differences in consonant discrimination performance for consonants with markedly different offset salience ('w'-'d') varied more strongly with our measure of offset sensitivity than differences in performance for consonants with similar offset salience ('f'-'sh'). These early findings suggest that individual differences in sound-offset sensitivity may be a factor contributing to inter-subject variation in speech-in-noise discrimination ability.

Anderson, L.A. & Linden, J.F. 2016. Mind the gap: two dissociable mechanisms of temporal processing in the auditory system. Journal of Neuroscience, 36 (6), 1977-95.

Ferguson, M.A., Hall, R.L., Riley, A. & Moore, D.R. 2011. Communication, Listening, Cognitive and Speech Perception Skills in Children With Auditory Processing Disorder (APD) or Specific Language Impairment (SLI). Journal of Speech Language and Hearing Research, 54, 211–227.

PS 802

Reconsidering the Efficient Coding Model of the Auditory Periphery under Reverberations

Hiroki Terashima; Shigeto Furukawa
NTT Communication Science Laboratories

Neurophysiological studies have succeeded in identifying the tuning properties of the auditory periphery. The sharpness of frequency tuning of the auditory nerve fibres seemingly follows a common distribution across mammals. Computational modelling has been used in attempts to understand why the tuning properties have been acquired. The sparse coding model explains the tuning properties in relation to natural sound statistics (Lewicki, 2002, Nature Neuroscience). Efficient codes or unsupervised learning of natural sounds like human voices exhibited tuning properties similar to those of the auditory nerve fibres.

The voices used by Lewicki were "dry" sounds recorded without environmental modulations. In realistic environments, however, the sound waveforms our ears receive are substantially altered by reverberations and other background sounds. In the present study, we attempted to establish a computational understanding of the auditory periphery with environmental modulations taken into consideration.

First, we tested whether the sparse coding model can also explain recordings in a natural environment. Instead

of the TIMIT database used by Lewicki, we employed adult-to-adult conversations in the NTT infant vocalization database, which were recorded in a home environment. Obtained sparse codes for the voices exhibited much sharper tunings than the auditory nerve. Next, to investigate the effect of reverberations, we convolved a set of natural impulse responses with sounds from the TIMIT database and applied the sparse coding model. Again, obtained filters showed similarly sharper tunings.

How can we gain an understanding of the relationship between reverberated sounds and the auditory periphery? In recent visual modelling, supervised learning has shown promising results. Inspired by this, we trained a convolutional deep neural network for a naturalistic auditory task: classification of waveforms into 39 phoneme classes. Waveforms of 125 ms were extracted from the TIMIT database as the inputs so that a target phoneme was located in the centre of the window. Each extracted waveform was convolved with an impulse response that was randomly chosen from a database recorded in natural environments. After training, the model predicted phonemes with more than 80% accuracy. Filters learned in the first layer showed frequency tunings whose sharpness was comparable with that of the auditory nerve fibres.

Overall, the results suggest that, although the auditory periphery adapts to natural sound statistics in some way, it does not adapt to the received sound waveforms themselves. Rather, it might be better understood as optimization to natural tasks such as speech recognition under reverberations.

PS 803

Envelope Cues in Notched Noise and Profile Analysis Tasks: Insights from Modeling

Braden Maxwell[1]; Laurel H. Carney[2]
[1]University of Rochester; [2]Departments of Biomedical Engineering, and Neurobiology & Anatomy, University of Rochester , Rochester

Background
Detecting a tone in a simultaneous notched-noise masker is a classic psychoacoustic task. The leading theory suggests that listeners accomplish this task by detecting an increase in energy at the output of an auditory filter tuned to the tone frequency. This view is challenged by the results of Lentz et al. (1999, JASA 106:2779), in which the levels of both stimulus intervals were randomly varied (roved) to make energy cues unreliable, but listener thresholds worsened only slightly. In this modeling study, we tested the hypothesis that envelope cues, manifested as changes in discharge rates of am-

plitude-modulation (AM)-sensitive cells in the inferior colliculus (IC), explain the robustness of human performance in the roving-level condition. We examined the usefulness of these types of cues in both notched-noise and profile-analysis tasks.

Methods
Stimuli matched those in Lentz et al. (1999). Model population responses were simulated using the Zilany et al. (2014, JASA 135:283) auditory-nerve (AN) model and models for IC cells with Band-Enhanced and Band-Suppressed modulation transfer functions (Carney et al., 2015, eNeuro 2:4). Thresholds for individual fibers or cells were calculated using a sensitivity index, d';, based on the difference in discharge rates during each interval. Overall sensitivity for each stage of the model was calculated by optimally combining the individual sensitivities of a population of cells with different best frequencies. The only source of internal noise in the model was the spontaneous activity of the model AN fibers.

Results
Envelope-related cues were observed in discharge rate differences of the model IC neurons for both roved and non-roved versions of the notched-noise task and for the profile-analysis task, which was roved. In band-enhanced IC responses to the notched-noise task, these cues included (1) an increase in discharge rate due to beating of the tone with edges of the noise bands and (2) a decrease in discharge rate due to 'flattening-out'; of modulation by the tone. These cues varied with stimulus parameters, characteristic frequency and best modulation frequency of each model cell. Model thresholds based on IC discharge rates approximated human thresholds in both tasks. Discharge rates of the model AN did not explain performance in the profile-analysis or notched-noise task, with or without rove.

Conclusions
Model results suggest that performance in both tasks depends on envelope cues present in the temporal properties of AN responses and in discharge rates of AM-sensitive cells in the IC.

Funding

PS 804

Modeling Amplitude-Modulation Masking of Frequency-Modulation Detection

Andrew J. King[1]; Léo Varnet[2]; Christian Lorenzi[3]
[1]*University of Oxford;* [2]*Laboratoire des systèmes perceptifs, Département détudes cognitives, École normale supérieure, PSL Research University, CNRS;* [3]*Laboratoire des systèmes perceptifs, Département d'études cognitives, École normale supérieure, PSL Research University, CNRS*

Background

Frequency modulation (FM) may be detected as amplitude modulation (AM) as the excitation pattern on the basilar membrane changes. Thus, FM detection in the presence of an AM masker should exhibit the main features of AM masking: tuning, effects of AM-masker depth, beating effects and phase effects (e.g., Strickland and Viemeister, 1996). Furthermore, the features of masking of FM by AM should be predictable by models of AM processing (e.g., Dau et al., 1997).

Methods

For 10 normal-hearing listeners, detection thresholds for sinusoidal FM (FMDTs) were measured with and without an AM masker as a function of FM rate (between 2 and 64 Hz) using a two-alternative, forced-choice task. Effects of AM rate (2 or 16 Hz), stimulus duration (0.5 or 1 s), carrier frequency (0.5 or 5 kHz), AM depth (50% or 25%) and phase relation between the FM and AM were tested. A computational model of modulation processing based on the modulation filter-bank concept and a template-matching decision strategy was developed to predict the FMDTs and masking effects. The model performed the same task as the listeners. The model parameters were adjusted to predict listeners'; AM detection thresholds from 2 to 32 Hz.

Results

FMDTs with an AM masker were elevated compared to FM detection thresholds without an AM masker, demonstrating masking broadly tuned to the AM masker rate. Carrier frequency had little effect, but masking increased with AM masker depth and stimulus duration. Mild phase effects were also observed. The model predicted FMDTs between 8 and 64 Hz, but overestimated them at 2 and 4 Hz. It only simulated the masking effects of a 16-Hz AM masker when the model was insensitive to modulation phase above 10 Hz. The model predicted beating effects that were not observed behaviourally and exaggerated phase effects. Removing the envelope beat cues from the template mitigated these effects. The model was unable to simulate the masking effect of a 2-Hz AM masker

Conclusions

AM masked FM with some AM-masking-AM features (tuning and the effect of AM-masker depth), but did not show beating or phase effects. Simulations indicate that i) masking of FM by AM results from the loss of sensitivity to envelope phase from modulation filters above about 5 Hz, ii) separate mechanisms drives low-rate FM and AM detection, and iii) human listeners do not build an internal template that incorporates envelope-beat cues generated by the interaction between the target FM and the AM masker.

References

Dau, T., Kollmeier, D., & Kohlrausch, A. 1997. Modeling auditory processing of amplitude modulation: I. Detection and masking with narrowband carriers. J Acoust Soc Am, 102, 2892-2905.

Strickland, E.A., & Viemeister, N.F. 1996. Cues for discrimination of envelopes. J Acoust Soc Am, 99, 3638-3646.

PS 805

Representation of Amplitude Modulation in a Deep Neural Network Optimized for Sound Classification

Takuya Koumura; Hiroki Terashima; Shigeto Furukawa
NTT Communication Science Laboratories

Sound envelopes are believed to convey important information about sound sources and the surrounding environment. Physiologists have intensively investigated how amplitude modulation is represented in the auditory nervous system (ANS). Those studies generally indicate that the characteristics of neural modulation tuning gradually change with the processing stages along the path from the periphery to the cortex (Joris et al., 2004, Physiol Rev). A natural hypothesis is that such physiological characteristics of the ANS are the results of its evolving to effectively process amplitude modulation. The present study examined this hypothesis computationally using a deep neural network (DNN), a state-of-art machine-learning model applicable to various tasks. Like the sensory nervous systems, a DNN consists of many layers with multiple units (or "neurons"), and a unit in a layer integrates outputs of multiple units in a lower layer and sends outputs to other units in an upper layer. Apart from this, the DNN we used was not designed to reproduce any physiological or anatomical properties of the ANS. The parameters of the DNN optimized for a task should reflect only the nature of the task and input data. We trained a DNN with a simple phoneme classification task. The model consisted of a stack of dilated convolutional layers, in which the first layer directly took samples of raw waveforms as inputs. We examined the

sensitivity of the units in the trained DNN to amplitude modulation by applying standard neurophysiological methods. We derived rate and temporal modulation transfer functions (rMTF and tMTF) from the unit activities in response to sinusoidally amplitude-modulated white noise and characterized them by the best modulation frequencies and the upper cutoff frequencies. Similarly to the ANS, the units in the trained DNN generally exhibited low-pass or band-pass characteristics to modulation frequency, with some units showing more complex patterns. The best and cutoff frequencies of the tMTFs generally decreased with the increasing level of the layers. A population of units with reliable rMTFs, indicating conversion from temporal to rate coding, were observed only at higher layers. A quantitative comparison of the model MTFs and the physiological MTFs revealed that lower/higher layers in the model were similar to the peripheral/central regions in the ANS. Such characteristics were not observed in the model before optimization. The results suggest that the characteristics of the response to amplitude modulation of the auditory neurons reflect optimization to behaviorally important tasks such as sound recognition.

PS 806

When FM echolocating bats determine echo delay, what frequency supplies the base reference?

James Simmons
Brown University

Echolocating big brown bats (Eptesicus fuscus) transmit FM sounds covering frequencies from about 23 to 100 kHz in two or three prominent downsweeping harmonics (FM1, 55-23 kHz; FM2, 100-45 kHz). The sounds are broadly directional, with a wide beam at low frequencies and less wide beams at progressively higher frequencies. During propagation, the sounds are weakened by spreading losses and by frequency-dependent atmospheric absorption. The incident sound has a flat spectrum only for a target on the beam';s axis at close range. Otherwise, for an off-axis or distant object the incident sound is lowpass filtered, which dominates the spectrum of echoes outside the immediate frontal region. Target images are compounded from overall echo delay estimates for target range and estimates of the target';s glint structure from the interference spectrum of the combined glint reflections. Due to amplitude-latency trading, the slope of the FM sweeps in echoes relative to broadcasts becomes the vehicle for focusing the images of a foreground target while focusing images of background clutter. The lowpass character of most echoes means that only the lowest frequencies in the FM1 sweeps of echoes (25-30 kHz) reliably indicate delay. As frequency increases, the accumulating effect of echo lowpass filtering, viewed through amplitude-latency trading, biases

delay estimates while also distinguishing clutter as different from the target. Perception of overall delay for target ranging requires the presence of 25-30 kHz in echoes, even for nominally easy discrimination of hundreds of microseconds in delay. Precise estimation of delay depends on the presence and coherence of both principal harmonics, FM1 and FM2. To accommodate the bat';s use of the lowest frequencies as the basis for delay imaging, the SCAT (Spectrogram Correlation and Transformation) model of biosonar processing accumulates responses to echoes until the end of the FM1 sweep has been received before initiating the formation of images. How this effect, so clearly manifested in behavior, might be manifested in auditory neurophysiology is an important problem for both theory and experimentation. (Work supported by the Capita Foundation and ONR.)

PS 807

Comparison of a standard front-end AGC with a newly adaptive multiband back-end AGC in speech

Florian Langner[1]; Andreas Büchner[1]; Waldo Nogueira[2]
[1]*Department of Otolaryngology, Hannover Medical School, Germany; Cluster of Excellence;* [2]*Department of Otolaryngology, Hannover Medical School, Germany; Cluster of Excellence Hearing4all*

The processing of Cochlear Implant (CI) sound coding strategies typically begins with a front-end automatic gain control (AGC) that reduces the broad acoustic dynamic range (DR). The usage of a front-end AGC introduces distortion into the signal and does not allow a direct mapping between the input signals energy to the electrical energy of the stimulus delivered to the patient. When listening to speech in noise, this reduction in DR typically results in lower speech intelligibility. Transients in for example (e.g. b and p in a logatome such as "aba" / "apa") inhibit spectral features that will be smeared when applying such a heavy DR reduction on a signal. It is therefore desirable to implement an AGC in a CI system that utilizes a full acoustic DR with adaptive multiband properties to preserve spectral features and improve speech intelligibility in noise. Such an algorithm has the potential to keep soft transients of speech, required to better distinguish consonants than a single channel front-end AGC.

Instrumental objective measurements based on STOI (short-time objective measure) and subjective tests in six normal hearing (NH) listeners and six CI users were used to compare speech performance with a standard single-stage dual-loop front-end AGC (StAGC) and the adaptive multiband back-end AGC VoiceGuard (VGAGC). The CI user group consisted of Oticon Medical CI users, which were directly stimulated via standard PC over the AuxIn connection of a research sound pro-

cessor, while NH were measured in a free-field condition. A logatome discrimination task was performed and consisted of the presentation of logatomes with different consonants in quiet and noise at +10 dB SNR. Speech intelligibility in quiet and noise at the same SNR was assessed with the Hochmair-Schulz-Moser sentence test which consists of everyday sentences.

A trend towards better speech intelligibility in quiet and in noise was found for the VGAGC condition in the CI group (16% and 14 % improvement respectively). Four CI participants could perform the logatome test in which they also performed better with the VGAGC condition (14%). The objective analysis via STOI revealed a 0.21 better intelligibility measure estimate for VGAGC than for the StAGC condition (U = 0, p < 0.001). Overall, a single stage multiband compression such as Voice-Guard can outperform a two-stage compression (AGC + static multiband compression) in both speech intelligibility and logatomes.

Temporal Bone Surgery

PS 808

Cochlear Implants in single sided deafness - its effect on speech discrimination and quality of life

Mark Praetorius[1]; Isabel Braun[1]; Sebastian Hoth[2]
[1]*Div.of Otology and Neurotology, Dept. of Otolaryngology;* [2]*Audiology, Dept. of Otolaryngology*

Background
Cochlear implants (CI) are the treatment of choice to restore hearing that can otherwise not be achieved. Here, we investigated the results of speech discrimination in quiet and noise, in directional hearing and quality of life in patients with one CI and usable acoustic hearing on the contralateral ear.

Methods
47 unilateral postlingually deafened patients treated wit a CI at the ORL department of the University of Heidelberg Medical Center were tested with the Freiburger monosyllable test, the Oldenburger and Göttinger Satztests and with a directional task. For the Quality of life, the NCIQ (Nijmegen Cochlear Implant Questionnaire), the APHAB (Abbreviated Profile of Hearing Aid Benefit) and the Visual Analog scale (VAS) was used.

Results
The speech discrimination scores in the Freiburg monosyllable test in the binaural condition were clearly im-

proved. In the Oldenburg sentence test, the speech discrimination threshold went to negative values in the binaural condition. In the Göttinger sentence test, in quiet the improvement was only seen in patients with an impaired contralateral hearing; in noise all patients showed improvement. The directional task was solved better regardless oft he second ear';s hearing. Quality of life tests showed high values in the NCIQ and the VAS. In the APHAB all but the subscale AV were improved. Sudden, loud sounds were perceived aversive with CI.

Conclusions
The results shown here for CI treatment in this study regarding speech discrimination, directional hearing and quality of life in patients with single sided deafness and normal or usable contralateral hearing are positive. This underlines that this is a good and efficacious option to treat these patients.

PS 809

Immunohistochemical evaluation of preservation of cells of the organ of Corti and innervating dendritic processes after cochlear implantation in the human

Takefumi Kamakura[1]; Jennifer T. O'Malley[2]; Joseph B. Nadol[3]
[1]*Osaka Women's and Children's Hospital;*
[2]*Massachusetts Eye and Ear Infirmary;* [3]*Department of Otolaryngology, Massachusetts Eye and Ear, Harvard Medical School, Boston, MA, USA*

Background
Surgical insertion of a cochlear implant electrode induces various pathologic changes within the cochlea including insertional trauma, foreign body response, inflammation, fibrosis, and neo-osteogenesis. These changes may result in loss of residual acoustic hearing, adversely affecting the use of hybrid implants, and may result in loss of putative precursor cells, limiting the success of future regenerative protocols.

Objectives
This study evaluated the degree of preservation of hair cells, supporting cells, and innervating dendritic processes after cochlear implantation in the human using immunohistochemical methods.

Methods
Twenty-eight celloidin-embedded temporal bones from fourteen patients with bilateral severe to profound sensorineural hearing loss and unilateral cochlear implants were studied. Two sections including the modiolus or basal turn from each temporal bone were stained using anti-neurofilament, anti-myosin-VIIa, and anti-tubulin antibodies in both implanted and unimplanted ears.

Results

Inner and outer hair cells: Immunoreactivity was reduced throughout the implanted cochlea and in the unimplanted cochlea with the exception of the apical turn. Dendritic processes in the osseous spiral lamina: Immunoreactivity was significantly less along the electrode of the implanted cochlea than in the other segments. Inner and outer pillars, inner and outer spiral bundles, and Deiters' cells: Immunoreactivity was similar in the implanted and unimplanted cochleae.

Conclusions

This study revealed that insertion of a cochlear implant electrode may significantly affect the inner and outer hair cells both along and apical to the electrode, and dendritic processes in the osseous spiral lamina along the electrode. There was less effect on pillar cells, Deiters' cells, and spiral bundles.

PS 810

Risk Factors and Management of Post-Operative Infection in Pediatric Cochlear Implantation

Eric J. Nisenbaum; David R. Friedmann; J. Thomas Roland; Susan B. Waltzman
New York University School of Medicine

Objective

Post-operative infection is a potential complication of cochlear implant surgery. In pediatric patients, these infections may require prolonged antibiotics and ultimately device explantation. Little is known about the factors – both constitutional and surgical – that may influence the occurrence and outcomes of these infections. We reviewed pediatric cochlear implants at our institution over a five-year period to examine factors associated with post-operative infection, management and resultant outcomes.

Study Design

Retrospective chart review

Methods

246 pediatric cochlear implant surgeries were identified by procedure code: 98 simultaneous bilateral and 148 unilateral or sequential procedures. Medical records were reviewed for patient data including age, presence of inner ear malformation, vaccination status, revision surgery, operative time, device manufacturer, and perioperative and postoperative antibiotic use. Infectious complications during the first postoperative year were recorded including location, time of infection, associated bacteria, management, and resolution.

Results

There were 16 infections among the 246 patients, for an overall infection rate of 6.5%. Nine occurred in simultaneous bilateral patients (9.2%) and 7 occurred in unilateral or sequential patients (4.7%). There was a significant difference in age between infected and non-infected patients both overall (17.2 vs 51.4 months, p=0.005) and for unilateral or sequential implants (20.9 vs 69.1, p=0.004).

Time from implant to infection ranged from 15 to 263 days, (mean = 82.9). The most common infectious complication was surgical site skin infection, followed by device infection. The most common cultured organism was S. aureus. The implant was salvaged in 9 of 16 patients. Of these, 5 received antibiotics alone, while 4 also underwent operative incision and drainage. In the simultaneous bilateral patients, 8 of 9 infections were unilateral. Of these, 2 occurred on the first side operated on, while 6 occurred on the second side. Explanted devices were analyzed for biofilm composition.

Conclusions

Post-operative infection is associated with age in unilateral but not bilateral pediatric cochlear implants. Infections are often culture-positive for skin microorganisms, and prompt therapy with antibiotics and operative washout can allow for high rates of device salvage. Though not statistically significant in this series, infections were more common on the second side of simultaneous implantations. While standard sterile technique was employed, this may suggest increased intraoperative exposure to pathogens during placement of the second implant.

Further analysis is ongoing to explore the association of our other collected constitutional and surgical variables with post-operative infection, as well as how outcomes vary for different infection types.

PS 811

Congenital CMV infection is associated with Sensorineural Hearing Loss (SNHL)

Cathy Yea Won Sung[1]; Keiko Hirose[2]; Stipan Jonjic[3]; William Britt[1]
[1]University of Alabama at Birmingham; [2]Washington University in St. Louis; [3]University of Rijeka

Congenital HCMV infection causes moderate to severe sensorineural hearing loss (SNHL) in approximately 15% of infected infants. However, the mechanism(s) of disease leading to SNHL in infants with congenital HCMV infection are unknown. We have developed a murine model of hearing loss that is associated with congenital

HCMV infection in newborn mice that follows hematogenous spread of virus to the inner ear (cochlea). Virus can be detected in the inner ear as early as fours days post infection and robust inflammatory responses were present in MCMV-infected inner ear. Moreover, we demonstrated that 50-60% of infected mice exhibited hearing loss with increased sound pressure level thresholds of approximately 20dB across all frequencies of sound. Surprisingly, histological analyses of the inner ear in MCMV-infected mice with hearing loss revealed uniformly preserved morphology and number of hair cells in the Organ of Corti. However, the number of spiral ganglion neurons (SGN) was decreased. Additionally, abnormalities in the synapses, which connect the cochlear hair cells and SGN nerve terminals, and SGN nerve fibers in the cochlear sensory epithelium were observed. MCMV infections in newborn mice were also associated with altered morphology of the stria vascularis. Specific findings in this model included decreased expression of potassium channels in the marginal cells and proteins associated with tight junctions in the stria vascularis. These findings coupled with normal hair cell morphology and number suggested several potential mechanisms of MCMV-induced hearing loss. Ongoing studies will be directed at dissection of the specific mechanisms responsible for the observed phenotypes in this model in hopes of identifying targeted interventions to limit hearing loss that could potentially be translated into clinical settings.

PS 812

Association Between Hearing Impairment and the Diameters of Bony Cochlear Nerve Canal and Internal Auditory Canal in Pediatric Sensorineural Hearing Loss Patients

Hun Yi Park; Hantai Kim
Dept.of Otolaryngology, Ajou University School of Medicine

Objectives
The association between morphological abnormalities of the inner ear such as Mondini dysplasia, Michel dysplasia, enlarged vestibular aqueduct syndrome , and hearing impairment in children is relatively well documented. But there are few studies about the correlation between the morphologic variation, internal auditory canal (IAC) and bony cochlear nerve canal (BCNC), and hearing in pediatric patients. The aims of this study are to investigate the relationships between the morphologic parameters and hearing impairment, and to identify radiologic morphological factors affecting hearing in pediatric sensorineural hearing loss (SNHL) patients representing normal inner ear anatomies.

Methods
One hundred ears from 50 pediatric patients diagnosed with SNHL in the Department of Otolaryngology, Ajou University Hospital (Republic of Korea) were enrolled in the study. As a control group, 100 ears from 100 pediatric patients with normal hearing also participated. High-resolution temporal bone-computed tomography was done on all of the enrolled patients. Temporal bone-computed tomography measures the BCNC and the width, height, and length of the IAC. We tried to find differences in radiologic morphology between the SNHL group and the normal hearing group.

Results
BCNC, IAC width, IAC height, and IAC length show a statistically significant mean difference between the two groups. Narrower and shorter BCNC and IAC width, height, and length are factors affecting SNHL by multivariate logistic regression; the odd ratios were 23.222 (5.970–90.324, 95% confidence interval), 1.719 (1.008–2.930), 1.637 (1.050–2.550), and 1.288 (1.075–1.543), respectively.

Conclusions
The diameters of BCNC and IAC are likely the factors affecting hearing function in pediatric patients. Although this study clarifies that they tend to be wider and longer in normal hearing ears, the physiologic and anatomic significances contributing to the management of SNHL remained investigated.

PS 813

Bone Thickness Estimation Software for Surgical Planning of a Bone-Conduction Implant

Carlos Salgado[1]; S. Alireza Rohani[1]; Sumit K. Agrawal[2]; Hanif M. Ladak[1]
[1]*Western University;* [2]*London Health Sciences Centre*

Background
The BONEBRIDGE (Med-El GmbH, Innsbruck, Austria) is a bone-conduction implant for patients with conductive and mixed hearing loss. The size of the device';s transducer (height of 8.7 mm) requires finding a suitably thick location on the temporal bone to house the implant. Software has been reported in the literature for estimating and spatially mapping bone thickness from computed tomography (CT) images for surgical planning purposes. However, the inclusion of air cells into the thickness estimates in current approaches can result in overestimation, which is problematic as the implant';s screws cannot be expected hold the transducer in place in highly pneumatized areas. The objective of this study was to develop and validate software to compute bone thickness maps from clinical CT images while excluding the air cells in the estimates.

Methods

CT images of four cadaveric temporal bones were used in this study. Each sample was segmented (i.e., classified) using manual thresholding to create a triangulated 3D surface model of the lateral surface of the temporal bone. A ray-tracing algorithm was used to calculate the thickness of the temporal bone. For each triangle on the 3D surface, a ray was projected towards the inside of the head and intersecting voxels were sequentially thresholded to find the first air cell voxel. Bone thickness was computed as the Euclidean distance from the ray';s starting point to the first identified air cell voxel. Three different thresholds were compared to determine the optimal one: 400 Hounsfield unit (HU), corresponding to D3 bone; 150 HU, corresponding to D4 bone; and -1000 HU, corresponding to air. To find the optimal threshold, manual measurements were performed by an experienced surgeon on a uniformly-distributed subset of triangles, and paired samples t-tests were conducted to compare the expert measurements and the automated thickness estimations.

Results

At the threshold of 150 HU, there was not a significant difference in the thicknesses for automated (mean=4.469 mm, standard deviation=2.553 mm) and expert measurements (mean=4.368 mm, standard deviation=2.439 mm), p=0.448. The absolute thickness difference was 1.01 mm ± 1.332 mm accounting for all measurement locations and samples.

Conclusions

Using an HU value of 150, the ray-casting algorithm can provide thickness estimations that are not significantly different to the measurements obtained by an experienced Otolaryngologist. This algorithm allowed consideration of the air cells to ensure adequate bone thickness for implant placement.

PS 814

Automated Digital Modeling of the Sigmoid Sinus from 3D Micro-CT Images for Surgical Training

Daniel G. Allen[1]; Kylen Ann Van Osch[1]; Bradley M. Gare[1]; Sumit K. Agrawal[2]; Hanif M. Ladak[1]
[1]*Western University;* [2]*London Health Sciences Centre*

Background

Accidental injury of the sigmoid sinus during mastoidectomy results in venous bleeding. To provide training opportunities in order to avoid such injuries, a virtual reality simulator has been developed to present realistic digital anatomy that can be operated upon in an intuitive manner with haptic (touch) feedback. To broaden the training experience, exposure to a wide variety of sigmoid sinus shapes within the simulated environment is required; however, segmentation or creation of digital models of the sigmoid sinus from image volumes is tedious, time-consuming and error-prone.

Objective

To develop and evaluate software for automatically segmenting the sigmoid sinus from 3D micro-computed tomography (micro-CT) images.

Algorithm

The automatically generated models were created using a technique called "atlas-based segmentation". First an exemplar image representing an average sigmoid sinus was selected, and a 3D digital model of the sigmoid sinus was created with a region growing segmentation technique and manual editing by an Anatomist; this manual step need only be done once during algorithm design. The exemplar image was then automatically registered (i.e., translated, rotated, scaled, and warped) to a new 3D image. The resulting transformation was applied to the exemplar digital model to create a model that fit the new image.

Accuracy

Forty cadaveric temporal bones were scanned with micro-CT. The 3D images were cropped, aligned, and digital models were manually created as before. This provided the ground truth models for evaluating the automatically generated models. Dice coefficients and Hausdorff distances were calculated to quantify the accuracy of the automatically generated models in comparison to ground truth models.

Results

Visual inspection of the automatically generated models showed that they fit well within the sigmoid sinus groove. The similarity metrics showed high overlap between the automated results and the ground truth models. Specifically, individual Dice coefficients were as high as 0.90, close to the ideal value of 1.0 (perfect overlap). The mean Dice coefficient was 0.73. The mean Hausdorff distance between the automatically generated and ground truth models was 0.379 mm which is low when compared to the models'; approximate average length of 60 mm, further indicating good overlap between the two sets of models.

Conclusions

Atlas-based segmentation has the ability to model the sigmoid sinus with reasonable accuracy from 3D micro-CT images. The automated nature of the atlas-based approach makes it a viable option for quickly and easily generating usable models of the sigmoid sinus.

PS 815

Virtual Consequences: The Development and Use of Surgical Complications for Virtual Training

Gregory Wiet[1]; Bradley Hittle[2]; Hector Medina-Fetterman[3]; Thomas Kerwin[2]; Don Stredney[2]
[1]*Nationwide Children's Hospital/The Ohio State University;* [2]*Ohio Supercomputer Center;* [3]*Interface Laboratory Consultant, Ohio Supercomputer Center*

Problem Statement

In surgical training, opportunities to manage complications are a double edged sword. They are valuable to the trainee but not for the patient. Ideally, learning to handle complications should be performed in a controlled environment, providing the capability to stop, consider conditions that predict the complication, how to avoid them and resolve the situation. High fidelity simulation provides such an environment. Representation of complications often requires high fidelity emulation to depict the real world; additionally, higher fidelity augments the user';s sense of immersion. The use of consequences serves to expand cognitive knowledge as it is integrated with surgical skills. By combining structural, spatial and sequential information with contextual cause and effect, a more engaging and effective learning experience can be achieved to provide expertise with and avoidance of complications.

Background

Although several groups, including our own, have generated virtual simulation of otologic surgery, previous representations of complications such as bleeding, have been limited. Current temporal bone surgery simulators do not incorporate fluid rendering or effects. We present a focused effort to depict real-time fluid interactions for emulating consequences associated with bleeding during mastoidectomy. Specifically we demonstrate a virtual surgical environment that supports the identification and management of the complication of surgical bleeding.

Methods

We employ direct volume rendering on the GPU to display the mastoid bone altered during the surgery. Haptics and real-time removal are processed on the CPU and the changes in the bone data due to removal from the drill are re-uploaded to the GPU for re-rendering. FLEX™, a library created by NVIDIA and released for free, provides fluid, fabric, and soft body real-time simulation for graphics applications. The interface for this simulation includes stereo visual and binaural displays. In addition, two haptic interfaces provide an avenue to learn for the deft orchestration of bi-dexterous tool manipulation.

Results

A Physics based fluid representation has been encorporated into our temporal bone simulator to provide bleeding and irrigation. Learners now can be exposed to small and large vessel bleeding during dissection and learn to prevent and manage this occurrence in mastoid surgery. See video links:

https://osu.box.com/s/d603mwg5nmkek7o7zofg373q-pqk4ed2j

https://osu.box.com/s/e4gu5h16s689kj41yncvtc-j6tw75odnn

https://osu.box.com/s/0jfgg9l4jpk4nfmx5w-7bysamgest0p

https://osu.box.com/s/u0mnyx7s2bxztsk4icyz9tiqwby-q35vn

Discussion

We have presented our approach to emulate both irrigation and bleeding associated with otologic surgery. The result is a visually plausible, three dimensional, real-time simulation of the consequences associated with bleeding and irrigation. This simulation allows for presenting complications in a controlled environment, providing a safe method for deliberate practice

Acknowledgement

PS 816

The clinical analysis of six patients with giant cell reparative granuloma of temporal bone

Liao Kaxi[1]; **Feng Bo**[2]; Shiming Yang[3]; Peng Tao[1]
[1]*Department of Otolaryngology-Head and Neck Surgery, Nanchong Central Hospital,The second affiliated hospital of North sichuan medical college;* [2]*Department of Otolaryngology-Head and Neck Surgery, PLA General Hospital, Beijing 100853, China;* [3]*Chinese PLA Medical School*

Objective

Giant cell repair granuloma(GCRG) of temporal bone is a rare clinical disease. Its pathogenesis is still unclear. GCRG of temporal bone can be invasive and be misdiagnosed because it has no specific manifestation.This study is aimed to summarize the clinical features of giant cell reparative granuloma of temporal bone in six cases, and to analyze the factors that lead to its misdiagnosis.

Method

The clinical data of six cases with GCRG of temporal bone admitted in Chinese PLA General Hospital from January 2011 to December 2016 were reviewed.

Result

There were 3 males and 3 females among the 6 cases in the study. The average age was 45.16 years old , and the course of disease range was from 5 months to 6 years. Clinical data shows hearing loss(conduction deafness), sensation of ear fullness were their major performance. In addition, tinnitus, facial paralysis, pain in temporal bone area might be accompanied symptoms. Computed tomography showed temporal bone area, fossa cranii media has dilatability space-occupying lesion, the main sign was osteolytic destrucion. Magnetic resonance imaging demonstrated low signal intensity on T1WI, and heterogeneous low signal intensity on T2WI. Completely surgical removal is the first choice treatment. One of the six cases received radiotherapy after surgery. The postoperative pathological examination of the six cases were diagnosed as GCRG of temporal bone. No recurrence and metastasis were found after a two to three years follow-up.

Conclusion

GCRG of temporal bone has various of manifestations and can be easily confused with other diseases. The final diagnosis depends on the consequence of pathological examination. Surgical resection is the first choice of treatment method.

Key words

Giant cell repair granuloma , GCRG, Temporal bone ,Definitive diagnosis, Surgical treatment.

The clinical analysis of six patients with giant cell reparative granuloma of temporal bone.docx

Vestibular Schwannoma

PS 817

Effect of MEK Inhibition on Cell Viability in Primary Human Vestibular Schwannoma Cells

Christine T. Dinh[1]; **Olena Bracho**[1]; Marisa Fuse[2]; Rahul Mittal[3]; Denise Yan[1]; Esperanza Bas[4]; Fred Telischi[1]; Cristina Fernandez-Valle[2]; Xue-Zhong Liu[1]

[1]University of Miami Miller School of Medicine, Department of Otolaryngology; [2]University of Central Florida Burnett School of Biomedical Science, Division of Neuroscience; [3]Hearing Research Laboratory, Department of Otolaryngology, University of Miami Miller School of Medicine, Miami, FL 33136, USA; [4]Department of Otolaryngology, University of Miami Miller School of Medicine

Background

Vestibular schwannomas (VS) are benign tumors originating from Schwann cells of the cochleovestibular nerve. Bilateral VS are diagnostic for Neurofibromatosis Type II (NF2) – a hereditary tumor disorder that causes hearing loss and other neurological sequelae. Treatment of NF2-associated VS is challenging. Microsurgical resection can cause significant cranial nerve morbidity, while radiotherapy can induce malignant transformation and progressive hearing loss in this population. Off-label use of FDA-approved chemotherapeutic drugs have been effective in improving hearing and reducing tumor burden in some patients. Our preliminary studies demonstrate that MEK (mitogen-activated protein ki-

nase kinase) inhibitors reduce growth of a merlin-deficient human Schwann cell line in vitro and an allograft mouse model of NF2.

Objective
Determine the effectiveness of two MEK inhibitors on reducing cell viability in primary human VS cells in vitro.

Methods
Fresh tumor was obtained from seven patients undergoing VS surgery at University of Miami/Jackson Memorial Hospital. NF2 mutational analysis was performed using Multiplex Ligation-Dependent Probe Amplification (MLPA). Dissociated primary human VS cells were cultured, and crystal violet assays to determine cell viability were performed after exposing cells to vehicle and three different concentrations of trametinib and PD0325901 for 3 days in vitro . Western blot was also performed to assess the levels of MEK and phosphorylated MEK (pMEK) in each tumor.

Results
The VS demonstrated NF2 mutations on MLPA. Two VS (~29%) demonstrated >20% reduction, three VS (~43%) demonstrated 10-20% reduction, and two VS (~29%) demonstrated <10% reduction in cell viability at the highest concentration of trametinib tested. A dose-dependent response was demonstrated in several tumors. The two VS that responded best to trametinib also responded favorably to PD0325901. All VS demonstrated expression of MEK and pMEK; however, there was no correlation between protein expression and cell viability (p>0.05).

Conclusion
MEK inhibition reduced cell viability in several VS. The effect of MEK inhibitors, trametinib and PD0325901, on cell viability was independent of the protein levels of MEK and pMEK in primary human VS cells with NF2 mutations. However, the degree of response to MEK inhibition was fairly consistent within each individual tumor. These findings suggest that other molecular factors, such as genetics, epigenetics, tumor cell composition, and competing signaling pathways, may contribute to drug resistance in each tumor. Future studies in NF2 therapeutics and precision medicine should consider utilization of primary human VS cultures as an additional preclinical tool in assessing drug efficacy and resistance in this heterogeneous population.

PS 818

Anti-tumor effect of cold atmospheric pressure plasma on vestibular schwannoma demonstrates its feasibility as an adjuvant treatment after surgery

Hyun Jin Lee[1]; Yeo Jun Yoon[2]; Michelle J Suh[1]; Hyun Young Lee[3]; Hae June Lee[3]; Eun Ha Choi[4]; Kiwon Song[2]; In Seok Moon[1]
[1]*Department of Otorhinolaryngology, College of Medicine, Yonsei University;* [2]*Department of Biochemistry, College of Life Science & Biotechnology, Yonsei University;* [3]*Department of Electrical Engineering, Pusan National University;* [4]*Plasma Bioscience Research Center and Department of Electrical and Biological Physics, Kwangwoon University*

Vestibular schwannoma (VS), although a benign intracranial tumor, can cause morbidities including hearing loss, tinnitus, dizziness, and possible mortality by brainstem compression. The treatment strategies of VS are conservative, because both microsurgery and stereotactic radiation therapy pose risks of morbidity. During the microsurgery of tumors with large volume, attempting the complete removal can increase the damage of cranial nerves, thereby leading to possible facial palsy or hearing loss. Minimizing the damage of cranial nerves during surgery may have a positive impact on the patient's wellbeing. On the other hand, incomplete resection can cause tumor recurrence. A novel adjunct therapy that efficiently removes the possible remnant tumor cells around cranial nerves would be helpful to minimize the surgical area to reduce the morbidity due to damage and the risk of recurrence. Cold atmospheric pressure plasma (CAP) is an ionized gas generated by electrical discharges in the atmospheric pressure at room temperature. Currently, CAP has been extensively studied for clinical applications since it can be easily generated, causes no thermal damage to cells, and can be controlled by adding gases and/or adjusting the electric field. CAP has been reported to induce cell death in various types of cancer cells via increasing the intracellular ROS. Here, we examined the feasibility of cold atmospheric pressure plasma (CAP) as an intra-operative adjuvant treatment for VS after surgery. Cell death was efficiently induced in both human HEI-193 and mouse SC4 VS cell lines upon exposure to CAP for seven minutes. Interestingly, both apoptosis and necroptosis were simultaneously induced by CAP treatment, and cell death was not completely inhibited by pan-caspase and receptor-interacting serine/threonine-protein kinase 1 (RIK1) inhibitors. Cell death phenotype was similarly observed in patient-derived primary VS cells and tumor mass upon CAP exposure. In addition, CAP exposure after the surgical removal of primary tumor efficiently inhibited tumor recurrence in SC4-grafted mouse mod-

els. Collectively, these results strongly suggest that CAP should be developed as an efficient adjuvant treatment for VS after surgery to eliminate the possible remnant tumor cells, and to minimize the postoperative complications.

Abstract.docx

PS 819

The Proteome of Perilymph in Patients with Vestibular Schwannoma gives some insight to the Tumor Associated Hearing Loss

Jesper Rasmussen[1]; Göran Laurell[2]; Helge Rask-Andersen[3]; Jonas Bergquist[2]; Po Eriksson[4]
[1]Department of surgical sceinces, Uppsala university; [2]Uppsala university; [3]University of Uppsala; [4]Uppsala university, Uppsala university hospital

Background
It is an axiom that samples from the inner ear cannot be taken for diagnostic purposes. In this study perilymph was aspirated from patients with vestibular schwannoma during skull-base surgery. The aim of the present study is to analyze the proteome of perilymph in individual patients.

Methods
Fifteen patients undergoing trans-labyrinthine surgery for sporadic vesibular schwannoma with varying degree of sensorineural hearing loss were included in the study. Perilymph was sampled by aspiration through the round window membrane and frozen in liquid nitrogen. Analysis was performed with online LTQ-orbitrap mass spectometer. The raw data from the masspectrometry was analyzed using Thermo Proteom Discovery to identify the total number of proteins. MaxQuant was used for quantification of proteins in individual samples using the implemented Andromeda search engine to correlate MS/MS spectra to the Uniprot human database. Hearing function was preoperatively assessed by pure ton audiogram.

Results
The proteome of perilymph from patients with vestibular schwannoma had in our samples 314 proteins. 91 proteins were identified in 12 or more of the patients. 184 were identified in only four or less patients. Alpha-2-HS-glycoprotein (P02765) was correlated to loss of hearing in the patients with vestibular schwannoma. The diameter of the tumor was possibly, but not confirmed, to be independent correlated to the Complement component C6 protein (P13671). Age, gender, and tumor diameter were rejected as parameters to predict hearing loss.

Conclusion
The perilymph proteome showed a stable section of 91 proteins found in the majority of the patients and a highly individual section of 184 proteins found in a minority of the patients. Correlation to tumor associated hearing loss was shown for the Alpha-2-HS-glycoprotein (P02765), indicating that this protein is part of the pathophysiologic process leading to the loss of hearing. The results need confirmation in a larger group of patients with vestibular schwanomma.

PS 820

Precision Medicine in Neurofibromatosis Type II

Christine T. Dinh[1]; Xue-Zhong Liu[1]; Cristina Fernandez-Valle[2]; Mislen Bauer[3]; Fred Telischi[1]
[1]University of Miami Miller School of Medicine, Department of Otolaryngology; [2]University of Central Florida Burnett School of Biomedical Science, Division of Neuroscience; [3]Nicklaus Children's Hospital

Background
Neurofibromatosis Type II (NF2) is a genetic tumor disorder that predisposes individuals to develop multiple nervous system tumors, including schwannomas, meningiomas, and ependymomas. Therapies to treat NF2 are limited, making the management of NF2 particularly challenging. The risks and benefits of each available treatment modality needs thorough assessment with the ultimate goals of balancing tumor control (to prevent intracranial complications) and quality of life (preserving hearing and neurological function). Precision medicine in NF2 refers to a methodical, systematic approach for identifying distinct and effective treatments, based on the genetic profiles of the individual and their tumors. However, the practice of personalized medicine in NF2 is elementary and impeded by our understanding of how variations in the type of NF2 mutations, presence of mutations in other genes, and epigenetic factors affect disease phenotype.

Objective
The objective is to present a preclinical, translational research, and clinical algorithm that incorporates broad investigations of the genome, epigenome, transcriptome, and proteome into predicting clinical outcomes and identifying effective, personalized treatments for NF2.

Methods
The participation of several basic science, translational, and clinical researchers and physicians from multiple disciplines was elicited at the University of Miami Miller School of Medicine, Burnett School of Biomedical Sciences at the University of Central Florida, and Nicklaus Children';s Hospital. A research and clinical strategy for addressing NF2 was developed.

Results

The algorithm incorporates: (1) identification and diagnosis of NF2 patients in the community, (2) NF2 mutational testing and disease phenotype stratification, (3) weekly clinical conferences with multi-specialists of the base of skull (MOBS), (4) referrals to appropriate sub-specialists, (5) a prospective and comprehensive clinical database, (6) genetic, epigenetic, transcriptional, and proteomic profiling of available tumor, (7) analysis of cerebrospinal fluid for biomarkers for disease and hearing loss, (7) high-throughput screening for candidate drug therapies using merlin-deficient Schwann cell lines, (8) low-throughput screening for best candidate drug therapies using primary human tumor cultures, (9) focused examination of top drug therapies in animal models, and (10) precision medicine clinical trials.

Conclusion

NF2 is a complex tumor disorder that requires a multidisciplinary approach for diagnosis and treatment. We present an organized strategy consisting of research and clinical elements to address the needs of NF2 patients. This algorithm is feasible, timely, and will provide the structured foundation to establish a network of scientific and patient-centered knowledge that will aid in the practice of precision medicine in NF2 in future years.

PS 821

Targeting the cMET pathway augments radiation response without adverse effect on hearing in NF2 schwannoma models

Yingchao Zhao[1]; Fu Zhao[2]; Na Zhang[1]; Jie Chen[1]; Lukas D. Landegger[3]; Takeshi Fujita[4]; Anat Stemmer-Rachamimov[5]; Jing Zhang[2]; Yanling Zhang[1]; Gino Ferraro[1]; Hao Liu[1]; Alona Muzikansky[6]; Pinan Liu[2]; Scott Plotkin[7]; Rakesh Jain[1]; **Konstantina M. Stankovic**[3]; Lei Xu[1]

[1]Edwin L. Steele Laboratories, Department of Radiation Oncology, Massachusetts General Hospital and Harvard Medical School, Boston, Massachusetts 02114; [2]Department of Neurosurgery, Beijing Tian Tan Hospital, Capital Medical University, Beijing, China; [3]Department of Otolaryngology, Massachusetts Eye and Ear; [4]Kindai University; [5]Molecular Pathology Division, Massachusetts General Hospital, Boston, Massachusetts 02114; [6]Division of Biostatistics, Massachusetts General Hospital, Harvard Medical School, Boston, MA 02114; [7]Department of Neurology and Cancer Center, Massachusetts General Hospital, Boston, Massachusetts 02114

In patients with progressive vestibular schwannoma (VS), radiotherapy is associated with the risk of debilitating hearing loss. There is an urgent need to identify an adjunct therapy that, by enhancing the efficacy of radiation, can help lower the radiation dose and preserve hearing. In our novel cerebellopontine angle (CPA) model of schwannomas that faithfully recapitulate the tumor-induced hearing loss, we observed that cMET blockade by crizotinib (CRZ) enhanced schwannoma radiosensitivity by enhancing DNA damage, and CRZ treatment combined with low-dose radiation was as effective as high-dose radiation. CRZ treatment had no adverse effect on hearing; however, it did not affect tumor-induced hearing loss in the CPA model, presumably because cMET blockade did not change tumor HGF levels. cMET gene knockdown study independently confirmed the role of cMET pathway in mediating the effect of CRZ. Furthermore, we evaluated the translational potential of cMET blockade in human schwannomas. We found that human samples of NF2-associated and sporadic VSs showed significantly elevated HGF expression and cMET activation compared to normal human great auricular nerves, and that HGF and activated cMET levels correlated with tumor growth and cyst formation. Using an organoid brain slice culture model, cMET blockade inhibited the growth of patient-derived schwannomas. Our study provides the rationale and critical data for the clinical translation of combined cMET blockade with radiation therapy in patients with vestibular schwannomas.

Vestibular: Meniere's Disease

PS 822

Cluster analysis identifies clinical subgroups in patients with uni- and bilateral Meniere's disease

Jose Antonio Lopez-Escamez; Lidia Frejo; on behalf of Meniere Disease Consortium
Centre for Genomics and Oncology Research (Genyo)

Background

Meniere';s disease (MD) is a heterogeneous syndrome of the inner ear characterized by episodes of spontaneous vertigo, with fluctuating low-to-medium frequency sensorineural hearing loss (SNHL), tinnitus and aural fullness. It is associated with the accumulation of endolymph within the cochlear duct. Some co-morbidities, such as migraine, allergy or autoimmune disorders (AD), have been associated with MD in epidemiological

studies. This heterogeneity may explain the poor results in most clinical trials.

Methods

We conducted a multicenter study in 1386 patients with MD from 21 hospitals within the MD Consortium. A two-step cluster analysis was performed in 988 patients with unilateral MD and 398 with bilateral involvement to identify the best predictors to define clinical subgroups with a potential different etiology.

Results

We have defined 5 clinical subgroups in patients bilateral MD according to 4 predictors: 1) another comorbid autoimmune disease (AD), 2) familial history with a first or second degree relative with MD; 3) comorbid migraine and 4) simultaneous onset of hearing loss. Groups were ranked according to their observed frequencies. Group 1 was the most frequently found, included 46% of patients, and is defined by metachronic hearing loss without migraine and without AD. Group 2 was found in 17% of patients, and it was characterized by synchronic hearing loss without migraine or AD. Group 3, with 13% of patients consisted of familial MD cases, while group 4, that includes 12% of patients, was associated by the presence of migraine in all cases. Group 5 was found in 11% of patients and was defined by AD. Of note, we also have found 5 clusters among patients with unilateral MD. Group 1 was the most frequently found (53% of patients) and it was defined as sporadic MD without migraine and without AD; Group 2 was observed in 8% of patients, and it is defined by hearing loss, which antedates the vertigo episodes by months or years (delayed MD). Group 3 included familial cases (13%); group 4 was associated with migraine and included 15% of patients. Group 5 was found in 11% of cases reporting a comorbid AD.

Conclusions

Cluster analysis defines clinical subgroups in MD, and it extends the phenotype beyond audiovestibular symptoms. This classification will help to improve the phenotyping in MD and the selection of patients for randomised clinical trials.

References

1. Frejo L et al. Clinical Subgroups in Bilateral Meniere Disease. Front Neurol. 2016;7:182.

2. Frejo L et al. Extended phenotype and clinical subgroups in unilateral Meniere disease: A cross-sectional study with cluster analysis. Clin Otolaryngol. 2017 Feb 6.

PS 823

PROINFLAMMATORY CYTOKINE LEVELS TO DIFFERENTIATE MENIERE'S DISEASE FROM VESTIBULAR MIGRAINE

Lidia Frejo[1]; Marisa Flook[1]; Alvaro Gallego-Martinez[1]; Juan Carlos Amor-Dorado[2]; Sofia Santos-Perez[3]; Andres Soto-Varela[3]; Angel Batuecas-Caletrio[4]; Juan Manuel Espinosa-Sanchez[5]; Eduardo Martin-Sanz[6]; Teresa Requena[1]; Jose Antonio Lopez-Escamez[1]
[1]Centre for Genomics and Oncology Research (Genyo); [2]Hospital Can Misses Ibiza; [3]Hospital Universitario Santiago; [4]Hospital Universitario Salamanca; [5]Hospital Virgen de las Nieves; [6]Hospital Universitario de Getafe

Background

Meniere disease (MD) and Vestibular migraine (VM) show an overlapping phenotype when MD is associated with migraine. An abnormal immune response has been suspected in a subset of patients with MD, and hearing loss may be restored by steroids in approximately 50% of cases. There are several evidences supporting the immune hypothesis in MD including, increased values of circulating immune complexes in some patients sera or the association of allelic variants in MICA, TLR10 or NFKB1 genes with hearing loss progression. The aim of this study was to characterize the cytokine profile in patients with Meniere';s disease (MD) and vestibular migraine (VM).

Methods

Isolated peripheral blood mononuclear cells (PBMC) from 113 patients with MD, 75 patients with VM and 54 controls were incubated at 37°C, 7% CO_2 overnight. Supernatant was collected and RNA harvested. Basal levels of TNFα, IL-1β, and IL-6 were quantified in supernatant of PBMC with a bead-based multiplex assay. RNA expression levels were measured using the HumanHT-12 v4 Expression BeadChip. Limma R package was used for expression data analysis and normalization and for differential expression analysis. Data were analyzed using SPSS Software and cluster analyses were performed using the heatmap.2 function from gplots R package.

Results

Two different subgroups of patients with MD were observed according to their cytokines profile. Eighty-nine patients (78.8%) presented low levels of cytokines (IL-1β = 1.5 ± 1.0; IL-6 = 4.83 ± 6.2 and TNFα = 6.2 ± 4.4), while 24 (21.2%) exhibited high levels of cytokines (IL-1β = 23.9 ± 14.8; IL-6 = 139.0 ± 151.3 and TNFα = 37.0 ± 20.3). All individuals with VM and controls showed low levels of cytokines.

The array data confirmed a differential expression of many immune-related genes in MD patients with higher levels of cytokines when they were compared to MD patients with low levels of cytokines, VM patients or healthy controls, retrieving significant pathways such as Toll-like receptor signaling (P=3.65x10^{-9}), TREM1 signaling (P=1.03X10^{-7}), IL-8 signaling (P=7.29x10^{-7}) and Th1 Pathway (P=1.76x10^{-6}). There were no significant differences between VM patietns and healthy controls.

Conclusions

1. Proinflammatory cytokines profiles suggest two subgroups of patients with MD.

2. VM patients show low levels of proinflammatory cytokines.

3. Cytokine profile could be a potential marker to differentiate MD and VM.

PS 824

SPI-1005 a novel investigational drug for the treatment of Meniere's disease

Jonathan Kil[1]; May Huang[2]; Shaun Nguyen[3]; Sujana Chandrasekhar[4]; Paul Lambert[3]
[1]Sound Pharmaceuticals; [2]Northwest Ear; [3]MUSC; [4]New York Otology

Background

Glutathione Peroxidase (GPx) is a critical cytoprotective enzyme in the brain, eye, ear, lung, and kidney. GPx1 is the dominant isoform in the inner ear and is highly expressed within the organ of Corti, spiral ganglia and stria vascularis of the cochlea. Ebselen is a selenorganic compound that mimics and induces GPx1 and has been show to prevent and treat sensorineural hearing loss in animals (Kil et al., Hear Res 2007). SPI-1005 is an investigational new drug that contains ebselen and is delivered orally (Lynch & Kil, Semin Hear, 2009). Recently, SPI-1005 was shown to prevent an acute noise induced hearing loss (NIHL) in a randomized double blind placebo controlled clinical trial (Kil et al., Lancet, 2017). Young adults treated with SPI-1005 showed a lower incidence and severity of NIHL when compared to placebos following a single noise exposure. Here, we report the first clinical data involving SPI-1005 in Meniere's disease (MD), where vertigo, hearing loss and tinnitus are documented and patient reported.

Methods

To determine the safety, pharmacokinetics and pharmacodynamics of SPI-1005 in probable or definitive MD by AAO-HNS 1995 criteria, we employed a randomized, double-blind, placebo-controlled, multi-center clinical trial in the US. 40 adults received either placebo or one of three different doses of SPI-1005 treatment for 21 days. Subjects were followed for an additional 28 days post-treatment. Repeat safety (hematology and serum chemistry) and audiologic testing (pure-tone audiometry, words-in-noise test (WINT), electrocochleography) were performed at baseline, at the end of treatment, and following treatment. Patient reported outcomes of tinnitus and vertigo severity were also determined before, during and following treatment. Multiple analyses were made during and following treatment and between SPI-1005 and placebo treated subjects.

Results

56 MD volunteers were screened, 42 enrolled and 39 completed the Phase 1b study: 22 males, 17 females, average age 53 (32-71). SPI-1005 was found to be safe and well tolerated following oral doses of 200, 400 or 600 mg bid for 21 days. No serious AEs were reported and all AEs were mild to moderate and consistent with earlier SPI-1005 studies. Several exploratory efficacy endpoints were analyzed. SPI-1005 showed clinically relevant improvements in low frequency hearing, which is most affected in MD. SPI-1005 also showed improvements in WINT, tinnitus loudness and vertigo severity. Given the initial safety and clinical improvements observed following SPI-1005 treatment in both auditory and vestibular symptoms, additional testing in Meniere's disease is warranted.

PS 825

DEVELOPMENT OF AN iPSCS-BASED MODEL FOR DTNA/FAM136A AUTOSOMAL DOMINANT MENIERE DISEASE

Lidia Frejo[1]; Jose Luis Rodriguez-Llamas[2]; Teresa Requena[1]; Ae-Ri Ji[1]; Ivan Velasco[2]; Veronica Ramos-Mejia[3]; Jose Antonio Lopez-Escamez[1]
[1]Centre for Genomics and Oncology Research (Genyo); [2]Instituto de Fisiología CelularNeurociencias, Universidad Nacional Autónoma de México, Mexico; [3]Gene regulation, Stem Cells and Development Group, Department of Genomic Oncology, GENYO

Meniere';s disease (MD) is an inner ear disorder characterized by sensorineural hearing loss, episodic vertigo and tinnitus. Using whole exome sequencing we have identified ultrarare mutations in the FAM136 and DTNA genes in a family with autosomal dominant MD. We generated an induced pluripotent stem cell (iPSC) line from a MD patient and a healthy control. Peripher-

al blood mononuclear cells were reprogrammed using non-integrative Sendai viruses containing Sox2, Oct3/4, c-Myc and Klf4 (CytoTune®-iPS 2.0 Sendai Reprogramming Kit). The first colonies started to emerge at 9 days after transduction and iPSC colonies were selected on day 19, with an efficiency of iPSC generation of 0.01% and 0.03% for patient and control, respectively. Two clones, MD-iPSCs (W8) and control-iPSCs (GRX-MCiPS4F-A2), were established and characterized (Cabrera et al.. 2015)

Control and MD-iPSCs were maintained in culture on irradiated human foreskin fibroblasts feeder cells and were also adapted to feeder-free cultures on matrigel. Exogenous reprogramming factors were silenced after 25 passages. . Both cell lines expressed the pluripotency markers hOCT4, hSOX2, hKLF4, hMYC and hNANOG at the mRNA levels, and they also expressed OCT4, SSEA4 and TRA-1-60 proteins as assessed by immunocytochemistry. Furthermore, both cell lines demonstrated pluripotency by differentiating into three germlayers by in vitro and in vivo differentiation tests. Of note, both cell lines showed different proliferation rates, as MD-iPSCs W8 have a doubling time of 48-53 hr, while GRX-MCiPS4F-A2 cells divide every 36-39 hr. We also perform neuron progenitors differentiation using a dual-SMAD inhibition and floor plate induction protocol (Kriks et.al., 2011).

Then, we analyzed DTNA and FAM136A expression in our iPSCs and found that in MD-iPSC DTNA expression was 3.75-fold lower (adjusted $P=1.65 \times 10^{-3}$) and FAM16A was 3.95-fold lower (adjusted $P=1.28 \times 10^{-3}$) when compared with control-iPSC. However, the expression of both genes in neural progenitors was higher in MD-iPSC (DTNA = 2.8-fold change ($P=2.2 \times 10^{-3}$); FAM136A = 2.7-fold change ($P=3.3 \times 10^{-3}$) when compared to Control-iPSC. Western blot and confocal microscopy analysis confirmed gene expression results at a protein level.

We describe the generation of DTNA/FAM136A patient-specific MD-iPSCs and their controlled differentiation to neural progenitors, showing a differential expression in both, iPSC and neural progenitor states. Future studies with this cellular model will improve the understanding of DTNA/FAM136A genes in MD.

References

1. Cabrera S et al. Stem Cell Res. 2015 Sep;15(2):337–40.

2. Kriks S et al. Nature. 2011 Nov 6;480(7378):547–51.

PS 826

Furosemide loading vestibular evoked myogenic potential testing in Meniere's disease - Confirmation of the rupturing of the membranous labyrinth theory -

Toru Seo; Takeshi Fujita; Katsumi Doi
Kindai University

Background

We reported that the p13-n23 peak-to-peak amplitude in vestibular evoked myogenic potential increased after furosemide administration in the patients with Meniere';s disease (Furosemide loading VEMP: FVEMP). The aim of this study is to investigate the factors which influence the results in unilateral Meniere';s disease.

Subjects and Methods

Subjects were 44 cases with unilateral Meniere';s disease who underwent FVEMP. The peak-to-peak amplitudes of VEMP were recorded before (AB) and after (AA) 20mg of furosemide administration. Improvement ratio (IR) was calculated by the following formula: IR = 100 x (AA-AB)/AB. Positive FVEMP test results; i.e., when IR was >14.2%, or when p13-n23 biphasic waves could be detected after the administration of furosemide in cases in which no such waves were detected before the administration of furosemide. The factors that affected the results of the FVEMP tests were also assessed.

Results

The FVEMP positivity rate for ears affected by Meniere';s disease was 63% and was not related to age, gender, disease stage, or illness duration (p>0.05). However, the rate was positively correlated with the time since the last vertigo attack (p=0.000647) and negatively correlated with the mean number of vertigo attacks per month (p=0.00294).

Discussion

Although positive FVEMP test results are indicative of endolymphatic hydrops, this study found that recent and frequent vertigo attacks are associated with negative results. This seemingly strange finding can be explained as follows: positive results mean the reduction of the accumulated endolymph; however, the examination results are negative if the endolymphatic space communicates to the perilymphatic space, because furosemide cannot affect reduction of endolymph. Thus, this study suggests that vertigo attacks are caused by the rupturing of the membranous labyrinth.

Evaluating Response to Intratympanic Gentamicin in Meniere's Disease using caloric Testing

James Naples[1]; Jason Brant[2]; Steven Eliades[2]; Michael Ruckenstein[2]

[1]University of Pennsylvania Hospital; [2]University of Pennsylvania

Background

Therapy for Meniere';s Disease (MD) aims at controlling symptoms through medical or surgical means. Intratympanic (IT) gentamicin is used to induce selective chemical labyrinthectomy. Although vestibular testing with caloric testing and videonystagmography are available to assess the degree of afferent labyrinthine loss following gentamicin, it is unclear how vestibular testing correlates with clinical response to IT gentamicin. We aim to evaluate whether vestibular testing provides information that correlates with clinical response or failure to IT gentamicin.

Methods

A retrospective chart review of patients receiving IT gentamicin (27mg/ml) for refractory MD from 2005-2017 was performed. All patients failed initial treatment. Failure was defined as recurrence of vertigo symptoms requiring more aggressive therapy. The number of IT injections was evaluated. Baseline and post-treatment vestibular testing data was collected, and response to treatment was evaluated based on vertigo resolution and need for further treatment.

Results

Sixty-seven patients were evaluated. A good clinical response to IT gentamicin was obtained in 90% of patients. Patients who failed IT gentamicin received a mean of 3.4 injections, whereas patients who responded received 2.4. Treatment failure patients had elevated mean (±SD) warm-caloric responses at 2 weeks (4.5±6.83) and 4 weeks (8.0±2.83) post-initial IT injection as compared to treatment-responsive patients (3.49±3.92 and 4.07±5.41)(p>0.05). Similarly, mean (±SD) ice-caloric responses in the failure groups were elevated at 2 weeks (18.6±10.53) and 4 weeks (13.67±10.5) compared to the responsive group (14.63±10.57 and 7.95±6.64, respectively). This difference trended toward statistical significance (p=0.49 and p=0.076, respectively)

Conclusions

Patients that failed IT gentamicin required more injections and had elevated warm-and ice-water caloric responses at 2 and 4 weeks post-injection compared to treatment-responders. The difference in response to warm- and ice-water caloric testing has potential to aid in predicting clinical response to treatment and guide treatment management. Further work is needed to fully understand clinical failures.
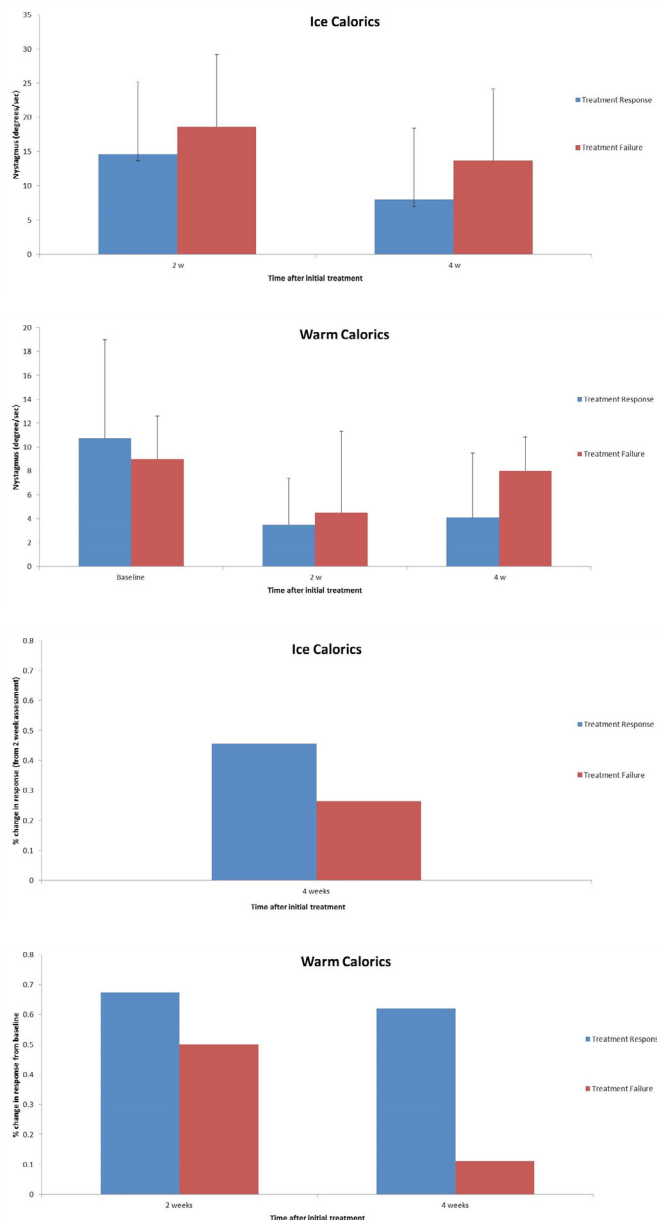
Effect of Intratympanic Gentamicin (ITG) Injection on VOR Gain in Vertical and Horizontal Canals using HIMPs and SHIMPs and Testing Vertigo Control

Qiwen Shen[1]; Christophe Magnani[1]; Catherine de Waele[2]; **Ian S. Curthoys**[3]

[1]Cognition and Action Group, CNRS UMR8257, University of Paris Descartes, Paris, France; [2]Universite Paris Descartes; [3]University of Sydney

Objective

This study is to determine whether intratympanic genta-

micin (ITG) injection similarly affects all three semicircular canals in patients suffering from Meniere';s disease as assessed by HIMPs and SHIMPs, and whether the decrease of angular vestibulo-ocular reflex (VOR) gain correlated with vertigo control.

Methods
50 normal subjects and 24 patients suffering from Meniere';s disease treated by ITG (13 with lesion on the left and 11 with lesion on the right) were recruited in this study. Patients treated by ITG were tested before the injection, one week post injection, four weeks after the last injection, and after six months. The gain of VOR in all three semicircular canals in each labyrinth was elicited by rapid head turns using HIMPs and SHIMPs using the video head impulse test device.

Results
In normal subjects, the VOR gain of left anterior, left posterior, left lateral, right anterior, right posterior and right lateral canal was 0.92, 0.95, 0.87, 0.94, 0.93, and 0.98, respectively. All patients treated by ITG injection showed decreased VOR gain (0.29-0.65) in the lesioned side of the horizontal plane. The majority of patients (83.3%) showed horizontal VOR (hVOR) gain lower than 0.6. 16.7% patients showed hVOR between 0.61-0.7. No patients had hVOR gain higher than 0.7. However, the VOR gain in the vertical canals varied in these patients. In posterior canals, only 37.5% showed posterior VOR (pVOR) gain less than 0.6. 16.7% of patients had the pVOR gain from 0.61-0.7, and 45.8% had gain more than 0.7. In the anterior canals, 45.8% of patients presented gain lower then 0.6, 12.5% had gain between 0.61-0.7, and 41.7% showed gain more than 0.7. Despite the variance in the gain of vertical canals, no patients reported vertigo after the last injection for at least the following six months. Moreover, there is no indication of whether posterior or anterior canal is more easily to be lesioned In ITG injection compared to the other one.

Conclusion
Our results suggest that ITG injection caused a significant decrease of hVOR gain in all patients treated with ITG injection. However, ITG appears to cause a differential loss of function across the three canals in the injected labyrinth: while the horizontal canal function was decreased, the vertical canal function could be within the normal range after the injection. Despite these differences between canals, the loss of horizontal canal function itself appears to ensure the control of vertigo recurrence.

PS 829

Eye Movement Response Patterns during Head Impulses; Healthy Subjects vs Patients with Meniere's Disease or Migraine Related Vertigo

Ian S. Curthoys[1]; Leonardo Manzari[2]; Ann Burgess[1]; Julia Dlugaiczyk[3]
[1]University of Sydney; [2]MSA ENT Academy Center; [3]Universitatsklinikum des Saarlandes

Objective
On video head impulse testing (HIMPs tested by vHIT) - to compare the eye velocity response profiles of healthy subjects to the response profiles of patients with early Meniere';s Disease or Migraine Related Vertigo. The stimulus was passive, unpredictable, horizontal head impulses.

Methods
Patients meeting guidelines set down by the Committee of Hearing and Equilibrium of the AAO-HNS for stage 3 Definite Meniere';s Disease (MD) were enrolled as well as patients diagnosed as Migraine Related Vertigo (MRV). Healthy subjects in the same age range were tested as controls. An inclusion criterion was MD patients had to be less than two years into MD – no patient was classed as long-term ("burnt out") MD patient. The ICS Impulse system measured the eye movement response to head impulses by vHIT using the HIMP paradigm was used: the subject or patient was instructed to maintain fixation on an earth-fixed target during small, abrupt, passive, unpredictable horizontal head turns in the plane of the horizontal canal.

Results
There are systematic differences between healthy subjects and both groups of patients in the eye velocity response. In healthy subjects the eye velocity closely matches head velocity at all parts of the head impulse, however typically MD and MRV patients show an early large eye acceleration, resulting in an eye velocity time series which looks saccadic, although the latency of this early enhanced phase is too short for it to be a saccade. The systematic pattern differences are reliable and are not due to artifacts. In some patients with enhanced eye velocity, the overall (area) VOR gain was 1.0, whereas the time series of eye velocity systematically departed from the usual response profile of healthy subjects.

Discussion and Conclusion
We suggest that this early onset trajectory is due to hydrops. Fluid dynamic modelling of the effect of hydrops on the semicircular canal response during the head impulse, predicted patterns of eye movements which closely match the patient patterns reported here (Gries-

er et al 2014). Some MD patients showed the same "early onset" eye movement response for stimulation of both labyrinths. Given the fact that hydrops may affect both ears, this is not unexpected. Not all MD and MRV patients showed this "early onset" eye movement pattern. Given the variability of hydrops, affecting different parts of the labyrinth differentially, again this is probably to be expected.

Grieser et al J Vest Research 2014: 24: 219

PS 830

Altered Resting-state Thalamo-cortical Functional Connectivity in Vestibular Migraine Patients

Taesu Kim
Kangwon National University

Vestibular migraine is a term used to describe episodic vertigo in patients with migraine spectrum disorders. The thalamus modulates the flow of vestibular sensory input to the cortex. Several studies showed abnormal thalamo-cortical functional connectivity in migraineurs. Recent studies showed the activity of overlapping vestibular and pain pathways from brainstem to cortical levels with particular attention on thalamus. The aim of this study is to investigate whether there are changes in thalamo-cortical functional connectivity of vestibular migraine patients and to determine the correlation with vertigo characteristics.

Thirteen vestibular migraine patients and 13 age- and sex-matched normal healthy controls underwent resting-state fMRI scan. We evaluated resting state functional connectivity using seed-based analysis.

We found the alteration of the right thalomo-cortical network in vestibular migraine patients compared to controls. Increased functional connectivity was detected between the right thalamus and two contralateral cortex regions (insular and orbitofrontal cortex). Decreased functional connectivity was detected between the right thalamus and several contralateral cortex regions (superior temporal gyrus, inferior parietal lobule and primary somatosensory cortex). Severity of subjective functional parameters of vestibular impairment correlated positively with right thalamic functional connectivity in insular and orbitofrontal cortex.

Areas in charge of pain modulation (for example insular and orbitofrontal cortex) have increased thalamo-cortical functional connectivity. But pain encoding area (e.g. primary somatosensory cortex) and vestibular integration area (e.g. superior temporal gyrus and inferior parietal lobule) showed decreased connection with right thalamus in vestibular migraine patients. These results provide evidence for functional connectivity between thalamus and pain control as a well as vestibular sensory integration areas are altered in vestibular migraine patients.

Activity-Dependent Development of the Auditory Brainstem

SYMP 57

Roles of auditory input in tonotopic differentiation of Kv1.1 expression in avian nucleus magnocellularis

Hiroshi Kuba
Cell Physiology, Graduate School of Medicine, Nagoya University

Avian nucleus magnocellularis is a homologue of mammalian anteroventral cochlear nucleus, and represents temporal information of sound with great precision for a wide frequency range. This precision is accomplished in part because the expression of voltage-gated K+ channel, Kv1.1, is differentiated tonotopically within the nucleus; it increases toward higher-characteristic-frequency regions. However, the mechanisms underlying this differentiation remained elusive. We examined the development of tonotopic differentiation of Kv1.1 channel expression, using in-vivo and in-vitro preparations of chickens. Our findings were; (1) the dependence of Kv1.1 expression on auditory input got strengthened specifically in neurons tuned to higher frequency sound at a late period of maturation, creating the difference in Kv1.1 expression among tuning frequencies; (2) attenuation of auditory input suppressed the differentiation in a level-dependent manner; (3) elevation of auditory input during earlier periods could not reproduce the differentiation; (4) treating cultured neurons with a high K+ media resulted in a higher expression of Kv1.1 only in those from higher-characteristic-frequency regions. The results indicated that the activity dependence of Kv1.1 expression could be determined in cell- and period-specific manners, which underlies the tonotopic differentiation of neurons in the nucleus.

SYMP 58

Paracrine ATP signaling is required for functional development of the endbulb of Held - bushy cell synapse

Sasa Jovanovic[1]; Tamara Radulovic[2]; Christian Keine[3]; Jana Nerlich[2]; Rudolf Rübsamen[4]; **Ivan Milenkovic**[2]
[1]Carl Ludwig Institute for Physiology, Faculty of Medicine, University of Leipzig, Germany; [2]Carl Ludwig Institute for Physiology, Faculty of Medicine, University of Leipzig; [3]University of Iowa; [4]Faculty of Biosciences, Pharmacy and Psychology, University of Leipzig

In the developing ventral cochlear nucleus, the first central station along the auditory pathway, paracrine ATP signaling enhances firing in a cell-specific and tonotopically-determined manner. Endogenously released ATP activates the P2X2/3R expressed only in bushy cells, and increases the synaptic efficacy of immature endbulb of Held input by facilitating AP generation and prolonging APs. Developmental down-regulation of P2X2/3R currents occurs simultaneously with an increase in AMPAR currents from high-to-low frequency area. Recent in vivo and slice experiments in P2X2/P2X3Dbl-/- mice demonstrate that the P2X2/3R is required for functional maturation of endbulb of Held synapses during the period of early auditory experience.

SYMP 59

Developmentally regulated inhibitory synaptic plasticity in the MSO

Nace L. Golding; Bradley D. Winters
Department of Neuroscience, University of Texas at Austin

Neurons of the medial superior olive (MSO) in the brain stem of mammals are coincidence detectors that signal interaural time differences (ITDs), cues used for sound localization along the horizontal plane. Glycinergic inhibitory inputs play a key role in this computation, providing well-timed, cycle-by-cycle hyperpolarizations which sharpen ITD tuning. After hearing onset, the number of inhibitory inputs is greatly reduced and remaining inputs are restricted to the soma and proximal dendrites, a process known to require normal auditory experience. However, the cellular mechanisms guiding the developmental reinforcement and preservation of inhibitory inputs with proper activation profiles and subcellular localization are unknown.

Using whole-cell current clamp recordings in gerbil brain slices, we found that in the first week of hearing (P12-15), pairing synaptic stimulation and action potentials (APs) at 200 Hz induced a long-term potentiation of inhibitory postsynaptic potentials (IPSPs) averaging 44%

above baseline (iLTP). iLTP depended on postsynaptic NMDA receptor activation and calcium dynamics. There was no dependence of iLTP magnitude on the relative phase of the IPSP and AP. However, iLTP was dependent on both frequency and number of stimuli.

Developmental changes in the size and backpropagation of the AP dictated the window over which iLTP can be induced. Using paired recordings, we found that just before hearing onset (P9-11), APs are overshooting (~ +15 mV) and backpropagate effectively into the dendrites. However, just a week later (P16-19) APs were smaller (~ -20 mV) and attenuated strongly in the dendrites. Accordingly, iLTP could not be induced at ~P30 when APs were small, but could be rescued by replacing the AP with larger depolarizations enforced via voltage clamp, demonstrating that the functional mechanisms for iLTP induction are still present at older ages.

Taken together, our results argue for a cumulative model of inhibitory plasticity in the MSO, the magnitude of which relies jointly on the number and frequency, but not the precise relative timing of paired synaptic and AP events. Nonetheless, linking reinforcement of inhibitory synapses to APs would select for inputs with activation timing in common with strong binaural excitation. We propose that the developmental decline of AP size and backpropagation deprives more distal inhibitory synapses of iLTP-mediated reinforcement, favoring those nearer the soma.

SYMP 60

GABA- and glutamate-dependent long-term potentiation of developing glycinergic MNTB-LSO synapses during tonotopic map refinement.

Eva Bach[1]; **Karl Kandler**[2]
[1]University of Pittsburgh School of Medicine; [2]Dept. Neurobiology, University of Pittsburgh School of Medicine

The lateral superior olive (LSO) in the auditory brainstem integrates binaural information to encode interaural sound intensity differences. Before the onset of hearing, the inhibitory pathway from the medial nucleus of the trapezoid body (MNTB) to the LSO undergoes substantial topographic refinement, which gives rise to the precise tonotopic map in mature animals. This developmental refinement involves the selective silencing and strengthening of MNTB-LSO connections and depends on the precise temporal patterns of spontaneous spike activity. During the period of topographic refinement, MNTB terminals in the LSO not only release glycine but also release GABA and glutamate.

To gain better insight into the developmental role of the transient GABA and glutamate release and to shed light on the synaptic mechanisms underlying the refinement of the inhibitory MNTB-LSO map, we investigated whether MNTB-LSO synapses can undergo activity-dependent long-term potentiation (LTP). In brainstem slices from one-week-old mice, LTP could be reliably induced by stimulation patterns that closely mimicked those that are present in the MNTB in vivo. In contrast, no LTP was observed with other high- or low-frequent stimulation patterns. Our results further indicate that this form of LTP is expressed postsynaptically, is mediated by an increase in glycinergic transmission, requires an increase in the postsynaptic calcium concentration, and depends on the activation of metabotropic GABA and glutamate receptors. This stimulus-specific form of LTP in immature MNTB-LSO synapses likely represents a synaptic mechanism by which the precise pattern of early spontaneous activity contributes to the formation of a precise, inhibitory tonotopic map. Supported by NIDCD (DC004199)

SYMP 61

Activity-dependent regulation of myelin in the mammalian auditory brainstem

James Sinclair[1]; Matthew Fischl[2]; **Conny Kopp-Scheinpflug**[3]
[1]UCL Ear Institute; [2]NIH / NIDCD Section on Neuronal Circuitry; [3]LMU Munich

Background
In the nervous system, myelin plasticity represents a mechanism to tune the flow of information along axons. The auditory system is heavily myelinated and operates at the upper limits of action potential generation rate and conduction speed observed in the mammalian CNS. It therefore provides an ideal model system to study circuit specific structure-function adaptations for speed. We previously characterized the development of myelin within the trapezoid body (TB), a central auditory fiber tract, and determined the influence of sensory experience on this process (Sinclair et al., J Neuroscience 2017). We found that fiber diameter and myelin thickness increased following hearing onset and that this process is accompanied by a doubling in conduction speed and an increasing ability to support high-frequency firing. In this study we probe the mechanisms leading to increased fibre diameter and myelin thickness in the developing auditory system.

Methods
Temporary sensory deprivation was induced by raising the animals with earplugs for a critical period between P10-20. Axon calibre and myelin thickness were measured in TB fibres by either electron microscopy or by using immunolabeling for neurofilament and myelin basic protein. Physiological measures of TB fibre activity in mice raised with earplugs and non-plugged controls were taken from in vivo single-unit recordings.

Results
In this study we characterised changes in activity and myelination of TB fibres in mice raised with earplugs (EPs) compared to control littermates. Recording neuronal firing in the medial nucleus of the trapezoid body as a measure of TB fibre activity in EP-raised mice revealed elevated thresholds (control: 17.9 ±2.3 dB SPL, n=18; plugged: 70.5 ±3.2dB SPL, n=11; t-test: p≤0.001) and decreased maximum firing rates (control: 177.7 ±9.3Hz, n=18; plugged: 70.7 ±25.4Hz, n=9; t-test: p≤0.001), but no significant change in the spontaneous firing rates or the distribution of characteristic frequencies. Yet, despite similar spontaneous firing rates, a smaller number of large calibre TB fibres and a significant reduction of myelin were observed in EP-raised animals compared to controls.

Conclusions
Our data suggest that spontaneous activity in the auditory pathway might be sufficient for some but not all developmental changes around and beyond hearing onset. Ongoing electrophysiological and anatomical experiments seek to answer the question of how increased, sensory-evoked activity following hearing onset is communicated to myelinating oligodendrocytes.

SYMP 62

Developmental Profiles of the MNTB and MSO Neurons Around Hearing Onset in the Non-Human Primate

Jun Hee Kim
UTHSCSA

The human fetus starts to hear as early as the third trimester of pregnancy, and notably the auditory system undergoes major developmental changes in utero. Although there are significant data regarding development of the auditory system in rodents, comparable research in the developing primate brain is very limited, and therefore our understanding of the physiological changes that occur during fetal development is less than adequate. In light of this, we have studied the intrinsic properties and synaptic functions of auditory brainstem neurons in the baboon at different gestational ages around hearing onset (at ~70% gestational age; GA). 1) In the MNTB, one of primary nuclei in the superior olivary complex (SOC), the frequency of spontaneous GABA/glycine receptor-mediated inhibitory postsynaptic synaptic currents was significantly reduced in term

MNTB neurons, compared to preterm MNTB neurons. In addition, preterm MNTB neurons had a higher input resistance than term neurons and fired in bursts, whereas term MNTB neurons fired a single action potential in response to suprathreshold current injection. The maturation of intrinsic properties and dominance of excitatory inputs in the primate MNTB allow it to take on its mature role as a fast and reliable relay synapse in the auditory brainstem. 2) In the MSO, another nucleus in the SOC, we observed an increase in the size of VGluT1- and VGAT- positive synaptic vesicles and in the complexity of dendrites of MSO neurons after hearing onset. In addition, the length of the axon initial segment (AIS), which is a specialized axonal region where action potentials are initiated, of MSO neurons became shorter during fetal development and this structural plasticity in the AIS occurs more distinctly in the ventral MSO. We tested the effect of different auditory experience in the Neonatal Intensive Care Unit (NICU) for preterm baboons on the structural plasticity of the AIS in MSO neurons. Interestingly, the previously observed developmental changes in AIS length was not observed in MSO neurons from preterm baboons exposed to 2 weeks in the NICU. Collectively, these results indicate that significant changes occur in the auditory circuit of developing non-human primates, and that the uterus provides important environmental factors that enable proper development of auditory neurons. From these results, we propose that sound-evoked neuronal activities in uterus results in the structural and biophysical changes we observed in the auditory neurons of developing baboons.

Plasticity, Learning & Adaptation to Hearing Impairment II

PD 81

Spontaneous activity in the developing auditory system persists in a mouse model of sensorineural deafness

Travis Babola[1]; Alexandra Gribizis[2]; Adam Lombroso[2]; Sally Li[1]; Michael Crair[2]; Dwight E. Bergles[1]
[1]Johns Hopkins University; [2]Yale University

Spontaneous electrical activity is a prevalent feature of the developing central nervous system, which influences the survival and maturation of neurons, as well as the refinement of neural circuits. Neurons in the developing auditory system exhibit bursts of activity that originate in the cochlea and propagate through auditory centers before hearing begins. However, the signaling events that initiate burst firing and the role of this activity in shaping development of auditory pathways remain uncertain, in part, because few mechanistic studies have been performed in vivo. To investigate the mechanisms responsible for this activity, we monitored neural activity in the inferior colliculus (IC) of unanesthetized Snap25-2A-GCaMP6s mice using widefield epifluorescence imaging. Time lapse imaging performed before hearing onset (postnatal day 7-9) revealed that neurons within tonotopic zones of the IC exhibit periodic increases in calcium that depend on input from the cochlea. Application of Gelfoam saturated with the AMPA receptor antagonist NBQX to the round window membrane (RWM) suppressed activity in the contralateral IC, mimicking the effect of unilateral cochlear ablation, indicating that spontaneous activity normally requires synaptic excitation of SGNs by inner hair cells (IHCs). To determine if spontaneous activity is abolished when hair cell output is silenced genetically, we visualized IC activity in VGLUT3–/– mice (Snap25-2A-GCaMP6s;V-GLUT3–/–), which lack functional vesicular glutamate transporters in hair cells and are profoundly deaf. Unexpectedly, correlated neuronal activity persisted in the IC of these animals. This activity was dramatically reduced after bilateral cochlear ablation, but unaffected by acute application of NBQX to the RWM, suggesting that activity in VGLUT3–/– mice originates in the cochlea, but is glutamate-independent. Previous studies have shown that spontaneous bursts of action potentials in SGNs are induced by release of K+ from supporting cells following activation of calcium-activated chloride channels; although these K+ waves depolarize afferent terminals, they are not normally sufficient to induce direct excitation of SGNs. However, SGNs in excised cochleae from VGLUT3–/– mice exhibited periodic calcium transients that were blocked by the calcium-activated chloride channel antagonist benzbromarone, which prevents K+ release from supporting cells. These data suggest that SGNs exhibit homeostatic increases in excitability when deprived of synaptic excitation by IHCs, allowing supporting cell-induced K+ transients to elicit SGN firing independent of IHC input. This preservation of early spontaneous activity in auditory centers despite IHC deficits may enhance the survival and maturation of auditory neurons, improving their response to cochlear implants.

PD 82

Long-Term Exposure to Low-Level Noise Induces Cochlear Functional Loss Underlying Different Mechanisms

Guang-Di Chen[1]; Xiaopeng Liu[2]; Richard Salvi[1]
[1]Center for Hearing and Deafness; State University of New York at Buffalo; [2]Xiaopeng Liu

Background
The maximum allowable noise exposure set by OHSHA is 90 dBA for an 8-hour daily exposure. With a 5-dB exchange rate, the maximum allowable noise exposure would drop to ~83 dBA for a 24-hour daily exposure.

Therefore, long term noise exposure in urban environment in the big city (65-71 dBA) would be considered safe and unlikely to induce hearing impairment. Indeed, prolonged exposure to sounds up to 80 dBA did not induce ABR threshold shift (TS) in cats. However, our recent studies revealed significant functional losses in the cochlear compound action potential (CAP) in rats after long-term narrow band noise exposure at 75 dB SPL. Therefore, we varied the intensity of the narrow band noise over a large range to identify which intensities were "safe" and no longer affected the CAP threshold or amplitude.

Methods

Rats were exposed to a narrowband noise (18-24 kHz) at 85, 75, 65, 55, or 45 dB SPL or ambient noise for 6 weeks. CAP input/output (I/O) functions were measured from 2-65 kHz at post-exposure 3 hour.

Results

The high-frequency noise exposure did not affect the low-frequency CAP I/O functions. However, at the frequencies around the noise band, the noise exposure reduced CAP-amplitude at low stimulation levels leading to CAP TS. Significant changes in the CAP were observed after exposures of 65 dB SPL. At the high frequencies, the 85 dB SPL exposure significantly reduced CAP amplitudes at high stimulus levels without causing a CAP TS; a slight reduction was observed at 75 dB, but no effect was seen at 65 dB or lower. As noise exposure intensity increased, changes in CAP amplitude and TS occurred over a wider frequency range.

Conclusion

Prolonged exposure to low-level noise at intensities far below the permissible exposure level for humans (~83 dBA) induced CAP amplitude reduction and TS. CAP TS mainly occurred at frequencies within the noise exposure band; these CAP TS are likely the result of outer hair cell dysfunction (loss of cochlear amplification). CAP amplitudes, but not TS, were greatly affected at frequencies above the noise exposure band. One interpretation of these results is that the exposure affected the high-threshold, low spontaneous rate fibers damaging the synaptic contact with inner hair cells.
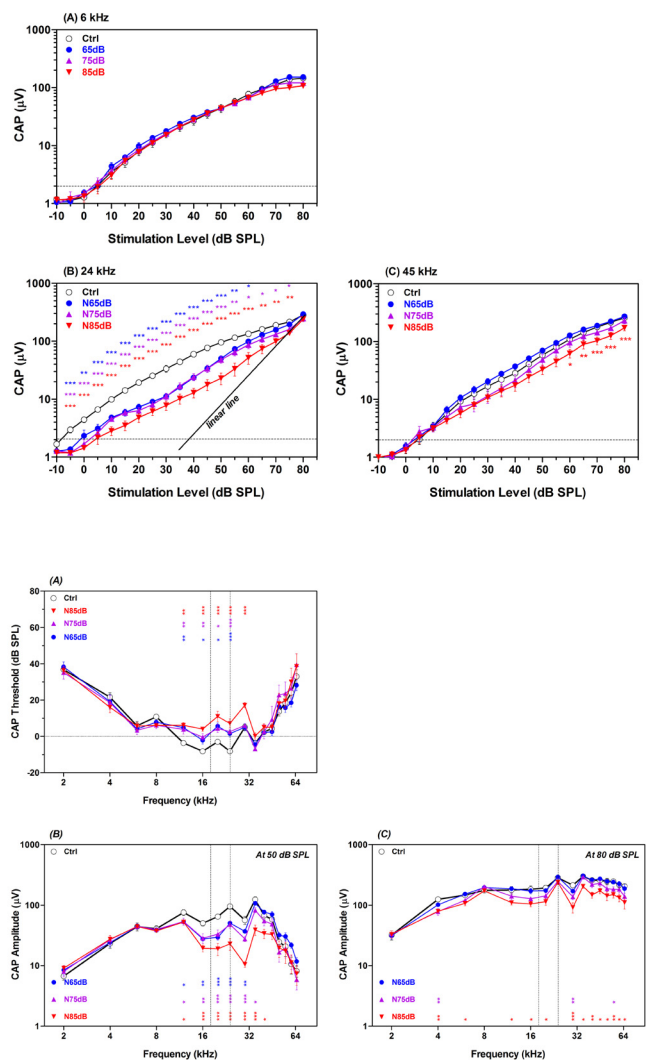
PD 83

Homeostatic Normalization of Central Gain in Corticofugal Neurons following Cochlear Synaptopathy

Meenakshi Asokan[1]; Ross S. Williamson[2]; Kenneth Hancock[3]; Daniel B. Polley[2]
[1]*Harvard University Program in Speech and Hearing Bioscience and Technology/Eaton-Peabody Laboratory, Massachusetts Eye and Ear Infirmary;* [2]*Massachusetts Eye and Ear Infirmary, Harvard Medical School;* [3]*Eaton-Peabody Laboratory, Massachusetts Eye and Ear Infirmary/ Department of Otolaryngology, Harvard Medical School*

Background

The auditory system features a massive set of descending efferent projections. The largest component of the efferent centrifugal pathway arises from corticofugal neurons in the deep layers of the auditory cortex, which are thought to modulate the gain and tuning selectivity in subcortical nuclei. Little is known about gain adjust-

ments in the corticofugal neurons themselves, due to technical challenges associated with targeted long-term recordings from the distributed deep layer cortical neurons. Here, we describe a chronic imaging approach to track day-by-day dynamics in the sensory response gain of corticocollicular (CCol) neurons following a noise exposure that causes a temporary shift in ABR thresholds but a permanent loss of Type-I synapses onto inner hair cells.

Methods
GCaMP6s was expressed in the auditory cortex of adult CBA/CaJ mice using a viral construct. A glass cranial window was installed atop the dorsal cap of ipsilateral inferior colliculus to enable daily widefield calcium imaging of sound-evoked activity in CCol axons. Temporary threshold shifts were induced with acoustic exposure to an octave band of noise (8-16 kHz) presented at 100 dB SPL for two hours. ABR thresholds and waveform amplitudes were also measured before and after noise exposure to contrast with CCol gain normalization.

Results
We found that sound-evoked CCol responses were suppressed immediately after moderate intensity noise exposure but returned to baseline levels within 24 hours, despite a substantial elevation of ABR thresholds and waveform amplitudes. CCol gain rose above baseline for several days following noise exposure before returning to pre-exposure levels within 6 days, while ABR wave 1 amplitudes remained suppressed due to a permanent loss of cochlear afferent synapses.

Conclusion
These findings demonstrate a homeostatic plasticity in auditory corticofugal neurons that compensates both for a temporary elevation of cochlear thresholds and a permanent loss of cochlear afferent synapses. Future work will reveal how this plasticity is coordinated with pre- and post-synaptic gain changes to shape adaptive and maladaptive changes in auditory perception following peripheral damage.

PD 84

The use of F0 and vocal-tract-length cues for voice discrimination: effects of early implantation and comparison to normal hearing

Yael Zaltz[1]; Raymond L. Goldsworthy[2]; Liat Kishon-Rabin[1]; Laurie S. Eisenberg[3]
[1]Department of Communication Disorders, Steyer School of Health Professions, Sackler Faculty of Medicine, Tel Aviv University, Israel; [2]University of Southern California; [3]Keck School of Medicine, USC

The ability to discriminate between different talkers is an essential skill, necessary for tracking the voice of a specific talker of interest in a multi-talker environment and thus important for speech perception in noisy environments. Adult cochlear implant (CI) users perform poorly in noisy environments, partly because of their limited ability to discriminate between different talkers. Results from recent studies have shown that postlingually deafened adult CI users, who had prior acoustic experience, relied entirely on fundamental frequency (F0) cues, making only limited use of vocal-tract length (VTL) cues for talker discrimination while performing gender categorization tasks. The present study assesses voice discrimination using F0 and/or VTL cues in prelingually deafened adult CI users compared to adults and children with normal hearing (NH). The NH group included 41 NH children aged 8-11 years and 30 young-adults. The CI users group included 18 young-adults with prelingual deafness. Half of the CI group (n=9) were "early-implanted" (less than 4 years of age) and the other half were "late-implanted" (6 years of age and older). A three-interval two-alternative forced choice adaptive procedure was used for discriminating between talkers based on changes of VTL only, F0 only, or the combination of both F0 and VTL. Nine of the NH adults listened to spectrally-degraded (vocoded) stimuli. Results showed that: (a) NH participants relied more on VTL cues than F0 cues for voice discrimination of non-vocoded speech but relied equally on both cues for vocoded stimuli; (b) NH children showed similar results to adults in terms of absolute thresholds and the use of the VTL compared to F0 cues with non-vocoded stimuli; (c) Voice discrimination of the CI users was worse than that of NH participants (both children and adults); (d) "Early-implanted" CI users relied equally on both VTL and F0 cues; (d) "Late-implanted" CI users had significant difficulties exploiting the VTL cues for talker discrimination; and (e) VTL perception of the CI users was positively associated with speech recognition scores in quiet and in noise. These results suggest that early implantation improves the utilization of the limited spectral resolution transmitted by the CI. Moreover, the ability to discriminate between talkers based on VTL cues may explain performance of speech recognition in noise.

PD 85

Video game players' auditory cognition and perception

Hannah J. Stewart[1]; Audrey Perdew[1]; Jasmin Martinez[1]; Shawn Green[2]; David R. Moore[1]
[1]Cincinnati Children's Hospital; [2]University of Wisconsin-Madison

People with listening difficulties have a variety of cognitive and perceptual problems including auditory spec-

tro-temporal resolution, executive function and attention switching. Auditory learning studies show that while a listener can train and improve performance on one task, it is very difficult for improved performance to transfer to a new task. This jump in training has been successfully shown in the visual domain by young adults completing action video game training. This study aims to assess whether that same training leads to improvements in auditory cognition and perception skills.

We are aiming to test 80 participants. So far, 45 young adults with video game experience ranging from zero to ten hours plus a week have been recruited. Recruitment was based on extensive questionnaires on current and prior experience of playing a variety of video game genres, adapted from the visual research. Each participant completed a battery of tests (outcome measures) assessing attention in the visual and auditory domains (Multiple Object Tracking, Test of Attention in Listening) and speech-in-noise comprehension (Enhanced QuickSIN Speech in Noise, Listening in Spatialized Noise-Sentences (LiSN-S)).

For initial analysis, participants were split into four groups: action video game (e.g. Call of Duty) players and non-players, and strategy game (e.g. Civilization) players and non-players. The visual attention outcome measures suggest that action players are able to track and remember more visual objects than action non-players ($p < .001$), thus replicating previous visual work. This result also extended into strategy players compared to strategy non-players ($p < .001$). Results from the auditory attention outcome measures suggest that video game players have better (larger) auditory processing capacities than non-players (action: frequency information $p = .051$, spatial information $p = .028$; strategy: $p = .006$, $p = .005$), but that game players were more negatively affected by conflicting auditory information than non-players (action: $p = .057$, $p = .031$; strategy: $p = .016$, $p = .006$). In the speech-in-noise intelligibility tests game players were no better on the Enhanced QuickSIN (action: $p \geq .82$; strategy $p \geq .27$) or LiSN-S (action: $p \geq .41$; strategy $p \geq .17$) than non-players.

Our results so far suggest that while playing action or strategy video games improves the ability to attend to more visual and auditory information, the players are less able to use the extra auditory information in their decision making. In turn, the players show no improvement in performance on speech-in-noise tests.

PD 86

Interactive Learning Environment for Use in Auditory Rehabilitation

Dragana Barac-Cikoja[1]; Kevin Cole[2]; Andrea Kottlowski[1]; Ashleigh Collis[1]; Kelsey Uguccioni[1]
[1]*Gallaudet University;* [2]*NOVA Web Development*

For individuals with profound hearing loss, cochlear implants provide the only access to sounds. However, to perceive speech, music or the environmental sounds based on the electric signals that implants deliver requires learning. Current clinical and home training programs for auditory rehabilitation use a supervised learning paradigm - an intensive training regime focusing on the better use of available acoustic and/or contextual cues. This contrasts with principles of implicit learning that model perceptual learning in real-life, natural circumstances, and include direct, self-structured and repeatable discovery of the auditory information. There is a growing realization that providing more realistic conditions, especially a variety of difficult listening situations, during training may lead to greater transfer of acquired skills. Similarly, the importance of realistic expectations in setting auditory rehabilitation goals both on the part of the cochlear implant user and the clinician/audiologist is universally acknowledged. To develop such expectations and ensure that the auditory rehabilitation goals are challenging yet attainable for the user, an individualized and interactive process is needed. We present a prototype computer-based auditory training/ counseling program that has been developed to allow a person to experience the benefits and limitations of his/her hearing device in a variety of simulated real-life listening situations (e.g., a restaurant, living room, office). The program is based on self-directed exploration of the relationship between (i) acoustic characteristics of the soundscapes that affect hearing, and (ii) technological solutions and communication strategies that are aimed at improving sound detection, speech comprehension and the overall listening experience. The software consists of thematic exercises (modules) that require the user to manipulate acoustic parameters and the hearing device settings using an intuitive visual interface and to rate the resulting sound quality, speech intelligibility, and listening effort. The user';s exploratory activities and ratings are tracked and saved for later analysis. Results of a study conducted on a sample of audiologists and speech-language pathologists to examine usability of this program in auditory rehabilitation will be reported.

Understanding Auditory Salience

SYMP 63

What Visual Saliency Tells Us

John Reynolds
Salk Institute

Studies of visual attention in the non-human primate have found that endogenously-generated attention signals modulate neuronal responses in ways that closely parallel changes that are observed with increases in salience. These include changes in response gain, modulation of center-surround interactions, and reductions in correlated neuronal response variability. This suggests that changes in attention and salience may both tap into some of the same neural circuitry. Evolution may thus have co-opted circuits that originally evolved to regulate sensitivity in response to changes the strength of sensory input, but now also mediate attention, where they adjust sensitivity to meet changing task demands.

SYMP 64

Eye Metrics as Indicators of Auditory Salience?

Shigeto Furukawa
NTT Communication Science Laboratories

In vision, salient (or attention-grabbing) objects can be identified by tracking the viewer's gaze, but what about in audition? Eye metrics, including the pupil dilation response (PDR) and microsaccades (small amplitude, jerk-like, involuntary eye movements), are good candidate indicators of auditory salience: Pupil diameter is known to reflect the activities of the locus-coeruleus noradrenarine system, which plays a key role in regulating alertness levels. Recent studies indicate that the microsaccade rate (the number of microsaccades per second) varies with aspects of covert attention or task demands. We confirmed that the PDR and microsaccade rate are sensitive to auditory stimulation and to acoustical and attentional factors that might be related to the salience of the sounds. The response sensitivities of the two measures to those factors often paralleled each other but differed in certain aspects, implying that they reflect more-or-less independent mechanisms of auditory processing. We also found that not only the occurrence rate but the detailed dynamics of individual microsaccade are modulated by voluntary and involuntary attention related to the auditory stimulus and task. It is expected that further explorations of the relationship between the detailed eye-metrical responses and auditory-related attentional factors will enable objective evaluations of auditory salience.

SYMP 65

Distraction as a measure of acoustic salience?

Maria Chait
University College London

A major stumbling block in the study of auditory salience is the lack of an operational definition and of a 'ground-truth' against which to measure it. I will present a series of experiments in which we measure a sound's capacity to elicit distraction as an objective measure of its salience. Distraction is quantified behaviorally (with standard laboratory experiments as well as mass-participant mechanical turk) as well as with pupilometry and EEG.

SYMP 66

Auditory Salience using natural soundscapes

Nicholas Huang; **Mounya Elhilali**
Johns Hopkins University

Studies of auditory salience have often relied on simplified or well-controlled auditory scenes to shed light on acoustic attributes that drive the salience of sound events. Unfortunately, the use of constrained stimuli in addition to a lack of well-established benchmarks of salience judgments hampers the development of comprehensive theories of sensory-driven auditory attention. Here, we will explore auditory salience in complex unconstrained scenes (e.g. Youtube, etc). By using natural scenes, the study takes a data-driven rather than experimenter-driven approach to exploring the parameters of auditory salience. We will discuss insights from using these unconstrained scenes and their implications for future work on auditory salience.

SYMP 67

Saliency of voice features: presenting a new Rapid Audio Sequential Presentation (RASP) paradigm

Clara Suied[1]; Vincent Isnard[2]; Franck Elisabeth[1]; Isabelle Viaud-Delmon[3]
[1]*Département Action et Cognition en Situation Opérationnelle, Institut de Recherche Biomédicale des Armées, Brétigny-sur-Orge, France;* [2]*Institut de Recherche et Coordination Acoustique/Musique, Paris, France;* [3]*Equipe Espaces Acoustique et Cognitif, Institut de Recherche et Coordination Acoustique/ Musique, Paris, France*

Human listeners seem to be remarkably able to recognize acoustic sound sources based on timbre cues. In this talk, we will describe a new psychophysical paradigm to estimate the inferred neural processing time it takes to recognize a set of complex sounds differing only in timbre cues, and explain how it helps to show

saliency effect of natural sounds presented in sequences. Sequences of short sounds are constructed and presented in rapid succession. Listeners are asked to report the presence of a single target (either voices or instrument) token that could occur at a random position within a sequence of sound distractors (instruments or voices). This method is analogous to the "rapid sequential visual presentation" paradigm (RSVP), which has been used to evaluate neural processing time for images. An unexpected and new result emerged from a series of experiment using this paradigm: a robust voice effect (better and faster performance for voice sounds). The voice pops out of the instrument distractors, probably because voice is coded as a specific feature.

SYMP 68

How screams and roughness hijack attention

Luc H. Arnal
University of Geneva

To survive in a complex sensory environment, it is essential for the brain to detect and prioritize the processing of biologically relevant signals. Salient stimuli capture attention, a process named bottom-up attention. However, whether specific features drive attention more efficiently than others is unclear. Here, I will attempt to elucidate how alarm vocalizations such as screams distress the brain to trigger efficient reactions. I will show that alarm vocalizations stimulate the auditory system using rough (30-120 Hz) amplitude modulations. These sounds selectively activate subcortical structures involved in arousal and danger processing by enhancing oscillatory dynamics involved in bottom-up attentional capture.

SYMP 69

Alarm fatigue and salience

Judy Edworthy[1]; Michael Kristensen[2]; Elif Ozcan[3]
[1]Plymouth University; [2]Cognition Institute, Plymouth University; [3]Delft University of Technology; Erasmus Medical Centre

The issue of auditory salience is clearly for important in the design and implementation of alarm sounds. Through understanding the perceptual and neurological mechanisms behind auditory salience, we can design alarm sounds that are attention-getting, and which elicit an appropriate response. However, doing this is arguably only helpful if we design for an environment which is conducive to such an approach, and the reailty is that most environments that would benefit from this approach are found seriously wanting. The way auditory alarms have typically been implemented in high-workload and safety-critical industries has been to attempt to elicit startle responses and to practise a 'better safe than sorry' approach - to make the alarm stand out from all other signals, and to signal about everything that might possibly need signalling - without consideration of all of those other factors which might contribute to safety performance in safety-critical areas, as well as ignoring the consequences of having working environments where auditory alarms are rife. The most obvious example of this is in clinical care, where the juxtaposition of unnecessary shrillness and loudness, high false alarm rates, and bad audio signal design has led to the coining of the term 'alarm fatigue', where patient deaths and serious incidents have been attributed to missed alarms, and where the missing of the alarm has then been attributed to alarm fatigue. Whilst widely accepted as a headline for a known problem, the details of alarm fatigue are not well understood and require further elaboration. The relative contributions of inaudibility, overly-loud alarms, false alarm rate, high numbers of alarms, confusing alarms and other issues to the overall alarm fatigue problem needs to be clarified in order to mitigate the problem. The issue here is that in real clinical environments the relevance of auditory salience - and the way(s) in which what we know about auditory salience can help in auditory alarm signal design - is somewhat lost in a sea of other problems. In this talk we will demonstrate some of those problems and talk about a project focusing on clinical audio alarm design for the future.

Gene Regulation in the Inner Ear II

PD 87

The gEAR portal v2: now integrating single cell RNA-seq, epigenomics and new data analysis tools

Joshua Orvis[1]; Dustin Olley[1]; Michael C. Kelly[2]; Jayaram Kancherla[3]; Beatrice Milon[1]; Yang Song[4]; **Carlo Colantuoni**[1]; Hector C. Bravo[3]; Seth Ament[1]; Anup A. Mahurkar[1]; Ronna Hertzano[5]
[1]University of Maryland School of Medicine, Baltimore, MD, USA; [2]NIDCD/NIH; [3]Center for Bioinformatics and Computational Biology, UMIACS, University of Maryland, College Park, MD, USA; [4]University of Maryland School of Medicine, Baltimore MD, USA; [5]University of Maryland School of Medicine, Baltimore, MD USA

The gEAR portal (gene Expression Analysis Resource, UMgEAR.org) is a portal for data visualization, sharing, and analysis designed for auditory and vestibular researchers. Next-generation sequencing is a common tool used by numerous molecular biology laboratories, cumulatively resulting in very large amounts of data. These data - which range from bulk/cell type-specific RNA-seq of wild type or mutant samples, to epigen-

etic analyses, and single cell RNA-seq – are a useful resource. However, accessing and analyzing multiple datasets in parallel requires time, and advanced informatics expertise. The gEAR allows researchers to instantly access these data in a meaningful way, without requiring further informatics training. This is done through simultaneous visualization of multiple datatypes across species in a user-friendly manner, using a variety of display options, keyed by gene names.

In this presentation, we reveal numerous updates/upgrades to the gEAR to further facilitate visualization, sharing, and analysis of multi-omic data. These include: integration of a viewer for epigenetic data (ChIP-seq, ATAC-seq and methylation analysis) in conjunction with expression data from the same gene across multiple datasets; New tools for visualization and analysis of single cell RNA-seq data; Improved dataset comparison tool, with gene selection and export capability; New analysis tools including hierarchical clustering, K-means clustering and principal component analysis; Improved dataset uploader; New data visualization formats; Faster response and analysis times thanks to experimental use of data formats such as HDF5, which are designed for large-scale storage, and a migration to cloud-based hosting, which allows us to dynamically increase resources as needed. We have also created a help-desk with a ticketing system.

PD 88

Single-cell RNA-Seq reveals novel mRNA transcript features in the mature organ of Corti

Paul T. Ranum[1]; Alex Goodwin[1]; Richard J. H. Smith[2]
[1]*The University of Iowa;* [2]*Molecular Otolaryngology and Renal Research Laboratories, Department of Otolaryngology—Head and Neck Surgery, Carver College of Medicine, University of Iowa*

Background
Single-cell RNA-Seq (scRNA-Seq) has revealed higher than anticipated levels of heterogeneity both in terms of transcript abundance and transcript structure, prompting researchers across disciplines to rethink assumptions about transcription. To date, mRNA transcript structure has not been interrogated at the single cell level in the highly specialized sensory and supporting cells of the functionally mature mammalian cochlea.

Methods
Using Illumina-based scRNA-Seq, we studied the tran-scriptomes of 42 individual inner hair cells (IHCs), 127 outer hair cells (OHCs) and 39 Deiters'; cells manually isolated from the murine cochlea across time points ranging from p15 to p228. We resolved and quantified full-length transcripts utilizing long-read Nanopore sequencing.

Results
Splicing analysis of Illumina reads revealed widespread and unanticipated splicing diversity, including the inclusion of highly conserved novel exons. The detection of these un-annotated, organ specific features expand the repertoire of mRNA transcripts produced by these key auditory cell types. For example, in 13 genes causally implicated in hereditary hearing loss, we identified 18 novel exons and a wide range of alternative spliceoforms.

Illumina sequencing facilitated the identification of splice sites and novel transcript features but it precluded reconstruction of full-length transcripts, especially for long genes with multiple alternatively spliced exons. To circumvent this limitation, we utilized long-read Nanopore sequencing technology to confirm the inclusion of novel exons and splicing patterns, allowing us to resolve and quantify full-length isoform structure.

Conclusion
Using scRNA-Seq, we have generated a high-resolution view of individual cell transcriptomes within the organ of Corti. In so doing, we have identified unappreciated mRNA structural diversity. These findings have important implications for the study, diagnosis, and treatment of deafness.

ARO FINAL FIGURE V1.pdf

PD 89

Organ-wide mapping of single-cell transcriptomes from the adult mouse cochlea

Matthew N. Nguyen; Kathy S. So; Ning Pan; Adam T. Palermo; Joseph C. Burns
Decibel Therapeutics

The adult mammalian cochlea houses diverse cell types that vary greatly in function and architecture. The large-scale gene expression patterns associated with this diversity remain poorly understood, not to mention how these patterns change during disease. This is particularly true for nonsensory cell types outside the organ of Corti, which appear to be essential for auditory function, despite incomplete understanding of their biological role.

Transcriptional profiling of the adult cochlea is challenging since its fragile cells are sensitive to mechanical manipulations, and it is encased in hard bone. We have overcome these barriers by developing optimized dissociation protocols that facilitate high-throughput single-cell RNA-Seq (scRNA-Seq) of the entire adult mouse cochlea. To date, we have captured >75,000 single cells from adult (>6 wko) CBA/CaJ mice. The median number of genes detected per cell is ~1700, which is well above the coverage required to distinguish gross cell types, subtypes, and cellular responses. Using unbiased clustering, we have identified over 40 distinct groups of cells. This level of diversity was somewhat surprising given that we identified roughly half this number in the neonatal cochlea, suggesting that substantial differentiation occurs after birth in the mouse. Based on known markers, we have been able to assign definitive identities to 16 of the clusters, which include hair cells, supporting cells, neurons, glia, and strial cells. The remainder fall into broad categories of immune, mesenchymal/fibrocyte, and epithelial. Immune cells appear to be the most diverse, comprised of at least 10 distinct types.

While scRNA-Seq provides a survey of cell-type transcriptomes, it lacks spatial information. Thus, to validate and localize the mRNAs that are unique to each cluster, we have paired scRNA-Seq with RNAscope technology. RNAscope overcomes issues with RNA degraded during cochlear decalcification by using tandem hybridization of independent "double Z" probes, thereby amplifying target signals and suppressing non-specific hybridizations. Using probes for different canonical and previously uncharacterized transcripts, we demonstrate that RNAscope provides high-quality detection of RNA transcripts in adult cochlea and correlates well with scRNA-Seq data.

Combined, the two technologies are enabling us to catalogue both transcriptomes and coordinates of all cell types within the adult cochlea. Not only is this data providing insights into the functional roles of a number of underappreciated cell types, but it is allowing us to understand how each cell responds to damage in unprecedented detail. We expect the results to provide new cellular targets for treating a dysfunctional cochlea.

PD 90

Locus-specific epigenetic repression of transcription factor expression in differentiating inner-ear organoid culture

Tyler M. Gibson[1]; Delia Sanders[2]; Albert Edge[3]
[1]*Eaton-Peabody Laboratories, Massachusetts Eye and Ear Infirmary; and Department of Otology and Laryngology, Harvard Medical School;* [2]*Eaton-Peabody Laboratories, Massachusetts Eye and Ear Infirmary; and Department of Neuroscience, Boston University;* [3]*Harvard Medical School*

Epigenetic regulation of gene expression provides an essential component of the gene regulatory pathways that drive both cell differentiation and the maintenance of somatic cell phenotypes. Intergenic enhancer elements that modulate the levels of gene expression play a central role in this regulation, and can vary dramatically between different cell lineages. Our current understanding of the different epigenetic regulatory elements that are functional in cochlear hair cell differentiation is highly limited due to the technical difficulty of harvesting sufficient cellular material for analysis and our limited ability to deliver DNA constructs to perturb epigenetic regulation at precise genomic loci.

The recent adaptation of CRISPR/Cas9 as a tool for genomic localization of protein domains that have known effects on the local chromatin marks provides an ideal tool to perturb putative enhancers. Loss-of-function studies can be easily run with the delivery of a nuclease-null dCas9 genetically fused to the KRAB repressor domain, which induces the formation of heterochromatin and recruits repressive marks to nearby histones including H3K9me3. Because there is no modification introduced to the target cells'; genetic sequences, this provides a reversible tool that can be used to drive short-term repression of enhancers.

Lgr5-expressing supporting cells of the cochlea have been shown to act as hair cell progenitors. We have recently developed methods for expansion of the Lgr5+ cochlear progenitors (LCPs) in an organoid model for hair cell differentiation. We are developing a method to deliver dCas9 epigenetic regulators into this in vitro model of cochlear progenitors.

Using the thoroughly-characterized enhancer 3'; of the Atoh1 gene as a model system, we have demonstrated targeted epigenetic repression of Atoh1. We introduce nuclease-inactivated dCas9 fused to the KRAB repressor domain together with short guide RNA sequences targeting either the Atoh1 promoter or either of the conserved regions of the 3'; enhancer. We demonstrated

Atoh1 downregulation when targeting either the promoter or the 3'; end of the enhancer, and consequently observed a repression of the expression of markers of hair cell differentiation such as Myo7a. These experiments demonstrate the feasibility of using dCas9-based tools for epigenetic modification in inner-ear organoid models to perform broader surveys of intergenic regulatory elements that play a necessary role in inner ear development. Ongoing work aims to use this tool to identify cell-type specific regulatory elements in our organoid models of hair and supporting cells.

PD 91

Genome-wide Methylation of the Mouse Inner Ear During Development and Maturation

Ofer Yizhar-Barnea[1]; Cristina Valensisi[2]; Kamal Kishore[3]; Naresh Doni Jayavelu[2]; Colin Andrus[2]; Tal Koffler-Brill[1]; Kathy Ushakov[1]; Kobi Perl[1]; Yael Noy[1]; Yoni Bhonker[1]; Mattia Pelizzola[3]; R. David Hawkins[2]; **Karen B. Avraham**[1]
[1]Department of Human Molecular Genetics & Biochemistry, Sackler Faculty of Medicine and Sagol School of Neuroscience, Tel Aviv University, Tel Aviv 6997801, Israel; [2]Division of Medical Genetics, Department of Medicine, Department of Genome Sciences, Institute for Stem Cell and Regenerative Medicine, University of Washington School of Medicine, Seattle, WA 98195, USA; [3]Center for Genomic Science of IIT@SEMM, Fondazione Istituto Italiano di Tecnologia, Milano 20139, Italy

DNA methylation is an epigenetic marker, playing a critical role in gene expression and silencing. DNA methylation patterns are established during development of an organism and are known to influence both health and disease. We have constructed the first genome-wide methylome map of the mouse inner ear across several key developmental time points. Whole genome bisulfite sequencing was performed on sensory epithelia at E16.5, P0 and P22. Genome-wide methylation signatures were evaluated in CpG, CHH, and CHG contexts. We detected an accumulation of non-CpG methylation, associated with establishment of neuroplasticity in the adult differentiated brain, suggesting similarities in regulation between neurons and sensory epithelia. Unmethylated (UMR) and low methylated (LMR) regions were annotated, providing a means to identify novel regulatory elements. We also determined transcription factor binding site (TFBS) motifs within UMRs and LMRs to identify putative regulators of target genes, and highlighted their differential enrichment across time points. As an example, several known inner ear TFs were found enriched within all LMRs analyzed, such as NeuroD1, Atoh1, Stat3, Sox10 and Sox2. Finally, we defined differentially methylated regions (DMRs) across developmental and maturation transition periods to identify candidate regulatory factors that may drive the development and maturation of the inner ear sensory epithelium. We subjected all DMRs to TFBS motif analysis to determine how differential methylation might impact gene regulation. A number of known inner ear regulators were enriched, including Six1, Stat3, Pou3f4, Wnt factors Tcf3 and Tcf4, Sox2, Atoh1 and NeuroD1. Our findings demonstrate that methylation will provide answers regarding the role of global epigenetic regulatory processes, as well as the dynamics of regulatory elements, in the inner ear, and will advance our understanding of auditory function.

PD 92

Characterizing Stria Vascularis Cell Type Heterogeneity at the Single Cell Level

Soumya Korrapati[1]; Rafal Olszewski[1]; Erich Boger[1]; Daniel Martin[2]; Robert J. Morell[3]; Michael Hoa[3]
[1]NIDCD; [2]NIDCR; [3]NIDCD/NIH

Introduction
The stria vascularis (SV) is responsible for generating the endocochlear potential (EP) in the inner ear which is necessary for proper hair cell functioning. The SV is a complex heterogeneous tissue consisting of multiple cell types thought to be required for EP generation and maintenance. Despite the importance of SV and the lateral wall in the development and maintenance of the EP, our understanding of the diversity of cells that comprise these structures remains limited. Similarly, our understanding of the signals involved in the development and maturation of those cell types is also minimal. EP develops between P8 and P15 and is considered mature at P30. While channels belonging to intermediate and marginal cells are known to play crucial roles in the generation of the EP, relatively little is known about the pathways and factors required to accomplish and maintain these functions. To establish a basis for understanding the molecular mechanisms responsible for these functions and possibly other unknown functions, we first set out to generate transcriptome profiles for isolated strial cells at P30.

Methods
SV was dissected from wild-type CBA/J P30 mice. Striae were dissociated to a single cell suspension or single nucleus suspension and isolated cells/nuclei were captured on the 10X Genomics platform. Expression profiles of SV subpopulations were analyzed using Seurat analysis pipeline. Pathway analysis was performed on different strial populations to gain insight into cell type-specific biological processes. A panel of established strial cell type-specific marker genes were utilized to validate unbiased clustering of strial cell types.

Results

Using the Seurat pipeline, P30 SV subpopulations were delineated using single whole cell and single nucleus RNA-Seq. Potential novel cell type-specific genes were identified. Utilizing pathway analysis, shared and cell type-specific gene regulatory networks and their associated biological processes were described. We validated a select group of novel cell type-specific genes for established strial cell types in the P30 adult mouse.

Conclusion

Characterization of cellular heterogeneity and transcriptional pathways of SV provides a foundation for identification and characterization of pathogenic mechanisms in studies of SV-related hearing loss.

PD 93

The Role of the Unfolded Protein Response and the Novel Gene, TMTC4, in the Pathogenesis and Treatment of Acquired Hearing Loss

Jiang Li[1]; Omar Akil[2]; Stephanie Rouse[3]; Ian Matthews[3]; Conor McLaughlin[3]; Lawrence R. Lustig[4]; Dylan Chan[3]; Elliott Sherr[1]
[1]Department of Neurology, UCSF; [2]University of California San Francisco, Epstein Lab, Dept Otolaryngology-HNS; [3]Department of Otolaryngology-Head and Neck Surgery, UCSF; [4]Department of Otolaryngology, College of Physicians and Surgeons, Columbia University and New York Presbyterian Hospital

Hearing loss is a significant public health concern, affecting over 250 million people worldwide. Both genetic and environmental etiologies have been identified, but in many cases the underlying cellular pathophysiology is not well understood, which underscores the critical importance of further discovery. We identified a novel gene, Tmtc4 (transmembrane and tetratricopeptide repeat 4), for which disruption causes acquired hearing loss in mice. Homozygous inactivation of this gene, which is broadly expressed in the mouse cochlea, leads to rapid progression of post-natal hearing loss followed by cochlear hair-cell degeneration and death. Intracellularly, TMTC4 is enriched in the endoplasmic reticulum, and our data suggest that it functions by regulating both Ca^{2+} dynamics and the unfolded protein response (UPR). Given this genetic linkage of the UPR to hearing loss, we hypothesized and subsequently demonstrated a direct link between the more common noise-induced hearing loss (NIHL) and the UPR. These experiments therefore suggested a novel approach to treatment. We then demonstrated that the small-molecule UPR and stress response modulator ISRIB (Integrated Stress Response Inhibitor), which activates eIF2B and leads to decreased synthesis of the pro-apoptotic protein Chop (C/EBP-homologous protein), prevents NIHL in a mouse model. Moreover, in an inverse genetic complementation approach, we demonstrate that mice with homozygous inactivation of both Tmtc4 and Chop have less hearing loss compared with knockout of Tmtc4 alone. This study implicates a novel mechanism for hearing impairment and highlights a potential approach for the treatment of a broad range of human hearing-loss disorders

PD 94

Proximal and Distal Cis Elements Regulate Expression of the Inner Ear-Specific Ubiquitin Ligase Subunit Fbx2

Byron Hartman[1]; Stefan Heller[2]
[1]Stanford | School of Medicine |Department of Otolaryngology - Head & Neck Surgery; [2]Stanford | School of Medicine | Department of Otolaryngology - Head & Neck Surgery

Fbx2 is a highly specific and abundant inner ear protein shown to be important for cellular homeostasis. Lack of Fbx2 in mice leads to age-related hearing loss beginning at two months, associated with degeneration of cochlear supporting cells and changes in membrane integrity, followed by progressive degeneration of hair cells and spiral ganglia (Nelson et al 2007). It is thought that Fbx2, a ubiquitin ligase substrate adapter protein with specificity for glycoproteins, plays an important role in protein quality control in the adult inner ear. Although it appears to function in cochlear maintenance, Fbx2 is expressed surprisingly early in otic development. In a previous microarray study, we found that Fbxo2 is one of the most abundant and specific genes in the developing otocyst as compared to other tissues of the early mouse embryo (Hartman et al. 2015).

We generated Fbxo2-VenusHC knock-in reporter mice to further characterize expression of this gene and exploit it to access the otic sensory lineage for developmental studies. The Fbxo2-VenusHC reporter drives expression of H2B-Venus (a nuclear-localized YFP) in otic sensory progenitors as well as nascent hair cells and supporting cells during embryogenesis. In the neonatal cochlea, H2B-Venus is expressed throughout the organ of Corti as well as the lesser epithelial ridge. Ultimately, in the adult, the reporter is expressed strongly in auditory hair cells and supporting cells, is exceptionally high in Boettcher and Claudius cells, and is found at lower levels in spiral ganglia, a subset of vestibular hair cells, and spiral ligament fibrocytes.

Here we aim to decipher how the robust and specific expression of Fbxo2 is regulated, and to identify cis-elements for directing future gene therapies specifically to

the inner ear. Phylogenetic comparison of the extended Fbxo2 locus across vertebrate species reveals several conserved noncoding regions, including a ~2kb promoter and nine highly evolutionarily conserved regions (ECRs) downstream of the 3';UTR. Several potential binding sites were identified in silico, including sites for Pax2/5/8, Gata3, and Sox10. Conservation and clustering of binding sites within the promoter and ECRs suggests combinatorial transcription factor binding. We used plasmid electroporation as a preliminary test of the activity of the 2kb promoter and found that it is sufficient to drive reporter expression in embryonic cochlea explants.

We hypothesize that Fbxo2 expression in the developing and adult mouse is regulated through multiple cis-regulatory modules located within the promoter and downstream ECRs. To test this, we produced a reporter mouse (Fbox2*tdTomato) with a transgene that mimics the native 100kb Fbox2 locus while condensing it to about 10kb by excluding non-conserved regions and replacing the Fbxo2 coding region with tdTomato. All nine of the ECRs were individually positioned similar to their native orientation and loxP and FRT sites were strategically included to allow subsequent excision of ECRs in two groups. The proximal ECRs 1-5 can be removed with Cre recombination while the distal ECRs 6-9 can be removed with Flip recombination. Germ line recombination was achieved by crossing the Fbox2*tdTomato mouse line to Cre and/or Flip recombinase-expressing mouse lines. The full-length transgene determines whether all of the conserved elements are sufficient to confer the normal pattern of Fbxo2 expression, while Cre/Flip excision tests for necessity within the ECR clusters. We find that the fully intact Fbox2*tdTomato reporter accurately recapitulates the major features of Fbxo2 expression and that downstream ECRs contain elements that enhance expression in otic cells and repress expression in off-target cells.

Middle Ear Potpourri

PD 95

Human middle-ear muscles rarely contract in anticipation of acoustic impulses

Heath Jones; Nathaniel Greene; William Ahroon
U.S. Army Aeromedical Research Laboratory

Repetitive exposure to high-level acoustic impulses, such as those from firearms, increases the susceptibility for hearing loss. As such, great effort over the past has been focused on developing a means for assessing the risk of auditory injury from acoustic impulses. Currently, the United States Department of Defense acquisition standard (MIL-STD-1474E) mandates the U.S. Army use the Auditory Hazard Assessment Algorithm for Humans (AHAAH) for calculating maximum permissible noise levels and exposure limits of military systems. The AHAAH is an electro-acoustic model designed to predict the auditory injury that results from intense pressure changes at the ear caused by blast overpressure and acoustic impulsive noise exposures. One concern with the model is that the middle-ear muscle contraction (MEMC) associated with the acoustic reflex is implemented as a protective mechanism for certain instances in which a person is 'warned' prior to the impulse. To date, there is limited evidence of acoustic reflex classical conditioning. In a technical report published by the developers, some older studies were cited as demonstrable evidence that the MEMC can be classically conditioned. However, the literature is equivocal concerning ability to condition the MEMC. The current project aimed to test some of these assumptions, such as whether the MEMC can be elicited by a conditioning stimulus prior to sound exposure (i.e., a "warned" response) and the effects of MEMC on sound transmission for these "warned" responses. In order to quantify the MEMC, we use laser-Doppler vibrometry to measure tympanic membrane motion in response to reflex-eliciting acoustic impulses presented to the contralateral ear. After verifying the MEMC, we attempted to classically condition the response by pairing a 110 dB peak SPL reflex-eliciting acoustic impulse (unconditioned stimulus, UCS) with various preceding stimuli (conditioned stimulus, CS). Changes in the magnitude and/or time-course of the MEMC following repeated UCS-CS pairings were considered evidence of MEMC conditioning. Out of the 36 subjects tested so far, both non-conditioned (n=34) and conditioned (n=2) responses have been observed. These findings suggest that a 'warned' MEMC may not be present in enough people to justify inclusion for being considered protective. Thus, the 'warned' option of the AHAAH model may not be appropriate to use when calculating auditory injury risk. Knowledge gained from this study indicates the need for updates to hearing health hazard assessments and will inform updates to Damage-Risk Criteria to better protect the hearing of Soldiers and civilians exposed to high-level impulsive noises.

PD 96

3D motion of the human ossicles with normal and stiffened ossicular joints during bone-conduction stimulation

Xiying Guan[1]; Sunil Puria[2]
[1]*Eaton-Peabody Laboratory, Massachusetts Eye and Ear; Department of Otolaryngology, Harvard Medical School;* [2]*Eaton-Peabody Laboratory, Massachusetts Eye and Ear; Department of Otolaryngology, Harvard Medical School; Speech and Hearing Bioscience and Technology, Harvard University Graduate School of Arts and Sciences*

The mammalian ossicular chain consists of three distinct bones typically connected by two synovial joints, comprising of a flexible circuitous coupling path between the eardrum and the cochlea. It has been hypothesized that this arrangement has several physiological advantages such as the ability to hear high-frequency sounds and to protect the inner ear from impulsive sounds and static pressures. While the utility of the ossicular flexibility for air-conducted sound transmission has been explored, its functional implications for the bone-conduction (BC) pathway are less well understood.

One possible benefit of the three-ossicle flexible structure is to minimize the perception of self-generated sounds such as chewing, neck movement, and footsteps. During BC stimulation, inertial motion of the ossicles can move differentially from their cochlear wall attachments and thus contributing to cochlear input. We hypothesize that having three ossicles with soft joints in-between may reduce the ossicular inertial effects and thereby attenuate the input to the cochlea during BC stimulation.

The present study aims to test this hypothesis. One difficulty in studying the dynamic behavior of the ossicular chain in BC is that the motion is usually three-dimensional (3D) and complex. Thus, we performed 3D velocity measurements of the malleus, incus and stapes of the human cadaveric ear with vibrational BC input at audio frequencies. The measurements were performed before and after we stiffened, with dental cement, the incudomalleolar joint, the incudostapedial joint, or both. The 3D motion and modes of vibrations of the bones in the normal and stiffened conditions were reconstructed and compared.

PD 97

OCT and LDV measurements of ossicular structure and function in chinchilla

John J. Rosowski[1]; Antoine Ramier[2]; Jeffrey T. Cheng[3]; Seok-Hyun Yun[4]
[1]Eaton Peabody Lab, Massachusetts Eye and Ear Infirmary, Harvard Medical School; [2]Helth Sciences and Techology, Massachusetts Insitute of Technology; [3]Eaton Peabody Laboratory, Massachusetts Eye and Ear Infirmary; Department of Otolaryngology, Harvard Medical School; [4]Harvard Medical School

Background
The sound-induced motion and in-situ structure of the ossicles and eardrum of the chinchilla have not been well described, and questions regarding the mode of motion and the ossicular structures that contribute to vibrational phase delays in the ossicular chain of this species remain.

Methods
Fourier-domain Optical Coherence Tomography (OCT) and OCT vibrography were used to characterize the three-dimensional structure and sound-induced motion of the eardrum and ossicular chain in post-mortem chinchillas. The data were gathered at A-line rates of 45,000 lines per sec, allowing complete volumetric scans of the ossicular chain in less than a minute and quantification of its motion in several minutes. Sound stimuli were sinusoids phase-locked to the OCT scan rate. The structural and vibrometer measurements were supplemented by Laser-Doppler Vibrometer (LDV) measurements made at multiple points along the ossicular chain - before and after opening a small hole on the eardrum over the stapes and incus. The LDV';s position was set by a computer-controlled positioner. LDV derived structural maps of the 2D projection of the malleus, incus and stapes were mapped to the OCT derived 3D structure.

Results
Preliminary results are consistent with simple rotation of the chinchilla ossicular chain about an axis determined by the elongated head of the malleus and incus in these animals. With tonal stimulation frequencies of 4000 Hz and below, the magnitude of the motion varies regularly along the length of the manubrium of the malleus, as would be expected of a simple lever arm, and the motion magnitudes of the incus and stapes are consistent with rigid motion of the shorter lever arm. In that same frequency range, the motions along the manubrium, and those of the incus and stapes vary little in phase. At higher frequencies in this range, we do see small deviations in the spatial-dependence of the motion that may be related to sound-induced motions of the ossicular axis, but we see little phase delay along the incus and malleus. The LDV measurements described the motion at frequencies as high as 30 kHz, and showed more evidence of sound-induced motion of the ossicular axis and also described near step-like changes in motion phase of the incus and stapes relative to the manubrium. at frequencies near 20 kHz

Discussion
These findings will be compared with earlier measurements of the ossicular motion in humans, cats, gerbils and mice.

PD 98

Preliminary application of intraoperative monitoring using tone-pip ABR via loudspeakers in middle ear surgery.

Hui Zhao[1]; **Wei Ren**[1]; Fei Ji[2]
[1]*PLA General Hospital;* [2]*Chinese PLA Medical School*

Background

Conductive hearing loss (CHL), a common disease caused by middle ear diseases, mainly affects hearing in low frequencies and leads to communication problems. It is reported that 69% of such group of patients benefit from ossicular reconstruction surgeries. However, the hearing improvement can only be assessed by post-operative pure tone audiometry (PTA). Thus, the undetermined surgery success rate and probable prolonged revision surgery are problems surgeons still facing. Therefore, we established a reliable and replicable system, the frequency-specific ABR via loudspeaker intra-operative hearing monitoring system (fs-ABR system), to optimize prosthesis's position and predict the post-operative hearing improvement during surgery.

Methods

Different from the previous studies, 1000Hz tone pip was chosen as the acoustic stimuli to assess the speech-frequencies threshold, loudspeaker was selected to replace the earplugs and put 30cm away from the eternal ear canal to guarantee the acoustic intensity and antiseptic principle. PTA and fs-ABR were applied to 13 normal hearing people in the acoustic booth to demonstrate its accuracy. After calibration, 18 unilateral CHL patients undergoing ossicular chain reconstruction were enrolled. They would experience four testes sequentially: standard PTA, fs-ABR in operation room under anesthesia before operation, fs-ABR after the prosthesis being implanted, standard PTA 3 months after operation. Blandman analysis and correlation analysis were used. All the subjects enrolled had signed a written informed consent before the experiment.

Results

1. Blandman analysis showed no difference between PTA and fs-ABR in normal hearing group, demonstrating the availability of our system. 2. For CHL group in operation room, the correlation coefficient was 0.761 between PTA and fs-ABR, demonstrating the availability of our system in the operation room. 3. For the following-up group, Blandman analysis showed no difference between afterward PTA and intra-operative fs-ABR, demonstrating that our system might predict the post-operative hearing improvement.

Conclusion and Discussion

Our study established a reliable and replicable fs-ABR intraoperative hearing monitoring system for middle ear surgeries. It might become a tool to optimize the prosthesis's position accordingly and predict the post-operative hearing improvement. However, several interference factors remain unsettled and how much they act on the threshold determination remain unknown, including the background noise, electromagnetic interference and especially blood in the external canal. The machine was covered by a copper net to shield it from electromagnetic factors. Other machines were closed to minimize the noise. However, further research would be needed to minimize the interference of blood.

figures.docx

PD 99

Importance of Radial Stiffness for High-Frequency Sound Conduction in 3D Printed Tympanic Membrane Grafts

Nicole L. Black[1]; Jeffrey T. Cheng[2]; Renee Friedman[1]; Iman Ghanad[3]; Elliott D. Kozin[3]; John J. Rosowski[4]; Aaron K. Remenschneider[3]; Jennifer A. Lewis[1]
[1]*Harvard John A. Paulson School of Engineering and Applied Sciences, Harvard University; Wyss Institute for Biologically Inspired Engineering, Harvard University;* [2]*Eaton Peabody Laboratory, Massachusetts Eye and Ear Infirmary; Department of Otolaryngology, Harvard Medical School;* [3]*Massachusetts Eye and Ear Infirmary, Harvard Medical School;* [4]*Eaton Peabody Lab, Massachusetts Eye and Ear Infirmary, Harvard Medical School*

Background

The tympanic membrane (TM) contains radial and circular collagen fibers within its medial, lamina propria layer. Previous modeling experiments have demonstrated that radial stiffness plays a role in allowing the tympanic membrane to conduct sound at high frequencies. Current tympanoplasty and myringoplasty graft materials, including fascia and cartilage, lack this microarchitecture, resulting in isotropic remodeled tissues and often poor hearing outcomes at high frequencies. Three-dimensional (3D) filamentary extrusion printing can mimic the fiber arrangement of the native TM and permit tuning of radial stiffness. We hypothesize that by tuning radial stiffness of 3D printed grafts, high frequency sound conduction can be altered.

Methods

Human cadaveric tympanic membranes are isolated from the ossicular chain to serve as a positive control.

Collagen sheets with random fiber arrangements serve as negative controls. A novel biodegradable polyurethane is synthesized and dissolved in acetone for printing. Filamentary extrusion printing with a 100 µm nozzle produces TM grafts with directed circular and radial fiber arrangements. The TM grafts are seeded with human neonatal dermal fibroblasts and maintained in standard tissue culture conditions to promote remodeling into anisotropic tissue. Cellular ingrowth and collagen deposition is determined by immunofluorescence staining and confocal laser microscopy. Laser holography and Doppler vibrometry (LDV) determine the acoustic responses of the grafts after 10 weeks of cellular remodeling.

Results

Confocal microscopy shows remodeled TM grafts maintain architecture of printed fiber arrangements.LDV demonstrates displacements at the center of the 3D printed grafts increase with the numbers of circular/radial fibers in the high frequency range (>10 kHz), bringing them closer to the umbo displacement of the human cadaveric TM tissue. The normalized velocity of the 50 circular / 50 radial (50C/50R) 3D printed graft is approximately 10x higher than that of the 50 circular only (50C) grafts above 10 kHz. Collagen sheets show lower velocities at most frequencies above 1 kHz. Holography demonstrates frequency dependent surface motion patterns ranging from simple at low frequencies to complex at higher frequencies. The complexity of motion patterns at 3000Hz and 6000 Hz are more pronounced for grafts with increased radial fibers, similar to the motion patterns of human TM.

Conclusion

3D printing with a novel biodegradable polyurethane produces TM grafts with micron-scale fiber arrangements that are remodeled by cellular ingrowth into anisotropic tissues. The anisotropy mimics the circular and radial fiber arrangements seen in native TMs, and radial fibers improve sound conduction in the high frequency range to more closely match the response of unloaded human TMs.
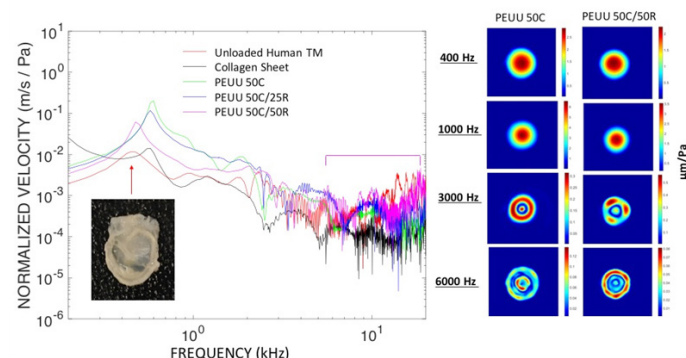
PD 100

Stenting the Eustachian Tube as a Novel Treatment Concept for Chronic Otitis Media

Tamara Wilfling[1]; Gerrit Paasche[1]; Robert Schuon[2]; Friederike Pohl[2]; Thomas Lenarz[3]
[1]Department of Otolaryngology, Hannover Medical School, Germany; Cluster of Excellence; [2]Department of Otolaryngology, Hannover Medical School, Germany; [3]Department of Otolaryngology, Hannover Medical School, Germany and DFG Cluster of Excellence Hearing4all

Introduction

Impaired function of the Eustachian tube (ET) is the main underlying pathophysiology of chronic otitis media. Several concepts have been tried to overcome chronic ET dysfunction but with moderate success rate. As the reason for ET dysfunction is typically located in the cartilaginous part of the tube, the stent concept might provide a solution for these patients. The stent shall be placed such that it facilitates natural opening and closure of the ET.

Methods

Cardiovascular stents were inserted into the Eustachian tube of cadavers of blackface sheep and humans, stenting the cartilaginous part lateral to the nasal orifice. The position of the stents was validated by endoscopy and CT-scans. Chronic sheep experiments were performed for 3 months and the position of the stents were checked by CT-scans and endoscopy. Ventilation of the middle ear was examined by tympanometry and tissue reaction by histology.

Results

Stents of a length of 20 mm can reliably be positioned in the cartilaginous part of the Eustachian tube with no signs of migration. The stents were well tolerated by the sheep and middle ears appeared ventilated. Only a mild tissue reaction was observed. The entire surface of the ET tissue was covered by ciliated epithelium, even on top of ingrown struts.

Conclusion

Stents for the Eustachian tube seem to be a feasible treatment option for patients with chronic Eustachian tube dysfunction. The design still has to be adapted to the human ET in order to ensure natural function of the tube and avoid possible autophony.

PD 101

Effect of Electronic Cigarettes on Human Middle Ear

Jiwon Chang[1]; Su-kyoung Park[1]; YooYeon Kim[2]; Jun Ho Lee[1]; Se Hee Lee[3]; Gi Jung Im[4]; Jae-Jun Song[4]
[1]*Department of Otolaryngology-Head and Neck Surgery, Hallym University College of Medicine;* [2]*Department of Medical Genetics, College of Medicine, Hallym University;* [3]*Korea University College of Medicine;* [4]*Department of Otolaryngology-Head and Neck Surgery, Korea University College of Medicine*

Electronic cigarettes (e-cigarettes) are the most commonly used electronic nicotine delivery system, and the e-cigarette market has been growing rapidly world-wide. However, the potential impact of e-cigarettes on public health has not been verified yet, and there are ongoing disputes about whether e-cigarettes produce significant organ toxicity or they are effective in quitting smoking and will replace the conventional tobacco or cigarettes in the future. Moreover, there are few reports about the potential effect of e-cigarettes on the upper airway and ENT diseases. Middle is connected to the nasopharynx through the eustatian tube, and is vulnerable from the bacterial infection and the environmental pollutant. Especially, since the smoking of family member is a well-known cause of otitis media, the use of e-cigarettes would probably increase the risk of inflammation in the middle ear. The purpose of our study is to identify the toxicity and possible mechanism of e-cigarettes on the middle ear. E-cigarette is composed of the battery, the vaporizing chamber and the electronic liquid (e-liquid). The main components of the e-liquid are propylene glycol (PG), vegetable glycerin (VG), flavoring agents with or without nicotine. We selected the most popular brands of e-liquids that dominate the domestic market after reviewing various and rapidly changing products. We examined the components of e-liquid and identified the heavy metal contents of them. We analyzed 73 bottles of 12 different brands purchased from local retailers, and investigated cell viability and inflammatory changes of human middle ear epithelial cells (HMEEC) after application of various concentrations of e-liquids. Trace elements such as Nickel, Arsenic, Cadmium, and lead were identified from various e-liquids. Although nicotine was not included in the E-liquids, they decreased cell viability to 50% in average concentration of 2.48 ± 0.93 %, and among various e-liquid flavors, menthol flavor demonstrated the lowest IC50 with 1.85 ± 0.80 %. When we analyzed the cytotoxicity of the different ratios of solvent (mixtures of PG and VG), the solvent with higher proportion of PG had lower IC50 values, and the concentrations of solvent which reduced cell viability to 50% were between 3.58 - 4.19 %. However, COX-2 and TNF-alpha were highly increased in tobacco flavor e-liquids.

We assume that e-liquids affect human middle ear cell and that flavors not alone nicontine influence the development of otitis media.

Non-Acoustic Influences on Speech Perception in Normal and Impaired Hearing

SYMP 70

Influences on children's perception of unfamiliar regional dialects and nonnative accents

Tessa Bent[1]; Rachael Holt[2]; Katherine Miller[2]
[1]*Indiana University;* [2]*Ohio State University*

During language acquisition, children must learn to recognize acoustic-phonetic variants of known words, which result from pronunciation variability both within and across talkers. One frequently encountered source of variability stems from nonnative accents and unfamiliar regional dialects. Our work suggests that perception of speech from talkers with unfamiliar accents and dialects exhibits a protracted developmental trajectory. The locus of children's immature abilities may arise from multiple sources such as continued development of foundational cognitive-linguistic skills (e.g., phonological awareness) or diminished ability to capitalize on top-down processing when mapping these unfamiliar speech signals.

SYMP 71

Talker familiarity improves speech understanding in the presence of simultaneous talkers

Emma Holmes[1]; Ysabel Domingo[1]; Ingrid Johnsrude[2]
[1]*Brain and Mind Institute, University of Western Ontario;* [2]*Brain and Mind Institute, University of Western Ontario; School of Communication Sciences and Disorders, University of Western Ontario*

Successful verbal communication requires listeners to understand speech spoken by a target talker in the presence of competing talkers. When two talkers speak simultaneously, listeners gain a 10-20% improvement in speech intelligibility when target speech is spoken by a familiar talker, such as a friend or spouse, than when it is spoken by an unfamiliar talker. Research in our lab has used closed-set speech intelligibility tasks to assess the magnitude of the benefit that listeners gain from a naturally familiar talker. We presented listeners with sentences spoken by a close friend or partner and with sentences spoken by the friends and partners of other participants in the experiment, who they had never met. Our results show that both older and younger listeners benefit from talker familiarity and this benefit is present after just 6 months of knowing someone. In addition, the familiar-talker benefit to speech intelligibility is robust to modifications of voice characteristics: the benefit is still

present when a familiar voice has been manipulated so much that it is no longer recognizable. Finally, we have used functional magnetic resonance imaging (fMRI) to compare the quality of the neural representations of familiar and unfamiliar voices, in order to determine whether a difference in the quality of the representations underpins their differences in intelligibility.

SYMP 72

Eye gaze and spatial release from speech-on-speech masking

Madeline S. Cappelloni; **Ross K. Maddox**
University of Rochester

Complicated auditory scenes are composed of multiple sound sources coming from many different directions. In such a setting, observers are likely to dynamically direct their eye gaze to different parts of the scene as they process it, but studies have typically not considered gaze as an independent variable. It is well known that the auditory system leverages the spatial separation between sound sources to improve processing of a single target sound, an effect known as spatial release from masking. This effect is dramatic: spatial separations of 45 degrees between target and masking sounds can have an effect on speech comprehension equivalent to reducing the masker intensity by about 10 decibels. Logically, this benefit should depend on both the physical separation and the listener's perception of that separation. Our previous work has shown that the processing of spatial cues is affected by the direction of eye gaze. Specifically, gazing toward probe sounds while keeping the head fixed yields improvements in spatial discrimination, particularly when those sounds are presented laterally instead of around the mid-line. In this talk we will discuss new work that investigates possible benefits to speech perception due to gaze-driven changes to spatial processing. We engaged listeners in a speech-on-speech masking task and determined target-to-masker ratio thresholds for a variety of conditions that manipulated auditory space and the subject's eye gaze. Our experiments were aimed at answering the question: could gaze-driven improvement in spatial processing also enhance the listening benefits of spatial release from masking?

SYMP 73

Linguistic Knowledge Affects Auditory Streaming of Speech: Insights from Intracranial Recordings and Functional Magnetic Resonance Imaging

Alexander Billig[1]; Kirill Nourski[2]; Ariane Rhone[2]; Phillip Gander[2]; Matthew Howard[2]; Ingrid Johnsrude[3]
[1]Brain and Mind Institute, The University of Western Ontario; [2]Human Brain Research Laboratory, Department of Neurosurgery, The University of Iowa; [3]Brain and Mind Institute, University of Western Ontario; School of Communication Sciences and Disorders, University of Western Ontario

Elements in a sound mixture are allocated to distinct perceptual objects based not only on their acoustic properties, but also on the extent to which they form familiar patterns. We demonstrate that sequences of repeated syllables (e.g. "stome stome stome …") can be perceived as one or two streams of sound according to spectral, spatial, and linguistic information. Using intracranial recordings and high-field fMRI we then exploit the bistable nature of such sequences to compare neural activity during the perception of one versus two streams of sound, and to examine the role of cortical language networks in auditory scene analysis.

SYMP 74

Examining the Relative Influence of Word Recognition and Word Recall on Speech Recognition in Speech Mixtures

Elin Roverud
Department of Speech, Language & Hearing Sciences, Boston University

There are many facets to understanding a talker in speech mixtures. The listener must be able to segregate the talkers, selectively attend to the target talker and recognize the words spoken. In addition, the listener must also rely on memory and linguistic processing to comprehend the message. Some laboratory studies of speech understanding in noise have examined the various cues (such as spatial separation of target and masker talkers) that may aid the listener in segregating and selectively attending to a target talker. However, in order to indicate that the target message was understood, the listener usually must also be able to recall a string of words spoken by the target talker. In this work, we aim to understand the relative influences and possible interactions of target selection and recall on recognition performance in speech mixtures. We employed a method of testing word recognition in various types of masking, comparing performance for individual words (where recall demands were low) to performance for progressively longer sequences of words (increasing demands

for recall). Based on current models of effortful listening (e.g., Rudner, 2016, Ear & Hearing, 37), we theorized that fewer cognitive resources would be available for word recall in the more challenging masked conditions. Furthermore, we hypothesized that performance differences among masking conditions would be more evident when resource demands placed on the recall task were high. This work has implications for experimental methods probing speech recognition in noise, which tend to assess word recognition performance using a fixed sequence length of words. This work also has potential implications for our understanding of the interactions of processes underlying speech understanding in noise. [Work supported by NIH NIDCD].

SYMP 75

Quantifying listening effort: Linking behavioral and physiological measures to underlying cognitive control networks

Stefanie E. Kuchinsky
University of Maryland

Understanding speech in noise often requires substantial effort, even for individuals with normal hearing. Myriad indices of listening-related effort have been proposed, however there is a gap in our understanding of how effort emerges and thus what is being measured. Recent research has aimed to address this issue by investigating the relative involvement of perceptual and cognitive processes in performing challenging listening tasks. I will present a dual-task study that varied acoustic, lexical, and attentional demands as 26 younger, normal-hearing participants recognized words in speech-spectrum noise. These factors had an interactive effect on dual-task reaction times, suggesting that listening effort comprises multiple component processes that support speech comprehension. I will describe how my ongoing work aims to further validate this finding by linking commonly used measures of effort with the engagement of well-studied perceptual and cognitive neural systems. I will present a preliminary functional magnetic resonance imaging (fMRI) study that tests the hypothesis that challenging speech recognition engages auditory, conflict monitoring, and cognitive control regions that may be differentially indexed by behavioral and pupillometry measures of effort in younger, normal-hearing adults. This research lays the groundwork for developing clinical assessments and interventions that target listening effort in older adults. This work is supported by NIH/NIDCD R03 DC015059.

SYMP 76

Factors influencing restoration of interrupted speech in cochlear implant users and normal hearing listeners

Pranesh Bhargava[1]; Etienne Gaudrain[2]; Deniz Baskent[2]
[1]Birla Institute of Technology and Sciences, Pilani, Hyderabad Campus; [2]University Medical Center Groningen, Dept. of Otorhinolaryngology / Head & Neck Surgery, The Netherlands

Cochlear implant (CI) users have difficulty understanding speech in noisy scenarios. This could, at least partially, be due to their reduced ability to deploy top-down processes in integrating and restoring speech glimpses across noise intervals. We measured the intelligibility of meaningful sentences, which had been interrupted at various rates and duty cycles. CI users' performance was compared with that of both young and age-matched normal-hearing listeners with full-spectrum and vocoded speech, in order to explore the effect of the loss of spectral resolution, advanced age, and baseline speech intelligibility. Loss of spectro-temporal resolution could not adequately explain impaired performance in CI users, indicating that additional factors associated with age and speech-cue transmission may play a role.

SYMP 77

Neural dynamics of attention to speech-in-noise: Ageing and hearing loss impair, but brain stimulation can enhance, auditory attention

Malte Wöstmann; Sarah Tune; Jonas Obleser
Department of Psychology, University of Lübeck

Do speech comprehension difficulties, as they often occur in older and hearing-impaired listeners, trace back to changes in neural activity? We will present results of human electroencephalography (EEG) experiments demonstrating that both, aging and hearing loss impact neural responses to speech in noise. First, the influence of a listener's intent (attend versus ignore) on 10-Hz alpha oscillatory power decreases with age. Second, amongst older listeners, differential phase-locking of ~4-Hz neural oscillations to envelopes of attended versus ignored speech decreases with hearing loss. These findings suggest that speech comprehension difficulties in older and hearing-impaired listeners are mediated by constraints in the neural dissociation of attended versus ignored speech. In a third study, we used brain stimulation in order to test whether neural activity is indeed a functionally significant substrate to speech-in-noise processing. Young, normal-hearing participants performed a dichotic listening task under continuous transcranial alternating current stimulation (tACS) at alpha (10 Hz,

vs sham) or gamma (47 Hz, vs sham) frequency, targeting left temporo-parietal cortex. As predicted, tACS modulated a listener's focus of spatial attention: Compared to sham, alpha-tACS contralateral to the attended ear decreased recall of attended targets, whereas gamma-tACS entirely reversed this effect. These results demonstrate that external amplification of neural oscillatory activity associated with processing attended versus ignored speech has the potency to facilitate attention to speech-in-noise.

Auditory Pathways Brainstem III

PD 102

Ventral cochlear nucleus small cells counteract medial olivocochlear suppression to preserve intensity coding

Calvin Wu[1]; Susan Shore[2]
[1]University of Michigan Ann Arbor; [2]University of Michigan

To encode sound intensity, auditory nerve fiber (ANF) firing rates must discriminate a range of stimulus levels. This "dynamic range" varies with ANF threshold, and can be altered by medial olivocochlear (MOC) suppression. By elevating hearing thresholds and shifting the dynamic range toward higher levels, MOC activation prevents firing-rate saturation in the presence of background noise, improving signal-in-noise detection at the expense of low intensity information. In order to account for this loss, it was suggested that MOC may facilitate ANF targets in the ventral cochlear nucleus (VCN) directly through collateral projections (Fujino & Oertel, J Neurosci 2001). To confirm this hypothesis, we characterized responses, in vivo, of two putative MOC-projection recipients: T-stellate and small cells. Small cells, located at the dorso-lateral edge of the VCN, exhibit higher thresholds, wider dynamic ranges, and narrower tuning at higher intensities than T-stellate cells, likely due to a paucity of low-threshold ANF inputs (Liberman, J Comp Neurol 1991). Electrically stimulating MOC neurons shifted T-stellate cell rate-level functions to the right, mirroring the responses of ANFs reflected in compound action potentials. MOC stimulation did not elevate small-cell response thresholds, but instead increased their firing rates at high intensities, further extending their dynamic ranges. These results not only confirm the hypothesis that MOC suppression of cochlear output is counteracted in VCN, but also highlight the unique properties of small cells and their novel role as putative conveyers of absolute intensity information.

PD 103

Kv3 K+ Currents Maintain Regular Spike-timing of Dorsal Cochlear Nucleus Fusiform Cells

Timothy Olsen[1]; Alberto Capurro[1]; Nadia Pilati[2]; Charles H. Large[2]; Martine Hamann[1]
[1]University of Leicester; [2]Autifony Therapeutics

Action potential timing is essential for sound processing in the dorsal cochlear nucleus (DCN), an auditory brainstem structure involved in sound localization in the vertical plane. Previous studies have shown that cross-unit synchrony and bursting activity in DCN fusiform cells are correlated with tinnitus (1). We have previously shown that DCN fusiform cells change from a regular to burst firing pattern in response to acoustic over-exposure, and this may be due to a down-regulation of Kv3-like K+ currents (2). Here we test whether AUT1, a positive modulator of Kv3 K+ currents (3) prevents the burst firing activity of fusiform cells after pharmacological reduction of K+ currents using tetra-ethyl-ammonium (0.5 mM TEA) or following exposure to loud sound. Whole cell current clamp recordings were performed on DCN fusiform cells of CBA mice (post-natal day 14 to 19). Action potential regularity was measured within and across trains, using coefficient of variation and coincidence ratio methods, respectively. We found that TEA or exposure to loud sound both reduced overall firing frequency, decreased the action potential after-hyperpolarisation (AHP), and disrupted action potential regularity. AUT1, applied in the presence of TEA, or following acoustic over-exposure, did not affect firing frequency, but did recover AHP amplitude, and maintained a regular action potential timing, preventing the occurrence of bursts under both conditions. In conclusion, modulation of Kv3 K+ currents could provide a means to treat sound discrimination deficits observed after acoustic over-exposure.

(1) Wu C1, Martel DT2, Shore SE3. Increased Synchrony and Bursting of Dorsal Cochlear Nucleus Fusiform Cells Correlate with Tinnitus. Journal of Neurosciences 36:2068-73.

(2) Pilati N, Large C, Forsythe ID, Hamann M (2012) Acoustic over-exposure triggers burst firing in dorsal cochlear nucleus fusiform cells. Hearing research 283:98-106.

(3) Rosato-Siri MD, Zambello E, Mutinelli C, Garbati N, Benedetti R, Aldegheri L, Graziani F, Virginio C, Alvaro G, Large CH (2015) A Novel Modulator of Kv3 Potassium Channels Regulates the Firing of Parvalbumin-Positive Cortical Interneurons. The Journal of pharmacology and experimental therapeutics 354:251-260.

PD 104

Signal integration at Spherical Bushy Cells - The multifaceted role of inhibition

Christian Keine[1]; Rudolf Rübsamen[2]; Bernhard Englitz[3]
[1]*University of Iowa;* [2]*Faculty of Biosciences, Pharmacy and Psychology, University of Leipzig;* [3]*Donders Institute for Brain Cognition and Behaviour, Radboud University*

Inhibition plays a crucial role in neural signal processing, shaping and limiting neuronal responses. In the auditory system, inhibition already modulates second order neurons in the cochlear nucleus, e.g. spherical bushy cells (SBCs). While the physiological bases of inhibition and excitation are well described, their functional interaction in signal transmission and their role in acoustic information processing has remained unclear. Using a combination of in vivo loose-patch recordings, iontophoretic drug application, and detailed signal analysis in the Mongolian Gerbil, we demonstrate that inhibition is widely co-tuned with excitation, and leads only to minor sharpening of the spectral response properties. Combinations of various complex synthetic stimuli and neuronal input-output analysis based on spectrotemporal receptive fields revealed inhibition to render the neuronal output temporally sparser and more reproducible than the input while effectively regulating the response gain of SBCs. Employing acoustically diverse environmental stimuli, e.g. rain, gravel, birdsong, sand, grass, forest, leaves, we demonstrate that the inhibitory gain control becomes even more effective, keeping acoustically-evoked response rates equal to spontaneous ones. Given this profound influence on signal transmission at the auditory nerve (ANF)-SBC synapse, it is relevant to address what the costs of this modulation are for the neuronal representation of acoustic signals. To address this question, we performed dynamic stimulus reconstructions based on the neural population responses for ANF input and SBC output to assess the influence of inhibition on signal representation. Compared to ANFs, reconstructions of natural stimuli based on SBC responses were temporally more precise, but the match between the acoustic and the represented signal decreased. Overall, subtractive inhibition seems to play a central role in preserving or even improving temporal response fidelity of SBCs across a wide range of input intensities and thereby provides the basis for high-fidelity signal processing. For natural sounds in particular, inhibition plays an even stronger role at SBCs in achieving sparse and reproducible neuronal activity, while compromising general signal representation.

PD 105

Principal Cells of the Brainstem's Interaural Sound Level Detector are Temporal Differentiators rather than Integrators

Tom P. Franken[1]; Philip H. Smith[2]; Philip X. Joris[3]
[1]*KU Leuven; The Salk Institute for Biological Studies;* [2]*University of Wisconsin - Madison;* [3]*KU Leuven*

The brainstem';s lateral superior olive (LSO) is thought to be crucial for localizing high-frequency sounds by coding interaural sound level differences (ILD). Its neurons weigh contralateral inhibition against ipsilateral excitation, making their firing rate a function of the azimuthal position of a sound source. Since the very first in vivo recordings from this nucleus, LSO principal neurons have been reported to give typically sustained and temporally integrating "chopper" responses to sustained sounds. Neurons with transient responses were observed but largely ignored and even considered a sign of pathology.

We have obtained the first in vivo patch clamp recordings from labeled LSO neurons, in the Mongolian gerbil. Light and electron microscopic analysis of labeled neurons allowed us to identify principal and non-principal neurons.

We find that both principal and non-principal neurons contribute to LSO tonotopy. Principal neurons, the most numerous projection neurons of the LSO, only respond at sound onset and show fast membrane features suggesting an importance for timing. In contrast, non-principal LSO neurons often generate sustained responses to sound, and have slower membrane features with larger action potentials. Similar responses to current injection and sound suggest that different intrinsic properties are primarily responsible for these features.

These results provide a new framework to interpret previously puzzling features of this circuit and suggest that principal LSO neurons have been undersampled in the existing literature.

PD 106

Tonotopic alterations to balance of excitation and inhibition in the auditory brainstem of Fragile X Syndrome Mice

Elizabeth McCullagh; Ernesto Salcedo; Molly Huntsman; Achim Klug
University of Colorado Anschutz

Hyperexcitability and the imbalance of excitation/inhibition are one of the leading causes of abnormal sensory processing in Fragile X syndrome (FXS). The precise timing and distribution of excitation and inhibition is crucial for auditory processing, especially at the level of the auditory brainstem, where the neural circuit for sound localization resides. Sound localization, and our ability to separate multiple simultaneous sounds in space, is one of the auditory symptoms of people with FXS. Using immunofluorescence staining we tested whether there were alterations in the number and size of presynaptic structures for the three primary neurotransmitters (glutamate, glycine and GABA) in the auditory brainstem of Fmr1 knockout mice. We found decreases in either glycinergic or GABAergic inhibition to the medial nucleus of the trapezoid body (MNTB) specific to the tonotopic location within the nucleus. MNTB is one of the primary inhibitory nuclei in the auditory brainstem and participates in the sound localization process with fast and well-timed glycinergic inhibition. Thus, a decrease in inhibitory afferents to MNTB neurons should lead to greater inhibitory output to the projections from this nucleus. In contrast, we did not see any other significant anatomical alterations in balance of excitation/inhibition in any of the other auditory brainstem nuclei measured, suggesting that the alterations observed in the MNTB are both nucleus and frequency specific. We furthermore show that glycinergic inhibition may be an important contributor to imbalances in excitation and inhibition in FXS and that the auditory brainstem is a useful circuit for testing these imbalances.

PD 107

Selective Auditory Attention At The Brainstem Level

Antonio E. Forte; Octave Etard; Tobias Reichenbach
Imperial College London

Background
The encoding of speech in the auditory cortex is modulated by selective attention. However, it remains debated whether such modulation occurs in subcortical auditory structures as well. Experimental investigations of an attentional modulation of the brainstem response have been hindered by the tiny magnitude of the brainstem response: its measurement normally requires a large number of repetitions of the same short sound stimuli which may lead to a loss of attention as well as to neural adaptation.

Methods
We sought to develop a method to measure the brainstem's response to natural continuous speech that does not repeat. The brainstem responds indeed at the fundamental frequency of voiced speech. Natural speech, however, has a fundamental frequency that varies in time, which compounds a readout of the brainstem's response. We employed empirical mode decomposition (EMD) of speech stimuli of several minutes in duration to identify an empirical mode that oscillates at the fundamental frequency of the speech signal; we refer to this mode as the 'fundamental mode' of the speech stimulus. EMD can indeed extract non-linear, irregular oscillations and has recently been used to determine the time-varying pitch of speech. We then presented subjects with a task of selective attention to either a male or a female voice. Both speech streams were presented simultaneously and diotically through earphones.

Results
We found that the complex correlation of the fundamental waveform with the brainstem response yields a significant response at a latency of around 9 ms. When analyzing the brainstem response to the fundamental waveform of the male as well as of the female speaker during selective attention, we found that the brainstem response is significantly larger when attending than when ignoring a speech signal. The attentional modulation is consistent across different subjects and speakers and evidences a role of the brainstem in selective attention for analyzing complex acoustic scenes.

Conclusions
We developed a computational methodology to detect the response of the auditory brainstem to the fundamental frequency of natural non-repetitive speech. The brainstem's response exhibits a characteristic latency of 9 ms. Moreover, we found that the brainstem response is modulated by selective attention to one of two competing speakers. Our results evidence a role of subcortical structures in actively analyzing complex acoustic scenes, presumably mediated through auditory centrifugal pathways that carry information from the cerebral cortex to more peripheral areas of the auditory system.

Auditory brainstem responses from apical portions of the cochlea evoked by a basilar membrane resonance induced by fast stimulus rates

Joaquin T. Valderrama Valenzuela[1]; Jaime A. Undurraga[2]; Lindsey N. Van Yper[2]; Angel de la Torre Vega[3]; David McAlpine[2]
[1]Macquarie University & National Acoustic Laboratories; [2]Macquarie University; [3]University of Granada

Background

Recording subcortical neural activity evoked by apical portions of the cochlea is a challenge using current electrophysiological approaches. The slowing travel time of the basilar membrane (BM) at apical regions, and the long 'ring'; time of low-frequency auditory filters leads to reduce neural synchronization and, consequently, smaller evoked brain potentials than at more basal regions of the cochlea. The objective of this study was to improve the recording of auditory brainstem responses (ABRs) evoked by neurons located at apical portions of the cochlea by generating a resonance in the BM displacement with short-duration stimuli presented at fast rates.

Methods

We generated a BM resonance at the 500-Hz characteristic frequency (c_f) using diotic presentation of 100000 auditory stimuli at 80 dBnHL, at a mean rate equal to the c_f. Since fast stimulus rates lead to overlapping ABR signals, obtaining transient ABRs required (a) a presentation rate with a certain jitter [rather than using a fixed stimulus rate], and (b) deconvolution of overlapping responses. The auditory stimulus consisted of one period of a sinusoidal signal of frequency equal to the c_f and phase $+\pi/4$, windowed with a Blackman window of the same duration. Deconvolution was achieved by the iterative randomized stimulation and averaging (IRSA) technique. This study evaluated deconvolved ABR signals obtained from stimulation sequences of different jitters. Simulations showed that a BM resonance would be generated by low-jittered stimulation sequences, and we hypothesized that this resonance would increase neural synchrony within an auditory filter.

Results

Our preliminary data in normal-hearing listeners indicate that our techniques for generating a low-frequency resonance in the apical end of the cochlea generates, following the deconvolution process - the typical morphology of ABRs, with waves I, III and V clearly present in most of the conditions. Further, ABR components showed longer latencies than standard ABRs evoked by clicks, consistent with the delays associated with the cochlear delay of the traveling wave. Finally, low-jittered stimulation sequences evoked ABR components of a larger amplitude, possibly as a result of an increased neural synchrony derived from the generated BM resonance.

Conclusions

The enhanced neural synchrony achieved by a BM resonance generated by short duration stimuli [only one period of a sinusoidal signal] presented at fast rates may have potential in the clinic to improve the recording of ABRs evoked by low-frequency stimuli, and opens a new perspective to study subcortical neural processes associated with binaural hearing.

Effect of Contralateral Acoustic Stimulation Measured with ABR and ECoG in the Mongolian Gerbil

Thomas Kuenzel
Institute for Biology 2, RWTH Aachen University

Descending cholinergic innervation of the inner ear and the cochlear nucleus mediates the olivocochlear reflex, which reduces the sensitivity of the inner ear to sound stimulation and supposedly plays an important role during hearing in noise. The majority of lateral and medial olivocochlear neurons are excited by responses from the same ear they project their axons to, thus forming an ipsilateral feedback loop. However, lateral and medial olivocochlear neurons are to a certain degree also excited by acoustic stimulation of the ear contralateral to their projection target. The exact function of the contralateral olivocochlear contribution is debated.

We eventually want to exploit the contralateral olivocochlear connection experimentally to study descending cholinergic influences on monaural neurons in the AVCN in vivo. To this end we needed to show the effectiveness of contralateral acoustic stimulation in our experimental animal, the Mongolian gerbil. Given reports of inter-individual variability of contralateral olivocochlear function, we also wanted to establish a simple screening method which can be applied to every experimental animal prior to more complex experiments. By applying scalp auditory brainstem recordings (ABR) and electrocochleography (ECoG) close to the round window we panoramically recorded electrical responses to broadband ipsilateral stimuli of the inner ear, auditory nerve and auditory brainstem.

We compared responses to ipsilateral clicks (0.1ms duration, alternating polarity; 0-90dB SPL) with responses to ipsilateral clicks preceded by contralateral noise bursts (50ms, 70dB SPL rms, 0.2-20kHz bandpass fil-

tered, 1ms cosine ramped). As a control we used contralateral noise bursts alone. We found that contralateral acoustic stimulation indeed reduces and delays early ABR waves (waves I/II) as well as the N1/N2 of the compound action potential. A reduced amplitude of the summating potential was also observed. Surprisingly, cochlear microphonic oscillations triggered by the click stimulus appeared more distinct after contralateral acoustic stimulation in some animals. Furthermore we found, that ABR waves attributed to structures in the auditory brainstem (waves III-V) were also reduced and delayed despite several reports of an excitatory effect of central cholinergic signaling in the auditory brainstem. In general, an increase of click ABR thresholds of more than 10dB SPL was observed, confirming a broad reduction of acoustic sensitivity upon contralateral acoustic stimulation in the Mongolian gerbil.

Hair Cell Injury and Repair in Hearing Loss from Mechanical Trauma

SYMP 78

Ca2+ homeostasis in cochlear outer hair cells

Robert Fettiplace
University of Wisconsin-Madison

Ca2+ enters cochlear hair cells via mechanoelectrical transducer (MET) channels in the hair bundle and voltage-dependent calcium channels in the basolateral membrane. The divalent ion is buffered in the cytoplasm by millimolar amounts of calcium-binding proteins such as oncomodulin and calbindin D28k (Hackney et al. 2005), and is extruded by PMCA2a calcium ATPase pumps concentrated in the stereocilia (Dumont et al 2001). Under physiological circumstances, 50 percent of the MET channels are open at rest in apical outer hair cells (OHCs), corresponding to a maintained Ca2+ load of as much as 4 pA. The current, although small, is significant because it flows into a tiny stereociliary compartment. The established PMCA2 density and pumping rate are predicted to extrude 20 pA of Ca2+ current, adequate to maintain homeostasis in apical OHCs (Beurg et al. 2010). However, the process may be marginal in basal high-frequency OHCs, where the MET currents are several-fold larger in amplitude (Johnson et al 2011), and the stereociliary volume is less than in apical OHCs. With strong acoustic stimulation, the larger Ca2+ load in basal OHCs might exceed the extrusion capacity of the PMCA2a pumps (Chen et al. 2012). In support of this notion, PMCA2 mutations with diminished pumping capacity, such as Oblivion and Tommy, cause progressive hearing loss (Mammano, 2011), beginning in basal OHCs. In IHCs, less than five percent of MET channels are open at rest which will reduce the steady Ca2+ load and make them less vulnerable. We suggest that Ca2+ overload may contribute to the greater ototoxic susceptibility of basal OHCs.

SYMP 79

Stereocilia bundle repair in mechanically damaged mammalian auditory hair cells

Gregory Frolenkov[1]; Jonathan Grossheim[1]; Ruben Stepanyan[2]; Mary Freeman[1]; A. Catalina Velez-Ortega[3]
[1]Dept. Physiology, Univ. Kentucky; [2]Dept. Physiology, Univ. Kentucky; Dept. Otolaryngology, Case Western Reserve University; [3]Department of Physiology, University of Kentucky

Damage to the stereocilia bundles of auditory hair cells has been known as a hallmark of noise-induced hearing loss for decades. Yet, it is still unclear what exactly is damaged in the bundle and whether the hair cell can repair these damages. Here we investigated the effects of intense (>1 um) stereocilia deflections on the mechano-electrical transduction (MET) current and stereocilia ultrastructure in the inner hair cells (IHCs) of organ of Corti explants. Three major effects were found: i) the loss of hair bundle stiffness similar to the one reported by Jim Saunders and co-authors in 1986; ii) a reduction of the MET current amplitude; and iii) a surprisingly dramatic reduction of the resting open probability of the MET channels.

Transmission electron microscopy (TEM) demonstrated that the overstimulation-induced changes in bundle stiffness may be attributed to sub-micron breaks in the actin core of stereocilia. These breaks were formed mostly at the base of the stereocilium, the site of the largest bending forces. Similar breaks were found in stereocilia of young adult (P18) mice exposed to white noise (100 dB SPL for 30 min), confirming that the observed effects of the in vitro overstimulation faithfully recapitulate the effects of noise trauma in vivo. In vitro, the actin core breaks partially recover within 24 hours, indicating an endogenous repair mechanism, which may involve gamma actin that accumulates selectively in the actin core gaps (Belyantseva et al., 2009). When the damage is unrepairable, it may result in calpain-dependent cytoskeleton disassembly. In correspondence with the latter hypothesis, we also found that the overexpression of calpastatin, an endogenous inhibitor of calpains, ameliorates permanent noise-induced hearing loss. To clarify the mechanism for MET current decrease after mechanical overstimulation, we imaged the IHC bundles with scanning electron microscopy (SEM) and found a proportional loss of tip links. Ultrastructural examination of the overstimulated IHC bundles also revealed the signs of the recently discovered MET current-dependent remodeling of the stereocilia actin core (Vélez-Ortega et al., 2017), indicating a potential mechanism for recovery of the resting open probability of the MET channels.

Thus, mammalian auditory hair cells show a remarkable ability for self-repair of mechanically-induced damages. These largely uninvestigated processes may determine whether noise-induced temporary hearing loss progresses into permanent hearing loss.

SYMP 80

Mechanisms of blast-induced hair cell trauma

John S. Oghalai
University of Southern California

Blast trauma is a frequent mechanism of injury to military personnel. We have fabricated a blast chamber to create pressure waves like an improvised explosive device and developed a reproducible mouse model to study blast- induced hearing loss. Using optical coherence tomography, we performed live cochlear imaging in vivo to dynamically assess cochlear morphology after blast trauma. Furthermore, we used genetic mouse mutants to alter cochlear physiology in targeted ways. Here, we will discuss how these studies have provided new insight into the mechanisms of injury after blast exposure that result in changes to hair cell morphology, physiology, and innervation.

SYMP 81

Time to hear: Glucocorticoid-dependent inflammation is regulating circadian sensitivity to noise exposure.

Barbara Canlon
Karolinska Institutet

The cochlea has been shown to contain a self-sustained circadian clock that regulates differential sensitivity to noise exposure throughout the day. Animals exposed to noise during the night are more vulnerable than when exposed during the day. Our findings support the notion that circulating glucocorticoids (GCs), which are highly controlled by circadian mechanisms, are regulating the day/night sensitivity to noise trauma. Surgical removal of adrenal glands (adrenalectomy, ADX) depleted the circulating glucocorticoids and allowed mice to completely recover from night noise trauma. To evaluate the circadian regulation of the cochlear transcriptome by GCs, we used a computational algorithm that allows the clustering of genes depending on their rhythmic or constant patterns of expression. Five models with distinct rhythmic patterns and phase specificity were generated. Model 1 is composed of genes that are non-rhythmic in ADX and sham conditions (7174 genes); model 2 is composed of non-rhythmic genes in sham cochleae that gained rhythmicity after ADX (455 genes); model 3 identifies rhythmic genes in both ADX and sham conditions (5941 genes); model 4 consists of genes with altered rhythmicity after ADX (129 genes); model 5 consists of rhythmic genes that lost their rhythmicity in ADX conditions (1141 genes). Gene expression of these models illustrated by heat maps show 22.5% of rhythmic genes being under the influence of GCs. Genes involved in the differential circadian regulation of noise sensitivity are predicted to appear in model 5, whereby the removal of circulating GCs leads to the loss of circadian transcription in the cochlea. The results from the GO analysis and the different models are showing a rise in expression of many pro-inflammatory signals at a time when noise sensitivity is increased at night. These findings are suggesting that the circadian response to noise trauma is driven by GC-dependent inflammatory processes and whose rhythmicity is abolished after removal of the adrenal glands by adrenalectomy (ADX). Finally, these findings reveal a novel pathway involving glucocorticoid-dependent inflammation that is likely contributing to the greater sensitivity of the afferent synapse to night noise. This work was supported by the Swedish Medical Research Council K2014-99X-22478-01-3, National Institute on Deafness and other Communication Disorders R21DC013172, Karolinska Institutet and the Tysta Skolan.

SYMP 82

Genetic regulators of the oxidative stress response and their roles in hearing after noise damage

Patricia White
Dept. of Neuroscience, University of Rochester School of Medicine

Long-lived cells, such as cochlear hair cells, must dynamically respond to a wide range of metabolic and oxidative stress. Certain genes that regulate cellular metabolism and the oxidative stress response have previously been implicated in age-related hearing loss. Here we present recent data investigating the roles of these regulators in the cochlear response to noise damage, by contrasting hearing function and anatomical structures in mutant mice and their wild-type littermates after exposure to a temporary-threshold shift-inducing noise. Surprisingly, we find differing requirements for these regulators in sustaining cochlear structures and function, consistent with distinct roles in hearing preservation.

SYMP 83

A Cell Type-Specific Blueprint of the Molecular Changes Following Noise Exposure

Ronna Hertzano[1]; Beatrice Milon[2]; Sunayana Mitra[2]; Yoko Ogawa[2]; Alok Shetty[2]; Xiaoyu Zhang[3]; Didier Depireux[4]; Ran Elkon[5]
[1]University of Maryland School of Medicine, Baltimore, MD USA; [2]University of Maryland School of Medicine, Baltimore, MD, USA; [3]Department of Otorhinolaryngology, University of Maryland School of Medicine, Baltimore, MD 21201, USA; [4]Institute for Systems Research, University of Maryland College Park, MD, USA; [5]Department of Human Molecular Genetics and Biochemistry, Sackler School of Medicine, Tel Aviv University, Tel Aviv, Israel

Detailed understanding of the cell type-specific molecular changes that occur in the inner ear following noise exposure is necessary for the rational design of therapeutics to treat and prevent noise-induce hearing loss (NIHL). A barrier to studying the cell type-specific molecular changes in response to noise has been the challenge of obtaining cell type-specific RNA from adult mice. In adult mice, tissue dissociation is traumatic, thereby likely to induce molecular changes which could mask changes specific to the noise exposure. The RiboTag mouse, in the presence of Cre-recombinase, allows for cell type-specific pulldown of translated mRNA (translatome), by marking the 60S ribosome subunit with a hemagglutinin (HA) tag. Importantly, as the mRNA is pulled-down from intact tissues, this approach avoids molecular changes induced by the stress of tissue dissociation. Here we crossed RiboTag mice with either Prestin(CreERT2) or Sox2(CreERT2) mice to allow for transcript pulldown from the outer hair cells and supporting/glia cells, respectively. At 10 week-of age, these mice were exposed to 94 or 105 dB SPL, 8-16 kHz octave band noise, for two hours, to induce a temporary or permanent threshold shifts, respectively. Cochleae were procured at baseline, 6 hours, and 24 hours after noise exposure. Gene expression from both whole cochleae as well as cell type-enriched immunoprecipitated (IP) mRNA was measured with RNAseq. We report our cell type-specific analysis of the molecular changes following these two types of noise exposure.

Auditory Cortex or Speech: Developmental, Comparative & Clinical

PS 831

Use of Speech Evoked Response Potentials to Assess Infant Speech Discrimination

Kristin Uhler[1]; Sharon Hunter[1]; Phillip Gilley[2]
[1]University of Colorado; [2]University of Colorado Boulder

Clinical Assessment of infant speech perception, under 5 months of age is greatly limited. However, for infants with hearing loss, knowledge of speech discrimination abilities with hearing aids could shape habilitation efforts. We compared two non-invasive speech evoked response potentials mismatch response (MMR) and acoustic change complex (ACC) to assess speech discrimination in infants.

Continuous EEG was recorded during sleep from 48 normally hearing infants aged 1.77 to 4.57 months (mean=2.96, s.d.=0.85; 28 male, 20 female). In an ACC task, two naturally produced vowels, /a/ and /i/, were presented in trials consisting of a three-vowel sequence (/i/-/a/-/i/). In an MMR task, the standard trials consisted of the /a/ vowel with a 15% probability of a deviant trial, the /i/ vowel. These comparisons were complete for two epochs short (-500-1500 ms) and long (-2.006 to 2.5 sec). A series of permutation t-tests (n-perms=10001, corrected for multiple comparisons using the false discovery rate) were used to assess differences between responses from each stimulus presentation at both the group level (comparisons of mean responses) and individual level (comparisons across trials).

ACC analyses only revealed significant differences from the offset to onset of the stimuli, but no defenses were observed to a change in speech stimuli for at the individual level and or group level. MMR/N analyses in revealed all participants with significant differences (p

Inconsistent ACC responses with no significant group-level differences highlight the limitation of the ACC as a biomarker of speech discrimination, at least in very young, sleeping infants. The positive findings from the MMR/N analyses suggest that these responses may prove useful for assessing an infant';s access to acoustic information necessary for the development of speech discrimination abilities.

PS 832

The Relationship Between Infant Speech Discrimination and Hearing Aid Signal Processing

Kristin Uhler[1]; Paige Mowery[2]; Melinda Anderson[1]
[1]University of Colorado; [2]University of Colorado Boulder

Current infant hearing aid (HA) fitting protocols are based on assuring audibility, and depend to a large extent on the evidence base drawn from older children and adults. In older children and adults, it has been established that HA signal processing, such as nonlinear frequency compression and wide dynamic range compression, affects a listener';s ability to discriminate speech sounds. However, a fundamental gap exists in the knowledge surrounding the impact of these HA settings on infant speech discrimina-

tion. These processing manipulations impact the temporal envelope (TE), as well as the temporal fine structure (TFS), of the original speech. Cabrera and Werner (2017) reported that adults and infants utilize TE and TFS cues differently. While it is clear that infants are able to utilize TE and TFS, it is not clear how these abilities relate to speech discrimination for hearing-aid-processed speech for this group. To examine this relationship, we related characteristics of the acoustic output of a hearing aid to performance on a behavioral speech discrimination task.

Subjects included 17 infants (age M=12 months; SD=5.81months), who used bilateral hearing aids. Visual Reinforcement Infant Speech Discrimination (VRISD) was used to assess infant speech discrimination of two speech contrasts (/a-i/ and /ba-da/). The acoustic analysis used the cumulative signal processing output with personal HA settings for the studied contrasts and quantified the amount of signal manipulation. The acoustic analysis of the personal HA settings was completed using two techniques. First, we established the output levels of the hearing aids for the VRISD contrasts for each presentation level (50, 60, 70 dBA). Second, we calculated the amount of cumulative distortion in the output of the HAs using a cepstral correlation technique.

The results indicate that the amount of audibility and the amount of signal modification may impact the discrimination abilities of infants with hearing loss. The relationship between audibility of /a-i/ is more significant than for /ba-da/, but there is a stronger relationship between ability to discriminate /ba-da/ and the amount of signal modification. Developing a better understanding of the relationship between hearing aid processing and speech discrimination in infancy will, overtime, allow us to broaden our knowledge base in this population. The increase in scientific literature has the potential to enhance our ability to fine tune hearing aid (HA) settings, making intervention more effective for infants with hearing loss.

PS 833

Speech processing, cortical activation and functional connectivity in children with and without listening difficulties: An MRI study

Hannah J. Stewart[1]; Scott K. Holland[1]; Thomas Maloney[1]; Nicholette Sloat[1]; Audrey Perdew[1]; Lisa L. Hunter[2]; Jennifer Vannest[1]; David R. Moore[1]
[1]Cincinnati Children's Hospital; [2]Cincinnati Children's Hospital and University of Cincinnati

Despite passing standard audiological testing, at least 5% of children experience listening difficulties (LiD), particularly in noisy conditions. As part of a larger project assessing the contribution of sensory, cognitive and linguistic processing to LiD, we investigated activation and connectivity of previously identified cortical hearing and speech areas. We predicted that children with LiD will have impaired activation and transmission within speech networks.

Ninety-two children (46 with LiD and 46 age-matched typically developing, TD; 6-14y.o.) have now completed a battery of MRI scans (3T Philips Ingenia). For functional MRI, Bamford-Kowal-Bench (BKB) sentences were presented to children in the scanner either as clear, spectrally rotated, or vocoded and rotated stimuli in the context of a simple discrimination game ("Was the talker a human or an alien"?). The planned contrasts between the three sentence types break down the skills required to listen to and comprehend language: intelligibility (intelligible vs. rotated sentences), speech (intelligible vs. rotated/vocoded sentences) and phonology (rotated vs. rotated/vocoded sentences). Listening and cognitive abilities were assessed respectively by the ECLiPS parent report questionnaire and the NIH cognition Toolbox battery. Preliminary results (n=61) show that the two groups were as fast and as accurate as one another processing intonation, phonetic and intelligibility features. However brain activation (with age and gender as covariates) suggests that children with LiD process intonation and phonetic, but not intelligibility features of speech similarly to TD children. For intelligibility, activation of the left paracingulate gyrus, a designated region of interest associated with theory of mind, was strongly related to listening (r(61) = -0.58, p < .01) and cognitive ability (r(61) = -0.37, p < .01).

Preliminary voxel-based morphometry showed that the children with LiD did not differ in brain structure from children without LiD. Resting state functional connectivity was used to examine the pathways that carry speech-related neural information from the auditory cortex to speech processing areas. Regions of interest (ROIs) in the frontal-parietal networks associated with auditory and language comprehension and production were selected using a meta-analysis of 528 published studies using the search term 'speech'; in Neurosynth. ROIs include the anterior and posterior superior temporal gyrus (bilateral), Broca';s area, planum temporale (bilateral) and supplementary motor area. Initial results show no significant differences in ROI-to-ROI connectivity between children with and without LiD. We plan to further assess attention and executive systems to examine whether these networks relate to these children';s listening and speech recognition abilities.

PS 834

A Novel Method of Measuring Phoneme Discrimination Using Pupillary Dilation Response

Keanu Shadron; Avinash Bala; Terry Takahashi
University of Oregon

Infants are tested for hearing impairments using multiple age-specific physiological and behavioral assays. These tests, however, cannot address language development due to time or efficacy constraints. Here we present a novel method of measuring phoneme discrimination using a subject';s pupillary dilation response (PDR), which has the potential use as a language development screen in infants. Sound-elicited PDR is an orienting response that habituates in response to repeated presentations of a given sound. Once habituated, the response recovers when presented novel sounds, allowing for a non-invasive measure of discrimination. In this pilot study with adult subjects, cameras recorded dilations evoked by habituating (/ba/) and oddball (/pa/) phonemes, while subjects recorded their precepts using a two-choice button press task. We found that dilations in response to habituating and oddball trials were significantly different. The non-invasiveness and speed of the test suggest that a PDR-based phoneme discrimination task may be useful in testing infant and toddler auditory perception.

PS 835

Relationships between listening skills and the brainstem response to speech in individuals at-risk for Central Auditory Processing Disorder

Rupa Balachandran; **Mateel Musallam**; Griffin Talan; Gabriella Musacchia
Department of Audiology, University of the Pacific

People with difficulties in processing auditory information are part of a heterogeneous group with multiple underlying and interconnected deficits. Difficulty processing speech in noise can result from, expressive and receptive language deficits, attention deficits, auditory processing deficits, and sensory integration deficits. Individuals who exhibit these problems are not always identified with typical tests of auditory processing. The speech-evoked, complex Auditory Brainstem Response (cABR), appears to be a promising "non-traditional" method to test this hypothesis because ample research has shown it to be an objective and reliable measure of encoding deficits in quiet and background noise. Additionally, the Auditory Processing Domains Questionnaire (APDQ) has recently been developed and validated to differentiate between populations with underlying problems of processing speech in the background noise. In the current study, we administered these two tests, in addition to standard tests, to 19 individuals who were referred for CAPD assessment. Our results showed that lower APDQ scores were correlated with delayed brainstem response latencies and weaker encoding of the speech fundamental frequency in noise. Individuals who had below average brainstem response measures performed 20-30% worse on Auditory Processing and Language portions of the APDQ than those with above average brainstem responses. Brainstem responses did not differ between CAPD+ and CAPD- groups and APDQ scores were significantly lower in the CAPD+ group, however no difference was observed between CAPD+/- groups on the standard protocol tests. This suggests that a subset of individuals who struggle with auditory information have concurrent deficits encoding speech sounds, especially in noise. People who have these difficulties may be missed by current evaluative methods. The data presented here suggest that electro-physiological tests of neuronal synchrony can assist in understanding the deficit diaspora of an individual at-risk for CAPD.

PS 836

Masked sentence recognition in children, young adults, and older adults: Age-dependent effects of semantic context and masker type

Emily Buss[1]; Sarah Hodge[2]; Lauren Calandruccio[3]; Lori J. Leibold[4]; John Grose[2]
[1]University of North Carolina - Chapel Hill; [2]UNC School of Medicine; [3]Case Western Reserve University; [4]Boys Town National Research Hospital

Purpose
Masked speech recognition in normal-hearing listeners depends on both listener age and masker type. Children and older adults are more susceptible to masking than young adults, particularly when the masker is speech. Semantic context has been shown to facilitate noise-masked sentence recognition in all age groups, but it not known whether age affects a listener';s ability to use context with a speech masker. The purpose of this study was to compare effects of masker type and target context as a function of age for listeners with normal hearing.

Method
Listeners were children (5-11 yrs), young adults (19-29 yrs), and older adults (67-81 yrs), all with normal or near-normal hearing. The task was to repeat target sentences presented either in speech-shaped noise or a two-talker masker. Target sentences were either semantically correct (high context) or semantically anomalous (low context). The masker was presented at 60 dB SPL, and the target level was adjusted adaptively to estimate the speech reception threshold (SRT).

Results

SRTs were lower for young adults than either children or older adults. Control conditions using low-pass filtered speech indicated that the poorer performance of older adults was not due to reduced high-frequency audibility. Age effects were more pronounced for the two-talker masker than the noise masker. Performance tended to be better for targets with high than low semantic context. The one exception was for young children tested in the two-talker masker, where little or no effect of semantic context was observed.

Conclusion

Both masker type and target context impact speech perception, with different effects observed at different points across the lifespan. While the two-talker masker was particularly challenging for both children and older adults, the speech masker appears to limit the use of target semantic context only in young children. Children';s inability to capitalize on context in a two-talker masker could reflect the greater cognitive demands associated with this listening condition; older adults'; use of context may require fewer cognitive resources due to their more extensive linguistic knowledge and life experience.

PS 837

Rapid changes in cortical evoked responses in a large cohort of children receiving cochlear implants bilaterally

Leticia Vicente[1]; Melissa J. Polonenko[2]; Stephanie Jewell[3]; Blake Papsin[2]; Karen Gordon[2]
[1]*University of San Paulo, Bauru Campus; The Hospital for Sick Children; [2]The University of Toronto; The Hospital for Sick Children; [3]The Hospital for Sick Children*

Objective

To evaluate cortical auditory asymmetries within the first 3 years of bilateral cochlear implant (CI) use in children.

Background

Multi-channel cortical responses have shown that early bilateral input through simultaneous implantation prevents the cortical reorganization that occurs with prolonged unilateral CI use in children who receive two implants sequentially. It may be possible to track some degree of cortical auditory development promoted by bilateral CIs using a more limited and clinically applicable electrode montage.

Methods

Electrically-evoked cortical responses were recorded in 86 children who received bilateral CIs simultaneously at age 3.12±3.72 years and in 112 children who received their first implant at 2.95±2.78 years and second implant after 3.95±2.76 years. Biphasic electrical pulse trains lasting 36 ms were presented at 1 Hz and delivered via an apical electrode. Two-channel responses were recorded from a surface electrode (Cz) referenced to each earlobe at multiple times post-bilateral implantation: ~1 week and 1, 6, 12, 18, 24 and 36 months. Area differences between unilateral and bilateral cortical responses were calculated from 44-200 ms and 200-400 ms latency for each time point and compared using mixed effects regression.

Results

In the simultaneously implanted group, right and left CIs evoked responses were similar but these unilateral responses differed from the bilateral response at initial bilateral CI use. This difference rapidly decreased by one month of bilateral CI use although the bilateral response remained slightly larger than either unilateral responses over the next 3 years. By contrast, the sequential group exhibited large asymmetries between the unilateral responses at second CI activation. These differences rapidly decreased over the first month of bilateral CI use but remained present around 200-400 ms even after 3 years. The bilateral response in the sequentially implanted group was initially more similar to that of the first implant in the 44-200 ms range but more similar to that of the second implant in the 200-400 ms range. Area difference between these conditions also decreased within one month, with changes beyond that occurring slightly over time. Differences between bilateral and unilateral responses remained in the 200-400 ms range after 3 years in this group.

Conclusions

Auditory cortical responses recorded from the midline of the head show large changes within the first month of bilateral CI use but limited differences thereafter. This suggests that a limited electrode montage may be most useful at identifying early and large effects of bilateral cochlear implantation in children.

PS 838

Rates of Neural Recovery and Speech Perception in Children with Auditory Neuropathy Spectrum Disorder and Sensorineural Hearing Loss

Rachael M. Jocewicz[1]; Sara M. Misurelli[1]; Christina L. Runge[2]; Ruth Y. Litovsky[3]
[1]*Waisman Center, University of Wisconsin-Madison; [2]Medical College of Wisconsin; [3]University of Wisconsin-Madison*

For children with auditory neuropathy spectrum disorder (ANSD) who do not benefit from hearing aids, co-

chlear implants (CIs) may be an option. However, there is need for evidence as to whether children with ANSD who received CIs perform similarly to their peers with sensorineural hearing loss (SNHL) who also use CIs. A hallmark of ANSD is underlying temporal auditory processing impairment. The purpose of this study was to investigate children with CIs who have ANSD or SNHL on two sets of measures: (1) temporal response from the auditory nerve, and (2) speech understanding in noise.

Children ages 6-16yrs with CIs participated (n=7 ANSD, n=7 SNHL). Participants in each group were matched for age, listening experience, and device manufacturer. All children with ANSD were bilateral CI users; in the SNHL group 5 children had bilateral CIs, 1 child used bimodal hearing, and 1 child had a unilateral CI. Speech recognition thresholds (SRTs) were assessed via an adaptive listening paradigm. Temporal recovery functions were obtained by presenting a masker and probe pulse to a medial electrode on the CI and varying the length of the inter-pulse-interval (IPI) via CI software specific to each manufacturer. A recovery constant value was obtained by fitting the function to an exponential, non-linear, regression curve. For the speech understanding measures target speech was presented from a loudspeaker at 0° azimuth, in three conditions: (1) quiet, bilateral; (2) 2-talker babble co-located with the target, bilateral; (3) quiet, unilateral with right ear; (4) quiet, unilateral with left ear.

Results thus far show that while high variability exists between individual children, on average, children with CIs who have ANSD or SNHL perform similarly when listening to speech in quiet (mean SRT=36dB) and in babble (mean SRT=58dB). Both groups also demonstrate comparable amounts of spatial release from masking (22 dB, difference between conditions 1 and 2), and show little advantage of bilateral summation (2.7 dB, difference between the average of conditions 3/4 and 1). In addition, the average recovery constant was slightly lower in the ANSD group (0.38 milliseconds) than the SNHL group (0.44 milliseconds). Further analyses of behavioral and objective data may reveal information regarding individual variability and possible relationships between the behavioral and objective measures.

PS 839

Tinnitus and cortical tonotopic maps

Elouise Koops[1]; Remco Renken[2]; Cris Lanting[2]; Pim van Dijk[3]
[1]Department of Otorhinolaryngology, University Medical Center Groningen, Netherlands; [2]University of Groningen; [3]Department of Otorhinolaryngology, University Medical Center Groningen, The Netherlands

Introduction

Clinical hearing loss, associated with neural plasticity, increases the chances of developing tinnitus, the perception of a sound in the absence of an external source. The specific plastic changes that are involved in tinnitus remain elusive. A striking feature of the auditory cortex is its tonotopic organization. Several studies have suggested a relation between hearing-loss-induced tonotopic reorganization and tinnitus. However, recent research has shown that the tonotopic organisation of tinnitus patients without hearing loss is not significantly different from that of normal hearing participants without tinnitus (Langers et al. 2012). We now focus on tinnitus patients with high-frequency sensorineural hearing loss to determine if any characteristics in the tonotopic maps are detectable that can be attributed to tinnitus.

Methods

In this study we use functional magnetic resonance imaging (fMRI) to gain insight in the association between tonotopic reorganization, hearing loss and tinnitus. In particular, we look into the changes of the tonotopic maps as a consequence of tinnitus and hearing loss. Three groups of participants were included: a tinnitus and hearing loss group, a hearing loss only group and a normal hearing control group. Pure tone stimuli were presented in the MRI scanner as the attention of participants was controlled by a non-related visual task. The loudness of the stimuli was matched across frequencies, within each participant.

Results

A preliminary analysis showed that tonotopic maps of the bilateral auditory cortices could be created, with opposing frequency gradients high-low-high in the posterior to anterior direction.

Conclusion

Tonotopic maps in hearing impaired participants with and without tinnitus, respectively, were similar to those observed in normal hearing subjects (e.g. Langers et al 2012). Further analysis will show whether maps differ between the participant groups.

PS 840

How can we reliably detect hearing loss induced cortical tonotopic reorganisation in humans?

Benjamin J. Gurer[1]; Susan T. Francis[2]; Deborah A. Hall[3]; Denis Schluppeck[4]; Julien Besle[5]; Katrin Krumbholz[1]
[1]Medical Research Council Institute of Hearing Research, School of Medicine, The University of Nottingham; [2]Sir Peter Mansfield Magnetic Resonance

Centre, School of Physics and Astronomy, University of Nottingham; [3]National Institute for Health Research Nottingham Biomedical Research Centre; [4]School of Psychology, The University of Nottingham; [5]Department of Psychology, American University of Beirut

Peripheral hearing loss (HL) not only causes reduction in hearing sensitivity (increase in hearing threshold), but also leads to problems in suprathreshold hearing such as difficulty understanding speech in noise and is also often associated with tinnitus. Animal research has suggested that such impairments may be related to changes in central auditory processing arising as a consequence of reduction in peripheral auditory output (Noreña & Farley, 2013). In animals, peripheral HL has been shown to cause large-scale tonotopic reorganisation in auditory cortex, whereby neurons responsive to frequencies affected by the HL (typically higher frequencies), shift their tuning towards less affected (lower) frequencies.

Cortical frequency tuning properties can now be assessed non-invasively in humans using functional magnetic resonance imaging (fMRI). For that, fMRI responses are recorded to sounds with a wide range of frequencies and, from these, local preferred frequencies and tuning widths are estimated. In HL, this estimation is potentially biased, because responses to frequencies affected by the HL should be reduced, thus skewing the shape of the measured frequency response functions. Here we evaluate a method to correct for this bias.

We simulated high-frequency HL in 8 normal-hearing controls using threshold-elevating noise. Cortical frequency tuning properties were estimated using "population receptive field" (pRF) modelling – a technique similar to methods for estimating tuning properties from neurophysiological data, which was first developed in the visual domain (Dumoulin & Wandell, 2008). Here, we modified the technique to take account of the simulated HL. By applying both the modified and unmodified pRF methods to data obtained both with and without HL simulation, we show (i) that using the unmodified method for HL data results in expected biases in preferred frequency and tuning width estimates, and (ii) that the modified method eliminates theses biases and results in similar tonotopic maps as for normal-hearing data. These results represent a key step towards studying the effects of HL on tonotopic organisation in human auditory cortex using BOLD fMRI, and understanding their potential perceptual consequences.

References

Dumoulin, S. O., & Wandell, B. A. (2008). Population receptive field estimates in human visual cortex. NeuroImage, 39, 647–660. http://doi.org/10.1016/j.neuroim-age.2007.09.034

Noreña, A. J., & Farley, B. J. (2013). Tinnitus-related neural activity: Theories of generation, propagation, and centralization. Hearing Research, 295, 161–171. http://doi.org/10.1016/j.heares.2012.09.010

PS 841

Optimising Detection of Subcortical Auditory Structure and Function Using MRI

Rebecca S. Dewey[1]; Deborah A. Hall[2]; Hannah Guest[3]; Garreth Prendergast[4]; Christopher J. Plack[4]; Susan T. Francis[5]
[1]*University of Nottingham;* [2]*National Institute for Health Research Nottingham Biomedical Research Centre;* [3]*Manchester Centre for Audiology and Deafness, University of Manchester;* [4]*University of Manchester;* [5]*Sir Peter Mansfield Magnetic Resonance Centre, School of Physics and Astronomy, University of Nottingham*

A current focus of auditory neuroscience concerns the physiological mechanisms that may underlie hidden hearing loss. Permanent noise-induced damage to hair-cell synapses for high threshold auditory nerve fibres, apparent as changes in the ascending auditory system, has been demonstrated following noise exposure in several mammalian species. It is as yet unclear whether or not similar patterns of altered responses can also be detected in humans. As such, we are conducting a study to assess the link between lifetime noise exposure and subcortical functional magnetic resonance imaging (fMRI) responses to auditory stimulation to determine:

which neuroimaging measures in the human central auditory system are associated with hidden hearing loss, and

whether these measures are also associated with tinnitus or hyperacusis.

Nuisance factors, such as EPI (echo planar image) distortion and physiological noise resulting from cardiac and breathing activity, make it difficult to locate fMRI responses within subcortical structures in an individual subject at 3.0 T. To ensure high quality fMRI data, optimisation of the image processing and statistical analysis pipeline is crucial. We report the optimum acquisition methods for subcortical fMRI of the ascending auditory pathway and assess the individual effects of each image processing step undertaken.

Structural and functional MRI data were collected on a Philips Ingenia 3.0 T MR scanner (Philips Medical Sys-

tems, The Netherlands) with a 32-channel head coil. Stimuli consisting of 24-seconds of broadband noise followed by a 42-second rest period were presented using the OptoACTIVE Optical MRI Communication System (Optoacoustics Ltd., Israel) system during active noise cancellation. Image analysis was performed using FSL (FMRIB Software Library) version 5, SPM12, and software toolboxes coded in Matlab. We evaluate the impact on the fMRI response of image processing steps to correct for (i) image distortion due to the EPI readout used, and (ii) physiological noise resulting in cardiac and respiratory artefacts. Statistical analyses were performed using a general linear model including motion parameters, and white matter and cerebrospinal fluid (CSF) noise regressors as covariates of no interest. We present findings from this optimisation procedure.

The overall aim of our MRC-funded programme is to understand the damage to the human auditory system that results from cumulative lifetime noise exposure, focussing on exploring behavioural and neuroimaging techniques for detecting and diagnosing hidden hearing loss.

PS 842

Electrophysiological Measurement of Auditory Cognition in Veterans with Blast-Exposure: Results of a P300 Go/No-Go Paradigm

Melissa Papesh[1]; Kelly Hanscom[2]; Curtis J. Billings[3]; Frederick Gallun[1]
[1]VA RR&D NCRAR; [2]University of Maryland, College Park; [3]VA RR&D National Center for Rehabilitative Auditory Research (NCRAR)

Military Veterans who have been exposed to high-intensity blast waves often experience both cognitive and auditory difficulties that persist long after the blast incident. These symptoms may be related in that auditory impairments place a greater demand on cognitive resources, while diminished cognitive resources impair a patient's ability to attend to desirable sound sources inhibit neural response to competing stimuli. To further explore this relationship, we used an electrophysiological P300 oddball Go/No-go paradigm and tested two groups of normally-hearing participants: those who had been exposed to a high-intensity blast since 2001 and a group of age- and hearing-matched control participants. During "go" trials, participants were instructed to press a response button only when they heard a rare high-pitched tone (1000 Hz tone presented during 20% of trials) in a sequence of low-pitched tones (500 Hz tone

presented during 80% of trials). This condition assesses participants' neural response to a change in the stimulus train and requires minimal cognitive effort. We hypothesized that neural responses to the rare stimulus measured in blast-exposed participants would be less robust compared to control participants, reflecting poorer auditory discrimination in blast-exposed participants. During the "No-go" trials, participants were instructed to press a response button following each presentation of a low-pitched tone but to suppress response to the rare high-pitched tones. The No-Go condition requires the ability to discriminate a change in the stimulus train, but also demands greater cognitive effort to suppress the conditioned button-press response to infrequent (high-pitch) stimulus presentations. We hypothesized the following results: 1). the neural response to rare stimuli be less robust in blast-exposed compared control participants, and 2). that group differences would be larger in the No-Go condition than in the Go condition, reflecting both poorer auditory processing and reduced cognitive control among blast-exposed participants. Preliminary data from 12 blast-exposed individuals and seven control participants support these hypotheses, and reveals that neural responses to the P300 No-go condition are well-correlated with self-perceived auditory deficits. Overall, this work supports the following conclusions: 1. Not only can auditory discrimination be impaired by exposure to high-intensity blasts, but that the addition of cognitive stress impairs these abilities even further, and 2. The No-go paradigm appears to tap into perceived auditory dysfunction more than the traditional oddball Go paradigm. The results of this study will be further discussed including the relationships between the P300 Go/No-go responses and multiple behavioral measures of cognitive and auditory function.

PS 843

No evidence for anti-retroviral drug effects on gap test performance in HIV positive adults

Abigail Fellows[1]; Albert Magohe[2]; Jiang Gui[3]; Enica Massawe[4]; Ndeserua Moshi[4]; Jay Buckey[3]
[1]Space Medicine Innovations Laboratory, Geisel School of Medicine at Dartmouth, Hanover, NH, United States; [2]Muhimbili University of Health and Allied Sciences, Dar es Salaam, Tanzania; [3]Geisel School of Medicine at Dartmouth; [4]Muhimbili University for Health and Allied Sciences

Background
Growing evidence shows a relationship between HIV infection and central auditory processing deficits. In our previous cross-sectional study in Tanzania we demonstrated elevated gap detection thresholds in HIV+ adults on anti-retroviral therapy (ART), compared to HIV+ adults not yet on therapy. These findings could be re-

lated to ART, or they could be related to more central nervous system damage in those on ART compared to those who had not yet been treated. To receive ART, the ART+ adults had to have had disease severe enough to warrant ART treatment. The central auditory findings may be an indication that those in the ART+ group had more advanced or more symptomatic HIV infections at one time. We have been following a cohort of HIV+ subjects in Tanzania longitudinally and we hypothesized that gap detection thresholds would not increase after starting ART.

Methods
As part of an overall study following HIV+ patients longitudinally, we had 96 HIV+ adults (68 women, 28 men, average age 39 at first visit) who began ART while they were being followed. They had an auditory evaluation including gap detection testing at each visit. Visits were scheduled for 6 month intervals, but the number and spacing of follow up visits varied. A linear model with gap threshold as the response variable and time in days as the predictor variable was fit to the data both before and after starting ART.

Results
A comparison of the 2 models showed a significant difference between pre and post ART models ($p<0.001$) indicating that the gap detection vs. time relationship changed after starting ART. Before starting ART the slope of the gap threshold vs. time line was not significantly different from zero. After starting ART, the slope had a tendency to be negative ($p=0.054$) indicating an improvement in gap detection scores with time while on ART.

Conclusions
Longitudinal data to date show no evidence for increased gap detection thresholds after starting ART. Instead there is a trend toward lower gap detection scores after ART initiation in this cohort. The elevated gap detection thresholds seen in the previous study may be related to the pre-ART severity of HIV infection, and not starting ART.

PS 844

Sex Differences in Behavioral Responses to the Four Main Categories of Mouse Vocalizations

Alexandra Niemczura[1]; Emily Hazlett[1]; Ahmad Alkhawaga[2]; Austin Poth[2]; Alyssa Carvalho[1]; Jeffrey Wenstrup[2]; Jasmine Grimsley[1]
[1]Northeast Ohio Medical University; [2]Northeast Ohio Medical University (NEOMED)

Adult mice emit four main categories of vocalizations: ultrasonic vocalizations (USV), mid-frequency vocaliza-tions (MFV), low-frequency harmonics (LFH), and noisy calls. Although we know how the proportion of each category emitted varies with context, the meaning of these categories to the listener remains unknown. Our goal is to determine the effect of these vocalizations on a listening mouse by assessing behaviors including fecal bolus quantity, locomotion, and vocal behavior during playback of the four categories of mouse vocalizations. Twenty-four sexually naïve adult CBA/CAJ mice (12m, 12f) were used in this study. Each animal underwent six 30-minute trials in an open-field arena: habituation, no-sound control, and 4 experimental trials (one for each vocalization category in a counterbalanced order). During experimental trials, 3 randomized exemplars of a single vocalization category were played for 20 minutes (80 dB SPL, 0.25 Hz).

In both male and female listeners, fecal bolus quantity was greater during playback of all vocalization categories than in the no-sound control trial ($F_{1,22} = 10.96$, $p < 0.05$), indicating that animals were aroused by all 4 categories of vocalizations. There was no interaction between sex and trial type for fecal bolus quantity ($F_{1,22} = 10.96$, $p > 0.05$), indicating that the amount of arousal evoked by each vocalization category does not depend on sex of the listener. Trial type and sex interact to affect distance traveled by the listener ($F_{1,22} = 3.04$, $p < 0.05$), supporting the hypothesis that different vocalization categories have different effects on locomotive behavior of the listener, depending on sex of the listener. Similarly, there was a 3-way interaction between sex, trial type, and category of vocalizations emitted by the listener on the duration of calls emitted ($F_{8,2492} = 2.01$, $p < 0.05$), indicating the trial type affects vocal behavior differently for males and females.

These preliminary data suggest that all vocalization categories are arousing to males and females, but their specific meaning varies depending on the sex of the listener. Greater understanding of what these vocalizations mean to the listener under baseline conditions will enable future investigations of altered auditory processing.

PS 845

Differential response of male and female mice to high-arousal mating vocal sequences

Zahra Ghasemahmad; Krish Nair; Austin Poth; Anthony Zampino; Sharad Shanbhag; Jeffrey Wenstrup
Northeast Ohio Medical University (NEOMED)

Introduction
Although studies have described the significance of mouse vocalizations from the sender';s perspective, fewer have investigated effects of these vocal signals

on the receiver. Here we identify acoustic features of vocal sequences associated with the most intense mating behaviors, then conduct playback experiments using exemplars of such vocal sequences to test behavioral responses of male and female mice.

Method
Mating vocalizations and behaviors of CBA/CaJ mice (n=16; ages p90-p180) were recorded. Vocalizations were divided into two categories: sequences emitted during mounting/head sniffing (high arousal) and vocalizations linked to less arousing aspects of the interaction. Several acoustic features of ultrasonic vocalizations (USVs) were analyzed, including syllable rate/type and spectrotemporal features. For playback, 10 exemplars of natural sequences of intermingled USVs and low frequency harmonics (LFH) linked to high arousal were presented. Both male and female mice (n=14) were used in behavioral tests; only females in estrous were included in the final analysis. Prior to testing, mice experienced mating and restraint in a counterbalanced order on consecutive days. On the test day, after 3-hour habituation, we video-recorded and analyzed 15 different behaviors before, during, and after stimulus presentation.

Results
Vocalization analysis: USVs emitted during high arousal were more complex and had more syllables with frequency jumps, harmonics and nonlinearities (p < 0.001). Further, dominant syllable types were significantly different in the higher arousal condition (more chevron and fewer flat USVs). During mounting/head sniffing, duration of syllables was significantly longer and inter syllable interval became shorter (mean=0.12, SD=0.09), resulting in emission of more syllables. Behavioral analysis: In response to playback of vocal sequences linked to high arousal, females decreased locomotion, adopted an alert posture and avoided the speaker after the sound onset; male mice increased exploratory behaviors (locomotion and rearing) in response to mating sequences and explored the speaker side more than females (p

Conclusion
The results demonstrate that the acoustic features of vocalizations during mating differ based on the intensity of the mating interaction. Thus, USVs linked to intense physical contact (mounting stage) are more complex and highly harmonic. Importantly, these sequences of vocalizations change the behavior of listening male and female mice, but do so in different ways consistent with their behaviors during mating: males are more exploratory, while females display reduced locomotion and more alert behavior. Overall, our findings show that mouse mating communication calls reflect the behavioral state of the sender and change the behavior of the listener.

CBA/CaJ Mouse Ultrasonic Vocalizations Depend on the Social Context

Kali Burke[1]; Laurel A. Screven[2]; Micheal L. Dent[3]
[1]University at Buffalo, SUNY; [2]University at Buffalo; [3]State University of New York at Buffalo

Mouse ultrasonic vocalizations (USVs) have variable spectrotemporal features, which researchers use to parse into different categories. USVs may be important for communication, but it is unclear whether the categories that researchers have developed are relevant to the mice. Instead, other properties such as the number, rate, peak frequency, or bandwidth of the calls may be what they are using to interpret the nature of the social interaction. To investigate this, we first must create a comprehensive catalog of the USVs that mice are producing across different social contexts. Forty male and female adult CBA/CaJ mice were recorded for five minutes following either a one-hour period of isolation or exposure to a same- or opposite-sex mouse. Vocalizations were extracted using Raven Pro, separated into nine categories, and quantified based on their bandwidth, duration, peak frequency, and the total number of calls. The sexual receptivity state of the females was controlled, such that all females were in the diestrus stage of their estrous cycle. Controlling the estrous cycles was essential in order to maximize the number of vocalizations that the females were producing and to control for any state dependent differences that fluctuations might cause in production by males. Results indicate that mice differentially produce their vocalizations across social encounters. There were significant differences in number, bandwidth, peak frequency, and duration of the calls they emitted when the mouse was alone compared to following a social exposure. Males and females both produce the most calls immediately following same sex exposures with the least vocalizations being produced following no exposure. Female mice produce calls with the largest bandwidth following opposite sex exposures, while males emit calls with the largest bandwidth following a period of isolation. Females on average produce calls with a higher overall peak frequency and longer duration than male mice across all conditions. This study shows that there are sex-specific differences in production of USVs in laboratory mice. It also provides important data about the effects of different types of social exposures on vocalizations in chronically socially isolated animals. Additionally, this study provides critical evidence that female mice produce calls, important since this is an often overlooked variable in mouse vocalization research. This work was supported by NIH DC012302.

PS 847

Spectral Modulation Depth Detection Predicts Spoken Language Abilities of Adolescents with Normal Hearing and Cochlear Implants

Susan Nittrouer; Joanna Lowenstein; Donal Sinex
University of Florida

Background
Good spectral processing is generally considered to be foundational to spoken language abilities, with two reasons being that it facilitates recovery of spectral cues to phoneme labeling and supports speech-in-noise recognition. Cochlear implants (CIs) interfere with spectral processing, a fact that probably helps to explain some of the poor spoken language abilities of listeners with CIs, particularly those with congenital hearing loss. Spectral modulation depth detection (SMDD) is a measure that has been investigated as a way to assess spectral processing and its relation to spoken language abilities, but mostly in post-lingually deaf adults. In this study, we measured SMDD both to assess spectral processing in normal-hearing (NH) adolescents and congenitally deaf adolescents who use CIs, and to predict abilities of these adolescents to: (1) attend to spectral cues to phoneme (fricative) labeling; (2) recognize speech in noise and quiet; (3) perform a phoneme awareness task; and (4) perform tasks of vocabulary and syntactic knowledge.

Method
14-year-old adolescents participated: 32 with NH and 22 with profound hearing loss who received CIs early in life. SMDD was measured with a 3-interval, forced-choice procedure in which two of the stimuli were unmodulated noises and one was a noise modulated at a rate of 0.5 ripples per octave. Modulation depth was manipulated in an adaptive manner to find the 70.7% threshold for modulation (SMDD). Measures were also obtained of: (1) attention to two spectral cues to syllable-initial fricative labeling (noise spectra and formant transitions); (2) speech recognition in noise and quiet; (3) phoneme awareness; and (4) vocabulary and syntactic knowledge.

Results
Compared to adolescents with NH, those with CIs had slightly larger mean SMDD thresholds, and: (1) reduced attention to both spectral cues to fricative labeling; (2) poorer speech recognition in noise and quiet; (3) poorer phoneme awareness; and (4) poorer vocabulary and syntactic knowledge. For adolescents with NH, SMDD thresholds were correlated with perceptual attention to spectral cues to fricative labeling, speech-in-noise recognition, and phoneme awareness. For children with CIs, SMDD thresholds were not correlated with perceptual attention to spectral cues to fricative labeling, but

were correlated with speech recognition in noise and quiet, and phoneme awareness. For neither group were SMDD thresholds correlated with vocabulary or syntactic knowledge.

Conclusions
SMDD is a sensitive measure of spectral processing for listeners with congenital hearing loss who use CIs that can predict sensitivity to phonemic structure and speech-recognition abilities, but not lexicosyntactic knowledge.

Table 1.docx

Table 2.docx

PS 848

Neural entrainment of the Speech Envelope in the Ageing Normal Hearing and Hearing Impaired Listeners

Lien Decruy; Jonas Vanthornhout; Tom Francart
KU Leuven - University of Leuven, Department of Neurosciences, ExpORL

Background
Given that the speech envelope is a primary cue for speech understanding, a measure of neural entrainment of the envelope, obtained from the EEG, can offer complementary information to behavioural speech audiometry. Indeed, Vanthornhout et al. (2017) found an increase in entrainment with increasing signal-to-noise ratio (SNR) in young normal hearing subjects. We investigated the effect of age and hearing loss on this method.

Methods
We recorded the EEG in 10 older (45-85 years) and 5 young normal hearing subjects (18-35 years). In addition to the normal hearing listeners, we also collected data of 3 older hearing impaired participants. In order to measure neural entrainment to the speech envelope in function of SNR, we trained a linear decoder to reconstruct the speech envelope from the EEG. Consequently, by correlating the reconstructed with the original envelope, entrainment was estimated. We presented two target stimuli spoken by female talkers: the Flemish Matrix sentences, to compare with behavioural speech audiometry, and audiobooks to resemble daily life speech. We used two maskers: speech weighted noise and a competing male talker, with the same long-term-average spectrum as the stimulus. Behavioural speech audiometry was administered during EEG recording.

Results
For all conditions, we found increased envelope entrainment with increasing SNR. Similar to Presacco et

al. (2016), neural entrainment to the speech envelope was higher in older normal hearing subjects compared to younger. As the behavioural speech understanding scores did not differ between age groups, these results indicate that older adults may need more cortical activation to perform in the same way. The results of the hearing impaired listeners will be presented.

Conclusions
There is a strong individual effect on neural envelope entrainment, depending on age. Therefore, the increase in entrainment with speech understanding only holds on an individual basis. Although ageing appears to induce the opposite effect, the results indicate that higher entrainment in older listeners can reflect an overactivation of the brain when trying to perform the same as the younger participants.

Acknowledgements

PS 849

Suppressing Auditory Background Speech: a Link to Auditory Hallucination in Schizophrenia

Pirazh Khorramshahi[1]; L Elliot Hong[2]; **Jonathan Z. Simon**[1]

[1]University of Maryland, College Park; [2]University of Maryland School of Medicine

Background
Schizophrenia is a severe brain disorder, where a hallmark symptom is auditory hallucination that is present in most patients sometime during the course of the illness. The origin of auditory hallucination may be a fundamentally a bottom-up problem, caused by erroneous processing of diverse external auditory inputs, or a top-down modulation problem, e.g., from attentional deficits or due to a failure to appropriately segregate/communicate internally-generated contents with the externally-oriented primary auditory pathway. This study uses magnetoencephalography (MEG) to investigate the latter hypothesis using a "cocktail-party" listening paradigm in which listeners attend to one speaker despite the interfering presence of another.

Methods
Subjects consisted of 24 schizophrenia patients (aged 21-61; 7 female), and 28 age- and sex-matched controls (aged 22-61; 8 female), all right-handed. Auditory hallucination (AH) was evaluated using the Psychotic Symptom Rating Scales - AH (PSYRATS-AH). During MEG scanning, participants listened to the stimuli which were 60 s duration segments of an audiobook story narrated by separate male and female speakers, digitally mixed into a single channel, and presented diotically. Subjects were instructed to listen to only one speaker at a time, and then asked to switch to the other speaker for the subsequent stimulus. Neural responses of each subject were transformed into corresponding Temporal Response Functions (TRFs), which characterize the auditory cortical processing of speech, both attended and unattended.

Results
As expected, TRFs were dominated by two peaks, the $M50_{TRF}$ and the $M100_{TRF}$ (speech-analogs of the tone-evoked M50/P1m and M100/N1m responses). Analysis focused on the $M100_{TRF}$, which is both larger and earlier for attended speech than unattended speech. This power enhancement of attended over unattended is significantly smaller for patients over controls (p=0.028); similarly, the latency difference is also significantly reduced for patients over controls (p=0.032). Additionally, within patients, the power enhancement of attended $M100_{TRF}$ over unattended is significantly correlated with AH score (r=0.557; p=0.0163).

Conclusion
The findings demonstrate significant cortical processing deficiencies in schizophrenia patents, in both power and latency measures, during the naturalistic task of listening to one speaker despite the presence of another. These neural deficiencies may underlie corresponding behavioral deficits in sustained attention and difficulty in appropriately segregating competing speech sources. In particular, a significant association was seen between the severity of auditory hallucination and a neural marker of the ability to distinguish and separate out conflicting auditory signals.

PS 850

Age effect on Cortical Auditory Evoked Potentials(CAEPs) elicited by vowels with the emotional salience.

Seungwan Lee[1]; Wondo Na[1]; Woojae Han[2]; Jinsook Kim[3]

[1]Department of Speech Pathology and Audiology, Graduate School, Hallym University, Chuncheon; [2]Division of Speech Pathology and Audiology, College of Natural Science, Hallym University; [3]Division of Speech Pathology and Audiology, Research Institute of Audiology and Speech Pathology, College of Natural Sciences, Hallym University, Chuncheon, Korea

Background

The Cortical Auditory Evoked Potentials(CAEPs) are usually classified as two types, such as obligatory or exogenous and cognitive or endogenous. It is known that CAEPs with the acoustic features of vowels reflect exogenous aspect while attentions, contents of sentences, and emotions of the stimuli reflect the endogenous aspect. Also, age effect of CAEP has been scarcely investigated. The purpose of this study was to investigate age, emotional, and vowel effects with the emotional statuses, neutral(N), anger(A), happiness(H), and sadness(S).

Methods

Participants were 20 younger adults(Mean: 22.1 years, range=21-27), and 20 older adults(Mean: 68.2 years, range=65-74), 10 females and 10 males per each group with normal hearing. They all had no significant neurological history and were right-handed. The stimuli were three vowels /u/, /a/, and /i/ out of Ling 6 sounds representing low, middle and high frequencies of vowels with emotional salience of N, A, H, and S. For recording CAEPs, bipolar channels with channel A for auditory evoked potential and channel B for monitoring of eye blink were applied. The experiments were performed in a quite environment and the participants were comfortably seated in bed. For analyzing components of CAEPs, the independent variables were 3 vowels(/u/, /a/, /i/), 4 emotions(N, A, H, S), 2 ages(younger, older adults), and gender(female, male). The dependent variables were latencies and amplitudes of the components of CAEP.

Results

Emotional effects in latency were statistically significant with P1, N2, P2, and N2, all components of CAEP. And, emotional effects in amplitude were statistically significant with P1, N2. Vowel effect was statistically significant with N1 latency. Age and gender effects were statistical

significance with P2 latency and N2 amplitude. The older group showed longer P2 latency and weaker N2 amplitude compared to younger group. Most components showed decreased in latency with A and H emotions.

Discussion

The age effect was agreed with the P2 latency and N2 amplitude of previous studies which investigated age-related factor of CAEPs(Rufener et al., 2014, Stenklev & Laukli., 2004). It may reflect decreased activity in synchronous firing among the neural ensemble and decreased efficiency in the neural generator related refractory period with aging. CAEPs were rarely affected by the vowels counting only acoustic features, but CAEPs were largely affected by the emotional effect, which can be counted more endogenous aspect. Therefore, it is plausible to speculate that the CAEP component revealed more endogenous aspects of brain.

PS 851

Emotional Modulation of the Early Cortical Representation of Speech Signals under "Cocktail-Party" Listening Conditions

Lingxi Lu; Liang Li

School of Psychological and Cognitive Sciences, Peking University

Background

Previous studies have shown that event-related potentials (ERPs) to a speech signal can be modulated by spatial attention against a noisy auditory background. Auditory emotion, on the other hand, is suggested to enhance attentional processes at an early stage of auditory processing in quiet environments. Using the paradigm of emotionally paired learning, which manipulates the emotional attribute of a target-speech voice, this study was to investigate the emotional effect on the early ERP representation of a speech signal under the speech-to-speech masking conditions.

Methods

Twenty-six younger-adult participants listened to a syllable /di/ articulated by two target female voices against a two-talker speech-masking background. The presentation of the emotionally-learned voice was immediately followed by the visual presentation of an identity-matched angry facial expression, while the control presentation was followed by an identity-matched neutral facial expression. Electroencephalograph (EEG) signals were recorded during the presentation. The scale of Self-Assementment Manikin (SAM) was used to obtain participants'; subjective emotional evaluations of the two voices and face pictures after the session of EEG recordings. Not only the peak amplitudes and the

latencies of central (vertex) P1 and N2 induced by the target voice, but also that of the occipito-temporal P2 induced by the identity-matched facial expressions were measured and analyzed.

Results

Participants'; subjective emotional ratings revealed more negative emotional valance of the emotionally-learned voice than the neutral one. The latency of voice-induced P1 was significantly shortened by emotional learning compared to neutral learning. Using the neutral learning as the baseline, the emotion-induced change of N2 amplitude elicited by the target voice was significantly correlated with that of P2 amplitude elicited by matched faces. These results suggest that conditionally associating a target voice with an emotionally negative event (an angry face) can modulate the ERP components to the voice at the latency from 100 to 200 ms.

Conclusions

After emotionally paired learning, the negative emotion associated with the target voice facilitates the early cortical representation of the target speech signal against a noisy background.

PS 852

Alpha Oscillations Within Human Auditory Cortex: An Intracranial Electrophysiology Study

Alexander Billig[1]; Björn Herrmann[2]; Ariane E. Rhone[3]; Phillip Gander[3]; Kirill Nourski[3]; Matthew Howard[3]; Ingrid Johnsrude[4]
[1]*Brain and Mind Institute, The University of Western Ontario;* [2]*The University of Western Ontario;* [3]*Human Brain Research Laboratory, Department of Neurosurgery, The University of Iowa;* [4]*Brain and Mind Institute, University of Western Ontario; School of Communication Sciences and Disorders, University of Western Ontario*

A prominent feature of the scalp-recorded electroencephalogram during rest and task performance is oscillatory activity in the alpha (8–14 Hz) range. Its strong posterior distribution derives largely from sources in occipital and parietal cortices. Due to its prominence when the eyes are closed (compared to when the eyes are open), early accounts described it as an "idling rhythm" (Adrian & Matthews, Brain 4:440-71, 1934). Subsequently, alpha oscillations have been implicated in modulation of population spiking, working memory, and detection (and suppression) of visual stimuli (reviewed in Basar, Int J Psychophysiol 86:1-24, 2012). The role of alpha activity in processing sensory information in other modalities, including audition, remains unclear. A handful of studies have revealed sources of an auditory alpha oscillator in

the temporal lobe (reviewed in Weisz et al., Front Psychol 2:73, 2011) but their projections to the scalp are much weaker than those from visual cortex, and precise locations have not been identified. As a first step toward a better characterization of auditory alpha activity, we analyzed data from patients who had multicontact depth electrodes implanted in Heschl';s gyrus (HG), including putative core auditory cortex in posteromedial HG, for monitoring of epileptic activity. Stimuli were spoken sentences (duration 1.2-4.7 s), presented either clearly or processed using a 3-band noise vocoder. For each recording site, cortical activity was characterized in the time-frequency plane as event-related band power (ERBP) between 1 and 150 Hz. Activity within anterolateral, but not posteromedial HG, was characterized by suppression of low frequency ERBP (theta/alpha; 4-14 Hz) approximately 300 ms following stimulus onset. This suppression effect was most prominent in the low alpha frequency range (8-10 Hz). The data suggest that event-related alpha power modulations reported in previous non-invasive studies may have sources within non-core auditory cortex in the anterolateral portion of HG. Future work will consider functional roles of activity in this frequency band, including its relationship to high gamma activity that tracks the acoustic properties of auditory stimuli.

PS 853

Evidence of Predictive Coding in Auditory Cortex for Lexical Judgements of Spoken Words

Andrew S. Liu[1]; Christopher Kovach[2]; Hiroto Kawasaki[3]; Matthew Howard[4]; Bob McMurray[5]
[1]*Human Brain Research Laboratory, Department of Otolaryngology-Head and Neck Surgery, University of Iowa Hospitals and Clinics;* [2]*Human Brain Research Laboratory, Department of Neurosurgery, University of Iowa Hospital and Clinics;* [3]*Human Brain Research Laboratory, Department of Neurosurgery, University of Iowa Hospitals and Clinics;* [4]*Human Brain Research Laboratory, Department of Neurosurgery, The University of Iowa;* [5]*The University of Iowa*

Cochlear implant users show marked variability in speech perception outcomes that are not well explained by peripheral and surgical factors. One possible explanation for this variability in outcomes is differences in the cognitive and perceptual processes that may be adopted after implantation to cope with a degraded peripheral signal. One such cognitive mechanism is offered by predictive coding accounts. In these accounts, top-down expectations about upcoming stimuli modulate the representation of stimuli in sensory and perceptual processing areas in cortex. Emerging evidence suggests that such mechanisms may play a role in speech perception. However, the neural basis of the predictive feedback signal during speech perception is not well established.

To better understand the role of predictive coding in speech perception, normal hearing (NH) listeners heard an isolated word (either unmodified or noise vocoded) preceded by an orthographic prime that either matched, mismatched, or was neutral. Listeners selected the auditory word from an array of four competitors. Subjects (N= 27) showed a performance benefit for matching primes, and a decrement for mismatching primes relative to an uninformative, neutral prime.

A second study measured cortical activity during this task in NH subjects with medically refractory epilepsy and had intracranial electrodes implanted for clinical seizure monitoring. Subjects were implanted with subdural grid and depth electrodes in frontal and temporal regions, including Heschl';s Gyrus (HG). The orthographic prime differentially modulated high gamma activity (70-150 hz) in HG between the posteriormedial (core) and anterolateral (belt/parabelt) during the first 100 ms and between 250-750 ms post stimulus onset. We also show, using a SVM-based neural decoder, that decoding performance is facilitated by matching primes for 4 ch noise vocoder stimuli compared to mismatch and neutral primes as well as for more intelligible stimuli. These results provide evidence of top-down feedback on auditory cortex consistent with a role of predictive coding in speech perception.

PS 854

Electrocorticographic (ECoG) Analysis of Auditory-verbal Short-term Memory (AVSTM) as Revealed During Performance of Digit Span (DS) and Reverse Digit Span (RDS) Tasks.

Mitchell Steinschneider[1]; Kirill Nourski[2]
[1]*Departments of Neurology and Neuroscience, Albert Einstein College of Medicine; *[2]*Human Brain Research Laboratory, Department of Neurosurgery, The University of Iowa*

AVSTM is a fundamental component of hearing, language and cognition. While lesion and functional neuroimaging data have stressed the importance of perisylvian regions of the dominant hemisphere in AVSTM, ECoG data obtained during a word repetition task suggest more bilateral involvement (Cogan et al., 2014. Nature, 507:94-98). DS and RDS tests are standard means by which AVSTM is assessed. Thus, in order to further clarify neural mechanisms underlying AVSTM, we examined ECoG data obtained from perisylvian and surrounding regions during performance of DS and RDS tasks. Subjects were consenting neurosurgical patients undergoing evaluation for treatment of medically intractable epilepsy. Analyses focused on high gamma cortical activity (70-150 Hz). Subjects performed an expanded version of the Mini Mental Status Exam that included DS and RDS tasks (Nourski et al., 2016. Front

Hum Neurosci, 10:202). Only data associated with correct behavioral responses were analyzed. High gamma power was measured within three time epochs; 1) listening to the digits, 2) recall of the digits, and 3) the delay period between these two events. Cortical sites where responses during the delay period were reliably greater than baseline were considered candidate locations for being involved in AVSTM. Responses during the delay period have been used as a physiological marker for AVSTM (e.g., Leonard et al., in press. Brain Lang, 2016) General findings include (1) larger, more sustained, and more expansive responses during the delay period of the harder RDS tasks, (2) bilateral activation, and (3) non-homogeneous activity patterns within a given brain region. Responses during the delay period were most prominent in the superior temporal, middle temporal, inferior temporal, supramarginal, and angular gyri. These regions have already been implicated in AVSTM (e.g., Baldo et al., 2012. Aphasiology, 26:338-354). Unexpectedly, prominent responses were also present in higher visual areas (fusiform, lingual, and middle and inferior occipital gyri), possibly representing evidence for visual imagery to complete the tasks. Responses during the delay period were not prominent in Heschl's gyrus, the superior temporal sulcus, and the temporal pole. We conclude that intracranial recordings are a valuable adjunct to non-invasive investigations in identifying brain regions associated with AVSTM. Data obtained via intracranial recordings indicate the presence of more extensive networks involved in AVSTM than previously recognized when probed using DS and RDS tasks. Supported by grants NIH R01-DC04290, NIH UL1-RR024979, NSF CRCNS-IIS-1515678, and the Hoover Fund.

PS 855

Neural responses to acoustic and linguistic features of spoken language recorded from EEG

Hugo Weissbart; Katerina Kandylaki; Tobias Reichenbach
Imperial College London

Background
Spoken language contains both acoustic and linguistic information, and the neural responses to both can be difficult to disentangle. In addition, research on spoken language processing often employs simplified stimuli such as single words or short sentences. However, such an approach cannot assess neural responses to statistical features of the word sequences of spoken language. To overcome this limitation, we measured cortical responses to continuous speech using electroencephalography (EEG) and modelled the obtained responses through acoustic and linguistic features, including a feature that emerges only from sequences of words.

Methods

We measured the cortical activity of healthy volunteers listening to audio books from EEG. We then described the acoustic and linguistic information in the spoken language through different acoustic and linguistic features characterizing word level features. Acoustic information was described through the word onset, and this was obtained by aligning the text with the audio signal. Linguistic information was included as word frequency obtained from Google Ngrams. We then added a second linguistic feature, the surprisal of a word, that denotes the negative logarithm of the probability of each word in its particular sequence. The surprisal could not be obtained from the word alone but only from the word in its context, and was computed through a recurrent neural network modelling prediction of words in th language. We then employed linear regression with ridge regularization to predict the EEG responses from the linguistic and acoustic features. We considered shuffled features, where the word onsets were left unchanged but the values of the linguistic features were taken from an unrelated text, as well as EEG responses to a foreign language as a control.

Results and Conclusion

We found that both the acoustic feature as well as the linguistic features elicited distinct neural responses. In particular, we obtained a specific electrophysiological correlate of the surprisal of a word in its sequence as computed from a deep neural network. This neural response was found in the delta and beta frequency bands and could not be explained by the acoustic properties or by word frequency alone. The cortical response to the surprisal of a word may support the predictive coding hypothesis where a sequence of words leads to the prediction of the next word. Our work can help to decode speech comprehension from EEG responses and may allow to better diagnose language deficit using EEG.

PS 856

Sound pattern processing: Neural synchronization and sustained neural activity

Björn Herrmann[1]; Ingrid Johnsrude[2]
[1]*The University of Western Ontario; [2]Brain and Mind Institute, University of Western Ontario; School of Communication Sciences and Disorders, University of Western Ontario*

Optimal perception and behavior requires an auditory system capable of detecting statistical regularities in sound environments. Two lines of research concern the neural operations involved in processing statistical regularities in sounds: one investigates how neural activity synchronizes with temporal regularity, whereas a different, unconnected line of research focuses on increas-es in sustained activity during stimulation with sounds that have spectro-temporally ordered structure. In three electroencephalography (EEG) studies we investigated the relation between these two measures: neural synchronization and sustained neural activity. We asked whether synchronization and sustained neural activity are dissociable, or whether they are functionally interdependent. Experiment I demonstrated that neural activity synchronizes with temporal regularity (i.e., frequency modulation) in sounds, and sustained activity increases concomitantly. In Experiment II, frequency modulation in sounds was parametrically varied. Manipulation of frequency modulation led to a parametric modulation of neural synchronization as well as sustained neural activity, but neural synchronization was more sensitivity to changes in frequency modulation compared to sustained activity. In Experiment III, participants either performed an auditory duration judgment task or a visual object tracking task. Neural synchronization was observed under auditory and visual tasks, whereas an increase in sustained activity with the sound';s frequency modulation was observed only during the auditory task. Together, the results show that neural synchronization and sustained activity levels are functionally linked, with both being sensitive to statistical regularities in sounds. However, neural synchronization might reflect a more sensory-driven response to regularity, compared with sustained activity which may be influenced by contextual or other experiential factors.

PS 857

Exploring speech-trained deep neural networks as models of human auditory behavior

Erica N. Shook[1]; Alexander J. E. Kell[1]; Josh H. McDermott[2]
[1]*Department of Brain and Cognitive Sciences, MIT; Center for Brains, Minds, and Machines, MIT;*
[2]*Department of Brain and Cognitive Sciences, MIT; Center for Brains, Minds, and Machines, MIT; Program in Speech and Hearing Biosciences and Technology, Harvard*

Machine perception systems have recently seen dramatic performance improvements, in large part due to advances in artificial neural networks and deep learning methods. Motivated by the human-level performance of such systems on some real-world recognition tasks, some neuroscientists have begun to consider them as models of sensory systems, including the auditory system. However, beyond absolute performance levels it remains unclear whether the detailed performance characteristics of deep neural networks are similar to those of human listeners, and thus whether they should be taken seriously as models of auditory neural computation. To address this gap, we explored similarities between

human listeners and deep neural networks trained on speech recognition tasks. Using millions of excerpts from labeled speech corpora, we trained a convolutional neural network to recognize words in the presence of real-world background noise (e.g., recordings from city streets, speech babble etc.). The network mapped cochleagrams to labels, indicating which word occurred in the middle of a two-second clip. The resulting network performed the task slightly better than human listeners, but also exhibited a similar pattern of errors across background types and signal-to-noise ratios. The results indicate that deep neural networks trained on realistic audio tasks recapitulate psychophysical phenomena observed in human listeners, suggesting that the networks are shaped by some of the same constraints that determine human behavior.

PS 858

Tracking Phoneme Processing During Continuous Speech Perception with MEG

Christian Brodbeck[1]; Jonathan Z. Simon[2]
[1]Univeristy of Maryland, College Park; [2]University of Maryland, College Park

A central task of the auditory cortex during speech perception is to analyze complex acoustic patterns to detect the words that make up the linguistic message. It is generally thought that this process includes at least one intermediate level of representation, that of phonemes. Because phonemes are defined at least partly through acoustic features, it is inherently difficult to distinguish representations of phoneme identity from acoustic representations. However, since phonemes mediate between a continuous, acoustic representation and discrete linguistic units, i.e. words, phonemes can be analyzed in terms of the information they convey for identifying words, with measures such as phoneme surprisal. Based on the assumption that information that is more surprising, or affords more cognitive processing, is associated with a modulation of brain activity, we used these measures to characterize neural transformations from acoustic to phonetic representations. We recorded brain responses to continuous speech using magnetoencephalography (MEG) while participants listened to audiobook segments. Source localized MEG responses were modeled as linear convolution of a multidimensional kernel with continuous predictor variables reflecting acoustic power and phoneme information content. Each predictor variable was evaluated by whether it significantly improved the model fit when compared to a permuted version of itself, while controlling for contributions from the other variables. Model improvements, as well as the kernels, were tested for significant regions in anatomical space and response time while controlling for multiple comparisons with permutation tests. Results indicate significant

brain responses associated with phoneme information content even when controlling for acoustic responses. Specifically, the resulting kernels indicate that the number of words excluded by a phoneme was associated with a response peak in posterior auditory cortex around 70 ms relative to phoneme onset. Phoneme surprisal was associated with a more anterior response peak in the superior temporal gyrus around the same time, and a later response around 200 ms in posterior auditory cortex. Furthermore, different models of speech processing make different predictions about how much information is conveyed by each phoneme, and consequently, these models can be compared by their ability to predict neural responses. A model assuming that words are analyzed in terms of their morphological components (e.g., 'building'; analyzed as 'build';+';ing';) made significantly better predictions than a model assuming that words are detected in their surface forms (i.e., 'building'; analyzed as one unit). Thus, our results demonstrate the feasibility of testing contrasting predictions from models of phoneme processing in natural, continuous speech.

PS 859

Temporal Response Functions Show that Collective Neural Processing Differs along the Speech-Music Continuum

Emily Graber[1]; Malcolm Slaney[2]; Shihab Shamma[3]
[1]Stanford CCRMA; [2]Google Research; [3]Ecole Normale Supérieure, University of Maryland

Different auditory tasks have been shown to modulate spectro-temporal receptive fields (STRFs) obtained from invasive neuroelectric recordings as well as temporal response functions (TRFs) obtained from scalp EEG recordings. Most studies modeling human EEG data with TRFs have used speech stimuli, however the processing of musical stimuli may also be evident in TRFs. Because behavioral and neuroimaging studies using the speech-to song illusion have found that speech and song are perceived and processed differently, we aimed to demonstrate that the neural processes associated with listening to speech and music are distinct in TRFs obtained from EEG recordings as well. In order to study the TRFs for stimuli falling in between the two categories, a continuum of stimuli ranging from speech to music were created and tested.

For two songs, a trained singer was recorded while reading the lyrics in a regular fashion, speaking the lyrics in rhythm, and singing. Various combinations of those recordings and separate accompaniment tracks were used to create the continuum of stimuli summarized in the supporting table below. Additionally, because speech and music have different acoustic features, a number of control conditions were designed to account for high

and low-level feature differences between the two most extreme stimuli. The accompaniment and plain speech conditions were scrambled in time to create controls where all low level acoustics were preserved, but high level organization was destroyed. Pink noise modulated by the envelopes of the accompaniment and speech were created as controls where low level features were removed while high level structures were preserved.

EEG was recorded while two subjects listened to the set of stimuli once through in a random order. TRFs were made for each stimulus via reverse correlation with the EEG and stimulus intensity. Finally the TRFs were compared with Pearson correlation. The preliminary results show that TRFs modeling responses to the musical side of the continuum are more similar to one another than those modeling responses to the speech side of the continuum. Future work will determine whether the TRFs from the controls with different low-level features were correlated, as well as those from the controls with different high-level features. These findings suggest that the TRFs derived from human EEG recordings can differentiate speech listening from music listening and that different TRFs must be used for decoding speech vs music, and potentially other signals.

SupportingTable.doc

PS 860

Decoding tension and resolution dynamics in naturalistic musical stimuli: EEG signals in the light of a theoretical predictive model

Claire Pelofi[1]; Daniel D.E. Wong[2]; Mohsen Rezaeizadeh[1]; Emily Graber[3]; Elizabeth Margulis[4]; Mary Farbood[5]; Malcolm Slaney[6]; Alain de Cheveigné[2]; Shihab Shamma[7]
[1]*Institute for Systems Research, University of Maryland; [2]Equipe Audition, Departement d'Études Cognitives, Ecole Normale Supérieure; [3]Stanford CCRMA; [4]Music Cognition Lab, University of Arkansas; [5]Music and Audio Research Laboratory, New York University; [6]Google Research; [7]Ecole Normale Supérieure, University of Maryland*

Decoding sensory information processing by merely observing the electrical signal measured from the brain is still a difficult endeavor. In the auditory domain, one of the challenges resides in the fact that acoustic signals are dynamically processed along different time scales. In music, tension and resolution patterns are triggered by different features, ranging from low-level acoustical cues such as amplitude modulations to higher-level structures such as harmony and melody progressions. It has been posited that tense portions of the music elicit

greater arousal in listeners, that may result in a higher attention to the content of what is happening. In this study, we propose to decode musical tension and release dynamics by collecting EEG signal while participants listen to musical excerpts and give continuous tension ratings. Specifically, we fit EEG recordings with different aspects of the acoustic signal using temporal and spectral filters and linear combination algorithms (De Cheveigné & Parra, 2014). In this manner, we obtain a projection of both signals to a space that extracts temporal similarities between the EEG and the acoustic signals. A profile of continuous correlations can then be computed from these projections: higher correlation score corresponds to a better fit between the two signals, which is also reflected in the behavioral measures. By observing the average of inter-subject correlation profiles, we could predict which parts in the music draw the most attention and supposedly, contain the most musical tension. This analysis was conducted along with a heuristic model of musical tension (Farbood, 2012) which combines weighted acoustic parameters believed to trigger musical tension and first designed to predict continuous rating (Farbood & Upham, 2013). By adapting the model to the specifics of EEG signals, we shall discuss which musical features best predict the brain signature of tension and release dynamics.

PS 861

Neural correlates of perceptual switching during auditory streaming of bistable stimuli

Nathan C. Higgins[1]; David F. Little[2]; Abin Kuruvilla-Mathew[2]; Karli M. Nave[2]; Breanne D. Yerkes[2]; Mounya Elhilali[3]; Joel S. Snyder[2]
[1]*Vanderbilt University Medical Center; [2]University of Nevada Las Vegas; [3]Johns Hopkins University*

Unchanging stimuli that evoke mutually exclusive percepts upon repeated or continuous presentation are known as 'bistable';. Bistable stimuli provide a powerful experimental paradigm for studying the underlying neural mechanisms of conscious perception and the influence of high-level factors such as attention. The majority of studies on the neural correlates of bistable perception have used visual stimuli (e.g., Necker cube, binocular rivalry), but more recent studies have used a number of auditory stimuli to study bistable perception. Here, we used an intermittent auditory stream segregation paradigm during electroencephalography recordings. On each trial, participants were presented with three triplets (700 ms duration each) of low (A) – high (B) – low (A) pitched tones, which were immediately followed by a 700 ms silent response period during which participants indicated via button press whether they perceived one integrated stream, or two separated streams. Each trial was then immediately followed by another trial so as

not to disrupt perceptual stability from trial to trial, thus allowing perception to alternate relatively naturally. This paradigm allows for 1) reduced temporal uncertainty in the electroencephalography data when relating perceptual responses to particular stimulus trials, and 2) comparison of neural activity during perception of one or two streams, and during trials in which a perceptual switch did or did not occur. Behaviorally, results demonstrated that the repeated trials of three ABA triplets first evoked perception of a single stream, followed by a switch to two streams after several trials and then periods of bistability (switching back and forth between trials) as the experiment progressed. Auditory evoked responses were characterized by sustained negative activity during the three triplets, as well as transient peaks, with greater sustained negative activity when participants reported two streams compared to one stream. This could result from enhanced top-down attention required to maintain perception of two streams and/or greater neural resources required to represent two segregated streams as opposed to just one integrated stream. A reversal negativity (RN) enhancement was present approximately 150-200 ms post-stimulus during trials in which a perceptual switch was reported compared to trials in which no switch was reported, collapsing across switch direction (i.e., one stream to two streams and two streams to one stream). The RN has been observed previously in studies on visual and auditory bistability and could reflect neural activity related to facilitating processing of the new percept and/or suppressing processing of the old percept.

PS 862

Steady State-Evoked Potentials Reflect Context-Induced Perception of Musical Beat in an Ambiguous Rhythm

Karli M. Nave; Erin Hannon; Joel S. Snyder
University of Nevada Las Vegas

Synchronous movement to music and other rhythmic stimuli is effortless, and yet relatively little is understood about the mechanisms that underlie this ability. Commonly listeners synchronize their movements with the beat of the music (a quasi-isochronous pattern of prominent time points). While top-down processes presumably influence listener perception of the beat, it has been difficult to disentangle stimulus-driven from listener-driven processes. Previous research has shown that the intended beat periodicity of a rhythmic stimulus can be observed in periodic neural activity, but it is still unclear whether this neural response reflects perception of musical rhythm or simply bottom-up processing of the stimulus. We used electroencephalography (EEG) to investigate whether steady-state evoked potentials (SS-EPs, the electrocortical activity from a population

of neurons resonating at the frequency of a periodic stimulus) arising from auditory cortex reflect beat perception when the physical information in the stimulus is ambiguous and supports two possible beat patterns. Participants listened to a musical excerpt that strongly supported a particular beat pattern (context phase), followed by an ambiguous rhythm consistent with either beat pattern (ambiguous phase). During the final probe phase, listeners indicated whether or not a superimposed drum matched the beat of the ambiguous rhythm. Accurate performance required that participants perceive the beat in the musical excerpt and also maintain that percept throughout the ambiguous rhythm, despite having no surface evidence to reinforce that perception exclusively. We found that participants perceived probes that matched the beat of the context as better fitting the ambiguous rhythm, compared to probes that did not match the beat of the context. We also found that SS-EPs during the ambiguous phase had higher amplitudes at frequencies corresponding to the beat of the preceding context. Finally, trial-by-trial analyses revealed that the amplitude of the beat-related SS-EPs was predictive of whether or not subjects correctly perceived the beat. These findings support the idea that SS-EPs arising from auditory cortex reflect perception of musical rhythm and not just stimulus encoding of temporal features.

PS 863

Language experience-dependent advantage in cortical pitch representation is maintained under reverberation

Ananthanarayan Krishnan; Chandan Suresh; Jackson Gandour
Purdue University

Long-term language and music experience enhances neural representation of temporal attributes of pitch in the brainstem and auditory cortex in favorable listening conditions. Herein we examine whether cortical pitch mechanisms shaped by long-term language experience are more resilient to degradative effects of reverberation. Cortical pitch responses were recorded from Chinese- (C) and English-speaking (E) natives using a Mandarin word exhibiting a high rising pitch (/yi^2/). Stimuli were presented diotically in quiet (Dry), and in the presence of Mild, Moderate and Severe reverberation conditions. At the Fz electrode site, both groups showed an increase in peak latency (Na, Pb, Nb) and a decrease in peak-to-peak amplitude (Na–Pb, Pb–Nb) with increasing reverberation. A language-dependent enhancement of Na–Pb amplitude (C > E) was restricted to Dry, Mild and Moderate conditions. As indexed by Pb–Nb amplitude, a similar group effect (C > E) was obtained pooling across stimuli. Pooling across groups, amplitude of the Dry condition was larger than the other three (Mild, Moder-

ate, Severe). At T7/T8 electrode sites, Na–Pb amplitude showed that the Chinese group exhibited a rightward asymmetry (T8 > T7) under Dry and Mild conditions. A language-dependent effect was restricted to T8 (C > E). These results taken together suggest that cortical pitch mechanisms shaped by long-term language experience provide an enhanced and stable neural representation of pitch-relevant information that is maintained in the presence of degraded effects of reverberation.

PS 864

Neural Resonance Theory: Testing Dynamical Predictions Using Missing Pulse Rhythms

Charles S. Wasserman[1]; Jung Nyo Kim[1]; Yi Wei[1]; Erika Skoe[2]; Heather Read[1]; Edward Large[1]
[1]University of Connecticut; [2]University of Connecticut, Department of Speech, Language, and Hearing Sciences

Many rhythm perception experiments employ simple isochronous rhythms, in which synchronous neural or behavioral responses are observed. However, responses at the stimulus frequency do not allow one to distinguish whether synchrony occurs as a response to a common input, or as the result of an emergent population oscillation that entrains at a particular frequency. However, It is possible to create a rhythm with no spectral energy at the pulse frequency by manipulating the number of events that occur anti-phase (180°) versus in-phase (0°) with the basic rhythmic cycle. Dynamical analysis predicts neural oscillation will emerge at such a missing pulse frequency. Previous studies have shown that subjects tap along to complex rhythms at the missing pulse frequency a finding that supports the prediction.

This study aimed to investigate whether the sensorimotor system, as measured by 32-channel cortical EEG, would entrain to a complex rhythm at the pulse frequency even when the complex rhythm contained no spectral power at that frequency. The experiment utilized four different rhythms of varying complexity (1 simple, 2 complex, and 1 random rhythm). Fast Fourier Transform (FFT) of the Hilbert envelope showed energy at the repetition frequency (2Hz) for the simple rhythm, but no spectral energy at the missing pulse frequency (2Hz) for the complex rhythms. EEG responses to these stimuli were examined for evidence of neural oscillations and power modulations at the missing pulse frequency predicted by dynamical analysis. We report evidence of 2Hz responses in the EEG to missing pulse rhythms. These data support the theory that rhythmic synchrony occurs as the result of an emergent population oscillation that entrains at this particular frequency. We also discuss generators of the 2Hz response component.

Wasserman_ARO_Abstract_FINAL.pdf

PS 865

Effects of Music Training on Cortical Auditory Potentials to Frequency Changes

Fawen Zhang[1]; Chun Liang[1]; Gabrielle Underwood[1]; Chelsea Blankenship[2]
[1]University of Cincinnati; [2]Cincinnati Children's Hospital and University of Cincinnati

Cochlear implant (CI) users generally have poor pitch perception performance, largely due to the limited spectral resolution transmitted by the CI. Thus, pitch-based speech tasks and music perception are extremely challenging for CI users. The objective of this project is to examine the effects of a short-term music training protocol on cortical auditory evoked potentials to frequency changes, a type of acoustic change complexes (ACC). This study is expected to have important impact on post-implantation intervention and assessment in CI users. Post-lingually deafened adult CI users were recruited. These subjects have worn there CI for at least 1 year. They have never received any music training. The music training protocol used in this study was as follows: participants used Pandora program downloaded on their home computer for music training. They only trained the self-selected CI ear that has unsatisfactory performance, with the device in their non-trained ear being switched off during the training. They were instructed to select the music genre they enjoy, but only pay attention to music melody, rather than other musical elements. The stimuli were at the most comfortable level. The training schedule was 40 minutes/day x 5 days/week x 4-8 weeks. They were required to log the training details each day. The pre-training and post-training tests included a psychoacoustic test of frequency change detection and an electroencephalographic (EEG) test. The stimuli were a series of 1-sec pure tones containing different magnitudes of upward frequency changes at 0.5 sec after the tone onset, which can evoke the ACC if the frequency change is perceivable. An adaptive, 2-alternative forced-choice procedure was employed to measure the frequency change detection threshold (FCDT). The EEG recordings were obtained using a 40-channel EEG system when the participants passively listened to the stimuli. The data collected showed that, compared to the pre-training results, there was an improvement in the FCDT and the ACC evoked by the frequency change. However, there was a variation on the training duration required for visible ACC improvement. In some participants, 1 month of training was enough to display a present ACC for a 5% frequency change. In some patients, the presence of the ACC for a 5% occurred after 2 months of training. While the data collecting is still ongoing to include more participants, the currently avail-

able data suggested that the short-term music training has positive effects on cortical processing of frequency changes and frequency change detection capability.

2018 ARO (music training).docx

PS 866

Neural correlates of training-related improvements during change detection in complex auditory scenes

Vanessa Irsik; Taylor Guthrie; Joel S. Snyder
University of Nevada Las Vegas

Research on change deafness--the inability to detect auditory changes--has shown that misdirected attention, memory limitations, and encoding failures contribute to change detection errors; however, the effects of practicing on change deafness are not well understood. The major goals of this experiment were to examine the efficacy of training on change deafness, to address whether observed learning reflects a true improvement in change detection ability while controlling for response bias, and to identify any training-related neural modulations by recording event-related brain potentials (ERPs). Participants completed change detection trials over a three-day period. During each trial, participants heard two auditory scenes separated by a 350 ms silent interval, after which they were asked to make a same/different judgment. Each scene was composed of five recognizable 1,000 ms sounds. On Day 1, each listener completed a pre-test. On Day 2, listeners practiced change detection with familiar sounds from the pre-test (n=15), or with a group of novel sounds (n=15). A third, control group (n=15) did not participate in any task on this day. Listeners who practiced received detailed feedback after each response, which told them the correct response and replayed the changed sound in isolation and both scenes. On Day 3, all listeners completed a post-test that contained sounds heard in the pre-test and a new group of novel sounds. ERPs were only recorded during the pre-test and post-test. Change detection error was substantially reduced at post-test following training, but false alarm rates also increased (p';sd';). During ERP analyses, we found a fronto-central sustained negative potential (FN) during scene 1 (same trials; 370-1000 ms), and a P3 response during scene 2 (different trials; 400-1000 ms) that showed a substantial reduction in amplitude at post-test. Using multiple linear regression, we found that changes in FN amplitude and response bias (c) were significant predictors of the amount of improvement in d'; (p';s< .05). In particular, participants with less FN reduction and less increase in response bias improved their perceptual sensitivitymore from pre-test to post-test. The FN component may reflect neural processing related to better sensitivity at post-test, perhaps due to better sustained attention in participants who improved their performance. Future studies should examine whether multiple days of training can improve change detection while keeping false alarm rates low and stable across a wider range of participants.

Auditory Pathways Brainstem IV

PS 867

FMRP regulates dendritic and synaptic properties of developing auditory neurons

Xiaoyu Wang[1]; Diego A. R. Zorio[2]; Leslayann Schecterson[3]; Edwin W. Rubel[3]; Yong Lu[4]; Yuan Wang[1]
[1]*Department of Biomedical Science, Program in Neuroscience, Florida State University College of Medicine;* [2]*Department of Biomedical Sciences, College of medicine, Florida State University;* [3]*Department of Otolaryngology, Bloedel Hearing Research Center, University of Washington;* [4]*Department of Anatomy and Neurobiology, Northeast Ohio Medical University*

Fragile X mental retardation protein (FMRP) is a mRNA-binding protein that regulates local protein translation. Reduced FMRP levels due to the silencing of Fmr1 gene results in fragile X syndrome (FXS), which is characterized by intellectual disabilities and auditory dysfunction. Knockout models in mouse and rat have shown dendritic and synaptic alterations, mostly in forebrain. How FMRP regulates neuronal cellular properties during development remains unknown. We examined the effects of knocking down FMRP expression in developing neurons of the chicken nucleus magnocellularis (NM), the avian homolog of the mammalian anteroventral cochlear nucleus.

To knock down FMRP protein in NM neurons, we introduced Fmr1 shRNA into NM precursors via in ovo electroporation at embryonic day 2 (E2). This approach transfects a subset, but not all, NM neurons, leaving neighboring non-transfected neurons as same-animal controls. As expected, non-transfected neurons in the rostral NM display extensive dendrites at E9, followed by dramatic dendritic pruning such that these neurons demonstrate adendritic morphology from E15 onwards. Neighboring transfected NM neurons, however, exhibit extensive dendrites at both E9 and E15, and gradually lose their dendrites at E19, indicating delayed dendritic pruning. We further examined the effects of postsynaptic FMRP knockdown on synaptic formation. As visualized by auditory nerve tracing studies as well as SNAP25 immunoreactivity, at E15 large Endbulb synapses form around the adendritic cell bodies of non-transfected NM neurons. In contrast, cell bodies and dendrites of neighboring transfected neurons were surrounded by small bouton-like presynaptic puncta. Finally, we com-

pared physiological properties between transfected and non-transfected neurons using whole-cell voltage clamp in acute brain slices from E15 embryos. Analyses of passive neuronal properties revealed significantly larger membrane capacitance in transfected neurons, indicating larger surface area of the neurons with less FMRP. The kinetics of spontaneous EPSCs (sEPSCs) in transfected neurons was also significantly slower in both 10-90% rise time and decay time constant than non-transfected cells, suggesting more distant input sites on dendrites and consequently stronger dendritic filtering. Consistently, both sEPSCs and evoked EPSCs (eEPSCs) in transfected cells showed smaller amplitude than recordings in non-transfected cells. Meanwhile, transfected neurons tended to have smaller voltage-gated K^+ current compared to non-transfected neurons, implying elevated excitability of the neurons with reduced FMRP.

Taken together, these data demonstrate that normal levels of FMRP are required for timely maturation of dendrites and synapses during important developmental periods, and that decreased levels of FMRP can lead to compromised neuronal properties and neurotransmission.

PS 868

Developmental Emergence of Phenotypes in the Auditory Brainstem Nuclei of Fragile X Model Mice

Sarah Rotschafer[1]; Karina Cramer[2]
[1]University of California, Irvine; [2]University of California Irvine

Fragile X syndrome (FXS) is the most common single-gene inherited cause of autism. In addition to symptoms associated with autism, individuals with FXS experience hypersensitivity to sound and demonstrate an enhanced response in the auditory cortex when presented with sound stimuli. Cellular and physiological abnormalities found in the FXS auditory brainstem may contribute to functional defects found throughout the auditory system. We used FXS model (Fmr1 KO) mice to study how FMRP loss effects auditory brainstem development at time points prior to and after hearing onset. We studied nucleus size, cell population size, cell size, VGLUT and VGAT expression, and glial populations in the ventral cochlear nucleus (VCN), medial nucleus of the trapezoid body (MNTB), and lateral superior olive (LSO) at postnatal day (P)1, P6, and P14. We found that the Fmr1 KO VCN gained cells at a reduced rate, and MNTB growth was slowed. Cell size was reduced in Fmr1 KO VCN after P6, in MNTB at all ages tested, and in LSO at P1 and P14. Neither the VCN nor LSO of Fmr1 KO mice showed any differences in synaptic protein expression, however, VGAT expression was elevated relative to VGLUT in the Fmr1 KO mouse MNTB. The number

of microglia present increased more slowly in all Fmr1 KO nuclei tested. Although the numbers of astrocytes in the Fmr1 KO VCN and MNTB was did not differ from those in wild type mice, the Fmr1 KO LSO had more astrocytes by P14. These data suggest that many of the auditory brainstem irregularities found in adult Fmr1 KO mice are rooted in atypical brainstem development.

PS 869

Spontaneous firing rate of unipolar brush cells is controlled by the action of ambient glutamate on inhibitory mGluR2 receptors and excitatory AMPA receptors

Timothy Balmer[1]; Carolina Borges-Merjane[2]; Laurence Trussell[1]
[1]Oregon Hearing Research Center, Vollum Institute, Oregon Health and Science University; [2]Institute of Science and Technology Austria

Unipolar brush cells (UBCs) are spontaneously firing glutamatergic interneurons present in the dorsal cochlear nucleus and cerebellum. UBCs receive input from mossy fibers carrying multisensory signals and project to granule cells and other UBCs. Glutamate released onto the UBC';s elaborate brush-like dendrite causes long duration currents that either increase or decrease spontaneous spiking. OFF UBCs have a large mGluR2-mediated outward K^+ current, and are thus inhibited by glutamatergic input – decreasing spiking. ON UBCs, which have a smaller mGluR2-mediated outward current, are dominated by AMPA receptor currents and are therefore excited by glutamate and increase firing.

Using acute mouse cerebellum slices we report that ambient glutamate at the mossy fiber-UBC synapse causes tonic currents. OFF UBCs (but not ON UBCs) had a tonic mGluR2 mediated outward current that slowed their spontaneous firing rate. ON UBCs (but not OFF UBCs) had a small tonic inward current mediated by AMPA receptors. AMPA receptor desensitization blocker cyclothiazide revealed that ambient glutamate causes tonic desensitization in both ON and OFF UBCs that reduces the evoked AMPA receptor current. These tonic currents were reduced by the activity of excitatory amino acid transporters. The glutamate transporter blocker TBOA increased the tonic inward current in ON UBCs and increased the tonic outward current in OFF UBCs. The source of the ambient glutamate is vesicular, as it was blocked by bafilomycin treatment. In the presence of TBOA, blockade of evoked release by TTX partially reduced the tonic current and was further blocked by mGluR2 or AMPA receptor blockers in OFF and ON UBCs, respectively. Restricted clearance of glutamate from the mossy fiber-UBC synapse affects the spontaneous firing rate of UBCs and shapes their synaptic re-

sponses to multisensory input.

PS 870

Variations in intrinsic and synaptic properties in MSO neurons confer a spectrum of ITD sensitivity

Brian J. Bondy[1]; Nace L. Golding[2]
[1]*Department of Neuroscience and Center for Learning and Memory, University of Texas at Austin;* [2]*Department of Neuroscience, University of Texas at Austin*

Neurons in the MSO display specializations that allow them to detect submillisecond interaural time differences (ITDs) in order to encode horizontal sound location. Previous studies have shown that this computation is mediated through the synergistic action of a small number of strong excitatory inputs and exceptionally fast membrane kinetics. However, there has been little focus on whether variability in MSO properties exists, and what implications variability may have on ITD tuning.

We performed whole-cell current clamp recordings of MSO neurons in gerbil brainstem slices (P18-P80, 35°C). In a subset of experiments ipsi- and contralateral inputs to MSO neurons were electrically stimulated. Excitatory and inhibitory postsynaptic potentials were isolated with strychnine and NBQX, respectively. Recorded MSO neurons were labeled with biocytin and mapped according to their location within the dorsal-ventral (tonotopic) axis and the rostro-caudal axis.

We found that MSO neurons exhibit substantial variations in synaptic and intrinsic electrical properties, and could be separated into three subcategories on the basis of firing pattern in response to current steps: phasic neurons, with low input resistances ($10.1\pm0.4M\Omega$, ±95% confidence interval), fast time constants ($0.3\pm0.01ms$), and onset-only spiking (n=256); oscillators, with higher input resistances ($36.6\pm5.1M\Omega$) and time constants ($0.9\pm0.2ms$), and a high-frequency, pausing firing pattern (n=95); and tonic neurons, with the highest input resistances ($96.1\pm24.4M\Omega$) and time constants ($5.2\pm1.5ms$), and regular firing (n=62). Oscillator and tonic neurons were primarily located in the ventral and dorsal-most fifths of the MSO. All MSO neurons received bilateral excitation and inhibition, and sent axons out of the MSO. In response to graded levels of electrical stimulation, phasic neurons displayed 4-5 discrete levels in EPSP amplitudes, likely reflecting the number of inputs per side. Oscillators displayed 7-10 levels, and in tonic neurons no discernable discrete levels were apparent, presumably reflecting large numbers of weaker inputs. EPSP widths were narrower in phasic neurons ($0.5\pm0.04ms$ n=12) vs. oscillators ($1.2\pm0.2ms$, n=11) and tonic neu-

rons ($3.8\pm1.6ms$, n=6). Accordingly, in coincidence detection experiments in vitro, phasic neurons exhibited narrow ITD curves vs. oscillator and tonic neurons (ITD halfwidths: phasic, $0.58\pm0.05ms$; oscillator, $0.92\pm0.3ms$; tonic: $3.6\pm1.2ms$, n=3,7,&3 respectively). Conversely, the strength and number of inhibitory inputs appeared similar across firing types.

While the physiological properties of phasic, oscillator, and tonic neurons are different on average, they nevertheless form a continuum. Thus we propose that these categories represent variations of a single principal neuron cell type that may carry out different integrative tasks.

PS 871

Relationship of Central Auditory Pathway Corticotropin Releasing Factor-positive Neurons to the Calcium-binding Proteins, Calbindin, Calretinin and Parvalbumin

Kathleen T. Yee; Douglas E. Vetter
University of Mississippi Medical Center

Introduction
We have previously reported that corticotropin releasing factor (CRF) is expressed throughout the central auditory pathway in neurons with varied morphologies. This expression pattern is of interest because CRF-based neurotransmission is known to significantly modulate glutamatergic-based neurophysiology (Liu et al., 2004), and as such, may play a role in shaping excitation-inhibition states of single neurons and more complex inhibitory surrounds and tuning curve widths of auditory-driven neuronal activity. To better define this population of neurons, we investigated whether CRF-expressing cells correlate with specific populations of the calcium-binding proteins, calbindin, calretinin and parvalbumin.

Methods
Homozygous CRF-IRES-Cre mice and ROSA26-tdTomato mice, expressing tdTomato preceded by a floxed STOP cassette (Ai14 line; Jackson Labs), were mated. The CRF:tdTomato reporter mice progeny carry both transgenes and express tdTomato in CRF-postive cells due to Cre recombinase deletion of the STOP cassette. Reporter expression faithfully mirrors CRF expression patterns based on immunohistochemical procedures (Chen et al., 2015). Brains from cardiac perfused (4% paraformaldehyde) CRF-Cre tdTomato mice were sectioned and stained with antibodies against calbindin, calretinin or parvalbumin. Native TdTomato protein was visualized either directly or following immunostaining with a red fluorescent protein antibody using fluorescence microscopy.

Results

We have examined auditory synaptic sites in the brainstem, midbrain, thalamus and cortex. Interestingly, CRF cells do not represent a single population of the three calcium-binding proteins examined. Neurons double labeled with calbindin, calretinin or parvalbumin exhibit varied morphologies represent only scattered CRF-expressing neurons in the auditory pathway and in many instances represent a small percentage of cells expressing CRF alone or one of the 3 calcium-binding proteins investigated. Intriguingly, the medial geniculate contained the greatest concentration of CRF-calcium-binding protein double labeled cells. CRF terminals were observed apposed to the soma of calcium-binding protein positive cells as well as cells that did not express calcium-binding proteins.

Conclusions

These results show that while some CRF-expressing neurons also express calcium binding proteins, most do not. The presence of CRF-positive terminals on calbindin, calretinin or parvalbumin neurons suggests that CRF may modulate these classes of neurons. However, the identity of the CRF-containing neurons along the auditory pathway remains largely unresolved. It is possible that no single classically defined neurochemical population of neurons represents the population of CRF expressing neurons, suggesting a wide-ranging modulatory effect through CRF expression across the central auditory pathways.

PS 872

Response properties of the human frequency-following response (FFR) to tones and speech: Level dependence, adaptation, and phase-locking limits

Gavin M. Bidelman; Louise Powers
University of Memphis

The frequency-following response (FFR) is a sustained neurophonic potential generated by auditory phase-locking used to assess the neural encoding of speech and musical sounds at subcortical levels. Despite a surge of recent FFR studies and its empirical and clinical applications, surprisingly little is known about basic response properties of this evoked potential. To this end, we measured FFRs in young, normal hearing adults in response to speech and nonspeech (pure tone, chirp sweeps) stimuli with similar fundamental frequencies (F0s). We quantified three key properties of auditory neural coding and FFRs: level-dependence, neural adaptation, and the upper limit of phase-locking. Stimulus intensity was varied parametrically to map input/output (I/O) functions. Neural adaptation was evaluated by assessing sweep-to-sweep changes in the accumulating FFR between 1 and 4000 trials. The upper limit of neural phase-locking was estimated from response spectrograms to chirp stimuli as the highest frequency where FFR energy remained above the signal noise floor. Expectedly, I/O functions showed FFR amplitude increased from 0.05 to 0.18 μV with increasing stimulus level between 25 and 85 dB SPL. However, growth of the FFR was steeper for tones than speech, despite being measured at the same F0. Similarly, FFR latency decreased for speech (tones) from 16 (19) ms to 11 (15) ms from 25 to 85 dB SPL. Adaptation analysis showed ~50% reduction in FFR amplitude over 4000 sweeps with stronger adaptation in the first ~500 trials and responses converging to their final amplitude by ~1500 trials. Lastly, estimates of neural synchronization revealed FFRs contained measurable phase-locking up to ~1150 Hz, consistent with the upper limit of phase-locking reported for single brainstem neurons. Our findings detail important normative aspects of the FFR and clarify signal conditions that provide the most robust and stable brainstem representations for speech and nonspeech inputs.

PS 873

Apoptosis-related Gene and Protein Expression in the Mouse Central Auditory System upon Acute Noise Exposure

Moritz Gröschel[1]; Dietmar Basta[1]; Arne Ernst[1]; Birgit Mazurek[2]; Agnieszka Szczepek[2]
[1]*Department of Otolaryngology, Unfallkrankenhaus Berlin;* [2]*Department of Otolaryngology, Charité University Medicine Berlin*

Beside peripheral pathologies of neuronal structures, noise trauma leads to changes in central neuroanatomy and neurophysiology. Several studies revealed an impact on the auditory pathway either by deprivation or acoustic overstimulation. An early significant loss of cells was shown in central auditory structures after noise trauma. Recently, cell death mechanisms have been detected after traumatizing single noise exposure in the auditory brainstem, midbrain and thalamus immediately postexposure, which lasted for several days. The present study should clarify the underlying mechanisms of acute degeneration in auditory brain structures on the gene and protein level. Due to the earlier results and observations during cochlear pathologies, the experiments focused on the expression of the pro-apoptotic gene Apaf-1 and the anti-apoptotic gene Bcl2a1a to analyze the contribution of mitochondria-related intrinsic apoptotic pathways on acute cellular damage immediately after traumatizing noise exposure. Normal hearing mice (NMRI strain) were exposed to a broadband noise (5-20

kHz) at a sound pressure level of 115 dB for 3 hours. Tissue samples from the cochlear nucleus, inferior colliculus and auditory cortex have been harvested immediately after exposure and mRNA and protein expression has been investigated for both genes by RT^{2}qPCR or western blot experiments, respectively. Unexposed animals served as controls and data have been compared statistically between groups. The results show an upregulation of Bcl2a1a mRNA immediately after trauma, whereby protein expression is reduced at least in the auditory brainstem. In contrast, Apaf-1 shows a downregulation in mRNA expression after acoustic overexposure. On the protein level, Apaf-1 expression tends to be increased in all investigated structures, although differences miss statistical significance. The data indicate that, among others, the intrinsic apoptotic pathway plays an important role during early damage of the central auditory system. It can be suggested from protein expression measurements that acute degeneration is triggered by direct hyperexcitation during acoustic overstimulation, leading to dysregulation of mitochondrial membrane potential and induction of apoptosis by overexpression of pro-apoptotic and downregulation of anti-apoptotic proteins. The inverse expression pattern on the mRNA level of both genes might reflect a protective cellular response to initiate subsequent inhibition of the intrinsic apoptotic pathway.

PS 874

Noise Induced Hearing Deficits in CBA/CaJ Mice Throughout the Lifespan

Laurel A. Screven[1]; Anastasiya Kobrina[2]; Katrina M. Schrode[3]; Omobalade Odedoyin[3]; Micheal L. Dent[4]
[1]University at Buffalo; [2]SUNY, University at Buffalo; [3]Johns Hopkins University School of Medicine, Department of Otolaryngology - Head and Neck Surgery, Center for Hearing and Balance; [4]State University of New York at Buffalo

Damaging noise exposure is a common cause of sensorineural hearing loss (SNHL) in adults. Despite the widespread impact of SNHL, the mechanisms underlying variability in the behavioral consequences of noise induced damage to the ear are currently unknown, including age- and sex-dependent differences observed in both humans and animal models. The goal of the present study was to measure absolute and masked threshold shifts following noise exposure in young and old mice. Cochlear and brainstem tissue were harvested from behaviorally characterized animals for immunohistochemical and electron microscopic analysis. We hypothesized that young mice would show an initial threshold shift but then return to pre-exposure levels, whereas older mice would show more permanent threshold shifts due to reduced capacity for central compensation for peripheral damage. Mice ranging from 1 to 2.5 years old were trained and tested using operant conditioning procedures and positive reinforcement to measure absolute and masked thresholds before and after traumatic noise exposure. Mice were placed in an anechoic chamber and exposed to 8-16 kHz narrow band noise at 100 dB SPL for 2 hours. Following noise exposure, thresholds were measured daily to track auditory acuity. Immunohistochemistry and transmission electron microscopy were conducted to quantify peripheral damage and central synaptic reorganization once behavioral testing was complete. Brains were collected, sectioned, and labeled against VGLUT1 or GAD65; we quantified labeling in the ventral cochlear nucleus. Cochleas were also collected, dissected, and labeled for either CTBP2 or SV2 to identify and quantify afferent or efferent terminals, respectively. Mice showed sex-dependent recovery following noise exposure in old animals, with males showing permanent and more extreme threshold shifts compared to females. Males also showed more instability in absolute thresholds measured across days. Additionally, mice exhibited age-dependent differences in recovery from noise exposure. Old mice were unable to recover masked thresholds compared to young animals. Furthermore, older mice showed evidence of reduced central plasticity after noise exposure, suggested by anatomical analysis of older brains. The present experiment investigates the influence of both sex and age on threshold shifts following damaging noise exposure. Older mice are more susceptible to the negative effects of acoustic trauma, particularly males, likely due to their inability to compensate for damage in the auditory periphery following the noise exposure. This work was supported by NIH DC012302 (MLD), NIH T32 DC000023, and the David M. Rubenstein Fund for Hearing Research.

PS 875

Fetal Development of the MSO around Hearing Onset in Baboon Neonates

Eun Jung Kim[1]; Blanco Cynthia[2]; Jun Hee Kim[3]
[1]Department of Cellular and Integrative Physiology, University of Texas Health Science Center; [2]Department of Pediatrics; [3]UTHSCSA

Children born prematurely suffer from reading-speaking disabilities and cognitive difficulties, which are associated with an auditory processing disorder. The human fetus starts to hear (at ~70% gestational age; GA) and undergo major developmental changes in the auditory system during the third trimester of pregnancy in the uterus. Human fetuses already have substantial capacity for auditory learning and memory in the uterus, whereas rats and mice cannot hear until postnatal day 13 (P13). Although auditory experiences in the early postnatal period around hearing onset significantly influence synaptic

plasticity and neuronal activities in rodents, there is little known about fetal development of the auditory nervous system before and after hearing onset in primates. We have studied whether sound experience after hearing onset in uterus critically influences the auditory development to ensure the anatomical and functional formation of synapses and neural circuitry of the auditory nervous system in primates. Using non-human primate, baboon brain tissues, we examined the effect of sound experience in uterus on developmental profiles: 1) excitatory and inhibitory inputs, 2) neuronal morphology, and 3) structural plasticity of axon initial segment (AIS) in the medial superior olivary nucleus (MSO) in the auditory brainstem from preterm (67% and 80% of GA) and term baboons. We observed an increase in the size of VGluT1- and VGAT -positive synaptic vesicles and also increase in the complexity of dendrites of MSO neurons from 80% of GA preterm and term baboon brains (after hearing onset), compared to the brain at 67% of GA preterm (before hearing onset). In addition, the length of the AIS, which is a specialized axonal region where action potentials are initiated, of MSO neurons became shorter during fetal development and this structural plasticity in the AIS length occurs more distinctly in that ventral MSO, which is in turns showing the tonotopic organization of the AIS after hearing onset. We tested the effect of different auditory environment in the NICU for preterm baboons on the tonotopy of the AIS of MSO neurons. We found that the tonotopy of AIS length (shorter ventral AIS and longer dorsal AIS) was not developed in MSO neurons from 2 weeks-NICU-experienced preterms (80% of GA). The results suggest that sound-evoked neuronal activities in uterus affect the tonotopic organization of the AIS in the MSO. Taken together, prenatal auditory inputs in uterus influence the structural and functional development of the auditory brain circuit. Funding: Southwest National Primate Research Center (SNPRC) Pilot Grant and NIDCD R01 to J.H.K.

PS 876

Audiometric and Histological Assessment of Serotonin Transporter (SERT) Mutant Mice

Ye-Hyun Kim[1]; Hamad A. Javaid[2]; Amanda M. Lauer[2]
[1]*Johns Hopkins School of Medicine, Department of Otolaryngology-Head and Neck Surgery, Center for Hearng and Balance;* [2]*Johns Hopkins University School of Medicine, Department of Otolaryngology - Head and Neck Surgery, Center for Hearing and Balance*

Background Recent advances in molecular genetic techniques are rapidly enhancing our understanding of functional role of specific neuronal populations or circuits in behavior, including hearing dysfunction. Critical to this approach is a thorough auditory phenotypic assessment of mutant strains to establish suitability for hearing re-

search. Previous work has implicated the serotonergic system as a neuromodulator in the peripheral and central auditory pathways. Serotonin transporter (SERT) is an important regulator for serotonin that is expressed in auditory pathway. As an initial step in exploring the role of SERT on auditory function, we characterized the auditory phenotypes of SERT mutant mice. Methods Two mutant strains, SERT Knock-out (KO) (Slc6a4 -/-; C57BL/6J background; The Jackson Laboratory) and SERT-EGFP reporter mice (Slc6a4-EGFP-BAC; CD1 background; GENSAT; line RP23-39F11 BAC BX86), were used. Hearing sensitivity and behavioral reactivity to sounds in these mice were assessed by auditory brainstem response (ABR) and acoustic startle response (ASR). To examine the expression pattern of SERT in peripheral and central pathways, cochleae and brain sections from SERT-EGPF reporter mice were processed for fluorescence imaging, and were compared against SERT immunoreactivity in CBA/CaJ mice. Results SERT KO mice are completely deficient of serotonin reuptake and have dysregulated serotonin level. SERT KOs and SERT Heterozygotes (HET) mice showed normal ABR and click thresholds during young adulthood. ASR reactivity to sounds was also normal in both SERT KO and SERT HET mice. SERT KOs, however, showed increased reactivity to loud sounds after unilateral sound exposure, while HETs did not. ABR threshold shifts were exaggerated in the sound exposed ear for both SERT KOs and HETs. SERT-EGFP reporter mice show targeted expression of enhanced green florescence under the Scl6a4 promoter. EGFP was heavily expressed in dorsal cochlear nucleus, granule cell domain of cochlear nucleus, and inferior colliculus. This expression pattern was similar to SERT expression in normal hearing mice. SERT-EGPF reporter mice, however, exhibited severe hearing loss during early adulthood that was progressive with age, as evidenced by elevated ABR thresholds (> 75 dB SPL) across all frequencies tested. Backcrossing of the SERT-EGPF reporter mice to CBA/CaJ background rescued the ABR thresholds to normal levels and remained stable throughout adulthood. Conclusions Our result highlights the importance of establishment of proper control and potential utility of SERT mutant mice in hearing research.

PS 877

Effects of Auditory Experience in Structural and Functional Development of Auditory Brainstem Neurons

Eun Jung Kim[1]; Michael Patton[1]; Jun Hee Kim[2]
[1]*Department of Cellular and Integrative Physiology, University of Texas Health Science Center;* [2]*UTHSCSA*

Auditory experience in the critical period, a time during which the nervous system is especially sensitive to cer-

tain environmental stimuli, is significantly involved in brain development. Many studies have reported a strong correlation between auditory experience in the early postnatal environment and topographical and structural development of the auditory system. Our previous study in non-human primate, baboon, suggests that early auditory experiences in uterus after hearing onset significantly influence synaptic plasticity and refinement in the auditory brainstem. In addition, heminodal sodium channel clustering is progressively formed around hearing onset while in deaf mouse, the sodium channels did not form clusters and maintained a broad expression. Here we investigate the effect of enhanced sound stimulation below the noise level immediately after hearing onset on the structural and functional plasticity of auditory brainstem neurons. We demonstrate that enhanced sound experience after hearing onset influence the structural and functional development of auditory neurons and consequently affect proper formation of the auditory circuit. Using the auditory brainstem response (ABR) test and immunostaining assay, we found that sound stimulation (80 dB, 16 kHz, 3 hrs for 7 days from P13 to P19) increase the amplitude of ABR waves without changes in the threshold, and c-fos expression in the MNTB of mouse auditory brainstem, comparing with control at the same age without additional sound stimulation. It suggests that neuronal activities in auditory brainstem neurons are increased in response to sound stimulation. To verify the effect of sound stimulation on the structural properties of neurons, we examined the axonal structure, the axon initial segment (AIS) of the MNTB principal neurons in control, deaf mice, and the sound-stimulation group. We found that the length of AIS in the MNTB was significantly decreased by ~20% in the sound-stimulation group, whereas it was significantly increased by ~40% in deaf mice, suggesting that sound-induced neuronal activities regulate the structural plasticity of the AIS in auditory neurons. In addition, in control with normal hearing, the length of the AIS depends on the tonotopic axis (shorter AIS in the medial MNTB neurons and longer AIS in lateral MNTB neurons). This tonotopic organization of the AIS was disappeared in deaf mice and enhanced in the sound stimulation group. Our results suggest that sound experience is critical in regulating the structural development of auditory neurons along the tonotopic axis in auditory system. Funding: NIDCD R01 to J.H.K.

PS 878

Multi-electrode Recording Analysis in the Rat Auditory Brainstem suggests that the Developmental Increase in Spontaneous Neuronal Activity before Hearing Onset is Mediated by Co-activation of Local Clusters.

Geng Pan[1]; Mariano N. Di Guilmi[2]; Krithikka Ravi[1]; Cheikh Babou[1]; Adrian Rodriguez-Contreras[1]
[1]City University of New York, City College; [2]Instituto de Investigaciones en Ingeniería Genética y Biología Molecular (INGEBI/CONICET)

Before the onset of hearing around postnatal day 12 (P12), auditory neurons in the medial nucleus of the trapezoid body (MNTB) and the inferior colliculus (IC) of rats fire spontaneous bursts of action potentials that originate in the inner ear (Tritsch et al. 2010. Nature Neurosci. 13:1050-1052). To fully understand the significance of spontaneous burst firing for the development of the central auditory system requires knowledge of the activity patterns in populations of auditory neurons, including how patterns of activity are affected by anesthesia, and eventually how experimental manipulations of activity during the prehearing stage affect hearing development in the short and the long term. In this study we recorded extracellular action potentials with multi-electrode arrays placed in the MNTB of Wistar rat pups anesthetized with isoflurane or ketamine/xylazine mix (n=30 pups). Electrophysiology recordings showed that multi-unit activity increased during postnatal development, being detected as early as P3 in ketamine/xylazine anesthetized pups (multi-unit range 0-10 spikes/s), but with a marked increase at P6 in both, isoflurane (multi-unit range 0-15 spikes/s) and ketamine/xylazine (multi-unit range 0-30 spikes/s) conditions. Cross correlation analysis of multi-unit activity simultaneously recorded across 16 recording sites at P9 revealed a moderate relationship between Pearson';s correlation coefficient and distance, with correlation coefficient values >0.6 observed predominately at distances of 50 µm and 100 µm (pairwise comparison range 50-450 µm; spike detection threshold 7 standard deviations above the mean; n=4 pups). Furthermore, spike sorting of multi-unit activity confirmed individual unit spike trains with inter-spike interval histograms that are consistent with burst firing described in previously published single-cell recordings. These preliminary results suggest that local activation of neuronal clusters is a predominant pattern of ensemble activity in the MNTB before hearing onset and that either changes in the number of neurons per cluster, the number of co-active clusters or both, can explain the increase in action potential firing recorded with multi-electrode arrays. Ongoing studies are focused in cross correlation analysis of simultaneously recorded individual spike trains, the cellular mechanisms that generate co-active clusters, and

how anesthesia affects burst firing and multi-unit activity levels in awake animals.

PS 879

Envelope-Following and Frequency-Following Responses Elicited by Signals of Increasing Complexity

Michelle R. Molis; William J. Bologna; Brandon M. Madsen; Amie Roten; Ramesh Muralimanohar; Caitlin E. Milligan; Curtis J. Billings
VA RR&D National Center for Rehabilitative Auditory Research (NCRAR)

Background According to the source-filter theory of speech production, voiced speech can be described as the output of a two-stage process where a periodic voicing source is generated by vocal fold vibration and then filtered by the shape of the vocal tract above the larynx. This process produces an acoustic signal in which the source can be related to the pitch of a voiced sound, and the filter to the spectral shape of the sound. Electrophysiological recordings of both the envelope-following response (EFR) and the frequency-following response (FFR) have demonstrated that the periodic envelope and fine structure of short syllables can be encoded by phase-locked brainstem neural responses. The motivation for this study was to determine the extent to which the acoustic characteristics of the vocal source and supralaryngeal filter are represented electrophysiologically in the brainstem in response to signals of increasing acoustic complexity. Methods EFRs/FFRs were recorded from younger adults with normal hearing in response to several stimulus types: a single 500 Hz tone, a multi-component harmonic complex approximating a vocal source with a 104.5-Hz fundamental frequency (F0), a combination of the tone and the harmonic complex, and a harmonic complex with a simulated formant-like peak at 500 Hz and an F0 of 104.5 Hz. All stimuli were 120 ms in duration and were presented at 80 dB SPL. Results As expected, the single tonal component elicited FFR responses at 500 Hz and minimal activity in the EFR. The synthetic vocal source elicited EFRs consistent with its F0 and harmonic structure. When both the 500-Hz tonal component and vocal source were present, EFRs and FFRs encoded the F0 of the periodic source and the frequency of the tonal component, respectively. Responses to the formant stimulus revealed robust representations of the F0 in the EFR and increased amplitude of the FFR at harmonic frequencies in the region of the formant peak (i.e., 418 Hz and 522.5 Hz). Conclusions These results suggest that physiological encoding of spectrotemporal features in the auditory system can be decomposed into corresponding source and filter components in the firing patterns observed in the brainstem. Implications will be discussed in terms of the extent to which formant transitions and other dynamic aspects of speech may be represented physiologically in the auditory system. [Work supported by NIH/NIDCD R01 DC12314 (Molis) and R01 DC015240 (Billings)]

PS 880

The Frequency-Following Response (FFR): Normative data in newborns for a potential cognitive disabilities biomarker

Teresa Ribas-Prats[1]; Laura Almeida[2]; Jordi Costa-Faidella[1]; Montse Plana[2]; Mj Corral[1]; M. Dolores Gómez-Roig[2]; Carles Escera[1]
[1]Institute of Neurosciences; [2]Institut de Recerca Sant Joan de Déu

The frequency-following response (FFR) is a non-invasive electrophysiological measurement of the encoding of the temporal and spectral characteristics of the evoking sound in a cortico-subcortical auditory network. Abnormal FFRs are found in children with auditory processing disorders, dyslexia and autism. Thus, the FFR may offers a neurophysiological marker of the efficient encoding of speech sounds related to literacy abilities. The FFR as a potential predictor of communication skills has been shown in school-aged children and in infants with ages between 3 and 10 months. Yet little is known about the neural transcription of speech sounds in newborns. The possibility to record FFR in newborns has been suggested in no more than ten studies so far, showing a remarkable similarity between the adult and the newborn responses. However, before the FFR can be used in the clinics, normative values need to be established.

The aim of this study is the establishment of a normative database depicting the standard variability found in different parameters extracted from the newborn FFR. The FFR was recorded from a sample of 50 neonates aged 12-144 hours after birth, to syllables /da/ and /ga/ (170 ms long; F0=113 Hz; intensity: 55 dB SPL, 2000 sweeps, delivered with alternating polarities). Newborns were included after passing the universal hearing screening. Four subjects were subsequently excluded because wave V could not be identified. The F0 signal-to-noise ratio (SNR) was strongly represented in most newborns (SNR /da/: mean=3.98, SD=2.44; SNR /ga/: mean=3.94, SD=2.10) and differed statistically between tokens ($t(45)=-3.49$, $p=0.001$), with two outliers (SNR<1.5). Higher harmonic components were not reliably present in all subjects. In the time domain, onset latencies were assessed (/da/: mean=10.06 ms, SD=1.42; /ga/: mean=9.70 ms, SD=1.01; $t(45)=3.084$, $p=0.003$), indicating that the stimulus with the highest second formant (/ga/) elicited a faster response than the stimulus with the mid-frequency formants (/da/), in agreement

with previous studies. Other objective indices have been studied to evaluate the accuracy and strength of pitch processing. Our study confirms the feasibility of recording the FFR in newborns at the maternity unit from the very onset of life and provides normative data from a preliminary sample of 46 newborns. Detecting an abnormal FFR in a newborn could lead to an early intervention that, given the plasticity of the underlying neurophysiological machinery, could promote an improvement in the encoding of speech sounds and thus avoid cognitive impairment.

PS 881

Mice with Cdh23/Ahl mutation show severe age-related deficits in temporal processing

Alice Burghard[1]; Nazli Morel[2]; Douglas Oliver[1]
[1]*UConn Health;* [2]*UConn*

Genetically modified mice are a powerful tool in various areas of research including the auditory system. Unfortunately, many genetically modified mice are created on a C57BL/6 background. A recessive point mutation on chromosome 10 of the Cdh23 gene (G>A at 753) leads to the age-related hearing loss phenotype commonly observed in this mouse strain. To investigate if this point mutation also affects temporal processing abilities earlier in life we compared Cdh23753A/A homozygote mice to Cdh23753G/A heterozygote mice at different ages. Both mouse strains were on a C57BL/6 background. The heterozygote strain was obtained since it contained one copy of the wildtype Cdh23 gene (B6.CAST-Cdh23Ahl+/ Kjn (B6.CAST)), and the other strain was cross-bred with it to introduce the wildtype gene into the colony (VGAT-ChR2 (H134R)-EYFP (VGAT) x B6.CAST). All experimental animals were genotyped via Saenger sequencing to define the experimental groups. The overall hearing abilities were tested using click-evoked auditory brainstem responses as well as the amplitude-modulation following response (AMFR). The latter was used to assess the temporal processing abilities of the animals in addition to generating an audiogram. Both groups of animals were tested at young (1-3 month), middle (6-7 month) and old age (11-12 month). For the audiogram, the AMFR stimuli had a 0.3 octave narrow-band noise carrier frequency and a 42.9 Hz modulation frequency (MF) shaped by a sine wave raised to the exponent 8. To test the temporal processing abilities, the frequency with the lowest threshold was stimulated at 30 dB above threshold and the MF was varied from 17-432 Hz in 1/3 octave steps. AMFR peak synchrony and jitter as well as peak amplitude were used to analyze temporal processing abilities. At young age, both strains did not differ in hearing threshold across the tested frequency range or in peak synchrony in response to different MFs. At 6 months of age, the Cdh23753A/A mice showed a

threshold shift for frequencies ≥ 16 kHz, but no change in peak synchrony at supra-threshold levels. The opposite was the case for the older Cdh23753G/A mice. They showed no change in hearing thresholds compared to younger mice of the same genotype, but they did show a mild decline in the peak synchrony at MFs > 100 Hz. The old Cdh23753A/A mice, however, showed a more pronounced decline in peak synchrony compared that started at MFs < 100 Hz in addition to a hearing threshold shift spanning the whole audiogram. In conclusion, mice which are homozygote for the single nucleotide mutation on gene Cdh23 show a greater decline of temporal processing abilities with increasing age as well as the expected hearing loss.

PS 882

Impaired Temporal Processing in the Auditory Brainstem and Midbrain of Alpha 7 Nicotinic Acetylcholine Receptor-deficient Mice

Richard Felix II[1]; Vicente Chavez[1]; Barbara Morley[2]; Christine Portfors[1]
[1]*Washington State University Vancouver;* [2]*Boys Town National Research Hospital*

Background
Resolving the coarse temporal structure of sound is critically important for speech recognition, which suggests that deficits in the extraction of temporal cues can contribute to auditory processing disorders. A potential key mediator of temporal feature extraction is the alpha 7 nicotinic acetylcholine receptor (α7 nAChR), which has been implicated in forming secure synapses in auditory brainstem circuits specialized for encoding coarse temporal information. This notion is supported by genetic studies that have linked the disruption of α7 nAChR expression to common neurodevelopmental disorders that include deficits in auditory temporal processing. Thus, a closer examination of the role of the α7 nAChR in auditory function is warranted.

Methods
We compared auditory responses in α7 nAChR knockout mice and age-matched colony controls. We measured auditory brainstem responses and recorded single-unit extracellular responses from the auditory brainstem and midbrain in unanesthetized, restrained mice of both sexes. We mapped the excitatory frequency response areas of neurons in the superior paraolivary nucleus, ventral nucleus of the lateral lemniscus, and inferior colliculus; regions that represent a presumptive circuit specialized for coarse temporal processing. In addition, these nuclei exhibit high levels of α7 nAChR expression in the developing auditory system. Temporal acuity to sound stimuli

was assessed by measuring gap detection and forward masking thresholds of responses, as well as spiking fidelity to changes in envelope modulation.

Results

We found degraded temporal responses for α7 nAChR knockouts versus controls in each nucleus despite no difference in audiometric hearing thresholds. For knockouts, neurons in each nucleus exhibited an average increase in the variability of evoked spike timing, an increase in gap detection thresholds, and a decrease in forward masking thresholds compared to controls. In addition, the overall strength of response synchronization to low rates of envelope modulation in knockouts was weaker than that of the control group.

Conclusion

The temporal response properties of neurons in the auditory brainstem and midbrain are shaped by α7 nAChRs. Disruption of α7 nAChR-mediated signaling may impair the extraction of temporal features of complex sounds, which could ultimately impact speech perception. Therefore, our findings have implications for understanding mechanisms of temporal processing in the normal-functioning auditory system as well as in conditions of deficient α7 nAChR function.

Auditory Pathways Brainstem V

PS 883

A Human Envelope-following Response Model for Studies of Hearing Impairment

Sarah Verhulst[1]; Alessandro Altoè[2]; Viacheslav Vasilkov[3]
[1]Ghent University; [2]Department of Signal Processing and Acoustics, Aalto University; [3]Oldenburg University

The increased interest in auditory-evoked potentials as a diagnostic tool for "hidden" hearing loss has resulted in a search for sensitive stimulus paradigms that can quantify synaptopathy in the presence of other hearing deficits (e.g., outer-hair-cell (OHC) loss). As patients may have unknown frequency-dependent combinations of peripheral hearing deficits, it is important to study how these deficits interact and affect auditory-evoked potentials. Broadband models of the human auditory periphery can help to disentangle the contribution of different hearing deficits to evoked potentials, because the model';s "hearing-loss" parameters can be modified independently to simulate specific combinations of hearing deficits.

In this work, we present a computational model of the human auditory periphery that was designed to capture both the level-dependent properties of auditory brainstem responses (ABR) and the amplitude modulation characteristics of envelope following-responses (EFR). This was achieved by: (i) representing the cochlear mechanics by a transmission-line model that can simulate different degrees of outer-hair-cell deficits in specific cochlear regions; (ii) including a biophysical model of the inner-hair-cell (IHC) and auditory-nerve (AN) complex that accounts for the voltage-dependent activation of IHC basolateral potassium channels, which improved single-unit AN phase-locking, dynamic range, modulation gain and synchrony-level responses over previous implementations.

The combination of a biophysical model of the IHC with a mechanical model of the cochlea accounts for key-features of human ABR and EFR simultaneously. Using this model, we estimated the relative contributions of on and off-frequency peripheral sources to the generation of the EFR. In particular, off-frequency neurons phase-lock to the stimulus envelope more strongly than on-frequency neurons for SPLs between 60 and 80 dB, thus greatly contributing to the generation of the pure-tone carrier EFR. Finally, we estimated how the contribution of the different EFR sources changes for various profiles of hearing impairment. Synaptopathy of LSR fibers resulted in shallower growth of the 70-90 dB pure-tone carrier EFR, whereas high-frequency OHC loss did not affect the growth slope but yielded overall higher EFR amplitudes in that same stimulus range. However, OHC loss did result in steeper EFR growth for stimulus levels between 50 and 70 dB than found for the LSR synaptopathy and normal-hearing models. Taken together, the EFR model offers a tool to develop sensitive ABR and EFR metrics that can disentangle different aspects of peripheral hearing loss.

PS 884

Impaired topographic map refinement and synaptic strengthening of an inhibitory auditory microcircuit in juvenile and adult Otoferlin knock-out mice

Nicolas Müller[1]; Mandy Sonntag[2]; Eckhard Friauf[1]
[1]Department of Biology, University of Kaiserslautern; [2]Paul Flechsig Institute for Brain Research

During development, sensory neural circuits are established broadly, becoming subsequently refined in an activity-dependent manner involving spontaneous activity prior to sensory input. In the auditory system, the impact of spontaneous activity on circuit refinement is less well

described than in the visual or somatosensory system, especially for inhibitory projections. Spontaneous pre-hearing activity is generated in the cochlea, and the activity pattern is conserved in downstream nuclei. Here we studied P11 Otoferlin^{deaf5/deaf5} mice to assess the role of spontaneous activity on circuit refinement of the inhibitory projection from the medial nucleus of the trapezoid body (MNTB) to the lateral superior olive (LSO). Otoferlin is highly expressed in the cochlea, but not in MNTB and LSO. Otoferlin^{deaf5/deaf5} mice show a strongly reduced vesicle exocytosis from inner hair cells. In line with this, in vivo recordings in the MNTB suggest a lower number of spiking units. Furthermore, the frequency of residual MNTB spike activity was reduced and showed atypical patterns. Focal flash photolysis of caged glutamate in the MNTB while recording from LSO neurons in acute slices from Otoferlin^{deaf5/deaf5} mice revealed a 2-fold broader mediolateral and dorsoventral input width. This strongly implies impaired synapse elimination, resulting in a distorted and imprecise topographic map. Besides synapse elimination, synaptic strengthening is a hallmark of circuit refinement. To address synaptic strengthening, we recorded from LSO neurons while stimulating MNTB fibers with stepwise increasing stimulus amplitude, thereby gradually recruiting convergent MNTB fibers. The number of MNTB fibers in Otoferlin^{deaf5/deaf5} mice was increased by 50%, confirming the impaired elimination seen in the glutamate uncaging experiments. Furthermore, the single fiber strength was reduced by 40%, demonstrating impaired synaptic strengthening. We determined quantal parameters and found a 40% lower quantal content per MNTB fiber. Fluctuation analysis revealed that the reduced quantal content was due to 40% fewer release sites per fiber, whereas the release probability of a release site was normal. Stepwise stimulation experiments in young adult (P30+) controls showed no further synapse elimination compared to P11. In P30+ Otoferlin^{deaf5/deaf5} mice, single fiber strength stayed immature, which can also be explained by a lower quantal content and fewer release sites. In conclusion, we demonstrate the requirement of spontaneous prehearing activity in topographic map refinement and strengthening of the inhibitory MNTB-LSO circuit. Our findings are novel in that they address effects of lacking spontaneous activity restricted to the cochlea and shed light on adult circuit refinement.

PS 885

Bimodal Hearing Disrupts Normal Brainstem ITD Processing in Children

Melissa J. Polonenko; Blake Papsin; Karen Gordon
The University of Toronto; The Hospital for Sick Children

Objective
To evaluate brainstem and behavioural processing of interaural timing differences (ITD) in children with bimodal compared to normal hearing.

Background
Perception of binaural cues is important for localizing sound and listening in noisy environments. While providing one cochlear implant (CI) and one hearing aid in the non-implanted ear (bimodal) stimulates the bilateral auditory pathways, delivering sound through two independent devices with substantially different timing delays to the auditory system may impede binaural processing in the brainstem and compromise binaural hearing development. Given these significant inter-device delays, we hypothesized that binaural brainstem processing and behavioural detection of ITDs would only occur at large ITDs lead by the slower hearing aid ear.

Methods
Seventy-eight children participated in this study: 28 children with normal hearing (mean±SD age 13.3±3.1 years) and 50 bimodal users (9.3±4.6 years) who received their CI (left:right ear n=29:21) at age 6.8±5.0 years and had used bimodal hearing for 2.4±2.3 years. Electrophysiological measures of brainstem activity were evoked in the implanted ear by biphasic electrical pulses and in all non-implanted ears by broad-band clicks at 11 Hz at maximum comfortably loud levels. Stimuli were presented unilaterally and bilaterally at ITDs ranging from 0 to 3 ms leading from both ears.

Results
Peak latencies of unilaterally evoked brainstem responses were more asymmetric (3.09±1.28 ms) in children with bimodal hearing than normal hearing peers (0.02±0.36 ms) (F(1,76)=225.6, p<0.001) and their responses to bilateral stimuli contained multiple peaks at most ITDs at latencies corresponding to the unilateral wave V latencies. As ITDs led increasingly from the non-implanted ear, asymmetries in the unilateral latencies decreased (mixed effects linear regression: $\chi^2(1)=125.6$, p<0.001) and a single peak was observed in the bilateral response. For children with normal hearing, multiple peak responses were only observed at ITDs beyond the physiological limit (≥1ms) for bilateral stimuli leading from either ear. To assess binaural integration, the single and multi-peak

bilateral responses were compared with the sum of the unilateral responses (binaural difference (BD)) across ITDs. BD amplitude and latency measures were compared with behavioural ITD detection assessed through binary logistic functions.

Conclusion

Bimodal users experience significant device-related peripheral timing delays that impacts brainstem processing of ITDs, potentially limiting spatial hearing compared to normal. Future studies will investigate whether correcting for large internal delays can promote a fused image of bilateral input and allow perception of ITDs leading from either ear.

PS 886

Tonic Activation of GluK1-Containing Kainate Receptors Regulates Inhibitory Circuitry in the Dorsal Cochlear Nucleus

Zhengquan Tang; Laurence Trussell
Oregon Hearing Research Center, Vollum Institute, Oregon Health and Science University

Unlike NMDA and AMPA receptors which dominate excitatory synaptic transmission in the brain, kainate receptors (KARs) act principally as modulators by modifying neuronal excitability and synaptic efficacy in the CNS. However, the role of these receptors in auditory processing is not well understood. To address this, we examined such modulation in the dorsal cochlear nucleus (DCN), a circuit in the first stage of auditory processing, by combining electrophysiological and pharmacological approaches in acute brain slices from P16-30 mice. Among different subunits including GluK1-5, GluK1 subunits are primarily expressed in interneurons and contribute to both pre- and post-synaptic KARs populations. Given pharmacological tools that are available to distinguish GluK1- from GluK2-/GluK3-containing KARs, we were particularly interested in determining how GluK1-containing KARs (GluK1-KARs) modulates DCN circuit activity.

Using extracellular recordings, bath application of UBP-302, a GluK1-selective KAR antagonist, decreased the spontaneous spike rate in a subpopulation of cartwheel interneurons. By contrast, ATPA, a GluK1-selective KAR agonist, increased spontaneous spike activity, as did nanomolar levels of domoic acid. In whole-cell current-clamp recordings, ATPA increased the probability of spikes evoked by somatic current injection, suggesting that GluK1-KARs enhance excitability. Dual recordings from synaptically connected cartwheel cell-fusiform cell pairs showed that ATPA did not affect unitary inhibitory postsynaptic currents in fusiform cells evoked by spikes

in cartwheel cells, and thus GluK1-KARs do not directly affect cartwheel cell-fusiform cell inhibitory synapses. Taken together, these data indicate that functional GluK1-KARs are present in neuronal processes or soma of cartwheel cells and are activated by ambient transmitter. Surprisingly, UBP-302 also decreased the amplitude of spontaneous or parallel fiber-evoked excitatory postsynaptic currents in cartwheel cells, suggesting that tonic activation of GluK1-KARs on presynaptic granule cell axons maintains a positive tone of glutamate release onto cartwheel cells. Based on these observations, we predicted that tonic activation of Gluk1-KARs enhances coupling between spike activity in parallel fiber and spike initiation in cartwheel cells. Accordingly, under current-clamp conditions, UBP-302 decreased the firing probability of cartwheel cells in response to parallel fiber spikes.

Our findings demonstrate that tonic activation of GluK1-KARs by ambient glutamate not only directly enhance excitability, but also maintain a tonic positive tone in excitatory inputs impinging on cartwheel cells. Given that cartwheel cells are spontaneously active, these results suggest a role of ambient glutamate in regulating such activity

PS 887

Characterization of Cholinergic Efferent Neurons Using ChAT-tauGFP mice.

Hiroki Takeda; Samuel Gubbels; **Anna Dondzillo**
University of Colorado, Department of Otolaryngology

Presbycusis, or age related hearing loss, affects 11% of the US population aged 50-59 and 25% of the population at ages 60-69 (2011-2012 survey[1]). Age related changes occur in the entire auditory system: peripheral and central nervous system at cellular and connectome levels. Hair cell death is well established as a causal factor of hearing loss with age. However, growing anatomical and physiological evidence suggests that the initial change seen in presbycusis involves synaptic rearrangements at the hair cells.

The inner ear both sends information to and receives feedback from the auditory brainstem. In the adult, the OHCs receive axosomatic input from Medial Olivocochlear (MOC) neurons. The Lateral Olivocochlear (LOC) axodendritic input terminates on the IHC afferent fibers. In contrast, in young mammals inner hair cells receive direct inhibitory cholinergic synaptic input from MOC neurons that disappears at around hearing onset in mice. Recent reports using electron microscopy and whole cell electrophysiology have shown that cholinergic inhibitory synapses re-emerge on IHCs in the aged

cochlea (Lauer et al., 2012; Zachary and Fuchs, 2015). To understand the role that these re-emerged synapses play in presbycusis it is necessary to establish where the projecting neurons are located. Whether they originate from the same population of neurons that send transient projections to the IHC before hearing onset, or whether they comprise a different neuronal population, is not well understood.

In this study we explore the feasibility of using a ChAT-tauGFP expressing mouse in tracing the neuronal pathways and synaptic terminals in mice at different ages. The ChAT-tauGFP mouse expresses tauGFP fusion protein under the promoter of choline acetyltransferase. We also use retrograde neuronal tracing delivered via round window membrane injection and immunohistochemistry to identify neurons projecting to the cochlear sensory epithelium. In both wild type C57BL/6 and ChAT-tauGFP, we analyze synapses on the inner ear hair cells, auditory dye or GFP labeled auditory pathways and source neurons projecting to the cochlea.

PS 888

Complex Statistical Model for Detecting the Auditory Brainstem Response to Natural Speech and for Decoding Attention from High-Density EEG Recordings

Mikolaj A. Kegler; Octave Etard; Antonio E. Forte; Tobias Reichenbach
Imperial College London

Background
The auditory brainstem responds to the fundamental frequency of a short repeated speech signal. A recent study showed that the brainstem response to continuous, non-repetitive speech can be measured as well. This involved the computation of a fundamental waveform that oscillates at the fundamental frequency of the voiced parts of speech. The correlation of this fundamental waveform with the neural activity measured from a few scalp electrodes revealed a brainstem response at a latency of 9 ms. In addition, the response was modulated by selective attention to one of two competing speakers. Here we sought to develop a statistical model to measure this response of the auditory brainstem to continuous speech from high-density EEG recordings, and to decode attention to one of two speakers from short time segments.

Methods
We employed linear regression with regularization to map the fundamental waveform of a speech signal to the high-density EEG signal at different delays. We then attempted to decode attention to one of two simultane-

ous speakers from the EEG data through the brainstem response. We employed linear regression models to reconstruct the fundamental waveform of an attended as well as of an ignored speaker from the neural recordings. We assessed the accuracy of each model through the correlation of the fundamental waveform and its reconstruction. We then employed linear discriminant analysis to classify the obtained accuracies according to the attentional focus.

Results
The developed regression model showed a brainstem response at a delay of 9 ms, and yielded a topographic map of the amplitude and phase of the brainstem response at each electrode. The delay and the topography of the response were consistent with previous studies that employed short repeated speech stimuli. We assessed the accuracy of the developed method for decoding attention and obtained a high accuracy of over 90% using short segments of neural data of a few seconds in duration only.

Conclusions
We showed that it is possible to detect the auditory brainstem response to natural speech from high-density EEG recordings. This allows to measure the response of the auditory brainstem as well as of cortical responses to continuous speech simultaneously. The decoding of a subject';s attentional focus from one second or more of EEG data demonstrates that attention can be assessed effectively from the auditory brainstem response to continuous speech.

PS 889

Evidence for the Origin of the Binaural Interaction Component of the Auditory Brainstem Response from Single-Unit Responses in the Gerbil Superior Olivary Complex

Sandra Tolnai[1]; Georg M. Klump[2]
[1]*Cluster of Excellence Hearing4all and Carl-von-Ossietzky University Oldenburg;* [2]*University of Oldenburg*

Auditory brainstem responses (ABR) allow for the objective measurement of a subject's hearing ability. Derived from the ABR, the so-called binaural interaction component (BIC) has gained attention as a potential tool to measure binaural auditory processing abilities. The BIC is revealed if the sum of the ABRs to monaural left and monaural right stimulation is subtracted from the ABR to binaural stimulation. The difference in activation under monaural versus binaural stimulation is indicative of neural binaural processing. To date, the sources of the BIC are still being discussed. Because an interac-

tion between excitation and inhibition might play the key role in the generation of the BIC, likely candidate source regions are the lateral superior olive (LSO) and the medial superior olive (MSO). Also, stimuli with interaural time differences (ITD) strongly affect the BIC; its amplitude decreases with increasing ITD and its latency increases. Determining the measures from single-unit (SU) responses and local-field potentials (LFPs) in the same way as for determining the BIC would allow for a comparison between these measures and the ABR-related BIC recorded at the same time. Observing similar properties of the BIC and SU and LFP measures would provide evidence about the source of the BIC.

We recorded LFPs and SU responses to monaural and binaural click stimuli with a range of ITDs from sites in the LSO and MSO of ketamine/xylazine-anaesthetised Mongolian gerbils while simultaneously acquiring ABRs from superficially placed electrodes. The BIC-like measure was calculated from averaged voltage traces (LFP, ABR) or, in the case of SU responses, from peri-stimulus time histograms (PSTH). The amplitudes of the largest negative deflection of those BIC-like measures were extracted.

In the LSO, the LFP-related BIC-like amplitudes did not mirror the characteristics of ABR-related BIC amplitudes while the PSTH-related BIC-like amplitudes did. In the MSO, neither the LFP-related nor the PSTH-related BIC-like amplitudes mirrored the ABR-related BIC amplitudes. Those results suggest that the output of units in the LSO contribute substantially to the BIC estimated from the ABR. The input to LSO units (measured in the form of LFPs) and the input and output activity of MSO units (measured in the form of LFPs and PSTHs, respectively) seem to play a rather marginal role in defining the ABR-related BIC. The results are consistent with the observation by Ungan and Yagcioglu (Hear Res 2002; 167(1-2):81-101) demonstrating the largest BIC measured from LFP at sites in the cat';s auditory brainstem at which lemniscal fibres terminate in the nuclei of the lateral lemniscus.

PS 890

Distribution patterns of low and high voltage activated potassium channel sub-units in neurons of the medial superior olive

Alisha Nabel[1]; Alexander Callan[1]; Sarah Gleiss[1]; Christian Leibold[2]; **Felix Felmy**[3]
[1]*Division of Neurobiology, Department Biology II, Ludwig-Maximilians-University München;* [2]*Bernstein Center for Computational Neuroscience Munich;* [3]*Institute for Zoology, Universtiy of Veterinary Medicine Hannover*

Neurons in the medial superior olive (MSO) perform ultra-fast coincidence detection of binaural inputs. The low input resistance of MSO neurons is one important factor in this rapid process. The accompanying leak current is partially based on the expression of low voltage activated potassium currents (KLT). The KLT amplitude is largest at the soma leading to a normalization of EPSP size propagating from dendrite to soma. Overall, somatic voltage excursions are kept small by KLT. Conversely, dendritic voltage excursions might become very large during episodes of high synaptic input because of the lower dendritic KLT density. The size of dendritic voltage excursions might reach levels that can gate high voltage activated potassium channels (KHT). So far it is unclear, whether MSO neurons express KHT channels and what their functional significance might be.

We determined from immunohistochemical stainings the sub-cellular distribution of KLT and KHT channel sub-units. The channel presence was verified pharmacologically with in vitro whole-cell recordings from MSO neurons of adult gerbils.

KLT sub-units Kv1.1 and Kv1.6 were more prominent at the soma, while Kv1.2 was also present at the dendrite. Two families of KHT sub-units were detected. Kv2.1 and Kv2.2 were located throughout the dendritic extent. A similar distribution pattern was found for Kv3.1b while Kv3.2 channels were biased towards the soma. In the presence of DTX, somatic potassium currents persisted, verifying the presence of channels other than KLT/Kv1.x. Application of low concentrations of TEA eliminated some of this residual current, supporting the presence of Kv3.x channels. Finally, when TEA and 4-AP were added, a remaining high voltage activated current was observed, consistent with the presence of Kv2.x channels. A multicompartmental model indicated that dendritic KHT channels are able to reduce the size of synaptically evoked voltage excursions. Moreover, the dendritic KHT channels amplify the peak advance of synaptic inputs when propagating along the dendrite. Thus, KHT channels contribute to the spatiotemporal profile of excitatory synaptic inputs. Simulating the integration of excitatory

inputs with different temporal disparities indicated that KHT will also limit the binaurally summed voltage signal.

Taken together, KLT currents are likely generated from Kv1.x heteromultimers, and additional KHT channels are present. Sub-units responsible for KHT are more localized to the dendrites and might interfere with excitatory voltage signaling, leading to smaller and faster EPSPs at the soma. Thus, the precision of postsynaptic integration in MSO neurons most likely relies on both KLT and KHT channels.

PS 891

A Nove Role of Oligodendroglia in Synapse Development and Plasticity in the Auditory Brainstem

Miae Jang[1]; Jie Xu[1]; Eun Jung Kim[2]; **Jun Hee Kim**[1]
[1]UTHSCSA; [2]Department of Cellular and Integrative Physiology, University of Texas Health Science Center

Oligodendrocytes (OLs) produce myelin and facilitate salutatory conduction along auditory axon fibers. During the early postnatal weeks, a number of OLs are present throughout the auditory brainstem including the MNTB nuclei. OLs near synapses detect and respond to neuronal activity. Thus, OLs may participate in modulating synaptic structure and functions during the development of the auditory circuitry. However, their physiological properties and roles in synapse development and plasticity in the auditory nervous system remains largely unexplored. Our recent study showed that a subpopulation of immature premyelinating OLs (CNPase+) is able to generate APs, and is referred to as excitable pre-OLs (Berret et al., 2017), indicating their active role in neuron-glia communication. Here, using electrophysiology, immunostaining, electron microscopy, and the auditory brainstem response test, we investigate the roles of OLs in presynaptic properties and synaptic transmission in the auditory brainstem. We found that OLs modulate neurotransmitter release at presynaptic terminals through secretion of brain derived neurotrophic factor (BDNF), an activity-dependent signal. Cell-specific ablation of BDNF in CNPase+ OLs significantly decrease vesicular glutamate release by reducing the available pool of glutamate vesicles, without altering presynaptic Ca^{2+} channel activation or release probability at the calyx terminal. This reduction was partially recovered by BDNF and tropomyosin receptor kinase B (TrkB) agonist application. The results suggest that OL-derived BDNF functions via TrkB to ensure fast, reliable neurotransmitter release and auditory transmission in the developing brain. This study highlights a novel function for OLs in synaptic transmission and their potential role in activity-dependent refinement of presynaptic terminals in the auditory brainstem. Funding: NIDCD R01 to J.H.K

PS 892

Neural responses to gap-in-noise stimuli in the inferior colliculus and medial geniculate body of BXSB/MpJ-Yaa mice

Jane Mattley; Lucy Anderson; Jennifer F. Linden
UCL Ear Institute

The BXSB/MpJ-Yaa mouse is a powerful animal model for studying the neural mechanisms of gap-detection deficits. Around 30-50% of BXSB/MpJ-Yaa mice have small cortical malformations called ectopias. Previous work has shown that mice with ectopias demonstrate impairment in detecting short gaps in noise compared to mice without ectopias (Clark et al., 2000). Extracellular recordings from the medial geniculate body (MGB) have indicated that neural gap-detection thresholds (defined as the minimum gap duration required to elicit a significant change in firing rate) are longer in ectopic than non-ectopic mice, particularly in the ventral MGB (Anderson and Linden 2016). The proportion of cells with offset responses is also reduced in ventral MGB of ectopic mice, suggesting that the thalamic gap-detection deficit might arise from an offset-response abnormality (Anderson and Linden 2016).

To determine whether neural deficits in gap-in-noise sensitivity and sound-offset responses in ventral MGB of BXSB/MpJ-Yaa mice are inherited from the auditory midbrain, we made extracellular recordings from the inferior colliculus (IC) in 10 ectopic and 10 non-ectopic mice. Mice were anaesthetised with urethane (as in the previous MGB study), and neural responses recorded with 16-channel microelectrode arrays (Neuronexus). We found that in contrast to the previous results from ventral MGB recordings, neural gap-detection thresholds were shorter in ectopic than non-ectopic mice for neurons with V-shaped tuning curves typical of the central IC (ranksum p<0.001; ectopic n=133, non-ectopic n=79). However, in agreement with previous results from the ventral MGB, we also found that the proportion of offset-responsive cells in IC was reduced in ectopic mice (15% in ectopic, 23% in non-ectopic across all IC recordings; Fisher's exact test p<0.01). These findings suggest that while the offset-response deficit in ventral MGB of ectopic mice could be inherited from the IC, the neural gap-detection deficit in the MGB is not.

References

Anderson, Lucy A, and Jennifer F Linden. 2016. "Mind the Gap: Two Dissociable Mechanisms of Temporal Processing in the Auditory System." The Journal of Neuroscience : The Official Journal of the Society for Neuroscience 36 (6): 1977–95. doi:10.1523/JNEUROSCI.1652-15.2016.

Clark, M G, G F Sherman, H a Bimonte, and R H Fitch. 2000. "Perceptual Auditory Gap Detection Deficits in Male BXSB Mice with Cerebrocortical Ectopias." Neuroreport 11 (4): 693–96.http://www.ncbi.nlm.nih.gov/pubmed/10757502.

PS 893

Binaural interaction component in American alligators

Lutz Kettler; Catherine Carr
University of Maryland

The auditory brainstem response (ABR) is an evoked potential that can be recorded with scalp electrodes and reflects auditory information traveling up the early auditory pathway. It is described by waves following the stimulus onset representing activity in consecutive auditory nuclei. Waves IV or V, typically identified by their latency, are the first waves considered to be of binaural origin, and thus, may correspond to activity in the superior olive in mammals and nucleus laminaris in birds. The binaural interaction component (BIC), reflecting binaural interaction, is computed by subtracting the sum of the ABR responses to both monaural stimulations, from the ABR with binaural stimulation. BICs have been identified in mammals but also in the barn owl. Although the neuroanatomy of the auditory pathway, detection of binaural cues, and the ABR shape in both groups are different, BICs differ only slightly. In general, the generation of the BIC is not sufficiently understood. We therefore measured ABRs and calculated BICs in the alligator. Crocodilians form a sister group of birds, and are considered to use the same mechanism of interaural time difference (ITD) detection. In contrast to the owl, however, alligators are predominantly sensitive to low frequency ITDs, similar to mammals. Their ears are also internally coupled. Alligator ABRs were remarkably similar to mammal ABRs with clearly distinguishable waves I-VI. In contrast, bird ABRs exhibit a reduced number of waves. The binaural interaction component, however, displayed a more complex shape, stretching from early

wave IV to wave VI. Small 'binaural'; interactions were also found in the early monaural waves, most likely due to the internally coupled ears, and therefore directional eardrum responses. Coupled ears generate additional interaural level cues, which could also influence the BIC in alligators and other animals with internally coupled ears, like most birds. Identifying the source(s) of the BIC and the different waves in the ABR could later help in identifying the mechanisms underlying the detection of binaural cues.

PS 894

Urocortin 3 modulates synaptic transmission at the calyx of Held synapse

Sara Pagella; Conny Kopp-Scheinpflug
LMU Munich

Background
Urocortin 3 (Ucn3), an orthologue of corticotropin releasing factor (CRF), has been shown to have wide-spread effects on peripheral organs and in the central nervous system. UCN3 binds with high affinity to the CRF receptor type 2 (CRFR2) and can act independently of the hypothalamus-pituitary (HPA) axis. While its role in many different circuits in the nervous system has been described to be protective against stress and crucial for mouse social behavior, its presence in nuclei of the auditory system is not understood. Previous results from our group showed Ucn3 expression in the auditory brainstem and the cochlea and revealed a protective effect of this neuromodulator against noise-induced hearing loss (NIHL). However, the underlying cellular mechanism of action is still unclear.

Methods
Anatomical description of the localization of Ucn3 expressing cells and axons was accomplished with the use of Ucn3 TdTom mouse model. Whole-cell patch clamp experiments were carried out on wild-type C57BL6 mice aged P15 to P22. Cells in the dorsolateral part of MNTB were selected based on their high expression of Ucn3 in the afferent calyx synapses. Miniature excitatory post-synaptic currents (mEPSCs) were recorded combined with pharmacological manipulations of Ucn3 signaling (Urocortin3: 100nM; CRFR2 inhibitor K41498: 400-600nM). Spontaneous activity and intrinsic properties of recorded cells were studied in current-clamp mode.

Results
Preliminary data suggest that Ucn3 acts via presynaptic mechanisms to potentiate the transmission at the calyx of Held-MNTB synapse. Pharmacological blockade of the endogenous UCN3 receptor CRFR2 resulted in a significant decrease of mEPSC frequencies by 68 ± 7%

(n=10 cells; paired t-test: p=0.015). Corroborating these results, bath application of UCN3 caused an increase in mEPSCs.

Conclusions
The expression of UCN3 in a population of calyx of Held synapses offers the possibility to thoroughly study the release characteristics of this neuromodulator from pre-synaptic terminals and its effects on synaptic transmission. We aim at transferring the knowledge of UCN3 action at the calyx of Held-MNTB synapse to understand how UCN3 signaling in the cochlea may account for the maintenance of normal hearing thresholds and noise protection we observed previously.

PS 895

A model of the human auditory brainstem response to running speech

Marina Saiz Alia; Amna Askari; Antonio E. Forte; Tobias Reichenbach
Imperial College London

Background
The auditory brainstem's response to many repeated short clicks as well as to the frequency of a pure tone (FFR) can be measured from scalp electrodes and serves as an important clinical assessment of hearing. Recently we have proposed a method for detecting the response of the auditory brainstem to the pitch of running speech that does not repeat. This has allowed us to establish a modulation of this brainstem response through selective attention to one of two competing speakers. A better understanding of the origin of the brainstem response to running speech as well as of the attentional modulation requires, however, a computational model that can trace sound processing from the auditory periphery to the different parts of the brainstem. Although computational models are available for click-evoked brainstem responses as well as for the FFR, no model has yet been developed for the brainstem response to running speech.

Methods
We combined an existing model of the middle and inner ear with models of the inner hair cells and the auditory-nerve fibers. We also developed a model of the globular bushy cells in the cochlear nuclei and combined it with a phenomenological model of the inferior colliculus. We then presented the integrated model with running speech. Following the methodology developed recently by ourselves for detecting the brainstem response to running speech, we correlated the fundamental waveform of the voiced parts of speech, which oscillates at the fundamental frequency, with the simulated brain-stem response.

Results
We found significant responses of the simulated brainstem activity to running speech. The responses occurred at delays that increased towards the midbrain. In particular, the auditory-nerve fibers responded at a latency of 3.5 ms, the cochlear nuclei at 8.1 ms, and the inferior colliculus at 9.6 ms. The latter latency matches the one found experimentally, suggesting that the scalp-recorded brainstem response to speech is dominated by the inferior colliculus.

Conclusions
We have developed a computational model of the auditory brainstem response to running speech. The simulations showed characteristic latencies for signals generated at the level of the auditory-nerve fibers, the cochlear nuclei and the inferior colliculus; they are consistent with physiological data. This simulation framework can be employed to investigate the contribution of different frequency bands of the speech signal, the loss of connections of auditory-nerve fibers as may occur in hidden hearing loss, as well as of the effect of background noise on the neural activity.

PS 896

Frequency-specific auditory brainstem response using parallel, pseudorandomly timed sequences of tonebursts

Ross K. Maddox
University of Rochester

The frequency-specific auditory brainstem response (ABR) is an objective electroencephalographic (EEG) method for estimating auditory thresholds when behavioral thresholds are not attainable, primarily in infants and toddlers. It is recorded by repeatedly presenting brief, band-limited tonebursts and averaging the scalp potential response. In a typical audiological exam, measurements are made at multiple intensities, at multiple frequencies, and in both ears, leading to a large combinatorial space and long test times. Here we present a method of recording the response at all frequencies and in both ears simultaneously. The work comprises two parts: 1) empirical proof of concept and 2) auditory nerve modeling. In part 1, we created ten toneburst trains: 5 frequencies (500, 1000, 2000, 4000, 8000 Hz) by 2 ears. Importantly, rather than the tonebursts being periodically timed according to standard practice, their timing was dictated by a homogeneous Poisson process. By using this randomized timing, we are able to separately compute the ABR to each of the ten toneburst trains as the cross-correlation of the click sequence and the EEG

recording. The amplitude of responses recorded in parallel was generally smaller than responses computed in serial, one frequency-ear-combination at a time. However, the ability to extend the analysis window arbitrarily (afforded by the mathematical properties of random timing) allowed response components out to 50 ms to be used. Additionally, the smaller response size is likely a direct result of improved frequency specificity, which is predicted by modeling. In part 2, we used a model of auditory nerve firing rates to examine the strengths and weaknesses of the approach. We found that at high intensities, current serial methods show very wide tuning due to spread of excitation. However, using our parallel approach, responses to simultaneous toneburst trains at high intensities are frequency specific, mitigating the problem. This improved tuning is similar to that provided by notched masking noise, with each toneburst train essentially acting as off-frequency masking for all the others. At lower intensities, where spread of excitation is less of a problem, the simultaneous toneburst trains have little effect on each other, suggesting the potential for large efficiency gains using parallel presentation over serial. This work represents a first step towards a new paradigm for objective audiometry. By presenting randomly timed tonebursts in parallel across frequencies and ears, we hope to substantially speed recording sessions while concurrently improving the accuracy of the estimated ABR thresholds.

PS 897

Functional Anisotropic Panglial Networks in the Inferior Colliculus

Simon L. Wadle[1]; Vanessa Augustin[2]; Julia Langer[3]; Roland Jabs[4]; Camille Philippot[4]; Dennis J. Weingarten[1]; Christine R. Rose[5]; Christian Steinhäuser[4]; Jonathan Stephan[1]
[1]*Animal Physiology Group, Department of Biology, University of Kaiserslautern;* [2]*Department of Biology, University of Kaiserslautern;* [3]*Institute of Neurobiology, Heinrich Heine University;* [4]*Institute of Cellular Neuroscience, University of Bonn;* [5]*Institute of Neurobiology*

Astrocytes form connexin (Cx)-mediated gap junctional networks, which participate in homeostasis by redistribution of ions and neurotransmitters within the syncytium. In the auditory brainstem, astrocytes are heterogeneously distributed and strongly aggregate in its nuclei. We immunohistochemically labeled Cx43 and Cx30 to investigate their developmental expression in the inferior colliculus (IC) at postnatal days (P) 7-30. In order to analyze astrocyte coupling and network shape in the IC, we utilized acute brainstem slices from C57Bl6 mice at P10-13. Astrocytes were identified a priori by sulforhodamine (SR) 101-labeling before subjecting them

to whole-cell patch-clamp recordings. The intracellular solution contained gap junction-permeable neurobiotin and gap junction-impermeable alexa fluor (AF) 568 to label the network and the patched cell, respectively. After tissue fixation, neurobiotin was labeled with avidin AF488. Additionally, we performed wide field sodium imaging in order to analyze the capability of ion redistribution within the IC. The expression of Cx43 was moderate during early development, peaked at P12 and decreased again with further age. In comparison, Cx30 onset started around P12 and remained high from P20 on. IC astrocytes formed networks, which showed great variability regarding their size and were restricted to the IC. Whereas astrocytic networks in many CNS regions are almost circular, those in the IC were often found to be anisotropic and to exhibit a predominant orientation orthogonal to the tonotopic axis. Electrical stimulation of individual IC astrocytes caused sodium elevations in their somata. Subsequently, sodium elevations were also present in neighboring cells, indicating a spread of sodium through gap junctions. Surprisingly, not only neighboring SR101-labeled astrocytes, but also SR101-negative cells responded to the stimulus. In order to analyze the contribution of non-astrocytic cells to the networks, we used PLP-GFP mice, in which oligodendrocytes are fluorescently labeled. Indeed, astrocytes as well as oligodendrocytes gave rise to panglial networks. Taken together, our results demonstrate the presence of heterogeneous astrocyte networks in the IC regarding their shape and orientation with respect to the tonotopic axis. Moreover, these networks do not only include SR101-positive astrocytes, but apparently include oligodendrocytes, together forming a panglial network. We assume that the topography of the networks in the IC lead to a spatially restricted homeostasis and therefore to a limited cross-talk between neighboring isofrequency bands. Thus, IC networks exhibit similar features like glial networks in the lateral superior olive (Augustin et al., Functional Anisotropic Panglial Networks in the Lateral Superior Olive, Glia, 2016, DOI: 10.1002/glia.23031).

PS 898

Cholinergic Influences on Spherical Bushy Cells in the AVCN of Gerbils

Charlène Gillet; Stefanie Kurth; Thomas Kuenzel
Institute for Biology 2, RWTH Aachen University

Spherical bushy cells (SBC) receive direct excitatory input from the auditory nerve with large axosomatic synapses. Furthermore, descending cholinergic axons from collaterals of the olivo-cochlear bundle and from the tegmentum enter into the cochlear nucleus. Goyer et al (2016) showed that the activation of muscarinic receptors had slow effects on SBC resting membrane potential (RMP). Here we investigate the cholinergic innerva-

tion and the underlying mechanisms of the long-lasting RMP modulation.

Immunohistochemical staining against the vesicular acetylcholine transporter (VAChT) were performed in coronal and parasagittal auditory brainstem slices of P5-P31 gerbils. Whole-cell patch clamp recordings from SBC were obtained in frontal slices of P14-22 gerbils. In current-clamp condition, the RMP and the input resistance (IR) were monitored over minutes before, during and after application of different pharmacologic agents acting on the cholinergic receptors (carbachol 500µM, 4-DAMP 1µM, oxotremorine 1µM).

Immunohistochemical data revealed that cholinergic terminals were present in AVCN at early stages and their density increased with development. In coronal slices, VAChT immunosignal was first detected on the medial side at P5 and spread progressively along the perimeter of the nucleus to finally innervate the whole AVCN at P28. VAChT immunosignal density significantly increased in the AVCN (from $145\pm37mm^{-2}$ at P5 to $500\pm107mm^{-2}$ at P28). Bath application of carbachol transiently depolarized SBC RMP in all cases ($+1.2\pm0.3mV$). However, wash-in of the muscarinic agonist oxotremorine lead in 52% of the cells to a negative shift of RMP ($-2.9\pm0.3mV$) while only 12% showed a depolarization ($+2.6\pm0.2mV$) accompanied with a fast decrease in IR ($-7.9\pm1.0M\Omega$), 36% cells did not show any significant response. Application of the m3 antagonist 4DAMP confirmed a significant contribution of m3 receptor signaling in both response types.

Our results indicate that cholinergic innervation of AVCN starts early in development. The divergent responses of SBC upon activation of muscarinic receptors imply physiological subgroups of SBC, which has not been described before. Despite the clear role of m3-receptors, its physiological action by itself cannot explain the complex muscarinic response we observed. This suggests the presence of another muscarinic receptor. In the future we will identify SBC subgroups by comparing the morphology of patched cells by 3D reconstruction as well as by imaging PIP_2 dynamics upon application of cholinergic agonist in the whole AVCN.

Auditory Pathways: Midbrain III

PS 899

Neural Representation of Interaural Correlation in Human Auditory Brainstem

Qian Wang[1]; Liang Li[2]
[1]Sanbo Brain Hospital; [2]School of Psychological and Cognitive Sciences, Peking University

Processing of interaural correlation (IAC), which is defined as the similarity of acoustic signals presented at the two ears, is essential in auditory perception. Calculation of IAC basically relies on the comparison of binaurally temporal information which conveyed by both quickly-varying temporal fine structures (TFSs) and slowly-varying envelopes. Previous animal studies suggest that the neurons of auditory brainstem are sensitive to IAC sensitivity, but it is still unclear how the TFS and envelope contribute to the neural representation of IAC. The current study investigated the subcortical mechanisms of IAC processing by recording frequency-following responses (FFRs) to the TFS component (i.e., FFR_{TFS}) and those to the envelope component (i.e., FFR_{Env}). The results showed that the both sustained FFR_{TFS} and FFR_{Env}, but not the transient brainstem responses, were sensitive to IAC. Using stimulus-to-response correlation analysis, the results also showed that both the acoustic TFS and envelope components could be entrained faithfully in auditory brainstem, but only the FFR_{TFS} contributed to the stimulus-specific representation. In addition, the IAC sensitivities of FFR_{TFS} and those of FFR_{Env} were significantly correlated. In conclusion, the faithful entrainment of TFS information in auditory brainstem neurons plays an essential role in binaural processing, while the source-specific correlation between the FFR_{TFS} and FFR_{Env} not only implies a functional binding between TFS and envelope in processing IAC in human brainstem level, but also suggests an possible mechanisms of auditory feature integrations at the higher neural and perceptual processing levels.

PS 900

Neurofeedback-mediated modulation of the frequency following response

Fernando Llanos[1]; Rachel Reetzke[1]; Madhumitha Sakthi[2]; Bharath Chandrasekaran[1]
[1]Communication Sciences and Disorders, The University of Texas at Austin; [2]Department of Electrical and Computer Engineering, The University of Texas at Austin,

Neurofeedback is a psychophysiological method in which real-time feedback of neural activation is delivered to participants in order to modulate neural function (Sitaram et al., 2016). In a typical EEG pipeline, neurofeedback is mediated by a brain-computer interface (BCI) that rewards specific modulations (e.g., attenuation) of EEG signal properties across trials. Because of its BCI design, neurofeedback provides a way to investigate neuroplasticity and to enhance/regulate neural function. Here, we investigate the extent to which neurofeedback can also be used to mediate changes in the frequency-following response (FFR), an electrophysiological component that reflects phase-locked ac-

tivity from neural ensembles involved in early auditory processing (Chandrasekaran & Kraus,2010). Although the FFR is often described as a pre-attentive response, FFR source generators (e.g., the midbrain and auditory cortex) are computational hubs that receive feedback connections from higher-level centers which are thought to promote egocentric selection of behaviorally-relevant elements in the signal (Chandrasekaran, Skoe & Kraus, 2014). Our goal here is to investigate the extent to which listeners can learn to exploit this feedback loop to induce FFR quality changes in real-time. To achieve this goal, we recorded EEG from young adults in response to multipe repetitions of a rising pitch pattern across 20 epochs. To remove the cochlear microphonic effect, alternating waveform polarities were presented across stimulus repetitions within each epoch. Participants were provided no instruction to guide response strategy and were probed on perceptual changes to the repetitive speech sounds ('verbal transformations';) that are known to modulate the FFR (Galbraith et al., 1998). After listening to each epoch, visual feedback using a score bar was provided based on online processing of FFR quality. FFRs were online segmented, band-pass filtered, baseline corrected, artifact rejected and averaged in line with standard FFR preprocessing methods. Our results indicate that participants can modulate the FFR online; however, the extent to which modulations enhanced or reduced FFR quality dependeded on the participant strategy. Strategies leading to increased perceptual transformation resulted in poorer FFR quality, while strategies leading to reduced perceptual transformation resulted in increased FFR quality. We discuss these results in the context of using neurofeedback to regulate the efferent auditory system in an effort to enhance listening skills.

PS 901

Machine learning decoding of listener identity from frequency following responses

Fernando Llanos; Bharath Chandrasekaran
Communication Sciences and Disorders, The University of Texas at Austin

The frequency following response (FFR) is a scalp recorded electrophysiological potential that reflects phase-locked activity from subcortical neural ensembles (Chandrasekaran & Kraus,2010). The FFR is often used to assess the quality of sensory auditory processing. Previous studies show that the FFR encodes information relative to the sound properties that are being processed (e.g., pitch) as well as the degree of familiarization with these properties via auditory experience (Krishnan, Gandour, & Bidelman, 2010). Here, we examine the extent to which the FFR can be also used to pick up on individual neural differences in a homogeneous population of normal hearing listeners. In particular, we test the extent to which listener identity can be reliable decoded from FFRs using a machine learning approach. Our database consisted of FFRs elicited from native speakers of English listening to 1000 repetitions of both Mandarin tone1 (high-level tone) and tone2 (rising tone) across three consecutive days (Xie, Reetzke, & Chandrasekaran,2017). Participants were normal hearing listeners with no significant experience with tonal languages and musical training. FFRs were recorded adopting a vertical montage of three electrodes. Stimulus waveform polarities were alternated across trials to reject the cochlear microphonic effect. We trained a series of hidden Markov Models (HMM) to decode listener identity from FFRs across different conditions. In the first condition, listener identity was decoded independently for each combination of day and tone; in the second condition, it was decoded across days; in the third condition, listener identity was decoded across tones. HMMs were input with the DFT coefficients extracted from the corresponding FFR spectrograms. HMM parameters (training, testing and averaging size) were set as described in Llanos, Xie & Chandrasekaran (2017) to provide optimal decoding FFRs in sets of 1000 trials. Listener identity was decoded with accuracy levels above chance (=20%). In particular, HMM accuracy was higher in the first condition, where days and tones were teased apart, ranging from M=53% (2nd day, tone2) to M=85% (1st day, tone1). Accuracy decreased when listener identity was decoded across tones (M=48, SD=9.8) or across days (M=29, SD=9). Implications and applications of these findings for future research will be discussed.

PS 902

Using acoustic and neural correlation statistics to categorize texture sounds in that auditory midbrain of unanesthetized rabbits

Fatemeh Khatami; Mina Sadeghi; Ian Stevenson; Heather Read; Monty Escabi
University of Connecticut

Barlow and others have suggested that organisms and the neural networks that underlie sensory perception are optimized to capture statistical regularities in sensory scenes. Accordingly, high-order statistical regularities in natural sounds are critical for perceptually discriminating and categorizing sounds (McDermott and Simoncelli, 2011; Geffen et al., 2011). Though neural responses in the central auditory system can vary with modulation and correlation sound statistics (Attias and Schreiner 1998; Escabi and Schreiner, 2002; Hsu et al 2004; Rodriguez et al., 2012) it remains unclear whether sensitivity to high-order statistics could be used to discriminate sound category and how this might be instantiated. Here we characterize single neuron activity neurons in

the inferior colliculus of awake rabbits in response to an ensemble of sound textures including water, fire, bird-song chorus, snake sounds, and speech babble. We synthetically manipulate each sound by selectively adding or removing high-order statistics using the synthesis algorithm developed by McDermott and Simoncelli (2011). First, we find neural response statistics including spike timing precision and firing reliability change systematically with the sound statistics. Second, we find correlated spiking across pairs of neurons varies with sound category and its synthetically manipulated statistics. Using neurometric and ideal observer analyses we demonstrate that neural response statistics can be used to discriminate sounds. Systematic removal of the high-order sound statistics decreases the neural-based sound classification performance whereas increasing the findings indicate that neural response statistics in the inferior colliculus have the capacity to capture statistical regularities in sounds that are critical for sound categorization. Moreover, our findings support the concept that mammalian systems have the capacity to perform sensory categorization through correlated activity in neuron populations. (Supported by NIDCD R01DC015138)

PS 903

Using nonstationary spectro-temporal correlation statistics for sound category identification

Mina Sadeghi; Ian Stevenson; Monty Escabi
University of Connecticut

Humans and animals can readily identify sounds and categorize them into behaviorally relevant categories. Yet, the acoustic cues and neural coding strategies that contribute to category identification phenomenon remain largely unknown. Motivated by recent studies showing that humans can utilize statistical regularities to identify texture sounds (McDermott & Simoncelli 2011) and work showing that central auditory neurons can respond selectively to various sound statistics (Attias and Schreiner 1998; Escabi et al 2003; Hsu et al 2004; Rodriguez et al 2010), we tested the hypothesis that non-stationary statistics obtained from computational auditory model can contribute to sound category identification phenomenon. Specifically, we developed a neural auditory model that measures the time-varying (nonstationary) spectro-temporal correlation statistics between frequency organized cochlear channels and use the output statistics to categorize sounds with a catalogue of natural and man-made sounds (containing 13 categories and 15 excerpts per category). A Bayesian classifier was applied to the time-varying correlation statistics and used to identify the sound category of each input sound. The classifier performance was always better than chance in a thirteen-alternative sound category identification task (7.7% chance level) and could reach 80% after parameter op-

timization. When tested independently, both the spectral and temporal correlation statistics appear to contribute equally since they individually achieved a similar level of performance. Furthermore, classifier performance improves with increasing sound duration and plateaus at ~7 sec mirroring human performance for texture identification (McDermott and Simoncelli 2012). The results also complement data from our accompanying poster (Khatami et al) which demonstrates that sound correlation statistics are reflected in the neuron-to-neuron correlation statistics of the auditory midbrain. Together the results suggest that non-stationary spectro-temporal correlation statistics in sounds contain viable information that the brain can potentially use to categorize sounds. (Supported by NIDCD R01DC015138)

PS 904

Direction-Dependent Effect of a Regularly Presented Sound on the Response to an Occasionally Presented Sound in the Rat's Inferior Colliculus

Mathiang Chot; **Huiming Zhang**
University of Windsor

The ability to sense a novel sound, i.e., an occasionally occurring acoustic event in an environment, is important for hearing. Studies have been conducted to investigate neural correlates of this ability using an oddball paradigm, i.e., a train of acoustic stimuli in which one sound occasionally and randomly replaces an otherwise repetitively presented sound. Oddball paradigms presented from earphones were used to find whether neurons reduce sensitivities to a regularly occurring sound while maintaining sensitivities to occasionally occurring sounds.

To understand neural mechanisms underlying the detection of a novel sound in a natural environment, we used two loudspeakers to present oddball paradigms. Each paradigm was created using two different tone bursts presented at different probabilities. In reference to the frontal midline (0° azimuth), the two sounds were either colocalized on the side contralateral to the recording site (c90° azimuth) or spatially separated with one sound at c90°. Action potential firing was recorded from single neurons in the rat';s inferior colliculus.

Results indicated that neurons generated stronger responses to a sound at c90° when it was presented at a low than high probability. Many neurons changed the strength of the response to a sound with a fixed location at c90° when the other sound of an oddball paradigm was relocated from c90° to another azimuth. Under most of the conditions of stimulation (i.e., angle of separation

between the sounds and probability at which the c90º sound was presented), the strength of response to the c90º sound was increased rather than reduced in the majority of neurons. The percentage of neurons showing increases was particularly high when a low probability sound was presented at c90º while a high probability sound was presented at an ipsilateral azimuth. It was also high when both sounds were presented at equal probabilities with one of them located at an intermediate but not extreme ipsilateral azimuth. These changes of responses to the c90º sound can';t be fully explained by direction-dependent alterations in excitatory/inhibitory inputs, suggesting that other yet unknown mechanisms have also contributed to shaping these responses.

Our results suggest that collicular neurons as a population had a better ability to detect a novel sound presented at one ear when a regularly occurring background sound is located within the opposite acoustic hemifield. The results provide important information for understanding auditory novelty detection as well as binaural hearing.

PS 905

Midbrain responses to Schroeder-phase harmonic complexes: Neurons and models

Laurel H. Carney[1]; Georg M. Klump[2]
[1]Departments of Biomedical Engineering, and Neurobiology & Anatomy, University of Rochester , Rochester; [2]University of Oldenburg

Schroeder-phase harmonic complex stimuli have been studied in numerous psychophysical and behavioral studies due to their interesting temporal, envelope, and masking properties. The stimuli were designed to have maximally flat envelopes for a given number of harmonics. The complexes have equal-amplitude harmonic components with phases that vary from 0 to $C\pi(N+1)$ radians, where N is the number of harmonics. Phase spectra can have positive (SCHR+) or negative (SCHR-) slopes, as specified by the sign of C. Because SCHR+ and SCHR- stimuli with a given F0 and C differ only in the sign of their phase spectra, they are time-reversed versions of each other. Each pitch period of SCHR+ stimuli is characterized by a linear downward frequency sweep from the fundamental (F0) to the highest component frequency, and SCHR- stimuli are upward frequency sweeps. The envelope and temporal-fine structure (TFS) properties of the stimuli lend them to experiments designed to explore the roles of different cues for discrimination and detection of complex sounds. We will

present physiological responses to Schroeder stimuli of midbrain neurons in both anesthetized gerbil inferior colliculus (IC) and in awake rabbit IC. Over much of the F0 and C parameter space, many neurons in the IC demonstrate marked selectivity for SCHR stimuli. In some cases, neurons respond briskly to SCHR- (or SCHR+) for a given F0 and C value, and weakly to the opposite signed SCHR stimulus with the same F0 and C. Thus, cells can respond strongly to an upward (or downward) frequency sweep, and weakly to a stimulus with the same magnitude spectrum but a frequency sweep in the opposite direction. These responses will be compared to other studies of IC cells in response to frequency-modulated (FM) stimuli. Models of IC neurons based on frequency tuning and periodicity tuning cannot explain the SCHR-selectivity that was observed. New models that include different potential mechanisms for FM-direction selectivity will be explored. Interactions between periodicity tuning and FM-direction selectivity in neural responses and models will be tested.

PS 906

Pitch of Harmonic Complex Tones: Temporal Coding in the Auditory Midbrain of Unanesthetized Rabbit

Yaqing Su[1]; Bertrand Delgutte[2]
[1]Boston University; Mass. Eye & Ear Infirmary;
[2]Massachusetts Eye and Ear

Pitch perception is closely related to the temporal periodicity of sound. Neural synchronization to the stimulus envelope provides a prominent temporal cue for periodicity in the auditory periphery, but becomes degraded and gives way to rate codes in higher centers. The inferior colliculus (IC) likely plays a key role in this temporal-to-rate code transformation. We previously identified a non-tonotopic rate code for envelope repetition rate and a rate-place code for resolved harmonics in the IC of unanesthetized rabbits. Here we complement these results with a characterization of temporal code in the IC.

We measured single-unit responses to harmonic complex tones (HCT) consisting of equal-amplitude harmonics with varying fundamental frequency (F0) (26-1792Hz). Envelope periodicity was manipulated by altering the phase relationship among harmonics: cosine phase (COS) gave strong envelope periodicity at 1/F0, cosine-sine (ALT) phase gave strong envelope periodicity at 1/2F0, and random phase (RAND) gave a nearly flat envelope. To test if temporal coding requires periodicity, we also tested pulse train stimuli of varying aver-

age repetition rate (ARR, 20-2560pps) and 0%-90% of random jitter in inter-pulse intervals.

For COS phase HCT, 66% of IC neurons showed significant synchrony to the stimulus periodicity for some F0. The highest F0 where synchrony was observed was 640 Hz. For these neurons, response to ALT stimuli yielded comparable synchrony at 2F0, not F0, indicating that responses were synchronized to the stimulus envelope. For RAND stimuli, neural synchrony was generally weak for F0 below 112 Hz, but comparable to COS at higher F0, consistent with an effect of cochlear filtering. For pulse train stimuli, over 40% of the neurons showed synchrony to periodic pulses (0% jitter) for some ARR, as determined by a stringent cross-correlation criterion. Both the prevalence and the strength of synchrony were comparable for 90% jittered pulse train of the same ARR, showing that envelope synchronization does not require periodicity.

Many IC neurons demonstrate strong synchrony to the envelope of both HCT and pulse train stimuli over a wide range of repetition rates, indicating that the temporal code in the periphery is largely preserved in the midbrain. Because this temporal code is not dependent on periodicity, it cannot provide a direct representation of pitch. However, in combination with the aforementioned rate codes, this temporal code can convey pitch cues to higher processing centers, especially for unresolved harmonics, which evoke relatively weak pitch sensations in humans.

PS 907

Neural correlates and sources of responses to pitch-shifted complex tones

Karl D. Lerud[1]; Erika Skoe[2]; Edward [...]
[1]*University of Connecticut;* [2]*University of Connecticut, Department of Speech, Language and Hearing Sciences*

The frequency following response (FFR) is an evoked potential recorded at the scalp, phase-locked to periodic auditory stimuli. It has been well-studied over many decades, but some aspects remain ill-characterized, including its precise frequency content and its neural origin. Like other auditory responses, the FFR is highly nonlinear and contains frequencies not present in the stimulus. The envelope frequency is typically present as well as other nonlinearities that are found with certain stimuli. When a harmonic complex is shifted slightly up or down in frequency, it becomes inharmonic in general and, while its envelope remains unchanged, its pitch

WITHDRAWN

perception shifts proportionally, though to a lesser degree. Inharmonic stimuli were used here to tease apart the various even- and odd-order nonlinearities, because they no longer align with one another as they do in responses to harmonic stimuli. This makes it apparent which response frequencies are related to the envelope and which are related to the primaries. We also sought to localize the source of these responses by collecting FFRs with a dense net of electrodes and constraining a source localization algorithm with individual structural MRI scans of each participant. A cPCA algorithm utilized the multielectrode setup to optimize the signal-to-noise ratio of the FFRs. Both low and high fundamental frequency stimuli were used, to ask whether a cortical contribution to the FFR was dependent on the ability of the neurons to fire once per stimulus period. FFRs were collected using alternating polarity to separate out the even- and odd-order portions of the response, and to be able to localize those two portions separately. Our results shed further light on the question of generating mechanisms of the FFR.

PS 908

Effect of Sound Pressure Level on Synaptic Inhibition Underlying Duration-Tuned Neurons in the Mammalian Inferior Colliculus

Roberto Valdizón-Rodríguez; Dominika Kovaleva; Paul A. Faure
McMaster University

Duration tuning in the mammalian auditory midbrain is created by the interaction of excitatory and inhibitory synaptic inputs that are offset in time. We used monotic paired-tone stimulation in combination with single-unit extracellular recording to measure the effect of stimulus amplitude on the evoked synaptic inhibition underlying duration-tuned neurons (DTNs) recorded from the inferior colliculus of the big brown bat (Eptesicus fuscus). We stimulated DTNs with two tones: a short duration, excitatory probe tone set to the cell';s best duration (BD), best excitatory frequency and presented at an amplitude of +10 dB above the excitatory (spiking) threshold, and a longer duration, non-excitatory (NE) suppressor tone that was varied in amplitude. Both tones were presented to the contralateral ear. The onset time of the BD tone was varied relative to the NE tone. When both tones were close in time, BD tone-evoked spikes were suppressed when the sound pressure level (SPL) of the NE tone was at or above the cell';s excitatory threshold. The effective duration of spike suppression increased as the NE tone amplitude increased. This occurred because the offset of the inhibition evoked by the NE tone systematically increased in latency with increasing SPL. In contrast, the onset of the NE tone-evoked inhibition, which preceded the evoked excitation, remained

constant at all SPLs above threshold. The amount of time that inhibition preceded excitation was related to a cell';s BD, duration filter class, and first spike latency at all SPLs except at threshold. We conclude that the strength of the synaptic inhibition that is responsible for creating duration-tuning in the mammalian inferior colliculus changes in proportion to the strength of the evoked excitation. We speculate that this may help to preserve the temporal selectivity of a DTN at different SPLs, as previously demonstrated in earlier reports.

PS 909

Frequency Tuning of Ipsilateral Synaptic Inhibition Underlying Duration-Tuned Neurons in the Mammalian Inferior Colliculus

Robert Mastroieni; Roberto Valdizón-Rodríguez; **Paul A. Faure**
McMaster University

Duration tuning in the mammalian auditory midbrain is created by the interaction of excitatory and inhibitory synaptic inputs that are offset in time. We used monotic and dichotic paired-tone stimulation in combination with single-unit extracellular recording to measure the spectral tuning of the ipsilateral inhibition acting on duration-tuned neurons (DTNs) recorded from the inferior colliculus of the big brown bat (Eptesicus fuscus). We stimulated DTNs with two tones: a short, excitatory probe tone set to the cell';s best duration (BD) and best excitatory frequency (BEF), and a longer duration, non-excitatory (NE) suppressor tone that was varied in frequency. The onset time of the BD tone was varied relative to the NE tone. In the monotic condition both tones were presented to the contralateral ear, and when they were close in time the NE tone suppressed BD tone-evoked spikes in all cells (100%). In the monotic condition the onset of the NE tone-evoked inhibition typically preceded the cell';s first spike latency. In the dichotic condition the BD tone was presented to the contralateral ear and the NE tone was presented to the ipsilateral ear, and when both tones were close in time BD tone-evoked spikes were suppressed in only ~50% of cells. In the dichotic condition the onset time of the NE tone-evoked inhibition typically followed the cell';s first spike latency. In both conditions, the evoked inhibition was strongest when the NE tone frequency fell within the monotic excitatory bandwidth (eBW), and the effective duration of spike suppression decreased as the NE tone frequency departed from the BEF. Moreover, the onset of inhibi-

tion did not vary as the NE tone frequency changed. The effective duration of the NE tone-evoked inhibition was used to generate an inhibitory frequency response area from which each cell';s best inhibitory frequency (BIF) and inhibitory bandwidth (iBW) were measured. In both monotic and dichotic stimulation, BIFs matched BEFs; however, monotic iBWs were significantly wider than monotic eBWs, whereas dichotic iBWs were broader than monotic eBWs in the same cell. These data suggest the temporal selectivity of midbrain DTNs is created by monaural auditory inputs, with binaural inputs playing less of a role in duration-tuning. We speculate that inhibition evoked in the ipsilateral ear shapes a cell';s spatial selectivity with contralateral inhibition creating the cell';s duration selectivity.

PS 910

Comparing Sound-Evoked Responses of Excitatory and Inhibitory Neurons in the Dorsal Inferior Colliculus of the Awake Mouse

Aaron B. Wong; J. Gerard G. Borst
Erasmus MC

The inferior colliculus (IC) is an auditory hub, receiving not only ascending input from most brainstem auditory nuclei.but also prominent feedback projections from the cerebral cortex, which preferentially target the non-lemniscal regions of the IC, the dorsal cortex (DCIC) and lateral cortex. Although the corticocollicular projections are glutamatergic in nature, direct stimulation of auditory cortex can have inhibitory effects on the IC, suggesting an important role for inhibitory neurons within the IC in the descending feedback. However, relatively little is known about the different responses of inhibitory and excitatory neurons within the DCIC. In the mouse, a large part of the DCIC lies superficially, making it a favorable structure for chronic in vivo two-photon Ca^{2+} imaging. Here, we measured GCaMP6s fluorescence in Gad2-IRES-Cre x Ai96 and GP4.3 mouse lines to monitor the spontaneous and sound-evoked activities in GABAergic and non-GABAergic neurons of the DCIC, respectively. In both GABAergic and non-GABAergic neurons, pure tone-evoked fluorescent responses in IC cells in awake mice could be classified into roughly four main categories: onset, sustained, inhibited and offset; these response types were in good correspondence to previous electrophysiological findings (e.g. Willott et al, 1988). GCaMP6s fluorescence kinetics were similar between the two mouse lines. No clear gradient in characteristic

frequency or response types was observed within the DCIC for individual animals, and adjacent cells showed large difference in their responses, in agreement with our earlier whole-cell recording data (Geis et al, 2011). Pupil size, whisker and body movements of the animals were recorded to further probe the effect of alertness on the activity of DCIC neurons.

Auditory Prostheses VI

PS 911

Platinum Black Plating Decreases the Impedance for Cochlear Implants to Stimulate Auditory Neurons

Hideaki Ogita[1]; Koji Nishimura[1]; Takayuki Nakagawa[2]; Juichi Ito[1]
[1]*Shiga Medical Center Research Institute;* [2]*Department of Otolaryngology - Head and Neck Surgery, Graduate School of Medicine, Kyoto University*

We are developing a novel cochlear implant (CI) called 'Hibiki device', which has a piezoelectric membrane. This new device converts sound oscillations of the basilar membrane and can be totally implantable in the cochlea. The new device converts sound oscillations of the basilar membrane into the electrical signals without any external sound processor. Since the output from the device depends on the input of sound oscillations, increasing the efficacy of mechano-electrical energy conversion by the device is needed for its clinical application. When an electrode is exposed to a fluid, an electrical double layer (EDL) appears on the surface of the electrode. An EDL acts as a capacitor and it inhibits the current flows and increases the impedance of the electrodes. Decreasing the impedance of the electrode-electrolyte interface is one of the solutions to decrease the power consumption for the electrode to stimulate the auditory neurons. Platinum black has the porous structure, which enlarges the surface area and lowers the impedance. However, platinum black electrodes have not been used in cochlear implants because most part of their platinum coating might be lost during mechanical insertion, and deteriorate in biological fluids (G. M. Clark et al., 1977). In recent years, some processing methods have been reported where mechanically stable platinum black was fabricated (S.A. Desai et al., 2010; R. Kim et al. 2013). In the present study, we evaluated the effect of platinum black electrodes whether it could decrease the impedance by measuring electrically evoked auditory brainstem responses (EABRs). We used two types of ball electrodes. The first one pure platinum without coating. The other one was platinum plated with platinum black. The diameter of the ball 0.6mm in length. After we inserted electrodes into the scala tympani of cochleae of Hartley guinea pigs, we measured EABR. A constant-current stimulator-generated electrical stimuli, which were biphasic current pulses with 100 μs phase durations. The intensity was increased by steps of 10 μA. During the EABR measurements, we measured the corresponding voltage excursion simultaneously. Here in we presented results of comparing the impedances, the thresholds, and the power consumption between platinum black electrodes and pure platinum electrodes.

PS 912

A Stem Cell-Alginate Coated Cochlear Implant for Chronic BDNF-Delivery is Stable and Neuroprotective In Vitro

Jana Schwieger[1]; Silke Hügl[1]; Annika Hamm[2]; Thomas Lenarz[3]; Andrea Hoffmann[2]; Thomas Rau[1]; Verena Scheper[4]
[1]*Department of Otolaryngology, Hannover Medical School, Germany;* [2]*Dep. of Orthopaedic surgery, Hannover Medical School, Germany;* [3]*Department of Otolaryngology, Hannover Medical School, Germany and DFG Cluster of Excellence Hearing4all;* [4]*Department of Otolaryngology, Hannover Medical School, Germany; Cluster of Excellence*

Background
The functionality of the cochlear implant (CI) is influenced by the nerve-electrode-interface. This interface might be improved by exogenous BDNF (brain-derived neurotrophic factor) application which protects the spiral ganglion neurons (SGN). A prerequisite for a longer lasting neuroprotective effect on SGN is a chronic BDNF application. One possibility for chronic drug delivery to the cochlea is the implantation of genetically modified cells. To avoid an uncontrolled migration of the cells or an enhanced immune reaction in the inner ear, the encapsulation of the cells in a bioinert alginate-matrix is one way to prevent patients from the named risks and let them benefit from neuroprotective effects of BDNF.

Methods
Bone marrow derived human mesenchymal stem cells (MSCs) were lentivirally modified for human BDNF-production. The MSCs were embedded in ultra-high viscosity alginate and linked to human-sized CI-electrode models after poly-L-lysine pre-coating. Multiple layers of embedded MSCs and final layers of cell-free alginate were applied by dip coating. For stability testing the coated electrodes were inserted three times into a cochlea model. Before and after first and last insertion microscopic images of the coating were taken and analyzed for amount and degree of abrasion. The neuroprotective effect of encapsulated MSCs was tested by co-cultivation of alginate-MSC-beads with dissociated neonatal rat SGN. The positive control included 50 ng/ml purified recombinant human BDNF, while the nega-

tive control lacked BDNF and beads. After 48 hours of cultivation, the bead-stability was macroscopically verified and the supernatant harvested for ELISA-detection of the BDNF content. The number of surviving neurons was counted after neuron-specific staining for survival rate calculation.

Results

It is possible to apply alginate-encapsulated MSCs by dip coating to the electrode array. After first insertion the amount and degree of abrasion was low but increased by repeated insertions. The alginate-MSC-beads were stable in culture and BDNF-secretion in a range of 50 to 600 pg/ml was detectable. The encapsulated MSCs significantly protected the SGNs from degeneration compared to negative control and were as neuroprotective as the positive control.

Conclusions

Alginate-encapsulated, BDNF-producing MSCs are a promising option for neuroprotection of SGN. A CI-coating with encapsulated cells is a feasible way for drug delivery. Further investigations have to verify the maintenance of the BDNF-production, the capacity of MSCs from different donors for lentiviral-mediated BDNF secretion and the survival of the MSCs in vivo. A technical optimization of the CI-coating might increase its stability. Supported by the German Research Foundation.

PS 913

Moldable Coupler for Round Window Stimulation - New Developments

Darcy Frear[1]; Hideko Nakajima[2]
[1]Harvard University, Mass Eye and Ear; [2]Department of Otology and Laryngology, Massachusetts Eye and Ear, Harvard Medical School, Boston, MA, USA

Instead of introducing sound to the inner ear by mechanically stimulating the oval window (as in normal air conduction - AC), the cochlea can be driven in reverse by mechanically stimulating the round window (RW). Commercially available middle-ear devices such as the Vibrant Soundbridge ® floating mass transducer (FMT) are used for RW stimulation, and other actuators have been proposed for this purpose. Today, RW stimulation with available devices produce variable hearing results the devices have been shown to work, however, with limitations and not consistently across ears. Furthermore they require surgical risk of removing bone near the RW membrane. In order to account for the variability among ears and ensure the safety of the delicate RW membrane and contents of the inner ear, we have developed a device that safely couples the motion of an actuator to the RW membrane (ARO 2015). Our original cylindrical fluid filled coupler equipped with two flexible membranes (with one end conforming to the RW niche space) was shown to have wide dynamic range, wide bandwidth and linearity. We are now making improvements for biocompatibility, consistency and ease of surgical implantation.

Anatomy from temporal bones and histological sections were studied for optimal shape and size of the RW coupler. Schematic drawings were first created to determine the necessary qualities desired (fit in ear, stimulation method, and safety). Intact temporal bones yielded measurements to create a simple prototype which was modeled in SolidWorks and printed with a 3D printer. Different shapes of the device were printed in order to determine the best overall fit of the device and actuator (how the device is stimulated) in the ear. Our new coupler design allows for the actuator motion to be orthogonal to the plane of the RW membrane, allowing for improved placement of the whole assembly. For the membranes of the coupler, silicone adhesive sealant is flexible and can be made very thin (<0.3mm). The device was tested outside the ear to determine the durability and compatibility of the device to different actuators.

Preliminary data indicate durability of the 3D printed structure and flexible membranes with different actuators. The device will be tested in human cadaveric temporal bones to determine the performance of the coupler to transmit sound to the inner ear. The major focus is on stabilizing the device with biocompatible materials and to make it an efficient and safe device.

PS 914

Preparation, characterization and application research of a sustained dexamethasone releasing electrode coating for cochlear implantation

Hongzheng Zhang[1]; Muqing Xu[1]; Dong Ma[2]; Dongxiu Chen[1]; Jieqing Cai[1]; Qiaofang He[3]; Fan Shu[1]; Jie Tang[4]
[1]Department of Otolaryngology, Zhujiang Hospital, Southern Medical University; [2]Key Laboratory of Biomaterials of Guangdong Higher Education Institutes, Department of Biomedical Engineering, Jinan University; [3]Operating Room of Anesthesiology Department, Zhujiang Hospital of Southern Medical University; [4]Department of Physiology, School of Basic Medical Sciences, 2Institute of Mental Health, Southern Medical University

Cochlear inflammatory response after cochlear implantation (CI) is an important mechanism for implantation trauma and hearing loss. The hearing loss was also

caused by damage to auditory hair cells (HCs), whereas ion homeostasis within the cochlea can ensure survival of HCs. In our study, pure hyaluronic acid (HA) was crosslinked with butanediol diglycidyl ether (BDDE) and the successful preparation of the cross-linked hydrogel (CHA) was confirmed by rheological characteristics and FTIR spectra. Artificial perilymph (APL) was prepared to simulate the ion homeostasis microenvironment within scala tympani of human cochlear, and served as the major component of artificial perilymph soaked CHA (APL-CHA). The conductivity experiment indicated that APL-CHA is more suitable to the requirements of the electrical conductivity in scala tympani. The electrode coating process found that the extrusion coating method have advantages of controllable adhesive capacity of APL-CHA, uniform coating thickness and smooth surface as compared to common method. Due to CI surgery application requirement, optimization of coating process was selected as follows: extrusion coating method, degree of 3.6vol%, pinhole diameter of 32G (110µm), pressure of 200±15.81Psi. Controlled dexamethasone 21-phosphate sodium salt (DSP) release of 20 days could be demonstrated using the hydrogel filled reservoir via a validated HPLC method. The morphological structure of CHA showed different sizes of porous structure among APL-CHA provided structural basis for drug delivery. L929 fibroblasts culture results in the CCK-8 assay revealed that APL-CHA possesses fine biological compatibility. APL-CHA shows a promising application in CI surgery and has great potential in preventing hearing loss with well simulation of ion homeostasis within the cochlear, local DSP delivery for target anti-inflammatory, approximate conductivity within the scala tympani and optimization of electrode coating process.

PS 915

Mechanisms underlying therapeutic hypothermia-induced protection of residual hearing in cochlea implantation

Rachele Sangaletti[1]; Caroline Williams[1]; Ilmar Tamames[2]; Fred Telischi[3]; Dalton Dietrich[4]; Curtis King[5]; Michael Hoffer[6]; Suhrud Rajguru[7]
[1]Department of Otolaryngology, University of Miami; [2]Department of Biomedical Engineering, University of Miami; [3]University of Miami Miller School of Medicine, Department of Otolaryngology; [4]Department of Neurological Surgery, University of Miami; [5]Lucent Medical Systems; [6]Department of Otolaryngology and Neurological Surgery, University of Miami; [7]Department of Biomedical Engineering and Otolaryngology, University of Miami

Background
Cochlea implantation (CI) causes inflammation and oxidative stress in the inner ear structures, leading to an acute and progressive hearing loss. We have shown that localized application of mild therapeutic hypothermia prevents and protects sensory hair cells against this trauma. However, the mechanisms by which hypothermia confers this protection in the inner ear remain poorly understood due its ability to activate several pathways simultaneously. In the present study, we characterized the efficacy of localized therapeutic hypothermia applied to the cochleae in reducing residual functional loss associated with electrode insertion trauma. Furthermore, we investigated the role of inflammatory and oxidative stress targets such as cytokines, chemokines as well as sirtuin proteins in hypothermia-induced otoprotection.

Methods
In chronic experiments, the auditory brainstem responses (ABRs) were recorded from anesthetized rats to assess their hearing function before and after CI. Changes in hearing following electrode insertion trauma were tested in the following groups of animals: 1) normothermic CI, 2) hypothermia-treated CI and 3) hypothermia-alone controls. Contralateral cochleae were used as intra-animal controls. In a separate set of animals, cochleae were harvested at several time points after each treatment for mRNA and protein extraction. Western Blot and rt-qPCR were performed to quantify gene and protein level expression of selected factors in CI hypothermic cochlea compared to CI normothermic and control cochlea. Immunostaining for reactive oxygen species (ROS) was performed 24 hours after cochlea implantation surgery.

Results
Results suggest that therapeutic hypothermia provided during cochlear implantation significantly reduced associated trauma and prevented residual functional loss. Additionally, hypothermia-treatment alone did not cause any adverse effects on residual hearing. Our preliminary results suggest a significant change in expressions of pro-inflammatory and oxidative stress indicators as well as of anti-apoptotic Bcl2. Experiments are under way to establish the role of NAD^+-dependent sirtuin proteins as targets of hypothermia preconditioning treatments.

Conclusion
Hypothermia protects residual hearing against electrode-induced trauma through inflammatory and oxidative stress pathways. Our data will highlight the role of hypothermia as beneficial therapy against traumatic effects caused by cochlear electrode insertion.

Conducting Polymer-Based Cochlear Electrodes

Guillaume Tourrel[1]; Mary J. Donahue[2]; Pierre Stahl[1]; George Malliaras[2]
[1]OTICON MEDICAL; [2]Ecole Nationale de Mines de Saint Etienne, Department of Bioelectronics

Background One of the major objectives in the development of cochlear implant systems is to further improve the efficiency of electrical stimulation by limiting energy consumption or improving the spatial selectivity. Various approaches have been explored, such as a better-fitted pulse shape, improved signal processing strategy, optimal placement of the electrode array inside the scala tympani, or modified design of the electrode array through variation of the electrode shape and material. Currently, all commercially available cochlear implant electrode arrays use electrode contacts made of an iridium/platinum alloy. Methods Among the multiple existing materials used for electric stimulation, conducting polymers are one of the most promising materials based on their electrical characteristics and the ability to interface with human tissues. In order to have a basis for comparison, we produced and tested iridium/platinum-based electrode in 2 configurations: (1) Unroughened (or smooth) iridium/platinum electrode, cylindric shape, Diameter 0.7mm * Thickness 0.47mm with a geometric area = 1.03mm². (2) Roughened iridium/platinum electrode, cylindric shape, Diameter 0.7mm * Thickness 0.47mm with a geometric area = 1.03mm². The poly(3,4-ethylenedioxythiophene) doped with poly(styrene sulfonate) (PEDOT:PSS) conducting polymer, was evaluated and fabricated according to two different processes: (3) Spin-coating deposition of PEDOT:PSS on a 2µm flexible Parylen C (PaC) substrate, with 100 nm thick gold interconnects. The electrode area was 0.07mm². (4) Direct coating by electrodeposition on the iridium/platinum electrodes with a cylinder shape, Diameter 0.7 mm * Thickness 0.46 mm with a geometric area = 1.03mm². We also used our current commercial electrode array: (5) Roughened iridium/platinum electrode, cylindric shape, Diameter 0.4mm * Thickness 0.47mm with a geometric area = 0.46mm². Results All the electrode samples were characterized with Electrochemical Impedance Spectroscopy (EIS) over a frequency range from 0.1 Hz to 10 kHz. - Impedance on roughened electrode (2) was 5 times lower compared to unroughened electrode (1). - Impedance on roughened electrode (2) with direct PEDOT coating (4) was 2.5 times lower compared to roughened electrode (2). Secondly, electrodes were connected to an OM cochlear implant stimulator to measure electrode impedances in clinical conditions: - Impedance on spin-coated PEDOT:PSS electrode on flexible PaC (3) was 2.5 times lower compared to roughened iridium/platinum electrode contact (5). Conclusions

Knowing the spin-coated PEDOT:PSS electrode area (3) was 6.5 times lower than iridium/platinum electrode (5), these results confirmed that PEDOT technology for cochlear implant stimulation is promising and could bring significant improvement for the stimulation.
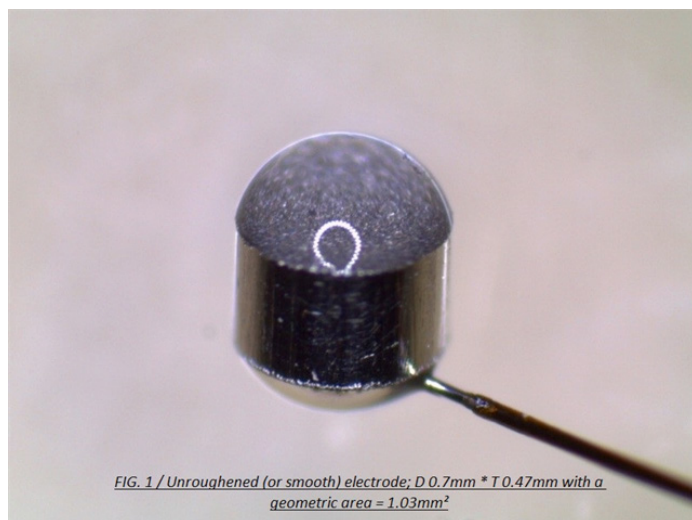

*FIG. 1 / Unroughened (or smooth) electrode; D 0.7mm * T 0.47mm with a geometric area = 1.03mm²*
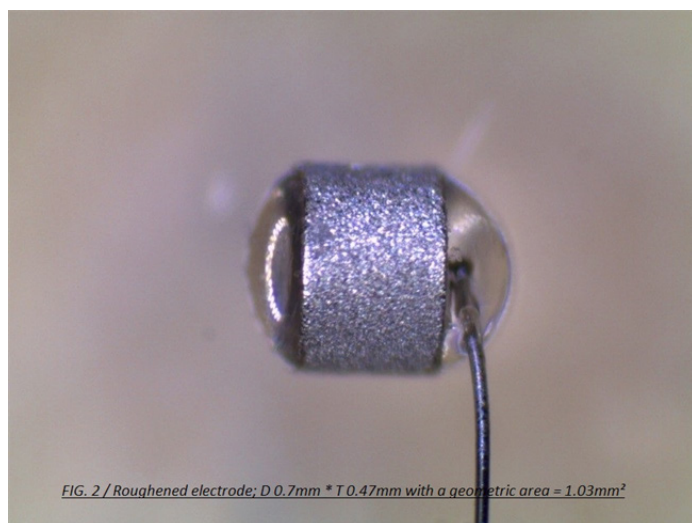

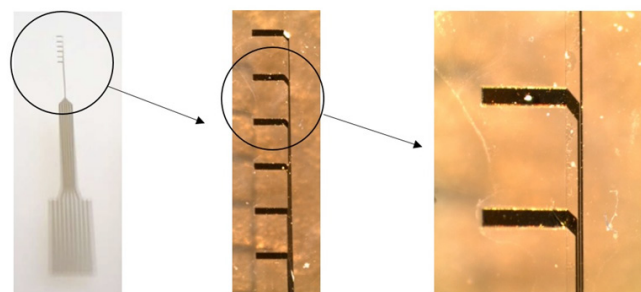*FIG. 2 / Roughened electrode; D 0.7mm * T 0.47mm with a geometric area = 1.03mm²*

FIG. 3 / Microfabricated array with spin-coating deposition of PEDOT:PSS on a 2µm flexible Parylene C (PaC) substrate, with 100 nm thick gold interconnects. The electrode area was 0.07mm²
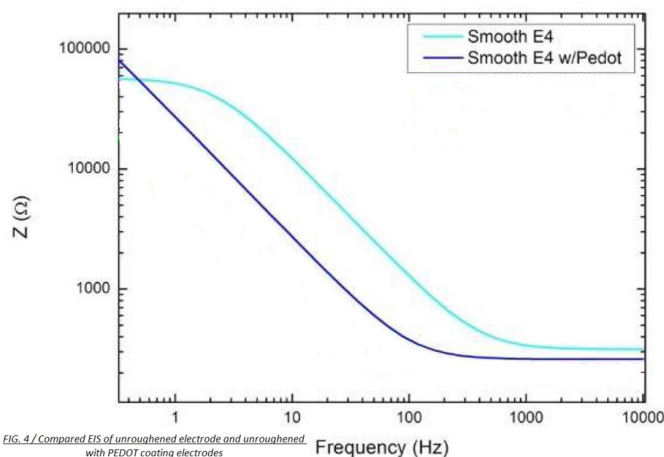
FIG. 4 / Compared EIS of unroughened electrode and unroughened with PEDOT coating electrodes
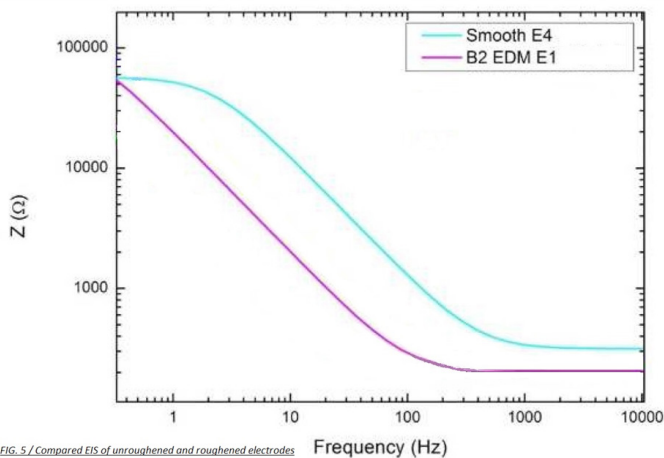

FIG. 5 / Compared EIS of unroughened and roughened electrodes

PS 917

Implantable Optrode Arrays of Edge Emitting Laser Diodes Evoked Auditory Responses in Vivo

Yingyue Xu[1]; Xiaodong Tan[1]; Nan Xia[1]; Claus-Peter Richter[2]

[1]Department of Otolaryngology-Head and Neck Surgery, Feinberg School of Medicine, Northwestern University; [2]Department of Otolaryngology-Head and Neck Surgery, Feinberg School of Medicine, Northwestern University & Resonance Medical, LLC, Chicago

Background

The use of infrared neural stimulation (INS) has been proposed as a novel method for neural stimulation in cochlear implants. INS has been shown to be more spatially selective than electrical stimulation, which could result in more independent perceptual channels for cochlear implants. In particular, for speech in noise recognition and for music perception it has been proposed that more independent may be beneficial. For the present study, we built arrays with small edge emitting laser diodes (Vixar Inc., Plymouth, MN), which were inserted in scala tympani of the basal cochlear turn of guinea pigs to test whether the light delivery system is able to evoke auditory responses.

Method

Edge emitting laser diodes (300 μm wide, 100 μm thick, and 250, 350, or 450 μm long) were assembled into arrays of multiple diodes and were inserted into the guinea pig cochlea. The emission wavelength of light sources is 1850 nm. Their output power is up to 50 mW for continuous wave mode at room temperature with a power efficiency up to 14%. For the measurements, the arrays were inserted into guinea pig cochleae. Compound action potentials (CAPs) were recorded in response to INS. Cochlear function was also determined by recording acoustically evoked CAPs before and after the cochleostomy surgery. During the stimulation, the arrays were operated with a 100 μs pulse width and 100 Hz repetition rate. The maximum output energy ranged from 8 to 20 μJ/pulse for individual laser diodes, which was measured in air using a Coherent J-50-LP-1A. For comparison, the light was delivered with an optical fiber, which was coupled to a table-top laser fiber (Lockheed Martin Aculight Corp., Bothell, WA).

Results

The threshold to evoke a CAP using INS and the optical fiber coupled to the table-top laser was on average 17 μJ/pulse. The edge emitting arrays were inserted into the cochleostomy to stimulate the base of the cochlea. CAPs were observed with edge emitting arrays with output energy over the INS evoked CAP thresholds. CAPs disappeared when the edge emitting arrays were partially extracted from the cochleostomy so that the emitting side was no longer towards the spiral ganglion.

Conclusion

Our data showed that auditory response could be evoked in vivo by optrode arrays made of edge emitting laser diodes. Future studies will focus on prototyping INS optrode arrays for cochlear implant users.

PS 918

Audio-frequency characterization of biomaterials for hearing prostheses

Nima Maftoon[1]; Nicole L. Black[2]; Payam Razavi[3]; Cosme Furlong[3]; Aaron K. Remenschneider[4]; Jennifer A. Lewis[2]; John J. Rosowski[1]; Jeffrey T. Cheng[5]
[1]Eaton Peabody Lab, Massachusetts Eye and Ear Infirmary, Harvard Medical School; [2]Harvard John A. Paulson School of Engineering and Applied Sciences, Harvard University; Wyss Institute for Biologically Inspired Engineering, Harvard University; [3]Center for Holographic Studies and Laser micro-mechaTronics, Mechanical Engineering Department, Worcester Polytechnic Institute; [4]Massachusetts Eye and Ear Infirmary, Harvard Medical School; [5]Eaton Peabody Laboratory, Massachusetts Eye and Ear Infirmary; Department of Otolaryngology, Harvard Medical School

In recent years our group has developed 3-D printed tympanic-membrane (TM) grafts for tympanoplasty in an effort to improve upon currently used autologous and non-autologous graft materials. 3-D printed grafts are designed with aims of ensuring reliable tympanopastly outcomes and improved vibroacoustic response. A range of biomaterials have been investigated. Successful development of effective TM grafts and other auditory prostheses requires knowledge of the mechanical properties of the employed materials at relevant audio frequencies. Such properties are currently unknown for most biomaterials. In this work we tested a mixed analytical-experimental approach to characterize biomaterials at audio frequencies. We 3-D printed biomaterials in circular plate geometries with varying thicknesses. We clamped the specimens on a holder with varying diameter and measured their motions in response to broadband sound stimuli using laser Doppler vibrometry and time-averaged optoelectronic holography techniques. We then fit the experimental measurements to analytical solutions and used experimental modal-analysis techniques to characterize the frequency-dependent mechanical properties of the biomaterials. In this report we demonstrate our methods by applying them to characterize frequency-dependent mechanical properties of Polydimethylsiloxane (PDMS), a commonly used biomaterial. Our results quantify the elastic modulus of PDMS up to 6 kHz and demonstrate a previously unknown frequency dependence of its damping. Knowledge of material properties is vital for establishing valid finite-element models that can be used to guide the optimization of prosthetic design. Findings have relevance for the establishment of effective TM graft materials with proper vibroacoustic response.

PS 919

Towards an Intracochlear Acoustic Receiver for a Totally Implantable Cochlear Implant System

Flurin Pfiffner[1]; Lukas Prochazka[1]; Ivo Dobrev[1]; Adrian Dalbert[1]; Jae Hoon Sim[2]; Francesca Harris[3]; Jérémie Guignard[4]; Joris Walraevens[3]; Christof Röösli[1]; Alexander Huber[1]
[1]University of Zurich, University Hospital Zurich, Department of Otorhinolaryngology, Head and Neck Surgery, Switzerland; [2]University Hospital Zurich; [3]Cochlear Technology Centre, Belgium; [4]Cochlear AG, European Headquarters, Basel, Switzerland

Background

Intracochlear sound pressure measurements are limited by the small dimensions of the human inner ear and the requirements imposed by the liquid medium. In-vivo evaluation methods of the pressure change in the cochlea are limited by the portability of existing devices. This project aims to develop intracochlear acoustic receivers (ICAR's) designed to measure the inner ear pressure in human temporal bones and in acute animal experiments. In addition, the ICAR is designed to replace external microphones of existing cochlear implant (CI) systems. This will be an important step towards a totally implantable CI system.

Methods

The presented ICAR concept consists of a MEMS condenser microphone (MEMS CMIC) with a passive protective diaphragm sealing the MEMS CMIC against the liquid medium and enabling insertion into the inner ear. These new sensors were used for intracochlear sound pressure measurements. Prototype I (PT I) sensors have been inserted at different locations in the inner ear of human and sheep temporal bones (scala tympani and scala vestibuli). The sensor's position was controlled by a custom micromanipulator system and verified with a subsequent CT-scan and 3D reconstruction of the temporal bone. Prototype II (PT II) sensors were designed for surgical insertion in the scala tympani in acute sheep experiments.

Results

A MEMS CMIC-based ICAR concept was developed to fulfill the major requirements for intracochlear sound pressure measurements in human and sheep temporal bones (prototype I sensors) and in acute experiments in sheep (prototype II sensors). Validation tests in human temporal bones at high stimulation levels (> 85 dB SPL) yielded data in agreement with the literature. We conclude that the presented ICAR concept is a useful sensor with a robust design for measurements of intracochlear sound pressure that could be applied in repeated measurements without marked sensitivity changes.

Conclusions

Results confirm that MEMS CMIC-based ICAR's are a useful technology for measurement of intracochlear fluid pressure. This presented ICAR concept has potential as an acoustic receiver in totally implantable cochlear implants.

PS 920

Plasmon-electric Hybrid Stimulation of Primary Neurons and its Applicability for Cochlear Implant Technologies

Ratka Damnjanovic[1]; Parveen Bazard*[1]; Robert D. Frisina[1]; Venkat Bhethanabotla[2]
[1]*Global Center for Hearing and Speech Research, University of South Florida- Tampa;* [2]*Chemical & Biomolecular Engineering Dept., Global Ctr. for Hearing & Speech Res., University of South Florida- Tampa*

Introduction

Cochlear implant technology is based on electrical stimulation, which has disadvantages due to the poorly controlled spread of electrical current, even with bipolar electrodes, resulting in low spatial/frequency resolution. Recently, it has been shown that infrared stimulation can excite neurons: peripheral, cranial, cochlear nerve, etc.; however infrared light can generate excessive heat in non-target, surrounding tissues. Most recently, an optical plasmonic stimulation of neurons has been demonstrated by our group, using green light (532 nm visible wavelength) pulsed by a monofilament laser fiber, aimed at the tip of a gold nanoparticle-coated micropipette positioned next (~2 μm) to a patched SH-SY5Y neuroblastoma cell (Bazard et al.; Sci. Rep. 2017). Electrophysiological recordings were achieved utilizing the whole-cell configuration patch-clamping method. This plasmonic methodology has the potential to be more selective than electrical stimulation, and less harmful to the surrounding tissue compared to infrared approaches.

Methods

The present study expands our previous plasmonic stimulation findings into a wider proof of concept arena; this time using primary trigeminal neurons cultured from 5-7 week old C57Bl/6 mice to demonstrate applicability and reproducibility. Plasmonic stimulation uses gold or other metal nanoparticles, which possess plasmonic properties that can be tuned, based on surface plasmon resonance phenomena, to respond to specific light wavelengths for modulating the firing patterns of electrically-excitable cells. The present study applies a novel hybrid neuron stimulation method which combines electrical and plasmonic stimuli at different ratios to fine-tune the response. This method is tunable to even more degrees of freedom compared to plasmonic stimulation alone.

Results

In-vitro recordings of trigeminal neurons were performed by patch clamping them and simultaneously applying electrical and optical laser pulses. We discovered that the electrical stimulus threshold required to evoke action potentials is reduced by 40-50% as the plasmonic stimulus (1-5 ms pulse width) is added, compared to electrical stimulation in the absence of plasmonic. Also, electrical action potentials were recorded after hybrid stimulation at a higher success rate as compared to after pure plasmonic stimulation. The reduction of current required to trigger action potentials, and the evidence that cells stay healthy after repeated exposure to hybrid stimulation, bode well for a new generation of tunable cochlear implants.

Conclusion

These principles and results will help develop improved cochlear implants that offer more precise frequency modulation enabled by more selective and tunable activation of auditory neurons.

PS 921

Implantation of conformable auditory brainstem implant arrays: a pilot human cadaveric study

Osama Tarabichi[1]; Nicolas Vachicouras[2]; Vivek V. Kanumuri[3]; Ruwan Kiringoda[1]; Samuel Barber[4]; Elliott D. Kozin[5]; M. Christian Brown[3]; Stéphanie Lacour[2]; Daniel J. Lee[3]
[1]*Massachusetts eye and ear Infirmary;* [2]*ÉCOLE POLYTECHNIQUE FÉDÉRALE DE LAUSANNE;* [3]*Eaton Peabody Lab, Massachusetts Eye and Ear Infirmary;* [4]*University of Arizona;* [5]*Massachusetts Eye and Ear Infirmary, Harvard Medical School*

Introduction

The auditory brainstem implant (ABI) electrically stimulates second order auditory neurons of the cochlear nucleus in deaf patients with severe cochlear or cochlear nerve abnormalities. The ABI provides sound detection that aids in lip-reading but mean outcomes are modest compared to the cochlear implant. Existing ABI designs include a rigid surface electrode array (700-μm thickness) that does not conform to the curved surface of the brainstem. We hypothesize that this condition is associated with poor contact of electrodes with the brainstem surface, leading to channel interaction and high activation thresholds. Recent advancements in bioelectronics have allowed for the microfabrication of soft conformable arrays that improve electrode-brainstem interactions. The conformability of arrays made with elastic materials can be tuned, in part, by varying the thickness of

the material in which they are held. Thin arrays (<50μm thick) have very high conformability, however, they fold easily and lack the rigidity necessary for insertion into the lateral recess of the brainstem. Herein, we aim to fabricate human-sized ABI array prototypes of different thicknesses using elastic materials (silicone rubber) and evaluate them in a human cadaveric model.

Methods
Paddle dimensions of the NucleusR ABI (8x3.5mm) (Cochlear Ltd.) were adapted from Rosahl et al (2012). Using histological axial slices of the CN, we defined the range of thickness (150-300 μm) for the array to enable conformability. Next we prepared, PDMS (poly(dimethylsiloxane)) membranes by spin-coating on glass wafers with thicknesses of 100, 200 and 300 μm. Mock-up electrodes and interconnects were embedded in the PDMS membranes to help with visualizing the paddle-tissue position. Standard retro-sigmoid and translabyrinthine craniotomies were performed on fresh human cadaveric heads to visualize the cerebellopontine angle, lower cranial nerves, and choroid plexus. PDMS ABI prototypes were inserted into the lateral recess of the IVth ventricle under rigid endoscopic guidance.

Results
PDMS ABI paddles with varying thicknesses were successfully fabricated. Paddles of 200 and 300μm thickness were easy to manipulate and insert into lateral recess using traditional surgical techniques. The 100μm thick paddle wrinkled and folded against the surface of the brainstem on insertion and placement was challenging.

Conclusion
Our novel ABI design is an important step towards translation of conformable neural implants for use in central auditory prostheses. Future studies will include integration of a clinical stimulator with functional conformable ABI electrode arrays in our cadaveric model.

PS 922

System for infrared neural stimulation in humans

Claus-Peter Richter[1]; Yingyue Xu[2]; Xiaodong Tan[2]
[1]*Department of Otolaryngology-Head and Neck Surgery, Feinberg School of Medicine, Northwestern University & Resonance Medical, LLC, Chicago;* [2]*Department of Otolaryngology-Head and Neck Surgery, Feinberg School of Medicine, Northwestern University*

Background
It has been demonstrated that neural stimulation with light can be spatially more selective when compared with electrical stimulation. Current spreads in the tissue and interactions between neighboring electrodes occur. The overlap in stimulation of spiral ganglion neuron populations limits the number of independent channels which can be used to parallel process acoustic information in cochlear implants (CIs). It has been postulated that better performance of CI users in noisy listening environments and improved music perception could be achieved by increasing the number of independent channels for stimulation. Here we propose a method to add optical sources to an electrode array used in contemporary CIs to increase the number of independent channels.

Methods and Results
The cochlear implant electrode of a contemporary CI system was used and was expanded at its tip with optical sources. First, a short array of side emitting laser diodes is fabricated. The cathode of the light sources was contacted with a single backbone, a 25 μm platinum-iridium wire. The anode of each of the light sources was then contacted with an additional platinum-iridium wire. Rather than ball bonding or wedge bonding of the wires, the optical sources were connected with conductive epoxy. The side emitting laser diodes were separated by 0.5 mm. The array was assembled and embedded in biocompatible Silastic, and then tested for function. The optical array was then fixed to the tip of a conventional CI electrode, and elongated the contemporary electrode by about 2 mm. Care was taken not to cover the electrical contacts of the contemporary electrode with Silastic during the fabrication of the optical array. Following the assembly of the hybrid electrode, its dimensions and physical properties were determined, including the insertion force of the electrode.

Conclusion
The resulting opto-electrical hybrid electrodes are a prototype for electrodes which can be used to evaluate novel coding strategies of optical and electrical stimulation in the cat animal model. The electrode also provides the human sized opto-electrical hybrid electrode, which can be used for testing in human cadaveric temporal bones for insertion and mechanical stability.

Funding

The Accuracy of Optical Pulse Amplitude Modulation at the Peripheral Hearing Level

Patricia Stahn[1]; Hubert H. Lim[2]; Marius Hinsberger[1]; Katharina Sorg[1]; Lukas Pillong[1]; Hans-Jochen Foth[3]; Achim Langenbucher[4]; Bernhard Schick[1]; Gentiana I. Wenzel[1]

[1]*Saarland University Faculty of Medicine, Department of Otolaryngology, Homburg, Germany; [2]University of Minnesota, Department of Biomedical Engineering; [3]University of Kaiserslautern, Department of Physics; [4]4Saarland University Faculty of Medicine, Experimental Ophtalmology, Homburg, Germany*

Introduction
Laser light applied at the tympanic membrane (TM) activates the hearing system. To develop a useful auditory prosthesis controlled modulation of the incoming optical signal for a precise activation of the peripheral hearing organ is mandatory. We previously demonstrated the possibility to frequency specific activate the hearing organ with our novel optical pulse amplitude modulation paradigm (ARO2015-2017). To prove the accuracy of our stimulation paradigm, we analyzed the distortions of the resulting vibrations in vitro and in vivo as well as the spread of activation in vivo.

Methods
Calculations and signal generation were performed with MATLAB® (R2014a, The MathWorks Inc., Natick). We inserted ex vivo a 365 µm diameter optic fiber into the outer ear canal of guinea pigs (n=9) and directed it towards the TM. Using a scanning laser Doppler Vibrometer (LDV, PSV-500, Polytec GmbH, Waldbronn), we recorded the vibration velocity of the TM after application of 10 ns laser pulses (532 nm Q-switched, INCA-laser system with acousto-optic modulator, Xiton Photonics, Kaiserslautern) modulated as sinusoids. We calculated the vibration displacement of the TM from the measured velocity data. The laser modulation rate (LMR) ranged between 1 and 10 kHz, the laser pulse rate (LPR) was 32 kHz or 50 kHz with the maximal energy/pulse between 0 and 12 dB re 1µJ/pulse. We compared the ex vivo results with the frequency specific recordings within the central nucleus of the inferior colliculus (ICC) in response to optical stimulation.

Results
Two main types of distortions occurred in vitro: The peak at the second harmonic depended on the LMR leading to a constant distortion ratio below 0.25 across all LPR/LMR combinations. The peak resulting from the LPR at 32 kHz or 50 kHz was not depending on the LMR. With our paradigm, resulting in a decreasing number of pulses per sinusoid period, the LPR distortion ratio increases with increasing the LMR. In vivo, the distortions at the 2nd harmonic observed in vitro could not be detected, most probably due to the middle ear damping and thresholds below neuronal detection. The spread of activation at ICC level after optoacoustic stimulation was at least as good as after pure acoustic stimulation

Conclusions
The results confirmed in vivo and in vitro that optical pulse amplitude modulation could be used for frequency specific activation of the peripheral hearing system. Studies to optimize different stimulation strategies to achieve high intensity pressure output under consideration of the biocompatibility margins are in progress.

Combined Electro-Optical Stimulation of Spiral Ganglion Neurons in a Mouse Model of an Optogenetic Cochlear Implant

Fadhel El May[1]; Xiankai Meng[2]; Vivek V. Kanumuri[2]; Osama Tarabichi[3]; Stéphanie Lacour[4]; Albert Edge[5]; M. Christian Brown[2]; Daniel J. Lee[2]

[1]*Massachusetts Eye and Ear Infirmary, Harvard Medical School; [2]Eaton Peabody Lab, Massachusetts Eye and Ear Infirmary; [3]Massachusetts eye and ear Infirmary; [4]ÉCOLE POLYTECHNIQUE FÉDÉRALE DE LAUSANNE; [5]Harvard Medical School*

Introduction
An optical cochlear implant may address limitations of electrically-based devices as light can be more spatially focused to create a greater number of independent auditory channels compared to existing designs. Light-driven stimulation of the cochlea is now feasible using optogenetics, which relies on the introduction of light-sensitive transmembrane ion channels to modulate spiral ganglion neuron (SGN) activity using pulsed visible light. A first generation optical CI will likely be a hybrid device combining both electrical and optical modalities to potentiate SGN responses. However, the interaction between electrical and optical stimulation is not well studied in the photosensitized cochlea. Here, we explore the effect of combined electrical and optical stimulation of SGNs on evoked auditory brainstem responses (ABRs) in a mouse model of cochlear optogenetics.

Methods
C57BL/6J mice expressing channelrhodopsin 2 (ChR2) driven by Cre-recombinase enzyme were used. The same strain mice with no ChR2 expression were used as controls. Following induction of anesthesia, a cochleostomy was performed distal to the round window niche using a postauricular approach followed by insertion of a conformable microelectrode array (École Polytechnique

Fédérale de Lausanne(EPFL))and flexible optical fiber (Thorlabs). Biphasic electric pulses (with alternating polarity, 0.4 ms duration) and blue light (488 nm, 1 ms duration) were presented in a 25 Hz pulse train. We examined the effect of five different co-stimulation paradigms on ABR threshold and morphology.

Results
ChR2-expressing mice showed evoked ABRs to either electric or optical stimulation. When tested near threshold, combined light and electrical stimulation usually resulted in larger peak amplitudes that approximated the sum of peak amplitudes from each modality alone. Paradigms where electrical stimulation was presented concurrently and immediately following light stimulation resulted in summation, but paradigms where electrical stimulation preceded optical stimulation did not. Control mice showed no optogenetic responses.

Conclusions
Co-stimulation using electrical and optogenetic approaches can produce larger evoked auditory responses. These results support the development of a hybrid electro-optical cochlear implant combining both stimulation modalities.

PS 925

In Vitro and In Vivo Models to Test the Effects of Electrical Stimulation on the Inner Ear

Adrien Eshraghi[1]; Christopher O'Toole[1]; Jorge Bohorquez[2]; Carolyn Garnham[3]; Rahul Mittal[1]; Emre Ocak[1]; Jeenu Mittal[1]
[1]*Hearing Research Laboratory, Department of Otolaryngology, University of Miami Miller School of Medicine, Miami, FL 33136, USA;* [2]*Department of Biomedical Engineering, College of Engineering, University of Miami;* [3]*MED-EL Corporation, Innsbruck, Austria*

Introduction
While there is a trend to implant patients with residual hearing, we know that cochlear implantation may cause some loss of this residual hearing. The direct effect of implantation of the electrode in macroscopic structures of the inner ear is well described, however, the effect of the electrical field generated by the implant has not been investigated to date. Some recent data suggests that the electrical stimulation can have a negative effect on the auditory system. However, the role of such stimulation on sensory cells in vitro and on hearing ability in vivo is not well established. The objective of this study was to determine the effect of electrical stimulation on auditory system employing in vitro and in vivo models.

Materials and Methods
A custom stimulator circuit that allows to study several parameters, including stimulation amplitude, pulse width, and total stimulation duration was designed. For the in vitro work, organs of Corti explant cultures from P3 rats were used. For in vivo work, the adult guinea pigs were implanted with a cochlear implant and subjected to a number of periods of electrical stimulation via constant activation of the implant. Stimulation was applied with varying parameters to determine the effects of the stimulation on the survival of hair cells. Survival was quantified by counting hair cells in organ of Corti explants using confocal microscopy. Auditory Brainstem Recordings (ABR) were performed to determine hearing thresholds in the guinea pig model.

Results
In the present study, a compact and easily-adjustable stimulator circuit was developed. It has sufficient flexibility to imitate a wide range of cochlear implant settings. By varying the amplitude, pulse width, and time parameters, we are able to achieve the simulation required for the electrical effects similar to a cochlear implant. There was a decrease in hair cell count in the explants exposed to higher duration of stimulation. In vivo testing revealed the possibility of testing the effects of changing various stimulation parameters on hair cell survival. Experiments are in progress in our laboratory to determine whether electrical stimulation induces oxidative stress and inflammation in the cochlea.

Conclusions
In summary, the electrical stimulator developed in this study can be used to understand the effect of electrical field on inner ear sensory cells. The models developed in this study using electrical stimulation can be used as a powerful tool to screen future otoprotective drugs for the preservation of residual hearing post-cochlear implantation.

Clinical Testing & Otopathology

PS 926

Cross Correlation and Machine Learning in the Analysis of Auditory Brainstem Response

Sihan Li; Jeewoo Kim; Hyun-Suk Ryoo; Jung-Bum Shin
University of Virginia

Auditory brainstem response (ABR) is a widely accepted method for testing hearing sensitivity. However, determination of hearing threshold is subjective and depends on the researcher';s experience. Additionally, characteristics of the ABR waves may differ between test subjects. It is important to develop a method to normalize the ABR

data and objectively determine the hearing threshold.

Here, we propose a novel method of combining Cross-correlation function (CCF) and deep neural networks for ABR wave evaluation and hearing threshold determination. CCF, which is used in signal processing and measures the similarity between two signals, is widely used for ABR analysis and quality assessment because it can provide information about ABR waves such as latency, intensity of response, and similarity between whole ABR plots. Deep neural networks are used for machine learning and can be applied to such experiments by using the CCF information as input to classify hearing sensitivity. Deep learning is a growing field where the use of deep neural networks has enabled scientists to analyze non-linear big data. Previously, there has been research of applying machine learning to ABR threshold determination. The development of deep learning has potential to build upon and improve the accuracy for this study.

In our study, CCF is used as a feature extraction method and enables normalization of the data by comparing the interleaved ABR responses. These features include the correlation coefficient at latency of zero and the maximum coefficient in a certain time window. Based on this, we created a training dataset with the information from the CCF results acquired from previous ABR data. For better variance, this dataset is acquired from mice with both normal and abnormal hearing. In the future, we plan to use this pre-classified dataset of CCF values to build a supervised deep learning model for hearing threshold classification.

PS 927

Tubomanometry in Children: Normative Data and Feasibility

Nicolas Gürtler; Götz Kuhlmann
Department of Otolaryngology University Hospital Basel Switzerland

Research Background Chronic dysfunction of the Eustachian tube is a frequent disease in children often requiring multiple interventions. Diagnostics is mainly limited to tympanometry and otomicroscopy. Tubomanometry, as developed by Esteve, represents a new diagnostic tool, potentially increasing diagnostic power. Tubomanometry has not yet been well validated and normative data for children does not exist. In this study we exmined the feasibility of tubomanometry in children and established normative values in children with normal Eustachian tube function. Methods A power analysis was performed to evaluate the number of children needed to analyze normative data. Dysfunction of the Eustachian tube was excluded by a questionnaire, otomicroscopy and tympanometry. Tubomanometry was performed twice at pressure level 30mBar, 40mBar and 5mBar for each side. Following parameters were analyzed : R-value, C1-C2, P1-P2 and age. Statistical analysis was done with SSPI. The study was approved by the Ethics Committee of the University Hospital, Basel, Switzerland. Results 38 children were included in the study. Age ranged from 5-16 years (mean 11 years). Measurements were completed in all cases. The results for the R-value, P1-P2 and C1-C2 according to age will be graphically depicted and statistically analzyed. Conclusions The findings and the value of tubomanometry in the diagnostics of chronic Eustachian tube dysfunction in children will be discussed and presented.

PS 928

An analysis of power reflectance in patients with superior canal dehiscence

Salwa Masud[1]; Xiying Guan[2]; Stephen Neely[3]; Hideko Nakajima[4]
[1]*Harvard Program in Speech and Hearing Bioscience and Technology;* [2]*Eaton-Peabody Laboratory, Massachusetts Eye and Ear; Department of Otolaryngology, Harvard Medical School;* [3]*Boys Town National Research Hospital;* [4]*Department of Otology and Laryngology, Massachusetts Eye and Ear, Harvard Medical School, Boston, MA, USA*

Superior canal dehiscence (SCD) is an opening in the bony wall of the superior semicircular canal. This defect alters the inner ear mechanics resulting in various auditory and vestibular symptoms. Often times, patients with SCD syndrome experience wrong and/or delayed diagnosis since SCD symptoms mimic a number of other common otologic pathologies. Diagnosis of SCD is generally confirmed with computed tomography (CT) imaging. However, CT cannot determine very small lesions that can produce significant symptoms. CT is also not often performed on patients with CHL or vertigo. Because SCD symptoms are due to a mechanical pathology, a mechanical measure – power reflectance can potentially be useful in diagnosing SCD.

Power reflectance (PR) is a measure of the ratio between the reflected sound energy from the eardrum and the forward sound stimulus. Because reflectance depends on the acoustic input impedance (Z_{in}) at the eardrum, PR is capable of detecting and differentiating middle ear pathologies that alter Z_{in} in a distinct way. PR also has the potential to inner-ear macro-mechanical lesions such as SCD. Previously, we found that in patients, SCD was commonly associated with a narrow-band decrease (notch) in PR near 1 kHz, and that generally after surgery this notch disappears. However, the mechanisms

of such patterns and the causes of inter-subject variation are not well understood.

The present study aims to elucidate the mechanisms of distinctive PR patterns in SCD patients and determine important factors that contribute to the inter-subject variation. We explore the use of a computational phenomenological lumped-element model to fit each subject';s PR as well as the Z_{in}. By using a nonlinear least squares approach, the model produces estimates of the dimensions of the ear canal (length and radius) and the critical parameters sensitive to the PR pattern for each patient';s ear. Variations in these critical parameters (i.e. the impedance of the dehiscence and the impedance of the round window membrane) in both SCD ears and normal ears are studied using the model.

PS 929

Smartphone Audiometry in Nicaraguan Schoolchildren

Isabelle Magro[1]; Karen Mojica[2]; Odile Clavier[3]; Catherine Rieke[4]; Abigail Fellows[4]; Jay Buckey[1]; James Saunders[5]
[1]Geisel School of Medicine at Dartmouth; [2]United Medical Center, Managua-EMP Central Hospital; [3]Creare, LLC; [4]Space Medicine Innovations Laboratory, Geisel School of Medicine at Dartmouth, Hanover, NH, United States; [5]Dartmouth-Hitchcock Medical Center

Background

Childhood hearing loss is prevalent, but often unrecognized in impoverished rural communities, leading to diminished language development, educational outcomes and employment opportunities. Hearing screening is challenging in these communities due to a lack of trained healthcare workers and testing locations with high ambient noise. Creare';s Wireless Automated Hearing Testing System (WAHTS) is a highly-noise-attenuating headset controlled through a mobile platform that requires minimal training (5-10 hours) to operate. If minimally trained personnel could perform high quality audiometry in schools using this device, children with hearing loss could be identified early and avoid lifelong disability.

Methods

A medical student (IM) completed 8 hours of training before using the WAHTS to screen 102 second and third graders (59 girls, 61 boys, average age 8) over 7 days at a school in Jinotega, Nicaragua. Ambient noise was measured with a sound level meter. Automated and manual audiometry was performed at 1, 2, and 4 kHz. Thresholds >25 dB HL for one or more frequencies were considered screening failures. A certified audiometric technician retested 101 children in an audio booth at the local hospital-based audiology clinic. IM also repeated manual screening with WAHTS in the audio booth for children who failed the school screening.

Results

All children with hearing loss (4 of 101) were detected with automated and manual screening using WAHTS in the school and confirmed using gold standard audiometry in an audio booth (sensitivity=100%). The false positive rate was significantly greater for automated screening, 23% (23 of 97) than manual screening, 3% (3 of 97), p<0.0001. Specificity was 76% for automated alone, 97% for manual alone, and 99% when a two-step process was used (those failing automated screening were tested manually) (Figure 1). The false positives from manual screening at the school passed manual WAHTS screening in the audio booth. Average ambient noise in the school (46 dBA± 0.4, n=95) was significantly higher than in the audio booth (23 dBA ± 1.4, n=7, p<0.0001). The average duration of testing was 20.2 minutes.

Conclusions

All children with hearing loss were identified with the WAHTS in a challenging field setting by minimally-trained personnel. Manual screening yielded a lower false positive rate than automated screening and may be a more reliable option for younger children. Automated screening may be used initially to screen children followed by manual screening for those who fail screening to reduce false positives and unnecessary referrals.

ARO Figure-1.pdf

PS 930

Preliminary Findings on the Prevalence of Decreased Sound Tolerance in Veterans with TBI

Sarah Theodoroff; Susan Griest; Kathleen Carlson; Frederick Gallun; Cody Blankenship; James Henry
VA RR&D NCRAR

Background

Traumatic brain injury (TBI) is considered the signature injury of the post-9/11 military conflicts in Iraq and Afghanistan and is associated with an abundance of sequelae including decreased sound tolerance (DST), often referred to as "sensitivity to noise." DST can have sensory and emotional aspects resulting in many negative consequences such that people who suffer from DST alter their lifestyles and social habits to avoid being around bothersome sounds. There are multiple components to DST which are not clearly defined. There is a critical need to address these gaps in our knowledge and determine the prevalence of DST in Veterans with TBI.

Methods

We examined preliminary data from the Noise Outcomes in Servicemembers Epidemiology (NOISE) Study, which addresses the etiology, prevalence, and effects of auditory complaints among recently separated Veterans. TBI history was assessed using a comprehensive TBI and blast-exposure questionnaire; DST was assessed using a screening question from the Tinnitus and Hearing Survey. Prevalence of DST was estimated for Veterans with versus without TBI history, and by categories of TBI source (e.g., military service-related TBI versus non-military TBI). Logistic regression analyses were performed to generate odds ratios (OR) and 95% confidence intervals (CI) estimating risk of DST by TBI history.

Results

From this sample [(N=278; mean age=33.5 years (SD=9.0)], the estimated prevalence of DST among Veterans with TBI history was 46%, compared to 36% among Veterans without TBI history. Prevalence of DST among Veterans with only military-related TBI was 50% while the prevalence among Veterans with only non-military TBI was 40%; among Veterans with both military and non-military TBI, prevalence was 43%. Of those with military-related TBI, the majority (72%) reported blast-exposure. Compared to Veterans without TBI history, those who experienced a military-related TBI were 1.8 times more likely to report DST; this association approached statistical significance (CI=0.97-3.23). Findings among those who experienced a non-military TBI, or who experienced both military and non-military TBI, compared to Veterans without TBI history were not statistically significant (OR=1.2; CI=0.58-2.40 and OR=1.4; CI=0.56-3.30, respectively).

Conclusions

Prevalence estimates from this preliminary analysis suggest DST is relatively frequent among Veterans with and without TBI. Preliminary findings suggest Veterans with military service-related TBI may be at increased risk of experiencing DST. Ongoing analysis include multivariable modeling to examine this association more closely while controlling for potential confounding variables. Additional work is needed to better define DST disorders. Supported by a Department of Defense grant (DoD-JW-MRP-60036)

PS 931

Otopathological Changes in the Cochlea Following Head Injury Without Temporal Bone Fracture

Reuven Ishai[1]; Renata Knoll[1]; Jenny Chen[1]; Kevin Wong[1]; Aaron K. Remenschneider[2]; David H. Jung[3]; Elliott D. Kozin[2]
[1]*Massachusetts Eye and Ear Infirmary; [2]Massachusetts Eye and Ear Infirmary, Harvard Medical School; [3]Eaton-Peabody Laboratories, Massachusetts Eye and Ear; Department of Otolaryngology, Harvard Medical School*

Introduction

Auditory dysfunction following temporal bone (TB) fracture may result from direct transection of the middle and inner ear. The pathophysiology of hearing loss due to head injury without TB fracture, however, is not well understood. Few reports describe pathologic findings in the auditory periphery of humans after head injury. Herein, we investigate inner ear pathologic findings in patients who sustained head injury without evidence of TB fracture.

Methods

Subjects from the National Temporal Bone Pathology Registry with documented history of head injury without TB fractures were included. Exclusion criteria included patients with history of noise exposure, clinical or histologic temporal bone fracture through the inner ear, otologic surgery, otologic dysfunction prior to head trauma, and/or severe post-mortem artifact. TBs were evaluated by light microscopy. Inner ear anatomy, including counts of spiral ganglion cells (SGC), hair cells (HC), pillar cells, health of stria vascularis and the presence of endolymphatic hydrops was evaluated. SGC counts were compared to normative historical age-matched controls.

Results

Five patients corresponding to six temporal bones met inclusion and exclusion criteria. The average age when head injury occurred was 60 (range from 44 to 78 years old). The average age of death was 81 years (range from 66 to 96 years old). All cases had evidence of inner ear pathology, and all cases had a decreased number of total SGC with an average of 65% loss (range 43% to 84%) compared to historical normative age-matched controls. The SGC count loss occurred along all parts of the Rosenthal';s canal (Segment I-IV) and was evenly-distributed. Four cases were found to have marked scattered atrophy of all three (marginal, intermediate and basal) layers of the stria vascularis. Three of six cases had cochlear endolymphatic hydrops, and one case had blockage of the endolymphatic duct.

Conclusions

This is the first contemporary otopathology study to investigate a series of human temporal bones from individuals with a history of head injury without evidence of temporal bone fractures. Otopathological analysis in patients with a history of head injury demonstrated significant inner ear pathology, even in the absence of TB fracture. Unrecognized peripheral auditory pathology in patients following head injury may in part mechanistically explain the development of hearing loss and tinnitus that has been clinically reported.

PS 932

Temporal Bone Histopathology of Furosemide Ototoxicity

Felipe Santos; Joseph B. Nadol
Department of Otolaryngology, Massachusetts Eye and Ear, Harvard Medical School, Boston, MA, USA

Objective

To describe the human temporal bone pathology in two patients who incurred furosemide induced ototoxicity.

Patients

A 46 year-old woman in acute liver and renal failure treated with high doses of furosemide for anasarca who developed a rapidly progressive severe to profound asymmetric sensorineural hearing loss.

A 65 year-old woman with undifferentiated small cell carcinoma of the lung who received intravenous furosemide one day prior to death for pulmonary edema.

Intervention(s)

Removal of temporal bones, histologic processing and light microscopy of temporal bones.

Main Outcome Measure(s)

Temporal bone histopathology and correlation with clinical and audiometric data.

Results

All three temporal bones demonstrated edema and cystic changes in the stria vascularis. In the first case the furosemide exposure was associated with hearing loss and the pathological changes were more extensive including cystic changes in the Hensen';s cells, collapse of Reissner';s membrane and the tectorial membrane and diffuse loss of inner and outer hair cells with only modest reduction in the spiral ganglion cell population. In the second case, without attributable hearing loss, there was only modest reduction in hair cell and spiral ganglion cell counts. Pathological changes were not observed in the ampullae of the semicircular canals or epithelium of the saccular or utricular maculae in either case.

Conclusion

The temporal bone pathologic correlate for furosemide-induced ototoxicity is edema and cystic degeneration of the stria vascularis. The degree of degenerative change appears dose-dependent. We infer that pathological changes may occur in the absence of a measurable immediate clinical effect.

PS 933

IgG4-Rlated Disease involving unilateral Temporal Bone

Liao Kaxi[1]; **Feng Bo**[2]; Shiming Yang[3]; Peng Tao[1]
[1]Department of Otolaryngology-Head and Neck Surgery, Nanchong Central Hospital,The second affiliated hospital of North sichuan medical college; [2]Department of Otolaryngology-Head and Neck Surgery, PLA General Hospital, Beijing 100853, China; [3]Chinese PLA Medical School

Background

IgG4-related autoimmune disease(IgG4-RD) has not been noted until recent years. Its etiology and pathogenesis are complex and unclear. IgG4-RD is characterized by higher serum IgG4 level than normal, lesion significantly infiltrated by IgG4(+) plasma cells and inflammatory fibrosis condition that may affect multiple organ systems including pancreas, salivary glands and ect.Cases on patients with IgG4-RD in temporal bone, however, has been rarely seen in recent literature reviews. Current literatures report only 4 cases of igG4 affecting temporal bone. And case on the Chinese population has still not been reported.Hence, We report the first case of a Chinese with IgG4-RD affecting temporal bone , and summarize its clinical features, pathological characteristics and treatment.

Methods

A retrospective analysis of a patient with IgG4-RD in temporal bone was diagnosed in October 2015.

Results

The patient was a 58-year-old Chinese woman presented with earache, tinnitus, hearing loss and 40 days temporal bone mass. . Otological examination showed dermohemia and bulge in Posterior superior wall of the left external auditory canal, and normal tympanic membrane.Computed tomography showed left temporal bone mastoid region has swelling bone destruction , the main sign was osteolytic lesion. Magnetic resonance imaging demonstrated T1 signal little longer than T2 , high signal intensity on DWI, and even enhancement, with the lesion size is approximately 23mm×3m-

m×5mm. Pathological examination result diagnosed as IgG4-RD, IgG4-positive plasma cells up to 50/HPF (high power field) on the left. The results of two years follow-up visit reported no relapse. Immunoglobulin level testing showed only IgG3 level higher than normal. General PETCT examination indicated that no abnormality was found in left temporal bone and other parts of the body.

Conculsion

The clinical presentation and radiological findings of temporal bone IgG4-RD are nonspecific or untypical, and can easily be confused with other diseases. Definitive diagnosis must be made by histopathology and immunostaining examination. Surgical resection is the first choice for the treatment of temporal bone IgG4-RD ,which can effectively improve long-term remission. Corticosteroids and immunosuppression have positive effect on management of the disease.

Key Words

IgG4-RD, definitive diagnosis, Surgical treatment, immunostaining examination.
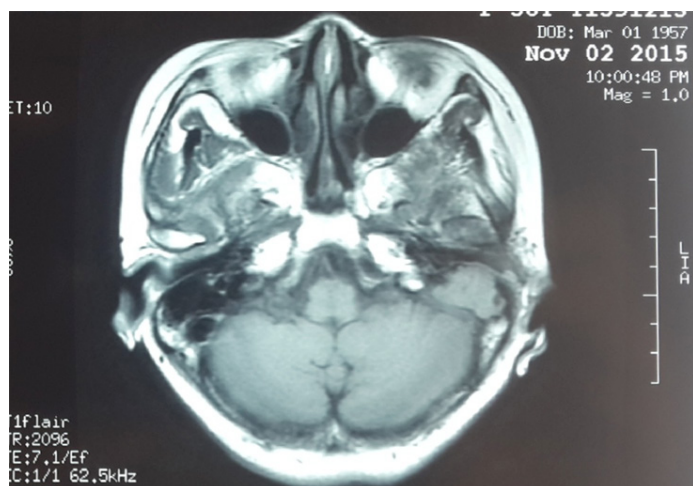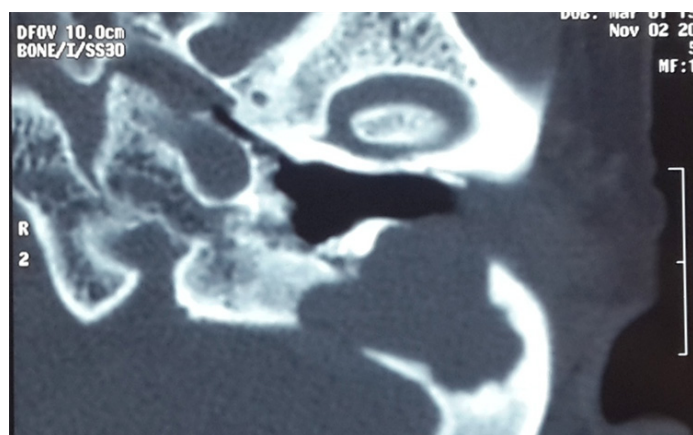
[IgG4-Rlated Disease involving unilateral Temporal Bone.docx](#)

Serum Total Bilirubin Level is Associated with the Severity of Hearing Loss in Bilateral Sudden Deafness

Dan Bing[1]; Lan Lan[1]; Dayong Wang[1]; Hongyang Wang[2]; Qiuju Wang[1]
[1]Chinese PLA General Hospital; [2]Eaton Peabody Lab, MEEI, Harvard Medical School/Chinese PLA General Hospital

Background

Hyperbilirubinemia has been well documented to be significantly associated with impaired auditory function. However, less is known about the impact of bilirubin within the normal or mildly elevated range on the auditory system. Recent studies indicated that bilirubin is a potent antioxidant with anti-inflammatory properties and high serum bilirubin may have cardio-cerebrovascular benefits. Since vascular dysfunction and viral infection are two of the main hypothesized etiologies in sudden sensorineural hearing loss (SSHL), the present study aimed to investigate the role of serum total bilirubin (TB) level in SSHL patients with bilateral involvement (BSSHL).

Methods

Thisobservational study enrolled 117 consecutive BSSHL patients who were stratified by tertiles of baseline TB levels (<10.5, 10.5-13.4µmol/L, 13.4 µmol/L). The dependent variables of interest included the hearing level across the affected frequencies (HL-AF) on admission and outcome measures defined as HL-AF at the end point, the hearing gain, or the dichotomized outcome of Siegel';s criteria.

Results

Elevated level of TB (> 21µmol/L) was only found in simultaneous BSSHL patients. Among them, four out of five had slightly elevation (21.1~24.2µmol/L) while only one had moderate increase (50.5µmol/L). The level of TB is significantly higher in male (13.8±6.2 µmol/L, 95%CI 12.7-15.0µmol/L) than female (10.4±4.2 µmol/L, 95%CI 9.5-11.4µmol/L) (P<0.0001). Participants with higher on-admission TB tended to be male and older, lower in hearing level before and after treatment in our hospital, more frequently had recovery, and less frequently had preceding infection history. Compared with lowest tertile, the regression coefficient (β) and 95% confidence intervals (CIs) for HL-AF on admission were -15.4 (-25.7, -5.0) in the highest tertile group after adjusting for possible confounding factors. These significant results persisted after excluding patients with mild hearing loss (HL-AF on admission ≤ 40 dB HL). The association between baseline TB and any outcome measures were not statistically significant.

Conclusion

Within the normal or mildly elevated range, higher levels of TB are independently and significantly associated with less severe hearing loss in BSSHL.

PS 935

Oxidative Stress in the Blood Labyrinthine Barrier in the Macula Utricle of Meniere's Disease Patients

Jacob L. Wester[1]; Ivan Lopez[2]; Akira Ishiyama[3]; Gail Ishiyama[4]
[1]*UCLA Department of Head and Neck Surgery;*
[2]*Department of Head & Neck Surgery, Geffen School of Medicine at UCLA;* [3]*David Geffen School of Medicine, University of California, Los Angeles;* [4]*UCLA Department of Neurology*

Background

There is mounting evidence for increased blood labyrinthine barrier (BLB) permeability in the inner ear of patients with Meniere';s disease (MD). Intravenous gadolinium, used in magnetic resonance imaging (MRI), is taken up into the perilymph presumably via perfusion through the BLB. In the ipsilateral MD perilymph, a pathologically increased uptake of gadolinium is noted, indicative of loss of BLB integrity. We recently published transmission electron microscopy of the BLB in the macula utricle of patients with intractable MD demonstrating destruction of the vascular endothelial cells (VECs) and degeneration of the BLB. We hypothesize that oxidative stress is involved in the pathogenesis of BLB degeneration and to date there are no studies of oxidative stress proteins in the human BLB.

Methods

We investigated ultrastructural and immunohistochemical changes of the BLB in the macula utricle from patients with MD (n=10), acoustic neuroma (AN) (n=3) and autopsy specimens (n=3) with no inner ear disease (normative). Each subject had a well-documented clinical history, audio-vestibular testing and MRI imaging. Utricular maculae were studied under TEM and double labeling immunofluorescence. VECs were identified using isolectin B4 (IB4) and pericytes were identified using alpha smooth muscle actin (aSMA).

Results

IB4 staining of the BLB in both AN and normative was universally identified. In contrast, IB4 was nearly undetectable in the MD specimens. aSMA was expressed in MD, normative, and AN specimens. Immunofluorescence of tight junction (TJ) proteins: ZO-1, claudin-1 and occludin, demonstrated no significant differences in MD specimens compared with normative and AN. Endothelial nitric oxide synthase (eNOS) and inducible nitric oxide synthase (iNOS) were used as markers of oxidative stress. The VEC in MD had significantly higher levels of expression of eNOS and iNOS compared with non-MD specimens.

Conclusions

The cellular and structural changes of the BLB in MD specimens are suggestive that while pericytes are relatively preserved, the VECs are subject to oxidative stress and undergo degenerative changes. These studies advance our scientific understanding of oxidative stress in the human inner ear BLB and otopathology.

Funding

PS 936

Mediation of Cigarette Smoke and Hearing Loss by Volatile Organic Compounds

Charles Pudrith[1]; William Dudley[2]
[1]*Northern Illinois University;* [2]*University of North Carolina at Greensboro*

Smoking cigarettes increases the chance of developing hearing loss. The mechanisms of cigarette-induced hearing loss are not well understood. Cigarette smoke contains volatile organic compounds, some of which are known to cause hearing loss. The purpose of this study was to determine if metabolites of volatile organic compounds found in cigarette smokers mediated the effect of smoking on hearing loss. To accomplish this, we downloaded hearing data, surveys on smoking status, and laboratory reports of metabolite concentrations in urine from the 2011-2012 cycle of the National Health and Nutritional Examination Surveys database. Among the 667 individuals that met the inclusion criteria of the study, those who indicating smoking at least 100 cigarettes throughout their lives had mean bilateral pure-tone thresholds at 4000 and 6000 Hz that were 3.7 dB higher ($t = 3.57$, $p = 0.0004$) than those who indicated that they did not smoke 100 cigarettes, after adjusting for age and gender. The PROCESS macro was used to measure the mediation of cigarette smoking on hearing loss by 12 VOC metabolites from 11 parent compounds. Of these 12 metabolites, two significantly (FDR = 0.05) mediated the effect of smoking. One mediator was N-acetyl-S-(2-hydroxyethyl)-L-cysteine, a metabolite of the ototoxic chemical, styrene. The other mediator was N-acetyl-S-(N-methylcarbamoyl)-L-cysteine, a mediator of N,N-Dimethylformamide. These results indicate that styrene and N,N-Dimethylformamide are toxins that may mediate cigarette smoke-induced hearing loss.

PS 937

Effects of Dosing on the Ototoxicity of Cisplatin Chemoradiation Treatment in Head and Neck Cancer

Ronald Maggiore[1]; Keri Bennett[2]; Garnett P. McMillan[3]; Shushan Rana[4]; S. Windy Lyle[5]; Marilyn Dille[2]; **Dawn Konrad-Martin**[3]

[1]*University of Rochester, Department of Medicine, Division of Hematology/Oncology; [2]VA RR&D National Center for Rehabilitative Auditory Research (NCRAR); [3]VA RR&D NCRAR; [4]Oregon Health & Science University, Department of Medicine, Division of Radiation/Oncology; [5]VA Portland Health Care System, Department of Hematology/Oncology*

Purpose

To characterize the effect of cisplatin dosing (bolus vs. weekly) on the risk of ototoxicity in a sample of Veterans undergoing chemoradiation for the treatment of head and neck cancer. Background The incidence of head and neck cancer (HNC) accounts for approximately 4% of all cancers in the United States and within the Veteran population. For patients with locally advanced, inoperable HNC, the treatment is generally concurrent cisplatin chemoradiation. Cisplatin is a known ototoxic agent. Bolus dosing, and radiation at or near the inner ear tissues may increase the potency of its effects. Importantly, many Veterans begin treatment with pre-existing hearing loss and up to half likely sustain ototoxicity from cisplatin. Even minor shifts in hearing, left untreated, can constrain effective provider-patient partnerships, family and workplace communication, and limit quality of life. A better understanding of the risk factors and clinical presentation of ototoxicity is needed to inform ototoxicity monitoring programs and treatment decisions.

Methods

Data were obtained prospectively in N=23 HNC patients at the VA Portland Health Care System receiving concurrent chemoradiation therapy with cisplatin for whom audiometry was obtained prior to treatment and at one or more fixed timepoints (35 days and 165 days) following initial treatment. We estimated the risk of audiogram shifts that met or exceeded the National Cancer Institute Common Terminology Criteria for Adverse Events (CTCAE) Grade 1, in relation to cisplatin dosing (>75mg/m2 or "bolus" vs. smaller weekly doses <40mg/m2). Effects of dosing were estimated using Bayesian analysis with priors informed by results of previous prospective studies on cisplatin ototoxicity. Descriptive statistics characterize the influence of additional treatment and patient factors (cisplatin cumulative dose, radiation dose, age, pre-existing hearing loss), and monitoring method (frequent hearing screening- vs. infrequent comprehensive hearing testing).

Results

Ototoxicity meeting CTCAE Grade 1 or greater within the conventional audiogram frequencies (through 8 kHz) was found at a rate of 40% for bolus dosing, whereas weekly smaller dosing generated about 2/3rds the risk (26%). The estimated risk of ototoxicity did not vary by hearing monitoring method.

Implications Evidence supports the view that CTCAE Grade 1 ototoxicity was associated with dosing in this sample. High dose regimens are more likely to cause ototoxic hearing loss. Implications for ototoxicity monitoring will be discussed.

PS 938

The localization of PENDRIN aggregation in Pendred syndrome patient specific iPSCs derived outer sulcus cells

Tsubasa Saeki[1]; Makoto Hosoya[2]; Takanori Nishiyama[2]; Saeko Matuzaki[2]; Shinsuke Shibata[3]; Tatsuo Matsunaga[4]; Masato Fujioka[2]; Kaoru Ogawa[5]; Hideyuki Okano[1]

[1]*Department of Physiology, School of Medicine, Keio University; [2]Department of Otolaryngology, Head and Neck Surgery, School of Medicine, Keio University; [3]Electron Microscope Laboratory, School of Medicine, Keio University; [4]Division of Hearing and Balance Research, National Institute of Sensory Organs/ Medical Genetics Center, National Hospital Organization Tokyo Medical Center; [5]Department of Otolaryngology, Head and Neck Surgery, Keio University School of Medicine*

Pendred syndrome (PDS) is the most frequent syndromic form of hereditary hearing loss. The disease is associated with the mutations in SLC26A4 which encodes an anion exchanger PENDRIN, yet the rodent models have not recapitulated human phenotype of progressive hearing loss. Furthermore, the ability to study human temporal bone pathology in nonlethal diseases is limited, as biopsy is precluded by cochlea anatomy. Therefore, we decided to conduct researches using patient derived-iPS cells directly examine human pathologies of PDS.

Previously, we have succeeded in inducing outer sulcus cells, the cochlear cells expressing PENDRIN from human induced pluripotent stem cells (iPSCs) and we examined the pathophysiology of Pendred syndrome patient derived cochlear cells. We found that the patient derived outer sulcus cells displayed aggregate of mutated PENDRIN protein and exhibited stress-induced cellular degeneration. Intracellular protein aggregation is one of the characteristics of neurodegenerative diseases such as Alzheimer';s diseases and Parkinson';s diseas-

es. The result suggests that the formation of PENDRIN aggregation may be involved in degenerative phenotypes of Pendred syndrome.

To further investigate the relationship between mutated PENDRIN aggregation and the pathophysiology of Pendred syndrome, we examined the detailed PENDRIN localization in the patient iPSCs derived-cochlear cells by using immunoelectron microscopy.

We found that all induced outer sulcus cells, either from healthy control individuals or patients, contain areas where electron density were relatively lower but were not surrounded by membrane structure. In the PDS patient derived cells treated by epoxomicin, however, some of these structures were fully covered by PENDRIN signals. The distribution is quite similar to that of aggregation-like PENDRIN immuncytochemistry in our previous study.

We also examined the ultrastructure of cochlear outer sulcus cell in a nonhuman primate common marmoset by electron microscope. The marmoset outer sulcus cells also had the similar low density organelle like-structures. The results suggest that the PENDRIN protein aggregation may be associated with the low density organelle like structures, which is well-developed in primate cochleae. Further investigation in human temporal bone will be awaited.

We previously revealed that the intracellular PENDRIN aggregates were co-localized with ubiquitin and LC3b. Furthermore, epoxomicin-induced cellular stress was inhibited by autophagy inducer, rapamycin. Taken together, we ask the organelle like structure may be involved in the function of protein degradation such as ubiquitin-proteasome or autophagy-lysosome. We will further examine the pathophysiology of Pendred syndrome by focusing on PENDRIN aggregation and protein degradation system.

PS 939

Low-dose rapamycin therapy proposed by an in vitro chronic disorder model of Pendred Syndrome using disease specific iPS cells

Makoto Hosoya[1]; Tsubasa Saeki[2]; Tatsuo Matsunaga[3]; Hideyuki Okano[2]; Masato Fujioka[1]; Kaoru Ogawa[4]
[1]*Department of Otolaryngology, Head and Neck Surgery, School of Medicine, Keio University;*
[2]*Department of Physiology, School of Medicine, Keio University;* [3]*Division of Hearing and Balance Research, National Institute of Sensory Organs/ Medical Genetics Center, National Hospital Organization Tokyo Medical Center;* [4]*Department of Otolaryngology, Head and Neck Surgery, Keio University School of Medicine*

Background

Pendred Syndrome is an autosomal-recessive disease characterized by congenital hearing loss and thyroid goiter. The incidence of the disease is estimated at 7.5 - 10 in 100,000. Pendred syndrome may account for as many as 10% of the cases of hereditary hearing loss, making it most common form of syndromic hearing loss. The hearing loss appears during childhood and is progressive. So far, we clarified the novel pathophysiology of Pendred syndrome, "Degenerative Cochlear Disease model", using in vitro cochlear cell models derived from patients'; specific iPS cells (Hosoya et al, Cell Reports, 2017). In this model we showed the cell stress susceptibilities, which finally caused cell death, were increased in patients'; derived cells with intracellular aggregation. Moreover, we also revealed the rapamycin can relief this cell death via activation of autophagy. We concluded that this cell death could explain the progression of hearing loss or fluctuations of hearing level of Pendred syndrome patients and rapamycin could be a potential therapeutic drug for Pendred syndrome. However, the long-term observation of cell survival that would be mimicking the natural course of this disease without the cell stressor and the rational minimum concentration of rapamycin that prevent the cell death has not been known. Here, we established an in vitro chronic disorder model of Pendred Syndrome and we report the possibilities of low-dose rapamycin therapy for Pendred Syndrome.

Methods

We induced PENDRIN positive inner ear cells from control and disease specific iPS cells via otic progenitors using specific induction medium as previously reported. We compared the long-term cell survival ratio and assessed the effect of the low-dose rapamycin.

Results

The survival of the PENDRIN positive cells derived from patient specific iPS cells were significantly decreased after long-term culture and low-dose rapamycin improved cell survival.

Discussion

Long-term cell culture of the neural cells induced from neurodegenerative disease specific iPS cells has been thought to be one of the potential in vitro chronic disorder model mimicking the progression of the neurodegeneration observed in the patients. In this report, we applied this technology for Pendred syndrome.

The inner ear cells derived from Pendred syndrome patients were more vulnerable for long-term culture and this weakness was relieved by the low-dose rapamycin. Our results suggest, this vulnerabilities for long-term culture of patient cells may account for the slow progression

of hearing loss in the patients and low-dose rapamycin therapy could rescue the patients of Pendred syndrome.

PS 940

FFR reveals acute and long-term auditory pathophysiology following sports-related concussion

Jennifer Krizman[1]; Tory Lindley[1]; Cynthia LaBella[2]; Danielle Colegrove[1]; Elaine C. Thompson[1]; Trent Nicol[1]; Travis White-Schwoch[1]; Nina Kraus[1]
[1]Northwestern University; [2]Ann & Robert H. Lurie Children's Hospital of Chicago

Diagnosis, assessment, and management of sports-related concussion requires a multi-modal approach. To date, this approach lacks an objective assessment of auditory processing. The auditory system is uniquely complex making it likely to be disrupted by a concussion. Brainstem, midbrain, and cortical auditory and non-auditory centers are highly interconnected; and, sound processing across these brain regions relies on exquisite temporal precision. Given this complexity and precision, together with the fact that axons are highly susceptible to damage from mechanical force, we hypothesize that auditory pathophysiology, defined as functional changes in auditory processing, are evident following a sports-related concussion. To test this hypothesis, we measured the speech-evoked frequency-following response (FFR), an objective electrophysiological measure of auditory processing, in normal-hearing collegiate and adolescent athletes at three points in the recovery process: acute (~24-48 hours post injury), intermediate (2-6 weeks post injury in symptomatic athletes), and long-term (1+ years post injury). We found that the FFR indicated auditory pathophysiology at all three time points. Immediately following a sports-related concussion, athletes had slower response timing and a weaker response to its fundamental frequency (F0), a pitch-based cue that facilitates speech understanding in complex listening environments. Weeks after the injury, athletes who were still symptomatic showed a smaller F0 response and timing delays (Kraus et al., (2016) Scientific Reports), coupled with poor hearing in noise. Over the long term, no timing delays were seen, however, the F0 response was still reduced (Kraus et al., (2017) Neuroscience Letters). Importantly, these athletes had suffered their concussion over a year prior and were deemed to have recovered from their injury, yet still showed auditory pathophysiology. While we saw improvement in auditory processing that tracked with symptom improvement in the acute and intermediate cases, the persistent reduction in F0 encoding years post injury suggests that concussion leaves a lasting imprint on auditory processing. From these findings we suggest that auditory processing is disrupted by concussion and should be evaluated following a head injury. Given that the FFR can reveal subtle processing deficits, we propose inclusion of this objective auditory measure in the multi-modal assessment of concussion.

Cochlea: Anatomy & Physiology

PS 941

Cochlear Parametric Shape Model and its Application for Cochlear Implantation Planning and Evaluation

Thomas Demarcy[1]; Clair Vandersteen[2]; Dan Gnansia[1]; Hervé Delingette[3]; Nicholas Ayache[3]; Charles Raffaelli[2]; Nicolas Guevara[2]
[1]Oticon Medical; [2]Nice University Hospital; [3]Inria

A parametric shape model of the scala tympani, the scala vestibuli and the full cochlea is presented.

The cochlear structures are defined as generalized cylinders, i.e. as cross-sections swept along a centerline. The centerline is parameterized in a cylindrical coordinate system by its radial and longitudinal coordinates within a given interval which defines the length of the centerline. The cross-sections are modeled by a closed planar shape on which a varying affinity is applied along the centerline. The scala tympani and the scala vestibuli are modeled with two half pseudo-cardioids while the cochlear cross-section corresponds to the minimal circumscribed ellipse of the union of the tympanic and vestibular cross-sections. The affinity of cross-section is parameterized by a rotation, a width and a height scaling. Eventually each of the derived component of the model is represented by a vector or a one-dimensional function of the angular coordinate. One-dimensional functions are themselves parameterized by combinations of simple functions (i.e. polynomial, logarithmic, etc.). The model is fitted to 9 cochleae which are manually segmented from a high-resolution micro-Computed Tomography (CT) images, the mean fitting error is equal to 0.15 mm. A compact set (N = 4) of cochlear model parameters are estimated for 987 CT images of temporal bones.

First, the parameters distributions estimated from a large dataset are used to generate random cochlear shape. By developing a cochlear insertion simulator, the surgical experience could be virtually augmented before the implantation, with patient specific or randomly generated cochlear shape. Second, the shape model is used to estimate the cochlear duct length and the a priori maximal atraumatic insertion length. Given such measures, the choice of the electrode design could be preoperatively optimized to be the least traumatic. Third, the cochlear shape model and inserted electrode array model are respectively fitted on pairs of pre- and post-

operative CT images. Pairs of CT images are rigidly registered using the FMRIB';s Linear Image Registration Tool from the FSL library. The resulting estimation of the position of the electrode with respect to the intracochlear cavities could be used to evaluate the surgical procedure and activate optimally the electrodes.

The three-dimensional cochlear model is of interest for cochlear implantation simulation, surgery planning and postoperative evaluation.

PS 942

Neonatal Morphology of the Apical Half of the Human Cochlea

Sebastiaan W.F. Meenderink[1]; Christopher A. Shera[1]; Michelle D. Valero[2]; M. Charles Liberman[3]; Carolina Abdala[1]
[1]Auditory Research Center, Caruso Department of Otolaryngology, University of Southern California; [2]Department of Otology and Laryngology, Harvard Medical School, Boston, MA, United States of America, Eaton-Peabody Laboratory, Massachusetts Eye & Ear Infirmary; [3]Harvard Medical School

Newborns have longer DPOAE phase-gradient delays than do adults in the apical half of the cochlea (<1.5 kHz). At the lowest frequencies, this difference is almost 1 ms. Because DPOAE phase is relatively independent of stimulus level, this immaturity cannot be explained by inefficiencies in middle-ear forward transmission. Neither is it easily explained by non-adult-like middle-ear delay, which is smaller (i.e., 0.2 ms round trip) than the observed difference due to age. We hypothesize that age-related differences in DPOAE delay are consistent with an immature frequency-place map secondary to immature stiffness and mass features of the neonatal cochlea. In this study, we seek to identify morphological properties in the apical turns of the neonatal cochlea that might contribute to the observed effects.

Human temporal bones from the collection at the Massachusetts Eye and Ear Infirmary were evaluated under light microscopy. We imaged mid-modiolar, horizontal temporal-bone sections from both neonates and adults with no history of inner ear disease. H&E-stained cross-sections of the organ of Corti (OoC) were imaged at locations approximately corresponding to characteristic frequencies of 3.5, 1.2, 0.75, 0.275, and 0.15 kHz. The positions of various anatomical structures/features were mapped, and the coordinates were used to calculate morphological metrics. These include the scala areas, the basilar membrane (BM) width (measured from spiral limbus to spiral lamina) and its thickness (i.e., height) at the mid-points of pars pectinata and pars tec-

ta, the width of the osseous spiral lamina (OSL), and the maximum height and area of the OoC.

Preliminary analysis suggests that the scala areas and the widths of the BM and OSL are similar in neonates and adults. This agrees with the notion that the human inner ear reaches adult size in utero. On a smaller scale, we observe differences between adult and newborn OoC morphology; its maximum height and total area are smaller in neonates. Future analyses will clarify whether these differences occur throughout the entire cochlea. Although BM width is not different between age groups, data suggest that in the pectinate zone its thickness is greater in the apical turns of the newborn cochlea compared to that of the adult. Since BM properties (e.g., stiffness) play an important role in shaping tuned cochlear responses and the tonotopic map, this difference in apical BM morphology may contribute to the age differences observed in low-frequency DPOAE phase.

PS 943

ELHnet: A convolutional neural network for classifying cochlear endolymphatic hydrops imaged with optical coherence tomography

George S. Liu[1]; Michael H. Zhu[1]; Jinkyung Kim[1]; Patrick Raphael[1]; Brian E. Applegate[2]; John S. Oghalai[3]
[1]Stanford University; [2]Texas A&M University; [3]University of Southern California

Detection of endolymphatic hydrops is important for diagnosing Meniere's disease, and can be performed non-invasively using optical coherence tomography (OCT) in animal models as well as potentially in the clinic. Here, we developed ELHnet, a convolutional neural network to classify endolymphatic hydrops in a mouse model using learned features from OCT images of mice cochleae. We trained ELHnet on 2159 training and validation images from 17 mice, using only the image pixels and observer-determined labels of endolymphatic hydrops as the inputs. We tested ELHnet on 37 images from 37 mice that were previously not used, and found that the neural network correctly classified 34 of the 37 mice. This demonstrates an improvement in performance from previous work on computer-aided classification of endolymphatic hydrops. To the best of our knowledge, this is the first deep CNN designed for endolymphatic hydrops classification.

PS 944

The developing concept of tonotopic organization of the inner ear, or, Where did I hear that?

Robert Ruben
Albert Einstein College of Medicine

Objective

To document historical conceptualization of the inner ear as the anatomical location for the appreciation of sound at a continuum of frequencies, and examine the evolution of current understanding of tonotopic organization.

Method

Primary sources from the 6th century BCE through the 20th century CE which had been noted in the various histories of otology, audiology, and acoustics were read, in the original language and/or in translation, to determine the view of the organization of the inner ear in that work/reference. Additionally, PubMed, Scopus, Google scholar and Index Med were searched for the terms tonotopic, cochlear mechanics and place theory of hearing. Each work/reference was categorized as to the methodology used to determine the role of the inner ear. The classifications were: theoretical; observation of anatomical structure which could account for localization of sound perception; physical models utilizing simulation; physical models utilizing biological material; physiological; animal behavioral studies; and human behavioral studies.

Results

Current understanding of the properties of the inner ear is a consequence of the acquisition over a long, complex history of the development of accurate information concerning acoustics, and the anatomy, physiology, and psychophysics of hearing. It was not until the 16th century that the physical and mathematical basis of resonance was described by Galileo. Concurrently, advances were made in the knowledge anatomy of the inner ear. This new knowledge led, in the 17th century, to the first theory of tonotopic organization in the 17th century, which stated that that high-frequency hearing was at the apex of the cochlea and low-frequency at the base of the cochlea. It was not until the 18th and 19th centuries that more accurate anatomical information became available which led to an opposite conclusion, and the formulation of the view we hold today: the localization of high tones at the base of the cochlea and low tones of the apex of the cochlea. During the end of the 19th century and beginning 20th century behavioral studies were carried out which in some instances were congruent of this concept. The discovery of physiological properties of the ear in 1930 allowed for physiological studies which were consistent with the concept of high low tone sensitivity continuum from base to apex. During the middle third of the 20th century both animal and human behavioral studies further supported this concept. Physical biological studies of the mid-20th century, however, while confirming the findings of greater sensitivity of high tones at the base and low tones at the apex, further demonstrated that for high-intensity sound there was a spread of effect through the entire cochlea, more so for low frequency tones than for high tones. This was consistent with animal and human behavioral studies.

Conclusion

Current understanding of tonotopic organization of the inner ear with regard to pure tones is the result of the acquisition over time of knowledge of acoustics, the anatomy, physical properties and physiology of the inner ear, and ultimately behavioral studies. Examination of this complex evolution leads to understanding of the way each approach through time builds upon those before it, culminating, through behavior studies, in a profound appreciation of empirical verification.

PS 945

Gadolinium-enhanced Magnetic Resonance Imaging of Induced Endolymphatic Volume Changes in the Murine Cochlea

Margarete Ueberfuhr[1]; Michael Czisch[2]; Benoit Boulat[2]; Markus Drexl[3]
[1]*German Center for Vertigo and Balance Disorders, Ludwig-Maximilians Universität München, Munich, Germany; Graduate School of Systemic Neurosciences, Ludwig-Maximilians Universität München, Martinsried, Germany;* [2]*Max Planck Institute of Psychiatry, Munich, Germany;* [3]*German Center for Vertigo and Balance Disorders, Ludwig-Maximilians Universität München, Munich, Germany*

Magnetic resonance imaging (MRI) has been proven to be a useful tool for gaining in-vivo access to the bone-enclosed mammalian inner ear. In a clinical setting, Gadolinium (Gd)-enhanced MRI can be employed to visualize volume changes of the inner ear fluids. Inner ear volume changes are the typical anatomical hallmark of Menières disease, a condition characterized by increased endolymph volume, termed endolymphatic hydrops. The mechanisms leading to endolymphatic hydrops are yet to be found and are most likely not exclusive to Menières disease, as simple manipulations of cochlear homeostasis can also lead to endolymphatic hydrops: In mice, endolymphatic hydrops, induced by systemic vasopressin administration, was successfully visualized by Gd-enhanced MRI (Degerman et al., 2015). Intense low-frequency sound, which causes transient changes of the cochlear activity, was also found to elicit endolymphatic hydrops in rodents. However, sound-induced endolymphatic hydrops has only been investigated in guin-

ea pigs by an indirect approach (Salt et al. 2004). Here, we used Gd-enhanced MRI (9.4 Tesla, T1-weighted 3D FLASH) to demonstrate the presence of endolymphatic hydrops or other (transient) structural changes in the cochlea after intense low-frequency sound exposure by directly visualizing inner ear fluid volumes. Four different experimental groups (male C57BL/6 mice, 8-11 weeks old) were included in the study: Group 1 was exposed to sound (100 Hz, 130 dB SPL, 50 min) during MRI session. Group 2 was subject to systemic vasopressin administration before MRI session (2 weeks of daily s.c. injections). Group 3 (control) was subject to administration of Ringers solution before MRI session (2 weeks of daily s.c. injections). Group 4 (control) was neither exposed to sound nor injected with any drug/solution. MRI data gathered in the present study will improve our understanding of the significance of endolymphatic hydrops in health and disease and how it relates to cochlear functional impairment. This work was funded by a grant (01EO1401) from the German Ministry of Education and Research (BMBF) to the German Center for Vertigo and Balance Disorders (DSGZ, project TRFII-6).

PS 946

Optimal Parameters for Cochlear Implant Visualization Using In-Line Synchrotron-Radiation Phase-Contrast Imaging

S. Alireza Rohani[1]; **Bradley M. Gare**[1]; John E. Iyaniwura[1]; Ning Zhu[2]; Sumit K. Agrawal[3]; Hanif M. Ladak[1]
[1]*Western University;* [2]*Canadian Light Source Inc.;*
[3]*London Health Sciences Centre*

Background

Visualization of a cochlear implant (CI) electrode relative to the basilar membrane (BM) is important for post-operative programming. Image processing techniques have been proposed to infer electrode and BM position using clinical computed tomography. To evaluate these algorithms, images are required that simultaneously show both the electrode and BM. Although micro-computed tomography (micro-CT) provides excellent visualization of the bony structures, soft tissues have low contrast and metallic objects create beam-hardening artifacts. We evaluated in-line synchrotron-radiation phase-contrast imaging (SR-PCI) combined with CT reconstruction. Regular CT is based on attenuation of X-rays as they traverse the sample, whereas with SR-PCI, the phase shift caused by the sample is transformed into detectable variations in X-ray intensity. In SR-PCI, imaging parameters such as object-to-detector distance (ODD) and beam energy (E) affect image quality.

Objective

To find optimum imaging parameters for in-line SR-PCI of the implanted cochlea.

Methods

One freshly-frozen cadaveric temporal bone was used. Following thawing, a CI (model Flex28, Med-El GmbH, Innsbruck, Austria) was inserted into the cochlea through the round window. The sample was then fixed using formalin. The specimen was imaged using in-line SR-PCI with CT reconstruction at the BioMedical Imaging & Therapy facility at the Canadian Light Source. Five different combinations of (ODD, E) pairs were evaluated. At the ODD of 2 m, three scans with E values of 47 keV, 60 keV and 72 keV were acquired. The remaining two scans were obtained with constant E value of 72 keV at ODD values of 1 m and 3 m. The detector used has isotropic pixel sizes of 8.5 μm, 8.6 μm and 8.9 μm for ODD distances of 3 m, 2 m and 1 m, respectively. The acquired 3D image volumes were compared using contrast-to-noise ratios (CNRs) of the BM and of the electrode. The extent of streaks caused by the electrode was quantified for each combination by computing standard deviations of voxels adjacent to it.

Results

Both intracochlear soft tissues and electrode were visible and discernable in all 5 imaging scenarios. However, artifacts were noticeably reduced in images with an E value of 72 keV. The maximum CNR and appropriate phase contrast were obtained with (ODD, E) = (1 m, 72 keV).

Conclusions

In-line SR-PCI with CT reconstruction is most effective in visualizing both the electrode and the intracochlear soft-tissues with maximum CNR and minimum metal artifacts with (ODD, E) = (1 m, 72 keV).

PS 947

Synchrotron radiation phase contrast imaging as an alternative to histological processing for study of the human inner ear

Janani S. Iyer[1]; Sergei Gasilov[2]; Ning Zhu[2]; Konstantina M. Stankovic[3]
[1]*Harvard University;* [2]*Canadian Light Source Inc.;*
[3]*Department of Otolaryngology, Massachusetts Eye and Ear*

The study of human inner ear morphology is presently limited by the fact that the sensory epithelium containing the cells that facilitate hearing, the organ of Corti, cannot be visualized at diagnostically-relevant resolution through standard clinical imaging technologies. As a re-

sult, the gold standard method for assessing the human organ of Corti';s structural integrity in cases of sensorineural hearing loss (SNHL) remains postmortem hematoxylin and eosin (H&E) histological processing, despite the artifacts known to result from the steps involved in implementing this technique (e.g. fixation, decalcification, sectioning and associated handling, and staining), and the time required for processing. Here, we present images of an intact human temporal bone acquired using synchrotron radiation-phase contrast imaging (SR-PCI), an ultra high resolution X-ray-based imaging technique, and demonstrate the technique';s potential to serve as a minimally-damaging alternative to histological processing for study of the human temporal bone. Specifically, we image the 3D-intact temporal bone from a patient with presbycusis-induced SNHL using SR-PCI, and compare the information gleaned from the resulting images to that provided through histological preparation of the contralateral ear from the same patient. Findings suggest that a) SR-PCI is sensitive to hair cell and neuronal damage in the cochlea, and b) damage visualized through SR-PCI corresponds to that visualized through H&E preparation. Given the short acquisition time and minimally-damaging nature of SR-PCI, in addition to the fact that the tomographic imaging method facilitates virtual sectioning and thus visualization along any plane in the cochlea, these results motivate further studies on SR-PCI';s diagnostic validity for human SNHL.

PS 948

A Novel Approach for Clinical Cochlear Duct Length Estimation

Max Eike Timm[1]; Daniel Schurzig[2]; Masoud Assadi[2]; Thomas Lenarz[3]
[1]*Department of Otolaryngology, Hannover Medical School;* [2]*MedEl;* [3]*Department of Otolaryngology, Hannover Medical School, Germany and DFG Cluster of Excellence Hearing4all*

Background
Prior to cochlear implantation (CI) surgery, the length of the cochlea (CDL) to be implanted should be taken into account for choosing an electrode array optimally suited for the individual patient. Hence, preoperative planning should ideally involve a measurement of the patient specific CDL. Alternatively, estimations of the CDL can be performed, e.g. using the basal diameter A as was proposed by Escudé et al. in 2006. These estimations are especially attractive from a clinical point of view since they can be done very quickly. However, within our studies we found that estimations with Escudé';s method a prone to error. This motivated the proposed development of a novel estimation method which covers the variability of the cochlear geometry in a more reliable manner and circumvents deviations resulting from implications of mathematical boundary conditions, e.g. cochlear spiral following a logarithmic profile.

Methods
Using Osirix MD, the cochlear lateral wall (LW) in cone beam CT (CBCT) scans of 217 CI patients was traced. In addition, a custom research tool was used for tracing the LW profile in 20 micro CT (μCT) datasets of temporal bones. The resulting 237 spirals were imported into Matlab and Python and analyzed to yield (a) to what extend the length profiles of CBCT and μCT differ, (b) if the length along the cochlea CDL(Θ) is dependent on the basal turn length (BTL) and (c) how simple measurements like the "A" value can be used to derive accurate BTL estimates. The results were then combined to derive a novel method for CDL estimation whose performance was compared to Escudé';s method.

Results
Differences in CBCT and μCT spline profiles could be observed especially in the apical cochlear region. However, the length along the cochlea spiral CDL(Θ) was found to be strongly dependent on the BTL in both CBCT and μCT data. Furthermore, it was shown that the employment of the basal diameters A and B for estimating the BTL yields significantly better estimates than Escudé';s method, i.e. the employment of A alone. The same holds true for the derived estimation method for CDL(Θ) in general, suggesting that the novel method is preferable to Escudé';s approach.

Conclusion
The determination of the patient specific CDL prior to CI surgery is important for optimal implantation outcomes. If measurements cannot be performed, the derived estimation approach is a feasible alternative and superior to approaches previously proposed in the literature.

PS 949

Eagles and Wind Turbines: Hearing Assessment as a Prelude to the Development of Acoustic Deterrence Tools

Edward J Walsh[1]; Peggy B. Nelson[2]; Jeff Marr[2]; Julia B Ponder[2]; Patrick Redig[2]; JoAnn McGee[1]
[1]*Boys Town National Research Hospital;* [2]*University of Minnesota*

Although controversial, the potential impact that wind energy installations have on bald (Haliaeetus leucocephalus) and golden (Aquila chrysaetos) eagle populations has recently arisen as an area of interest at the Department of Energy (DOE). According to a report published by Erickson et al. (2001), between 10,000 and 40,000 birds are killed annually in collisions with turbines, and an average of 0.03 raptor fatalities/turbine occurs each year. This report was filed over 15 years ago and the number of wind facility installations has increased dramatically in the interim. To address concerns and develop turbine collision mitigation strategies, DOE is supporting efforts to develop and implement protocols that employ acoustic signals engineered to discourage eagles from encroaching into the air space surrounding wind farms. As a prelude to the design and deployment of acoustic deterrence devices, the auditory and vocal attributes of both bald and golden eagles are being studied at the University of Minnesota and the Sia Mission (Comanche National Ethno-Ornithological Initiative) tribal aviary in Oklahoma. Because access to both eagle species is limited, the hearing of red-tailed hawks (Buteo jamaicensis), a surrogate species that will be studied under some circumstances, is also being assessed. Findings from preliminary auditory brainstem response studies suggest that the red-tailed hawk threshold-frequency curve resembles those reported in other raptors and passerine birds. The curve is bowl-shaped and the bandwidth of greatest sensitivity ranged between approximately 1.5 and 3 kHz. The lower and upper cutoff frequencies were approximately 400 Hz and 5 kHz, respectively, 30 dB above the best frequency threshold. Input-output curves were similar to those of other avian species, as were response latency-level curves. Findings from bald eagle recording sessions currently underway, or scheduled, will be compared with those observed in red-tailed hawks, and questions related to the impact of wind energy systems on wildlife will be considered in the context of fatalities related to collisions and the impact of noise produced by wind energy farms. Finally, we ask the question, how many wind turbine related eagle fatalities constitute too many in the context of eagle ecology and conservation biology. The low reproductive potential of eagles suggests that the loss of a relatively small portion of the existing population has the potential to promote the rapid decline in population abundance, a particularly alarming consideration given the expanding base of the wind energy industry. This study was supported by a grant from the DOE #DE-EE0007881.

PS 950

Cochlear Hair Cells, Supporting Cells and Nerve Fibers with Cholinergic Evoked Calcium Modulation During Early Development in a GAD2-Cre GCaMP5G Transgenic Mouse

Holly A. Holman[1]; Ali Almishaal[1]; Yong Wan[2]; Micah Frerck[1]; Richard D. Rabbitt[1]
[1]University of Utah; [2]Scientific Computing and Imaging Institute

Background

Developing inner hair cells (IHCs) fire spontaneous calcium-based action potentials (APs) that disappear upon IHC maturation and by the onset of hearing in mice (~P14). These APs trigger glutamate release in the absence of sensory stimuli, and are modulated by cholinergic (ACh) inputs from efferent contacts on IHCs and by ATP from inner phalangeal cells (IPCs) of Kölliker';s organ. We imaged ACh-evoked intracellular calcium [Ca^{2+}] modulation during this dynamic period in GCaMP5G expressing hair cells and supporting cells.

Methods

Transgenic mice expressing GCaMP5G in GABAergic cells were generated by crossing a floxed GCaMP5G-IRES-tdTomato (G5-tdT) line with GAD2-IRES-Cre driver line. Immunolabeling of fixed tissues was performed to examine expression patterns of calretinin, ChAT, GABA, GAD65, and myosin VIIa. For live cell [Ca^{2+}] imaging the bony labyrinth was resected, to access the organ of Corti, which was carefully immobilized and continuously perfused. Confocal images of GCaMP fluorescence modulation ($\Delta F/F$) were acquired in time sequences and z stacks to study the action of 500 ms application of 1mM ACh.

Results

The G5-tdT reporter was highly expressed in IHCs, IPCs, outer hair cells (OHCs) and nerve fibers/terminals in an age dependent manner. Spontaneous [Ca^{2+}] transients were present in excised tissue, but were infrequent at rest. Rates increased when the tissue was exposed to ACh. ACh-evoked [Ca^{2+}] modulation in IPCs initiated at the base and travelled toward the apex with an apparent intracellular propagation speed of ~25 µm-s^{-1}, magnitude $\Delta F/F$~1, and total duration ~1-10s. Calcium modulation in IHCs initiated inside the basolateral plasma membrane with magnitude of $\Delta F/F$~0.2 and subsequently appeared in the cell body with a total duration ~5-10s. The time course in IPCs and IHCs was consistent with activation of calcium induced calcium release (CICR). Calcium modulation in OHCs were spatially compact (~1 µm), small in magnitude $\Delta F/F$~0.08, and occurred during each brief ACh pulse, consistent with kinetics of α9/α10 nAChRs and putative local action of the synaptoplasmic

reticulum. Immunolabeling demonstrated expression of GAD65 puncta within both IHCs and OHCs at their basolateral membranes. GABA immunolabeled in efferent boutons at the base of IHCs.

Conclusions

ACh-evoked [Ca^{2+}] modulation reveals cell-specific kinetics and spatial extent in the postnatal developing cochlea. Immunolabeling further showed GABA containing efferent boutons synapsing with GAD65 expressing IHCs, and GABAergic nerve fibers innervating OHCs with GAD65 puncta. ACh-evoked [Ca^{2+}] modulation in these GAD2 positive cells suggests the presence of a multi-transmitter feedback loop in the developing cochlea.

PS 951

Imaging cochlea in vivo: first step towards watching hair cells in action

Jinkyung Kim[1]; Anthony J. Ricci[2]
[1]Stanford University; [2]Department of Otolaryngology, Head and Neck Surgery, Stanford School of Medicine, Stanford, CA, USA.

In vivo imaging with cellular resolution enables us to identify and characterize receptive field properties of a sensory system. However, cochlear in vivo imaging remain challenging, owing to not only its deep location but also bony structure filled with fluids. Here we demonstrate a method to resolve individual cochlear hair cells with hearing function in live mice. For imaging cochlea with preserved function, we place an imaging window on otic capsule bone following cochleostomy. Results from the surgical approach elevate auditory thresholds approximately 20 dB, however the mice retain stable hearing function. Two-photon in vivo imaging with long working distance objectives clearly shows each outer and inner hair cells at 11 kHz region of the cochlea through the imaging window. AM1-43 dye is injected through vestibular canal for imaging at postnatal day one. Our in vivo cochlear imaging strategy will set a solid foundation to study dynamics of auditory function. In future work, either GCaMP calcium or voltage sensor will be applied to the strategy for watching cochlea in action. (This project was funded by NIH R01 DC003896-16)

PS 952

Effect of Loud Sound Exposure on Cochlear Blood Flow and Metabolic Stress Pathways in Salsa Mice

Suzan Dziennis[1]; George Burwood[1]; Teresa Wilson[1]; Ruikang Wang[2]; Jianlong Yang[1]; Gangjun Liu[1]; Sarah Foster[1]; Alfred L Nuttall[1]
[1]Oregon Health & Science University; [2]University of Washington

The mammalian cochlea has an extremely high metabolic demand, in order to maintain sensitive hearing function. This demand is met by blood flow through the vascular network in the lateral wall of the scala media, the stria vascularis (SV). Loud sound exposure (LSE) results in immediate metabolic stress which can lead to irreversible hearing loss. LSE decreases blood flow, and it is likely that this change plays an important role in noise-induced deafness mechanisms. However, it is unclear whether this change in blood flow is driven by local metabolism. Furthermore, it is unknown whether or not loud sound causes direct mechanical insult to the SV.

We have attempted to separate the metabolic and mechanical pathways to SV flow regulation during loud sound exposure, by using Cadherin23-missense mutant mice (salsa) mice which lack Cadherin23 for tip links required for the activation of mechanosensitive (MET) channels, but have intact outer hair cells (at p56). We hypothesized that damage caused by sound stimulation would be attributed to the activation of mechano-electrical (MET) channels rather than physical forces applied to the organ of Corti leading to overactive and harmful metabolic pathways ultimately leading to hearing loss. To determine whether the lack of normal MET transduction pathways prevents LSE-induced metabolic signal transduction pathways and vasoconstriction, 8 week old male age-matched salsa and CBA/CaJ control mice were exposed to acute intense broadband noise. Changes in flow relative to baseline measurements were examined using Optical Coherence Tomography Angiography (OCTA). Known noise-induced metabolic stress pathways including STAT3 and NADPH oxidase 4 were investigated by immunohistochemistry.

As expected, LSE decreased blood flow in control mice. Noise-induced blood flow changes in salsa mice differed substantially from controls. Despite this, noise-induced metabolic stress pathways examined did not differ in comparison to controls. Although compensatory mechanisms may occur, these results suggest that the MET channel is possibly part of a feedback loop regulating cochlear blood flow, but may not contribute to how the cochlea responds to changes in metabolic demand.

PS 953

Exposure to Continuous Light Disrupts the Cochlear Circadian Oscillation in CBA/CaJ Mice

Chao-Hui Yang[1]; Chung-Feng Hwang[1]; Ming-Yu Yang[2]; Jiin-Haur Chuang[3]
[1]*Department of Otolaryngology, Kaohsiung Chang Gung Memorial Hospital and Chang Gung University College of Medicine;* [2]*Graduate Institute of Clinical Medical Sciences, Chang Gung University College of Medicine, Taiwan;* [3]*Department of Pediatric Surgery, Kaohsiung Chang Gung Memorial Hospital and Chang Gung University College of Medicine*

Circadian rhythm is present in almost all eukaryotes with a 24 hour cycle. Daily rhythmic changes are found in several physiological processes, including sleep, appetite, hormone level, metabolism and gene expression. There are at least nine core circadian clock genes that regulate central and peripheral circadian oscillators using transcriptional-translational feedback loops. Disruption of circadian rhythm or altered circadian clock genes (CCGs) are associated with plenty of diseases. However, little is known about the circadian oscillation in the cochlea.

Therefore, we used two models - continuous light (LL) and continuous dark (DD) to test if the alteration of light-dark cycle will affect the circadian oscillation of CCGs expression in the cochlea of CBA/CaJ mice. As expected, the cochlea, like the liver, had the oscillations of CCGs expression in the normal 12-12 hours light-dark (LD) cycle. Among the 11 circadian clock genes (CCGs), PER2 showed similar amplitudes in the cochlea and liver. The circadian rhythm was still found in the cochlea and liver of DD mice. However, in the mice exposed to continuous light (LL), the oscillation of CCGs expression was disrupted in the cochlea and liver. Our result demonstrates that the change of light-dark cycle, especially continuous light, affects the cochlear circadian oscillation.

PS 954

Different distribution and contribution of ion channels along the tonotopic turns of the rat cochlea

Gi Jung Im[1]; Eunyoung Yi[2]; Se Hee Lee[1]; Euyhyun Park[1]; Sung Won Chae[1]; Hak Hyun Jung[1]
[1]*Korea University College of Medicine;* [2]*College of Pharmacy and Natural Medicine Research Institute, Mokpo National University*

Background
The Cochlea is tonotopically mapped, and sensitive to specific frequencies of the sound. High frequency sounds stimulate the basal turn of the cochlea, whereas low frequency sounds stimulate the apex. Various ion channels are distributed through the hair cells of cochlea, and tonotopic distribution of ion channels may be different. The aim of this study was to investigate the tonotpic distribution/contribution of ion channels in rat cochlea using both whole-cell patch-clamp recordings and molecular works.

Methods
Electrophysiology and molecular experiments were performed using organs of Corti dissected from the cochlea of rat postnatal days 8-11. Three tonotopic regions of the organ of Corti were examined: the apex, middle, and base. The electrophysiological responses of ACh were recorded in the inner hair cells of three regions. Multiple ion channels were analyzed in three regions using RT-PCR: ACh receptor 9 & 10, BK channel, SK channel, Ryanodine receptor 1-2-3, SERCA pump.

Results
The patch-clamp recordings showed that the efferent response of inner hair cells was different along the tonotopic turns of the cochlea, and ACh response of basal region was stronger than apex. From apex to base, mRNA expression of BK channels was significantly increased. Application of high concentration potassium solution evoked synaptic events, which were significantly increased from apex to base.

Conclusion
This is a challenging study for investigation of the tonotopic distribution of ion channels in the three regions of rat cochlea. Both efferent response using path-clamp and the distribution of ion channels using RT-PCR were different along the tonotopic turns of cochlea. Different distribution and contribution of Ion channels can play a role in tonotopical detection of sound in the cochlea, and may be related to ion exchange, especially potassium using BK channel. It also may be related to different sensitivity against both ototoxic drugs and noise damages. Funding: This work was supported by the National Research Grant funded by the Korea Health Industry Development Institute (R1606512, R1621961, R1429733), and research fund (K1609821). These funding sources provided only financial support and played no specific scientific role in this study.

Im ARO 2018 abstract.doc

PS 955

Strong suppression found on the basilar membrane in echolocating bats to extract the terminal frequency of their echo

Hiroshi Riquimaroux[1]; Zhiqiang Ma[2]
[1]*Shandong University;* [2]*Shandong University*

Flying bats have to extract a signal contained in a weak echo to avoid obstacles and to catch preys. However, they need to eliminate interfering frequency components close to the signal frequency in their echo. In the central auditory system a network may inhibit interfering frequency components by inhibitory synapses. However, in the peripheral system an active suppression on the basilar membrane may work well to extract a weak signal by eliminating interfering frequency components. We examined the cochlear microphonics (CM) of echolocating FM bats (Eptesicus fuscus and Pipistrellus abramus) to investigate frequency specific suppressive activities on the basilar membrane. In FM bats their terminal frequency of FM sweep has been reported to serve as a carrier to convey echo signals from a distant place. Our findings show strong suppression for frequencies on both sides of the terminal frequency of FM sweep, around 20 kHz for Eptesicus fuscus while around 40 kHz for Pipistrellus abramus. The suppression may eliminate interfering frequency components on both sides of the terminal frequency on the basilar membrane for extraction of the terminal frequency component in the echo. [Research supported by Grant-in-Aid for Scientific Research (B) 26280064 to H.R. from the MEXT of Japan and Shandong University Startup Research Grant to H.R.]

External Ear

PS 956

Microtia as a common feature of hearing loss syndromes

Juan Manuel Fons Romero; Abigail Tucker
King's College London

There are several human syndromes characterized by hearing loss with mutations affecting the development of the three ear components (external, middle and inner ear), leading to malformation of the hearing apparatus. Microtia is a common feature of a diverse range of syndromes and encompasses auricle defects with variable severity, classified as grade I (small auricle), grade II (some recognizable structures remain), grade III (only soft tissue is present) and grade IV (Anotia or absence of auricle). Examples of syndromes associated with microtia and hearing loss include Branchio-oto-renal syndrome (BOR), DiGeorge or 22q11.2 deletion syndrome, and lacrimo-auricular-dento-digital (LADD) syndrome.

Mutations in Eya1, which is a kinase that can function as a signal transducer or transcription factor, has been found as the main cause in 40% of the cases of BOR syndrome. Tbx1, a transcription factor involved in mesoderm differentiation, is one of the principal genes within the 22q11.2 deletion that leads to DiGeorge syndrome. Mutations in FGF10, a signalling factor involved in many aspects of embryonic development, such as cartilage differentiation and epithelial-mesenchymal interactions, leads to LADD syndrome. In this study, we aim to uncover the genetic interactions between Eya1, Tbx1 and FGF10 during auricle development using the mouse as a model. Mice mutant for Eya1 display microtia, similar to that in BOR patients. Tbx1 mutant mice show a more severe microtia, resembling that observed in DiGeorge syndrome patients. We found that Eya1 is expressed in the mesodermally-derived auricle muscle, downstream of Tbx1. Loss of function of either gene led to a lack of cartilage differentiation due to a downregulation of Sox9 in the ectomesenchyme. Eya1 and Tbx1 are needed for auricle muscle differentiation, as shown by the downregulation of MyoD and Myf5, but not for auricle muscle determination, as MyR is not affected. However, Sox9 deletion does not interfere with the initial stages of auricle development suggesting that cartilage is not essential for auricle induction, in contrast with the critical function of the auricle muscle in auricle development. FGF10 mutant mice display a mild microtia, characteristic of patients with LADD syndrome. We observed that FGF10 is not needed for auricle induction but for auricle morphogenesis, as mutant auricles are arrested during development in Fgf10 null mice. In contrast toTbx1 and Eya1, loss of FGF10 does not affect Sox9 expression. We propose a model in which Tbx1/Eya1 positive mesodermal muscle instructs the ectomesenchyme to induce auricle development and to differentiate into elastic cartilage by upregulation of Sox9.

PS 957

Cartilage conduction hearing

Tadashi Nishimura[1]; Hiroshi Hosoi[2]; Osamu Saito[3]; Ryota Shimokura[4]; Sakie Akasaka[3]; Toshiaki Yamanaka[5]; Tadashi Kitahara[6]
[1]*Otolaryngology - Head and Neck Surgery, Nara Medical University;* [2]*Nara Medical University;* [3]*Department of Otolaryngology-Head&Neck surgery, Nara Medical University;* [4]*Interdisciplinary Graduate School of Science & Engineering;* [5]*Otolaryngology - Head and Neck Surgery;* [6]*Department of Otolaryngology - Head and Neck Surgery, Nara Medical University*

Background
A clear sound can be heard when a vibration signal is delivered to the aural cartilage. This new form of sound

transmission was found by Hosoi and referred to as Cartilage conduction (CC). The conventional forms of sound transmission to the cochlea are classified into air or bone conduction (AC or BC). The purpose of this study is to elucidate which conduction CC is classified into.
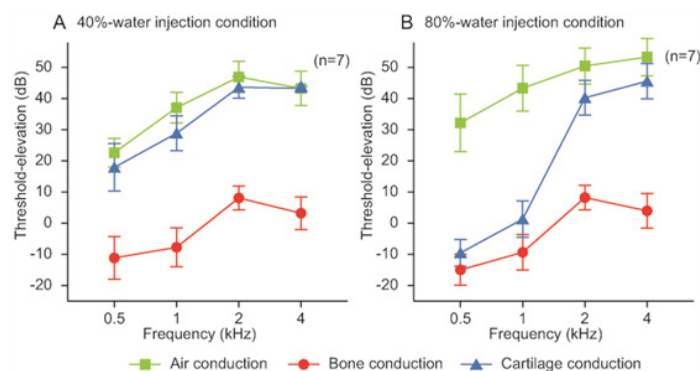
Methods
Seven volunteers with normal hearing participated in this experiment. AC, BC, and CC thresholds at 0.5-4 kHz were measured in the 0%-, 40%-, and 80%-water injection conditions. The vibrations of the cartilaginous portion of the ear canal induced by AC, BC, and CC were evaluated by the threshold shifts when water was injected into the ear canal.

Results
The water injection elevated the AC thresholds by 22.6-53.3 dB, and the threshold shifts for BC were within 14.9 dB. For CC, when the water was filled within the bony portion, the thresholds were elevated to the same degree as AC. When the water was additionally injected to reach the cartilaginous portion, the thresholds at 0.5 and 1 kHz dramatically decreased by 27.4 and 27.5 dB, respectively. In addition, despite blocking AC by the injected water, the CC thresholds in force level were remarkably lower than those for BC.

Conclusion
The vibration of the cartilaginous portion contributes to the sound transmission, particularly in the low frequency range. Although the airborne sound is radiated into the ear canal in both BC and CC, the mechanism underlying its generation is different between them. CC generates airborne sound in the canal more efficiently than BC. The current findings suggest that CC is not classified into AC or BC.

A 40%-water injection condition   B 80%-water injection condition

Air conduction   Bone conduction   Cartilage conduction

Wideband measures of the ear canal and middle ear properties: Quality Markers for Probe Fit and Calibration

Samantha M. Stiepan[1]; Danielle Hojnicki[1]; Stephen Neely[2]; Sumitrajit Dhar[1]; Jonathan Siegel[3]
[1]Northwestern University; [2]Boys Town National Research Hospital; [3]Hugh Knowles Center, Roxelyn and Richard Pepper Department of Communication Sciences and Disorders, Northwestern University

Background
Wide frequency band measures of middle ear transmission and methods of in-situ calibration for acoustic probe measurements are undergoing rapid innovation. Normative values of wideband acoustic immittance (WAI) are emerging as are population characteristics of different types of otoacoustic emissions. All of these measures are only valid and reliable when the measurement probe is tightly sealed in the ear canal. Air leaks can compromise the validity of the measurements, interfere with calibration, and increase variability. Here we report ear canal characteristics and WAI from a relatively large sample of human subjects. We also investigate the utility of these ear canal acoustic measures in determining goodness of the probe seal in the ear canal.

Methods
In-situ calibrations of a custom acoustic probe were performed in 1,199 human subjects between the ages of 10 and 68 years. Acoustic immittance characteristics were estimated between 0.125 to 20 kHz. Ear canal characteristics (e.g., diameter and length) were also estimated from each ear evaluated. Finally, various acoustic properties were examined to determine the presence of air leaks due to inadequate seals of the probe tip in the ear canal.

Results
The influence of age, gender, and ear (left/right) on ear-canal geometry and WAI measures will be reported. Additionally, admittance and absorbance will be used to assess and characterize the presence of acoustic leaks marking suboptimal probe seals.

Conclusions
These results will add to the extant information about normative values for WAI measures as well as provide critical information about the dependence of these measures on age, gender, and ear (left/right). Markers of failed or suboptimal probe seal in the ear canal can also be useful in automatic flagging so the clinician has an opportunity to revise the probe seal prior to initiating clinical measurements. Such warning systems will improve the quality of data collected.

PS 959

Optogenetic Stimulation of the Facial Nerve in a Murine Model

Vivek V. Kanumuri[1]; Bishoy Ameen[2]; Nate Jowett[2]; Osama Tarabichi[3]; Fadhel El May[4]; Xiankai Meng[1]; Elliott D. Kozin[4]; Christopher Knox[2]; Tessa A. Hadlock[2]; M. Christian Brown[1]; Daniel J. Lee[1]
[1]Eaton Peabody Lab, Massachusetts Eye and Ear Infirmary; [2]Massachusetts Eye and Ear; [3]Massachusetts eye and ear Infirmary; [4]Massachusetts Eye and Ear Infirmary, Harvard Medical School

Introduction

Facial Nerve (FN) paralysis occurs in approximately 40,000 individuals in the United States annually. FN paralysis can result in significant morbidity including oral incompetence, speech difficulties, exposure keratopathy, and reduced quality of life due to social isolation. Current rehabilitative options include medical, physical, and surgical options that can restore only limited facial function and have variable outcomes. Microelectrode array implantation and electrical stimulation of facial nerve distal to the site of injury have been proposed as an alternative approach but current spread may hamper the ability to activate discrete nerve branches. Novel paradigms of neuronal activation, such as optogenetics, may address limitations in current techniques. Optogenetics allows for cell specific light sensitivity via delivery and activation of light-gated transmembrane ion channels. Optogenetic stimulation has been shown to have a number of benefits over traditional electrical stimulation in the peripheral nervous system, including recruitment of motor units in a more physiologically consistent manner and reduction in stimulation artifact. Our current research explores optogenetic activation of the facial nerve to elicit whisker movement in a mouse model.

Methods

We generated a transgenic mouse line by crossing Bhlhb5-Cre mice with mice with a flox-stop cassette containing Channelrhodopsin2 (ChR2) coupled with eYFP. Confocal microscopy was used to verify expression of ChR2 in facial nerve axons and in brainstem facial motor nucleus. Following induction of anesthesia, the facial nerve was exposed using a retro-auricular incision. Pulsed blue light (473nm) was delivered using a stripped 400M multimodal optical fiber aimed at to the pes anserinus. Optically evoked EMGs recorded with needle electrodes and high-resolution, high speed video recordings of whisker motion were analyzed.

Results

ChR2-eYFP was expressed in the facial motor nucleus and in sections of the facial nerve at the pes anserinus. Stimulation of all ChR2+ mice with pulsed blue light resulted in large amplitude facial EMG responses and visible whisker motion. This motion was quantified using custom whisker tracking software and correlated with optical EMG responses. The signals demonstrated shorter latency and increasing amplitude with increasing optical power. Reliable EMG responses were elicited at rates up to 100Hz. Control animals showed no response to optical simulation.

Conclusion

This study is the first to describe optogenetic stimulation of the facial nerve in an murine model. Future work will examine the utility of optogenetics to modulate facial nerve activity following acute and chronic injury.

Hair Cells VI

PS 960

A Mouse Model for Human Deafness DFNA5 Links Hearing Loss to Pyroptosis/Secondary Necrosis in Sensory Hair Cells.

Suzan Harris; **Martin Schwander**
Rutgers University

Abstract

DFNA5 is the causative gene of autosomal dominant progressive hearing loss (DFNA5) and a putative tumor suppressor gene. All DFNA5 mutations identified to date lead to skipping of exon 8 at the mRNA level, giving rise to a truncated protein that is toxic for yeast and mammalian cells. Recent studies have shown that, upon "apoptotic stimulation" by chemotherapeutic drugs, caspase-3 can cleave DFNA5 to release autoinhibition on its N-terminal gasdermin domain, which causes pyroptosis/secondary necrosis via its pore-forming activity. It is therefore possible that hearing loss (DFNA5) is caused by a similar toxic-gain-of-function mechanism but direct in vivo evidence for this hypothesis is missing. Genetic ablation of exon 8 in mice has been attempted but abrogated expression of DFNA5 protein and did not result in hearing loss. Thus, the precise mechanism of pathogenesis underlying hearing loss DFNA5 remains unknown.

Methods

To define the role of DFNA5 in inner ear development and its contribution to progressive hearing loss we analyzed the phenotype of novel DFNA5 conditional transgenic mice. In these mice, a conditional cassette containing a human mutant DFNA5 transgene (Δ exon 8) and an IRES-eGFP immediately preceded by a loxP-flanked transcriptional termination sequence (neo-tpA), and followed by a FRT-flanked human DFNA5 wild-type transgene with an IRES-mCherry was targeted to the TARGATT landing pad at the Hipp11 locus. We induced expression of human wild-type or mutant DFNA5 in co-

chlear hair cells and neurons using Atoh1-CreER™ and Ngn1-CreER^T2 mice, respectively. To assess the effect of DFNA5 overexpression on hearing function we recorded auditory brainstem responses (ABRs) and distortion product otoacoustic emissions (DPOAEs) from ketamine/xylazine anesthetized DFNA5 transgenic mice and littermate controls, aged 4 and 12 weeks. To characterize the potential role of DFNA5 in regulating hair cell survival we evaluated their morphology by immuno-histochemistry and electron microscopy.

Results
We show that mice overexpressing mutant but not wild-type DFNA5 in sensory hair cells display rapid hair cell degeneration and progressive hearing loss. By contrast, expression of mutant DFNA5 in auditory neurons had no effect on auditory function. Hair cell death in DFNA5 mutant mice includes activation of caspase-3 and morphological features of apoptosis and necrosis.

Conclusions
These findings support the idea that DFNA5-induced pyroptosis/secondary necrosis in hair cells contributes to the pathogenesis of human deafness DFNA5, offering a new angle to understand cell-death mechanisms in hearing loss with the potential for drug-based therapy.

PS 961

Examining the Contribution of the Ribbon Synapse to Adaptation of Spike Trains in the Zebrafish Lateral Line.

Daniil Frolov[1]; Samuel Short[2]; Christina Hansen[2]; Cristian Ramirez[2]; Emily Isko[2]; Thomas Sommers[2]; Josef Trapani[2]
[1]University of Massachusetts, Amherst; [2]Amherst College

In hair-cell containing sensory systems, including the lateral line, trains of action potentials (spikes) in afferent neurons show robust adaptation and delayed rates of recovery in response to prolonged stimulation. The encoding of spike trains in the afferent neuron relies on the precise recruitment, release, and recycling of distinct pools of synaptic vesicles by the hair cell';s presynaptic specializations, which includes the synaptic ribbon. Thus, the ribbon synapse is uniquely poised to play a major role in spike train adaptation, but its quantitative contribution to the overall time course of adaptation and its recovery is not well understood. We hypothesized that different recovery times of two spike train parameters, first spike latency (FSL) and spike rate (SR), would suggest at least two different underlying mechanisms that contribute to adaptation. To test this hypothesis, we used both mechanical and mechanotransduction-inde-

pendent, optogenetic activation of hair cells and also direct optogenetic stimulation of afferent neurons in the zebrafish lateral line. By separating mechanotransduction- and afferent neuron-based adaptation mechanisms from the ribbon synapse, we aimed to produce different levels of synaptic pool depletion. Specifically, we varied the stimulus duration of paired-pulse stimuli and then increased the inter-stimulus interval (ISI) to generate a recovery time course of spike train adaptation. Construction of dose-response curves for recovery times across different stimulus durations allowed us to calculate time constants for recovery of both parameters. Preliminary results show that FSL and SR have different rates of recovery from adaptation, which in turn may correspond to the recovery of two distinct vesicle pools at the ribbon synapse. We also examined the time course of recovery of spontaneous spiking following delivery of single stimuli at different durations. Rates of recovery for the first spontaneous spike latency (FSSL) and spontaneous spike rate (SSR) occur at time scales that are longer than those for recovery of FSL and SR, respectively. Together, our findings that parameters of the afferent spike train recover from adaptation at different time courses support the notion that adaptation mechanisms at the ribbon synapse play a central role in determining the temporal patterns of hair-cell encoded spike trains.

PS 962

Does membrane lipid fluidity modulate hair cell mechanotransduction?

Shefin Sam George; Anthony J. Ricci
Department of Otolaryngology, Head and Neck Surgery, Stanford School of Medicine, Stanford, CA, USA.

Hair cells are the specialized mechanoreceptors for the sense of hearing and balance. Cochlear hair cells bear a specialized organelle called the hair bundle, which is composed of three rows of actin-filled microvillae, termed stereocilia. Stereocilia are connected via extracellular protein linkages, with the tip-link spanning the distance between the top of the shorter row and the next taller row of stereocilia such that hair bundle deflection results in the opening and closing of mechano-electrical-transduction (MET) channels residing at the tip of the shorter stereocilia. Recent data from our lab demonstrate that, in mammalian cochlear hair cells, the resting open probability (P_{open}) of the MET channel is modulated by membrane potential through a mechanism involving the lipid membrane (Peng, A. et al. 2016). As the first step toward understanding how manipulating membrane potential affects the lipid membrane mechanics to change force translation to MET channels, we combined whole-cell patch-clamp with two-photon FRAP (fluorescence recovery after photo bleaching). FRAP

provides an estimate of lateral diffusion within the membrane, thus allowing us to directly assess the effects of voltage on the stereocilia lipid membrane and the MET channel gating in rat inner hair cells. Two-photon FRAP allowed us to confine the photo-bleaching within 3 μm of the stereocilia tip. Our results suggest that the diffusivity of Di-3-ANEPPDHQ within the stereocilia membrane of the first row is slower than that of the second row under control conditions. Additionally, the diffusivity measurements of the first row stereocilia were dependent on the angle at which the stereocilia were orientated. Depolarization of the cell resulted in faster diffusivity of Di-3-ANEPPDHQ within the stereocilia membrane, and increased the P_{open} of the MET channel as seen previously. Our data support the hypothesis that the lipid bilayer can modulate force transfer to the MET channel. Funding: This work is supported by NIDCD RO1 DC003896 and NIDCD RO1 DC014658 to AJR

PS 963

Multiple Hair Cell Conductances Modulate [K+] in the Synaptic Cleft Between Type I Hair Cell and Calyx Afferent in the Posterior Semicircular Canal of the Turtle

Donatella Contini[1]; Gay R. Holstein[2]; Jonathan J. Art[1]
[1]University of Illinois College of Medicine; [2]Icahn School of Medicine at Mount Sinai

Background

Prior studies in mammals and reptiles have demonstrated that K^+ flowing out of the hair cell (HC) into the synaptic cleft elevates the local [K^+], and depolarizes the HC, which, in turn, permits Ca^{2+} influx and synaptic vesicle fusion. At present, however, it is unclear how the kinetics, voltage-, and ion-dependences of the K channels within this ensemble contribute to the total potassium accumulation within the synaptic cleft. Previous studies have suggested that there are three K channel types that might participate, but little quantitative data exists comparing their relative contributions to the modulation of transmission over different voltages and ion concentration.

Methods

Simultaneous patch-electrode recordings from type I HCs and their enveloping calyces were made with KF/KCl and KCl, dye-filled pipettes, in the epithelia of the posterior semicircular canal of the turtle, Trachemys scripta elegans. Both pre- and postsynaptic elements were examined in voltage clamp, under conditions of ionic substitution and pharmacological block. Steady-state and instantaneous I-V curves were constructed to analyze changes in conductance and driving force on the presynaptic HC, and the postsynaptic afferent terminal. Stacks of confocal fluorescent images were used to confirm the synaptic relation between HCs and their enveloping calyx afferents.

Results

HCs held at -100 mV, demonstrated large outward K currents when depolarized above -90 mV. The total current was half activated at -60 mV, but decreased from its maximum, when depolarized above +30 mV. The current could be separated into two of its components by differential sensitivity to 4-AP, TEA-Cl, and BAPTA. Inclusion of 15 mM 4-AP in the recording electrode, blocked a slow current that activated from -90 mV, and isolated a rapid component that activated from -60 mV. Upon repolarization, the tail current kinetics of this rapid component were insensitive to changes in $[K^+]_{cleft}$. The rapid component was sensitive to external TEA-Cl, however, with a half-blocking dose of ~300 μM. Conversely, inclusion of 10 mM BAPTA in the pipette, blocked the rapid current, while sparing the slower current, whose tail kinetics were sensitive to $[K^+]_{cleft}$.

Conclusion

In the central dimorphic region of the canal epithelium, there are two K conductances that activate in the voltage range between E_K, the potassium equilibrium potential, and 0 mV, the transducer equilibrium potential. When activated from -100 mV, one is a relatively slow, 4-AP-sensitive current, and the other is a rapidly activating current that bears the hallmarks of a Ca-activated K conductance.

PS 964

Atoh1-reporter system to study hair cell differentiation in inner ear organoids

Dunia Abdul-Aziz[1]; Albert Edge[2]
[1]Eaton-Peabody Laboratories, Massachusetts Eye and Ear Infirmary; and Department of Otolaryngology, Harvard Medical School; [2]Harvard Medical School

Mammalian hair cells do not regenerate to a significant degree once lost, and their loss is a major cause of deafness. Formation of hair cells relies on the expression of Atoh1, a key regulator of hair cell fate

Because Atoh1 expression is critical to hair cell fate determination, we seek to investigate the regulatory elements that control the Atoh1 gene. The Atoh1 3′ enhancer itself contains a binding site for Atoh1, which is the basis for its autoregulation. While key developmental pathways, such as Notch and Wnt signaling, have been shown to act on this enhancer, the temporal and combinatorial effects of these factors are unknown. High throughput screening of drug libraries for compounds or genetic factors that may promote hair cell regeneration has until now been precluded by the relatively small number of cells that can be derived from the mammalian cochlea, the unique microenvironment of the organ of

Corti, which limits long-term viability in primary culture, and the largely non-regenerative nature of the mammalian inner ear. Our lab has recently established a protocol for >2000-fold expansion of inner ear progenitor cells in 3D culture, thereby generating inner ear organoids which can be used to study pathways in inner ear development. Atoh1 enhancer and Atoh1 enhancer-promoter constructs were engineered upstream of luciferase and delivered into murine inner ear progenitor cells upon harvest. Following proliferation, progenitor cells were exposed to different genetic and drug treatments, and luciferase signal analyzed. We demonstrate that, relative to limited de novo differentiation, treatment with a Notch inhibitor and Wnt activator, together increased Atoh1 activity in these progenitor cells and drove hair cell transdifferentiation. This organoid-based Atoh1-reporter system can be applied to the study of other genetic and chemical modulators of Atoh1 activity.
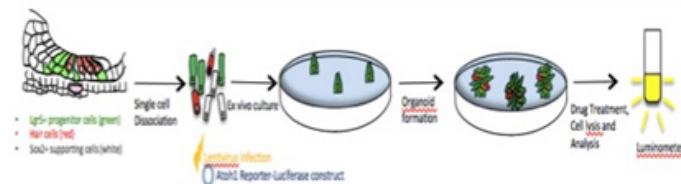
Schematic diagram of inner ear organoids generated from neonatal mouse organ of Corti. The sensory epithelium of the cochlea are harvested and dissociated into single cells which contain Lgr5+ inner ear progenitor cells (green). These progenitor cells are then expanded in Matrigel-based three-dimensional culture system that can then be used to study differentiation into hair cells (red) under different conditions and drug treatments.
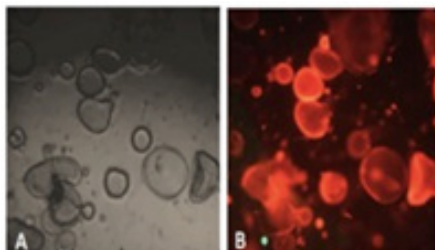
A. Live brightfield image showing clonally expanded inner ear organoids after 10 days *in vitro*. B. CY3 (red) channel showing mCherry expression in essentially all the clonally-derived organoids. Inner ear progenitor cells were infected with lentivirus containing mCherry plasmid at day 0 and allowed to clonally expand into spheroid organoids. (10X magnification).

PS 965

The Potassium Channel Repertoire of Auditory Inner Hair Cells

Marlen Dierich; Saskia Evers; Dominik Oliver; **Michael G. Leitner**
Department of Neurophysiology, Institute of Physiology and Pathophysiology, Philipps-University Marburg

The extraordinary acuity of mammalian hearing is determined by sensory hair cells located in the organ of Corti of the inner ear. Inner hair cells (IHC) are the primary detectors of sound directly modulating the activity of auditory neurons. Outer hair cells (OHC) are the cellular basis of cochlear amplification, as they actively amplify sound-induced vibrations of the basilar membrane. The function of hair cells critically depends on an exclusive set of K$^+$ currents that have been denoted as $I_{K,f}$, $I_{K,n}$ and $I_{K,s}$ according to biophysical properties. These currents shape the hair cell´s receptor potential in response to incoming sound and thus intrinsically specialize IHCs for accurate detection of sound frequency and intensity. Whereas it is known that $I_{K,f}$ and $I_{K,n}$ are mediated by $K_{Ca}1.1$ (BK channels) and $K_v7.4$ subunits, respectively, the molecular identity of channels underlying the slow current $I_{K,s}$ remains unknown.

We aimed at identifying the molecular components of $I_{K,s}$ to elucidate the physiological relevance of K$^+$ channels in auditory IHCs. Using whole cell patch clamp, we found that $I_{K,s}$, in fact, was mediated by at least three independent K$^+$ current components. Through detailed biophysical and pharmacological characterisation these currents could be attributed to members of the K_v1, K_v11 and K_v12 families of voltage-gated K$^+$ channels. Reverse transcription polymerase chain reaction (RT-PCR) and antibody staining revealed that these channels actually were expressed in auditory IHCs. Based on these findings, we present a refined biophysical model of IHCs that allows for evaluation of physiological relevance of the identified currents.

In summary, we found that auditory IHCs express a repertoire of at least five independent K$^+$ current component with distinct biophysical properties. Our data suggest that these different K$^+$ currents are required for adequate encoding of sound frequency and/or intensity.

PS 966

Hair cell specific pattern of expression in the adult cochlea in a Gm1714-cre transgenic mouse line

Michael Hoa[1]; **Rafal Olszewski**[2]; Caroline Rieger[3]; Brittany Whitley[2]; Inna A. Belyantseva[1]; Thomas B. Friedman[4]; Robert J. Morell[1]
[1]*NIDCD/NIH;* [2]*NIDCD;* [3]*Georgetown University School of Medicine, Department of Otolaryngology-HNS;* [4]*Laboratory of Molecular Genetics, National Institute on Deafness and Other Communication Disorders (NIDCD), Bethesda, MD, USA*

Introduction

Attempts at hair cell regeneration will benefit from both an understanding of the developmental steps to convert cochlear supporting cells into hair cells and insight into the final transcriptional state and proteome of adult cochlear hair cells. Assessing the final transcriptional state of adult hair cells is difficult due to their fragility and relative low abundance. To this end, we characterized a new transgenic mouse model that can be used to isolate RNA specifically from adult cochlear hair cells.

Method

An IRES-Cre expression construct replaced portions of exons 4 and 5 corresponding to locus Gm32742 (GENCODE version M11). This predicted transcript overlaps a novel, highly alternatively spliced gene expressed almost exclusively in cochlear hair cells. Adult heterozygotes and homozygotes had normal ABRs and were unchanged from wild-type littermates. Gm1714-cre mice were bred to two fluorescent reporter mouse lines: B6.Cg-Gt(ROSA)26Sor$^{tm14(CAG-tdTomato)Hze}$/J (Ai14) and B6;129S6-Gt(ROSA)26Sor$^{tm1(CAG-tdTomato*,-EGFP*)Ees}$/J (ROSA $^{nT-nG}$). Fluorescence immunohistochemistry combined with confocal laser scanning microscopy was performed on whole mount and mid-modiolar cross-sections of adult cochlea to demonstrate the pattern of expression of Gm1714-cre.

Results

Adult cochlea showed an explicit pattern of Gm1714-cre recombination in adult hair cells. We demonstrate hair-cell specific expression of the transgene in the adult mouse cochlea and characterize the apical-to-basal pattern of recombination. Fluorescence-activated cell sorting of adult cochlear hair cells will be discussed.

Conclusion

The expression of the transgene in the Gm1714-cre mouse is a useful tool with which to isolate and study adult inner ear hair cells.

PS 967

Signatures of Friction from Transduction Channels' Gating in Spontaneous Hair-Bundle Oscillations

Jérémie Barral[1]; Frank Jülicher[2]; **Pascal Martin**[1]
[1]*Institut Curie; [2]Max Planck institute for the Physics of Complex Systems*

Hair cells of the inner ear can power spontaneous oscillations of their mechanosensory hair bundle, resulting in amplification of weak inputs near the characteristic frequency of oscillation. Recently, dynamic force measurements have revealed that delayed gating of the ion channels responsible for mechanoelectrical transduction produces internal friction forces on the hair bundle. Here, to determine whether channel friction plays a role in spontaneous hair-bundle oscillations, we characterized key oscillation properties over a large ensemble of cells. In addition, we measured how viscosity of the endolymph that bathes the hair bundles affects these properties. In combination with a model of active hair-bundle mechanics, our observations rule out viscous drag on the hair bundle as the dominant source of friction during a spontaneous oscillation. Instead, they indicate that the friction coefficient owing to channel gating is 3-8 fold larger than that resulting from viscous drag. We further exploit our analysis of hair-bundle dynamics to estimate that the channels'; activation time is about 1 ms. Our results suggest that channel friction affects the waveform of oscillation and that the channel activation time can tune the characteristic frequency of the hair cell. We conclude that the kinetics of transduction channels'; gating plays a fundamental role in the dynamic process that shapes spontaneous hair-bundle oscillations.

PS 968

In Depth-Analysis of the Cochlea-Specific Deletion of Cav1.3 Before Birth and Around the Onset of Hearing

Stephanie Eckrich[1]; Kerstin Blum[1]; Dietmar Hecker[2]; Katharina Sorg[3]; Barbara Fell[1]; Bernhard Schick[3]; Dusan Bartsch[4]; Jutta Engel[1]
[1]*Center for Integrative Physiology and Molecular Medicine (CIPMM) and Department of Biophysics, Saarland University, Homburg, Germany; [2]Dept. of Otorhinolaryngology, Saarland University, Homburg, Germany; [3]Saarland University Faculty of Medicine, Department of Otolaryngology, Homburg, Germany; [4]Dept. of Molecular Biology, Central Institute of Mental Health, Mannheim, Germany*

Throughout life inner hair cells (IHCs) require $Ca_v1.3$ voltage-gated Ca^{2+} channels. Before the onset of hearing at postnatal day 12 (P12) in mice, IHCs generate Ca^{2+} action potentials that drive terminal maturation of IHCs and the auditory pathway. In mature IHCs, Ca^{2+} currents elicit transmitter release. In $Ca_v1.3^{-/-}$ mice, which are deaf due to missing transmitter release, lack of Ca^{2+} action potentials before the onset of hearing disrupts terminal differentiation of IHCs. The $Ca_v1.3^{-/-}$ mouse is therefore not an appropriate model to study the role of $Ca_v1.3$ in mature IHCs. Furthermore, tissue-specific deletion of $Ca_v1.3$ in brainstem nuclei adds to the auditory phenotype of $Ca_v1.3^{-/-}$ mice [Hirtz (2011) J Neurosci 31:8280]. To separate the multiple roles of $Ca_v1.3$ in IHCs and the auditory pathway, conditional mouse models with cell- and age-specific deletion are required.

We used $Ca_v1.3^{flex}$ mice with cre-dependent ablation of $Ca_v1.3$ coupled to eGFP expression [Satheesh (2012) HumMolGen 21:3896]. These mice were crossbred with i) Pax2::cre mice with embryonic cre expression in the cochlea [Ohyama (2004) Genesis 38:195] or ii) Prestin::cre mice with hair-cell specific cre expression starting from around P10 [Tian (2004) DevDyn 231:199]. We analyzed Ba^{2+} currents (I_{Ba}) through $Ca_v1.3$ channels using whole-cell patch clamp recordings of IHCs and expression of IHC proteins using whole-mount immunolabeling. Auditory brainstem responses (ABR) and distortion product otoacoustic emissions (DPOAE) were evaluated to assess hearing function.

Because homozygous $Pax2::cre;Ca_v1.3^{flex/flex}$ mice showed i) mosaic deletion of $Ca_v1.3$ and ii) degeneration of IHCs most likely due to high levels of GFP expression we used $Ca_v1.3^{-/flex}$ mice. Embryonic cochlea-specific deletion of $Ca_v1.3$ in $Pax2::cre;Ca_v1.3^{-/flex}$ mice, eliminating effects of central $Ca_v1.3$ deletion, caused a phenotype very similar to systemic $Ca_v1.3^{-/-}$ mice. Cre expressed from around P10 in $Prestin::cre;Ca_v1.3^{-/flex}$ mice did not simultaneously excise $Ca_v1.3$ in all IHCs resulting in diverse IHC phenotypes ranging from $Ca_v1.3^{-/-}$-like to nearly wildtype-like between P14 and P35. A slow turnover rate of $Ca_v1.3$ might further add to the heterogeneity. We found a requirement for $Ca_v1.3$ for maintaining the general IHC phenotype even after the onset of hearing. Funded by CRC894, EU-project MRTN-CT-2006-35367 („CavNet") and Saarland University.

PS 969

Role of Serum Response Factor in Hair Cell Function and Maintenance

Tingting Du; Jung-Bum Shin
University of Virginia

Filamentous actin (F-actin) constitutes the structural basis of all hair cell features required for mechanoreceptor function, most prominently the hair bundle and the cuticular plate. Characterizing how the hair cell governs its F-actin dynamics is thus imperative for understanding the development, function and maintenance of the hair cell. Serum response factor (SRF) is a versatile transcription factor that is abundantly expressed in many cell types. It has been described in depth as an essential regulator of actin microfilament-related cytoskeletal genes which are important for cellular processes that involve dynamic actin changes. SRF, therefore, likely plays an important role in regulating actin cytoskeleton homeostasis and mechanotransduction function in the hair cell.

To investigate the role of SRF in hair cell development and function, we developed hair cell-specific conditional Srf knockout mouse lines. Initial studies demonstrate that hair cell specific deletion of Srf does not affect hair cell development, but causes rapid deterioration of stereocilia and the cuticular plate postnatally. Differential phenotypes are seen in inner versus outer hair cells: while inner hair cell bundles exhibit severe thinning and shortening, the outer hair cells have normal bundles, but present with significantly reduced F-actin density in the cuticular plate. Consistent with this hair cell degeneration pattern, ABR thresholds are severely affected at P18 (80-100 dB SPL), but DPOAEs are not affected, with the exception of a mild defect at low frequencies. Overall, our current results suggest that SRF governs a major pathway required for hair cell maintenance. Roughly 25% of genetic hearing loss is caused by mutations in genes coding for components of the actin cytoskeleton. We thus expect that elucidating the role of SRF, a master regulator of actin homeostasis, will be significant for understanding a broad spectrum of sensorineural hearing loss phenotypes.

Hair Cells VII

PS 970

Chaotic Dynamics of Inner Ear Hair Cells

Justin Faber; Dolores Bozovic
University of California, Los Angeles, Department of Physics & Astronomy

Hair cells of the auditory and vestibular systems are capable of detecting sounds that induce sub-nanometer vibrations of the hair bundle, far below the stochastic noise levels of the surrounding fluid. Hair cells of certain species are also known to oscillate without external stimulation. The role of these spontaneous oscillations is not yet understood, but they are believed to be a manifestation of an underlying active mechanism. As this active process constitutes an important topic in auditory research, a deeper understanding of spontaneous motility could impact our understanding of the extreme sensitivity of hearing. We will present experimental measurements of spontaneous hair bundle oscillations, which were obtained from the sacculus of the American bullfrog. Our experiments suggest that low-dimensional chaos exists in the dynamical system of the active hair cell. Chaotic systems are a subclass of nonlinear systems that have been shown to be highly sensitive to small perturbations. Using Poincaré maps, we observe a transition from chaos to order as increasingly stronger stimulus is applied to the hair bundle. This transition is also accompanied by an increase in information transmission from the stimulus to the hair bundle, indicative of signal detection. Further, we use a simple theoretical model to describe the observed chaotic dynamics. The model exhibits an enhancement of sensitivity to weak

stimuli when the system is poised in the chaotic regime. We propose that chaos may play a role in the hair cell's ability to detect low-amplitude sounds.

PS 971

Actin-spectrin structures in inner ear hair cells

Jieyu Qi; Renjie Chai
Southeast University

In mammalian hearing the cuticular plate of the mechanosensory cochlear hair cells (HCs) is a specialized region in the inner ear that converts sound-induced mechanical vibrations into electrical signals through the deflection of stereocilia. These stereocilia are inserted into the cuticular plate and they play a key role in the function of HCs. While the proteins F-actin and βII-spectrin are essential to many of the HC';s functions and therefore hearing, their structural organization remains poorly understood. Here we show that previously unknown F-actin and βII-spectrin structures develop synchronously with a rodent';s ability to hear and are disrupted in those with hearing impairment suggesting they are prerequisite to the development of hearing. Using two super-resolution fluorescence imaging methods we find that F-actin develops a fan-shaped meshwork in the cuticular plate of outer HCs while the F-actin and βII-spectrin rings wrap around the circumference of stereocilia rootlets, likely providing elasticity and durability to the stereocilia rootlet which are spaced nearly evenly along their core regions.

PS 972

Autonomous and evoked calcium signals in inner hair cells and coupling to calcium waves in the developing mouse cochlea

Tobias Eckrich[1]; Kerstin Blum[2]; Ivan Milenkovich[3]; Stefan Münkner[1]; **Jutta Engel**[2]
[1]Dept. of Biophysics & CIPMM, Saarland University, Homburg, Germany; [2]Center for Integrative Physiology and Molecular Medicine (CIPMM) and Department of Biophysics, Saarland University, Homburg, Germany; [3]University of Leipzig, Faculty of Medicine, Carl Ludwig Institute for Physiology, Leipzig, Germany

During final differentiation of the cochlea before the onset of hearing, inner hair cells (IHC) generate Ca^{2+} action potentials in the absence of sound whereas inner supporting cells (ISCs) of the great epithelial ridge (Kölliker';s organ) generate intercellular ATP-mediated Ca^{2+} waves. There is a debate as to whether Ca^{2+} action potentials of IHCs are independent of Ca^{2+} waves or not. Using the Ca^{2+} indicator Fluo 8-AM and a confocal laser scanning microscope (Zeiss LSM 710) we performed Ca^{2+} imaging in acutely dissected inner ear explants at postnatal day 4-5. Using small fields of view and scan rates of $\geq$ 30 Hz, we were able to resolve fast Ca^{2+} transients in IHCs simultaneously to the slower Ca^{2+} waves in adjacent supporting cells. Three signal types of IHCs were observed, single fast Ca^{2+} transients (FCaT), minibursts of 2 to 5 fCaTs, and bursts of 6 to ~70 fCaTs. Time-to-peak of a fCaT was 16.3 ± 5.5 ms whereas the total length amounted to 896 ± 381 ms. The overall frequency of fCaTs was 0.32 ± 0.11 Hz but increased to 4 10 Hz within bursts. IHC fCaTs critically depended on the presence of extracellular Ca^{2+} and of $Ca_v1.3$ Ca^{2+} channels, indicating that fCaTs reflected Ca^{2+} action potentials in IHCs. ATP superfused from the strial side caused fCaTs in IHCs first and ~0.97 s later Ca^{2+} waves in ISCs. In summary, IHCs were able to generate fCaTs and minibursts autonomously without Ca^{2+} wave activity in adjacent ISCs. IHC bursts however were mostly triggered by Ca^{2+} waves, which invaded the IHC region and synchronized the activity of many IHCs. The mechanisms behind the Ca^{2+} transients and waves remain to be elucidated.

PS 973

A glutamate scan identifies an electrostatic switch for prestin activity

Dmitry Gorbunov[1]; Julia Hartmann[1]; Vijay Renigunta[1]; **Dominik Oliver**[2]
[1]Philipps University Marburg, Institute for Physiology and Pathophysiology; [2]Department of Neurophysiology, Institute of Physiology and Pathophysiology, Philipps-University Marburg

The structural architecture of SLC26 transporters has recently been revealed. Accordingly, these transporters including prestin (SLC26A5) belong to the 7TMIR (7 transmembrane domain inverted repeat) class of solute transporters, together with SLC4 and SLC23 transporters. Recent structures indicate that these proteins are generally dimers, with each monomer organized into two rigid helix bundles (gate and core). Dimerization is exclusively mediated by the gate domains, whereas the core domain contains the substrate binding site.

It is thought that prestin mediates outer hair cell electromotility by alternating between to major conformations, with the transition driven by membrane voltage and accompanied by translocation of electrical charge. Intracellular anions are essential in this process; detailed kinetic measurements recently suggested that anion binding and one or more rate-limiting transitions precede the voltage-sensitive electromotile step.

A series of structures recently obtained across all 7TMIR families suggests that transport is mediated by a rigid body movement of the core domain against a static gate domain scaffold. Translocation of the central substrate binding site along with the core domain allows for alternating access of bound substrate to intracellular and extracellular sides, which mediates transmembrane transport.

We were interested in understanding whether this mechanism may also explain the electromotile activity of prestin. Therefore, we conducted a glutamate scan of TM3 and TM10, that make up most of the predicted anion binding site, by replacing individual amino acids with glutamate. Among all mutants generated, S396E retained electromotile function as deduced from wild-type-like charge movement. This position is located centrally in the putative anion binding site of prestin. Notably, functioning of this mutant (and to a lesser degree S398E) was independent on intracellular anions and insensitive to competitive anionic inhibitors like salicylate. This indicated that the presence of a negative electrical charge at this site is necessary and sufficient to enable the electromotile transition, thus acting as an electrostatic switch. Moreover, fixation of the anionic charge (396E) to the central site refutes the previous idea that movement of anions into the protein produces charge movement. Rather, movement of the entire core domain with combined electric dipole contributions from bound anion and protein may translocate charge, thus acting as an unconventional 'voltage sensor domain';. Of note, since electromotile transitions in this mutant should occur undamped by prior anion binding and intermediate slow transitions, a detailed kinetic examination will allow to experimentally test current biophysical models of prestin function.

PS 974

Precise control of presynaptic Ca2+ signal is required to maintain phase-locking at the hair cell ribbon synapses

Adolfo E. Cuadra; Burt Lindsay; Anastasia Chobany; William Edmonds; Geng-Lin Li
University of Massachusetts

Phase-locking is a phenomenon observed in the auditory system in which excitatory responses of the auditory nerve is synchronized with input sound wave oscillations that stimulate the auditory hair cells. Voltage oscillations in hair cells, driven by sound stimulation, activates Ca^{2+} influx, via voltage gated Ca^{2+} channels. Ca^{2+} entering the ribbon synapse triggers secretion of the excitatory neurotransmitter, glutamate. Following depolarization the endogenous Ca^{2+}-buffering system in hair cells modulates local intracellular Ca^{2+} concentration ($[Ca^{2+}]i$) to

control release. Phase-locked signaling can occur very rapidly for long durations. In some hair cells release rates can exceed several kHz with high fidelity. We questioned whether phase-locking can be maintained in the presence of excess $[Ca^{2+}]i$ load mediated by suppression of different Ca^{2+} extrusion pumps in the hair cell. We started by comparing the kinetics of voltage stimulated Ca^{2+} spark decay from Ca^{2+} hot spots in the adult bullfrog amphibian papilla. We employed Ca^{2+} indicator dye, Fluo-4, in patch clamp pipette solution to visualize and compare the kinetics of Ca^{2+} modulation. Hair cells were depolarized for 200 ms to -30 mV, from a holding potential of -90 mV, to evoke $[Ca^{2+}]i$ sparks, which were focused at ribbon synapses. Upon repolarization, spark fluorescence decreased with a fast and a slow decay component. Inhibition of PMCA- and mitochondrial-Ca^{2+} extrusion mechanisms markedly slowed the clearance of $[Ca^{2+}]i$ spark decay compared to untreated controls. In contrast, inhibition of NCX pump showed no effect on $[Ca^{2+}]i$ clearance. We then tested how these treatments affected phase-locked EPSC formation. Experiments were performed using paired patch recordings technique, with one pipette patched to the hair cell and the second patched to the associated afferent neuronal fiber. Sine wave stimulation (-55 mV center voltage with 20 mV oscillation, peak to peak at 400 Hz) was applied to the hair cell and EPSCs were recorded from a synapsed afferent neuronal fiber. Our results demonstrate that conditions affecting normal presynaptic $[Ca^{2+}]i$ clearance, exhibited by impairment of PMCA- and mitochondrial-clearance mechanisms, further disrupted phase-locked EPSC synchronization. On the other hand, NCX inhibition, which did not affect $[Ca^{2+}]i$ spark decay, did not affect phase-locked synchronization. These results demonstrate that precise $[Ca^{2+}]i$ clearance is required in order to maintain phase-locked signaling fidelity in the hair cell ribbon synapse. Furthermore, we found that PMCA- and mitochondrial-Ca^{2+} extrusion mechanisms are essential in maintaining effective presynaptic $[Ca^{2+}]i$ clearance and phase-locked signaling.

PS 975

The Extracellular Loop of Pendrin and Prestin Modulates Their Voltage-Sensing Property

Makoto Kuwabara[1]; Koichiro Wasano[2]; Satoe Takahashi[3]; Justin Bodner[4]; Tomotaka Komori[1]; Sotaro Uemura[1]; Jing Zheng[3]; Tomohiro Shima[1]; **Kazuaki Homma**[3]
[1]*University of Tokyo;* [2]*Department of Otolaryngology Head and Neck Surgery, Keio University School of Medicine;* [3]*Northwestern University;* [4]*DePaul University*

Background

Pendrin (SLC26A4) and prestin (SLC26A5) belong to the solute carrier 26 family of anion transporters, and

their functions are essential for normal hearing. Prestin is unique among the SLC26 family members in that it displays voltage-driven motor activity (electromotility) and concurrent gating currents that manifests as nonlinear cell membrane electrical capacitance (NLC). Although the anion transport mechanism of the SLC26 proteins has begun to be elucidated, the molecular mechanism of electromotility still remains largely elusive.

Methods
Doxycycline-inducible stable cell lines that heterologously express pendrin or prestin constructs with C-terminally attached mTurquoise2 (for pendrin-based constructs) or ECFP (for prestin-based constructs) were established. NLC was measured in the whole-cell configuration using a sinusoidal voltage stimulus (2.5-Hz, 120-150 mV amplitude) superimposed with two higher frequency stimuli (390.6 and 781.2 Hz, 10 mV amplitude). Recording pipettes were filled with an intracellular solution containing (mM): 140 CsCl, 2 $MgCl_2$, 10 EGTA, and 10 HEPES (pH 7.3). Cells were bathed in an extracellular solution containing (mM): 120 NaCl, 20 TEA-Cl, 2 $CoCl_2$, 2 $MgCl_2$, 10 HEPES (pH 7.3). The resting cell membrane potentials of the cell lines were determined in HBSS using recording pipettes filled with an intracellular solution containing (mM): 140 KCl, 2 $MgCl_2$, 10 EGTA, and 10 HEPES (pH 7.2). Bicarbonate/chloride anitiport activities of the pendrin and prestin constructs were assessed using a ratiometric pH indicator, SNARF-5F, which was loaded into the stable cell lines.

Results
We found that NLC, which is the electrical signature of electromotility, is evidently present in pendrin as well. We also found that charged residues present in one of the extracellular loops of pendrin and prestin plays significant roles in setting the voltage-operating points of NLC.

Conclusions
Our results suggest that the molecular mechanism responsible for sensing voltage is not the unique asset equipped only in prestin among the members of the SLC26 family, and that this voltage-sensing mechanism may not be rooted in the anion transport mechanism.

PS 976

Sea anemone as a model to study Usher proteins interactions in inner ear hair bundle.

Vincent Michel[1]; Cécile Sabourault[2]; Christine Petit[3]
[1]*Institut Pasteur, INSERM UMRS 1120, Université Pierre et Marie Curie; [2]Université Côte d'Azur, Nice, France; [3]Institut Pasteur, INSERM UMRS1120, Université Pierre et Marie Curie, Institut de la Vision, Collège de France*

Cnidarians use a very specialized structure to capture their preys and protect themself : the nematocyst. Nematocyt discharge is controlled by a mechanosensitive actin made structure located on the tentacles : the hair bundle.

Hair bundles of sea anemones are structurally close ancestors of vertebrate hair bundles and may constitute a valuable model to study inner ear vertebrate hair bundle functions. It has been previously shown that some molecules crucial for vertebrate hair bundles shaping and function are present in sea anemone. In the inner ear of superior vertebrates, including human, USH1 and USH2 proteins (defective in the Usher syndrome type 1 and type 2, respectively associating deafness and blindness) are localized in the auditory hair bundle, the mechanosensitive structure receptive to sound stimulation. The presence of a homolog of cadherin 23, i.e. the USH1D protein in vertebrates, has been demonstrated some years ago in sea anemone. Here we show that other USH1-protein homologues could also be observed by in situ immunohistochemistry within Nematostella viridis hair bundles, by using antibodies designed against specific vertebrates USH1 proteins. In parallel, by using scanning electron microscopy approach, we have done a morphological comparison between the different types of sea anemone hair bundles structures and frog and mouse inner ear mechanoreceptor neurons hair bundles.

PS 977

Characterization of a Possible Crosslinker between Tectorial Membrane Proteins and Outer Hair Cell Stereocilia

Jing Zheng[1]; Satoe Takahashi[1]; Daniel Li[1]; Caroline Tilley[1]; Mary Ann Cheatham[2]
[1]*Northwestern University; [2]Department of Communication Sciences and Disorders, Northwestern University*

Acoustic signals delivered to the cochlea generate fluid-born sound that activates the cochlear partition and induces a radial shear between the tectorial membrane (TM) and reticular lamina. The resulting deflection of the stereocilia stretches the tip links and opens the mechanoelectrical transduction channels. The resulting receptor currents represent the transformation of mechanical motions into electrical responses. Although this process requires the tallest stereocilia of outer hair cells (OHC) to be firmly attached to the TM, little is known about the molecules that physically mediate this connection.

The TM is composed of radially-oriented collagen fibers imbedded within a striated-sheet matrix consisting of several secreted proteins including a-tectorin (TECTA),

b-tectorin (TECTB), and carcinoembryonic antigen-related cell adhesion molecule 16 (CEACAM16). In contrast to tectorin proteins that are not synthesized after the onset of hearing (Rau et al., 1999), CEACAM16 continues to be secreted from supporting cells throughout adulthood to maintain the integrity of TM. CEACAM proteins commonly contain one N-terminal Ig variable (Ig-V)-like domain (N domain), which is generally involved in protein-protein interactions. However, unlike other CEACAM family members, CEACAM16 has N domains at both N- and C-termini (N1 and N2 domains, respectively). Thus, CEACAM16 has the potential to interact with two distinct protein targets through its two N domains. Our previous work showed that the N1 domain of CEACAM16 binds to the ZP domains of both tectorins, which also form an Ig-like fold (Lin et al., 2011; Monné et al., 2008).

Neuroplastin-55 (Np55), an OHC stereocilia membrane protein, was recently suggested to function as a linker to the TM (Zeng et al., 2016). Np55 was also reported to have two Ig-like domains. Because Np55, CEACAM16, and the ZP domains of a- and b-tectorin all form Ig-like domains, we hypothesize that the connections between TM and OHC stereocilia are via immunoglobulin interactions between Np55, CEACAM16 and the two tectorins. To test this hypothesis, we transiently expressed different domains of CEACAM16, TECTA, TECTB, and Np55 in HEK293T cells and tested their interactions in vitro. Our data suggest that Np55 can bind tectorin and CEACAM16 proteins. As tectorins are not synthesized in mice after weaning, our data imply that CEACAM16 not only serves to stabilize the tectorin-based matrix, but also to maintain the linkage between the TM and OHCs (Work supported by NIDCD grant DC011813).

PS 978

Rapid Frequency Mapping and Quantification of Murine Hair Cells Along the Organ of Corti in Three Dimensional Images

Nancy Paz[1]; Benjamin Holmes[1]; Trevor W. Lancon[2]; Ning Pan[1]; Ada Silos-Santiago[1]
[1]*Decibel Therapeutics;* [2]*Thermo Fisher Scientific*

Background Place-frequency mapping of the organ of Corti (OC) has been established (Mueller et al, 2004; Taberner and Liberman, 2004) and routinely used for characterization and quantification of hair cells in a frequency-specific manner. The process is generally performed manually using image processing programs such as ImageJ (National Institute of Health). Here we propose a workflow to automate frequency mapping of the murine OC and segmentation of the inner (IHC) and outer hair cell (OHC) using Amira 6.4 (Thermo Fisher Scientific). The ultimate goal is to create an efficient fully-automated image analysis workflow to quantify the IHCs and OHCs at all given frequencies along the whole murine cochlea. Methods The whole mouse cochlea was microdissected into 3-6 pieces along the basal-apical longitudinal axis and stained with antibodies for specific cell markers. All the pieces were then imaged using multi-channel fluorescent microscopy. We generated a workflow in Amira to identify the OC region using various filtering, thresholding and masking. A line was then extracted and smoothed from the region (Sato et al, 2000). The line for each component piece was then connected to make one continuous object from most basal to most apical location and the frequency map was generated using the logarithmic function that describes the relation between normalized distance from the base and frequency. Individual IHCs and OHCs were segmented from nuclear stained channels using Otsu criteria (Otsu, 1979) and morphologically cleaned before being separated using watershed. False positives are removed from potential cell candidates using modules that support size exclusion and nuclear separation. The centroid from each unique cell is then correlated to the closest point along the extracted frequency line. The cell centroid positioning and the frequency line mapping data is subsequently merged in Matlab to support the cell quantification. Results Qualitative evaluation of the frequency line segmentation routine shows agreeable results. Relevant IHCs and OHCs are shown to be successfully thresholded and identified. Comparison of automated and manual counts resulted in high agreement. Determination of the points describing the frequency line throughout the cochlea allows correlation of the centroid of each segmented cell to the nearest point along the line and the corresponding frequency according to the species-specific place-frequency function. Conclusion A robust method has been developed that streamlines place-frequency mapping and quantification of murine hair cells along the OC. Future work includes merging processing routines against manual segmentation and additional automation steps.

PS 979

NMDA Receptors Suppress Glutamatergic Transmission at the Hair Cell Afferent Synapse

Joy Sebe
University of Washington, Department of Biology

We recently reported that synaptic transmission and excitotoxic damage at the hair cell synapse are mediated by Ca^{2+} permeable AMPA receptors (CP-AMPARs). We now show that another type of Ca^{2+} permeable glutamate receptor, the NMDA receptor (NMDAR), is present at the hair cell synapse where it suppresses glutamatergic transmission and may protect against excitotoxic damage. Using a combination of immunohistochemistry

and in vivo Ca²⁺ imaging in the larval zebrafish lateral line system, we examined glutamate receptor localization at the synapse and Ca^{2+} responses of both hair cells and terminals to mechanical stimulation. Immunohistochemical studies show that NMDAR NR1 subunit expression at the hair cell synapse is widespread and overlaps with expression of the AMPAR GluR4 subunit and postsynaptic density marker MAGUK. We show that certain NMDAR antagonists (D-AP5 and CPP) significantly enhance hair cell and terminal Ca^{2+} responses to mechanical stimulation while MK-801, which blocks only ionic current through the receptor, does not affect Ca^{2+} responses. We have previously shown that AMPA application (100 mM) causes afferent terminal excitotoxic damage by inducing Ca^{2+} accumulation and that the terminal can be protected by blocking CP-AMPARs. We now show that while a lower dose of AMPA alone (30 mM) does not cause terminal damage, pretreatment with antagonists that block Ca^{2+} entry via voltage-gated Ca^{2+} channels and NMDARs sensitizes terminals to a low dose of AMPA. Future work will examine the mechanisms by which NMDARs suppress glutamatergic transmission and protect the terminal against excitotoxic damage.

Inner Ear: Mechanics & Modeling III

PS 980

An operating principle of the turtle utricle to detect wide dynamic range

Jong-Hoon Nam
University of Rochester

Background

The utricle encodes both static information such as head orientation, and dynamic information such as vibrations. The macular surface of the utricle has two distinguished zones—striolar and extra-striolar zones. The shapes hair cells are distinctly different between these zones. In the striolar region, the kinocilium has similar height with the tallest row of stereocilia, and the stereocilia height gradient is steep. In contrast, in the extrastriolar region, the kinocilium is often several times taller than the rest of the bundle, and the stereocilia height gradient is gentle.

Methods

Two hair bundles were modeled using the finite element method—one representing the striolar hair cell (Cell S), and the other representing the medial extrastriolar hair cell (Cell E). A mechano-transduction (MET) channel model was incorporated to compute MET current (i_{MET}) due to hair bundle deflection. A macro-mechanical model of the utricle was used to compute otoconial motions from head accelerations (a_{Head}). According to known anatomical data, Cell E has a long kinocilium that

is plugged into the stiff otoconial layer. Unlike Cell E, the hair bundle of Cell S falls short of the otoconial layer. Considering such difference in the mechanical connectivity between the hair cell bundle and the otoconial layer, two cases were simulated: displacement-clamped (X-clamped), viscously-coupled (V-clamped) cases.

Results

Quasi-static motion with the stimulation amplitude level of 0.3g that is equivalent to 17 degrees of head tilt saturated the X-clamped Cell S. When the utricle is consisted with the combination of different types of hair cells such as the X-clamped Cell E and the V-clamped Cell S, it could encode a wide range of head acceleration (0.02g and 3g) over a wide range of frequency (DC to 3 kHz). When a realistic head motion was simulated (a 30 degrees of head tilt followed by a feeding strike), the X-clamped Cell E encoded the head tilt well, but saturated during the feeding strike. The V-clamped Cell S was unresponsive during the tilt, but responded well during the feeding strike. In contrast, the X-clamped Cell S fully saturated during the tilt.

Conclusions

By incorporating two mechanical stimulation modalities (firm coupling and viscous coupling between the hair bundles and the otoconia), the turtle utricle can perform a dual sensor: as a static head orientation sensor, and a motion detector over a wide operating range both in stimulating amplitude and in frequency.

PS 981

Stochastic Resonance in Nanometric Sensors Explain the Pressure Induced Motility of Outer Hair Cells in Mammals

Eitan Kimmel[1]; Einat Shapira[1]; Itai Friman[1]; Remy Pujol[2]
[1]*Technion;* [2]*University of Montpellier*

Questions regarding the identity of the mammalian cochlear amplifier and its mechanism have intrigued scientists for decades. It is common to assume that when sound reaches the inner ear it initially induces vibrations of the basilar membrane (BM); only then, outer hair cells (OHCs) detect and amplify these vibrations. We challenge this notion, claiming that in a passive element like the BM, the induced distortion at low sound pressure levels would be too small compared to the noise and, therefore, cannot be detected or magnified. Moreover, this concept has difficulties in explaining a significant characteristic of mammalian hearingamplification of high frequencies. Based on the morphology of the mam-

malian cochlea, and in particular of OHCs, we suggest that sound induced motility of OHCs could result from a synchronized action of hundreds of thousands of actuators in OHC';s lateral wall. They were denoted by us as nanometric acoustic motile sensors (NAMSs). We show that a mechanism of stochastic resonance in the NAMSs can account for the major features of mammalian hearing: wide dynamic range, attributed to amplification of low sound pressure levels (SPLs) and compressive nonlinearity at higher SPLs; sharp frequency selectivity; generation of spontaneous otoacoustic emissions; and the ability to process relatively high frequencies. Another unique, unexplained feature of mammalian OHCs is that their length (L), which span between 10 μm and 80 μm, is inversely correlated with the logarithm of the frequency coding (f) of the cochlea, which varies between 10 Hz and 10^5 Hz. This is often named "the xylophone". Surprisingly, we were able to derive from the NAMS model, an explanation for the L-f relationship for the OHCs of all mammals by combining fundamentals of statistical mechanics with the energy balance of a NAMS ensemble in a single OHC.Finally, the NAMS model is expanded to address the experimental electro-mechanic characteristics of the OHCs, with a focus on a plasma membrane's molecular motor - Prestin. We hypothesize that the Prestin, while embedded in the NAMS'; plasma membrane, it can wrap the membrane around to some degree, thus controlling the contraction force that the NAMS applies on the OHC, to shorten it. We show that this rolling induced contraction force is modulated by membrane potential and is the reason for potential dependent OHC elongation and non-linear capacitance.

PS 982

Bone conduction sound transmission in the human head based on model simulations

Stefan Stenfelt; You stenfelt
Linköping University

Bone conduction hearing in the human is caused by sound that is transmitted to the inner ear by means of vibrations in the skull bone and soft tissues. Due to its complexity, the exact mechanisms of hearing by bone conduction has not yet been clarified. In an effort to understand the pathways involved in hearing by bone conduction, models of the human hearing for bone conduction was developed. One such model was a finite element model of the human head comprising eight tissue domains. This model predicts that during bone conduction stimulation on the mastoid, most of the sound energy is concentrated to the skull bone and the sound energy in the soft tissues decrease with frequency indicating that it may only be important for bone conduction hearing at the very low frequencies. It further suggest that the vibration pattern in the cranial vault differs from the skull base where the cranial vault show wave transmission by bending and transversal waves and the skull base have longitudinal wave propagation. The sound energy in the skull bone spreads radially from the stimulation position and decreases with distance on the ipsilateral side. At the contralateral side, the sound energy increases slightly with distance from the stimulation position as a result of a refocus of the sound energy. The contralateral sound energy increase is also caused by sound energy that is transmitted from the skull bone to the skull interior on the ipsilateral side and transmitted back to the skull bone on the contralateral side. This effect is apparent at frequencies at and above 2 kHz while at frequencies between 0.6 and 1.8 kHz, there is sound energy transmission from the skull bone to the skull interior at both the ipsilateral and contralateral sides. When the stimulation is at a surface of $175mm^2$ at the mastoid skin, at 1 kHz the skin vibrates with almost 30 dB greater level than the skull bone beneath the stimulation point, and the ipsilateral cochlea motion is close to 10 dB lower than at the mastoid bone. At 10 kHz, these numbers have increased to more than 40 dB difference between the skin and skull bone motion, and around 30 dB less motion at the cochlea than at the surface of the mastoid bone.

PS 983

Mechanically facilitated ion transportation in the organ of Corti

Catherine A. Knox; Douglas H. Kelley; Jong-Hoon Nam
University of Rochester

Background

The organ of Corti (OoC) separates two lymphatic fluids—the endolymph and the perilymph. The electro-chemical gradient between the two fluid spaces drives mechano-transduction (MET) current, mostly carried by K^+. There exists substantial silent (standing) MET current, and the current is greater toward the basal end of the cochlea. This implies that it takes greater effort to clear K^+ toward the base. It is believed that ion transportation in the Corti fluid (extracellular fluid space in the OoC) is diffusion limited. Using a computational model, we investigated if advection in the Corti fluid can contribute to the cochlear fluid homeostasis.

Methods

A 2-D computational model of the Corti fluid space was created to investigate the ion transportation along the length of the cochlea. To consider two modes of ion transportation (diffusion and advection), two governing equations were solved. First, fluid motion was represented by the Navier-Stokes equations for an incompressible fluid. Second, ion transportation was computed by solving the diffusion-advection equation. The top

and bottom boundaries of the fluid domain represent the top and bottom surfaces of the OoC, that vibrate to carry traveling waves. When the two surfaces vibrate out-of-phase, peristaltic agitation can occur, inducing local longitudinal flow along the tunnel of Corti.

Results

Different patterns of OoC vibration were simulated and the ion transportation along the Corti fluid space were analyzed. The mixing (homogenization) due to ion transport was quantified in two ways. The change in standard deviation of ion concentration over the Corti fluid space was computed—as mixing occurred the standard deviation decreased. Additionally, the time for a concentrated source at one end of the cochlea to reach a certain longitudinal distance from the source was computed. The model shows that the advection can be an effective means for the ion transportation in the Corti fluid. The efficiency of the transportation depends on the pattern of OoC vibrations. The out-of-phase motion between the top and bottom surfaces of the OoC was more effective than in-phase motion.

Conclusions

Our theoretical results show that 1) there can exist ion transportation due to fluid advection in the OoC; 2) OoC vibrations due to the outer hair cell motility can help transport ions longitudinally.

PS 984

The Effects of Endolymphatic Hydrops on Hearing Thresholds in Air conduction and Bone Conduction: Finite Element Analysis

Yoonkyung Oh; Myungjoon Han; Jongwoon Choi; Namkeun Kim
Incheon National University

A three-dimensional finite element model of human middle ear and cochlea, with a tapered box geometry, was used to explore the effects of endolymphatic hydrops on hearing threshold. Because the scala media was combined with scala vestibuli in the model, the hydrops was implemented by giving static pressure on the basilar membrane (BM) surface. The deformed displacement of the BM due to the static pressure stiffened its elastic modulus. While maintaining the stiffened BM, both air conduction (AC) and bone conduction (BC) were simulated. The AC was implemented by applying dynamic pressure on the tympanic membrane whereas the BC was simulated by applying sinusoidal displacement on the bony surface of the cochlea and the ends of ligaments connecting middle-ear structure and skull. The re-

sults show that about 100 Pa pressure increase causes hearing loss at low frequencies below 300 Hz in both AC and BC. However, over 300 Hz, there was insignificant effect on hearing from the hydrops in the simulation. In addition, results from the BC show similar patterns to those from the AC at all the simulated frequencies. In theory, as the pressure on the BM increases, the deformed displacement of the BM should increase from the apex, which in turn increases the Young';s moduli of the BM from the apex as well. However, due to the geometry of the cochlea, the maximum deformed displacement was limited to the height of the scala tympani (or scala vestibule). Therefore, there was restriction on the pressure range affecting hearing threshold. In other words, for the BM velocities to be affected by the endolymphatic hydrops at high frequencies, the basal parts of the BM should be fully stiffened by the deformation. However, it is physically difficult to obtain the pressure in the scala media high enough to deform the basal parts of the BM due to the limited geometry. Hence, the BM velocities cannot be mechanically affected by the hydrops at high frequencies.

PS 985

A comparison of the capacity of different cochlear models to predict neural responses in the mammalian auditory midbrain and primary auditory cortex

Monzilur Rahman[1]; Benjamin D.B. Willmore[1]; Andrew J. King[2]; Nicol Harper[2]
[1]Department of Physiology, Anatomy, and Genetics, University of Oxford; [2]University of Oxford

Previous studies have developed various models of the auditory periphery from the mechanistic to the phenomenological. These models range from modelling in detail the biophysical characteristics of the cochlea and auditory nerve to very pared-down spectrogram-like approximations of the information processing in these structures. In encoding models of the neural responses of higher auditory areas such as the auditory midbrain or primary auditory cortex, cochlear models often provide the first stage of transformation of sound input. However, detailed quantitative evaluation of the capacity of different cochlear models to help explain the time-courses of neural responses in such brain regions has been somewhat limited, although progress has been made by Gill et al. (2006, J Comput Neurosci: 21) in birds. In the current work, we compared the capacity of a wide range of cochlear models to predict the time-course of single-unit neural responses in the auditory midbrain and the auditory cortex of mammals (ferrets), when combined with a linear non-linear encoding model. Using multi-electrode probes, neural responses to various natural sounds were first recorded. Then the majority

of this dataset was used to train the models to predict neural responses and a remaining proportion was used to test the prediction capacity. Comparison between the actual and predicted neural responses were made using the normalized correlation co-efficient (CCnorm) (Hsu et al. 2004, Network: Comput Neural Syst: 15; Schoppe et al. 2016, Front Comput Neurosci: 10). We found that simple phenomenological models of the auditory periphery outperform the more biophysically detailed models. Specifically, a simple model based on a log-spaced spectrogram with either a log or Hill compression function performs better (cross-validated CCnorm 0.64-0.66) than more complex models involving features such as a gammatone filterbank, lateral inhibition, gain control or various detailed biophysically-inspired hair cell or basilar membrane dynamics (cross-validated CCnorm 0.12-0.49). These findings emphasize the value of using simple pre-processing models when building LN-like encoding models of the nervous system and perhaps also imply that the complex mechanisms of the auditory periphery may together result in a simpler than expected functional transformation of the inputs.

PS 986

Analyzing the current distributions of the Multi-Mode Grounding cochlear stimulation

Pierre Stahl[1]; Kai Dang[2]; Clair Vandersteen[3]; Nicolas Guevara[3]; Dan Gnansia[2]; Maureen Clerc[4]
[1]OTICON MEDICAL; [2]Oticon Medical; [3]Nice University Hospital; [4]Inria

Introduction

Modern cochlear implants can adopt different stimulation modes in order to achieve the predicted current distribution in the inner ear. While the Monopolar mode forces the current to return to a reference electrode placed between the skull and scalp in order to reduce the energy consumption, the common ground mode allows the current to return to allnon-stimulating electrodes of thearray in order to achieve better focusing.

The Multi-Mode Grounding (MMG) is provided by Oticon Medical. This mode combines both Monopolar and common ground modes with the assumption that MMG leads to an optimized balance between efficiency and focus. However, the current distribution of this stimulation mode has not yet been studied.

Objectives and Methods

The present study uses both experimental measures and simulations to estimate the current flow into a 3D cochlear model. This procedure was more specifically used to evaluate current spread with MMG stimulation. The proportion of returning current on each pathway during MMGstimulation was acquired through a XP implant produced by Oticon Medical implanted in a dead human specimen . During each stimulation, the current waveform on all non-stimulating electrodes was recorded, resulting in a map of the returning current distribution in relation to the place of stimulation in the cochlea. The measured current distribution was finally used as an input parameter in a 3D cochlear model to simulate the current field accrossthe inner ear, especially at the position of the auditory nerve fibers. This model was previously used to estimate the current pathways of the Monopolar and bipolar stimulations.

Results

This combination of experimental measurements and simulations provided a powerful and easy tool to estimate the current pathway into a 3D modeled cochlea. While the Monopolar and the bipolar lead respectively to the largest and smallest current patterns, the MMG current spread was shown to be in between.

PS 987

Evaluation of the performance of a novel subcutaneous bone conduction device

Ivo Dobrev; Alexander Huber; Christof Röösli
University of Zurich, University Hospital Zurich, Department of Otorhinolaryngology, Head and Neck Surgery, Switzerland

Objectives

Evaluation of the transfer function efficiency of a newly-developed subcutaneous bone conduction actuator (OSI).

Methods

Experiments were conducted on five Thiel embalmed whole head cadaver specimens.A subcutaneous bone conduction actuator (OSI) is sequentially implanted on three positions: 1) traditional Baha® position 5cm posterior of the tragus in the temporal line, 2) superior to the external auditory canal as close to the cochlea as possible, 3) a posterior position 7cm behind the tragus in the temporal line. For each stimulation location two types of measurements were performed: 1) motions of the cochlear promontory were measured on the ipsilateral and contralateral side, at a single point using a 3-dimensional laser Doppler vibrometer (3D LDV) system, and measurements were repeated after mastoidectomy on the ipsilateral side; 2) three-dimensional motions of the bone surrounding the OSI were quantified at 70-90 points, covering an area of approximately 8×8 cm^2, using the 3D LDV system, supported on an automated robotic arm. All measurements at stimulation position 1 were done with both OSI (piezo-electric transducer) and the actuator from Baha® Cordelle II system (elec-

tro-magnetic transducer), sequentially, for comparison purposes.

Results

Surface wave patterns of the skull surface, for stimulation with OSI and Baha actuators, are comparable for both the magnitude and phase of motion. The magnitude of motion at the promontory, normalized by the driving voltage, is higher for stimulation with Baha actuator compared to OSI, at low frequencies (i.e. < 0.6 kHz), and vice-versa at mid and high frequencies (i.e., 1.5 – 10 kHz).

Conclusion

The sound transfer function efficacy of a novel subcutaneous bone conduction device has been quantified, and the influence of stimulation position and the state of the mastoid have been analyzed.

PS 988

Stimulation site and coupling type dependence of bone conduction pathways

Ivo Dobrev; Alexander Huber; Christof Röösli
University of Zurich, University Hospital Zurich, Department of Otorhinolaryngology, Head and Neck Surgery, Switzerland

Objectives

Investigation of bone conduction sound propagation by the osseous and non-osseous pathways and their interaction depending on stimulation site and coupling method of the bone conduction hearing aid (BCHA).

Methods

Experiments were conducted on five Thiel embalmed whole head cadaver specimens. The electromagnetic actuators from a commercial bone conduction hearing aids (BCHA) (Baha® Cordelle and BoneBridge®) were used to provide stepped sine stimulus in the range of 0.1-10 kHz. Osseous pathways (direct bone stimulation or transcutaneous stimulation) were sequentially activated by mastoid stimulation via a percutaneously implanted screw, Baha® Attract transcutaneous magnet and a 5-Newton steel headband. Non-osseous pathways (only soft tissue or intra-cranial contents stimulation) were activated by stimulation on the eye, neck and dura via a 5-Newton steel headband, as were compared with equivalent stimulation on the mastoid or forehead. The response of the skull was monitored as motions of the ipsi- and contra-lateral promontory and the intracranial pressure (ICP) measured in central, anterior, posterior, ipsilateral and contralateral temporal regions of the cranial space. Promontory motion was monitored a three-dimensional laser Doppler vibrometer (3D LDV) system.

Results

Direct dura and eye stimulation induce comparable or even higher (at frequencies below 1 kHz) ICP, relative to percutaneous mastoid stimulation. Phase data indicates lower phase delays in ICP, when stimulated via non-osseous means (i.e. eye, dura) versus osseous means (i.e., mastoid, forehead). 3D LDV data indicates that the promontory undergoes complex spatial motion with similar contributions from all motion components, under all stimulation modes.

Conclusion

Comprehensive experiments, including simultaneous motion and pressure measurements, with various stimulation positions and coupling methods allow for detailed exploration and differentiation of the individual contributions of the various bone conduction pathways.

PS 989

Finite Element Cochlea Modeling under Inertial and Compressional Bone Conduction

Liu-Jie Ren; Lin Yang; Tian-Yu Zhang
Eye &ENT Hospital of Fudan University

Background

Both inertial and compressional bone-conducted vibration induces frequency dependent traveling wave along the basilar membrane (BM), but with slightly different mechanism. Inertial bone conduction, which dominates the low frequency range, involves the inertia of cochlear fluid and the ossicular chain. While compressional bone conduction, which matters at higher frequencies, is associated with the deformation of the bony walls. A three dimensional finite element cochlea model is developed to simulate the BM traveling wave under bone-conducted stimulation.

Methods

Reconstructed from human head CT slices, the finite element model consists of the middle ear, semicircular canals and a coiled cochlea, which is covered by bony structures. The cochlea structure is simplified into the classical 'box model' - two scalae filled with cochlear fluid, and separated by an elastic membrane with longitudinal varied width, thickness and Young's modulus. Firstly, the model parameters are tuned and verified under air-conducted stimulation, by applying sinusoidal pressure on the tympanic membrane. Then loads are directly applied to the cochlear bony walls as inertial or compressional bone-conducted stimulation. We compare the BM vibration, oval and round window motion, and fluid pressure under air-conducted stimulation and two types of bone-conduction stimulations.

Results and Discussions

Our preliminary results show similar traveling wave type and frequency-location relation under bone-conducted and air-conducted stimulations. Moreover, under inertial bone-conducted stimulation, the oval and round windows move in phase, and the BM response is proportional to their motion, which is significantly influenced by the impedance of the middle ear. While under compressional bone-conducted stimulations, the two windows moves out of phase, and the BM response is more complicated. This research is still in progress. More results and discussions would be available during the meeting.

Acknowledgements

ARO-ABSTRACT-REN.pdf

PS 990

Relating the Cohesiveness of Auditory Hair Bundles in Mammals to their Function

Wisam Reid[1]; Anthony J. Ricci[1]; Daibhid O Maoileidigh[2]
[1]Department of Otolaryngology, Head and Neck Surgery, Stanford School of Medicine, Stanford, CA, USA.; [2]Department of Otolaryngology - Head and Neck Surgery, Stanford University School of Medicine

Hair bundles are comprised of a set of stereocilia connected by links that ensure their cohesion in vestibular systems and nonmammalian auditory organs. In contrast, bundles from the mammalian cochlea exhibit weak coherence in response to experimental stimuli. Although coherence between stereocilia determines how hair cells transduce stimuli, we do not fully understand the relationship between a bundle';s cohesiveness and its function.

To connect a hair bundle';s structure with its response to stimulation, we construct a mathematical model of hair-bundle mechanics describing inner and outer hair cells. The model consists of a set of stereocilia connected by tip links and top connectors and includes the viscosity of the surrounding fluid. We vary the geometry and material properties of the bundle and analyze its responses to sinusoidal and step stimuli. These simulations are compared to the observed displacements of real hair bundles in response to experimental stimuli applied using a fluid jet or a stiff probe.

There are several consequences arising from a lack of bundle cohesion. We find that the measured stiffness and drag of a bundle depends on how the stimulus is applied and that a bundle may not be accurately described by a single spring constant and drag coefficient. Moreover, in response to a stimulus, tip links between different stereocilia do not extend the same amount and their extensions are not in phase with one another.

We conclude that the responses of a weakly coupled hair bundle to stimuli are considerably more complex than those of a tightly coupled bundle. To more completely characterize the exact role of cohesion, intrinsic noise, mechanotransduction channels, and adaptation need to be taken into account. Nonetheless, our reduced description reveals that bundle cohesion strongly affects how a hair cell detects external signals.

PS 991

Modelling polarity and pulse shape effects on a Spiral Ganglion Neuron with KLT channels under electro-stimulation

Matthieu Recugnat; Jaime A. Undurraga; David McAlpine
Macquarie University

Computational models of spiral ganglion neurons (SGNs)—from single cells to neural populations are important in understanding how the electrode-neuron interface might be enhanced in cochlear implants (CIs). Electrode-neuron distance, spread of excitation within the cochlea, neuron survival, and the status of the SGNs, are known factors in the efficiency of the neural encoding of sound in CI users. Current research focuses on improving that interface; biologically through increased 'bio-mimicking'; of electrical stimulation strategies, pharmacologically with neuro-trophic or –protective drug coatings applied to the electrode array, or through parallel advances in signal processing.

Successful models of the SGNs that use realistic morphology and physiologically derived ionic channels dynamics have been efficient in predicting action-potential firing. Although these models help understand the behavior of SGNs when subjected to external electrical stimuli, they often fail to account for key characteristics of SGN firing, such as adaptation or refractoriness. Recent work has shown that this could be caused by the use of an impoverished set of ionic channels and that said models could be improved by adding sub families of ionic channels such as low-threshold potassium conductances (KLT) or hyperpolarizing cation channels (HCN).

Here, using cable-equation methods, we focus on the effects of polarity and the shape of electrical pulse on the electrically stimulated auditory nerve by means of

a physiologically inspired model of a single SGN. This study investigates the effect of electrical stimulation in a realistic SGN model in order to evaluate stimulation strategies and determine the efficacy of other proposed improvements in CI devices. The model compares predictions from ionic channel models with and without the KLT and HCN channels.

The model incorporates relevant physiological characteristics that generate action potentials, and results in refractoriness, facilitation, accommodation and spike-rate adaptation. The model also allows for parameterization of ionic channels dynamics as well as geometry characterization. Specifically, we study the effects of polarity and pulse shape on the firing pattern on separate SGNs undergoing several degrees of degeneration – from partial (decrease of peripheral myelination) to total peripheral degeneration. Results are compared with published data from animal and computational models.

PS 992

Identifying the Cellular Sources of the Low-Frequency Cochlear Response

Aryn M. Kamerer; Mark E. Chertoff
University of Kansas Medical Center

Medical and technologic treatments for hearing loss are quickly outpacing current clinical diagnostic techniques. In order to knowledgeably treat patients and accurately predict treatment outcomes, we need diagnostic tools that can identify the anatomic damage or dysfunction underlying the loss of hearing. The cochlear microphonic –a reflection of current flow through hair cells –in conjunction with high-pass noise or suppressing tones, shows promise as a method of assessing the health of hair cells at specific locations along the cochlear partition in rodent models. In this study, we propose that the electrical potential recorded from the round window in gerbils to low-frequency tones contains significant responses from the auditory nerve and inner hair cells in addition to the outer hair cell response. A model is created from data found in existing literature and our previous studies, which provides evidence for identifying each cellular source contributing to this low-frequency round window potential, termed the cochlear response (CR).

The CR was recorded via an electrode placed in the round window niche of 16 Mongolian gerbils and elicited with a 45 Hz tone burst embedded in 18 high-pass filtered noise conditions, which in theory, target responses from increasing apical-to-basal regions along the cochlear partition. Independent component analysis and filtering of the response recovered several contributing

sources whose spectral and temporal content provided clues to their identification. These suspected sources were modeled using previously-published hair cell and auditory nerve response data, and then weighted and combined using linear regression to produce a model response that fits closely to the mean CR waveform.

We conclude that the low-frequency CR contains contributions from several cellular sources, for which the model provides evidence of the most significant contributors being outer hair cells, inner hair cells, and apical auditory nerve fibers. Therefore, the CR shows the capacity to be developed into a diagnostic tool that can assess the health of multiple structures in the cochlea objectively, simultaneously, and independently.

PS 993

In Search of the Outer Hair Cell Mechanoelectrical Transduction Nonlinearity

Mackenzie L. Mills[1]; Robert H. Withnell[1]; Kevin Ohlemiller[2]
[1]*Department of Speech and Hearing Sciences, Indiana University;* [2]*Department of Otolaryngology-Head and Neck Surgery, Washington University School of Medicine*

Background
Previous research suggests that cellular mechanical events within cochlea add energy to cochlear hydrodynamics. Cochlear nonlinearity stabilizes this amplification process by saturating the voltage-driven positive feedback from mechanical outer hair cell (OHC) vibration. Previous efforts to model cochlear amplification have accepted the Boltzmann equation as an adequate representation of this cochlear nonlinearity. However, a local saturation-feedback model of DPOAE generation, solved as a function of time, with the OHC mechano-electrical transduction (MET) represented by a Boltzmann function, suggests an alternative equation to describe cochlear nonlinearity is necessary. In this study, we investigate various sigmoid functions as alternative descriptors of OHC MET.

Methods
DPOAEs were measured in normal hearing CBA/CaJ mice (age 12-18 weeks) at stimulus frequencies of 17, 25, and 33 kHz. Stimulus frequency ratio was 1.2. Stimulus levels were varied between 20 and 90 dB SPL in 5 dB steps. Mice were anesthetized with ketamine/xylazine (80/15 mg/kg, IP) with the pinna resected for access to the ear canal. Animal respiration was unassisted. A custom-made probe (EPL acoustic system design) for sound delivery and recording was used with signal generation and data acquisition was computer controlled

using EMAV (Neely and Liu, BTNRH). Hearing sensitivity was monitored using auditory electrophysiology.

A local saturation feedback model (Zwicker, 1979) was used for DPOAE generation, solved in the time domain. The feedback gain parameter was found from a nonlinear least-squares-fit of the model to DPOAE data at one stimulus level, and then DPOAE model I/O functions were generated. Various sigmoid functions representing OHC MET nonlinearity were investigated in terms of the fit to DPOAE data. All model calculations were performed using Matlab R2016b.

Results
A Boltzmann function, first or second order, representing OHC MET in the model of DPOAE generation, did not provide a good fit to mouse DPOAE data. It was found that a sigmoid function with a more rapid stimulus-level dependent saturation provides a closer fit to DPOAE data.

Conclusion
Zwicker';s model of cochlear mechanical amplification, solved in the time domain, provides insight into the form of the nonlinearity responsible for OHC MET and may, in the future, inform our understanding of hair bundle ion channel kinetics. Alternatively, given experimental findings reported in the literature that support OHC MET being well described by a Boltzmann function, these results may suggest that a saturating positive feedback model is not a good descriptor of cochlear mechanical amplification.

PS 994

A theoretical model for multi-vesicular release of synaptic ribbon in auditory hair cells

Kang-Hun Ahn[1]; Sul-Ah Park[1]; Ruth Anne Eatock[2]
[1]*Chungnam National University;* [2]*University of Chicago*

The auditory synapse has distinct properties from other synapse. It has high release rates without fatigue. It has wide range of EPSC amplitude probably due to multivesicular release. It transfers sound stimuli with high fidelity so that it exhibits phase locking of 5 kHz signal. Timing of action potential does not vary with stimuli amplitude. The synapses of auditory hair cells have ribbon-like structure where vesicles are tethered. Each vesicle contains glutamate molecules which are negatively charged and it contains charges of the protein on the vesicle surface. Here, we investigate the consequence of vesicle charging effects on two stage; the dynamics of mobile vesicles on the ribbon and the glutamate release. The inter-vesicle interaction form certain quasi-equidistant structure of the vesicles. At the stage of glutamate release, our stochastic dynam-

ics simulations show the synchronization of vesicle release due to charging effects.

PS 995

Membrane Models of Outer Hair Cell Motility

Kuni H. Iwasa
National Institutes of Health

Electromotility of outer hair cells (OHC), a key factor for the performance of the mammalian ear, has been described by either membrane models (MemMs) or by one- dimensional models (1DimMs). The simplicity of 1DimM helped describing the effect of the motile element with extra states [1-3] in addition to the two states essential for electromechanical coupling. Those treatments are for motile activity under load-free condition. A 1DimM has been also employed to describe the motion of OHCs under mechanical load to evaluate energy production by these cells [4]. More physical but complex MemMs have so far been formulated for motile elements with only two states for describing quasi static behaviors. An advantage of MemMs is that they can describe the effect of stresses other than axial, such as turgor pressure, unlike 1DimMs.

The goal of the present study is two fold: to extend a MembM to describe the motion of OHCs under mechanical load and to incorporate multiple states to the motile element. This extension enables to predict the effect of turgor pressure on the energy output of OHCs. It also extends Song and Santos-Sacchi';s theory, where the motile element has four conformational states [2]. In addition to the two states essential for electromechanical coupling, the theory proposes transitions which depend only on turgor pressure, which cannot be adequately described by 1DimMs.

The equation of motion for a MemM with two-state motile element shows that turgor pressure affects the energy output primarily due to shifts in the operating point of the motile activity. Since mechano-electric transitions are sensitive to turgor pressure, in a MemM with multi-state motile element, transitions between three states must be turgor pressure sensitive, not just between two states as proposed by the original 1DimM version [2]. For this reason, the dependence of energy production on turgor pressure is more complex than that of two-state motor. For a given value of turgor pressure, the MemM can be reduced to a 1DimM, revealing the physical origins of its phenomenological parameters in the 1DimM.

References
[1] Homma K and Dallos P, J Biol Chem 286(2011)2297–2307.

[2] Song L and Santos-Sacchi J, Proc Natl Acad Sci USA 110(2013)3883-3888;

[3] Santos-Sacchi J and Song L, Biophys J 107(2014)126–133.

[4] Iwasa KH, Biophys J 111(2016)2500-2511; Iwasa KH, Sci Rep (in press).

PS 996

Volumetric Model of the Actin Core in Shaft and Taper as revealed by Cryo-Electron Tomography of Vitrified Whole-Mount Stereocilia

Jun Ha Song[1]; Jocelyn Krey[2]; Roma Patterson[1]; Ting Chih Lin[1]; Samantha Hao[1]; Jennifer Wiederspahn[1]; Julio Kovacs[3]; Tom Goddard[4]; William Tivol[1]; Niels Volkmann[5]; Willy Wriggers[3]; Jing He[3]; Dorit Hanein[5]; Peter G. Barr-Gillespie[6]; **Manfred Auer**[1]
[1]*Lawrence Berkeley National Laboratory;* [2]*Oregon Hearing Research Center and Vollum Institute;* [3]*Old Dominion University;* [4]*University of California, San Francisco;* [5]*Sanford Burnham Prebys Medical Discovery Institute;* [6]*Oregon Health & Science University | Oregon Hearing Research Center and Vollum Institute*

Stereocilia ultrastructure to date is based on transmission electron microscopy (TEM) of resin-embedded, ultra-thin sections, which provide longitudinal or cross-sectional views. Using electron tomography of resin-sections we had shown 3D ultrastructural insight into the actin-rich stereocilium, including actin-actin crosslinkers and actin-membrane connectors (1). We found that while the stereocilia actin core was less ordered than expected, our tomography-based estimate of connector proteins was in excellent agreement with estimates from quantitative proteomics (1). Being concerned that high pressure freezing/freeze-substitution and resin-embedding may have been prone to sample preparation artifacts, we developed a cryo-EM approach that allows imaging of intact vitrified stereocilia. Stereocilia were blotted off the sensory epithelial apical surface onto an electron microscopy grid and immediately plunge-frozen.

Cryo-EM/tomography of such unstained frozen-hydrated intact stereocilia revealed that the membrane resealed at the point of insertion into the cell body. Judging by visual inspection as well as 2D Fourier analysis of tomographic slabs, wild type stereocilia contained both regions of high order, as well as regions of low order. We found evidence of gaps and forking in the actin core, suggesting that the actin filaments were structured more like a gel rather than a paracrystalline monolith. Given the higher order of the actin core in plastin-1 knockout mice (Pls1^{-/-}) (2), we imaged Pls1^{-/-} stereocilia, which are currently used for development of automated filament tracking approaches. We have obtained simplified volumetric models of the actin core as well as an unexpected 3D volumetric arrangement of the actin in the taper and rootlet region. We are currently probing the space between the actin core and the membrane for unconventional myosin macromolecules.

Furthermore, data collection is currently underway using beam-induced specimen motion-correcting direct electron detector- and phase plate-imaging, which promise even higher resolution density maps. Such maps may be of high enough quality to detect known protein structures via template matching.

While our focus lies on the 3D cryo-EM imaging of stereocilia , we have begun to use focused ion beam SEM imaging to reveal the 3D architecture of entire hair bundles and hair cells. We are currently developing multiscale, multimodal imaging work-flows that will allow correlative linking of fluorescence imaging studies of entire animals (e.g. zebrafish larvae) at the millimeter scale and submicron resolution to FIBSEM at the 10-50 micron scale and ~10 nanometer resolution imaging of individual cells and organelles via advanced X-ray tomography of resin-embedded tissues or entire small animals.

References
1. Shin JB, Krey JF, Hassan A, Metlagel Z, Tauscher AN, Pagana JM, Sherman NE, Jeffery ED, Spinelli KJ, Zhao H, Wilmarth PA, Choi D, David LL, Auer M, Barr-Gillespie PG. Molecular architecture of the chick vestibular hair bundle. Nat Neurosci. 2013 Mar;16(3):365-74. doi: 10.1038/nn.3312. Epub 2013 Jan 20. PubMed PMID: 23334578; PubMed Central PMCID: PMC3581746.

2. Krey JF, Krystofiak ES, Dumont RA, Vijayakumar S, Choi D, Rivero F, Kachar B, Jones SM, Barr-Gillespie PG. Plastin 1 widens stereocilia by transforming actin filament packing from hexagonal to liquid. J Cell Biol. 2016 Nov 21;215(4):467-482. Epub 2016 Nov 3. PubMed PMID: 27811163; PubMed Central PMCID: PMC5119939.

ARO MWM2018 Abstract_FINAL170913.docx

PS 997

Bone conduction hearing in Guinea Pigs

Stefan Stenfelt; Mingduo Zhao; Anders Fridberger
Linköping University

Although bone conduction hearing is well investigated in the human, it is less so in animals. In the human, the

amount of conductive loss is estimated as the difference between the air and bone conduction thresholds compared with normal hearing thresholds. Similar estimations for animals are difficult since in most species, the normal bone conduction hearing has not been established. In the current study, the normal bone conduction thresholds in the frequency range between 2 kHz and 20 kHz are investigated for the Guinea Pig. Air conduction stimulation was provided by a calibrated speaker that was coupled to the ear of the Guinea Pig by a short tube. Bone conduction stimulation was applied at the top of the skull of the Guinea Pig where a connector was attached to the cranial bone with bone cement, and a special built bone conduction transducer was rigidly screwed to the connector. The hearing of the Guinea Pig was registered by a silver electrode on the round window capturing the compound action potentials. These potentials were obtained at multiple levels between 25 and 75 dB SPL. Where clear potentials were obtained a regression analysis were performed to estimate the stimulation level that caused 0 Volts compound action potential and this level was used as the threshold for both air and bone conduction stimulation. The bone conduction stimulation used levels that gave similar response levels as with air conduction stimulation. After the electrophysiology testing of the Guinea Pig, the vibration of the cochlea during bone conduction stimulation was estimated by a three-dimensional laser Doppler vibrometer (Polytec CLV-3D). In this way, air conduction thresholds in dB SPL could be compared to bone conduction thresholds in vibration units of the cochlea facilitating transducer independent comparison between labs. The bone conduction threshold levels could also be computed as vibration or force at the stimulation position (top of the Guinea Pig skull). In general, the air conduction thresholds have a U-shaped function when measured in dB SPL (between 0 and 35 dB SPL as measured here) while the bone conduction thresholds seem to be related to a relatively constant acceleration of the cochlea. When the middle ear ossicles were either artificially severed or glued to the surrounding bone, the air conduction thresholds increased by 30 to 50 dB while the same increase in bone conduction thresholds were between 0 and 10 dB leading to a 30 to 40 dB air-bone gap. The compound action potential growth functions indicated a slightly steeper slope with bone conduction stimulation compared to air conduction stimulation.

Inner Ear: Membranes & Fluids

PS 998

Role of the distal endolymphatic sac epithelium in endolymphatic ion homeostasis and Meniere's disease

David Bächinger[1]; Hannes Egli[2]; Madeline Goosmann[1]; Sabina Wunderlin[3]; Arianne Monge Naldi[1]; Joseph B. Nadol[4]; Joe C. Adams[4]; Andreas H. Eckhard[1]
[1]*Department of Otorhinolaryngology, Head and Neck Surgery, University Hospital Zurich, Zurich, Switzerland;* [2]*University of Zurich, Zurich, Switzerland;* [3]*Institute of Veterinary Pathology, University of Zurich, Zurich, Switzerland;* [4]*Department of Otolaryngology, Massachusetts Eye and Ear, Harvard Medical School, Boston, MA, USA*

Background

The unique ionic composition of the endolymphatic fluid in the inner ear is crucial for proper auditory and vestibular function. The endolymphatic sac (ES) has previously been proposed to be critically involved in maintaining endolymphatic ion concentrations. However, the molecular determinants of ion transport in the ES epithelium are only partially identified, and a conclusive model of endolymphatic ion homeostasis by the ES is still missing.

Methods

1) DAB- and immunofluorescence labeling of sodium (Na^+) and calcium (Ca^{2+}) transport-associated proteins on paraffin-embedded murine ES tissue sections (male, 6 – 8 weeks). 2) Quantification of immunolabeled epithelial cells along the proximal-to-distal axis of the ES. 3) In situ proximity ligation assay (PLA) for aldosterone-regulated Na^+-transport proteins on ES tissue sections from mice kept for seven days on high and low Na^+-diets.

Results

Na^+- and Ca^{2+}-transport proteins – known to be expressed in the aldosterone-sensitive distal nephron (ASDN) of the kidney – were identified in the distal portion of the ES epithelium. Most transport proteins exhibited a proximal-to-distal intraepithelial labeling gradient, showed a cell-type specific localization pattern, and a distinct subcellular distribution in mitochondria-rich cells (MRCs) and ribosome-rich cells (RRCs). The extracellular Ca^{2+} sensing receptor (CaSR) was found to be exclusively located in MRCs; CaSR was not located in any other epithelial site of the inner ear membranous labyrinth. In situ PLA demonstrated the aldosterone-dependent expression and translocation of Na^+-transport-associated proteins, such as the epithelial Na^+-channel (ENaC), in the distal ES epithelium; high plasma aldosterone levels increased apical membrane abundance of ENaC mediated by the serum and glucocorticoid regulated kinase 1

(SGK1), whereas low plasma aldosterone levels led to an internalization of channel proteins mediated by the E3 ubiquitin-protein ligase NEDD4-2.

Conclusions

Several Na⁺- and Ca²⁺-transporters and their regulatory proteins were identified in the mature murine ES epithelium. Distinct subpopulations of epithelial cells with supposedly different functions in endolymphatic ion homeostasis, including cellular "sensors" of endolymphatic Ca²⁺ concentration and cellular "mediators" of transepithelial ion fluxes were identified. Loss of the ES';s ion transport mechanisms is of potential pathophysiological significance in diseases associated with ES pathologies, such as in Meniere';s disease.

PS 999

Molecular Architecture of Endolymphatic Sac underlying Fluid Absorption by the Developing Inner Ear

Keiji Honda[1]; Sung Huhn Kim[2]; Michael C. Kelly[1]; Joseph C. Burns[3]; Laura Constance[2]; Xiangming Li[2]; Fei Zhou[2]; Michael Hoa[1]; Matthew W. Kelley[1]; Philine Wangemann[2]; Robert J. Morell[1]; Andrew J. Griffith[4]
[1]NIDCD/NIH; [2]Kansas State University; [3]Decibel Therapeutics; [4]Otolaryngology Branch, National Institute on Deafness and Other Communication Disorders (NIDCD), Bethesda, MD, USA

Background

Mutations of SLC26A4 are a common cause of hearing loss associated with enlargement of the vestibular aqueduct (EVA), which encompasses the endolymphatic sac and duct. SLC26A4 encodes a transmembrane anion exchanger, pendrin, which is expressed in a subset of nonsensory epithelial cells in the cochlea, vestibular organs and endolymphatic sac. Slc26a4 expression in the developing mouse endolymphatic sac is required for acquisition of normal inner ear structure and function. The objective of our present study was to gain insight into the functional, molecular and cellular architecture of the endolymphatic sac and to identify the components of the physiologic-developmental pathway that is disrupted in EVA.

Methods

Endolymphatic sacs were isolated from E14.5 Slc26a4^Δ/+ and Slc26a4^Δ/Δ 129S6 mice, filled with a solution containing a fluorescent dye, and maintained in organ culture in the absence and presence of inhibitors of channels and transporters. The rate of fluid absorption was quantified by volume measurements with 3D confocal microscopy. Single-cell RNA-seq was performed on endolymphatic sac epithelial cells isolated from E12.5, E16.5, P5 and P30 C57BL/6J mice to identify cell groups and differentially expressed genes. Gene array analysis was performed on embryonic endolymphatic sacs from E13.5, E14.5, E16.5, and E17.5 Slc26a4^Δ/+ and Slc26a4^Δ/Δ mice to determine temporal gene expression profiles and differences between genotypes. Expression of selected genes was validated by RT-qPCR and immunohistochemistry.

Results

Endolymphatic sacs from E14.5 Slc26a4^Δ/+ mice engaged in fluid absorption. The rate of fluid absorption at E14.5 was higher in endolymphatic sacs from Slc26a4^Δ/+ than from Slc26a4^Δ/Δ mice, sensitive to ouabain and gadolinium and insensitive to benzamil, bafilomycin and S3226. Single-cell RNA-seq analysis of pre- and postnatal endolymphatic sacs demonstrated two types of differentiated cells. Early ribosome-rich cells (RRCs) had a transcriptomic signature suggestive of production and secretion of proteins, while mature RRCs express genes implicated in innate immunity. Mitochondria-rich cells (MRCs) expressed genes encoding transporters, ion channels and pumps and four genes (Slc26a4, Foxi1, Atp6v0a4, Atp6v1b1) known to cause EVA, suggesting that MRCs mediate vectorial ion transport.

Conclusion

Based on functional and pharmacological data and expression profiles, we propose a molecular mechanism for fluid absorption in the endolymphatic sac during development based on the absorption of NaCl by MRCs. We conclude that disruption of this mechanism by mutations of SLC26A4 or other factors is the root cause of hearing loss associated with EVA.

PS 1000

Steady Streaming as a Method for Drug Delivery to the Inner Ear

Laura Sumner; Tobias Reichenbach
Imperial College London

Background

Sensorineural hearing loss occurs when the hair cells inside the inner ear that are responsible for converting the mechanical sound stimuli into electrical signals, are impaired. Research has identified several promising drugs to prevent hair cell damage or to regenerate hair cells, but delivering the drugs to these cells remains an important problems. The inner ear is encased in the body's hardest bone, and drugs can only be injected through the round window or oval window at its base. Passive diffusion from the base through the spiral-shaped cochlea is comparably ineffective. Here we seek to investigate if steady streaming may be employed to efficiently

distribute drugs from the base of the cochlea along its longitudinal extent. Steady streaming is indeed present in fluid systems with a fluctuating flow and results in a non-zero mean flow. In the cochlea, the fluctuating flow results from the motion of the basilar membrane. This membrane has a spatially-varying impedance which allows to spatially segregate frequencies At a particular frequency the basilar membrane responds maximally at a frequency-specific location. Distributing drugs through steady streaming may thus employ a series of sounds of different frequencies to transport drugs from the high- to the low-frequency region.

Method

We model the basilar-membrane motion at a particular frequency through the WKB approximation. We then used this motion as input to a computational fluid-dynamics (CFD) simulation that we implemented using OpenFOAM. The simulation used a dynamic mesh solver combined with a particle tracking solver to enable the coordinates of individual particles across the entire domain to be determined. The data were post processed to find the steady streaming velocities.

Results

Steady longitudinal streaming at 3kHz showed a reasonable agreement with the theoretically proposed values. These values were also large enough to enable effective transport. The boundary layer thickness was also an almost exact match to theoretical vales, validating the simulation.

Conclusions

We show that the simulation predicts considerable steady streaming over timescales reasonable for therapies, and plan to use it to investigate different types of complex sound stimulation for efficient drug transport.

PS 1001

The Human Cochlear "Battery"— Ion Transport Proteins and Claudin 11 Barrier in the Lateral Wall of the Cochlea. Confocal and Structured Illumination Microscopy

Wei Liu[1]; Rudolf Glueckert[2]; Göran Laurell[3]; Anneliese Schrott-Fischer[2]; Heval Benav[4]; Hao Li[1]; Charlotta Kämpfe[1]; Helge Rask-Andersen[5]
[1]*Department of surgical sceinces, Uppsala university, Uppsala, Sweden; [2]Department of Otolaryngology, Medical University of Innsbruck , Austria; [3]Uppsala university; [4]MedEl; [5]University of Uppsala*

Background

The cochlea produces an electric field potential essential for hair cell transduction and hearing. This biological "battery" is situated in the lateral wall of the cochlea and contains highly organized molecular/cellular arrangement that secretes and recycles K+ ions. Its functioning depends on ion-transporting machinery and junctional proteins that guarantee a unidirectional delivery of K+ and restrict the para-cellular escape of the ion. Claudin 11 protein has been found to be one of the major constituents at tight junction that maintains ion gradients (Gow et al., 2004; Kitajirietal., 2004). We are the first to elucidate the human Claudin 11 framework and the associated ion transporters (channels/pumps/carriers) using super-resolution structured illumination microscopy (SR-SIM).

Methods

Archived cochleae obtained during meningioma surgery were used for SR-SIM, together with confocal laser scanning microscopy and transmission electron microscopy after ethical permission as well as patients'; consent.

Results

Claudin 11-expressing cells formed parallel tight junction lamellae that insulated the epithelial layers of the stria vascularis and extended to the suprastrial region. Intercellular gap junctions were found between the barrier cells and fibrocytes.

Conclusion

Transmission electron microscopy, confocal laser scanning microscopy and SR-SIM revealed exclusive cell specialization in the various subdomains of the lateral wall of the human cochlea. The Claudin 11-expressing cells exhibited both conductor and isolator characteristics, and these microporous separators may selectively mediate the movement of charged units (mainly K+) to the intrastrial space in a manner that is analogous to a conventional electrochemical "battery." The function and relevance of this "battery" for the development of inner ear diseases are discussed.

PS 1002

Generation of inner ear Cx26-gap junction plaque forming cells derived from induced pluripotent stem cells

Ichiro Fukunaga[1]; Kaori Hatakeyama[1]; Ayumi Fujimoto[1]; Osamu Minowa[2]; Katsuhisa Ikeda[1]; Kazusaku Kamiya[1]
[1]*Department of Otorhinolaryngology, Juntendo University Faculty of Medicine; [2]BioResource Center, RIKEN*

Introduction

Mutation of the Gap Junction Beta 2 gene (GJB2) encoding connexin 26 (Cx26) is the most frequent cause of he-

reditary deafness worldwide. Recently, we reported that disruption of the Cx26-dependent gap junction plaque (GJP) is associated with the pathogenesis of GJB2-related deafness (Kamiya et al., J Clin Invest. 2014) and the cochlear gene transfer of GJB2 using an adeno-associated virus significantly improved GJP formation and the auditory function (Iizuka et al., Hum Mol Genet. 2015). Embryonic stem (ES)/induced pluripotent stem (iPS) cells are an important tool for studying the molecular mechanisms underlying inner-ear pathology as well as for generating cells for replacement therapies. However, previous studies have targeted the generation of inner-ear hair cell-like cells from ESCs/iPSCs. It has not been reported that ES/iPS cells differentiate into Cx26-GJP forming cells such as cochlear supporting cells. In this study, we developed a new strategy for differentiation of mouse iPS cells into Cx26-GJP forming cells.

Method
We examined the strategy to induce Cx26-GJP forming cells from mouse iPS cells using modified methods of previous studies (Koehler et al., Nature. 2013).

Results
After the aggregate formation, Cx26-expressing GJP-forming cells (iCx26GJC) were observed in a part of the aggregate. Aggregates were subcultured in adherent culture, and proliferation of iCx26GJCs were observed. In proliferated iCx26GJCs, Cx30 protein, another causative gene product frequently encountered in hereditary deafness, co-assembled with Cx26 in the formation of gap junctions between cells as in the cochlear supporting cells—specifically the outer- and inner-sulcus cells. To investigate whether the iCx26GJC were functional, we performed scrape-loading assay and Ca^{2+} imaging. In the iCx26GJC culture, we observed that Lucifer yellow diffused beyond the wounded parental cells. Furthermore, iCx26GJC exhibited spontaneous Ca^{2+} transients and their propagation. The spontaneous Ca^{2+} signaling activity was reversibly inhibited by the p2x receptor antagonist PPADS and the connexin hemichannel blocker FFA (flufenamic acid) as in the developing cochlea.

Conclusion
In this study, we demonstrate the differentiation of mouse iPS cells into functional Cx26-GJP forming cells, as in the cochlea (Fukunaga et al, Stem Cell Reports, 2016). By using these cells, it is expected to establish the inner ear cell therapy for hearing recovery in GJB2-related hereditary deafness.

PS 1003

Quantitative Analysis of Aquaporin Expression Levels during the Development and Maturation of the Inner Ear

Takushi Miyoshi[1]; Taro Yamaguchi[2]; Kiyokazu Ogita[2]; Yasuko Tanaka[3]; Ken-ichi Ishibashi[3]; Hiroaki Ito[4]; Taisuke Kobayashi[4]; Takayuki Nakagawa[5]; Juichi Ito[6]; Koichi Omori[7]; Norio Yamamoto[1]

[1]Department of Otolaryngology, Head and Neck Surgery, Graduate School of Medicine, Kyoto University; [2]Department of Pharmacology, Faculty of Pharmaceutical Sciences, Setsunan University; [3]Department of Medical Physiology, Meiji Pharmaceutical University; [4]Department of Otolaryngology, Head and Neck Surgery, Kochi Medical School; [5]Department of Otolaryngology - Head and Neck Surgery, Graduate School of Medicine, Kyoto University; [6]Shiga Medical Center Research Institute; [7]Department of Otolaryngology-Head and Neck Surgery, Graduate School of Medicine, Kyoto University

Introduction
Aquaporins (AQPs) are a family of small channels that transport water molecules across the membrane. Mammals express 13 subtypes of AQPs, including the recently reported AQP11 and 12. However, the contribution of individual AQPs, including AQP11 and 12, to the inner ear water homeostasis is still unclear. To elucidate the contribution of these AQPs, we tracked their expression levels during the development of the inner ear using quantitative reverse transcription polymerase chain reaction (qRT-PCR). For further analysis, we also performed in situ hybridization (ISH) of Aqp11 and immunohistochemistry (IHC) of AQP5 and 9. Considering both quantitative and localization data, we discuss the contributions of these AQPs to the establishment of inner ear function.

Methods
Whole inner ears were dissected from C57BL6/J mice at embryonic days (E) 10, 13, and 18, and at postnatal days (P) 3, 10, and 21. Total mRNA was extracted and expression levels were determined by qRT-PCR. ISH and IHC were performed using frozen sections (E10–P21). The template sequence for Aqp11 ISH was amplified from mouse cDNA. The antibodies for AQP5 and 9 were purchased from Millipore and Abcam. The audiological thresholds of Aqp11-knockout mice were determined by click ABR (auditory brainstem response).

Results
In the mature inner ear (P21), Aqp1, 4, 9, and 11 were majorly expressed. Longitudinal quantification indicated that the expression levels of several AQPs followed

characteristic patterns: increasing (Aqp0, 1, and 9), decreasing (Aqp6, 8, and 12), and E18 peak expression (Aqp2, 5, and 7). ISH of Aqp11 revealed its unique expression in the outer hair cells. However, the ABR thresholds were similar between knockout and wild-type mice. IHC of AQP9 indicated its gradual emergence in the supporting cells involved in K^+ recycling. AQP5 was localized in root cells, which expanded toward the apical turn during E13–E18, and regressed from the basal turn after P3.

Conclusions

Combining the expression levels and localization of AQPs, we revealed the unique contribution of AQP11 to the water homeostasis of outer hair cells. We also demonstrated that AQP9 is possibly involved in establishing endolymphatic potential through K^+ recycling. AQP5 might be responsible for the development of endolymphatic spaces.

PS 1004

Otolin-1 in Biological Fluids: A Possible Biomarker for Inner Ear Disease.

Emlio Avallone[1]; Giorgio Lilli[1]; Warneke Athanasia[2]; Anke Lesinski-Schiedat[1]; Thomas Lenarz[2]; Kerstin Willenborg[1]; Heike Schmitt[3]
[1]Department of Otorhinolaryngology and Head and Neck Surgery, Hannover Medical School; [2]Department of Otolaryngology, Hannover Medical School, Germany and DFG Cluster of Excellence Hearing4all; [3]Cluster of Excellence of the German Research Foundation (DFG; "Deutsche Forschungsgemeinschaft") "Hearing4all".

Objective

The expression of Otolin-1 mRNA is highly restricted to the inner ear. In particular, it is identified in the supporting cells of the maculae and cristae. It is also a component of the tectorial membrane. A previous study showed that Otolin-1 is present in a significantly higher level in serum samples of patients with benign paroxysmal positional vertigo (BBPV) compared to healthy patients. Menières disease leads to changes in the inner ear volumes and pressure. We therefore hypothesize that significantly increased levels of the protein Otolin-1 can be detected in blood, urine or saliva of patients suffering from Menières disease.

Material and Methods

Ten patients suffering from acute vertigo and diagnosed with Ménière's disease according to the AAO-HNS criteria were included in the present study. The control group consists of 10 subjects without any history of otoneurological disease. Blood, urine and saliva sampling was performed in the morning after at least 12 hours of fasting. All samples were stored at -20 °C until analysis. Detection of Otolin-1 concentration was performed by the use of a highly sensitive ELISA-kit for human Otolin-1.

Results

Otolin-1 was detected in pg/ml range in all collected samples (i.e., urine, saliva and serum). The highest values were detected in saliva whereas the lowest ones were detected in urine. Serum samples of 9 out of 10 patients suffering from Menières disease showed significantly higher Otolin-1 values than control samples (n = 10; $p < 0.001$). There was no significant difference in the saliva or urine concentrations of Otolin-1 between patients of the Menière (n = 10) and of the control group (n=10).

Conclusion

Our results indicate that Otolin-1 is present in serum and also in saliva, but rarely in urine of patients with the Menières disease and controls. The highly significant difference in serum samples of Menière patients and controls seems indicative for a biomarker function of Otolin-1 in the acute state of the Menières disease. However, high levels can also be found in patients with BPPV or increased age. Further investigations in a subset of patients with different otological diseases are necessary to elucidate the role of Otolin-1 in inner ear disorders.

PS 1005

Underlay myringoplasty using high-density collagen sheet in rat

Takenori Miyashita[1]; Shigehisa Aoki[2]; Ai Matsubara[1]; Ryuhei Inamoto[1]; Shinjiro Fukuda[1]; Nozomu Mori[1]; Toshiaki Takezawa[3]; Hiroshi Hoshikawa[1]
[1]Department of Otolaryngology, Faculty of Medicine, Kagawa University; [2]Department of Pathology and Microbiology, Faculty of Medicine, Saga University; [3]Division of Animal Sciences, National Institute of Agrobiological Sciences

Background Tympanic membrane perforation is one of the common aural diseases, and causes conductive hearing loss. The gold standard treatment is myringoplasty (type 1 tympanoplasty). Myringoplasty applies a graft as a scaffold to tympanic perforation. The graft should be applied to the middle ear side of tympanic per-

foration, because on the external auditory canal side, epithelial cell migration may extrude the attached graft. In human myringoplasty, this underlay graft applying technique is widely used but there is no animal model of underlay myringoplasty. Therefore we developed the underlay myringoplasty rat model and evaluated a new high-density collagen sheet as a graft for myringoplasty. Method Ten Sprague-Dawley rats were anesthetized with isoflurane (4% induction and 2-3% maintenance). On the posterior half area of each side of eardrums, a perforation was made with the original instrument for myringotomy. A piece of high-density collagen sheet was placed on the perforated eardrums of 10 ears using the underlay procedure. The other 10 ears was left untreated as the control. After 7 days, all rats were deeply anesthetized and decapitated. The temporal bones were removed. The tympanic membrane of bilateral sides, including the malleus and the bony annulus, were dissected carefully under stereomicroscopy. The samples were fixed in 4% PFA in PBS for 8 h at 4°C. The tympanic membrane was observed with a stereomicroscope and fluorescence microscope to evaluate the residual perforation size. Then the samples were decalcified in 0.12 M EDTA and embedded in paraffin. HE staining and immunohistochemical analysis was subsequently performed on the deparaffinized sections. Results All 10 ears of control perforation were not closed in 7 days and the average size in the residual perforation of the control group was 0.52± 0.24 mm2. The average size in the residual perforation of high-density collagen sheet treatment group was 0.070± 0.086 mm2. The size of the residual perforation of high-density collagen sheet treatment group was significantly smaller than that in the control group. Conclusion We successfully developed the underlay myringoplasty rat model and evaluated the new high-density collagen sheet as a graft for myringoplasty. The high-density collagen sheet was useful for underlay myringoplasty and effective for regeneration of the tympanic membrane. This new high-density collagen sheet is one of the ideal material for the graft of myringoplasty and tympanic membrane regeneration.

PS 1006

microRNA Profiling in Human Inner Ear Perilymph

Matthew Shew[1]; Athanasia Warnecke[2]; Thomas Lenarz[2]; Sumedha Gunewardena[3]; **Hinrich Staecker**[4]
[1]Department of Otolaryngology, University of Kansas School of Medicine; [2]Department of Otolaryngology, Hannover Medical School, Germany and DFG Cluster of Excellence Hearing4all; [3]Department of Molecular and Integrative Physiology, University of Kansas School of Medicine; [4]Department of Otolaryngology , University of Kansas School of Medicine

Objective

Hearing loss is common and caused by a wide range of molecular and cellular pathologies. Diagnosis of hearing loss depends of a combination of physiologic testing, patient history and in some cases genetic testing. No biopsy or equivalent procedure exists to diagnose inner ear disorders. MicroRNAs are short ribonucleic acids that regulate a variety of cellular processes. They have been found to be reliable markers for a variety of disease processes. In particular, a variety of miRNAs that are markers for neurodegenerative disease have been identified in cerebrospinal fluid. The goal of this study was to determine if miRNA populations could be identified in human perilymph.

Study design

Prospective sampling and analysis

Subjects and Methods

Patients undergoing surgery in which the inner ear is opened as part of the procedure (cochlear implantation, stapedectomy, labyrinthectomy) were recruited. Two to 5 ml of perilymph was collected and analyzed using Affymetrix GeneChip miRNA 4.0 microarrays. A functional analysis of significant miRNAs was done using the IPA Ingenuity software package.

Results

miRNAs could be isolated from the inner ear fluid of all patients. Evaluation of miRNAs demonstrated the presence of miRNA populations that are predicted to interact with genes expressed in the inner ear. Additional analysis of miRNA populations demonstrated that perilymph miRNAs could be linked to pathways associated with hearing disorders

Conclusion

Sampling of human perilymph is feasible and can potentially identify miRNAs associated with hearing disorders

Bioinformatic analysis of the human inner ear: presence of BDNF-regulated proteins in human perilymph and their correlation to audiophysiological data

Athanasia Warnecke[1]; Ines deVries[2]; Thomas Lenarz[1]; Nils Prenzler[2]; Martin Durisin[2]; Heike Schmitt[3]; Hinrich Staecker[4]
[1]*Department of Otolaryngology, Hannover Medical School, Germany and DFG Cluster of Excellence Hearing4all;* [2]*Department of Otolaryngology, Hannover Medical School, Germany;* [3]*Cluster of Excellence of the German Research Foundation (DFG; "Deutsche Forschungsgemeinschaft") "Hearing4all".;* [4]*Department of Otolaryngology , University of Kansas School of Medicine*

Despite improvements in implant design, cochlear implant outcomes are still variable. Among the factors that can influence outcomes, the functional quality and integrity of the peripheral auditory system seem to be an important measure. Due to the fact of limited in-vivo access to the cochlea, most causes of inner ear disorders are unknown or poorly understood. Accessing the cochlea during implantation opens a possibility for investigating molecular pathology of the inner ear and potentially increases our understanding of cochlear implant outcomes. The neurotrophin brain-derived neurotrophic factor (BDNF) has been implicated with the function of the auditory nerve at least in experimental settings. However, nothing is known about the role of BDNF and about the proteins regulated by this neurotrophin in the human inner ear. Proteomics of human perilymph obtained during surgery and the human transcriptome of surgical specimen of the inner ear were analyzed with respect to BDNF and the regulated proteins. Ingenuity pathway analysis delineated putative intracellular pathways connected to BDNF and Trk signaling. The obtained results were correlated to the patients' audiophysiological data following cochlea implantation. Initial proof was achieved that bioinformatics analysis may aid in the identification of predictive factors for cochlear implant performance. Additionally, this approach offers new possibilities for identification of patients in need of additional biological intervention in order to support the state of the auditory nerve

Comparison of the Perfusates for Underwater Endoscopic Ear Surgery in Guinea Pig Model.

Daisuke Yamauchi; Yohei Honkura; Yosuke Hara; Kazuya Arakawa; Hiroshi Hidaka; Yukio Katori
Department of Otolaryngology-Head and Neck Surgery, Tohoku University Graduate School of Medicine

Background
Preservation of inner ear function is always a priority for ear surgeons in difficult cases such as cholesteatoma with labyrinthine fistula, superior semicircular canal dehiscence syndrome (SCDS) and petrous apex lesions, for which a trans-labyrinth approach is recommended. Furthermore, cochlear implantation, especially electro-acoustic stimulation (EAS), has recently been encouraged for preservation of inner ear structure and residual hearing. Ideal surgical techniques for inner ear preservation have been a topic of debate, and require a logically based and thorough understanding of local anatomy and physiology. We have clinically previously proposed "underwater" endoscopic ear surgery (UWEES) as a novel technique for treatment of inner ear conditions. This technique yields a clear operative field without the need for suction, and protects the inner ear from unexpected aeration that may impair its function. Initially saline was used for perfusate but which kind of solution is most suitable for UWEES has not been investigated yet.

Methods
Female Hartley guinea pigs (total nine ears) were divided into three groups and UWEES was performed for each with saline, UromaticS (Baxter) and artificial cerebrospinal fluid (ARTCEREB, Otsuka). All animals were anesthetized with an intraperitoneal injection of ketamine and xylazine and were measured auditory brainstem response (ABR) before and after UWEES. The middle ear was opened by dorsal approach. Then the vestibule was opened and both the utricle and the saccule were excised and plugged with bone wax by UWEES. An Endosheath (KOKEN) covering a 0-degree, 2.7-mm-diameter high-definition endoscope (Storz) was used for UWEES.

Results
In UromaticS group, the ABR threshold was significantly higher after surgery. In saline group, the ABR threshold was also significantly higher after surgery but not so much as UromatisS group. In artificial cerebrospinal fluid group, the ABR threshold was not significantly changed after surgery.

Conclusions
The artificial cerebrospinal fluid is likely suitable for UWEES to preserve hearing in acute animal experiment.

PS 1009

ATP-purinergic receptor P2X2 null mice have no hearing loss but diminish the regulation of active cochlear amplification

Yan Zhu[1]; Hong-Bo Zhao[2]

[1].University of Kentucky Medical Center; [2]1. University of Kentucky Medical Center

Background

ATP purinergic receptor P2X2 mutations can induce nonsyndromic hearing loss (DFNA41), indicating that ATP-purinergic signaling has a critical role in hearing. P2X2 predominantly expresses in the cochlea including outer hair cells (OHCs) and other cochlear structures. In our previous studies, we reported that ATP can activate P2X receptors to mediate OHC electromotility (Zhao et al., PNAS, 102: 18724-18729, 2005; Yu and Zhao, Eur J Physiol, 457: 453-461, 2008), gap junctional coupling between supporting cells, and K+-sinking in cochlear supporting cells (Zhu and Zhao, Purinergic Signal. 6: 221-229, 2010; Biochem Biophys Res Commun. 426: 528-532, 2012). In this study, we have further investigated ATP-purinergic hearing function by use of P2X2 null mice.

Methods

P2X2 null mice were purchased from Jackson Lab (Stack No: 004603). ABR threshold, DPOAE, and cochlear microphonics (CM) were recorded to assess cochlear and hearing function. Wild-type (WT) littermates were used as control.

Results

We found that ABR thresholds in P2X2 KO mice had no significant difference in comparison with WT mice. However, the regulation of the active cochlear amplification gain in P2X2 KO mice was diminished. In comparison with WT mice, the gain of DPOAE in P2X2 KO mice was not reduced as sound stimulation levels increased. For exposure to moderate levels of noise, both WT and P2X2 KO mice had similar initial temporary threshold shift (TTS). However, P2X2 KO mice showed less recovery in comparison with WT mice, or even had no any recovery.

Conclusions

P2X2 null mice have no apparent hearing loss under normal conditions but diminish the regulation of active cochlear amplification, thereby increasing susceptibility to noise stress. Supported by NIH R56 DC 015019

PS 1010

The regulation of ER stress-induced autophagy through XBP1-FoxO1 interaction in auditory cells

Akihiro Kishino[1]; Ken Hayashi[2]; Chiaki Hidai[1]; Yasuyuki Nomura[1]; Takeshi Oshima[1]

[1]Nihon University School of Medicine; [2]Kamio Memorial Hospital

Background

Endoplasmic Reticulum (ER) stress is caused by the accumulation of unfolded proteins in ER lumen and induces an adaptive mechanism known as Unfolded Protein Response (UPR). UPR failure results in cell death. Recent findings indicated that ER stress was involved in the pathogenesis of sensorineural hearing loss or age-related hearing loss. XBP1 is a key transcriptional regulator of the UPR. IRE1α-mediated XBP1 mRNA splicing has been found to induce autophagy to alleviate ER stress. In addition, FoxO1 is also involved in the induction of autophagy. Several reports demonstrated the potential interaction of FoxO1 with XBP1. However, the correlation of UPR and autophagy under ER stress remains unclear in auditory cells. The purpose of this study was to clarify the crosstalk among XBP1, FoxO1 and autophagy in the auditory cells under ER stress.

Methods

HEI-OC1 was used as an auditory cell line. Tunicamycin was used as an ER stress inducer. The cell viability was determined by cell viability assays. Western blot analysis, co-immunoprecipitation and RT-PCR were performed. TEM was performed to analyze ultrastructure of cells. siRNA was transfected into cells by lipofection.

Results

We report that ER stress induced by tunicamycin treatment resulted in IRE1α-mediated XBP1 mRNA splicing and autophagy. XBP1 mRNA splicing and FoxO1 were involved in ER stress-induced autophagy, based on the observation that the expression of LC3-II was suppressed by knockdown of IRE1α, XBP1 and FoxO1. In addition, XBP1u interacts with XBP1s in auditory cells under ER stress, functioning as a negative feedback regulator based on the following three important findings; (1) There was a significant inverse correlation between XBP1u and XBP1s expression, (2) The expression of protein XBP1 showed different dynamic state as compared with the level of XBP1 mRNA, and (3) There was the direct physical interaction between XBP1u and XBP1s. Furthermore, our results regarding the relationship among XBP1 and FoxO1 by siRNA paradoxically showed that XBP1 negatively regulated FoxO1 expression.

Conclusion

Our findings suggested that the interaction of XBP1 and FoxO1 regulates ER stress-induced autophagy which serves as a cell survival mechanism in auditory cells.

PS 1011

Role of Bcl6 in Hair Cell Maintenance and Survival

Seth Morrill; Huizhan Liu; David Z. He
Creighton University

Although inner and outer hair cells (IHCs and OHCs) of the inner ear are both vulnerable to noise and ototoxic drugs, IHCs are less susceptible to those insults. The molecular mechanisms of such differential vulnerability are unknown. Hair cell-specific transcriptome analysis shows that Bcl6, a known anti-apoptotic gene, is differentially expressed in IHCs compared to OHC with an 3 fold difference. We hypothesize that higher expression of Bcl6 in IHCs contributes to relative resilience of IHCs to ototoxic and mechanical assault. Here, we examine the role of Bcl6 on survival and differential vulnerability of IHCs and OHCs using a Bcl6 conditional knockout mouse model generated by mating the B6.Cg-Tg(Atoh1-cre)1Bfri/J mouse line with the B6.129S(FVB)-Bcl6 [tm1.1Dent]/J from Jackson Labs. Exons 7-9 were deleted from the Bcl6 gene. Auditory Brainstem Response(ABR)-based thresholds were determined using tone pips with frequencies between 4-50 kHz in homozygous, heterozygous, and wild type littermate mice at 1 and 3 months of age. The cochlear microphonic and endocochlear potential were also measured. Hair cell survival and morphology from the three cochlear locations (representing apical, middle and basal turns of the cochlea) were examined using confocal microscopy. A diminished hearing threshold and loss of hair cells, especially IHCs, would suggest that Bcl6 is necessary for hair cell maintenance and survival. Two lines of future work are currently under way: 1) assessing changes in gene expression (transcriptomes) and identification of downstream targets of Bcl6 in hair cells using hair cells isolated and collected from three genotypes, and 2) applying mechanical and ototoxic insult to mice to determine whether loss of function due to Bcl6 deletion would make IHCs equally vulnerable to noise and ototoxic insults.

PS 1012

FISHing for a New Method to Quantify mRNA in the Mouse Cochlea

Pezhman Salehi[1]; Charlie Nelson[1]; Yingying Chen[1]; Jianxin Bao[2]
[1]NEOMED; [2]Northeast Ohio Medical University (NEOMED)

Quantitative analysis of gene expression is essential to understanding key biological mechanisms and discovering the biomarkers for diseases. Real-time quantitative PCR (RT-qPCR) is an effective method for measuring RNA transcript expression, but this technique can';t be used for tissues composed of multiple cell types.

Single-molecule fluorescence in situ hybridization (smFISH) is an emerging technique used to achieve quantitative, morphological visualization of single mRNA transcripts at high resolution among different tissue types. Until now, smFISH has not been successfully performed in murine cochlear tissue samples because target RNAs are easily degraded and staining-induced background artifacts are substantially increased. This technique employs multiple single-stranded short 20 base pairs long DNA probes to target multiple regions of the same mRNA transcript.

We have successfully performed smFISH in tandem with immunohistochemistry of mouse cochleae and demonstrated the sensitivity and specificity of RNA transcripts to distinct regions of the auditory system, including spiral ganglion neurons (SGNs) and the inner and outer hair cells of the organ of Corti. A combined manual segmentation of an SGN marker and an automated transcript analysis were used to quantify individual RNAs and localize them to specific cells in a cross-section of the cochlea.

This study introduces a unique opportunity to analyze gene expression at the cellular and subcellular levels in murine cochlea.

PS 1013
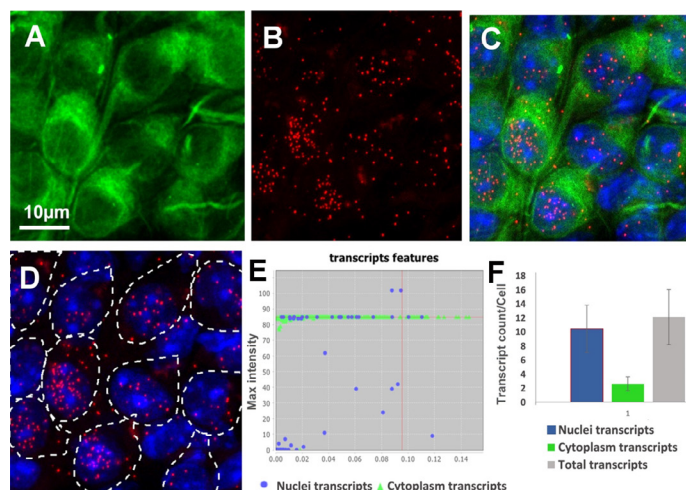
Postsynaptic Density Proteins in the Inner Hair Cell Afferent Synapses

Daniel Reijntjes; Sonja Pyott; Nick Schubert
University Medical Center Groningen

Background

In the central nervous system (CNS), interactions between glutamate receptors and other components of the postsynaptic density (PSD) govern glutamate receptor cycling, scaling of synaptic strength, and excitotoxic damage of glutamatergic synapses. Similar interactions likely occur at glutamatergic synapses between the inner hair cells and spiral ganglion neurons in the cochlea. The extent to which these interactions occur and the degree to which they are specialized at afferent PSDs in the organ of Corti are not known, largely because little is known about the molecular composition of these PSDs, especially in comparison to those of the CNS. Therefore, we applied transcriptomics, immunofluorescence and quatitative image analysis to investigate the similarity between the PSDs in the CNS and organ of Corti.

Methods

Organs of Corti and cerebellums of six week old C57BL/6 mice were dissected for RNA extraction. RNA was processed to c-DNA and further prepared for Lexogen RNA sequencing. A shortlist of 136 genes encoding known PSD proteins in the CNS was created with a focus on proteins involved in glutamate receptor function and/or clustering. Expression of genes and fold-changes in expression were compared between the two tissues. For several proteins of interest, immunofluorescent labeling was performed and immunovolume size assessed using confocal microscopy and quantitative image analysis.

Results and Conclusions

For the 136 genes examined, 93% were expressed in both the CNS and organ of Corti. This suggests a similar structural composition of PSDs in both tissues. Analysis of fluorescently labeled images confirmed the expression of several PSD proteins in the afferent PSDs. The 7% unshared genes do not suggest specific functional differences. Examination of fold-changes in expression indicate the highest dissimilarity in the genes encoding glutamate receptors. Of these genes, the genes encoding GluA2 and GluA3 are the most abundantly expressed in the organ of Corti, followed by lower expression of the gene encoding GluA4 and low/no expression of the gene encoding GluA1. The genes encoding for the NMDA beta/gamma/delta subunits, kainate receptors, and metabotropic glutamate receptors are lowly expressed except for those encoding GluK4/5 and mGluR7/8. These results support previous work that calcium impermeable glutamate receptors consisting of the GluA2 and GluA3 subunits dominate afferent PSDs, and the recent finding of calcium permeable GluA3/GluA4 glutamate receptors. The overall high similarity in PSDs with the exception of the glutamate receptors suggests a functional redundancy in the glutamate receptors with subtle specific advantages for the afferent signaling complex.

PS 1014

Optical tissue clearing of the temporal bone: Application to LacZ reporter transgenic mice

Rebecca Cook[1]; Arnaud Giese[2]; Zubair Ahmed[2]; Tomoko Makishima[3]
[1]*University of Texas Medical Branch;* [2]*University of Maryland Baltimore;* [3]*Department of Otolaryngology, University of Texas Medical Branch*

The inner ear is difficult to study due to its organs being encapsulated within a small, hard, boney shell. Tissue clearing techniques enable whole organs to be studied without tedious manipulation. While many different organs have been successfully cleared, bone is one of the most difficult to process. Another challenge is the choice of labeling method for the cells of interest. LacZ reporters are widely used in transgenic mice and result in strong blue colorimetric labeling of cells when processed with the substrate Xgal. Compared to fluorescent labeling, Xgal colorimetric labeling is more stable lasting for months. Therefore, our goal was to utilize Xgal colorimetric labeling in combination with tissue clearing methods to obtain long-lasting stable temporal bone samples. We modified clearing protocols for use in the mouse temporal bone.

Temporal bones of wild type C57BL6J and transgenic CIB2 mice were used (age ≤ P30). In CIB2 mice, the LacZ reporter is expressed in inner ear hair cells in both the cochlea and the vestibule.

The whole temporal bone was dissected, processed for Xgal labeling, fixed and decalcified. Then they were cleared by incubating in a series of tissue clearing solutions. We tested protocols: SeeDB, ScaleS, and Visikol. Imaging was obtained using Zeiss Lightsheet Z.1 system with 5x objective lens. Evaluation of the temporal bones was done by light microscopy to produce 2D images as well as light sheet microscopy along with the Imaris software to obtain 3D reconstructions.

We were successful in clearing the mouse temporal bone and imaging by light microscopy as well as the light sheet microscopy. We found Xgal labeling could be converted to fluorescent signals by applying different wavelength lasers. The signal was strongest when

using the 488 nm wavelength laser for excitation on the whole temporal bone and recorded under the 638 nm wavelength laser.

The LacZ reporter/Xgal labeling system can be successfully used in combination with tissue clearing methods and can be applied to fluorescent labeling, imaging and 3D reconstruction. We hope to use these methods to find the relationship of the inner ear organs as they relate and orient with each other.

PS 1015

Calcium signaling of interdental cells during the critical developmental period of the neonatal mouse cochlea

Thore Schade-Mann[1]; Pauline Schepsky[1]; Jutta Engel[2]; Tobias Eckrich[3]
[1]*Saarland University, Dept. of Biophysics, CIPMM;* [2]*Center for Integrative Physiology and Molecular Medicine (CIPMM) and Department of Biophysics, Saarland University, Homburg, Germany;* [3]*Dept. of Biophysics & CIPMM, Saarland University, Homburg, Germany*

Introduction

The tectorial membrane (TM), an acellular structure consisting of collagens and the glycoproteins α- and β-tectorin and otogelin, is essential for normal hearing. It stretches between the spiral limbus and the sterocilia of the outer hair cells along the longitudinal axis of the cochlea. During the first postnatal week, interdental cells (IDCs) of the spiral limbus and presumably inner supporting cells of Kolliker';s organ secrete TM proteins into the endolymphatic space. So far, little is known about the physiology of IDCs and how they contribute to the generation of the TM.

Methods

Ca^{2+} imaging experiments were performed using acutely dissected explants of the organ of Corti from mice at postnatal day 1 (P1) to P18. Apical or medial turns were incubated with the Ca^{2+} indicator Fluo-8 AM, washed and imaged with a confocal laser scanning microscope (Zeiss LSM 710). Specimens were bathed with standard buffer or were superfused with buffer containing either ATP or UTP at 1 – 10 μM.

Results

Neonatal IDCs generated different types of spontaneous calcium signals at low frequencies (interspike intervals ≥ 100 s). These were (i) Ca^{2+} transients with a fast upstroke and fast mono-exponential decay and (ii) longer signals with a fast upstroke and a prolonged, complex decay. All Ca^{2+} signals were confined to single IDCs and did not propagate. Before the onset of hearing, stimulation by both ATP and UTP lead to robust intracellular calcium oscillations in IDCs at concentrations as low as 1 μM. This response fundamentally changed after the onset of hearing.

Conclusion

IDCs generated spontaneous and evoked Ca^{2+} signals that varied in shape and duration as a function of age. Differential responses to ATP/UTP suggest a change in purinergic receptor expression during postnatal development. Whether IDC Ca^{2+} signals contribute to the formation of the tectorial membrane requires further studies.

PS 1016

Expression pattern of SOD1(Cu/Zn SOD) in the cochlea of common marmoset (Callithrix jacchus)

Kento Kasuya[1]; Makoto Hosoya[1]; Saeko Matuzaki[1]; Hideyuki Okano[2]; Masato Fujioka[1]; Kaoru Ogawa[3]
[1]*Department of Otolaryngology, Head and Neck Surgery, School of Medicine, Keio University;* [2]*Department of Physiology, School of Medicine, Keio University;* [3]*Department of Otolaryngology, Head and Neck Surgery, Keio University School of Medicine*

Oxidative stress and free radical production have been shown to contribute to deafness, including age-related hearing loss (AHL) or noise-induced hearing loss (NIHL). Normal cellular respiration results in the production of highly toxic superoxide radicals that damage cells if they are not quickly eliminated. SOD1 is one of three human superoxide dismutases. It is said that SOD1(Cu/Zn SOD), coded by the Sod1 gene, is abundantly expressed in the cochlea and plays a key role in reducing oxidative stress that have been shown to contribute to AHL. A study of $Sod1^{-/-}$ mice showed that the absence of SOD1 resulted in hearing loss at an earlier age than in wild-type mice.

We have been investigating the cochlea of a non-human primate common marmoset, because this species has similar basic morphology and gene expressions to those of human. Our previous results revealed discrepancies of gene expression patterns in between primates and rodents. Here, we examined expression of SOD1 protein by immunohistochemistry in cochleae of common marmoset.

Materials and Methods

We performed immunohistochemical analysis of adult common marmoset (N=4) cochlea with an SOD1-specific antibody (ab52950 , abcam , 1 : 200).

Results

In the marmoset cochlea, SOD1 immunoreactivity was observed in the stria vascularis (marginal cells, intermediate cells and basal cells), spiral ganglion neurons, supporting cells including inner and outer piller cells, Deiter';s cells and Hensen cells. Weakly immunoreactivity was observed in spiral ligament. No immunoreactivity was observed in outer and inner hair cells, Reissner';s membrane and the other supporting cells. There was no difference in the expression pattern between the basal and the apical cochlear turns.

Discussion

Although oxidative stress is known as a critical element especially in the hair cell survival, there were no report showing detailed pattern of Sod1 in the Organ of Corti, except one showing negative expression in all hair cells and supporting cells (Park et al, 2017). In our presenting result in a primate, immunoreactivity for SOD1 was observed in the supporting cells within Organ of Corti but no expression was observed in hair cells. Recent studies revealed that the polymorphisms of SOD1 associated either with AHL (Kitoh R, 2016) or with NIHL (Liu YM, 2010; Li SD,2011) in human. Taken together, further study of primate supporting cells and lateral wall cells should be awaited to understand the relations of SOD1 and hearing loss.

PS 1017

Functional Characterization of Glial P2X7 Receptors in the Rat Cochlea

Silvia Prades; Gregory Heard; Katie Smith; Jonathan Gale; Dan Jagger
UCL Ear Institute

The auditory nerve transmits acoustic signals from cochlear hair cells to the brain. The spiral ganglion neurons (SGNs) forming the primary afferent pathway may be reliant on glial cells for their long-term survival, but their interactions remain largely uncharacterized. Purinergic signaling is recognized as a regulator of auditory nerve physiology, following the detection of various P2X and P2Y receptors, and demonstration of neuronal ionotropic and metabotropic responses. Here, we examined P2X7 receptors (P2X7Rs) as potential mediators of cochlear neuro-glial communication.

In rat cochlear vibratome sections, P2X7R immunofluorescence was first detected at postnatal day 6 (P6) in Schwann cells wrapping SGN peripheral neurites and in satellite cells surrounding the SGN cells bodies, but not in oligodendrocytes in the central portion of the auditory nerve within the cochlear modiolus. This expression pattern was conserved through to adulthood. Elsewhere in the peripheral nervous system P2X7Rs are non-selectively permeable to small cations when stimulated transiently, but during prolonged agonist exposure there is an increased permeability to larger cationic molecules up to 1kDa (e.g. dyes). To investigate the properties of P2X7Rs in cochlear glia, we prepared dissociated spiral ganglion cultures from juvenile hearing rats (P13-14) for electrophysiology or dye uptake experiments. P2X7Rs were stimulated using BzATP (10μM) and blocked by the specific antagonist A-740003 (100nM). Patch clamp recordings demonstrated BzATP-activated currents that increased in magnitude with prolonged exposure time, and that were inhibited by A-740003. BzATP activated rapid YOPRO-1 uptake into glia during time series confocal imaging, but BzATP-mediated YOPRO-1 uptake was prevented by pre-incubation of A-740003. Where an SGN and its satellite cell remained paired, BzATP-mediated YOPRO-1 uptake could be detected only within the satellite cell.

The present study demonstrates functional expression of P2X7Rs in glial cells within the peripheral portion of the auditory nerve, raising the possibility that these enigmatic ion channels play roles in cochlear neuro-glial communication. We suggest that P2XRs may act as sensors of tissue stress during periods of damaging noise or ischemia.

PS 1018

Identifying novel calcium signalling pathways in the mammalian cochlea

Fraser Todd[1]; Charlotte Brown[1]; Andrei Lukashkin[2]; **Snezana Levic**[3]
[1]*Brighton and Sussex Medical School;* [2]*University of Brighton, UK;* [3]*Brighton and Sussex Medical School, University of Sussex; University of Brighton*

Calcium ions (Ca^{2+}) are fundamental to the most important roles in sensory processing played by vertebrate hair cells (HCs), including those of the mammalian cochlea, (Organ of Corti, (OC)), such as mechano-transduction, synaptic release and frequency selectivity. The remarkable capability of hair cells as mechanoelectrical signal transducers relies on tightly regulated intra and extracellular Ca^{2+} microdomains.Therefore in addition to $[Ca^{2+}]_{int}$, $[Ca^{2+}]_{ext}$ levels could play important roles at the apical domain in regulating mechanosensory adaptation and at the basal domain for controlling synaptic transmission, spontaneous electrical activity during development and frequency tuning.

The main objective of this work is to discover the localization and function of Ca^{2+}-sensitive receptor (CaSR) signalling pathway, that we recently identified in the OC. CaSR is a G-protein coupled receptor (GPCR) involved in calcium homeostasis in vertebrates by monitoring extracellular levels of Ca^{2+} ($[Ca^{2+}]_{ext}$) and responding to a wide range of stimuli. Several inherited disorders of systemic Ca^{2+} homeostasis result from mutations in the gene for the CaSR. CaSR mutations often alter the sensitivity of the expressed receptor protein to extracellular Ca^{2+}, affecting pathways known to be necessary for normal hearing. This is the first report identifying the presence, location and function of the CaSR in Ca^{2+} signalling and maintaining Ca^{2+} homeostasis in the OC.

We employ immunohistochemical and electrophysiological techniques using acutely isolated OC to assess the expression pattern and the role of CaSR in the sensory epithelium. We show that CaSR is widely expressed in the mammalian cochlea, including apical domain of OHCs, basal domain of IHCs, supporting cells, spiral ganglion neurons, fibrocytes and the cells of stria vascularis. We also report the effects of CaSR on biophysical properties of cells identified to express CaSR.

Functional alterations in CaSR should have profound consequences on the OC development and function, including altered intracellular $[Ca^{2+}]_{int}$ handling, expression of ion channels, altered synaptogenesis and electromechanical coupling, leading to compromised hearing function. This knowledge is fundamental to understanding the mechanisms responsible for the sensitive, finely tuned, acoustical, mechanical and electrical responses of the mammalian cochlea.

PS 1019

Expression pattern of EYA4 in the common marmoset (Callithrix jacchus) cochlea

Saeko Matuzaki[1]; Makoto Hosoya[1]; Hideyuki Okano[2]; Masato Fujioka[1]; Kaoru Ogawa[3]
[1]Department of Otolaryngology, Head and Neck Surgery, School of Medicine, Keio University; [2]Department of Physiology, School of Medicine, Keio University; [3]Department of Otolaryngology, Head and Neck Surgery, Keio University School of Medicine

The eyes absent (EYA)-like genes are essential for the formation of sensory organs among fly (Drosophila melanogaster) and mammals. EYA4, one of the vertebrate genes of Eya family, is reported to be causative for late-onset mid-frequency sensorineural hearing loss in humans. EYA4 was mapped to chromosomes 6q22.3–q23.2 and it encodes a 639-amino-acid protein called the EYA4 protein. Mammalian EYA proteins translocate into the nucleus in association with members of the sine oculis homeobox (SIX) family of transcription factors. While Eya4-deficient mice exhibited congenital profound deafness and otitis media with effusion due to the eustachian tube dysmorphology. Because of the species difference in the phenotype, the pathophysiology of EYA4 in the human cochlea has yet to be elucidated. Here, we examine the expression pattern of EYA4 in the cochlea of common marmoset (Callithrix jacchus), a non-human primate. In the marmoset cochlea, EYA4 immunoreactivity was observed in spiral ganglion neurons, inner/outer hair cells, all supporting cells including the Deiters';, Hensen';s, and Claudius cells, inner/outer pillar cells, and inner/outer sulcus cells. No immunoreactivity was observed in the stria vascularis, lateral wall fibrocytes, and Reissner';s membrane. There was no difference in the pattern of expressions among the turns of the cochlear spiral. Furthermore, our results revealed an EYA4-SIX1 co-localization in the cells of the organ of Corti including the inner/outer hair cells, supporting cells and the spiral ganglion neurons. The expression pattern of EYA4 in the adult marmoset cochleae was different from the mouse cochlear expression pattern. Interestingly, EYA4 expression in the auditory hair cells and neurons was co-localized with sine oculis homeobox–SIX1, a transcription factor essential for the transcriptional activity of EYA4. The expression pattern of EYA4 in the adult marmoset cochleae was different from the mouse cochlear expression pattern; .In rodents, it has been previously reported, using in situ hybridization, that Eya4 is expressed in the early stage of the otic vesicle, mostly restricted to the upper cochlear duct within cells that develop into the stria vascularis and Reissner';s membrane, and eventually to spiral limbus, organ of Corti, and spiral prominence. A reproduce testing with an immunohistochemistry of ours also showed the same tendency: Expression in the supporting cells were narrower and weaker as the age develops to adult, which was quite different from those in In contrast with these findings in rodents, our present results revealed the expression of EYA4 in several different parts of the adult marmoset cochlea. The inter-species differences in the expression pattern of EYA4 gene between primates and rodents suggestsalso indicated a fundamental role of EYA4 in the primate auditory cochleacells. (Experiments with primate models such as marmosets or with human cochlear cells may provide cues about the unknown pathogenesis of EYA4-related hearing loss.)

Acetylcholine Evoked Calcium Modulation in Crista Hair cells and Afferents in a GAD2-Cre GCaMP5G Transgenic Mouse

Holly A. Holman[1]; Lauren Poppi[2]; Micah Frerck[1]; **Richard D. Rabbitt**[1]
[1]University of Utah; [2]University of Newcastle

Background
The efferent neurotransmitter acetylcholine (ACh) acts on vestibular hair cells and afferents by activating nicotinic (nAChR) and/or muscarinic (mAChR) receptors, both of which modulate intracellular $[Ca^{2+}]$ in postsynaptic targets. The present study examined ACh evoked $[Ca^{2+}]$ responses in a subset of hair cells and afferent neurons in the crista using the fluorescent calcium indicator GCaMP, with expression driven by GAD2-Cre. The GAD2 gene encodes an isoform of glutamate decarboxylase, GAD65 that catalyses the decarboxylation of glutamate to the neurotransmitter GABA. Driving floxed expression with GAD2-Cre provides a means to examine GABA positive targets of ACh in the inner ear.

Methods
Transgenic mice used for this study express the Ca^{2+} reporter GCaMP5G along with an identifying marker td-Tomato (G5-tdT) under the CAG promoter in cells containing GAD2-IRES-Cre. Expression patterns and $[Ca^{2+}]$ transients were imaged in excised cristae of P1-mature mice. For immunohistochemistry, semicircular canals were fixed, blocked and reacted with different primary antibodies, including calretinin, ChAT, GABA, GAD65, and myosinVIIa, and imaged using a confocal microscope. For live cell GCaMP $[Ca^{2+}]$ imaging, the anterior crista, horizontal crista and utricle were dissected, overlying epithelial membrane was excised, and organs were secured in a recording chamber continuously perfused and imaged with a swept field confocal microscope. GCaMP5G was excited at 488 nm and fluorescence responses were imaged at 10-20 s^{-1} following 0.5-2s puffs of 1mM ACh.

Results
G5-tdT expression in cristae was predominantly in a subset of type I hair cells (type 1g), and a subset of newly identified cells (myosinVIIa-negative) in the eminentia cruciatum (EC). Low-level G5-tdT expression was also noted in calyces and neural dendritic fields. G5-tdT allowed for identification of expressing cells and live $[Ca^{2+}]$ imaging in response to ACh. ACh evoked $[Ca^{2+}]$ modulation was observed in type Ig hair cells, afferents, and EC cells. Type Ig hair cells showed decreased GCaMP fluorescence following ACh application, while calyces enveloping the same cells exhibited an increase in GCaMP fluorescence. EC cells exhibited a strong ACh-evoked

GCaMP fluorescence transients that were reversibly blocked by the mAChR antagonist, atropine.

Conclusions
ACh evoked $[Ca^{2+}]$ responses were present in type Ig hair cells, calyx terminals, afferent dendrites and uniquely identified EC cells. Expression of G5-tdT and reactivity against anti-GAD65 antibody in these cells suggests the ACh targets in the present experiments were GABAergic, and reveals potential feedback interactions between these important inner ear transmitters.

CD68 a marker for macrophages in archival human temporal bones comparing the implanted vs. non-implanted sides after cochlear implantation

Ivan Lopez[1]; Gail Ishiyama[2]; Akira Ishiyama[3]
[1]Department of Head & Neck Surgery, Geffen School of Medicine at UCLA; [2]UCLA Department of Neurology; [3]David Geffen School of Medicine, University of California, Los Angeles

Background
The presence of inflammatory cells of the innate immune defense system in the human cochlea following cochlear implantation (CI) is an active field of research. There are prior studies reporting evidence for foreign body stimulating an inflammatory cellular infiltrate. We used antibodies against CD68, a lysosomal membrane marker indicative of phagocytic activity, to identify and localize macrophages in the implanted side and compared results with the contralateral non-implanted side. We also compared results with CD68 immunostaining in normative control archival human temporal bone cochlea from patients with no documented audio vestibular diseases and other auditory disorders including presbycusis.

Methods
Monoclonal antibodies anti- human CD68 were used and immunostaining was visualized using HRP-DAB. Comprehensive analysis of the CD68 positive cells was assessed. Eight human temporal bones with CI and their non-implanted side were immunostained, six cochleas from patients with presbycusis were also evaluated. The presence of melanocytes was also taken into account, by distinguishing the pigmented cells demonstrating greenish color which can be clearly distinguished from dark amber-colored CD-68 immunoreactivity cells.

Results
CD68 immunoreactivity macrophages were detected, and the quantity and regional distribution of CD68+ cells were similar in the CI and the non-implanted side in all

temporal bones examined. There were no CD68+ infiltrations noted in any of the temporal bone specimens. CD68 + cells were present in the three cochlea regions (apical middle and base) specifically with cells in the organ of Corti, the mid-modiolus, implanted site and cells in the stria vascularis with CD68+ cells surrounding the microvasculature in the intermediate zone. The stroma of the macula utricle and saccule also exhibited CD68 + cells.

Conclusions

The results are suggestive that the presence of macrophages in the temporal bones are a part of normal inner ear homeostasis and or a normal response to inner ear pathologies rather than a pathological reaction. In the cochlea with CI, the contralateral non-implanted cochlea, the cochlea from normal aging and from presbycusis, the regional distribution of CD68+ macrophages is relatively similar, implicating that these macrophages are responsible to maintain normal inner ear homeostasis.

Support

PS 1022

PECAM-1 immunoreactivity in the blood vessels of the human cochlea

Seiji Hosokawa[1]; Kumiko Hosokawa[1]; Gail Ishiyama[2]; Akira Ishiyama[3]; Ivan Lopez[4]
[1]*Hamamatsu University Department of Otorhinolaryngology - Head & Neck Surgery;* [2]*UCLA Department of Neurology;* [3]*David Geffen School of Medicine, University of California, Los Angeles;* [4]*Department of Head & Neck Surgery, Geffen School of Medicine at UCLA*

Introduction

PECAM-1 (platelet/endothelial cell adhesion molecule-1) is a major constituent of the endothelial cell intercellular junction and is widely used as a molecular marker for mature endothelial cells. To the date there are very few studies related to identify the components of the blood labyrinthine barrier (BLB) in the human inner ear. Traditional hematoxylin and eosin staining do not delineate the thin blood vessels of the cochlea. As part of a project related to investigate the components of the BLB in the human inner ear, we used immunohistochemical markers to identify vascular endothelial cells (VECs) in the microvasculature of the human cochlea.

Methods

In this study, we used indirect immunohistochemistry and specific antibodies against human PECAM-1 in for-

malin-fixed celloidin-embedded (FFCE) sections of the human cochlea obtained from temporal bones with no inner ear diseases (n=3), and also with patient diagnosed with different inner ear diseases (n=12). Results: In normal and pathological specimens, PECAM-1-immunoreactivity-(IR) was easily visualize in large size blood vessels (more than 10 microns, cross sectional diameter) located in the mid-modiolar area of the cochlea. In contrast PECAM-1-IR in small blood vessels (less than 10 microns, cross sectional area), was not easily identified. Small size blood vessels were located in the stroma of the spiral ligament, stria vascularis, and vestibular endorgans.

Conclusion

The use of PECAM-1 allows to delineate the blood vessels of the human inner ear in both the cochlea and vestibule. The identification of BLB components in the human inner ear allow to determine the involvement of the microvasculature in different inner ear diseases like Meniere's diseases, normal aging and presbycusis.

Grant Support

PS 1023

Sex Determination of Archival Fixed and Immunolabeled Guinea Pig Cochleas

Frederic F. Depreux; Lyubov Czech; Donna S. Whitlon
Northwestern University

Outbred guinea pigs have been used in research for decades for as models of infection, drug studies, cardiology, receptors and audiology. Some of these studies use measures that, unknown at the time, may be significantly affected by the sex of the animal. For example, recent studies have suggested that males show more hearing loss than females under several conditions. In fact, in recent years, NIH has begun to formally consider sex as a biological variable and has taken steps to try to balance data from male and female animals in preclinical studies. When visual inspection is insufficient (for example in fetal or young postnatal animals), evaluation of the sex of an individual is carried out in various species by PCR amplification of X and Y chromosome specific genes. When tissue is fixed, immunolabeled and archived, genomic DNA extraction and gene PCR amplification are more challenging. Conditions to process cochlear turns for sex typing in general and in guinea pig in particular were absent from the literature. Using our tissue collection archive, we established a protocol for genomic DNA extraction and sex typing of paraformaldehyde fixed, im-

munolabeled and slide-mounted guinea pig cochlear half turns, some as old as 3 years. Using QIAmp DNA FFPE tissue extraction kit, the average amount of genomic DNA extracted from archival fixed cochlea half turn was 173 ± 117 ng for an average half turn surface area of 1.21 ± 0.67 mm2. The amount of genomic DNA extracted was not affected by duration of sample storage. Using various databases, specific primers for dystrophin (X-chromosome) and SRY (Y chromosome) guinea pig genes were designed. The dystrophin detection was immediately successful, but SRY gene amplification required the creation of a degenerative PCR primer set. After PCR amplicon sequencing from unfixed guinea pig pinna and liver tissues, we found that the published guinea pig SRY gene sequence was significantly different from that in our population of guinea pigs. Thus, we have successfully developed a new protocol for sex typing unfixed tissues and fixed, immunolabled, archival tissues from guinea pig that should allow new evaluations of sex differences in auditory physiology from previously completed experiments. Funded by grant #N00014-16-1-2508 from the Office of Naval Research and by the Department of Otolaryngology, Northwestern University.

PS 1024

Change of Hearing Threshold in Apolipoprotein E Knockout Mice Fed High Fat Diet

YooYeon Kim[1]; Harry Jung[1]; Boyoung Kim[1]; Jiwon Chang[2]; Hajin Nam[1]; Jun-Gyo Suh[1]; Jun Ho Lee[3]
[1]Department of Medical Genetics, College of Medicine, Hallym University; [2]Department of Otolaryngology-Head and Neck Surgery, Hallym University College of Medicine; [3]Department of Otorhinolaryngology-Head and Neck Surgery, College of Medicine, Hallym University

In recent years, prevalence of metabolic diseases with hyperlipidemia, atherosclerosis, heart disease, and high blood pressure has been increasing by westernized eating habits and aging. Apolipoprotein E knockout (ApoE KO) mouse is an animal model for hyperlipidemia and atherosclerosis. To investigate the association between hypercholesterolemia and hearing loss, the cholesterol level in the blood and hearing levels were assessed in ApoE KO mice induced hypercholesterolemia. 8-week-old C57BL/6J male mice were fed chow diet; fat, 10% kcal (B6-CD) and ApoE KO male mice were fed chow diet (ApoE KO-CD) or western diet; fat, 40% kcal (ApoE KO-WD) for 16 weeks. Weight-corrected chow monthly intake, total cholesterol (Chol), high-density lipoprotein cholesterol (HDL-Chol), and low-density lipoprotein cholesterol (LDL-Chol) were measured at 0 to 4 months after the diet. Auditory brainstem response (ABR) thresholds were measured for click sound at 2 and 4 months after the diet. After the diet for 4 months, histological analy-

sis of the cochlea was performed in mice. Weight-corrected chow monthly intake was higher in ApoE KO-WD than that in B6-CD and ApoE KO-CD mice groups until 2 months after the diet. Total cholesterol and LDL-Chol were elevated in ApoE KO-CD than those B6-CD, and ApoE KO-WD remarkably increased compared with those B6-CD and ApoE KO-CD at 1 to 4 months after the diet. HDL-Chol was significantly increased in ApoE KO-WD compared with that B6-CD and ApoE KO-CD at 1 to 4 months after the western diet. ABR thresholds of left ear at click sound showed statistically significant increase in ApoE KO-WD at 4 months than that B6-CD and ApoE KO-CD at 4 months after the western diet. Also, histological changes of the cochlea were aggravated in the ApoE KO-WD compared with that B6-CD and ApoE-CD at 4 months after the western diet. Taken together, these results indicate that hypercholesterolemia may cause the hearing loss of left ear in ApoE KO male mice. Therefore, this study suggests that hypercholesterolemia associated with the unilateral hearing loss in ApoE KO male mice.

Inner Ear: Noise-Induced Hearing Loss II

PS 1025

Are Recovery Processes Activated During Longer-Duration TTS-Producing Noise Exposures?

Dan Guo[1]; Albert Edge[2]; John J. Guinan[3]; Sharon G. Kujawa[4]
[1]Eaton-Peabody Laboratories, Massachusetts Eye and Ear Infirmary; and Department of Otology and Laryngology, Harvard Medical School; [2]Harvard Medical School; [3]Massachusetts Eye and Ear Infirmary; [4]Eaton-Peabody Laboratories, Massachusetts Eye and Ear Infirmary and Department of Otolarynology, Harvard Medical School, Boston, Massachusetts

Background Prior work has provided extensive characterization of threshold sensitivity and hair-cell losses as functions of noise exposure energy. This work has informed noise-risk estimates that are incorporated in federal exposure guidelines and regulations. It is now clear that such losses can be preceded by dramatic loss of inner-hair-cell (IHC) synapses with cochlear afferent neurons (synaptopathy), which permanently silences affected fibers. Most synaptopathy observations have been made after exposures producing large (40-50 dB at 24 hr), but temporary, threshold shifts (TTS). Such shifts are arguably excessive compared to much human TTS. Thus, a question with human health importance is whether and how noise-induced cochlear synaptopathy and deafferentation scale with acute threshold loss and the overall energy of the exposures that produce them. Methods Here, we consider noise-induced injury for a series of equal-level, TTS-producing exposures of varying durations delivered to awake, adult CBA/CaJ mice.

The noise, an 8-16 kHz band, had an overall level of 100 dB SPL. We adjusted exposure energy by varying duration, from 7.5 min to 2 hr, and studied outcomes at post-exposure times from <1 hr to 2 wk. Noise-induced pathophysiology was characterized by assaying electro-physiologic and otoacoustic responses, in comparison with unexposed cohorts. For the same ears, we quanti-fied hair cells (OHC, IHC) and IHC-afferent synapses in immunostained cochlear whole mounts at cochlear-frequency locations from 5-64 kHz. Results Depending on frequency, these equal-level exposures produced elevations in both OHC- and neural-based response thresholds ranging from trivial (~5 dB) to large (>50 dB) at 24 h, followed by complete threshold recovery by 2 wk. In tonotopically-relevant regions, shortest-duration exposures unexpectedly produced larger TTS than longer-duration exposures. This outcome suggests hair-cell recovery processes already active during exposures that are non-lethal to hair cells. Importantly, the short-dura-tion exposures that produced large threshold shifts also yielded the smallest IHC synaptic losses, suggesting that OHC injury, by reducing input to the IHCs, reduces consequences of the exposure (perhaps excitotoxic) that instigate the synaptic loss. Conclusions Risk for cochle-ar synaptopathy and deafferentation cannot be directly predicted by the magnitude of temporary noise-induced threshold shifts. The surprising result that less energy applied (by shorter noise duration) yielded more acute injury suggests stimulation-dependent recovery. Beyond informing noise-risk estimates, findings have important implications for efforts to characterize protective vs. re-generative outcomes of cochlear therapeutics. Funding Funding support from DoD W81XWH-15-1-0103 (SGK). DG received support from the Department of Medicine, Henan Medical College.

PS 1026

Darc deficiency ameliorates cochlear damage from noise exposure

Hongzhe Li; Alisa Hetrick; Liana Sargsyan; Bouchra Edderkaoui
VA Loma Linda Healthcare System

Introduction
Cochlear inflammatory response has been increasing-ly studied with various environmental insults, including acoustic and ototoxic overexposures. As the immune response is associated with both pathology and protec-tion, targeting a specific immune component will unravel the interactions between the cellular damage and the inflammatory associated protection and repair in the co-chlea. Duffy antigen receptor for chemokines (Darc) is a member of atypical chemokine receptors, and essential for chemokine-regulated leukocyte/neutrophil traffick-ing during inflammation. Previous studies have report-ed that Darc deficiency alters chemokine bioavailability and leukocyte homeostasis and therefore, led to signifi-cant anti-inflammatory effects post tissue injuries. In this study, we have used Darc knockout mice to determine the impact of gene deficiency in the stressed cochlea.

Methods
Darc-knockout (KO) (Dr. Chaudhuri, New York Blood Center, NY) and control C57Bl/6 (JAX stock #0664) mice were studied. Animals were housed in a Specif-ic Pathogen Free-modified room, without sound treat-ment of ambient noise. Auditory brainstem responses to a broad frequency range, from 4 to 32 kHz, were measured with or without intense noise exposure (112 dB SPL, octave-wide). Posttraumatic hair cell survival and ribbon synapse density were examined. Temporary threshold shifts were introduced by exposing the animal to sustained broad-band noise at 95 dB with closed-field sound delivery under ketamine/xylazine anesthesia. Gene expression changes due to noise exposure was evaluated by Real Time PCR at three time points for both lines of mice.

Results and Conclusion
DARC is not required for normal development of cochle-ar function, as suggested by typical hearing sensitivity in juvenile Darc-KO mice, compared to C57Bl/6 control. Darc-KO mice exhibited improved recovery after intense noise exposure. The ABR threshold shift between Darc and control mice was most evident at one week after noise exposure. At higher frequency cochlear locations, both hair cell survival and ribbon synapse density were improved with Darc deficiency. Furthermore, the mRNA levels of some major inflammatory effectors were re-duced in Darc-KO mice compared to control mice at one and three days post noise exposure. These data suggest Darc-dependent inflammatory response slows down the recovery process, and exacerbates cellular damage in the cochlea post noise exposure. Further research is required to determine the long-term effect of Darc-deficiency under acoustic overexposure, and to identify the degree of inflammatory dependent hearing damage that contributes to the overall hearing deficits by noise exposure, ototoxic compounds or during the aging process.

PS 1027

Hair cell cytotoxicity model of zebrafish lateral line by ultrasonic generator

Yoshinobu Hirose; Kazuma Sugahara; Yosuke Takemoto; Makoto Hashimoto; Hiroshi Yamashita
Department of Otolaryngology, Yamaguchi University Graduate School of Medicine

Introduction

Zebrafish lateral line hair cells are physiologically and morphologically similar to inner ear hair cells. As the zebrafish lateral line is located on the body surface, damage to the hair cells can be rapidly assessed. Therefore, the zebrafish lateral line is an effective system for the evaluation of drugs that damage or protect hair cells. Zebrafish have been used to examine protection from aminoglycosides in hair cells. We have been used to screen protective effect of supplement and herbal medicines drugs.

On the other hand, hair cell damage model with aminoglycoside have some disadvantages (1) drug attenuat the toxicity of neomycin itself, (2) drug inhibits uptake of neomycin into hair cells, (3) neomycin damege model are considered to be different from physiological disorders such as noise-induced deafness. In consideration of the above, we considered physiologically hair cells damege model by sonic models.

Materials and Methods

[Evaluation of used animals and hair cells] 5dpf Zebrafish embryos of the AB wild-type strain were produced by paired mating of adult fish. Anti-parvalbumin was used as a primary antibody, hair cells were immunostained. Hair cells from the SO1, SO2, O1, and OC1 neuromasts were counted with a fluorescent microscope. [Hair cell damage by sound speaker] The 48 plate was placed under the speaker, and the acoustic load was exposed in the octave band noise of 4 kHz center, 130 dB SPL, 3 hours. Larvae were fixed in 4% paraformaldehyde at 48 and 72 hours after the exposure. [Hair cell damage by ultrasonic washing machine] Washing machine (Shimazu Corp, SUS-103, frequency:28, 45, and 100 kHz,100 W) was used. 48 plates was placed in the machine and floated on the water . Exposure time was 5 to 180 minutes and specimens were fixed at 24, 48 and 72 hours after exposure. [Hair cell disorder by ultrasonic generator] Ultrasonic generator (Kaijo, QUAVA mini reactor, frequencies:35, 100, 160 kHz, 1-50W) was used. Condition were (1) 35 kHz, 1-10 W, 30 min (2)100 kHz, 1-10 W, 30-160min, (3)160 kHz, 1-10 W, 30-180 min, and specimens were fixed was 72 hours after the exposure.

Results

[Hair cell damage by sound speaker] At 72 hours after acoustic injury, hair cells were partially damaged.
[Hair cell damage by ultrasonic washing machine] (1) 28 kHz,100 W, 5 min, (2) 28 kHz,100 W, 5 min, larva could not survive. (3)100 kHz, 100 W, 3 h, (4)100 kHz, 100 W, 1h, hair cells were damaged about 20%, but some larva could not survive. These results showed that it was difficult at high power of 100 W. [Hair cell damage by ultrasonic generator] (1) 35 kHz, 10 W, 30 min, hair cells are damaged, but some larva could not survive. (2) 35 kHz, 1 W, 30 min, hair cells (3)100 kHz, 1 and 10 W, 30 to 180 min (4)160 kHz , 1 and 10 W, 30 to 180 min, hair cells were damaged without damage fish.

Conclusions

Zebrafish larva were damaged in low frequency (28-45kHz) with high output(100W). Optimal conditions of hair cell cytotoxicity model by ultrasonic generator are high frequency (100-160kHz) with low output (1-10W).

PS 1028

Macrophages Promote Synaptic Recovery and Neuronal Survival Via Fractalkine Signaling After Noise-Induced Excitotoxicity

Tejbeer Kaur[1]; Kevin Ohlemiller[2]; Anna Clayman[1]; Angela Schrader[1]; Mark Warchol[1]
[1]*Washington University School of Medicine;*
[2]*Department of Otolaryngology-Head and Neck Surgery, Washington University School of Medicine*

Background

Noise-induced excitotoxicity causes rapid and permanent loss of inner hair cell-afferent nerve fiber (IHC-ANF) synapses, followed slowly by death of spiral ganglion neurons (SGNs). Similar forms of excitotoxic injury have been extensively studied in the CNS, where microglia (brain resident macrophages) and fractalkine signaling are important regulators of neuronal survival. Fractalkine (CX_3CL1) is a transmembrane chemokine involved in the adhesion and migration of leukocytes. Fractalkine binds to its exclusive receptor, CX_3CR1, which is expressed by macrophages, microglia and peripheral leukocytes. The role of innate-immune system in cochlear excitotoxicity is unknown. The present study characterized the immune response following noise exposure as well as the function of fractalkine signaling on the recovery of synapses and the survival of SGNs.

Methods

Adult $CX_3CR1^{+/+}$, $CX_3CR1^{GFP/+}$ and $CX_3CR1^{GFP/GFP}$ mice were exposed for 2 hours to an octave band (8-16 kHz) noise at either 90 or 120 dB SPL. The $CX_3CR1^{+/+}$ and $CX_3CR1^{GFP/+}$ line retains fractalkine signaling, while

CX$_3$CR1$^{GFP/GFP}$ lack the fractalkine receptor. ABRs, DPOAEs, ABR wave I amplitudes were characterized prior to noise exposure, immediately after noise exposure, at two weeks recovery, and immediately prior to sacrifice. Temporal bones were fixed and processed for immunohistochemistry to label hair cells, macrophages, neurons or synapses. Animals exposed to ambient noise levels served as controls.

Results

Exposure to 120 dB SPL noise resulted in permanent elevation in hearing thresholds accompanied by afferent nerve fiber degeneration and hair cell loss, while exposure to 90 dB SPL noise caused temporary threshold shifts without any evident hair cell loss. Enhanced macrophage migration towards the IHC-synaptic region was observed immediately after noise exposure, followed by an increase in macrophage density in the spiral ganglion at 1 week post exposure. Synaptic immunolabeling revealed a rapid ~50% loss of synaptic ribbons throughout the basal half of the cochlea. These synapses had recovered by two weeks post exposure in mice with intact CX$_3$CR1. However, CX$_3$CR1knockout mice displayed enhanced synaptic degeneration and IHC damage that correlated with attenuated suprathreshold neural responses at higher frequencies. Finally, lack of fractalkine signaling resulted in enhanced SGN loss after loud noise exposure compared to wild type mice.

Conclusions

Results suggest that chemokine-fractalkine signaling influence synaptic remodeling and afferent neuronal survival after noise-induced hearing loss and that macrophages may play a protective role in cochlear excitotoxicity.

PS 1029

Effects of noise exposure on neonatal auditory brainstem response thresholds in pregnant guinea pigs at gestational periods

Chihiro Morimoto[1]; Nario Kazuhiko[1]; Tadashi Nishimura[2]; Ryota Shimokura[3]; Hiroshi Hosoi[4]; Toshiaki Yamanaka[1]; Tadashi Kitahara[5]
[1]Otolaryngology - Head and Neck Surgery;
[2]Otolaryngology - Head and Neck Surgery, Nara Medical University; [3]Interdisciplinary Graduate School of Science & Engineering; [4]Nara Medical University; [5]Department of Otolaryngology - Head and Neck Surgery, Nara Medical University

Noise exposure during pregnancy has been reported to cause fetal hearing impairment. However, little is known about the effects of noise exposure during various gestational stages on postnatal hearing. In the present study, we investigated the effects of noise exposure on auditory brainstem response (ABR) at the early, mid-, and late gestational periods in newborn guinea pigs.

Pregnant guinea pigs were exposed to 4-kHz pure tone at a 120-dB sound pressure level for 4 h. We divided the animals into four groups as follows: the control, early gestational exposure,mid-gestational exposure, and late gestational exposure groups. ABR thresholds and latencies in newborns were recorded using 1-, 2-, and 4-kHz tone burst on postnatal days 1, 7, 14, and 28. Changes in ABR thresholds and latencies were measured between the 4 × 4 and 4 × 3 factorial groups mentioned above (gestational periods × postnatal days, gestational periods × frequencies).

The thresholds were low in the order of control group < early gestational exposure group < midgestational exposure group and late gestational exposure group. Noise exposure during pregnancy influenced ABR thresholds in neonatal guinea pigs.

This is the first study to show that noise exposure during the early, mid-, and late gestational periods significantly elevated ABR thresholds in neonatal guinea pigs.

PS 1030

Noise Exposure, Self-Reported Speech-in-Noise Perception, and the Auditory Brainstem Response in Normal-Hearing Human Ears

Nikki Go; Tiffany A. Johnson
University of Kansas Medical Center

Background

Difficulty understanding speech in noise (SIN) is a common complaint among many listeners. There is emerging evidence that noise exposure is associated with difficulties in speech discrimination and temporal processing despite normal audiometric thresholds. Recent data from animal studies have revealed significant deafferentation of select auditory nerve fibers after full recovery of threshold responses following noise exposure. While there is some evidence suggesting noise-induced synaptopathy in human ears, the perceptual consequences of this phenomenon remain unclear. This study explores the link between recreational noise exposure, evoked potential estimates of neural survival and temporal processing, and perceptual deficits in humans with normal thresholds.

Methods

Data were collected from 30 normal-hearing subjects (18-35 years old) who fell into two categories based on their annual noise exposure (ANE) estimate as quantified by a questionnaire: low-noise (LN) exposure (ANE

< 75; n = 15) and high-noise (HN) exposure (ANE ≥ 79; n= 15). ANE ≥ 79 LAeq was classified as high-noise exposure based on Johnson et al. (2017) where these individuals were judged to be at highest risk for noise-induced hearing loss. ANE < 75 LAeq was required for inclusion in the LN group to increase differences in ANE between the LN and HN groups. Auditory brainstem responses (ABR) were recorded to both a click (as a measure of neural survival) and speech stimulus (/da/; as a measure of temporal processing). To reduce the confounding effects of sex on the ABR variables, equal numbers of males and females were recruited for each noise group. The speech hearing subscale of the Speech, Spatial and Qualities of Hearing Scale (SSQ) was also administered to quantify individual self-reported SIN abilities.

Results and Conclusion

Preliminary analyses showed no significant difference in the wave I amplitude of the click-ABR (cABR) between the LN and HN groups. Likewise, no significant association was found between the SSQ-speech hearing scores and the cABR wave I amplitude. Analyses of the differences in speech-ABR variables between the noise-exposure groups and the relationship to SSQ-hearing scale scores is ongoing. Failure to find differences for any of ABR variables (click- or speech-evoked) between the noise-exposure groups will call into question the extent to which recreational noise exposure produces synaptopathy. In contrast, if systematic associations are revealed for speech-ABR variables, this would suggest that noise exposure can lead to temporal processing deficits implicated in SIN perception difficulties. [Work supported by the American Academy of Audiology Foundation.]

PS 1031

Noise damage and repair in Vglut3 wild-type, heterozygous, and knockout mice

Aizhen Yang-Hood[1]; Shelby Payne[1]; Song-Zhe Li[1]; Bethany Davis[1]; Kyunghee Kim[1]; Kevin Ohlemiller[2]; Keiko Hirose[1]; **Mark Rutherford**[1]
[1]Washington University in St. Louis; [2]Department of Otolaryngology-Head and Neck Surgery, Washington University School of Medicine

This dissociation of cochlear ribbon synapses that occurs during noise exposure is thought to be glutamate-induced. The excitotoxic mechanisms are unknown, but may involve Ca^{2+} permeable AMPA receptors (Sebe et al., 2017). Although glutamate is recognized as the afferent neurotransmitter released from hair cell synapses (Seal et al., 2008; Ruel et al., 2008), other excitotoxic substances may be released from synaptic vesicles. Moreover, cell swelling and fragmentation may involve mechanisms upstream of glutamate release, such as voltage-gated Ca^{2+} influx at the hair cell presynaptic ribbon. To address these issues, we studied mice having one, two, or zero copies of the vesicular glutamate transporter-3 (Vglut3).

Despite the lack of glutamatergic transmission, many afferent synapses develop and persist as AMPA receptors juxtaposed with presynaptic ribbons. However, the ring-shaped arrays of AMPA receptors on auditory nerve fiber (ANF) post-synaptic terminals from KO mice tended to be larger and more complex in structure, as did the inner hair cell (IHC) presynaptic ribbons. Outer hair cell number and DPOAE levels were similar to WT in 1-3 month old Vglut3 HET and KO mice. Although KO mice are profoundly deaf, hearing thresholds in HET mice are not different from WT. After noise exposure, DPOAEs reduced and recovered similarly in WT, HET, and KO mice.

In Vglut3 WT and HET mice aged 9 weeks, 2 hours of 8-16 kHz noise at 100 dB SPL caused a threshold shift at 1 day that partially recovered by 2 weeks post-exposure. Interestingly, recovery of ABR threshold was significantly better in WT compared with HET mice, by approximately 20 dB. This was accompanied by loss of ~50% of synapses at 1 day, which partially recovered by 2 weeks post-exposure. Recovery of ribbon synapse number was significantly greater in WT compared with HET. Noise-induced synaptopathy was evident as disintegration between the presynaptic ribbon and postsynaptic AMPA receptors. In Vglut3 KO littermates the same noise exposure resulted in no synaptic disintegration. AMPA receptors remained paired with ribbons, suggesting that synaptopathy depended on glutamate.

Two hours of 94 dB SPL noise caused ABR threshold shifts that recovered to control levels by 4 weeks post exposure in Vglut3 WT and HET mice. Amplitude of ABR wave 1 tended to recover faster in WT. This difference was relatively small. Subsequent analysis will determine if differences exist between ribbon synapse numbers in WT and HET cochleae.

In Vglut3 KO IHCs, voltage-gated calcium channels (CaV1.3) clustered at presynaptic active zones, as in wildtype. However, we did not observe presynaptic damage after overexposure to sound in the Vglut3 KO IHCs, suggesting that presynaptic Ca^{2+} influx was not alone sufficient to damage the presynaptic active zone.

The Role of ECRG4 in Early-Onset Hearing Loss and Noise-Induced Cochlear Damage

Lauren Rynders[1]; Arwa Kurabi[1]; Kwang Pak[2]; Allen F Ryan[3]
[1]*University of California, San Diego; [2]UCSD; [3]UCSD and San Diego VA Medical Center*

Introduction

Esophageal Cancer Related Gene 4 (ECRG4) is a candidate tumor suppressor gene that is also involved in aging and injury responses. It has been found to induce senescence of oligodendrocyte and neural precursor cells, inhibit cell proliferation, and regulate apoptosis in various cell types in numerous tissues in the body. ECRG4 is expressed in the inner ear, but its role in the cochlea is currently unknown, including any potential role in hearing loss due to acoustic trauma or aging.

Methods

This study used auditory brainstem response (ABR) to investigate the hearing sensitivity of ECRG4 knock-out (KO) mice compared to C57/BL6 wild type (WT) mice before and after acoustic trauma and over the aging process, to see if loss of ECRG4 rendered the cochlea more sensitive to noise damage and to age-related hearing loss.

Results

Results showed a high-frequency hearing deficit in four-week-old ECRG4 KO mice. There was no significant difference between ECRG4 KO and WT mice for temporary or permanent threshold shift after acoustic trauma. Hearing sensitivity across aging did not indicate a rapid progression of hearing loss.

Conclusions

This is the first report showing that loss of ECRG4 expression leads to high frequency hearing loss in mice. Future research, including cochlear histology and ABR waveform amplitude growth analysis, will explore the nature of this genetic hearing loss defect.

Mechanical overstimulation of zebrafish lateral-line organs produces morphological damage resembling noise-exposed cochleae

Lavinia Sheets[1]; Michael E. Ravicz[2]; Kenneth Hancock[2]
[1]*Washington University School of Medicine in St. Louis; [2]Eaton-Peabody Laboratory, Massachusetts Eye and Ear Infirmary/ Department of Otolaryngology, Harvard Medical School*

Noise-induced damage to sensory hair cells depends on the intensity and duration of stimuli, with moderate and prolonged noise levels leading to synaptic damage and loss of a subset of synaptic contacts. Currently, the cellular mechanisms underlying synaptic-ribbon damage and loss following noise exposure are poorly defined. Zebrafish have proven to be a valuable model system for studying cellular pathways underlying hair-cell damage, as zebrafish lateral-line hair cells are both optically and pharmacologically accessible in whole, intact larvae. While pharmacological mimics of noise exposure, i.e. glutamate receptor agonists and L-type calcium channel activators, are informative, they do not fully replicate actual noise exposure and mechanical overstimulation of hair cells. Exposing zebrafish larvae to calibrated, traumatic noise stimuli allows investigation of cellular pathways mediating hair-cell synapse loss using a more physiologically relevant paradigm.

We therefore built a device controlled by custom software to expose 7-day-old free-swimming larvae to strong current by vibrating their enclosure. Larvae exposed tointense 60Hz sinusoidal acceleration for 1.5-2 hours experienced water displacement sufficient to overstimulate their lateral-line neuromast (NM) hair cells. While two consecutive 1h. exposures at >1.3 m/s^2 (-17.5 dB re 1 g) contributed to hair-cell death, larvae exposed to 2 showed lateral line afferent retraction and the loss of synaptic ribbons from a subset of NM hair cells. We also observed smaller synaptic ribbons and orphan postsynaptic densities, indicating synaptic-ribbon loss in exposed larvae relative to unexposed control. These results indicate we can induce noise damage, both hair cell and "synaptopathic", in zebrafish lateral-line organs that appears morphologically similar to noise-exposed mammalian cochlea.

We subsequently compared changes in synapse morphology of noise-exposed larvae with two pharmacological mimics of noise exposure. Overactivation of AMPA/Kainate iGluRs, while leading to afferent terminal swelling and hair-cell loss, did not contribute to synaptic-ribbon loss in remaining NM hair cells. By contrast, exposure to (S)-(-)-Bay-K 8644 at a concentration previ-

ously shown to significantly increased Ca^{2+} influx in NM hair cells led to both a reduction in synaptic-ribbon size and the loss of a subset of synaptic ribbons similar to what we observed in "noise-exposed" hair-cells. Notably, these phenomena were also observed in Bay-K exposed larvae lacking hair-cell glutamate release (vglut3 -/-), suggesting that noise-induced synaptic-ribbon loss may occur independent of glutamate signaling. Overall, these data support the utility of the zebrafish lateral line toward determining the contributions of specific cellular processes to noise-induced hair-cell damage and synapse loss.

PS 1034

Hearing Impairment Induced by Shock Wave Exposure

Eiko Harada; Kunio Mizutari; Akihiro Shiotani
National Diffense Medical College

Background
Blast injuries to head and neck area have increased because of terrorism and conflicts. The ear is one of high-risk organs for blast injury as well as intestinal tract and lung. Sensorineural hearing loss caused by a shock wave is the most critical etiology relating to blast-induced hearing loss. In this study, we analyzed the pathological condition of hearing impairment in mice using a shock wave generator capable of faithfully reproducing shock waves due to explosion.

Method
Shock wave was generated by compressed nitrogen in the SUS-tubing (length of low pressure part: 800 mm, length of high pressure part: 400 mm, ID: 25 mm). Polyester membrane was set between these two parts. Nitrogen gas was inflated into high pressure part, then shock wave was generated by breaking the membrane using a thin needle. The pressure and waveform of the shock wave were measured using pressure sensor and an oscilloscope. The shock wave peak pressure was set to 25 kPa.

Six-week-old male CBA / J mouse (BW: 17-20 g) was used, and shock wave was irradiated from the front of the mouse head. We observed tympanic membrane using a small endoscope (AVS) immediately after irradiation. Measurement of auditory function was performed using auditory brainstem response (ABR) on before and 1, 7, and 28 days after irradiation. Immunohistochemistory was performed 28 days after shock wave exposure, using Myosin VIIA, CtBP2, and GluR2 on the organs of Corti, for evaluation of the morphology of the hair cells and the synapses.

Result
Although the ABR thresholds were elevated immediately after shock wave irradiation, there were no any side injuries such as perforation of tympanic membrane or cerebral hemorrhage, therefore the observed hearing impairment considered as sensorineural hearing loss. The peak of ABR threshold elevation was observed one day after the irradiation, and threshold shifts were remained at the higher frequencies up to 1 month after irradiation, whereas recovered at the lower frequencies. Histopathology revealed mild loss of outer hair cells and reduction of synapses mainly at basal turn.

Conclusion
Our mouse model revealed that shock wave irradiation generated by shock tube could generate sensorineural hearing loss. This model would replicate important characteristics of blast-induced hearing loss.

PS 1035

Localized Therapeutic Hypothermia Mitigates Noise-Induced Hearing Loss

Samantha Rincon[1]; Rachele Sangaletti[2]; Anne Feliciano[1]; Curtis King[3]; Suhrud Rajguru[4]
[1]Department of Biomedical Engineering , University of Miami; [2]Department of Otolaryngology, University of Miami; [3]Lucent Medical Systems; [4]Department of Biomedical Engineering and Otolaryngology, University of Miami

Background
Noise-induced hearing loss (NIHL) is caused either by acute acoustic trauma or by repetitive exposure to loud sounds and remains one of the leading global occupational diseases, with nearly 30–40 million Americans exposed to hazardous noise levels on a regular basis. In the present study, we assessed the therapeutic benefit and mechanisms of localized therapeutic hypothermia in preservation of residual hearing and mitigation of cochlear injury following acoustic trauma in a rat model.

Methods
All procedures were approved by the University of Miami Institutional Animal Care and Use Committee. Female Brown Norway rats were separated into three groups: (1) Control Group, receiving neither trauma nor treatment, (2) normothermic NIHL, (3) hypothermic-treated NIHL. Auditory brainstem response (ABR) and distortion product otoacoustic emission (DPAOE) were measured to quantify changes in hearing threshold in anesthetized rats (44 mg/kg ketamine, 5 mg/kg xylazine) prior to NIHL and at various time points following trauma. NIHL was delivered in anesthetized rats (isoflurane) during 2 hours of continuous noise exposure using a 4-8 kHz narrow-

band noise emitted from a speaker with intensities of 105 or 120dBSPL. Hypothermia was applied to cool the cochlea (~33ºC) for 2 hours. Following measurements at multiple time points over 30 days, cochleae were harvested for immunolabeling and cell counting. In a separate set of animals, cochleae were harvested at several time points after each treatment for mRNA and protein extraction. Western Blot and rt-qPCR were performed to quantify gene and protein level expression of selected anti-inflammatory targets.

Results

Previous studies have suggested that animals exposed to noise when hypothermic show significant less elevation of hearing thresholds than those exposed when euthermic. Our preliminary results confirm that hypothermia treatment even post NIHL preserves significant residual function. Hypothermia treatment alone did not cause adverse effects on residual hearing. Furthermore, a significant increase in oxidative stress within the cochlea follows noise exposure.

Conclusions

It is known that multiple mechanisms must be targeted to reduce acute and chronic inflammation, prevent cell death and loss of function following trauma to the inner ear. Hypothermia is known to reduce oxidative stress and increase activity of anti-apoptotic pathways, providing mechanisms whereby it might also reduce adverse effects of noise on hearing.

PS 1036

A metabolomics approach to investigate the acute effects of noise on the inner ear

Lingchao Ji[1]; Ho Joon Lee[2]; Guoqiang Wan[1]; Guo-Peng Wang[3]; Jochen Schacht[3]; Costas Lyssiotis[2]; **Gabriel Corfas**[3]
[1]*Kresge Hearing Research Institute, University of Michigan;* [2]*Department of Molecular and Integrative Physiology, University of Michigan Medical School;* [3]*Kresge Hearing Research Institute, University of Michigan Medical School*

Exposure to loud sound alters cochlear structure and function, and leads to hearing loss. Much of the exploration of the effects of noise-exposure on the inner ear at the molecular level has focused primarily on nucleic acids and proteins. Changes in these macromolecules are usually detectable only hours after the exposure, thus they are unlikely to be the key initiators of noise-induced degenerative processes. We hypothesize that the triggers to the damaging effects of noise are acute and likely to involve rapid changes in metabolites which directly compromise cell and tissue homeostasis. To explore this model, we are using targeted metabolomics to measure metabolite levels and identify key metabolic pathways acutely altered by noise exposure.

To characterize robust metabolome changes induced by noise exposure, several cohorts of mice of different strains (FVB/N, CBA/J and C3H) were subjected to different levels of noise (98 dB/100 dB/110 dB) for different exposure durations (1 hour/2 hour), and to several different noise bands (2-20 kHz/8-16 kHz). Temporal bones were dissected immediately after noise exposure, metabolites were isolated by methanol extraction and then analyzed by liquid chromatography-mass spectrometry. Preliminary meta-analysis of metabolomic data identifies several dozen metabolites whose levels are consistently changed by noise exposure. Pathway analysis based on the affected metabolites indicates that aminoacyl-tRNA biosynthesis, which includes several amino acids, is consistently and statistically significantly altered.

Our results indicate that metabolomics analysis of mouse temporal bones can be used to investigate early molecular events triggered by noise exposure and could help in the identification of the underlying associated metabolic processes. Such knowledge will further the understanding of noise-induced hearing loss and will be vital for metabolic profiling to identify robust biomarkers for disease states and drug efficacy.

PS 1037

Immune Response to Noise Damage is Altered in Mice Lacking Adaptive Immunity

Megan Wood[1]; Tetsuji Yamashita[2]; Jian Zuo[2]
[1]*St. Jude Children's Research Hospital;* [2]*Department of Developmental Neurobiology, St. Jude Children's Research Hospital, Memphis, Tennessee, USA*

Cells of the immune system respond to noise damage to the cochlea which may lead to hair cell loss. The best characterized immune cells present in the ear before and entering the cochlea after noise damage are macrophages. However, many different types of immune cells are present in the cochlea before and after noise damage. We and others have demonstrated, by using immunofluorescent confocal microscopy and flow cytometric analysis, that cell types of both the innate and adaptive immune systems are present in the normal ear. Additionally, we have used single cell RNA sequencing to identify innate and adaptive immune cells in the adult cochlea. After noise damage, an increase in immune

cell types of the innate and adaptive system was observed as well. Here we sought to understand the role of the adaptive immune system in the response to noise damage by using a mouse model known to lack these cells. Mice deficient in the recombination activating gene 1 (Rag1) lack B and T cells which make up the adaptive immune system. Rag1 knockout mice (Rag1^{-/-}) and mice heterozygous for the Rag1 mutant gene (Rag1^{+/-}) have normal ABR thresholds when compared to wildtype C57BL/6 mice. After noise damage, Rag1^{-/-} mice exhibit significantly higher ABR thresholds at 32kHz than wildtype animals. In adult cochleae at the steady state, increased numbers of CD45+ cells are present in Rag1^{-/-} mice compared to in wildtype mice. After noise damage, the number of immune cells in the cochlea of Rag1^{-/-} mice increases as in wildtype animals. However, the makeup of the immune cell population shifts from predominantly monocytes and macrophages to include a larger proportion of neutrophils and natural killer (NK) cells in the Rag1^{-/-} mice than in the wildtype mice. These data indicate that the adaptive immune system may be an important contributor to the immune response after noise damage. Our studies show that the population of immune cells in the cochlea is a heterogeneous mix of innate and adaptive cell types in the absence of damage; but, after noise damage, cells of the adaptive immune system may play a protective role in preventing neutrophil and NK cell infiltration.

PS 1038

Estimating Risk of Noise-Induced Hearing Loss Caused by Portable Listening Device Using One-month Tracking Method

Gibbeum Kim[1]; Ji Hun Shin[2]; Woojae Han[3];
Changgeun Song[4]; Saea Kim[1]
[1]Department of Speech Pathology and Audiology, Graduate School, Hallym University; [2]Department of Convergence Software, Graduate School, Hallym University; [3]Division of Speech Pathology and Audiology, College of Natural Science, Hallym University; [4]Department of Convergence Software, College of Information and Electronic Engineering, Hallym University

Purpose
Occupational noise exposure is widely recognized as one of the causes of hearing loss. More recently, recreational activity that involves a high level of noise has also been shown to have a negative effect on the human auditory system. Contemporary researchers have been concerned about the overexposure to MP3 players by adolescents and young adults who habitually listen to music at high levels of volume for long periods of time. The purpose of the present study was to measure preferred listening levels of MP3 players by college students and their listening duration in actual daily life for one month (i.e., 4 weeks), and to find a pattern for noise-induced hearing loss while comparing the results to currently proposed risk criteria.

Methods
Before conducting the experiments, we developed an application for Android that measured participants' preferred listening levels when they listened to music in real time. Thirty-four college students (16 male and 18 female) with normal hearing participated in the study. They were asked to listen to music similar to what they listened to in their daily lives for four weeks and also asked to control the volume steps of the personal listening device as they wished.

Results
Results of the study showed that the mean of the preferred listening level was 69.88 dB during the four weeks. Fridays and Tuesdays had significantly the highest (71.08 dB) and the lowest (67.42 dB) levels, respectively. Although there were a few differences based on time of day, the highest preferred listening level was recorded between 3 pm and 8 pm. In addition, 56.72% of subjects listened to music more than one hour per day. Based on noise standards that can be used to estimate damage risk, such as those established by NIOSH (1998) and OSHA (2003), risk of occupational noise exposure was 0% and 26.4% of the subjects, respectively. However, 56% of the subjects remained below WHO's "60/60" rule (i.e., keep the volume on the MP3 player below 60 percent and only listen for a maximum of 60 minutes a day).

Conclusion
In summary, the preferred listening levels of college students using their MP3 players were not high enough to induce temporary hearing loss when they used MP3 players. However, there were large individual differences among the preferred listening levels and use time. Thus, we concluded that appropriate and specific criteria for avoiding noise-induced hearing loss by recreational users should be proposed.

Mechanisms of Oxidative Stress and Outer Hair Cell Death in Noise-Exposed Foxo3 Knock-Out Mice

Holly Beaulac[1]; Patricia White[2]
[1]*University of Rochester;* [2]*Dept. of Neuroscience, University of Rochester School of Medicine*

Noise-induced hearing loss (NIHL) is attributed to over-stimulation of the inner and outer hair cells (IHCs and OHCs) on the organ of Corti and increased oxidative stress (OS). We have previously demonstrated that the forkhead transcription factor FOXO3 is required for auditory function and OHC preservation after noise exposure (NE). FOXO3 regulates an array of cellular processes including the oxidative stress response (OSR). FOXO3';s pro-survival actions depend on mechanisms not yet fully understood. A mild NE produces profound, persistent hearing deficits and dramatic OHC loss in adult mice with Foxo3 deletion (Foxo3[KO/KO]), whereas their wild type (WT) littermates rapidly recover with minor OHC loss (Gilels et al., 2017). I hypothesize that damage recovery pathways used to preserve OHCs during cochlear stress are regulated by FOXO3.

The ability of our NE to induce OS and OHC death has been assessed with specific OSR markers.

Methods

NE was performed on adult WT and Foxo3[KO/KO] mice and cochleae were extracted at 0, 30min post-NE (MPN), 4hrs post-NE (HPN), and 24HPN. Cochleae were sectioned and OSR factors labeled. Results: Under control conditions for both genotypes, activated pJNK was present beneath both IHCs and OHCs. At 30MPN in the WT, the IHC and supporting cells displayed increased activated pJNK. At 30MPN in the KO, increased pJNK activity was found in the supporting cells, IHC, and nerve terminals. KO OHC nuclei sizes were comparable to WT at 30MPN and to controls. However, disruption of the OHC morphology was visible in the mid-basal cochlear turn and activated pJNK appeared within the Deiter cells. In an effort to prevent more damage, the Deiter cells could be phagocytizing the OHCs.

FOXO3 primarily regulates via transcription and its absence may result in altered gene expression. Methods: To identify this transcription factor';s downstream targets prior to and after noise, adult WT and Foxo3[KO/KO] mice were exposed to 105 dB noise for 30 min in the 8-16 kHz band. Cochleae were removed at 0, 4HPN, and 24HPN for mRNA extraction. Changes in cochlear gene expression between WT and Foxo3[KO/KO] mice were examined using RNA-sequencing. Gene Ontology was used to perform enrichment analysis on our derived gene set. Three significant, differentially expressed genes in control conditions and five with FOXO3 binding sites were selected for further analysis.

Results

Two target proteins have demonstrated strong reproducibility of the RNA-sequencing with RT-qPCR and may be important targets for FOXO3 in maintaining cell homeostasis during OS.

Middle Ear Devices & Clinical

Stapes Prosthesis Position Along Incus Long Process Affects Sound Induced Velocity

Iman Ghanad[1]; Danielle R. Trakimas[1]; Elliott D. Kozin[1]; John J. Rosowski[2]; Jeffrey T. Cheng[3]; Aaron K. Remenschneider[1]
[1]*Massachusetts Eye and Ear Infirmary, Harvard Medical School;* [2]*Eaton Peabody Lab, Massachusetts Eye and Ear Infirmary, Harvard Medical School;* [3]*Eaton Peabody Laboratory, Massachusetts Eye and Ear Infirmary; Department of Otolaryngology, Harvard Medical School*

Background

Stapedectomy is a procedure used to restore hearing in condititions of stapes fixation, such as stapedial otosclerosis, or malformation. A stapes prosthesis, typically consisting of a piston that is placed in the vestibule attached to a wire affixed to the incus long process, provides hearing rehabilitation. While surgical outcomes generally improve conductive hearing losses, the complete closure of air-bone-gap is variable. In addition, high frequency hearing is often post-operatively poor. Little is known about how prosthesis position along the incus long process affects middle ear sound transmission. In this study, we aim to determine if prosthesis position influences sound induced displacement. We hypothesize there is an optimal position of the prosthesis along the incus long process to 1) decrease the air-bone-gap, and 2) provide for high frequency hearing.

Methods

Cadaveric temporal bones without history of otologic diseases underwent laser stapedotomy through a facial recess approach. The tympanic membrane (TM) was kept intact. A nitinol-fluroplastic stapes piston was placed into a 6mm fenestration within the intact stapes footplate. The wire was positioned and crimped at three different positions at 1mm increments from the lenticular process of the incus (eg: distal, middle and proximal). Sound induced velocity measurements were taken by Laser Doppler Vibrometry (LDV) from the 'shoulder'; of

the piston. Calibrated probe microphone sensors were placed lateral to the TM for pressure measurement and normalization of results. A sound source was sealed to the external ear canal opening to deliver pure tones between 200-10000 Hz.

Results
Prosthesis position along the incus long process influenced sound induced displacement of the prosthesis. 'Middle'; positioning of the prosthesis demonstrated measurably greater overall displacement compared to distal and proximal positions. At low frequencies, middle positioning provided greater displacement than proximal and distal positioning, although the differences were small. Above 5 kHz, however, the 'middle'; postioning demonstrated up to two times greater displacement than the 'proximal'; positioning and up to four times greater displacement than the 'distal'; positioning.

Conclusion
The positioning of the stapes prostheses along the incus long process following stapedectomy affects sound induced displacement of the prosthesis. Middle positioning appears to provide the highest high frequency displacement when compared to proximal or distal positions. Further study is still needed to determine optimal prosthesis location. These findings are relevant for understanding the physiology of post-operative hearing outcomes in stapedectomy.

PS 1041

Application of high-speed Digital Image Correlation to study blast damage to thin membranes

Payam Razavi[1]; **Hami Tang**[1]; Koohyar Pooladvand[1]; Michael E. Ravicz[2]; Aaron K. Remenschneider[3]; John J. Rosowski[4]; Jeffrey T. Cheng[5]; Cosme Furlong[1]
[1]Center for Holographic Studies and Laser micro-mechaTronics, Mechanical Engineering Department, Worcester Polytechnic Institute; [2]Eaton-Peabody Laboratory, Massachusetts Eye and Ear Infirmary/ Department of Otolaryngology, Harvard Medical School; [3]Massachusetts Eye and Ear Infirmary, Harvard Medical School; [4]Eaton Peabody Lab, Massachusetts Eye and Ear Infirmary, Harvard Medical School; [5]Eaton Peabody Laboratory, Massachusetts Eye and Ear Infirmary; Department of Otolaryngology, Harvard Medical School

Background
High-intensity impulsive sounds caused by blast waves (e.g., explosion, jet engines or large caliber military ordnance, etc.) can damage the Tympanic Membrane (TM), which often leads to mild to severe conductive hearing loss. In order to improve the design of hearing protec-

tion and TM rehabilitation surgeries, it is important to understand the dynamics of TM rupture by high amplitude excitations. To achieve this goal, a high-speed non-intrusive full-field-of-view metrology is developed and applied to study blast damage to membranes.

Method
Thin membranes (i.e., PolyTetraFluoroEthylene (PTFE) sheets) with orthotropic material properties resembling the human eardrum are ruptured by static air pressure produced from a custom made loading apparatus. The orthotropic material properties are verified and measured by scanning electron microscope and micro-tensile-tests. High-speed cameras are deployed to capture the rapid-time course of the acoustic to solid interaction over the full 20 mm2 surface area at high frame rates (i.e., 2 million fps). The dynamic rupture process of thin membranes are quantified using stereo High-Speed Digital Image Correlation (HS-DIC) in both 3D and 2D.

Results
Images of PTFE microstructure shows that it has fibers aligned in primary and orthogonal secondary direction. Micro-tensile-tests illustrate significant differences in the stiffness and yield strength in the two directions. HS-DIC results indicate that the rupture process can be divided into three stages: global expansion, bulging and crack propagation. The average strain rate in the global expansion is about 100 microstrain/μs; however,the strain rates of bulging and crack propagation cannot be determined because of speckle pattern decorrelation. During propagation, the crack initializes along the primary fiber direction, and then it further opens along the secondary direction, with velocities estimated by edge detection as high as 0.73 Mach and 1.05 Mach, respectively. The directions of initialization and propagation of crack are related to the orthotropic material properties.

Conclusion
The HS-DIC system can describe the high-strain rates measurements of soft membranes during fracture, which could provide a better understanding of sound-matter interaction during blast-induced injury to the TM, and help development of hearing protection. Test parameters and results obtained from this study provide valuable information to guide future experimental designs and procedures on real eardrum samples.

Funding

PS 1042

Tympanoplasty Graft Material Affects Sounds Induced Stapes Velocity in Human Cadaveric Temporal Bones

Iman Ghanad[1]; Danielle R. Trakimas[1]; Elliott D. Kozin[1]; John J. Rosowski[2]; Jeffrey T. Cheng[3]; Aaron K. Remenschneider[1]
[1]*Massachusetts Eye and Ear Infirmary, Harvard Medical School; [2]Eaton Peabody Lab, Massachusetts Eye and Ear Infirmary, Harvard Medical School; [3]Eaton Peabody Laboratory, Massachusetts Eye and Ear Infirmary; Department of Otolaryngology, Harvard Medical School*

Background
Autologous graft materials used in tympanoplasty have imperfect sound conduction properties. Histopathologic study has shown relatively little remodeling of preimplantation graft materials after healing, thus preimplantation sound conduction properties of graft materials are relevant in predicting post-surgical outcomes. Recent developments in synthetic and non-autologous, biologic graft materials have shown controllable acoustic properties, which may ultimately improve audiometric outcomes in tympanic membrane (TM) repair. Sound transmission to the middle ear with reconstructed TM perforations is not well understood. In this study, we aim to understand 1) the impact of various graft material patches on stapes displacement in human cadaveric temporal bone model of TM perforation and 2) differences in sound conduction between autologous and non-autologous graft materials.

Methods
Two cadaveric temporal bones without history of otologic diseases were used to assess graft material influence on sound induced stapes displacement. Controlled perforations of the TM were created after Laser Doppler vibrometry (LDV) measurement of baseline stapes velocity with intact TM. Calibrated probe microphone sensors were placed lateral to the TM into the external ear canal and in the middle ear to monitor pressure changes in the sealed temporal bone. A sound source is sealed to the external ear canal opening to produce sine sequence tones between 200-20000 Hz to vibrate the TM. Graft materials (human fascia, porcine intestinal submucosa (SIS), paper patch, cartilage and 3D printed grafts) were used to reconstruct the perforation with repeat measurements of stapes velocity recorded.

Results
Perforation closure was detected with each utilized graft material and was confirmed by expected external and middle ear pressure changes. Normalized stapes displacement is detectably different when comparing graft materials. In all reconstructed TMs the stapes displace-ment was higher than in perforated TMs. Peak displacement was seen consistently in lower to mid frequencies, ranging between 500 Hz to 2 kHz, depending upon the graft. Several grafts (SIS, fascia and 3D printed grafts) demonstrated higher normalized stapes velocity in low and mid frequencies than the non-perforated TM. Paper patch demonstrated high stapes displacement at 1-2 kHz, while cartilage patched TMs showed decreased stapes displacement in those frequencies.

Conclusion
Synthetic and autologous graft materials utilized in to reconstruct TMs in cadaveric temporal bones demonstrate varied effects on stapes velocity. Materials structure and scaffold viscoelastic properties may influence postoperative hearing outcomes. The study has implications for further design and implementation of synthetic graft materials for tympanoplasty.

PS 1043

Evaluating active transport across the tympanic membrane of various species using an in vitro assay

Arwa Kurabi[1]; Volker Noack[2]; Kwang Pak[3]; Marlen Bernhardt[4]; Daniel Schaerer[4]; Allen F Ryan[5]
[1]*University of California, San Diego; [2]Ruhr-Universität Bochum; [3]UCSD; [4]University of California San Diego; [5]UCSD and San Diego VA Medical Center*

Using in vivo phage display biopanning, we previously discovered peptides that are actively transport bacteriophage across the intact tympanic membrane (TM) of rats. To determine whether this transport mechanism is present in other species we developed an in vitro assay. To assess feasibility, we first isolated the tympanic bulla from rats and evaluated transport ex vivo over time. Transport was observed up to 6 hours post-mortem, validating an in vitro approach. The assay consists of two cylindrical chambers, separated by a silicon membrane gasket with an appropriately sized opening. A TM fragment is placed external side up over the opening of the fluid-filled lower chamber (representing the middle ear space), followed by the gasket and the upper chamber, and compression sealed. The upper chamber, representing the external ear, is filled with fluid containing peptide-bearing phage or free peptide for varying periods of time. We exposed phage bearing a TM-transiting peptide identified in rat, to the freshly-dissected TMs of rats, guinea pigs and rabbits. We then measured the concentration of phage in the lower chamber. Two experimental controls were employed. In the first, trypan blue was placed in the upper chamber during the experiment. Colorimetry was used to detect any penetration of dye into the lower chamber that would indicate a leak. Trypan blue did not affect the transport of TM-transiting

peptide phage, and was used in all experiments. Any detection of dye in the fluid of the lower chamber led to data discard. For the second control, wild-type (WT) phage not displaying a peptide was placed in the upper chamber. Movement of TM-transiting phage through the TM was comparable in rat, guinea pig and rabbit. Transit of WT phage was extremely low or absent in all species. Transport of peptide-bearing phage was similar in all species. Active transport across the TM in three mammals separated by ~80 million years of evolution indicates a well-conserved transport mechanism. We also found that free peptide, not attached to phage, is transported at a comparable rate to peptide expressed by phage. The assay is currently being used to evaluate transport across human TM fragments obtained during reconstructive surgery.

PS 1044

Single-Cell RNA Sequencing Identifies Cell Types in the Murine Tympanic Membrane

Stacey M. Frumm; Kevin Shengyang Yu; Lauren E. Byrnes; Julie B. Sneddon; Aaron D. Tward
University of California, San Francisco

The tympanic membrane (TM) conducts sound waves from the external auditory canal (EAC) to the ossicular chain. The basic structure of the TM is known: it is comprised of epidermal, fibrous, and mucosal layers. Prior studies have shown that the TM epidermis has anatomically defined proliferative zones near the malleus and annulus, and that keratinocytes migrate radially outward to join the EAC epidermis. However, little is known about the molecular biology underlying these behaviors or the cells residing in the proliferative niches. This study aimed to define the cells that make up the murine TM via single-cell RNA sequencing (scRNA-seq), and to characterize their behavior with EdU pulse-chase experiments.

TMs from adult mice were enzymatically split into two fractions: (1) the epidermal layer and (2) the fibrous and mucosal layers. Each fraction was dissociated and scRNA-seq was conducted. Cumulatively, gene expression profiles from 1,319 cells were obtained. An initial round of unsupervised clustering yielded 12 distinct clusters of cells in the fibrous/mucosal fraction, including: endothelial cells, smooth muscle cells, neurons, Schwann cells, two discrete groups of mucosal cells (non-ciliated and ciliated), and several mesenchymal cell types (Figure A). In the epidermal fraction, six clusters of keratinocytes were identified that spanned differ-

entiation states (Figure B). Some keratinocyte clusters had higher expression of Krt5, Krt14, Itga6, and Trp63, typical of relatively undifferentiated cells, while others upregulated Krt10, Ivl, and Flg, markers of maturation. Among the less differentiated keratinocytes, proliferating cells were in a unique cluster defined by upregulation of genes associated with the cell cycle. Novel markers of the different populations were identified, including Krt23 in the mature keratinocytes and Sox2 in the mucosal cells. The scRNA-seq findings were validated with detection of protein expression by immunohistochemistry and immunofluorescence, and of RNA expression using RNAscope technology. Furthermore, the proliferation and migration dynamics of keratinocytes were characterized with EdU pulse-chase experiments. It was confirmed that TM keratinocytes proliferate proximal to the malleus and annulus, but not in the intervening body of the pars tensa. Additionally, continuous EdU exposure demonstrated that the entire keratinocyte population on the murine TM turns over in approximately three weeks.

Overall, these studies describe the cellular composition of the murine TM and lay the groundwork for future investigation of the clonal architecture of the TM and of the molecular biology underlying TM maintenance.

2017.09.21_ARO_Abstract_Fig.pptx

PS 1045

A Surgical Model for Long-Term Repeat Administration to the Middle Ear in Guinea Pigs

Kelly Tenneson; Jean-Francois Lafond; Frederick Emond
Charles River Laboratories

The otic route of administration has applications for many classes of compounds, most notably for antibiotics and gene therapy, and is increasingly used to target the otic and vestibular systems. In animal studies, investigating long term, repeated exposure that mimics potential clinical dosing regimens remains a challenge due to the lack of suitable models. Transtympanic injections are not suitable for long-term studies due to the increased risk related to tympanic membrane rupture and repeated periods of anesthesia, and surgical models previously used have not been reliable for longer than 4 weeks and resulted in elevated stress levels. We refined an existing surgical model in order to permit repeat dosing up to 9 weeks or longer after implantation of a catheter into the middle ear of Guinea Pigs.

Guinea pigs (Cavia porcellus; 9 males) were group housed (up to 6 animals) and surgically implanted with catheters bilaterally in the middle ear via an opening

created in the temporal bone. Catheters were secured and then passed subcutaneously to connect with a dual channel access port placed in the interscapular region. Following a two-week recovery period, 70 uL saline or gentamicin (42 mg/dose) were administered to the middle ear on Days 1, 4, 8 and 11 with. Animals underwent auditory brainstem response (ABR) assessment at 4, 8 and 16 kHz following surgery and 4 and 7 weeks after dosing start. Nine weeks after surgery, animals were sent to necropsy for collection of the ears for either microscopic evaluation or cytocochleogram analysis.

Following surgical implantation, transient body weight loss was observed during the first week. Overall, the recovery was very good, with return to normal food intake and grooming behaviour within days and body weight gains by the second week of recovery. ABR responses were unaffected by the procedure. Following dosing, some animals given gentamicin had some vestibular effects (headtilt, uncoordination and abnormal gait), elevated ABR thresholds and hair cell loss observed microscopically. Saline control animals remained in good condition and had normal or slightly elevated ABR threshold (15 to 30 dB) prior to necropsy. Catheters remained implanted and patent throughout the study period.

In conclusion, this refined surgical method was considered suitable for use in studies requiring repeated administration to the middle ear for at least 9 weeks in duration, and expected ototoxic effects were detected using ABR and microscopy following repeat middle-ear administration.

PS 1046

Predicting clinical efficiency of a Direct Acoustic Cochlear Implant actuator from measurements of intracochlear pressure in cadaver ears

Ute Alice Gamm[1]; Martin Großöhmichen[2]; Thomas Lenarz[3]; Hannes Maier[2]
[1]Cochlear Deutschland GmbH & Co. KG; [2]Department of Otolaryngology, Hannover Medical School, Germany; Cluster of Excellence; [3]Department of Otolaryngology, Hannover Medical School, Germany and DFG Cluster of Excellence Hearing4all

Introduction
Measurements in temporal bones are the gold standard for preclinical testing of active middle ear implants (AMEI). We have recently been able to show that clinical data of patients with an AMEI actuator coupled to the incus correlate with experimental data on temporal bones with high accuracy. In this study we investigate the correlation between clinical actuator efficiency in patients with a direct acoustic cochlea implant (Cochlear™ Co-

dacs™ System) and intracochlear pressure measurements in cadaver with the same implant.

Methods
Twenty-two temporal bones were implanted with the Codacs actuator. Intracochlear pressure in scala vestibuli (SV) and scala tympani (ST) was measured between 100 Hz and 10 kHz. To simulate tissue growth around the implant, especially around the piston stimulating the cochlear fluid, we sealed 8 of the stapedotomies around the piston with fibrin glue (Tisseel) and in 7 cases additionally the cavity surrounding the actuator. Actuator output was expressed as equivalent free field sound pressure levels at 1 Vrms. Actuator output in patients was calculated from bone conduction and direct implant thresholds.

Results
Medians of the clinical and cadaver data at frequencies from 100 to 400 Hz were equally about 110 dB SPLeq and about 100 dB SPLeq above 4000 Hz. However, between 400 and 4000 Hz, actuator output in patients was higher than in temporal bone experiments with a maximum deviation of 25 dB at 1000 Hz. Sealing of the piston as well as covering the round window and the actuator with fibrin glue did not have a significant effect on the measured actuator output. A slight increase in output however was observed for frequencies up to 1000 Hz with a maximum of 8 dB.

Conclusion
Previously we were able to show close correlation of clinical data of patients with an AMEI actuator coupled to the incus with data from temporal bone experiments. However in this study we observed deviations from clinical data for experiments with the Codacs actuator by up to 25 dB at 400-4000 Hz. We could not prove the hypothesis that tissue growth would cause this discrepancy

PS 1047

Evaluating intracochlear pressure measurements for best prediction of clinical performance of an implantable hearing actuator

Ute Alice Gamm[1]; Martin Großöhmichen[2]; Bernd Waldmann[1]; Thomas Lenarz[3]; Hannes Maier[2]
[1]Cochlear Deutschland GmbH & Co. KG; [2]Department of Otolaryngology, Hannover Medical School, Germany; Cluster of Excellence; [3]Department of Otolaryngology, Hannover Medical School, Germany and DFG Cluster of Excellence Hearing4all

Introduction
Intracochlear pressure measurements in temporal bone

have shown to be a valid tool to evaluate sound transmission to the inner ear. Intracochlear pressure differences are measured by inserting two pressure probes into both scala vestibuli (SV) and scala tympani (ST). However, when using intracochlear pressure differences to investigate the output of middle ear implants, net pressure signals are not considered but rather the relationship between signals recorded upon acoustical stimulation and actuator stimulation. This study aims to investigate whether intracochlear pressure difference measurements are still the superior measure when actuator output is investigated or whether pressures measured in either of the scalae are sufficient.

Methods

We have investigated the output of the Cochlear™ Carina™ T2 actuator coupled to the incus through intracochlear pressure on 14 temporal bones. The actuator output was expressed as equivalent free field sound pressure levels at 1 Vrms, i.e. the free field sound pressure stimulation level that is necessary to elicit the same intracochlear signal as ossicular stimulation via the actuator driven with 1V. The output was calculated for intracochlear pressure measurement results of either scala vestibuli, scala tympani and for the pressure difference between both scalae. Results were compared with clinical data of actuator output in patients through bone conduction and direct implant threshold measurements.

Results

As earlier shown actuator efficiency calculated from intracochlear pressure measurements in human temporal bones showed a very good correlation with clinical data. No significant differences in results were found between actuator efficiency calculated from pressure measurements in scala tympani or scala vestibuli alone, or the pressure differences between the two scalae.

Conclusion

These result suggest that in applications stimulating the ossicles measurements in only one scala is sufficient to evaluate actuator output in temporal bones.

PS 1048

Effect of static loading forces on actuator output, conductive losses and guidance for effective coupling

Martin Großöhmichen[1]; **Ute Alice Gamm**[2]; Thomas Lenarz[3]; Hannes Maier[1]
[1]Department of Otolaryngology, Hannover Medical School, Germany; Cluster of Excellence; [2]Cochlear Deutschland GmbH & Co. KG; [3]Department of Otolaryngology, Hannover Medical School, Germany and DFG Cluster of Excellence Hearing4all

Introduction

Instructions for implantation of the Cochlear™ Carina™ active middle ear implant include the use of a transducer loading assistant that measures the impedance of its actuator (T2) at the resonance frequency. Upon contact with the incus, the actuator impedance drops by at least 50 Ω and for best coupling results the manufacturer recommends to advance the actuator forward by a quarter turn of the adjustment screw (63μm). It has not been investigated yet which static loading forces are applied to the incus following these instructions, furthermore, it is unknown which consequences higher or lower forces have on coupling efficiency. In this study we aimed to close this knowledge gap and performed an extensive investigation of loading forces on actuator coupling efficiency and normal sound transmission via the ossicular chain, and the potential to use electric actuator impedance measurements as loading guidance.

Methods

The T2 actuator was coupled to a force sensor attached to a micromanipulator. Incus coupling was investigated at static loading forces up to 100 mN in 14 human temporal bones. Actuator output was measured through laser Doppler vibrometric measurement of stapes motion for a frequency range between 100 Hz and 10 kHz. The actuator output was expressed as equivalent free field sound pressure levels at 1 Vrms actuator input. Additionally we investigated whether high loading forces would induce conductive losses by measuring changes in stapes motion in response to the acoustic input to the tympanic membrane. Furthermore actuator impedance over the whole frequency spectrum was measured for each loading force to investigate the validity of direct electrical impedance measurements during surgical implantation as feedback tool for coupling efficiency.

Results

Loading forces below 1 mN did not lead to effective coupling and maximum coupling efficiency was observed at forces above 10 mN. Additionally no decrease in actuator output was observed for high loading forces (10-100 mN). Conductive losses were not observed for static loading forces up to 100 mN. Impedance measurements showed a rapid decrease of the actuator resonance peak upon coupling to the incus which completely vanished at 5-10 mN loading forces.

Conclusion

Above a minimum coupling force of 10 mN, the T2 actuator has been shown to couple to the incus with high efficiency, and no conductive losses were observed even up to high forces. Direct electrical impedance measurements via the transducer loading assistant are a useful measure to indicate effective coupling.

Predicting clinical efficiency of the T2 actuator as Direct Acoustic Cochlear Implant (DACI) from measurements of intracochlear pressure in cadaver ears

Ute Alice Gamm[1]; Martin Großöhmichen[2]; Bernd Waldmann[1]; Thomas Lenarz[3]; Hannes Maier[2]
[1]*Cochlear Deutschland GmbH & Co. KG; [2]Department of Otolaryngology, Hannover Medical School, Germany; Cluster of Excellence; [3]Department of Otolaryngology, Hannover Medical School, Germany and DFG Cluster of Excellence Hearing4all*

Introduction
The Cochlear™ Carina™ active middle ear implant (AMEI) has regulatory approval for coupling to incus, stapes head and round window. In this cadaver study we explored the potential for future use of the Carina actuator in a Direct Acoustic Cochlear Implant (DACI) configuration. We used intracochlear pressure difference (ICPD) measurements in human temporal bones to predict actuator output of the T2 in a DACI configuration and compared results with to experimentally determined actuator output in the Cochlear™ Codacs™ DACI.

Methods
Twenty-two temporal bones were implanted with the Codacs actuator and intracochlear pressure differences measurements were used to determine actuator output for a frequency range between 100 Hz and 10 kHz. The actuator output was expressed as equivalent free field sound pressure levels at 1 Vrms, i.e. the free field sound pressure stimulation level that is necessary to elicit the same intracochlear signal as stimulation via an actuator driven with 1V. Fourteen of the twenty two temporal bones were subsequently stimulated with Carina's T2 actuator with a customized piston which describes the same angle as the artificial incus and piston of the Codacs™ implant.

Results
Median of 22 Codacs actuator output values was 115 dB SPLeq at 100 Hz and decreased slightly to 100 dB SPLeq at 1000 Hz. A small peak of 111 dB SPLeq was visible at 2000 Hz. In comparison, the median output of 14 T2 actuators was slightly lower and rather flat with maximum values of 108 dB SPLeq and minimum values of 97 dB SPLeq and no pronounced peak.

Conclusion
By attaching a customized piston to the T2 actuator we were able to stimulate cochlear liquid in a similar way to Codacs direct acoustic cochlear stimulation. Output of the T2 actuator was observed to be only slightly lower that Codacs output. From these results we can conclude that the Carina T2 actuator, with an appropriate coupling element, is capable of being used in a DACI configuration.

Modelling Round-window Hearing Stimulation with a Piezoelectric Disc Actuator

Ainhitze Mendizabal[1]; Daniela Wildenstein[1]; Andreas Wagner[1]; Anthony W. Gummer[2]; Ernst Dalhoff[2]
[1]*Section of Physiological Acoustics and Communication, University of Tübingen; [2]University of Tübingen*

Background
Patients with conductive or mixed conductive-sensorineural hearing loss are often unable to use or receive significant benefit from conventional hearing aids due to medical conditions or insufficient amplification. Active Middle Ear Implants (AMEI) can potentially solve these problems, since they do not occlude the ear canal and also bypass a pathologic middle ear. AMEI are surgically inserted into the middle ear to produce vibrations that are mechanically coupled to the auditory organ.

In this work, a lumped-element circuit is used to model reverse stimulation of the cochlea and the ensuing middle-ear vibrations when the round window is driven by a piezoelectric thin-film actuator furnished with a silicone cap.

Methods
Experimental vibration data for the actuator were obtained using a Laser Doppler vibrometer under well-defined load conditions, in human temporal-bone experiments where the actuator drives the cochlea and the middle-ear from reverse at the round window. Middle-ear vibrations were also measured in response to sound-pressure stimulation of the eardrum.

Model parameters were fitted in separate steps to series of experiments of different load and stimulus conditions.

Results
Simulations show that the developed analytical model describes the performance of the piezoelectric actuator acting on the round window membrane as well as the coupling to the anatomical structures, in fair agreement with the experimental data up to frequencies of 10 kHz.

Conclusion
The model enables analysis of coupling losses in individual experiments and optimization of the actuator, its fixation, and the silicone cap.

Feedback pathways in patients with a direct acoustic cochlear implant

Bernd Waldmann[1]; Eugen Kludt[2]; Thomas Lenarz[3]; Hannes Maier[4]

[1]*Cochlear Deutschland GmbH & Co. KG;* [2]*Hannover Medical School;* [3]*Department of Otolaryngology, Hannover Medical School, Germany and DFG Cluster of Excellence Hearing4all;* [4]*Department of Otolaryngology, Hannover Medical School, Germany; Cluster of Excellence*

Introduction

In some of the patients with the Cochlear™ Codacs™ Direct Acoustic Cochlear Implant implanted at Hannover Medical School, feedback squealing was observed when the device was programmed for prescription gain. Possible pathways for feedback are: (i) air-conducted sound radiated by the actuator, and passed via ear drum and ear canal to the behind-the-ear (BTE) processor, or bone vibration emanating from (ii) the actuator mounting system or (iii) the cochlea itself, which propagates to the surface of the skull and vibrates the BTE processor. In order to decide on a mitigation strategy for those cases, as well as understanding the phenomenon, we performed a series of qualitative observations designed to discriminate between these hypotheses regarding feedback pathway, as well as quantitative measurements of sound and feedback transfer function.

Methods

Tests were performed on 6 ears (6 patients) with feedback issues, and an additional 6 ears (4 patients) without. Qualitative tests: we observed whether feedback was audible for the subject and for the investigator, in multiple conditions: (a) BTE processor in regular position, (b) lifted off the ear, which should disrupt vibration pathways, (c) placed on contralateral ear, which should disrupt air conduction pathways, and (d) in regular position, but with the ear canal blocked with a foam eartip, which should disrupt air conduction feedback through the ear canal. Quantitative measurements: an Etymotics ER-7C probe microphone was used to measure sound near the microphone port of the BTE processor while driving the implant with a test signal. The BTE microphone signal itself was also recorded in response to the actuator test signal, this enabled calculation of the maximum stable gain.

Results

Observations regarding audibility of feedback in the four conditions are consistent with a hypothesis of an air conduction feedback path (sound from actuator – ear drum – ear canal – processor) or a mixed air and bone conduction feedback path (vibration from actuator or co-chlea – skin radiates sound – processor), and were not consistent with a pure bone conduction path (vibration from actuator or cochlea – vibration of skull – vibration of processor). Maximum stable gain in the no-issues group was 50-70 dB, but in the group with feedback issues as low as 20-30 dB at some frequencies.

Conclusion

The dominant feedback pathway with the direct acoustic cochlear implant is via airborne sound.

Silk Multi-Layered Scaffold for Tympanic Membrane Tissue Engineering

Filippo Valente[1]; Ben Allardyce[2]; Philip Wijesinghe[3]; Brendan Kennedy[3]; Lawrence Liew[1]; Hsern Ern Tan[1]; Xungai Wang[2]; Marcus Atlas[4]; Rodney Dilley[4]

[1]*Ear Science Institute Australia;* [2]*Institute for Frontier Materials, Deakin University;* [3]*BRITElab, The University of Western Australia;* [4]*Ear Sciences Centre, The University of Western Australia, Nedlands, Australia*

Background

The integrity of the tympanic membrane is essential for hearing function: chronic perforations can produce hearing loss and serious complications. Driven by persistent failure rates for conventional surgical methods, we have developed novel tissue engineering scaffolds for tympanic membrane repair. Silk fibroin-based biomaterials have a broad range of applications, with proven biocompatibility, excellent acoustic energy transfer and high tensile strength. The aim of the present study was to evaluate an innovative protein crosslinking method to enable rapid prototyping of silk devices that can support the growth of specific cell types.

Methods

Silk fibroin solution was combined with a photo-crosslinking agent exposed to light to create solid silk films. Stability of the film over two weeks in culture and under rapid degradation conditions were assessed using optical coherence tomography (OCT). Two different human cell lines, HaCaT (keratinocytes) and skin fibroblast, were cultured on different crosslinked silk scaffolds and their growth assessed by molecular biology and microscopy.

Results

Films of varying thickness and stiffness could be rapidly formed with this method and dried to make a transparent, stable and durable solid film. Using various soluble porogens we created porous films and delivered them onto a preformed solid film to make multi-layered composite devices, to model tympanic membrane. In vitro

models showed that these tympanic membrane scaffolds supported culture of keratinocytes on solid layers and fibroblasts in porous layers. Analysis of OCT images was able to detect dimensional changes of the device in routine culture. The crosslinked scaffolds retained their shape and physical characteristics during cell culture. Some material compositions underwent swelling immediately upon wetting but maintained dimensional stability over the longer period. With enzymatic degradation the rate of material loss over time was dependent on composition, so we were able to generate rapidly degrading devices and long-term stable devices. In vitro models of tympanic membrane supported two cell lines of the eardrum. It was easily handled while supporting the cell growth.

Conclusions

This production method allowed the design of stable silk structures with tuneable degradation properties. The method has potential to revolutionize rapid prototyping for surgical reconstruction applications in the ear and the technology developed could be applied also to ocular and skin tissue engineering.

PS 1053

Osteogenesis for Postoperative Temporal Bone Defects Using Human Ear Adipose-derived Stromal Cells and Tissue Engineering: an animal model study

Oak-sung Choo[1]; Beomyong Shin[2]; Seung Won Kim[3]; Xiang Yun Yin[4]; Byoung Hyun Min[4]; Jeong Hun Jang[1]; Yun-Hoon Choung[1]
[1]*Department of Otolaryngology, Ajou University School of Medicine, Suwon, Republic of Korea;* [2]*Department of Otolaryngology, Ajou University School of Medicine;* [3]*Department of Burns and Plastic Surgery, Hospital of Yanbian University;* [4]*Department of Orthopedic Surgery, Ajou University School of Medicine*

Mastoidectomy, the removal of infected mastoid bones, is a common surgical procedure for the treatment of chronic otitis media. Persistent and recurrent otorrhea and accumulation of keratin debris following open cavity mastoidectomy are still bothersome issues for both patients and otologists. In this study, we used human ear adipose-derived stromal cells (hEASCs) in combination with polycaprolactone (PCL) scaffolds and osteogenic differentiation medium (ODM) to regenerate temporal bone defects. The hEASCs showed stem cell phenotypes, and these characteristics were maintained up to passage 5. Mastoid bulla and cranial bone defects were induced in Sprague-Dawley rats using $AgNO_3$ and burr hole drilling, respectively, and the rats were then divided into five groups: (1) control, (2) hEASCs, (3) hEASCs + ODM, (4) hEASCs + PCL scaffolds, and (5) hEASCs

+ PCL scaffolds + ODM. Osteogenesis was evaluated by micro-computed tomography and histology. Compared with the control group, the groups transplanted with hEASCs and PCL scaffolds had significantly higher bone formation along the periphery of the mastoid bulla area. Moreover, ODM synergistically enhanced bone formation in mastoid bulla defects. Our results suggest that combining hEASCs with PCL scaffolds represents a promising method for anatomical and functional reconstruction of postoperative temporal bone defects following mastoidectomy.

Molecular Landscape of Hearing Loss III

PS 1054

Copy Number Variants in the STRC Gene are a Common Cause of Moderate Hearing Loss in a Japanese Population

Hideaki Moteki[1]; Yoh Yokota[1]; Shin-ya Nishio[1]; Tomomi Yamaguchi[2]; Keiko Wakui[2]; Shin-ichi Usami[1]
[1]*Department of Otorhinolaryngology, Shinshu University School of Medicine;* [2]*Department of Medical Genetics, Shinshu University School of Medicine*

Background

Sensorineural hearing loss (SNHL) affects at least 1 in 1,000 newborns, with genetic causes accounting for 50-70% of all childhood hearing loss. Hereditary hearing loss is a genetically heterogeneous disorder with 89 causative genes and more than 2,000 identified disease causing mutations. The majority of those mutations are single nucleotide variants (SNVs) or small indels. Recently, copy number variants (CNVs) have been recognized as a major cause of genetic hearing loss. The STRC gene is a well-known deafness gene involved in autosomal recessive hearing loss (ARHL) resulting from a large deletion in chromosome 15q15.3. The interpretation of sequence data for the STRC gene is difficult due to the existence of the pseudo-STRC gene (pSTRC), which facilitates genomic alterations within the region. Massively parallel sequencing (MPS) has emerged as a powerful platform for the diagnosis of genetic hearing loss. We undertook CNV analysis of the STRC region using the MPS dataset and custom array CGH. The aims of this study were to elucidate the frequency of CNVs in the STRC region and their phenotypic features.

Methods

We examined DNA from 40 probands with SNHL segregated as autosomal recessive inheritance. We used the MPS platform, a social health insurance-approved method, to identify the genetic cause of hearing loss. We then performed CNV calling using two methods; 1) Ion reporter (Thermo Fisher Scientific) which was commercial application, and 2) read-depth approach we developed.

Both analyses were curated through manual inspection. The CNV results were confirmed with customized array comparative genomic hybridization (array CGH).

Results

We identified 23 probands with deafness-causing CNVs of the STRC genetic region. CNV analysis revealed that a deletion involving STRC and pseudogene with functionally null STRC. We also identified one copy loss involving STRC in the 42 probands that appear to be a carrier. Their audiograms showed congenital mild-moderate down-sloping hearing loss, and hearing loss phenotype was consistent with previously reported cases.

Conclusion

We identified CNVs of the STRC genetic region as an important cause of hearing loss. The present study indicated that a considerable number of deafness patients, particularly among mild-moderate ARHL patients, caused by CNVs in the STRC gene.

PS 1055

NLRP3 is Expressed in the Spiral Ganglion Neurons and Associated with both Syndromic and Non-syndromic Sensorineural Deafness

Penghui Chen; Hao Wu; Tao Yang
Department of Otolaryngology Head & Neck Surgery, The Ninth People's Hospital, Shanghai Jiao Tong University School of Medicine, Shanghai, China. Ear Institute, School of Medicine, Shanghai Jiao Tong University, Shanghai, China. Shanghai Key Laborato

Background

Non-syndromic deafness is genetically heterogeneous but phenotypically similar among many cases. Though a variety of targeted next-generation sequencing (NGS) panels has been recently developed to facilitate genetic screening of non-syndromic deafness, some syndromic deafness genes outside the panels may lead to clinical phenotypes similar to non-syndromic deafness.

Methods

All the affected family members received a clinical evaluation including pure tone audiometry. Targeted NGS and whole-exome sequencing were performed to identify the deafness gene and immunostaining of the mouse cochlea was to detect expression of the deafness gene in inner ear.

Results

No pathogenic mutation was identified by targeted NGS in 72 non-syndromic and another 72 syndromic deafness genes. Whole exome sequencing identified a p.E313K mutation in NLRP3, a gene reported to cause

syndromic deafness Muckle-Wells Syndrome (MWS) but not included in any targeted NGS panels for deafness in previous reports. Follow-up clinical evaluation revealed only minor inflammatory symptoms in addition to deafness in six of the nine affected members, while the rest three affected members including the proband had no obvious MWS-related inflammatory symptoms. Immunostaining of the mouse cochlea showed a strong expression of NLRP3 in the spiral ganglion neurons.

Conclusions

Our results suggested that NLRP3 may have specific function in the spiral ganglion neurons and can be associated with both syndromic and non-syndromic sensorineural deafness.

fig 1.pptx

fig 2.pptx

fig 3.pptx

fig 4.pptx

PS 1056

Characterization Of A New Mouse Model With A Non-Sense Mutation In LOXHD1/DFNB77

Nicolas Grillet; Alix Trouillet
Stanford University

We previously identified the gene LOXHD1 as responsible for an autosomal-recessive form of hearing loss in mice and human (Grillet N., AJHG, 2009). Interestingly all human DFNB77 patients have missense or frame-shift mutations, and present a large variability of the hearing loss onset. The gene LOXHD1 encodes a protein made of 15 PLAT (Polycystin Lipoxygenase Alpha-Toxin) domains and is expressed exclusively by hair cells. The LOXHD1 protein is found in the stereocilia and the cuticular plate, at the junction between membrane and the actin-cytoskeleton. The function of LOXHD1 is unknown. We hypothesize that LOXHD1 is necessary for the function of the hair bundle by forming a physical link between the membrane and the actin-core of the stereocilia.

The deaf Samba mutant mouse presents a missense mutation in the PLAT domain #10 of LOXHD1. However the protein is still found in the stereocilia bundle. Even in the adult animal, no major morphological defect is observed in the stereocilia bundle. We asked if truncating the LOXHD1 protein would induce a structural phenotype of the hair bundle. We generated a new mouse model for LOXHD1/DFNB77 where we introduced

a non-sense codon and deleted the exons coding for PLAT domain #10. We characterized the consequence of the presence of the nonsense mutation on the mRNA level by RT-PCR. The auditory phenotype was assessed by ABR and DPOAE and the hair cell morphology by Scanning Electronic Microscopy.

Results
The presence of a missense mutation in LOXHD1 induces mRNA splicing that skip the mutated exon. The spliced mRNAs of the mutant can produce either a truncated protein or a full protein missing only the PLAT domain#10. The morphology of the hair bundle is not affected by the missense mutation. The auditory phenotype of the mutants is comparable but with more variability between animals in the missense mutant. We conclude that the non-sense mutation in PLAT10 is slightly less deleterious than the missense mutation. We propose that this residual response is generated by the production of a full protein missing only the PLAT domain#10 by splicing. The Nonsense-associated altered splicing could participate in the variability of hearing loss onset of DFNB77 patients.

PS 1057

A Relational Database to Efficiently Manage and Analyze Diverse Auditory and Vestibular Data Sets

J. Beth Kempton; Dennis Trune; Edward Porsov; John V. Brigande
Oregon Hearing Research Center, Oregon Health & Science University

Background
Copious amounts of data can be generated from a single rodent during its participation in an auditory and vestibular study that tracks inner ear function longitudinally. For the study of autoimmune disease, a routine experimental subject may undergo multiple quantitative measures: auditory-evoked brainstem responses (ABR); hematocrit, anti-nuclear antibody titer, and immune complex levels; and tissue harvest for PCR-based assessments, histological analyses, or electron microscopy. For fetal gene therapy studies, a routine experiment involves: preoperative, operative, and postoperative care of the dam; parameters for the virus- or electroporation-mediated gene transfer, or the pharmacological agent delivered; genotyping; ABRs, distortion product otoacoustic emissions, compound action potentials, and startle reflex tests; balance assessments by Rota-Rod, open field, reaching, and swimming tests; and finally histological and ultrastructural analyses. The data set associated with a single mouse in a longitudinally-focused study is voluminous. To define an integrated data management solution for multiple users with diverse experimental responsibilities, we created a relational database to catalog all interventions throughout the life of each mouse.

Methods
The FileMaker Pro platform (FM Pro and FM Server) was adopted for ease of customization in developing database structure, mobile device capability, and the extensive online technical support. The OHSU Institutional Animal Care and Use Committee (IACUC) approved our use of the database under IACUC Protocol IS3723. A redundant database backup scheme was achieved with Retrospect software (version 12.5.0.177) and a Synology network associated server (DS2415+).

Results
The Animal Information Record is the fulcrum of the database management portal and holds core data such as mouse identification number, date of birth, strain, and gender (see attached Database Schema). The Animal Information Record links to the Survival Surgery, the Neurophysiology, and the Tissue Analysis Records as well as an integrated Calendar that presents daily workflow. Representative database records will demonstrate the content of each field and their connectivity. To date we have over 3,000 ABR records which are easily searchable by strain, age, and experimental intervention allowing access to historical records with ease.

Conclusions
We defined a relational database to manage mouse auditory and vestibular studies that satisfies IACUC compliance requirements; permits unfettered access to all of the data originating from an individual mouse; and allows construction of targeted searches to group auditory and vestibular neurophysiology data sets for quantitative analyses. This efficient management of data ensures that the minimum number of mice are used to cost-effectively complete an experimental trial.

Database Schema Kempton et al., 2018.pdf

PS 1058

Variations of the LOXHD1 Mutation and its Phenotypic Features

Karuna Maekawa; Shin-ya Nishio; Hideaki Moteki; Shin-ichi Usami
Department of Otorhinolaryngology, Shinshu University School of Medicine

Background
Hearing loss (HL) is one of the most common sensory impairments, observed in one in one thousand new-

borns, with the hearing loss in approximately half of them due to genetic factors. Approximately one hundred genes have been reported to be associated with inherited HL. The LOXHD1 gene, mapped on chromosome 18q12-21 and expressed in the mechanosensory hair cells of the cochlea and vestibule, is a known cause of DFNB77, a progressive form of autosomal recessive sensorineural hearing loss. Only a limited number of HL patients (11 patients from 9 pedigrees from various ethnic groups) have been reported to have mutations in this gene. LOXHD1 gene mutations present various phenotypic features in HL. This study was intended to elucidate the mutation spectrum of this gene as well as its phenotypes.

Methods
We conducted a study on 5,563 unrelated Japanese hearing loss patients, utilizing massively parallel DNA sequencing of 68 target genes, to identify the genomic variations responsible for HL. Among them, we selected 35 candidates who carried LOXHD1 probable pathogenic variants, and applied Sanger sequencing and segregation analysis using exon-specific custom primers to confirm those variations. To elucidate the genotypic-phenotypic correlations, we assessed the auditory brain stem response, pure-tone audiometry and computed tomography findings from the probands and their family members. Their vestibular symptoms and test results (e.g. electronystagmography and Caloric stimulation) were also collected.

Results
We successfully identified 12 probands with LOXHD1gene mutations, with seven of them showing likely pathogenic variants, five of which were novel variants. These probands showed a relatively similar phenotypic pattern with severe to profound HL, but presented no other symptoms or malformations, though several exceptions, e.g. progrssive HL, were also observed.

Conclusion
We identified 12 probands with HL due to LOXHD1mutations. Mutations in LOXHD1 are quite rare, with only a limited number of patients with associated HL reported to date. By continuing this research, we aim to more fully ascertain the properties of this gene, and apply this information in the treatment of patients.

PS 1059

Contribution of Changes in the Inner Ear to the Disease Processes Seen in the NPC1 Mouse

Joyce J. Repa[1]; Sarath Vijayakumar[2]; Timothy A. Jones[3]; **Karen S. Pawlowski**[1]
[1]UT Southwestern Medical Center; [2]University of Nebraska-Lincoln; [3]University of Nebraska, Lincoln

Hearing loss has been linked to abnormal cholesterol metabolism for some time, with little direct evidence of their association. Now, with a wealth of available animal models, improvement in assessment techniques and collaborative efforts from many different areas of expertise, a link between cholesterol balance and hearing is emerging. Early-onset hearing loss and inner ear pathology have been demonstrated in the debilitating cholesterol storage disease, Niemann-Pick disease, type C1 (NPC1, King, et al, 2014 PMID 24839095). We will present additional data on the pathologic changes in the inner ear of the NPC1 mouse model (BALB/cNctr-Npc1m1N/J strain, Npc1-/-, KO) and discuss the contribution of these changes to the observed hearing loss and vestibular dysfunction. Existing evidence shows KO mice demonstrate abnormal auditory brainstem response (ABR) thresholds by 20 days of age (P20) that progressively worsen. New information shows ABR responses at P15 are also elevated in KO mice and by P70 responses in KO mice are elevated across all frequencies tested. Amplitudes and latencies for wave I-III in KO mice are similar to WT mice at P20, indicating the early changes are non-neural, arising from within the cochlea. By P65, KO mice have significantly longer latencies than controls for all the waveforms, indicating a worsening neural condition along the auditory system. DPOAEs are present, but significantly smaller in KO versus WT mice at P20 and, although amplitudes increase for all groups over time, differences between KO and WT mice remain. Differences in vestibular sensory-evoked potentials (VsEP) between KO and WT mice are also apparent by P39-57. Prolonged response latencies with little change in interpeak intervals indicate an effect on the peripheral nerve. Cochlear changes in the spiral ganglion of KO mice are present at P30. Over time, an accumulation of lipophilic inclusions develops within the organ of Corti and stria vascularis. Changes in the vestibular ganglion in KO mice, specifically swelling of nerve calyxes, also appear by P30. Cochlear pathology in this mouse appears to be occurring prior to changes in the central auditory system. This could also be the progression pattern for the vestibular apparatus. However, there is clear pathology in the Purkinje cells within the cerebellum by 3-4 weeks of age. This and the presence of swelling of the afferent nerve calyces at P30 suggests a combined central and peripheral neural loss.

What Rescues Partial Hearing in Human Connexin26-linked Hearing Impairment

Hongyang Wang[1]; Jing Guan[2]; Monkol Le[3]; Jun Shen[4]; Zheng-Yi Chen[5]; Qiuju Wang[2]
[1]Eaton Peabody Lab, MEEI, Harvard Medical School/ Chinese PLA General Hospital; [2]Chinese PLA General Hospital; [3]Broad Institute; [4]Harvard Medical School Center for Hereditary Deafness; [5]1. Department of Otolaryngology, Harvard Medical School, 2. Eaton Peabody Laboratory, Massachusetts Eye and Ear Infirmary

Background

Pathogenic variants in GJB2, which encodes the gap junction protein Connexin 26, are responsible for the most common form of autosomal recessive non-syndromic hearing loss (DFNB). Among over 300 GJB2 variants associated with hearing loss, 235delC is the most common one in some East Asian populations, with a carrier frequency of 1%. A majority of patients homozygous for GJB2 235delC manifest pre-lingual severe to profound hearing impairment. Here we report a family in which all six affected members in three generations manifest delayed moderate hearing loss despite being GJB2 235delC homozygotes and the study to identify the possible mechanism underlying the phenotype.

Methods

Mutation screening of GJB2 was performed on all ascertained six affected members from three generations from one family and three sporadic cases by polymerase chain reaction (PCR) amplification and Sanger sequencing. Targeted capture and next-generation sequencing (NGS) of the coding and splicing regions of 307 hearing loss related genes was carried out on affected probands to explore additional genetic variants. Whole genome sequencing (WGS) was performed on six individuals (three affected and three unaffected) from the family. Reverse transcriptase–quantitative PCR was conducted on some of these cases by extracting RNA from white cells to study expression of GJB6 (Connexin30).

Results

Mutation screening identified GJB2 235delC homozygous mutations in all six affected members of a Chinese family with autosomal recessive hearing loss. The affected members have delayed onset (4-5 years of age) hearing loss that became moderate to severe at later stage (50-60 years of age). We further identified three sporadic GJB2 235delC homozygous cases with delayed onset moderate hearing impairment. Targeted NGS did not detect any single nucleotide variant, small insertions or deletions among 307 deafness genes in any of the GJB2 235delC homozygotes. Overexpression of GJB6 in some of these cases was detected. By WGS of six family members we identified a distinct haplotype of 92kb marked by a private non-coding 6 bp deletion in the genomic region surrounding the GJB2 locus. This haplotype is shared among the affected family members but not in 15 East Asian alleles carrying 235delC in the Genome Aggregation Database. Samples from patients with congenital profound hearing loss who are homozygous for 235delC will be tested to compare the haplotype

Conclusion

1) Identification of multiple affected members with delayed onset moderate to severe hearing loss reveals phenotypic heterogeneity in hearing loss caused by GJB2 235delC homozygosity.

2) WGS study may enable us to identify genetic modifier(s) whose function may delay the onset and reduce the severity of congenital profound hearing loss generally associated with GJB2 235delC homozygosity, with implications for the development of potential therapy to target hearing loss caused by GJB2 deficiency.

Whole Exome Sequencing of Thirty Adults with Different Patterns of Adult Onset Hearing Loss

Morag Lewis[1]; Lisa Nolan[2]; Barbara Cadge[3]; Lois Matthews[4]; Bradley A. Schulte[4]; Judy R. Dubno[4]; Karen Steel[5]; Sally Dawson[3]
[1]King's College London; [2]UCL Ear Institute; [3]University College London; [4]The Medical University of South Carolina; [5]King's College London and Wellcome Trust Sanger Institute

Hearing loss is one of the most common sensory deficits in the human population, and it has a strong genetic component. However, although to date more than 140 loci relating to human hearing loss have been mapped, and over 100 genes identified, the vast majority of genes involved in hearing remain unknown. In order to explore the landscape of variation associated with hearing loss, we sequenced the exomes of thirty patients selected for distinct phenotypic sub-types from well-characterised cohorts of 1479 people with adult-onset hearing loss. After sequencing, variants were called with SAMtools and Dindel, and filtered based on quality, frequency in the non-Finnish European population, predicted consequence and predicted severity of impact. We examined the results for genes which carried mutations in more than one individual and also compared them to a list of genes known to be associated with deafness in mice or humans.

From these comparisons, we have identified multiple candidate mutations for further investigation and follow-up. We also found that every patient carried predicted pathogenic mutations in at least ten deafness-associated genes; similar findings were obtained from an analysis of the 1000 Genomes Project data unselected for hearing status. The high frequency of predicted-pathogenic mutations in known deafness-associated genes in the population was unexpected and has significant implications for current diagnostic sequencing in deafness. Our results illustrate the complexity of genetic contributions to hearing loss and the power of stratified analysis in complex disease to identify candidate variants for further study.

PS 1062

Mitochondrial tRNA mutations in 894 Chinese Han subjects with Hearing Loss

Jing Zheng[1]; Min-Xin Guan[2]
[1]*Northwestern University;* [2]*Zhejiang University*

Mutations in the mitochondrial tRNAs have been associated with hearing loss. However, the prevalence and spectrum of mitochondrial tRNA mutations in patients with hearing loss remain poorly understood. In this report, we have investigated the mutational frequency and spectrum of 22 mitochondrial tRNA genes in a cohort of 894 Han Chinese subjects with hearing loss. A total of 147 variants (142 known and 5 novel) on 22 tRNA genes were identified by next generation sequencing sequencing analysis. These variants were further evaluated for the pathogenicity using criteria as follow: (1) present

Guan abstract 3.docx

PS 1063

Hereditary Hearing Loss in the Slovak Roma Population: Still a Mystery?

Lukas Varga[1]; Ivica Masindova[2]; Daniel Danis[2]; Martina Skopkova[2]; Lucia Demesova[1]; Livia Majernikova[1]; Zuzana Slobodova[1]; Milan Profant[1]; Daniela Gasperikova[2]
[1]*Department of Otorhinolaryngology—Head and Neck Surgery, Faculty of Medicine and University Hospital, Comenius University;* [2]*Biomedical Research Center, Slovak Academy of Sciences*

Background

Roma (Gypsy) people represent about 8% of the total population of Slovakia. Most of them live in isolated communities, characterized by high degree of consanguinity. In a number of Slovak Roma settlements, sensorineural hearing loss (SNHL) is among the most common chronic disorders with obvious hereditary pattern. Routine genetic testing, however, has much lower yield of confirmed etiology than in the majority (Caucasian) population. The aim of our research is to identify genetic causes contributing to SNHL in this unique population.

Methods

Samples of whole blood were collected at boarding schools for deaf children throughout Slovakia or directly in selected Roma settlements. DNA analysis in probands included direct sequencing of GJB2 gene in all cases, followed by testing for common GJB6 deletions (D13S1830 and D13S1854) by multiplex PCR and MARVELD2 by direct sequencing in GJB2 wild type subjects or heterozygotes. Ten individuals from seven families with no mutation found in aforementioned genes were selected for whole exome sequencing (WES). The WES data were filtered using a virtual gene panel of 179 hearing loss related genes in human and mice. Hearing loss phenotype in the affected subjects was evaluated from the available patients´ clinical files, and by otoscopy, OAE and pure tone audiometry.

Results

Our cohort included 338 Roma individuals from affected families (138 probands and 200 family members). Biallelic GJB2 mutations accounted for deafness in 29 (21%) families, with mutations c.71G>A and c.35delG detected in the majority of the cases. Subsequently, of the 69 tested probands, we only identified 3 (4.4%) harboring biallelic mutation in MARVELD2 gene (c.1331+2T>C). None of the tested patients carried any of the analyzed GJB6 deletions. Of the 7 probands selected for the WES virtual panel analysis, we detected 2 with candidate variants in TSPEAR and KCNQ4 genes. In additional five probands, the whole exome sequencing revealed no pathogenic variants in 179 known deafness genes.

Conclusion

Apart from GJB2 gene, to date we were not able to identify any other common genetic cause of deafness in our Roma population. The preliminary results of WES analysis in the first 7 families indicate that focusing on known deafness genes may not be sufficient approach in this ethnicity and further search out of the virtual panel is necessary to identify candidate deafness genes. Supported by APVV-15-0067, VEGA 1/0214/16.

PS 1064

Genetic Screening for Hearing Loss: Characteristics of Infants who Passed and Failed the Newborn Hearing Screening - Preliminary Results

Christine D'Aguillo[1]; Denise Yan[2]; Xue-Zhong Liu[2]
[1]University of MIami; [2]University of Miami Miller School of Medicine, Department of Otolaryngology

Background
The Universal Newborn Hearing Screening (UNHS) uses otoacoustic emissions testing and auditory brainstem response testing to screen all newborn infants for hearing loss (HL), but may not identify infants with mild, late onset, or progressive HL. Advances in genetic technology have made it feasible to screen large populations of infants for hundreds of mutations for HL and could supplement the current UNHS.

Objective
1) Identify the characteristics of infants who passed and failed the UNHS and later developed HL. 2) Characterize the specific mutations for HL in infants who passed and failed the UNHS.

Methods
Children with sensorineural HL and documented UNHS results were recruited for the study. Retrospective chart review was done to identify characteristics of HL. Saliva was collected from each patient for genetic analysis. Probands were tested for 9 common mutations among Caucasian populations using the CapitalBioMiamiOto Array chip and verified with Sanger sequencing. If no mutations were identified, probands were analyzed using MiamiOtoGenes panel, which screens for 180 known deafness causing genes.

Results
At this time, 21 children have been enrolled. 13 children passed the UNHS and 8 children failed. The mean age of HL diagnosis in the "pass" group is 3.2 years old and the mean age in the "fail" group is 1.9 years old. Eight mutations were identified in total, 4 in "pass" probands and 4 in "fail" probands. Four mutations were pathogenic mutations and 4 were heterozygous mutations or polymorphisms. The overall mutation detection rate was 38.1% (n=8). Pathogenic mutations were identified in 23.1% (n=3) of "pass" patients. Among UNHS "pass" patients, the mutation detection rate was 19.0% (n=4).

Conclusion
In this small cohort, eight mutations were identified. Four mutations were identified in "pass" probands, and three of these were pathogenic. Mutations in rare genes were more commonly seen in "pass" probands. Ultimately, genetic screening may supplement UNHS by identifying HL in infants who might otherwise go undetected.

PS 1065

FDXR mutations cause sensorial neuropathies and expand the spectrum of mitochondrial Fe-S synthesis diseases

Antoine Paul[1]; Anthony Drecourt[2]; Floriane Petit[2]; Delphine Dupin Deguine[3]; Cécile Masson[2]; Crystel Bonnet[4]; Saber Masmoudi[5]; Isabelle Mosnier[6]; Laurence Mahieu[7]; Didier Bouccara[6]; Josseline Kaplan[8]; Georges Challe[9]; Christelle Domange[10]; Fanny Mochel[11]; Oliviers Sterkers[6]; Sylvie Gerber[8]; Christine Bole-Feysot[2]; Agnès Rötig[2]; Agnès Delahodde[12]; Sandrine Marlin[13]
[1]Laboratory of Embryology and genetics of human malformation, INSERM UMR1163, Institute of Genetic Diseases, Imagine; [2]INSERM laboratory, UMR1163, Institut Imagine, Université Paris Descartes, Sorbonne Paris Cité; [3]Department of Medical Genetics, Purpan Hospital; [4]UMRS 1120, Institut de la Vision; [5]Laboratory of Molecular and Cellular Screening Processes, Center of Biotechnology of Sfax; [6]Department of Otolaryngology, Pitié-Salpêtrière hospital, APHP; [7]Ophthalmology department, Rangueil Hospital; [8]Laboratory of Genetics in Ophthalmology, INSERM UMR1163, Institute of Genetic Diseases, Imagine, Paris Descartes University; [9]Department of Ophthalmology, Pitié-Salpêtrière Hospital, APHP; [10]Department of Otolaryngology, Lariboisière Hospital; [11]Department of Medical Genetics, Pitié-Salpêtrière Hospital, APHP; [12]Institute for Integrative Biology of the Cell (I2BC), CEA, CNRS, Univ. Paris-Sud, Université Paris-Saclay; [13]Necker Enfants Malade Hospital, APHP, Laboratory of Embryology and genetics of human malformation, INSERM UMR1163, Institute of Genetic Diseases, Imagine, Paris Descartes University

Hearing loss and visual impairment in childhood have mostly genetic origins, some of them being related to sensorial neuronal defects. Here, we report eight subjects from four independent families presenting with auditory neuropathy and optic atrophy. Whole-exome sequencing revealed biallelic mutations in FDXR in affected subjects of each family. FDRX encodes the mitochondrial ferredoxin reductase, the sole human ferredoxin reductase which is implicated in the biosynthesis of iron-sulfur clusters (ISC) and in the heme formation. ISC proteins are involved in enzymatic catalysis and gene expression, DNA replication and repair. We observed deregulated iron homeostasis in FDXR mutant fibroblasts and indirect evidence of mitochondrial iron overload. Functional complementation in a yeast strain deleted for ARH1, the human FDXR ortholog, estab-

lished the pathogenicity of these mutations. These data emphasize the wide clinical heterogeneity of mitochondrial disorders related to ISC synthesis.

Figure 1.docx

PS 1066

Application of next-generation sequencing to identify mitochondrial mutations: report on m.7511T>C in hearing loss patients

Monika Oldak[1]; Agnieszka Pollak[2]; Urszula Lechowicz[1]; Agnieszka Fraczak[2]; Małgorzata Rydzanicz[3]; Piotr Stawiński[2]; Artur Lorens[4]; Piotr H. Skarżyński[5]; Henryk Skarżyński[6]; Rafał Płoski[7]
[1]Department of Genetics, Institute of Physiology and Pathology of Hearing, Warsaw, Poland; [2]Department of Genetics, Institute of Physiology and Pathology of Hearing, Warsaw/Kajetany, Poland; [3]Department of Medical Genetics, Medical University of Warsaw, Warsaw, Poland; [4]epartment of Implants and Auditory Perception, Institute of Physiology and Pathology of Hearing, Warsaw/Kajetany, Poland; [5]World Hearing Center, Institute of Physiology and Pathology of Hearing, Warsaw/Kajetany, Poland; Department of Heart Failure and Cardiac Rehabilitation, Second Faculty, Medical University of Warsaw, Warsaw, Poland; Institute of Sensory Organs, Kajet; [6]Oto-Rhino-Laryngology Surgery Clinic, Institute of Physiology and Pathology of Hearing, Warsaw/Kajetany, Poland; [7]Department of Medical Genetics, Warsaw Medical University, Warsaw, Poland

Interruptions in the activity of mitochondria induced by mutations in the mitochondrial genome (mtDNA) can be the source of numerous diseases including hearing loss (HL). One of the mitochondrial variants responsible for HL is m.7511T>C mutation located in the MT-TS1 gene. Next-generation sequencing was used to search for the HL mutations in the whole mtDNA in two patients with maternal type of inheritance and real time PCR was applied for population screening of the m.7511T>C mutation in a group of 1644 HL patients. Sequencing of the whole mtDNA in two probands revealed a homoplasmic m.7511T>C mutation. Inheritance of the m.7511T>C mutation has been confirmed in examined matrilineal relatives in both families. The mean age of HL onset was 14.1 y.o. with the mean degree of HL equaling 74.8 dB. Large-scale searching for the m.7511T>C mutation among HL patients allowed us to establish the frequency of m.7511T>C mutation at 0.12% among Polish HL patients. In conclusion, this first report on central European patients harboring the m.7511T>C mutation reveals that the m.7511T>C shall not be forgotten when diagnosing patients with maternally inherited HL.

PS 1067

Whole exome sequencing identifies TRIOBP pathogenic variants as a cause of post-lingual bilateral moderate-to-severe sensorineural hearing loss

Monika Oldak[1]; Agnieszka Pollak[2]; Urszula Lechowicz[1]; Victor Abel Murcia Pieńkowski[3]; Piotr Stawiński[2]; Joanna Kosińska[3]; Henryk Skarżyński[4]; Rafał Płoski[3]
[1]Department of Genetics, Institute of Physiology and Pathology of Hearing, Warsaw, Poland; [2]Department of Genetics, Institute of Physiology and Pathology of Hearing, Warsaw/Kajetany, Poland; [3]Department of Medical Genetics, Warsaw Medical University, Warsaw, Poland; [4]Oto-Rhino-Laryngology Surgery Clinic, Institute of Physiology and Pathology of Hearing, Warsaw/Kajetany, Poland

Background
Implementation of whole exome sequencing has provided unique opportunity for a wide screening of causative variants in genetically heterogeneous diseases including nonsyndromic hearing impairment. TRIOBP in the inner ear is responsible for proper structure and function of stereocilia and is necessary for sound transduction.

Methods
Whole exome sequencing followed by Sanger sequencing was conducted on patients derived from Polish hearing loss family.

Results
Based on whole exome analysis, we identified two TRIOBP pathogenic variants (c.802_805delCAGG, p.Gln268Leufs*610 and c.514G>T,p.Gly1672*, the first of which was novel) causative of nonsyndromic, peri- to postlingual, moderate-to-severe hearing loss in three siblings from a Polish family. Typically, TRIOBP pathogenic variants lead to prelingual, severe-to-profound hearing loss, thus the onset and degree of hearing impairment in our patients represent a distinct phenotypic manifestation caused by TRIOBP variants. The pathogenic variant p.Gln268Leufs*610 disrupts the TRIOBP-4 and TRIOBP-5 isoforms, whereas the second pathogenic variant c.514G>T,p.Gly1672* affects only TRIOBP-5.

Conclusions
The onset and degree of hearing impairment, characteristic for our patients, represent a unique phenotypic manifestation caused by TRIOBP pathogenic variants. Although TRIOBP alterations are not a frequent cause of hearing impairment, this gene should be thoroughly analyzed especially in patients with a postlingual hearing loss. A delayed onset of hearing impairment due to TRI-

OBP pathogenic variants creates a potential therapeutic window for future targeted therapies.

PS 1068

Further evidence for "gain-of-function" mechanism of DFNA5 related hearing loss

Hongyang Wang[1]; Jing Guan[2]; Qiuju Wang[2]
[1]Eaton Peabody Lab, MEEI, Harvard Medical School/ Chinese PLA General Hospital; [2]Chinese PLA General Hospital

Introduction

DFNA5 is the fifth locus of ADNSHL and the related gene is DFNA5 (no indication for its function, so the gene was called DFNA5 for now), only 6 splice-site variations have been reported to be pathogenic for hearing loss up to date. Here we reported a novel and a known DFNA5 splice-site mutations in two large autosomal dominant non-syndromic hearing loss families, as well as a DFNA5 novel benign frameshift variation, further supporting the gain-of-function mechanism of DFNA5 related hearing impairment.

Methods

After excluding common deafness related genes in China, members from Family 1007208, Family 1007081 and a sporadic case with hearing loss were performed next generation sequencing. Candidate genes mutations were verified by polymerase chain reaction (PCR) amplification and Sanger sequencing on all of the ascertained members in these families. Reverse transcriptase-quantitative PCR was conducted on the proband from Family 1007208 by extracting RNA from peripheral blood to test how the splice-site mutation affects the transcription in RNA level.

Results

A novel heterozygous splice-site mutation c.991-3C>A in DFNA5 was found in Family 1007208, and a known recurrent heterozygous splice-site mutation c.991-15_991_13delTTC was identified in Family 1007081. Both of the splice-site mutations were segregated with the hearing loss phenotype, leading to the skipping of exon 8 at RNA level. In addition, a novel DFNA5 frameshift variation c.116_119delAAAA was found in the sporadic case, but was not segregated in the family.

Conclusion

We identified a novel and a known DFNA5 splice-site mutation in two Chinese ADNSHL Families, which is supposed to be pathogenic, and a novel DFNA5 frameshift mutation in a sporadic case, which does not the cause for the hearing loss case. All of the two pathogenic splice-site mutations and the nonpathogenic frameshift

variation provide further support for the specific gain-of-function mechanism of DFNA5 related hearing loss.
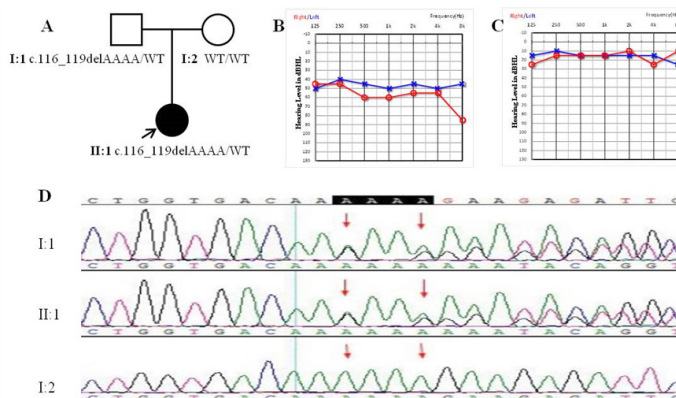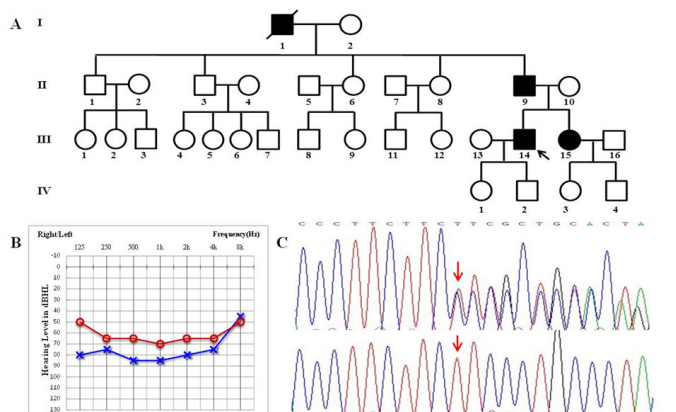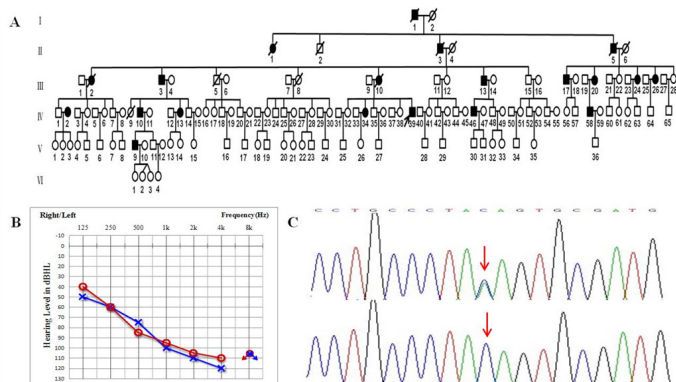
PS 1069

Detection of De novo Chromosome 2q36.1q36.3 Interstitial Deletion Involving 17 Genes in a Family with Syndromic Hearing Loss via WES and SNP-array

Jing Guan[1]; Hongyang Wang[2]; Linwei Yin[1]; Lidong Zhao[1]; Dayong Wang[1]; Qiuju Wang[1]
[1]Chinese PLA General Hospital; [2]Eaton Peabody Lab, MEEI, Harvard Medical School/Chinese PLA General Hospital

Objective

To detect and confirm genetic diagnosis in a family of

one affected individual with severe syndromic hearing loss who has normal parents and to assess recurrence risk and genetic counseling.

Methods
The family was recruited subject to informed consent as approved and underwent clinical evaluation. The subjects underwent a full medical history and comprehensive audiological evaluation, including otoscopic examination, pure-tone audiometry, tympanometry, acoustic reflex, distortion product evoked otoacoustic emissions (DPOAEs), and auditory brainstem responses (ABRs). The proband additionally underwent rotational chair testing (RCT) and colic vestibular evoked myogenic potential (cVEMP) testing. Temporal bone CT and cranial MRI scans were also performed. We performed conventional cytogenetic analysis on the peripheral blood lymphocytes and whole exome sequencing (WES) and SNP array analysis on DNA samples from the family. The microarray scanning profiles were processed by Agilent Feature Extraction 10.7.3.1. The extracted data was analyzed and plotted by Agilent Workbench 7.0. ADM-2 was selected as statistical algorithm with the threshold of 6.0 and the Fuzzy Zero turning on. Each CNV was called by at least four consecutive probes with log_2Ratio (fluorescence value ratio of subject-associated Cy5 to control-associated Cy3) consistent with deletion or duplication. The CNV records archived in Database of Genomic Variants were used as references to exclude common CNVs in human populations and help identified rare CNVs that may cause the clinical conditions in our pedigree.

Results
The affected subject was a 5-year-old boy who presented with bilateral profound sensorineural hearing loss, mental retardation, developmental delay, dystopia canthorum, congenital camptodactyly, low set ears and facial dysmorphism. The temporal bone CT and cranial MRI were all normal. RCT assesses the vestibular ocular reflex (VOR) using gain, asymmetry and phase outcome variables. The RCT disclosed normal VOR for the proband. The parents were not consanguineous, and there was no familial history, aged 36 and 34 years for the father and the mother. Cytogenetic analysis showed a 46, XY karyotype. WES was performed and no likely pathogenic single nucleotide variants (SNVs) were subsequently confirmed. We confirmed the presence of 5.175 Mb heterozygous deletions on chromosome 2q36.1 to q36.3 in the proband using SNP-array. This deletion was not detected in the parents tested by the same SNP-array. The deletion occurred a de novo copy number variation (CNV) in the proband. Seventeen genes were located in the deleted segment including: EPHA4, PAX3, CCDC140, SGPP2, FARSB, MOGAT1, ACSL3, KCNE4, SCG2, AP1S3, WDFY1, MRPL44, SERPINE2, FAM124B, CUL3, DOCK10, KIAA1486. Among them PAX3 is involved in the several clinical characteristics of the proband. PAX3 is involved in the development of the central nervous system, somites, skeletal muscle, NC-derived lineages including cardiac tissue, melanocytes, and enteric ganglia.

Conclusion
Here we report the detection of deleterious CNVs of chromosome 2q in a severely syndromic hearing loss. These findings raise the potential that failure to identify SNVs may lead to the misinterpretation of genetic testing results. CNVs should not be uncommon considering of genomic variation. PAX3 is mainly involved in the several clinical characteristics of the proband. There is no obvious correlation between the PAX3 gene deleted, truncating, or missense nature of the mutation, its location, and the severity of the disease. The identification of genetic diagnosis in the proband is important in recurrence risk assessment.

PS 1070

A common SLC26A4-linked haplotype underlying non-syndromic hearing loss with enlargement of the vestibular aqueduct

Parna Chattaraj[1]; **Tina Munjal**[2]; Keiji Honda[3]; Nanna Rendtorff[4]; Jessica Ratay[1]; Julie Muskett[1]; Davide Risso[5]; Isabelle Roux[1]; Edward Gertz[6]; Alejandro Schaffer[6]; Thomas B. Friedman[7]; Robert J. Morell[3]; Lisbeth Tranebjaerg[4]; Andrew J. Griffith[1]
[1]Otolaryngology Branch, National Institute on Deafness and Other Communication Disorders (NIDCD), Bethesda, MD, USA; [2]Otolaryngology Branch, National Institute on Deafness and Other Communication Disorders (NIDCD), Bethesda, MD, USA; Department of Otolaryngology - Head & Neck Surgery, Stanford University School of Medicine, Palo Alto, CA, USA; [3]NIDCD/NIH; [4]Institute of Clinical Medicine, University of Copenhagen, The Panum Institute; Department of Otorhinolaryngology, Head & Neck Surgery and Audiology, Rigshospitalet; Department of Clinical Genetics, Rigshospitalet/ The Kennedy Center; [5]Laboratory of Communication Disorders, National Institute on Deafness and Other Communication Disorders (NIDCD), Bethesda, MD, USA; [6]Computational Biology Branch, National Center for Biotechnology Information, Bethesda, MD, USA; [7]Laboratory of Molecular Genetics, National Institute on Deafness and Other Communication Disorders (NIDCD), Bethesda, MD, USA

Background
Enlargement of the vestibular aqueduct (EVA) is the most common radiological abnormality in children with

sensorineural hearing loss. Mutations in coding regions and splice sites of the SLC26A4 gene are often detected in Caucasians with EVA. Approximately one-fourth of patients with EVA have two mutant alleles (M2), one-fourth have one mutant allele (M1) and one-half have no mutant alleles (M0). The M2 genotype is correlated with a more severe phenotype.

Methods

We performed genotype–haplotype analysis and massively parallel sequencing of the SLC26A4 region in patients with M1 EVA and their families.

Results

We identified a shared novel haplotype, termed CEVA (Caucasian EVA), composed of 12 uncommon variants upstream of SLC26A4. The presence of the CEVA haplotype on seven of ten 'mutation-negative'; chromosomes in a National Institutes of Health M1 EVA discovery cohort and six of six mutation-negative chromosomes in a Danish M1 EVA replication cohort is higher than the observed prevalence of 28 of 1006 Caucasian control chromosomes (p<0.0001 for each EVA cohort). The corresponding heterozygous carrier rate is 28/503 (5.6%). The prevalence of CEVA (11 of 126) is also increased among M0 EVA chromosomes (p=0.0042).

Conclusions

The CEVA haplotype causally contributes to most cases of Caucasian M1 EVA and, possibly, some cases of M0 EVA. The CEVA haplotype of SLC26A4 defines the most common allele associated with hereditary hearing loss in Caucasians. The diagnostic yield and prognostic utility of sequence analysis of SLC26A4 exons and splice sites will be markedly increased by addition of testing for the CEVA haplotype.

PS 1071

Exonic mutations and exon skipping: lessons learned from DFNA5

Kevin Booth[1]; Hela Azaiez[2]; Kimia Kahrizi[3]; Donghong Wang[2]; Yuzhou Zhang[4]; Kathy Frees[2]; Carla Nishimura[2]; Hossein Najmabadi[5]; Richard J. H. Smith[2]

[1]Molecular Otolaryngology and Renal Research Laboratories, Department of Otolaryngology—Head and Neck Surgery; Interdisciplinary Graduate Program in Molecular Medicine, Carver College of Medicine, University of Iowa; [2]Molecular Otolaryngology and Renal Research Laboratories, Department of Otolaryngology—Head and Neck Surgery, Carver College of Medicine, University of Iowa; [3]Genetics Research Center, University of Social Welfare and Rehabilitation Sciences; [4]Molecular Otolaryngology and Renal Research Laboratories, Department of Otolaryngology - Head & Neck Surgery, University of Iowa; [5]University of Social Welfare and Rehabilitation Sciences, Tehran Iran.

Mutations in the DFNA5 gene are responsible for postlingual and progressive autosomal dominant non-syndromic hearing loss (ADNSHL). Currently, all known pathogenic variants occur in the intronic regions surrounding exon 8 of DFNA5. These mutations alter essential RNA-splicing signals, resulting in dysregulation of exon 8 splicing. The loss of exon 8 at the mRNA level results in a deleterious constitutively active truncated protein.

To investigate the genetic cause of hearing loss segregating in five families with postlingual, progressive ADNSHL, we employed two next generation sequencing platforms: OtoSCOPE and Whole Exome Sequencing. Variant filtering and prioritization based on minor allele frequency and functional consequence were achieved using a customized bioinformatic pipeline. The predicted effects of candidate variants on splicing were computationally assessed using Human Splicing Finder and confirmed in vitro using mini-genes with wildtype or mutant DFNA5 exon 8.

We identified three novel and two recurrent mutations in DFNA5 segregating with hearing loss in the ascertained families. All three novel missense mutations are within exon 8 and are computationally predicted to alter splicing efficiency of exon 8 or oblate it. Functional assessment of these novel variants using mini-genes confirmed their deleterious effect. While all 5 mutations identified in this study and the previously reported mutations are unique at the DNA level, at the mRNA level they are equivalent – they all cause skipping of exon 8 to yield the same truncated DFNA5 protein.

This report is the first to identify exonic mutations in the DFNA5 gene that cause deafness. As such, this work expands the mutational spectrum of DFNA5-related deafness to include missense mutations and highlights the importance of assessing the effect of coding variants on splicing. (Supported in part by NIDCD RO1s DC003544 and DC012049)

Ototherapeutics II

PS 1072

Twice versus Once Daily Oral Dosing of SENS-401 for 28 Days Reveals Exposure Duration Driven Treatment Effect Against Severe, Acoustic Trauma Induced Hearing Loss in Rat

Mathieu Petremann; Christophe Tran Van Ba; Charlotte Romanet; Jonas Dyhrfjeld-Johnsen
Sensorion

Currently no approved pharmaceutical treatment exists for sudden sensorineural hearing loss and recent meta-analysis of the standard-of-care, off-label use of corticosteroid therapy has concluded that neither systemic nor intratympanic administration has any significant treatment effect (Crane et al., 2015). Noise-induced hearing loss is among the most common types of permanent hearing loss for adults (American Speech-Language-Hearing Association - ASHA; Hearing Loss Association of America - HLAA) and acoustic trauma is the most validated preclinical model of sudden sensorineural hearing loss.

SENS-401 is small molecule, clinical stage drug candidate with orphan drug designation for the treatment of Sudden Sensorineural Hearing Loss, which achieves dose-dependent local exposure in inner ear tissue (C_{max} = 35, 177 and 361 ng/mL; AUC_{last}= 146, 503 and 1566 ng*h/mL) lasting ~8 hrs for single 6.6, 13.2 and 26.4 mg/kg oral doses in rats.

Following baseline audiometry (ABRs at 8/16/24 kHz; DPOAEs at 4/8/16/24/32 kHz), 7 week old awake and behaving male Wistar rats were exposed to 120 dB octave band noise (8-16 kHz) for 2 hours. Daily oral SENS-401 treatment with 6.6 or 13.2 mg/kg SENS-401 (twice daily at 7 hrs interval), 26.4 mg/kg SENS-401 (once daily) compared to placebo treatment for 28 days.

Analyzing recordings from animals with initial severe hearing loss (mean threshold shift ≥ 55 dB at t=24h) on D28 showed limited ABR threshold shift (mean recovery across frequencies 9.3 dB) and DPOAE amplitude (mean recovery across frequencies 5 dB) recovery in placebo treated rats (n=5). All three SENS-401 treated groups showed statistically significant ABR threshold shift recoveries (mean recoveries across frequencies 18.9-21.4 dB, n=6-7, p=0.004-0.041) while DPOAE amplitude recovery only reached statistical significance in the 13.2 mg/kg SENS-401 twice daily group (mean recovery across frequencies 9.9 dB, n=7, p=0.023). Construction of cochleograms using fixed tissue from animals sacrificed after audiometry on D28, statistically significant enhancement of outer hair cell survival was found in the basal turn for 6.6 mg/kg and 13.2 mg/kg twice daily treatment with SENS-401 compared to placebo (1.2-3.6 fold mean enhancement of survival, p=0.003-0.035).

These results demonstrate that twice daily oral administration of lower doses of SENS-401 is comparable to, if not better than, a single high daily oral dose. This suggests that maximal drug exposure is less important than extended local exposure for the otoprotective efficacy of SENS-401, with twice daily administration rendering effective the 6.6 mg/kg dose which was not effective with single daily administration in previous experiments.

PS 1073

Protective Effect of Honokiol Against Cisplatin Ototoxicity - In Vitro Studies

Xiaodong Tan[1]; Michelle Lim[1]; Yueming Zhu[2]; Joseph O'Brien[2]; David Gius[2]; Jing Zheng[3]; Claus-Peter Richter[4]
[1]*Department of Otolaryngology-Head and Neck Surgery, Feinberg School of Medicine, Northwestern University;* [2]*Department of Radiation Oncology, Feinberg School of Medicine, Northwestern University;* [3]*Northwestern University;* [4]*Department of Otolaryngology-Head and Neck Surgery, Feinberg School of Medicine, Northwestern University & Resonance Medical, LLC, Chicago*

Background
Cisplatin-induced hair cell death is related to the generation of reactive oxygen species (ROS). To protect from cisplatin-induced hearing loss, anti-ototoxicity agents working as free radical scavengers have limited use because they compromise the antitumor effects of cisplatin. Honokiol, an anti-tumor agent having synergistic effects with cisplatin, showed strong cytoprotective effects against oxidative stress in multiple tissues and organs. The mechanism by which honokiol interacts with cells is related to the direct activation of SIRT3 in mitochondria. In this study, honokiol has been tested for its potential otoprotective effects against cisplatin treatment in cell and tissue cultures. A prostate cancer cell line was also tested to rule out the interference of honokiol with the anti-tumor effect of cisplatin.

Methods

Standard cell and tissue culture techniques were applied for cochlear-derived House Ear Institute-Organ of Corti 1 (HEI-OC1), Prostate cancer cells (C2-4B) and cochlear explants with the co-application of cisplatin (50 or 100 μM, respectively) and honokiol (0, 5, 10, 25 μM, respectively). Cell counting with a hemocytometer and western blot were performed to examine the survival of the cultured cells, the expression levels of SIRT3, caspase 3 and the cleaved poly ADP ribose polymerase (PARP). Tissue culture of cochlear whole mount is still ongoing. Immuno-staining and confocal microscopy will be used to verify the changes of the organ of Corti on cellular and molecular levels.

Results

1) Cisplatin treatment induced a dose-dependent cell loss (62% or 38% cell survival, respectively) in cultured HEI-OC1 cells while co-application of honokiol decreased the effect (100% or 65% cell survival, respectively). Honokiol treatment alone did not show a significant increase in cell proliferation. 2) Cisplatin treatment induced massive prostate cancer cell death (over 97%) while co-treatment with honokiol did not improve cancel cell survival. 3) SIRT3 expression level increased and apoptosis gene expression level decreased with the co-application of honokiol in cisplatin treatment.

Conclusions

1) Honokiol has a strong protective effect against cisplatin-induced HEI-OC1 cell death but not prostate cancer cell death. 2) The protective effect of honokiol is associated with increased SIRT3 expression level. This otoprotective effect of honokiol will be further verified in cochlear tissue culture and in vivo.

Funding

PS 1074

Hydrogen inhalation against hearing damage induced by impulse noise

Pernilla Videhult Pierre[1]; Kristian Pirttilä[2]; Curt Pettersson[2]; Jakob Haglof[2]; Torbjorn Arvidsson[2]; Marta Kisiel[2]; **Göran Laurell**[2]
[1]Karolinska Institutet; [2]Uppsala university

Background

Pharmacological treatment to prevent noise-induced hearing loss is lacking. Gaseous hydrogen (H2) can act as an antioxidant and reduce cytoplasmatic levels of reactive oxygen species. A few earlier studies demonstrate that inhaled H2 can have otoprotective properties. Gaseous H2 could easily be available for rescue of hearing after impulse noise trauma to workers exposed to occupational exposure. The emergence of omics techniques can give new insights into physiological and pathological conditions in the inner ear. Metabolomics deals with the study of chemical processes involving metabolites. Aim The aim of the present preclinical in vivo study was to investigate the effects of impulse noise on the hearing and on the metabolome of scala tympani perilymph and whether these effects could be altered by gaseous H2.

Methods

Anesthetized albino guinea pigs were exposed to noise (156 dB, 400 impulses, ~3 min) only (Noise group; n=11) or immediately followed by gaseous H2 (2% in air, 60 min; Noise+H2 group; n=10). Effects on the hearing were assessed by measuring frequency specific ABR thresholds shifts before and 4 days after the exposure. After the final ABR measurement, scala tympani perilymph was sampled from the basal turn of the cochlea in order to analyze the polar metabolome using LC-MS. After the perilymph sampling the animal was deeply anesthetized and decapitated. One cochlea was collected to evaluate loss of inner and outer hair cells. Surface preparation was performed for hair cell counting.

Results

At each frequency, there was a statistically significant difference in threshold shift between the Noise and the Noise+H2 groups (p<0.05). PCA scores plot of the metabolomics data demonstrated a clear separation between perilymph samples from the Noise and the Noise+H2 groups, and a number of interesting metabolites were identified.

Conclusion

We have characterized the impact of inhalation of H2 after impulse noise exposure. Inhalation of H2 immediately after impulse noise exposure partially protected the hearing, and alterations of metabolites in perilymph was shown to be a measure of otoprotection.

PS 1075

Quinoxaline Otoprotective Effects in Zebrafish Hair Cells

Marisa Zallocchi[1]; Linda Goodman[1]; Shikha Tarang[2]; Sonia Rocha-Sanchez[2]
[1]Boys Town National Research Hospital; [2]Creighton University

Hair cell loss is the leading cause of hearing and balance disorders in humans. Their loss can be caused by multiple insults, including noise, aging or treatment with

certain therapeutic drugs. Aminoglycoside antibiotics used to treat bacterial infections, and platinum-based drugs, used as a chemotherapeutic for certain types of cancer, are among the main groups of compounds known to cause hair cell damage. Increasing evidence suggests that there are multiple mechanisms by which hair cells can be damaged by these drugs, complicating possible therapeutic interventions and ultimately the search for otoprotective treatment. Hair cells of the lateral line organ in zebrafish are homologous to mammalian hair cells not only morphologically but also functionally, as well as in their responses to ototoxic drugs. As such, these cells provide a good model for screening potential otoprotective compounds. Here we present the results of preliminary studies on the otoprotective effect of quinoxaline (Qx), an anti-inflammatory compound, and some of its derivative against cisplatin and neomycin ototoxicity. 5-6 dpf (days post fertilization) zebrafish were incubated with vehicle alone or with different concentrations of Qx in the presence/absence of cisplatin or neomycin. After incubation, animals were washed and immediately fixed for confocal microscopy studies. The number of hair cells per neuromasts was quantified and compared versus vehicle controls. Alternatively, after treatment, animals were incubated with 30 µM FM1-43 for 40sec to evaluate mechanotransduction channel activity. Total fluorescence intensity per neuromast was calculated and compared versus control. In a different set of experiments, animals were incubated with Texas Red-conjugated Qx and Qx uptake evaluated over time by confocal microscopy. Statistical significance was evaluated by one-way ANOVA followed by Dunnetts multiple comparisons test. Qx protects neuromast hair cells from the deleterious effects of cisplatin and neomycin, with an optimal concentration of 300µM. Moreover, as determined by the FM1-43 fast uptake, Qx does not block mechanotransduction channels activity making it an attractive potential otoprotective compound. Likewise, the intracellular detection of Texas Red-conjugated Qx incorporation into the hair cells in the absence or presence of ototoxins suggests that Qx functions at the intracellular level. Overall, the results support Qxs otoprotection against the deleterious effect caused by ototoxic drugs while preserving hair cells normal function. This work was supported in part by the National Institutes of Health grant 5P20RR018788, the Tobacco Settlement Fund from the State of Nebraska (M. Zallocchi), and the National Institute of Health grant 1R21OD019745 (S.M. Rocha-Sanchez).

PS 1076

Rescue Effect of the Novel Peptide Vaccine GV1001 in an Aminoglycoside-Furosemide-induced Deaf Mouse Model

Ye Ji Shim[1]; Shin Hye Kim[2]; Gaon Jung[3]; Ja-Won Koo[3]
[1]*Seoul National University, Boramae Medical Center;* [2]*Korea University Medical Center;* [3]*Seoul National University Bundang Hospital*

The cell-penetrating peptide GV1001 has been investigated as an anticancer agent and recently demonstrated anti-oxidant and anti-inflammatory effects. It has shown a protective effect on a kanamycin (KM) induced ototoxicity mouse model. In the present study, we administered GV1001 at different time points after inducing hair cell damage, and examined if it rescues hair cell loss and restores hearing. A deaf mouse model was created by intraperitoneal injection of KM and furosemide. Firstly, to test the early temporal change of hearing and extent of hair cell damage after KM and furosemide injection, hearing and outer hair cell loss were evaluated on day 1, day 2 and day 3 after injection. In the second experiment, following KM and furosemide injection, GV1001, dexamethasone, or saline were given for 3 consecutive days at different time points: D0 group (days 0, 1, and 2), D1 group (days 1, 2, and 3), D3 group (days 3, 4, and 5) and D7 group (days 7, 8, and 9). The hearing thresholds were measured at 8, 16, and 32 kHz before ototoxic insult, and 7 days and 14 days after KM and furosemide injection. After 14 days, each turn of the cochlea was imaged to evaluate outer hair cell (OHC) damage. GV1001-treated mice showed significantly less hearing loss and hair cell damage than the saline control group in the D0, D1, and D3 groups (p<0.0167). The rescue effect of GV1001 was superior to that of dexamethasone in the D0 group. However, in the D7 group there was no hearing restoration or hair cell survival in any group. GV1001 protected against cochlear hair cell damage, and furthermore, delayed administration of GV1001 up to 3 days rescued hair cell damage and hearing loss in KM-furosemide-induced deaf model.

PS 1077

Investigating the Potential Role of Salicylate in Preventing HPβCD-induced Ototoxicity in the NPC1 Mouse Model

Yingjie Zhou[1]; **Satoe Takahashi**[2]; Kazuaki Homma[2]; Mary Ann Cheatham[1]; Jing Zheng[2]
[1]*Department of Communication Sciences and Disorders, Northwestern University;* [2]*Northwestern University*

2-hydroxypropyl-β-cyclodextrin (HPβCD) is a cholesterol-chelating agent that is currently undergoing clin-

ical trial for the treatment of Niemann-Pick Type C1 (NPC1) disease. Though promising in alleviating neurological symptoms, HPβCD unfortunately causes hearing impairment in NPC1 patients by inducing outer hair cell (OHC) death. Recently, we identified prestin, an OHC-specific motor protein, as a possible contributor to HPβCD-induced ototoxicity based on the observation that OHCs lacking prestin were less vulnerable to HPβCD (Takahashi et al., 2016). Since cholesterol influences prestin's membrane targeting and function, we speculate that HPβCD may affect interactions between prestin and cholesterol, thereby implicating prestin as a novel therapeutic target to mitigate hearing loss in NPC1 patients undergoing HPβCD treatment. Because salicylate directly binds to prestin, we examined whether pretreatment with salicylate might reduce the ototoxic effect of HPβCD by changing the prestin/cholesterol relationship within the plasma membrane. To this end, we first carried out a detailed evaluation of the properties of OHCs in the NPC1 mutant mouse model (NPC1-/-) using the following methods: 1) Nonlinear capacitance (NLC) measurements of OHCs isolated from wildtype (WT) and NPC1-/- mice to assess prestin function. 2) Immunohistochemistry, using antibodies against prestin and potassium voltage-gated channel subfamily KQT member 4 (KCNQ4), on cochlear tissue harvested from NPC1 -/- mice to examine protein localization in OHCs. 3) In vivo electrophysiology using distortion product otoacoustic emissions (DPOAE) and auditory brainstem responses (ABR) to evaluate auditory function in NPC1-/- mice treated with HPβCD and salicylate alone or in combination using three procedures to evaluate different chemical doses, animal ages, and methods of delivery. Our data show that OHCs dissociated from mice lacking NPC1 have similar amounts of functional prestin protein with the appropriate lateral membrane localization. Notably, the membrane potential at the peak of the NLC function of OHCs harvested from NPC1-/- mice is significantly depolarized, consistent with less cholesterol in the plasma membrane. NPC1-/- mice also exhibited progressive high-frequency hearing loss as previously reported (King et al., 2014). Salicylate, however, did not prevent OHC loss in this mouse model of NPC1 disease using any of the methods we employed. Although potentially attractive, co-administration of salicylate does not mitigate HPβCD-induced OHC death. (Work supported by the Ara Parseghian Medical Research Fund and the Knowles Hearing Center).

PS 1078

Experimental study of hyperbaric oxygen therapy on noise - induced hearing loss

Ning Yu
Chinese PLA General Hospital & Ear Institute

Objective

By discussing the relationship between the timing of the hyperbaric oxygen therapy and curative effect in treatment of noise-induced hearing loss, and provide reference for clinical application.

Methods

Fifty healthy guinea pigs with a normal ABR threshold, weighing 250-300 g were used. The guinea pigs were randomly divided into 3 groups: control group, noise group, noise + hyperbaric oxygen therapy group (2ATA, 10 days). HBOT was given immediately, 7 days and 14 days after noise exposure. The other five guinea pigs were randomly selected as draw materials group immediately after noise exposure. Impulse noise (pressure peak 142 dB SPL, pulse width 0.25 ms) was given 100 times in succession. The auditory brainstem response (ABR) was measured before exposure to pulse noise, immediately after exposure, and twice、 six times、 ten times after hyperbaric oxygen therapy. At the end of treatment, changes in the metabolism of cochlea were observed by measuring the levels of inflammatory cytokines and oxygen free radicals.

Results

Compared with the noise group, hyperbaric oxygen therapy immediately after noise exposure reduced the ABR threshold of 16 kHz, which was significant (P<0.05). hyperbaric oxygen therapy after 7 days of exposure to noise the ABR thresholds at click,4, 8, and 16kHz were lower (P noise group and the group of hyperbaric oxygen therapy after 14 days of exposure to noise, even the threshold of ABR in thehyperbaric oxygen therapy group was higher than that in the noise group at click、 4kHz. The levels of 8-OHdG, TNF-α and IL-1β in the noise + hyperbaric oxygen treatment group were lower than those in the noise group (P HIF-1α in noise + hyperbaric oxygen treatment group was lower than that in noise group, but there was no statistical significance.

Conclusion

HBOT has a significant effect in the treatment of noise-induced hearing loss. After 7 days of exposure to noise, hyperbaric oxygen therapy is the best. The result is not only poor after 14 days of exposure to noise, but also has some adverse effects.

PS 1079

AP-001/NPD1 Prevents Cisplatin-induced Hearing Loss in the Rat and Confers Protection Through Unique Pleiotropic Actions on Multiple Targets

Debashree Mukherjea[1]; Asmita Dhukhwa[1]; Sumana Ghosh[1]; Kelly Sheehan[1]; Leonard Rybak[2]; Vickram Ramkumar[1]; Per Gjorstrup[3]
[1]SIU School of Medicine; [2]Southern Illinois University School of Medicine; [3]ANIDA Pharma

Background

Neuroprotectin D1 (NPD1; Anida Pharma: AP-001) belongs to the class of endogenous "Specialized Pro-resolving Mediators" (SPM) acting as homeostatic regulators (Serhan, Nature 2014;510:92-101). AP-001 is shown to regulate acute inflammatory responses while inhibiting apoptosis and stimulating repair in tissues of neuroectodermal origin. It was now of interest to see if AP-001 could prevent the ototoxic effects of cisplatin.

Methods

The male Wistar rat in vivo model: pre-treatment ABRs (8, 16 and 32 kHz) were recorded in naïve animals, followed by transtympanic injection of AP-001 (as its ester prodrug to enhance delivery to target tissues) dissolved in PBS, which was used for controls. Cisplatin (11 mg/kg i.p.) was infused 1 hour later and ABRs recorded at 72 hours. UB/OC1 cells were used to explore AP-001 actions at cellular level: ROS generation was determined using CellROX dye, and NOX3, TRPV1, TNF-α and iNOS by quantitative q-PCR (for all: cisplatin at 2.5μM for 24 hours). Apoptosis was quantified by using Annexin V/PI flow cytometry or Tunnel staining following exposure to cisplatin at 20μM for 48 hours. In additional experiments live Ca^{2+} imaging was performed by confocal microscopy using Flup-4-AM dye. AP-001 was throughout added 30 min prior to cisplatin.

Results

AP-001 dose-dependently protected from cisplatin-induced hearing loss: Control ears had shifts of 7.8 ± 2, 18.9 ± 1.8, 26.7 ± 1.9 dB, respectively. Following AP-001 at a dose of 5μg the corresponding shifts were 1.4 ± 1.1, 2.1 ± 1.2 and 2.8 ± 2 dB. At an AP-001 dose of 3μg threshold shifts were 4 ± 2.4, 8 ± 2 and 10 ± 3.2 dB, while a further reduced dose of 0.3μg offered no protection.

Consistent with 5μg being efficacious in vivo, AP-001 in vitro was remarkably potent: stress and inflammation markers were completely inhibited at concentrations of 1nM or lower. AP-001 action was concentration-dependent with half-maximal responses observed at 1-10pM. At higher concentrations, up to 10μM, AP-001 retained full efficacy without any obvious negative effects, including cell viability. The effect by AP-001 on TRPV1 was further confirmed by complete inhibition of cisplatin-induced calcium-flux/spike observed at 60-90 seconds after cisplatin exposure.

Conclusion

AP-001 protects against cisplatin-induced hearing loss, supported by it regulating several pathways implicated in hair cell loss. The effective concentration range of AP-001 could afford protection not only at the cochlear base, but also the apex where drug concentrations following transtympanic injection are commonly low.

PS 1080

Targeted local nanoparticle delivery of D-JNKi-1 to the inner ear protects from noise-induced hearing loss

Julian Wooltorton; Andrew R. Ramsey; Mohammad N. Kayyali; Qiang Song; Daqing Li
University of Pennsylvania

Hearing loss is the most prevalent sensory disability worldwide and may be caused by age, drug exposure and excessive noise exposure. We have previously developed a non-invasive nanohydrogel drug delivery system for the inner ear which can successfully deliver multifunctional nanoparticles (MFNPs) through the round window membrane to the inner ear. We extended substantially this technique by conjugating a targeting peptide to the MFNP to deliver payload to specific inner ear cell types. Targeting can prevent off-target cell exposure to drugs and hence reduce side effects. The peptide used here recognizes prestin, a transmembrane electromotile protein uniquely expressed in outer hair cells of the inner ear. We delivered targeted MFNPs with a JNK inhibitor payload (D-JNKi-1) specifically to outer hair cells in 6-8 week old CBA/J mice and partially protected mice from noise induced hearing loss.

MFNPs were produced using a method for liposomes modified from Lajud et al., 2015, Otol Neurootol, 36:341-7). Functionalization of the liposomes was achieved by replacing 20% DSPE-PEG2K with DSPE-PEG2K-DBCO (which reacts with azides). The prestin targeting peptide, PrTP1, was conjugated to DBCO to produce the targeted MFNP. Hydrogel was mixed with targeted D-JNKi-1, untargeted D-JNKi-1 and targeted empty MFNPs (n=5 per group) and applied to the round window niche of anesthetized 6-8 week old CBA/J mice (see Lajud et al., 2015). Mice were exposed to 115-120 dB white noise (6.3-20 kHz) for 4 h in a reverberant wooden box. Auditory brainstem responses (ABRs) from 4, 8, 16, 24 and 32 kHz and clicks were recorded between 20

and 100 dB SPL at time points: pre-noise, noise+1, 3, 7 and 14 days.

Immunostaining of cochlear tissues demonstrated that noise exposure produced an increase in phosphorylated c-Jun expression indicating activation of the JNK apoptotic pathway. ABRs showed significant shifts in hearing thresholds which were attenuated by targeted D-JNKi-1 MFNPs, especially for clicks and low frequencies (4, 8 kHz). There were small improvements at other frequencies but not as pronounced as for the low frequencies. In contrast, untargeted D-JNKi-1 MFNPs did not convey significant protection from noise induced hearing loss at any frequency or timepoint.

This is the first demonstration of a successful prophylactic protection from noise induced hearing loss using a novel targeted payload delivery system which is non-invasive to the inner ear and, as such, is an appealing technique for use in clinical applications to prevent noise-induced hearing loss.

PS 1081

Resveratrol and N-acetylcysteine Combined Treatment Modulates the Expression of Oxidative Stress Response Genes and Ameliorate Cochlear Damage in a Ototoxicity Rat Model

Silvia Murillo-Cuesta[1]; Sara Pulido[1]; José M. Bermúdez-Muñoz[1]; Fernando García-Alcántara[2]; Raquel Martínez-Vega[3]; Teresa Rivera[2]; Marta Milo[4]; **Isabel Varela-Nieto**[5]
[1]Institute of Biomedical Research "Alberto Sols", Spanish National Research Council-Autonomous University of Madrid; Centre for Biomedical Network Research in Rare Diseases (CIBERER), Institute of Health Carlos III (ISCIII).; [2]Príncipe de Asturias University Hospital, Universidad de Alcalá; Institute of Biomedical Research Alberto Sols (IIBM), Spanish National Research Council-Autonomous University of Madrid; [3]Institute of Biomedical Research "Alberto Sols" (IIBM), Spanish National Research Council-Autonomous University of Madrid; [4]Department of Biomedical Science, University of Sheffield; [5]Institute of Biomedical Research "Alberto Sols", Spanish National Research Council-Autonomous University of Madrid; Centre for Biomedical Network Research in Rare Diseases (CIBERER), Institute of Health Carlos III (ISCIII); Hospital La Paz Institute

Background
Aminoglycoside antibiotics are widely used in medicine but they show ototoxic side-effects. The generation of reactive oxygen species is a central element in ototoxicity, leading to oxidative stress, inflammation and ultimately activation of caspase-dependent apoptosis. Several antioxidants have been used independently in clinical trials against ototoxicity, with positive but limited effects. The combination of antioxidant drugs with complementary mechanisms of action is a novel approach that could provide stronger ROS scavenging potentiate the otoprotection and prevent the oxidation of the drugs themselves.

Objective
Toevaluate the protective effect of a treatment with resveratrol plus N-acetylcysteine (NAC) on the ototoxic actions of kanamycin and furosemide in the rat. Methods: Resveratrol (10 mg/kg) and NAC (400 mg/kg) were administered together intraperitoneally to male 2 month-old Wistar rats on 5 consecutive days. The second day, a concentrated solution of kanamycin and furosemide was placed unilaterally on the round window by bullostomy to induce ototoxicity. Auditory brainstem responses were registered before and 5, 16 and 23 days after the beginning of the treatment. Cochlear samples were taken at day 5 and 23 to analyze oxidative balance and inflammation related genes by targeted PCR arrays or RT-qPCR, respectively. The cytoarchitecture and the presence of apoptosis, oxidative stress and inflammation markers were evaluated in cochlear sections.

Results and Conclusions
Co-administration of resveratrol plus NAC reduced the threshold shifts induced by ototoxic drugs, although this protective effect fades after the cessation of the treatment. The treatment modulated the expression of genes involved in the cellular oxidative (Gpx1, Sod1, Ccs and Noxa1) and inflammatory (Il1b, Il4, Mpo and Ncf) responses to injury.

Funding

Honokiol, an Anti-Tumor Agent, Protects Against Cisplatin-Induced Ototoxicity

Xiaodong Tan[1]; Yingjie Zhou[2]; Mary Ann Cheatham[2]; Yueming Zhu[3]; Joseph O'Brien[3]; Yingyue Xu[1]; David Gius[3]; Jing Zheng[4]; Claus-Peter Richter[5]
[1]*Department of Otolaryngology-Head and Neck Surgery, Feinberg School of Medicine, Northwestern University;* [2]*Department of Communication Sciences and Disorders, Northwestern University;* [3]*Department of Radiation Oncology, Feinberg School of Medicine, Northwestern University;* [4]*Northwestern University;* [5]*Department of Otolaryngology-Head and Neck Surgery, Feinberg School of Medicine, Northwestern University & Resonance Medical, LLC, Chicago*

Background
The ototoxicity of cisplatin, a major sequela during chemotherapy, is mainly associated with outer hair cell (OHC) death. To date, no effective FDA approved treatment is available to protect against cisplatin-induced hearing loss. We identified a compound, honokiol, which has merit as a hearing protective agent. Honokiol has a synergistic effect with cisplatin (in tumor suppression), is permeable to the blood-brain-barrier and provides cytoprotection against oxidative stress in multiple tissues and organs. In our pilot study, a protective effect of honokiol against cisplatin ototoxicity was observed in cell culture using mouse HEI-OC1 cells, a cochlear primary cell line. Expanding on our cell culture experiments, we demonstrate in this study the protective effect of honokiol against cisplatin ototoxicity in vivo.

Methods
Honokiol (in total 10-20 mg/kg) was injected intraperitoneally 1 hour prior to cisplatin injections (15 mg/kg) on two consecutive days in adult C57BL/6J mice of both sexes. Auditory brainstem responses (ABR) and distortion product otoacoustic emissions (DPOAE) were measured pre- and post-treatment up to 14 days to examine changes in hearing threshold and to assay hair cell survival and function. After euthanasia and fixation, immunohistochemistry and confocal microscopy of cochlear whole mounts were used to verify the changes in OHCs, as well as other cell types and structures.

Results
1) Cisplatin treatment induced a 20 dB elevation of acoustically evoked ABR thresholds to clicks and 10-35 dB elevation to tone-burst stimuli above 12 kHz. Significantly decreased DPOAE amplitudes were also observed at frequencies over 16 kHz. 2) Pre-treatment with honokiol significantly reduced the threshold elevation (Student';s t-test) and the decrease in DPOAEs. In fact, no cisplatin-induced hearing loss was observed after pre-treatment with high doses honokiol (20 mg/kg). 3) Confocal imaging also showed that honokiol increased OHC survival compared to mice receiving cisplatin only.

Conclusions
Honokiol protects against cisplatin-induced ototoxicity in mice. Further studies are required to verify the molecular mechanism of honokiol oto-protection in order to establish its role in alleviating the clinically significant complications associated with cisplatin chemotherapy in humans.

Funding

Effect of Local Administration of Mesenchymal Stem Cell Therapy on Auditory System in a Rat Model.

Rahul Mittal; Emre Ocak; Hyunseo Jung; Jeenu Mittal; Adrien Eshraghi
Hearing Research Laboratory, Department of Otolaryngology, University of Miami Miller School of Medicine, Miami, FL 33136, USA

Background
Mesenchymal stem cell (MSC) therapy is an emerging treatment modality for a number of human diseases. Although induced pluripotent stem cells (iPSCs) have been explored for the restoration of hearing, the potential of MSCs as a therapeutic strategy for various cochlear insults is not determined. MSCs possess anti-inflammatory, anti-apoptotic and neuroprotective properties, making them an attractive target for the treatment of inner ear disorders such as hair cell damage in response to inflammation. However, the first step is to determine the safety of MSC in the cochlea. The aim of the present study was to examine the effects of mesenchymal stem cell therapy on the auditory system.

Methods
MSCs were generated from rat bone marrow and phenotypically characterized using flow cytometry. MSCs were locally administered into the rat ear through intratympanic injection. Animals injected with PBS or untreated served as control group. Cochlea were harvested at different days of post-treatment and stained with FITC phalloidin to visualize hair cells. The Stereocilia hair cell bundle morphology was determined by scanning electron microscopy. Cochlea was also subjected to immunostaining with CellROX deep red staining and 4-Hydroxy-2-nonenal (HNE) to determine the levels of

oxidative stress and lipid peroxidation. The levels of proinflammatory cytokines in cochlear homogenates (TNF-α, IL-1β and IL-6) was determined by ELISA.

Results
We observed that MSCs have no adverse effect on the auditory hair cells. There was no statistical difference in number of hair cells between MSC treated and control group. Stereocilia hair cell bundle morphology was also preserved in MSC treated animals similar to control group. No oxidative stress was evident in cochlea from MSC treated animals as indicated by absence of CELL-ROX deep red and HNE staining. There was no statistical difference in the levels of proinflammatory cytokines between MSC treated and control group.

Conclusions
The results of this study suggest that MSC therapy is well-tolerated in the auditory system. Experiments are in progress in the laboratory where we are exploring the potential of MSC therapy in providing otoprotection against cochlear insults. MSCs possess a tremendous potential for the treatment of inner ear disorders that needs to be harnessed in the future investigations.

Vestibular: Clinical and Epidemiology

PS 1084

Active Spatial Orientation During a Navigation Task Depends on More Than Passive Spatial Orientation Ability

Dara Bakar[1]; Matthew Ehrenburg[2]; Yuri Agrawal[3]; **Eric Anson**[4]
[1]*School of Medicine, Brown University;* [2]*Department of Otolaryngology - Head & Neck Surgery, Johns Hopkins University School of Medicine;* [3]*Johns Hopkins School of Medicine;* [4]*Johns Hopkins Medical Institutes*

Background
Spatial orientation and navigation require an internal representation of one';s self and the world. Vestibular function has been linked to visuospatial ability and navigation. Individuals with unilateral or bilateral vestibular loss demonstrate path deviations while walking a remembered path when blindfolded. Vestibular disease negatively impacts walking ability through a combination of altered postural control, abnormal gaze stability, and impaired spatial orientation. Vestibulo-ocular reflex (VOR) performance is enhanced with active compared to passive head rotation, and spatial orientation ability may also be better during active behavior. Here we investigate the relationship between a passive test of rotational spatial orientation and an active rotational navigation task in healthy older adults.

Methods
97 healthy adults participating at the Baltimore Longitudinal Study on Aging were tested for passive perception of spatial orientation (PSO) using position steps in a rotating chair, VOR gain using video head impulse test, and vestibular navigation ability with the Triangle Completion Test (TCT). Briefly, the PSO test consisted of 12 passive rotations and the participant indicated how large each rotation was. During the TCT participants had to turn and walk the final leg of a triangle (hypotenuse) after being passively guided along the other 2 legs for each of 4 triangles. Multivariate linear regression was used to determine the relationship between the average rotational error on the TCT and the average PSO error while controlling for VOR gain, age, and gender.

Results
The average age of the participants was 70.2 (12.8) and 54 were female. The average rotational error on the TCT was 21.6 (12.0) degrees. The average PSO error was 12.6 (8.7) degrees. Average rotational error on the TCT increased by 0.28 degrees for every 1.0 degree of error on the PSO ($\beta = 0.28$, $p = 0.041$) while controlling for age, and gender. Average rotational error on the TCT also increased by 0.29 degrees for each year of increasing age ($\beta = 0.26$, $p = 0.005$).

Conclusions
Errors during perceptual tests of passive rotation are related to but incompletely explain navigation heading errors during a blindfolded walking task. Vestibular-proprioceptive integration during locomotor behavior could explain some of the discontinuity between active and passive evaluations of spatial orientation. These results add to the existing evidence highlighting the importance of both active and passive assessments of vestibular function to determine the true impact of impaired vestibular function.

PS 1085
Persistent deficits in heading perception with chronic unilateral vestibular lesions
Benjamin T. Crane; Raul Rodriguez
University of Rochester

Heading perception can be determined from both visual and inertial cues. This study examined visual and inertial heading perception in the horizontal plane in human subjects with chronic unilateral vestibular lesions. Subjects were 35-58 (mean 47) years old. Four were female and four had right sided lesions. Lesions were surgical in 3 cases and due to vestibular neuritis in 2. None had a caloric response on the lesioned side. Lesions were present from 3-15 years (mean 8.6). Subjects experienced 2s of inertial motion during which the platform moved

15 cm. An analogous visual stimulus at 75% coherence was also delivered independently or synchronized with the inertial movement. During the inertial only condition, the point of subjective equality (PSE) was deviated to the side opposite in the lesion in all subjects by a mean of 7.5 ± 4.0° (range 4 to 12.5°) such that a forward heading would be more likely to be perceived towards the side of the lesion. The average sigma was 6.9 ± 1.3°. With the visual only stimulus, one subject had a 10.6° deviation of the PSE to the side of the lesion, but the average deviation was only 3.0 ± 4.6° so there was not a consistent deviation across subjects. There was no consistent deviation in the combined visual-inertial heading perception with the average deviation 0.7 ± 3.5° (range -4.5 to 5.0) of the PSE towards the lesion. The average sigma for the visual-inertial stimulus was 5.2 ± 2.4°. Figure 1 shows the PSE with the full range of the error bars representing the standard deviation. These results indicate that in darkness, perception of forward inertial motion remains deviated towards the side of a lesion for years afterwards. However, there is no bias in visual heading or combined visual-inertial heading perception. Support: R01 DC013580

Summary plot.pdf

PS 1086

Influence of Cross-Modal Cues on Heading Perception

Raul Rodriguez
University of Rochester

Background
Heading perception is established using visual and inertial cues, but the relative influence of these cues on each other is uncertain. This study examined visual and inertial heading perception in the horizontal plane in human subjects presented with concurrent visual and inertial stimulius.

Methods
Four Eexperiments were conducted with varying offsets between visual and inertial heading stimuli in the horizontal plane. The experiments were divided into two blocks, one reporting inertial heading and one another reporting visual heading. Visual and inertial headings were reported using by orienting a dial to point in the perceived direction of perceived motion. Visual headings was were determined reported by pointing the dial in the direction of suggested self-motion (where the visual field originated). There were two trials performed for each block. The first experiment (1) had an inertial stimulus range of ±30° in 10° increments and a visual stimulus range of -±60° with 20° increments (maximum

visual heading 90°). The second experiment (2) had an inertial stimulus range of ±140° in 35° increments and a visual stimulus range of ±120° in 30° increments. The third Eexperiments 3 and 4(3) had the same inertial and visual stimulus ranges as experiments 1 and 2, but subjects were instructed to reverse reporting opposite the direction of suggested motionof visual motion (where the visual field is headed, suggesting external motion). The final experiment (4) used the same inertial and visual stimulus range as experiment 2, but subjects were instructed to report opposite the direction of suggested motion (where the visual field is headed).

Results
The results for each experiment at reflective offset angles (e.g. -60° and 60°) were combined. For experiment 1, as visual offset angles increased, the influence of visual stimuli on inertial perception decreased (fig. 1A). Experiment 2 demonstrated a similar trend, but the visual influence was less than experiment 1 (fig. 1B2) due to the relatively larger offsets. Experiment 3 had negligible visual influence on inertial perception (fig. 1A1). Experiment 4 resembled experiment 2 in visual influence (fig. 1C3). Inertial stimuli influence on visual perception was approximately 8%, 25%, 3%, and 27% across all offsets in experiments 1-4 respectively and was not did not appear related to the degree of visual offset.

Conclusion
There was a decreasing influence of visual stimuli on inertial perception as visual offset increases. Influence of visual offsets persistedVisual and inertial stimuli influenced each other at even with 150° offsets indicating they are never perceived completely independently larger than expected. Influence of visual offsets were larger in experiment 1 than 2, possibly due to the smaller inertial stimulus range of in experiment 1. The influence of inertial stimulius may have been consistent due to the reliability of inertial sensing. The larger inertial influence of experiments 2 and 4 relative to experiments 1 and 3 may be due to an increased visual stimulus range.

Support
R01-DC013580

Figure1.pdf

PS 1087

Hearing aids and postural control: Vestibular status modulates the benefit of auditory cues

Maxime Maheu; Lydia Behtani; Audrey Delcenserie; François Champoux
Université de Montréal

Background

Auditory cues have been suggested to play a role in postural control in hearing-impaired individuals. However, only a few studies have focused on the effect of hearing aids on postural control. However, the large prevalence of vestibular impairment and the variability of hearing thresholds between groups could be important confounding factor. Objectives The main goal of the present study was to evaluate the influence of auditory input restitution through hearing aids on postural control. A secondary goal was to determine if vestibular impairment modulates the benefits of auditory input for postural control. Finally, we wanted to examine the possibility that weighting could be modified by the use of hearing aids during postural control.

Method

We evaluated 19 hearing impaired participants: 11 with vestibular impairment (HIVL) and 8 without vestibular impairment (HI). Each participant was tested in four postural conditions (A: eyes open on firm surface; B: eyes closed on firm surface; C: eyes open on foam; D: eyes closed on foam) with and without hearing aids on a force platform.

Results

The two groups were found to significantly differ (p = 0.014) on the use of auditory input. Indeed, the HIVL group showed a significantly greater improvement in postural control than the HI group on condition C (p = 0.017) as well as on condition D (p = 0.025). Moreover, the HIVL group had a significantly lower somatosensory reliance to maintain postural control when using hearing aids than the HI group (p = 0.006).

Conclusion

Our results are in line with previous evidence showing that hearing-impaired individuals with hearing aids have improved postural control. Of interest, our results deepen previous findings by suggesting that vestibular impairment not only modulates the use of auditory cues in postural control, but also modifies somatosensory reliance.

PS 1088

Comparison of Haptic and Visual Perception of Upright and the Effect of Handedness

Min Jung Kim[1]; Jorge Otero-Millan[2]; Amir Kheradmand[2]
[1]Min Jung Kim; [2]Department of Neurology, The Johns Hopkins Hospital

A stable spatial perception is dependent upon sensing gravity through vestibular sensors and its integration with visual, proprioceptive, and other sensory inputs. Here we investigated the role of laterality in cerebral function for processing proprioceptive inputs that contribute to perception of upright. Upright perception was measured using a tactile stimulus in a forced choice paradigm (subjective haptic vertical or SHV), using the right and left hands in three different head positions: upright, right lateral head tilt of 20°, and left lateral head tilt of 20°. The role of hemispheric laterality was studied by comparing the SHV results with upright perception measured in a visual task (subjective visual vertical or SVV) between 15 right-handed and 15 left-handed participants. In the right-handed group, head tilt induced comparable systematic biases in all three tasks (SVV, SHV with left hand, and SHV with right hand). Averaging the three tasks for left head tilt, there was a bias of 4.4° ± 0.9° with respect to the same task performed in upright position; for right head tilt this bias was -4.7° ± 1.0°. There was an additional systematic bias related to the hand used in the SHV task that was comparable in all three head positions. Averaging the three head positions, the bias in performing the task with the left hand was -3.2° ± 1.5° with respect to the SVV at the same head position; with the right hand, this bias was 7.0° ± 1.5°. The asymmetry of the bias by the specific hand used did not reverse when left-handed subjects performed the task (-3.8° ± 1.4° for the left hand and 6.0° ± 1.2° for the right hand), indicating that the dexterity of the hand was not a clear factor in the SHV bias. Thus, while the hand used had an asymmetric effect on the haptic perception of upright, this asymmetry did not reverse between the right and left-handed subjects. This finding suggests that the effect of the hand used in the SHV task could be related to the hemispheric laterality in the representation of space, rather than the representation of the hand. We also found a robust effect of head tilt that was independent of the type of the task (haptic or visual), which suggests that both haptic and visual tasks share a common pathway for perception of upright.

PS 1089

Noisy galvanic vestibular stimulation induces a sustained improvement in body balance in patients with bilateral vestibulopathy

Chisato Fujimoto[1]; Shinichi Iwasaki[1]; Naoya Egami[1]; Yoshiharu Yamamoto[2]; Tatsuya Yamasoba[1]
[1]Department of Otolaryngology and Head and Neck Surgery, Graduate School of Medicine, The University of Tokyo; [2]Educational Physiology Laboratory, Graduate School of Education, The University of Tokyo

Objective

To examine whether long-term noisy galvanic vestibular stimulation (nGVS) keep improving body balance after the cessation of the stimulus in patients with bilateral vestibulopathy (BV).

Methods

Thirteen BV patients underwent two nGVS sessions at 2-week interval. In each session, the BV patients received nGVS for 30 min and were monitored without stimuli for 6 h. Two-legged stance tasks were performed with eyes closed with and without nGVS. The velocity of the center of pressure (COP) movement, the area enclosed by the COP movement, and the root mean square of the displacement of COP were measured using posturography, and power spectrum of the COP sway were assessed. Subjective improvement of body balance was also scored.

Results

In each session, the velocity of the COP movement was significantly improved for 6 h after the cessation of the stimulus. Power spectrum of the COP sway was significantly shifted to lower frequencies after the cessation of the stimulus. Subjective symptom of imbalance was also improved during the post-stimulation effect of nGVS.

Conclusions

nGVS can lead to the improvement in body balance that lasts for several hours after the cessation of the stimulus in BV patients, especially in the velocity of the COP movement. The shift to lower frequencies of the COP power spectrum, which was caused by nGVS, has a strong association with the ameliorating effect on the postural stability.

PS 1090

Does nocturnal Hypoxia cause Vestibular dysfunction in Patients with Obstructive Sleep Apnea?

Angela Wenzel[1]; Richard Birk[2]; Miriam Dietz[3]; Karl Hörmann[1]; Ulrich Sommer[1]
[1]University Hospital Mannheim, Department of Otorhinolaryngology, Head and Neck Surgery;
[2]University Hospital Marburg, Department of Otorhinolaryngology Head and Neck Surgery, Marburg;
[3]University Hospital Mannheim, Department of Otorhiolaryngology, Head and Neck Surgery

Introduction

It known that nocturnal hypoxia may lead to cochlear dysfunction in patients with obstructive sleep apnea (OSA). Less is known about whether hypoxia during sleep also impacts vestibular function in those patients. Thus, the present study aimed to assess the potential vestibulotoxic effect of nightly desaturations with hypoxia in patients suffering from OSA by investigating a possible correlation between the sleep apnea parameters and the vestibular function test results.

Patients and Methods

Vestibular function was assessed using a video head-impulse-test (vHIT) to evaluate horizontal semicircular canal function and cervical vestibular evoked myogenic potential (cVEMP) and ocular vestibular evoked myogenic potential (oVEMP) to measure otolith function in 54 patients that underwent cardiorespiratory polysomnography (PSG) at our sleep lab. Kendall's tau was performed to determine if there was a correlation between vHIT and the cVEMP and oVEMP results with polysomnographic parameters (e.g., apnea-hypopnea index [AHI], oxygen desaturation index [ODI])

Results

A correlation between horizontal semicircular function and polysomnographic parameters could not be demonstrated in the study ($p>0.05$). The cVEMP and oVEMP results showed a trend towards a correlation with ODI and AHI.

Conclusion

Although a correlation between the pathological vHIT results and the pathologically-elevated AHI and ODI could not be demonstrated in the study, the VEMP results showed a trend towards a correlation with AHI and ODI. Vestibulotoxicity due to nocturnal hypoxia in patients with OSA should be considered when the otolith organs seem to react more sensitively to potential damage.

PS 1091

Effect of Intratympanic Steroid Injection in Light Cupula

Min-Beom Kim Kim; Jin Su Park; Jung Yup Lee
Department of Otorhinolaryngology-Head and Neck Surgery, Kangbuk Samsung Hospital, Sungkyunkwan University School of Medicine, Seoul, Republic of Korea

Objective

To evaluate the effects of intratympanic steroid injection in light cupula. Study Design: Prospective cohort study.

Setting

Tertiary otology clinic Patients and Interventions: A total of 47 patients with persistent geotropic direction changing positional nystagmus with null point (light cupula) participated in this study. All study populations were randomly classified into three groups on initial visit day: intratympanic steroid injection (ITS, N = 15), vestibular suppressant (VS, N = 16) and canalith repositioning procedure (CRP, N = 16). Main Outcome Measure: Positional nystagmus and dizziness severity by dizziness handicap inventory (DHI) and visual analogue scale (VAS) were completed before first treatment. Three days

and 1 week after the first treatment, positional nystagmus, DHI, and VAS were re-evaluated to compare the effect of each treatment.

Results
DHI and VAS scores had decreased after treatment in all groups. However, there were no differences among the three groups during follow-up. At 1 week after the first treatment, there were 7, 6 and 7 patients who showed resolution of persistent geotropic DCPN in the ITS, CRP, and VS groups, respectively. There were no significant differences between the three groups. In the ITS group only, however, reversal of the stronger side on head roll test was observed in 6 patients, and 2 of them showed resolution of DCPN at the third day.

Conclusion
ITS wasn't effective for patients with light cupula at 1 week follow-up. However, some patients in the ITS group showed change and resolution of DCPN at earlier follow-up.

Light cupula.docx

PS 1092

Vestibular Function and Hippocampal Volume in the Baltimore Longitudinal Study of Aging (BLSA)

Rebecca Kamil[1]; Athira Jacob[2]; Tilak Ratnanather[3]; Susan Resnick[4]; Yuri Agrawal[5]
[1]Johns Hopkins Department of Otolaryngology-Head and Neck Surgery; [2]Johns Hopkins Center for Imaging Science; [3]Johns Hopkins University; [4]National Institute of Aging; [5]Johns Hopkins School of Medicine

Background
Vestibular loss in aging adults has been linked to decline in spatial orientation. Spatial cognition encompasses spatial memory and navigation, which represent the brain';s ability to generate a mental map and navigate through a given environment. Several animal and human experiments have shown that vestibular information is critical for accurate spatial memory and navigation behaviors. The hippocampus is a vital component of the network of brain regions involved in spatial cognition, and is known to receive peripheral vestibular input. In this study, we evaluated whether vestibular loss in aging adults is associated with hippocampal atrophy, which may underlie the relationship between vestibular loss and impaired spatial memory and navigation.

Methods
Participants for this cross-sectional study were selected from the Baltimore Longitudinal Study of Aging (BLSA), a long-running cohort study of healthy aging.

Eligible participants were age ≥60 years and had both vestibular physiological testing and brain MRI at the same visit. Vestibular function testing consisted of the cervical vestibular-evoked myogenic potential(cVEMP) to assess saccular function, the ocular VEMP(oVEMP) to assess utricular function, and the video head-impulse test(VHIT) to assess semicircular canal function based on vestibular ocular reflex(VOR). Brain MRI scans were performed on a 3T Philips Achieva scanner and hippocampal volumes were calculated using diffeomorphometry. Multivariate linear regression was used to investigate the relationship between vestibular function and hippocampal volume.

Results
The study sample included a total of 74 participants with mean(±SD) age of 77.0(±8.15) years and mean hippocampal volume of 3102.8(±371.5) mm^3. Multivariate linear regression models showed that among the 24 participants with present cVEMP, every 1μV amplitude increase of cVEMP had a significant increase of 258.0 mm^3 (p=0.049) in mean hippocampal volume. This relationship was not observed with oVEMP amplitude or VOR gain. There was no significant difference between the relationships of right hippocampal volume with right-sided vestibular tests and left hippocampal volume with left-sided tests. Only the relationships between right-sided oVEMP and right-sided hippocampal volume and left-sided VOR and left-sided hippocampal volume were significant. All other laterality-specific vestibular tests were not significantly associated with their corresponding laterality-specific hippocampal volume.

Conclusions
We observed a significant association between cVEMP amplitude and mean hippocampal volume in adjusted models in the BLSA. This finding is in line with prior work demonstrating a link between saccular function and spatial cognition in older adults. Further studies are ongoing using longitudinal data to assess the causal direction of this relationship.

Abstract_Tables_ARO_Final.docx

PS 1093

Preliminary Results of a Small-Scale Epidemiologic Study of Vestibular Disorders in Houston

Helen S. Cohen[1]; Haleh Sangi-Haghpeykar[1]; Ajitkumar P. Mulavara[2]; Jacob J. Bloomberg[3]
[1]Baylor College of Medicine; [2]KBRWyle; [3]NASA/ Johnson Space Center

Having tested a group of screening tests of vestibular function (see ARO abstracts 2017) we reduced the bat-

tery to the tests with the best ROC values, sensitivity and specificity. Those tests were a variation of 10 steps of Tandem Walking with eyes closed and Romberg on compliant foam sharpened with head movements. Then we added to the battery with Dix-Hallpike maneuvers, because positive, classical responses are pathognomonic for benign paroxysmal positional vertigo. We also included a well-written set of questions about vertigo currently in use in the National Longitudinal Study of Adolescent to Adult Health (Add Health study) – an on-going, survey-based epidemiologic study). The goals of the present study are to determine if the entire screening battery predicts the presence of any type of abnormality of the vestibular system and to determine the percentage of supposedly healthy people who have vestibular disorders. Therefore, we are testing the results of the screening battery against the results of objective diagnostic testing with a standard battery of bi-thermal caloric tests, positional tests, c-VEMP, and low frequency sinusoidal tests of the vestibulo-ocular reflex in darkness in the rotatory chair. Preliminary findings will be presented.

PS 1094

Current status of treatment of the Mal de Debarquement syndrome (MdDS) in 384 cases

Sergei B. Yakushin[1]; Bernard Cohen[1]; Catherine Cho[2]; Susan Shin[1]; Mingjia Dai[1]
[1]Icahn School of Medicine at Mount Sinai; [2]NYU Langone Medical Center

The Mal de debarquement syndrome (MdDS) is postulated to be caused by maladaptation of THE Velocity Storage Integrator in the vestibulo-ocular reflex (VOR), and it has been successfully reversed with readaptation of the VOR (Dai et al 2014, 2017). There are two forms of MdDS: motion triggered (classic) or non-motion triggered (spontaneous) MdDS. Both forms are characterized by persistent rocking, swaying and bobbing sensations that are temporarily relieved with passive or active motions. MdDS is debilitating not only because of the constant motion experience but also because of the companion symptoms, i.e., fatigue, inability to concentrate, headaches, motion sickness, sensitivity to light and sound and brain fog';. Over the past 4 years we have treated 384 MdDS patients in whom 83% cases were classic and 17% were spontaneous. The MdDS was diagnosed by Otolaryngologists (43%), Neurologists (15%), Physiotherapists (4%), by self-online (32%), or by other means (6%). All diagnoses were confirmed by our questionnaire survey for MdDS. The majority of classic'; cases occurred after travel on water *(cruise 46%, boating -19%), from flight (20%) and other motion triggers that inflicted unusual vestibular and visual stim-

uli (15%). The average age of MdDS patients was 48±14 yr (range 14-87). Treatment was considered a success if symptoms were reduced by at least 50% on a 10-point scale. The initial success rate was 74% for classic and 52% for spontaneous MdDS patients. These success rates have not changed throughout the years of studies since the commencement of our treatment. Thus, maladaptation of the velocity storage integrator in the VOR by roll-while-rotation could be a major triggering source of the MdDS. The success rate of MdDS treatment could be improved if we have a better understanding of how learning in the VOR occurs.

Vestibular: Injury, Recovery, Prosthetics

PS 1095

Exposure to Primary Blast Overpressure via the Ear Canal Induces Loss of Vestibular Stereocilia Bundles and Deficits in the Vestibulo-ocular Reflex in Rats

David S. Sandlin; Jun Huang; Yue Yu; Robby Tianwen Chen; Yiji Tu; Yang Ou; Alberto Arteaga; Kelsey Bounds; Youguo Xu; Hong Zhu; Wu Zhou
University of Mississippi Medical Center

Background

Primary blast injury, i.e., that due to the pressure shockwave of a blast, is a frequent cause of injury both in military and civilian populations. U.S. soldiers exposed to blast during conflict in Iraq and Afghanistan reported symptoms of vestibular deficits such as dizziness and vertigo during initial treatment and during follow-up examination. In this study, we tested the hypothesis that primary blast induces vestibular injuries by investigating effects of blast exposure on vestibular stereocilia bundles and the vestibulo-ocular reflex (VOR) responses to sinusoidal and transient head rotations.

Methods

Adult female Long-Evans rats were implanted with a head-holder for measuring their VOR responses to sinusoidal (0.2~4Hz) and step (40~90/d/s peak velocity) head rotation. After establishing VOR baseline levels by 3 separate tests, the rats were anesthetized and exposed to a single blast of 275kPa (80% of lethal dose determined in previous studies) to the left ear. VOR responses were measured after 1 day, 3 days, 1 week, and then weekly out to two months. A second group of rats were exposed to blast in the same manner, were allowed to age for periods ranging from one day to two months, and were sacrificed for histology at the same intervals as the VOR tests. The vestibular end organs were dissected and stained with FITC-conjugated phalloidin to mark actin, were imaged on a confocal microscope, and the stereocilia bundles were counted for the five vestibular end organs.

Results

A small number of sheared stereocilia bundles were noted immediately after blast exposure. However, substantial loss of stereocillia bundles in vestibular end organs were observed at 2 weeks after blast exposure. While steady state VORs exhibited little changes over 4 weeks after blast exposure, transient VORs exhibited a substantial reduction at 4 weeks after blast exposure. Interestingly, although blast was delivered into the left ear, reduced transient VOR responses were observed for both leftward and rightward head rotations, indicating that effects of blast exposure on the vestibular system was not confined to the stimulated side.

Conclusions

These results validated our model of blast-induced vestibular injuries. They also provided evidence for the hypothesis that primary blast-induced vestibular deficits were mediated by a progressive process, which induces loss of vestibular stereocilia bundles and deficits in transient VORs over several weeks. Furthermore, compared to steady state VOR responses, transient VORs are more sensitive biomarkers of blast-induced vestibular injuries.

PS 1096

Cisplatin-induced toxicity decreases the mouse vestibulo-ocular reflex

Yasumitsu Takimoto[1]; Takao Imai[1]; Makoto Kondo[2]; Yukiko Hanada[1]; Atsuhiko Uno[1]; Yusuke Ishida[3]; Takefumi Kamakura[4]; Tadashi Kitahara[5]; Hidenori Inohara[6]; Shoichi Shimada[2]
[1]Department of Otorhinolaryngology—Head and Neck Surgery, Osaka University Graduate School of Medicine; [2]Department of Neuroscience and Cell Biology, Osaka University Graduate School of Medicine; [3]Department of Anatomy, Tohoku Medical and Pharmaceutical University Graduate School of Medicine; [4]Osaka Women's and Children's Hospital; [5]Department of Otolaryngology - Head and Neck Surgery, Nara Medical University; [6]Department of Otorhinolaryngology-Head and Neck Surgery, Graduate School of Medicine, Osaka University

Cisplatin is a chemotherapeutic agent commonly used for the treatment of solid tumors, and its side effects include vestibulotoxicity. Previous studies have reported cisplatin-induced vestibulotoxicity in various animal models, but no study has investigated in vivo mouse vestibular dysfunction after cisplatin. The aim of this study was to investigate cisplatin-induced vestibulotoxicity in C57BL/6J mice. Vestibular function was assessed by recording the vestibulo-ocular reflex (VOR).

This was done during sinusoidal rotations in the horizontal plane at three frequencies (0.5, 1.0 and 2.5 Hz). A high-resolution, highfrequency digital infra-red camera was used with eye-tracking algorithms. Cisplatin at 16 mg/kg, but not 8 mg/kg, decreased the VOR gain at 2.5 Hz compared with the vehicle control. Following 16 mg/kg cisplatin treatment, the animals showed no change in the optokinetic nystagmus response, suggesting that no major changes in visual or oculomotor functions had occurred. This mouse model may be useful for studying cisplatin-induced vestibulotoxicity and its treatment.

Cisplatin-induced toxicity decreases the mouse vestibulo-ocular reflex.pdf

PS 1097

Correction of Vestibular Dysfunction and Spatial Organization in Usher Mice Using Antisense Oligonucleotide Therapy

Frederic F. Depreux[1]; Sarath Vijayakumar[2]; Tia N. Donaldson[3]; Kelsey T. Jennings[3]; Lucia A. Cherep[3]; Adam M. McNeela[3]; Francine M. Jodelka[4]; Frank Rigo[5]; Jennifer J. Lentz[6]; Douglas G. Wallace[3]; Timothy A. Jones[7]; **Michelle L. Hastings**[4]
[1]Northwestern University; [2]University of Nebraska-Lincoln; [3]Northern Illinois University; [4]Rosalind Franklin University of Med; [5]Ionis Pharmaceuticals; [6]Louisiana State University Health Sciences University; [7]University of Nebraska, Lincoln

Usher syndrome type 1C (USH1C/harmonin) is characterized by auditory, vestibular and retinal dysfunction. We have developed an antisense oligonucleotide (ASO-29) that improves auditory function and balance in mice homozygous for the human harmonin mutation USH1C c.216G>A. The findings were suggestive of improved vestibular function; however, no direct vestibular assessment has been previously performed. Here, we measured vestibular sensory evoked potentials (VsEPs) to directly assess vestibular function in Usher mice. We find that VsEPs are absent or abnormal in Usher mice, indicating profound loss of vestibular function. Strikingly, Usher mice receiving ASO-29 treatment have normal vestibular response thresholds when treated during a critical period shortly after birth, but the thresholds increase with later treatment times. Treatment of mice with ASO-29 at P15 was minimally effective at rescuing vestibular function. Interestingly, despite differences in vestibular function, ASO-29 treatment at all treatment times up to P15 resulted in sufficient vestibular recovery to support normal balance behaviors, suggesting a therapeutic benefit to balance with ASO-29 treatment at later times despite the profound vestibular functional deficits.

The discrepancy between sensory function and behavior, suggests that the two are differentially affected by therapeutic intervention. To evaluate in more detail the effect of ASO-based therapy on pathological behavior in Usher mice, we next assessed in more detail the open-field behavior of Usher mice with and without ASO-29 treatment. For this, we evaluated the organization of exploratory movements to assess spatial organization. Usher and heterozygous mice received ASO-29, or a control, non-specific ASO treatment at P5. Organization of exploratory movements was assessed under dark and light conditions at two and six month post-treatment. Disruptions in exploratory movement organization observed in control-treated Usher mice were consistent with impaired use of self-movement and environmental cues. In general, ASO-29 treatment rescued organization of exploratory movements at two and six month testing points. These observations are consistent with ASO-29 rescuing processing of multiple sources of information.

Overall, these findings provide the first direct evidence of an effective treatment of peripheral vestibular function and spatial organization in a mouse model of USH1C, and reveal the potential for using antisense technology to treat vestibular dysfunction and topographical disorientation associated with other disorders.

PS 1098

Variability in Recovery of Vestibular Evoked Potentials in Rats after Low Frequency Noise Exposure

Courtney E. Stewart; Ariane Kanicki; Tarana Joshi; Halima Haque; Richard Altschuler; W Michael King
University of Michigan

Introduction
The vestibular system plays a critical role in precise detection of head movements and is essential for normal postural control and balance. Because of their anatomical proximity to the cochlea, the otolith organs are selectively exposed to sound pressure and are at risk for noise overstimulation. Although clinical reports suggest a link between noise-induced hearing loss and balance problems, the physiology underlying this linkage is not well understood. It has recently been shown that low frequency noise is associated with signs of short-term injury. The first of these is a transient reduction in head postural stability during normal locomotion which recovers over approximately seven days. The second is a reduction in VsEP amplitude, which shows variable, and incomplete recovery within three days but is not consistently observable until after 7 days in most animals. Until recently, it has been unclear if recovery continues to occur after 21 days; however, recent evidence suggests that approximately half of noise exposed animals are able to recover some VsEP function, and that a few have successfully recovered to baseline over two months. The reason for variability in recovery is unclear. Therefore, the goal of the current study is to examine noise-induced changes in VsEP amplitude over extended periods of time at multiple time points during recovery, in order to better understand individual differences in animals and mechanisms involved in maximum recovery from a single intense low frequency noise exposure. Results of this work will identify key otopathological changes in the ear after recovery from noise exposure, and examine qualitative differences in waveforms produced from noise-exposed rat otolith organs. These findings will offer insight into functional changes occurring in the vestibular periphery associated with noise overstimulation.

Methods
Adult male Sprague-Dawley rats (400-450 g) were exposed to either 120 dB pSPL (0.5-4 kHz) noise or sham conditions for six hours on a single day. Changes in auditory function were evaluated by measuring auditory brainstem response (ABR) before and after noise exposure. Before, immediately following, and until VsEP waveforms were no longer statistically different from baseline, or different but stable over three weeks, VsEP was evaluated. After completing the final measurements, animals were transcardially perfused and inner ears were collected for dissection, staining, and whole mount confocal microscopy.

Results and Conclusions
Preliminary analysis suggests that approximately 50% of animals show recovery at time points greater than or equal to 7 days. Additionally, it appears that of the three waveforms which are observed in VsEP responses, the first must be present for the second to recover, and the third is generally unable to recover in the absence of the second. This may be associated with variable injury to the otolith organs in animals which are noise exposed.

Conclusions
Awake and freely moving animals may experience variable levels of noise based on head and body position during noise exposures, leading to variable recovery.

PS 1099

Vestibular Otopathological Changes Following Head Injury Without Temporal Bone Fracture

Renata Knoll[1]; Reuven Ishai[1]; Jenny Chen[1]; Kevin Wong[1]; Aaron K. Remenschneider[2]; David H. Jung[3]; Elliott D. Kozin[2]

[1]Massachusetts Eye and Ear Infirmary; [2]Massachusetts Eye and Ear Infirmary, Harvard Medical School; [3]Eaton-Peabody Laboratories, Massachusetts Eye and Ear; Department of Otolaryngology, Harvard Medical School

Background
The pathophysiology of vestibular symptoms following head injury without temporal bone (TB) fracture is not well understood. Vestibular symptoms may be caused by both central and peripheral etiologies. Proposed peripheral etiologies of vestibular dysfunction include labyrinthine concussion, benign paroxysmal positional vertigo, perilymphatic fistula, unilateral vestibular loss, traumatic endolymphatic hydrops, and / or utriculosaccular injury. Peripheral vestibular injury has been reported in animal models of head injury and include rupture of the membranous walls of the utricle and saccule, as well as degenerative changes in the macula of the saccule. To date, such findings in humans are not well described. Herein, we investigate the histopathology of the peripheral vestibular system in patients who sustained head injury without evidence of a TB fracture.

Methods
Subjects from the National Temporal Bone Pathology Registry with history of head injury without TB fractures were included. Exclusion criteria included evidence of TB fracture, otologic surgery, significant noise exposure, and/or auditory or vestibular dysfunction prior to head injury. All cases were evaluated by light microscopy. Inner ear anatomy including evaluation of the superior and inferior vestibular nerve and vestibular hair cells were evaluated. The presence of endolymphatic hydrops was also investigated.

Results
Six TB from five patients (four men and one woman) met inclusion and exclusion criteria. All TB had evidence of inner ear pathology. There was a 46% decrease (range 44 to 60%) of the mean Scarpa ganglion cell (ScGC) count compared to normative historical age-matched control. No difference was seen in ScGC between superior and inferior vestibular nerve. Moderate to severe degeneration of the vestibular membranous labyrinths was identified in posterior, superior, and lateral canal in several cases (n=3). Additional findings include vestibular hydrops (n=3) and blockage of the endolymphatic duct (n=1).

Conclusions
Otopathological analysis in patients with history of head injury without temporal bone fracture demonstrated peripheral vestibular otopathology. These findings have implications for mechanism and unrecognized peripheral vestibular pathology in patients following head injury. Additional research is needed to correlate otopathological findings with clinically observed vestibular symptoms in patients with head injury.
*RMN and RI contributed equally

PS 1100

A disparity fusion test for objective diagnosis of vergence abnormalities after mild traumatic brain injury

Carey Balaban[1]; Alex Kiderman[2]; Mikhaylo Szczupak[3]; Michael Hoffer[4]

[1]Otolaryngology, Biomedical Engineering, and Neuroscience, Univeristy of Pittsubrgh; [2]Neuro-kinetics, Inc.; [3]Department of Otolaryngology, University of Miami Miller School of Medicine; [4]Department of Otolaryngology and Neurological Surgery, University of Miami

Abnormal convergence eye movements (convergence insufficiency) have been reported in individuals with mild traumatic brain injury (mTBI). Convergence eye movements are a component of the near response, which includes synkinetic pupil constriction and lens accommodation. This study examined dynamic coordination between disconjugate vergence eye movements and pupil size in 15 control subjects and 15 subjects with acute mTBI. These responses were evaluated during a step retinal disparity fusion task, using an i-PAS virtual display platform (Neuro Kinetics, Inc, Pittsburgh, PA). Each eye viewed a white square with red center (0.1 degrees visual angle); the task consisted of disparity shifts in the horizontal plane equivalent to symmetric, approximately $\pm 1.4°$ vergence eye movement steps. Because neither stimulus luminance nor size changed it provided a pure disparity fusion stimulus for vergence. Eye movements and pupil area were sampled with a video-oculographic system at 100 Hz; pupil size data were normalized to responses to 0.42 to 65.4 cd/m² homogeneous illumination steps. Data were detrended prior to analysis. Visual angles (re: calibration phoria) for vergence eye movements were symmetric ($1.50 \pm 0.16°$ (SE) converging; $-1.51 \pm 0.16°$ diverging) in the control subjects; the pupil constriction was -11.9 ± 2.3 % (normalized area) during convergence steps and dilation was 9.8 ± 2.2 % (normalized area) during divergence steps. One control subject did not perform the task; another performed eye movements without a pupil near response (data included). Both the vergence eye movement ($0.63 \pm 0.16°$ (SE) converging; $-0.65 \pm 0.16°$ diverging) and pupil

modulation (-5.9 ± 2.3 % (normalized area) converging; -3.0 ± 2.3 % (normalized area) diverging) were reduced significantly in the mTBI group (ANOVA, p<0.01). Nine mTBI subjects were below the 93rd percentile for vergence eye movement magnitudes. The detrended pupil responses were also modeled as a sum of high and low pass filtered representations of the vergence eye movements; R-squared values were greater (p<0.05) in the control (0.43 ± 0.06) than the mTBI group (0.21 ± 0.06). Residuals showed strong pupil hippus activity unrelated to vergence. These findings suggest that a retinal disparity vergence test has utility in objective diagnosis of convergence insufficiency in acute mTBI.

PS 1101

Clinical value of 4-hour delayed gadolinium-enhanced 3D FLAIR MR images in acute vestibular neuritis

Hayoung Byun; Jae Ho Chung; Seung Hwan Lee; Chul Won Park
Hanyang University

Objective
To investigate the clinical significance of 4-hour delayed-enhanced 3.0 Tesla 3D-fluid attenuated inversion recovery (FLAIR) MR imaging in acute vestibular neuritis.

Study Design
A prospective observational study

Methods
Twenty-nine vestibular neuritis patients were enrolled between January 2017 and June 2017. Vestibular function tests, comprising the caloric and video head impulse tests and vestibular evoked myogenic potential measurements, were performed. Pre-contrast, 10-minute and 4-hour delayed-enhanced 3D-FLAIR MR images using double-dose IV gadolinium were obtained. After the laterality and extent of inner ear enhancement were defined, the patients were divided into groups based on the patterns of enhancement, and clinical parameters were analyzed according to the groups.

Results
Twenty patients (20/29, 69.0%) had obviously asymmetric enhancement of the affected inner ear structures on 4-hour delayed images, while only 3 patients (10.3%) had marked enhancement on 10-minute delayed images. The duration of spontaneous nystagmus (DurSN) was significantly longer in the patients with enhancement, especially with enhancement of the whole inner ear including vestibule and SCCs (p < 0.033). Spontaneous nystagmus resolved within 12 days in patients without laterality of enhancement, and within 16 days in

ipsi-lesional enhancement confined to the inner auditory canal (IAC) and fundus. Other results of vestibular function tests did not reveal any significant associations with MR enhancement.

Conclusions
Contrast enhancement of the vestibular nerve and inner ear structures can be identified on 4-hour delayed-enhanced 3T 3D-FLAIR MR images in acute vestibular neuritis. The extent of inner ear enhancement may be associated with the DurSN.

PS 1102

A comparison of materials used in the repair of superior canal dehiscence and their effect on inner ear pressure measurements

Deepa Galaiya[1]; Xiying Guan[2]; Raphaelle Chemtob[3]; Hideko Nakajima[3]
[1]*Massachusetts Eye and Ear Infirmary;* [2]*Eaton-Peabody Laboratory, Massachusetts Eye and Ear; Department of Otolaryngology, Harvard Medical School;* [3]*Department of Otology and Laryngology, Massachusetts Eye and Ear, Harvard Medical School, Boston, MA, USA*

Introduction
The effects of repairing superior canal dehiscence (SCD) on the vestibular and auditory system are poorly understood. By measuring inner-ear pressures, we can determine the input drive for the cochlea and the superior canal ampulla in a controlled manner, furthering our knowledge of such repairs. Using this technique, we studied the effect of different repair materials for SCD on inner ear pressures evoked by air and bone conduction (AC and BC) stimulation. Many different surgical materials and methods are used for repairing an SCD, but little is known about the relative effectiveness of these different materials. Previous data has shown that stiffer materials may produce a more effective repair of superior canal dehiscence based on measured inner ear pressures using bone conduction stimulation.

Methods
Intracochlear pressures in the scala vestibuli (Psv) and scala tympani (Pst) were measured in 3 human cadaveric temporal bones using micro-fiberoptic pressure sensors sealed and firmly glued to the otic capsule near the oval and round windows. Psv, Pst, ear-canal pressure (Pec) and stapes velocity were measured while stimulated by AC (with speaker at ear canal) or BC (with a bone anchored hearing aid) in normal intact superior canal, with SCD, and with repaired SCD. Repairs were made using a plugging method with the following sur-

gical materials: fascia, fascia with bone dust and fibrin glue, fascia with bone dust and cement, and bone wax.

Results

With AC, SCD reduced both Psv and Pst, and reduced the cochlear and ampulla input drives at low frequencies. Patching the dehiscence with various materials reversed this effect to the normal initial pressures, as long as a hermetic seal was achieved. In BC, SCD reduced Psv across a limited low-frequency bandwidth, but did not generally change Pst. Estimates of cochlear and ampulla input drives were reduced at limited low-frequency bandwidths. As long as a plugging method was used, each material used to repair the SCD was able to fully reverse the SCD effect during BC.

Discussion and Conclusion

Reversing SCD effects on bone-conducted inner-ear pressures were more challenging than reversing air-conducted inner-ear pressure effects. Unlike what has been previously shown, as long as a plugging method with a hermetic seal was used, the type of surgical material used for SCD repair may not impact reversal of the SCD effect on the input drive to the auditory and vestibular systems during BC.

PS 1103

First-in-Human Clinical Trial of the MVI™ Multichannel Vestibular Implant in Individuals with Bilateral Sensorineural Vestibular Loss: Effects on Gait and Posture

Margaret Chow[1]; Yoav Gimmon[1]; Desi P. Schoo[1]; Carolina Trevino[2]; Peter Boutros[1]; Mehdi Rahman[3]; Nicolas Valentin[3]; Andreas Hofner[4]; Aitor Morillo Rascon[4]; Andreas Marx[4]; Ross Deas[4]; Gene Y. Fridman[1]; Andreas Jaeger[4]; Michael C. Schubert[5]; John Carey[1]; Charles C. Della Santina[5]
[1]*Johns Hopkins University School of Medicine;* [2]*Johns Hopkins School of Medicine;* [3]*Labyrinth Devices, LLC;* [4]*Med-El GmbH;* [5]*Johns Hopkins University*

Background

Bilateral sensorineural vestibular loss (BVL) due to ototoxic hair cell injury is disabling, with affected individuals suffering chronic oscillopsia, disequilibrium and postural imbalance. While rehabilitation exercise helps many affected individuals improve stability, those who fail to compensate for profound BVL currently have no adequate treatment options. The Labyrinth Devices MVI™ Multichannel Vestibular Implant system is intended to treat chronic, adult-onset, severe-to-profound BVL in individuals who remain severely symptomatic despite vestibular rehabilitation. This system encodes head rotation information via motion-modulated pulsatile electrical stimulation of vestibular afferent nerve branches, mimicking normal semicircular canal function. We investigated the efficacy of the MVI™ system on gait and balance of three study participants enrolled in the Multichannel Vestibular Implant Early Feasibility Study.

Methods

Device implantations in the left ears of 3 participants took place between August 2016 and February 2017. After onset of chronic, continuously motion-modulated stimulation, subjects wore their MVI™ systems 24 hr/day and were evaluated 1, 2, 3, 6, 8, ~20 and ~45 wk after activation. To assess MVI™ efficacy in restoring gait and balance function, we compared performance on several posture and gait tests while the MVI™ system delivered either motion-modulated or constant-rate stimulation. We quantified performance using the Modified Romberg Test, Bruininks-Oseretsky Test Edition 2, Subtest 5 (BOT™), Timed Up and Go (TUG), Dynamic Gait Index (DGI) and gait metrics collected by a GAITRite™ system. We fit a general linear mixed-effect model to quantify outcomes as functions of subject, condition (modulation vs. baseline) and time.

Results

All subjects reported improvement in balance symptoms and activity level. As expected due to the small sample size, there was no statistically significant difference between conditions (modulation/baseline) over all participants. BOT™ score and walking pattern metrics such as gait speed, stride length, stride time and rhythmicity did not exhibit consistent changes. Base of support decreased in all three participants from pre-activation to their most recent visit; however, there are no significant differences between motion-modulated and baseline stimulation conditions. DGI improved more than the clinical minimal detectable change (3.2 points) in two of the three patients. One subject exhibited a clinically significant increase in time to failure during a modified Romberg test with eyes closed and standing on foam. TUG scores improved significantly ($p < 0.05$) for two of the three participants.

Conclusions

These data demonstrate that motion-modulated prosthetic input from the MVI™ system provides sensory input that may influence gait and balance in subjects with BVL.

PS 1104

First-in-Human Clinical Trial of the MVI™ Multichannel Vestibular Implant: Continuous Restoration of the Human Vestibulo-Ocular Reflex

Peter Boutros[1]; Mehdi Rahman[2]; Nicolas Valentin[2]; Desi P. Schoo[1]; Yoav Gimmon[1]; **Margaret Chow**[1]; Andreas Hofner[3]; Aitor Morillo Rascon[3]; Andreas Marx[3]; Ross Deas[3]; Gene Y. Fridman[1]; Natan Davidovics[2]; Bryan Ward[1]; Carolina Trevino[4]; Stephen Bowditch[1]; Dale Roberts[4]; Michael C. Schubert[5]; Andreas Jaeger[3]; John Carey[1]; Charles C. Della Santina[5]
[1]Johns Hopkins University School of Medicine; [2]Labyrinth Devices, LLC; [3]Med-El GmbH; [4]Johns Hopkins School of Medicine; [5]Johns Hopkins University

Background

The angular vestibulo-ocular reflex (VOR) drives eye movements that keep retinal images stable during head rotation. Individuals with bilateral sensorineural vestibular loss (BVL) suffer poor visual acuity during head motion, chronic disequilibrium and postural instability. Affected individuals who fail to compensate despite rehabilitative exercises have no adequate treatment options. Electrical stimulation of vestibular afferent neurons to partially restore the VOR has been effective in animal models of BVL. The Labyrinth Devices/MED-EL MVI Multichannel Vestibular Implant was designed to sense 3D head motion and continuously provide artificial stimulation to branches of the vestibular nerve that normally encode different components of that motion. Here we describe initial results from a first-in- human early feasibility study of the MVI as a treatment for BVL. Methods

Three subjects with chronic BVL were implanted in the left ear with MVI stimulators, which comprise a modified cochlear implant stimulator and array of electrodes inserted into each semicircular canal. An earth vertical rotary chair was used to provide en blocsinusoidal rotations in darkness over 0.12Hz at peak velocity 100°/s. Eye movements were recorded using 3DBinoc video-oculography goggles (Labyrinth Devices, LLC) pre-operatively and post-op/pre- activation (in subjects MVI002R004 and MVI003R140) and up to 8 weeks post-activation (all subjects including MVI001R019). This report focuses on the two complete data sets.

Result

In response to 100°/s peak velocity sinusoids at 0.1, 0.2, 0.5, 1 and 2 Hz, MVI002R004 had preoperative VOR gains of 0.05±0.02, 0.1±0.04, 0.19±0.05, 0.36±0.09 and 0.33±0.08, respectively. In response to the same sinusoidal stimuli, MVI003R140 had preoperative gains of 0.02±0.01, 0.05±0.03, 0.16±0.05, 0.46±0.06, 0.45±0.09,

respectively. After device activation, both subjects reported improvement in visual and postural stability with prosthetic stimulation, which has persisted throughout >6 months of continuous use. After 16 weeks of continuous use, MVI002R004';s VOR gain at the above frequencies was 0.15±0.02, 0.18±0.03, 0.25±0.03, 0.30±0.04 and 0.37±0.05, respectively, signifying a modest but significant increase in gain above preimplantation levels. Over the same duration, MVI003R140';s gain was 0.09±0.02, 0.08±0.02, 0.09±30.03, 0.25±0.06, and 0.29±0.03 respectively, showing a moderate increase in low frequency function and decrease at high frequency gain likely due to electrode implantation. VOR gain was greater during motion-modulated stimulation than with placebo stimulation for all 3 subjects.

Conclusions

Coupled with durable and significant subjective benefit, VOR responses measured in humans during whole-body rotation with and without motion-modulated MVI stimulation support the hypothesis that prosthetic vestibular nerve input effectively drives vestibulo-cerebellar VOR circuits.

Boutros_MVI_ClinicalTrial_RotChair_MVI002MVI003_FUNDING_FINAL.pdf

PS 1105

Long-term Audiometric Results from the first 3 subjects of the MVI™ Multichannel Vestibular Implant Early Feasibility Study

Desi P. Schoo[1]; Stephen Bowditch[1]; Dawn Marsiglia[1]; Peter Boutros[1]; Margaret Chow[1]; Yoav Gimmon[1]; Mehdi Rahman[2]; Nicolas Valentin[2]; Bryan Ward[1]; Carolina Trevino[3]; Natan Davidovics[2]; Andreas Hofner[4]; Aitor Morillo Rascon[4]; Andreas Marx[4]; Ross Deas[4]; Gene Y. Fridman[1]; Andreas Jaeger[4]; John Carey[1]; Charles C. Della Santina[5]
[1]Johns Hopkins University School of Medicine; [2]Labyrinth Devices, LLC; [3]Johns Hopkins School of Medicine; [4]Med-El GmbH; [5]Johns Hopkins University

Background

Bilateral vestibular loss (BVL) is a disabling diagnosis characterized by chronic imbalance and oscillopsia. Analogous to cochlear implants, vestibular implants (VI) aim to restore semicircular canal (SCC) function. For patients with BVL, the Labyrinth Devices MVI™ Multichannel Vestibular Implant system intends to continuously encode angular head velocity into a motion-modulated electrical stimulus delivered unilaterally to afferent vestibular nerve branches. The risk of hearing loss from implantation of devices like the MVI™ is a key safety concern. Currently, data are sparse and conflicting: hear-

ing preservation was demonstrated in 7/12 nonhuman primates, but one study reported 4/4 human subjects with Meniere';s disease experienced profound hearing loss after implantation of SCC stimulating electrodes. The likelihood of hearing preservation will be a key determinant of VI';s acceptance as a treatment option for patients with chronic, disabling BVL with intact hearing in a candidate ear. Here, we present long-term audiometric outcomes from the first three participants in the Multichannel Vestibular Implant Early Feasibility Study (NCT02725463).

Methods
Three participants with confirmed BVL on caloric testing were consented and enrolled in this first-in-human study. Preoperatively, subject MVI001 had normal hearing up to 1kHz and a severe high frequency sensorineural hearing loss (HF-SNHL), while the other two had normal hearing except for a mild HF-SNHL. The left ear was implanted in each participant between August 2016 and February 2017. Hearing was measured preimplantation, post-implantation, and at regular intervals after device activation. Audiometric tests included pure tone audiometry, word recognition score, speech reception threshold, distortion product otoacoustic emissions and tympanometry.

Results
All 3 subjects exhibited directionally-appropriate, electrically-evoked vestibulo-ocular reflex, confirming targeted intralabyrinthine placement of VI electrodes. Hearing in the implanted ear was mostly, but not completely, preserved and has remained stable up to 5-10 months post-implantation. Air conduction pure tone thresholds are within 10dB of preimplantation (0.125-8kHZ) in MVI001. Subjects MVI002 and MVI003 retained hearing in the normal or mild loss range for 125-2000Hz and exhibited a new 40-70 dBHL HF-SNHL at 4-8kHz. All 3 subjects have ear-specific speech discrimination scores similar to preimplantation and can use a telephone with the implanted ear. All subjects experienced self-limited symptoms consistent with a third mobile window syndrome after implantation.

Conclusions
While a larger sample size is needed for a statistically robust risk estimation, this data demonstrates that implantation of MVI™ electrodes can be performed in humans while preserving hearing to a degree sufficient to support unaided communication.

PS 1106

Temporal Dynamics of Electrically-Evoked Eye Movements Elicited by a Vestibular Prosthesis Designed to Restore Sensation of Gravitoinertial Acceleration

Margaret Chow[1]; Kristin Hageman[2]; Dale Roberts[2]; Charles C. Della Santina[3]
[1]Johns Hopkins University School of Medicine; [2]Johns Hopkins School of Medicine; [3]Johns Hopkins University

Background
The vestibular labyrinth comprises two classes of end organs: three semicircular canals (SCCs), which sense rotational head velocity, and two otolith end organs (utricle and saccule), which sense gravitoinertial acceleration (vector summation of linear and gravitational accelerations). Each end organ encodes head motion by modulating neuronal firing rates to drive ocular and postural reflexes that maintain visual acuity, stable gait and balance. Efforts to develop a vestibular prosthesis have until now focused almost entirely on stimulation of the SCCs; however, the SCCs and otolith end organs encode head movements with different kinematics and different temporal dynamics. In the present study, we examined the temporal dynamics of eye movements evoked by individual and combined stimulation of electrodes in SCCs and otolith end organs.

Methods
We fit three chinchillas with head posts and binocular scleral coils for tracking 3D eye movements. After charactering normal 3D eye movement responses to head rotation, tilt and translation, we implanted a polyimide vestibular electrode array with 26 otolith and 24 SCC contacts into the left ear. Bipolar current pulses were delivered while the animals were kept still, in the dark, eliciting sensation of a 'virtual'; movement and driving purely electrically evoked eye movements in response to that sensation. Eye movements were recorded during a constant pulse train (encoding a virtual 40 sec static tilt) delivered via multiple electrode configurations.

Results
The temporal dynamics to reach the final ocular counter-roll position during a virtual static tilt depended on location of the stimulating and reference electrodes. Stimulation with a SCC/distant reference or otolith/distant reference combination resulted in quick onset of eye movement (consistent with the SCCs'; high pass characteristic and suggesting current spread to SCCs when using otolith/distant reference combination). Otolith/near reference stimulation resulted in a significantly slower rise-time to final ocular counter-roll position (consistent with the otolith end organs'; low pass characteristic and suggesting more selective otolith stimulation). Addition-

ally, combining SCC and otolith stimulation resulted in an eye response similar to that of a mechanical static head tilt in a normal animal.

Conclusions
Responses differed in temporal dynamics for SCC and otolith stimulation, with the former being quick and transient and the latter having slower onset but able to generate a static tilt response. These results indicate that semi-selective prosthetic stimulation of the otolith end organs is possible and suggest that it may be necessary to restore sensation of low frequency head motion and static tilts.

Chow-ARO2018-Funding.pdf

PS 1107

Spatial Selectivity of Electrically-Evoked Eye Movements Elicited by a Vestibular Prosthesis Designed to Restore Sensation of Gravitoinertial Acceleration

Kristin Hageman[1]; **Margaret Chow**[2]; Dale Roberts[1]; Charles C. Della Santina[3]
[1]*Johns Hopkins School of Medicine; *[2]*Johns Hopkins University School of Medicine; *[3]*Johns Hopkins University*

Background
The vestibular labyrinth comprises two classes of end organs: three semicircular canals (SCCs), which sense rotational head velocity, and two otolith end organs (utricle and saccule), which sense gravitoinertial acceleration (vector summation of linear and gravitational accelerations). Each end organ encodes head motion by modulating neuronal firing rates to drive ocular and postural reflexes that maintain visual acuity, stable gait and balance. Efforts to develop a vestibular prosthesis have until now focused almost entirely on stimulation of the SCCs; however, the SCCs and otolith end organs encode head movements with different kinematics and different temporal dynamics. In the present study, we examined the spatial selectivity and range of eye movements evoked by individual and combined stimulation of electrodes in SCCs and otolith end organs intended to encode head tilts about different Earth-horizontal axes.

Methods
We fit three chinchillas with head posts and binocular scleral coils for tracking 3D eye movements. After charactering normal 3D eye movement responses to head rotation, tilt and translation, we implanted a polyimide vestibular electrode array with 26 otolith and 24 SCC contacts into the left ear. Bipolar current pulses were delivered while the animals were kept still, in the dark,

eliciting sensation of a 'virtual'; movement and driving purely electrically evoked eye movements in response to that sensation. Eye movements were recorded during a constant pulse train (encoding a virtual 40 sec static tilt) delivered via multiple electrode configurations.

Results
Providing a step change in pulse rate to different stimulating/reference electrode pairs resulted in an ocular counter-roll for the duration of the virtual static tilt. A linear increase in pulse rate or pulse amplitude on the same pair of electrodes elicited a linear increase of the magnitude of the eye movement without significantly changing response direction. The direction and magnitude of ocular counter-roll responses depended in a deterministic way on the relative locations of the pairs of electrodes intended to stimulate different locations on the otolith end organs.

Conclusions
Spatially selective stimulation of different regions within a utricular or saccular macula is possible, and prosthetic stimuli can systematically and repeatedly elicit eye movement responses consistent with those expected for static head tilts about different axes. These findings indicate that prosthetic stimulation of the utricle and saccule is feasible and may serve as a useful complement to prosthetic SCC stimulation for encoding head tilt and translation.

Hageman-ARO2018-Funding.pdf

PS 1108

Eye-Head Tracking Virtual Reality System for Vestibular Rehabilitation and its Neural Evidence for Clinical Implication

Jeong-Hye Park[1]; Han Jae Jeon[2]; SeJik Park[1]; Eun Cheon Lim[1]; Chang-Guen Song[2]; Sung Kwang Hong[1]
[1]*Department of Otorhinolaryngology-Head and Neck Surgery, Hallym University Sacred Heart Hospital; *[2]*Department of Convergence Software, Hallym University*

Research Background
It is clearly evident that vestibular rehabilitation exercises (VREs) can be effective to alleviate functional disability caused by many vestibular deficits. However, since it is self-directed exercise program requiring active efforts, lack of interest or tedious manner may negatively affect outcome of VREs. In this study, we introduce virtual reality contents which are working on eye-head tracking head-mount display headset, which allow patients to follow their eye or head exactly at the target presented on virtual reality for eye-head exercise with interactive man-

ner. In addition, we explored functional neural dynamics for VREs under the platform for clinical implication using electroencephalogram.

Methods
VREs contents were made by the Unity 3D program (Unity technologies, CA, USA) and provided via head mount display connected with eye and head-inertial tracker (SMI, TelTow, Germany). 21 healthy subjects were included; they conducted VREs under two experimental task-paradigms consisted of 2 blocks of eye tracking on and off conditions (50 trial per block). Recorded EEG data using 32 channels arrays (Brain product, Gilching, Germany) was analyzed for the neural oscillations and the directional functional connectivity.

Results
Our results showed that VREs under eye tracking on condition yielded significantly higher evoked alpha (8-12 Hz) and delta (1-4) power ($p < 0.05$). In addition, we observed significant higher theta power synchrony under saccade eye tracker-on condition compared to eye tracker off condition ($p < 0.05$). Further, the result of brain connectivity revealed eye tracking on condition had additional connectivity with frontal eye filed and more complex interaction between our interest regions (vestibular networks).

Conclusions
Integration of eye tracking system enable subjects to exercise with a top down attention and showed abundant functional connectivity on vestibular networks, while VREs on immersive virtual reality without feedback like those tracking system may induce adverse effect for functional recovery because of possible of passively viewing on virtual reality rather than active exercise, which will be established through our follow up study.

eyetracking.pptx

PS 1109

A Wearable System for the Prevention of Motion Sickness and VR-induced Sickness

Didier Depireux[1]; Robert True[2]; Jack Daggitt[3]; Thomas Hardart[3]; Samuel Owen[3]
[1]*Institute for Systems Research, University of Maryland College Park, MD, USA;* [2]*True Technologies Inc;* [3]*OtolithLabs*

Background
Most people are subject to motion sickness in some way, either as passengers in a car, or when experiencing virtual reality with one of the recent developed virtual reality (VR) headsets and systems. For most, it is a quality of life issue, but in many cases it is also an economic issue, which can impact modern developments in unexpected ways, such as the motion sickness experienced by the majority of users of autonomous vehicles. Current solutions to motion and VR induced sickness are few, with the most common ones involving the use of pharmaceuticals, with their side-effects (particularly sleepiness) which far outlast the length of the typical car or bus ride. Thus there is a real need for a device that would be easy to use, wearable, and could mitigate or eliminate motion- and VR-induced dizziness and discomfort, and would lead to no lasting effects the moment it is turned off. We show that a simple mechanical transducer of a new design, worn as a bone conduction device, can significantly improve the car passenger and VR user experience, and that it can prevent motion- and VR-sickness with no lasting side-effects.

Objective
To evaluate the effectiveness of a bone-conduction transducer of our design at preventing motion sickness, whether induced by being a passenger reading in a moving car, or as a user of a Virtual Reality game.

Methods
In the VR setting, subjects wore an Oculus Rift headset and watched a target rotating at accelerating angular velocities, or accelerated through a field of obstacles (somewhat similar to visual motion back and forth or sideways through a star field). The value of the maximal angular velocity and linear velocity without the transducer or with a control device was compared to the same value obtained with our custom transducer, as a function of the power, frequency, waveform and placement of the transducer. The optimal working parameters of the transducer were determined.

In a separate set of experiments, subjects played a VR game (Eve:Walkyrie) for up to 15 minutes, on separate days, without and with our transducer at the optimal settings determined from the first set of experiments. Ten minutes after they stopped playing the game, they filled out a Motion Sickness Assessment Questionnaire.

In a final set of experiments, subject were passengers in a car and read an article on their smartphone. In random order, subjects either did not wear any device, or wore a sound generator, or a wrist worn commercial device purported to prevent motion sickness, or our bone conduction transducer. The 20-minute itinerary was fixed and consistent. The time to first symptoms of motion sickness was recorded, and the questionnaire filled out at the end of each ride.

Results

Not every subject experienced motion- and/or VR-induced sickness in our comparatively short tests. With the optimal working parameters for the bone conduction transducer, no subject felt worse with our device. For the subjects that did experience motion sickness, over 95% displayed significant improvement with the device active. For the subjects that experienced VR-sickness, all of them experienced significant improvement when wearing the active device.

Conclusions

We are developing a non-pharmaceutical intervention that is remarkably effective at mitigating and sometimes completely preventing motion- and virtual reality- induced sickness. In the near future, we hope to expand our research to medical conditions for which reduction of dizziness would result in improvement of quality of life, such as vestibular migraines, vestibular neuritis and Ménière';s disease. Conflict of Interest

All authors have a financial interest in OtolithLabs, a start-up dedicated to improving the quality of life of those suffering from motion sickness and VR-induced sickness.

Aging: Processes & Prevention

PD 110

CBA/CaJ mice (Mus musculus) as a behavioral model for hearing loss

Anastasiya Kobrina[1]; Micheal L. Dent[2]
[1]*SUNY, University at Buffalo;* [2]*State University of New York at Buffalo*

Age related hearing loss (ARHL), or presbycusis, is the most common disorder among older humans. Thus, it is critical to establish a reliable anatomical, physiological, and behavioral animal model for ARHL in order to understand the basis of presbycusis, and for developing future diagnostic and treatment strategies. Mice are frequently used to study and model ARHL due to similarities in human and mouse cochleae and in genetic makeup. Mice also emit ultrasonic vocalizations (USVs) that may be used for communication purposes, similar to speech in humans. Previous electrophysiological research established that the CBA/CaJ mouse strain is an appropriate model for late-onset hearing loss. These mice exhibit ARHL sex differences in auditory brainstem responses (ABRs) for pure tones between 12 and 15 months of age, with males showing higher ABR thresholds than females. Although much is known about electrophysiological measures of hearing loss in mice, behavioral research has been severely underrepresented in the aging literature. The only longitudinal behavioral study to date by Kobrina and Dent (2016) used operant conditioning procedures with positive reinforcement to show that CBA/CaJ mice exhibit ARHL, however much later in life than established by ABR studies in the same strain of mouse. In fact, this strain is capable of detecting 42 kHz pure tones and USVs up to 34 month of age. The behaviorally measured ARHL sex differences were present for detecting USVs, but not for 42 kHz tones, conflicting with previous ABR findings. The goal of current research is to use operant conditioning procedures to establish a complete pure tone audiogram, to examine the effects of stimulus duration on signal detection across lifespan, and to assess the effects of aging on USV and pure tone detection in quiet and noise in adult CBA/CaJ mice. The results revealed that adult mice retain their hearing late into their lifespan as assessed by behavioral methodologies. Similarly to humans, mice lose hearing for high frequency pure tones earlier than for low frequency pure tones. Not surprisingly, mice showed lower thresholds for longer pure tone stimuli than for shorter ones. This duration benefit disappears with age, particularly at a faster rate for high frequency tones. Mice are also capable of detecting pure tones and USVs in silence and noise across their lifespan, with older mice exhibiting higher thresholds in noise than in silence. The results highlight the necessity for behavioral measures of hearing in mouse models of ARHL.

PD 111

Hearing Loss and Associated Risk Factors among Older Adults: The Age, Gene/Environment Susceptibility-Reykjavik Study (AGES-RS)

Chuan-Ming Li[1]; Howard J. Hoffman[1]; Christa L. Themann[2]; Robert A. Dobie[3]; Gudny Eiriksdottir[4]; Johanna E. Sverrisdottir[4]; Lenore J. Launer[5]; Vilmundur Gudnason[4]; Hannes Petersen[6]
[1]*Epidemiology and Statistics Program, National Institute on Deafness and Other Communication Disorders (NIDCD), National Institutes of Health (NIH);* [2]*Hearing Loss Prevention Team, Division of Applied Research and Technology, National Institute for Occupational Safety and Health (NIOSH), Centers for Disease Control and Prevention (CDC);* [3]*Department of Otolaryngology-Head and Neck Surgery, The University of Texas Health Science Center at San Antonio;* [4]*The Icelandic Heart Association;* [5]*Laboratory of Epidemiology and Population Sciences, Intramural Research Division, National Institute of Aging (NIA), National Institutes of Health (NIH);* [6]*Department of Otolaryngology-Head and Neck Surgery, Landspitali-University of Iceland*

Introduction

Age-related hearing loss (ARHL) is a common sensori-neural disorder in older adults, who typically experience gradual rather than sudden onset of disabling hearing impairment (HI).

Objective

To estimate prevalence and identify risk factors associated with HI in a well-characterized cohort of older adults. Methods: The Age, Gene/Environment Susceptibility–Reykjavik Study (AGES-RS) 2002–2006, interviewed and examined a population-based cohort of 5,764 adults aged 66–96 years. We performed analysis on 5,171 subjects who completed air-conduction, pure-tone audiometric examinations after removal of clinically significant cerumen. Hearing in the better ear was analyzed using the pure-tone average (PTA: 0.5–1–2–4 kHz) threshold classification recommended by the Global Burden of Disease (GBD) 2010 Hearing Loss Expert Group: "mild" (20–34 dB hearing level [HL]), "moderate" (35–49 dB HL), "moderately severe" (50–64 dB HL), "severe" (65–79 dB HL), "profound" (80–94 dB HL), and "deaf" (≥95 dB HL). Disabling HI has been defined as BE, PTA ≥35 dB HL. Multivariable-adjusted prevalence ratios (PRs) and 95% confidence intervals (CI)s were calculated using logistic regression models.

Results

The prevalence of (only) mild HI was 43.2% (males, 44.0%; females, 42.5%), while disabling HI was 32.5% (males, 38.9%; females, 27.8%). Males had higher prevalence of disabling HI compared to females (PR:1.43; 95% CI:1.32-1.54). Prevalence of disabling HI increased with age (66-69, 70-74, 75-79, 80-84, and 85+ years): males, 13.0%, 24.0%, 39.1%, 55.4%, and 73.7%; females, 5.7%, 13.6%, 24.7%, 45.9%, and 70.9%, respectively. After adjusting for age, sex, and education, the risk factors associated with disabling HI were: "fair" (PR:1.15; 95% CI:1.03-1.28) and "poor" general health status (PR:1.22; 95% CI:1.03-1.45); underweight (PR:1.37; 95% CI: 1.07-1.75); hypertension (PR:1.16; 95% CI:1.02-1.33); mild (PR:1.16; 95% CI:1.04-1.30) and moderate-to-severe depression (PR:1.39; 95% CI:1.08-1.79); mild (PR:1.44; 95% CI:1.29-1.61) and greater cognitive impairment (PR:1.27; 95% CI:1.10-1.47); vertigo (PR:1.10; 95% CI:1.01-1.19); frequent falls (PR:1.31;95% CI:1.14-1.51); tinnitus (PR:1.37; 95% CI:1.25-1.50); self-reported hearing loss (PR:4.69; 95% CI:4.09-5.37); wearing hearing aids (PR:3.67; 95% CI:3.42-3.93); history of repeated ear infections (PR:1.35; 95% CI:1.18-1.55); and history of work-related noise exposure (PR:1.43; 95% CI:1.32-1.54). Lifetime moderate or higher physical activity was protective, i.e., associated with decreased prevalence (PR:0.91; 95% CI:0.83-0.99).

Conclusion

In AGES-RS, disabling HI prevalence increased markedly with age. ARHL is a permanent condition with limited rehabilitation success. Hence, reliable information for ways to delay onset of ARHL is a priority. Findings from epidemiological studies can suggest preventive strategies, e.g., moderate or higher physical activity.

PD 112

Exaggerated temporal processing deficits as animals age after synaptopathic noise

Aravindakshan Parthasarathy[1]; Gerard Encina-Llamas[2]; Sharon G. Kujawa[3]

[1]Eaton-Peabody Laboratory, Massachusetts Eye and Ear Infirmary/ Department of Otolaryngology, Harvard Medical School; [2]Hearing Systems group, Department of Electrical Engineering, Technical University of Denmark; [3]Eaton-Peabody Laboratories, Massachusetts Eye and Ear Infirmary and Department of Otolarynology, Harvard Medical School, Boston, Massachusetts

Background

Normal aging results in a progressive loss of synapses between inner hair cells and auditory nerve fibers. An early overexposure to sound exacerbates this loss, even when thresholds recover. The functional consequences of this synaptopathy are poorly understood, though it is thought to affect suprathreshold coding of sound, especially in challenging listening conditions like the presence of background noise. Here, population level auditory brainstem responses (ABRs) and envelope following responses (EFRs) were used to study suprathreshold temporal processing with aging after an early noise exposure in a rodent model of synaptopathy.

Methods

ABRs and EFRs were obtained from an age-graded series of CBA/CaJ mice with or without a single exposure to a known synaptopathic noise that does not cause permanent hearing threshold elevations. ABRs were obtained to tone pips at various sound levels and frequencies. EFR stimuli were sinusoidally amplitude modulated (sAM) tones. Stimuli were centred on synaptopathic or non-synaptopathic cochlear regions. The modulation frequency, depth, sound levels and signal-to-noise ratio of the sAM stimuli were systematically varied to test temporal processing with degraded envelope cues. DPOAE thresholds and growth functions provided information about outer hair cell (OHC) functional integrity, and immunostained cochlear whole-mounts were used to quantify hair cells and synapses.

Results

ABR wave 1 and EFRs measured from early neural sources both show progressive loss of amplitudes with age. Prior exposure to TTS-producing noise exaggerated these ongoing declines: As animals aged after noise, amplitude declines for both metrics exceeded those of age-matched controls in frequency regions of largest noise-induced synaptopathy. Pre-neural responses (DPOAEs, EFRs from pre-neural sources) were minimally affected until advanced age, when hair cell losses occur. Synaptopathic animals also showed a reduced dynamic range of encoding AM depth and noise masking in EFRs. These changes were present even though ABR and DPOAE thresholds and DPOAE amplitudes were similar to age-matched controls. Together, these changes are consistent with decreased temporal processing, exaggerated in the previously noise-exposed ears.

Conclusions

Age-related cochlear synaptopathy is accompanied by deficits in temporal processing at the earliest neural generators, resulting in a decrease in the dynamic range of encoding degraded envelope cues. These deficits are accelerated, but not fundamentally altered by an early over-exposure to noise. These results suggest that even a single exposure to synaptopathic noise can result in increased deficits in temporal processing throughout the lifespan.

Funding

PD 113

Auditory Processing and Hidden Hearing Loss in Elderly Subjects.

Mariela Torrente[1]; Alexis Leiva[2]; Kattalin Elespuru[2]; Paul H. Delano[3]
[1]Department of Otorhinolaryngology, Universidad de Chile; [2]Neuroscience Department, Faculty of Medicine, University of Chile; [3]Otolaryngology Department, Clinical Hospital of the University of Chile

Introduction

Temporal processing of the auditory signal and hearing in noise are two events that could be impaired in elderly subjects. One of the possible mechanisms involved in these observations might be hidden hearing loss (cochlear neuropathy). The purpose of this work is to evaluate an eventual relation between hidden hearing loss, auditory processing, and aging in elderly subjects.

Material and Method

Subjects: adults over 60 years of age enrolled in the Au-ditory and Dementia Study (ANDES). Exclusion criteria: cognition impairment (Mini Mental test score < 23, previous ear disease, hearing aid user, asymmetric hearing loss.

Auditory Processing Assessment

Non verbal tests: frequency pattern (Auditec), and gap in noise (Beta Adult version of the Adaptive Tests of Temporal Resolution (ATTR)). Verbal tests: speech in noise, dichotic digits, and Spanish version of staggered spondaic words (S-SSW), all of them available from Auditec. Auditory brainstem evoked responses were assessed with supra threshold click stimulus 80-90 dB nHL, filtered between 100 and 3000 Hz. Amplitude of wave I and V was defined from peak to through. Hidden hearing loss was determined by measuring the amplitude of wave I, and by the ratio between amplitudes of wave I and V.

Project approved by local ethics committee, and volunteers gave consent.

Statistical Analysis

Spearman correlation p<.05; and backward stepwise regression.

Results

72 subjects were included. Average age 74 years (SD 12), 66.7% female. Average PTA 0.5 to 4 KHz 26.9 dBHL (SD 11.8). Performance in the speech in noise test, both for the right and left ear, and dichotic digits for the left ear had a significant negative correlation with age (Table 1). Total number of errors in S-SWW for both ears had a significant correlation with age (Table 1). Amplitude of wave I and the ratio between amplitude of wave I and V had a significant correlation with correct answers in speech in noise for the left ear only (table 2). Temporal processing (gap in noise and frequency pattern) had no significant relation with aging.

Backward stepwise regression showed that the correlation of speech in noise was dependent on PTA rather than age, and for the left ear HHL was also significant.

Discussion

We provide evidence that speech in noise discrimination has a significant decline with aging, and this phenomenon could be dependent on hidden hearing loss.

tabla ARO word.docx

PD 114

Aging effects on neural representation and perception of temporal speech cues

Samira Anderson; Lindsey Roque; Alanna Schloss; Hanin Karawani
University of Maryland

Objective

Older adults often report that they have difficulty with the clarity of speech when conversing with others. This lack of clarity may arise from deficits in temporal processing that reduce the ability to distinguish one word from another. The duration cue is a key temporal feature for identifying words based on the final consonant. Compared to younger adults, older adults require longer vowel durations to perceive final voicing and longer silent interval durations to perceive final affrication. The aim of this study was to investigate the age-related changes in temporal coding underlying phoneme identification based on silent interval and vowel durations, and to determine how well neural representation of these cues can predict behavioral performance.

Methods

Participants comprised 15 younger normal-hearing adults (YNH, ages 18-30) and 15 older normal-hearing adults (ONH, ages 55-70) who had no history of middle ear surgery or neurological disorder. Behavioral identification functions were obtained for the words ditch and dish on a 7-step continuum of silence duration and for wheat and weed on a 9-step continuum of vowel duration. Auditory brainstem responses (ABRs) were recorded to a 100-μs click to provide an indirect measure of cochlear nerve function through calculation of Wave I amplitude. Frequency-following responses (FFRs) to the end-points of the dish-ditch and wheat-weed continua were recorded. Phase-locking factor obtained from the FFR was used to assess spectrotemporal precision. Multiple linear regression modeling was used to predict behavioral performance.

Results and Conclusion

The cross-over points of identification functions revealed that ONH listeners require longer silence durations to discriminate between "dish" and "ditch" and longer vowel durations to discriminate between "wheat" and "weed" compared to YNH listeners, replicating previous behavioral studies. ABR Wave I amplitude was equivalent between groups, but phase-locking factor of the FFR was higher in the YNH than in the ONH participants. The multiple linear regression model revealed that the phase-locking factor to the fundamental frequency significantly predicted variance in behavioral performance. Wave I amplitude did not significantly contribute to the model. Overall results suggest that central process-ing deficits may limit the older adult';s ability to use duration cues to identify temporal contrasts in words.

PD 115

Loss of Mitochondrial IDH2 Accelerates Age-related Hearing Loss in Mice

Shinichi Someya[1]; Karessa White[1]; Mi-Jung Kim[1]; Dalian Ding[2]; Hyo-Jin Park[1]; Chul Han[1]; Kevin Boyd[1]; Zaimary Meneses[3]; Cole Slade[3]; Jonathan Hirst[3]; Richard Salvi[4]
[1]*University of Florida, Department of Aging and Geriatric Research;* [2]*University at Buffalo, USA;* [3]*University of Florida;* [4]*Center for Hearing and Deafness; State University of New York at Buffalo*

Background

Isocitrate dehydrogenase (IDH) 2 participates in the TCA cycle and is a major source of NADPH for the mitochondrial antioxidant defenses. There are three isozymes for IDH: cytosolic IDH1, and mitochondrial IDH2 and IDH3. All isozymes catalyze the conversion of isocitrate to α-ketoglutarate. While IDH1 and IDH2 converts NADP+ to NADPH, IDH3 converts NAD+ to NADH. In the current study, we investigated whether loss of Idh2 affects the progression of age-related hearing loss (AHL) using wild-type (WT) and Idh2-/- mice that were backcrossed onto the CBA/CaJ strain, a well-established model of late onset AHL.

Methods

To investigate whether loss of Idh2 affects hearing function in young and old mice, we measured ABR (auditory brainstem response) thresholds, wave I amplitudes, and wave I latencies in WT, Idh2+/- and Idh2-/- mice at 5 and 24 months of age that were backcrossed onto the CBA/CaJ strain for 5 generations (CBA/CaJ- Idh2-/-). Following the ABR tests, we performed histological analyses to assess hair cell loss and spiral ganglion neuron density in the cochlea of young and old WT and Idh2-/- mice. We also measured the activities of IDH2, glutathione reductase and thioredoxin reductase 2 and the levels of oxidative DNA damage and apoptosis markers in the cochlea of young and old WT and Idh2-/- mice.

Results

We found that 24-month-old Idh2-/- mice displayed a 27-35 dB increase in ABR threshold at 8, 32 and 48 kHz, a 40-46% decrease in wave I amplitude at 8 and 48 kHz, and a 49% increase in wave I latency at 48 kHz compared to age-matched WT mice. In agreement with the hearing test results, 24-month-old Idh2-/- mice displayed

a 54-59 % increase in OHC loss, a 6-13 % increase in IHC loss, a 30-50% decrease in SGN density in the cochlea compared to age-matched WT mice. This was associated with increased oxidative DNA damage and increased apoptotic cell death in the cochlea of 24-month-old Idh2-/- mice. In young mice, loss of Idh2 resulted in decreased NADPH redox state and decreased activity of thioredoxin reductase 2 in the mitochondria of the inner ear.

Conclusions

Therefore, these results provide evidence that loss of IDH2 accelerates the progression of AHL in mice. Funding: This study was supported by NIH/NIDCD grants R01 DC012552 (S.S.) and R01 DC014437 (S.S.).

PD 116

Investigating the Impact of Hearing Aid Use and Auditory Training on Cognition, Mood and Social Interaction in Older Adults with Hearing Loss: the Study Protocol of a Crossover Trial

Joanna A. Nkyekyer[1]; Denny Meyer[1]; Peter Blamey[2]; Andrew Pipingas[1]; Sunil Bhar[1]
[1]Swinburne University of Technology; [2]Blamey and Saunders Hearing Pty Ltd

Background

Sensorineural hearing loss is the most common sensory deficit among older adults. Some of the psychosocial consequences of this condition include difficulty in understanding speech, depression and social isolation. Studies have shown that older adults with hearing loss show some age-related cognitive decline. Although hearing aid use and auditory training have been proven as successful interventions to alleviate sensorineural hearing loss, no research has been designed to look at the effect of simultaneous hearing aid use and auditory training on cognitive performance in older adults. This study will investigate whether wearing hearing aids will improve the impact of auditory training on cognition, mood and social interaction for older adults with sensorineural hearing loss.

Methods/Design

This is a crossover trial targeting elderly men and women between 50 and 90 years with either mild or moderate symmetric sensorineural hearing loss. Participants will be assigned in random order to receive hearing aid (intervention) for either the first three or last three months of the six month auditory training program. Each participant will be tested at baseline, three and six months. Speech tracking rates will be calculated, for each participant, from the six month auditory training program. The primary outcome, cognitive performance, will be as-

sessed by a neuropsychological test battery. Secondary outcomes, mood and social interaction will be assessed by self-reported measures. The effectiveness of hearing aids and auditory training on speech perception will be evaluated using a mathematical learning model, an online speech perception test and the Abbreviated Profile of Hearing Aid Benefit (APHAB).

Discussion

This study will investigate whether using a hearing aid augments auditory training to improve a person's cognition, mood and social interactions with family and friends. Results from the study will inform strategies for aural rehabilitation, hearing aid delivery and future hearing loss intervention trials. Trial registration: This trial is retrospectively registered at ClinicalTrials.gov, on April 13, 2017, identifier: NCT03112850.

Keywords

Sensorineural hearing loss, hearing aids, auditory training, crossover design.

PD 117

Prevention of age-related hearing loss (ARHL) via antioxidant and energy-modulating approaches in a novel mitochondrial mouse model of ARHL

Alla V. Ivanova[1]; Winston Tan[2]; Joseph Santos-Sacchi[3]
[1]Yale University School of Medicine; [2]Department of Surgery (Otolaryngology), Yale University School of Medicine, New Haven, Connecticut, USA; [3]Department of Surgery (Otolaryngology), Neuroscience, and Cellular and Molecular Physiology, Yale University School of Medicine, New Haven, Connecticut, USA

Background

Age-related hearing loss has become an epidemic of the 21st century. Hearing loss impairs the ability to communicate, disrupts daily activities and social life, and may lead to cognitive decline and dementia. No pharmacological treatment for prevention or mitigation of ARHL exists due to the complexity of underlying mechanisms and lack of information on key molecular targets. While it is becoming increasingly clear that mitochondrial dysfunction is one of the key mechanisms of aging, understanding its role in hearing loss is lagging due to shortage of adequate animal models.

Novel mitochondrial ARHL model. We developed a novel mitochondrial model of premature hearing loss of strial/neural origin via targeted deletion of a small mitochondrial protein, Fus1. Auditory brainstem response (ABR) measurement showed that hearing in Fus1 KO mice progressively declined leading to severe hearing loss in

8-10 m.o. KO mice as compared to WT animals that had relatively good hearing even at the age of 16-18 months. The dynamics of hearing deterioration in Fus1 KO mice is reminiscent of that seen in patients with hearing loss suggesting that the Fus1 KO mouse is a faithful model of ARHL. Molecular and metabolic analysis of KO and WT demonstrated that, in addition to oxidative stress, the cochleae of young Fus1 KO mice prematurely activated age-related AKT and mTOR pathways as well as anaerobic (non-mitochondrial) glycolysis suggesting inefficient ATP production by mitochondria.

Methods

We supplemented female Fus1 KO mice for 3 months either with a common antioxidant N-acetylcysteine (NAC), mTOR inhibitor Rapamycin (RAPA), or glucose mimetic and glycolytic inhibitor 2-deoxiglucose (2-DG) in drinking water. ABR and cochlear RNA and protein expression analyses (Affymetrix microarray and Western blot) were performed before and after treatment to measure hearing and molecular changes, respectively.

Results and Conclusion

NAC treatment delayed hearing loss, restored endocochlear potential, mitochondrial architecture, and attenuated molecular signaling affected in Fus1 KO mice. However, beneficial NAC effects were observed only at high doses, which resulted in side effects and increased mortality in Fus1 KO mice. Seeking more effective treatment, we targeted the mTOR and anaerobic glycolysis pathways responsible for energy sensing and energy production, respectively. We demonstrated that 2-DG and RAPA are safe and efficient in protecting hearing in Fus1KO mice. Interestingly, we found drug-specific parts of the response, which we are currently pursuing further. Molecular analysis identified common and drug-specific effects on multiple Fus1-dependent processes including immune and brain responses, calcium signaling, metabolism, and cell adhesion. Thus, our study reveals pathways critical for hearing and provides a foundation for developing novel approaches to protect and improve hearing.

Auditory Nerve III

PD 118

Speech-in-Noise Performance is Primarily Governed by Outer Hair Cell rather than Auditory Nerve Function

Richard Hoben[1]; Maeve Salinger[2]; Sofia Pevzner[3]; **Mark Parker**[4]

[1]St. Elizabeth's Medical Center; [2]University of Maryland; [3]St Elizabeth's Medical Center; [4]Tufts University School of Medicine

The overall goal of this research was to determine the contribution of outer hair cell (OHC) and auditory nerve (AN) functions in speech discrimination in complex listening environments. Subjects (N=120) from our clinic with standard audiometric thresholds ranging from normal to moderate degree of sensorineural hearing loss were recruited to participate in this study. OHC function was measured using Distortion-Product Otoacoustic Emissions (DPOAEs). AN function was measured using peak-to-trough amplitude and SP/AP ratios of the Compound Action Potential (CAP) obtained during electrocochleography (analogous to wave I of the Evoked Auditory Brainstem Response), and 45% Time-Compressed NU-6 word lists in 10% reverberation. Speech-in-Quiet (SIQ) was measured using the NU-6 wordlist presented at 50 dB SL. Speech-in-Noise (SIN) performance was measured using the QuickSIN test, and with the NU-6 word list presented at equivalent levels (+0 dB SNR) with competing filtered noise. These functions were then correlated with subject variables such as age, gender, subjective perceived rating of difficulty hearing in noise, and High Frequency Audiometry (9-20k Hz).

Patient responses were rank ordered and divided into groups based on degree of hearing loss, high frequency audiometry, SIN performance, DPAOE thresholds and amplitudes, CAP amplitude, and CAP SP/AP ratios. Correlations between the group variables were conducted the using non-parametric Kendall's tau-b correlation coefficient. Statistically significant trends between groups were measured by the non-parametric Jonckheere–Terpstra test. Linear Mixed Effects modeling was used to predict the main and mixed effects of the measured and subject variables.

The results from these analyses indicate that 1) differences in CAP amplitude can be measured in persons with normal hearing thresholds (pure tone average < 15 dB HL) and normal OHC function, which suggests that Auditory Synaptopathy can be present in persons with normal hearing thresholds, 2) these persons exhibit normal SIN performance, which suggests that Auditory Synaptopathy does not correlate with SIN performance

in a general clinical population, and 3) SIN performance correlates strongly with DPAOE function and the degree of hearing loss. In aggregate, these results suggest that SIN performance in the general clinical population is primarily governed by OHC rather than AN function.

PD 119

Does Synaptopathy Correlate with Hearing Aid Performance?

Richard Hoben[1]; Sofia Pevzner[2]; Maeve Salinger[3]
[1]St. Elizabeth's Medical Center; [2]St Elizabeth's Medical Center; [3]University of Maryland

This study aimed to determine whether auditory nerve (AN) function or outer hair cell (OHC) function correlated with hearing aid benefit in patients recruited from our clinic. Synaptopathy was measured by the ratio of summating potential to action potential (SP/AP ratio) obtained during electrocochleography and 45% Time Compressed NU-6 word list plus 10% echo (TC). Outer hair cell function was measured by distortion product otoacoustic emission (DPOAE) amplitudes. These measurements were correlated with objective subject variables including age, degree of sensorineural hearing loss, speech in quiet (SIQ) using the NU-6, speech-in-noise (SIN) using Quick SIN, and self-perceived rating of difficulty hearing in noise (HIN). All subjects were fit to prescribed NAL-NL1 targets with binaural Phonak Audeo B90 hearing aids programmed with linear compression and subjected to aided SIQ and SIN testing on the day of initial fitting, after 1 week, and after 1 month of full time (greater than 8 hrs) daily use.

Patient responses were rank ordered and divided into groups based on aided SIQ performance, aided SIN performance, and aided self-perceived HIN. Correlations between the group variables were conducted the using non-parametric Kendall's tau-b correlation coefficient. Statistically significant trends between groups were measured by the non-parametric Jonckheere–Terpstra test. Linear Mixed Effects modeling was used to predict the main and mixed effects of the measured and subject variables.

Preliminary results obtained by 11 persons who have successfully completed this study showed that aided SIQ performance after 1 month positively correlated with both OHC function (greater DPOAE amplitudes) and better AN function (lower SP/AP ratios, increased TC score). In contrast, SIN performance was positively correlated with better AN function but was independent of OHC function. Although preliminary, these results suggest that both AN and OHC function play roles in hearing aid benefit in quiet environments, however, hearing aid benefit in noise is positively dependent on AN function.

PD 120

A Simple and Novel Method to Diagnose Noise-induced "Hidden" Hearing Loss and Cochlear Synaptopathy

Hong-Bo Zhao[1]; Yan Zhu[2]; Ling Mei[2]; Brian Earl[3]; Simone Mariotti Roggia[4]; Audrey Frederick[3]; Joseph Pinkl[3]
[1]1. University of Kentucky Medical Center; [2]1.University of Kentucky Medical Center; [3]2. University of Cincinnati; [4]3. Federal University of Santa Catarina

Background

Recent animal studies demonstrate that short-term, moderate noise exposure that does not result in apparent hair cell loss could still have irreversible neural degeneration, in particular, loss of low spontaneous rate (LSR) auditory neurons and their synapses with inner hair cells. This can eventually lead to difficulty hearing in noisy environments. Such 'hidden' hearing loss is not readily detectable by standard clinical audiology tests, which mainly focus on threshold testing. Based on their spontaneous rate (SR), auditory nerves can be divided into high-SR and low-SR fibers. High-SR fibers have low-threshold and their discharges are quickly saturated as sound intensity increases, whereas low-SR fibers have high-threshold and their discharge rates can still increase at high intensity levels. Thus, most threshold-based hearing tests mainly reflect high-SR fiber function and cannot efficiently detect low-SR fiber and synapse loss, thereby leading to "hidden" hearing loss.

Methods

In this study, we used moderate levels of white noise to conditionally saturate high-SR fiber discharge so that the low-SR fiber activity can be detectable. CBA/CaJ mice were used. ABR and DPOAE were recorded under both quiet and conditional noise masking (CNM). Ribbon synapse loss was examined by CtBP2 labeling. The CNM procedure was then adapted for studies in normal-hearing adults with positive noise exposure history and mild speech-in-noise difficulties. Chirp-evoked compound action potentials (CAPs) were recorded in quiet and in CNM. DPOAEs were recorded and speech-in-noise performance was assessed with the QuickSIN test.

Results

ABR thresholds in noise-exposed mice were significantly increased in comparison with those of a normal control group under the moderate level of CNM. The dynamic response range in the noise-exposed group with CNM was also significantly reduced. However, DPOAEs in the noise-exposed group had no significant changes compared to those in the control group. Morphological examination confirmed that ribbon synapses (positive CtBP2 labeling) were significantly reduced, correspond-

ing well to the increase of CNM ABR threshold in the noise-exposed group. The human studies also revealed a significant increase in CAP threshold in CNM for the noise-exposed group with mild speech-in-noise loss compared to the unexposed control group with normal speech-in-noise performance. DPOAE levels did not differ significantly across groups.

Conclusions
These data demonstrate that this novel, simple, and clinically-feasible method can detect cochlear synaptopathy in a well-established mouse model and provide physiologic evidence for hidden hearing loss in noise-exposed humans who have speech-in-noise loss. Supported by NIH R56 DC 015019

PD 121

The Effect of Elicitor Bandwidth on a Wideband Measure of the Middle-ear-muscle Reflex in Young Normal-hearing Individuals

Magdalena Wojtczak; Jordan A. Beim
University of Minnesota

Background
A recent study in our lab showed that individuals with normal audiometric thresholds who experience chronic tinnitus have significantly weaker middle-ear-muscle reflex (MEMR) than age- and sex-matched normal-hearing individuals without tinnitus. The similarity of the finding of weaker MEMR in humans with tinnitus to the weaker MEMR in mice with noise-induced cochlear synaptopathy is consistent with the hypothesis that tinnitus in the absence of hearing loss may be triggered by a loss of synaptic connections between the inner hair cells and the auditory nerve fibers. Consistent with this interpretation, the results also suggest that the MEMR may be used to detect cochlear synaptopathy in humans. However, we only used broadband-noise (0.5-10 kHz) elicitor of the MEMR and because hearing thresholds were not measured for frequencies beyond 8 kHz, there remains a possibility that differences in hearing sensitivity at frequencies above the audiometric range could account for the difference in MEMR strength between the tinnitus and control group. In this study, the strength of the MEMR was measured as a function of the upper cutoff frequency of MEMR noise elicitor.

Methods
Contralateral noise bands with upper cutoff frequencies of 10, 8, 4, and 2 kHz were used to elicit the MEMR. The probe was a click with a flat spectrum between 250 Hz and 8 kHz presented at 90 dB peSPL. The widest elicitor had an overall level of 85 dB SPL and the spectrum level of the noise was held constant as the upper cutoff fre-

quency was decreased. The strength of the MEMR was estimated by comparing the sound pressure in the clicks before and during the elicitor. Young normal-hearing listeners with no tinnitus participated in the study.

Results
Preliminary data suggest that removing the elicitor components above 4 kHz did not have a significant effect on the strength of the wideband measure of the MEMR and removing the components above 2 kHz reduced the strength of the reflex, but not sufficiently to make it comparable to the reflex strength observed for the tinnitus group in our previous study.

Conclusions
Our preliminary results suggest that a loss of hearing sensitivity that is limited to frequencies at the higher end and above the audiometric range cannot account for the weaker MEMR in individuals with tinnitus and normal audiometric hearing thresholds. [Supported by NIH grant R01DC015987].

PD 122

Effectiveness of TrkB and TrkC agonists at promoting neuron survival, neurite extension, and synapse restoration in rat cochlea ex vivo models

Alan C. Foster[1]; Stephanie Szobota[1]; Pranav D. Mathur[2]; Sairey Siegel[2]; Kristen Black[2]; H. Uri Saragovi[3]
[1]Otonomy Inc; [2]Otonomy Inc.; [3]McGill University, Lady Davis Institute-Jewish General Hospital

Background
Hearing loss is the most common sensory disorder, affecting approximately 15% of adults in the US. In many of these cases, especially for those with mild-to-moderate hearing loss or decreased speech-in-noise discrimination, hearing loss may be reversible with treatments that promote the survival of cochlear neurons and restoration of their synaptic contacts with hair cells. One approach that has been investigated is the application of BDNF and NT-3, neurotrophins which are known to provide trophic support to spiral ganglion neurons (SGNs) in the cochlea through activation of TrkB and TrkC receptors. Monoclonal antibodies (mAbs) with agonist activities also have the potential to activate TrkB or TrkC, while providing therapeutic advantages such as high affinity and biostability. Several mAb TrkB or TrkC agonists were generated and characterized alongside BDNF and NT-3 in Trk receptor assays and ex vivo models using rat cochlear tissue.

Methods
AlphaLISA and Biacore assays were used to evaluate the binding properties of BDNF, NT-3, and the Trk ago-

nist mAbs. Functional activity was tested by measuring several known downstream effectors using Western Blot and AlphaLISA in stable cell lines that express Trk receptors. The ability of BDNF, NT-3, and mAbs to activate native cochlear TrkB and TrkC and stimulate pro-survival signaling was evaluated by counting surviving neurons in cultures containing dissociated SGNs prepared from postnatal Sprague Dawley rats. The most active molecules were then tested in SGN explants and organotypic cochlea cultures from postnatal rats to examine their ability to stimulate neurite growth and synaptogenesis.

Results

The mAbs selectively bound to either TrkB or TrkC with low nanomolar affinity. Activation of downstream signaling in TrkB or TrkC -expressing cell lines was potent and dose-dependent. The degree of agonism of the different mAbs varied, ranging from partial to full, relative to BDNF and NT-3. Survival of dissociated SGNs was increased significantly with BDNF, NT-3 and mAbs, compared to untreated cultures. In explants of intact spiral ganglion or cochlea, treatments increased the length and number of neurites and number of synaptic puncta.

Conclusions

BDNF, NT-3, and the Trk agonist mAbs evaluated are potent activators of neurotrophin signaling in ex vivo cochlea cultures. Their ability to promote survival, neurite extension, and synapse restoration make them attractive therapeutic candidates for the treatment of hearing loss.

PD 123

Characteristic of Firing Pattern of Type I and Type II Spiral Ganglion Neurons

Jeong Han Lee[1]; Wenying Smith[2]; Seojin Park[2]; Mincheol Kang[2]; Maria C Perez-Flores[1]; Ebenezer Yamoah[1]

[1]University of Nevada Reno; [2]University of Nevada, Reno

The spiral ganglion neurons (SGNs) participate in the physiological process of hearing by relaying signals from sensory receptors to the cochlear nucleus. Two subtypes of SGNs exist as type I and type II. The type I comprise the vast majority of SGNs (~95%), and exclusively innervate the inner hair cells (IHC), whereas ~5% of them are type II SGNs. They are responsible for the sensory innervation of outer hair cells (OHCs). We investigated the functional difference between type I and type II spiral ganglion neurons. Type I and type II SGNs were isolated from the topographic axis of the cochlear contour from peripherin-EGFP transgenic mice. In stark contrast to type I SGNs, the input resistance of type II

neurons was at least 6-fold greater than that of type I neurons. Other glaring differences included prolonged action potential (AP) duration, reduced AP amplitude, reduced whole-cell K+ current density, and pronounced transient outward current (Fig. 1). Table 1 outlines a summary of the properties of type I and type II SGNs. The underlying macroscopic and elementary properties of ionic currents of type II SGNs that determine their electrical properties will be identified.

Figure 1. Distinct properties of type I and II SGNs. A-B. Current-clamp recordings from type I (red) and type II SGNs (blue), showing visible differences in the action potential (AP) duration and amplitude. C-E. From the RMP, positive and negative current was injected to determine the resting input resistance. Type I SGNs voltage response properties (C) had input resistance, which was determined from the slope of the regression line = ~55 + 2 MW (n = 13). D. In contrast, the voltage response properties of type II SGNs was steep with input resistance of ~320 + 15 MW (n = 17) (p < 0.001 comparing data from type I and II SGNs (E). F-H. Voltage-clamp data from type I (red traces) and type II (blue traces) SGNs and the corresponding current-voltage (I-V) relationships (H). Neurons were held at -80 mV and stepped from -120 to 60 mV with DV = 10 mV and tail current voltage was at -40 mV. The peak currents are denoted with solid symbols and the steady-state current are in open symbols (n = 15). The summary data of the differences in AP profiles between type I and II SGNs are summarized in Table 1.
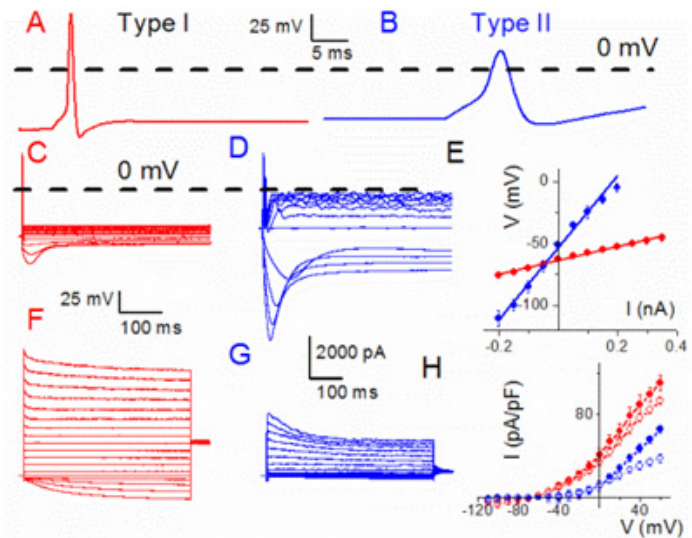

Table 1: Summary of the properties of AP in type I and II SGNs.
Data were obtained from 11 DTMs

	RMP (mV)	Threshold (mV)	Amplitude (mV)	Duration (ms)	AHP (mV)	Latency (ms)
Type I	-57.8 ± 2.8	-37.6 ± 2.4	90.2 ± 9.8	1.8 ± 0.2	-29.3 ± 4.3	2.5 ± 0.3
Type II	-53.7 ± 3.4*	-46.8 ± 3.2**	79.9 ± 8.7**	4.9 ± 0.9**	-5.7 ± 4.2**	1.1 ± 0.1**

*p < 0.05, **p < 0.01 (n = 15). RMP = resting membrane potential, AHP = after-hyperpolarization

PD 124

A Simple Physiological Model of Spike-Conducting Auditory Nerves -- towards the Application of Cochlear Implant Modeling

Go Ashida[1]; Waldo Nogueira[2]
[1]*University of Oldenburg; *[2]*Department of Otolaryngology, Hannover Medical School, Germany; Cluster of Excellence Hearing4all*

Modeling spike conduction of auditory nerves has served as a useful tool to evaluate the performance of cochlear implants by producing quantitative predictions of the electric interaction between the nerves and implanted electrodes. Previous physiological models of spike-conducting axons used Hodgkin-Huxley(HH)-type (or Frankenhaeuser-Huxley-type) equations that describe the dynamics of various ionic currents on the neuronal membrane. To precisely simulate the electrical activity of an auditory nerve, a number of model parameters (typically more than 20) need to be tuned or optimized. However, since the amount of available physiological data is largely limited especially in humans, it is generally difficult to justify the selection of model parameters. Furthermore, optimizing a large number of parameters incurs enormous computational costs, which hinders efficient simulations of the electrode-nerve interface. Thus it is desired to have a simple model that still holds the fundamental characteristics of the auditory nerves with a small number of unknown parameters to be tuned. Here we present a novel type of spike-conducting axon model based on the exponential integrate-and-fire (EIF) model, which is much more compact (in terms of the number of parameters and equations) than the conventional HH-type models but still able to faithfully replicate the neuronal spike initiation. Modifying the standard EIF model by limiting the maximum depolarization current and introducing a repolarization current, our model can reproduce the entire neuronal spike waveform with a small number of parameters (less than 10) and reduced computational costs. This new model was applied to simulate the spike propagation of both myelinated nerves and unmyelinated nerves. Our series of simulations showed that both EIF-based model and HH-type model have almost identical dependencies of morphological parameters such as the axonal diameter and internodal length, confirming the validity of the new model for the examination of axonal spike conduction. As an application of our new approach, we modeled the central axons of auditory nerves. By tuning a few parameters, our model can simulate distinct spiking activity of high and low characteristic frequency nerves that was reported in previous animal studies. Our simulations predict that the axonal spike conduction of high frequency nerves is faster than that of low frequency nerves, which should be tested in future experimental measurements. In the presentation, possible application of the new model to simulate the electrode-nerve interface between the cochlear implant and auditory nerves will also be discussed.

PD 125

A Comprehensive Approach to Quantifying Age-Related Differences in Auditory Nerve Function

Kelly C. Harris[1]; Carolyn M. McClaskey[1]; James W. Dias[1]; Judy R. Dubno[2]
[1]*Medical University of South Carolina; *[2]*The Medical University of South Carolina*

Several pathophysiological processes are known to underlie age-related changes in the auditory system. Recent results suggest that hair cells may not be the most vulnerable elements in the inner ear; rather, synapses between hair cells and nerve terminals appear to degenerate first following noise exposure and with increasing age. Although the loss of synaptic connections may not result in significant elevation of detection thresholds, cochlear synaptopathy disrupts auditory nerve (AN) function and may contribute to suprathreshold auditory processing deficits. Because procedures to assess AN activity in humans are limited, the functional effects of synaptopathy and subsequent AN degeneration have been difficult to quantify. Traditionally, analysis of the compound action potential (CAP), an extracellular potential reflecting the summed response of a population of AN fibers, is limited to differences in peak amplitudes and latencies. Although amplitudes and latencies of individual fiber responses are conceptually independent, these measures can be confounded in averaged responses. To better characterize the effects of age on AN function, we developed and analyzed five metrics derived from averaged CAP waveforms recorded from younger and older adults with normal hearing; we also analyzed responses to individual stimuli in the frequency domain to quantify neural synchrony. We hypothesized that younger adults, with their larger population of functioning AN fibers, would have larger and broader CAP waveforms and stronger phase locking than older adults. This increase in the width of the CAP response in younger adults, along with age-related delays in response onset, is hypothesized to result in greater age-related differences in response onset latency than peak latency. To test these hypotheses, CAPs were elicited using 100-µs click trains presented at 70-110 dB pSPL. Modified Matlab ERPlab functions estimated the onset of the averaged CAP response, response area, and width. Peak amplitudes and latencies of the averaged waveforms were recorded for N1 of the CAP. EEGlab performed time-frequency analyses across trials and estimated phase locking value (PLV) across frequency. Compared to younger adults, older adults exhibited reduced peak amplitudes and shallower slopes

of CAP amplitude-intensity functions. These age-related differences in response amplitude were associated, in part, with poorer neural synchrony. As predicted, at higher stimulus intensities, age-related differences in onset latency were greater than differences in peak latency. This comprehensive approach may better define the functional effects of age-related changes in neural synchrony and AN loss and provide a means to better identify underlying pathological processes.

Development IV

PD 126

Par3 integrates planar cell polarity (PCP) signaling to regulate hair bundle morphogenesis

Andre Landin Malt[1]; Zachary Dailey[1]; Julia Holbrook-Rasmussen[1]; Steven Gercken[1]; Yuqiong Zheng[1]; Maxwell Madani[2]; Xiaowei Lu[3]
[1]University of Virginia School of Medicine; [2]University of VIrginia School of Medicine; [3]University of Virginia Health System

During development, cochlear hair cells form V-shaped hair bundles that are uniformly oriented across the organ of Corti (OC). This process is controlled by the coordinated action of tissue-level PCP signaling, and a hair cell-intrinsic polarity machinery. The cell-intrinsic machinery is also required for hair bundle morphogenesis through basal body positioning and consists of Rac-PAK, Cdc42-aPKC signaling modules and LGN/Gαi/dynein, an evolutionarily conserved complex for mitotic spindle orientation. LGN mutations have been implicated in congenital deafness, underscoring the importance of this pathway in hearing.

To further understand how PCP signaling is coupled with hair bundle morphogenesis, we investigated the role of Par3 (aka Pard3), a PDZ scaffold protein and an evolutionarily conserved regulator of cell polarity, in hair cell PCP.

In the developing cochlea, we found that Par3, but not its binding partner Par6, is asymmetrically localized at intercellular junctions in the OC during hair bundle morphogenesis, consistent with a role in PCP establishment. Indeed, analysis of inner-ear specific Par3 conditional knockout (Par3^{cKO}) cochleae revealed defects in both hair bundle orientation and morphogenesis. To elucidate the underlying mechanisms, we first tested whether Par3 promotes asymmetric cortical localization of LGN, similar to its role in mitotic spindle orientation. To our surprise, asymmetric distribution of LGN/Gαi was

unaffected in Par3^{cKO} hair cells. Instead, levels of PAK activity were decreased in Par3^{cKO} cochleae, suggesting a positive role of Par3 in regulating Rac-PAK signaling. We hypothesized that Par3 promotes Rac-PAK signaling on the lateral hair cell cortex through its interaction with TIAM1, a guanine nucleotide exchange factor for Rac, as reported in other systems. Co-IP experiments confirmed that Par3 forms a complex with Tiam1 in the ear in vivo. Moreover, Tiam1 localization was altered in Par3^{cKO} hair cells. We further demonstrated that Par3 regulates microtubule organization and stable attachment of microtubules at the lateral hair cell cortex. Taken together, the results demonstrated a critical function of Par3 in regulating basal body/kinocilium position through the Tiam1-Rac-PAK axis.

At the tissue-polarity level, we found that Par3 and the core PCP molecule Vangl2, mutually regulate each other';s subcellular localization. Thus, we propose that Par3 integrates tissue-level and cell-intrinsic PCP signaling pathways to regulate hair bundle morphogenesis

PD 127

Daple coordinates organ-wide and cell-intrinsic polarity to pattern hair bundles

Kimberly Siletti[1]; Basile Tarchini[2]; A. James Hudspeth[3]
[1]The Rockefeller University; [2]The Jackson Laboratory; [3]Howard Hughes Medical Institute and Laboratory of Sensory Neuroscience, The Rockefeller University

The planar polarization of mammalian cells necessitates the integration of diverse pathways. In the inner ear, at least two systems regulate the planar polarity of the hair bundle. The core planar-cell-polarity (PCP) proteins coordinate the orientations of hair cells across the epithelial plane. The cell-intrinsic patterning of each hair bundle is implemented independently by the alpha subunit of a heterotrimeric G-protein complex (Gαi) and G-protein signaling modulator 2 (Gpsm2). Classically known for orienting the mitotic spindle, these proteins form an apical blueprint for hair-bundle development. Although the primary cilium also participates in each of these pathways, the mechanism that links tissue-wide and cell-intrinsic polarity is not yet understood.

To address this issue, we performed a yeast two-hybrid screen with a central component of the cell-intrinsic pathway, Gαi3. One of the most promising candidates, Dishevelled-associating protein with a high frequency of leucine residues (Daple), interacts with both core PCP and cell-intrinsic signals. Regulated by the cell-intrinsic polarity pathway, Daple is required to maintain core PCP signals and to position the primary cilium at the abneural side of the apical surface. Our results suggest more-

over that the primary cilium or an associated structure influences the cell-intrinsic blueprint that shapes the hair bundle. Daple is therefore essential to orient and pattern sensory hair bundles.

PD 128

The Planar Cell Polarity Protein VANGL2 acts Non-autonomously to Direct Type II Spiral Ganglion Neuron Innervation of the Developing Cochlea.

Satish Ghimire; Evan Ratzan; Michael Deans
University of Utah

The cochlea is innervated by sensory neurons of the spiral ganglia that relay sound information from hair cells to central auditory targets. A subset of these are the Type II spiral ganglion neurons (SGN) which have nociceptive features and may contribute to a feedback circuit that provides neuroprotection in extreme noise. The morphological development of Type II SGNs is unique because their peripheral axons project beyond inner hair cells, pass underneath the supporting cells and always turn towards the cochlear base before synapsing with 10 or more outer hair cells (OHC). The mechanisms underlying the stereotyped turning of the Type II fibers remain poorly understood. We hypothesized that components of the planar cell polarity (PCP) signaling pathway could contribute to Type II fiber development because several studies have shown the involvement of the core PCP proteins in the navigation of commissural axons in spinal cord and the polarized migration of facial branchiomotor neurons in hindbrain. In this study, we examined the role of the core PCP protein VANGL2 in Type II SGN innervation of the cochlea using mouse genetic tools.

In Vangl2 knockouts, NF200 immunostaining revealed that Type II growth cone turning is randomized in the basal turn of cochlea and approximately 50% turn incorrectly towards the cochlear apex. Similar turning errors in Celsr1 KO and Fzd3 KO mice suggesting a contribution from the PCP signaling pathway in Type II peripheral axon pathfinding. Using a series of transgenic Cre lines to restrict Vangl2 gene deletion to either the SGN or the cochlear duct, we demonstrate that Vangl2 functions non-autonomously in the cochlea and is not required in the growth cone. This is in contrast to commissural axons where PCP signaling occurs in the growth cone to guide a similar axon turning event. Moreover, whole mount immunostaining reveals that VANGL2 is asymmetrically distributed at intercellular junctions between the basolateral surfaces of cochlear supporting cells. Super resolution microscopy further demonstrated that VANGL2 is enriched on one side of supporting cell facing the cochlear apex. We propose that this distribution would allow VANGL2 to interact with the Type II peripheral axon growth cones and bias the turning of

these fibers towards the cochlear base. Altogether these data demonstrate a novel function for PCP signaling in the developing cochlea and suggests that VANGL2 acts non-autonomously from the tissue that is innervated rather than autonomously in the navigating growth cone.

PD 129

The Planar Cell Polarity gene Ptk7 regulates SGN peripheral projections

Yuqiong Zheng[1]; Andre Landin Malt[1]; Michelle Lynskey[2]; **Xiaowei Lu**[2]
[1]University of Virginia School of Medicine; [2]University of Virginia Health System

During tissue morphogenesis, planar cell polarity (PCP) signaling acts in both epithelial and non-epithelial cells to drive polarized cell behaviors within the plane of the tissue. We have shown previously that the receptor pseudo-kinase Ptk7 acts in concert with the core PCP genes to coordinate the uniform orientation of the hair bundles in the organ of Corti (OC). Ptk7 is broadly expressed in the developing cochlea, including the spiral ganglion neurons (SGNs) that innervate hair cells. We therefore generated inner ear conditional knockout of Ptk7 (Ptk-7[cKO]) in order to determine the function of Ptk7-mediated PCP signaling in SGN development.

During embryonic development, SGNs extend peripheral processes to form ribbon-type synapses with inner or outer hair cells. The majority afferents (type I) contact IHCs, while type II afferents extend across the tunnel of Corti and turn towards the base of the cochlea to connect with multiple OHCs. SGN neurite outgrowth appeared normal in Ptk7[cKO] cochleae, with well-organized radial bundles and inner and outer spiral bundles. However, immunostaining of markers for type II cochlear afferents revealed that some type II afferent turned towards the apex instead of the base. Sparse labeling of SGN projections in Ptk7 null cochleae furthered confirmed that about 50% type II afferent made turning errors, indicating that this turning event requires Ptk7-mediated PCP signaling. We hypothesize that Ptk7 either regulates planar polarity cues in the OC to guide type II afferents, or control the response to planar polarity cues by SGN growth cones. To determine cell autonomy of Ptk7 in type II peripheral projections, we are testing the effect of deleting Ptk7 either in SGNs or the sensory epithelium on turning behavior of type II afferents. Experiments are ongoing to test whether Ptk7 regulates other components of the non-canonical Wnt signaling pathway.

PD 130

Hair cell-driven activity shapes diversification of Type I spiral ganglion neurons

Brikha R. Shrestha; Chester Chia; Lorna Wu; Lisa V. Goodrich
Harvard Medical School

In the developing auditory system, spontaneous spiking of inner hair cells (IHCs) before the onset of hearing causes rhythmic bursts of action potentials in spiral ganglion neurons (SGNs), which in turn drive activity onward in the circuit. This spontaneous cochlear activity influences maturation of central auditory circuits. However, it is unknown whether IHC-driven activity is also necessary for proper development of Type I SGNs, which exhibit heterogeneity in threshold sensitivities that likely contributes to the fidelity of sound encoding in the auditory periphery.

To analyze how SGN subtypes develop, we first derived an unsupervised transcriptome-based classification of these neurons in mice (P25-P27) by single-cell RNA sequencing (scRNA-seq). Three major molecular subtypes of Type I SGNs, which we name Ia, Ib, and Ic, were found across the tonotopic axis of the cochlea. Fibers of Ia and Ic SGNs preferentially innervate the pillar and modiolar faces of IHCs, respectively, and flank those of the Ib subtype, indicating that they correspond to the high, low and medium spontaneous firing rate (SR) SGN subgroups defined classically based on physiology. Examination of subtype marker expression in situ revealed that SGN molecular identities begin to emerge around birth and are gradually refined over early postnatal stages, a time of abundant spontaneous activity in the cochlea.

To examine whether activity plays a role in the establishment of SGN subtype identity, we examined Vglut3$^{-/-}$ mice, in which IHC-driven excitation of SGNs is abolished at all stages. SGNs expressed Ia, Ib, and Ic subtype markers in comparable proportions in control and Vglut3$^{-/-}$ mice at birth. However, by P7, there was a dramatic decrease in the number of SGNs expressing Ib/Ic markers and a concomitant increase in those expressing Ia markers. Transcriptomic analysis of SGNs in Vglut3$^{-/-}$ mice by scRNAseq at P25-P27 confirmed that the vast majority of Type I SGNs (73% vs. 33% in wildtype) had molecular profiles resembling the Ia subtype. Thus, lack of IHC-driven activity impaired consolidation of Ib/Ic SGN identities in the first postnatal week, leading to an overabundance of Ia SGNs in the mature cochlea.

In summary, we found three molecular classes of Type I SGNs whose identities are shaped by IHC-driven spontaneous activity, thereby determining their proper proportion in the mature cochlea. Since mutations in Vglut3 causes deafness in humans (DFNA25), our findings underscore a need to assess the impact on SGN differentiation in forms of congenital deafness expected to affect hair cell activity. In addition, these results have important implications for the correction of congenital sensorineural hearing loss with genetic etiologies, as well as the use of cochlear implants.

PD 131

Combining Molecular Manipulations and Targeted Transplantation to Elucidate Central Afferent Pathfinding Properties

Karen L. Elliott-Thompson[1]; Jeremy S. Duncan[2]; Douglas W. Houston[1]; Bernd Fritzsch[1]
[1]University of Iowa; [2]Western Michigan University

Background
Inner ear afferents establish stereotyped connections between hair cells at the periphery and nuclei in the hindbrain, such that inner ear afferents terminate between trigeminal and lateral line nuclei. Inner ear afferents from transplanted ears find the correct target nuclei, even when transplanted across species or to the spinal cord, suggesting molecular guidance by diffusible factors. Given that Wnt/planar cell polarity signaling patterns the dorsal hindbrain and spinal cord and that the Wnt/PCP effector Prickle1 has been shown to affect afferent guidance (Yang et al., 2017), we hypothesize that Wnt signaling plays a role in dorsoventral guidance of inner ear projection within the hindbrain and plays a major role in guiding growing fibers in the CNS.

Methods
Cochlea of mice mutant for the Wnt receptor, Frizzled3 (upstream of Prickle1), were injected with lipophilic dyes to reveal their central projections. To eliminate signal redundancy of substrate and diffusible factors in pathfinding we eliminate normal substrate guidance properties by transplanting ears from frogs injected with Fzd3 morpholino at the two-cell stage to an uninjected frog, with or without replacing the native ear. Thus, only the ear lacks the Fzd3 receptor, and does so prior to afferent differentiation. To further elucidate Wnt as a diffusible molecule for afferent navigation, ears from a control frog were transplanted to a frog injected with Wntless morpholino (eliminates all Wnt secretion

Results

Mice mutant for Fzd3 show aberrant central projections. In these mice, afferents do not maintain a normal tonotopic organization somewhat similar to Prickle1 null mice. In addition, transplantation of an ear from a frog injected with Fzd3 morpholino to replace the native ear of a control frog resulted in misrouting of central projections, such that afferents overlapped with the more dorsal lateral line afferents. Finally, transplantation of a control ear to replace the native ear in a Wntless frog also results in misrouting of inner ear afferents to even more ventral positions.

Conclusions

These results implicate the Wnt pathway in dorsoventral targeting of inner ear afferents within the hindbrain. Further work will need to determine which Wnts are secreted and how many different Fzd receptors are present in placodally-derived neurons relative to neural crest derived neurons that allow them to find a specific gradient to home onto. Such analysis is possible through the combination of molecular defects of afferents forced to rely solely on diffusible factors by excluding substrate guidance cues through transplantation.
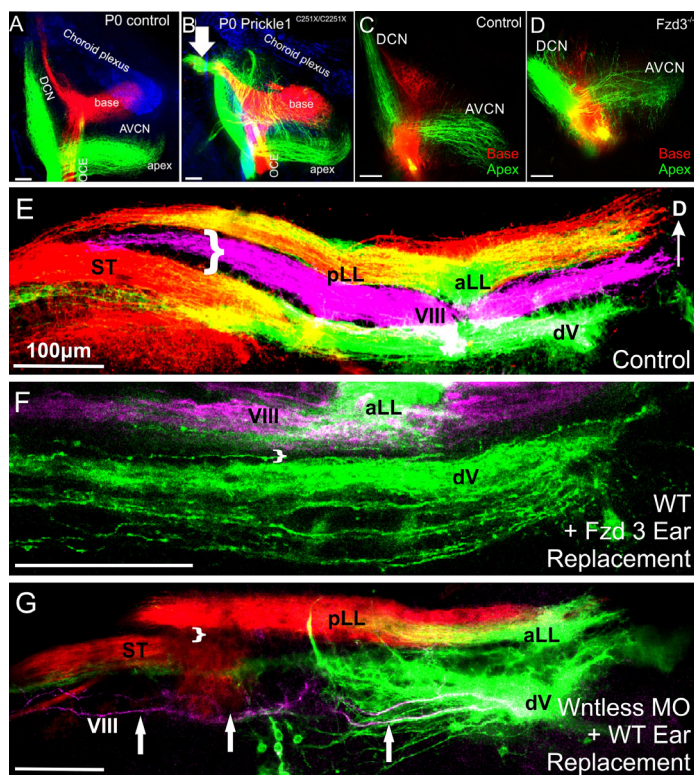

Figure 1. Manipulations of the Wnt/PCP pathway lead to altered central projections. (A,B) Image from Yang et al. (2017) showing aberrant central projections in mice following Prickle1 mutation. (C,D) Compared with control (C), Fzd3⁻/⁻ mice (D) have aberrant central projections. (E) Control central projections of a frog showing lateral line most dorsal (aLL/pLL), followed by inner ear (magenta, VIII), and then trigeminal (dV). (F) Wild type frog with an ear transplanted from a frog injected with Fzd3 morpholino in place of the native ear showing overlap of inner ear afferents with the lateral line. (G) Frog injected with Wntless morpholino with a wild type ear transplanted in place of the native ear showing inner ear projections ventral to trigeminal afferents (arrows). Normal projection region of inner ear afferents is marked with a bracket (}).

PD 132

Reduction of retinoic acid signaling mediates striolar formation in the mouse maculae

Kazuya Ono[1]; Omar López Ramírez[2]; Antonia Gonzalez Garrido[2]; Sarath Vijayakumar[3]; Ruth Anne Eatock[2]; Sherri Jones[4]; Doris Wu[1]
[1]NIDCD; [2]University of Chicago; [3]University of Nebraska-Lincoln; [4]Department of Special Education and Communication Disorders College of Education and Human Sciences, University of Nebraska-Lincoln

The striola, a central swath of the sensory epithelium in the otolithic organs (maculae), is conserved and found among inner ears of mammals, birds, reptiles, and amphibians. This specialized region differs from the rest of the macula in the anatomy, gene expression and functional properties of its sensory hair cells and innervating neurons. Notably, afferents of the striolar region exhibit irregular firing patterns and transient responses to current steps and those that innervate the extra-striolar region have regular firing and sustained responses to current steps. A number of specializations suggest that the striola may be critical for mediating rapid vestibular reflexes. However, the significance of striolar function in vestibular reflexes or maintenance of balance has not been demonstrated experimentally because there is no existing animal model that specifically lacks the striola. Here we report a transgenic mouse in which the maculae are largely normal in size and total HC number but the striola formation is compromised. We found that normal striolar formation requires a low level of retinoic acid (RA) signaling during development, mediated by the expression of one of the RA degradation enzymes, Cyp26b1, whereas the peripheral region of maculae expresses a gene that encodes a RA synthesizing enzyme, Raldh3. The lack of Cyp26b1 resulted in a severe reduction of the striolar domain based on the loss of several striolar-specific markers such as oncomodulin expression in striolar Type I HCs, b-tectorin expression in supporting cells, and anti-calretin or anti-calbindin staining in afferents. The afferent firing pattern evoked by injected currents was more likely to be sustained than transient in mutant striolar region, also consistent with a reduction in striolar specialization in the Cyp26b1 conditional null mutant. Whether there is any vestibular deficit caused by this compromised striola is currently under investigation.

PD 133

Gjb2 is required in supporting cells of the organ of Corti in a developmental stage- and cell type-specific manner

Jennifer M. Skidmore[1]; Lisa A. Beyer[2]; Gilson J. Sanchez[3]; Donald L. Swiderski[4]; Donna M. Martin[5]; Yehoash Raphael[4]

[1]Department of Pediatrics and Communicable Diseases University of Michigan, Ann Arbor, MI, USA.; [2]Kresge Hearing Research Institute University of Michigan, Ann Arbor, Michigan, USA; [3]Departments of Pediatrics and Communicable Diseases University of Michigan, Ann Arbor, MI, USA.; [4]Kresge Hearing Research Institute, University of Michigan; [5]Departments of Pediatrics and Human Genetics, University of Michigan, Ann Arbor, MI, USA

Mutations in GJB2, encoding Connexin26 (Cx26), are the most common cause of autosomal recessive hereditary deafness. Despite this high prevalence, the specific pathogenic mechanisms leading to GJB2-related hearing loss are not understood, and there are no curative treatments. Individuals with GJB2-related hearing loss typically exhibit normal organ of Corti morphology and spiral ganglion neurons (SGNs), suggesting the mechanisms contributing to hearing loss may not involve major disruptions in morphology of auditory epithelia or nerves. In contrast, mice with conditional loss of Gjb2 in supporting cells of the auditory epithelium (Sox10-Cre;Gjb2$^{flox/flox}$) exhibit profound loss of hair cells and SGNs. Here we used inducible Sox10-iCre^{ERT2}-mediated loss of Gjb2 to ask whether auditory epithelial integrity and function are sensitive to Gjb2 loss in supporting cells at various developmental stages (i.e. embryonic vs. early postnatal vs. adult). Reporter assay confirmed Cre expression in supporting cells of the organ of Corti in Sox10-iCre^{ERT2} mice after early (E10.5) or later (E17.5) tamoxifen induction. To delete Gjb2, tamoxifen was administered to Sox10-iCre^{ERT2};Gjb2$^{flox/flox}$ mice by intragastric injection at postnatal day 1 (P1) or intraperitoneal injection at day 14 (P14). Littermate Gjb2$^{flox/flox}$ mice were injected as controls. At least 8 mice were analyzed for each experimental condition. The mice were allowed to mature until postnatal day 21 (P21), when their hearing was analyzed using auditory brainstem response audiometry. Histological analysis of the auditory epithelium was also performed. Deletion of Gjb2 was confirmed by reduced anti-Connexin26 staining in ears from mice injected at both P1 and P14. Interestingly, Gjb2 deletion at P1 led to coat hypopigmentation, severe to profound hearing loss, but no major changes in hair cell organization. In contrast, Gjb2 deletion at P14 had no effects on coat color or inner ear hair cell morphology, but resulted in mild-moderate hearing loss at P21. These results indicate that reduced Gjb2 dosage has important developmental stage- and cell type-specific effects on both coat color and on auditory epithelial morphology and function. Further studies are necessary to determine whether the difference is due to age or duration. These findings highlight the role of Cx26 in the developing organ of Corti, and shed light on specific developmental stages and cell types that are critical for Cx26 function. The results also suggest that development of therapies to correct GJB2-related hearing loss in humans may need to target specific developmental stages or cell types.

Auditory Prostheses VII

PD 134

Heterogenous Demyelination Alters Response Properties of Simulated Neuron Populations to Implant Stimulation

Jesse M. Resnick; Jay T. Rubinstein
University of Washington

Cochlear implants (CIs) function by directly depolarizing spiral ganglion neurons (SGNs) with current applied through an intracochlear array. While with prolonged deafness, SGN soma are lost, progressive structural changes, including loss of internodal myelin, precede complete degeneration and the ramifications of these more modest changes remain poorly understood. In this work, we simulated populations of neurons, heterogenous with respect to their myelination state, to explore how within population variation alters coding of electrically delivered signals.

We have introduced a modification to our, previously reported, biophysical model of SGN activation by applied extracellular current in which, by varying only the membrane capacitance for subsets of internode segments, variable amounts of axonal demyelination can be simulated. This approach enabled the creation of single fibers with any combination of simulated myelin thickness and extent of fiber affected. However, current applied through an individual channel will activate many neurons simultaneously and pathological myelination does not impact fibers uniformly. Here we have expanded our strategy to simulate a population of spiral ganglion nerves with axolemma diameters distributed as in a healthy cochlear nerve but with heterogenous demyelination. Populations'; myelination states were set probabilistically by constructing bounded normal distributions representing the probability density functions for myelin loss severity. Individual fibers'; myelination was then determined via random draws from these distributions, enabling the creation of SGN populations differing both in average severity and between fiber variability of myelin loss.

As in our single fiber studies, with modest to moderate demyelination the input-output curves of populations are nearly normal. With more severe demyelination-distribution means, populations become less sensitive, resulting in elevated thresholds; these shifts are relatively modest except in the event of extreme myelin loss. Substantial myelination variance lead to shallower slopes of population input-output curves due to slower recruitment of fibers with different myelination states. Moreover, in populations including some extremely demyelinated fibers, these fibers failed to respond even at the highest current intensities tested, yielding submaximal population firing efficiencies.

Response-latency distributions were even more sensitive to both the averages and variances of the severity distribution. As average myelin loss increased, slowed conduction velocities lead to increased latencies and broadening of latency distributions. In populations containing severely demyelinated fibers, central initiation dramatically reduced response latencies in some fibers, yielding bimodal latency distributions. Modest increases in myelination variance at these elevated average demyelination levels further increased jitter and the incidence of bimodality.

PD 135

Prediction of eCAP responses to electrical pulse train stimulation using a fast combined biophysical and phenomenological model

Margriet van Gendt[1]; Jeroen Briaire[2]; Randy Kalkman[2]; Johan H. Frijns[3]
[1]ENT department, Leiden University Medical Center; [2]Leiden University Medical Center; [3]Leiden University Medical Center, The Leiden Institute for Brain and Cognition

Research Background
ECAPs (electrically evoked compound action potentials) are measurements of the auditory nerve';s response to electrical stimulation. In the most conventional ECAP measure, the N1-P2 peak in the response to single pulses is recorded. In a different approach, the peak amplitudes over time in response to a pulse train are measured. This shows temporal alternation in peak amplitudes at specific stimulus rates, which diminishes over time during stimulation. This pattern is different per subject, but it is not yet known how it relates to the state and behavior of the nerve. We hypothesize that the number of neurons, stochasticity, refractoriness, adaptation and jitter influence the temporal ECAP responses and investigated this using a computational model. Methods: Thirty thousand auditory nerve fibers were modelled, spatial and pulse-shape effects, as well as temporal and stochastic effects were incorporated [1,

2]. A 3D conductance-based model was coupled to a biophysical neural model, and extended with stochasticity, refractoriness, adaptation and accommodation to calculate responses to pulse trains in a computationally efficient manner. ECAPs in response to pulse trains of different rates and amplitudes were predicted for fibers with different morphologies and the effects of model parameters were investigated.

Results
The model predictions show alternation of peak amplitudes similar to the human data, which is strongly related to refractoriness. The number of fibers used in the model affects the depth of the alternating pattern in the responses. A larger number of fibers causes a decrease in, and earlier disappearance of the alternating pattern. Stochasticity has no clear effect on rates and amplitudes of alternation. Increased adaptation reduces the amplitude of the alternation. Published data of neural survival and ECAPs from animal experiments were replicated by variation of the adaptation parameter.

Conclusion & Discussion
Using the comprehensive model with average parameter settings ECAP predictions similar to human data were obtained. Variation of adaptation and number of fibers changes the predicted eCAP responses similar to variations seen in experimental data. These parameters are related to factors such as duration of deafness and neural survival. This research therefore suggests that the temporal ECAP pattern can be used to determine the state of the nerve, and could be used to monitor neural survival post-implantation.

1. van Gendt MJ, Briaire JJ, Kalkman RK, Frijns JHM: A fast, stochastic, and adaptive model of auditory nerve responses to cochlear implant stimulation. Hear Res 2016, 341:130–143.

2. van Gendt MJ, Briaire JJ, Kalkman RK, Frijns JHM: Modeled auditory nerve responses to amplitude modulated cochlear implant stimulation. Hear Res 2017, 351:19–33.

PD 136

Systematic Design and Application of Atraumatic Electrode Arrays

Thomas Lenarz[1]; Andrej Kral[2]; Theodor Doll[3]; Rolf Salcher[4]

[1]Department of Otolaryngology, Hannover Medical School, Germany and DFG Cluster of Excellence Hearing4all; [2]Institute of AudioNeuroTechnology (VIANNA), Hannover Medical School; [3]Medical University Hannover; [4]Department of Otolaryngology, Hannover Medical School, Germany

Today';s cochlear implant (CI) recipients commonly have some low-frequency residual hearing that can be combined with electrical stimulation to improve speech understanding and enhance sound quality. The reliable preservation of residual hearing in the large majority of cases is a challenge to both CI manufacturers and surgeons.

A careful microCT analysis of 16 human temporal bones provided detailed design information for specification of parameters. Several generations of prototype lateral array design were developed and inserted into temporal bones using a 3-dimensional force measurement system, refining the prototype to a 23 mm length; targeting a 420 degree insertion depth. A series of 10 fresh-frozen temporal bones were implanted with the candidate design. Round window (RW), extended RW and bony cochleostomy approaches were used, with the facial recess maintained to reflect a live surgical approach. MicroCT and histological analysis were conducted. Finally, human implantations have begun with a series of 5 implantations using a RW approach. To control insertion, ECochG was recorded intra-operatively. In bench experiments hydrogel has been added to the electrode array with the goal of a self-bending device allowing a consistent peri-modiolar location for any individual';s size or shape of cochlea.

No trauma was observed for 9 of the 10 bones implanted with the lateral array design. In one case the basilar membrane was slightly elevated. A mean insertion depth of 432 (SD ±13) degrees was obtained: consistent with the 420 degree design intent. All live surgeries progressed smoothly. The ECochG signal was used as a real-time warning system. If ECochG dropped, insertion was halted, or the electrode withdrawn until the signal recovered. Following 4 of the 5 surgeries ECochG was recorded on completing the insertion, indicating successful hearing preservation. In one case technical problems prevented a final ECochG measurement. Hydrogel bench experiments confirm that curvature of the electrode array can be controlled.

A rigorous design process appears to have resulted in a lateral lying electrode array with positive surgical handling properties that appears capable of high levels of hearing preservation. In some cases a partial insertion may be required to truly preserve hearing. Initial hydrogel experiments indicate that a fully peri-modiolar location will be possible across differing anatomy while maintaining surgical handling and atraumicity. Further temporal bone work with hydrogel will be reported. Experience shows that both electrode design and surgical technique are important for reliable hearing preservation, with ECochG bringing useful real-time surgical feedback during insertion.

PD 137

Zwitterionic coatings control fibroblast, Schwann cell and spiral ganglion neuron behavior adhesion and alignment

Elise Cheng[1]; Braden Leigh[2]; Allan Guymon[2]; Marlan R. Hansen[3]

[1]University of Iowa; [2]University of Iowa Department of Chemical and Biochemical Engineering; [3]Department of Otolaryngology - Head & Neck Surgery, University of Iowa Hospitals and Clinics, Iowa City, IA

Introduction
Intracochlear fibrosis is an expected outcome following cochlear implantation with standard silastic and platinum electrode arrays. Emerging evidence suggests that intracochlear fibrosis may adversely affect hearing outcomes in CI users. Fibrosis may increase the voltage required to stimulate the target spiral ganglion neurons, causing current spread and reduction of the number of effective channels of stimulation. In the case of hearing preservation CIs, fibrosis may contribute to late loss of native hearing. We hypothesize a UV polymerizable zwitterionic antifibrotic coating can resist cell adhesion. We also hypothesize that when patterned, this coating may influence directional growth of Schwann cells and spiral ganglion neurons. These coatings may therefore be useful cues for spiral ganglion neurite guidance.

Methods
Fibrinogen or laminin were applied to glass and silastic substrates with or without zwitterionic coatings and protein adhesion was compared by quantitative immunofluorescence. Primary rat fibroblast, spiral ganglion, and Schwann cell cultures were cultured on glass or silastic substrates that were a) uncoated b) zwitterionic coated uniformly or c) zwitterionic coated using a striped photomask with a periodicity of 100mm. For fibroblasts and Schwann cells, cell density was measured by counting cell nuclei. To quantify Schwann cell alignment to the pattern, an ellipse was fit to the outline of the cell and the angle of the long axis of the ellipse relative to the

pattern feature was calculated. Spiral ganglion neurite alignment to the pattern was calculated as the ratio of neurite length divided by the end to end distance over the pattern feature.

Results

Zwitterionic coatings inhibited protein adhesion to glass and silastic substrates. Fibroblasts, Schwann cells, and spiral ganglion neurons adhere to uncoated glass but do not adhere to uniformly coated zwitterionic coated glass substrates. Furthermore, fibroblasts failed to adhere to zwitterionic coated silastic substrates. Fibroblasts on striped substrates extended their cytoplasmic borders to the edges of uncoated glass but do not extend cystoplasm into the coated region. Schwann cells cultured on striped substrates oriented themselves nearly parallel to the striped pattern with an average angle of 1.82° (SD 1.43°). Spiral ganglion neurites were also closely aligned to the pattern with an alignment ratio of 1.08 (SD 0.15).

Conclusions

Zwitterionic coatings strongly resist protein, fibroblast, Schwann cell, and spiral ganglion neuron adhesion. Patterned coatings strongly guide cell adhesion and Schwann cell and spiral ganglion neurite alignment.

PD 138

Pilot Evaluation of Cochlear Implant Electrode Position Control System in a Sheep Model

Christopher R. Kaufmann[1]; Viral D. Tejani[2]; Daniel Sun[1]; Douglas Fredericks[3]; Paul Abbas[2]; Marlan R. Hansen[4]

[1]Department of Otolaryngology - Head & Neck Surgery, University of Iowa Hospitals and Clinics; [2]University of Iowa Department of Communication Sciences and Disorders; [3]University of Iowa Department of Orthopedics & Rehabilitation; [4]Department of Otolaryngology - Head & Neck Surgery, University of Iowa Hospitals and Clinics, Iowa City, IA

Background

Hearing preservation cochlear implants (CIs) provide significant benefits in speech understanding, yet there can be continued progressive hearing decline following surgery.[1] This may leave CI recipients with the need to undergo a repeat surgery or experience limited hearing outcomes after hearing preservation cochlear implantation with a short array. We developed a novel implantable electrode position control system prototype with the goal of non-surgically advancing and optimizing intracochlear electrode position to account for post-surgical hearing loss. Here, we present initial in vivo evaluation of our prototype system in a sheep model. We aim to assess the ability of the implantable electrode positioning device to both perform atraumatic electrode insertions and wirelessly advance the intracochlear electrode array after 30 days.

Methods

Adult female Suffolk/Dorset crossbred sheep underwent unilateral (n=2) or bilateral (n=6) retrofacial approach to access the round window. Standard length, full size human CI electrodes were inserted through the round window membrane utilizing either prototype devices or manual insertions. For bilateral procedures, the prototype device was implanted and utilized for controlled CI insertions while manual by-hand CI insertions were used on the contralateral side. After 30 days, prototype devices were wirelessly accessed to remotely advance the electrodes further into the cochlea. X-ray fluoroscopy confirmed electrode position. Electrocochleography (ECoG) was performed pre- and post-implantation, as well as at 1 month post-operatively using both surface needle electrodes and a ball electrode placed at round window niche. The sheep were euthanized at 30 days post-op and necropsy, microCT, and cochlea histology was performed.

Results

Electrodes from three manufacturers interfaced with the prototype device and were inserted into the cochleae of 8 sheep at robotically-assisted control rates and distances ranging from 0.1 to 1 mm/sec and 4 to 12 mm, respectively. The prototype device was capable of wirelessly advancing an intracochlear electrode array. Histological, imaging, and ECoG measures were used to assess for insertion trauma. Histology and microCT imaging suggested correct intrascalar positioning and limited intracochlear fibrosis. ECoG measures were stable to a varying degree post-insertion with across sheep variability in amplitude changes noted.

Conclusion

The results support continued development of the implantable electrode insertion control system and further evaluation in long-term animal studies. Both atraumatic insertion and non-surgical optimization of intracochlear electrode position may lead to improved hearing outcomes for patients undergoing hearing preservation CI surgery.

1. Scheperle RA, Tejani VD, Omtvedt JK, Brown CJ, Abbas PJ, Hansen MR, Gantz BJ, Oleson JJ, Ozanne MV. (2017). Delayed changes in auditory status in cochlear implant users with preserved acoustic hearing. Hear Res. 350:45-57.

PD 139

Hearing Preservation after the Implantation of an Artificial Auditory Epithelium in the Guinea Pig Cochlea

Koji Nishimura[1]; Hideaki Ogita[1]; Takayuki Nakagawa[2]; Juichi Ito[1]
[1]*Shiga Medical Center Research Institute;* [2]*Department of Otolaryngology - Head and Neck Surgery, Graduate School of Medicine, Kyoto University*

Inner ear disorders such as sensorineural hearing loss are incurable by conventional therapeutic strategies. Hence, new therapeutic strategies for the protection and recovery of inner ear function need to be investigated. The aim of this project is to investigate a newly-invented artificial auditory epithelium which can be implanted in the inner ear. We created a device, consisting of a 40-micrometer-thick piezoelectric material fixed in a trapezoid-shape to mimic the shape of the basilar membrane and its frequency characteristics. We previously showed that this device can imitate the function of the cochlear sensory epithelia and transform vibrations into electric signals with frequency characteristics. We also showed that the electrical potentials generated by this device in response to sound stimuli can induce auditory brain stem responses (ABRs) in deafened guinea pigs, indicating its capacity to mimic basilar membrane function. In this study, we evaluated the degree of surgical trauma after insertion of the device into the cochlea and evaluated its potential for recovery of hearing. Four-week-old male Hartley guinea pigs were partially deafened by subcutaneous injection of kanamycin (100 mg/kg) followed by intravenous injection of furosemide (100 mg/kg). One week later, an artificial cochlear epithelium was implanted into the scala tympani of the basal cochlea. ABRs were measured every week after implantation for eight weeks until animals were sacrificed for histology. After implantation, there was minimal hearing deterioration and one animal demonstrated hearing recovery at 8 kHz. Therefore, we have shown that this artificial auditory epithelium has the potential to become an effective tool for the treatment of hearing impaired patients.

PD 140

Optogenetic stimulation of the cochlea—critical mechanisms and first models

Robin Weiß; Andrej Voss; **Werner Hemmert**
Technical University of Munich

We evaluate the potential of optogenetic methods for the stimulation of the auditory nerve and assess the feasibility of optogenetic cochlear implants (CIs). We provide an estimation of all critical steps: light source properties, beam divergence, attenuation due to absorbtion and scattering, the activation of channelrhodopsins, and finally, the activation of action potentials. From these foundations, quantitative estimates for the number of independent stimulation channels and the temporal precision of optogenetic stimulation of the auditory nerve are derived and compared with state-of-the-art electrical CIs. We conclude that optogenetic CIs have the potential to increase the number of independent stimulation channels by up to one order of magnitude to about 100, but only if light sources are able to deliver confined illumination patterns. Our calculations indicate that the large beam divergence of LEDs will severely limit the number of maximal channels, similar to the case in electric CIs, when they are placed at a distance larger than about 300μm from the spiral ganglion neurons SGNs without focusing elements. Vertical-cavity surface-emitting laser diodes would be a more promising solution, if they become available in the required wavelengths. On the other hand, the light sources with narrow beams require means for precise alignment towards their target. Another yet unknown factor is the modiolar bone, which is likely to severely attenuate and scatter light, but here data for modeling is scarce. The temporal properties of fast opsin variants like ChETA and Chronos enable driving of the auditory nerve up to rates of 200 spikes/s. This value is already close to the physiological value for the maximum sustained firing rate of auditory nerve fibers to acoustic stimulation. Apart from the activating time constants, also opsins with fast deactivating time constants are required to limit Na^+ influx and therefore the metabolic load imposed on the neurons.

We conclude that technical challenges for optogenetic CIs involve the delivery of sufficient light to the neurons, energy efficacy of the implant, the alignment and the long-term stability of the implanted optrode array. From the viewpoint of biology, the safety of gene transfection and the achievement of high expression levels are the most critical steps. Finally, the implantation of the optrode is expected to be much more delicate than with purely passive electrical arrays and preservative implantation will be a challenge for the surgeon. In summary, optogenetic CIs still face major hurdles, which require extensive research to overcome, before they are an option to replace electrical CIs.

PD 141

Auditory Attention Decoding: What Anatomical Locations and Neural Frequency Bands Contribute?

James O'Sullivan[1]; Jose Herrero[2]; Elliot Smith[1]; Sameer A. Sheth[1]; Guy M. McKhann[1]; Ashesh D. Mehta[2]; Nima Mesgarani[1]
[1]Columbia University; [2]Feinstein Institute for Medical Research

Decoding an attended speaker from neural recordings (termed auditory attention decoding; AAD) has many applications. The most pertinent is probably the development of a cognitively controlled hearing aid that can automatically track and amplify an attended speaker. Such devices will likely be limited to either non-invasive or minimally invasive neural recordings. Non-invasive recordings such as electroencephalography (EEG) can typically only record from low frequency (LF; < 50Hz) neural data, and have relatively poor spatial resolution. However, multiple electrodes can be used to target cortical areas using source-localization signal processing strategies. Minimally invasive approaches can place a restricted number of electrodes over specific cortical areas, and can also record from higher neural frequencies. In both cases, knowledge of the anatomical locations and neural frequency bands that contribute to AAD is crucial.

To investigate, we used an invasive recording methodology known as electrocorticography (ECoG) that can record from both low and high frequency (HF; < 200Hz) neural data, and can also localize neural activity to within ~3mm from both deep and surface brain regions, spanning the full extent of auditory cortex. We show that both LF and HF data can be used to decode attention, however with distinct differences between the two: When using HF data, single electrodes can perform AAD, with superior temporal gyrus (STG; a surface brain region) producing the most robust encoding of attended speech. However, LF data requires the combined use of multiple electrodes, with both deep structures such as Heschl';s gyrus (primary auditory cortex) and STG contributing to AAD. These results provide the first extensive exploration of the neural frequency bands and anatomical locations that contribute to AAD, and will inform future work on the development of cognitively controlled hearing aids.

Hair Cells VIII

PD 142

Single-molecule nanomechanics of a tip-link protein

Tobias F. Bartsch[1]; Felicitas E. Hengel[1]; Aaron Oswald[1]; Gilman Dionne[2]; Iris V. Chipendo[1]; Muhammad El Shatanofy[1]; Simranjit S. Mangat[1]; Ulrich Mueller[3]; Lawrence Shapiro[2]; A. James Hudspeth[4]
[1]The Rockefeller University; [2]Columbia University; [3]Johns Hopkins University; [4]Howard Hughes Medical Institute and Laboratory of Sensory Neuroscience, The Rockefeller University

The astounding sensitivity and dynamic range of mammalian hearing result from hair cells, the sensory receptors of the inner ear. Each hair cell features a hair bundle, a cluster of stiff stereocilia whose deflection opens mechanically gated ion channels. An enduring question in sensory neuroscience concerns the properties and identity of the "gating spring," the mechanical element that converts bundle deflection into a force capable of opening the channels. A strong candidate for this spring is the tip link, a dimer of dimers of protocadherin 15 and cadherin 23 molecules that connects each pair of adjacent stereocilia. The link';s elasticity results from the elasticity of individual cadherin domains, from the Ca^{2+}-stabilized rearrangement of the domains relative to each other, and potentially from the unfolding and refolding of individual domains. Although the mechanics of fragments consisting of a few cadherin domains from protocadherin 15 and cadherin 23 has been explored by molecular-dynamics simulations, the results do not account for the in vivo properties of the gating spring, and the mechanical properties of the full-length proteins and their dimers remain unknown.

Here we measure the force-extension curves and energy landscapes of the full extracellular domain of protocadherin 15 at subnanometer resolution and with physiologically relevant forces. When we confine a single protocadherin 15 molecule between a glass substrate and a polystyrene bead 1 μm in diameter, the bead experiences thermal forces and undergoes a random walk defined by the energy landscape of protocadherin 15. Using a stiff optical trap, we can also apply forces up to 30 pN, beyond the range accessible by thermal forces alone. After measuring the position distribution of the particle, we can infer through Boltzmann statistics the energy landscape and force-extension relation of protocadherin 15.

We explore the mechanics of protocadherin 15 at different Ca^{2+} concentrations and for different pathologically relevant mutations. For 20 μM Ca^{2+}, a concentration

typical of the endolymph in the mammalian cochlea, we observe the unfolding of individual cadherin domains under physiologically relevant forces. This behavior might act as a stress relief to protect the integrity of the tip link during loud sounds. The unfolded polypeptide chain then acts as an entropic spring that considerably diminishes the molecule';s stiffness. We find that such unfolding events are much less frequent at the millimolar Ca^{2+} concentrations usually employed in experiments conducted ex vivo, in vitro, or in silico.

PD 143

Hair-Bundle Stiffness and Tip-Link Tension along the Tonotopic Axis of the Rat Cochlea

Mélanie Tobin[1]; Nicolas Michalski[2]; **Pascal Martin**[1]
[1]*Institut Curie;* [2]*Institut Pasteur, INSERM UMRS 1120, Université Pierre et Marie Curie*

Auditory processing of complex natural sounds relies on acute frequency discrimination over a broad frequency range. Frequency analysis is initiated in the cochlea by mechanosensory hair cells, which are each tuned to respond at a characteristic frequency that varies monotonically along the longitudinal axis of the auditory organ. This tonotopic map is associated with morphological gradients of the hair bundle– the mechano-receptive antenna of the hair cell– but their significance for frequency tuning has remained elusive. Here, we studied micromechanical properties of the hair bundle along the tonotopic axis of the rat cochlea. We combined fluid-jet stimulation to deflect the hair bundle, iontophoresis of a calcium chelator (EDTA) to break the tip links and measure bundle movements resulting from tension release by these links, and patch-clamp recordings of transduction currents to count the number of intact tip links contributing to the response. From these measurements, we were able to estimate hair-bundle stiffness and mechanical tension in the whole hair bundle as well as in a single tip link. We found that the tip links contributed up to 50% of the hair-bundle stiffness. In outer hair cells, as the characteristic frequency increased from 1 to 4 kHz, we observed steep gradients of hair-bundle stiffness and single tip-link tension, which varied from 2.2±0.2 mN/m to 7.5±0.4 mN/m and from 3.0±0.2 pN to 26±6 pN, respectively. In contrast, inner hair cells only showed weak mechanical gradients of their hair bundles. Although hair-bundle stiffness and single tip-link tension were comparable in the two types of cells at the 1-kHz location, they were about twofold lower in inner hair cells than in outer hair cells at the 4-kHz location and increased to only 5.4±0.3 mN/m and 16±4 pN at the 15-kHz location. Remarkably, in both inner and outer hair cells, we observed that EDTA iontophoresis evoked a two-fold increase of tip-link tension before the tip links broke, resulting in active hair-bundle movements. Thus,

calcium changes might provide feedback on tip-link tension, as observed in other classes of vertebrates such as the frog and the turtle. Our results indicate that the transduction apparatus of the hair cell is mechanically tuned according to the cell';s characteristic frequency, more so in outer hair cells, which serve primarily as mechanical amplifier of sound-evoked vibrations, than in inner hair cells, the true sensors of the inner ear.

PD 144

Ribeye protein is intrinsically dynamic but is stabilized in the context of the ribbon synapse

Zongwei Chen; Shih-Wei Chou; Brian McDermott
Department of Otolaryngology, University Hospitals Cleveland Medical Center, Case Western Reserve University School of Medicine

Ribeye protein is a major constituent of the synaptic ribbon, an organelle that coordinates rapid and sustained vesicle release to enable hearing and balance. The ribbon is considered to be a stable structure. However, under certain physiological conditions such as acoustic overexposure that results in temporary noise-induced hearing loss or perturbations of ion channels, ribbons may change shape or vanish altogether, suggesting greater plasticity than previously appreciated. The dynamic properties of ribeye proteins are unknown. Here we use transgenesis and imaging to explore the behaviors of ribeye proteins within the ribbon and also their intrinsic properties outside the context of the ribbon synapse in a control cell type, the skin cell. By fluorescence recovery after photobleaching (FRAP) on transgenic zebrafish larvae, we test whether ribeye proteins are dynamic in vivo in real time. In the skin, a cell type devoid of synaptic contacts, Ribeye a-mCherry exchanges with ribbon-like structures on a minute timescale ($t_{1/2}$ = 3.2 min). In contrast, Ribeye a of the ear and lateral line and Ribeye b of the lateral line each exchange at ribbons of hair cells an order of magnitude slower ($t_{1/2}$ of 125.6 min, 107.0 min, and 95.3 min, respectively) than Ribeye a of the skin. These basal exchange rates suggest that long-term ribbon presence may require ribeye renewal. In addition, we show that Ribeye a exchange is independent of mechanotransduction. Our studies demonstrate that ribeye proteins are inherently dynamic but are stabilized at the ribbons of sensory cells in vivo.

PD 145

Regulation of Prestin by Anion Exchangers

Maria C Perez-Flores[1]; Jeong Han Lee[1]; Xiaodong Zhang[2]; Michael Anne Gratton[3]; Ebenezer Yamoah[1]
[1]*University of Nevada Reno;* [2]*University of California Davis;* [3]*Washington University*

Background

The mammalian hearing organ has exquisite mechanical sensitivity and frequency selectivity that surpasses any known sensory system in the body. An important technical quality of outer hair cells (OHCs) is their high-gain mechanical amplification of sound. Prestin (slc26a5) is a motor protein, and member of the solute carrier (SLC) gene family. The mechanism of prestin functions and regulation to confer OHC properties remains unknown. We studied the interaction between prestin and AE2 (slc4a2), an anion exchanger protein.

Methods

To meet our goals, we used heterologous CHO cell expression system and slc4a2$^{+/+}$, slc4a2$^{+/-}$, and slc4a2$^{-/-}$ mice. We recorded the non-linear capacitance (NLC) in CHO cells and OHCs from semi-intact cochlear tissue.

Results

In contrast to the current notion that the cochlear amplifier consists of prestin alone, lining the lateral wall of OHCs, we hypothesize that the authentic cochlear amplifier consists of prestin and a cavalry of other proteins, including slc4a2. We predicted that slc4a2 regulate the intracellular pH microdomain and Cl$^-$ to control prestin activity. We tested our hypothesis by demonstrating that 1) slc4a2 is expressed in OHCs. 2) Co-expression of prestin and slc4a2 in CHO cells revealed results in keeping with the prediction that prestin activity is modulated by slc4a2. 3) We evaluated the auditory function of mice with null deletion of slc4a2 and to our surprise; the mice had increased ABR threshold and reduced DPOAE, signifying OHC dysfunction. Consistent with the in vivo data, analyses of NLC of OHCs from slc4a2$^{+/-}$ and slc4a2$^{-/-}$ showed that OHCs from slc4a2$^{-/-}$ have a leftward shift in the voltage-dependence of NLC (-52 ± 6 mV; n = 3) compared with the OHCs from wildtype mice (-44 ± 4 mV; n = 3), the maximum charge (Qmax) in slc4a2$^{-/-}$ was reduced by ~2-fold (0.53 ± 0.04 pC; n = 3) compared with wild type (1.05 ± 0.1 pC; n = 3).

Conclusion

These results suggest that prestin activity is regulated by slc4a2 to optimize the sensitivity of the cochlear amplifier.

PD 146

Ultrastructural Localisation of Transmembrane Channel-like protein 1 (TMC1) in Cochlear Hair Bundles

Shanthini Mahendrasingam; **David Furness**
Keele University

TMC1 is a putative subunit of the mechanoelectrical transduction (MET) channel and expected to be part of the transducer complex at the lower end of the tip link (Pan et al, 2013; Neuron 79:504-515; Beurg et al., 2015; PNAS 112(5):1589-1594). We have shown by high resolution immunogold labelling for transmission electron microscopy (TEM) that another component of this apparatus, lipoma HMGIC fusion partner-like 5 (LHFPL5), localises precisely in this region (Mahendrasingam et al., 2017; PLoS 1 (in press)). LHFPL5 is thought to interact with TMC1, connecting the channel to the tip link (Xiong et al., 2012; Cell, 151(6):1283-1295). We have attempted to localise TMC1 to confirm its presence in this region and an association with LHFPL5. Custom antibodies were made to a synthetic peptide near the N-terminus of the TMC1 sequence (residues 82 – 101, Life Technologies UK). Immunofluorescence labelling of postnatal day (P)9 and P12 CD/1 wild type and P12 TMC1$^{-/-}$ mice was performed to validate the antibody, followed by pre-embedding immunogold for TEM. For immunofluorescence, cochleae were fixed for 20 min in 4% paraformaldehyde in phosphate buffer, dissected, washed, permeabilised in 0.5% Triton-X-100, pre-blocked in 10% goat serum (GS) in PBS - Tween 20 (T20), and incubated in anti-TMC1 diluted 1:25 in 1% GS-PBS-T20 for 48 h followed by TRITC-goat anti-rabbit secondary antibody (diluted 1:50) for 2 h and examined in an MRC1024 confocal microscope. For TEM, P9, P12 and P21 cochlea were processed the same way except that 10-nm gold-conjugated secondary was used (diluted 1:20), followed by postfixation and embedding in Spurr resin. Sections were examined in a JEOL 1230 TEM. Confocal microscopy revealed positive, punctate labelling of hair bundles but no distinct labelling elsewhere in the hair cells. There was labelling in the apical cytoplasm of supporting cells. All labelling was absent in the TMC1$^{-/-}$ mouse. Pre-embedding immunogold labelling was sparse at all ages examined; occasional gold particles were found on the shafts of all rows of stereocilia, but there was specific localisation of 2 – 3 particles at the tips of short and intermediate stereocilia. These data are consistent with TMC1 being part of the MET complex in animals from P9 onwards, and localised to the lower end of the tip link. This study thus provides further evidence that this protein may be part of the MET channel.

Human CLRN1 Complements Zebrafish Clrn1 in the Hair Cells

Suhasini Gopal[1]; Yvonne Tsui[1]; Daniel Chen[1]; Ruben Stepanyan[2]; Brian McDermott[1]; Kumar Alagramam[1]
[1]Department of Otolaryngology, University Hospitals Cleveland Medical Center, Case Western Reserve University School of Medicine; [2]Dept. Physiology, Univ. Kentucky; Dept. Otolaryngology, Case Western Reserve University

Usher syndrome type III (USH3) is characterized by progressive loss of hearing and vision with varying degrees of vestibular dysfunction. USH3 is caused by mutations that affect the human clarin-1 protein (hCLRN1), a member of the tetraspanin protein family. hCLRN1[N48K] is a common causative USH3 mutation among people of Ashkenazi Jewish descent; the affected individuals hear at birth but lose that function over time. We developed an animal model system using zebrafish transgenesis and gene targeting to provide an explanation for this phenotype. Wild-type (WT) zebrafish that express either hCLRN1 or hCLRN1[N48K] in hair cells were generated to examine the subcellular localization of these proteins. hCLRN1 localized to the hair bundles similar to zebrafish Clrn1, leading to the hypothesis that clarin-1 function is conserved across species. In contrast, hCLRN1[N48K] largely aggregates in the endoplasmic reticulum (ER) with a small amount reaching the hair bundle. We proposed that this small amount of hCLRN1[N48K] reaching the hair bundle provides clarin-1-mediated function during the early stages of life; however, the presence of the mutant protein in the hair bundle diminishes over time because of ERAD (ER-associated degradation) of the mutant protein, leading to progressive loss of hair bundle integrity and hair cell function. The zebrafish Clrn1 null mutant displayed compromised hearing and balance function associated with aberrant hair bundle morphology, but null mutants expressing hCLRN1 in hair cells were indistinguishable from those of WT. However, Clrn1 null zebrafish expressing hCLRN1[N48K] in hair cells displayed progressive loss of hearing and balance. These results are consistent with our hypotheses and demonstrate that hCLRN1 can complement zebrafish Clrn1. These findings and genetic tools provide an understanding and a path forward to identify therapies to mitigate hearing loss linked to CLRN1 mutation.

Hair-cell Ribbon Synapse Formation is Controlled by Calcium levels in Synaptic Mitochondria and downstream NAD(H) redox homeostasis

Hiu-tung C. Wong; Katie Kindt
National Institutes of Deafness and Other Communication Disorders, National Institutes of Health

Background

Sensory hair cells rely on specialized ribbon synapses to facilitate rapid and sustained vesicle release. The structural protein Ribeye is a major component of the presynaptic ribbon. Ribeye has a putative NAD(H) binding domain that has been shown in vitro to regulate Ribeye-Ribeye interactions, an effect which has not been demonstrated in vivo. Previous work has shown that during synapse development, Ribeye localization to the ribbon increased when the presynaptic L-type calcium channel $Ca_v1.3$ function is blocked. We aim to investigate how ribbon formation is affected by NAD(H) redox homeostasis, and if $Ca_v1.3$-dependent activity promotes Ribeye localization to the ribbon through NAD(H) redox homeostasis.

Methods

To study ribbon synapse development, we examined hair cells in the zebrafish lateral line. Lateral line hair cells resemble mammalian type II vestibular hair cells in structure and are easy to access for in vivo pharmacology, stimulation and visualization. Our work uses pharmacology to disrupt hair cell calcium and NAD(H) redox homeostasis in the developing hair cells. We also use transgenic zebrafish lines that express fluorescent calcium sensors and NAD(H) redox indicators to visualize calcium dynamics and NAD(H) redox in hair cells during pharmacological treatments. Synaptic ribbon morphology is quantified by immunofluorescence staining of Ribeye.

Result

We have found that similar to pharmacological block of $Ca_v1.3$, exogenous NAD^+ treatment increased ribbon size during ribbon formation. We predicted that mitochondrial calcium uptake of $Ca_v1.3$-dependent synaptic calcium may alter NAD(H) redox and Ribeye self-assembly via Ribeye';s NAD(H)-binding domain. To test the role of mitochondrial calcium uptake on Ribeye localization, we blocked the mitochondrial calcium uniporter (MCU) and found that, similar to $Ca_v1.3$ block and exogenous NAD^+ treatment, more Ribeye localized to the presynaptic ribbon. Interestingly, we also observed strong $Ca_v1.3$-dependent mitochondria calcium uptake in developing hair cells. We also observed that pharmacologically blocking of either MCU or $Ca_v1.3$ decreased baseline mitochondrial calcium levels. To examine the

relationship between Ca$_v$1.3, MCU and NAD$^+$ further, we expressed the NAD$^+$/NADH ratio indicator protein Rex-YFP in hair cells. We found NAD$^+$/NADH ratio increased in hair cells after exogenous NAD+ treatment and when MCU or Ca$_v$1.3 was pharmacologically blocked.

Conclusion

These result suggests that in vivo, Ca$_v$1.3-dependent mitochondrial calcium uptake may control ribbon assembly through cytosolic levels of NAD$^+$. This mechanism couples synaptic function to synapse formation in the hair cell through changes in cellular metabolism.

Human Auditory Cortex & Speech

PD 149

The phase of pre-stimulus ~6-10 Hz EEG oscillations predicts auditory pattern recognition performance

Matthew Wisniewski[1]; Natalie Hansen[2]; Nandini Iyer[1]; Brian D. Simpson[3]; Assaf Harel[2]
[1]U.S. Air Force Research Laboratory; [2]Wright State University; [3]Air Force Research Lab, 711th HPW

Recent electroencephalographic (EEG) research suggests that the state of ongoing oscillatory activity influences perceptual processes in humans. Specifically, pre-stimulus power and phase differs for correct and incorrect trials. The present work examines such effects in an auditory pattern recognition task. On each trial, participants heard a sequence of three 40-ms sinusoidal tones separated by 40-ms inter-stimulus intervals. Participants'; task was to indicate each tone';s frequency (low-low-high, low-high-low, etc.). An adaptive one-up, one-down procedure was used to determine the frequency separation associated with individuals'; 50% correct identification threshold. Afterwards, individuals completed 250 trials while EEG was collected from a 68-channel array of electrodes. No significant differences were found between correct and incorrect trials for pre-sequence power. Using a phase-opposition sum measure, 6-10 Hz oscillations were found to have opposing phases for correct and incorrect trials at ~-200 to -100-ms pre-sequence onset. Further, after separating single-trials into different phase bins, and computing mean accuracy for each bin, a clear continuous relationship between accuracy and phase was apparent. Several control analyses, including analyses of event-related potentials (ERPs) and alternative time-frequency decompositions, ruled out the possibility that effects were caused by contamination from post-sequence activity. Results suggest that ongoing oscillatory brain states can impact auditory perception in a similar way to the visual domain.

PD 150

Cortical Hierarchical Processing of Auditory Novelty in Awake and Anesthetized States: An Intracranial Electrophysiology Study

Kirill Nourski[1]; Ariane Rhone[1]; Mitchell Steinschneider[2]; Hiroto Kawasaki[3]; Matthew Howard[1]; Matthew I. Banks[4]
[1]Human Brain Research Laboratory, Department of Neurosurgery, The University of Iowa; [2]Departments of Neurology and Neuroscience, Albert Einstein College of Medicine; [3]Human Brain Research Laboratory, Department of Neurosurgery, University of Iowa Hospitals and Clinics; [4]Deparment of Anesthesiology, University of Wisconsin - Madison

Predictive coding models of sensory processing emphasize the integration of feedforward and feedback information streams across cortical regions. Studies employing local/global deviant (LGD) auditory stimulus paradigms (e.g. Bekinschtein et al., 2009, PNAS 106:1672-7) offer promise for elucidating the cortical hierarchy underlying sensory awareness. Non-invasive studies show that responses to local (within-trial) deviance are robust to changes in the level of consciousness, whereas responses to global (across-trial) deviance are not. However, non-invasive recordings offer limited opportunity to investigate the contributions of specific cortical regions to these processes. This study used electrocorticography to refine the localization of LGD responses and test their sensitivity to general anesthesia.

Subjects were neurosurgical patients undergoing removal of intracranial electrodes placed to identify epileptic foci. Stimuli were four repetitions of a vowel, followed by the same or different 5th vowel (local deviance; LD). Global deviance (GD) was manipulated by varying the percentage of "same" and "different" patterns. Subjects responded to GD with a button press. The stimuli were presented during an awake baseline and during induction of general anesthesia with propofol. Recordings were made with multicontact depth electrodes, and subdural strip and grid electrodes. Analysis of cortical activity focused on averaged evoked potentials (AEPs) and high gamma (70-150 Hz) event-related band power.

Changes in AEP amplitude associated with LD were broadly distributed across temporal, frontal and parietal regions. High gamma LD effects were more spatially restricted and localized primarily to auditory cortex in the superior temporal plane and on the lateral surface of the superior temporal gyrus. Latencies of LD effects increased from core to non-core to auditory-related areas. GD effects were most prominent in non-core auditory cortex, auditory-related and prefrontal areas, had longer latencies and a nearly opposite hierarchical la-

tency profile compared to LD effects. During induction of general anesthesia, LD effects became progressively more restricted to auditory cortex and, within core auditory cortex, were resistant to loss of consciousness. GD effects were suppressed under anesthesia, even at sub-hypnotic doses.

The data identifies differential cortical activation profiles associated with preattentive (LD) and higher-level (GD) auditory novelty detection in the human brain. The latency profiles of LD and GD effects highlight feedforward and feedback signal pathways, respectively. Sedation is associated with suppression of higher-level predictive coding processes, followed by attenuation of preattentive components of auditory novelty detection.

PD 151

Neural Correlates of Auditory Enhancement

Lei Feng; Anahita H. Mehta; Andrew J. Oxenham
University of Minnesota

Introduction
A target tone in a simultaneous masker becomes perceptually more salient if the masker itself, termed precursor, is presented first. This phenomenon, known as "auditory enhancement", reflects the general principle of contrast enhancement, and may help in the detection of new acoustic events and in the perceptual constancy of speech under varying and noisy acoustic conditions. However, the physiological mechanisms underlying auditory enhancement are still largely unknown. In this study, we used the envelope following response (EFR) and auditory steady state response (ASSR) to explore potential neural correlates of auditory enhancement at both subcortical and cortical levels simultaneously.

Methods
Sixteen normal-hearing (NH) listeners were tested in a passive listening EEG setup. For the simultaneous masking (MSK) condition, each trial consisted of a five-component inharmonic complex, including one target and four masker tones (two maskers on each side). The frequencies of the complex were roved within a one-octave range as a whole from trial to trial. In the enhancement (ENH) condition, the masker-plus-target complex was preceded by a precursor with the four maskers alone and separated by a 10-ms silent gap. The level of the target was tested at three target-to-masker ratios (TMRs) in both conditions. The target was amplitude modulated by a sum of two sinusoids with frequencies of 34.28 and

98.28 Hz to tag cortical and subcortical representations, respectively. The masker components were amplitude modulated at 43.43 and 91.42 Hz. The phase locking value (PLV) was calculated from the Fast Fourier Transformation (FFT) of the EEG waveforms. The subcortical and cortical responses to the target and maskers were quantified as the PLVs at the slow and fast modulation frequencies, respectively.

Results
Preliminary data revealed robust neural responses to both target and masker at cortical and subcortical levels. The response to the target embedded in the simultaneous maskers increased as the TMR increased. An initial trend was observed for increased neural responses to the target when the precursor was presented at both subcortical and cortical levels.

Conclusions
The preliminary data demonstrate that the double-modulation paradigm can be used to probe the neural correlates of auditory enhancement at both cortical and subcortical levels simultaneously.

PD 152

Temporal Effects on Word-in-Noise Recognition for Normal-Hearing Listeners and Cochlear-Implant Users

Miriam I. Marrufo-Pérez; Almudena Eustaquio-Martín; Milagros J. Fumero; Enrique A. Lopez-Poveda
University of Salamanca

The amplitude fluctuations in speech signals are useful cues for speech recognition. Several adaptation mechanisms can theoretically enhance the coding of these cues in competing noise, something that might facilitate the recognition of speech in noise. Among those mechanisms are the linearization of basilar membrane responses and/or the restoration of the dynamic range of auditory nerve fibers by the medial olivocochlear (MOC) reflex (Almishaal et al., 2017, J. Acoust. Soc. Am. 141:324-333; Marrufo-Pérez et al., 2017, ARO abstract #PS395), or the dynamic-range adaptation of central auditory neurons toward the most frequently occurring level (e.g., Dean et al., 2005, Nat. Neurosci. 8:1684-1689). Because these mechanisms have rather slow activation time constants (> ~130 ms), we hypothesized that word recognition may be easier when words are presented later than earlier in background noise. To test this hypothesis, we measured speech reception thresholds (SRTs) (the signal-to-noise ratio for 50% word recognition) for natural and tone-vocoded disyllabic words presented

monaurally at the onset (early condition) and delayed 300 ms from the onset (late condition) of simultaneous bilateral, ipsilateral, and contralateral speech-shaped noise. SRTs were 0.5 to 2.1 dB SNR lower (better) in the late than in the early condition for the three noise lateralities. The magnitude of the temporal effect was comparable for natural and vocoded words, suggesting that the temporal fine structure in speech is not affected by temporal adaptation. We also observed a similar temporal effect for bilateral cochlear-implant (CI) users tested in the same conditions with a sound processing strategy that lacked any form of dynamic processing. Because CI users lack both acoustic and MOC reflexes and since we used a time-invariant sound processing strategy, this suggests that the temporal effect on word-in-noise recognition is probably mostly due to central dynamic-range adaptation for both normal-hearing listeners and CI users. [Work supported by the University of Salamanca, Banco Santander, MED-EL, and MINECO (BFU2015-65376-P).]

PD 153

Rapid, Simultaneous EEG Assay of the Speech Processing Hierarchy, from Brainstem to Cognition: New Approaches to Improve Real-World Comprehension

Lee M. Miller[1]; Andrew S. Kessler[2]; Britt W. Yazel[1]; Kristina C. Backer[1]; Markham H. Anderson[1]; Fernando Espinosa-Iniguez[1]; Sanjay S. Joshi[1]; David P. Corina[1]
[1]*University of California, Davis;* [2]*University of Washington, Seattle*

Understanding speech in noisy 'cocktail party'; environments is the most profound daily challenge for listeners with hearing loss. Unfortunately, present approaches are limited both in i) rapidly diagnosing how different listeners fail to understand speech and ii) designing aids and other assistive devices to cope with dynamic, acoustically cluttered scenes. Recent work in our lab uses auditory neuroscience with neuroengineering to advance both these aims. First, we have developed a novel EEG method that provides a rapid (~5 min), hierarchical view into the functional health of the auditory-speech system – from brainstem to cortex – including how different processing stages may interact. Combining natural speech acoustics with FM sweep chirps, this CHEECH (chirp-speech) approach is adaptable to virtually any speech corpus and real-world perceptual, linguistic, or cognitive task. We will describe how it allows us to characterize auditory/speech development and auditory-visual cross-modal plasticity in children with cochlear implants, and how it may reveal fine temporal processing deficits in older adults with 'hidden hearing loss';. A related project in our lab develops an assistive device that uses eye gaze tracking and microphone array beamforming to serve as an "attentional prosthetic": wherever a listener looks, she will hear that sound best. The system is implemented on a mobile platform (Android) and incorporates virtual 3-D acoustic cues (HRTFs or head related transfer functions) to improve real-world comprehension both in individuals with hearing loss as well as healthy listeners in 'cocktail parties';.

PD 154

Does the way speech intelligibility is manipulated matter for the auditory efferent system?

Heivet Hernandez-Perez[1]; Catherine McMahon[1]; Sriram Boothalingam[2]; Sumitrajit Dhar[3]; David Poeppel[4]; Jessica J M Monaghan[1]
[1]*Macquarie University;* [2]*University of Wisconsin-Madison;* [3]*Northwestern University;* [4]*New York University*

Although it is well accepted that auditory efferent activity, particularly the mediolivocochlear reflex, increases signal-to-noise ratio when transient sounds are presented in noise, its potential role in speech perception remains unclear. Here it is hypothesized that the auditory efferent system aids speech perception by affecting a reduction in cochlear gain when speech signals are degraded. We also hypothesize that the change in cochlear gain is correlated with behavioural and cortical responses associated with speech perception.

Speech intelligibility was manipulated in a series of three experiments: 1) "active" and "passive" listening of noise-vocoded speech; 2) "active" and "passive" listening of speech-in-speech-shaped noise and 3) "active" and "passive" listening of speech-in-babble noise. Fifty normal-hearing, native Australian English speakers between 18-35 years old were assessed using lists of monosyllabic words and non-words. In the "active" listening condition, the subjects were instructed to make a lexical decision and press a button every time they heard a non-word, while in the "passive" listening condition they were instructed to ignore all the auditory stimuli and watch a non-subtitled movie. Click-evoked OAEs (CEOAE) were continuously obtained from the contralateral ear to the speech stimuli with a probe in the external ear canal. Synchronised, 64-channels EEG and CEOAE recording systems allowed the measurement of speech onset auditory-evoked event-related potentials (ERPs), click-evoked auditory brainstem responses (ABRs), CEOAEs and behavioral responses.

As expected, behavioral results from the three experiments showed that task accuracy (d';) decreases as the speech signal is degraded. A decrease in cochlear gain, manifested as a reduction in CEOAE amplitude, with increasing task difficulty was observed for vocoded speech, but not consistently for the speech-shaped-noise or babble maskers. For all three experiments, ERP components were modulated by the "active" listening of speech sounds while brainstem activity remained invariable across both "active" and "passive" listening conditions. These data suggest that differentially manipulating the intelligibility of speech targets can indeed affect how the cochlear gain is subsequently modulated via the auditory efferent system.

PD 155

EEG-measured Correlates of Comprehension in Speech-in-noise Listening

Octave Etard; Tobias Reichenbach
Imperial College London

Background
Humans excel at analysing complex acoustic scenes. Independent sources can be detected and segregated to extract perceptually relevant and distinct auditory objects, even when they are acoustically overlapping. This process is especially relevant in the context of the cocktail party problem where an effective segregation of different competing speech signals is necessary for communication. Brain activity in the delta and theta frequency band has recently been found to track the speech envelope. This neural correlate of speech processing is enhanced for an attended speaker in a setup of competing speakers (attentional modulation). Moreover, variations of the neural response to the speech envelope in the delta and theta frequency bands with speech comprehension have been established. However, variations in comprehension levels were obtained through acoustic manipulations (acoustic degradations) of the stimuli, making it arduous to tease apart the effect of the comprehension from the acoustic modifications.

Methods
We employed electroencephalography (EEG) with 64 scalp electrodes to record neural responses of native English speakers listening to naturalistic continuous speech in varying conditions of noise (speech in quiet, competing speakers and different levels of speech-in-babble-noise). We obtained EEG recordings in response to English stimuli as well as in response to a foreign unknown language with similar acoustic properties (Dutch). When listening to English the subjects'; comprehension was systematically modulated by the noise level, but remained nil in the acoustically matched Dutch conditions. This allowed us to separate neural correlates of changes in the acoustic properties of the stimuli and of speech comprehension. We used regularised linear spatio-temporal models to correlate the speech envelopes to the EEG waveforms, and reconstructed speech comprehension for all acoustic conditions.

Results
We were able to accurately reconstruct the stimulus envelopes, and to reliably predict speech comprehension in the different acoustic conditions. We showed that comprehension could be estimated using data segments of only a few seconds in duration. We investigated the relative importance of the delta, theta and alpha frequency bands, and found the delta band activity at 100 ms and 260 ms post-stimulus to be critical for predicting comprehension.

Conclusion
We have developed a procedure to infer speech-in-noise comprehension from neural responses to continuous speech in background noise. The obtained results demonstrate that the speech envelope, a low-level acoustic feature, can be used to recover comprehension, a high level cognitive construct. This approach may thus prove useful to investigate auditory processing disorders.

PD 156

Th Effect of Eye-controlled Beamforming on Speech Intelligibility in a Dynamic 'Cocktail Party'

Ľuboš Hládek[1]; Bernd Porr[2]; Owen Brimijoin[1]
[1]*MRC/CSO Institute of Hearing Research - Scottish Section;* [2]*Glasgow University*

Pointing the eyes, not the nose, is a natural strategy when following a moving conversation involving multiple talkers. This strategy is even more pronounced for hearing impaired people because they often rely on visual cues in adverse listening conditions. Directional microphones on hearing aids can provide benefit in terms of increased signal-to-noise ratio but these are pointed with respect to the head, not the eyes. In the current experiment, we tested head-controlled and eye-controlled beamforming in a 'dynamic cocktail party' scenario. We expected that the intelligibility of speech immediately after a change in target location would be the most enhanced under the eye-controlled condition. The task of the normal hearing and hearing impaired participants was to listen to a sequence of numbers (presented among speech-shaped noise distractors) and report them back to the experimenter. The numbers could originate either from the left or right, such that the switch between the sides occurred randomly after a few presentations. The beamforming technology was simulated in the loudspeaker ring using

head tracking and eye tracking. In the analysis, we focused on the overall performance over the course of a block of measurements as a function of the width of the acoustic beam, the performance during the switching periods, and the patterns of any head and eye movements. The data show that the participants were likely to follow the targets with their eyes, the head angles usually underestimated the angles of the target speech which interacted with the pattern of the acoustic beam and influenced speech intelligibility. Moreover, the narrow patterns of the acoustic beams led to more error-prone speech perception than did the wider patterns. Our data suggest that the eye-controlled beamforming is a promising technology; however, it will be of critical importance to understand how it depends on width of the acoustic beam.

Acknowledgements

Binaural Hearing & Sound Localization

PD 157

Pediatric congenital unilateral hearing loss: Longer transmission time between cochlea and brainstem results in worse aided sound localization

Marlin Johansson[1]; Filip Asp[2]; Erik Berninger[3]
[1]Department of Clinical Science, Intervention and Technology, Karolinska Institutet, Stockholm, Sweden; [2]Department of ENT diseases, Section of Cochlear Implants, Karolinska University Hospital, Stockholm, Sweden; Department of Clinical Science, Intervention and Technology, Karolinska Institutet, Stockholm, Sweden; [3]Department of Audiology and Neurotology, Karolinska University Hospital, Stockholm, Sweden; Department of Clinical Science, Intervention and Technology, Karolinska Institutet, Stockholm, Sweden

Background

It is known that the auditory system reorganizes after longer periods with unilateral hearing. It is not known if this neural reorganization may be avoided if a hearing aid (HA) providing sufficient audibility to the impaired ear is delivered within a sensitive period.

Methods

We studied whether 10-11 year old children with congenital unilateral sensorineural hearing loss (uSNHL) benefit from introduction of HA amplification after 5 years of age. Auditory brainstem responses (ABRs), sound localization accuracy (SLA), speech recognition in competing speech and subjective benefit was measured. The subjects were tested in an unaided and an aided condition, and the ABRs were recorded in both ears.

Results

The mean pure tone average was 45 dB HL and 6 dB HL in the impaired and normal ear, respectively (n=6). SLA was poorer in the aided compared to unaided condition (p<0.05, n=6). A distinct correlation between aided SLA and the ABR interpeak I-V interval from the worse ear existed (r=0.98, p=0.02, n=4), and the relationship likewise existed in a post-hoc analysis including an estimated I-V interval for the fifth individual (r=0.98, p=0.004, n=5). Linear regression analysis showed a significant relationship between aided SLA and the Wave-V latency, further confirming a relationship between transmission time and aided SLA.

A significant benefit with HAs existed in one-to-one communication assessed with questionnaires. Compared to normal hearing children, SLA, aided speech recognition in competing speech, and subjectively assessed hearing disability and aural/oral performance were degraded. No significant aided to unaided difference existed in neither measurements of speech recognition in competing speech nor rated subjective benefit in demanding listening situations.

Conclusion

A close relationship existed between aided SLA and the ABR wave I-V interval. This suggests that a longer transmission time between the cochlea and brainstem may lead to worse aided SLA for children with congenital uSNHL with late fitted HAs (after 5 years of age). The longer ABR I-V interval may be due to auditory deprivation and/or reorganization, that prevents optimal adaptation to a HA introduced late in hearing development.

PD 158

Larger than Typical Spatial Release from Masking and Binaural Squelch for Normal-hearing Children

Z. Ellen Peng; Sara Misurelli; Alan Kan; Ruth Y. Litovsky
University of Wisconsin-Madison

Segregation of target speech improves with spatial separation between target and background talkers. Understanding the abilities of children to segregate sounds is important because they need to communicate effectively in daily noisy environments. Among normal-hearing (NH) children, speech reception threshold (SRT) typically improves by 6-7 dB when a masker is moved from the front (i.e., co-located with target) to either side of the listener. Quantifying the amount of spatial release from masking (SRM) in NH children has been overall inconsistent when compared to NH adults, who can achieve up to 12 dB SRM. With most studies using free-field or dichotic listening paradigms, the contribution of binaural

squelch and monaural head shadow (i.e., SRT improvement when listening with an additional ear with poorer target-to-masker ratio) has yet to be clearly quantified for NH children. The present study aimed to quantify each of these in NH children using a paradigm that maximizes SRM. The long-term goal is to use the same approach to investigate emergence of binaural abilities in children fitted with hearing-aids and/or cochlear implants.

Stimulus presentation was tightly controlled using virtual auditory space techniques. Speech materials were convolved with head-related transfer functions of a KEMAR manikin, and presented to listeners via headphones. Target stimuli were short sentences adapted from the Australian Sentence Test in Noise, whereas the maskers consisted of two continuous unrelated stories spoken by same-gender talkers. The target was always at +90° azimuth. SRT was measured for each listener in three conditions: (1) Co-located: target and masker at +90° azimuth; (2) Separated: masker at -90° azimuth to achieve maximum target-masker separation of 180°; (3) Monaural: masker at -90° azimuth, ear contralateral to the target muted. We quantified SRM by subtracting SRT in Condition (2) from (1), and binaural squelch by subtracting SRT in Condition (2) from (3).

Preliminary data from five NH children aged 11-15 years showed an average SRM of 13 dB, much higher than those reported in existing literature. The larger SRM is likely due to: (1) Larger target-masker spatial separation of 180° compared with 90° in prior studies; (2) More informational masking and better access to context in the target sentences. These children also demonstrated 6 dB averaged binaural squelch similar to NH adults, suggesting that binaural squelch may be adult-like by adolescence.

PD 159

Interaural time difference sensitivity in the inferior colliculus of neonatally deafened rats after cochlear implantation

Jan Schnupp[1]; Alexa N. Buck[2]; Kongyan Li[2]; Ambika Prasad Mishra[2]; Nicole Rosskothen-Kuhl[3]
[1]City University of Hong Kong; [2]1Hearing Research Group, Biomedial Science Department, City University of Hong Kong, Hong Kong; [3]1Hearing Research Group, Biomedial Science Department, City University of Hong Kong, Hong Kong; 2 Neurobiological Research Laboratory, Section for Clinical-Experimental Otology, Medical Center, University of Freiburg, Germany

Sound localization is one of the major challenges for bilateral cochlear implant (CI) users. One important hub for the binaural processing of auditory inputs is the inferior colliculus (IC). To derive maximum benefit from two CIs, further research is needed in animal models to understand how parameters such as interaural synchronization influence the binaural processing in central auditory hubs of CI patients.

We present the adult Wistar rat as a new model to investigate binaural hearing with acoustic or electrical intracochlear stimulation. We used hearing rats to study the sensitivity for interaural time differences (ITDs) in a normal developed system, and bilaterally CI-implanted deaf rats were used to study ITD sensitivity in a hearing-inexperienced system. Deafness was induced neonatally by daily intraperitoneal injection of kanamycin from postnatal day 10 to 20, inclusively. Auditory brainstem responses to click stimuli of varying intensity via in-ear headphones were recorded to measure hearing thresholds and confirm deafness in kanamycin treated animals. When the deafened animals reached young adulthood (8-12 weeks) bilateral acute CI implantation was performed under anesthesia by a cochleostomy over the middle turn of the cochlear. On both sides, five electrode rings were completely inserted in direction towards the cochlear apex, even if only the two tip electrodes were used for binaural, biphasic stimulation.

ITDs varied over the rat';s physiological range, from 0.16 ms left ear leading to 0.16 ms right ear leading in 0.02 ms steps. In this manner, electrical ITD tuning curves were recorded for 898 multi-units in the IC of 4 deaf rats. All multi-units were driven by the electrical stimuli, and, perhaps surprisingly for these completely hearing inexperienced animals, the overwhelming majority (779/889 or 87.6%) of the multi-units were significantly sensitive to ITD (ANOVA), with most multi-units tuned to contralateral, or sometimes central locations. Tuning was often quite sharp and reproducible, and a mutual information analysis showed that responses can carry substantial amounts of information about these sub-millisecond ITDs, up to 1.6 bits / response. Comparison with preliminary data for ITD tuning curves recorded with acoustic click stimuli in age matched, normal hearing rats indicates that acutely CI implanted deaf rats had broadly comparable ITD sensitivity to that seen in normal animals.

Thus, IC neurons in young adult rats frequently show substantial ITD sensitivity independent of early hearing experience. Overall, we showed that rats are a good model to investigate the central binaural processing of acoustic or electrical sensory stimulation in an auditory system with different hearing history.

Behavioral sensitivity for interaural time differences in normal hearing rats and rats with cochlear implants

Nicole Rosskothen-Kuhl[1]; Alexa N. Buck[2]; Kongyan Li[2]; Ambika Prasad Mishra[2]; Jan W Schnupp[2]
[1]1Hearing Research Group, Biomedial Science Department, City University of Hong Kong, Hong Kong; 2 Neurobiological Research Laboratory, Section for Clinical-Experimental Otology, Medical Center, University of Freiburg, Germany; [2]1Hearing Research Group, Biomedial Science Department, City University of Hong Kong, Hong Kong

Sound localization is one of the major challenges for bilateral cochlear implant (CI) users. To derive maximum benefit from two CIs, further research is needed in animal behavioral models to understand how parameters such as interaural synchronization influence the binaural hearing of CI patients.

We present the adult Wistar rat as a new model to investigate binaural hearing with acoustic or electrical intracochlear stimulation. We trained normal hearing rats on sound lateralization tasks using acoustic click train stimuli, and bilaterally CI-implanted deaf rats were trained on sound lateralization using electrical pulse trains. Deafness was induced neonatally by daily intraperitoneal injection of kanamycin from postnatal day 10 to 20, inclusively. Normal hearing or loss of hearing function was verified by measuring auditory brainstem responses to click stimuli presentation via in-ear headphones. Bilateral CI implantation occurred in adulthood (8-12 weeks) by a cochleostomy over the middle turn of the cochlear. On both sides, two electrode rings were completely inserted in direction towards the cochlear apex. We studied the sensitivity for interaural time differences (ITD) by training hearing rats and CI-implanted deaf rats on two-alternative forced choice stimulus lateralization tasks. For the acoustic ITD discrimination training, hearing rats were trained in a closed-field stereo audio setup using click stimuli. For the electrical training, CI rats were connected to an external stimulator by means of a commutator and trained on ITD discrimination by using binaural, biphasic stimuli.

Both groups of rats showed good ITD sensitivity within their physiological range of +/- 0.15 ms, distributed as a psychometric function. Acoustically stimulated hearing rats showed peak ITD discrimination around +/- 0.15 ms, while electrically stimulated deaf rats had peak performances from +/- 0.075 to +/- 0.1 ms. Although there was some individual variation, the sensitivity of rats to ITDs did depend somewhat on click rate, but for relatively slow click rates (e.g. 50 Hz) electrically stimulated and normal-

ly hearing rats showed comparable sensitivities, with their probability of a correct choice increasing up to 95% and 93%, respectively, for their peak ITD parameters.

In contrast to Wesolek et al. (2010), we have demonstrated that rats can use ITD cues for sound localization. Furthermore, even hearing-inexperienced adult rats can learn to use ITDs to localise sound sources with electric auditory stimulation through bilateral CIs. Here, we established a new behavioural animal model which allows the study of binaural hearing in bilateral CI users.

Poor Monaural Temporal Encoding in Bilateral Cochlear Implants: Interactions with Place-of-Stimulation Mismatch in a Normal-Hearing Simulation

Sean R. Anderson; Caroline M. Swords; Alan Kan; Ruth Y. Litovsky
University of Wisconsin-Madison

Bilateral cochlear-implant (CI) users show poorer sensitivity to interaural time differences (ITDs) compared with normal-hearing (NH) listeners. Accurate computations of ITDs rely on factors including precise temporal encoding in each ear, and matched place-of-stimulation across the ears. Both factors are poorly controlled in bilateral CI listeners. Interaural place-of-stimulation mismatch (IPM) has been argued as a main factor reducing ITD sensitivity in bilateral CI users.

This project explored the influence of poor monaural temporal sensitivity on ITD sensitivity. We tested two predictions: First, that monaural temporal sensitivity will influence the ability to use ITD cues for perceived intracranial position; that is, if monaural temporal encoding in one ear is poor, then the range of lateralization of ITDs will be reduced (so long as there is some overlap in excitation across the ears). Second, we predicted that the impact of monaural sensitivity will be greater for perceived position than for IPM.

CI stimulation was simulated in NH listeners, to carefully control temporal encoding and IPM. Stimuli were 300 ms, Gaussian enveloped tones (GET) presented at 500 pulses per second, with a pure tone carrier at 4000 Hz, and 100 Hz second-order sinusoidal amplitude modulation (AM). Interaural mismatch was introduced by changing the carrier frequency to 4697, 5511, or 6426 Hz in one ear, corresponding to an IPM of 1.5, 3, or 4.5 mm. Poor temporal encoding was simulated by reducing the depth of AM from 50% to 20% in one ear. In each condition, ITDs of 0, 100, 200, 400, and 800 µs were applied to the stimuli and listeners respond-

ed by indicating the perceived intracranial position. Preliminary evidence showed small effects of AM depth when place-of-stimulation was matched across the ears. Consistent with previous reports, IPM within 3 mm produced no reduction in the range of lateralization for NH listeners when AM depth was 50% in both ears. However, a significant interaction was found between IPM and AM depth such that when AM depth was 20% in one ear, IPM greatly decreased the range of lateralization.

Results from this experiment suggest that the state of monaural temporal encoding becomes increasingly important as the amount of overlap in excitation across ears decreases. Thus, unless perfect matching in place-of-stimulation across the ears is achieved, poor monaural temporal encoding will negatively affect binaural sensitivity.

PD 162

Effects of magnitude of interaural delay, center frequency, and hearing status on precision of binaural processing: Empirical data and quantitative modeling

Leslie R. Bernstein; Constantine Trahiotis
University of Connecticut Health Center

Background
We recently published binaural detection thresholds taken as a function of the magnitude of interaural temporal disparity (ITD) imposed on masker-alone and signal-plus-masker waveforms [Bernstein and Trahiotis, J. Acoust. Soc. Am. 140, 3540-3548 (2016)]. Listeners were those classified, audiometrically, as having no more than "slight" hearing loss. The stimuli and procedures yielded estimates of precision of binaural processing along the putative internal delay-line common to theoretical accounts of measures of binaural processing (e.g., detection, discrimination, and lateralization/localization). The results indicated that listeners internally "compensated" for the external ITDs and that the compensation enhanced binaural detection performance. As expected, the precision of ITD-compensation declined as the magnitude of the ITD increased. In addition, the data revealed additional degradations in binaural detection performance for listeners whose monaural pure-tone thresholds at 4 kHz were elevated (i.e., >= 7.5 dB HL) but whose overall audiometric profile would still be characterized as normal or "slight loss."

Methods
Data Collection: In the current study, binaural detection was measured in three stimulus conditions. One was (NoSπ)τ and another was (No)±τ(Sπ)τ, in which the masker is the sum of two independent noises, one with an ITD favoring the left, the other with an equal ITD favoring the right. (No)±τ(Sπ)τ stimuli have the same interaural correlation as their (NoSπ)τ counterparts, but their ITDs cannot be internally compensated. The third stimulus condition, (NoSo)τ, served as a control because it conveyed no interaural cues to foster detection. We measured binaural detection as a joint function of ITD and center frequency for stimuli spanning the five octaves from 250 Hz to 8 kHz.

Quantitative analyses: Predictions were made via an interaural cross-correlation-based model incorporating commonly employed stages of peripheral and central auditory processing. The inputs to the model were condition-specific multiple tokens of masker-alone and signal-plus-masker waveforms. Following Fisher';s z transformation of the values of correlation, a decision variable (da) was formed by computing the difference between the means of the distributions of the interaural correlations of masker-alone and signal-plus-masker waveforms divided by the estimate of their combined standard deviation. We assumed that 1) listeners'; performance was constrained by the inherent variability of sample-to-sample values of interaural correlations of both masker and signal-plus-masker waveforms; 2) a constant value of da would yield a constant level of performance at each center frequency; 3) listeners'; performance was limited by two different sources of internal noise: one having a power that increases with the power of the external masker, the other having a power that grows with the magnitude of the ITD.

Results and Conclusions
Compensation of ITD consistently provided advantages for binaural detection for center frequencies spanning 250 Hz to 8 kHz and for ITDs ranging from 0 to 3000 µs. For the same sets of stimuli, binaural processing appears to be less precise for listeners having HL > 7.5 dB @ 4 kHz. Overall, the predictions of the cross-correlation-based model captured the complex patterning of the data obtained across center frequency and ITD. In addition, the model successfully accounted for the differences in binaural detection measured between listeners having hearing levels at 4 kHz less than vs. greater than 7.5 dB (those that might be classified by some as having hidden hearing loss). According to the model, the differences in binaural detection thresholds found between the two groups of listeners result from the listeners with HLs at 4 kHz greater than 7.5 dB also having elevated levels of additive, stimulus-dependent, internal noise.

PD 163

Adaptation to spatial statistics in brain stem neurons focally improves sound source separability by optimizing population coding efficiency

Helge Gleiss[1]; Joerg Encke[2]; Andrea Lingner[3]; Todd Jennings[1]; Benedikt Grothe[3]; **Michael Pecka**[3]
[1]Division of Neurobiology, Department of Biology II, Ludwig-Maximilians Universitaet Muenchen, Martinsried, Germany; [2]Technical University of Munich; [3]Ludwig-Maximilians-Universitaet Munich

Our ability to discriminate individual sound sources in complex environments is conveyed by brainstem neurons that translate physical spatial cues into activity rates. Yet the nature of the spatial code based on these neuronal activity patterns is still debated. Here we studied the effects of spatially complex stimulation on the processing of interaural level differences (ILD) in gerbils and human listeners and provide evidence for a new concept of differential auditory space coding. We show that during naturalistic stimulation, activity rates of individual neurons in the Lateral Superior Olive (LSO) adapted to the concurrent spatial statistics, demonstrating a lack of absolute encoding of space by neuronal firing rate. Rather, the observed rate adaptation maximized the efficiency of neuronal separability specifically for those ILDs that were most likely to occur in the concurrent statistical environment (high probability region, HPR). Importantly, the selective improvement of ILD separability was only found on the level of the average LSO population response. In contrast, rate adaptation on the level of individual neurons failed to cature stimulus-specific coding improvements. This lack of spatial information content by single neurons was caused by large response variability to a given ILD, which was reliably compensated on a population level. A simple LSO model explained that a LSO gain control mechanism is required to generate such efficient population coding. The stimulus-specific enhancements in neuronal population coding were paralleled by human listeners exhibiting a selective improvement in just noticeable differences in ILDs within the respective HPR. We conclude that, already on the primary detector level, the processing of ILDs is not tuned towards an absolute representation of space, but optimizes efficient sound source separation by population decoding of ILDs.

PD 164

Complex Acoustic Environments: Recordings, Processing, Experiments

S. Theo Goverts[1]; **H. Steven Colburn**[2]
[1]VU University Medical Center; [2]Boston University

Motivated by the social importance of environments with multiple acoustic sources and the challenges experienced by hearing-impaired listeners in these environments, we are working to characterize the acoustical signals that reach the earcanals in these environments and to use the recorded signals in various behavioral tests. The recordings were made using binaural microphones in the ear canals while the listeners were behaving and moving normally; examples include sitting at their table in a restaurant, driving in a car, walking down a city street, or riding on a city bus. The recordings are available for analysis and experiments for other investigators upon request. The results of various analysis procedures that we have applied to the recordings will be presented and discussed. These analyses include the characterization of the interaural time and intensity differences, measurements of the speech-likeness of the modulation patterns as characterized by combining across frequency bands. Finally, results of speech intelligibility experiments, including tests with controlled speech waveforms added to the complex-environment recordings will be reported. One of the goals of this work is to develop clinical tests that can be used to characterize the abilities of hearing-impaired listeners to understand speech from sources in complex (multiple-source) environments, with and without their hearing aids. [Work supported by the Hearing Industry Research Consortium (IRC), a research consortium including GN Resound, Starkey, Oticon, Sivantos, Widex, and Phonak.]

PD 165

Gene therapy approach to protect hearing from age-related and noise-induced hearing loss

Yu-Juan Hu[1]; Hongyang Wang[2]; Yong Tao[3]; Mingqian Huang[4]; Veronica Lamas[3]; Adam Ruprecht[3]; Qiuju Wang[5]; Weijia Kong[6]; Zheng-Yi Chen[7]

[1]*Department of Otorhinolaryngology, Union Hospital, Tongji Medical College, Huazhong University of Science and Technology;* [2]*Chinese PLA General Hospital/Harvard Medical School;* [3]*Eaton Peabody Laboratory, Massachusetts Eye and Ear Infirmary;* [4]*1. Department of Otolaryngology, Harvard Medical School, 2. Eaton-Peabody Laboratory, Massachusetts Eye and Ear Infirmary;* [5]*Chinese PLA General Hospital;* [6]*Huazhong University of Science and Technology;* [7]*1. Department of Otolaryngology, Harvard Medical School, 2. Eaton Peabody Laboratory, Massachusetts Eye and Ear Infirmary*

Introduction

Age-related hearing loss (ARHL) affects one third of the population older than 65 years of age and approximately 5% of the population is suffering from hearing loss caused by intense noise exposure. While multiple factors are likely to be involved in ARHL, one main pathological feature shared by ARHL and noise-induced hearing loss (NIHL) is the loss of hair cells. Thus promotion of hair cell survival could serve as an approach to preserve hearing during aging and after exposure to intense noise. We have previously shown that hair cell specific over-expression of Isl1, a LIM-homeodomain transcription factor critical in the development and differentiation, promotes hair cell survival and ameliorates ARHL and NIHL in a transgenic mouse model (C57BL/6J). To further explore if overexpression of Isl1 in postnatal hair cells by AAV-based gene delivery could protect hearing in different mouse models with ARHL and after noise exposure, we delivered AAV-Isl1-GFP into P0-P3 mouse cochleae by cochleostomy and studied hearing during aging and after noise exposure.

Methods

CD1 and DBA/2J, two strains with ARHL due to different genetic mutations, were injected with AAV-Isl1-GFP at P0-P3. AAV-Isl1-GFP was further injected into the cochleae of P0-P3 CBA/CaJ, which were then exposed to the noise of 100 dB at 8-16 kHz for two hours at 8 weeks of age. Uninjected and AAV-GFP injected inner ears served as control. Hearing studies, including ABR (auditory brainstem response) and DPOAE (distortion product otoacoustic emissions), were performed at 1 to 10 months for CD1, DBA/2J and at two weeks after noise exposure in CBA/Caj mice. The cochleae were harvested for comparative study of inner ear pathology.

Results

CD1 and DBA/2J exhibit early onset of ARHL starting at one month with continuous hearing deterioration during aging. In CD1, compared to uninjected or AAV-GFP injected ears, injected ears displayed significantly smaller ABR and DPOAE thresholds at high frequency at one month, with persistent hearing protection extended to 10 months at low frequency. For DBA/2J, significantly smaller ABR but not DPOAE thresholds were detected at one and two months at middle frequency in the injected ears. Two weeks after noise exposure that induced permanent threshold shifts, injected CBA/CaJ ears manifested significantly lower ABR and DPOAE thresholds compared to uninjected controls ears. In the experimental inner ears of ARHL group, AAV-Isl1 delivery led to significant survival of all hair cells. After noise exposure, significantly better survival of outer hair cells was detected in the injected ears.

Conclusion

The study illustrates that AAV-Isl1 gene therapy could be used to provide long-term hearing protection in different ARHL mouse models as well as NIHL mouse models. In both ARHL and NIHL models hair cell survival is significantly improved by AAV-Isl1 overexpression, supporting a common mechanism underlying some forms of ARHL and NIHL that can be ameliorated by the function of Isl1. Together with a previous study in a transgenic model, we have demonstrated hearing protection by Isl1 hair cell expression in three distinct mouse ARHL models including C57BL/6J, CD1 and DBA/2J, and in C57BL/6J and CBA/CaJ models exposed to noise. The study laid the foundation to use AAV-Isl1 gene therapy as a general approach to treat ARHL and NIHL by rescuing hair cells with clinical application in humans.

PD 166

Inner Hair Cell-specific Expression of Vesicular Glutamate Transporter 3 by Fetal Gene Transfer Restores Hearing in a Mouse Model of Cochlear Synaptopathy

Lingyan Wang[1]; J. Beth Kempton[1]; Wenxuan He[2]; Han Jiang[1]; Rebecca P. Seal[3]; Omar Akil[4]; Tianying Ren[1]; Lawrence R. Lustig[5]; John V. Brigande[1]

[1]*Oregon Hearing Research Center, Oregon Health & Science University;* [2]*Oregon Hearing Research Center;* [3]*University of Pittsburgh;* [4]*University of California San Francisco, Epstein Lab, Dept Otolaryngology-HNS;* [5]*Department of Otolaryngology, College of Physicians and Surgeons, Columbia University and New York Presbyterian Hospital*

Background

Recent advances in gene therapy to treat hearing loss and vestibular dysfunction in mouse models of human inner ear disease have relied on adeno-associated virus (AAV)-mediated gene transfer to the neonatal membranous labyrinth or systemic administration of pharmacological agents to neonates. The neonatal mouse inner ear is functionally immature until the second week of postnatal life. Gene and pharmacotherapies conducted after postnatal day 7 (P7) are dramatically less effective or fail to restore sensory function. A corollary window of therapeutic efficacy in humans is anticipated prior to the emergence of hearing at 16-19 weeks gestation. To evaluate the feasibility of fetal gene therapy to treat congenital hearing loss, we previously showed that transuterine microinjection of AAV1 encoding VGLUT3 to the embryonic day 12.5 (E12.5) otic vesicle restores auditory thresholds at P40 in 22% of VGLUT3 knockout mice to near wild type levels and that significant rescue persists through P340. We speculate that off target expression of VGLUT3 in outer hair cells (OHC) and spiral ganglion neurons (SGN) reduces effectiveness. We hypothesize that constraining expression of VGLUT3 to inner hair cells (IHC) will enhance the efficiency and longevity of hearing restoration in VGLUT3 knockout mice.

Methods

A Cre recombinase-dependent AAV1 vector encoding the chick beta actin promoter driving VGLUT3 (2.4 x 10^14 vector genomes/mL) was microinjected into the E12.5 otic vesicle of VGLUT3 knockout mice carrying a VGLUT3-Cre allele. Hearing function was assessed by auditory-evoked brainstem responses (ABR) and compound action potentials (CAPs). VGLUT3 expression was determined by cochlear whole mount immunofluorescence to assess AAV1 transduction efficiency.

Results

IHC transduction efficiency at P30 was >95% in the apex and midbase and 40% in the base (n=6). In a cohort of 8 P30 Cre-bearing VGLUT3 knockout mice, 7 (87.5%) demonstrated significantly improved ABR thresholds: 8 kHz/40 ± 6.5 dB SPL; 16 kHz/48 ± 4.9 dB SPL; 24 kHz/24 ± 3.4 dB SPL; and 32 kHz/34 ± 5.0 dB SPL. Remarkably, average ABR thresholds at P400 remained significantly improved averaging from 38-61 dB SPL. CAPs at P21-28 show >20-dB threshold improvement across a broad frequency range up to 45 kHz.

Conclusion

Constraining VGLUT3 expression to IHCs dramatically improves the efficiency of AAV1-mediated gene therapy in the VGLUT3 knockout mouse and suggests that cell type-specific expression may emerge as a prerequisite for the most efficacious rescue of cochlear synaptopathies.

PD 167

A666 peptide-conjugated biodegradable naonoparticles as a carrier to target dexamethasone to outer hair cells in inner ear

Xueling Wang[1]; Yuming Chen[2]; Yunge Gao[3]; **Dehong Yu**[4]; Hao Wu[3]

[1]1.Department of Otolaryngology Head & Neck Surgery, Shanghai 9th People's Hospital /Shanghai Ninth People's Hospital , School of medicine, Shanghai Jiao Tong University 2. Ear Institute Shanghai JiaoTong University School of Medicine ） 3.; [2]shanghai 9th peoples hospital Shanghai jiaotong university school of medicine; [3]1.Department of Otolaryngology Head & Neck Surgery, Shanghai 9th People's Hospital / Shanghai Ninth People's Hospital , School of medicine, Shanghai Jiao Tong University 2. Ear Institute Shanghai JiaoTong University School of Medicine ） ; [4]1.Department of Otolaryngology Head & Neck Surgery, Shanghai 9th People's Hospital /Shanghai Ninth People's Hospital , School of medicine, Shanghai Jiao Tong University 2. Ear Institute Shanghai JiaoTong University School of Medicine ） 3. Shanghai K

Targeted delivery of treatment agents to the inner ear using nanoparticles (NPs) has shown a great potential to overcome the limitations of the conventional therapeutic approach to curing or alleviating hearing loss. We developed a drug delivery system, consisting of NPs conjugated with A666-(CLEPRWGFGWWLH) peptides for targeting drug delivery to inner ear outer hair cells (OHCs). Dexamethasone (DEX), a glucocorticoids with potential otoprotective activity, was used as a prototype drug. We designed the maleimide poly(ethylene glycol)-poly(lactide) (Mal-PEG-PLA) block copolymer. A666 ligand, a peptide that can bind to the prestin receptor predominantly expressed on the surface of OHCs in the inner ear with high affinity and specificity, was conjugated to the maleimide group of the PEG chain via the maleimide-thiol coupling method. The A666 peptides-conjugated dexamethasone-loaded NPs (A666-DEX-NP) had a hydrodynamic diameter of 157.80 ±14.33 nm. The A666 density on NPs surface was 3490 ± 1148 per particle and the mean distance between two neighboring PEG chains linked to A666 peptide was 4.85 ± 0.80 nm. The A666-conjugated coumarin 6-labeled NPs (A666-coumarin 6-labeled NP) could be significantly internalized by House Ear Institute-Organ of Corti 1 (HEI-OC1) cells through the A666-prestin interaction. This facilitated uptake of pretreated with A666-DEX-NP, following by cisplatin-treated group, led to the expected enhanced cell viability, reduced apoptotic properties, and decreased ROS levels compared to cells pre-treated with DEX and

DEX-NP, following by cisplatin-treated groups. A666-coumarin 6-labeled NP placed onto the round window membrane (RWM) of guinea pigs showed better RWM penetration and active targeting to OHCs of organs of Corti after 2 h of administration, as compared with coumarin 6-labeled NPs. This nanoparticulate drug delivery system offers a new strategy for delivery of DEX and it could also be used to carry other glucocorticoids, antibiotics, genes, and proteins for treatment of inner ear diseases.

PD 168

GSTA4 Plays an Essential Role in Removing Cisplatin in Female Mice

Shinichi Someya[1]; Hyo-Jin Park[1]; Mi-Jung Kim[1]; Dalian Ding[2]; Karessa White[1]; Chul Han[1]; Maria Ticsa[3]; Isabela Caicedo[1]; Aaron Gomez[3]; Kevin Boyd[1]; Richard Salvi[4]
[1]University of Florida, Department of Aging and Geriatric Research; [2]University at Buffalo, USA; [3]University of Florida; [4]Center for Hearing and Deafness; State University of New York at Buffalo

Background
The glutathione transferase (GST) detoxification system converts a toxic compound into a less toxic form by conjugating the compound to reduced glutathione by GST enzymes. Cisplatin is one of the most widely used chemotherapeutic agents for the treatment of a broad spectrum of cancers. However, one-third of all cisplatin-treated patients develop hearing loss. In the current study, we investigated the role of glutathione transferase α4 (GSTA4), a member of the GST family, in cisplatin detoxification in the cochlea of wild-type (WT) and Gsta4 homozygous knockout mice that were backcrossed onto the CBA/CaJ strain, a well-established model of late onset AHL.

Methods
To investigate how cisplatin treatment affects hearing function in young WT and Gsta4-/- mice, 3-4-month-old mice received cisplatin (3 mg/kg) each day for 4 days followed by 10 days of recovery. This protocol was repeated one additional time for a total of two cycles of cisplatin treatment. Before and after cisplatin treatment, we measured ABR (auditory brainstem response) thresholds, wave I amplitudes, and wave I latencies in young WT and Gsta4-/- mice. Following the ABR tests, we performed histological analyses to assess hair cell loss, spiral ganglion neuron density and stria vascularis thickness in the cochlea of WT and Gsta4-/- mice.

Results
We found that cisplatin treatment resulted in increased ABR thresholds at 32, 48, and 64 kHz in both WT and Gsta4 KO mice. However, under cisplatin treatment,

Gsta4 KO female mice showed significantly higher ABR thresholds at 32 and 48 kHz, higher wave I amplitudes, and lower wave I latencies compared to age-matched WT female mice, while there was no difference in ABR thresholds, wave I amplitudes or wave I latencies between cisplatin-treated WT and Gsta4 KO male mice. In agreement with the hearing test results, cisplatin-treated Gsta4 KO female mice showed increased loss of IHCs and OHCs, decreased SGN density, and decreased SV thickness in the cochlea compared to WT female mice. Furthermore, WT female mice showed significantly higher GSTA4 activities in the inner ear compared to WT male mice under cisplatin treatment.

Conclusions
Together, these results provide evidence that GSTA4 plays an essential role in detoxifying cisplatin in the cochlea of female mice.

Funding

PD 169

A Surrogate in vitro Model for Assessing Compound Permeability Through the Round Window Membrane

Paul Liebesny; Brendan Arsenault; Changsuk Moon; Gabriela Pregernig; Kathy S. So; Fuxin Shi; John Lee
Decibel Therapeutics

Introduction
Understanding the permeability of potential therapeutic compounds through the tight junction barrier of the round window membrane (RWM) is essential for predicting concentrations in the cochlea following intra-tympanic or trans-tympanic delivery. While in vivo studies provide the most accurate and relevant data for characterizing delivery of potential therapeutics, they are time consuming and expensive. Likewise, while ex vivo RWM tissue can be used to determine permeability, the specimens are fragile, and the approach is low throughput. As a simplified surrogate, we developed an in vitro transwell permeability assay using primary mouse tracheal cells that form a tight junction monolayer barrier culturable utilizing an air-liquid interface approach. This 2D model system recapitulates the air-liquid interface of the RWM and allows permeability testing for compounds in solution or hydrogel suspension.

Methods
Primary tracheal epithelial cells isolated from the tracheas of CD-1 mice were cultured in Matrigel to form organoids. Prior to use, organoids were broken into

single cells, plated on transwell filters, and cultured for 1 week until tight junctions formed, as determined by transepithelial electrical resistance values >200 Ω*cm^2. Compounds were added to the top of the transwell in artificial perilymph solution (AP) or 20% poloxamer-407, while the bottom chamber was filled with a AP bath. Compound concentrations were measured by LC-MS/MS (Agilent 1260 HPLC/AB Sciex QTRAP 4500) over a 26-hour time course using multiple reaction monitoring (MRM) in ESI positive ion mode. To compare the characteristics of the primary trachea cells to native round window membrane cells, the transcriptional profiles of each were examined by RNA-Seq. RNA extracted from primary mouse tracheal cells and guinea pig round window membrane was amplified and prepped for Illumina sequencing.

Results & Discussion

When delivered in solution in AP, metoprolol and dexamethasone were highly permeable in this system (>10e-6 cm/s), whereas atenolol and lucifer yellow were moderate (5-10e-6 cm/s) and low (<5e-6 cm/s) permeability compounds, respectively. Delivery by encapsulation in 20% poloxamer-407 generally reduced the measured flux of the compound in a dose-dependent manner, with a larger effect observed for highly permeable compounds. Analysis of the RNA-Seq data revealed several drug transporters, including members of the ABC and SLC families, as well as tight junction and adherens junction genes, which are robustly expressed in both the RWM and primary tracheal cells. Transcriptional profiling thus indicates that this system may serve as a rough surrogate for native round window membrane in assessing compound permeability.

PD 170

Murine Round Window Membrane Inner Ear Drug Delivery with a Wirelessly Controlled Implantable Micropump

Farzad Forouzandeh[1]; Xiaoxia Zhu[2]; Ahmed Alfadhel[1]; Meng-Chun Hsu[1]; Joseph P. Walton[3]; Denis Cormier[1]; Robert D. Frisina[4]; David Borkholder[1]
[1]Rochester Institute of Technology; [2]Global Center for Hearing & Speech Research, University of South Florida- Tampa; [3]Department of Communication Sciences & Disorders, and Chemical and Biomedical Engineering, Global Center of hearing and Speech Research, University of South Florida, Tampa, FL; [4]Global Center for Hearing and Speech Research, University of South Florida- Tampa

Recent advances in protective and restorative biotherapies have created new opportunities to address auditory and vestibular disorders with site-directed, programmable drug delivery systems. Successful therapy development leveraging the transgenic, knock-in, and knock-out variants of human disease in the mouse model system requires advanced microsystems specifically designed to function with nano-liter precision and with system volumes suitable for implantation. Here we present a novel biocompatible, fully implantable, scalable, and wirelessly controlled peristaltic micropump. The structure of the micropump is built around a commercially available catheter microtubing (250µm OD, 125µm ID), which can provide a biocompatible leak-free flow path while avoiding complicated microfluidic interconnects. Peristaltic pumping is achieved by sequentially compressing the microtube via expansion and contraction of a thermal phase-change material that is located in three chambers integrated adjacent to the microtube. Direct write micro-scale printing technology was used to build the mechanical components of the pump around the microtubing directly on the backside of a printed circuit board assembly (PCBA). The custom PCBA is fabricated with standard commercial processes, providing microprocessor control of actuation and Bluetooth wireless communication through an Android application. In vitro pump characterization results are presented, demonstrating a precise control over the drug delivery flow rate in the desired range by changing the actuation frequency. It is also shown that the pump can provide desired flow rates (15-50nl/min) in the presence of physiological back pressures (0.3-0.6 kPa). Three different pumps were tested on eight mice for in vivo implantation of the microcatheter tubing into the round window membrane niche for infusion of a known ototoxic compound, sodium salicylate at 50 nL/min. Real-time shifts in distortion product otoacoustic emission (DPOAE) thresholds and amplitudes (DPgrams) as a function of infusion time were consistent with our previously published results using syringe pump delivery of salicylate at the same flow rate. This proof of concept in vivo success of our advanced micropump technology in the mouse, where the entire volume of the mouse cochlea is less than 1 µL, indicates translational opportunities. The pump is inherently scalable to larger species and for clinical applications in children and adults by appropriate scaling of the microtubing size and actuator volume. Advanced micropumps like this provide organ-targeted drug delivery to avoid systemic side effects and maximal control of drug concentration and timing parameters.

PD 171

A Surgical Procedure for the Administration of Drugs to the Inner Ear in a Non-Human Primate Common Marmoset (Callithrix jacchus)

Sho Kurihara[1]; **Masato Fujioka**[2]; Tomohiko Yoshida[3]; Makoto Koizumi[4]; Hiromi Kojima[3]; Kaoru Ogawa[5]; Hirotaka James Okano[6]
[1]Department of Otorhinolaryngology, Jikei University School of Medicine, Tokyo, Japan; [2]Department of Otolaryngology, Head and Neck Surgery, School of Medicine, Keio University; [3]Department of Otorhinolaryngology, Jikei University School of Medicine; [4]Laboratory Animal Facilities, Jikei University School of Medicine, Tokyo, Japan; [5]Department of Otolaryngology, Head and Neck Surgery, Keio University School of Medicine; [6]Division of Regenerative Medicine, Jikei University School of Medicine

Hearing research has long been facilitated by rodent models; but in some diseases, human symptoms cannot be recapitulated. The common marmoset (Callithrix jacchus) is a small, easy-to-handle New World monkey which has a similar anatomy of the temporal bone, including the middle ear ossicular chains and inner ear to humans than in comparison with that of rodents. Here, we report a reproducible, safe, and rational surgical approach to the cochlear round window niche for the drug delivery to the inner ear of the common marmoset.

Methods

We adopted posterior tympanotomy, a procedure used clinically in human surgery, to avoid manipulation of the tympanic membrane that may cause conductive hearing loss. All experiments were approved by an institutional animal committee (2015-099) in accordance with NIH guideline. Marmosets were immobilized by general anesthesia and their respiratory state was maintained by a ventilator. In a supine position, post-auricular incision was made and the lateral part of the temporal bone was exposed by peeling muscles. Opened up the bone by drilling, the lateral semicircular canal was identified. After confirming the incus, posterior tympanotomy was performed: a small hole was made with 0.6 mm diameter diamond bar in between posterior wall of the external auditory canal and the vertical portion of the facial nerve. Thru the hole, promontory and round window niche can be observed. In case with the over-hanged facial nerve at its vertical portion that interferes with the access to the round window niche, the posterior wall of the external auditory canal should be drilled as thin as possible so the niche can be visualized. In these cases, particularly, endoscopic inspection helps to confirm the round window niche and, directly, membrane.

Discussion

This approach was possible due to the large bulla structure of the common marmoset, although the lateral semicircular canal and vertical portion of the facial nerve should be carefully considered. Variation can be sometimes recognized in the level of aeration or the development of mastoid structure, which can be easily and safely coped with.

Conclusion

Presenting surgical method allows us to perform safe and accurate administrations of drugs without making hearing loss, which is of great importance in obtaining pre-clinical proof of concepts for new therapeutics in the translational research.

Inner Ear: Innate Protection

PD 172

The Essential Role of Cannabinoid Receptor (CB2) in the Cochlea in Otoprotection

Debashree Mukherjea[1]; Sumana Ghosh[1]; Kelly Sheehan[1]; Asmita Dhukhwa[1]; Sandeep Sheth[1]; Leonard Rybak[2]; Vickram Ramkumar[1]
[1]SIU School of Medicine; [2]Southern Illinois University School of Medicine

CB receptors include cannabinoid receptor 1 (CB1), cannabinoid receptor 2 (CB2) and non-CB1/CB2, such as transient potential vanilloid 1 receptor (TRPV1) and G protein-coupled receptor 55 (GPR55). CB1 are abundant in the brain where they modulate neuronal activities, while CB2 are predominantly expressed in the immune cells and regulate the growth and proliferation of different immune cells and modulate the activities of cytokines network and anti-oxidant machinery in stress conditions. CB2 are localized to the cochlea and are induced by cisplatin. In an organ of Corti-derived cell cultures, activation of CB2 protected against cisplatin-induced apoptosis. In the current study, we provide a detailed distribution of CB2R in the mouse and rat cochleae and showed that these receptors protects against cisplatin-induced hearing loss. In a knockin mouse model expressing CB2 tagged with green fluorescent protein (GFP), we show distribution of CB2 in the organ of Corti, stria vascularis (SV), spiral ligament (SL) and spiral ganglion cells. A similar distribution of CB2 was observed in the rat cochlea using a polyclonal antibody. Activation of these receptors with trans-tympanic administration of the agonist JWH-015 protected against cisplatin-induced hearing loss which was reversed by the antagonist, AM630. Protection was associated with reduced loss of outer hair cells (OHCs), preservation in inner hair cell (IHC) ribbon synapses and maintenance of Na$^+$/K$^+$ ATPase immunoreactivity in the SV and SL. AM630

alone produced significant hearing loss independent of loss of OHCs, but associated with loss of IHC ribbon synapses and loss of Na⁺/K⁺ ATPase in the SV and SL. Knock-down of CB2R by trans-tympanic siRNA sensitized the cochlea to cisplatin-induced hearing loss at low and middle frequencies. Hearing loss induced by cisplatin and AM630 in the rat was associated with increased genes for oxidative stress and inflammatory proteins in the rat cochlea. These data unmasked a protective role of the cochlear endocannabinoid/CB2 system which is active under normal, low level stress conditions. However, application of exogenous agonist is needed to boost the activity of CB2 for protection against a more traumatic insult, such as cisplatin.

PD 173

Estrogenic Protection from Noise-Induced Hearing Loss in Females But Not in Males

Ryan M. Casserly[1]; Sunayana Mitra[1]; Shaun Viechweg[1]; Benjamin Shuster[2]; Allen Myers[3]; Yang Song[4]; Beatrice Milon[1]; Didier Depireux[5]; Jessica A. Mong[1]; Ronna Hertzano[6]
[1]University of Maryland School of Medicine, Baltimore, MD, USA; [2]University of Maryland School of Medicine; [3]University of Maryland School of Medicine, Baltimore, MD; [4]University of Maryland School of Medicine, Baltimore MD, USA; [5]Institute for Systems Research, University of Maryland College Park, MD, USA; [6]University of Maryland School of Medicine, Baltimore, MD USA

Background

Hearing loss remains a major health concern with little in the way of treatment or prevention. Prior literature has demonstrated 1) a sex difference in the response to acoustic trauma in mice, and 2) estrogen as an otoprotective agent against temporary threshold shift-inducing acoustic trauma in females. However, it is unknown whether estrogen has a similar effect for females in response to more intense noise, at a level that would induce a permanent threshold shift (PTS), and whether estrogen has any otoprotective effect in males.

Objectives

To 1) determine whether estrogen can provide otoprotection from PTS-inducing noise exposure, in both male and female mice, and 2) physiologically and histologically characterize the estrogenic otoprotective effect.

Methods

Thirty two 8-week old B6CBAF1/J (16 males, 16 females) were gonadectomized. Animals were simultaneously implanted with an Alzet® micro-osmotic pump loaded with estradiol or vehicle alone (polypropylene glycol)

with a dose of 1 mg/kg/day. With these four groups, animals underwent baseline auditory brainstem response (ABR) testing at one week post-surgery/implantation. At 10 weeks of age, they were exposed to 102.5 dB SPL of octave-band noise (8-16 kHz) for two hours. Hearing thresholds were measured at 24 hours post-exposure for compound threshold-shift (CTS) and 15 days post-exposure for permanent threshold-shift (PTS). After the final ABR, blood was collected, estrogen-responsive reproductive organs were photographed, and cochleae were procured for cytocochleograms and synaptic ribbon counts using CtBP2 antibody.

Results

ABR thresholds shifts were analyzed separately by sex and by frequency. In females, estrogen had a significant protective effect for both CTS (at 8, 24 and 32 kHz) and PTS (at 8, 16, 24 and 32 kHz). In males, however, there was only significant protection for both CTS and PTS at 16 kHz. Conversely, PTS for males receiving estrogen at 32 kHz demonstrated higher threshold shifts than those who received vehicle alone.

Conclusions

Our data show a strong otoprotective effect by estrogen in females but not in males. Furthermore, we demonstrate a rescue of PTS-inducing NIHL in females in this hormone-controlled ovariectomy model for the first time. By studying sex differences in hearing we could further our knowledge of protective mechanisms from NIHL, which could then be used to develop therapeutics for both sexes.

PD 174

Netrin1 Mediates the Protection of Cochlear Hair Cells by IGF1 through its Canonical Receptor, UNC5B

Norio Yamamoto[1]; Kohei Yamahara[2]; Takayuki Nakagawa[3]; Kazuo Kinoshita[4]; Koichi Omori[5]; Juichi Ito[4]
[1]Department of Otolaryngology, Head and Neck Surgery, Graduate School of Medicine, Kyoto University; [2]Department of Otlaryngology, Head and Neck Surgery, Graduate School of Medicine, Kyoto University; [3]Department of Otolaryngology - Head and Neck Surgery, Graduate School of Medicine, Kyoto University; [4]Shiga Medical Center Research Institute; [5]Department of Otolaryngology-Head and Neck Surgery, Graduate School of Medicine, Kyoto University

Sensorineural hearing loss (SNHL) is mainly caused by the damage of cochlear hair cells (HCs). As HCs and supporting cells (SCs) that exist around HCs do not proliferate in postnatal mammals, the loss of HCs and SCs

is irreversible, emphasizing the importance of preserving their numbers to prevent SNHL. It is shown by our group that insulin-like growth factor 1 (IGF1) is instrumental in the treatment of SNHL (Lee et al., 2007). Our previous study indicates that IGF1 protects HCs against aminoglycoside by activating the IGF1 receptor and its major downstream pathways in SCs (Hayashi et al., 2013), which results in the upregulation of the expression of the Netrin1-encoding gene (Ntn1) (Hayashi et al., 2014).

To determine if NTN1 acts as a downstream molecule of IGF1 to protect cochlear HCs against inner ear damage, we performed several experiments. First, we demonstrated that NTN1 promoted HC survival as we observed for IGF1. Secondly, we found that NTN1 blocking antibodies attenuated IGF1-induced HC protection from aminoglycoside, indicating that NTN1 is the effector molecule of IGF1 signaling during HC protection.

To elucidate the responsible receptors among six canonical NTN1 receptors that mediated the effect of cochlear HC protection, the localization of canonical NTN1 receptors were examined using in situ hybridization. UNC5B is the only receptor that was expressed in the organ of Corti through whole turns of cochleae. Addition of blocking antibodies of UNC5B attenuated the cochlear HC protection by NTN1, indicating that UNC5B is the NTN1 receptor involved in the HC protection. The effect of IGF1 on the protection of HCs against aminoglycoside was also attenuated by UNC5B blocking antibodies. These results suggested that NTN1 and its receptor, UNC5B, mediate the effect of IGF1 to protect HCs.

Apoptosis was significantly suppressed by NTN1 when HCs were protected from aminoglycoside although the proliferation of SCs was not affected by NTN1. Considering that IGF1 protects HCs from aminoglycoside through the inhibition of apoptosis and the promotion of SC proliferation, this observation indicates that NTN1 mediates a part of the downstream of IGF1.

Our results provide new insights into the mechanisms underlying IGF1 protection of cochlear HCs, suggesting a possibility of using NTN1 as a new treatment for SNHL.
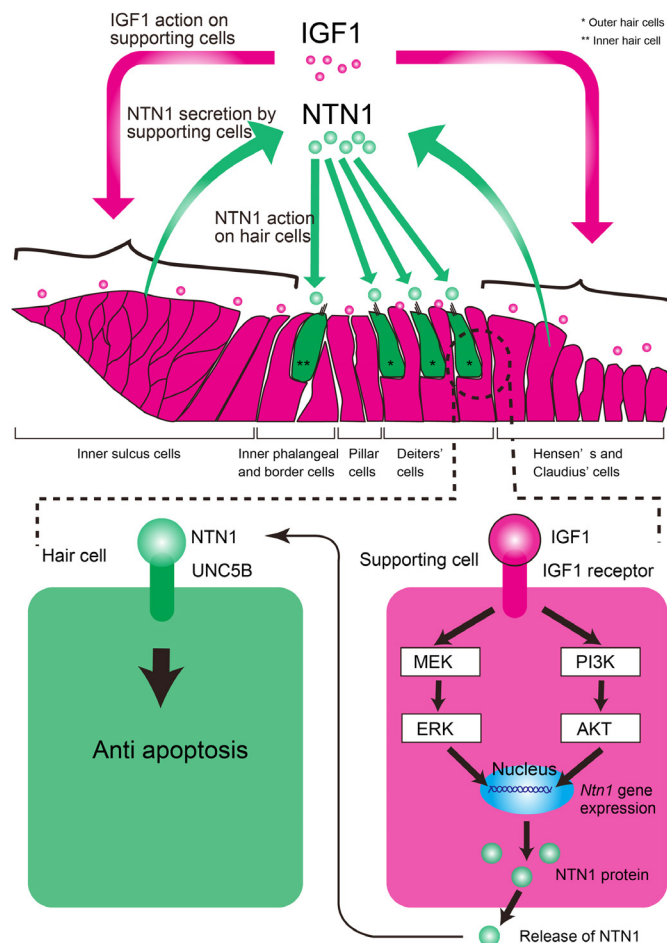
PD 175

Restoration of Methionine sulfoxide reductase B3 in the inner ear rescues hearing in a mouse model of congenital sensorineural hearing loss by in utero gene therapy

Min-A Kim; Byeonghyeon Lee; Nari Ryu; Un-Kyung Kim; Kyu-Yup Lee
Kyungpook National University

Methionine sulfoxide reductase B3 (MsrB3) is specifically repairs methionine-R-sulfoxide, which is important for the maintenance of hair cells, and the mutations in the MsrB3 gene are associated with human autosomal recessive nonsyndromic hearing loss due to the apoptotic death of cochlear hair cells and the degeneration of stereociliary bundles. Here, we investigated a fundamental treatment strategy in an MsrB3 deficiency mouse model and confirmed the biological significance of MsrB3 in the inner ear using MsrB3 knockout (MsrB3−/−) mice. We delivered a recombinant adeno-associated virus (rAAV) encoding the MsrB3 gene directly into the otocyst at embryonic day 12.5 using an in-utero approach. We observed hearing restoration in the treated ears of MsrB3−/− mice at postnatal day 28, and we identified MsrB3 mRNA and protein expression in cochlear ex-

tracts. Additionally, we demonstrated that the morphology of the stereociliary bundles in the rescued ears of MsrB3−/− mice was similar to those in MsrB3+/+ mice. To our knowledge, this is the first study to demonstrate functional and morphological rescue of the hair cells of the inner ear in the MsrB3 deficiency mouse model of congenital genetic sensorineural hearing loss using an in utero, virus-mediated gene therapy approach. Our results provide insight into the role of MsrB3 in hearing function and bring us one step closer to hearing restoration as a fundamental therapy.

PD 176

The cochlear lateral wall as a stress manager

Anni Herranen; Kuu Ikäheimo; Ulla Pirvola
Department of Biosciences/University of Helsinki, Finland

Differential susceptibility to noise trauma between mouse strains has been acknowledged for a long time. To understand the mechanisms behind these differences, we compared two mouse strains, one susceptible and one resistant to noise trauma, and studied the possible differences in the stress response of the cells of their cochleas. Mitogen-activated protein kinase (MAPK) pathways are important components of the large stress response network in cells, similar to NF-kB signaling. Several studies have described the activation of these pathways in the cochlea following noise trauma. By studying the response acutely after noise exposure, we found that the MAPK stress responses are activated in the organ of Corti of both noise-susceptible and –resistant mouse strains. In contrast, striking differences between the strains were found in the cochlear lateral wall; the spiral ligament and stria vascularis. The MAPK stress responses were largely absent in the lateral wall of noise-resistant mice, while they were prominently present in noise-susceptible mice. NF-kB transcriptional activation, detected with a transgenic reporter mouse line, was not seen in the organ of Corti of neither noise-resistant nor –susceptible mice and this activation in the lateral wall was very limited.

To further address the absence of stress responses in the cochlear lateral wall of the noise-resistant mouse strain, we triggered systemic stress that is transmitted to the lateral wall mainly via the microcirculation in the stria vascularis. Systemic stress alone and particularly systemic stress combined with noise exposure elicited strong and broad MAPK activation in the lateral wall. This response was found both in the noise-resistant and –susceptible mouse strains. These findings show that also the lateral wall of noise-resistant mice is capable of sensing stress and eliciting a stress response. Our results suggest that the stress response mounted in the organ of Corti is not efficiently transmitted to the cochlear lateral wall in these mice. The mechanisms involved are not understood.

Our results show the importance of the lateral wall in noise trauma by revealing the link between the loss of outer hair cells of the organ of Corti and MAPK activation in the lateral wall. Our results suggest that several compartments of the lateral wall can potentially be targeted by systemic effects via stria vascularis. Modulating the stress response in the lateral wall through systemic effects might be useful as an intervention to treat noise-induced hearing loss.

PD 177

Autophagy protects auditory hair cells against neomycin-induced damage

Zuhong He[1]; Lingna Guo[1]; Yilai Shu[2]; Qiaojun Fang[1]; Han Zhou[3]; Xiaoli Zhang[3]; Suhua Sa[4]; Weijia Kong[5]; Huawei Li[6]; Xia Gao[3]; **Renjie Chai**[1]
[1]*Southeast University;* [2]*1. Department of Otolaryngology, Harvard Medical School, 2. Eaton-Peabody Laboratory, Massachusetts Eye and Ear Infirmary, 3. Department of Otolaryngology, Hearing Research Institute, Affiliated Eye and ENT Hospital of Fudan University;* [3]*Affiliated Drum Tower Hospital of Nanjing University;* [4]*Medical University of South Carolina;* [5]*Huazhong University of Science and Technology;* [6]*Department of Otolaryngology, Hearing Research Institute, Affiliated Eye and ENT Hospital of Fudan University*

Aminoglycosides are toxic to sensory hair cells (HCs) by inducing the production of reactive oxygen species (ROS) that in turn activate apoptotic pathways. Autophagy is an essential and highly conserved self-digestion pathway that plays important roles in the maintenance of cellular function and viability under stress. However, the role of autophagy in aminoglycoside-induced HC injury is unknown. In this study, we systematically investigated the role of autophagy in aminoglycoside-induced HC damage. First we found that autophagy activity was significantly increased, including enhanced autophagosome-lysosome fusion, in both the cochlear HCs and HEI-OC-1 cells after neomycin/gentamicin injury. This suggested that autophagy might be correlated with aminoglycoside-induced cell death. We then used rapamycin, an autophagy activator, to increase the autophagy activity and found that the ROS level, apoptosis, and cell death were significantly decreased after neomycin/gentamicin injury. In contrast, treatment with the autophagy inhibitor 3-methyladenine (3-MA) or knockdown of autophagy-related proteins (ATGs), including ATG5, BECN1, and ATG7, resulted in reduced autophagy activity and significantly increased ROS levels, apoptosis,

and cell death after neomycin/gentamicin injury. Lastly, after neomycin injury, the antioxidant N-acetylcysteine could successfully prevent the increased apoptosis and HC loss induced by 3-MA treatment or ATG knockdown, suggesting that autophagy protects against neomycin-induced HC damage by inhibiting oxidative stress. We also found that the dysfunctional mitochondria were not eliminated by autophagy (mitophagy) in HEI-OC-1 cells after neomycin treatment, suggesting that autophagy might not directly target the damaged mitochondria for degradation. This study demonstrates that moderate ROS levels can promote autophagy in order to recycle damaged cellular constituents and maintain cellular homeostasis; while the induction of autophagy can inhibit apoptosis and protect the HC by suppressing ROS accumulation after neomycin/gentamicin injury. Our results suggest that autophagy might be a new therapeutic target for the prevention of aminoglycoside-induced HC death.

PD 178

### The protective effect of autophagy on ischemia/reperfusion induced hearing loss: implication for sudden hearing loss

Jiaqi Pang[1]; Haidi Yang[2]; Hao Xiong[3]; Zhengfei Yang[2]; Yiqing Zheng[1]
[1]Sun Yat-sen Memorial Hospital, Sun Yat-sen University, China; [2]Sun Yat-sen Memorial Hospital, Sun Yat-sen University; [3]Medical University of South Carolina

The present study aimed to determine the effects of ischemia/reperfusion (IR) injury for the carotid system on hearing, particularly, the role of autophagy in this process. Sixty-three Sprague-Dawley rats were divided randomly into three groups: sham surgery animals (S), temporary carotid artery occlusion (ischemia) for 30 min (I30), and temporary carotid artery occlusion for 60 min (I60). Auditory brainstem response measurements were performed on mice. After 72 h of reperfusion, the microcirculation was measured in mice after ischemia injury. Immunofluorescence was used to examine the expression of caspase-3 and light chain 3B in the cochlear sections. Temporary carotid artery occlusion lasting for 30 (I30) or 60 min (I60) caused significant hearing loss in the ischemia phase. Following a recovery during the postreperfusion phase, the temporal threshold shift occurred in the I30 group, whereas a permanent threshold shift occurred in the I60 group. Moreover, both microcirculation and autophagy affected hearing 24 h after reperfusion, whereas at 72 h, autophagy works as an intrinsic cellular process that protects against death from the IR effect. These results suggest that the sooner the reperfusion, the better the hearing recovery. In conclusion, autophagy promotes cell survival in the co-

chlea; however, excessive IR damage overwhelms the beneficial potential of autophagy protection and leads to a permanent threshold shift.

hearing teated ischemia_victor revised 2017.pdf
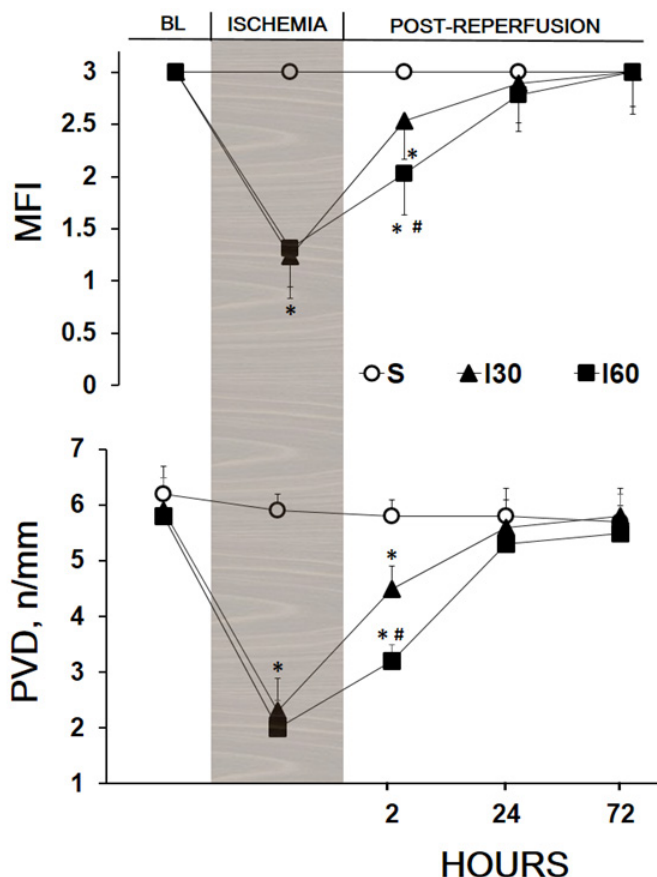
PD 179

Exosome-associated HSP70 protects against aminoglycoside-induced hair cell death.

Nora Welsh[1]; Andrew M. Breglio[2]; Ronald S. Petralia[3]; Ya-Xian Wang[3]; Lindsey May[1]; Lisa Cunningham[4]
[1]Section on Sensory Cell Biology, National Institute on Deafness and Other Communication Disorders, National Institutes of Health; [2]National Institute on Deafness and Other Communication Disorders & University of Oxford; [3]Advanced Imaging Core, National Institute on Deafness and Other Communication Disorders, National Institutes of Health; [4]National Institute on Deafness and Other Communication Disorders

Background
Heat shock proteins (HSPs) are highly-conserved molecular chaperones that mediate re-folding of misfolded proteins, respond to a wide-range of cellular stresses, and can help prevent apoptosis. Previously, we have

shown that heat shock can protect against aminoglycoside-induced hair cell death in utricles in vitro, and that this otoprotective response is mediated through extracellular HSP70 (May et al 2013). Extracellular HSP70 is commonly associated with exosomes, a type of extracellular vesicle. We hypothesized that the protective effect of heat shock is mediated by exosomes carrying HSP70.

Methods
Utricles from CBA/J mice were heat-shocked in a 43°C water bath for 30 minutes and then allowed to recover at 37°C. Following recovery, expression of HSP70 was analyzed by immunohistochemistry. Transmission electron microscopy (TEM) was used to visualize vesicles within heat-shocked and control utricles. Exosome release was quantified by nanoparticle tracking analysis (NTA) of conditioned media from heat-shocked utricles. An enzyme-linked immunosorbent assay (ELISA) was used to measure concentrations of inducible HSP70 in utricles and their conditioned media. Exosomes were isolated from this conditioned media via differential ultracentrifugation or ultrafiltration.

Results
Following heat shock, HSP70 was robustly expressed in all supporting cells and a small fraction of hair cells. NTA analysis revealed an increase in the production of exosomes from heat-shocked utricles, as compared to controls. TEM showed multivesicular bodies containing exosome-like vesicles present in both hair cells and supporting cells following heat shock. ELISA analysis demonstrated that HSP70 is upregulated in heat-shocked utricles and their conditioned media. A portion of extracellular HSP70 was associated with exosomes.

Conclusions
HSP70 expression is significantly induced after heat shock and this expression is largely limited to supporting cells, suggesting that supporting cells are central to the otoprotective role of HSP70. Exosome release also increases significantly after heat shock, and these exosomes contain HSP70. Together, these data suggest that exosomes carrying HSP70 help mediate the protective heat shock response. Additionally, these results suggest that exosomes may play an innate protective role in hair cell survival and may hold potential for further therapeutic development.

SAVE THE DATES

FEBRUARY 9-13 2019
42nd Annual MidWinter Meeting
Baltimore Marriot Waterfront
Baltimore, Maryland, USA

JANUARY 25-29, 2020
43rd Annual MidWinter Meeting
San Jose Convention Center
San Jose, California

FEBRUARY 20-24, 2021
44th Annual MidWinter Meeting
Renaissance SeaWorld
Orlando, Florida

FEBRUARY 5-9, 2022
45th Annual MidWinter Meeting
San Jose Convention Center
San Jose, California

Association for Research in Otolaryngology
19 Mantua Road
Mt. Royal, NJ 08061
www.aro.org